

# Late Cainozoic rainforest vertebrates from Australopapua: evolution, biogeography and extinction

**Author:**

Hocknull, Scott Alexander

**Publication Date:**

2009

**DOI:**

<https://doi.org/10.26190/unsworks/22854>

**License:**

<https://creativecommons.org/licenses/by-nc-nd/3.0/au/>

Link to license to see what you are allowed to do with this resource.

Downloaded from <http://hdl.handle.net/1959.4/44580> in <https://unsworks.unsw.edu.au> on 2024-05-05

# LATE CAINOZOIC RAINFOREST VERTEBRATES FROM AUSTRALOPAPUA: EVOLUTION, BIOGEOGRAPHY AND EXTINCTION

**Scott A. Hocknull**

Thesis submitted in fulfilment of the requirements for the degree of Doctor of  
Philosophy in the School of Biological, Earth and Environmental Sciences  
University of New South Wales Sydney, Australia  
January 2009

**THE UNIVERSITY OF NEW SOUTH WALES  
Thesis/Dissertation Sheet**

Surname or Family name: Hocknull

First name: Scott

Other name/s: Alexander

Abbreviation for degree as given in the University calendar:

PhD

School: Biological, Earth and Environmental Sciences

Faculty: Science

Title: **Late Cainozoic rainforest vertebrates from Australopapua: evolution, biogeography and extinction.**

**Abstract 350 words maximum: (PLEASE TYPE)**

Understanding the evolution, biogeography and extinction of Australopapuan vertebrate lineages is fundamental to determining baseline responses of those groups to past environmental change. In light of predicted climatic change and anthropogenic impact, it is imperative to determine the trajectories of Australia's modern flora and fauna. In particular, mesothermic rainforest faunas are among Australia's most vulnerable terrestrial biota under threat from both natural and anthropogenic causes. There is a gap in knowledge of past patterns of change and, in particular, a conspicuous lack of direct evidence of response of rainforest faunas to past climatic change.

This study documents the late Cainozoic Australopapuan rainforest vertebrate record and its response to environmental change via adaptive radiation, biogeographical change and extinction. In particular, it provides the first detailed systematic appraisal of Quaternary fossil sites and local faunas from northern Australia. The study documents the only known Quaternary mesothermic rainforest fauna in Australia and its transition to a xeric-adapted fauna during the middle Pleistocene.

The fossil assemblages analysed are comprised of dozens of species, including several new genera and species. Each fossil taxon shares a close phylogenetic relationship with others either known only from the Australian Tertiary record or from Quaternary-Recent New Guinea and Wet Tropics rainforests. The presence of many species is evidence of previously much larger distributions followed by subsequent massive range retractions.

Detailed documentation of this rare fauna testifies to rainforest stability in central eastern Queensland until approximately 280,000 years ago, when the development of an El Nino dominated climate generated variable climatic patterns that could not support aseasonal rainforest. Extinction of this late Pleistocene rainforest fauna serves as one of only two examples of major rainforest faunal turnover in Cainozoic Australia, the other occurring in the late Miocene. These two major extinction events are compared. The late Pleistocene faunal extinction differs from the late Miocene event in being biased towards large-bodied, terrestrial herbivores and carnivores (both reptile and mammal).

This study also combines fossil and phylogenetic data with latest understanding of palaeogeography, tectonics and sea level history along Australia's northern margin to provide hypotheses of faunal dispersal between New Guinea and mainland Australia throughout the Neogene.

**Declaration relating to disposition of project thesis/dissertation**

I hereby grant to the University of New South Wales or its agents the right to archive and to make available my thesis or dissertation in whole or in part in the University libraries in all forms of media, now or here after known, subject to the provisions of the Copyright Act 1968. I retain all property rights, such as patent rights. I also retain the right to use in future works (such as articles or books) all or part of this thesis or dissertation. I also authorise University Microfilms to use the 350 word abstract of my thesis in Dissertation Abstracts International (this is applicable to doctoral theses only).

**Signature****Witness****Date**

**The University recognises that there may be exceptional circumstances requiring restrictions on copying or conditions on use. Requests for restriction for a period of up to 2 years must be made in writing. Requests for a longer period of restriction may be considered in exceptional circumstances and require the approval of the Dean of Graduate Research.**

FOR OFFICE USE ONLY

**Date of completion of requirements for Award:****THIS SHEET IS TO BE GLUED TO THE INSIDE FRONT COVER OF THE THESIS**

**ORIGINALITY STATEMENT**

'I hereby declare that this submission is my own work and to the best of my knowledge it contains no materials previously published or written by another person, or substantial proportions of material which have been accepted for the award of any other degree or diploma at UNSW or any other educational institution, except where due acknowledgement is made in the thesis. Any contribution made to the research by others, with whom I have worked at UNSW or elsewhere, is explicitly acknowledged in the thesis. I also declare that the intellectual content of this thesis is the product of my own work, except to the extent that assistance from others in the project's design and conception or in style, presentation and linguistic expression is acknowledged.'

A handwritten signature in black ink, featuring a large, stylized 'S' and 'H' followed by a long horizontal stroke.

Signed  
Dated

31<sup>st</sup> March, 2009



## Dedication

*I dedicate this thesis to,*

*my small family,*

*Pop, Gran, Granny, Grandad, Dad, Mum, Dad M, Mom M, Craig,  
Laura, Aston, my daughter Angie and my wife Shona...*

*my best mates,*

*Paul, Noel and Dave...*

*The members of the Central Queensland Speleological Society,  
for their dedication to fighting the good fight and introducing me to  
the amazing world of Mt Etna, Queensland.*

*Henk Godthelp,  
for taking the time.*

*my close colleagues,  
who have stood by and waited for me to finish this bloody thing!*

*“Back off, man, I’m a Scientist...”*

(Bill Murray as Dr. Peter Venkman in *Ghostbusters*<sup>TM</sup>, 1984)

## Acknowledgements

I would like to acknowledge the following people for their tireless support of me in my pursuit of this thesis. As always, I list these people in alphabetical order and in no list of hierarchy as I believe everyone has assisted me in many different and meaningful ways. To not acknowledge you all would be a disservice.

Aaron Sands, Alex Cook, Allan Greer, Alan Andrews, Amy Sands, Amanda Laner, Andrew Amey, Angelique Ford, Angelica Wilson, Anna Gillespie, Aston Marks, Bernard Cooke, Ces & Doris Wilkinson, Christina Cook, Chris Bell, Chris White, Clive Cavanah, Craig Hocknull, Dave Pickering, David Elliott, Debra Lewis, Diane Vavyrne, Dirk Megirian, Don Kiem, Durumbal People, Eric Fitzgerald, Gavin Prideaux, Gilbert Price, Gregg Webb, Heather Janetski, Henk Godthelp, Jan Williams, Jeanette Sands, Jian-xin Zhao, Jim McNamarra, Jim Mead, Joanne Ford, Joanne Wilkinson, John Hocknull, John Hooper, John Long, John Scanlon, Jonathan Cramb, Joshua Moulds, Joyce McNeil, Judy Elliott, Julian Louys, Karen Black, Karen Roberts, Ken Aplin, Ken McNamarra, Kristen Spring, Laura Hocknull, Laurie Beirne, Libby Cannon (& Family), Linda Deer, Lindal Dawson, Liz Reed, Luke Berrill, Luke Nothdurft, Lynne Angrews, Mark Hutchinson, Mary Dettmann, Maria Zammit, Mathew Ng, Michael Archer, Mike Lee, Mike Tyler, Mina Bassarova, Morag Hocknull, Natalie Camilleri, Noel Sands, Pat Vickers-Rich, Patrick Couper, Patrick Moss, Paul Tierney, Paul Willis, Peter Berrill, Peter Kershaw, Philip Marks, Ralph Molnar, Robyn Mackenzie, Rod Wells, Ross Sadler, Sandrine Martinez, Sandy Ingleby, Sarah Perrott, Saskia Dyke, Shona (nee Marks) Hocknull, Stuart Mackenzie, Steve Bourne, Steve Donnellan, Steve McGlouchlin, Steve Van Dyck, Susan Hand, Tim Flannery, Tish Ennis, Tom Rich, Trevor Clifford, Troy Myers, Wendy Marks, Yuexing Feng, Work for the Dole participants and countless volunteers.

## Table of Contents

<b>Dedication .....</b>	<b>iv</b>
<b>Acknowledgements .....</b>	<b>vi</b>
<b>Table of Contents.....</b>	<b>vii</b>
<b>List of Tables and Figures .....</b>	<b>x</b>
 <b>Chapter 1 .....</b>	 <b>1</b>
1.1 Introduction & Study Area .....	1
1.2 Introduction .....	1
1.3 Study Area 1: Mt Etna Region, central eastern Queensland .....	4
1.4 Study Area 2: Marmor Quarry, central eastern Queensland. ....	20
1.5 Present Day Environment.....	22
1.6 Methods .....	25
 <b>Chapter 2.....</b>	 <b>33</b>
2.1 Ecological succession during the late Cainozoic of central eastern Queensland: extinction of a diverse rainforest community. ....	33
2.2 Preface .....	33
2.3 Abstract .....	33
2.4 Introduction .....	35
2.5 HISTORY OF COLLECTION .....	37
2.6 METHODS.....	40
2.7 FAUNAL ASSEMBLAGES (LOCAL FAUNA). ....	43
2.8 FAUNAL ASSEMBLAGE AGE.....	43
2.9 GEOLOGICAL SETTINGS .....	44
2.10 SITE LIST.....	46
2.11 MOUNT ETNA LIMESTONE MINE AND NATIONAL PARK 47	
2.12 LIMESTONE RIDGE.....	62
2.13 NORTHWEST LIMESTONE RIDGE.....	62
2.14 SOUTHEAST LIMESTONE RIDGE .....	64
2.15 OLSEN’S CAVE SYSTEM .....	67
2.16 KARST GLEN SYSTEM .....	68
2.17 MARMOR QUARRY .....	70
2.18 UNDESCRIBED TAXA .....	71
2.19 SYSTEMATIC PALAEONTOLOGY .....	72
2.20 BIOCHRONOLOGY.....	169
2.21 ASSEMBLAGE AGE.....	171
2.22 FAUNAL SUCCESSION .....	173

2.23	PALAEOECOLOGICAL SUCCESSION EARLY PLIOCENE.	184
2.24	CONCLUSION .....	196
2.25	ACKNOWLEDGEMENTS .....	199
2.26	Appendix 1. Small-sized mammalian fauna data matrix. 0 = Absent, 1 = Present.....	200
<b>Chapter 3</b>		<b>203</b>
3.1	Additional notes on fossil deposits, their formation and age. ....	203
3.2	Introduction .....	203
3.3	Mount Etna Limestone Mine and National Park .....	203
3.4	Limestone Ridge National Park .....	242
3.5	Karst Glen.....	246
3.6	Olsen's Cave System (Figs 3-57 – 3-59) .....	247
3.7	Summary of Chronometric Ages. ....	249
3.8	Hypothesised Cave and Cave Deposit Formation .....	249
<b>Chapter 4</b>		<b>265</b>
4.1	Additional Pleistocene vertebrate fauna from central eastern Queensland, Australia. ....	265
4.2	Introduction .....	265
4.3	Systematic Palaeontology.....	266
<b>Chapter 5</b>		<b>392</b>
5.1	Dragon's Paradise Lost: Palaeobiogeography, Evolution and Extinction of the Largest-Ever Terrestrial Lizards (Varanidae). ....	392
5.2	Preface .....	392
5.3	Authors .....	392
5.4	Abstract .....	393
5.5	Introduction .....	393
5.6	Methods.....	394
5.7	Results .....	397
5.8	Discussion.....	413
5.9	Conclusion.....	417
5.10	Acknowledgements .....	418
5.11	References .....	418
5.12	Supporting Online Material .....	423
5.13	Supplementary Figures .....	423
5.14	Chapter Conclusions.....	437
<b>Chapter 6</b>		<b>439</b>
6.1	Responses of Quaternary rainforest vertebrates to climate change in Australia. ....	439
6.2	Abstract .....	439

6.3	Introduction .....	439
6.4	Methods .....	441
6.5	Results .....	444
6.6	Discussion.....	451
6.7	Conclusions .....	460
6.8	Acknowledgements.....	461
6.9	Appendix A. Supplementary material.....	462
<b>Chapter 7</b>	<b>.....</b>	<b>478</b>
7.1	Responses of Australian Neogene rainforest vertebrates to late Cainozoic environmental change: a synthesis of current knowledge.....	478
7.2	Introduction .....	478
7.3	The Australian Neogene vertebrate literature (1960-2008). ....	479
7.4	Temporal and spatial coverage of Neogene vertebrate fossil sites...481	
7.5	Palaeogeographic evolution of the Australopapuan region. ....	482
7.6	Palaeoclimatic and rainforest floral evolution of the Australopapuan region. ....	494
7.7	Biochronology and evolutionary radiations of vertebrate groups during the Cainozoic.....	506
7.8	Palaeobiogeography of Australopapuan rainforest vertebrates .....	524
7.9	New Guinean rainforest connectivity to northern Australian rainforest. 538	
7.10	Extinction of Neogene rainforest faunas .....	543
7.11	Guild decline and extinction in tropical rainforests during the Quaternary.....	548
7.12	Responses of Pleistocene rainforest vertebrates to climate change 563	
7.13	Conclusions.....	586
<b>Chapter 8</b>	<b>.....</b>	<b>588</b>
8.1	Conclusions .....	588
<b>References</b>	<b>.....</b>	<b>594</b>
<b>Appendices</b>	<b>.....</b>	<b>627</b>
8.2	Submitted/Published Papers by S. Hocknull .....	627

## List of Tables and Figures

Figure 1-1. Satellite imagery of the Mt Etna and Limestone Ridge Study Area.....	4
Figure 1-2. Eastern face of Mt Etna.....	6
Figure 1-3. The northern face of Mt Etna Caves National Park.....	7
Figure 1-4. Western Quarry of Mt Etna during the study period. A. 2002, B. 2003, C. 2004, D. 2005, E. 2006, F. 2007, G. 2008. ....	9
Figure 1-5. Stockpiling operations during the study period. A. Removal of deposits via excavation. B. Supervised removal of sediment in relative stratigraphic context. C. Trucking of stockpiled material to scientific research area. D. Stockpiling of material in discrete sections representing individual deposits. E. Perpetual access to stockpiled material in a designated Scientific Research Area (National Park as of 2008). ....	10
Figure 1-6. Scientific Research Area Stockpiles. A. Stockpiles originally laid on ramp toward Main Cave entrance re-stockpiled onto flat accessible land. B. Final stockpile arrangement and fossil deposits. ....	11
Figure 1-7. Limestone Ridge National Park showing the Northern and Southern Section. ....	13
Figure 1-8. Aerial photograph of Limestone Ridge from the Northern aspect, showing the locations of Johansen's and Old Timbers Caves. ...	14
Figure 1-9. Limestone Ridge National Park (Southern Section) showing general locations of Mini, Ballroom and Larynx Labyrinth Caves. ....	15
Figure 1-10. Satellite imagery of Cammoo Caves section of Limestone Ridge National Park.....	16
Figure 1-11. Satellite imagery of the Capricorn Caves Tourist Park, including Olsen's and Gigas Hall Caves.....	17
Figure 1-12. Closer imagery of Olsen's Cave showing general location of three important fossil deposits (Icicle Chamber, Honey Moon Suite Chamber and Colloseum Chamber). ....	17
Figure 1-13. Satellite imagery of Karst Glen limestone showing the general locations of cave and exposed bone breccias, including KG3, Ladder Cave.....	18
Figure 1-14. Satellite imagery of Marmor Quarry and surrounds showing extent of limestone quarrying and untouched limestone sections to the north. ....	20
Figure 1-15. Aerial photograph of Marmor Quarry (north-eastern aspect) showing the positions of cave entrances and fossil deposits on unmined limestone karst. ....	20
Figure 1-16. Fifteen Mile creek running south-west from Cammoo Caves with extent of tuffa deposits marked on map. ....	22
Figure 1-17. Fifteen Mile Creek Tuffa deposits.....	23
Figure 1-18. Fossilised remains of plant material found within Tuffa. A. Root casts. B. <i>Casuarina</i> pinnae. C. Broad-leafed angiosperm. ....	24

Figure 1-19. Dry Rainforest (Semi-evergreen Vine Thicket) at Mt Etna...	25
Table 1-1. Lithified deposits investigated during this study.....	28
Figure 1-20. Collecting from surface breccias (Karst Glen). ....	28
Table 1-2. Unconsolidated sediments investigated during this study. ....	29
Figure 1-21. Excavation of unconsolidated cave sediments at Colloseum Chamber, Olsen's Cave, Capricorn Caves Tourist Park.....	29
Figure 1-22. Mt Etna Fossils Open Day, Aug 2006. ....	30
Figure 1-23. Sieving of fossiliferous sediment. A. Large-scale wet sieving of mullock heaps. B. Small-scale wet sieving of cave sediments. ....	31
Figure 1-24. Acetic Acid Etching of lithified sediments. A. Two-sized acid vats, large vat for bulk processing, small vat for smaller items. B-C. Results of acid-etching process, showing delicate bones etching free of the matrix.....	32
Figure 1-25. Mechanical tools used in fossil preparation.....	32
Figure 2-1. Map of fossil localities. A, Major localities mentioned in text, 1. Riversleigh; 2. Lynch's Crater; 3. Bluff Downs; 4. ODP815, Marion Plateau; 5. Aquarius Well, Capricorn Trough; 6. Mt Etna/Marmor; 7. Chinchilla; 8. Bow; 9. Big Sink, Wellington; 10. Hamilton; 11. Curramulka; 12. Tirari Formation, Lake Eyre. B, 6. expanded. C, The Caves area.....	42
Figure 2-2. Fossil localities on the western benches of Mount Etna Limestone Mine. 1. QML1419; 2. QML 1313, 3. QML1383, 4. QML1310 Unit 1, 5. QML1310 Unit 2, 6. QML1311 A/B, 7. QML1311 C/D, 8. QML1311 F, 9. QML1311 H, 10. QML1398U, 11. QML1384L, 12. QML1385.....	45
Figure 2-3. Schematic diagram illustrating the relationships between fossil deposits on the western benches of the Mount Etna Limestone Mine, Mount Etna. * Fauna collected. ** Fauna presented herein. ....	49
Table 2-1 TABLE 1. Faunal lists for fish and amphibians.....	76
Figure 2-4. (FIG. 4.) A, <i>Crinia</i> sp.; QMF51472, right ilium. B, <i>Litoria</i> sp. 3; QMF51447, left ilium. C, <i>Litoria</i> sp. 4; QMF51450, right ilium. D, <i>Litoria</i> sp. 1; QMF51445, left ilium. E, <i>Litoria</i> sp. 2; QMF51446, left ilium. F. <i>Nyctimystes</i> sp. 1; QMF51465, left ilium. G. <i>Cyclorana</i> sp.; QMF51443, left ilium. Scale bar = 1mm.....	80
Figure 2-5 (FIG. 5.) A, <i>Limnodynastes</i> sp. 3; QMF51486, right ilium. B, <i>Limnodynastes</i> sp. cf. <i>L. peronii</i> ; QMF41793, left ilium. C, <i>Limnodynastes</i> sp. 1; QMF51473, right ilium. D, <i>Limnodynastes spenceri</i> ; QMF51484, left ilium. E, <i>Limnodynastes</i> sp. 2; QMF51476, right ilium. F. <i>Kyarranus</i> sp.; QMF51489, right ilium. Scale bar = 1mm.....	82
Figure 2-6 (FIG. 6.) A, <i>Lechriodus</i> sp.; QMF51492, right ilium. B, <i>Etnabatrachus maximus</i> ; QMF44208, left ilium. C, <i>Neobatrachus</i> sp.; QMF51487, right ilium. D-E, microhylid sp. 3; QMF51498, left ilium in mesial and lateral view. F, microhylid sp. 2; QMF51496, left ilium. G, microhylid sp. 1; QMF51493, right ilium. Scale bar= 1mm.....	89
Figure 2-7 (FIG. 7.) A-F, Mekosuchinae; A, QMF17071, premaxillary. B, QMF52064, scute. C, QMF52065, scute. D, QMF51503, ziphodont tooth. Scale bar = 5mm. E, QMF51593 closeup of carinae (Scale bar = 1mm). F. QMF51505, scute. G-H, Chelidae; G. QMF52061, carapace. H, QMF52062, plastron. ....	93



- Figure 2-8 (FIG. 8.) A-D, Agamidae; A, *Tympanocryptis* sp. cf. *T. cephalus*; QMF41963, right maxilla. B, *Diporiphora* group 2; QMF51507, left maxilla. C, *Pogona* sp.; QMF41969, left maxilla. D, *Amphibolurus* sp.; QMF43893, right maxilla. E-K, Scincidae; E, *Sphenomorphus* group (robust morph); QMF51543, left dentary. F, *Egernia* sp.; QMF51529, left dentary. G, *Sphenomorphus* group (gracile morph); QMF51537, right dentary. H, *Cyclodomorphus gerrardii*; QMF51519, right maxilla. I-J, *Eugongylus* group; QMF51535 & QMF51536, right dentaries. K, *Tiliqua* sp.; QMF51516, left dentary. Scale bar = 5mm. .... 96
- Figure 2-9 (FIG. 9.) A-C, Gekkonidae; A&C, gekkonid (large morph); QMF51508, right dentary, QMF51510, left dentary. B, gekkonid (small morph); QMF51511, left dentary. Scale bar = 1mm. D-H, Varanidae; D-E, *Varanus* sp. 2; D, QMF51548, dorsal vertebra. E, QMF51549, femur. F, *Megalania prisca*; QMF1418, caudal vertebra. G-H, *Varanus* sp. 2; G, QMF51550, cervical vertebra. H, QMF52066, dorsal vertebra. Scale bar = 5mm. .... 103
- Figure 2-10 (FIG. 10.) A-B, Pythoninae; A, QMF51560, dorsal vertebra. B, QMF51561, dorsal vertebra. C, Elapidae; QMF51551, dorsal vertebra. Scale bar = 5mm. D-E, Typhlopidae; D, QMF51578, dorsal vertebra. E, QMF51579, three articulated dorsal vertebrae. Scale bar = 1mm. .... 105
- Figure 2-11 (FIG. 11.) A-C, Galliformes; QMF51607-51609 (left to right), humeri. D-H, Gruiformes; D-F, QMF51610-51612 (left to right), humeri. G-H, QMF33458 & QMF33460 (left to right), carpometacarpi. I-L, Passeriformes; QMF51601-51604 (left to right), humeri. Scale bar = 5mm. .... 107
- Figure 2-12 (FIG. 12.) A-K, Strigiformes; A-B, QMF51578 & 51579, femora. C-D, QMF51580 & 51581, carpometacarpi. E-F, QMF51582 & 51583, ulnae. G-H, QMF51584 & 51585, carpometacarpi. I-K, QMF51586, 51581, 33361, phalanges. L-M, QMF33863 & 33864, claws. Scale bar = 5mm. .... 111
- Figure 2-13 (FIG. 13.) A-G, Peramelidae; A, *Perameles* sp. 1; QMF51613, LM<sup>1</sup>. B, *Perameles* sp. 2; QMF51621, RM<sup>1</sup>. C-E, *Perameles bougainville*; QMF51627, RM<sup>1</sup>. Scale bar = 1mm. D, QMF51628, left mandible. E, QMF51529, right mandible. Scale bar = 5mm. F, *Isoodon obesulus*; QMF51632, RM<sup>2</sup>. G, *Isoodon* sp.; QMF51635, RM<sup>2</sup>. Scale bar = 1mm. .... 115
- Figure 2-14 (FIG. 14.) A-D, Peramelidae; A-D, *Chaeropus ecaudatus*; A, QMF51637, RM<sup>3-4</sup>. Scale bar = 5mm. B-C, QMF515638, RM<sup>2</sup>, occlusal & anterior views. D, QMF51639, RM<sup>3</sup>. E, Thylacomyidae; *Macrotis lagotis*; QMF51642, RM<sup>1</sup>. Scale bar = 1mm. .... 118
- Figure 2-15 (FIG. 15.) A-B, Family incertae sedis; A, Gen. et sp. nov. 1; QMF51644, LP1-M3. B, Gen. et sp. nov. 2; QMF51645, RM1-3. Scale bar = 5mm ..... 122
- Figure 2-16 (FIG. 16.) A-K, Dasyuridae; A-C, *Antechinus*; A, *Antechinus* sp. 1; QMF51651, RM1-4. B, *Antechinus flavipes*; QMF51681, LP3-M4. C, *Antechinus swainsoni*; QMF51686, LM2-4. D, *Planigale maculate*; QMF51707, RM1-4. E-F, *Sminthopsis*; E, *Sminthopsis macroura*; QMF51715, LC1-M4. F, *Sminthopsis murina*, QMF51724, RP2-M4. G-H, Gen et sp. nov.; QMF51743, lingual and occlusal views. Scale bar = 1mm. I-J, *Phascogale*; I, *Phascogale* sp.; QMF51704, LM1-4. J, *Phascogale topoatafa*; QMF51699, LC1-M4. K, *Dasyurus viverrinus*; QMF51690, RM3-4. Scale bar = 5mm. .... 126

Figure 2-17 (FIG. 17.) A-D, Dasyuridae; <i>Sarcophilus</i> ; A, <i>Sarcophilus harrisii</i> ; QMF51712, left mandible. B-D, <i>Sarcophilus lanianus</i> ; B, QMF41997, LM <sup>1</sup> . C, QMF51713, LM1. D, QMF1872, partial skull. E-F, Thylacinidae; <i>Thylacinus cynocephalus</i> ; E, QMF1737, RM2. F, QMF51755, RM1. Scale bar = 5mm. ....	129
Table 2-3 (TABLE 3.) Faunal lists for large-sized mammal species.....	132
Table 2-18 (FIG. 18.) A, Vombatidae; <i>Vombatus ursinus mitchelli</i> ; QMF1420, LM1-4. B, ?Zygomaturine; QMF1419, fragmentary mo Zar. C-D, Palorchetidae; <i>Palorchestes</i> sp. cf. <i>P. parvus</i> ; C, QMF51759, RM <sup>2</sup> (partial M <sup>1</sup> ). D, QMF51760, LI <sup>1</sup> . Scale bar = 10mm. ....	135
Figure 2-19 (FIG. 19.) A-I, Macropodidae. A-H, <i>Dendrolagus</i> sp.; A, QMF51770, RI1-M4. B, QMF1739, LM1-4. C-D, QMF51771, RP <sup>3</sup> -M <sup>1</sup> in lingual and buccal view (showing postero-buccal cuspule on P <sup>3</sup> ). E-H, Calcanea; QMF51772-51775 (left to right). I. <i>Bohra</i> sp.; QMF51783, calcaneum. Scale bar = 5mm.....	137
Figure 2-20 (FIG. 20.) A-H, Macropodidae. A-D, <i>Kurrabi</i> sp.; A-B, QMF51767; RP <sup>3</sup> in lingual & occlusal views. C, QMF51768, LP <sup>3</sup> . D, QMF51769, LP <sup>3</sup> . Scale bar= 1mm. E-H, <i>Protemnodon</i> sp. cf. <i>P. devisi</i> ; E, QMF41737, LP3. F, QMF41953, LM <sup>1</sup> . G-H, QMF51763; LP <sup>3</sup> in buccal & lingual views. Scale bar = 5mm. ....	142
Figure 2-21 (FIG. 21.) A-G, Macropodidae; A-B, <i>Macropus</i> sp. cf. <i>M. agilis siva</i> ; A, QMF51829, RM1-3. B, QMF51830, LM1-2. C-D, <i>Petrogale</i> sp.; C, QMF51812, RP3. D, QMF51813, LM2-4. E-G, <i>Macropus titan</i> ; QMF 1697 in lingual (E), buccal (F) & occlusal (G) views. Scale bar = 5mm. ....	143
Figure 2-22 (FIG. 22.) A-C, Macropodidae; <i>Thylogale</i> sp.; A, QMF51784, LI1-M2. Scale bar = 5mm. B, QMF51785, LM2. C, QMF51786, LM <sup>2</sup> . Scale bar= 1mm. ....	145
Figure 2-23 (FIG. 23.) A-I, Pseudocheiridae. A, B, D, E & H, <i>Pseudocheirus</i> spp.; A, QMF51898, RM1. B, QMF51899, RI1-M3. D, QMF51900, RM2-3. E, QMF51901, RP3. Scale bar = 5mm. H, QMF51840, LM1, (Scale bar = 1mm). C, <i>Pseudochirulus</i> sp. 2; QMF51871, RI1 & M1. F, G & I, <i>Pseudochirulus</i> sp. 1; F, QMF51838, LM1. G, QMF51839, LI1 & M1-3. Scale bar = 5mm. I, QMF51841. Scale bar = 1mm. ....	149
Figure 2-24 (FIG. 24.) A-F, Pseudocheiridae; A-D, <i>Pseudocheirus</i> sp.; A, QMF51920, LP <sup>3</sup> . B-C, QMF51921, LP <sup>3</sup> in buccal & occlusal views. E, <i>Pseudochirulus</i> sp. 1; QMF51870, RP <sup>3</sup> -M <sup>3</sup> (broken). Scale bar= 1mm. F, <i>Pseudochirulus</i> sp. 2; QMF51887, partial skull. Scale bar = 5mm. ....	150
Figure 2-25 (FIG. 25.) A-H, Pseudocheiridae; A-C, <i>Petauroides</i> sp.; A, QMF51923, RM1. B, QMF51924, LM <sup>2</sup> . C, QMF51925, RM <sup>2</sup> . D-F, <i>Pseudocheirops</i> sp.; D-E, <i>Pseudocheirops</i> sp. 1; D, QMF51934, RM <sup>3</sup> . E, QMF51935, RM <sup>2</sup> . Scale bar= 1mm. F, <i>Pseudocheirops</i> sp. 2; QMF51937, RM2. Scale bar= 5mm. G-H, Pseudokoala sp.; G, QMF51934, RM <sup>2</sup> . H, QMF51939, RM2. Scale bar = 1mm.....	154
Figure 2-26 (FIG. 26.) A-F, Petauridae, A-D, Gen. et sp. nov.; A, QMF51949, LP <sup>1</sup> -M <sup>3</sup> . B, QMF51950, RP <sup>3</sup> -M <sup>3</sup> . C, QMF54951, partial skull. D, QMF54952, left mandible (M1-2). E, <i>Dactylopsila</i> sp. 1; QMF51947, LM <sup>1</sup> . F, <i>Dactylopsila</i> sp. 2; QMF51948, RI1 & M1. G-H, Burramyidae; <i>Cercartetus</i> sp.; G, QMF51984, LP3-M2. H, QMF51985, LP <sup>2</sup> -M. Scale bar= 1mm. ....	158

Figure 2-27 (FIG. 27.) A, Acrobatidae; <i>Acrobates</i> sp.; QMF51982, RP3-M1. Scale bar = 1mm. B-C, Superfamily incertae sedis; QMF51974 in buccal & occlusal view. Scale bar = 1mm. D-F, Phalangeridae; D, <i>Trichosurus</i> sp. 1; QMF52009, right mandible. E, <i>Trichosurus</i> sp. 2; QMF52012, partial skull. F, <i>Strigocuscus</i> sp.; QMF52003, LP3-M3. Scale bar = 5mm. ....	162
Figure 2-28 (FIG. 28.) A-E, Thylacoleonidae; A-C, <i>Thylacoleo</i> sp.; QMF52069, RP <sup>3</sup> in lingual, buccal & occlusal views. D-E, <i>Thylacoleo hilli</i> ; QMF52013, RP <sup>3</sup> in buccal & lingual views. Scale bar = 5mm. ....	167
Figure 2-29 (FIG. 29.) A-E, Megadermatidae; <i>Macroderma gigas</i> ; A-B, QMF48021, partial skull in dorsal & ventral views. C, QMF48022, partial skull. D, QMF48006, RP3-M3. E, QMF48591, LP4-M3. Scale bar = 5mm. ....	168
Figure 2-30 (FIG. 30.) A-I, Muridae; A, <i>Conilurus</i> sp.; QMF52052, LM <sup>1-2</sup> . B, <i>Leggadina</i> sp.; QMF52040, LM <sup>1</sup> . Scale bar = 1mm. C-D, <i>Uromys/Melomys</i> sp.; QMF52014, skull in dorsal & ventral views. Scale bar = 5mm. E-F, <i>Pseudomys</i> spp.; E, QMF52043, LM <sup>1-2</sup> . F, QMF52044, RM <sup>1-3</sup> . G, <i>Pogonomys</i> sp.; QMF52022, RM <sup>1-3</sup> . H, <i>Zyzomys</i> sp.; QMF52053, RM <sup>1-3</sup> . Scale bar = 1mm. I, <i>Notomys</i> sp.; QMF52036, RM <sup>1-3</sup> . J, <i>Rattus</i> sp.; QMF52033, partial skull. Scale bar = 5mm. ....	169
Figure 3-31 (FIG. 31.) Dendrogram illustrating faunal similarity derived from small-sized mammal species from sites presented herein. Present day small-sized mammal fauna placed as the outgroup. ....	170
Table 2-5 (TABLE 5.) Summarised ages for The Caves & Marmor fossil sites. ....	176
Figure 3-1. Northern and western margin of Mt Etna showing location of Main Cave. ....	203
Figure 3-2. Main Cave Bone Breccia, showing breccia made up of mostly cemented clay and angular pieces of parent limestone. Bone bearing sediment light yellow-pink colour. ....	205
Figure 3-3. Main Cave Bone Breccia shown as rocky scree to the north and down slope of the Main Cave entrance. ....	205
Figure 3-4. Speaking Tube Cave as mapped by UQSS prior to mining operations destroyed it. A. Plan view. B. Cross-sectional view of main chamber system (AA). ....	207
Figure 3-5 QML1419. Bench 0, solution pipe running from Bench 0 to Bench 1. Photo taken from Bench 1. Insitu material referable to QML1313 is located to the left of this solution pipe. ....	207
Figure 3-6. QML1419 Unit A and B, divided by massive flowstone. ....	209
Figure 3-7. ROK E. Speleothem collection used to date the minimum age of QML1419 Unit A. ....	210
Figure 3-8. ROK D. Calcite Vug found within QML1419 Unit B, used to find minimum age of Unit B. ....	211
Figure 3-9. QML1383 'Northwest Chamber', Bench 1. Units A & B divided by flowstone (black line). ....	213
Figure 3-10. QML1383 'Northwest Chamber', Bench 1 breccia showing sedimentological sample of Unit A with white flecks being fossil bone. .	213

Figure 3-11. QML1383 'Northwest Chamber', Bench 1. Flowstone intersecting Units A and B used to provide a minimum age for Unit A...	214
Figure 3-12. QML1313 and QML1419, Bench 1 as they were exposed on the western side of Mount Etna in 1992 (24/12/92). Note QML1419 mostly covered by limestone, subsequently exposed in collapse in 2002-2003.	215
Figure 3-13. QML1383 and QML1313, Bench 1 remnants relocated on the western side of the Mount Etna Mine in 2003.	216
Figure 3-14 QML1313, Bench 1 with original chamber walls of Speaking Tube Cave showing QML1313 which was stockpiled in 1992, rediscovered in 2003. Note covered entrance to Speaking Tube. This entrance is now exposed on the western face of Bench 1.	217
Figure 3-15. QML1313, Bench 1. Discovered in 2003, speleothem associated with remnant sediments of QML1313 exposed in 1992. Additional QML1313 were discovered further to the north from this section.	218
Figure 3-16. Basal section of flowstone found to be capping QML1313 deposit was used to return the youngest minimum age of the QML1313 deposit.	218
Figure 3-17. QML1310, Unit A, Bench 2. Showing large continuous capping flowstone that demarcates Unit A from B above.	221
Figure 3-18. QML1310, Unit B, Bench 2. Showing flowstone contact (top of picture) with Unit C, massive cemented breccia with clasts of parent limestone and allochthonous clasts of surrounding claystones/siltstones and limestones. Bone present. Scale Bar 20cm.	222
Figure 3-19. QML1310 Unit C, Bench 2. Showing large angular clasts of allochthonous rock derived from surrounding Devonian units (centre), surrounded by brown colours cemented clays and dirty flowstone. 20cm Scale Bar.	223
Figure 3-20 QML1310 Units 2 and 1, Bench 2. Scale Bar = 2m.	224
Figure 3-21. QML1310 Units 1 & 2, Bench 2. Showing calcite vug in Unit 2 used for dating; speleothem layers; gastropod layer; and division between Units 2 and 1.	225
Figure 3-22. QML1310 Unit 2, Bench 2. Showing calcitic vug within wall of Unit 2.	226
Figure 3-23. Collected calcite vug showing U-Th dates returned from each section of calcite growth, total timeframe spanning approximately 200,000 years.	226
Figure 3-24. QML1310 Unit 2, Bench 2. Isolated block from base of Unit 2 above basal flowstone, showing semi-associated and articulated juvenile specimen of <i>Dendrolagus</i> . Scale Bar = 5cm.	227
Figure 3-25. QML1310 Unit 2, Bench 2. Showing mid gastropod layer. Scale Bar = 10cm.	227
Figure 3-26. QML1310, Unit 2, Bench 2. Close-up image of mid gastropod layer showing packing of gastropods. Scale Bar = 1cm	228
Figure 3-27. QML1310, Unit 2 & 1, Bench 2. Showing flowstone capping Unit 2 and basal to Unit 1.	229

Figure 3-28. QML1310 Unit 1, Bench 2. Showing capping flowstone over both Units 1 and 2. Note the sculpted surface showing old cave wall surface.....	230
Figure 3-29. QML1310 Unit 1 & 2, Bench 2 with chronometric ages detailed for relevant flowstone horizons. ....	231
Figure 3-30. Bench 3 deposits. A. Location of QML1311A, B, C, D, F, H and J. B. Dotted line tracing of parent limestone phreatic pendants exposed during stockpiling operations.....	232
Figure 3-31. QML1311 A, Bench 3. Showing massive angular clasts of parent limestone isolated in thick lithified clay matrix. ....	232
Figure 3-32. Speleothem between QML1311 A and B used for U-Th dating.....	233
Figure 3-33. QML1311 CD, Bench 3. Showing gross morphology, colour and sedimentological characteristics in the field.....	233
Figure 3-34. QML1311 C, Bench 3. Block of consolidated sediment seen in cross-section showing random bone orientations, size and sedimentological character.....	234
Figure 3-35. QML1311 CD basal flowstone providing the contact between QML1311F and QML1311CD. This speleothem was used to return a series of ages showing that the minimum age for QML1311F was ~430ka, the maximum age for QML1311CD is ~330ka and that the growth of this speleothem took approximately 100,000 years. ....	234
Figure 3-36. QML1311F, Bench 3. Piece of matrix in cross-section showing dominant fine-grained matrix with large individual allochthonous clasts and post-depositional calcite formation within porous sediment matrix.....	235
Figure 3-37. QML1311 F & H, Bench 3. Showing decalcified flowstone contact between QML1311 F and H.....	236
Figure 3-38 QML1311 F&H, Bench 3. Close up of old flowstone of F now incorporated within H. Also shows sedimentological differences between F and H, notably the massive increase in surface allochthonous clasts. ..	237
Figure 3-39. QML1311H, Bench 3. Showing distinctive phreatic pendants within QML1311H sediment. Minimal, if any calcite precipitation indicative of a non-vadose system. ....	237
Figure 3-40. QML1311H, Bench 3. Matrix showing random bone orientations, increased percentage of allochthonous sediment with some post-depositional calcite formation with vugs and bone hollows.....	238
Figure 3-41. QML1311F-H Contact zone with inter-layered calcite formations dated using U-Th techniques to >500ka. ....	238
Figure 3-42. QML1311F. Calcitic Vug found within QML1311 F, used to determine minimum age of deposit. Returned an age ~280ka, which indicates speleothem deposition at this time. ....	239
Figure 3-43. QML1311J, Bench 3. Location of QML1311J on western quarry face. ....	239
Figure 3-44. QML1311J. Note the small size of this deposit. It may have been considerably larger before mining operations. ....	240

Figure 3-45. QML1311J. Speleothem used to date QML1311J. A. Calcite vug within QML1311J, used to provide a minimum age. B. Flowstone within QML1311J used to provide a close approximation of the deposits age. ....	240
Figure 3-46. QML1384 UU and LU, Bench 3. Showing solution pipe and chamber being excavated for stockpiling.....	241
Figure 3-47. QML1384UU. Capping flowstone considered to represent the minimum age of QML1384UU. ....	241
Figure 3-48. QML1314, Lower Johansen's Cave, Limestone Ridge (northern section). Showing capping flowstone and guano beneath. ....	242
Figure 3-49. QML1314, Lower Johansen's Cave flowstone lithified sediment in cross-section. Note, the cementation of the sediment below the flowstone indicating that the sediment deposit below the flowstone accumulated before the flowstone. ....	242
Figure 3-50. QML1314, Lower Johansen's Cave Guano deposit below flowstone level. Note the distinct colouration difference between the guano floor sediment and the sediment wall (dotted orange line). ....	243
Figure 3-51. QML1284, Mini Cave, Limestone Ridge (southern section). Example of cave wall flowstone, inter-bedded within fossiliferous deposit, used for dating the sequence presented in Hocknull et. al. (2007). ....	243
Figure 3-52. Mini Cave – Lost Paradise – Lion's Den Section of Limestone Ridge (southern section). ....	244
Figure 3-53. Demarcation of karst exposed bone-bearing fossiliferous cave sediment deposits. QML1284a (Above Mini Cave) and QML1382 (Leo's Lunch Site).....	245
Figure 3-54. QML1284a. Sedimentological sample cut in cross-section to show matrix composition. ....	245
Figure 3-55. QML1412, near KG3 B entrance, Karst Glen. Showing exposed bone-bearing fossiliferous deposits.....	246
Figure 3-56. QML1411, exposed fissure deposit, Karst Glen. Showing unique sedimentological deposit in cross-section. Goethitic pisolites, dirty speleothem, bone fragments, limestone clasts and clay matrix.....	247
Figure 3-57. Honey Moon Suite Chamber deposit, Olsen's Cave. ....	247
Figure 3-58. QML1456, Colloseum Chamber excavation.....	248
Figure 3-59. QML1456, Colloseum Chamber dating materials. A. Lower incisor from a <i>Petrogale</i> . B. Straws. C. Snail shell.....	248
Figure 3-60. Summary of Chronometric ages discussed in text and throughout Chapters 1-7.....	249
Figure 3-61. An example of a fissure deposit high on the western face of Mt Etna mine, showing angular limestone clasts and irregular limestone wall. ....	251
Figure 3-62. An example of a sediment-filled solution pipe, Bench 0, Mt Etna Mine. ....	252
Figure 3-63. Hypothesised cave formation, sedimentation and karst development on the western margin of Mt Etna. A. Phreatic and Fissure Development. B. Phreatic sedimentation and vadose cave development.	

C. Karstic and major vadose development. D. Karstic exposure and guano deposition. WT = water table. ....	258
Figure 3-64. Hypothesised cave formation, sedimentation and karst development at Limestone Ridge (southern section). A. Phreatic Development. B. Vadose cave and open doline development. C. Extant Cave development. D. Karstic exposure and guano deposition. WT = water table. ....	260
Figure 3-65. Hypothesised cave formation, sedimentation and karst development at Olsen's Cave. A. Phreatic Development. B. Karstic and joint development. C. Cave sedimentation. D. Karstic exposure, collapse and guano deposition. WT = water table. ....	262
Figure 3-66. Hypothesised cave formation, sedimentation and karst development at Karst Glen. A. Phreatic and Fissure deposition. B. Karst and joint development. C. Vadose cave development. D. Karstic exposure and collapse. WT = water table. ....	264
Figure 4-1. <i>Cyclorana</i> sp. cf. <i>C. cultripes</i> , right partial ilium, QML1456. ....	267
Figure 4-2. <i>Cyclorana</i> sp. 2, right ilium, QML1456. ....	267
Figure 4-3. <i>Neobatrachus</i> 1., left ilium, QML1312. ....	268
Figure 4-4. <i>Neobatrachus</i> sp. 2., right ilium, QML1456. ....	268
Figure 4-5. <i>Uperoleia</i> sp., right ilium, QML1385. ....	269
Figure 4-6. <i>Taudactylus</i> sp. cf. <i>T. diurnus</i> , left ilium, QML1284. ....	270
Figure 4-7. <i>Assa</i> sp., A. right ilium, B. left ilium, C. left ilium; QML1385. ....	271
Figure 4-8. <i>Philoria</i> sp., A. Left ilium, B. Left ilium, C. Right ilium, QML1385. ....	271
Figure 4-9. <i>Pseudophryne</i> sp.1, A. Left ilium, B. Right ilium, C-D. <i>Pseudophryne</i> sp. 2 Right ilium, QML1385. D. Right ilium, QML1284a. ....	272
Figure 4-10. <i>Kyarranus</i> sp. 1, A. Right ilium, B. Left ilium, QML1284a; C. Right ilium, QML1385. ....	273
Figure 4-11. <i>Kyarranus</i> sp. 2, A. Left ilium, B. Right ilium, C. Right ilium, QML1313; D. Left ilium, QML1284. ....	273
Figure 4-12. <i>Lechriodus</i> sp. cf. <i>L. platyceps</i> , A. Right ilium, QML1313; B. Right ilium, C. Right ilium, QML1385. ....	274
Figure 4-13. <i>Cophixalus</i> sp., A. Right ilium, B. Right ilium, C. Left ilium, QML1385. ....	275
Figure 4-14. microhylid ?gen. nov. A. Left ilium, QML1313; B. Left ilium, QML1284. ....	276
Figure 4-15. <i>Rheodytes</i> sp. cf. <i>R. leukops</i> , first left pleural, QML1384LU. ....	277
Figure 4-16. indeterminate chelid remains; A-D. dorsal vertebra in anterior (A), posterior (B), left lateral (C) and right lateral (D) views, QML1384LU. E. carapace fragment, QML1311H. ....	278
Figure 4-17. <i>Quinkana</i> sp. A-E. Isolate osteoderms from QML1384LU (A-C), QML1311CD (D), QML1311H (E). F-G. Postorbital bone in dorsal (F) and ventral (G) views. H. ungual, I-J. isolated tooth in mesial (I) and lateral view (J), QML1311H. ....	279

Figure 4-18. A. <i>Arua modestus</i> (modern Aru Island) anterior right maxilla. B. <i>Hypsilurus/Arua</i> sp. anterior right maxillary fragment, QML1313. ....	280
Figure 4-19. <i>Tiliqua</i> sp. nov.. (QMF 51516) Fossil dentary compared with dentaries of extant species of <i>Tiliqua</i> and <i>Cyclodomorphus</i> (lingual view). .....	283
Figure 4-20. <i>Tiliqua</i> sp. nov.. Fossil dentary compared with dentaries of extant species of <i>Tiliqua</i> and <i>Cyclodomorphus</i> (dorsal (occlusal) view). Species comparisons as above. ....	284
Figure 4-21. <i>Cyclodomorphus gerrardii</i> . A. Left maxilla (QML1313), B. Ontogenetic series from QML 1311 H. ....	285
Figure 4-22. <i>Egernia major</i> . Isolated dentaries from QML 1311 H. ....	286
Figure 4-23. <i>Sphenomorphus</i> group skinks. Isolated maxillae (left column) and dentaries (right column) from QML1312. ....	287
Figure 4-24. gekkonid fossils. Isolated maxillae and dentary fragments from QML1313. ....	288
Figure 4-25. Histogram of fossil varanid dorsal vertebral measurements (Pre-Postzygophysis Length), compared with variation seen in three different-sized varanids ( <i>V. gouldii</i> , <i>V. varius</i> and <i>V. giganteus</i> ).....	289
Figure 4-26. Varanid fossils. A. Quadrate (QML1312), B. Frontal (QML1311H), C. Parietal (QML1312), D. Osteoderm (QML1311J), E. Sacral vertebra (QML1311H), F. Ilium (QML1311H), G. Cervical (QML1312), H. Dorsal vertebrae (left to right): QML1311 H, QML1311 C/D, QML1384LU, QML1312, QML1312, QML1311 H. ....	290
Figure 4-27. Bivariate plot of total Body Length to maximum pre- postzygopophysis length (dorsal vertebrae) for Australian elapids. Used to estimate the total body length of fossil elapid vertebrae. ....	292
Figure 4-28. A Histogram of estimate body lengths for fossil elapid dorsal vertebrae from middle Pleistocene sites at Mt Etna. B. Comparison between the size range of elapids from older middle Pleistocene rainforest sites to arid fauna of QML1312. ....	293
Figure 4-29. Elapid fossils. A. Maxilla from QML1313 in ventral, mesial, lateral and anterior views. B. Elapid dorsal vertebrae in dorsal view from (left to right) QML1312, QML1311 H, QML1384LU, QML1311 J, QML1312. C. Elapid dorsal vertebrae in dorsal view from (left to right) QML1312, QML1313, QML1312, QML1312. ....	294
Figure 4-30. Histogram of pythonine fossil vertebral lengths (Pre- postzygopophysis Length) compared with the variation in lengths seen in a variety of python species. ....	295
Figure 4-31. Pythonine fossils. A Dorsal vertebrae in anterior view from (left to right) QML1311H, QML1312, QML1312, QML1312. B. QML1311H, QML1384LU, QML1311CD, QML1311H. C. Articulated series in lateral and ventral view (QML1311 H). ....	296
Figure 4-32. Typhlopod vertebrae in dorsal, ventral posterior and anterior views (QML1284). ....	297
Table 4-1. Fossil madtsoiid vertebral measurements compared with published fossil specimens. ....	298



Figure 4-33. Madtsoiid vertebrae in, A. anterior, posterior and lateral views (QML1384LU). B. Dorsal (QML1384LU) and anterior views (QML1311H, QML1311J) .....	298
Figure 4-34. Fossil tachyglossid ungual (QML1311J).....	299
Figure 4-35. Fossil peroryctid M <sub>1</sub> s in occlusal view. ....	301
Figure 4-36. Fossil peroryctid M <sup>1</sup> s in occlusal view. ....	302
Figure 4-37. Fossil peramelid lower M <sub>1</sub> s in occlusal view and M <sup>1</sup> s in near-occlusal view. ....	303
Table 4-2. Table of Character states for fossil peroryctid and peramelid fossils from Mt Etna. ....	304
Figure 4-39. Consensus phylogeny of Mt Etna perameloid taxa, including bootstrap values over 50%. ....	305
Figure 4-40. Fossil thylacinid specimens, including, A. Right maxillary molar row, B. Proximal humerus and C. Calcaneum (QML1313). ....	306
Figure 4-41. Fossil vombatids, A. Left mandible (QMF 1420), B. Isolated molar (QML1311 H), C. Right maxillary fragment (QML1311 J). ....	307
Figure 4-42. Possible new vombatid (isolated incisor from skull) (Lower Johansen's Cave).....	307
Figure 4-43. <i>Palorchestes</i> sp. cf. <i>P. pickeringi</i> from Mt Etna. A. QMF 51759 RM <sup>2</sup> , partial M <sup>1</sup> . B. M <sub>3</sub> (QML1384LU). C-D. QMF 51760, LI <sup>1-2</sup> . ...	308
Figure 4-44. <i>Palorchestes</i> sp. cf. <i>P. parvus</i> , Marmor Quarry LM <sub>3</sub> . ....	310
Figure 4-45. Fossil diprotodontid fragments from Mt Etna. A. Fragment of maxilla (QML1311 H). B. molar loph (QMF 51761) .....	310
Figure 4-46. <i>Troposodon</i> sp. cf. <i>T. minor</i> from Mt Etna, RP <sup>3</sup> (QML1311 H). ....	311
Figure 4-47. cf. <i>Lagostrophus</i> sp. LM <sub>2</sub> .....	312
Figure 4-48. <i>Protemnodon</i> sp. cf. <i>P. devisi</i> from Mt Etna. A. Right maxilla with P <sup>2</sup> - M <sup>2</sup> in occlusal, lingual and buccal views (QML1311J). Isolated M <sup>1</sup> (QML1311 H) compared with <i>P. devisi</i> (left) and <i>P. anak</i> (right).....	313
Figure 4-49. <i>Protemnodon</i> sp. nov. Mt Etna, A. Left partial mandible showing posterior position of the mental foramen, close to the base of P <sub>3</sub> (left) and the posterior placement of the dental symphysis (right) (QML1311 H). B. Isolated low-crowned M <sup>2or3</sup> (QML1311 H) .....	314
Figure 4-50. <i>Protemnodon brehus</i> from Mt Etna, isolated P <sup>3</sup> (QML1311H) and partial skull (QML1311J).....	315
Figure 4-51. <i>Wallabia</i> sp. from Mt Etna, isolated P <sup>3</sup> s, A. QML1311 H; B. QML1311 H. ....	316
Figure 4-52. <i>Thylogale stigmatica</i> from Mt Etna, right mandible with P <sub>2</sub> -M <sub>1</sub> (compared with isolated molar of <i>Thylogale</i> sp. nov. (above).....	317
Figure 4-53. Bivariate plot of dP <sub>3</sub> length to anterior width, showing the very small size of <i>Thylogale</i> sp. nov. from Mt Etna, compared with <i>T. christenseni</i> and all other species of <i>Thylogale</i> . ....	319
Figure 4-54. <i>Thylogale</i> sp. nov. from Mt Etna. A. Isolated upper M <sup>2or3</sup> . B-C, isolated dP <sup>3</sup> s. D. four isolated lower M <sub>2-3</sub> s.....	319
Figure 4-55. <i>Dendrolagus</i> sp. cf. <i>D. mbasio</i> from Mt Etna, isolated RP <sup>3</sup> , compared with modern specimen (right). ....	321

Figure 4-56. <i>Dendrolagus</i> sp. cf. <i>D. spadix</i> from Mt Etna, isolated LP <sup>3</sup> , compared with modern specimen.....	321
Figure 4-57. <i>Dendrolagus</i> sp. cf. <i>D. ursinus</i> from Mt Etna, RP <sup>3</sup> -M <sup>1</sup> QMF51771. ....	322
Figure 4-58. <i>Dendrolagus</i> sp. nov. 1 from Mt Etna, right maxilla P <sup>3</sup> -M <sup>3</sup> , QML1313.....	323
Figure 4-59. <i>Dendrolagus</i> sp. nov. 2 from Mt Etna. A. Isolated RP <sup>3</sup> (QML1311 H) compared with modern specimens, B. <i>D. dorianus</i> and C. <i>D. goodfellowi</i> . ....	323
Figure 4-60. <i>Bohra</i> sp. nov. 1 from Mt Etna (QML1311 H), isolated RP <sup>3</sup> . ....	325
Figure 4-61. <i>Bohra</i> sp. nov. 2 from Mt Etna (QML1311 CD), isolated RP <sup>3</sup> . ....	326
Figure 4-62. <i>Bohra</i> sp. nov. 3 from Mt Etna QML1311 H, isolated RP <sup>3</sup> . ....	327
Figure 4-63. <i>Kurrabi</i> sp. 1 from Mt Etna, isolated P <sup>3</sup> s. A. QML1311 H and B. QML1311 H.....	328
Figure 4-64. <i>Kurrabi</i> sp. 2 from Mt Etna, isolated P <sup>3</sup> s. A, QML1311 H, B. QML1311H. ....	329
Figure 4-65. cf. <i>Simosthenurus</i> sp. from Mt Etna, isolated M <sub>1or2</sub> . (QML1311 H).....	330
Figure 4-66. Bivariate plot of M <sub>1</sub> Length to Width of large pseudocheirids, including a new genus, <i>Pseudochirops</i> and <i>Pseudokoala</i> from Mt Etna. ....	331
Figure 4-67. New genus of pseudocheirid from Mt Etna, isolated M <sub>2or3</sub> from Mt Etna (QML1311 C/D).....	331
Figure 4-68. <i>Pseudokoala</i> sp. nov. 1 from Mt Etna. A. RM <sub>1</sub> QML1384LU, B. RM <sub>2</sub> QML1311H.....	332
Figure 4-69. <i>Pseudokoala</i> sp. cf. <i>P. curramulkensis</i> from Mt Etna QML1311C/D (RM <sub>2</sub> ). ....	333
Figure 4-70. <i>Pseudokoala</i> sp. cf. <i>P. erlita</i> from Mt Etna. A. LM <sub>2</sub> (QML1385), B. M <sup>2or3</sup> (QML1385). ....	333
Figure 4-71. Bivariate plot of M <sup>1</sup> length to width for fossil and modern <i>Pseudochirops</i> .....	334
Figure 4-72. Fossil <i>Pseudochirops</i> from Mt Etna, isolated upper molars. A. M <sup>1</sup> s QML1311CD, QML1311CD, QML1311CD. B. M <sup>2</sup> QML1311CD, M <sup>1</sup> QML1311H, M <sup>1</sup> QML1311H. C. M <sup>x</sup> s QML1385, QML1385.....	335
Figure 4-73. Bivariate plot of M <sup>1</sup> length to width for fossil and modern <i>Petauroides</i> and <i>Pseudochirulus</i> .....	336
Figure 4-74. Fossil <i>Petauroides</i> from Mt Etna. A. M <sup>1</sup> QML1311CD, B. M <sup>1</sup> QML1311CD. C, P <sub>3</sub> QML1311CD, QML1311CD, QML1311H, QML1311H, D. M <sub>1</sub> QML1284. E. RP <sub>3</sub> -M <sub>3</sub> QML1313. ....	337
Figure 4-75. Bivariate plots of M <sub>1</sub> /M <sup>1</sup> length to width for fossil and modern <i>Petauroides</i> , <i>Pseudochirulus</i> and <i>Pseudocheirus</i> . ....	338
Figure 4-76. Fossil <i>Pseudocheirus</i> from Mt Etna, lower dentition. A. P <sub>3</sub> s, B-E. M <sub>1</sub> s. ....	339

Figure 4-77. Bivariate plots of $M_1/M^1$ length to width for fossil and modern <i>Pseudochirulus</i> .....	340
Figure 4-78. Fossil <i>Pseudochirulus</i> from Mt Etna, lower dentition. $P_3$ s and $M_1$ s. ....	342
Figure 4-79. Phylogenetic analysis of pseudocheirids using upper dentition and lower dentitions. Both phylogenies report bootstrap values >50%. ....	348
Table 4-3, pseudocheirid character matrix for upper dentition.....	349
Table 4-4, pseudocheirid character matrix for lower dentition. ....	350
Figure 4-80. Taxonomic diversity of petaurids through the Middle Pleistocene to present day at Mt Etna. ....	350
Table 4-4, Character matrix for petaurids (from Williams & Hocknull, in Prep).....	350
Figure 4-81 Phylogeny of petaurids at Mt Etna, showing bootstrap values over 50%. ....	351
Figure 4-82. Bivariate plots of Incisor length to depth for fossil and modern <i>Dactylopsila</i> . ....	352
Figure 4-83. Bivariate plots of $M_1/M^1$ length to width for fossil and modern <i>Dactylopsila</i> . ....	353
Figure 4-84. Fossil <i>Dactylopsila</i> from Mt Etna. A-C. $M^1$ s (QML1284, QML1284a, QML1311H). D. <i>D. tatei</i> . ....	354
Figure 4-85. <i>Cercartetus</i> sp. nov. 1 from Mt Etna QML1313. A. Left maxilla showing alveoli for $P^1$ , preserved $P^{2-3}$ . B. $M^{1-2}$ . C. $P_3$ - $M_1$ . ....	355
Figure 4-86. Fossil <i>Cercartetus</i> from Mt Etna, <i>Cercartetus</i> sp. nov. 2 (top two mandibles) compared with <i>C.</i> sp. nov. 1 (lower two mandibles). ....	356
Figure 4-87. Fossil acrobatoid (sp. nov. 1) from Mt Etna (QML1313). A. $P^2$ , $P^3$ , $M^1$ . B. $M^{2-3}$ (alveoli), $M^{3-4}$ alveoli. C. Isolated $M^1$ .....	357
Figure 4-88. Fossil acrobatoid (sp. nov. 2) from Mt Etna, isolated $M^1$ . ...	358
Figure 4-89. Fossil <i>Acrobates</i> from Mt Etna, isolated $M_1$ .....	358
Figure 4-90. <i>Madakoala</i> sp. nov. 1 from Mt Etna (A&B) compared with <i>M. devisi</i> (C&D) and <i>Phascolarctos</i> (E&F), from Price & Hocknull (submitted). ....	359
Figure 4-91. “ <i>Milliyowi/Aepyprymnus</i> ” sp. nov. from Mt Etna. A. $P_3$ - $M_2$ (buccal and lingual views). B. $M_{1-2}$ occlusal view.....	361
Figure 4-92. Bivariate plot of lower molar length vs width of fossil and modern potoroiids, compared with the new species from Mt Etna. ....	362
Figure 4-93. <i>Phalanger gymnotis</i> from Mt Etna. A. $P^3$ (QML1284), B. $P^3$ - $M^2$ (QML1311H), C. $P_3$ - $M_3$ (QML1284), D. $P_3$ - $M_2$ (QML1384LU). E. $M^1$ (QML1311CD). ....	363
Figure 4-94. <i>Phalanger</i> sp. cf. <i>P. mimicus</i> from Mt Etna. A. $P^3$ - $M^2$ (QML1384LU), B. $P_3$ - $M_1$ (QML1284) C. $M^1$ (QML1311H).....	364
Figure 4-95. <i>Spilocuscus</i> sp. from Mt Etna, QMF52006 $M^1$ .....	365
Figure 4-96. Miralinid fossils from Mt Etna. A-B. $M^1$ (QML1311H), C. $M^{2 \text{ or } 3}$ (QML1311H).....	366
Figure 4-97. <i>Thylacoleo hilli</i> from Mt Etna. A. QMF52013 compared with <i>T. hilli</i> from Childers Cove, Victoria (buccal and lingual views). B.	

QMF52013 compared with <i>T. hilli</i> from Childers Cove, Victoria (occlusal view). C. right maxillary fragment preserving P <sup>2</sup> -P <sup>3</sup> and M <sup>1</sup> alveolus (QML1311H).....	368
Figure 4-98. <i>Thylacoleo hilli</i> calcaneum from Mt Etna (QML1311H) compared with <i>T. carnifex</i> from the eastern Darling Downs. ....	369
Figure 4-99. Bivariate plot of P3 length to width for species of thylacoleonid, to compare against <i>T. hilli</i> specimens (marked). ....	370
Figure 4-100. Phylogeny of thylacoleonids. Above, bootstrap valued phylogram showing supported groupings. Below, strict consensus tree. ....	373
Figure 4-101. Sympatry in <i>Thylacoleo</i> . Box plot of proportional prey species (divided into terrestrial and arboreal herbivores) with the presence of 1 or 2 species of <i>Thylacoleo</i> . ....	375
Figure 4-102. Fossil <i>Leggadina</i> from Mt Etna, M <sup>1</sup> s (QML1312).....	376
Figure 4-103. Fossil <i>Pseudomys</i> from Mt Etna, M <sup>1</sup> s.....	377
Figure 4-104. Fossil <i>Zyzomys</i> from Mt Etna, M <sup>1</sup> s (QML1312). ....	378
Figure 4-105. Fossil <i>Notomys</i> from Mt Etna (QML1312) compared with <i>N. aquilo</i> (far right) M <sup>1</sup> s and maxillae. ....	379
Figure 4-106. Fossil <i>Notomys</i> from Mt Etna (QML1312) compared with <i>N. fuscus</i> (right) maxillae.....	379
Figure 4-107. Fossil <i>Notomys</i> from Mt Etna (QML1312) M <sup>1</sup> compared with <i>N. cervinus</i> (right) maxillae. ....	380
Figure 4-107. Fossil <i>Pogonomys</i> M <sup>1</sup> s from Mt Etna (QML1313). ....	381
Figure 4-108. Fossil ' <i>Mesembriomys</i> ' from Mt Etna (middle Pleistocene localities) compared with extant <i>Mesembriomys gouldii</i> (top right) and <i>M. macrurus</i> (bottom right), M <sup>1</sup> s. ....	383
Figure 4-109. <i>Uromys</i> sp. nov. from Mt Etna (QML1313), compared with <i>Melomys</i> sp. from Mt Etna (QML1313), maxillae.....	384
Figure 4-110. Box plot of M <sup>1-3</sup> molar row length compared with extant species of <i>Uromys</i> . ....	384
Figure 4-111. Bivariate plot of M <sup>1</sup> length to width of fossil and modern <i>Uromys</i> and <i>Melomys</i> specimens.....	385
Figure 4-112. <i>Uromys hadrourus</i> from Mt Etna (QML1313) M <sup>1</sup> s. ....	386
Figure 4-113. Fossil <i>Melomys</i> from Mt Etna QML1311H, QML1311 CD and QML1313, M <sup>1</sup> s.....	386
Table 4-5. Taxonomic methodology and coverage for the taxa identified during this work. Apomorphy-based versus comparative-based method for identification; literature-based or direct comparisons to extant and extinct taxa; geographical and temporal coverage of comparisons. ....	391
Figure 5-1. Morphometric measurements. A. Pre-postzygapophysis length. B. Centrum length. C. Cotylar width. D. Post-postzygapophysis width. E. Pre-prezygapophysis width. F. Tooth crown height. G. Tooth base length. H. Diaphysis width (humerus). I. Distal condyle width (humerus). ....	396
Figure 5-3. <i>Varanus komodoensis</i> (Neogene, Australia). A-B, E-G. Pliocene <i>V. komodoensis</i> (Australia)A-B. QMF 53955, partial left humerus	

in dorsal view showing position of insertion for the *latissimus dorsi* (lat dors). C-D. Left and right humerus of a modern *V. komodoensis* (NNM 17504). E-F. QMF 53954, partial right humerus in ventral and dorsal views, showing the position of the ectepicondyle (ect). G. QMF 866, partial scapulocoracoid. H-P. Pleistocene *V. komodoensis* (Australia). H-I. QMF 54605, partial left maxilla in lingual and labial views. J. QMF 54606, partial right quadrate in anterior view. K. QMF 54607, supraoccipital bone in posterior view. L. QMF 54608, proximal left tibia. M. QMF 54604, ulna diaphysis. N-P. QMF 1418, proximal mid-caudal in cranial, oblique lateral and dorsal views. Scale bar = 1 cm. .... 403

Figure 5-4. *Varanus komodoensis* (Pliocene, Australia). A-F. QMF 42104, posterior dorsal vertebra compared with modern *V. komodoensis* (white), in anterior (A-B), posterior (C-D) and left lateral (E-F) views. G-L. QMF 42096, mid-dorsal vertebra compared with modern *V. komodoensis* (white), in anterior (G-H), posterior (I-J) and right lateral (K-L) views. M-R. QMF 42102, mid-dorsal vertebra compared with modern *V. komodoensis* (white), in anterior (M-N), posterior (O-P) and left lateral (Q-R) views. S-V. QMF 23684, cervical vertebra compared with modern *V. komodoensis* (white), in left lateral (S-T) and anterior (U-V) views. W-X. QMF 23686, anterior dorsal vertebra compared with modern *V. komodoensis* (white) in anterior view. Scale bar = 1 cm. .... 404

Figure 5-5. *Varanus komodoensis* (Pleistocene, Flores). A-B. Sacral vertebrae from modern (A) and fossil (LB558a) *V. komodoensis* in anterior view. C. Articulated dorsal vertebrae (LB19/20-9-04) in dorsal view. D. Cervical vertebra (LB517b) in dorsal view. E. Four isolated teeth (LB04 unreg) in lingual view. F-H. Ulna diaphysis (LB-447a/16.8.04) in medial (F), cranial (G) and lateral (H) views. I. Radius diaphysis (LB-28.7.03) in medial view. Scale bar = 1 cm. .... 407

Figure 5-6. *Varanus* sp. cf. *V. komodoensis* and *V. salvator* (Pleistocene, Java). A-F. *V. sp. cf. V. komodoensis*. Anterior dorsal vertebra (CD 6392) compared with modern *V. komodoensis* in anterior (A-B), dorsal (C-D) and left lateral view (E-F). G-K. *V. salvator*. G-I. CD 8873, mid-dorsal vertebra, compared with modern *V. komodoensis* in dorsal (G-H) and anterior (H-I) views. J-K. CD 216, sacral vertebra, compared with modern *V. komodoensis* in anterior view. Scale bar = 1 cm. .... 409

Figure 5-7. *Varanus sivalensis* (Pliocene, India). A-B. NNM 17504, modern *Varanus komodoensis* humerus. C-D. NHMR 40819, distal humerus in dorsal (C) and ventral (D) views. E-I. NHMR 740, posterior dorsal vertebra compared with modern *V. komodoensis* (white) in anterior (E-F), left lateral (G-H) and dorsal (I) views. J-N. NHMR 739, anterior dorsal compared with modern *V. komodoensis* (white) in left lateral (J-K), anterior (L-M) and posterior (N) views. Scale bar = 1 cm. .... 411

Figure 5-8. *Varanus* sp. nov. (Pleistocene, Timor). A-F. Mid-dorsal vertebra (CV Raebia 1) compared with modern *V. komodoensis* in anterior (A-B), left lateral (C-D), dorsal (E-F) views. G-L. Anterior caudal vertebra (CV Raebia 2) compared with modern *V. komodoensis* in anterior (G-H), dorsal (I-J) and oblique posterior (K-L) views. M-R. Sacral vertebra (CV Raebia 3) compared with modern *V. komodoensis* in anterior (M-N), dorsal (O-P) and ventral (Q-R) views. S. QMF 8968, sacral vertebra of *Varanus prisca* in anterior view. .... 413

Figure 5-9. Palaeogeography and chronology of giant varanids. Schematic diagram illustrating the proposed taxonomy, chronology and dispersal sequence of giant varanids from mainland Australia to the Indonesian islands of Timor, Flores and Java during the Pliocene-Pleistocene..... 417

Figure 6-1. Location of the post-Miocene Australopapuan rainforest vertebrate fossil record in relation to the present day Wet Tropics rainforests of north-eastern Australia, including the early Pliocene Hamilton fauna from south-eastern Australia, the Quaternary faunas from New Guinea and the eastern Australian Quaternary fauna presented herein. .... 441

Figure 6-2. Chronometrically constrained, bootstrapped, similarity cluster analysis of dated fossil and modern faunas of the present study. .... 447

Figure 6-3. Similarity cluster analysis of modern and fossil faunas associated with hydric (1-14), mesic (15-26) and xeric (27-38) habitats. Dashed lines indicate fossil faunas. Site locations and references are provided as a supplementary table in Appendix A. .... 448

Figure 6-4. Species richness and faunal turnover through time for medium and small-sized mammal species for the study area. (a) species richness (count of spp.), (b) percentage of new species, (c) percentage of species loss. .... 450

Table 6-1. Representative U/Th dates for fossil sites at Mt Etna, central-eastern Queensland. .... 451

Figure 6-5. Australia's middle Pleistocene palaeoclimatic record showing the differential timing of the shift to intensifying aridity and climatic variability in northern, central and southern Australia. The vertical grey bar represents the time of faunal turnover during the middle Pleistocene at Mt Etna (~280-205 ka). 1-13. Intensifying aridity in northern Australia since ~300 ka; 1. Mt Etna faunal turnover, 2-3. Aeolian dust records from the Tasman [31] and Coral Seas [32], 4-5. Lake level reduction and playa deflation [33], 6. Magela Ck. net sedimentation post 300 ka [34], 7-9. Sea Surface Temperature (SST) increase along the East Australian Current with reef development [35, 38, 39, 43, 44], 10-13. Palynological records from northwest Australia [27,45,46]. 14-15. Intensifying aridity in central Australia since 4 Ma; 14. Gibber-Stony desert formation [47], 15. Lake Amadeus arid shift [49]. 16-20. Intensifying aridity in southern Australia since ~600 ka; 16-17. Southern lakes shift to aridity [50-54], 18-19. Southern weathering shift to aridity [55], 20. Dry phase between 270-220 ka at the Naracoorte Caves recorded from speleothems [21,22]..... 456

Table 6-2. Middle Pleistocene fossil taxa considered to be rainforest or arid specialists with the annual precipitation range\* of their closest living relatives. .... 457

Figure 6-6.  $^{230}\text{Th}/^{238}\text{U}$  vs.  $^{234}\text{U}/^{238}\text{U}$  evolution diagram for flowstone and calcite filling samples from Mt Etna. Curved lines are closed-system isotopic evolution for initial  $^{234}\text{U}/^{238}\text{U}$  activity ratios of 1.3, 1.6, 1.9, 2.2 and 2.5. Straight lines are isochrons with numbers corresponding to isochron ages (ka). The plot shows that the vast majority of samples plot in between the 300 and 600 ka isochrons. .... 462

Figure 6-7. Stratigraphy of Mt Etna Limestone Mine and QML1284 with dates, adapted and revised [15]. A. Exposed fossil deposits at Mt Etna

Limestone Mine, western benches. 1-5 QML1311; 1. A/B, 2. C/D, 3. F, 4. H, 5. J. 6-7 QML1384; 6. LU, 7. UU. 8. QML1310 Unit 2, 9. QML1383 A, 10. Open chamber to Speaking Tub Cave System, 11. QML1313, 12. Bench 0 (A/B), 13. QML1385. Blue coloured text represent minimum ages, red coloured text represents maximum ages. ....	463
Figure 6-8. Images of selected flowstones with dating loci. Flowstone ROK04 was dated at three loci, i.e. ~4, 15 and 46 mm below the top surface of the flowstone. Samples ROK02-4 and 02-5 represent different sections of one flowstone (ROK02), and the bottom parts of both samples yield identical ages. ROK-G is a flowstone-like calcite vug growing within the void of Unit-2 deposits at site QML1310 (somehow like a micro-cave). Its top, middle and bottom portions yield three different ages corresponding to Marine Isotope Stages 7, 11 and 13. ....	464
Table 6-4. Faunal lists for fossil sites and present day. 0=absent, 1=present. ....	471
Table 6-5. Detailed U-series data for fossil sites. ....	473
Table 6-6. Generic-level mammal list used for Fig. 3 cluster analysis. Abbreviations, H, hydric, M, mesic, X, xeric. ....	477
Figure 7-1. Publications relating to the Neogene vertebrate record showing the marked decline (red arrow) over the last ca. 20 years in the study of vertebrate faunas, alpha-taxonomy and palaeoecology. This is compared with the significant proportional shift with increasing (blue arrow) molecular studies and a focus on megafauna extinction. ....	481
Figure 7-2. Palaeogeographic reconstruction of the northern Australian region through the mid-late Cainozoic. A. Oligo-Miocene (convergent margins, subduction zone), B. Middle-Late Miocene, carbonate platform development, C. early-Late Pliocene, cratonic basin subsidence and siliciclastic in fill (emergent northern islands) D. Late Pliocene-Pleistocene, upthrust and basin filling (orogen fully developed), exposed basin floor during lowered sea level. E. Late Pliocene-Pleistocene during lowered Sea Level (cool and wet), F. Late Pliocene-Pleistocene during high sea level (warm and wet), G. Late Pliocene-Pleistocene during low sea level (cold and dry). ....	488
Figure 7-3. Middle Miocene palaeogeographic map showing plate movements and the development of carbonate platforms. ....	489
Figure 7-4. Late Miocene, showing the beginning of emergent land and cratonic basin sedimentation. Arrival of other oceanic terranes from the north. ....	490
Figure 7-5. Early Pliocene, burial of carbonate platforms and subsidence of the intracratonic basin (Gulf of Carpentaria), lateral development of carbonate platforms off Gulf of Papua. ....	491
Figure 7-6. Late Pliocene, major up thrust and basin fill, lowered sea level exposes basin, total land connection for the first time. ....	492
Figure 7-7. Pleistocene, Last Glacial Maximum margin (100-120m) lowered sea level. Lake Carpentaria, Bass Strait Lake. Black represents the present day mesothermic rainforest archipelago. ....	493
Figure 7-8. Mid-late Cainozoic Sea Level Change from Bintanja et al (2005) and Haq et al (1987). ....	494

Figure 7-9. Middle Miocene, illustrated extent of rainforest vegetation based on records available (most-likely more extensive than this).....	495
Figure 7-10. Middle-late Miocene development of the western Pacific warm pool (From Li et al, 2006).....	496
Figure 7-11. Late Miocene vegetation, showing the reduction in western, central and northern rainforest habitats. ....	497
Figure 7-12. Early Pliocene vegetation, only marginal increase in rainforests during the early Pliocene. Continued aridification in the southwest and central Australia. Expansion of dry-adapted flora. ....	498
Figure 7-13. Mid-late Pliocene vegetation. Disconnection of the southern rainforests, still relatively continuous connection of northern rainforests, allowing for southern expansion of New Guinea rainforest fauna (e.g. rainforest-obligate rodents and microhylids).....	500
Figure 7-14. Present-day mesothermic rainforest patches in northern Australia, associated with uplands ~600m +. ....	501
Figure 7-15. Abundance of warm-water planktonic forameniferans, showing dramatic increase from ~283ka. From Lopez-Otálvaro et al (2008).....	502
Figure 7-16. Summarised palaeogeography, palaeoclimate, sea level and impact history of the Australasian region.....	505
Figure 7-17. Biochronology of non-volant marsupial families from the Late Oligocene to the present day.....	511
Figure 7-18. Bioclimatic distribution prediction map for <i>I. obseulus</i> and <i>I. auratus</i> based on mean annual precipitation and mean monthly temperature. ....	514
Figure 7-19. Palaeobiogeography of Middle Pleistocene and present day frog species. ....	526
Figure 7-20. Palaeobiogeography of Middle Pleistocene and present <i>Egernia major</i> . ....	527
Figure 7-21. Palaeobiogeography of Middle Pleistocene and present day species of <i>Hypsilurus</i> .....	527
Figure 7-22. Palaeobiogeography of Middle Pleistocene and present day <i>Pseudocheirus</i> .....	529
Figure 7-23. Palaeobiogeography of Early Pliocene, Middle Pleistocene, Holocene and present day <i>Petauroides</i> .....	530
Figure 7-24. Palaeobiogeography of Mio-Pliocene, Early Pliocene, early Pleistocene and Middle Pleistocene species of <i>Pseudokoala</i> . ....	530
Figure 7-25. Palaeobiogeography of Early Pliocene, Middle Pleistocene, Holocene species of 'plesiomorphic' thylogale. ....	531
Figure 7-26. Palaeobiogeography of Early Pliocene, late Pliocene and Middle Pleistocene species of <i>Bohra</i> .....	531
Figure 7-27. Palaeobiogeography of Mio-Pliocene, Early Pliocene, early Pleistocene and Middle Pleistocene <i>Thylacoleo hilli</i> .....	532
Figure 7-28. Palaeobiogeography of Middle Pleistocene and present day species of <i>Dendrolagus</i> . ....	533



Figure 7-29. Palaeobiogeography of Middle Pleistocene, Holocene and present day species of <i>Dactylopsila</i> .	533
Figure 7-30. Palaeobiogeography of Middle Pleistocene and present day <i>Micromurexia</i> .	534
Figure 7-31. Palaeobiogeography of Middle Pleistocene and present day species of <i>Phalanger</i> and <i>Spilocuscus</i> .	534
Figure 7-32. Palaeobiogeography of Middle Pleistocene and present day species of <i>Pogonomys</i> .	535
Figure 7-33. Palaeobiogeography of Pleistocene species of <i>Protemnodon</i> .	535
Figure 7-34. Palaeobiogeography of Middle Pleistocene and present day species of <i>Pseudochirops</i> .	536
Figure 7-35. Palaeobiogeography of Middle Pleistocene and present day species of <i>Pseudochirulus</i> .	536
Figure 7-36. Palaeobiogeography of Middle Pleistocene and present day species of <i>Pseudochirulus</i> .	537
Figure 7-37. Palaeobiogeography of Middle Pleistocene and present day <i>Uromys hadrourus</i> .	537
Figure 7-38. Palaeobiogeography of Middle Pleistocene and present day species of <i>Uromys</i> .	538
Figure 7-39. Locomotary guilds for marsupial family dispersal to New Guinea (NG).	539
Figure 7-40. Body-size guilds for marsupial family dispersal to NG.	540
Figure 7-41. Dietary guilds for marsupial family dispersal to NG.	540
Figure 7-42. Linear regression of Successful dispersal versus candidate representation, showing a positive relationship between candidate representation versus success in dispersing to NG. $R^2$ value high: 0.79.	541
Figure 7-43. Biochronology of non-volant marsupial families from the late Oligocene to present day, showing extinctions during the late Miocene and late Pleistocene. Extinction events broken down into guild types (body-size, locomotion and diet). Overall family-level diversity has fallen through time to the present levels with extinction peaking both during the late Miocene and late Pleistocene.	545
Figure 7-44. Body-size guild extinction between the Quaternary rainforests (Mt Etna) and present day Wet Tropics rainforests (species-level).	549
Figure 7-45. Dietary guild extinction between the Quaternary rainforests (Mt Etna) and present day Wet Tropics rainforests (species-level).	550
Figure 7-46. Locomotary guild extinction between the Quaternary rainforests (Mt Etna) and present day Wet Tropics rainforests (species-level).	550
Table 7-1. Middle Pleistocene and Present day (Wet Tropics) frog fauna and guilds.	552
Table 7-2. Middle Pleistocene and Present day (Wet Tropics) frog fauna.	553

Table 7-3. Middle Pleistocene and Present day (Wet Tropics) reptile fauna and guilds. ....	554
Table 7-4. Middle Pleistocene and Present day (Wet Tropics) reptile fauna. ....	554
Table 7-5. Middle Pleistocene and Present day (Wet Tropics) carnivore fauna and guilds. ....	555
Table 7-6. Middle Pleistocene and Present day (Wet Tropics) carnivore guilds. ....	556
Table 7-7. Middle Pleistocene and Present day (Wet Tropics) terrestrial herbivore fauna and guilds. ....	557
Table 7-8. Middle Pleistocene and Present day (Wet Tropics) terrestrial herbivore guilds. ....	557
Table 7-9. Middle Pleistocene and Present day (Wet Tropics) arboreal herbivore fauna and guilds. ....	559
Table 7-10. Middle Pleistocene and Present day (Wet Tropics) arboreal herbivore guilds. ....	559
Table 7-11. Middle Pleistocene and Present day (Wet Tropics) 'invertivore' fauna and guilds. ....	560
Table 7-12. Middle Pleistocene and Present day (Wet Tropics) 'invertivore' guilds. ....	560
Table 7-13. Middle Pleistocene and Present day (Wet Tropics) exudivore fauna and guilds. ....	562
Table 7-14. Middle Pleistocene and Present day (Wet Tropics) exudivore guilds. ....	562
Table 7-15. Middle Pleistocene and Present day (Wet Tropics) omnivore (perameloid) fauna and guilds. ....	562
Table 7-16. Middle Pleistocene and Present day (Wet Tropics) murid (omnivore-granivore) fauna. ....	563
Figure 7-47. Summary of prevailing climatic changes over the last 1.2 million years in the Australasian region. ....	564
Figure 7-48. Bioclimatic distribution of fauna between middle Pleistocene rainforest fauna and the xeric-adapted QML1312 fauna. Showing overall decrease in mean annual precipitation (see text for explanation). Top (all taxa), Bottom (obligate taxa only). ....	566
Figure 7-49. Frog succession at Mt Etna between the middle Pleistocene and present day. MP1 (>280ka), MP2 (205-170ka), LP (<80ka), H (<10ka) PD (present). ....	567
Table 7-17. Mt Etna frog succession. ....	568
Figure 7-50. Middle Pleistocene (Mt Etna) and present day occurrence of <i>Neobatrachus</i> . ....	569
Table 7-18. Mt Etna murid succession. ....	570
Figure 7-51. Murid succession at Mt Etna between the middle Pleistocene and present day. MP1 (>280ka), MP2 (205-170ka), LP (<80ka), H (<10ka) PD (present). ....	571
Figure 7-52. Middle Pleistocene (Mt Etna) and present day occurrence of <i>Notomys</i> . ....	571

Figure 7-53. Middle Pleistocene (Mt Etna) and present day occurrence of <i>Zyzomys</i> .	572
Figure 7-54. Middle Pleistocene (Mt Etna) and present day occurrence of <i>Leggadina</i> .	572
Figure 7-55. Middle Pleistocene (Mt Etna) and present day occurrence of <i>Conilurus</i> .	573
Table 7-19. Mt Etna possum succession.	575
Figure 7-56. 'Possum' succession at Mt Etna between the middle Pleistocene and present day. MP1 (>280ka), MP2 (205-170ka), LP (<80ka), H (<10ka) PD (present).	575
Table 7-20. Mt Etna kangaroo-potoroo succession.	576
Figure 7-57. Non-megafaunal macropod succession at Mt Etna between the middle Pleistocene and present day. MP1 (>280ka), MP2 (205-170ka), LP (<80ka), H (<10ka) PD (present).	576
Table 7-21. Mt Etna 'megafauna' succession.	577
Figure 7-58. Very large and megafaunal mammal succession at Mt Etna between the middle Pleistocene and present day. MP1 (>280ka), MP2 (205-170ka), LP (<80ka), H (<10ka) PD (present).	578
Table 7-22. Mt Etna dasyurid succession.	579
Figure 7-59. Dasyurid succession at Mt Etna between the middle Pleistocene and present day. MP1 (>280ka), MP2 (205-170ka), LP (<80ka), H (<10ka) PD (present).	579
Figure 7-60. Middle Pleistocene (Mt Etna) and present day occurrence of <i>Planigale tenurostris</i> .	580
Figure 7-61. Middle Pleistocene (Mt Etna) and present day occurrence of <i>Sminthopsis macroura</i> .	580
Table 7-23. Mt Etna bandicoot succession.	581
Figure 7-62. Perameloid succession at Mt Etna between the middle Pleistocene and present day. MP1 (>280ka), MP2 (205-170ka), LP (<80ka), H (<10ka) PD (present).	582
Figure 7-63. Middle Pleistocene (Mt Etna & Chillagoe) and present day occurrence of <i>Chaeropus ecaudatus</i> .	582
Figure 7-64. Middle Pleistocene (Mt Etna) and late Pleistocene (Broken River) and present day occurrence of <i>Macrotis lagotis</i> .	583
Figure 7-65. Middle Pleistocene (Mt Etna) and late Pleistocene (Darling Downs) and present day occurrence of <i>Perameles bouganville</i> .	583
Table 7-24. Mt Etna reptile succession.	584
Figure 7-66. Middle Pleistocene (Mt Etna) and present day occurrence of <i>Tympanocryptis</i> .	585
Figure 7-67. Middle Pleistocene (Mt Etna) and present day occurrence of <i>Pogona</i> (small).	585
Figure 8-1. Summary of major events since the Late Miocene that shaped Australian mesothermic rainforest vertebrate faunas	589

# Chapter 1

## 1.1 Introduction & Study Area

## 1.2 Introduction

Study of the late Cainozoic environmental record provides the fundamental background to our understanding of the modern environment and its responses to past change. Documentation of the late Cainozoic record provides the baseline knowledge from which we can determine the mode and trajectory of future natural environmental change.

Projections of future climate change indicate that the 21<sup>st</sup> century will be a period of unprecedented and extremely rapid change. It is most likely that some regions of the world will experience major environmental impacts, associated with variable rainfall, rising temperatures and sea levels. Queensland's most treasured natural environments, such as the World Heritage Areas of the Wet Tropics (WT) and Great Barrier Reef (GBR) of north-eastern Australia, are particularly sensitive to regional changes in temperatures and sea level (Walsh et al., 2002; Williams et al., 2003; Shoo et al., 2005a, b; Thomas et al., 2004a, b; Williams & Hilbert, 2006).

The IPCC 2007 report predicts a massive reduction in WT biodiversity by 2020 with increased temperatures, whilst substantial declines in the GBR are predicted by an increase in Sea Surface Temperatures (SST) and sea level rise by 2050 (Hoegh-Guldberg & Hoegh-Guldberg, 2004). Therefore there is a critical need to develop and integrate the baseline data of past environmental alterations (both climatic and anthropogenic) of this internationally significant bioregion to determine the long term vulnerability and responses of them to future climate change.

Of particular importance are the mesothermic rainforests and their associated endemic and isolated faunas of the Wet Tropics of north-eastern Queensland, which are considered to be on the brink of catastrophic extinction under future projections of climatic change (Williams et al., 2003). These assertions are

founded on an understanding of current species distributions and bioclimatic tolerances. However, there is a considerable knowledge gap between these data and known past responses of rainforest species to similar levels of environmental change. How can the palaeontological record help?

Although considerable effort has been focused on documenting the vertebrate fossil record of Australia's late Cainozoic, very little is known of the responses of vertebrate faunas to past climatic change. This is primarily due to the lack of systematic collections and long term research efforts involved with documenting extensive fossil deposits. Primarily there is a lack of detailed faunal studies that include all major faunal groups, most having been focussed on mammalian taxa over others. This has led to the disproportionate understanding of the terrestrial fauna and is due to an overall lack of primary alpha taxonomy and detailed taxonomic reviews that include morphological features preserved as fossils (in particular shell, bones and teeth).

With the exception of mammals, most Australian vertebrate groups are very poorly known with regard to their osteological diversity, variation, and, therefore, their fossil record. Due to this simple artefact, practically nothing is known about our non-mammalian vertebrate fossil record, save for a few attempts (e.g. frogs, Tyler, 1976; and squamates, Meredith-Smith, 1976 and Hutchinson, 1992).

The late Cainozoic vertebrate record for Australia is better known in the southern periphery and centre of the continent, with practically no systematic collections in northern Australia. This lack of detailed information has particularly significant impacts on our understanding of some of the most vulnerable habitats of the present day, such as monsoonal rainforest, dry rainforest and closed tropical rainforests. Southern studies have indicated overall faunal stability during periods of climate change and, therefore, application of this view across the continent could be misleading if past climatic changes are proven to impact areas of the continent in different ways.

The research presented here aims to document for the first time and in as much detail as possible the faunal record for a single northern Australian region, the Mt Etna region of central eastern Queensland, and included within it the only representation of a mainland Quaternary mesothermic lowland rainforest fauna.

**Chapter 1** introduces the study and documents the study area, its history and the methodologies for collection and preparation of the fossil material.

**Chapter 2** “Ecological succession during the Late Cainozoic of central eastern Queensland: extinction of a diverse rainforest community” (Hocknull, 2005) presents the first systematic paper to document the fauna, together with an attempt to reconstruct the palaeoecology and biocorrelation of the fossil sites.

**Chapter 3** “Additional notes on fossil deposits, their formation and age” presents additional information on localities collected during and since Hocknull (2005), including dating of localities which refute the initial age determination of Hocknull (2005). This includes a hypothesised depositional regime for the major deposits in the Mt Etna region.

**Chapter 4** “Additional vertebrate fauna from central eastern Queensland, Australia” presents additional faunal systematics on fauna collected during and since Hocknull (2005), presenting the most up-to-date taxonomic appraisal of the Mt Etna and Marmor Quarry faunas.

**Chapter 5** “Palaeobiogeography, evolution and extinction of the largest-ever terrestrial lizards (Varanidae)” presents a submitted paper on the palaeobiogeography of large-bodied varanids, including identification of the Komodo Dragon on mainland Australia from the Early Pliocene to the Middle Pleistocene (including Mt Etna). The palaeobiogeographic implications of this are addressed in Chapters 5 and 7.

**Chapter 6** “Responses of Quaternary rainforest vertebrates to climate change in Australia” (Hocknull et al., 2007) presents dated faunal successions and provides a correlation of Middle Pleistocene climatic records to understand the extinction of Middle Pleistocene rainforest fauna in central eastern Queensland.

**Chapter 7** “Responses of Australian rainforest vertebrates to late Cainozoic climate change: a synthesis of current knowledge” brings together the data from Chapters 2-6 along with current palaeogeographical, tectonic and palaeoclimatic history through the late Cainozoic and looks at and characterises the major extinctions within Australian mesothermic rainforests throughout the Late Miocene to present day. It also discusses the biogeographic history of New Guinea and the impact of the new Quaternary rainforest record on previous biogeographic models.

**Chapter 8** “Conclusions” summarises the major findings of this work and presents a chronology for the Australian Neogene with particular reference to the evolution of Australia’s mesothermic rainforests.

### 1.3 Study Area 1: Mt Etna Region, central eastern Queensland

#### 1.3.1 Mt Etna & Limestone Ridge National Park (including Mt Etna Quarry)



**Figure 1-1. Satellite imagery of the Mt Etna and Limestone Ridge Study Area**

The Mount Etna region is located near the township of The Caves, 25kms to the north of Rockhampton, central eastern Queensland, Australia (Fig. 1-1).

Cavernous isolated limestone massifs are present in the region and are distributed in a general west-east direction with Mt Etna being the western-most section.

#### **Mt Etna**

The cavernous limestone of Mt Etna includes an area approximately 1.17km long running along an axis in a north-west south-east direction. At its widest point the limestone spans approximately 440m of exposed karst, however, extensive non-karstic limestone horizons can be found flanking the NW and NE sides of the mountain. The southern margin of Mt Etna is made up of silici-clastic and volcanogenic sediments and are non-cavernous. Mt Etna possesses the highest exposed karst in the region, exposed some 20-30m below the summit of Mt Etna. Mt Etna is made up of four major limestone areas: the eastern face, northern face, western face and western ridge.

### **Eastern Face (Eastern Quarry) (Fig. 1-2)**

The eastern face of Mt Etna was sporadically quarried between 1903 and 1966, when significant operations began by Central Queensland Cement Ltd. Mining ceased on this section of Mt Etna in 1974, when operations moved onto the western benches. Two main cave systems were present on this face (E2 & E22), and one such system may have contained bone-bearing breccias (E2) (Armstrong Osborne *pers. com.* 2008). Since mining ceased on this face, significant restoration works have been undertaken, including bench blasting to provide less steep bench faces and significant revegetation.

#### *Resurrection Cave*

Resurrection Cave (E22) is the only remaining cave system on the eastern benches and can be accessed via a locked door at the base of the benches. Resurrection Cave contains significant speleothem formations and silt deposits, but is yet to yield any significant bone deposits. This cave system, being low on the mountain, is considered to be a closed cave and therefore, accumulation of bone material is highly unlikely. At the base of the eastern face, several thousand tonnes of fossiliferous deposit have been stockpiled, having originally been discovered on the western face. The stockpiled deposits have been removed and placed in stratigraphic sequence. Both the stockpiled and insitu deposits are designated as a scientific collecting areas, forming part of the Mt Etna and Limestone Ridge Caves National Park in 2008.





**Figure 1-2. Eastern face of Mt Etna**

### **Northern Face (National Park) (Fig. 1-3)**

The northern face of Mt Etna was gazetted as the Mt Etna Caves National Park in 1990 and consists of a large section of karstic limestone with cave systems. Caves in this section have been described by Shannon (1970a) and include several systems yielding fossil bone deposits, both within the cave systems and exposed palaeocave breccia deposits.

## Main Cave

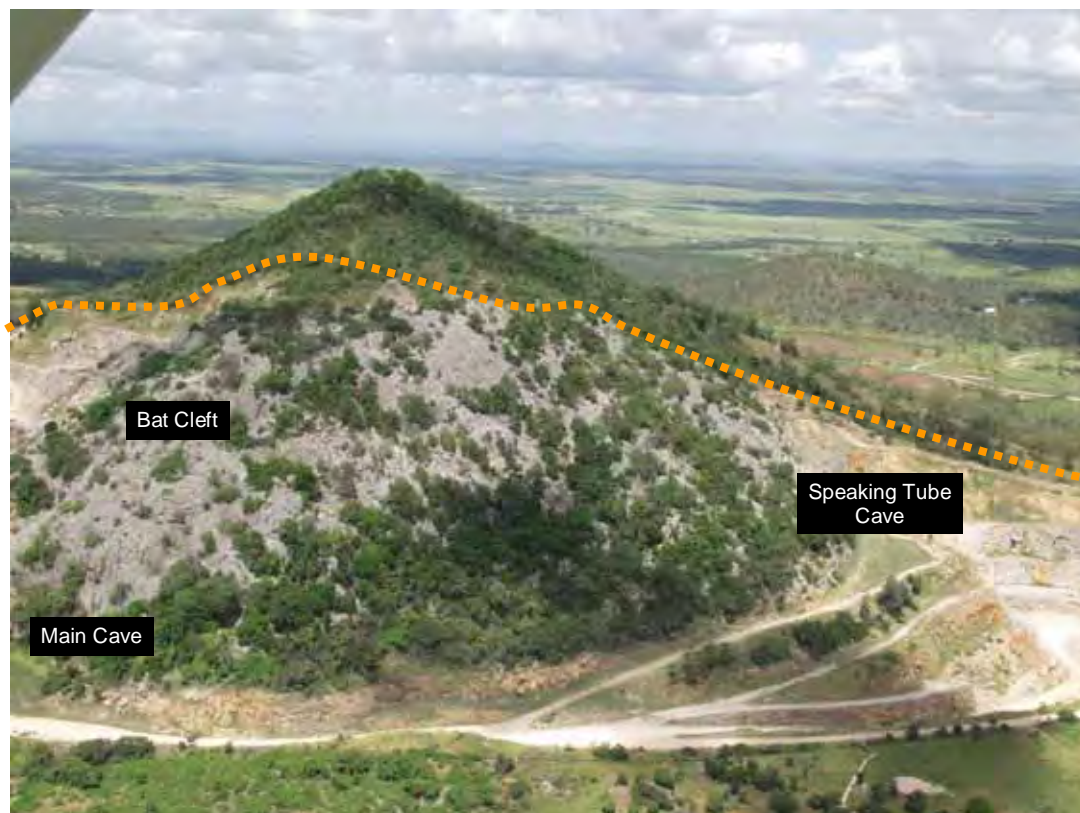


**Figure 1-3. The northern face of Mt Etna Caves National Park**

### **Western Face (Western Quarry) (Fig. 1-4)**

The western face of Mt Etna has undergone significant mining since 1974, which ceased in 2007 and was formally handed over to National Parks in 2008.

Considerable and significant fossil deposits are located on the western benches of the Mt Etna mine. Several of these fossil deposits have been sampled and extensive collections of material taken for study. Large quantities of each deposit have been stockpiled at the base of the eastern face in a designated resource area for scientific study and collection.

The fossiliferous material recovered from the western benches was once part of two major cave systems, Speaking Tube and Elephant Hole Cave Systems.

Hocknull (2005) and Hocknull et al. (2007) detail these deposits and their preliminary faunas.

**Deposit Stockpiling (Fig. 1-5; 1-6)**

In 1992 some fossiliferous material removed from the western benches was stockpiled on the bench running up to the Main Cave entrance. Some of this material was also sent to the Queensland Museum. This stockpiled deposit was 're-discovered' in 2002 along with remnants of the original deposit on the western face of Mt Etna.

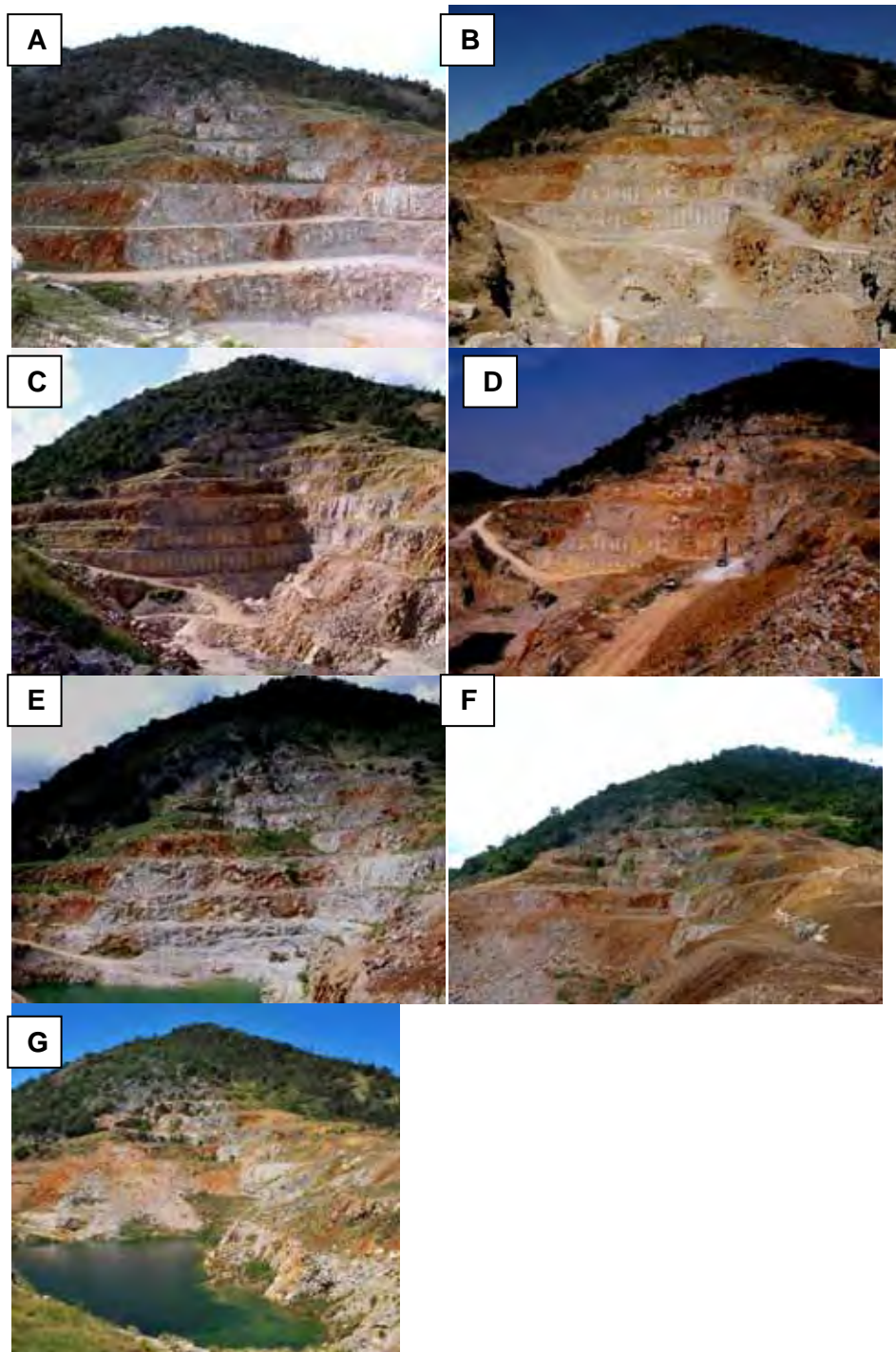


**Figure 1-4. Western Quarry of Mt Etna during the study period. A. 2002, B. 2003, C. 2004, D. 2005, E. 2006, F. 2007, G. 2008.**



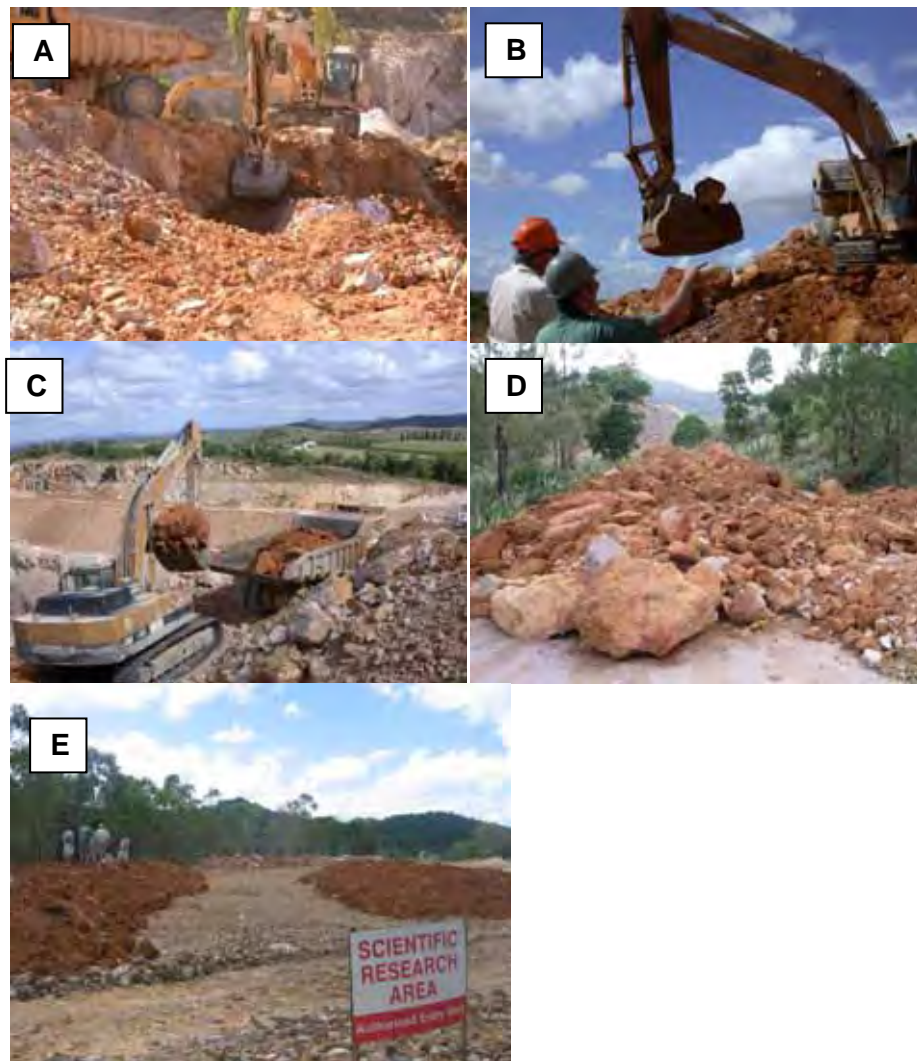


**Figure 1-5. Stockpiling operations during the study period. A. Removal of deposits via excavation. B. Supervised removal of sediment in relative stratigraphic context. C. Trucking of stockpiled material to scientific research area. D. Stockpiling of material in discrete sections representing individual deposits. E. Perpetual access to stockpiled material in a designated Scientific Research Area (National Park as of 2008).**

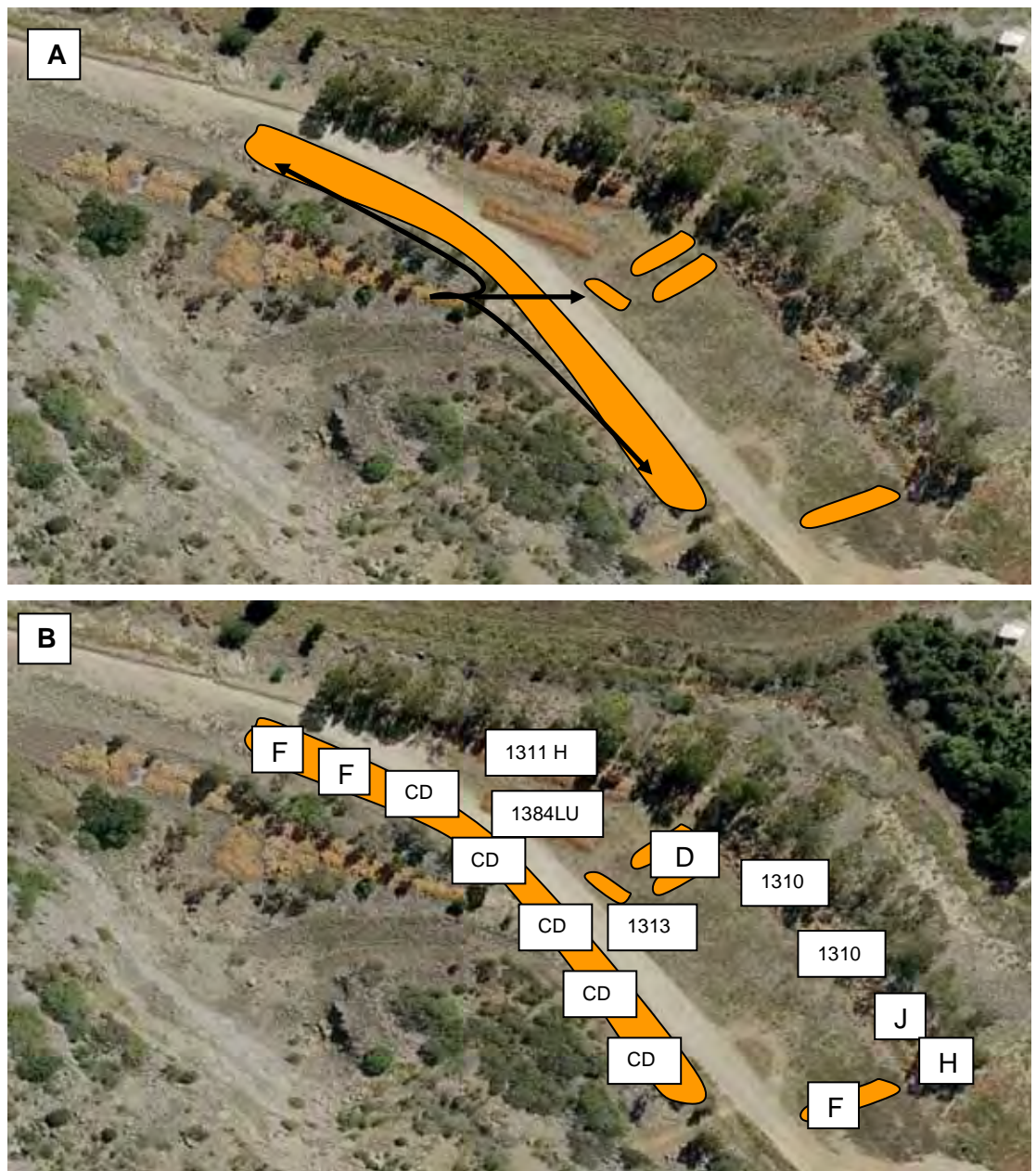


**Figure 1-6. Scientific Research Area Stockpiles. A. Stockpiles originally laid on ramp toward Main Cave entrance re-stockpiled onto flat accessible land. B. Final stockpile arrangement and fossil deposits.**

### **Limestone Ridge (Fig. 1-7).**

Limestone Ridge is located approximately 1km east of the Mt Etna summit and includes three major limestone bodies: a northern, southern and ‘Cammoo Caves’ section. Bisecting the northern and southern areas of limestone is a saddle made up of mostly silici-clastic and volcanogenic sediments. The long axis of Limestone Ridge runs in a near north-south direction for approximately 1.43kms

and is 500m wide at its widest exposed karst. The Cammoo Caves section is a smaller area of limestone directly south of the southern section and is bisected from the southern section by a saddle.

### **Northern Section (Fig. 1-8).**

The northern section of Limestone Ridge has undergone some limestone quarrying from 1932 to 1963 (Pilkington's Quarry) and guano mining in the late 1800s and early 1900s (Hocknull, 2005), however, significant fossil deposits have been located in several of these cave systems.

#### *Johannsen's Cave*

The largest cave system in the northern section of Limestone Ridge is divided into two levels, 'Upper' and 'Lower' Johansen's Cave. Johansen's Cave has been subject to considerable disturbance through the activities of limestone quarrying on the outside north-western face and guano mining within the chambers. Hocknull (2005) reports on the fossil faunas and deposits within this system.

#### *Old Timbers Cave*

Old Timbers Cave has been subjected to disturbance from guano mining (Hocknull, 2005), although significantly deep sediment deposits have been discovered in this cave. Collections made in 2006 reveal a diverse small fauna which is most likely Late Pleistocene to Recent in age, including murids, bats, dasyurids, reptiles and birds.





**Figure 1-7. Limestone Ridge National Park showing the Northern and Southern Section.**





**Figure 1-8. Aerial photograph of Limestone Ridge from the Northern aspect, showing the locations of Johansen's and Old Timbers Caves.**

### **Southern Section (Fig. 1-9)**

The Southern Section of Limestone Ridge has extensive exposed karst with minimal vegetation on the eastern flanks. Large caves are found throughout this section and include several with significant sediment and bone-breccia deposits. Hocknull (2005) details the sedimentology of the fossil deposits from the Mini Cave system and Leo's Lunch Site.

#### *Ballroom Cave*

Ballroom Cave is a large horizontally developed cave system following both limestone and andesitic bedding plains. In the upper eastern section of the cave, under a crawl-way, is a small bone-breccia deposit. Throughout the cave system, Recent, subfossil and reworked fossil material can be found concentrated in the wash pools toward the lower southern section of the cave. Concentrations have been found around washpools in the centre of the chambers and near washouts below large fig tree root masses.

#### *Larynx Labyrinth Cave*

Larynx Labyrinth Cave is very large cave system towards the base of the eastern flank of Limestone Ridge. Fossil deposits are well known in this system, but very few specimens have been collected. A large chamber deep within the system possesses a vast number of bones in situ. Throughout the cave are small pockets of breccia, usually found high within the chambers.

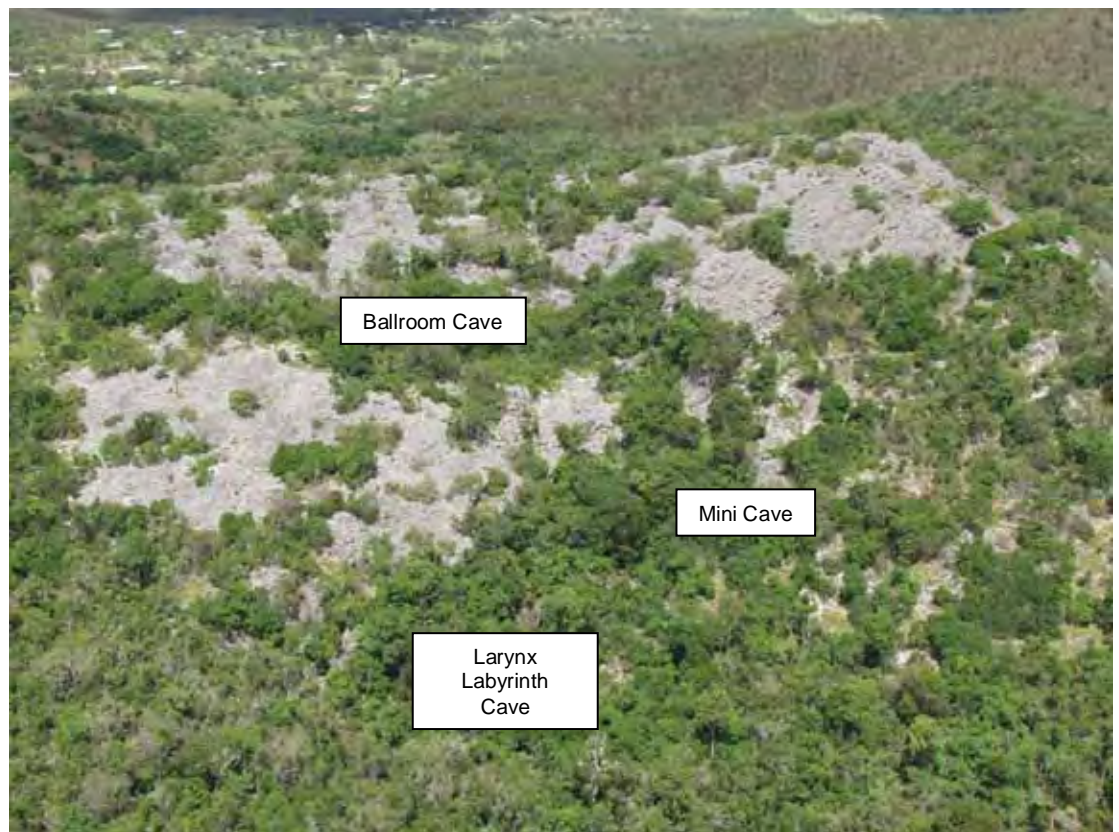


**Figure 1-9. Limestone Ridge National Park (Southern Section) showing general locations of Mini, Ballroom and Larynx Labyrinth Caves.**

### *Lost Paradise Cave*

Lost Paradise Cave is a medium-sized cave with small sediment deposits within the main chamber. As with Ballroom Cave, Recent, subfossil and reworked bone material is concentrated in washpools and washouts toward the lower sections of the chambers.

### **Cammoo Caves Section (Fig. 1-10)**

Cammoo Caves have been disturbed as the result of previous tourist activities throughout the caves. As yet no fossil deposits have been discovered or recovered from these caves. This has primarily been due to the unsafe entrance to these caves at the present time (2008/2009). The Cammoo and Southern Sections of Limestone Ridge provide the output for a small creek that runs southwest from the limestone and carries the carbonates that form tufa barrages further downstream.



**Figure 1-10. Satellite imagery of Cammoo Caves section of Limestone Ridge National Park.**

### 1.3.2 Capricorn Caves (Figs 1-11, 1-12).

Capricorn Caves are approximately 3.9km east of the Mt Etna summit. Two main cave systems occur in the area, Olsen's Cave and Gigas Hall Cave. Olsen's Cave has been used as a tourist cave since the early 1900s, and was also mined for guano (Hocknull, 2005). Within the cave, several bone-rich deposits are present in individual chambers. Three main deposits have been excavated from Icicle, Honey Moon and Colloseum Chambers. Gigas Hall is a low-lying karst with joint-controlled long chambers. Small bone deposits can be found throughout the cave system, including false-floor bone breccias.





**Figure 1-11. Satellite imagery of the Capricorn Caves Tourist Park, including Olsen's and Gigas Hall Caves.**



**Figure 1-12. Closer imagery of Olsen's Cave showing general location of three important fossil deposits (Icicle Chamber, Honey Moon Suite Chamber and Colloiseum Chamber).**

### 1.3.3 Karst Glen (Fig. 1-13)



**Figure 1-13. Satellite imagery of Karst Glen limestone showing the general locations of cave and exposed bone breccias, including KG3, Ladder Cave.**

Karst Glen is located approximately 4.6km south-east of the Mt Etna summit and approximately 800m south-east of the Olsen's Cave system. Fossiliferous deposits are found on the western and northern exposures of karst, including several localities close to extant cave entrances (Ladder Cave, KG3). Considerable bone breccias occur throughout, with several large bone-bearing deposits within individual chambers.

Preliminary inspection of the bone-bearing horizons at Karst Glen has identified a significant component of the fauna to be typical of the mid-Pleistocene and older deposits that occur to the west at Mt Etna. These fauna include a diverse range of pseudocheirids, rodents and some megafaunal remains (e.g. *Palorchestes*).

Based on the faunal remains so far studied, most of the cemented bone-bearing deposits are most similar to the Middle Pleistocene-aged deposits at Mt Etna. Opportunities are available in several of the deposits to glean speleothem.





#### 1.4 Study Area 2: Marmor Quarry, central eastern Queensland.



**Figure 1-14. Satellite imagery of Marmor Quarry and surrounds showing extent of limestone quarrying and untouched limestone sections to the north.**



**Figure 1-15. Aerial photograph of Marmor Quarry (north-eastern aspect) showing the positions of cave entrances and fossil deposits on unmined limestone karst.**

**Marmor Quarry (Figs 1-14, 1-15).**

Marmor Quarry is located approximately 63kms south of Rockhampton. The limestone quarry has been worked for over 100 years (1906-2008) with several fossilised specimens deposited in the Queensland Museum over this timeframe (Hocknull, 2005). The limestone stratigraphy is generally horizontal, with some shallow folding.

During an inspection of the mine in 2006, no significant fossil-bearing deposits were discovered in the limestone quarry itself. However, to the east of the quarry, untouched limestone bears both caves and surface fossil deposits. Cave entrances are relatively small and the karst relatively low, in comparison to Mt Etna and Limestone Ridge. Surface fossil deposits are found along the southern flank of the karst, with the northern flank disappearing below a soil profile.

Hocknull (2005) describes some faunal remains attributed to fossil deposits collected from Marmor Quarry. Material described by Longman (1924, 1925a, 1925b) and breccias recovered by Batholomai (1968) appear to be very similar in overall preservation and lithology. Fossil localities at Marmor recorded in 2006 produce specimens markedly different from those already within the Queensland Museum collection and therefore must be considered separately.

Fossil teeth recovered from bone breccias collected by Batholomai in 1968 were dated using U/Th technique, returning an age for calicitic infill within the tooth of  $153 \pm 1.3$ ka, which should be considered a minimum age. Based on faunal similarities, I suspect that the Marmor fauna is younger than the rainforest faunas of Mt Etna (e.g. <280ka) but older than the major arid-zone fauna from Mt Etna (>170ka), and, therefore, Marmor Quarry breccia collected by Batholomai is most likely an intermediate fauna between 280-170ka. Higher resolution dating and faunal analysis will further refine this age estimate.



## 1.5 Present Day Environment

### 1.5.1 Tuffa Dams (Figs 1-16, 1-17, 1-18)

To the southwest of Cammoo Caves runs a small tributary of the Fitzroy River (Fifteen Mile Creek). The creek runs from the south-western base of Limestone Ridge in a southwest direction for approximately 1.43kms before it is truncated by the Bruce Highway. Along this creek are the preserved remains of palaeotufa and active tufa barrages. Fifteen Mile Creek forms the major efflux from Limestone Ridge, forming major tufa barrages along the length of the creek. The tufa consists of active and inactive dams with several barrages up to approximately 2m thick. Plant and wood fossils are preserved within the tufa.



**Figure 1-16. Fifteen Mile creek running south-west from Cammoo Caves with extent of tuffa deposits marked on map.**

The age range of the tufa deposits is unknown, but several of the deposits must be relatively young because they have grown up and around living vegetation, including tree roots.



**Figure 1-17. Fifteen Mile Creek Tuffa deposits.**

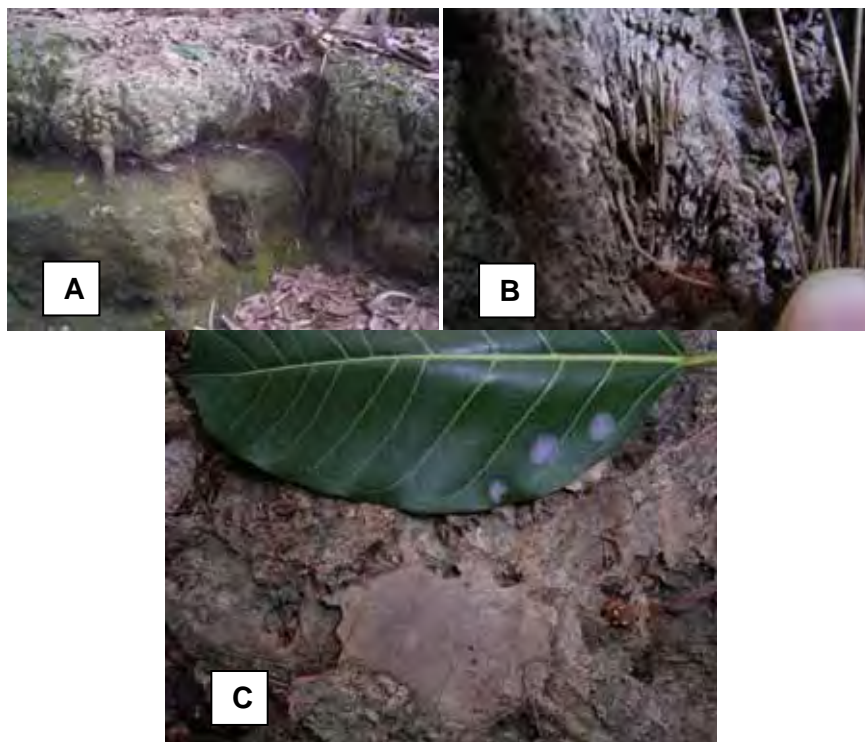


**Figure 1-18. Fossilised remains of plant material found within Tuffa. A. Root casts. B. *Casuarina* pinnae. C. Broad-leafed angiosperm.**

#### 1.5.2 “Dry Rainforest” Semi-evergreen Vine Thicket (Fig. 1-19).

The present day vegetation on Mt Etna considered under the classification of Webb & Tracey (1981) is semi-evergreen vine thicket (SEVT), which occurs almost exclusively on the limestone outcrops, although significant land clearance around the base of these limestone hills and along water courses has significantly reduced the amount of dry rainforest available in the area. SEVT is sensitive to fire and cannot survive in areas where mean annual rainfall falls below 500mm. Fensham (1995) considers the dry rainforest of northern Queensland, including the area of Mt Etna, to be a recent formation due to the probability that rainfall reduced to below 500mm annual precipitation during glacial maxima. If this is the case, then the Late Pleistocene-Holocene faunas of the region should reflect this glacial extinction and subsequent reintroduction. However, dry rainforest situated on limestone may present a different hydrological system, which could provide long-term refugia in an area below the threshold for dry rainforest to exist.





**Figure 1-19. Dry Rainforest (Semi-evergreen Vine Thicket) at Mt Etna.**

## **1.6 Methods**

### **1.6.1 Collecting Methods**

#### **Bone-bearing lithified sediments**

Collections of bone-bearing sediments that have been lithified and cemented with carbonate were collected using sledge-hammers, geological picks and chisels.

Exposed deposits on karst were easily accessible and usually included isolated pieces that were removed without breaking (e.g. QML1284a & KG3; Fig. 1-20). Lithified deposits found within cave systems were removed using chisels to crack loose slabs from roof and wall deposits (e.g. Mini Cave; QML1284).

Areas discovered off-mine were sampled if they met one or more of the following three criteria (Table 1-1):

- Significance.
- Location/accessibility
- Size of resource (Small  $<0.5\text{m}^3$ , Medium  $0.6\text{-}3\text{m}^3$ , Large  $4\text{-}10\text{m}^3$ , Very Large  $10\text{-}50\text{m}^3$ , Massive  $>50\text{m}^3$ ).

Site	Significance	Location/Accessibility	Size of Resource	Resource Collected (as a percentage of resource available)
<b>Mini Cave</b>	Rainforest fauna  First to be discovered.  Bone-breccia not collected since 2003.	Small cave, no permanent bat colony, no significant cave formation. Hard to access.	Large.	<10%
<b>Above Mini Cave</b>	Rainforest fauna  Bone-breccia not collected since 2003.	Exposed Limestone	Large.	<10%
<b>Karst Glen</b>	Rainforest fauna	Exposed Limestone	Very Large.	<5%
<b>Karst Glen (Ladder Cave)</b>	Rainforest fauna	Large cave system. Hard to access.	Very Large.	0%
<b>Marmor Quarry</b>	New fauna	Exposed Karst, easy access.	Very Large.	<5%
<b>Ballroom Cave</b>	?	Large cave system, easy access.	Medium.	<5%
<b>Larynx Labyrinth Cave</b>	Rainforest fauna (Megafauna)	Large cave system, easy to access deposit.	Medium.	<2%
<b>Lower Johansen's Cave (Flowstone Unit)</b>	Pleistocene (Mekosuchine)	Large cave system disturbed by guano miners.	Medium.	<10%
<b>Main Cave (Outside)</b>	?	Exposed, easy to access	Medium.	0%
<b>QML1385</b>	Rainforest fauna (dated)	Exposed on mine, easy access. Subsequently lost.	Large. (deposit covered)	~60%
<b>QML1313</b>	Rainforest fauna (dated)	Stockpiled, easy access	Large.	<20%
<b>QML1311 A/B</b>	?	Stockpiled, easy access	Large.	<5%
<b>QML1311 C/D</b>	Rainforest fauna (dated)	Stockpiled, easy access	Massive	<5%
<b>QML1311 H</b>	Rainforest fauna (dated)	Stockpiled, easy access  Exposed on mine.	Massive	<5%
<b>QML1311J</b>	Rainforest fauna	Stockpiled, easy access	Large	~20%

		Exposed on mine		
Site	Significance	Location/Accessibility	Size of Resource	Resource Collected (as a percentage of resource available)
QML1384 LU	Rainforest fauna	Stockpiles, easy access	Massive	<5%
QML1310	Rainforest fauna	Stockpiles, easy access  Exposed on mine	Very Large.	<5%

**Table 1-1. Lithified deposits investigated during this study.**



**Figure 1-20. Collecting from surface breccias (Karst Glen).**

**Cave Sediment (unconsolidated) (Table 1-2; Fig. 1-21).**

Collections of compacted (unlithified) cave floor sediment was collected insitu via standard excavation techniques. Areas discovered off-mine was chosen to excavate if they met one or more of the following set of criteria.

- Significance of the deposit.
- Areas already significantly disturbed via limestone or guano mining, or tourism traffic.
- Areas clearly representing insitu cave floor accumulations sourced from Owl and/or Ghost Bat (*Macroderma*) Roosts.

Cave	Significance	Prior Disturbance	Roost	Resource Collected as a percentage of total.
<b>Johansen's Cave</b> (below flowstone)	Late Pleistocene fauna	Guano Mining	<i>Macroderma</i>	<5%
<b>Johansen's Cave</b> (upper chamber)	New species of Wombat	Guano Mining	N/A	<1%
<b>Colloseum Chamber</b>	Late Pleistocene fauna  High concentration of bone	Tourism	Owl (? <i>Tyto</i> sp.)	<10%
<b>Honey Moon Chamber</b>	Late Pleistocene-Holocene fauna	Guano Mining	N/A	<10%
<b>Icicle Chamber</b>	Late Pleistocene-Holocene fauna	Tourism (cement floors)	Owl (? <i>Tyto</i> sp.)	<20%

**Table 1-2. Unconsolidated sediments investigated during this study.**



**Figure 1-21. Excavation of unconsolidated cave sediments at Colloseum Chamber, Olsen's Cave, Capricorn Caves Tourist Park.**

**Stockpiles (sediments removed during mining operations available for Scientific Study) (Fig. 1-22).**

Collecting from fossiliferous stockpiles is a very productive way of returning large numbers of specimens for taxonomic work and research. Many eyes pick over the stockpiles after periods of rain which tend to expose fossil bones and teeth. Large groups of people have been involved in this process, including two



Open Day events (August 2006 and September 2008) during which more than 3000 visitors assisted collection of material for scientific study.



**Figure 1-22. Mt Etna Fossils Open Day, Aug 2006.**

#### 1.6.2 Processing Methods

##### **Sieving (Fig. 1-23)**

Sieving of sediments was undertaken using three different mesh sizes: 10mm, 5mm and 1mm meshes. Sieving of unconsolidated sediment was either through wet or dry sieving depending on the situation available at the time. The majority of material collected underwent wet sieving using large water tubs and 50cm diameter metal sieves. Larger sieving benches were erected to process greater quantities of the stockpiled sediment.



**Figure 1-23. Sieving of fossiliferous sediment. A. Large-scale wet sieving of mullock heaps. B. Small-scale wet sieving of cave sediments.**

#### **Acid Etching (Fig. 1-24)**

Lithified bone-bearing rocks were transported back to the Queensland Museum where they were processed using dilute (c. 10%) acetic acid.



**Figure 1-24. Acetic Acid Etching of lithified sediments. A. Two-sized acid vats, large vat for bulk processing, small vat for smaller items. B-C. Results of acid-etching process, showing delicate bones etching free of the matrix.**

### **Mechanical Preparation (Fig. 1-25)**

Some specimens preserved in lithified sediments, or with clay adhering to the bone or enamel, were processed using an ARO™ pneumatic air scribe.



**Figure 1-25. Mechanical tools used in fossil preparation.**

## Chapter 2

### 2.1 Ecological succession during the late Cainozoic of central eastern Queensland: extinction of a diverse rainforest community.

### 2.2 Preface

The following chapter is a published work:

Hocknull, S.A. 2005. Ecological succession during the late Cainozoic of central eastern Queensland: extinction of a diverse rainforest community. *Memoirs of the Queensland Museum* **51** (1): 39-122. This paper is a direct copy of what was published in 2005 without any alterations. Since its publication, the taxonomic understandings of some taxa (in particular the bandicoots) recorded herein have been updated. Chapter 4 details these new allocations and includes the addition of several dozen new taxa of frogs, reptiles and mammals, which have come to light in the intervening time.

### 2.3 Abstract

New late Cainozoic faunal assemblages are preliminarily identified and described from central eastern Queensland. Biocorrelation of the sites has determined that the oldest faunal assemblages are Early Pliocene in age, with younger faunas from the Plio-Pleistocene, late Pleistocene and Holocene. Pliocene faunal assemblages are characterised by rainforest-specialist frog, squamate and mammalian taxa. These include new Pliocene records for frogs; *Kyarranus*, *Lechriodus*, *Nyctimystes* and microhylids, squamates; *Cyclodomorphus gerrardii*, a new species of *Tiliqua* and typhlopids, and mammals; *Bohra* sp., *Pseudochirulus* spp., new petaurids and dasyurids, *Dactylopsila*, petauroid *incertae sedis*, *Acrobates*, *Cercartetus*, *Uromys/Melomys*, *Mesembriomys* and *Pogonomys*. Ecological signals derived from the faunal assemblages correlate well with dated palynological records from central eastern and northern Queensland (ODP815, Aquarius Well and Lynch's Crater). Combined Early Pliocene palynological and faunal records strongly indicates a nonseasonal, mesothermal, angiosperm-dominant rainforest with

emergent gymnosperms at Mount Etna. A Plio-Pleistocene seasonal, open ecology indicated by the palynological record is corroborated by fauna from similar-aged sites, although several rainforest taxa persist. Increasing aridity during the late Pleistocene is suggested by a distinctly arid-adapted faunal assemblage in late Pleistocene sites, including eastern-most records of *Tympanocryptis*, *Macrotis lagotis*, *Chaeropus ecaudatus*, *Perameles bougainville*, *Sminthopsis macroura* and *Notomys*. Faunal succession from the Early Pliocene to Holocene is characterised by the extinction of most rainforest groups by the late Pleistocene, being replaced by more xeric-adapted forms. Several of the Early Pliocene taxa show resilience to extinction by remaining, albeit rare, in the late Pleistocene fauna, probably in local refugia. These include *Dendrolagus* sp., a new petauroid, *Thylogale*, *Macroderma gigas*, *Sarcophilus lanarius* and *Thylacinus*. Presence of rainforest murids in the Early Pliocene of Australia significantly predates previous estimates for their dispersal onto mainland Australia.

## 2.4 Introduction

The succession of faunal assemblages during the late Cainozoic of Australia is unknown for large parts of the continent. Where present, the records are extremely patchy when compared with similar-aged faunal records for other continents (e.g. North America (Stirton, 1936); Africa (Bishop et al., 1971); China (Flynn et al., 1991); and Eurasia (Azzaroli et al., 1988)). A majority of the Australian late Cainozoic Local Faunas have either been the focus of long term, low yield, sporadic collecting with little systematic documentation or once-off, large-scale excavations of a single fossil specimen, site or horizon (Rich, 1991). Typical examples of these sites include the Plio-Pleistocene sites of the Darling Downs southeast Queensland, which, for over 150 years have yielded large collections of specimens with little or no field data due to the ad hoc nature of the collecting (Molnar & Kurz, 1997). These specimens are usually collected as single miscellaneous finds from along creek banks and riverbeds and have, until recently, possessed little documentation associated with the specimen. Such specimens are mostly out of stratigraphic context making them basically useless for detailed palaeoecological reconstruction and biostratigraphy.

In contrast, one-off large-scale excavations have either occurred in response to a major find, such as a complete skeleton(s), or the impending destruction of a fossil site by human impact (Archer, 1978; Long & Mackness, 1994). Material recovered from these sites usually possesses good field data, however, very rarely spans the temporal scale needed to document the succession of faunas for a single region over large periods of time.

There have been several attempts to tie together Pliocene and Pleistocene sites in an effort to develop a biochronological and evolutionary framework for the late Cainozoic fossil communities of Australia (Archer & Wade 1976; Lundelius, 1983,

1989; Woodburne et al., 1985; Rich, 1991; Tedford et al., 1992; Tedford, 1994; Archer et al., 1995a; Archer et al., 1999; Dawson et al., 1999).

A review of literature for Australian Plio-Pleistocene faunas show some distinctive trends: 1) The majority of sites determined as Pliocene in age are considered to be from the Early Pliocene (5.2-3.4 Mya); Bluff Downs (Mackness et al., 2000); Chinchilla (Tedford et al., 1992); Rackham's Roost (Archer et al., 1995b): QLD; Curramulka (Pledge, 1992; Tedford, 1994), Tirari Formation (Tedford et al., 1992), Sunlands (Pledge, 1987): SA; Forsyth's Bank (Tedford, 1994); Hamilton (Rich, 1991); Parwan (Tedford, 1994); Boxlea (Tedford, 1994); Coimadai (Turnbull et al., 1992) VIC; Big Sink (Dawson et al., 1999); and Bow (Flannery & Archer, 1984) NSW. These sites include the only radiometrically or magnetostratigraphically dated sites of the Pliocene: Bluff Downs 3.6 Mya; Hamilton 4.5Mya and the Tirari Formation 3.4-3.9Mya. 2) When Early Pliocene faunas are compared with the few identified Late Pliocene sites (3.4-2.0Mya): Dog Rocks in Victoria (Tedford, 1994); Bone Gultch and Fisherman's Cliff in New South Wales (Tedford, 1994); and Quanbun in Western Australia (Flannery, 1984; Rich, 1991), there is a distinct 'modernisation' of the fauna as suggested by Tedford (1994). These faunas possess several extant and extinct genera and species that become dominant during the Pleistocene and are the typical suite of taxa found in the late Pleistocene (Bartholomai, 1977; Archer, 1978; Hope, 1978; McNamara, 1990; Dawson & Augee, 1997; Molnar & Kurz, 1997; Reed & Bourne, 2000). The apparent faunal mixing of plesiomorphic and stratigraphically older taxa with younger, derived taxa, makes biochronology of the Late Pliocene and early Pleistocene difficult via stage-of-evolution criteria. Direct dates are needed to calibrate the timing of faunal changeover from the Pliocene to Pleistocene.

One notable near absence from the Pliocene to Pleistocene record is that of the diverse rainforest communities that distinguished many of the older

Oligo-Miocene faunas of Australia (Archer et al., 1995a; Archer et al., 1999). A palaeoecological succession for the Pliocene through medial Pleistocene of southeastern Australia has been proposed by Tedford (1994). This includes the Early Pliocene Hamilton Fauna (Turnbull & Lundelius, 1970; Flannery, 1992; Rich, 1991; Macphail, 1996), the only representation of a post Early Miocene rainforest community in southern Australia. Additional Pliocene and Pleistocene faunas from southeastern Australia support several rainforest components, however, these accounts are usually interpreted as part of a patchy assemblage and do not dominate the ecological reconstruction (Tedford, 1994; Archer et al., 1999).

Tedford (1994) concluded that the rainforest communities of southeastern Australia are missing by the Late Pliocene. Archer et al. (1995a) reviewed the Tertiary biotic change in Australia and concluded that by the Late Pliocene central Australia was becoming arid, coastal regions were forested and open, and rainforest persisted in northeastern Queensland as refugia. Macphail (1997) showed distinctly drier-adapted flora throughout the Late Pliocene of Australia.

A unique opportunity to access a late Cainozoic terrestrial fossil record from central eastern Queensland has been made possible via a series of open-cut limestone quarries and cavernous systems running along the coast to the north and south of Rockhampton (Fig. 1). Exposures of extensive fossiliferous deposits in stratigraphic context allow for this first account of a faunal succession spanning the Pliocene to Holocene in Queensland, including a distinctive Pliocene-aged rainforest community.

## **2.5 HISTORY OF COLLECTION**

Collection of vertebrate remains from cave and fissure deposits in central eastern Queensland (CEQ) occurred sporadically for over 90 years, but few papers have appeared on fossils collected from these sites (Longman 1921, 1924, 1925a, 1925b;



Hocknull, 2003).

Central eastern Queensland contains several limestone blocks with known karstification. Of these, Marmor and The Caves are the only two areas where vertebrate fossils have been found prior to 2002.

In 1910 G.E. Blundell collected a tooth from Marmor Quarry, South of Rockhampton, which made its way to the British Museum of Natural History (BMNH10257) identified as *Macropus brehus*, now identified as *Palorchestes*.

First vertebrate remains acquired by the Queensland Museum QM were from guano mining in caves on Reserve Holding 272, Limestone Ridge, east of Mount Etna (R444), between 1920-1921. A mandible assigned to *Sarcophilus laniarius* was presented to Heber A. Longman in 1921 by P.H. Ebbott of Mount Etna Fertilisers Ltd (Longman, 1921). Shortly thereafter, Samuel Evans, mine manager of Marmor Quarry, presented several small collections of fossils unearthed during quarrying. In 1924, Longman collected the QM's first representative samples from CEQ; from Olsen's Cave, SE of Mt Etna and Marmor Quarry, publishing the combined material collected from Marmor Quarry (Longman, 1924, 1925a & b). Longman's faunal records from Marmor Quarry included; *Diprotodon australis* (herein ?Zygmaturinae), *Phascalomys* sp. (herein, *Vombatus urinus mitchellii*), *Thylacoleo carnifex* (herein *Thylacoleo* sp.), *Thylacinus spelaeus* (herein *Thylacinus cynocephalus*), *Sarcophilus laniarius*, *Macropus anak* (herein *Macropus titan*), *Phascogale flavipes* (herein *Antechinus* sp. 2), *Petrogale* sp. cf. *P. inornata* (herein *Petrogale* sp.) and *Megalania prisca*. Smaller fauna included snake and rodent remains. Fossils collected from Olsen's Cave remained unpublished.

In 1925 Evans presented a second Marmor Quarry collection to Longman. F.W. Whitehouse collected bones from Johannsens Cave on Limestone Ridge in 1926, during the peak of guano mining. A hiatus of nearly 30 years followed. In 1954 and 1957 two collections of bones were presented to the QM from Marmor Quarry,

by O. Anderson and J.E. Joyce, respectively. Final collections of large pieces of bone-bearing cave breccia were taken from Marmor Quarry in 1964-5 by Bartholomai and Joyce. This breccia is currently being prepared and contains remains of some very large vertebrates, including *Macropus titan*, as well as many smaller-sized species. No collecting has been possible from Marmor Quarry since 1964.

In 1972, Mike Murray donated small surficial collections from Old Timbers, Lion's Den and Johansen's Cave, Mount Etna area.

A second hiatus from the 1970's to mid 1980's occurred when concerns regarding the conservation of several caves on Mount Etna were at their greatest (Bourke, 1970; Vavryn, 1987). Two cave systems, Speaking Tube Cave and Elephant Hole Cave, were under threat from quarrying operations on the W flank of Mt Etna. In 1986, Kerry Williamson & Dianne Vavryn removed two sacks of loose bone and sediment from the floor of Elephant Hole Cave before mining operations broke into the cave. The small collection was sent to the QM later that year.

Mining operations continued on the western ridge of Mount Etna until early 2004. During the initial stages of operation, the two known caves were broken into and cave breccias exposed. A deposit was unearthed in 1992 when breaking into Speaking Tube Cave. Then mine manager M. Barton, with assistance from David Kershaw and Don Keim, kindly donated bone-breccia samples to the QM and kept a stockpile of bone breccia material on the eastern side of Mount Etna on a flat bench below Main Cave (QML1313).

The author, Paul Tierney and members of the Central Queensland Speleological Society, mounted expeditions to Mt Etna in 1998, 2000 and 2001. Several sites were successfully located and collected within the Mt Etna Caves National Park and Mt Etna Limestone Mine.

Extensive fossiliferous deposits on Limestone Ridge were found in 1998 which

included considerably diverse faunas from several distinct ecologies, including rainforest. Twice in 2000, the QM and University of New South Wales systematically collected material from sites on Limestone Ridge and Mt Etna.

In 2001 collections were made from the Mt Etna Limestone Mine, with the discovery of, *inter alia*, faunal assemblages of similar diversity and age to those from Limestone Ridge. Deposits represent a series of cave-fills exposed in cross-section by mining operations. Examination of these units has enabled development of a preliminary chronology of the faunas. Continued fieldwork in 2002 and 2003 increased the number of distinct sites on the mining lease and located a remnant chamber of Speaking Tube Cave. In mid-2002 a limestone at Mount Princhester, 50kms north of Mount Etna, was investigated and small deposits of exposed fossiliferous cave floor sediment collected. Further fieldwork (2003) resulted in discovery of new sites in Olsen's Cave and Karst Glen, SE of the main Mount Etna and Limestone Ridge blocks.

## 2.6 METHODS

**FOSSIL SITES** (Figs. 1-3). Preliminary site geology, including simplified sedimentological descriptions are provided herein. Cave names follow (Shannon, 1970b). Fossil sites are given a QML number (Queensland Museum Locality).

Superpositional and stratigraphic data was collected from all localities with the exception of Marmor Quarry. Data collected included, stratigraphic context, breccia components, bone preservation, tooth preservation, shell preservation and a facies interpretation. Where possible, sampling bias was reduced by collecting and processing equal amounts of material from each site.

**TAXONOMY.** A brief systematic account of the taxa found from each site is tabulated (Table 1-3, Appendix 1) with abbreviated systematic descriptions of relevant taxa given below. A selection of the best-preserved specimens was used to provide the

identifications that follow. All specimens are held at the Queensland Museum, (prefix QMF). Frog osteological nomenclature and taxonomy follows Tyler (1976) and Cogger (2000) respectively. Squamate nomenclature follows; Hutchinson (1992) for scincids, Hutchinson (1997) for pygopodids and gekkonids, Hecht (1975) for varanids, Hocknull (2002) for agamids, Smith (1976) for elapids and Holman (2000) for typhlopids. Squamate taxonomy follows Cogger (2000); crocodylian nomenclature and taxonomy follows Willis (1995); mammalian nomenclature follows Archer (1984) for tooth morphology and Luckett (1993) for tooth positions. Mammalian taxonomy follows Strahan (1995) and Flannery (1994). Fossil mammal taxonomy follows Long et al. (2002). Avian nomenclature follows Gilbert et al. (1981) and taxonomy Lindsey (1992).

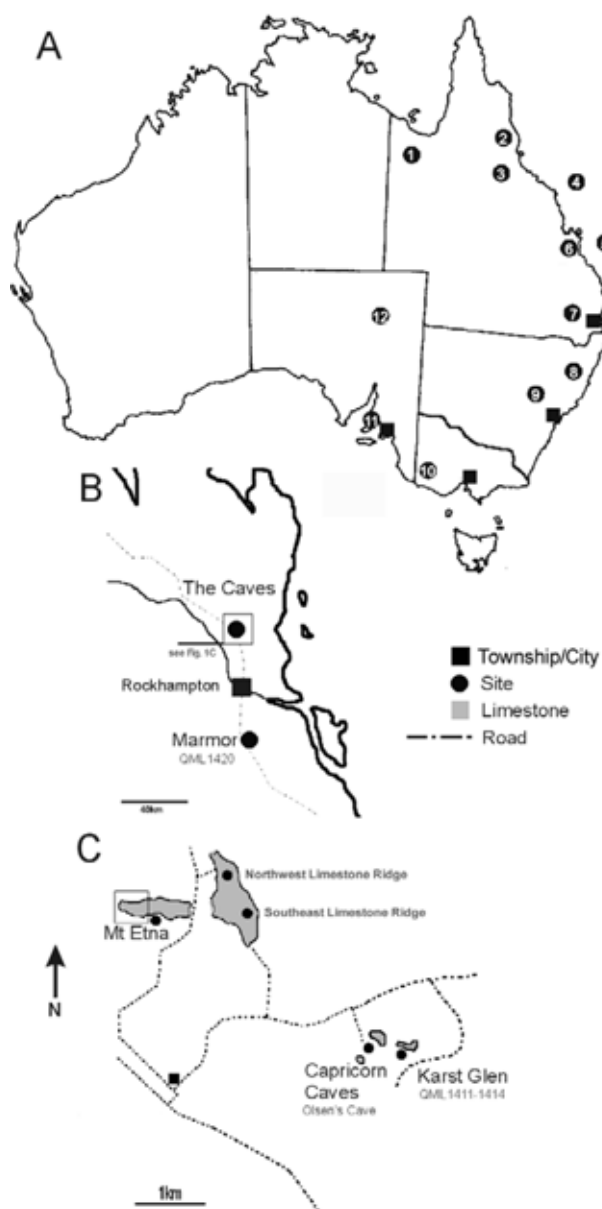


**Figure 2-1. Map of fossil localities. A, Major localities mentioned in text, 1. Riversleigh; 2. Lynch's Crater; 3. Bluff Downs; 4. ODP815, Marion Plateau; 5. Aquarius Well, Capricorn Trough; 6. Mt Etna/Marmor; 7. Chinchilla; 8. Bow; 9. Big Sink, Wellington; 10. Hamilton; 11. Curramulka; 12. Tirari Formation, Lake Eyre. B, 6. expanded. C, The Caves area.**

## 2.7 FAUNAL ASSEMBLAGES (LOCAL FAUNA).

Similarities between site faunas were computed using PAUP (Swofford, 2000) and MacClade software (Maddison & Maddison, 2000), where sites defined as 'taxa' and the taxa as 'characters'. 'Characters' were given the states of either being absent (0) or present (1) (Appendix 1).

Small-sized mammals (smaller than and including *Petrogale*) were chosen for the analysis because they were represented in all of the sites and are least affected by taphonomic bias. The dominant accumulating agent for each site was either via a pit-trap and/or owl/bat roosts. This biases the preservation of large-sized vertebrate taxa, thus they are excluded from the analysis.

A mammal list was constructed to define the present day small mammal fauna for Mount Etna. This list was derived from mammal species surveyed directly at Mount Etna (Horsup et al., 1993; Dwyer, 1970) and those species found in habitat similar to that of present day Mount Etna (semi-evergreen vine thicket), which are also found within the central eastern Queensland region today (Horsup et al., 1993). The present day fauna was fixed in position for the analysis as the 'outgroup'. Present day mammal species not found in the fossil record were excluded from the 'ingroup' analysis because they were simply counted as autapomorphies and uninformative. A dendrogram of relationship was constructed using both PAUP and MacClade parsimony analyses (heuristic search; 1000 replicates).

## 2.8 FAUNAL ASSEMBLAGE AGE.

Biocorrelated taxa were used to provide an estimated date for each of the sites. Palaeoecological signals generated from well-constrained palynological records off the coast of central eastern Queensland (Hekel, 1972; Martin & McMinn, 1993) were correlated with palaeoecological signals generated from site faunas. Direct

dating of one site, QML1312, was possible via Thermal Ionisation Mass Spectrometry (TIMS) Uranium-series dating. Dating was carried out on a *Petrogale* jaw. The date is considered to be a minimum age based on late-stage uptake of Uranium into bone and dentine (Ayliffe & Veeh., 1988; Shen et al., 2001; Zhao et al., 2002).

## 2.9 GEOLOGICAL SETTINGS

The geological history of the limestone blocks containing cave and fissure deposits of the present study have been subject to debate (Kirkgaard et al., 1970; Shannon, 1970a; Willmott et al., 1986; Barker et al., 1997; Simpson et al., 2001). Sites occur in cavern and fissure systems within Early Devonian limestone blocks (Philip & Pedder, 1967) of the Mount Alma Formation (*sensu* Barker et al., 1997). Limestone blocks are irregular in shape and are scattered randomly throughout the formation. The southern extremity of the limestone blocks occurs in the Marmor-Raglan area 50 kms S of Rockhampton. The northern extension of the limestone outcrops as a series of small limestone bluffs at The Caves township (25km N of Rockhampton) and at Princhester (50km N). Sediments from these sites have yielded an enormous and varied vertebrate fossil record.

Palaeontological and structural evidence suggests the limestones are allochthonous blocks within Late Devonian Mount Alma Formation (Barker et al., 1997).



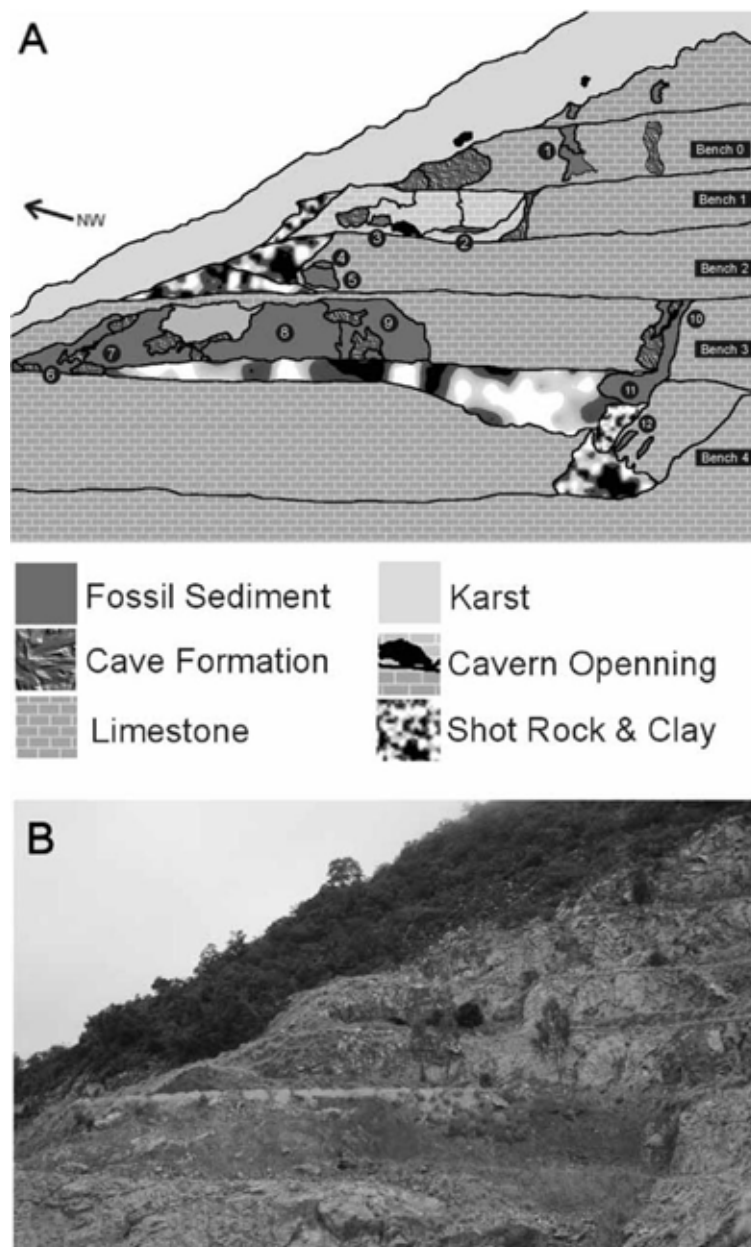


Figure 2-2. Fossil localities on the western benches of Mount Etna Limestone Mine. 1. QML1419; 2. QML 1313, 3. QML1383, 4. QML1310 Unit 1, 5. QML1310 Unit 2, 6. QML1311 A/B, 7. QML1311 C/D, 8. QML1311 F, 9. QML1311 H, 10. QML1398U, 11. QML1384L, 12. QML1385.

The structural history of these limestone blocks which includes their distance and position from one another, irregular bedding planes, faulting, and complex joint systems, has had a direct influence on the sedimentology of the varying vertebrate fossil deposits found within them (Willmott et al., 1986). Structural history has also influenced the terrestrial communities occupying the limestone (caverns and surrounds) through the past and in the present. Modern ecologies on these limestones strongly reflect this influence because most of the bluffs act as present day refugia for flora and fauna (Horsup et al., 1993).

## **2.10 SITE LIST**

### **Mount Etna Limestone Mine and National Park**

#### *Speaking Tube Cave System*

Bench 0, QML1419\*

Bench 1, QML1313 (=QML1313 & QML1288)\*\* Bench 1, QML1383\*

Bench 2, QML1310 Unit 1 Bench 2, QML1310 Unit 2\* Bench 3,

QML1311 Unit A\* Bench 3, QML1311 Unit B\* Bench 3, QML1311

Unit C\*\* Bench 3, QML1311 Unit D\*\* Bench 3, QML1311 Unit F\*

Bench 3, QML1311 Unit H\*\*

#### *Elephant Hole Cave System*

Williamson & Vavym Collection, QML1312\*\*

Bench 3, QML1384 Upper Unit\*\* Bench 3, QML1384 Lower Unit\*\*

Bench 4, QML1385\*\*

### **Northwest Limestone Ridge**

*Johansen 's Cave System* QML1314, Guano deposit\*\*

QML368, Flowstone (False Floor) Unit\*\* Southeast Limestone Ridge

### *Mini Cave System*

Mini Cave Chamber Deposit, QML1284\*\*

Mini Cave Surface Deposit, QML1284a\*\* Leo's Lunch Site, QML1382\*

### **Olsen's Cave System\*\***

Karst Glen System

KG3 Surface Deposits, QML1411-1414\*

### **Marmor Quarry**

Marmor Bone Breccia collection, QML1420\*\* \* Sites with fauna

\*\* Sites with fauna presented herein

## **2.11 MOUNT ETNA LIMESTONE MINE AND NATIONAL PARK**

Approximately 40% of Mount Etna is massive recrystallised limestone with the remainder a combination of faulted sedimentary and volcanogenic units of the Mount Alma Formation (Shannon, 1970a; Barker et al., 1997). Limestone on Mount Etna dips steeply to the SW, with major joints oriented along a NW axis. Joints are predominantly vertical and control cave development (Shannon, 1970b). Phreatic enlargement has occurred along these vertical planes producing deep chambers with sculptured phreatic pendants. Vadose cave development is marked by extensive speleothem formation and cave entrance development. Bone breccias and cemented cave floors are common throughout, occurring within functional cave systems or exposed on weathered and collapsed dolines. Two major cave systems on Mount Etna are the focus of the present study; Speaking Tube and Elephant Hole Cave systems.

Speaking Tube Cave system occupies two major joint controlled rifts running down the mountain in a NW-SE direction. Phreatic chambers developed at depth are linked to the surface by long solution pipes. Elephant Hole Cave system is a third joint-controlled rift to the SE of the Speaking Tube Cave system. It is also linked to the surface by large solution pipes. A geochronological summary of sites found on the western benches of Mount Etna Limestone Mine is provided in Fig. 3.

### **Speaking Tube Cave System**

SPEAKING TUBE CAVE: E7. *“This cave has nine entrances at middle to highest levels on the West flank of Mt Etna. It is a very complicated active inflow cave with three active sumps.”* (Shannon, 1970b: 25)

It is obvious from the many and varied bone breccias recovered that Speaking Tube Cave system has had a long and complex history. No substantial collections were made from Speaking Tube Cave before it was broken into by mining operations. In 1992, bone breccias were exposed close to surface karst and stockpiled by Pacific Lime Pty Ltd operators. A small sample of these bone breccia blocks was sent to the Queensland Museum marked “Speaking Tube Cave”. In 2000 the stockpile was located on the eastern side of

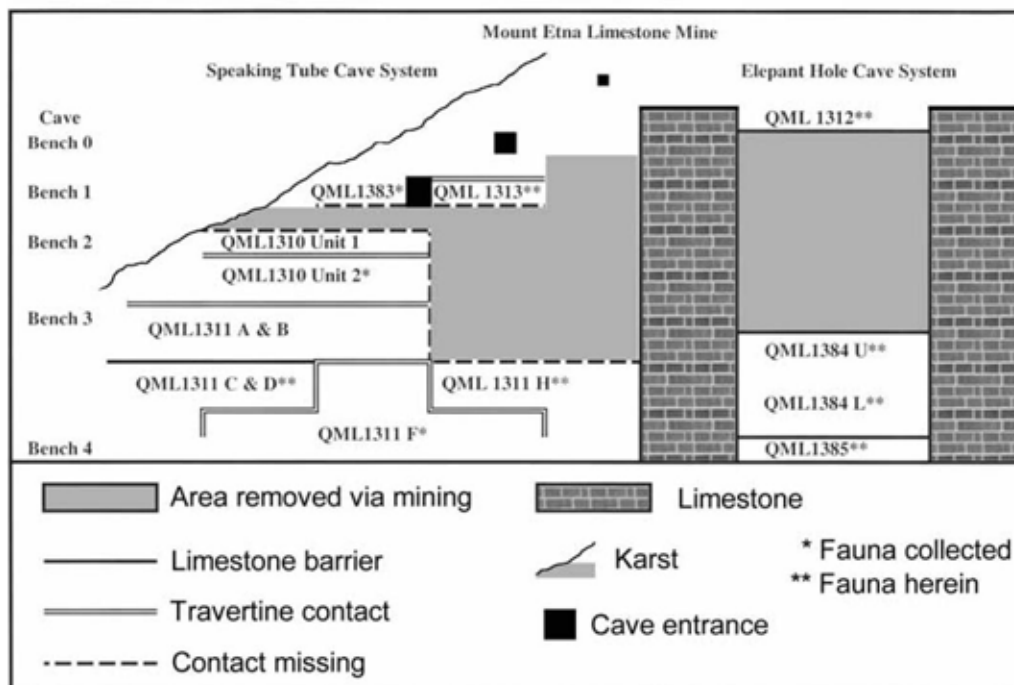


Figure 2-3. Schematic diagram illustrating the relationships between fossil deposits on the western benches of the Mount Etna Limestone Mine, Mount Etna. \* Fauna collected. \*\* Fauna presented herein.

Mount Etna by the QM and collected, given the site name ‘Mat’s Menagerie’ (QML1313). The original location of the bone breccia was unknown until 2002 when equivalent material was found in situ on Bench 1 of the western benches. Five main benches are considered to preserve portions of the Speaking Tube Cave system, including an entrance to the cave through an exposed chamber on Bench 1.

BENCH 0, QML 1419. A thin veneer of limestone covered a solution tube until 2003 when it collapsed and revealed a breccia-filled tube. It was discovered in mid 2003. The solution pipe contains several levels of varying indurated fossiliferous sediment.

BENCH 1, QML1313 (=QML1313 & QML1288). A small amount of bone breccia received from Pacific Lime in 1992 and labeled as ‘Speaking Tube Cave’ (QML1288) was rediscovered by the Queensland Museum as a stockpile on the eastern face of Mount Etna, subsequently named “Mat’s Menagerie Site” (QML1313). The bone breccia originated on the western benches where its exact locality was unknown. Inspection of the Bench 1 cliff line relocated lithologically identical bone breccia adhering to an exposed cave chamber wall. The material follows a cave wall demarcated by cave formations along the middle length of the bench. The breccia runs in a northwest/southeast axis toward an opened chamber. The chamber constitutes a known chamber within Speaking Tube Cave. Bone breccia received by the museum, stockpiled on the eastern face and adhering to the southeast side of the cave wall on Bench 1, western benches, constitutes the same unit.

*Stratigraphic context.* There is no preserved contact of this unit with any of the other deposits on the mountain. The area in which a contact may have occurred has been mined. There are no clasts of other bone breccias within the matrix. The only breccia that shows similarities in sedimentology to QML1313 is QML1311 (Unit A) of Bench 3, which indicates that this unit was very extensive and formed deep within

the system. It is sedimentologically distinct from the only other breccia found on Bench 1 (QML1383), which occurs to the northwest of the open chamber.

*Breccia components.* Distinctly bright yellow to orange coloured, heavily cemented containing large angular clasts of parent limestone, flowstone and smaller clasts of allochthonous rock; abundant bone, teeth and skulls of variable sizes; snails common; large calcite vugs. Small clasts of red to brown clay; pisolites of ironoxide and calcite; bedding chaotic.

*Bone preservation.* Articulated and semi-associated skeletal elements; well-preserved material with no apparent dominant bone orientation; calcite growth within bone vacuities; bones variable in size, from large limb bones (10-15cm) to grain-sized bone fragments.

*Tooth preservation.* Teeth usually in jaws.

*Shell preservation.* Shells complete and isolated. *Facies Interpretation.* Abundant large angular clasts, articulated and semi-articulated large-sized bones, large complete shells and no dominant bedding or clasts indicates an entrance facies talus and scree.

BENCH 1, QML1383. Located to the northwest of the open chamber, QML1383 is a large fossiliferous unit.

*Stratigraphic context.* Sedimentologically this unit is similar to QML1311 (Unit B) of Bench 3 and QML1310 (Unit 2) of Bench 2. QML1310 (Unit 1) of Bench 2 divides the contact between QML1383 and QML1310 (Unit 2) so it is suggested here that QML1383 is stratigraphically younger than both QML1310 and QML1311. The site has an analogous depositional facies.

*Breccia components.* Dark red to pink clay, heavily cemented with minor clasts of decalcified limestone, allochthonous sediments and pisolites; abundant bones, teeth and shell.

*Bone preservation.* Bones fragmentary and small; no distinct large bone orientation; smaller bone fragments occur in fine lenses which are horizontally bedded.



*Tooth preservation.* Usually isolated and well preserved.

*Shell preservation.* Abundant in small lenses.

*Facies Interpretation.* Lack of large angular clasts, large bones and the lack of distinct large bone orientation indicates a depositional facies away from an entrance and having not been subject to significant water transport. Abundance of small fragments of bones and isolated teeth indicates a possible predator accumulation. Thin irregular lenses of material suggest that accumulation occurred from slumping of upper roost deposits, probably *Macroderma*. The deposit seems to occur within an old aven when viewed in sectional profile.

BENCH 2, QML1310. Bench 2 lacks large deposits of breccia, with the two units described here only found on a small pinnacle left from mining operations.

**Unit 1; Stratigraphic context.** Unit 1 is younger than Unit 2 with a distinct cave floor formation between the two horizons.

*Breccia components.* Mottled red/grey horizons; lacks bone and teeth; small clasts of allochthonous sediments; heavily cemented.

*Bone, tooth and shell preservation.* Rare to nil.

*Facies Interpretation.* Lack of fossil material and major clasts indicates a non-entrance facies. The mottling of the rock indicates the presence of dense rootlets and thus the base of a chamber.

**Unit 2; Stratigraphic context.** Occurs below and is older than Unit 1. Several thick bands of flowstone occur through the top of this unit, demarcating different levels of formation. Toward the base there is a considerable reduction in flowstone. The base of Unit 2 appears to be very similar in depositional style to QML1311 (Unit B) of Bench 3 and is interpreted as the top of this unit.

*Breccia components.* Flowstone-dominated light red coloured, heavily cemented bone breccia; flowstones irregular in shape and domed at the middle of the exposure; bones abundant and small; shell abundant in small lenses, associated with flowstones; small, grain-sized clasts of allochthonous sediment.

*Bone preservation.* Disarticulated, disassociation within the accumulation; large numbers of bones from small animals, usually broken into grain-sized particles.

*Tooth preservation.* Isolated teeth, well preserved, no rounding.

*Shell preservation.* Small snail shells, in bands usually associated with flowstone unit.

*Facies Interpretation.* The mass of banded flowstones at the top of QML1310 Unit 2 indicates a major increase in speleothem genesis over that found in QML1311, Unit B. It is unknown whether this was a rapid phase of precipitation or it was a gradual increase over time. The reason for this is because the contact between QML1311, Unit B and the base of QML1310 Unit 2 has been removed by mining. The presence of the flowstones and a domed lamination indicates a series of cave floors, probably in the shape of a sediment cone. Absence of large angular clasts and large bones indicates a chamber facies. The sediment cone was probably produced at the base of a bat roost because there are no additional chambers above the deposit that could have acted as a sump.

### BENCH 3, QML1311

**Unit A; Stratigraphic context.** Unit A in contact with Unit B. Unit A formed before Unit B. Unit A is considered lithologically equivalent to QML1313 sediment although found deeper within the system. This is reflected in the breccia components, bone preservation, greater bedding and speleothem genesis of Unit A sediments.

*Breccia components.* Yellow, grey and pink coloured clay; heavily cemented; massive flowstones and travertine throughout (ranging from 5-20cm thick); cave formations preserved within breccias. Large clasts of allochthonous sediments and semi-rounded parent limestone. Drusy calcite vugs and well preserved bone.

*Bone preservation.* A semi-articulated, associated accumulation with some patches of sorted large bone; limb bones well preserved with most elements complete; small bones in apparent association; bone vacuities in filled with calcite.

*Tooth preservation.* Teeth usually found in complete or near complete jaws.

*Shell preservation.* Snails abundant, isolated, and well preserved.

*Facies Interpretation.* Unit A is considered a talus accumulation below the entrance facies of QML1313.

**Unit B; Stratigraphic context.** Unit B occurs in two areas along Bench 3. Unit B contacts Unit A on its north-western extremity and occurs above Unit C/D toward the center of Bench 3. Unit B is divided from Unit C/D by a massive limestone wall, varying from 5-10m thick. Unit B is considered so close in lithology to the sediment at the base of QML1310 Unit 2, Bench 2, that it is considered here to have had a conformable contact between these two units.

*Breccia components.* Light red heavily cemented clay; numerous clasts of decalcified parent limestone, cave wall travertine and allochthonous sediments, including gravel. Cave formation dominates the clasts, followed by allochthonous sediment and parent limestone.

Bone and tooth fragments abundant; small drusy calcite vugs; isolated iron-oxide pisolites.

*Bone preservation.* Disarticulated accumulation with some sorting of small bone elements. Sorting is localised and not common; large bones are rare; small bone well preserved with teeth in jaws. Long bones badly preserved, mostly broken at both proximal and distal ends; numerous grain-sized bone particles occur in irregularly graded lenses. Calcite growth within bone vacuities.

*Tooth preservation.* Well preserved tooth rows.

*Shell preservation.* Shell abundant and usually associated with bone sorting.

*Facies Interpretation.* Unit B is considered the base of a talus from a well-developed sediment cone. The base being Unit B and the top being QML1310 Unit 2 Bench 2. The lack of large bone accumulations and the abundance of small bone fragments suggest a similar predator accumulation as to QML1310 Unit 2 Bench 2 within an aven chamber.

**Unit C; Stratigraphic context.** Unit C grades into Unit D but with less mottling. Unit C and D are considered equivalent in age. Unit C is separated from Unit A & B by a

large limestone wall, varying from 5-10m thick. Units C and D unconformably overlies Unit F on a decalcified and eroded travertine surface formed on Unit F and included as clasts in Units C & D. Units C and D are thus considered to be younger than Unit F.

*Breccia components.* Red/yellow/grey clay, moderately cemented; drusy calcite vugs formed within rootlet vacuities; isolated iron-oxide pisolites; small clasts of decalcified parent limestone and allochthonous sediments. Isolated clasts of broken and transported travertine; large bones, isolated teeth and numerous complete small bones; large bones fractured and exploded by clay matrix; no travertine formation other than calcite formation between Unit C and F. Small clasts of Unit F at the southeast extremity of unit C.

*Bone preservation.* Disarticulated accumulation with little bone sorting; large long bones missing proximal and distal ends; vertebrae missing processes. Large bones have been transported some distance. Small bones variably preserved; complete elements to grain-sized particles; bone vacuities filled with clay.

*Tooth preservation.* Large teeth usually preserved within the jaw. Small teeth usually isolated and associated with edentulous jaws.

*Shell preservation.* Rare to absent.

*Facies Interpretation.* Unit C is considered to be a deep chamber deposit based on the lack of large angular inclusions and large well-preserved, semi articulated or associated bone. There are no indications that this deposit is a predator accumulation. The lack of sorting of clasts and no distinct bedding planes indicate that stream and channel action was not the main mode of transport and deposition here. The presence of large bones and very few well-preserved snails indicates a deposit where the larger elements have been transported from an entrance facies into a lower chamber probably via extensive slumping, requiring little water transport.

**Unit D; Stratigraphic context.** Unit D is a mottled breccia very close in lithology to Unit C and is considered equivalent in age. Unit D conformably grades into Unit C

without any distinctive demarcation.

*Breccia components.* Mottled red/yellow/grey clay, loosely cemented; drusy calcite vugs formed within rootlet vacuities. Unit D possesses distinctive mottling due to penetration of the clay load by rootlets. Isolated iron-oxide pisolites; small clasts of decalcified parent limestone and allochthonous sediments; rare large bones and isolated teeth; no travertine formation other than calcite formation between Unit C/D and F.

*Bone preservation.* Disarticulation accumulation with little bone sorting; large long bones missing proximal and distal ends. Bone vacuities filled with clay.

*Tooth preservation.* Small teeth usually isolated and associated with edentulous jaws.

*Shell preservation.* Rare to absent.

*Facies Interpretation.* As for Unit C but with a greater influence from rootlets altering the general colouration and texture of the sediments.

**Unit F; Stratigraphic context.** Unit F is located between Units C & D and Unit H. There are contacts between Unit F and Unit C on the northwest flank, and with Unit H on the southeast flank. These contacts are demarcated by cave wall formation in the form of travertine and decalcified, detached flowstones with Units C, D and H. All three Units have been secondarily capped by a more recent travertine. Based on the contact zone, Unit F formed before Units C, D and H.

*Breccia components.* Bright yellow sandy, clay-rich; cemented; travertine distinct and demarcates contacts with younger sediment; little internal flowstone formation. Interspersed small, rootlet-shaped drusy calcite vugs; minor clasts (0.5-2cm) of decalcified parent limestone with chalky texture. Small patches of highly fragmented bones and teeth.

*Bone preservation.* Disarticulated accumulation with no bedding or sorting; bones small and hollow in cross section; no large elements, mostly postcranial.

*Tooth preservation.* Mostly fragmented rodent incisors.

*Shell preservation.* Shell absent.

*Facies Interpretation.* The sediment is unlike any other found in the study area. The paucity of bone, internal speleothem genesis and clasts indicates a possibly dry accumulation. Further investigation of this deposit is needed. The lack of fossil specimens may also indicate a relatively old age for the deposit, before there was major connection of the solution pipes with the surface and well before karstification.

**Unit H; Stratigraphic context.** Unit H contacts the travertine wall enclosing Unit F and is younger. Unit H has formed at a similar depth to Units C, D and QML1384 Lower Unit, however, their superpositional relationships are unknown, possibly contemporaneous.

*Breccia components.* Red to dark brown clay, heavily compacted but not heavily cemented; numerous small clasts of altered serpentinite, clasts of decalcified parent limestone and iron-oxide pisolites; large and small bone fragments; isolated teeth and jaws. Minor travertine inclusions from Unit F.

*Bone preservation.* Dissarticulated accumulation with no distinct bedding or sorting of elements. Tightly packed bone accumulations; large bones are commonly long bones. Long bones usually with broken proximal and distal ends; shafts fractured and exploded by clay matrix; vertebrae usually missing transverse processes and neural spines; metatarsals commonly missing one distal end; small bones include variously fragmented skeletal elements; usually preserving epiphyses. Ranging from complete bone elements to grain-sized bone particles.

*Tooth preservation.* Mostly edentulous jaws and numerous isolated teeth. Large (e.g. large macropodid) teeth usually remain within the jaw. Teeth variably preserved with tooth roots.

*Shell preservation.* Nil.

*Facies Interpretation.* Absence of angular limestone blocks and dipping beds indicates a non-entrance facies. The lack of cementation indicates a period of saturation of the sediment or the inclusion of humic acids into the cavern, both similarly retarding the precipitation of calcite within the sediment, however, geochemical

analyses will be needed to clarify this.

### **Elephant Hole Cave System**

ELEPHANT HOLE CAVE: E8. “*On the West flank of Mt Etna. The cave [Elephant Hole Cave] has three middle level entrances, all containing vertical pitches. An active inflow cave. From the main entrance a talus slope leads to the drop into two large caverns. ...The cave has little decoration, but has some breccia deposits which include bone material.*” Shannon (1970b: 25)

**Williamson & Vavryn Collection, QML1312;** a sample of unconsolidated floor sediment from an earth floor within Elephant Hole Cave in 1986.

*Stratigraphic context.* Of unknown stratigraphic context. TIMS U-series date based on *Petrogale* dentition (minimum age)  $149,000 \pm 611$  ybp. Considered to be young based on the preservation state of the material. Younger than QML 13 84 and QML1385 deposits.

*Breccia components.* Sediment and bone that was collected is derived from a loosely compacted cave floor (Vavryn & Williamson pers coms.) which is almost entirely made-up of fine, dark to light brown or red clay. Sediment breaks down easily in water and contains small, angular fragments of cave wall and roof, which show some signs of weathering and decalcification. Bone appears to be subfossil, with minimal bone discolouration, except for black manganese-oxide surface stains.

*Bone preservation.* Disarticulated, semi associated; bone small to medium-sized (<100mm in length) with portions of larger limb elements; very well preserved with most of the long bones retaining epiphyses and skull bones intact. Bone cavities free of calcite and sediment.

*Tooth preservation.* Most mandibles and maxillae retain teeth and most molar rows.

*Shell preservation.* Fragmentary and rare.

*Facies Interpretation.* Abundance of small bones of mammals, lizards, frogs and passerine birds suggests that a fraction of the deposit be derived from a predator accumulation. Some gnaw marks have been found and identified as rodent



gnawing. Present in the deposit are owl (*Tyto* sp.) and ghost bat (*Macroderma gigas*) remains indicating that typical cave dwelling predators were present in Elephant Hole Cave during

deposition. Well-preserved and semi-associated large vertebrate remains attaining a maximum size of the macropodine *Petrogale*, indicate an accumulation close to an entrance.

No orientations of the bones were taken with the collection so it is unclear whether water was involved in the accumulation. No speleothem or cementing has occurred, suggesting the sediment was not water transported. Some sediment clods remained within the deposit and were not broken down during collection, transport or preparation. These compacted sediment clods are thick with bones and teeth with their orientations relatively random. The lack of water transport, compaction and calcite precipitation indicates a very dry accumulation close to an entrance, with input from a predator's roost.

**BENCH 3, QML1384 UPPER UNIT.** In 2000 whilst collecting on the western benches of Mount Etna Mine, a site (QML 1384U) was discovered with a similar sedimentology to that seen in the material recovered from Elephant Hole Cave by Williamson & Vavym in 1986 (QML1312). Based on the position of the deposit on the mine site, it would have occupied a deep chamber within the Elephant Hole Cave system.

*Stratigraphic context.* QML 1384 is considered to be older than QML1312 because it is found much deeper and is more compacted and lightly cemented. There is no distinct reworking of bone material and the bone has a greater degree of alteration than the bone from QML1312.

*Breccia components.* Cave earth compacted, only lightly cemented, breaking down easily in weak acidic solution. Sediment possesses a strikingly similar colour and texture to QML1312, including an abundance of brown to red clay, angular cave wall and roof inclusions.

*Bone preservation.* Bones disarticulated; subfossil preservation; similar in preservation to QML1312, especially by the presence of the black manganese oxide staining. The completeness of cranial and postcranial bones also indicates close similarities because no other site at Mt Etna, other than the Elephant Hole Cave collection, has such a high density of perfectly preserved elements. Bones in filled with clay.

*Tooth preservation.* Complete jaws with tooth rows preserved.

*Shell preservation.* Rare and fragmentary.

*Facies Interpretation.* The chambers of Elephant Hole Cave were large and vertical. It is therefore considered that QML1384U is simply a lower and older extension of the entrance and predator accumulation identified as the QML1312 deposit.

#### BENCH 3, QML1384 LOWER UNIT.

*Stratigraphic Context.* QML1384L is lithologically similar to QML1384U. There is no distinct contrast between the upper and lower unit except for a darker colour of the clay in the Lower Unit. The Lower Unit is considered to be continuous with and therefore older than the sediments collected from the upper unit.

*Breccia components.* Sediment unconsolidated, extremely clay-rich, dark brown in colour. The clay is very greasy in texture; isolated allochthonous cobbles and gravel are dispersed throughout the clay load. Bone rare; little flowstone and few autochthonous clasts are present in the sediment.

*Bone preservation.* Bone rare and fragmented, where present relatively unaltered, possessing simple manganese staining. Larger bone vacuities free of clay. Similar in preservation to the upper unit, except for greater manganese staining.

*Tooth preservation.* Rare and isolated.

*Facies interpretation.* Lower Unit is simply an extension of a large vertically oriented solution pipe which fed into a large chamber housing phreatic pendants. The lack of distinctive vadose developed flowstones within the sediment suggest that, like

QML1311 Units C, D and H, the lower unit was accumulating within a water-saturated chamber, or one with sufficient acidity to prevent carbonate precipitation. This would also explain the lack of carbonate to indurate the clay sediment. The sediment looked to continue deeper within the system and certainly down to the level of Bench 4 (QML1385) deposit. This lower unit may contact QML1385 and be a source for the bone accumulations in it.

**BENCH 4, QML 1385.** In 2002 a small deposit of bones was discovered further down the mine site benches, in a direct line below QML1384L. The deposit is the lowest found so far on Mount Etna. This deposit is unlike any found on Mount Etna, however, it occurs closest to the base of the QML1384L. It is here considered to be part of the Elephant Hole Cave system, however, it may be independent of all accumulations on the mountain. A large wedge of limestone covers any potential connection between QML1384L and QML 1385 below it.

*Stratigraphic context.* Although the relationship of the deposit to the Elephant Hole Cave system is unclear, it is considered older than both QML1312 and QML1384 based primarily on the preservation of the bones, cementing of the breccia and great depth on the mountain.

*Breccia components.* The bone breccia contains deep red coloured clays, well sorted, well rounded pebbles and gravel and abundant fossilised bones and teeth. The breccia is heavily cemented but lacks distinctive speleothem genesis. Clasts of gravels are distinctly allochthonous with few parent limestone fragments.

*Bone preservation.* Disarticulated, slight reworking and rounding of dark-coloured bones. The majority of the bones are discoloured to some degree with crystallisation occurring within the bone. Long bones are usually found in parallel orientations but are not associated.

*Tooth preservation.* Variably preserved either within jaws, isolated and complete, or isolated and tumbled with smoothed edges.

*Shell preservation.* Rare.

*Facies Interpretation.* QML1385 is a complex mixture of accumulation processes. Bones and teeth are variably preserved and show differing degrees of preservation and alteration. A small portion of the bones and teeth are tumbled and rounded indicating stream or channel deposition. Many bones, especially frog ilia and mammal and bird limb bones show signs of predation, including bite marks (bat) and semi digestion (owl). The site is interpreted as a mixed deposit of material accumulated by reworking and water transportation of a predator accumulation. The material was then washed deep within the mountain to form well-sorted stream gravel deposits. Lack of travertine clasts or travertine development may indicate the deposition into a water-filled pool or a recently opened chamber.

## **2.12 LIMESTONE RIDGE**

Limestone Ridge occurs directly to the east and southeast of Mount Etna (Fig. 1, C) and may have been connected to Mt Etna in the past. The ridge is bisected by a large siltstone/mudstone unit of the Mount Alma Formation, therefore, the cave systems presented herein are best described in two sections, northwest Limestone Ridge and southeast Limestone Ridge. The limestone blocks do not dip to the southeast as seen at Mount Etna and overall cave system development is along a horizontal joint axis.

Within a horizontally controlled joint system phreatic enlargement has developed long, ‘ballroom’ shaped and sized chambers. The presence of massive speleothems illustrates a long vadose history. Some horizontal development of the caves has been due to the influence of intrusive sills of volcanogenic material, such as Ball Room Cave J8 and Lost Paradise Cave J7 (Shannon, 1970a).

## **2.13 NORTHWEST LIMESTONE RIDGE**

### **Johansen's cave system**

JOHANSEN'S CAVE J1 AND J2. "*This is at present the largest cave in the Mt Etna district*" Shannon (1970b: 29).

Johannsens Cave is characterised by its abundance of bat guano. In 1919 guano mining began in Johansen's Cave. A discovery by P.H. Ebbott of a mandible of *Sarcophilus lanarius* (Longman, 1921) from within a guano matrix may be attributed to guano mining in Johansen's or Bee Cave. In 1926 Whitehouse recovered a small surface collection of bones from the guano in Johansen's Cave, all being from modern local species. In 1972 Mike Murray collected kangaroo mandibles, an edentulous *Sarcophilus harrisii* mandible and a crocodilian premaxilla from Lower Johansen's Cave. The mandibles were obviously from guano accumulations as guano still adheres to the bone. A note on the specimen label for the crocodile premaxilla (QMF 17071) reads "In flowstone bed, above Tas. Devil level, Lower Johansen's Cave."

In 2002 the author visited Johansen's Cave, in particular Lower Johansen's Cave (J2), to relocate the flowstone bed with a guano unit below it. A distinctive thick (10-30cm) flowstone bed occurs along a small section of the back chamber with a large unit of mined guano below it. Preliminary inspection of the chamber located large vertebrate bones, including macropod metatarsals within the flowstone and similar-sized but differently preserved bone in the guano. The flowstone bed forms a false floor across a small portion of the chamber with a secondary filling of guano.

QML1314, Guano bed below flowstone *Stratigraphic context.* Guano occurs throughout the cave and has an amorphous sedimentological structure. It is considered younger than the flowstone unit because of the false floor nature of the flowstone.

*Breccia component.* Fine-grained dark brown to black guano, heavily organic; large and small bones of variable size and parent limestone fragments.

*Bone preservation.* Disarticulated, well preserved bone with long bones preserving epiphyses.

*Tooth preservation.* Variably preserved jaws with teeth preserved or isolated.

*Snail preservation.* Abundant, complete snail shells. Colour patterning present.

*Facies Interpretation.* A guano deposit with minor stream and channel movement within a large chamber.

QML368, FLOWSTONE (FALSE FLOOR) UNIT *Stratigraphic context.* A distinct false floor developed over an older sediment, which has been subsequently eroded leaving the false floor. Guano fills within a vacuity under the false floor. Thus, the flowstone unit is considered to be older than the guano beneath it.

*Breccia components.* Fine-grained yellow to brown clays with very well preserved, heavily cemented travertine. Numerous large bones and land snails occur within these flowstone bands.

*Bone preservation.* Disarticulated. Well preserved bones with most epiphyses preserved.

*Facies Interpretation.* Flowstone false floor. *Surface collection:* no stratigraphic context.

SHUFFLE CAVE NO E NO: bone collection QML371

OLDER TIMBERS CAVE J31: surface collection QML372 & 1315

## 2.14 SOUTHEAST LIMESTONE RIDGE

### Mini cave system

MINI CAVE J12. “*Small horizontal ... active inflow cave. The single entrance leads to a tunnel cavern 60 feet long then a short crawl to an end [second] chamber*”

(Shannon, 1970b: 32).

At the end of the first chamber is a small shelf of heavily cemented bone breccia. The existing breccia is the remainder of a more substantial deposit that would have filled at

least 40% of the first chamber.

QML1284, MINI CAVE CHAMBER BRECCIA, *Stratigraphic context*. The chamber breccia occurs lower on Limestone Ridge than both surface breccias (QML1284a and QML1382), however, they are considered to be contemporaneous deposits. QML1284a illustrates an entrance facies, which would be expected to occur above the QML1284 section, feeding material into the chamber.

*Breccia components*. Consists of fine-grained yellow to red coloured clay, bedded travertine, small angular clasts of parent limestone, allochthonous siltstone and serpentinite, small black goethitic and lighter coloured carbonate pisolites. The oxide pisolites are considered to be allochthonous, the carbonate pisolites autochthonous (cave pearls). The sediments are layered with speleothem, producing distinct sections throughout the deposit. These layers are continuous throughout the deposit and are interpreted as a series of sump deposits flowing into permanent rim pools.

*Bone preservation*. An articulated assemblage of small cave dwelling species such as snakes, frogs and bats. Bones well preserved in a halo of carbonate. Bones vary in size from tiny osteoderms to pockets of larger bone up to 100mm in size. All skeletal elements are well preserved, even the minute osteoderms from skinks. Little evidence of bone gnawing or digestion from predators.

*Tooth preservation*. Teeth usually in jaws and well preserved tooth rows, mostly molar rows and isolated incisors. Majority of teeth are from small taxa, however, isolated teeth from large-sized taxa occur randomly in the lenses.

*Shell preservation*. Snail shells well preserved, usually complete shells of varying sizes.

*Facies Interpretation*. Presence of distinct rim pool formations (basin-shaped travertine, abundant carbonate pisolites, and sorting of sediment matrix) indicates the deposit was at the base of a chamber being fed from above. The entrance is thought to have been higher than the current Mini Cave entrance and QML1284a is in a suitable position to be this entrance facies. The abundance of articulated or associated specimens



indicates that many vertebrates including frogs, bats, rodents and snakes inhabited the chamber.

**QML1284A, ABOVE MINI CAVE.** Located above and to the northwest of the Mini Cave entrance is a heavily weathered bone breccia, which is interpreted as the upper level of the Mini Cave System, and an old cave chamber collapse.

*Stratigraphic context.* QML1284a deposit sits above QML1284 sediments but is considered to be relatively contemporaneous as it is believed that QML1284a is the entrance facies for the

same series of accumulations making up the deeper rim pool deposits of QML1284. QML1382 is a lateral extension of the QML1284a entrance facies, therefore, is of similar age also.

*Breccia components.* Pink-grey coloured clay, heavily cemented with thinly bedded travertine throughout. Irregular bedding within breccia blocks. Large clasts of parent limestone, with smaller clasts of oxide and carbonate pisolites, allochthonous gravels and large calcite vugs.

*Bone preservation.* Well preserved, complete bones and associated specimens. Bones showing predation and partial digestion. Snail shells complete and associated with travertine.

*Tooth preservation.* Teeth usually in jaws and well preserved.

*Shell preservation.* Well preserved, complete.

*Facies Interpretation.* Large angular limestone clasts and irregular bedding suggests a facies close to an entrance. The presence of a distinct predator accumulation and a small contribution of larger vertebrate remains suggests a chamber was close to an entrance, which was big enough to support a bat or owl's roost.

**QML1382, LEO'S LUNCH SITE.** Located to the north of QML1284a, QML1382 is interpreted as a lateral extension of the QML1284a collapse line.

*Breccia components.* A grey-pink, heavily cemented bone breccia with large clasts of parent limestone, smaller clasts of flowstone, pisolites and allochthonous sediment.

*Bone preservation.* Small grain-sized fragments, isolated limbs and vertebrae within flowstones.

*Tooth preservation.* Isolated teeth.

*Shell preservation.* Snail shells associated with flowstone.

*Facies Interpretation.* A lateral extension of the entrance facies of QML1284a, with greater flowstone development and irregular bone accumulations.

*Surface collections:* no stratigraphic context.

LOST PARADISE CAVE J7: bone collection, stream channel first chamber.

BALL ROOM CAVE J8: bone collection, stream channel southern end of main chamber.

## 2.15 OLSEN'S CAVE SYSTEM

### **Olsen's cave.**

*"Essentially only one cave system of sixteen interconnected caverns, usually joint-controlled and of varying dimensions..."* Shannon (1970b: 36).

*Stratigraphic context.* Unknown, however, bone preservation suggests relatively young deposit.

*Breccia components.* Dark brown coloured clay sediment. Loosely consolidated and cemented cave floor sediment. No major clasts present.

*Bone preservation.* A mass of disarticulated, unsorted, tightly compacted fragmentary bone.

*Tooth preservation.* Jaws with teeth and most molar rows. Exclusively small vertebrates.

*Shell preservation.* Nil.

*Facies Interpretation.* Tightly compacted bone accumulation of predominantly small

vertebrate remains suggests atypical predator accumulation such as an owl's roost accumulation. Some incorporation of isolated macropod teeth.

## **2.16 KARST GLEN SYSTEM**

To the southwest of Olsen's Cave is another isolated outcrop of limestone known as Karst Glen. Several small to medium sized caves occur in this limestone block and possess associated fossil deposits. Tall karst towers on the northern aspect of the limestone outcrop demarcate a collapsed cliff line following an intersecting vertically jointed system. These collapses have exposed a series of bone breccias and cemented cave floor sediments. Amongst the karst scree, several in situ fossil deposits can be found, generally near to, or beneath, a present cave entrance. Within the chambers, deep sequences of breccia are associated with extensive speleothems. Collections were not made within the caves of these breccias, however, outcrops of surface breccia were located and collected.

### **QM1411-1414, KG3 surface breccia**

QML1411, KG3 BRECCIA UPPER BRECCIA SITE. Located as an exposed fissure deposit near the top of the karst limestone at Karst Glen, QML1411 connects with the sediment found deeper within the limestone caverns. Lithologically it is unique amongst the cave deposits for central eastern Queensland being a markedly pisolitic conglomerate rather than a breccia..

*Stratigraphic context.* QML1411 occurs high on the open karst as a fissure deposit dipping at approximately 45° and running the length of a NW joint. It is stratigraphically higher than any of the other units currently at Karst Glen and is considered to be a very old fissure fill system.

The age of the sites in relation to the other sites on Karst Glen is unknown.

*Breccia components.* The rock unit at QML1411 is best considered a pisolitic conglomerate. The majority of the unit contains large and small, well rounded

conglomerate of black oxide pisolites. The rock is heavily cemented with the matrix a grey-coloured carbonate clay. Small clasts of parent limestone occur throughout the conglomerate.

*Bone preservation.* Very well rounded and reworked medium-sized bones that are heavily oxidised and shiny black in colour and luster.

*Tooth preservation.* Nil. *Shell preservation.* Nil.

*Facies Interpretation.* A heavily reworked channel fill occurring within the confines of a limestone fissure.

#### QML1412 & QML1413, KG3 B ENTRANCE BRECCIA.

QML1412 and QML1413 occurs beneath and to the southeast of “B” entrance within the KG3 Cave complex at Karst Glen. The unit follows a collapsed joint running NE-SW. The breccia is the remnant sediment fill within the vertical joint that has collapsed. Several of the blocks are *in situ*, forming the source for a large breccia scree found working its way down slope throughout the thick vegetation. Large patches of flowstone exposed on the surface can also be found closer to the present cliff line.

*Stratigraphic context.* QML1412 and QML1413 are of unknown stratigraphic context to other sites on KG3 and within the Cave systems. As the deposits are all joint controlled, each joint may contain contemporaneous sediment without stratigraphic contact.

*Breccia components.* A fine grained, red coloured matrix that is heavily cemented. Very small allochthonous gravel and pisolitic clasts. Sediment is clay dominant. Weathered flowstone found in patches throughout the site.

*Bone preservation.* Bone mostly small and well sorted into fine lenses forming the main irregular bedding planes. Finest portion of bone material, small and sand grain-sized. Bone well preserved, however, most elements are fragmentary with epiphyses missing.

*Tooth preservation.* Teeth usually associated with jaws. Almost entirely comprised of small jaws of rodents, possums, bats and dasyurids. Very few larger vertebrates present.

*Shell preservation.* Very little shell present. Some well preserved isolated large snails.

*Facies Interpretation.* The lack of large angular limestone clasts, patchy travertine and abundant clay load indicates a non-entrance facies. The fine lenses of grain-sized bones and massive accumulation of small vertebrates indicates a possible predator accumulation.

## 2.17 MARMOR QUARRY

QML1420.

Bone breccia collected by Bartholomai in 1964

*Stratigraphic context.* Unknown. QML1420 has been treated as a single fauna because none of the fossils are in stratigraphic context. Two factors suggest that the fossils have been derived from similarly aged sediment, probably the same breccia: 1. The lithology of the matrix adhering to all of the material collected is very similar. When known sites of different age are compared at Mount Etna, the matrix differs dramatically in sediment colour, cementation and bone preservation (e.g. QML1312 versus QML1311). Therefore, it seems likely that the material from Marmor Quarry is derived from the same unit. 2. Two collections have been used for this analysis: One by Longman in the 1920's and one by Bartholomai in the 1960's. Both collections used the mine manager of-the-day as a source of historical knowledge for site location, plus they both collected similar fauna, such as *Macropus titan*, *M. agilis siva*, and *Sarcophilus laniarius*.

Both collections contain similar species of rodents and bandicoots, with the small mammals derived from Bartholomai's collection via acid etching of bone breccia. This breccia also contained megafauna such as *Macropus titan*.

*Breccia components.* Grey to brown clay, lightly cemented; clasts of limestone only.

*Bone preservation.* Bone preserved as grain-sized fragments, isolated large long bone elements and occasional large vertebrate remains.

*Tooth preservation.* Small-sized vertebrates are generally preserved as isolated teeth without jaws. Large-sized vertebrates present as isolated mandibles and maxillae with preserved teeth.

*Shell preservation.* Isolated large snails.

*Facies Interpretation.* The sediment type and bone preservation is very similar to the guano found in Lower Johansen's Cave, the major difference being the degree of cementation. Marmor Quarry sediment is considerably more cemented than the guano found at Lower

Johannsen's Cave. It is therefore considered that the breccia recovered by Bartholomai in 1964 comes from a cemented guano deposit.

## FAUNAS

Many of the sites individually represent diverse faunas and their constituent taxa are tabulated (Tables 1-3, Appendix 1). Higher level taxa which are represented by few or one elements but are noteworthy are listed below. In addition the murids are listed below but will be described in another work.

## 2.18 UNDESCRIBED TAXA

Teleost indet. QMF51442, vertebra, QML368.

Micro chiropterans; QMF48001-48108; QMF48160-QMF48165; All localities (except QML1420).

Bats are found in all faunal assemblages except QML1420 and range in size from very small species of *Miniopterus*, to the very large *Macroderma gigas* (Fig. 29A-E.).

Identification of the numerous small species of bats was outside the scope of the present study.

Murids: Rodents are a conspicuous element of all sites and faunal assemblages. At least ten genera have been identified (Author and H. Godthelp). The taxa range in size from the large arboreal *Melomys/Uromys* and aquatic *Hydromys*, to the very small arboreal

*Pogonomys* and terrestrial *Leggadina*. Specific identifications will be determined in a full review of the rodents. A preliminary list is provided below with identified specimens.

**Conilurus** sp. Fig. 30A: QMF52052; QML1312. **Hydromys** sp. QMF52056; QML1420.

**Leggadina** sp. Fig. 30B: QMF52040- QMF52042, QML1312; Olsen's Cave; QML1314.

**Uromys/Melomys** sp. Fig. 30C-D; QMF52014- QMF52021; QML1284; QML1284a; QML1313; QML1420; QML1311; QML1384L.

**Mesembriomys** spp. QMF52028- QMF52032, QML1284; QML1384L; QML1385; QML1313; QML1311.

**Notomys** spp. Fig. 30I; QMF52036-52039; QML1312.

**Pogonomys** sp. nov. Fig. 30G QMF52022-QMF52027; QML1313; QML1284; QML1284a; QML1384U; QML1384L; QML1385; QML1311.

**Pseudomys** spp. Fig. 30E-F; QMF52043- QMF52051; All Localities **Rattus** spp. Fig. 30J; QMF52033- QMF52035; QML1312; QML1384U; Olsen's Cave; QML1420.

**Zyzomys** spp. Fig. 30H; QMF52053- QMF52055; QML1284; QML1284a; QML1312.

## 2.19 SYSTEMATIC PALAEOLOGY

Order ANURA Rafinesque, 1815

Family HYLIDAE Rafinesque, 1815

**Cyclorana** Steindachner, 1867

**Cyclorana** sp.

(Fig. 4G)

MATERIAL. QMF51443 & QMF51444 ; Olsen's Cave.

Two ilia represent this genus. Both ilia possess very large acetabular fossae with thin acetabular rims; distinct but small dorsal acetabular expansion; small and rounded ventral acetabular expansion; narrow preacetabular zone; slight curvature of the ilium; distinct dorsal prominence; anteroventrally and laterally orientated dorsal protuberance. Dorsal prominence almost entirely anterior of the acetabular rim. Superior acetabular rim margin above the level of the ventral margin of the ilial shaft. Lateral rim and medial groove absent. Iliac crest absent.

Identified as *Cyclorana* on comparison with Tyler's description of the genus (Tyler, 1976; Tyler et al., 1994). Identified as being close to *Cyclorana cultripes* by the presence of the large acetabular fossa, distinct dorsal prominence and protuberance and laterally projecting protuberance. Comparative specimens of the many species of *Cyclorana* were not available for this study, therefore, no specific assignment is warranted.

### **Litoria/Nyctimystes**

Menzies et al. (2002) illustrated the problems associated with identifying fossil hyliids from their pelvic elements, especially differentiating species of *Litoria* and *Nyctimystes*. Using the diagnostic features described by Tyler (1976) and Menzies et al. (2002) for *Litoria* and *Nyctimystes*, it was clear that both these taxa are present within the faunal assemblages. Identification to species level was not possible, except for those fossil specimens closely allying taxa with available comparative specimens such as *Litoria caerulea*.

Specimens assigned to *Litoria* were so based on the presence of the following distinctive features; 1. Ovoid dorsal protuberance, 2. Dorsal iliac crest absent, 3. Large acetabular fossa. Specimens assigned to *Nyctimystes* were so based on the presence of the following additional features to those seen in *Litoria*; 1. Ventral acetabular expansion rounded. 2. Very broad preacetabular zone.



**Litoria** Tschudi, 1838

**Litoria** sp. 1

(Fig. 4D)

MATERIAL. QMF51445; QML1385.

Small *Litoria* with: 1. acetabular fossa large and shallow with distinct peripheral rim. 2. dorsal prominence anterior to acetabular rim. 3. dorsal protuberance a distinct ovoid, laterally developed, knob. 4. small fossa posterior of the protuberance and at the base of prominence. 5. ridge runs anteriorly from base of protuberance to medial side of ilial shaft. 6. Ilial shaft slightly curved. 7. dorsal acetabular expansion and ventral acetabular expansion reduced. 8. narrow preacetabular zone. 9. broad ilial shaft. Differs from all other *Litoria* within the assemblages by possessing an anterior ridge of the dorsal prominence running from the base of the dorsal protuberance to the medial side of the ilial shaft. Differs from *Litoria* sp 2 by possessing a narrow preacetabular zone and a shorter dorsal acetabular expansion. Differs from *Litoria* sp. 3 by being smaller and possessing a smaller dorsal protuberance and a narrower preacetabular zone. Differs from *Litoria* sp. 4 by being smaller and having a more ovoid, and better-developed dorsal protuberance.

**Litoria** sp. 2

(Fig. 4E)

MATERIAL. QMF51446; QML1385.

Medium-sized *Litoria* with the following: 1. broad, oval, and shallow acetabular fossa. 2. distinct acetabular rim. 3. Narrow preacetabular zone. 4. Elongate dorsal acetabular expansion. 5. Well developed and rounded ventral acetabular expansion. 6. Low dorsal prominence. 7. Dorsal protuberance ovoid and laterally developed. 8. Ilial shaft straight.

Differs from *Litoria* sp. 3 by being larger, having a smaller dorsal protuberance and an elongate dorsal acetabular expansion, which extends superiorly of the line of the dorsal protuberance. Differs from *Litoria* sp. 4 by being larger, possessing a well-developed dorsal protuberance and broad preacetabular zone.

### ***Litoria* sp. 3**

(Fig. 4B)

MATERIAL: QMF51447-51449; QML1385.

A medium-sized *Litoria* possessing the following features: 1. Large, half-moon shaped acetabular fossa. 2. Reduced dorsal acetabular expansion. 3. Ventral acetabular expansion well developed and rounded. 4. Narrow preacetabular zone. 5. Dorsal prominence reduced. 6. Dorsal protuberance as a massive ovoid knob with a distinct ventral groove.

	QML368	QML1284	QML1284a	QML1312	QML1314	QML1384LU	QML1385	Olen's Cave
Teleosti indet	x							
<i>Cyclorana</i> sp.								x
<i>Litoria</i> sp. 1							x	
<i>Litoria</i> sp. 2							x	
<i>Litoria</i> sp. 3							x	
<i>Litoria</i> sp. 4		x					x	
<i>Litoria caerulea</i>					x			
<i>Nyctimystes</i> sp. 1							x	
<i>Nyctimystes</i> sp. 2		x	x					
<i>Etnabatrachus</i>		x					x	
<i>Crinia</i> sp.							x	
<i>Kyarranus</i> sp.		x	x			x	x	
<i>Limnodynastes</i> sp. 1							x	
<i>Limnodynastes</i> sp. 2		x		x			x	
<i>Limnodynastes</i> sp. 3			x					
<i>L. tasmaniensis</i> sp.							x	
<i>L. spenceri</i> sp. >~							x	
<i>L. sp. cf. L.</i>		x		x				

<i>Lechriodus</i> sp.		x						
<i>Neobatrachus</i> sp.							x	
microhylid sp. 1		x	x					
microhylid sp. 2		x	x					
microhylid sp. 3		x						

**Table 2-1 TABLE 1. Faunal lists for fish and amphibians**

Differs from *Litoria* sp. 4 by being larger and possessing an enormous ovoid dorsal protuberance with a ventral groove.

***Litoria* sp. 4**

(Fig. 4C)

MATERIAL. QMF51450-51456; QMF51463-51464, QML1385; QML1284.

A small-sized *Litoria* possessing the following features; 1. Reduced, triangular-ovoid acetabular fossa. 2. Dorsal acetabular expansion and ventral acetabular expansion reduced. 3. Dorsal prominence reduced. 4. Dorsal protuberance conical-shaped and laterally produced. 5. Iliac shaft straight.

Differs from *Litoria conicula* by possessing a larger conical protuberance, smaller acetabular fossa, less developed ventral acetabular expansion and a narrow preacetabular zone.

***Litoria caerulea* (White, 1790)**

MATERIAL. QMF51457-51462; QML1314.

A large-sized *Litoria*, possessing the following features: 1. Medial and lateral groove absent. 2. Dorsal acetabular expansion reduced. 3. Ventral acetabular expansion gently curved. 4. Dorsal prominence and protuberance low on the iliac shaft. 5. Dorsal protuberance elongate-ovoid and slightly produced laterally.

Closely resembles comparative material available for *L. caerulea* from Queensland, especially the distinctly low dorsal prominence and ovoid protuberance.

Two smaller morphs of *Litoria* are present in subfossil accumulations from QML1314. It is uncertain whether these represent different taxa or a highly variable *Litoria caerulea*.

### **Nyctimystes Stejneger, 1916**

#### **Nyctimystes sp. 1**

(Fig. 4F)

**MATERIAL.** QMF51465; QML1385.

A large *Nyctimystes* possessing the following features of the ilium; 1. Moderately large triangular acetabular fossa. 2. Reduced dorsal acetabular expansion. 3. Ventral acetabular expansion gently rounded and expanded, spatulate-shaped. 4. Preacetabular zone broad. 5. Dorsal prominence low with small indistinct ovoid protuberance. 6. Posterior ridge of dorsal prominence tapers to anterior base of dorsal acetabular expansion. 7. Iliac shaft straight, medio-laterally compressed and broad. Differs from *Nyctimystes* sp. 2 by lacking a well-developed dorsal prominence and laterally developed dorsal protuberance. Further differs by lacking a distinctive groove ventral of the dorsal protuberance.

#### **Nyctimystes sp. 2**

**MATERIAL.** QMF51466-51468; QMF51469-51471, QML1284; QML1284a.

A large *Nyctimystes* possessing the following features of the ilium; 1. Large ovoid acetabular fossa. 2. Reduced and pointed dorsal acetabular expansion. 3. Ventral acetabular expansion rounded and very broad. 4. Preacetabular zone broad and gently curved to the base of the iliac shaft. 5. Dorsal prominence and protuberance low on the iliac shaft. 6. Dorsal protuberance distinct and laterally developed into an elongate-ovoid knob. 7. Beneath the dorsal protuberance runs a distinct lateral groove. 8. Dorsal protuberance above anterior-most margin of acetabular rim. *Nyctimystes* sp. 2 most closely resembles *N. disrupta* and *N. zweifeli* from

illustrations and descriptions available from Tyler (1976) and Menzies et al. (2002).

**Etnabatrachus** Hocknull, 2003

**Etnabatrachus maximus** Hocknull, 2003

(Fig. 6B)

MATERIAL. QMF44207, QMF44208; QML1385, QML1284.

A giant frog probably from the Hylidae, based on the large rounded dorsal protuberances. Previously described by Hocknull (2003) and currently endemic to the Plio-Pleistocene of Mount Etna and Limestone Ridge.

Family LEPTODACTYLIDAE Werner, 1896

**Crinia** Tschudi, 1838

**Crinia** sp. (Fig. 4A)

MATERIAL. QMF51472, QML1385.

A small leptodactylid. Only the rim of acetabular fossa preserved, indicating a large rounded and shallow fossa. Other features include: 1. Dorsal acetabular expansion short and pointed. 2. Ventral acetabular expansion broken and insignificant. 3. Preacetabular zone narrow. 4. Dorsal prominence low and long, running halfway anterior of the acetabular rim. 5. Dorsal protuberance inconspicuous. 6. Long thin median groove running the length of the ilial shaft. 7. Ilial shaft curved and slender. *Crinia* sp. is identified as *Crinia* based on its small-size, reduced dorsal prominence and protuberance, slender curved ilial shaft, large acetabular fossa and longitudinal medial groove.

**Kyarranus** Moore, 1958

**Kyarranus** sp.

(Fig. 5F)

MATERIAL. QMF51488, QMF51489, QMF51490, QMF51491; QML1284a; QML1284, QML1385, QML1384U.

Large sub-triangular acetabular fossa. Acetabular rim distinct and high. Dorsal acetabular expansion expressed as a triangular point at an equivalent height to the dorsal prominence and protuberance. Ventral acetabular expansion narrow and anteriorly projecting. Preacetabular zone narrow. Dorsal prominence high and anterior of acetabular rim. Dorsal protuberance is an elongate antero-dorsally projecting process from dorsal prominence. Small fossa at the posterior base of the dorsal prominence. Iliac shaft long, slender and curved.

*Kyarannus* is a distinctive leptodactylid, possessing an elaborate dorsal prominence and anteriorly projecting protuberance. The combination of this feature with a long, curved iliac shaft and a high acetabular rim identify *Kyarannus* here. Specific placement will be considered in later works.

### ***Limnodynastes* Fitzinger, 1843**

Tyler et al. (1998) describes all species of *Limnodynastes* as possessing an extremely large dorsal prominence and protuberance, and a high and steep dorsal acetabular expansion of the ilium. Within the genus there is considerable variation of these features, with the development of an iliac crest in some taxa (Tyler 1976). Specimens possessing these features are here assigned to *Limnodynastes*.

### ***Limnodynastes* sp. 1**

MATERIAL. QMF51473-51474; QML1385.

Acetabular fossa large and high, with a distinct acetabular rim. Dorsal acetabular expansion rises steeply from the shaft to an acute point. Ventral acetabular expansion is gracile and rounded. Preacetabular zone narrow and runs beneath the rim of the acetabulum. Dorsal prominence rises high above iliac shaft and positioned anterior of the acetabular margin. Dorsal prominence antero-dorsally oriented and distinct. A short lateral groove runs 1/3 the length of the iliac shaft, originating just anterior to the

base of the dorsal prominence. A long median groove runs the length of the ilial shaft. Iliac shaft slightly curved.

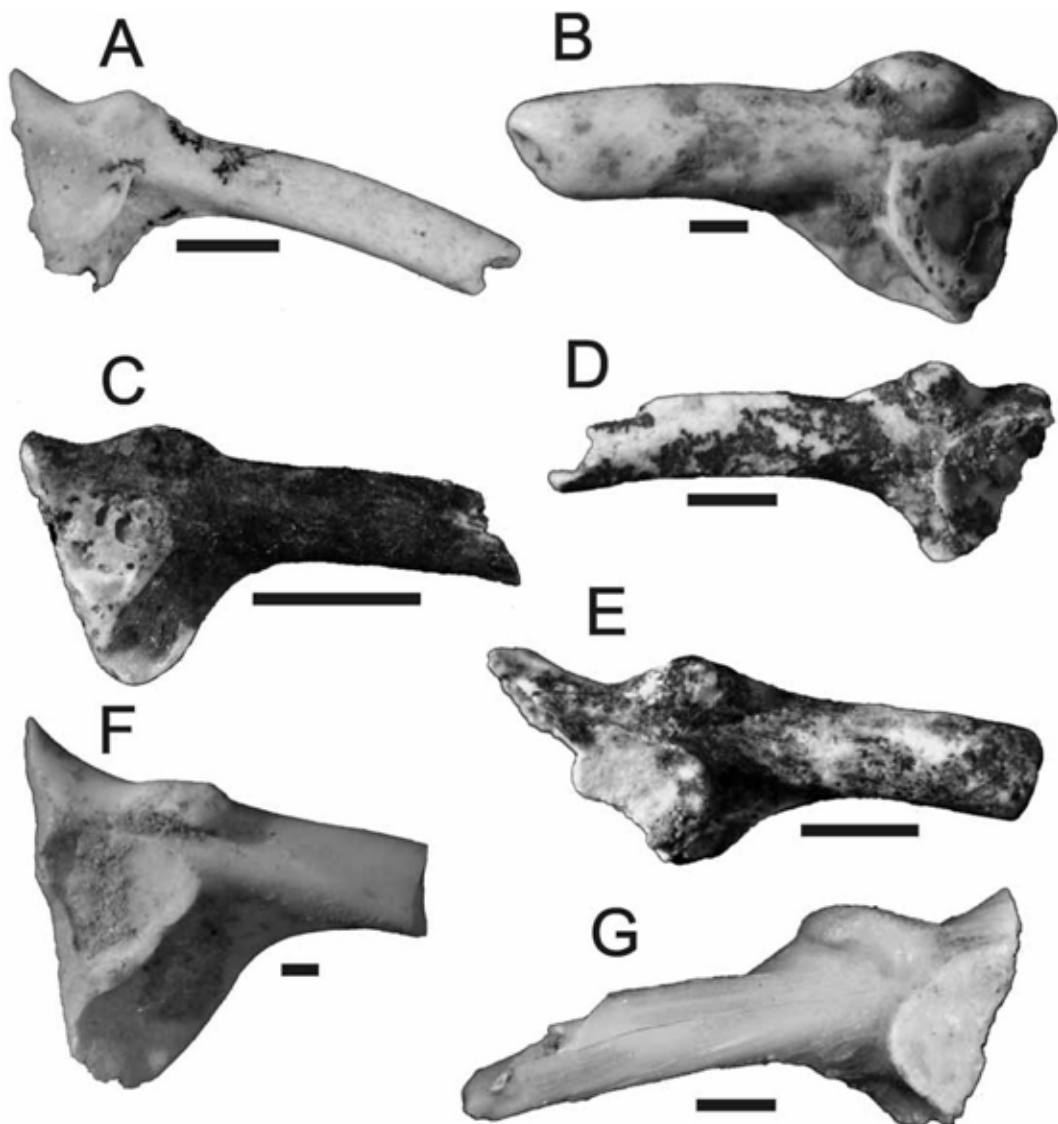


Figure 2-4. (FIG. 4.) A, *Crinia* sp.; QMF51472, right ilium. B, *Litoria* sp. 3; QMF51447, left ilium. C, *Litoria* sp. 4; QMF51450, right ilium. D, *Litoria* sp. 1; QMF51445, left ilium. E, *Litoria* sp. 2; QMF51446, left ilium. F, *Nyctimystes* sp. 1; QMF51465, left ilium. G, *Cyclorana* sp.; QMF51443, left ilium. Scale bar = 1mm.

Differs from *Limnodynastes* sp. 2 by possessing a median groove, a larger dorsal prominence and protuberance and missing a pocket on the ventral acetabular expansion, situated beneath the acetabular rim. Differs from *Limnodynastes*

sp. 3 by lacking a lateral groove ventral to the dorsal prominence and possessing a better-developed dorsal protuberance. Differs from *Limnodynastes tasmaniensis* sp. group by possessing a median groove on the ilium. Differs from *Limnodynastes spenceri* sp. group by lacking a dorsal ilial crest. Differs from *Limnodynastes peronii* by being much smaller and lacking the massive development of the dorsal prominence and protuberance.

**Limnodynastes sp. 2**

(Fig. 5E)

MATERIAL. QMF51476-51477, QMF51478-51481, QMF41864, QMF41856, QMF33383; QML1284, QML1385, QML1312.

Acetabular fossa broad and shallow, subtriangular in lateral view. Acetabular rim high. Dorsal acetabular expansion elongate and pointed reaching much higher than the tip of the

dorsal protuberance. Ventral acetabular expansion rounded. Preacetabular zone narrow, running beneath the acetabular rim. A dorsal pocket occurs beneath the rim and at the origin of the ventral acetabular expansion. Dorsal prominence low and inconspicuous. A small fossa is located at the posterior base of the prominence. Dorsal protuberance equally inconspicuous being low and only slightly conical. Iliac shaft laterally compressed, narrow and curved.

Differs from *Limnodynastes* sp. 3 by possessing a pocket on the ventral acetabular expansion and a lower dorsal prominence. Differs from *Limnodynastes tasmaniensis* group by possessing a lower prominence, indistinct protuberance and lacking a lateral groove. Differs from *Limnodynastes spenceri* group by lacking a dorsal ilial crest. Differs from *Limnodynastes peronii* by lacking a massively developed dorsal prominence and protuberance.



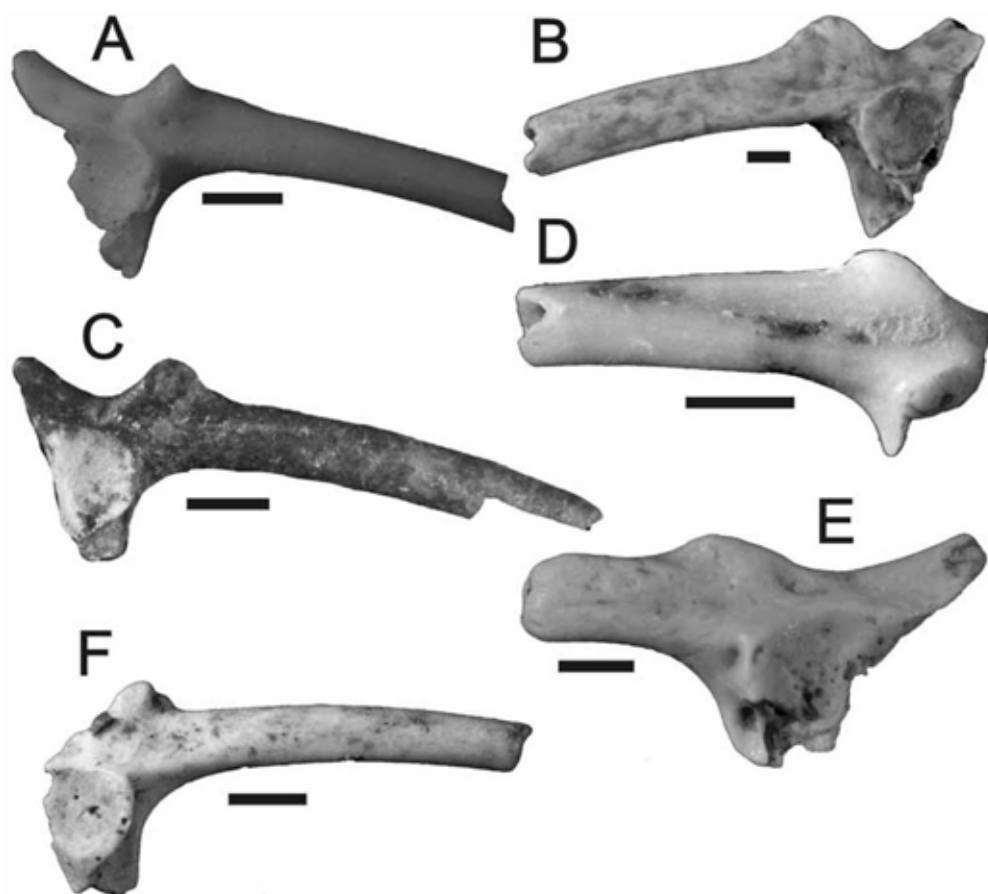


Figure 2-5 (FIG. 5.) A, *Limnodynastes* sp. 3; QMF51486, right ilium. B, *Limnodynastes* sp. cf. *L. peronii*; QMF41793, left ilium. C, *Limnodynastes* sp. 1; QMF51473, right ilium. D, *Limnodynastes* spenceri; QMF51484, left ilium. E, *Limnodynastes* sp. 2; QMF51476, right ilium. F. *Kyarranus* sp.; QMF51489, right ilium. Scale bar = 1mm.

**Limnodynastes sp. 3**

(Fig. 5A)

MATERIAL. QMF51486; QML1284a.

Acetabular fossa ovoid and deep, rim elevated. Dorsal acetabular expansion elongate and pointed dorsally. Ventral acetabular expansion rounded and gracile. Preacetabular zone narrow. Lateral groove absent. Dorsal prominence low. Dorsal protuberance distinct, as a point projecting antero-dorsally from the prominence. Iliac shaft slightly curved. Median groove running the length of the iliac shaft. Differs from *Limnodynastes tasmaniensis* group by possessing a median groove along the shaft and lacking a lateral groove. Differs from *Limnodynastes spenceri* group by lacking an iliac crest. Differs from *Limnodynastes peronii* by lacking a massive dorsal prominence and protuberance.

**Limnodynastes tasmaniensis** Günther, 1858

sp. group.

MATERIAL. QMF51482-51483; QML1385.

Acetabular fossa distinctly rounded and elevated from the shaft. Dorsal acetabular expansion elongate, tapering to a point at an equivalent level to the dorsal protuberance. Ventral acetabular expansion narrow and tapered. Preacetabular zone narrow and concave. Lateral groove present on the shaft just ventral to the dorsal prominence. Dorsal prominence distinct, triangular shaped. Dorsal protuberance elongate, ovoid and projecting antero-dorsally. Iliac shaft curved. Differs from *Limnodynastes spenceri* group by lacking a dorsal iliac crest. Differs from *Limnodynastes peronii* by lacking the massive dorsal prominence distinctive of *L. peronii*.

***Limnodynastes spenceri* Parker, 1940 sp.**

group.

(Fig. 5D)

MATERIAL. QMF51484-51485; QML1385.

Small ilium possessing a distinct dorsal ilial crest and prominent antero-dorsally oriented dorsal protuberance. Acetabular fossa small and rounded. Acetabular rim distinct. Dorsal acetabular expansion unknown in the specimens. Ventral acetabular expansion unknown in

specimens. Preacetabular zone narrow and close to the acetabular rim. Ilial shaft relatively straight.

Differs from all other *Limnodynastes* species by possessing an ilial crest. Differs from the only other taxa with ilial crests, *Rana*, *Mixophyes* and *Lechriodus*, by lacking the extreme dorsal development of the crests.

***Limnodynastes* sp. cf. *L. peronii* Duméril &**

Bibron, 1841

(Fig. 5B)

MATERIAL: QMF41793, QMF41801, QMF41812, QMF41821, QMF41827, QMF33380, QMF41863, QMF41865-41866; QML1284; QML1312.

Acetabular fossa large and rounded. Rim elevated and thick. Dorsal acetabular expansion elongate and tapered, steeply pointed. Ventral acetabular expansion rounded and broad. Preacetabular zone narrow and concave. Fossa present at the posterior base of the dorsal prominence. Dorsal prominence distinct and anterior of acetabular rim. Dorsal protuberance large and well developed. Protuberance anterior projecting. Ilial shaft broad and slightly curved.

Specimens assigned to *L. peronii* from QML1284 differ from conspecific

specimens from QML1312 in possessing a distinct fossa and a more anteriorly projecting dorsal prominence. This variation is considered to be within the possible range of variation for this taxon.

### **Lechriodus** Boulenger, 1882

#### **Lechriodus** sp.

(Fig. 6A)

MATERIAL. QMF51492; QML1284.

Iliac crest present. Dorsal protuberance ovoid and level with the acetabular rim. Dorsal acetabular and ventral acetabular expansions narrow and short. Preacetabular zone narrow. Broad semicircular acetabular fossa. Shallow lateral groove runs the length of the iliac crest.

### **Neobatrachus** Peters, 1863

#### **Neobatrachus** sp.

(Fig. 6C)

MATERIAL. QMF51487; QML1385.

Acetabular fossa very small and rounded. Acetabular rim low and distinct from preacetabular zone. Dorsal acetabular expansion very broad and high, coalescing with the posterior margin of the dorsal prominence. Ventral acetabular expansion narrow and pointed. Preacetabular zone narrow and close to acetabular rim. Dorsal prominence is large with a tiny point making up the dorsal protuberance. Iliac shaft nearly straight and laterally compressed.

*Neobatrachus* possesses distinct iliac characteristics not found in other

leptodactylids, including the elaboration of the dorsal acetabular expansion and its coalescence with the dorsal prominence, small acetabular fossa and reduced ventral acetabular expansion. Specific assignment is not justified at this stage due to the lack of comparative specimens.

#### Family MICROHYLIDAE Günther, 1858

Microhylids have been identified from some of the faunal assemblages based on their small size, very large acetabular fossa, curved shaft and diminutive posteriorly placed dorsal prominence and protuberance.

##### microhylid sp. 1

(Fig. 6C)

MATERIAL. QMF51493-51494, QMF51495; QML1284, QML1284a.

Large rounded acetabular fossa which is distinct from the shaft and possesses a distinct acetabular rim. Dorsal acetabular expansion short and pointed. Ventral acetabular expansion short and rounded. Preacetabular zone narrow and constricted toward the acetabular rim. Dorsal prominence low with a conical protuberance posterior of acetabular rim. Iliac shaft recurved without dorsal crest.

Differs from microhylid 2 by possessing a curved shaft and less ridged dorsal protuberance. Differs from microhylid 3 by lacking a dorsal crest.

##### microhylid sp. 2

(Fig. 6F)

MATERIAL. QMF51496, QMF51497; QML1284, QML1284a.

Acetabular fossa large and rounded. Distinct acetabular rim. Dorsal acetabular

expansion and ventral acetabular expansion unknown, however, inferred to be reduced. Preacetabular zone narrow. Dorsal prominence low, dorsal protuberance small and ridged. Iliac shaft slightly curved and slender. Differs from microhylid 3 by lacking a dorsal crest.

microhylid sp. 3 cf. **Hylophorbus** Macleay,

1878

(Fig. 6D-E)

MATERIAL. QMF51498; QML1284.

Large rounded acetabular fossa. Distinct acetabular rim, set high above iliac shaft. Dorsal acetabular expansion elongated to a sharp dorsal point. Ventral acetabular expansion anteriorly deflected and rounded. Preacetabular zone narrow. Dorsal prominence inconspicuous, forming the posterior margin of a dorsal crest. Dorsal protuberance elongate and antero-dorsally projecting. Iliac shaft curved. Dorsal crest laterally compressed, angled medially, running almost the entire length of the iliac shaft.

The form of the ilium, distinct iliac crest, and curvature of the shaft ally this taxon very closely to *Hylophorbus* from Papua New Guinea as described and figured in Menzies et al. (2002). More specimens and access to comparative *Hylophorbus* will be needed to clarify its taxonomic placement within the Microhylidae.

Order TESTUDINES Linnaeus, 1758

Family CHELIDAE Gray, 1825a

chelid indet. (Fig. 7G-H)

MATERIAL. QMF52061, QMF52062, QMF52063; QML1311(H); QML1384L; QML1311(C/D).

Several pieces of carapace and plastron represent remains of freshwater turtles. The portions of carapace are thick, with distinct suture lines. A single posterior portion of a plastron is very thin and preserves pelvic sutures from the left side.

Order NEOSUCHIA Benton & Clark, 1988

Family CROCODYLIDAE Cuvier, 1807

Mekosuchinae indet.

(Fig. 7A-F)

MATERIAL. QMF51499-51505, QMF52064-52065, QMF17071; QML1311 (H), QML1384L, QML368, QML1313.

Fragmentary remains, including a serrated ziphodont tooth, a portion of an edentulous premaxilla, two partial vertebrae, three scutes, the proximal end of a femur and an ungual represent crocodilians. The tooth has distinctly serrate carinae and is ziphodont in form. A wear facet can be seen on the mesial margin of the tooth. The premaxilla is rounded with three alveoli, linked to one another by thick ridges on the lateral premaxillary margin. The vertebrae are antero-posteriorly compressed and squat, preserving both the condyle and cotyle. Scutes, small and thin, with a flat ventral surface and a keeled dorsal surface. Rows of pits occur on the dorsal surface of the scutes.

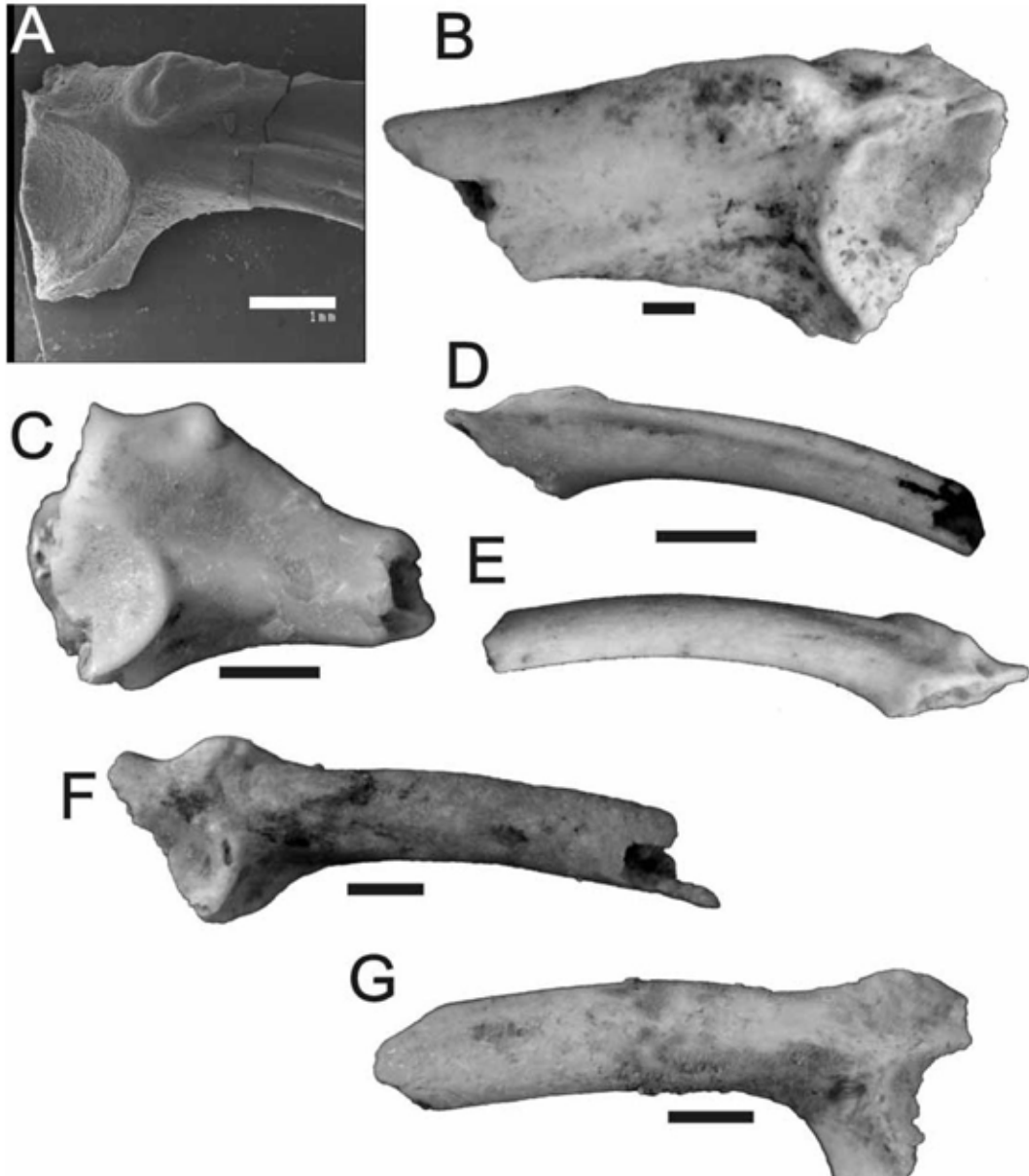


Figure 2-6 (FIG. 6.) A, *Lechriodus* sp.; QMF51492, right ilium. B, *Etnabatrachus maximus*; QMF44208, left ilium. C, *Neobatrachus* sp.; QMF51487, right ilium. D-E, microhylid sp. 3; QMF51498, left ilium in mesial and lateral view. F, microhylid sp. 2; QMF51496, left ilium. G, microhylid sp. 1; QMF51493, right ilium. Scale bar= 1mm.



The overall shape and size of the premaxillary bone, tooth and femur are similar to that of *Baru huberi* (QMF31061) but differs by having a deep reception pit for the first dentary tooth, that breaks the dorsal surface of the premaxilla.

Order SQUAMATA Oppel, 1811

Family AGAMIDAE Hardwicke & Gray, 1827

***Amphibolurus*** Wagler, 1830

***Amphibolurus*** sp.

(Fig. 8D)

MATERIAL. QMF43893; QML1312.

Right maxilla bearing two pleurodont tooth loci, both broken at the base. Nine acrodont tooth loci. The dorsal maxillary process is broken dorsal to the narial basin.

QMF43893 is placed within *Amphibolurus* on the basis of the following combined features: 1. Possessing a significantly reduced, near absent, naris ridge. 2. Dorsal maxillary process constricted superiorly and broad inferiorly. 3. Two pleurodont teeth with <sup>P1</sup> approximately three quarters the size of P<sup>2</sup>. 4. Less than fifteen acrodont teeth. 5. Angular dorsal maxillary process. 6. Hooked anterior profile.

***Diporiphora*** Gray, 1842

***Diporiphora*** group 2 (*sensu* Hocknull, 2002)

(Fig. 8)

MATERIAL. QMF51507; Olsen's Cave.

A left maxilla bearing one large pleurodont and six acrodont teeth. Maxilla broken posterior to A<sup>6</sup>. Pleurodont tooth large, recurved and orientated labially.

Angulate dorsal maxillary process.

Identified as a species within *Diporiphora* group 2 *sensu* Hocknull (2002) on the basis of the following combined features: 1. Naris ridge absent. 2. Broad dorsal

maxillary process, narrowed superiorly. 3. One large caniniform maxillary pleurodont tooth.

**Hypsilurus** Peters, 1867

**Hypsilurus** sp.

MATERIAL. QMF51506; QML1313.

Half of a badly preserved right dentary (Length: 12.13+mm) bearing 11 acrodont and one tiny pleurodont tooth represents a medium-sized agamid. The dentary is broken posteriorly of A11 and is gracile, tapering anteriorly with little curvature. Four visible foramina are present on the labial side of the dentary, with the last occurring below A11. The dental sulcus is narrow along its length and tapers markedly anteriorly. The dentary symphysis is small and ovoid. Acrodont dentition is badly weathered, however, there are distinct mesoconids and small antero and posterconids. Tooth size changes markedly between tooth position A5 and A6.

Agamid dentaries are difficult to identify, however, only five Australian agamid genera possess such distinctively diminutive pleurodont dentition of the dentary; *Chelosania*, *Hypsilurus*, *Physignathus*, *Moloch* and *Pogona* (Hocknull, 2002). The fossil is most similar to *Hypsilurus* by sharing one very tiny pleurodont tooth (*Hypsilurus* possesses one or two) and a very gracile, tapered dentary outline. The fossil dentary differs from all of the other four genera by possessing a much more gracile dentary and narrowly tapered dental sulcus. The fossil specimen differs further from *Chelosania* by being larger and possessing less tricuspid acrodont dentition. The fossil differs further from *Physignathus* by being smaller and possessing one versus three pleurodont dentary teeth. The fossil differs further from *Pogona* by possessing less rounded acrodont dentition and relatively shallower posterior and anterior margins.

**Pogona** Storr, 1982

**Pogona** sp. (small morphotype)

(Fig. 8C)

MATERIAL. QMF41969; QML1312.

Left maxilla with the anterior and posterior margins broken. Twelve acrodont teeth present.

*Pogona* has been identified from QML1312 by the presence of the following feature of the maxilla: 1. Posterior region deep. 2. Rounded acrodont teeth with large mesocones. Based on its size, the specimen allies the smaller *Pogona* species, such as *P. mitchelli* and *P. minor*.

**Tympanocryptis** Peters, 1863

**Tympanocryptis** sp. cf. **T. cephalus** Günther,

1867

(Fig. 8A)

MATERIAL. QMF41963; QML1312.

A nearly complete right maxilla, which is broken posteriorly to A<sup>12</sup>. Twelve acrodont and two pleurodont teeth preserved. Dorsal maxillary process broken at the dorsal margin.

Specimens referred here to a species of *Tympanocryptis* have been identified based on the following combined features; 1. Naris ridge present. 2. Naris ridge borders narial basin. 3.

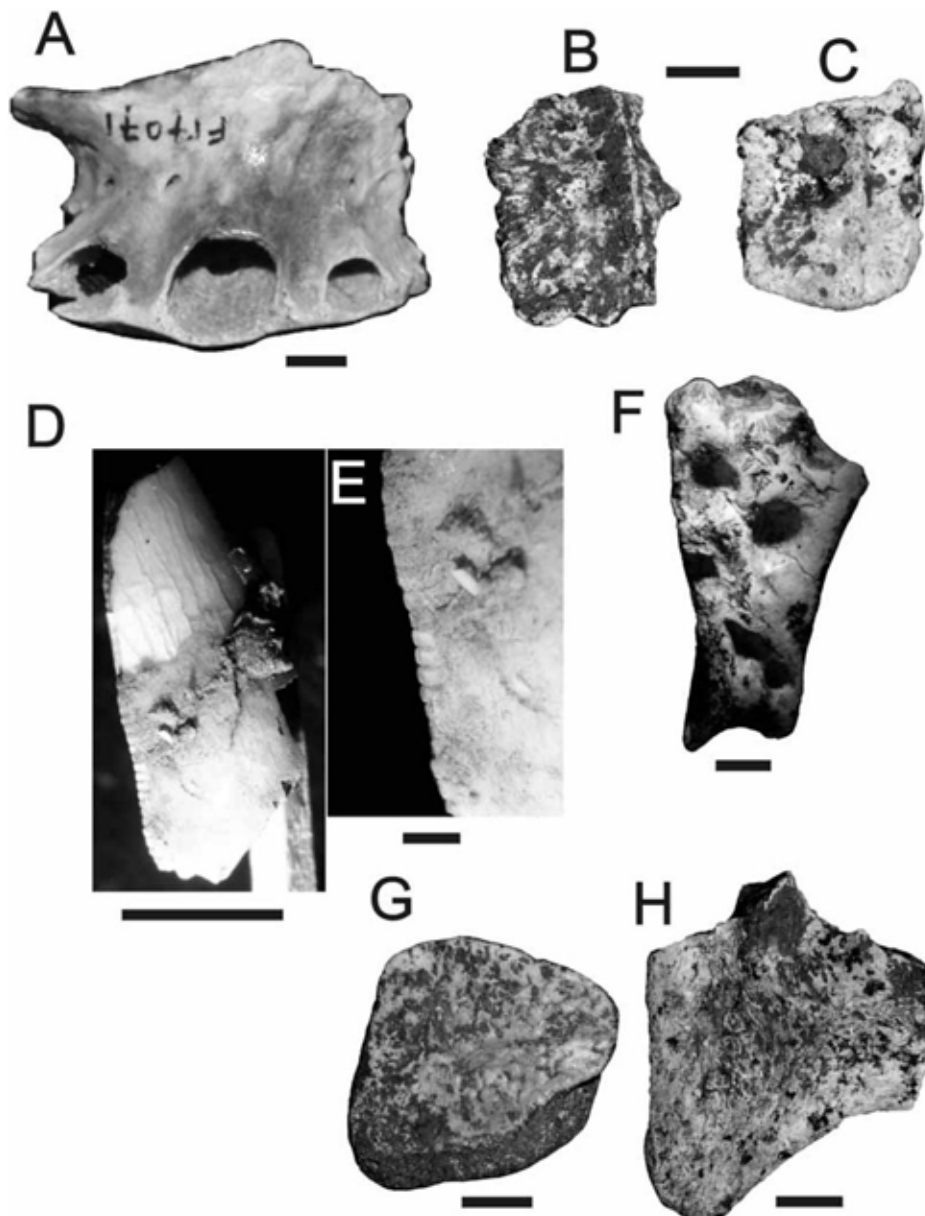


Figure 2-7 (FIG. 7.) A-F, Mekosuchinae; A, QMF17071, premaxillary. B, QMF52064, scute. C, QMF52065, scute. D, QMF51503, ziphodont tooth. Scale bar = 5mm. E, QMF51593 closeup of carinae (Scale bar = 1mm). F. QMF51505, scute. G-H, Chelidae; G. QMF52061, carapace. H, QMF52062, plastron.

TABLE 2. Faunal lists for reptiles and birds.

[illegible]

Two unequally-sized pleurodont teeth with P<sup>2</sup> caniniform. 4. Distinct notch anterodorsally of P<sup>1</sup>. QMF41963 shares very close similarities to *T. cephalus*. P<sup>1</sup> and P<sup>2</sup> are parallel to one another, which is not found in *T. tetraporophora* and *T. intima*. Also, *T. intima* is considerably larger than the specimen and comparative *T. cephalus*. The posterior “molar” acrodont teeth do not show the marked size change typical of *T. lineata* and *T. intima* (Hocknull, 2002). The lateral margin of the premaxillary/maxillary suture is higher and the naris ridge contributes more to this than it does in *T. lineata*. The p1 is very small, which is more usual in *T. cephalus* specimens, than *T. lineata*. The total number of acrodont teeth is unknown in this specimen, however, judging from the amount of missing maxilla, the number of teeth would be thirteen or more. Thirteen or more acrodont teeth in the maxilla is more commonly found in *T. cephalus* with tooth counts of 13-14 than *T. lineata* with 11-13. agamid indet.

MATERIAL: QML1284, QML1284a, QML1311, QML1313, QML1384, QML1385; QML1420

Several maxillary and dentary fragments bearing acrodont dentition are recorded in most sites, however, most of these are unidentifiable because they do not preserve the anterior diagnostic elements needed (Hocknull, 2002). The majority of the specimens show characteristics typical of juvenile agamids, including large acrodont teeth relative to jaw depth, lack of distinct wear facets on the acrodont teeth and dental bone, and overall bone fragility.

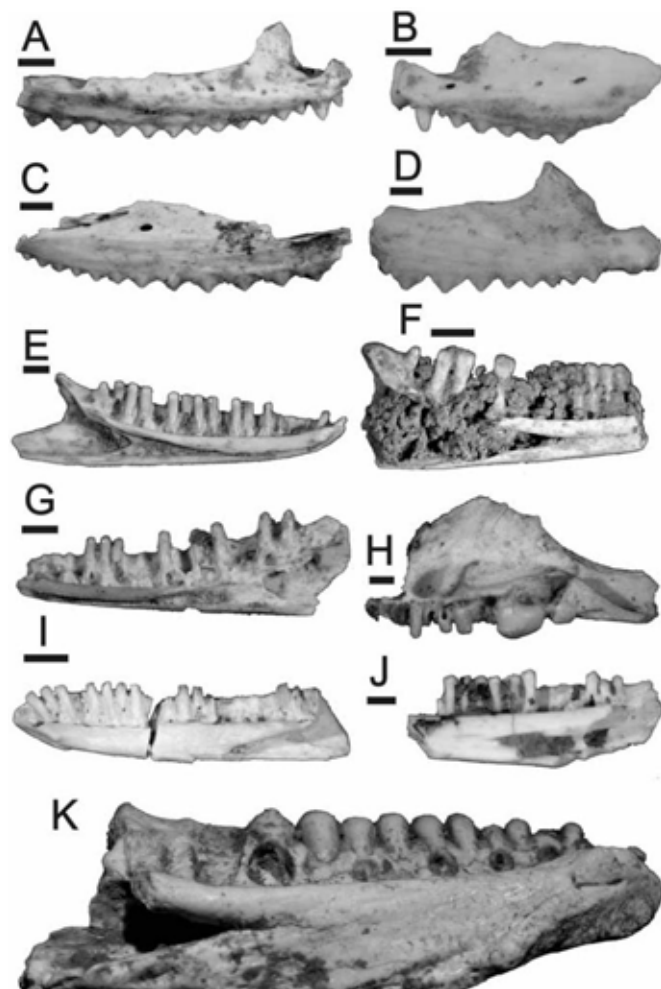


Figure 2-8 (FIG. 8.) A-D, Agamidae; A, *Tympanocryptis* sp. cf. *T. cephalus*; QMF41963, right maxilla. B, *Diporiphora* group 2; QMF51507, left maxilla. C, *Pogona* sp.; QMF41969, left maxilla. D, *Amphibolurus* sp.; QMF43893, right maxilla. E-K, Scincidae; E, *Sphenomorphus* group (robust morph); QMF51543, left dentary. F, *Egernia* sp.; QMF51529, left dentary. G, *Sphenomorphus* group (gracile morph); QMF51537, right dentary. H, *Cyclodomorphus gerrardii*; QMF51519, right maxilla. I-J, *Eugongylus* group; QMF51535 & QMF51536, right dentaries. K, *Tiliqua* sp.; QMF51516, left dentary. Scale bar = 5mm.

Family SCINCIDAE Oppel, 1811

**Egernia** Group *sensu* Greer, 1979

**Tiliqua** Gray, 1825

***Tiliqua* sp nov.**

(Fig. 8K)

MATERIAL. QMF51516; QML1284.

A robust left dentary, broken posterior to the splenial notch. Eleven conical, haplodont teeth are preserved with four addition tooth loci. Symphysial crest extends to below the eighth haplodont tooth locus. Symphysis elongate, tapering sharply to the posterior and rounded anteriorly. The labial side of the dentary bone is distinctly inflated to the posterior, giving the dentary a very robust appearance in lateral view. Teeth gradually increase in width toward the posterior, all retaining their conical grooved tooth crowns. Dental shelf deep along its length.

The closed Meckelian groove places this specimen with the *Egernia* and *Eugongylus* groups within the Lygosominae (Greer, 1979). The enlarged posterior conical teeth place this specimen within the *Tiliqua* lineage (Shea, 1990). The presence of a long symphysial crest, bunched haplodont dentition and the absence of a single massive posterior durophagous tooth excludes this specimen from being *Cyclodomorphus*. *Tiliqua* sp. differs markedly from all living and fossil *Tiliqua* so far described and is most probably a new species.

***Tiliqua scincoides* (White, 1790)**

MATERIAL. QMF51517; QMF51518; QML1313, QML1314.

*Tiliqua scincoides* is best represented by a single right dentary possessing nine teeth and twelve tooth loci. The largest tooth is toward the posterior and is characterised by having a rounded durophagous tooth crown. The elongate symphysial crest places this specimen within *Tiliqua*, its size and tooth morphology place it firmly within *Tiliqua scincoides* by being much smaller and more gracile than both *T. gigas* and the large *Tiliqua* species from Mini Cave.

***Cyclodomorphus* (Fitzinger, 1843)**



***Cyclodomorphus gerrardii* (Gray, 1845)**

(Fig. 8H)

MATERIAL. QMF51519-QMF51527; Olsen's Cave, QML1284, QML1284a, QML1311(H), QML1311(C/D), QML1384 U, QML1313, QML1385, QML1420.

Several isolated maxillae and dentaries possess a massively rounded posterior tooth in both jaw elements, a short symphyseal crest and a concave anterior portion of the dental sulcus. Maxillae preserve up to ten haplodont teeth in varying degrees of replacement. Dentaries usually exhibit some form of abrasion on the smaller anterior haplodont teeth.

The identification of *Cyclodomorphus gerrardii* was based on the presence a single massive durophagous maxillary and dentary tooth, concave anterior dental sulcus and short symphyseal crest.

***Egernia* Gray, 1838**

***Egernia* spp.**

(Fig. 8F)

MATERIAL. QMF51529-51534; all localities.

Dentaries and maxillae large, possessing at least 12 haplodont teeth with chisel-shaped crowns. Meckelian groove closed. Posterior portion of the jaw robust and deep.

Large inferior mental foramen.

***Eugongylus* group (*sensu* Hutchinson, 1992)**

(Fig. 8I-J)

MATERIAL. QMF51535-QMF51536; QML1284, QML1284a.

Large-sized scincid possessing a slender dentary, wedge-shaped, tightly spaced haplodont teeth and a closed Meckelian groove.

The large size, slender dentary, closed Meckelian groove ally these specimens to

the *Eugongylus* Group *sensu* Hutchinson (1992).

**Sphenomorphus** Group (*sensu* Greer, 1979)

gracile morphotype

(Fig. 8G)

MATERIAL. QMF51537-QMF51541; QML1284a; QML1284, QML1312, QML1313, QML1385.

Small-sized dentary with closely-spaced haplodont teeth. Teeth with pointed crowns. Meckelian groove open along its length to symphysis. Dentary shallow and symphysis small.

The small gracile form of the dentary and the open Meckelian groove place these specimens within the gracile morphotype of *Sphenomorphus* Group *sensu* Hutchinson (1992).

robust morphotype

(Fig. 8E)

MATERIAL. QMF51543, QMF51544; QML1312, Olsen's Cave.

Large-sized dentary with elongate blunt-crowned haplodont teeth. Meckelian groove open along its length to symphysis. Dentary deep at posterior, tapering markedly to ovoid symphysis.

The open Meckelian groove, large size, robust tooth morphology and deep jaw place these specimens within the robust morphotype of *Sphenomorphus* Group *sensu* Hutchinson (1992).

Family GEKKONIDAE Oppel, 1811

Fossil gekkonids have been found in several deposits and are abundant throughout. Unfortunately most of the maxillae and dentaries are preserved as fragments, which make identification very difficult. In addition to this, there is no

premise for identification of fossil Australian gekkonid taxa based on maxillary and dentary characteristics, therefore, gekkonid specimens described here were only compared with the limited comparative collection available to the author.

gekkonid (large)

(Fig. 9A-C)

MATERIAL. QMF51508, QMF51509, QMF51510; QML1284, QML1284a, QML1313.

Several large maxillary and dentary fragments preserving rows of closely-set, needle-like homodont teeth. Maxillae possess a dorsal process of the maxilla, which lies anterior to the orbit and contacts the nasal bones. The process borders the posterior margin of the narial opening. The morphology of this margin varies between gekkonid taxa and is distinctly broad in the fossil specimens. The most complete fossil dentaries indicate the presence of a very large gekkonid. The dentaries are characterised by being long and curved mesially, possessing many closely-spaced homodont teeth, a splenial notch and a small dental symphysis.

Based on its overall very large size, the fossil taxon must have reached a snout-to-vent length of 16 cm or more, making it similar in size to the largest extant Australian gekkonids (*Phyllurus*, *Cryptodactylus*). The maxillae and dentaries of all three genera show similarities with the fossil taxon.

gekkonid (small)

(Fig. 9B)

MATERIAL. QMF51511-51515; All localities.

Several small fragmentary dentaries and maxillae are preserved throughout the deposits,

probably representing several taxa. A small maxilla (QMF51511; QML1284) is distinctive in possessing a relatively narrow dorsal process originating posterior of the

narial opening and tapering markedly to the posterior of the maxilla. The dentition is simple, however several of the teeth are bicuspid. Dentaries are small, curved and slender.

On comparison with small-sized gekkonids, most of the gekkonid specimens cannot be adequately identified.

#### Family VARANIDAE Hardwicke & Gray, 1827

Varanids are a conspicuous member of the lizard fauna. Varanids have been identified from isolated, recurved small and large-sized serrated teeth, an isolated parietal, quadrate, femur, dentary fragments and several isolated cervical, dorsal and caudal vertebrae.

#### **Varanus** Merrem, 1820

##### **Varanus** sp. 1

MATERIAL. QMF51546, QMF51547; QML1312, QML1311(H).

A medium-sized species of *Varanus* is represented by a parietal, two dentary fragments, an isolated dorsal and several caudal vertebrae. The fossils compare favourably with a similarly sized *Varanus varius*, particularly in the broad flat parietal with narrow, slender temporal ridges; small-sized teeth and a dorsal vertebrae that falls within measurements provided by Smith (1976) for *Varanus*. The dorsal vertebrae compare in size to either *V. varius* or *V. gouldi*.

##### **Varanus** sp. 2

(Fig. 9D-E, G-H)

MATERIAL. QMF51548-QMF51550, QMF52066; QML1312, QML1311(H), QML1311(C/D), QML1313.

A very large varanid is represented by an isolated right quadrate, a cervical and several dorsal and caudal vertebrae. On prezygopophysis to postzygopophysis length alone, these specimens fall within the range of dorsal vertebral measurements

provided by Smith (1976) for *V.giganteus* and below the range provided for a small species of *Megalanina* from Chinchilla provided by Hutchinson & Mackness (2002). The dorsal vertebrae are most similar in length to *V. giganteus*, however, differ remarkably in the ratio defined by Smith (1976) as prezygopophysis-prezygopophysis (Pr-Pr) width over prezygopophysis- postzygopophysis (Pr-Po) length. In particular, when comparing this ratio to modern and fossil varanids the dorsal

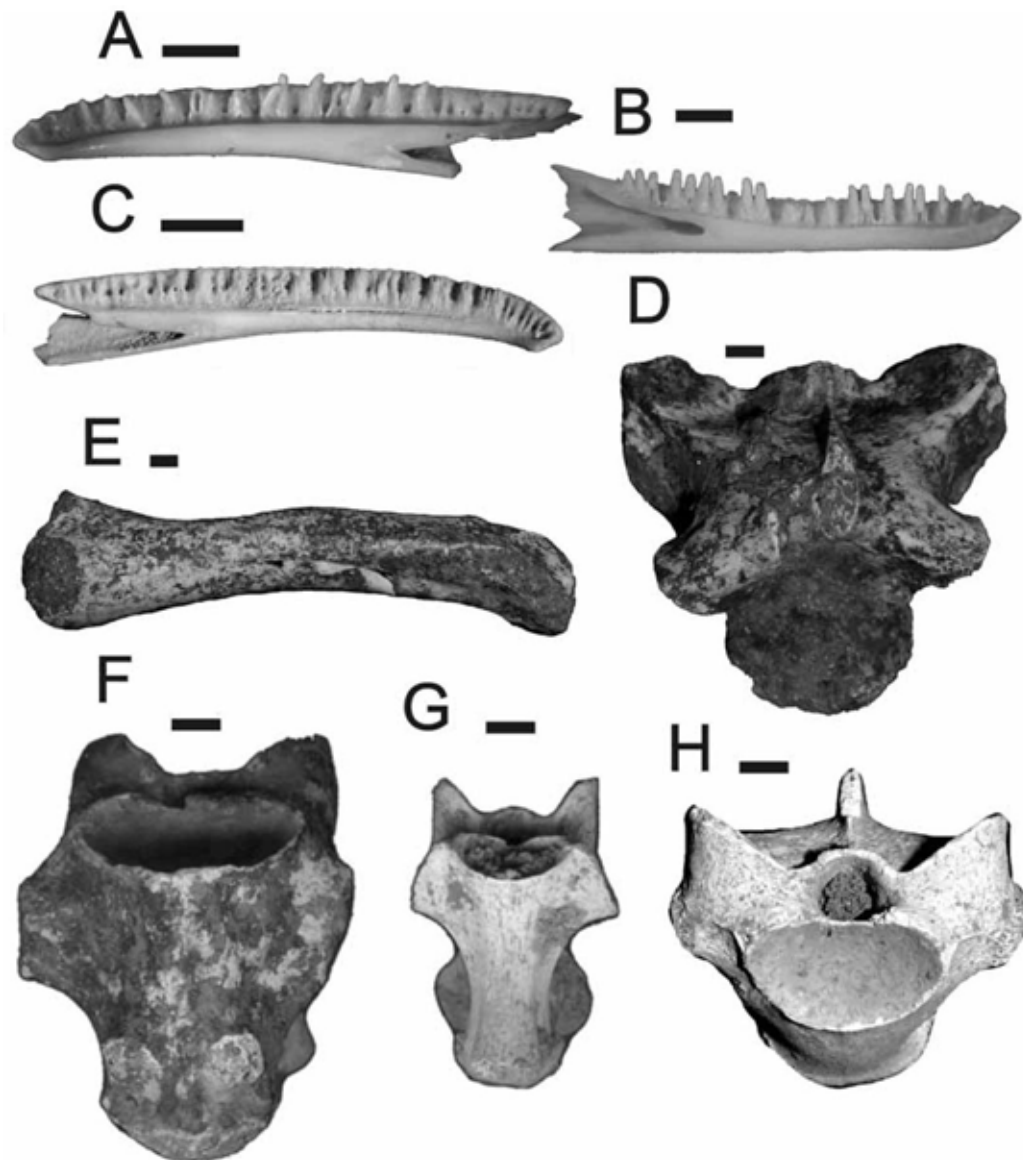


Figure 2-9 (FIG. 9.) A-C, Gekkonidae; A&C, gekkonid (large morph); QMF51508, right dentary, QMF51510, left dentary. B, gekkonid (small morph); QMF51511, left dentary. Scale bar = 1mm. D-H, Varanidae; D-E, *Varanus* sp. 2; D, QMF51548, dorsal vertebra. E, QMF51549, femur. F, *Megalania prisca*; QMF1418, caudal vertebra. G-H, *Varanus* sp. 2; G, QMF51550, cervical vertebra. H, QMF52066, dorsal vertebra. Scale bar = 5mm.

vertebrae measured here attain a ratio of between 1.07 and 1.22. This indicates that the Pr-Pr width of the vertebrae are generally wider than the Pr-Po length.

Interestingly, the measurements provided by Smith (1976) show that dorsal vertebrae of extant *Varanus* are mostly longer than broad with some being nearly equally as long as broad. Very few measured slightly broader than long.

Specimens referable to *Megalania* from both Chinchilla, Bluff Downs (Mackness & Hutchinson, 2000; Hutchinson & Mackness, 2002) and the Darling Downs (Hecht 1975; pers. obs.) possess dramatically broader than long dorsal vertebrae. This feature is easily seen in the largest *Megalania prisca* dorsal vertebrae. Further comparisons of *Varanus* spp larger than *V. giganteus*, such as *V. komodoensis*, will be needed to verify the validity of these differences.

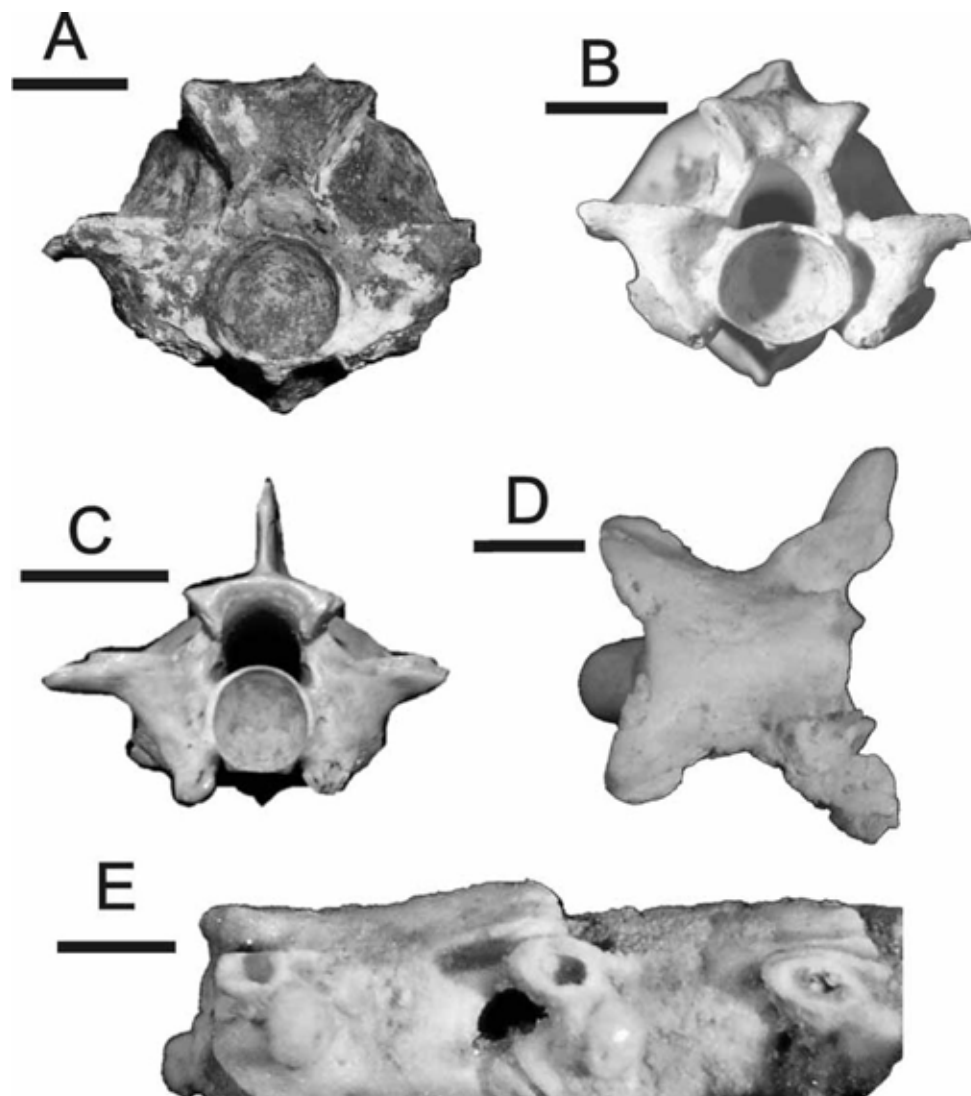


Figure 2-10 (FIG. 10.) A-B, Pythoninae; A, QMF51560, dorsal vertebra. B, QMF51561, dorsal vertebra. C, Elapidae; QMF51551, dorsal vertebra. Scale bar = 5mm. D-E, Typhlopidae; D, QMF51578, dorsal vertebra. E, QMF51579, three articulated dorsal vertebrae. Scale bar = 1mm.



**Megalania** (Owen, 1860)

**Megalania prisca** (Owen, 1860)

(Fig. 9F)

MATERIAL. QMF1418; QML1420.

*Megalania prisca* is represented by a single varanid distal caudal vertebra, cotylecondyle length: 28.80mm. The massive size of the vertebra and the fact that it is a distal caudal vertebra indicates that the varanid was enormous, attaining the dimensions only seen in *Megalania*. Until the debate surrounding the generic validity of *Megalania* is resolved (Hecht, 1975; Molnar, 1990; Lee, 1996), this giant varanid will be placed within *Megalania*.



Figure 2-11 (FIG. 11.) A-C, Galliformes; QMF51607-51609 (left to right), humeri. D-H, Gruiformes; D-F, QMF51610-51612 (left to right), humeri. G-H, QMF33458 & QMF33460 (left to right), carpometacarpi. I-L, Passeriformes; QMF51601-51604 (left to right), humeri. Scale bar = 5mm.

Family ELAPIDAE Boie, 1827

elapid indet.

Fig. 10C

MATERIAL. QMF51551-51559; All Localities.

Elapids have been identified based on the following features of the trunk vertebrae: 1. Elongate and high vertebrae, longer than broad. 2. Distinct hypopophyses. 3. High neural spine. 4. Accute prezygopophyses. 5. Spherical condyle-cotyle articulation. Elapid specimens are variable in size with the largest specimen from QML1312, being at least twice the size of the largest elapids from QML1284, 1284a and 1311.

Subfamily PYTHONINAE Fitzinger, 1826

pythonine indet.

(Fig. 10A-B)

MATERIAL. QMF51560-51569; All Localities.

In addition to maxillary and dentary remains, pythonines have been identified from the deposits based on the following features of the trunk vertebrae: 1. Short, stout vertebrae, as wide as long. 2. Robust zygantrum. 3. Thick zygosphen. 4. Ovoid condylar-cotylar articulation. 5. Hypopophysis tiny or absent. 6. Large ovoid prezygopophyses. 7. High neural spines with overhanging anterior and posterior margins.

Family TYPHOLOPIDAE Gray, 1825

typholopid indet.

(Fig. 10D-E)

MATERIAL. QMF51578-51582, QMF51583-51587; QML1284, QML1284a.

Typhlopids have been identified on the basis of the following features of the trunk vertebrae: 1. Neural spine absent. 2. Neural arch low and thin.

3. Zygantrum narrow and deep. 4. Accute prezygopophyses. 5. Hypopophysis absent. 6. Hemal keel absent or only slight. 7. Neural canal very large relative to vertebral size.

## AVES

Bird postcranial elements are numerous throughout all of the sites, especially from those sites interpreted as predator accumulations with owls as the major accumulator. The largest bird elements are currently attributed to the owls (Strigiformes), the smallest from the song birds (Passeriformes).

### Galliformes (Fig. 11A-C)

MATERIAL. QMF51607-51609; QML1312.

Quails are represented by several postcrania, including very distinctive humeri and carpometacarpi. The size of the humeri and presence of two proximal pneumatic fossae in the head of the humerus suggests the presence of a species of *Coturnix*.

### Gruiformes (Fig. 11 D-H)

MATERIAL. QMF33458, QMF33460, QMF51610- QMF51612; QML1312.

Buttonquails are represented by several postcrania, including humeri, carpometacarpi, femora, tarsometatarsi and sternal fragments. The distinctive larger pneumatic fossa in at the proximal head of the humerus and the large triangular intermetacarpal tuberosity ally these specimens closest to a species of *Turnix*.

### Passeriformes (Fig. 11 I-L)

MATERIAL. QMF51601, QMF51602-51606; QML1284 QML1312.

Passeriformes were identified from humeri possessing a distinct entepicondylar prominence, ectepicondyle distinct and distal to internal condyle, and a shallow pneumatic fossae.

#### Strigiformes (Fig. 12 A-K)

MATERIAL. QMF51578-51587; All localities except QML1420.

Owls were identified from numerous postcranial specimens including humeri, ulnae, carpometacarpi, phalanges, claws, femora and tarsometatarsi. Owls possess a distinct first phalange of the pes digits, with four tuberosities in each corner of the phalange. The phalange tends to be short and squat with a deep facet on the dorsal and distal margin.

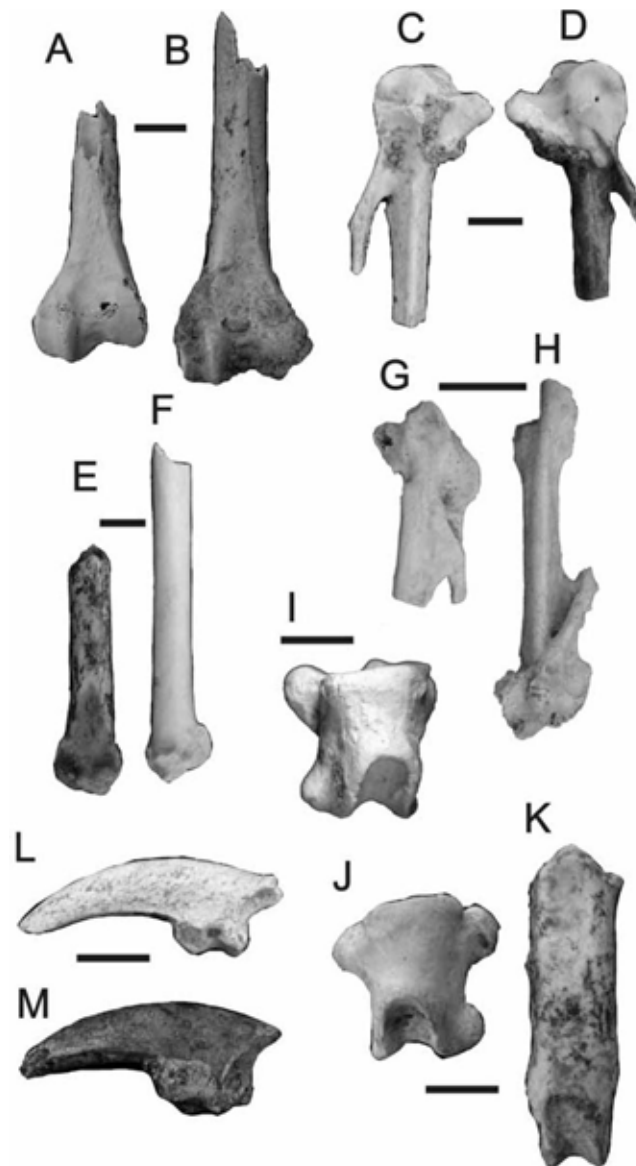


Figure 2-12 (FIG. 12.) A-K, Strigiformes; A-B, QMF51578 & 51579, femora. C-D, QMF51580 & 51581, carpometacarpi. E-F, QMF51582 & 51583, ulnae. G-H, QMF51584 & 51585, carpometacarpi. I-K, QMF51586, 51581, 33361, phalanges. L-M, QMF33863 & 33864, claws. Scale bar = 5mm.

## MAMMALIA

Family PERAMELIDAE Gray, 1825b

**Perameles** Geoffroy, 1803**Perameles** sp. 1

(Fig. 13A)

MATERIAL. QMF51613-QMF51620; QML1284, QML1284a, QML1311(H), QML1313, QML1384U, QML1385, QML1420, QML1311(C/D).

A species of *Perameles* on the basis of the following combination of features: 1. Presence of fully developed anterior and posterior cingulae on  $M^{1-3}$ . 2. Triangular tooth crown with the para and metastylar corners outside the margin of the tooth crown. 3. Equidistant protoconid-metaconid, protoconid-paraconid distances on  $M_{1-4}$ . 4. Absence of the anterior cingulid on M1.

When compared with the modern species of *Perameles* the fossils differ as follows:

*Perameles* sp. 1 is larger than *P. bougainville* and has a more buccally developed posterior cingulum on  $M^{1-3}$ . The posthypocristid runs to the hypoconulid on M1-3 whereas the posthypocristid only runs to the hypoconulid in M1-2 of *P. bougainville*

*Perameles* sp. 1 is smaller than *P. nasuta*. The meta- and parastylar corners in unworn molars of the fossil taxon are bicuspid whereas *P. nasuta* possess single conical meta- and parastyle.

*Perameles* sp. 1. is smaller than *P. gunnii* and possesses a more buccally developed posterior cingulum on  $M^{1-4}$ . The posthypocristid runs to the hypoconulid on all lower molars in the fossil *Perameles*, whereas it only runs to the hypoconulid in  $M_{2-3}$  of *P. gunnii*.

*Perameles* sp. 1. differs from *P. bowensis* by being larger, possessing larger hypoconulids, and a posthypocristid that runs to the hypoconulid on M3. *Perameles* sp. 1. differs from *P. allinghamensis*, which is only known by an isolated upper

molar, by being much smaller and possessing a posterior cingulum that terminates below and buccal to the metacone. *Perameles* sp. 1. differs from *P. sobbei*, which is only known from lower dentition, by possessing larger hypoconulids on M1-3, a posthypocristid that runs to the hypoconulid on M1-3, and by being smaller.

***Perameles* sp. 2**

(Fig. 13B)

MATERIAL: QMF51621-QMF51626; QML1284, QML1284a, QML1311(H), QML1313, QML1384U, QML1385.

A second medium-sized species of *Perameles* possesses the following features: 1. Anterior cingulid of M1 absent. 2. Hypoconulid reduced on M1-3. 3. Posthypocristid contacts the base of the entoconid M1-3. 4. Trigonid cusps approximated. 5. Entoconid conical with a small preentocristid crest. *Perameles* sp. 2 differs from *Perameles* sp. 1 by being larger, possessing a posthypocristid that contacts the entoconid and a preentocristid crest. *Perameles* sp. 2 differs from *P. nasuta*, *P. bougainville*, *P. eremiana*, *P. bowensis* by possessing an M1 with a posthypocristid that contacts the entoconid instead of the hypoconulid. *Perameles* sp. 2 differs from *P. gunnii* by being markedly smaller, possessing a more mesially terminating cristid obliqua and not possessing a simple conical entoconid. *Perameles* sp. 2 differs from *P. sobbei* by its smaller size, larger hypoconulid on M1, narrower protoconid-metaconid distance and smaller paraconid.

***Perameles bougainville* Quoy & Gaimard,**

1824

(Fig. 12C-E)

MATERIAL. QMF51627-51630, QMF51631; QML1312; Olsen's Cave.

A small species of *Perameles* is present in the fauna recovered from QML1312 and a single specimen in Olsen's Cave. The fossils are identified as *Perameles* on the



basis of the following combined features: 1. Para- and metastylar corners angular, occurring outside the peripheral margin of the tooth crown base, 2. The presence of a variably complete posterior cingulum. 3. Anterior cingulum on M2-4 that originates well below the apex of the paraconid. 4. Gently curved ascending ramus. 5. Reduced metaconule.

When compared with the three available species of modern *Perameles* (*P. nasuta*, *P. gunnii* and *P. bougainville*) this fossil species was closest to *P. bougainville* in size. The fossils referred to here as *P. bougainville* differ from both *P. nasuta* and *P. gunnii* by; being considerably smaller; possessing small, isolated parastyles on M1 instead of large, curved parastyles that are connected to the main tooth crown by a distinct preparacrista; possessing distinct protocones and metaconules on M<sup>1-3</sup>; acute angle made by the postprotocrista and premetaconule crista; possessing a lower angle of the postmetacrasta to the longitudinal axis of the tooth crown; more lingually oriented stylar cusp B & D. They differ from *P. allinghamensis* by being much smaller and possessing a more triangular outline in occlusal view. They differ from *P. bowensis* by being larger and better developed posterior cingulum on M<sup>3</sup>.

The fossils compare favourably with *P. bougainville* on the basis of: 1. Small size, though they are slightly larger than the samples measured by Freedman & Joffe (1966). 2. Form of the parastyle on M<sup>1</sup>, being small, isolated and not connected to the preprotocrista. 3. Higher angle of the postmetacrasta to the longitudinal axis of the tooth crown. 4. Lingually oriented stylar cusps B & D. 5. Incomplete posterior cingulum on M<sup>1-2</sup> with a short posterior cingulum on M<sup>3</sup>.

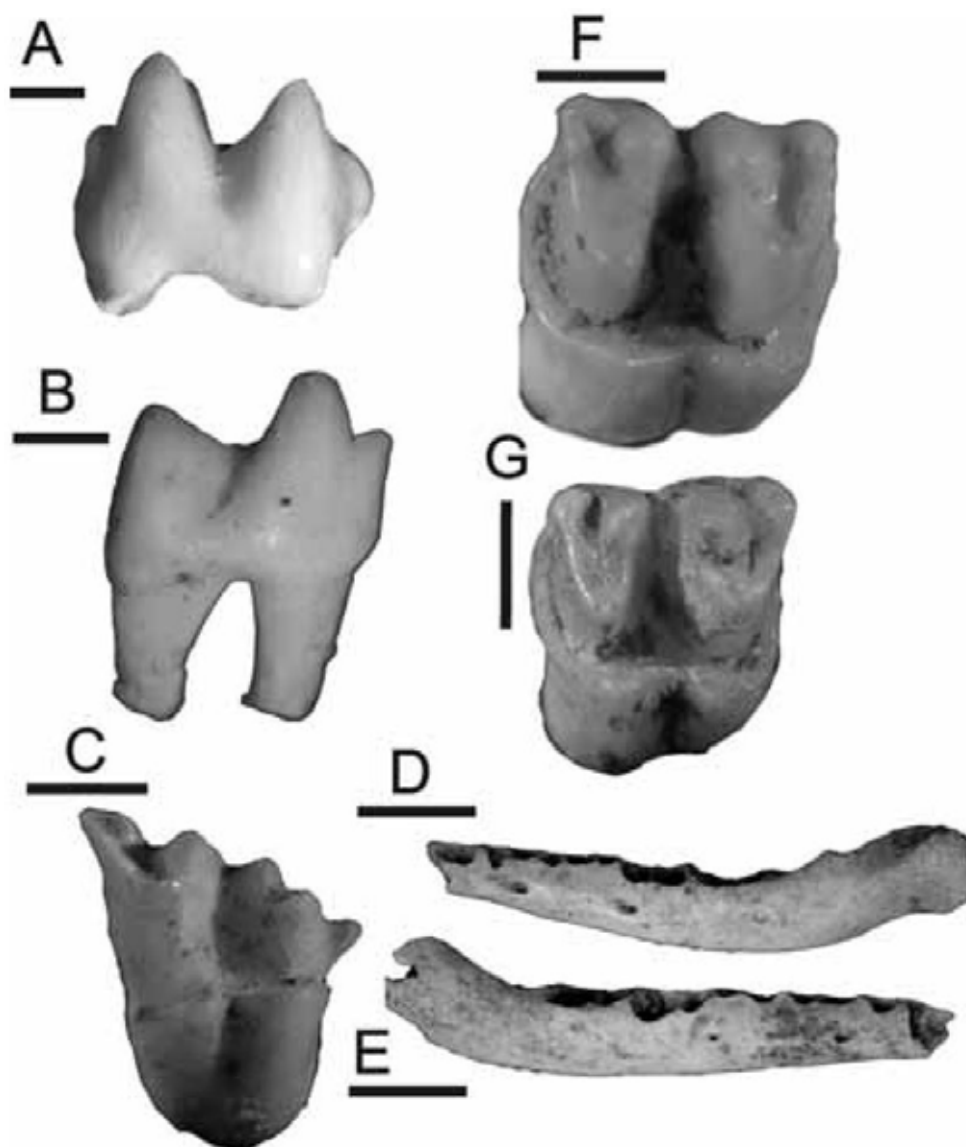


Figure 2-13 (FIG. 13.) A-G, Peramelidae; A. *Perameles* sp. 1; QMF51613,  $LM^1$ . B, *Perameles* sp. 2; QMF51621,  $RM$ . C-E, *Perameles bougainville*; QMF51627,  $RM$ . Scale bar= 1mm. D, QMF51628, left mandible. E, QMF51529, right mandible. Scale bar = 5mm. F, *Isoodon obesulus*; QMF51632,  $RM^2$ . G, *Isoodon* sp.; QMF51635,  $RM^2$ . Scale bar= 1mm.

The identification presented here is made with some caution due to the absence of *P. eremiana* from comparative collections available. However, Muirhead (1994)

provides characteristics to split these two species. These features included the development of the posterior cingulum (complete on  $M_1$  in *P. eremiana* and incomplete on  $M_1$  of *P. bougainville*) and the hypoconulid. Features characteristic of *P. bougainville* are shared with the fossil over *P. eremiana*. It is unlikely that the fossil taxon represents an extinct species based on the closeness in morphology to *P. bougainville*. Instead, it may represent a larger-sized eastern population of the arid-adapted *P. bougainville*. This record represents the most easterly and northerly record of the small-sized, arid-adapted members of *Perameles*.

**Isoodon** Desmarest, 1817

**Isoodon obesulus** (Shaw, 1797)

(Fig. 13F)

MATERIAL. QMF51632-QMF51634; QML1312, QML1384U, QML1420.

*Isoodon* fossils are abundant in the QML1384U and QML1312 deposits. These specimens are referred to *Isoodon* based on the following combined features: 1. Well developed anterior and posterior cingulae on  $M^{1-3}$ ; 2. Styler corners well within the tooth crown margins on  $M^{2-3}$ ; 3. Styler cusps B & D oriented lingually; 4. Deep, dumb-bell shaped lingual root on upper molars; 5. Cuspid at the anterobuccal base of the hypoconid, 6. Anterior cingulae on  $M_2-4$  terminates just ventral to the paraconid.

Morphologically, the fossils differ from *I. macrourus* and *I. auratus* in possessing distinct metaconules and protocones on  $M^{1-3}$ , where the postprotocrista and premetaconule crista form an acute angle between the two cusps. They also agree in size with modern *I. obesulus*.

**Isoodon** sp. (Fig. 13G)

MATERIAL. QMF51635-QMF51636; QML1384U, QML1312.

Specimens of a species of *Isoodon* represent a second species. The specimens are smaller than all three extant *Isoodon* species, being closer to *I. obesulus* than *I. macrourus* and *I. auratus*. In morphology the specimens differ from all species of *Isoodon* by possessing an incomplete anterior cingulum on  $M_2$  and narrower metastyle-stylar cusp D and parastyle-stylar cusp B distances. The fossil specimens are all smaller than those teeth assigned to *I. obesulus* from the same deposit.

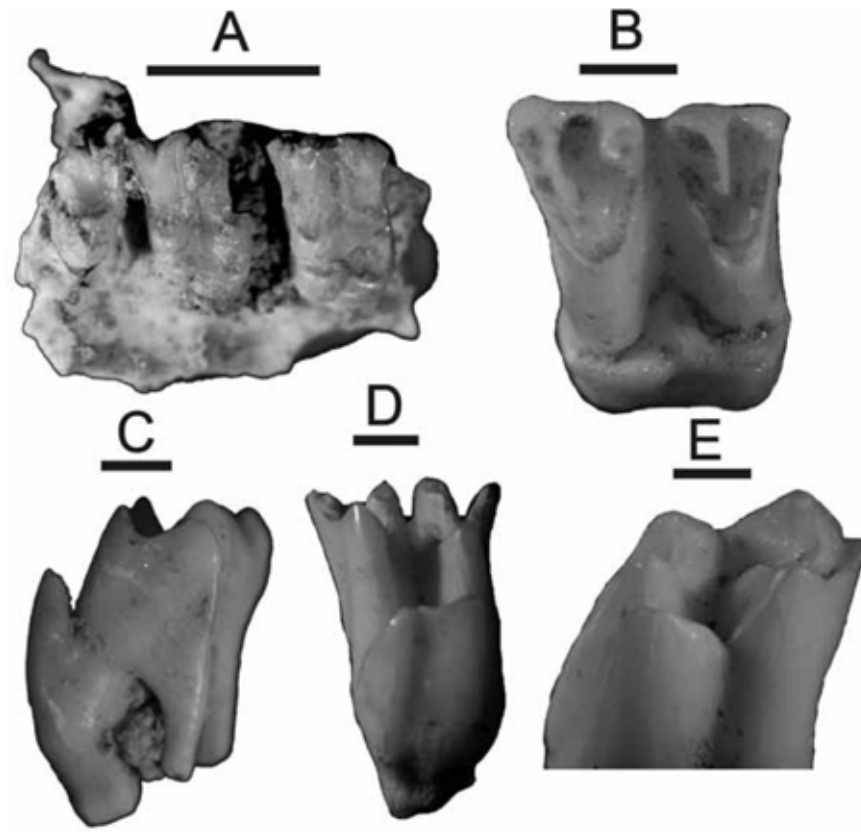


Figure 2-14 (FIG. 14.) A-D, Peramelidae; A-D, *Chaeropus ecaudatus*; A, QMF51637, RM<sup>3-4</sup>. Scale bar = 5mm. B-C, QMF515638, RM<sup>2</sup>, occlusal & anterior views. D, QMF51639, RM<sup>3</sup>. E, Thylacomyidae; *Macrotis lagotis*; QMF51642, RM<sup>1</sup>. Scale bar= 1mm.

### *Chaeropus* Ogilby, 1838

#### *Chaeropus ecaudatus* (Ogilby, 1838)

(Fig. 14A-D)

MATERIAL. QMF51637-51641; QML1312.

*Chaeropus ecaudatus* is only known from QML1312 and is the third most abundant bandicoot in that deposit. *C. ecaudatus* has been identified from upper molars using the following combination of characteristics defined by Muirhead

and Godthelp (1995): 1. Near parallel preparacristae and postmetacristae to each other and almost perpendicular to the long axis of the tooth crown. 2. Absence of both an anterior and posterior cingulae. 3. Very tall and slender molar crowns. 4. Preprotocristae and postprotocristae terminate at the base of the paracone and metacone respectively. 5. Preparacristae straight with no anterior curvature.

Family THYLACOMYIDAE (Bensley, 1903)

**Macrotis** Reid, 1837

**Macrotis lagotis** (Reid, 1837)

(Fig. 14E)

MATERIAL. QMF51642-51643; QML1312.

The Greater Bilby is an enigmatic species of bandicoot with a highly specialised and distinctive tooth morphology. Two molars have been recovered from QML1312. Identification of the teeth as *M. lagotis* was based on the following combination of features. 1. Absence of the paraconid, 2. Absence of the metaconule, 3. Rectangular-ovoid molar crowns, 4. Dumbell-shaped molar roots and 5. Large cuspid on the anterobuccal side of the lower molars (considerably larger than that found in *Isoodon*).

Family INCERTAE SEDIS

Two new bandicoots are present in the fauna with uncertain family-level taxonomic position. Several indications of new bandicoot groups within the Late Tertiary have been made in the literature (Muirhead, 1994, 1999; Dawson et al.,

1999; Long et al., 2002) without formal description. One family, the Yaralidae, are described from the Oligo-Miocene (Muirhead, 2000) and are thought to occur into the Pliocene (Long et al., 2003). Based on dentition alone, family-level taxonomy becomes complicated with several previously definitive features now thought to be plesiomorphies (Muirhead, 1994; 2000; Muirhead & Filan, 1995). It is for this reason that these two distinct bandicoots will remain *incertae sedis* with the possibility of their placement within the plesiomorphic family Yaralidae.

Recently, Turnbull et al., (2003) erected a new bandicoot taxon, cf. *Peroryctes tedfordi* from the Early Pliocene Hamilton Fauna. Although they place the taxon in the Peroryctidae, they did note its plesiomorphic features and similarity to *Yarala*. The taxa identified below are morphologically very similar to cf. *Peroryctes tedfordi*, however, I reserve the placement of these taxa into any perameloid family until a full revision of both the Hamilton and Mt Etna material is available.

Gen. et sp. nov. 1

(Fig. 15A)

MATERIAL. QMF51644; QML1311 (H).

A large species of perameloid, similar in size to *Echymipera rufescens*, possessing the following features: 1. A distinct anterior cingulum on M1. 2. Trigonid extremely compressed with protoconid and metaconid cusps high and approximated. 3. Paraconid small. 4. Bladed entoconid. 5. Hypoconulid heavily reduced on M1-2, less so on M3. 6. M2-3 trigonid with protoconid-metaconid relatively more broader than corresponding cusps on M1. 7. Posthypocristid contacts the base of the entoconid on M1-3. 8. Cristid obliqua terminates on the posterior trigonid flank, buccally of the tooth midline.

This taxon shares a complete and distinctive anterior cingulum with only one other

published bandicoot, *Yarala burchfieldi* from the Oligo-Miocene of Riversleigh, Far North Queensland (Muirhead & Filan 1995). It differs from *Yarala burchfieldi* by possessing a bladed entoconid, smaller hypoconulids, posthypocristid that contacts the entoconid and a less posteriorly placed metaconid.

Gen et sp. nov. 2

(Fig. 15B)

MATERIAL. QMF51645-QMF51650; QML1284, QML1284a, QML1311(H), QML1384U, QML1313, QML1385, QML1311 (C/D).

A medium-sized bandicoot possessing the following dental characteristic: 1. M1 with anterior cingulid present as distinct antero-dorsally projecting cuspule. 2. A small buccal cuspule between metaconid and hypoconid. 3. Compressed trigonid with all three main cusps closely approximated. 4. Bladed entoconid on <sub>M1</sub>. 5. Posthypocristid runs to the base of the entoconid on M1-3. 6. Hypoconulid reduction on M1, further reduction on M2 and near absent on M3. 7. Cristid obliqua runs to the middle of the posteroventral flank of the trigonid. 8. Talonid broadens consecutively along molar row.



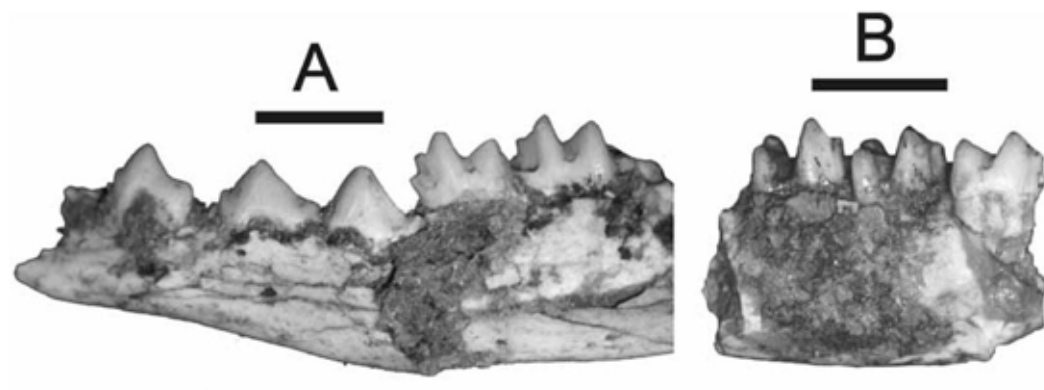


Figure 2-15 (FIG. 15.) A-B, Family incertae sedis; A, Gen. et sp. nov. 1; QMF51644, LP1-M3. B, Gen. et sp. nov. 2; QMF51645, RM1-3. Scale bar = 5mm

Family DASYURIDAE Goldfuss, 1820 *sensu*  
Waterhouse, 1838

Dasyurids are a conspicuous part of all of the faunas, being represented by isolated teeth, nearly complete mandibles and maxillae, or even partial skulls. Identification of dasyurids follows the character states defined by Wroe and Mackness (1998) for *Dasyurus*, Van Dyck (2002) for *Antechinus*, Archer (1981) for *Sminthopsis*, Dawson (1982a) for modern and fossil *Sarcophilus*, Archer (1976) for *Planigale* and Wroe et al. (2000) for other dasyurid genera.

**Antechinus** Macleay, 1841

*Antechinus* is a morphologically diverse group as defined by Van Dyck (2002).

Specimens were identified as *Antechinus* on the basis of the combined features: 1. Complete posterior cingulum on upper molars. 2. P3 / P<sup>3</sup> reduced. 3. Meta- and hypocristids not transverse to the longitudinal axis of the jaw. 4. Entoconid variably present.

**Antechinus** sp. 1

(Fig. 16A)

MATERIAL. QMF51651-51653, QMF51654-51657; QML1313, QML1284a.

*Antechinus* sp. 1 is allied very closely to *Antechinus adustus* based on maxillary morphology. The fossil maxillae possessed the greatest number of maxillary character-states provided by Van Dyck (2002) for *A. adustus*, which included characters; 18-19, 22, 25-28, 30, 33, 36-37. Mandibles and isolated lower molars conform in size to the maxillary specimens, however, they do not conform in the character-states that are present in *A. adustus*. Instead, the mandibles show a greater similarity to *A. godmani* or *A. minimus* (characters 40-46; 48-54). Due to the very small sample size, these morphological variations may either constitute a single morphologically distinct new taxon or two similarly-sized known

species of modern *Antechinus*. The most convincing characteristics seem to be from the maxilla, thus *A. adustus* would be considered the most likely taxon present in the deposits.

***Antechinus* sp. 2**

MATERIAL. QMF51663-51680; QML1284a, QML1385, QML1311(C/D), QML1420, QML1311(H), QML1313, QML1284.

A second species of *Antechinus* is present and differs from *Antechinus* sp. 1 by being larger in overall dimensions and possessing a relatively larger P3. This species of *Antechinus* does not possess any greater similarity to any of the modern species of *Antechinus*.

***Antechinus flavipes* (Waterhouse, 1838)**

(Fig. 16B)

MATERIAL. QMF51681-51685; QML1312, QML1384U.

*Antechinus flavipes* has been identified by numerous fragmentary and complete maxillae and mandibles. The most complete specimens, which are also the easiest to identify, are the mandibles. Using the characteristics provided by Van Dyck (1982, 2002) and Smith (1972), which included: 1. Tiny and crowded P3. 2. Transversely orientated P3. 3. Small entoconids. 4. Small paraconid. 5. Size (7.54-7.66mm<sub>M1-4</sub> Length), I am able to differentiate this species from a second species present in the same deposit, *Antechinus swainsoni*.

***Antechinus swainsoni* (Waterhouse, 1840)**

(Fig. 16C)

MATERIAL. QMF51686-51688; QML1312.

*Antechinus swainsoni* is also represented by numerous maxillae and mandibles. Using features in Van Dyck (1982) that differentiate *A. flavipes* from *A. swainsoni*, this smaller species was able to be distinguished. The premolar row is not crowded as in *A.*

*flavipes*, the mandible is gracile and  $M_{1-4}$  length reaches 7.30-7.34mm.

***Dasyurus* Geoffroy, 1796**

*Dasyurus* was identified by the absence of  $P^3$  or  $P3$  (except *Dasyurus dunmalli*) and its moderately large-sized molars and total mandibular dimensions (larger than *Phascogale*, smaller than *Sarcophilus* and *Glaucodon*).

***Dasyurus hallucatus* Gould, 1842 MATERIAL.** QMF51689, QML1312.

A small-sized *Dasyurus*, differing from other modern and extinct *Dasyurus* by possessing a relatively shorter metacrista length on  $M^3$  than  $M^2$ , and a metacone on  $M^1$  perpendicular to stylar cusp D.

***Dasyurus viverrinus* (Shaw, 1800)**

(Fig. 16K)

**MATERIAL.** QMF51690-51695; QML1312; QML1384U.

A medium-sized *Dasyurus*, differing from other modern and extinct *Dasyurus* by possessing a longer metacrista on  $M^3$  than on  $M^2$ ; metacone anterior to stylar cusp D; reduced paracones; not bulbous (as in *D. maculatus*); reduced metaconid.

Differs specifically from *D. geoffroyi*, a species most similar to *D. viverrinus*, by having relatively longer metacristae. Fossil specimens show similarities to *D.*

*maculatus*, including a small entoconid and a reduced posterior cingulid on  $M_{1-3}$ .

These features are intriguing and with more specimens may constitute further review, however, at the present time there are significantly more morphological features shared with *D. viverrinus*.

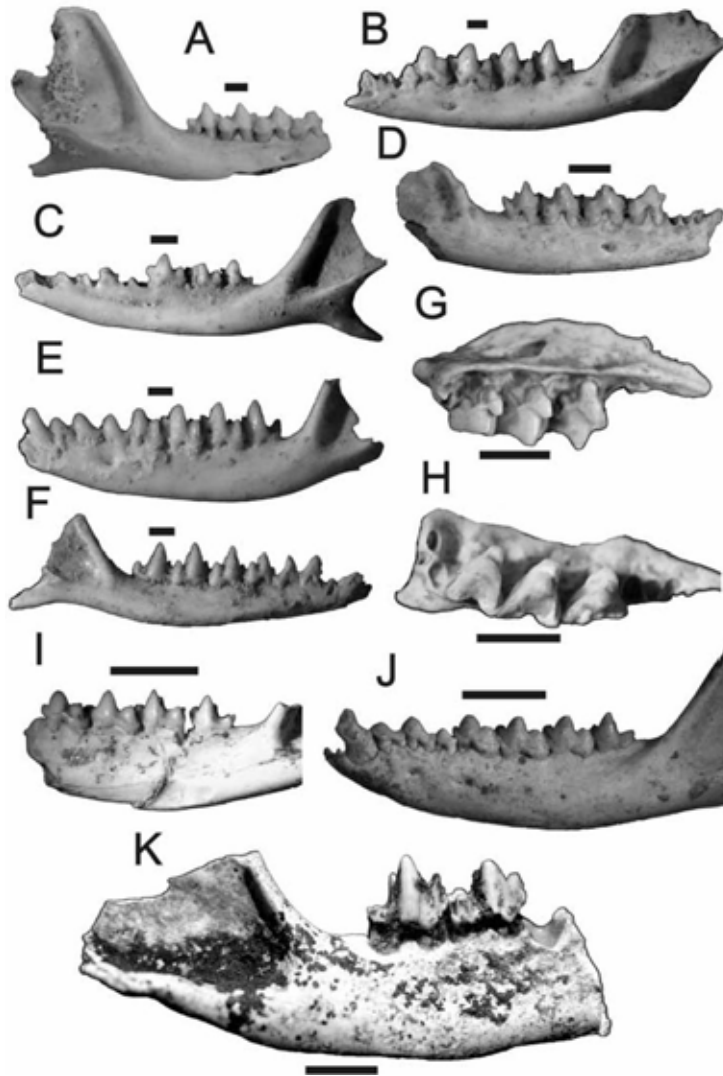


Figure 2-16 (FIG. 16.) A-K, Dasyuridae; A-C, *Antechinus*; A, *Antechinus* sp. 1; QMF51651, RM1-4. B, *Antechinus flavipes*; QMF51681, LP3-M4. C, *Antechinus swainsoni*; QMF51686, LM2-4. D, *Planigale maculate*; QMF51707, RM1-4. E-F, *Sminthopsis*; E, *Sminthopsis macroura*; QMF51715, LC1-M4. F, *Sminthopsis murina*, QMF51724, RP2-M4. G-H, Gen et sp. nov.; QMF51743, lingual and occlusal views. Scale bar = 1mm. I-J, *Phascogale*; I, *Phascogale* sp.; QMF51704, LM1-4. J, *Phascogale topoatafa*; QMF51699, LC1-M4. K, *Dasyurus viverrinus*; QMF51690, RM3-4. Scale bar = 5mm.

**Dasyurus** sp. MATERIAL. QMF51696-51698; QML1313.

A medium-sized species of *Dasyurus* is represented by an isolated M2, M<sup>2+3</sup>.

There are not enough features available on the specimen to warrant specific placement at the present time.

**Phascogale** Temminck, 1824

Species of *Phascogale* are distinguished from other similar dasyurids by the P3 being higher than P2 and by being considerably larger than the only other dasyurid exhibiting the former trait, *Sminthopsis*.

**Phascogale topoatafa** (Meyer, 1793)

(Fig. 16J)

MATERIAL. QMF51699-51703; QML1312.

*Phascogale topoatafa* is distinguished from *Phascogale calura* by being larger, possessing a small posterior cusp on P<sup>3</sup> and possessing a smaller protocone on M<sup>1-3</sup>.

**Phascogale** sp.

(Fig. 16I)

MATERIAL. QMF51704-51706; QML1420, QML1313.

A small, possibly undescribed, species of *Phascogale* is tentatively identified here based on the great number of similarities (as defined by Van Dyck (2002)) shared with both *P. topoatafa* and *P. calura*. Its smaller size seems to differentiate it from the two extant species of *Phascogale*, however, further analysis of *P. calura* is needed to determine whether the fossil specimens are within the variation for this species.

**Planigale** Troughton, 1928

**Planigale maculata** (Gould, 1851)

(Fig. 16D)

MATERIAL. QMF51707-QMF51711, QML1312; Olsens Cave.

A species of *Planigale* was identified based on its diminutive size, reduced single-rooted P3, absent entoconid, present posterior cingulum and reduced styler cusps, especially styler cusp D on M<sup>2-3</sup>. *P. maculata* was distinguished by its size, being smaller than *P. novaeguineae*, larger than *P. ingrami* and *P. tenuostris*, and by possessing P3 (versus *P. gilesi*, which does not).

#### **Sarcophilus** Cuvier, 1837

Species of *Sarcophilus* were determined by using criteria described by Dawson (1982a) for *Sarcophilus lanianus* and *Sarcophilus harrisii*. No site has yet been found where both taxa can be said to occur sympatrically, however, a fragment of a mandible which is referred to here as *Sarcophilus lanianus* may have been derived from sediments from within Lower Johansen's Cave, a site containing the only representative of *Sarcophilus harrisii*.

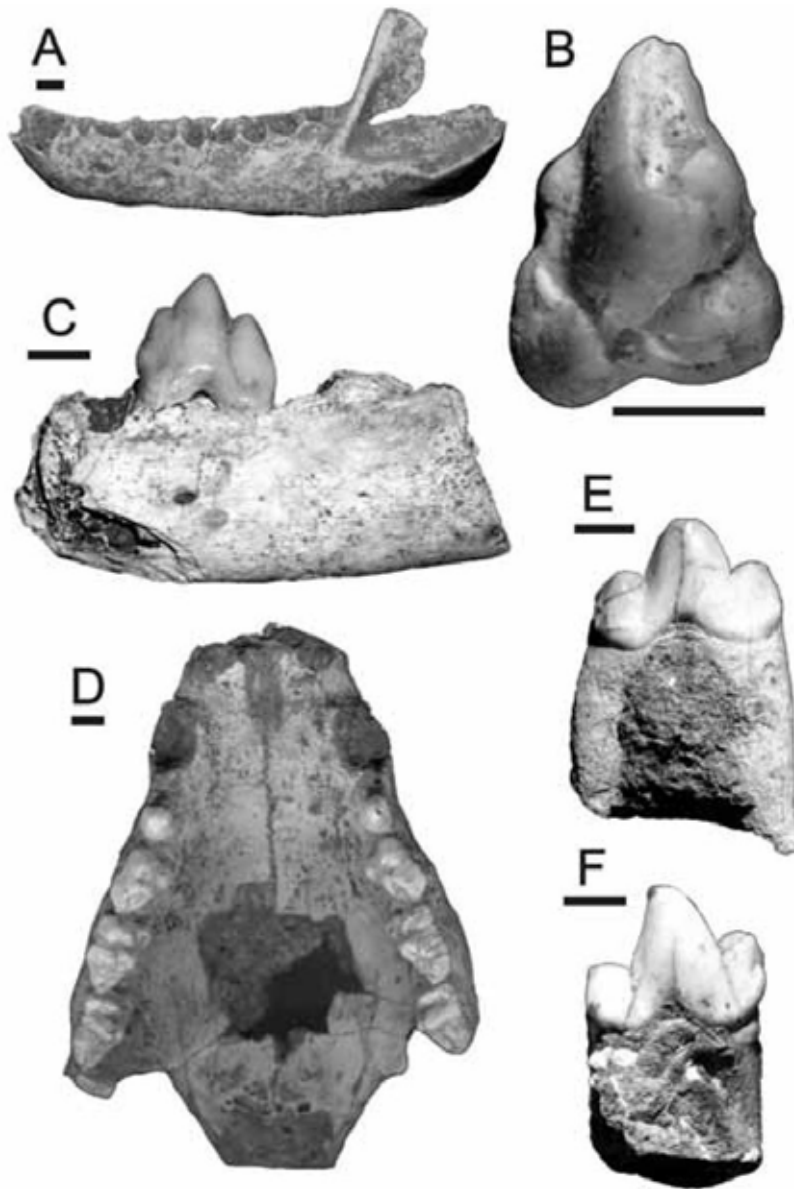


Figure 2-17 (FIG. 17.) A-D, Dasyuridae; *Sarcophilus*; A, *Sarcophilus harrisii*; QMF51712, left mandible. B-D, *Sarcophilus lanarius*; B, QMF41997, LM<sup>1</sup>. C, QMF51713, LM1. D, QMF1872, partial skull. E-F, Thylacinidae; *Thylacinus cynocephalus*; E, QMF1737, RM2. F, QMF51755, RM1. Scale bar = 5mm.

***Sarcophilus harrisii* (Boitard, 1841)**



(Fig. 17A)

MATERIAL. QMF51712; QML1314.

*Sarcophilus harrisii* is represented by an edentulous left mandible (M1-4 alveoli length: 39.50mm). The specimen differs markedly from *Sarcophilus lanarius* known from the Darling Downs and specimens from Marmor Quarry by being much smaller in size and having a more gracile lateral profile.

***Sarcophilus lanarius* (Owen, 1838)**

(Fig. 17B-D)

MATERIAL. QMF693, QMF1872, QMF51713- QMF51714, QMF41997; QML1420, QML1311(H), QML1312, QML1384U, QML1384L.

*Sarcophilus lanarius* is represented by isolated molars, a partial mandible and an almost complete palate. The distinctive large triangular dasyurid molars unquestionably place these specimens within *Sarcophilus*. The large size and robust nature of the palate and molars allies these specimens with those of typical *Sarcophilus lanarius* from the eastern Darling Downs and those measured by Dawson (1982a).

***Sminthopsis* Thomas, 1887**

Archer (1981) reviewed the taxonomy of *Sminthopsis*, providing keys to the species using either external or skeletal features. Species of *Sminthopsis* were identified on the basis of their compressed upper and lower molars; absent posterior cingulum on upper molars; transverse meta- and hypocristids; and subequal premolar heights.

***Sminthopsis macroura* (Gould, 1845)**

(Fig. 16E)

MATERIAL. QMF51715-QMF51723; QML1312, QML1384, QML1314.

*Sminthopsis macroura* was identified by possessing the following features: large

and distinct entoconid; hypocristid that does not contact the entoconid; C1 not enlarged; premolars longer than broad; medium-sized species (M1-4L = 5.8mm).

***Sminthopsis murina*** (Waterhouse, 1838)

(Fig. 16F)

MATERIAL. QMF51724-51739; QML1312, QML1313, QML1420, QML1284, QML1284a, QML1385, Olsen's Cave.

Difficulty was experienced in identifying a second species of *Sminthopsis*, distinguished by the absence of the entoconid. Very few features were available from Archer (1981) to distinguish species of this group based simply on mandibular or maxillary features. Three species were possible candidates; *S. butleri*, *S. leucopus* and *S. murina*. *S. butleri* was excluded because it apparently shows signs of tiny entoconids on M1-3, the fossil specimens do not. *S. leucopus* was excluded because the fossil specimens show premolars that do slightly contact each other, a feature generally not seen in *S. leucopus*, however, this is a relatively variable trait. *S. murina* is preferred until further analysis is possible.

Gen. et sp. nov. (Fig. 16G-H)

MATERIAL. QMF51743-51754; QML1311(H), QML1385, QML1284, QML1284a, QML1313, QML1384U.

A tiny dasyurid, similar in size to *Planigale* and *Ningaui*, possesses heavily reduced upper dentition, including a significantly reduced protocone on M<sup>1-3</sup>; an extremely reduced paracone on M<sup>1</sup>; absent styler cusps D and B on all molars; and a distinct ectoloph indentation. There are only four roots found between the canine root and M<sup>1</sup> suggesting the loss of p<sub>3</sub> as in *Planigale gilesi*. The possession of these distinctly derived traits (*sensu* Wroe et al., 2000) suggests the possible need to erect a new genus of dasyurid to accommodate this highly distinctive taxon. More complete material will soon be available and a more formal description and analysis is underway.

Family THYLACINIDAE Bonaparte, 1838

**Thylacinus** Temminck, 1824

**Thylacinus cynocephalus** (Harris, 1808)

(Fig. 17E-F )

MATERIAL. QMF1737, QMF51755-QMF51757; QML1420, QML1313, QML1311(H), QML1311 (C/D), QML1312.

Several isolated molars and an almost complete skull and mandibles represent the marsupial carnivore, *Thylacinus cynocephalus*. They compare favourably with modern and fossil specimens assigned to *T. cynocephalus*, falling within the variation provided by Dawson (1982b).

**Table 2-3 (TABLE 3.) Faunal lists for large-sized mammal species**

	QML1284	QML1284a	QML1311H	QML1311CD	QML1312	QML1313	QML1384U U	QML1384LU	QML1420
<i>Thylacinus</i>			X	X	X	X			X
<i>Vombatus ursinus</i>				X					X
?zygomaturine									X
<i>Palorchestes</i> sp. cf. <i>P.</i>			X	X					X
?diprotodontid indet			X						
<i>Bohra</i> sp.				X					
<i>Kurrabi</i> sp.			X	X					
<i>Protemnodon</i> sp. cf. <i>P.</i>	X		X	X					
macropodine indet.	X	X	X				X	X	X
<i>Macropus</i> sp. 1					X				X
<i>Macropus</i> sp. cf. <i>M. agilis</i>			X						X
<i>Macropus titan</i>									X
<i>Thylacoleo</i> sp.								X	X
<i>Thylacoleo hilli</i>			X						

Family VOMBATIDAE Burnett, 1830

**Vombatus** Geoffroy, 1803

**Vombatus ursinus mitchellii** (*sensu* Dawson,

1983)  
(Fig. 18A)

MATERIAL. QMF51758, QMF1420; QML1311 C/D, QML1420.

The only large marsupial with hypsodont molars, wombats are easily identified from any deposit. *Vombatus* is represented from QML1420, Marmor Quarry, by an incomplete left mandibular ramus with molars and incisor root preserved, and a partial right maxilla. A single tooth, within a partial maxilla has also been recovered from QML1311 Unit C/D. Based on size comparisons, the three specimens are much smaller than *Phascolonus* and slightly smaller than *Phascolomys medius*, falling within the size range of the Late Pleistocene *Vombatus ursinus mitchelli* (*sensu* Dawson 1983; Murray 1998) from the eastern Darling Downs.

Family DIPROTODONTIDAE Gill, 1872

?zygomaturine  
(Fig. 18B )

MATERIAL. QMF1419, QML1420.

Tooth fragments of a diprotodontid from Marmor Quarry which were initially identified by Longman (1925a) as *Diprotodon australis* are revised to ?zygomaturine. Two of the three tooth fragments come from the same molar. The fragments consist of a protolophid which possesses a narrow anterior cingulum. The third tooth fragment may come from the same molar and represents the posterior lingual side of the molar, preserving the lingual edge of the hypolophid. The tooth is low crowned and the lophs are relatively straight and narrow. Based on this, and comparing the molars to specimens of *Zygomaturus*, *Euryzygoma* and *Diprotodon*, it seems most likely that the tooth came from a species *Zygomaturus*. Phalanges and fragments of vertebrae have also come from Marmor Quarry, however, these do not aid in the identification of this relatively large form of diprotodontid.

Family PALORCHESTIDAE (Tate, 1948)

**Palorchestes** Owen, 1873

**Palorchestes** sp. cf. **P. parvus** De Vis, 1895

(Fig. 18C-D)

MATERIAL. QMF51759-51760, QMF42635 (cast) / BMNH10257;  
QML1311(H); QML1311 (C/D), QML1420.

*Palorchestes* is represented by an isolated M2, a left maxillary fragment preserving the posterior portion of M and a complete M<sup>2</sup>, and a left I<sup>1-2</sup>. Left<sub>1</sub> large, curved and broad distally. LI<sup>2</sup> broad with tapering root. LM<sup>1</sup> preserves a double mid-link and a posterior-lingual fossette. LM<sup>2</sup> ovo-rectangular in occlusal view, lophs relatively narrow with the metaloph slightly narrower than paraloph. Single mid- and forelink. Anterior cingulum deep and completely running the length of the molar, bisected by forelink. Buccal cingulum present between paracone and metacone. Postero-lingual pocket. No posterior cingulum. M2 rectangular in occlusal view, lophids high and narrow, distinct fore- and mid-link, posterior cingulid absent.

These specimens cannot be assigned to a species of *Palorchestes* because they lack diagnostic features of the M<sub>1</sub> (Black, 1997). Based simply on size, the specimens are from a small species of *Palorchestes*, much smaller than *P. azael* and very similar in size to *P. parvus*. The M2 is larger than the species recovered from the Hamilton LF, which was considered by Turnbull & Lundelius (1970) to be *Palorchestes painei*. This identification has been challenged by Rich (1991) who considers it to represent a new taxon, illustrating the taxonomic uncertainty surrounding the smaller members of the Palorchestidae.

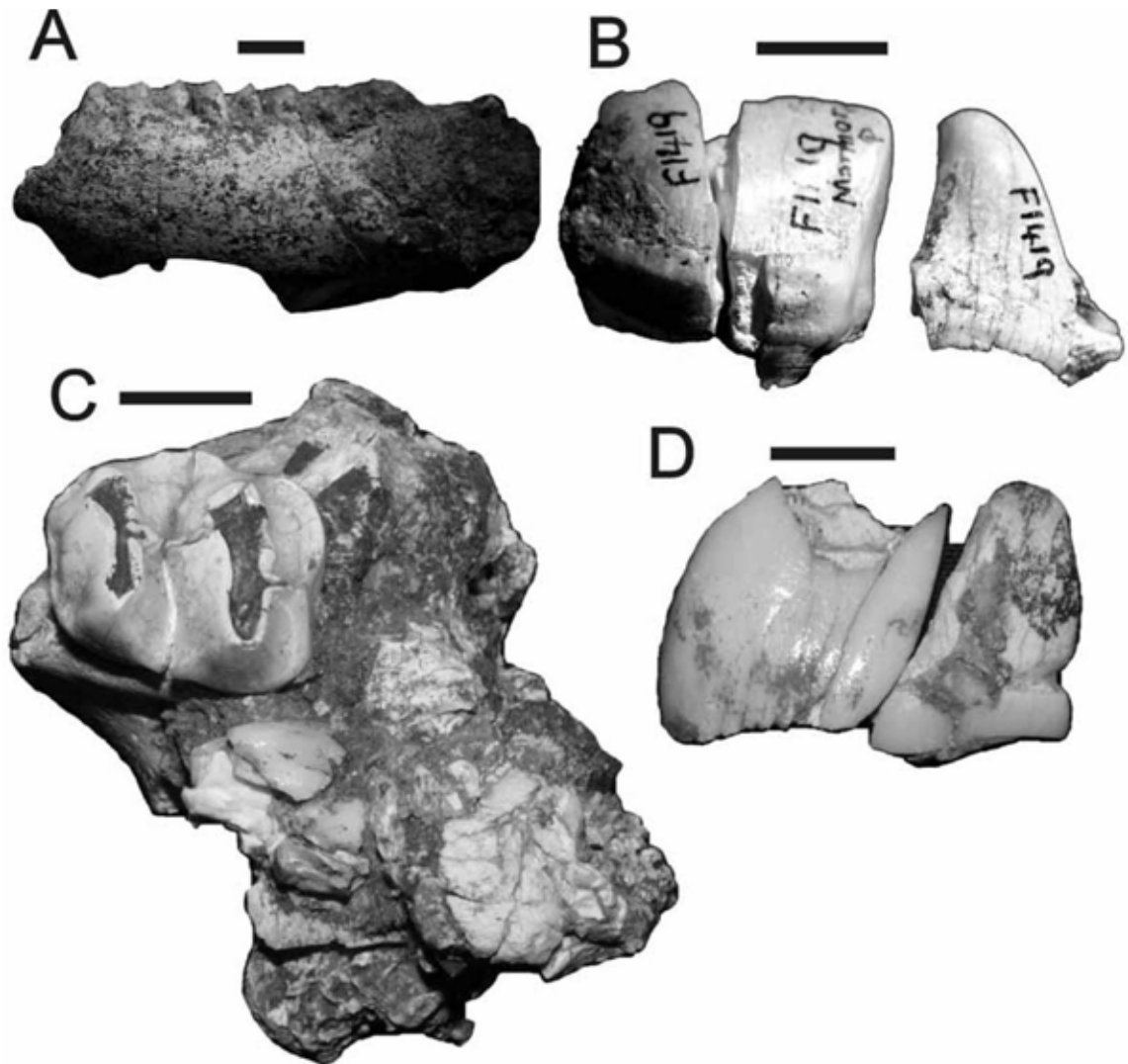


Table 2-18 (FIG. 18.) A, Vombatidae; *Vombatus ursinus mitchelli*; QMF1420, LM1-4. B, ?Zygomaturine; QMF1419, fragmentary mo Zar. C-D, Palorchetidae; *Palorchestes* sp. cf. *P. parvus*; C, QMF51759, RM<sup>2</sup> (partial M<sup>1</sup>). D, QMF51760, LI<sup>1</sup>. Scale bar = 10mm.

?diprotodontid indet.

MATERIAL. QMF51761; QML1311H.

Approximately a quarter of a lower molar possibly represents a small diprotodontid. The tooth is low crowned, lophodont and bears thick slightly crenulated enamel distinctive in several diprotodontian groups. The molar is distinctly not macropod based on the thickness of the enamel and the crenulations are not as distinct as those found in the Sthenurinae. The lophids are lower than those found in palorchestids.

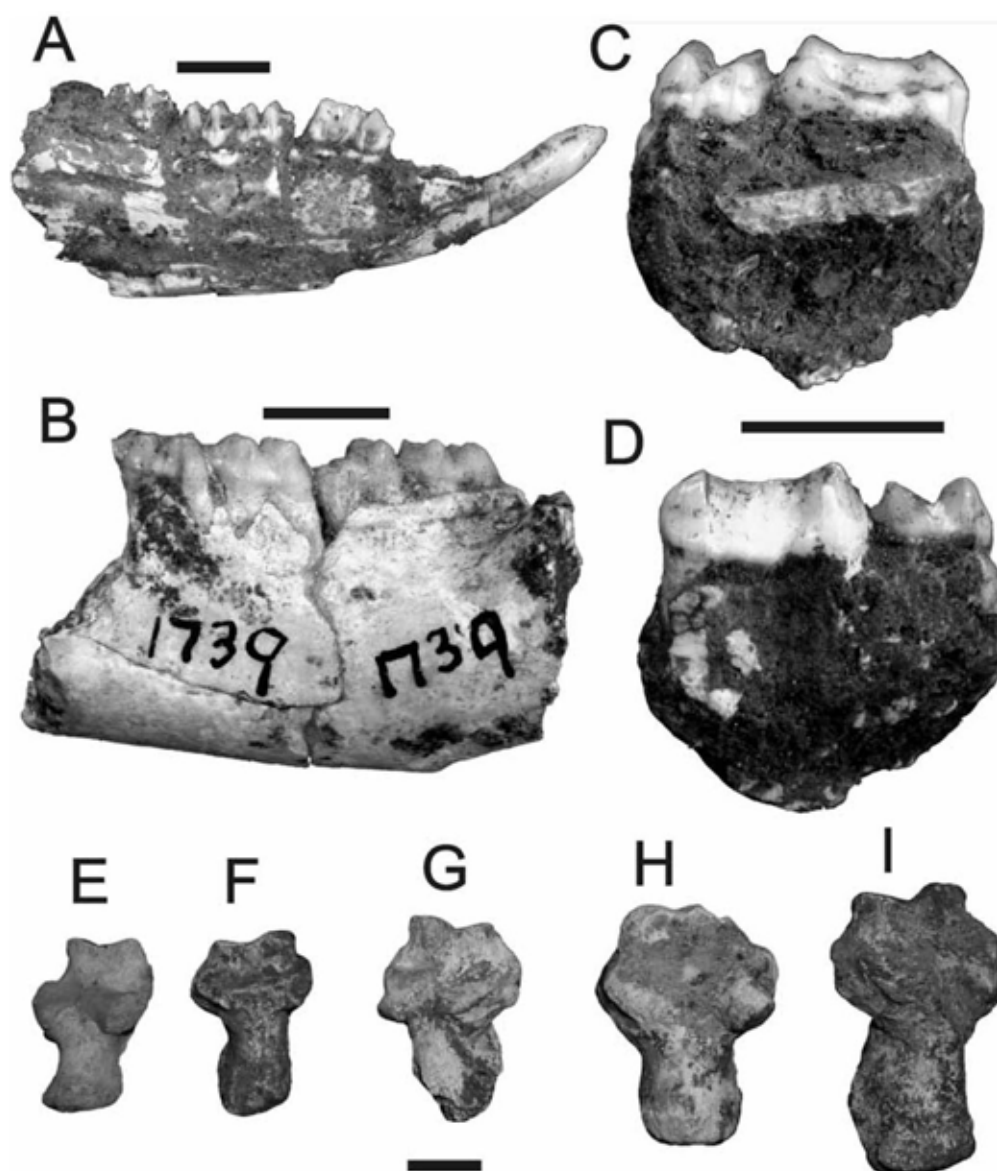


Figure 2-19 (FIG19.) A-I, Macropodidae. A-H, *Dendrolagus* sp.; A, QMF51770, RI1-M4. B, QMF1739, LM1-4. C-D, QMF51771, RP<sup>3</sup>-M<sup>1</sup> in lingual and buccal view (showing postero-buccal cuspule on P<sup>3</sup>). E-H, Calcanea; QMF51772-51775 (left to right). I. *Bohra* sp.; QMF51783, calcaneum. Scale bar = 5mm.



Family MACROPODIDAE Gray, 1821

**Bohra** Flannery & Szakay, 1982

**Bohra** sp. (Fig. 19I)

MATERIAL. QMF51762; QML1311C/D.

*Bohra* sp. is represented by a complete right calcaneum (Calcaneal Length: 46.79mm; Calcaneal-Cuboid articulation height 12.43mm and width 18.96; Astragalar-calcaneal articulation length 23.01mm). The calcaneum is placed within *Bohra* on the basis of the following features it shares with *Bohra paulae*: 1. Massive calcaneal size relative to all other dendrolagine macropods. 2. Height to width of calcaneal-cuboid articulation (Flannery & Szakay, 1982) (0.65). 3. Calcaneal length to astragalar-calcaneal articular length (Flannery & Szakay, 1982) (0.49).

**Dendrolagus** Muller & Schkegel, 1839

**Dendrolagus** sp.

( Fig. 19A-H)

MATERIAL. QMF51770-QMF51783; QML1284, QML1311(H), QML1311(C/D), QML1312, QML1385, QML1420.

*Dendrolagus* is represented by two nearly complete mandibles, three maxillary fragments, isolated premolars, molars and three calcanea. The mandibles are characterised by possessing low crowned, square molars and an elongate, blade-like P3. P3 blade bounded by a large anterior cusp and posterior cusp. A single intermediate cuspule is situated a third the way along the crest. The upper dentition is characterised by an ovo-rectangular P<sup>3</sup> in occlusal view, possessing low-crowned square molars with weak midlinks and absent forelinks. P<sup>3</sup> with both postero-buccal and postero-lingual cuspules. Paracone linked to metacone via a crested blade. A single vertical ridge runs to a small cuspule near the centre of the

blade. A tiny accessory cuspule is present posterior to the main cuspule. Lingual cingulum runs the length of the tooth, terminating below the paracone. When compared with extant species of *Dendrolagus* the fossil taxon shares closest lower dentition morphology with *D. matschiei*, whereas the upper dentition most closely resembles *D. ursinus*. At present there are no morphological or morphometric features that suggest that the mandibles represent one taxon and the maxillae another. Further material will be needed to clarify the specific placement of these specimens,

however, it seems most probable that the fossils represent an extinct taxon with phylogenetic links to both *D. matschiei* and *D. ursinus*.

Calcanea have been identified by possession of a distinctive squat shape, short calcaneal tuberosity, and broad anterior articular facets. Four specimens have been recovered so far and all four are distinctly different in size. The largest is from QML 1420 Marmor Quarry (QMF51781), the second largest from QML1311 (QMF51780) and the smallest from QML1312. With so few calcanea available to compare, morphometric comparison with extant populations was not possible, however, the great difference in size between the largest and smallest calcanea may illustrate the presence of several species.

**Kurrabi** Flannery & Archer, 1984

**Kurrabi** sp. (Fig. 20A-D)

MATERIAL. QMF51767-51769; QML1311(H), QML1311 (C/D).

Three isolated P<sup>3</sup>'s represent a species of *Kurrabi*. Each premolar is elongate with two small vertical ridges on the longitudinal crest between the paracone and metacone. A moderate-sized fossette occurs on the posterior lingual side of the tooth. A lingual cingulum runs the length of the tooth, terminating just posterior of the base of the paracone. In size, the specimens are closest to *K. merriwaensis* (L: 9.2-

11.5mm). Without more material specific diagnosis is not warranted.

**Protemnodon** Owen, 1874

**Protemnodon** sp. cf. **P. devisi** Bartholomai,

1973

(Fig. 20E-H)

MATERIAL: QMF41737, QMF41953, QMF51763- QMF51766, QMF52068; QML1284, QML1311(H), QML1311 (C/D).

*Protemnodon* sp. cf. *P. devisi* has been identified from an isolated premolar; a badly preserved palate with portions of  $RP^2$ ,  $RdP^3$ ,  $RM^{1-3}$  and  $LdP^3$ ,  $RM^{1-2}$  preserved; a left mandible with M23; left mandible preserving P3; isolated  $RM^1$ , LM,  $LM^4$ ,  $LdP3$ , LM2, LM3 and an isolated I1. Dimensions of the premolar and molars are within the range given for *P. devisi* by Bartholomai (1973). However, the specimens here differ from *P. devisi* from Chinchilla, but are similar to those of *P. sp. cf. P. devisi* described by Dawson et al. (1999) from Big Sink, in the following ways: 1. Lower molars lack a posterior cingulum. 2. Upper molars lack a secondary link across the median valley. 3.  $P^3$  has weak vertical ridges. The specimens do possess premetacristae, which the Big Sink specimens do not. The overall variation seen in the specimens of *P. devisi* from Chinchilla, Big Sink and Mount Etna is within that seen for similar cosmopolitan species such as *P. anak*.

macropodine sp. indet

MATERIAL. QMF51802-51811; QML1284, QML1284a, QML1420, QML1384, QML1311(H).

Several isolated molars appear to represent a large species similar to species of *Thylogale*, however, being much greater in size. Other distinctive features of the molars include sharply crested postpara- and premetacrista running into the median valley; a sharply crested preparacrista linking onto the anterior cingulum, and a

well-developed forelink.

The molar is high crowned, and similar in shape to some species of *Macropus*, however, the mid-link is weakly developed and the cristae are sharp and elaborated unlike *Macropus*.

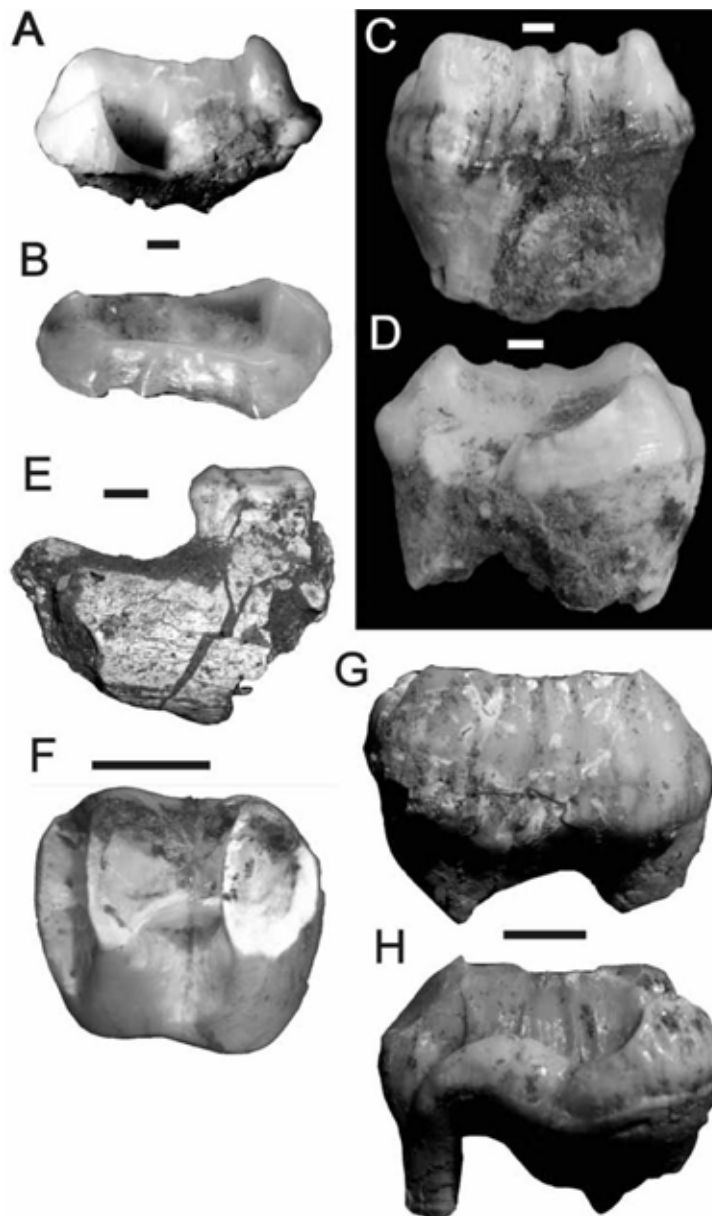


Figure 2-20 (FIG. 20.) A-H, Macropodidae. A-D, *Kurrabi* sp.; A-B, QMF51767; RP<sup>3</sup> in lingual & occlusal views. C, QMF51768, LP<sup>3</sup>. D QMF51769, LP<sup>3</sup>. Scale bar= 1mm. E-H, *Protemnodon* sp. cf. *P. devisi*; E, QMF41737, LP<sup>3</sup>. F, QMF41953, LM<sup>1</sup>. G-H, QMF51763; LP<sup>3</sup> in buccal & lingual views. Scale bar = 5mm.

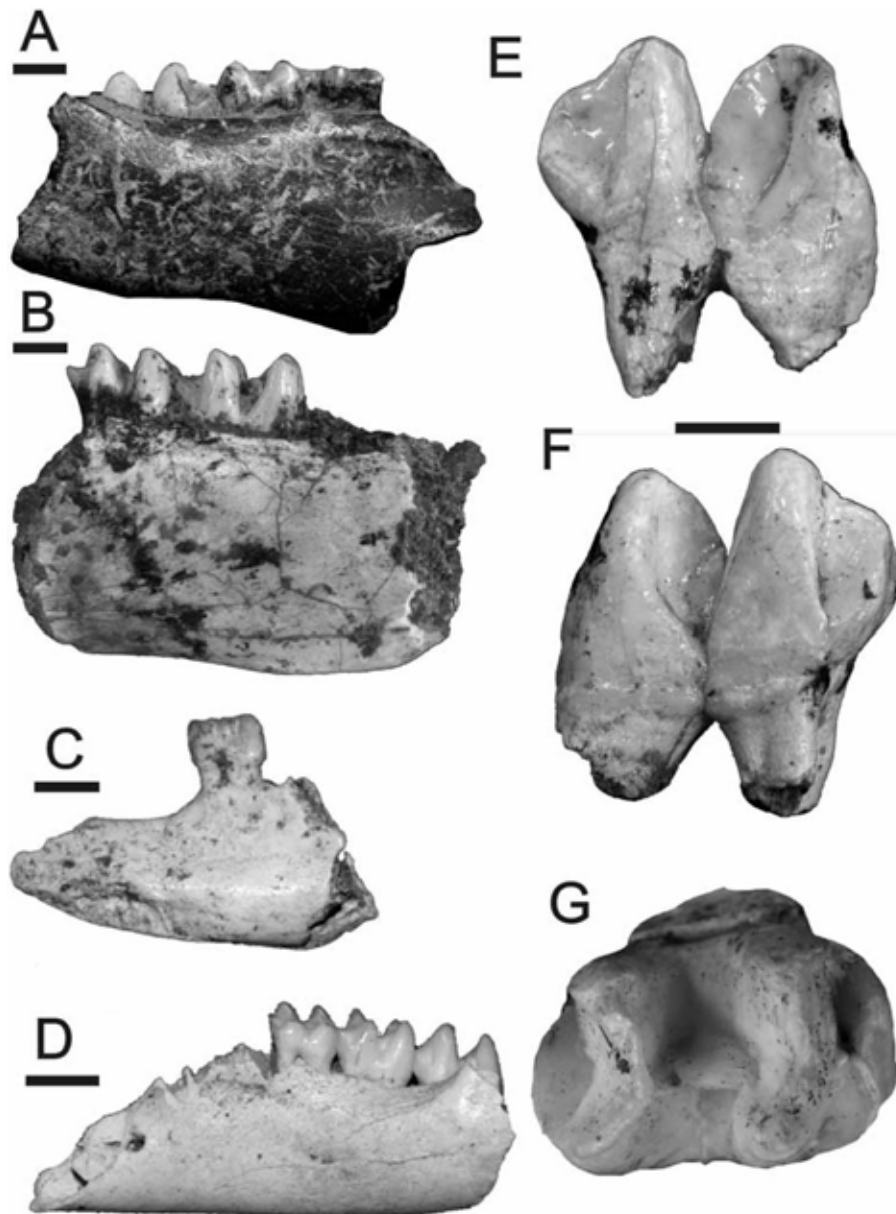


Figure 2-21 (FIG. 21.) A-G, Macropodidae; A-B, *Macropus* sp. cf. *M. agilis siva*; A, QMF51829, RM1-3. B, QMF51830, LM1-2. C-D, *Petrogale* sp.; C, QMF51812, RP3. D, QMF51813, LM2-4. E-G, *Macropus titan*; QMF 1697 in lingual (E), buccal (F) & occlusal (G) views. Scale bar = 5mm.

**Petrogale** Gray, 1837

**Petrogale** sp. (Fig. 21C-D)

MATERIAL. QMF51812-51824; All localities.

*Petrogale* is represented by dozens of isolated mandibles, maxillae, molars, premolars, incisors and postcrania. The only taxa close to *Petrogale* are *Thylogale* and small members of *Macropus*. *Petrogale* differs from *Thylogale* in having lower-crowned molars, in the I<sup>3</sup> morphology (not having a longitudinal groove along the length of the I<sup>3</sup> crown) and the anterior morphology of the

P<sup>3</sup> (not having a well-developed lingual cingulum with an anterior-lingual pocket).

*Petrogale* differs from small-sized *Macropus* by being generally smaller, having a relatively longer P3 and smaller I<sup>3</sup>. The taxonomic diversity of modern species of *Petrogale* is not reflected in dental morphology, thus species placement is not warranted on the basis of available material.

**Macropus** Shaw, 1790

Isolated molars and partial jaws represent species of *Macropus*. Bartholomai (1975), Archer (1978) and Dawson & Flannery (1985) illustrate the difficulty in identifying species of *Macropus* on the basis of isolated molars or jaws without premolars and incisors. Distinction of different species of *Macropus* requires almost complete mandibles or maxillae. When dealing with isolated teeth, absolute size comparisons are the only features available for comparison to available data such as Bartholomai (1975). More complete specimens are required before specific allocations can be made.

**Macropus** sp. 1

MATERIAL. QMF51825-51828; QML1312, QML1420.

A medium-sized *Macropus*, close to *Macropus dorsalis*, is represented by isolated molars that are larger in absolute size than those species of *Petrogale* but smaller than modern species of the size of *Macropus agilis*.

***Macropus* sp. cf. *M. agilis siva* (De Vis, 1895)**

(Fig. 21A-B )

MATERIAL. QMF51829-51834; QML1420, QML1311(H).

Isolated molars and a partial right mandible represent a medium-sized species of *Macropus*. *Macropus agilis agilis* is closest in overall size to the fossil specimens from Marmor Quarry, however, there is overlap with *Macropus agilis siva* when comparing the mandible from Lost Paradise Cave (J7) and the maxilla and mandible from QML1311. All dental measurements fall within the range for *Macropus agilis siva* defined by Bartholomai (1975).

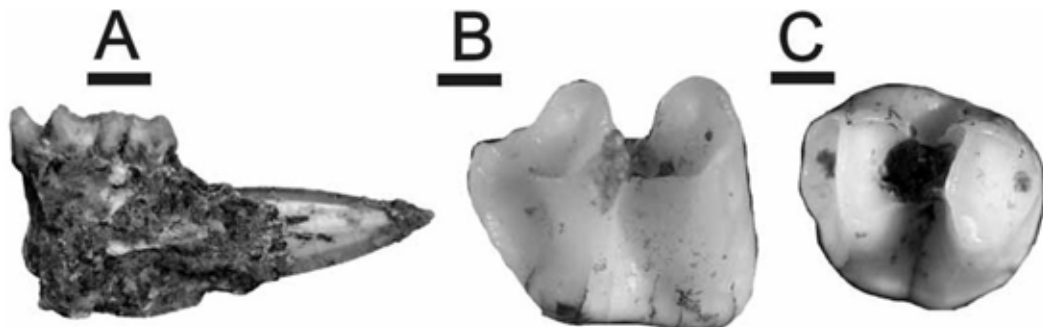


Figure 2-22 (FIG. 22.) A-C, Macropodidae; *Thylogale* sp.; A, QMF51784, LI1-M2. Scale bar = 5mm. B, QMF51785, LM2. C, QMF51786, LM<sup>2</sup>. Scale bar= 1mm.



**Macropus titan** (Owen, 1838)

(Fig. 21 E-G)

MATERIAL. QMF1697, QMF51835-51837; QML1420.

*Macropus titan* is a large macropod easily distinguished by its large high crowned molars, distinct mid- and fore-links and posterior hypolophid groove. Specimens referred to here are placed within *M. titan* based on these features and their similar size to samples taken from the Darling Downs (Bartholomai, 1975).

**Thylogale** Gray, 1837

Two species of *Thylogale* have been identified based on the presence of high-crowned (relative to *Dendrolagus*), rectangular molars, poorly developed midlinks, an anterior cingulum that does not extend across the entire width of the upper molars, and an I<sup>3</sup> that has a complete longitudinal groove on the occlusal face. They have been differentiated from *Petrogale* by having weaker midlinks, an incomplete anterior cingulum on upper molars, smaller-sized molars, and better-developed cristae on dP3s and upper molars.

**Thylogale** sp. 1

(Fig. 22A-C)

MATERIAL. QMF51784-51797; QML1284, QML1284a, QML1385, QML1384U.

A very small-sized new species of *Thylogale*, smaller than any extant or extinct species, including the smallest known species, *Thylogale christenseni* from Irian Jaya. The upper molars possess weakly developed midlinks, a reduced forelink and an anterior cingulum that only extends slightly more than half way across the front of the molar. These features are shared to a greater extent with *T. christenseni* and *T. billardierii*. With further specimens, this taxon will probably be a new species closely related to *Thylogale christenseni*.

### **Thylogale** sp. 2

MATERIAL. QMF51798-51801; QML1312, QML1420.

On the basis of molar size and morphology, differentiation of *Thylogale thetis* and *Thylogale*

*stigmatica* is extremely difficult. The fossil specimens are within the range of both taxa and are very similar in overall morphology.

### Family PSEUDOCHEIRIDAE (Winge, 1893)

Pseudocheirids are represented by hundreds of isolated premolars and molars, molar rows and jaw fragments. The apparent morphological diversity in the collection is corroborated by the diversity in sizes, ranging from very small ringtails of similar size to *Pseudochirulus mayeri*; medium-sized similar to *Pseudochirulus forbesi*; large-sized *Pseudocheirops* and giant *Pseudokoala*. On reviewing the morphology of modern and Tertiary pseudocheirid taxa it became obvious that the most useful features for identification are found in the P3 and M1 of the upper and lower dentition. Based on characters from these key teeth, several groups emerged. More specific formal taxonomy will be provided in a future analysis as more complete material becomes available.

### **Pseudochirulus** Matschie, 1915

*Pseudochirulus* has been identified based on the following combined features: P<sup>3</sup> morphology; elongate-ovoid, preparacrista variably linked to paraconule by blade or valley, only two cusps, posterolingual cingulum variably expressed. M1 morphology; molar profile elongate-rectangular, preprotoconule crista variably expressed, lingual cingulum absent. P3 morphology; metaconid blade-like or absent, paraconid distinct and not linked to protoconid by blade, cristid obliqua distinct running from the hypoconid to protoconid. M1 morphology; distinct paraconid; preprotocristid kinked buccally to paraconid, metaconid variably expressed,

entostylid absent. Three species of *Pseudochirulus* have been identified, two small species similar in size to *Pseudochirulus mayeri* and one medium-sized species similar in size to *Pseudochirulus forbesi*.

***Pseudochirulus* sp. 1 (Fig. 23 G-I, Fig. 24 E)**

MATERIAL. QMF51838-51870; QML1385, QML1311(H), QML1311(C/D), QML1284, QML1284a, QML1313, QML1385L.

*Pseudochirulus* sp. 1 is the smallest of the pseudocheirid taxa represented and possesses the following distinctive features that distinguish it and differentiate this species from *Pseudochirulus* sp. 2 and 3: 1. Simple preprotoconule that does not connect to any other cristae. 2. Protostyle absent. 3. Lingual cingulum absent. 4. Anteriorlingual para- and metacristae absent. 5. Posterolingual para- and metacristae absent. 6. P<sup>3</sup> elongate-ovoid in occlusal view. 7. P<sup>3</sup> preparacrista does not connect to paraconule. 8. Distinct posterolingual cingulum on P<sup>3</sup>.

*Pseudochirulus* sp. 1 is closest in morphology to the living *Pseudochirulus canescens* and *Pseudochirulus mayeri* and the Early Pliocene *Pseudocheirus marshalli*.

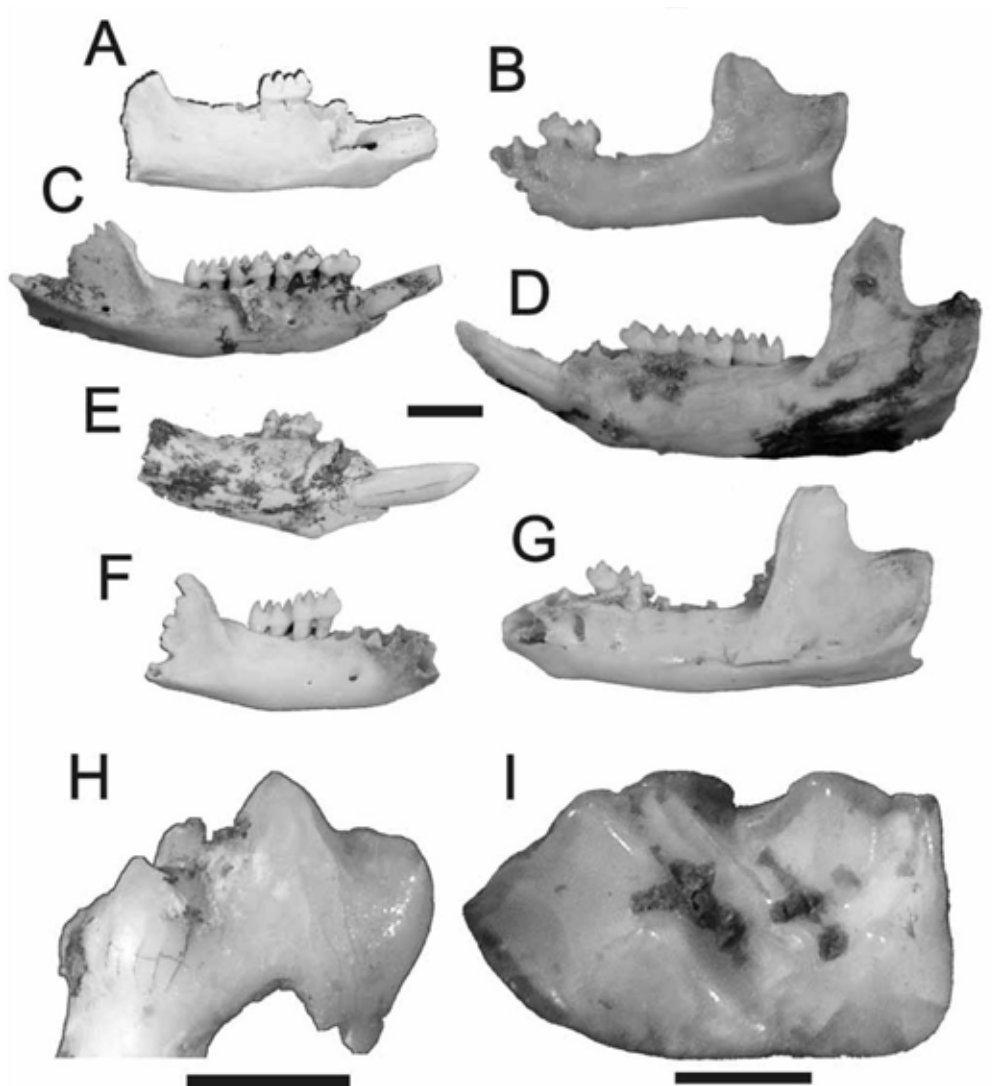


Figure 2-23 (FIG. 23.) A-I, Pseudocheiridae. A, B, D, E & H, *Pseudocheirus* spp.; A, QMF51898, RM1. B, QMF51899, RI1-M3. D, QMF51900, RM2-3. E, QMF51901, RP3. Scale bar = 5mm. H, QMF51840, LM1, (Scale bar = 1mm). C, *Pseudochirulus* sp. 2; QMF51871, RI1 & M1. F, G & I, *Pseudochirulus* sp. 1; F, QMF51838, LM1. G, QMF51839, LI1 & M1-3. Scale bar = 5mm. I, QMF51841. Scale bar = 1mm.

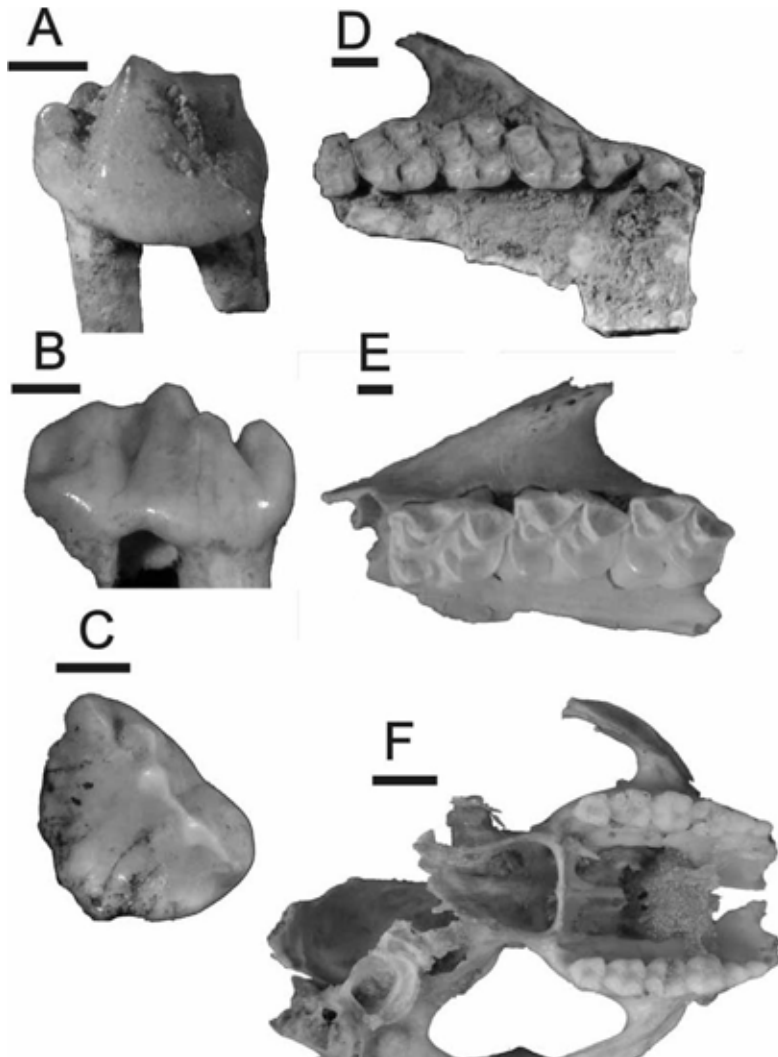


Figure 2-24 (FIG. 24.) A-F, Pseudocheiridae; A-D, *Pseudocheirus* sp.; A, QMF51920, LP<sup>3</sup>. B-C, QMF51921, LP<sup>3</sup> in buccal & occlusal views. E, *Pseudochirulus* sp. 1; QMF51870, RP<sup>3</sup>-M<sup>3</sup> (broken). Scale bar= 1mm. F, *Pseudochirulus* sp. 2; QMF51887, partial skull. Scale bar = 5mm.

***Pseudochirulus* sp. 2 (Fig. 23C, Fig. 24F)**

MATERIAL. QMF51871-51887; QML1284, QML1284a, QML1313, QML1311(H), QML1384U, QML1384L, QML1385.

*Pseudochirulus* sp. 2 possesses the following distinctive features, that when combined differentiate it from *Pseudochirulus* sp. 1 and 3: P<sup>3</sup> morphology; 1. P<sup>3</sup> elongate-ovoid. 2. Distinct paraconule. 3. Preparacrista contacts paraconule. 4. Broad posterolingual margin with indistinct cingulum. 5. Postparaconule crista distinct and terminates at the base of the paracone. M1 morphology; 1. Preprotoconule crista contacts paracone buttress. 2. Protostyle present and well-developed. Overall size larger than *Pseudochirulus* sp. 1.

When compared with modern species the fossil taxon is most similar to *Pseudochirulus cinereus* and *Pseudochirulus forbesi* in overall size. The P<sup>3</sup> of *Pseudochirulus* sp. 2 is distinctly more ovoid than the morphology seen in the modern species. The P<sub>1</sub> has large double roots, a feature seemingly unique to this taxon, having not being observed in any of the modern or fossil taxa.

### ***Pseudochirulus* sp. 3**

MATERIAL. QMF51888-51897; QML1284, QML1284a, QML1313, QML1311(H), QML1385, QML1384U, QML1384L.

*Pseudochirulus* sp. 3 possesses the following features that in combination differentiate it from *Pseudochirulus* sp. 1 and 2: P<sup>3</sup> morphology; 1. P<sup>3</sup> elongate-ovoid. 2. Preparacrista contacts paraconule. 3. Distinct posterolingual cingulum, variably cuspidate. 3. Kink in the posterobuccal end of the postparacrista.

When compared with modern species, the fossils are closest in morphology to both *Pseudochirulus mayeri* and *Pseudochirulus herbertensis*. The fossil specimens differ from these species in being larger than *Pseudochirulus mayeri* and smaller than *Pseudochirulus herbertensis*.

### ***Pseudocheirus* Ogilby, 1837**

#### ***Pseudocheirus* spp.**

(Fig. 23A-B, D-E, H, Fig. 24A-D)

MATERIAL. QMF51898-51922; QML1284, QML1284a, QML1313, QML1311(H), QML1385, QML1384U, QML1384L.

*Pseudocheirus* has been identified on the basis of the following combined features:  $P^3$  morphology; 1. Tricuspid, possessing a paracone, paraconule and an accessory cusp between and buccal to them. 2. Ovoid shape to the premolar in occlusal view. 3. Shallow, indistinct posterolingual basin.  $M^1$  morphology; 1. Preprotoconule terminating at the base of the parastyle. 2. Protostyle distinct. 3. Lingual cingulum present between protocone and metaconule. 4. Lack postero- and anterolingual para- and metacristae.  $P^3$  morphology; 1. Metaconid present as a distinct and high cusp.  $M^1$  morphology; 1. Preprotocristid blade-like running to tip of paraconid. 2. Paraconid in line with protoconid. 3. Protostylid tall and crested, closely set against protoconid. 4. Entostylid absent. There are three species of *Pseudocheirus* represented from the sites, all three being markedly different in size but all significantly smaller than extant *Pseudocheirus*. Three species are considered to be new extinct species.

### **Petauroides** Thomas, 1888

#### **Petauroides** spp.

(Fig. 25A-C)

MATERIAL. QMF51923-51935; QML1284, QML1284a, QML1313, QML1311(H).

*Petauroides* has been identified on the basis of the following combined features:  $P^3$  morphology; 1. Ovoid shape in occlusal view. 2. Distinctly straight blade made by the crests running between the paraconule, paracone and posterobuccal margin of the premolar. 3. Posterolingual postparacrista running into posterolingual basin. 4. Posterolingual cingulum present.  $M^1$  morphology; 1. Preprotoconule connects to preprotocrista. 2. Posterolingual para- and metacristae well developed as crests. 3.

Protostyle absent. 4. Lingual cingulum absent. P3 morphology; 1. Paraconid, protoconid and metaconid in a line along the longitudinal axis of the tooth crown. 2. Cristids variably expressed and probably constitute several species. 3. Small posterior pocket below the metaconid developed in some specimens.

The morphological diversity seen in specimens referred to here as *Petauroides* indicates a very complex fossil history leading to the modern *Petauroides* and *Hemibelideus*.

The only P<sup>3</sup> specimen available is closest in morphology to *Hemibelideus*. P3 morphology shows great degrees of morphological diversity albeit retaining typical *Petauroides* characteristics.



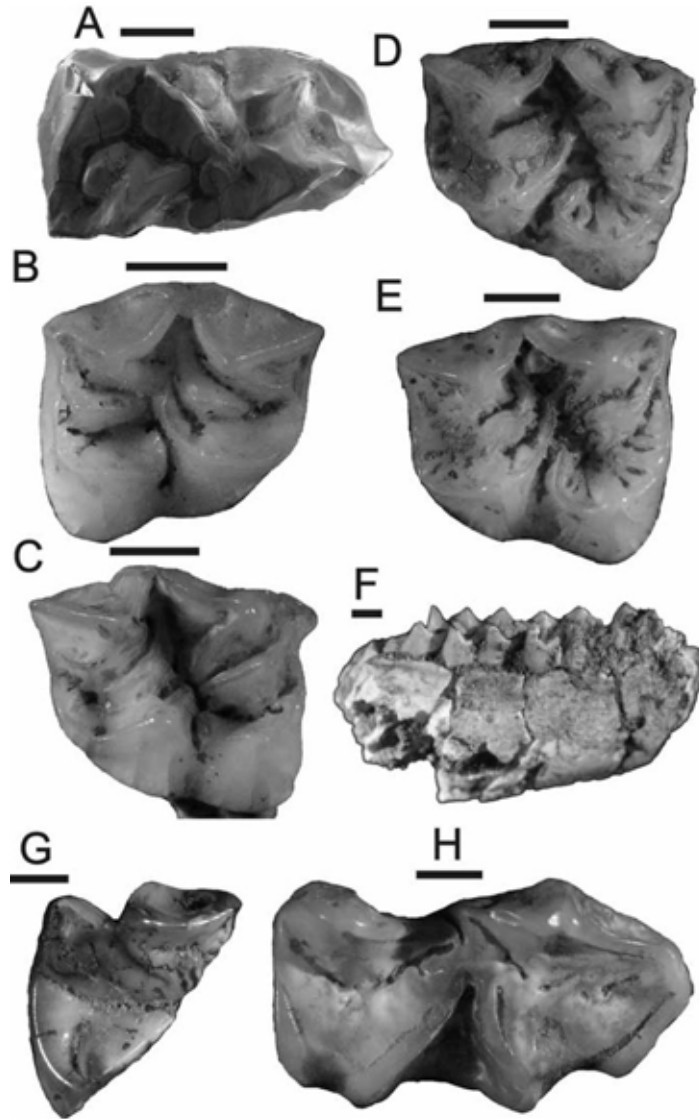


Figure 2-25 (FIG. 25.) A-H, Pseudocheiridae; A-C, *Petauroides* sp.; A, QMF51923, RM1. B, QMF51924, LM<sup>2</sup>. C, QMF51925, RM<sup>2</sup>. D-F, *Pseudocheirops* sp.; D-E, *Pseudocheirops* sp. 1; D, QMF51934, RM<sup>3</sup>. E, QMF51935, RM<sup>2</sup>. Scale bar= 1mm. F, *Pseudocheirops* sp. 2; QMF51937, RM2. Scale bar= 5mm. G-H, *Pseudokoala* sp.; G, QMF51934, RM<sup>?</sup>. H, QMF51939, RM2. Scale bar = 1mm.

Five distinct morphologies are present, however, these will be treated as polymorphic until

a larger collection is available. Even so, no P3 clearly represents known species of *Petauroides* or *Hemibelideus*. M1 morphology shares greater similarities with extinct species of *Petauroides* (*Petauroides stirtoni* and *Petauroides ayamaruensis*, see Long et al., (2002)) than with the modern *Petauroides volans* and *Hemibelideus lemuroides*.

### ***Pseudocheirops* Matschie, 1915**

*Pseudocheirops* has been identified on the basis of the following features: 1. Protostylid basin on M1-3. 2. Elaborate crenulations on upper and lower molars. 3. Entostylid present. 4. Posterior bifurcation of protoconule. 5. Protostyle present. 6. Crest present labial to protostyle. Two species of *Pseudocheirops* have been identified so far.

#### ***Pseudocheirops* sp. 1**

(Fig. 25D-E)

MATERIAL. QMF51936, QMF51934-51935; QML1311(H), QML1384L. *Pseudocheirops* sp. 1 is a right mandible preserving a partial M1, complete M2-3 and a partial M4. Two upper right molars are also considered to be conspecific. The fossils compare favourably with *Pseudocheirops archeri* both in size, crenulations and development of the protostylid basin.

#### ***Pseudocheirops* sp. 2**

(Fig. 25F)

MATERIAL. QMF51937; QML1284.

The second, much smaller species *Pseudocheirops* sp. 2, is only known from a right M2. The crenulations are indistinct with a narrow entostylid and very small protostylid basin. The fossil is much smaller than any of the modern *Pseudocheirops* available to study, yet it is similar in size to the Pliocene *Pseudocheirops winteri* from Bluff Downs. The fossil differs from *Pseudocheirops winteri* by possessing a

complete preentocristid-metacristid connection.

**Pseudokoala** Turnbull & Lundelius, 1970

**Pseudokoala** sp.

(Fig. 25G-H)

MATERIAL. QMF51938-51939; QML1385; QML1311 (C/D).

*Pseudokoala* has been identified from an isolated M2 and a fragment of upper molar.

It has been placed within *Pseudokoala* based on the

following combined features: 1. Very large size. 2. Crenulations present but forming large buttresses, less crenulated than *Pseudocheirops* spp. 3. Lack of an entostylid. 4. Truncated posthypocristid. 5. Buccally buttressed protoconid.

When compared with the three species of *Pseudokoala*, *Pseudokoala* sp. is closest to *Pseudokoala erlita* in size (M2L: 6.78mm *Pseudokoala* sp., M2L: 6.2-7.3mm *Pseudokoala erlita* Turnbull & Lundelius (1970), M1L: 10.7mm *Pseudokoala curramulkensis*, M1L: 10.9mm *Pseudokoala cathysantamaria* Archer et al. (1997). The molar crown is simplified as in *Pseudokoala erlita*, however, due to the worn nature of the tooth no more specific comparisons can be made.

pseudocheirid indet. MATERIAL. QMF51940; Olsen's Cave.

A posterior fragment of an upper molar with distinctly selenodont morphology represents the only material of a pseudocheirid from the Olsen's Cave collection. The lack of crenulations and an anterolingual metacrista allies the specimen to a large member of *Pseudochirulus* or *Pseudocheirus peregrinus*.

Family PETAURIDAE (Gill, 1872)

Petaurids are represented by several nearly complete maxillae, fragmentary mandibles, isolated incisors, premolars, molars and postcrania. Two genera are recorded, *Dactylopsila* and a new undescribed genus.

### **Dactylopsila** Gray, 1858

*Dactylopsila* has been identified based on the following combined features: 1.

Possession of a distinct and large M<sup>1</sup> parastyle. 2. Reduction of the styler margin with a distinct indentation between the paracone and metacone. 3. Reduced metaconule. 4. Procumbent I1. 5. Bulbous, rectangular-ovoid lower molars.

### **Dactylopsila** sp. 1

(Fig. 26E)

MATERIAL. QMF51943-QMF51946; QML1284; QML1284a; QML1384U; QML1385.

*Dactylopsila* sp. 1 is 10-12% smaller than the species of *Dactylopsila* available for study, *Dactylopsila trivirigata* and *Dactylopsila palpator*. The fossil species also differs from *D. trivirigata* and *D. palpator* by possessing less rounded and more gracile lower molars, a more buccal placement of the protoconid on M1 and a less distinct postprotocristid. When compared with the extinct *D. kambuayai* the fossil is approximately 20% larger, however, it does possess a similar gracile profile of the M2.

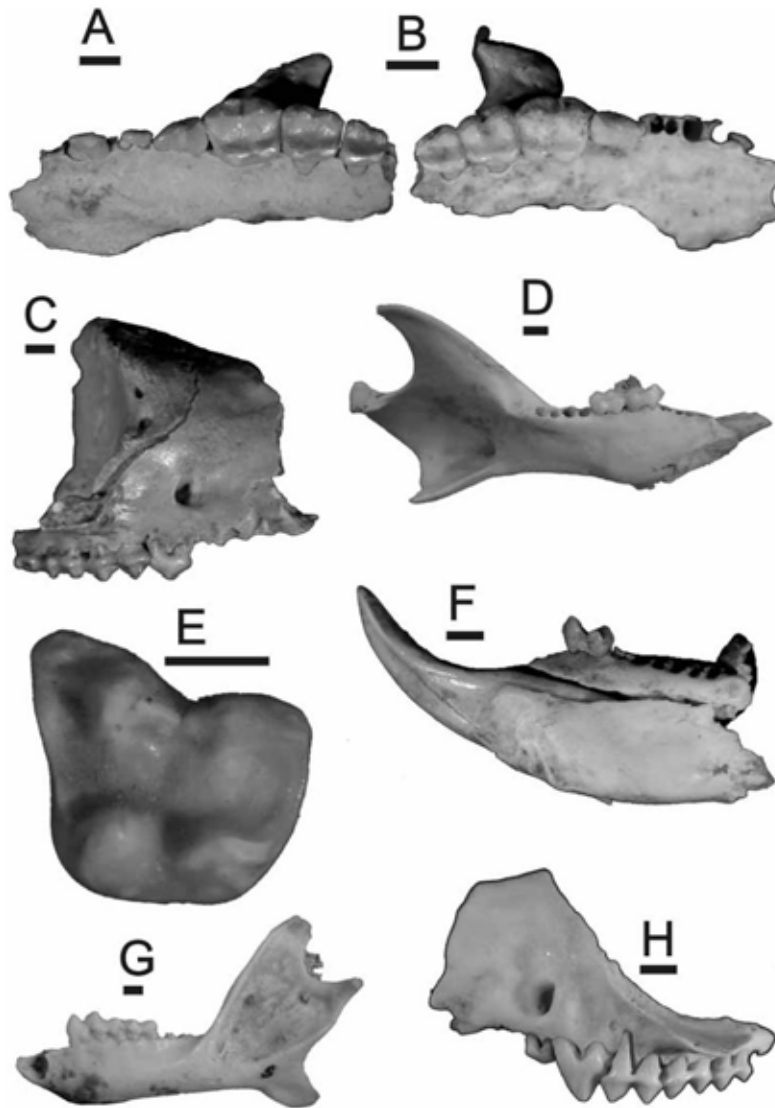


Figure 2-26 (FIG. 26.) A-F, Petauridae, A-D, Gen. et sp. nov.; A, QMF51949, LP<sup>1</sup>-M<sup>3</sup>. B, QMF51950, RP<sup>3</sup>-M<sup>3</sup>. C, QMF54951, partial skull. D, QMF54952, left mandible (M<sup>1-2</sup>). E, *Dactylopsila* sp. 1; QMF51947, LM<sup>1</sup>. F, *Dactylopsila* sp.<sub>3</sub>, 2; QMF51948, RI1 & M1. G-H, Burramyidae; *Cercartetus* sp.; G, QMF51984, LP3-M2. H, QMF51985, LP<sup>2</sup>-M. Scale bar= 1mm.

***Dactylopsila* sp. 2**

(Fig. 26F)

MATERIAL. QMF51947-51948; QML1284.

A second, smaller species of *Dactylopsila* is represented by a fragmentary left mandible with I1 and M1. The I1 is large and recurved, procumbent. M1 gracile in occlusal profile, rectangular ovoid with conids without bulbous exterior margins. Protoconid mesially produced. Masseteric fossa inserts below  $M_{2-3}$ . Very small alveoli for P2-3.

When compared with *D. trivirigata* and *D. palpator*, *Dactylopsila* sp. 2 differs by being much smaller, a less recurved I1, possessing a more gracile and unbuttressed hypoconid, and a more mesially oriented protoconid on M1.

*Dactylopsila* sp. 2 is similar in size and I1 morphology to *D. kambuayai*, however, there are no specimens of M2 available for direct comparison.

Gen. et sp. nov. 1 & 2

(Fig. 26A-F)

MATERIAL. Sp 1: QMF51949-51969; QML1284, QML1284a, QML1313, QML1312, QML1385. QML1384U; QML1384L; QML1420, QML1311.

MATERIAL. Sp 2: QMF51970-51973; QML1284, QML1284a.

Two species of a new medium-sized petauroid are characterised by a dentition that possesses a combination of both plesiomorphic features found in Oligo-Miocene petauroid *Djaluganji yadjana* (Brammal, 1998), and the derived characteristics seen in modern *Petaurus*. The upper molar row is distinctly straight, not possessing the upward inflexion toward the posterior as seen in all modern petaurids. The presence of a distinct styler basin in  $M_1$  and  $M_2$  distinguish this taxon from both the modern and described Oligo-Miocene petaurids. The reduction of the premolars and molar gradient is shared with *Petaurus* and *Gymnobelidius*, but not

to the extent seen in these taxa. Two distinct species are present from the sites and can be distinguished from each other (and the Hamilton Fauna petaurids) on the state of the metaconule, postprotocristae, premetaconule cristae and stylar basin. The greater number of features shared with *Petaurus* and *Gymnobelidius* warrant its placement in the Petauridae at the present time.

#### Family BURRAMYIDAE (Broom, 1898)

Burramyids were identified on the basis of their small-sized, square molars with reduced stylar shelf and distinctly high paracone and metacone. They were differentiated from acrobatids by possessing reduced P 1 and P2 and the presence of M4. Burramyid specimens comprise the majority of the very small possums collected from the possum-rich localities of the present study. A conspicuous absence from the burramyid fauna is *Burramys*, with all of the specimens being placed within *Cercartetus*.

#### **Cercartetus** Gloger, 1841

#### **Cercartetus** sp. (Fig. 26G-H)

MATERIAL. QMF51984-52002; QML1284, QML1284a, QML1385, QML1311(H), QML1313.

Several nearly complete mandibles, well preserved maxillae, dozens of isolated molars and premolars represent *Cercartetus*. These specimens have been placed within *Cercartetus* based on their size and the absence of the distinctly plagiaulacoid  $p_3/P_3$ , which is distinct in the only other burramyid, *Burramys*. On comparison with the four known species of *Cercartetus*, the fossil specimens differ least from *Cercartetus caudatus* by being very close in size, retaining M4 and possessing a  $P^3$  with a single conical cusp. The specimens differ from all other species of *Cercartetus* by possessing an M4. *Cercartetus* sp. differs from *Cercartetus caudatus* by possessing a larger and double rooted  $p_1$  and  $P^2$ , a larger  $c_1$  root and a shorter diastema between  $c_1$  and  $P^1$ . Additionally, it differs from all extant species of

*Cercartetus* by only possessing two individual roots between I1 and P3, instead of three. The homology of the missing root is unknown. With further analysis, *Cercartetus* sp. probably represents a new extinct species closely related to *Cercartetus caudatus*.

#### SUPERFAMILY INCERTAE SEDIS

Gen et sp. nov. (Fig. 27B-C)

MATERIAL. QMF51974-51981; QML1284, QML1284a, QML1311(H), QML1385.

A medium-sized possum, similar in size to *Petaurus*, represents a new taxon of uncertain affinities. The closest morphologies to this taxon can be found within both the Acrobatidae and the Burramyidae, where features they share include: 1. Enlarged paracones and metacones on  $M^{1-4}$ . 2. Very reduced styler margin. 3. Distinct molar size gradient from  $M^{1-4}$ . 4. Double-rooted P2-3. The taxon differs from the majority of these taxa by features that are considered plesiomorphic within the two families (Archer, 1984), including: 1. Presence of  $M^4$  (*Burramys parvus* and *Cercartetus caudatus*). 2. Subequal metaconule with protocone. 3. Double-rooted  $P^2$ .

The taxonomic placement within either of these families would require further material and a review of pygmy-possum higher taxonomy, which is under considerable confusion at present (Archer, 1984; Strahan, 1998).



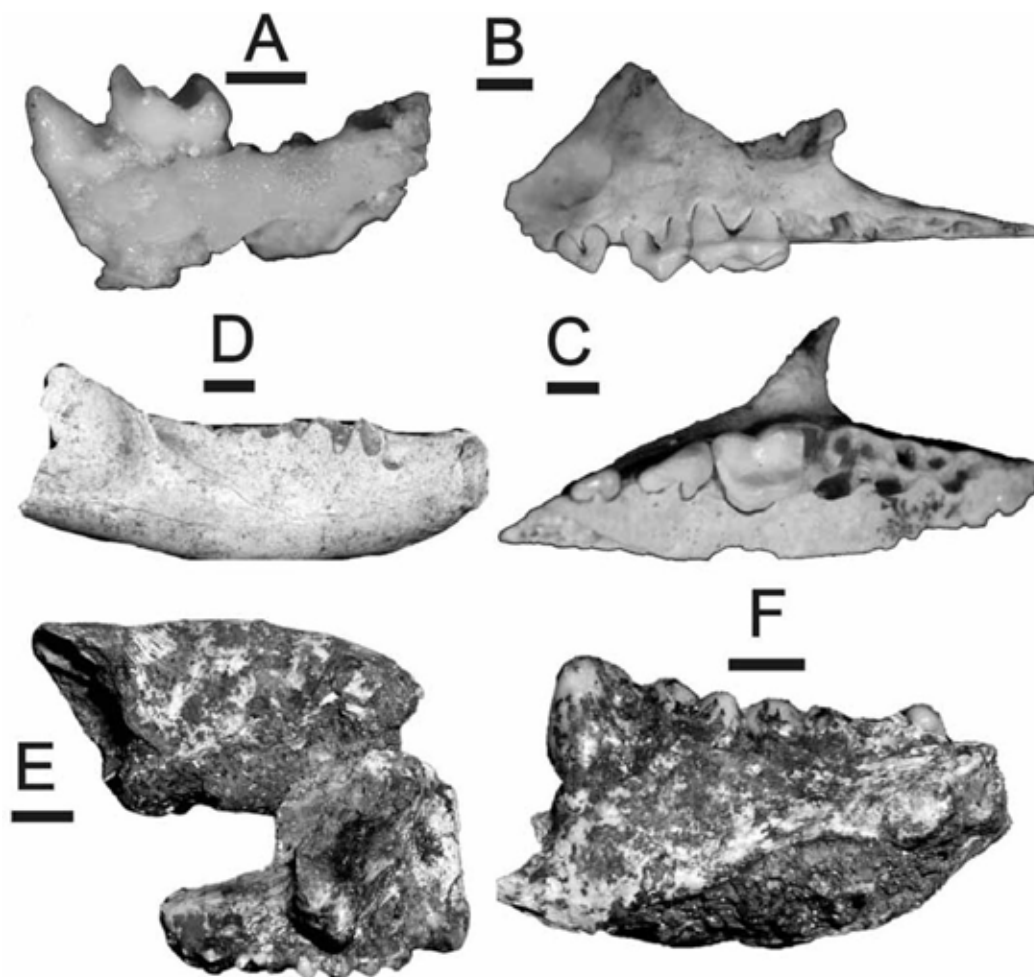


Figure 2-27 (FIG. 27.) A, Acrobatidae; *Acrobates* sp.; QMF51982, RP3-M1. Scale bar = 1mm. B-C, Superfamily incertae sedis; QMF51974 in buccal & occlusal view. Scale bar = 1mm. D-F, Phalangeridae; D, *Trichosurus* sp. 1; QMF52009, right mandible. E, *Trichosurus* sp. 2; QMF52012, partial skull. F, *Strigocuscus* sp.; QMF52003, LP3-M3. Scale bar = 5mm.

#### Family ACROBATIDAE Aplin, 1987

Acrobatids are easily distinguished and are here represented by the very small-sized *Acrobates*. The fossil specimens have been identified as acrobatid based on

the large sized premolars and the premolariform shape to the M1 trigonid (Archer, 1984).

**Acrobates** Desmarest, 1818

**Acrobates** sp.

(Fig. 27A)

MATERIAL. QMF51982- QMF51983; QML1385, QML1284.

*Acrobates* sp. has been identified based on its diminutive size and the presence of a large P3, which distinguishes it from the only other member of the Acrobatidae, the New Guinea genus *Distoechurus*. On comparison with *Acrobates*, the specimens are very similar in size and overall morphology. There is only a slight difference in the posterobuccal morphology of the P3. The variation of this feature is unknown, therefore, the identification will remain conservative.

Family PHALANGERIDAE Thomas, 1888

Phalangerids have been found in most localities and either represent rainforest phalangerids or the more sclerophyll woodland species of *Trichosurus*. There is considerable difficulty when identifying phalangerids from partial jaws and isolated teeth because the best diagnostic features seem to be from the periotic (Crosby, pers.com.) and basicranial region (Flannery et al., 1987). Morphological conservatism obvious in fossil phalangerid taxa, including the Miocene *Strigocuscus reidi* and Early Pliocene *Strigocuscus notialis*, makes identification of this material particularly difficult. However, using features defined by Flannery et al. (1987) it is possible to refine the identification of phalangerids to generic level.

**Strigocuscus** Gray, 1862

**Strigocuscus** sp.

(Fig. 27F )

MATERIAL. QMF52003-QMF52008, QMF52071; QML1284, QML1284a,

QML1384U, QML1385, QML1384L.

*Strigocuscus* sp. is represented by two partial right mandibles, a partial left mandible and several isolated premolars and molars. The specimens are placed within *Strigocuscus* based on the presence of the following features: 1. P3 at an oblique angle to the molar row. 2. P3 has more than four cuspules. 3. P3 hypertrophic. 4. P3 highest anteriorly. 5. Molars without complex crenulations. 6. Preprotocrista contacts parastyle

on M<sup>1</sup>. The fossils share their greatest similarity with *S. gymnotis* and *S. notialis*, which includes a distinctly large, antero-buccally oriented P3 and a single-rooted P2. The specimens differ from *S. gymnotis* by being only slightly larger, possessing more cuspules on P3 and having a distinct contact of the preprotocrista to parastyle. [Note: AMR22155, *S. gymnotis* from Parkop Village PNG does possess an M<sup>2</sup> with a preprotocrista contacting the parastyle albeit not as distinct as the fossil]. *S. reidi* Flannery & Archer, 1987 from the Miocene and *S. notialis* Flannery et al., 1987 from the Early Pliocene are phenetically very similar to *S. gymnotis*, however both possess distinct preparacristae contacting the parastylar corner of M. Additionally *S. reidi* is larger than *S. gymnotis* and *S. notialis* is smaller. On balance, *Strigocuscus* sp. shares most features with *S. notialis*, except for being larger.

### **Trichosurus** Lesson, 1828

#### **Trichosurus** sp. 1

(Fig. 27D)

MATERIAL. QMF52009-QMF52011; QML1312, QML1314, QML1420.

*Trichosurus* sp. 1 is represented by an edentulous right and a partial left mandible, two left partial maxillae, isolated molars and premolars. *Trichosurus* sp. 1 has been identified based on the following combined features: 1. P2 absent. 2. P3, rectangular-shaped in lateral profile (as high anteriorly as posteriorly). 3. Gracile mandible in lateral profile.

Archer (1978) could not adequately differentiate modern species of

*Trichosurus* based on molar morphology and size, this mainly being due to the extreme variation seen in the cosmopolitan *T. vulpecula*. One feature of note, present in both fossil mandibles, is a large cavity situated above the posterodorsal margin of the mandibular symphysis, which penetrates the lower incisor alveolus. This feature has not been seen in any phalangerid examined for this study yet the feature is present in both mandibles referred to *Trichosurus* sp. 1. Also, both jaws are from different faunas, being split by almost 100km. The association of the cavity with the incisor root suggests that this may be a pathology, which affected a large population of *Trichosurus* in central eastern Queensland.

### **Trichosurus sp. 2**

(Fig. 27E)

MATERIAL. QMF52012, QMF52070; QML1311(H), QML1384L.

A second, small species of *Trichosurus* is known from a single left mandible fragment preserving P3 and M1 and a portion of skull with right maxilla (P<sup>3</sup>-M<sup>4</sup>). The specimen is placed within *Trichosurus* based on: 1. A rectangular P3 in lateral profile. 2. M1 with distinct metaconid, positioned posterolingually to protoconid. 3. Reduced P3 cuspules. 4. P3 smaller than M1. 5. Preprotocristid crest to paraconid. When compared with *T. vulpecula* and *T. caninus*, the fossil species is markedly smaller with a relatively larger M1 to P3. *Trichosurus* sp. 2 differs from the Early Pliocene *T. hamiltonensis* by possessing a smaller P3 relative to M1 and by being smaller in overall size. *Trichosurus* sp. is closest in morphology and size to *T. dicksoni* from the Miocene of Riversleigh. Because direct comparison to all trichosurin phalangerids, such as *T. arnhemensis*, was not possible a specific assignment will be left for a later analysis.

Family THYLACOLEONIDAE Gill, 1872

**Thylacoleo** Gervais, 1852

**Thylacoleo** sp. (Fig. 28A-C)

MATERIAL. QMF1338, QMF52069; QML1420, QML1384L.

An isolated P<sup>3</sup> (QMF1338) and P<sup>3</sup> (QMF52069) represent the distinctive marsupial carnivore, *Thylacoleo*. Comparison of the premolars with *Thylacoleo carnifex* and *T. crassidentatus* does not resolve its taxonomic position, because the posterior portions of both premolars are broken, thus a full morphometric analysis was not possible. Interestingly, both specimens show very little wear.

***Thylacoleo hilli* Pledge, 1977**

(Fig. 28D-E)

MATERIAL. QMF52013; QML1311(H).

A single left P<sup>3</sup> represents the smallest known species of *Thylacoleo*, *Thylacoleo hilli*. Identification of small thylacoleonid P<sup>3</sup>'s has been subject to speculation that they may be deciduous premolars of larger species (Pledge, 1977; Archer, 1984; Archer & Dawson, 1982b). Archer & Dawson (1982) suggest that *Thylacoleo* probably did not have a significant deciduous premolar since no thylacoleonid material so far found preserves a dP<sup>3</sup>. The lack of a molariform premolar, resorption pits for the premolar roots and the presence of a relatively well used wear facet along the longitudinal shearing blade of the fossil premolar indicate that this specimen was from an adult. Comparison to obvious juvenile *T. carnifex* from Naracoorte Caves, shows that *Thylacoleo* did not have any deciduous dentition (pers. obs.). The specimen is therefore assigned to the Late Miocene to Pliocene *T. hilli* based on its diminutive size (24.4mm in *T. hilli* (Pledge, 1977) and 22.23mm for QMF52013), simplified posterior margin of the premolar and overall similarity to the holotype described by Pledge (1977).

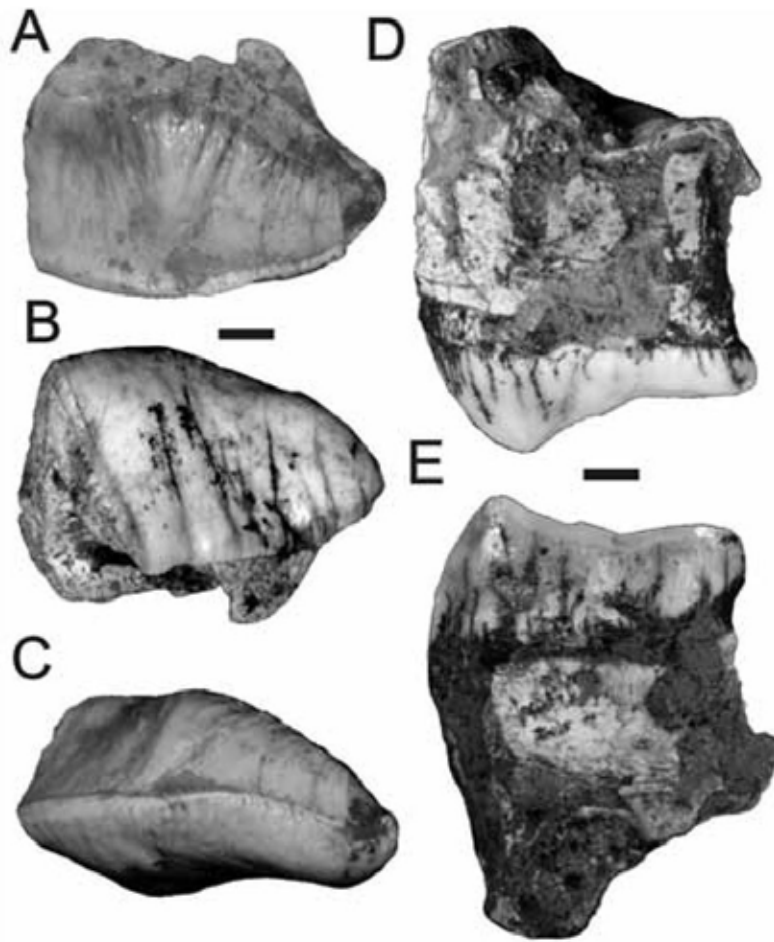


Figure 2-28 (FIG. 28.) A-E, Thylacoleonidae; A-C, *Thylacoleo* sp.; QMF52069, RP<sup>3</sup> in lingual, buccal & occlusal views. D-E, *Thylacoleo hilli*; QMF52013, RP<sup>3</sup> in buccal & lingual views. Scale bar = 5mm.

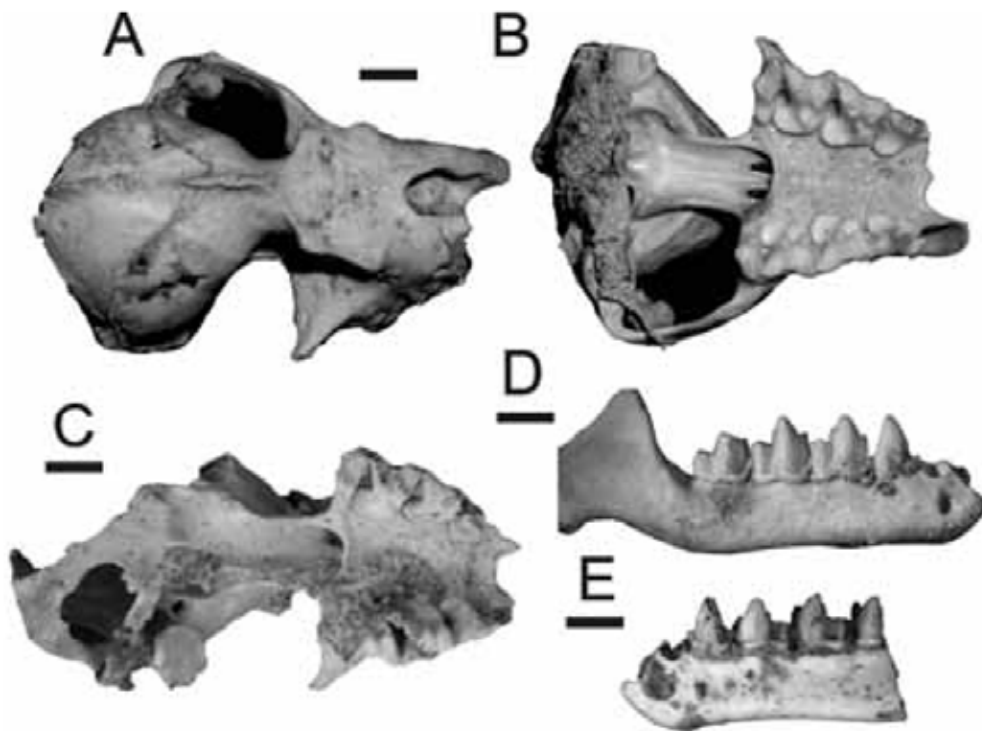


Figure 2-29 (FIG. 29.) A-E, Megadermatidae; *Macroderma gigas*; A-B, QMF48021, partial skull in dorsal & ventral views. C, QMF48022, partial skull. D, QMF48006, RP3-M3. E, QMF48591, LP4-M3. Scale bar = 5mm.

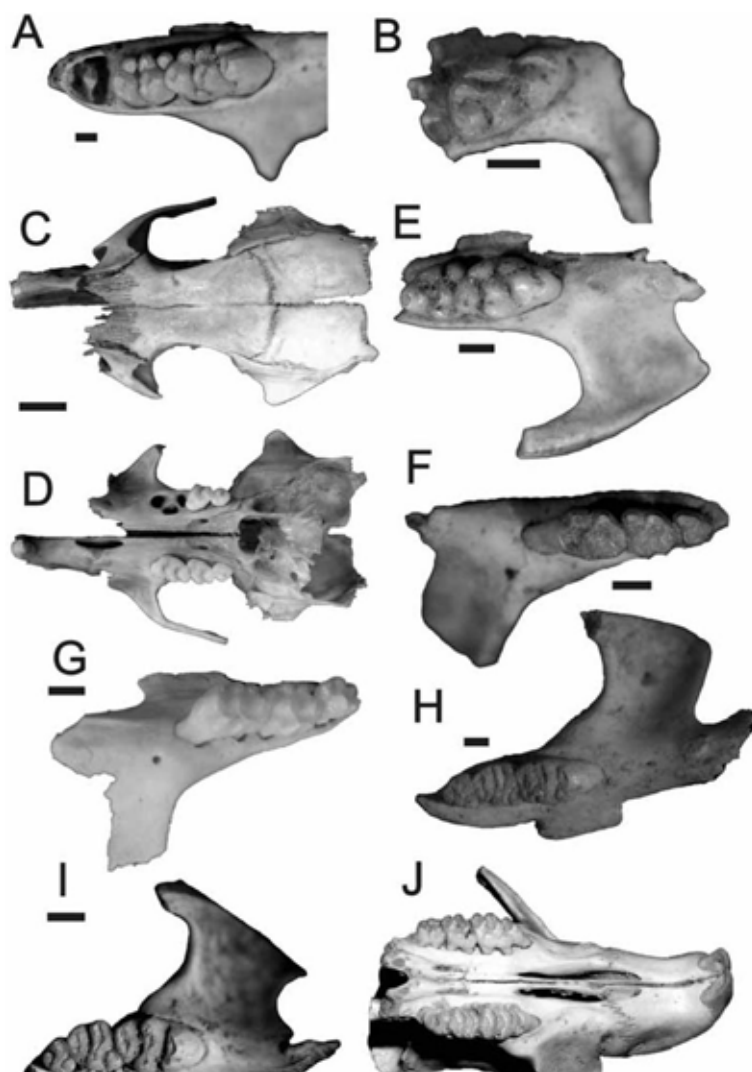


Figure 2-30 (FIG. 30.) A-I, Muridae; A, *Conilurus* sp.; QMF52052, LM<sup>1-2</sup>. B, *Leggadina* sp.; QMF52040, LM<sup>1</sup>. Scale bar = 1mm. C-D, *Uromys/Melomys* sp.; QMF52014, skull in dorsal & ventral views. Scale bar = 5mm. E-F, *Pseudomys* spp.; E, QMF52043, LM<sup>1-2</sup>. F, QMF52044, RM<sup>1-3</sup>. G, *Pogonomys* sp.; QMF52022, RM<sup>1-3</sup>. H, *Zyzomys* sp.; QMF52053, RM<sup>1-3</sup>. Scale bar = 1mm. I, *Notomys* sp.; QMF52036, RM<sup>1-3</sup>. J, *Rattus* sp.; QMF52033, partial skull. Scale bar = 5mm.

## 2.20 BIOCHRONOLOGY

In order to develop a faunal chronology of the sites, each site needed to be grouped based on their faunal similarity and these groups placed in geochronological order. Presence/absence data was used to produce a dendrogram of similarity for sites using



small-sized mammalian taxa (excluding bats) represented at each site (Appendix 1; Fig. 31). The analysis grouped sites with progressively dissimilar faunas from those of the present day. Fig. 31 shows the relationship of sites based on small-sized mammal fauna.

Olsen's Cave fauna shares the greatest similarity with the present day fauna. Five faunas fall successively further away from the Olsen's Cave fauna, first QML1312, then QML1420, QML1384U, QML1384L and QML1311C/D. A final group of five faunas (QML1284, 1284a, 1385, 1313 and 1311H) remain unresolved (polytomy) by the analysis and are considered to possess, equally, the least number of taxa shared with the present day.

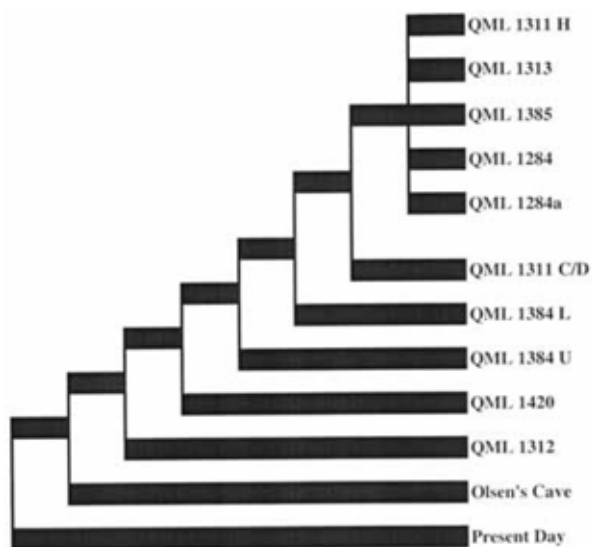


**Figure 3-31 (FIG. 31.) Dendrogram illustrating faunal similarity derived from small-sized mammal species from sites presented herein. Present day small-sized mammal fauna placed as the outgroup.**

When compared with the available site geochronologies, the faunal dendrogram correlates well with the sites from the Elephant Holes Cave System but not as well with the sites from the Speaking Tube Cave System.

Geochronologically, the Elephant Hole Cave System sites range from the oldest (QML1385) through QML1384L and QML1384U to the youngest (QML1312). The

faunal dendrogram correlates with the geochronology, by QML 1312 sharing the most taxa with the present day and QML1385 the least. Within the Speaking Tube Cave System, QML1311(H) and QML1311 (C/D) are considered to be geochronologically contemporaneous, with QML1313 possibly being younger. The faunal dendrogram does not provide any further resolution to these sites, all of which share similarly few taxa with the present day.

## 2.21 ASSEMBLAGE AGE

A complete absence from the sites of mammalian taxa known from the Oligocene-Miocene (possible exceptions being *Thylacoleo hilli* and *Trichosurus* sp. 2) confines biocorrelation to sites of post Late Miocene age. Radiometrically-dated and biocorrelated vertebrate faunas from the Pliocene were used to hypothesise the age of the oldest of the sites at Mount Etna and Limestone Ridge. Table 4 presents a summary of the taxa shared between the Mount Etna and Limestone Ridge sites and other Pliocene vertebrate communities throughout eastern Australia. Two sites possessed mixed faunas of Pliocene and Pleistocene taxa. These two sites were simply classified as Plio-Pleistocene, being younger than the biocorrelated Early Pliocene sites and older than the dated late Pleistocene, QML1312. Table 5 summarises the hypothesised ages for each site yielding fauna identified herein.

**Early Pliocene.** The most dissimilar assemblages to those of the present day fauna possess several taxa confined to the Pliocene in other parts of Australia. These taxa include, *Thylacoleo hilli*, *Kurrabi* sp., *Protemnodon* sp. cf. *P. devisi* and the new perameloids. Of these taxa, *Thylacoleo hilli* and *Kurrabi* sp. are confined elsewhere in Australia to the Early Pliocene (Pledge, 1977; Flannery & Archer, 1984; Flannery et al., 1992). Several undescribed taxa presented here share their closest morphological similarities with taxa only known from the Early Pliocene. These taxa include, *Strigocuscus* sp. close to *Strigocuscus notialis* (Hamilton LF); *Trichosurus* sp. 2 close to *Trichosurus hamiltonensis* (Hamilton LF); *Petauroides* spp. close to *Petauroides stirtoni* (Hamilton LF; Big Sink LF);

*Pseudochirulus* sp. 1 close to *Pseudocheirus marshalli* (Hamilton LF); *Pseudokoala* sp. close to *P. erlita* (Hamilton LF); and *Kurrabi* sp. close to *K. merriwaensis* (Bow LF; Big Sink LF).

Noticeable occurrences of believed Pleistocene-aged taxa are also present in these assemblages, including *Macropus agilis siva* and *Sarcophilus lanianus*. There is uncertainty surrounding the identification of *Macropus agilis siva* in the fauna, therefore it may be incorrectly identified. *Sarcophilus lanianus* is positively identified here and is considered to be the earliest age for this taxon, rather than a younger age of the fauna. The previously oldest record of *Sarcophilus* is from the early Pleistocene of Nelson Bay (Gerdtz & Archbold, 2003) although Tedford (1994) has identified possible *Sarcophilus* from Parwan (Early Pliocene). Gerdtz & Archbold (2003) record the presence of *Sarcophilus harrisii* and *Sarcophilus moornaensis* during the early Pleistocene of Victoria, indicating a pre-Pleistocene origin of *Sarcophilus* and supporting the presence of *Sarcophilus* in the Pliocene of Australia.

Overall, the majority of biocorrelatable taxa indicate an Early Pliocene age for the following sites: QML1284, QML1284a, QML1384L, QML1311 C/D, QML1311 H, QML1313 and QML1385.

**Plio-Pleistocene.** Two sites, QML1384U and QML1420 are considered to be dated sometime between the Late Pliocene and middle Pleistocene. Both sites possess similar small mammal faunas, with QML1384U sharing a similar large portion of its small mammal fauna with the Early Pliocene sites. Unfortunately QML1384U is yet to yield megafauna, however, it is considered to be faunally intermediate between the Early Pliocene assemblage and QML1420. QML1420 fauna lacks the restricted Early Pliocene taxa and possesses Plio-Pleistocene and Pleistocene species, including; *Palorchestes* cf. *P. parvus*, *Macropus titan*, *Macropus agilis siva*, and *Megalanina prisca*. Additionally, QML1420 is considered to be pre-late Pleistocene in age based on its intermediate small mammal fauna between the Pliocene-aged assemblages and the dated late Pleistocene QML1312 fauna.

**Late Pleistocene.** QML1312 has been TIMS U-series dated using *Petrogale* dentition, providing a minimum age of 149,000 +/- 611 ybp. Faunally, QML1312 is intermediate between QML1420 and Olsen's Cave. The only distinctly Pleistocene taxon within the deposit is *Sarcophilus lanarius*. There are some elements of the fauna that show a lingering relationship to the older faunas, namely *Dendrolagus*, new genus of petauroid and *Thylacinus cynocephalus*.

**Holocene.** Olsen's Cave and QML1314 are considered to be post-late Pleistocene and probably Holocene in age based on the complete lack of megafauna (even though QML1314 site does collect large-sized macropodines) and the exclusive presence of extant taxa. Olsen's Cave fauna possesses the most similar small mammal fauna to the present day and the accumulation is subfossil in preservation.

## 2.22 FAUNAL SUCCESSION

To adequately reconstruct the faunal and palaeoecological succession from Early Pliocene through to the present day taphonomic processes must be considered and the maximum available source area of fauna must be estimated for each fossil site. This may be predicted by examining the gross taphonomic processes dominating the deposition of each faunal assemblage.

Two predominantly allochthonous accumulation modes are identified as accounting for all of the sites; these being pit-trap and/or predator accumulations. Thus, all large-sized fauna, which would have been too large for owls and Ghost Bats to dispatch, would have been derived from the immediate vicinity of the cave/fissure entrance. There is no indication for dening of large marsupicarnivores or major fluvial deposition as evidenced by the lack of gnaw marks on long bones and fluvially transported sediments. Smaller vertebrates would have been collected from the vicinity of the cave entrances as either allochthonous or autochthonous (cave dwelling) assemblages. Additionally, small vertebrates would have also been collected within the hunting ranges of both the Ghost Bat and owl, the only known cave-dwelling predators within the deposits.

	Mount Etna LF	Bluff Downs LF	Rackham's Roost LF	Chinchilla LF	Big Sink LF	Bow LF	Kanunka LF	Town Well Cave	Hamilton LF
	QLD	QLD	QLD	QLD	NSW	NSW	SA		VIC
MYA	Early Pliocene	Early Pliocene	Early Pliocene	late Early Pliocene	Early Pliocene	Early Pliocene	Late Pliocene	Mio-Pliocene	Early Pliocene
		3.8	3-5	3.4	3-5	3-5	3.4		4.46
<i>Thylacinus</i>	<i>cynocephalus</i>			<i>cynocephalus</i>	sp.				
<i>Antechinus</i>	spp.				sp.				sp.
<i>Sminthopsis</i>	<i>murina</i>		sp.		spp.				
<i>Dasyurus</i>	sp.	<i>dunmalli</i>		<i>dunmalli</i>		<i>dunmalli</i>			
Perameloid	gen. nov.				gen. nov.	gen. nov.			cf. <i>Peroryctes tedfordi</i>
<i>Perameles</i>	sp. 1 & sp. 2			<i>bowensis</i>		<i>bowensis</i>			
		<i>allinghamensis</i>				<i>allinghamesis</i>			
<i>Thylacoleo</i>	sp.	<i>crassidentatus</i>		<i>crassidentatus</i>	<i>crassidentatus</i>	<i>crassidentatus</i>			
<i>Thylacoleo</i>	<i>hilli</i>					<i>hilli</i>		<i>hilli</i>	
<i>Protemnodon</i>	cf. <i>devisi</i>	<i>snewini</i>	cf. <i>snewini</i>	<i>devisi</i>	<i>devisi</i>	<i>chinchillaensis</i>	cf. <i>devisi</i>		sp.
<i>Kurrabi</i>	sp.				cf. <i>merriwaensis</i>	<i>merriwaensis</i>	sp.		<i>plechenorum</i>
<i>Bohra</i>	sp.			<i>wilkinsonorum</i>					
<i>Dendrolagus</i>	sp.					sp.	sp.		sp.
<i>Macropus</i>	sp.	spp.		spp.		spp.	spp.		sp.
<i>Thylogale</i>	spp.								<i>ignis</i>
<i>Palorchetes</i>	cf. <i>parvus</i>	<i>selestiae</i>		<i>parvus</i>		cf. <i>parvus</i>			sp. nov.
Vombatidae	<i>Vombatus</i>	<i>Ramsayia</i>		? <i>Vombatus</i>		<i>Phascolonus</i>	<i>Vombatus</i>		gen. indet.
<i>Strigocuscus</i>	sp.								<i>notialis</i>
<i>Trichosurus</i>	sp. 2								<i>hamiltonensis</i>
Burramyidae	<i>Cercartetus</i>				<i>Cercartetus</i>				<i>Burramys</i>
<i>Pseudokoala</i>	sp.								<i>erlita</i>
<i>Pseudocheirus</i>	spp.								<i>marshalli</i>
<i>Petauroides</i>	spp.				cf. <i>stirtoni</i>				<i>stirtoni</i>
<i>Pseudocheirops</i>	spp.	<i>winteri</i>							
Petauridae	gen. nov.								<i>Petaurus</i>
<i>Macroderma</i>	<i>gigas</i>		<i>gigas</i>		<i>koppa</i>				

TABLE 4. Biocorrelations of taxa in the hypothesised Early Pliocene Mount Etna Local Fauna.

Owls have hunting ranges of up to 10km<sup>2</sup> (Lindsey, 1992) and *Macroderma gigas* ranges over an area of 2km<sup>2</sup> (Toop, 1985; Nelson, 1989). Thus owls would have had the potential to collect vertebrates from both the limestone bluff and the surrounding lowlands. The present day range of an owl at Mount Etna would encompass both closed vegetation typical of limestone bluffs out into lowland open vegetation. Small creeks are present within the owl's range and thus provide a third possible hunting habitat along riverine areas. Ghost Bat foraging areas would be considerably smaller and source the majority of its prey from the immediate vicinity of the feeding roost.

Owls are not considered to be an active accumulator at Marmor Quarry and Ghost Bats are considered to have had little input into the small vertebrate accumulation, therefore, Marmor Quarry is considered to have collected most of its fauna from the immediate vicinity of the pit-trap entrance.

Where possible, fossil sites were equally sampled to remove any potential collecting bias at each of the sites. Only presence/absence data are used for faunal and palaeoecological successions, with no analysis of relative abundance, which would be most affected by sample size. Collections from QML1312 are restricted due to the site's destruction prior to the expeditions in 2000.

On balance, the majority of faunas described here are considered to have been representative of the ecologies in direct vicinity of the cave entrances for both Mt Etna and Marmor Quarry.

*Anurans.* Greatest diversity of frogs occurs in the Early Pliocene sites from Mount Etna and Limestone Ridge. Of the 22 frog taxa identified here, 20 are found in the Early Pliocene sites. *Cyclorana* is restricted to the Holocene Olsen's Cave fauna and is not present in any of the older sites. New fossil frog records for Australia include the Early Pliocene species of *Nyctimystes*, *Etnabatrachus maximus* and microhylids. New frog records for the Early Pliocene include species of *Crinia*,

*Kyarannus*, *Lechriodus*, *Limnodynastes* and *Litoria*. The majority of the species present in the Early Pliocene are locally extinct by the late Pleistocene, leaving only a single species of *Limnodynastes*. Species of *Litoria* and *Cyclorana* occur in the Holocene assemblages. The present day frog fauna includes at least, *Cyclorana*, *Litoria*, *Limnodynastes* and

**Table 2-5 (TABLE 5.) Summarised ages for The Caves & Marmor fossil sites.**

Holocene	Olsen's
Late Pleistocene	QML1312
Plio-Pleistocene	QML1420
Early Pliocene	QML1313
	QML1384L
	QML1311C/D

*Pseudophryne*. The retention of *Litoria* and *Limnodynastes* into the present day fauna is not surprising as these genera are cosmopolitan in their distribution and habitat preferences.

Occurrence of *Neobatrachus* in the Early Pliocene is peculiar, representing a burrowing frog with a present day distribution restricted to arid areas. *Neobatrachus* has been recorded from the Pliocene of South Australia (Tyler, 1988; Tyler, 1994) in a palaeoecology that was wetter than today. Its presence within a predominantly rainforest frog fauna may be explained in a similar way as to the presence of the marsupial mole family, Notoryctidae, which occurs in a predominantly rainforest mammal fauna in the Oligo-Miocene of Riversleigh, yet it is confined to the arid zone of Australia today (Long et al., 2002). Adaptation for burrowing in soft rainforest soils may have allowed notoryctids to be pre-adapted to a later arid environment with soft sands. Similarly, it may be conceived that a burrowing frog that

originated in rainforest would then be pre-adapted to life in the arid zone.

*Chelids.* Turtle fossils are restricted to the Early Pliocene localities and are a rare component of the assemblages. Freshwater turtles occur throughout the region today and are almost never encountered on the limestone karst. Turtle fossils would become absent from the record as karstification developed inhospitable ground for turtles to traverse.

*Crocodylians.* Crocodile specimens are generally restricted to the Early Pliocene sites and are rare. A single specimen is known from QML368 which has yet to yield a contemporaneous large-sized fauna that can be biocorrelated, however, the small-mammal fauna suggests a Pleistocene age.

*Squamates.* Agamids (Dragons) are rare, but have been found in all deposits from the Early Pliocene through to the present. Early Pliocene agamid remains are mostly unidentifiable, however, a single specimen is referable to a species of *Hypsilurus*. Diversity of agamids is greatest in the late Pleistocene with species of *Amphibolurus*, *Pogona* (small-morph) and *Tympanocryptis* present. *Diporiphora* replaces these in the Holocene. The present agamid fauna includes, *Diporiphora*, *Chlamydosaurus* and *Pogona barbata* (large-morph).

Gekkonids (Geckoes) have been found throughout the Pliocene to present, except in QML1420. Absence of gekkonids from QML1420 is considered an artefact of small collection size and the absence of a distinct predator accumulation. The large gekkonid form is present in the Early Pliocene sites but missing in the late Pliocene to present day. Due to their general rareness within the Early Pliocene sites, it is uncertain whether the absence of the large gekkonid from younger sites is a taphonomic bias or a Plio-Pleistocene extinction. The small gekkonid forms are present throughout the Pliocene to the present, however, they probably constitute several distinct taxa.



Large scincids (Skinks) are conspicuous in the Early Pliocene deposits. *Tiliqua* is known from the Early Pliocene and Holocene, but does not occur in the Late Pliocene-Pleistocene or late Pleistocene faunas. Species of *Tiliqua* are rare within any assemblage, represented by single specimens. Its absence from sites cannot be determined as either ecological or taphonomic. *Cyclodomorphus gerrardii* is the most common large skink and is found from the Early Pliocene to the present day, with the exception of site QML1312. The absence of *Cyclodomorphus* from QML1312 is not considered to be due to taphonomic bias because abundant remains of other large-sized skinks are present in this fauna. Instead, *Cyclodomorphus* is considered to have become locally extinct due to late Pleistocene aridity. By the present day, *Cyclodomorphus* had dispersed back into the Mt Etna region. *Egernia* sp. is present throughout the Early Pliocene to Holocene. Large skinks found at Mount Etna today include *Tiliqua scincoides* and *Cyclodomorphus gerrardii*.

Varanids (Goannas & Monitors) are found from the Early Pliocene to the present day, with the exception of the Holocene faunal assemblage. This absence at Olsen's Cave is considered to be a taphonomic bias against large squamates (as with large mammals) because the deposit is derived from an owl roost. Two varanids are present in the Early Pliocene, one the size of modern *Varanus varius*, the second much more massive but not attaining the size of Pliocene or Pleistocene species of *Megalania*. These two taxa persist into the late Pleistocene, however, are missing from QML1420. Varanids are represented at QML1420 by the giant varanid *Megalania prisca*.

Elapids (Venomous snakes) are found from the Early Pliocene to the present day. Conspicuous size difference can be seen when comparing the largest vertebrae of elapids in the Pliocene-Pleistocene with those from the late Pleistocene. The late Pleistocene elapids are up to twice the size of their Early Pliocene relatives.

Pythonines are found from the Early Pliocene to the present day. Madstoids have

not been found. Python vertebrae tend to remain large-sized throughout the Pliocene to present day.

Typhlopids (Blind snakes) are only found in the Early Pliocene sites. This is the second record of fossil blind snakes in Australia and the first from the Pliocene. The first record was from the Oligo-Miocene Riversleigh deposits from far north Queensland (Archer et al., 1995b).

Typhlopids are a peculiar fossorial group with a cosmopolitan range today. A nocturnal ant/termite feeder, typhlopids represent a specialised niche within the Early Pliocene faunal assemblage at Mount Etna. The typhlopids seem to represent yet another group of fossorial animals, like the notoryctids (marsupial moles) and leptodactylids (*Neobatrachus*), which have utilised their adaptation for burrowing in ancient rainforests as an adaptative advantage with subsequent increasing aridity.

*Aves*. Four bird groups have been identified, including the quails (Galliformes), button quails (Gruiformes), song birds (Passeriformes) and owls (Strigiformes). The owls are a conspicuous component of all the fossil assemblages except QML1420. Their absence at QML1420 is considered to be due to taphonomic processes. All four groups exist in the area today. The Early Pliocene occurrence of owls is the oldest known in Australia.

*Thylacinidae*. *Thylacinus cynocephalus* is present from the Early Pliocene to late Pleistocene. *Thylacinus cynocephalus* is absent from the Plio-Pleistocene site QML1384U, which is probably due to the taphonomic bias in that deposit toward smaller-sized mammals. *Thylacinus* is absent by the Holocene.

*Dasyuridae*. *Antechinus* spp. are present from the Early Pliocene through to the present day. During the Early Pliocene, *Antechinus* is represented by two species. By the late Pleistocene, these two species are extinct, having been replaced by *Antechinus*

*flavipes* and *Antechinus swainsoni*. *Dasyurus* spp. are also present from the Early Pliocene through to the present day. During the Pliocene *Dasyurus* is represented by a medium-sized species. This species is replaced by *Dasyurus hallucatus* and *Dasyurus viverrinus* during the late Pleistocene. *Dasyurus hallucatus* and *Dasyurus maculatus* are found in the Holocene and present day fauna respectively. *Phascogale* has a possible appearance in the Early Pliocene with a small undescribed species. This species continues into the Pleistocene, however, it is extinct by the late Pleistocene, having been replaced with *Phascogale topoatafa*. *Planigale maculata* appears in the late Pleistocene and remains in the Holocene and present day fauna. An extinct, undescribed, small planigale-like dasyurid is present in the Pliocene but is extinct by the Pleistocene. Species of *Sarcophilus* are present from the Early Pliocene to late Pleistocene and possibly Holocene. *Sarcophilus lanianus* is known to occur from the Early Pliocene to late Pleistocene. A single specimen of *Sarcophilus harrisii* is present in the late Pleistocene-Holocene from Lower Johansen's Cave (QML1314). Species of *Sminthopsis* occur in the Early Pliocene but are rare within the Pliocene assemblages. During the late Pleistocene *Sminthopsis* represents the most abundant small-sized dasyurid, represented by two species, *Sminthopsis murina* and *Sminthopsis macroura*.

*Vombatidae*. A species of *Vombatus* is represented by three specimens, one in the Early Pliocene and two in the Plio-Pleistocene site QML1420. *Vombatus* is not present in the area by the late Pleistocene.

?*Zygomaturine*. This large-sized diprotodont is only known in the region from the Plio-Pleistocene (QML1420).

*Palorchestidae*. *Palorchestes* sp. cf. *P. parvus* is present in the Early Pliocene and in the Plio-Pleistocene (QML1420).

*Macropodidae*. *Bohra* sp. is only present in the Early Pliocene. Species of *Dendrolagus* are present from the Early Pliocene to late Pleistocene. Species of *Thylogale*, *Petrogale* and *Macropus* are all present from the Early Pliocene to the present day. *Protemnodon* sp. cf. *P. devisi* and *Kurrabi* are only present in the Early Pliocene. *Macropus titan* is restricted to the Plio-Pleistocene of Marmor Quarry and is absent from the late Pleistocene. This is the first record in Australia of *Dendrolagus* in the Pleistocene and the second record of *Bohra* in the Pliocene (Dawson, 2004).

A conspicuous absence from the macropod fauna are the morphologically distinct potoroids, in particular *Potorous* and *Hypsiprymnodon*. Although they may turn up in future collections, the sample sizes at present suggest that this may be unlikely and that this group of macropods was absent from the Early Pliocene of Mt Etna.

Interestingly, the small macropod fauna at Mt Etna includes several small-sized macropodids, namely *Thylogale* sp. 1, which is very similar to the Irian Jaya *Thylogale christenseni*. Furthermore, there are no potoroids known from the present day or fossil record of Papua New Guinea and Irian Jaya, yet the small macropodid faunas tend to be either species of *Thylogale* or *Dorcopsis*. The disjunctive nature of this macropodid fauna, where the Early Pliocene Mt Etna fauna more closely resembles those from Papua New Guinea and Irian Jaya, is also seen in the *Pseudocheiridae*.

*Pseudocheiridae*. *Pseudocheirids* are considerably diverse during the Pliocene but are locally extinct by the late Pleistocene, returning in the Holocene as a rarity and abundant in the present day as a single taxon, *Pseudocheirus peregrinus*.

*Pseudochirulus* spp. are present in the Early Pliocene, including *Pseudochirulus* sp. 1 which is very similar to the Early Pliocene Hamilton Fauna *Pseudochirulus marshalli* and the modern Papua New Guinean *Pseudochirulus canescens* and *Pseudochirulus mayeri*. Similarly, taxa referred to here as *Petauroides* share

closer taxonomic affinities with species from both the Early Pliocene Hamilton Fauna and the late Pleistocene Irian Jayan Fauna, than they do to the modern *Petauroides* and *Hemibelideus* from far north Queensland forests and rainforests.

*Petauridae*. The new genus of petaurid is present with two species in the Pliocene and one species in the Plio-Pleistocene and late Pleistocene. It is extinct by the Holocene. *Dactylopsila* is present in the Pliocene but is locally extinct by the Pleistocene. This is the first post Miocene, and pre Holocene, record of *Dactylopsila* in Australia. *Dactylopsila* sp. 2 is diminutive in size relative to any living species, however, it is very close to the extinct Irian Jayan taxon, *Dactylopsila kambuayai*, which along with the macropodids and pseudocheirids illustrates a possible faunal connection to Papua New Guinea and Irian Jaya during the Early Pliocene.

*Superfamily incertae sedis*. A new genus and species of possum with unknown phylogenetic and taxonomic affinities is present in the Early Pliocene but has yet to turn up in younger sediments.

*Acrobatidae*. *Acrobates* occurs in the Early Pliocene and has not been found in younger sediments. This is the first record of acrobatids in the Pliocene of Australia.

*Burramyidae*. *Cercartetus* occurs in the Pliocene but is not found in younger sediments. The only other Pliocene record of *Cercartetus* is from the Big Sink Fauna (Dawson et al., 1999).

*Phalangeridae*. *Strigocuscus* is present in the Pliocene but is absent by the Pleistocene. *Trichosurus* is represented by two species, the first confined to the Early Pliocene and the second found in the Pleistocene, Holocene and present day.

*Thylacoleonidae*. Two species of *Thylacoleo*, one small and one large species, occur in the Early Pliocene whilst one large species has been found in the Plio-Pleistocene (QML1420). No remains of *Thylacoleo* have yet been found in late Pleistocene

deposits.

*Peramelidae*. Species of *Perameles* occur throughout the Pliocene and into the present day. During the Pliocene and Plio-Pleistocene times, *Perameles* was represented by two extinct species. By the late Pleistocene to Holocene, these species were replaced by *Perameles bougainville* and eventually *Perameles nasuta*. *Isoodon* occurs in the Plio-Pleistocene to present day. *Isoodon* is represented by two small-sized species in the Plio-Pleistocene and late Pleistocene sites, *Isoodon obesulus* and *Isoodon* sp. During the Holocene, small-sized *Isoodon* were replaced with the larger *Isoodon macrourus*. During the late Pleistocene both *Chaeropus* and *Macrotis* appeared, leaving no further record.

*Perameloid* incertae sedis. An enigmatic family of bandicoots possibly related to the Oligo-Miocene Yaralidae are restricted to the Pliocene-aged deposits.

*Muridae*. Rodents are a conspicuous element of every deposit. Early Pliocene rodents include the first records of many rainforest taxa with no previous fossil records in Australia. Several taxa are found to dominate the Pliocene sites with possible Plio-Pleistocene records. These include *Melomys/Uromys*, *Pogonomys* and *Mesembriomys*. *Zyzomys* is present from the Pliocene to late Pleistocene.

*Leggadina* is found in the late Pleistocene to Holocene. *Conilurus* is found in the late Pleistocene. *Rattus* is found from the Plio-Pleistocene to present day.

*Pseudomys* is found from the Pliocene to present day. *Notomys* is restricted to the late Pleistocene. *Hydromys* has been recovered from the Early Pliocene, Plio-Pleistocene (QML1420) and present day faunas.

*Microchiropterans*. Bats are found in all deposits, except QML1420.

*Macroderma gigas* is found from Early Pliocene to the present day.

## 2.23 PALAEOECOLOGICAL SUCCESSION EARLY PLIOCENE.

*Nonseasonal, Mesothermal, angiosperm- dominant rainforest with emergent gymnosperms; minor grassy understory.*

Rainforest has been indicated both locally by the fauna and regionally through palynological studies of the Early Pliocene. Two pollen cores, Aquarius Well (Fig. 1A,5) (Hekel, 1972) and ODP815 (Fig. 1A,4) (Martin & MacMinn,1993), located off the central eastern Queensland coast are close to the fossil sites. The Aquarius Well core was taken from the edge of the Capricorn Trough, which is located to the NE of Mount Etna and Marmor Quarry (Fig. 1). Hekel (1972) published the palynological record of Aquarius Well, showing a dramatic increase in rainforest flora in the region post Late Miocene and dominating the entire Early Pliocene.

ODP815 drill core (Martin & MacMinn,1993) from the Marion Plateau to the NE of Mount Etna shows an Early Pliocene dominated by rainforest flora. Macphail (1997) reviewed both the Aquarius Well and ODP815 records and concluded that the dominant vegetation type during the Early Pliocene would have been an angiosperm-dominated mesothermic rainforest with Araucaraceae. Low pollen counts for rainforest angiosperm taxa were considered to be an artefact of taphonomic bias toward more dispersible taxa, however, no conclusions could be drawn as to how dominant or complex the rainforest angiosperms were. Macphail (1997) suggests that the climate required to support such a vegetation structure would include temperatures greater than 20<sup>0</sup>C, and an annual precipitation rate of between 1300 and 2000mm.

Fauna recovered from Early Pliocene-aged sites within the local area of Mount Etna and Limestone Ridge support the presence of rainforest at the time, as follows;

*Anurans.* Microhylids are recorded from the Early Pliocene deposits and,

although rare, indicate a very moist rainforest environment. *Nyctimystes* is presently known from rainforests of far north Queensland and Papua New Guinea, whilst *Lechriodus* is known from rainforest in southeastern Queensland and Papua New Guinea. *Kyarranus*, although not exclusively rainforest dwelling, is restricted to areas of constant moisture in areas close to or within montane rainforest or wet sclerophyll. Interestingly, the suite of frog genera identified in the Early Pliocene is similar to that recorded from the interpreted rainforest ecologies present during the Oligo-Miocene of Riversleigh (*Litoria*, *Limnodynastes*, *Kyarranus*, *Lechriodus*, and *Crinia*) (Tyler, 1991; Tyler 1994) and to those identified from the montane rainforests of Papua New Guinea (Menzies et al., 2002).

The overall abundance and diversity of small-sized frogs and the presence of only a single, rare, monotypic giant frog (*Etnabatrachus maximus*) indicates that the area experienced a reliable (non-seasonal) precipitation regime (Tyler, 1994).

*Squamates*. Several squamates indicate a predominantly rainforest ecology during the Early Pliocene. The most abundant large-sized squamate present in any of the Early Pliocene deposits is *Cyclodomorphus gerrardii*. Although also found in dry sclerophyllic vegetation today, *Cyclodomorphus gerrardii* is most frequently encountered in wet sclerophyll and rainforest. *Hypsilurus* sp. has been identified from the Early Pliocene. This agamid genus is rainforest-restricted, present only in rainforests of southeastern Queensland, the Wet Tropics and Papua New Guinea.

*Mammals*. Several analyses of Australian mammal biogeography have focused on determining correlative values that describe the patterns seen in rainforest mammal distributions (Braithwaite et al., 1985; Williams, 1997; Kanowski et al., 2001; Kanowski et al., 2003; Winter, 1988; Winter, 1997; Laurance, 1997; Nix & Switzer, 1991). These correlative values encompass several different categories



into which the mammals found in rainforests have been placed. These categories include broad definitions such as “Rainforest Specialists Species”, “Forest Generalists Species”, “Rainforest Ecotone Species”, “Generalist Species” and “Independent Species” (Winter, 1988); or more specific definitions, such as the eleven defined tropical mammal guilds of Braithwaite et al. (1985). Williams (1997) used Braithwaite et al.’s guilds to describe patterns seen in mammal species of the Wet Tropics rainforest. Other authors (Kanowski et al., 2001; Kanowski et al., 2003; Winter, 1997; Laurance, 1997; Nix & Switzer, 1991) have either focused on a single or a combination of ecological parameters to describe patterns in rainforest mammal species-richness. These parameters include; modeled palaeoclimate, floristics, altitude, geology, precipitation, rainforest shape and size, latitude, temperature, habitat fragmentation and predators. These criteria developed for modern rainforest mammals have been utilised here in identifying the palaeoecological parameters of the Early Pliocene environment, since several extant mammal genera (and possibly species) with obvious rainforest affinities occur in the Early Pliocene sites.

#### *Ecological Specialisation.*

Forteen extant mammal species were identified by Winter (1988) to be rainforest specialists and restricted to northern Queensland. Of these taxa, eight are considered to be rainforest specialist genera (*Phalanger*, *Uromys*, *Pogonomys*, *Pseudocheirops*, *Pseudochirulus*, *Hypsiprymnodon*, *Hemibelideus* and *Dendrolagus*). In the Early Pliocene assemblages, five of these eight genera are present, with the absence of *Phalanger*, *Hypsiprymnodon* and *Hemibelideus*.

Rainforest-restricted mammal species were determined for Australia and New Guinea by using Strahan (1995) and Flannery (1994) respectively. The genera

*Strigocusus* and *Dactylopsila* are presently rainforest-restricted and are found in the Early Pliocene at Mt Etna. Additionally, *Cercartetus* sp. is considered to be very close to, if not conspecific with, *Cercartetus caudatus*, and although *Cercartetus* is not a rainforest-restricted genus, *Cercartetus caudatus* is a distinct rainforest specialist (Winter, 1988). *Antechinus* sp. 1 is considered to be very close to the rainforest-restricted *Antechinus adustus* (Van Dyck & Crowther, 2000).

#### *Mammal guilds and species richness*

Palaeoecological reconstruction using extant rainforest-restricted and specialist taxa as analogues provides good evidence for the presence of rainforest during the Early Pliocene. Defining the different mammalian guilds and the species richness present at sites allows for an extension of the palaeoecological reconstruction to include possible correlations with floristic diversity and climate as seen in modern day rainforest studies (Braithwaite et al., 1985; Heads, 2002; Williams, 1997).

Braithwaite et al. (1985) defined Australian tropical mammal guilds on the basis of three traits; 1. Body size (small <200g, medium 200-3kg, and large 3kg-10kg); 2. Microhabitat (arboreal, scansorial and terrestrial); and 3. Diet (insectivore, nectarivore, folivore/frugivore (here classed as herbivore), carnivore, omnivore and granivore).

Allocation of these three traits to the taxa from the Early Pliocene was achieved by choosing the closest living analogue or determining each trait from morphology. Table 6 lists the Early Pliocene mammalian fauna, their modern analogues and defined guild type based on Braithwaite et al's traits.

Most of the fossil taxa were able to be assigned to their equivalent modern day analogue by means of genus-level identity. Most species within the analogue genus shared traits defined for that genus' guild, with the possible exception of size. For genera with unknown modern analogues, the closest living taxon to the extinct taxon was used, with inferences drawn for each trait based on family-level trait

similarity. For example, *Pseudokoala* was defined as being a large-sized ( $>3\text{kg}$ ), arboreal herbivore, based on its much larger size when compared with the largest living pseudocheirid (*Pseudocheirops* -  $<3\text{kg}$ ); and because all living pseudocheirids are arboreal and herbivorous.

Fossil Taxon	Present Day Analogue	Guild
Thylacinidae		
<i>Thylacinus</i>	<i>Thylacinus cynocephalus</i>	VLTC
Dasyuridae		
<i>Antechinus sp. 1</i>	<i>Antechinus</i>	SSI
<i>Antechinus sp. 2</i>	<i>Antechinus</i>	SSI
<i>Dasyurus sp.</i>	<i>Dasyurus</i>	MSI/C
<i>Phascogale sp.</i>	<i>Phascogale</i>	SSI
<i>Sarcophilus laniarius</i>	<i>Sarcophilus harrisii</i>	LTC
<i>Sminthopsis murina</i>	<i>Sminthopsis murina</i>	SSI
dasyurid new	<i>Planigale</i>	STI
Vombatidae		
<i>Vombatus ursinus mitchelli</i>	<i>Vombatus ursinus</i>	VLTH
<i>Palorchestes sp.</i> cf. <i>P. parvus</i>	None	VLTH
diprotodont indet	None	VLTH
Macropodidae		
<i>Bohra sp.</i>	None	LSH
<i>Dendrolagus spp.</i>	<i>Dendrolagus</i>	LAH
<i>Thylogale sp. 1</i>	<i>Thylogale christenseni</i>	MTH
<i>Thylogale sp. 2</i>	<i>Thylogale stigmata</i>	LTH
<i>Petrogale</i>	<i>Petrogale</i>	LTH
<i>Macropus sp. 1</i>	<i>Macropus dorsalis</i>	LTH
<i>Protemnodon cf. P. devisi</i>	None	VLTH
<i>Kurrabi</i>	None	LTH
Pseudocheiridae		
<i>Pseudocheirulus sp. 1</i>	<i>Pseudocheirulus mayeri</i>	SAH
<i>Pseudocheirulus sp. 2</i>	<i>Pseudocheirulus canescens</i>	MAH
<i>Pseudocheirulus sp. 3</i>	<i>Pseudocheirulus herbertensis</i>	SAH
<i>Pseudocheirus spp.</i>	<i>Pseudocheirulus spp.</i>	SAH
<i>Petauroides</i>	<i>Petauroides/Hemibelidius</i>	SAH
<i>Pseudocheirops sp. 1</i>	<i>Pseudocheirops</i>	MAH
<i>Pseudocheirops sp. 2</i>	<i>Pseudocheirops</i>	MAH
<i>Pseudokoala</i>	None	LAH
Petauridae		
<i>gen. et sp. nov. 1</i>	<i>Petaurus</i>	SAN-I
<i>gen. et sp. nov. 2</i>	<i>Petaurus</i>	SAN-I
<i>Dactylopsila sp. 1</i>	<i>Dactylopsila</i>	SSI
<i>Dactylopsila sp. 2</i>	<i>Dactylopsila</i>	SSI
Incerti Sedis		
<i>gen. et sp. nov.</i>	None	SAN-I
Acrobatidae		
<i>Acrobates sp.</i>	<i>Acrobates</i>	SAN-I
Burramyidae		
<i>Cercatetus sp.</i>	<i>Cercatetus</i>	SAN-I
Phalangeridae		
<i>Strigocuscus</i>	<i>Strigocuscus</i>	LAH
<i>Trichosurus sp. 2</i>	<i>Trichosurus</i>	LAH

Fossil Taxon	Present Day Analogue	Guild
Thylacoleonidae		
<i>Thylacoleo hilli</i>	None	LSC
<i>Thylacoleo sp.</i>	None	VLSC
Peramelidae		
<i>Perameles sp. 1</i>	<i>Perameles</i>	MTO
<i>Perameles sp. 2</i>	<i>Perameles</i>	MTO
Perameloid fam. Incertae sedis		
<i>gen. et sp. nov. 1</i>	<i>Perameles/Peroryctes</i>	MTO
<i>gen. et sp. nov. 2</i>	<i>Perameles/Peroryctes</i>	MTO
Muridae		
<i>Hydromys</i>	<i>Hydromys</i>	MQO
<i>Pseudomys spp.</i>	<i>Pseudomys</i>	STO
<i>Zyomys</i>	<i>Zyomys</i>	STO
<i>Uromys/Melomys</i>	<i>Uromys/Melomys</i>	SSH
<i>Pogonomys</i>	<i>Pogonomys</i>	SSH
<i>Mesembriomys</i>	<i>Mesembriomys</i>	MSO

**Table 2-6 (TABLE 6.) Mammalian guilds defined for the Early Pliocene. Guild traits expanded from Braithwaite et al., (1985). Abbreviations: Size; S. Small, <200g; M. Medium 200g-3kg; L. Large 3kg-20kg, VL Very Large >20kg. Microhabitat: A. Arboreal, T. Terrestrial, S. Scansorial, Q. Semi-aquatic. Diet: N- Nectarivore, I - Insectivore, O – Omnivore, C - Carnivore, H - Herbivore.**

The remaining taxa are those with no family-level trait similarities to modern groups (Diprotodontidae, Palorchestidae and Thylacoleonidae). All three of these families are characterised by being very large-sized (>20kg), with the exception of *Thylacoleo hilli*, which is considered here to be large-sized (between 10 and 20kg) (Wroe et al., 2004). Based on the very-large size of these mammals, a fourth body size trait is added here. Two mammal families are considered to be terrestrial in their microhabitat due to their very large size, with the exception of *Thylacoleo*, which is here considered to be scansorial. Diprotodontidae and Palorchestidae are considered to be herbivores and members of the Thylacoleonidae to be carnivores.

All of the guilds defined by Braithwaite et al. (1985) were present in the Early Pliocene at Mt Etna. Nine new guilds were identified that did not fit the 11 guilds defined by Braithwaite et al. (1985) and are here considered to be either present in the Wet Tropics, Papua New Guinea/Irian Jaya or extinct from rainforests today. These nine guilds were; 1. Small-sized, arboreal, herbivore (SAH) (e.g. *Pseudochirulus mayeri*, *Pseudochirulus* sp 1., *Pseudocheirus* sp. 1-2). This guild is present today in Papua New Guinea and Irian Jaya; 2. Medium-sized arboreal herbivore (MAH) (e.g. *Pseudochirulus* spp., *Pseudocheirops* spp.). Today present in the The Wet Tropics, Papua New Guinea and Irian Jaya; 3. Large-sized, scansorial carnivore (LSC) (e.g. *Thylacoleo hilli*), which is extinct; 4. Medium-sized terrestrial herbivore (MTH) (e.g. *Thylogale* sp. 1, *Thylogale christenseni*), recently extinct in Irian Jaya (Hope, 1981); 5. Medium-sized, semi-aquatic omnivore (MQO) (e.g. *Hydromys*), present in the Wet Tropics, PNG and Irian Jaya; 6. Large-sized, scansorial herbivore (e.g. *Bohra* sp.), which is now extinct; 7. Very large-sized, terrestrial herbivore (VLTH) (e.g. *Palorchetes*, diprotodont), extinct; 8. Very large-sized terrestrial carnivore (VLTC) (e.g. *Thylacinus*), extinct; and 9. Very large-sized scansorial carnivore (VLSC) (e.g. *Thylacoleo*), extinct.

Braithwaite et al. (1985) illustrates that the greatest number of mammalian guilds found in the Australian tropics are located in the habitat classified as rainforest. Williams (1997) illustrates that three guilds; small, scansorial, insectivores; large, arboreal, herbivores; and small, scansorial, omnivores, are important in determining species richness in modern rainforest of the Wet Tropics and are also the most extinction prone. All three of these guilds are present in each of the interpreted Early Pliocene sites at Mt Etna.

Williams (1997) also shows that overall species richness in rainforest is positively influenced by guild diversity, rainforest shape, area and habitat diversity (rainfall and vegetation diversity). According to Williams (1997), the number of small to large-sized mammalian guilds present in the most species rich locations of the present day Wet Tropics is nine. The number of small to large sized mammalian guilds from individual sites in the Early Pliocene of Mount Etna ranges from ten to thirteen.

Williams (1997) identifies two regions of the northern Queensland Wet Tropics that possess the greatest species richness (21-26 spp), greatest number of endemic mammal species (4-8 spp.) and thus the greatest number of guilds (9) of rainforest mammals in Australia. These two areas are defined by Williams as the Windsor and Carbine Uplands, and the Lamb, Atherton, Bellenden-Ker/Bartle-Frere & Kirrama Uplands. Both regions have their greatest area above 1000m altitude and possess the greatest vegetation diversity of the Wet Tropics. The present day climatological parameters needed to sustain such a large number of guilds and high species richness for these two upland regions is a high consistent (nonseasonal) precipitation rate (>2000mm) with a moderately cool to cool annual temperature regime (meso-megathermal; 21-23°C) (Nix, 1982; Winter, 1997).

Rainforest areas of the Papua New Guinean central highlands show similar species richness of mammals (24-29 spp) (Halls, 2002). These regions are defined by Nix (1982) as a nonseasonal mesothermal-microthermal (12-14°C) climate.

The similarities seen here for both the Wet Tropics and Papua New Guinea suggest that both regions possess their greatest mammalian species richness and guild diversity in areas that have a relatively cool climate with nonseasonal high annual rainfall. Each of the Early Pliocene sites from Mt Etna possess from at least 21 to 30 small to large-sized mammal species. This species richness is similar to that found in Papua New Guinea and the Wet Tropics of today, however, this does not account for the very large-sized taxa also present in the Early Pliocene.

When considered together; guild diversity, species richness, specialist and endemic taxa, the Early Pliocene faunal assemblage strongly indicates the presence of a diverse rainforest habitat, which was subject to regular nonseasonal high rainfall in a mesothermal climate regime (20-23°C). The entire fauna strongly indicates a vegetation structure that included several levels of complexity to house diverse guilds containing, arboreal, scansorial, terrestrial, fossorial, semi-aquatic and aquatic niches. On the basis that the fossil sites are not found higher than 200m above sea level today, the Early Pliocene rainforest could be considered to be lowland rainforest. The diversity of mammalian nectarivores, herbivores and insectivores indicates the presence of an equally diverse angiosperm flora, possibly more diverse than what is indicated in the ODP 815 and Aquarius Well pollen cores. The very rare occurrence of grazing macropods and a single wombat specimen indicates the presence of small areas of grasslands or grassy understory within the Mt Etna area.

#### PLIO-PLEISTOCENE.

*Seasonal, mesothermal, mosaic rainforest sclerophyll forest with chenopod, Asteraceae and grassy understory.*

The Plio-Pleistocene pollen record for central eastern Queensland shows an increased seasonality toward the end of the Late Pliocene and into the Pleistocene

with an increase in the sclerophyllous vegetation and decrease in several rainforest groups (Martin & McMinn, 1993). Podocarps, aruarcarians and ferns decrease with an increase in Casuarinaceae in the Aquarius Well core (Hekel, 1972). Similarly gymnosperms, rainforest angiosperms and ferns decrease during the Plio-Pleistocene of ODP815. A sudden increase in Chenopodaceae and Asteraceae is seen in the Plio-Pleistocene Aquarius Well record (Hekel, 1972), and a steady increase in these two floristic groups is seen toward the Late Pliocene and Pleistocene in the ODP815 core (Martin & McMinn, 1993).

Two sites record the Plio-Pleistocene vertebrate record of central eastern Queensland (QML1384U and QML1420). This is due to the intermediate faunal similarity between the Early Pliocene rainforest faunal assemblage and the late Pleistocene faunal assemblage. QML1384U retains the distinct rainforest signal found in the Early Pliocene, however, there are a number of differences that may reflect a more seasonal climate. Additionally, QML1420, has a fauna that shows a more seasonal, open habitat.

*Frogs.* Only two frog species have been identified in the Plio-Pleistocene faunal assemblage, *Litoria* and *Kyarranus*. Although specimens are abundant at QML1384U, the presence of so few frog taxa may reflect a less complex vegetation and precipitation regime during this time. Neither taxon is specifically rainforest-dwelling, however, *Litoria* sp. indicates an arboreal environment and *Kyarranus* sp. indicates areas of permanent moisture.

*Squamates.* The presence of *Cyclodomorphus gerrardii* indicates a closed, wet, forest system.

*Mammals.* Although the mammal species are similar to those from the Early Pliocene, several taxa have been replaced by species with a broader environmental tolerance. *Antechinus flavipes* is present in the Plio-Pleistocene and possibly possesses a broader ecological range than that hypothesised for *Antechinus* sp. 1 and



*Antechinus* sp. 2, which it replaces. *Sminthopsis macroura* also appears in Plio-Pleistocene, which may indicate a dry, open environment based on its present day distribution. Extant *Sminthopsis macroura* are commonly found in chenopod shrublands throughout central Australia (Strahan, 1998), therefore the presence of chenopods in the Plio-Pleistocene pollen record could have provided suitable habitat for this species.

Arboreal possums continue to constitute a large portion of the QML1384U fauna, less so QML1420. Pseudocheirids are represented by three genera (*Pseudochirulus*, *Pseudocheirus* and *Petauroides*), petaurids with two genera (*Dactylopsila* and new genus), burramyids by *Cercartetus*, and phalangerids by *Strigocuscus*. The abundance of arboreal herbivores, insectivores and nectarivores, indicates the retention of some rainforest and a dominance of angiosperms in the vicinity of Mt Etna. Bandicoot diversity shows changes from the Early Pliocene with the appearance of two species of *Isodon*. *Isodon obesulus* possibly indicates a more mosaic vegetation structure (Strahan, 1998).

Macropod diversity remains high at QML1420, with a strong component of grazing macropodids, indicating the presence of more extensive grasslands at Marmor Quarry.

The mammal assemblage at QML1420 indicate a mosaic of environments present in the area, including open areas with grasses (*Macropus* spp, *Vombatus*, *Megalania prisca*, zygomaturine), closed forest (*Dendrolagus*, *Thylogale* sp. 2, *Trichosurus*, Petauroid new genus and *Melomys/Uromys*) and semi-aquatic (*Hydromys*).

## LATE PLEISTOCENE (ca. 149,000 ybp)

*Dry, open arid-zone with closed 'refugial' forest.*

The pollen record for the late Pleistocene is absent at Aquarius Well and ODP815, demarcated by a hiatus of deposition and correlated with sea level fall (Hekel, 1972; Martin & McMinn, 1993). As an alternative, Lynch's Crater (Fig. 1A, 2), far north Queensland provides a better late Pleistocene record for Queensland (Kershaw, 1986). Kershaw (1986) estimates an annual precipitation rate which is 50% lower than the present day approximately 150,000 years ago. If it is hypothesised that the Mt Etna area experienced a similar relative decrease in annual precipitation rate during this period of time, then the annual precipitation rate would have been less than 500mm (present day annual rainfall is between 800-1000mm, Data from Bureau of Meteorology: [www.bom.gov.au](http://www.bom.gov.au)). An annual precipitation rate of below 500mm is equivalent to the precipitation rate currently recorded in central western Queensland, approximately 600kms to the west of Rockhampton. The late Pleistocene faunal assemblage reflects the very dry components of this ecology, however, it also records remnants of more mesic, probably refugial, environments.

*Frogs.* Frog diversity is low with only a single taxon so far positively identified and a complete absence of hylids (tree frogs).

*Squamates.* Squamate diversity is high, with most taxa identified, presently existing in the Australian arid zone. The squamates comprise, three agamids, all of which are currently restricted to the arid zone of central Australia; at least three species of skink; two large-sized varanids and several elapids. The absence of *Cyclodomorphus gerrardii* supports the contention for a very dry habitat.

*Mammals.* A distinct faunal change demarcates the late Pleistocene mammal assemblage from the older faunas of the same area. The small to large-sized dasyurids illustrate a diversity of insectivorous and carnivorous niches available within the ecology. There is retention of *Antechinus flavipes*, *Dasyurus*

*hallucatus*, *Sminthopsis murina* and *Sminthopsis macroura* from older assemblages, with the addition of *Antechinus swainsonii*, *Dasyurus viverrinus*, *Planigale maculata* and *Phascogale topoatafa*. *Antechinus swainsonii* indicates the presence of closed wet environments, as do *Antechinus flavipes*, *Sminthopsis murina* and *Planigale maculata*. The remaining three new taxa lend evidence to the presence of dry sclerophyll in the region because all three extend into these environments today. Macropodines also indicate the presence of both open and closed environments with *Macropus* indicating grasses and *Thylogale* sp. 2 and *Dendrolagus* occupying closed forest. Possums are almost entirely absent with only two taxa present, *Trichosurus* sp. 1 and the new genus of petauroid.

*Perameles bougainville* appears in the record during the late Pleistocene, indicating the presence of dry open environments with shrubby, possibly chenopod-dominant ground cover. *Isodon obesulus* remains in the faunal assemblage, supporting the mosaic nature of the palaeoenvironment. *Chaeropus ecaudatus* and *Macrotis lagotis* both strongly indicate a dry climate. Additionally, they illustrate the presence of grasses, possibly tussock grasses, in the area (Strahan, 1998). The rodent fauna also suggests a combination of distinctive dry and woodland species. The presence of species of *Notomys* and *Leggadina* suggest an open environment, whilst *Conilurus* sp. suggests woodland.

On balance, the faunal assemblage indicates mosaic vegetation with areas of open grassland/chenopod shrubland, sclerophyll forest and a closed refugial forest. Such refugial forest is seen today in the semi-evergreen vine forest on Mount Etna, where the vine thickets are restricted to the wetter microclimates of limestone, whilst being surrounded by dry sclerophyll woodlands.

## 2.24 CONCLUSION

Analysis of faunal and palaeoecological succession spanning the Early Pliocene

to Holocene in central eastern Queensland is made possible by the long accumulation histories of cave and fissure systems in this region. As with the Wellington Caves of New South Wales (Dawson et al., 1999), Mount Etna provides a unique opportunity to document environmental change over ca. 4 million year period and the fauna associated with this change.

The Pliocene sites from Mount Etna are distinguished from all other sites in Australia of similar age by the presence of a distinct and dominant rainforest fauna, with the exception of the Hamilton Local Fauna. All other Pliocene sites in Australia differ from those at Mount Etna and Hamilton by possessing none or minor components of the fauna which are rainforest-adapted. In addition, the Mount Etna Fauna provides biogeographic links to Papua New Guinea and Irian Jaya by possessing taxa that are now restricted to these areas today or have only recently gone extinct there.

The mammalian fauna of the Early Pliocene at Mount Etna suggests biogeographic connectivity to Papua New Guinea and Irian Jaya during or just prior to this time. The murid fauna indicates a much earlier dispersal event of rainforest murids into Australia and questions the late Pleistocene or Holocene arrival previously suggested (Flannery, 1995; Winter, 1997). Combining an Early Pliocene record of rainforest specialist murids at Mount Etna with the incredibly diverse and endemic murid fauna from Rackham's Roost, Riversleigh, far north Queensland, substantially increases the probability that murids entered Australia before the Early Pliocene and probably in the Late Miocene (Archer et al., 1991; Long et al., 2002). The Pliocene possum and macropod faunas from Mount Etna illustrate connectivity between New Guinea and Australia also, by possessing taxa (or lineages) with affinities to taxa now extant or recently extinct in New Guinea.

Although the fossil record is patchy between the Early Pliocene and late Pleistocene, there is a distinct trend in the fauna to become arid-adapted, with an arid-

adapted fauna by the late Pleistocene. The late Pleistocene fauna adds new records for the palaeodistribution of arid-adapted taxa, with several extant central Australian taxa being found extremely close to the eastern Australian coastline. Even so, several mesic-adapted taxa persist into the late Pleistocene, probably existing in refugia offered by the limestone bluffs in the Mount Etna area, as is seen today.

The Mount Etna and surrounding fossil deposits offer a unique opportunity to document the evolution of the central Queensland environment over 4 million years of climate change, including the extinction of a diverse rainforest community, the expansion of the arid zone interior and the isolating affects on fauna utilising the refugial nature of limestone bluffs.

## **2.25 ACKNOWLEDGEMENTS**

Henk Godthelp is thanked for his assistance in rodent identifications. Jian-xin Zhao is thanked for his provision of preliminary dating results. The following people and groups are acknowledged for their encouragement and assistance in developing this study: Aaron Sands, Alex Cook, Amy Sands, Aust. Skeptics, Ayla Tierney, Bernie Cooke, Chris White, Deb Lewis, Gilbert Price, Gregg Webb, Henk Godthelp, Jan Williams, Jeannette Sands, Jian-xin Zhao, Joanne Wilkinson, John Hocknull, John Walsh, Jonathan Cramb, Kristen Spring, Liz Reed, Lyndall Dawson, Mary Dettmann, Merv Barton, Michael Archer, Mina Bassarova, Morag Hocknull, Noel Sands, Paul Tierney, Peter Jell, Shona Marks, Steve Bourne, Sue Hand and numerous volunteers. This study (in part) has been assisted by funds provided by an Australian Research Council Linkage Grant LP0453664, with the following Industry Partners: Queensland Museum, Cement Australia, Central Queensland Speleological Society, Rockhampton Regional Development. Tourism Queensland is thanked for additional funding.

**2.26 Appendix 1. Small-sized mammalian fauna data matrix. 0 = Absent, 1 = Present.**

QML	I31H	I31CD	I313	I385	I384L	I384U	I312	I284	I284a	I420	Oisans	Present
<i>Antechinus</i> sp. 1	0	0	1	0	0	0	0	0	1	0	0	0
<i>Antechinus</i> sp. 2	1	1	1	1	1	0	0	1	1	1	0	0
<i>Antechinus flavipes</i>	0	0	0	0	0	1	1	0	0	0	0	1
<i>Antechinus swainsoni</i>	0	0	0	0	0	0	1	0	0	0	0	0
<i>Dasyurus hallucatus</i>	0	0	0	0	0	0	1	0	0	0	0	1
<i>Dasyurus viverrinus</i>	0	0	0	0	0	1	1	0	0	0	0	0
<i>Dasyurus</i> sp.	0	0	1	0	0	0	0	0	0	0	0	0
<i>Phascogale</i> sp.	0	0	1	0	0	0	0	1	0	1	0	0
<i>Phascogale topoatafa</i>	0	0	0	0	0	0	1	0	0	0	0	1
<i>Planigale maculata</i>	0	0	0	0	0	0	1	0	0	0	1	1
<i>Sarcophilus lanianus</i>	1	1	0	0	1	1	1	0	0	1	0	0
<i>Sarcophilus harrisii</i>	0	0	0	0	0	0	0	0	0	0	0	0
<i>Sminthopsis macroura</i>	0	0	0	0	0	1	1	0	0	0	1	0
<i>Sminthopsis murina</i>	0	0	1	1	0	1	1	1	1	1	1	1
<i>dasyurid</i> (gen. et sp. nov.)	1	0	1	1	0	1	0	1	1	0	0	0
<i>Dendrolagus</i> spp.	1	1	1	1	1	0	1	1	1	1	0	0
<i>Thylogale</i> sp. 1	1	1	0	1	1	1	0	1	1	0	0	0
<i>Thylogale</i> sp. 2	0	0	0	0	0	0	1	0	0	1	0	0
<i>Petrogale</i>	1	1	1	1	1	1	1	0	0	1	1	1
<i>Pseudochirulus</i> sp. 1	1	1	1	1	1	0	0	1	1	0	0	0
<i>Pseudochirulus</i> sp. 2	1	1	1	1	0	1	0	1	1	0	0	0
<i>Pseudochirulus</i> sp. 3	1	1	1	1	0	1	0	1	1	0	0	0
<i>Pseudocheirus</i> cf <i>peregrinus</i>	0	0	0	0	0	0	0	0	0	0	1	1
<i>Pseudocheirus</i>	1	1	1	1	0	1	0	1	1	0	0	0
<i>Petauroides</i>	1	1	1	1	0	0		1	1	0	0	0
<i>Pseudocheirops</i> sp. 1	1	0	0	0	1	0	0	0	0	0	0	0
<i>Pseudocheirops</i> sp. 2	0	0	0	0	0	0	0	1	0	0	0	0
<i>Pseudokoala</i>	0	1	0	1	0	0	0	0	0	0	0	0
gen. et sp. nov. 1	1	1	1	1	1	1	1	1	1	1	0	0
gen. et sp. nov. 2	1	0	1	0	0	0	0	1	1	0	0	0
<i>Dactylopsila</i> sp. 1	1	0	1	1	0	1	0	1	1	0	0	0
<i>Dactylopsila</i> sp. 2	0	0	0	0	0	0	0	1	0	0	0	0
Incerti sedis gen. et sp. nov.	1	0	0	1	0	0	0	1	1	0	0	0
<i>Acrobates</i> sp.	0	0	0	1	0	0	0	1	0	0	0	0
<i>Cercatus</i> sp.	1	1	1	1	1	0	0	1	1	0	0	0
<i>Strigocuscus</i>	1	1	0	1	1	1	0	1	1	0	0	0
<i>Trichosurus</i> sp. 1	0	0	0	0	0	0	1	0	0	1	0	1
<i>Trichosurus</i> sp. 2	1	0	0	0	1	0	0	0	0	0	0	0
<i>Perameles</i> sp. 1	1	1	1	1	1	1	0	1	1	1	0	0
<i>Perameles</i> sp. 2	1	1	1	1	0	1	0	1	1	0	0	0
<i>Perameles bouganville</i>	0	0	0	0	0	0	1	0	0	0	1	0
<i>Isodon obesulus</i>	0	0	0	0	0	1	1	0	0	1	0	0
<i>Isodon</i> sp.	0	0	0	0	0	1	1	0	0	0	0	0
<i>Chaeropus ecaudatus</i>	0	0	0	0	0	0	1	0	0	0	0	0
<i>Macrotis lagotis</i>	0	0	0	0	0	0	1	0	0	0	0	0
perameloid gen. et sp. nov. 1	1	1	1	1	1	1	0	1	1	0	0	0



QML	I31IH	I31ICD	I313	I385	I384L	I384U	I312	I284	I284a	I420	Oleans	Present
perameloid gen. et sp. nov. 2	1	0	0	0	0	0	0	0	0	0	0	0
<i>Notomys</i> sp. 1	0	0	0	0	0	0	1	0	0	0	0	0
<i>Notomys</i> sp. 2	0	0	0	0	0	0	1	0	0	0	0	0
<i>Hydromys</i>	0	0	0	0	0	0	0	0	0	1	0	1
<i>Pseudomys</i>	1	1	1	1	1	1	1	1	1	1	1	1
<i>Rattus</i>	0	0	0	0	0	1	1	0	0	1	1	1
<i>Conilurus</i>	0	0	0	0	0	0	1	0	0	0	0	0
<i>Zyzomys</i>	1	1	0	1	0	0	1	0	0	0	0	0
<i>Leggadina</i>	0	0	0	0	0	0	1	0	0	0	1	0
<i>Uromys/Melomys</i>	1	1	1	1	1	1	0	1	1	1	0	0
<i>Pogonomys</i>	1	1	1	1	1	1	0	1	1	0	0	0
<i>Mesembriomys</i>	1	1	1	1	0	0	0	1	1	0	0	0
<b>Microchiropteran</b>	1	1	1	1	1	1	1	1	1	0	1	1
<i>Macroderma gigas</i>	1	1	1	1	1	1	1	1	1	0	1	1

Appendix 1. Small-sized mammalian fauna data matrix. 0 = Absent, 1 = Present.

## Chapter 3

### 3.1 Additional notes on fossil deposits, their formation and age.

### 3.2 Introduction

Vertebrate fossil deposits at Mt Etna and Marmor Quarry were initially described by Hocknull (2005) with subsequent additional information, including chronometric dating, detailed in Hocknull et al. (2007). Here I present further notes and descriptions of these new fossil deposits, including chronometric dates now available for the Mt Etna and Marmor Quarry fossil deposits. In summarising this chapter, I present a series of possible scenarios to explain the process of cave formation, chamber sedimentation and karstic development at Mt Etna, Limestone Ridge, Olsen's Cave and Karst Glen.

### 3.3 Mount Etna Limestone Mine and National Park

#### 3.3.1 Main Cave System (Fig. 3-1)

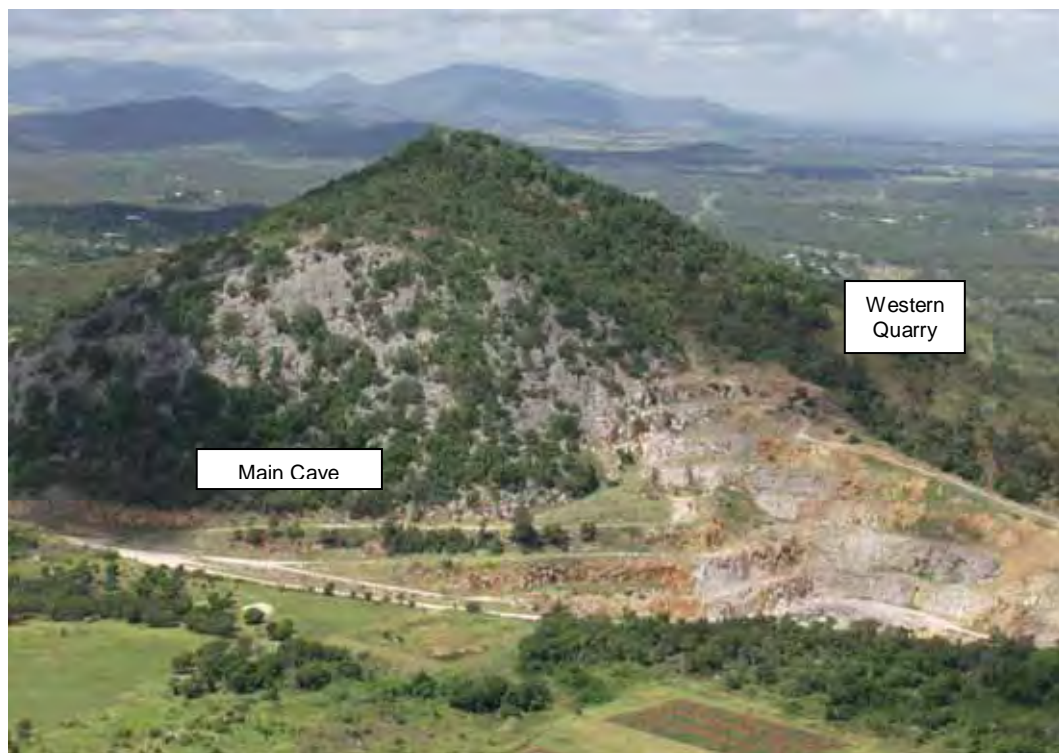


**Figure 3-1. Northern and western margin of Mt Etna showing location of Main Cave.**

### Main Cave Bone Breccia

The Main Cave bone breccia deposit is located on the scree slope below the main entrance to Main Cave, which is located on the northern face of Mt Etna (Fig. 3-1). The breccia is made up of large parent limestone blocks cemented within a fine lithified clay matrix (Fig. 3-2).

*Stratigraphic context.* The Main Cave breccia is exposed on karst limestone and most blocks have dislodged and moved away from their original position. Consequently it is likely that the majority of the deposit is ex-situ with no direct stratigraphic context (Fig. 3-3).

*Breccia components.* Large clasts of autochthonous limestone; fine-grained bedded speleothem; clay matrix.

*Bone preservation.* Small fractured bone shards.

*Tooth preservation.* No dental remains have been identified.

*Shell preservation.* Small gastropods and broken pieces of large individual gastropods.

*Facies interpretation.* Most likely an old fissure-fill deposit made up of mostly angular parent limestone cemented together with fine matrix and dirty speleothem.

*Chronometric age.* None available, most likely much greater than 500,000 years old.



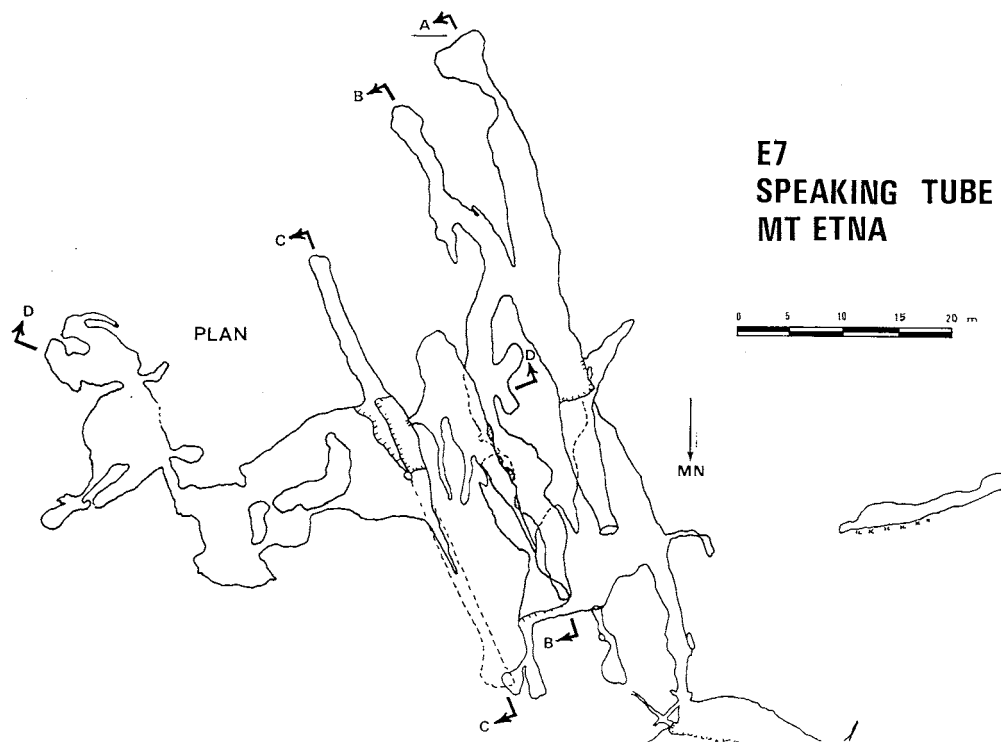
**Figure 3-2. Main Cave Bone Breccia, showing breccia made up of mostly cemented clay and angular pieces of parent limestone. Bone bearing sediment light yellow-pink colour.**



**Figure 3-3. Main Cave Bone Breccia shown as rocky scree to the north and down slope of the Main Cave entrance.**

### 3.3.2 Speaking Tube Cave System (Fig. 3-4)

The Speaking Tube Cave System was a large active system throughout its life with long deep chambers that followed the jointing and bedding planes of the parent limestone. Several large chambers, along with blind-ending avens, constituted the Recent cave chamber morphology. Based on the sediment deposits within the Speaking Tube Cave System, it is most likely that this same overall morphology was operating for over 500,000 years with subsequent vadose overprinting on some of the old cave chamber deposits. Figure 3-4 illustrates a plan and cross sectional view of the Recent cave morphology before mining operations destroyed it between 1991-1993.





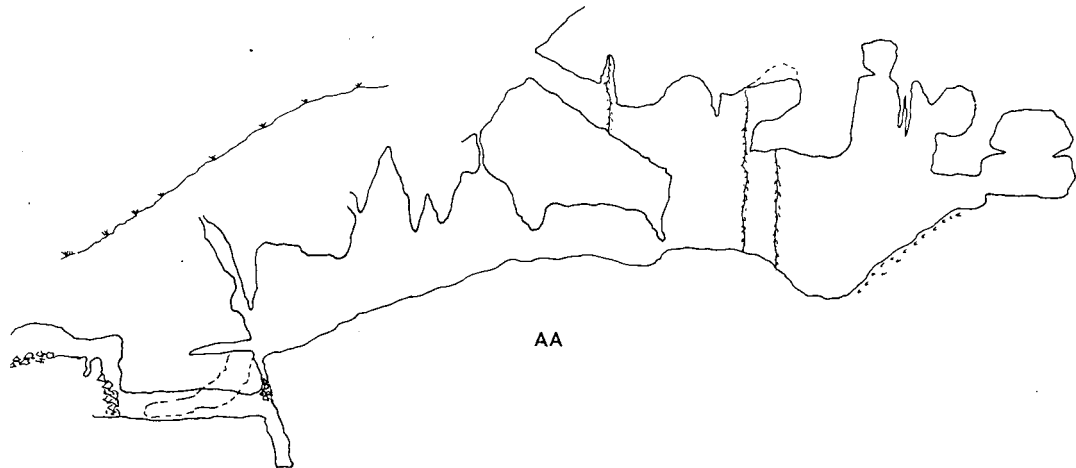


**Figure 3-4. Speaking Tube Cave as mapped by UQSS prior to mining operations destroyed it. A. Plan view. B. Cross-sectional view of main chamber system (AA).**

**Bench 0, QML1419 (Fig. 3-5)**



**Figure 3-5 QML1419. Bench 0, solution pipe running from Bench 0 to Bench 1. Photo taken from Bench 1. Insitu material referable to QML1313 is located to the left of this solution pipe.**

The highest vertebrate bearing deposit of the Speaking Tube Cave System occurs in a large solution pipe, approximately 10-15m in depth which was exposed through mining operations. The solution pipe runs below into Bench 1, but no deposits connect below this solution pipe. Based on photographic evidence of the area as exposed in 1992, this solution pipe ran to the south of chambers that contained QML1313 and QML1383. The solution pipe constitutes an old, now filled, solution pipe that would have exposed the Speaking Tube Cave System to the surface, high on the present day limestone karst. Therefore, the entry point for the fossil material that constitutes QML1419 was much higher than the current entry points to the functional Speaking Tube Cave. The walls of the solution pipe preserve old flowstone wall formations. The deposit is divided into two distinct units (A and B), divided by a thick band of flowstone.

#### **QML1419, Unit A (Fig. 3-6).**

Unit A is lower than Unit B and is a cemented breccia containing abundant faunal remains. A small entrance to the present day Speaking Tube Cave occurs on the open karst to the north of the solution pipe. Fossiliferous bone breccia adheres to the lip of this entrance and indicates a similar old solution pipe into the old Speaking Tube Cave System.

*Stratigraphic context.* Unit A underlies Unit B, being divided by a massive flowstone (20-40cm thick). Dating of the flowstone that divides these two units indicates that Unit A has a minimum age of >500ka.

*Breccia components.* Light pink to red clay sediments, heavily cemented. Minor clasts of parent limestone. Similar to that which constitutes QML1310 Unit 2 (see below). The thick flowstone band includes decalcified and recrystallised regions. There is evidence of 'dog tooth' spar, although the upper and lower layers are finely laminated.

*Bone preservation.* Well preserved, disarticulated assemblage small bones; no distinct bone orientations.

*Tooth preservation.* Isolated, well preserved teeth.

*Shell preservation.* Shell rich horizons.

*Facies interpretation.* Sedimentologically Unit A is most similar to QML1310 Unit 2 (Hocknull, 2005) and QML1383 Unit A.

*Chronometric age.* A flowstone speleothem located at the base of Unit B and above Unit A was dated using the U-Th dating technique and returned an age outside the maximum limit of the technique (500ka); the minimum age of Unit A is older than 500ka (Fig. 3-7).

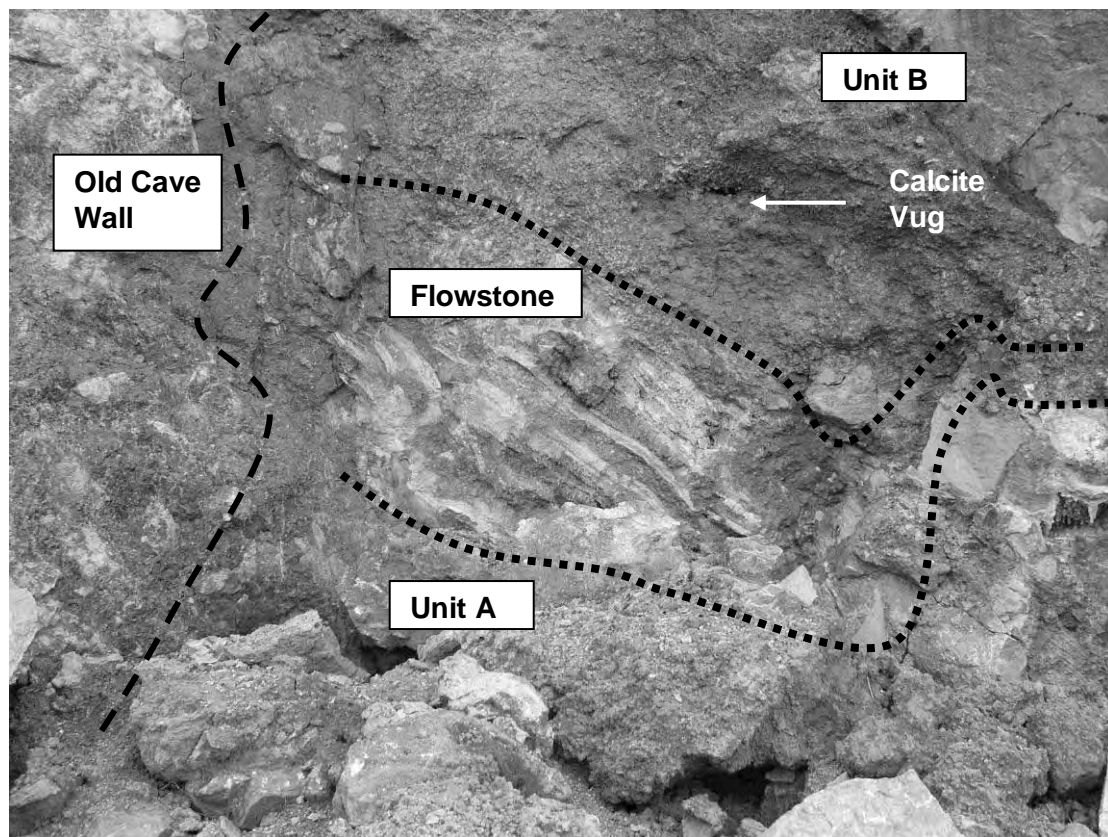


Figure 3-6. QML1419 Unit A and B, divided by massive flowstone.





**Figure 3-7. ROK E. Speleothem collection used to date the minimum age of QML1419 Unit A.**

#### **Bench 0, QML1419 Unit B (Fig. 3-6).**

*Stratigraphic context.* Unit B overlies Unit A, being divided by a massive flowstone (20-40cm thick). Dating of the flowstone that divides these two units indicates that Unit B has a maximum age of >500ka. A calcite vug occurs within Unit B and has been dated to 60.9 +/-0.7ka, indicating the deposit is older than ~61ka.

*Breccia components.* Unit B is mottled brown clay with small gravelly inclusions and rounded carbonate nodules.

*Bone preservation.* Bone is abundant but not well preserved

*Tooth preservation.* Isolated, well preserved teeth.

*Shell preservation.* Isolated fragments of snail shell.

*Facies interpretation.* Sedimentologically Unit B is most similar to QML1311 C, D and H deposits.

*Chronometric age.* A calcite-filled vug provides a minimum age for Unit B which accumulated prior to the vug formation. U-Th series dating of the calcite within the vug returned an age of ~61ka. Based on the considerable antiquity of Unit A, which is below Unit B, the minimum age returned is most likely too young to represent a viable age for Unit B. Instead, the calcite probably represents a later precipitation event (Fig. 3-8).

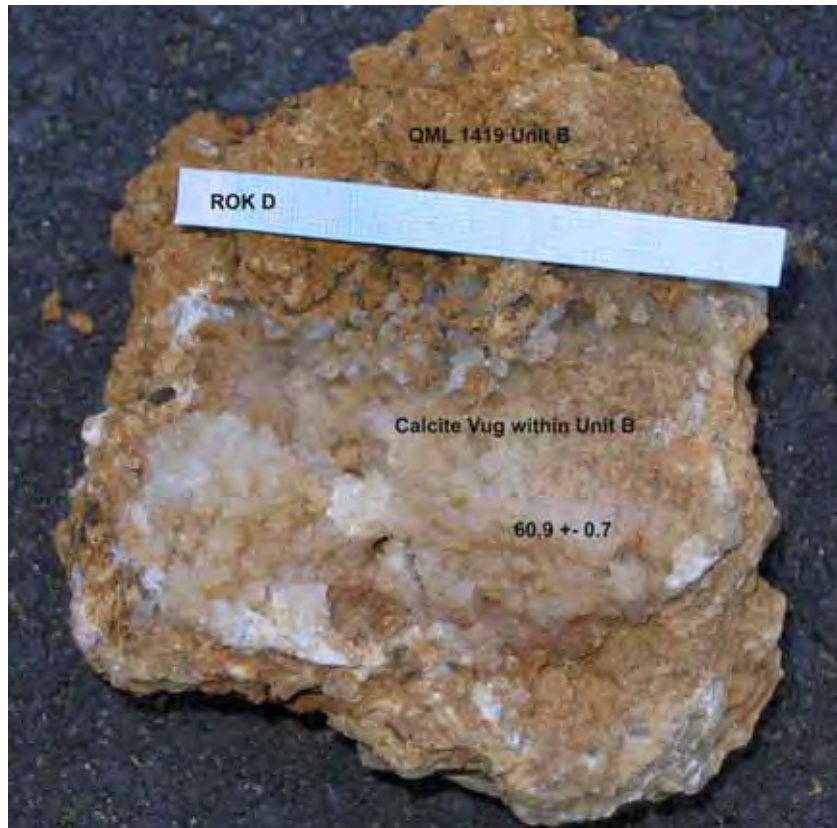


**Figure 3-8. ROK D. Calcite Vug found within QML1419 Unit B, used to find minimum age of Unit B.**

### **Bench 1, QML1383 (Northwest Chamber) Figs 3-9, 3-10.**

The following data supplement those in Hocknull (2005).

*Stratigraphic context.* QML1383 was excavated in 2005 and revealed two distinct deposits, identified in Fig. 3-9 as Unit A and Unit B. These units are divided by a thick flowstone, following the upper surface topography of Unit A. Unit A is distinctly faunally rich, whereas unit B is not. Additional flowstone covers both Units A and B, forming the functional cave wall surface that was present in Speaking Tube Cave before it was exposed during mining activities in the early 1990s. Hocknull (2005) considered QML1383 to be stratigraphically younger than QML1310 and QML1311 due to its higher position within the Speaking Tube Cave system. However, radiometric dating of the intersecting flowstone subsequently provided a minimum age for the top of Unit A of approximately 419ka (Hocknull et al., 2007). The top of Unit A is interbedded with silty flowstone layers and therefore this date is considered to be close to the actual age of the top of Unit A.

*Breccia components.* For Unit A see Hocknull (2005) and Hocknull et al. (2007). Unit B is not as heavily cemented as Unit A, being a dark brown colour instead of red-pink as in Unit A. Unit B also differs from Unit A by being depauperate of fossils.

*Bone preservation.* Unit A (Hocknull, 2005; Hocknull et al., 2007). Unit B, minor bone fragments.

*Tooth preservation.* For Unit A see Hocknull (2005) and Hocknull et al. (2007). Unit B, no teeth identified.

*Shell preservation.* For Unit A see Hocknull (2005) and Hocknull et al. (2007). Unit B, no shell identified.

*Facies interpretation.* Unit A see Hocknull (2005) & Hocknull et al. (2007).

Deposition of Unit A occurred before Unit B and the intervening flowstone. Cessation of deposition of Unit A and subsequent deposition of speleothem and the poorly fossiliferous Unit B was apparently due to the closure of the cave entrances leading to this chamber. Unit B is therefore considered here to be a closed chamber accumulation.

*Chronometric age.* The flowstone dividing Units A and B has been dated using U-Th series techniques and returning a minimum age for Unit A of approximately 420ka (Fig. 3-11).

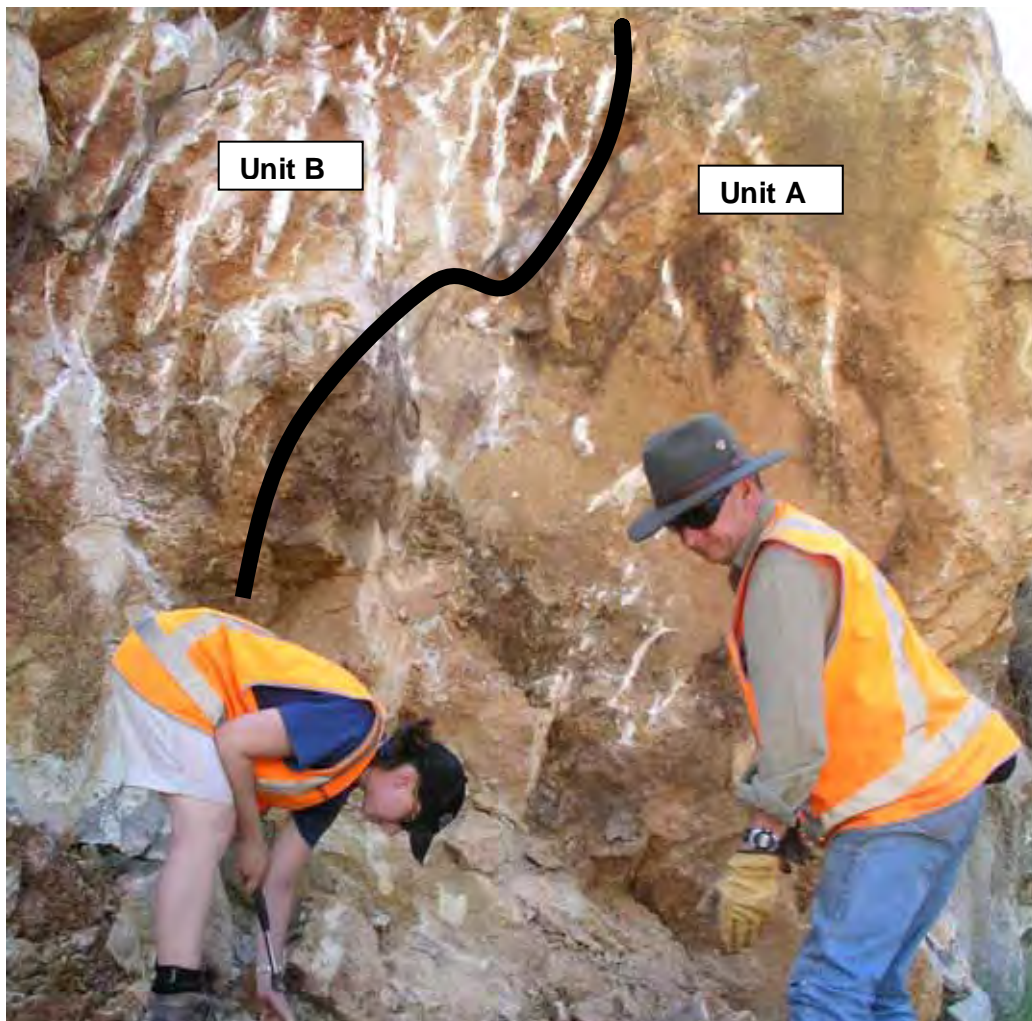


**Figure 3-9. QML1383 'Northwest Chamber', Bench 1. Units A & B divided by flowstone (black line).**



**Figure 3-10. QML1383 'Northwest Chamber', Bench 1 breccia showing sedimentological sample of Unit A with white flecks being fossil bone.**





**Figure 3-11. QML1383 'Northwest Chamber', Bench 1. Flowstone intersecting Units A and B used to provide a minimum age for Unit A.**

### **Bench 1, QML1313 (Figs 3-12 – 3-16)**

The following data supplement those in Hocknull (2005) and Hocknull et al. (2007).

QML1313 has a complex history of discovery, removal, stockpile and relocation.

Hocknull (2005) details this site, with additional information provided below.

Images of the western mine benches in 1992 during mining operations illustrate the position of QML1313 in relation to other deposits prior to their removal.

QML1313 originated as a cemented bone breccia at the base of a relatively continuous series of deposits within a single very large chamber (Figs 3-12 & 3-14). Figures 3-12 and 3-14 show QML1313 overlain by another sequence of less well cemented sediments, between 1-2m thick. These upper sediments include a brown-yellow sediment, that, based on the photographs, was not as well cemented as QML1313. A thin layer of dark brown to black sediment demarcates the top of the deposit, lying directly below the chamber roof. This sediment looks strikingly like a layer of guano ranging from about 10-30cm depth. Close inspection of the images available suggests the absence of any distinct flowstones between the dark brown-black layer and the mottled brown-yellow layer. A distinct flowstone was subsequently discovered that overlays the lower sediment level. Figure 3-12 shows a distinctive sediment scree that covered a chamber exposed by mining operations. Aligning this chamber, the

surrounding karst and the general bench shape allowed for the rediscovery of QML1313 remnants on these benches in 2002-2003.



**Figure 3-12. QML1313 and QML1419, Bench 1 as they were exposed on the western side of Mount Etna in 1992 (24/12/92). Note QML1419 mostly covered by limestone, subsequently exposed in collapse in 2002-2003.**

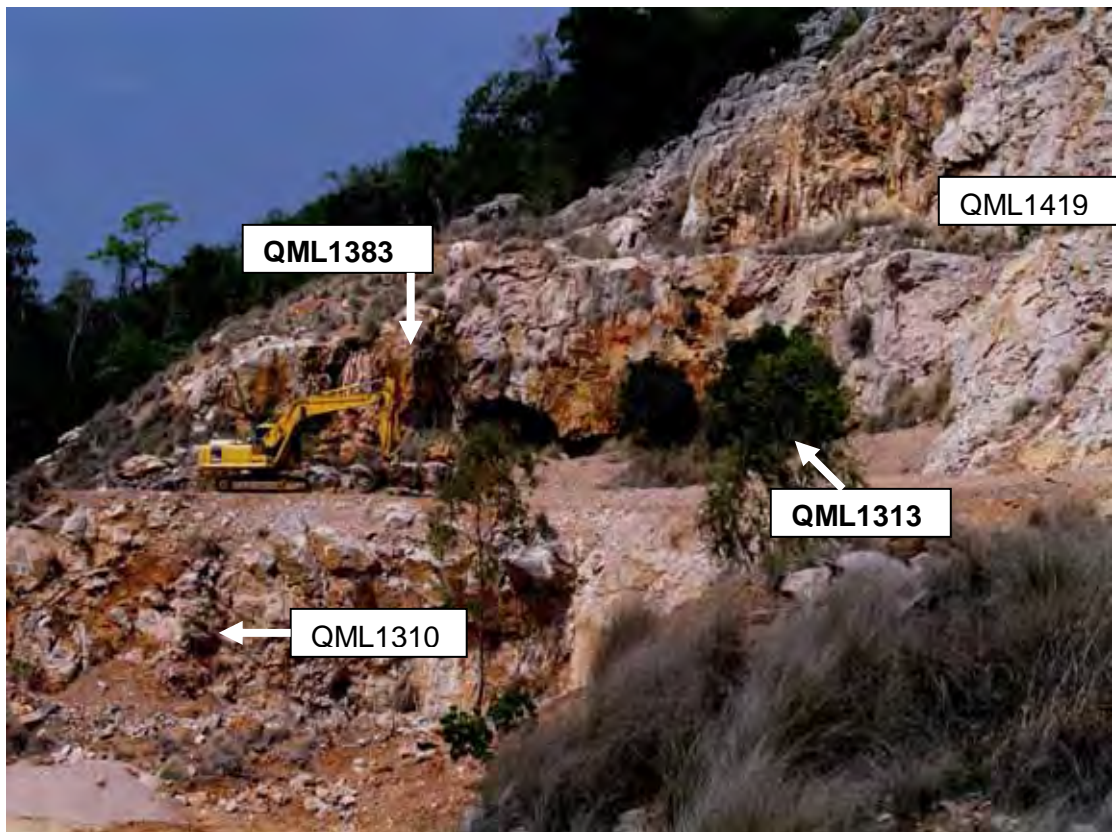


**Figure 3-13. QML1383 and QML1313, Bench 1 remnants relocated on the western side of the Mount Etna Mine in 2003.**



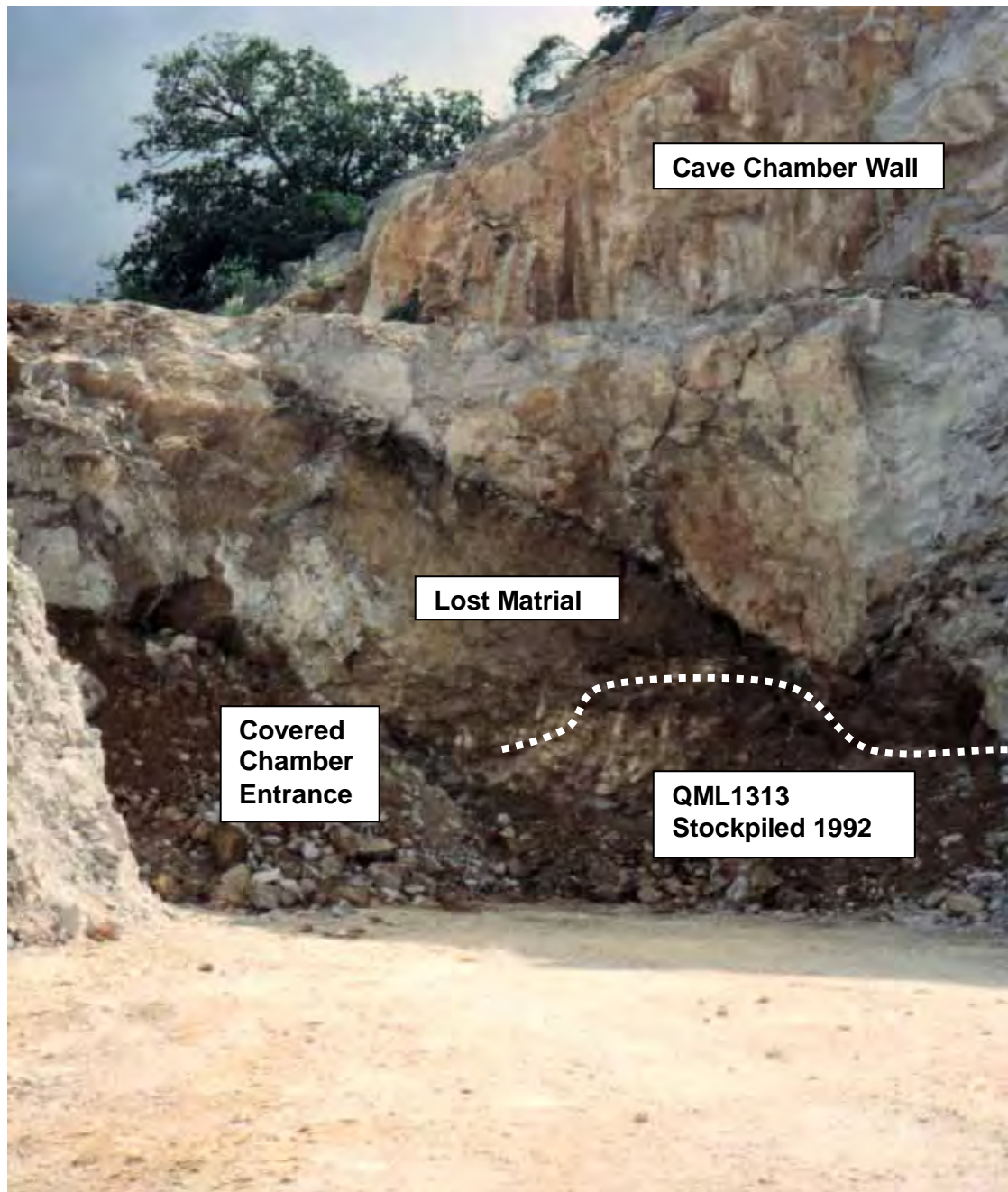


**Figure 3-14 QML1313, Bench 1 with original chamber walls of Speaking Tube Cave showing QML1313 which was stockpiled in 1992, rediscovered in 2003. Note covered entrance to Speaking Tube. This entrance is now exposed on the western face of Bench 1.**





**Figure 3-15. QML1313, Bench 1. Discovered in 2003, speleothem associated with remnant sediments of QML1313 exposed in 1992. Additional QML1313 were discovered further to the north from this section.**



**Figure 3-16. Basal section of flowstone found to be capping QML1313 deposit was used to return the youngest minimum age of the QML1313 deposit.**

## **Bench 2, QML1310. (Figs 3-17 – 3-29)**

The following data supplement those in Hocknull (2005) and Hocknull et al. (2007).

During major excavations on the Mt Etna Limestone quarry during 2004-2005 Bench 2 QML1310 was extended westward from its original exposure (Units 1 and 2 of Hocknull, 2005). West of these units, three additional deposits were found to lie in general stratigraphic sequence, Unit C overlying units A and B, and Unit B overlying Unit A. All three units are separated from QML1310 Units 1 and 2 by a large wedge of parent limestone.

### **Bench 2, QML1310 Unit A**

*Stratigraphic context.* Unit A is overlain by Units B & C and is laterally at a similar depth to QML1310 Unit 2. A capping flowstone demarcates Unit A from Unit B. Deposition ceased and flowstone growth began. Undated, but interpreted to be >500ka due to its similarity to QML1310 Unit 2 deposit.

*Breccia components.* Unit A is a fine grained fossiliferous deposit, pink-red in colour with minor allochthonous clasts and parent limestone.

*Bone preservation.* Bone fragmented and sparse. Small bone preserved throughout deposit.

*Tooth preservation.* No teeth identified from the deposit.

*Shell preservation.* No shell identified from the deposit.

*Facies interpretation.* Unit A is interpreted to be a chamber floor facies, with minor bone accumulations.

*Chronometric age.* Unknown

### **Bench 2, QML1310 Unit B**

*Stratigraphic context.* Unit B overlies Unit A and is overlain by Unit C. A capping flowstone demarcates Unit B from Unit C. Undated, age uncertain.

*Breccia components.* Large angular clasts suspended in a heavily cemented fine grained pink-red matrix. Angular clasts include parent limestone and allochthonous clasts of serpentinite and siltstone. Large fragments of bone are also preserved.

*Bone preservation.* Large pieces of fragmented bone preserved.

*Tooth preservation.* No teeth identified.

*Shell preservation.* No shell identified.

*Facies interpretation.* The angular clasts and typical breccia morphology indicate that this deposit most likely formed at the base of an entrance scree.

*Chronometric age.* Unknown.

## **Bench 2, QML1310 Unit C**

*Stratigraphic context.* Unit C is the uppermost deposit within the sequence, overlying both Units A and B. An irregular flowstone caps both Unit C and forms a crust over all three units, suggesting that this flowstone formed a portion of a functional cave wall. Undated, but in sedimentology and preservation of snail shells it is very similar to the false-floor deposit found in Lower Johansen's Cave on Limestone Ridge. Deposit regarded to be late Pleistocene in age.

*Breccia components.* Dark to light brown heavily cemented fine grained sediment with isolated large allochthonous clasts and parent limestone.

*Bone preservation.* Minor bone inclusions, usually broken pieces.

*Tooth preservation.* No teeth identified.

*Shell preservation.* Large snail shells found within the capping flowstone and other associated speleothem.

*Facies interpretation.* Silty chamber floor, typical of extant chambers on Mt Etna and Limestone Ridge.

*Chronometric age.* Unknown

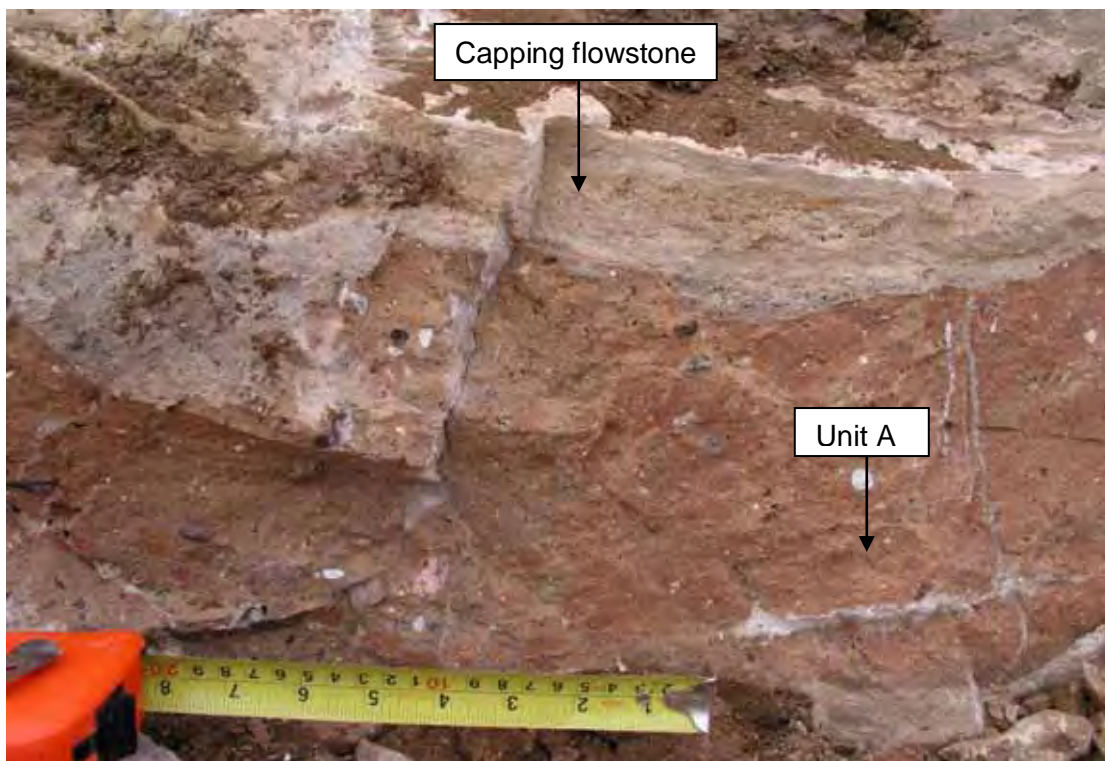


**Figure 3-17. QML1310, Unit A, Bench 2. Showing large continuous capping flowstone that demarcates Unit A from B above.**



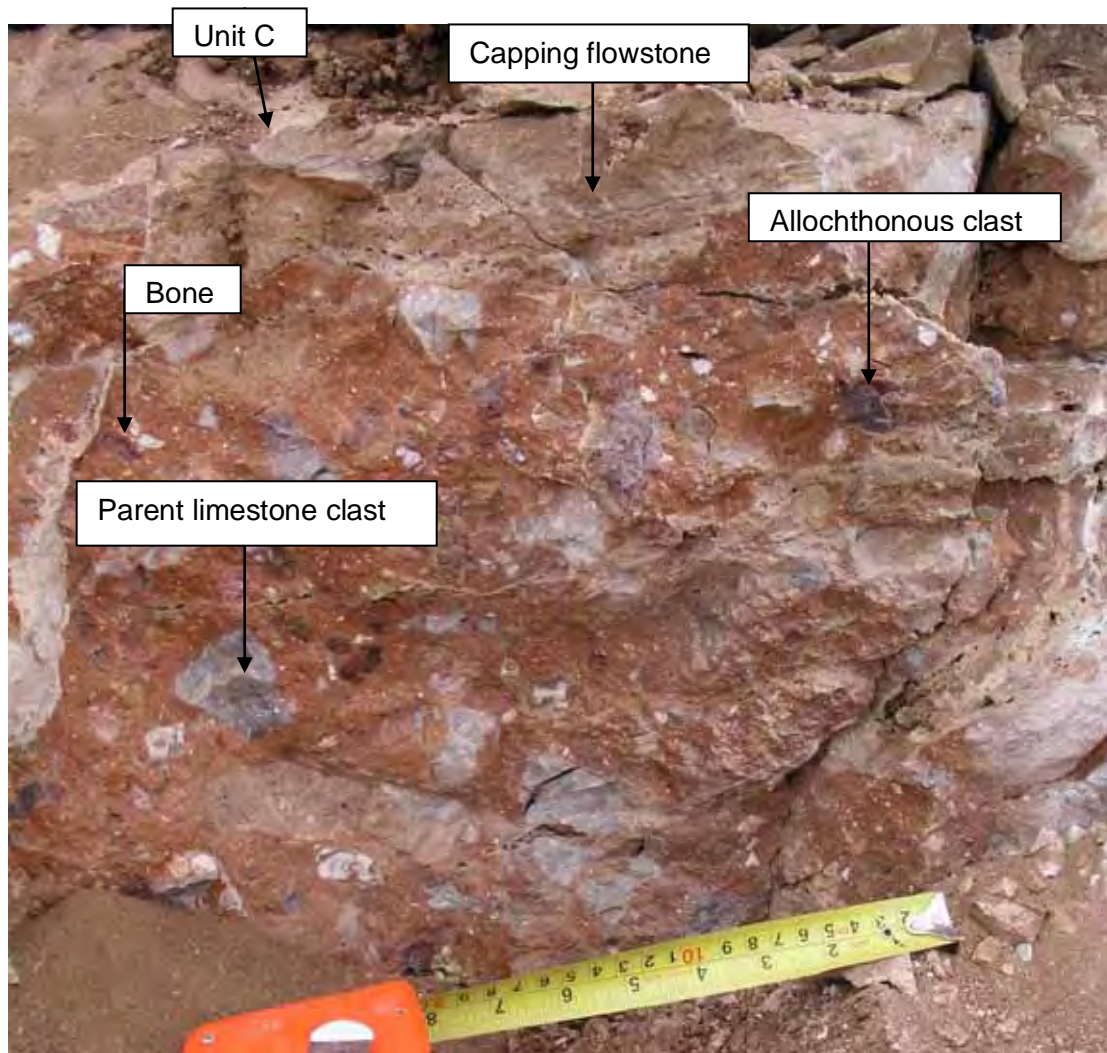


**Figure 3-18. QML1310, Unit B, Bench 2. Showing flowstone contact (top of picture) with Unit C, massive cemented breccia with clasts of parent limestone and allochthonous clasts of surrounding claystones/siltstones and limestones. Bone present. Scale Bar 20cm.**



**Figure 3-19. QML1310 Unit C, Bench 2. Showing large angular clasts of allochthonous rock derived from surrounding Devonian units (centre), surrounded by brown colours cemented clays and dirty flowstone. 20cm Scale Bare.**

## QML1310 Unit 1 & 2

Since Hocknull (2005), QML1310 Units 1 and 2 were excavated to reveal a more significant section of the deposit (Fig. 3-20).

### Unit 1

Unit 1 is divided by a thick, dirty, weathered flowstone that runs the length of the exposure. Above this flowstone Unit 1 is preserved as dark to light brown mottled clay with no sign of bone within it. This unit is referred to by Hocknull (2005) as a 'non-entrance facies'. Based on the deposition of a significant flowstone and subsequent deposition of clay-rich, yet poorly allochthonous and fossiliferous sediments, it is here suggested to have accumulated during a time of entrance closure.

Below the Unit 1 mid flowstone, a second deposit is preserved. This deposit contains fine-grained heavily cemented clays bearing very little bone. The sediment is dark brown in colour and contains minor clasts of parent limestone. At the base of this deposit, a second very thick flowstone, up to 35cm deep occurs, capping Unit 2.

Chronometric ages for Unit 1 are shown in Fig. 3-29.

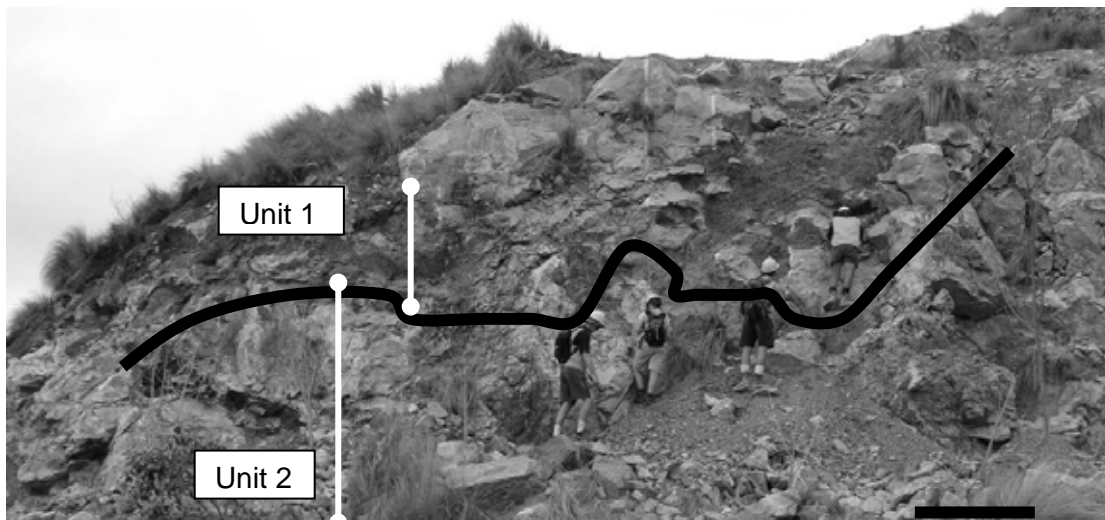


**Figure 3-20 QML1310 Units 2 and 1, Bench 2. Scale Bar = 2m.**

Unit 2 is divided into several discrete sections, demarcated by flowstones and a thick gastropod lens. Below the thick flowstone that demarcates Units 1 from 2, the sediment is densely packed, heavily cemented and very fine-grained, pink in colour. Minor clasts of limestone and allochthonous sediments are preserved with occasional pockets of densely packed, broken up bone. This deposit is relatively thick and occurs above a layer of gastropods, cemented together in a single laterally continuous layer. The gastropod layer ranges from 5cm – 20cm in thickness and is interspersed by small flowstones.

Below the gastropod layer is the largest section of Unit 2, being sedimentologically similar to the unit above the gastropod layer. Small pockets of bones are preserved within this massive deposit, most of which are semi-associated and articulated. A single skeleton of a juvenile *Dendrolagus* species was discovered at the base of this unit. Located within this layer are large calcitic vugs, having grown within holes in the unit. One such vug preserves a micro-cave like formation with small flowstones and calcite straws. Finally, capping both units 1 and 2 is a surface flowstone, which would have been a flowstone wall in the extant Speaking Tube Cave system. Chronometric ages for Unit 2 are illustrated in Fig. 3-29.



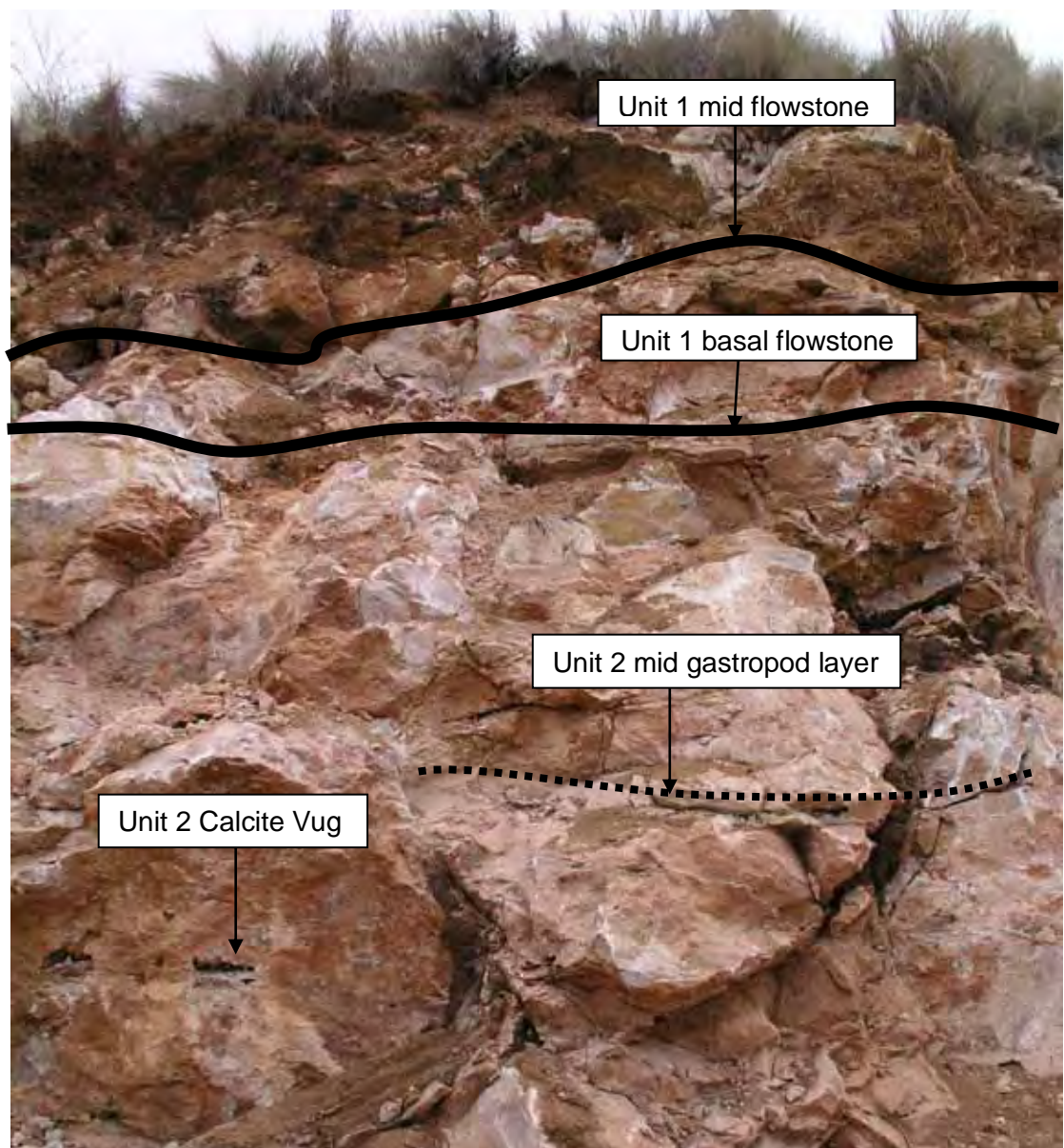


**Figure 3-21. QML1310 Units 1 & 2, Bench 2. Showing calcite vug in Unit 2 used for dating; speleothem layers; gastropod layer; and division between Units 2 and 1.**





Figure 3-22. QML1310 Unit 2, Bench 2. Showing calcitic vug within wall of Unit 2.



Figure 3-23. Collected calcite vug showing U-Th dates returned from each section of calcite growth, total timeframe spanning approximately 200,000 years.



Figure 3-24. QML1310 Unit 2, Bench 2. Isolated block from base of Unit 2 above basal flowstone, showing semi-associated and articulated juvenile specimen of *Dendrolagus*. Scale Bar = 5cm

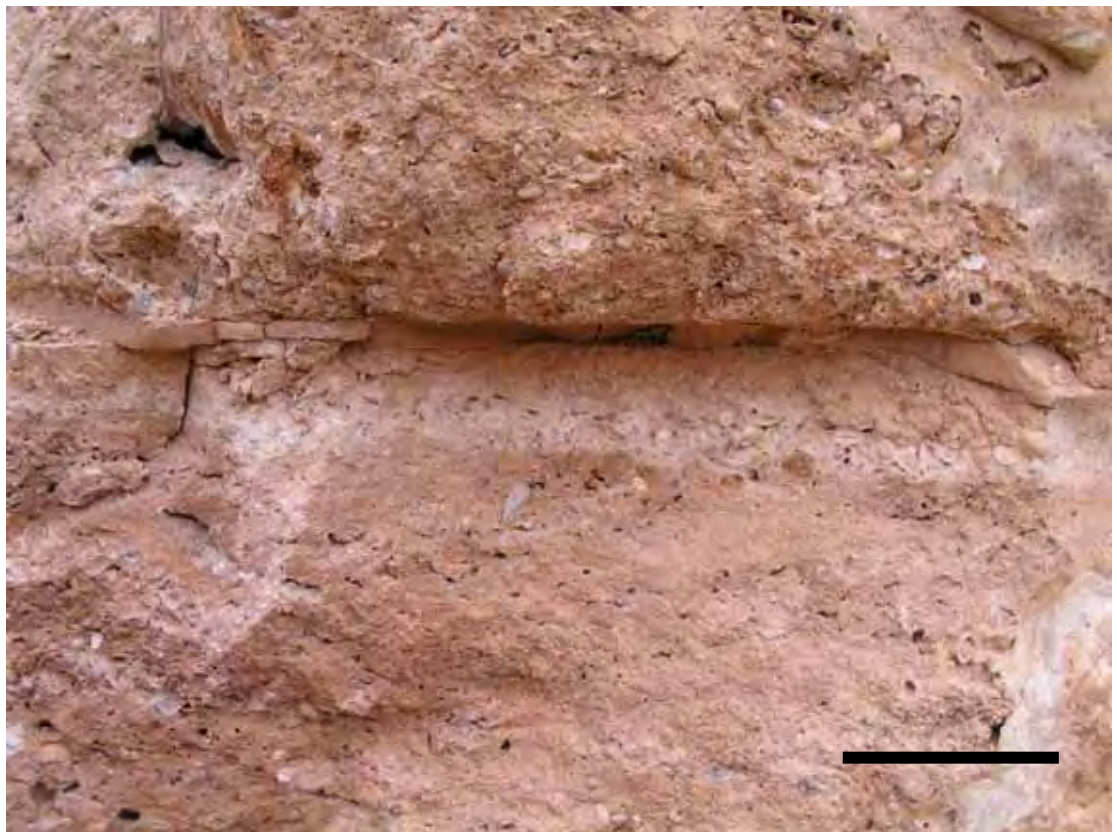
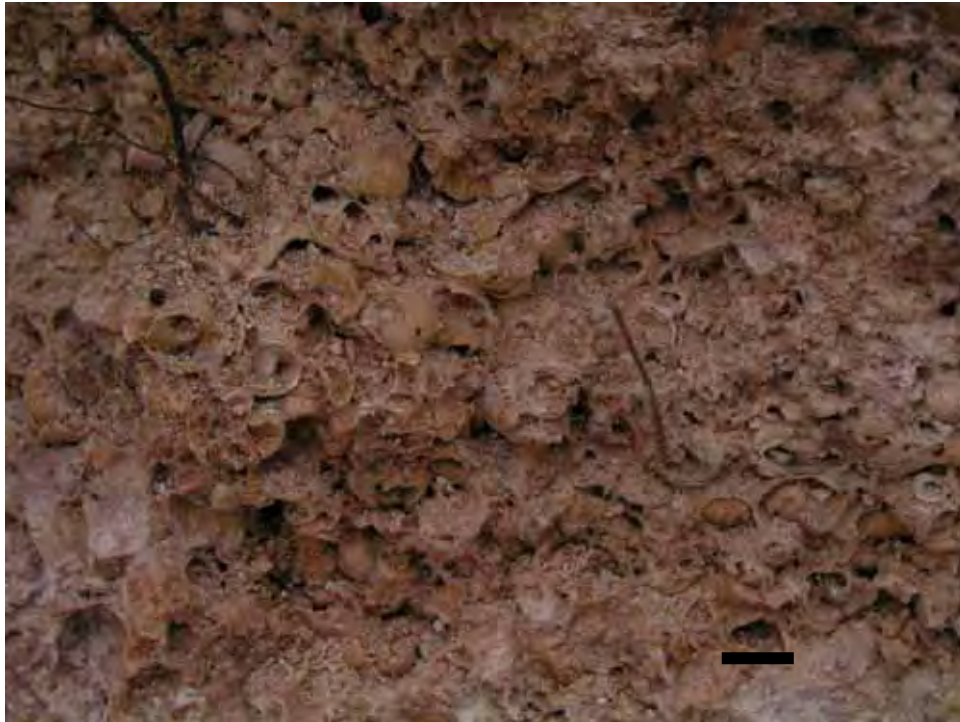


Figure 3-25. QML1310 Unit 2, Bench 2. Showing mid gastropod layer. Scale Bar = 10cm.



**Figure 3-26. QML1310, Unit 2, Bench 2. Close-up image of mid gastropod layer showing packing of gastropods. Scale Bar = 1cm**



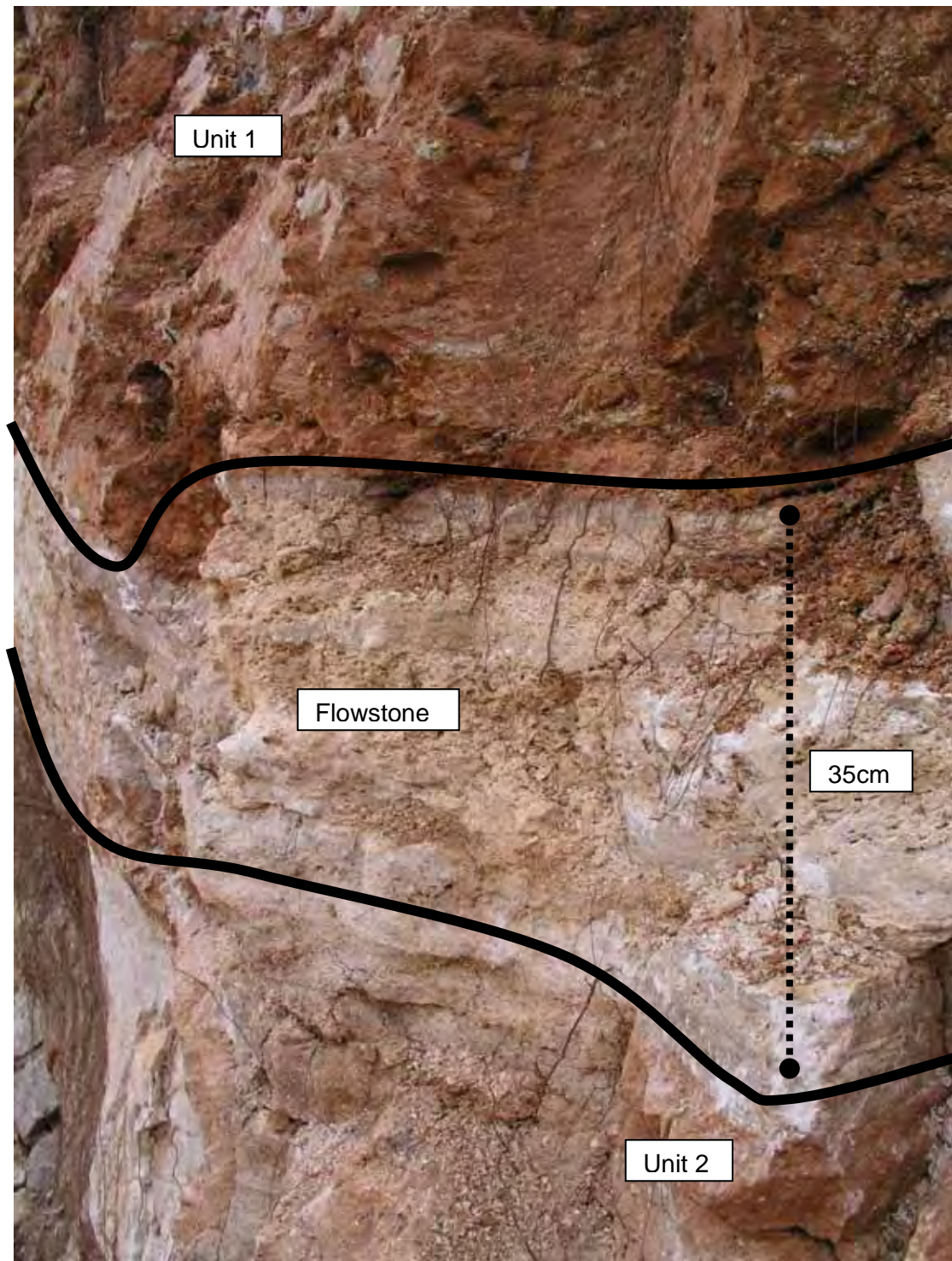
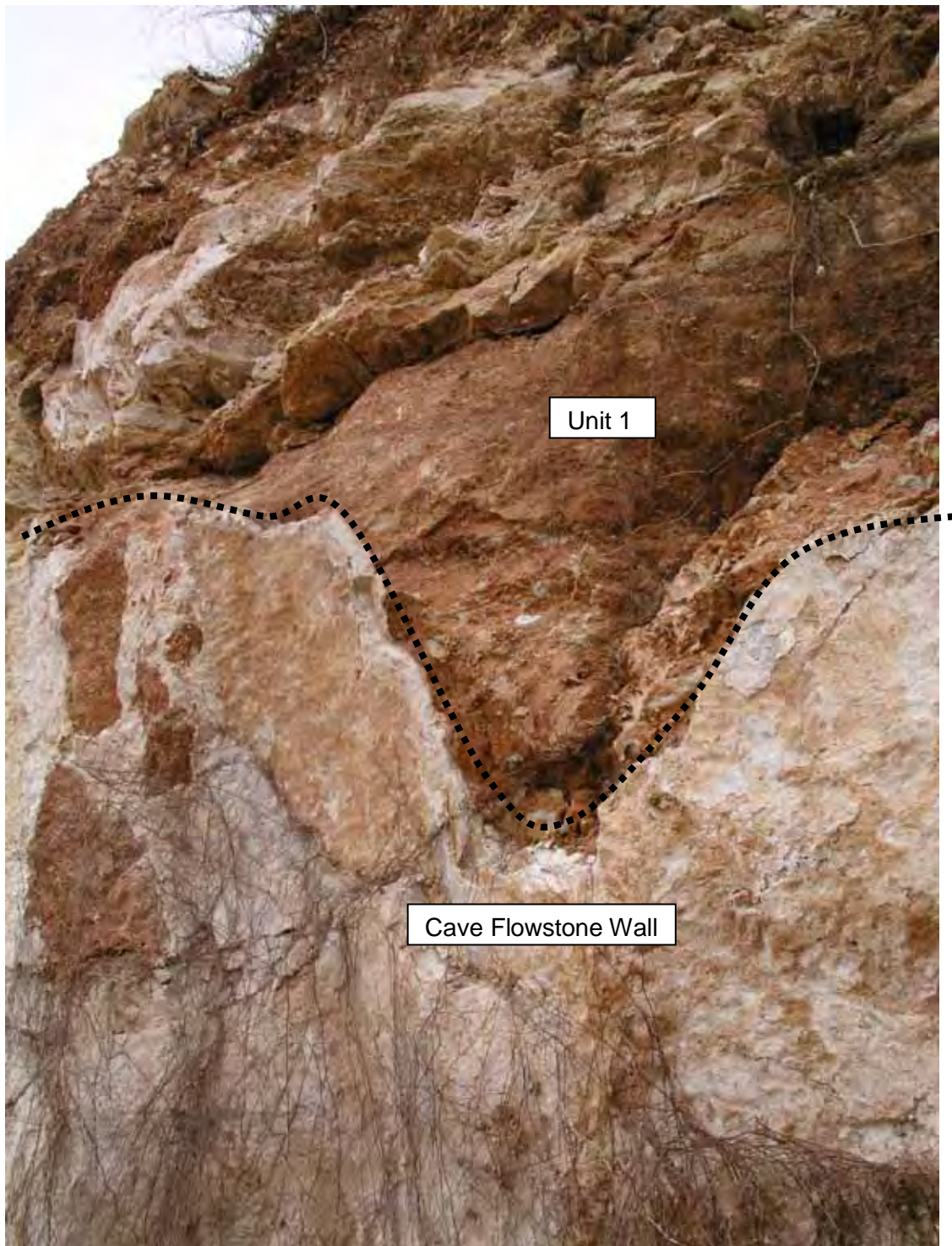


Figure 3-27. QML1310, Unit 2 & 1, Bench 2. Showing flowstone capping Unit 2 and basal to Unit 1.





**Figure 3-28. QML1310 Unit 1, Bench 2. Showing capping flowstone over both Units 1 and 2. Note the sculpted surface showing old cave wall surface.**



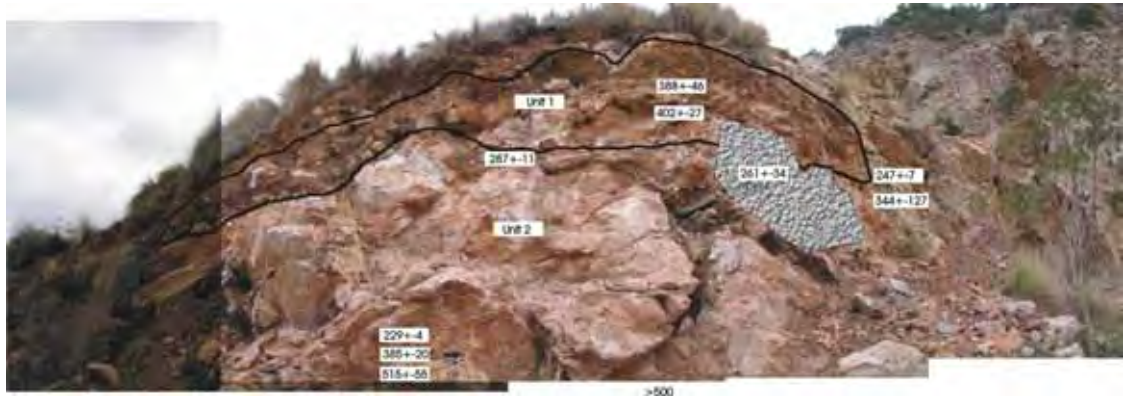


**Figure 3-29. QML1310 Unit 1 & 2, Bench 2 with chronometric ages detailed for relevant flowstone horizons.**

### **Bench 3, QML1311 (Fig. 3-30 – 3-45)**

Hocknull (2005) and Hocknull et al., (2007) describe the major deposits of Bench 3 allocated the locality number 1311 and figured here.

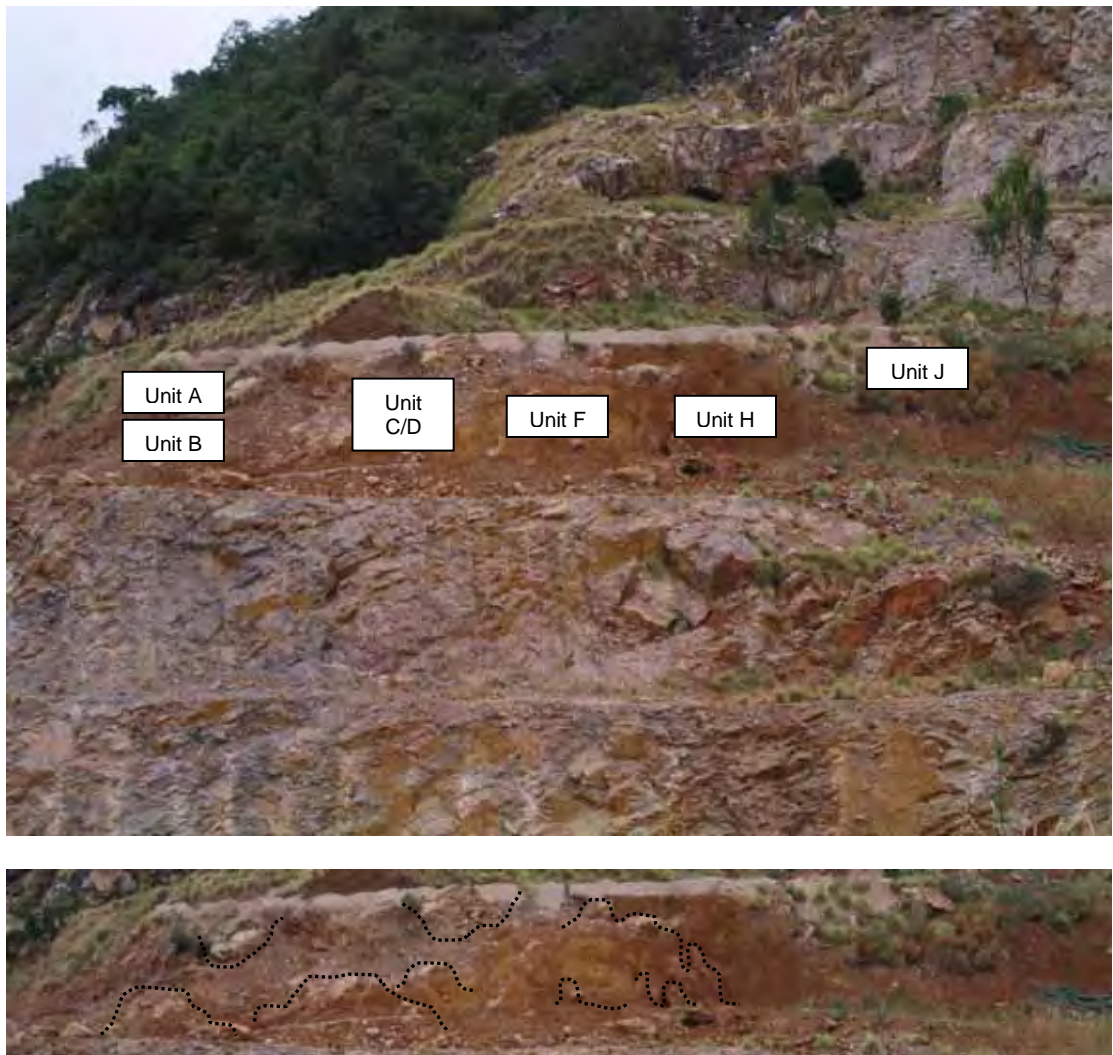


**Figure 3-30. Bench 3 deposits. A. Location of QML1311A, B, C, D, F, H and J. B. Dotted line tracing of parent limestone phreatic pendants exposed during stockpiling operations.**

### **QML1311 A/B, Bench 3.**

The following supplements Hocknull (2005).

*Chronometric age.* Flowstone between Units A and B dated to 398.6+- 46.6ka (Hocknull et al., 2007).



**Figure 3-31. QML1311 A, Bench 3. Showing massive angular clasts of parent limestone isolated in thick lithified clay matrix.**



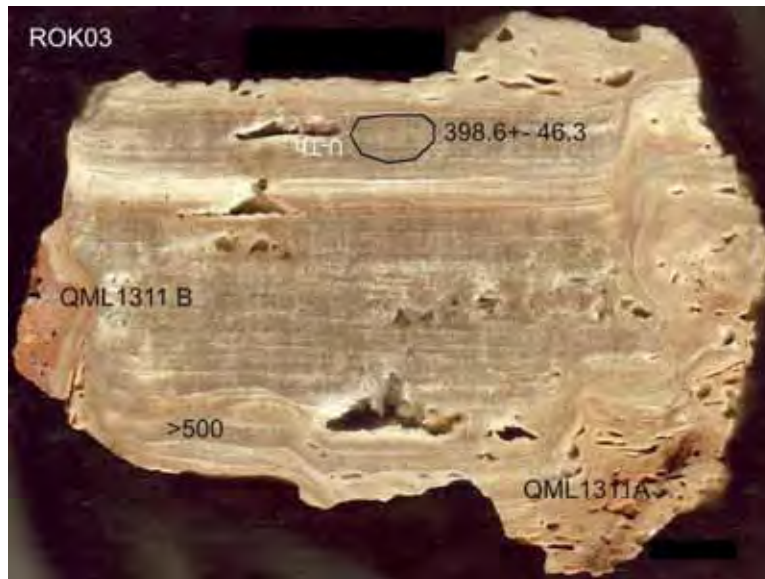


Figure 3-32. Speleothem between QML1311 A and B used for U-Th dating.

### QML1311 C/D, Bench 3.

*Chronometric age.* Basal flowstone dated to approximately  $326 \pm 26$ ka (Hocknull et al., 2007). (Fig. 3-35).



Figure 3-33. QML1311 CD, Bench 3. Showing gross morphology, colour and sedimentological characteristics in the field.





Figure 3-34. QML1311 C, Bench 3. Block of consolidated sediment seen in cross-section showing random bone orientations, size and sedimentological character.

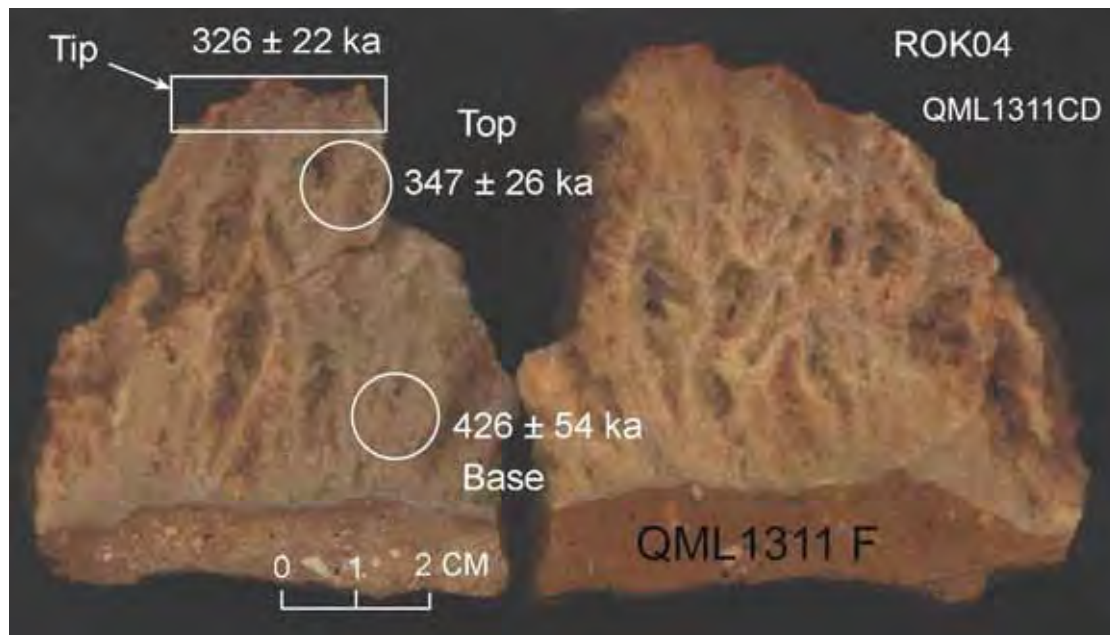


Figure 3-35. QML1311 CD basal flowstone providing the contact between QML1311F and QML1311CD. This speleothem was used to return a series of ages showing that the minimum age for QML1311F was ~430ka, the maximum age for QML1311CD is ~330ka and that the growth of this speleothem took approximately 100,000 years.

**QML1311 F, Bench 3.**

*Chronometric Age. Unknown, >>500ka.*



**Figure 3-36. QML1311F, Bench 3. Piece of matrix in cross-section showing dominant fine-grained matrix with large individual allochthonous clasts and post-depositional calcite formation within porous sediment matrix.**



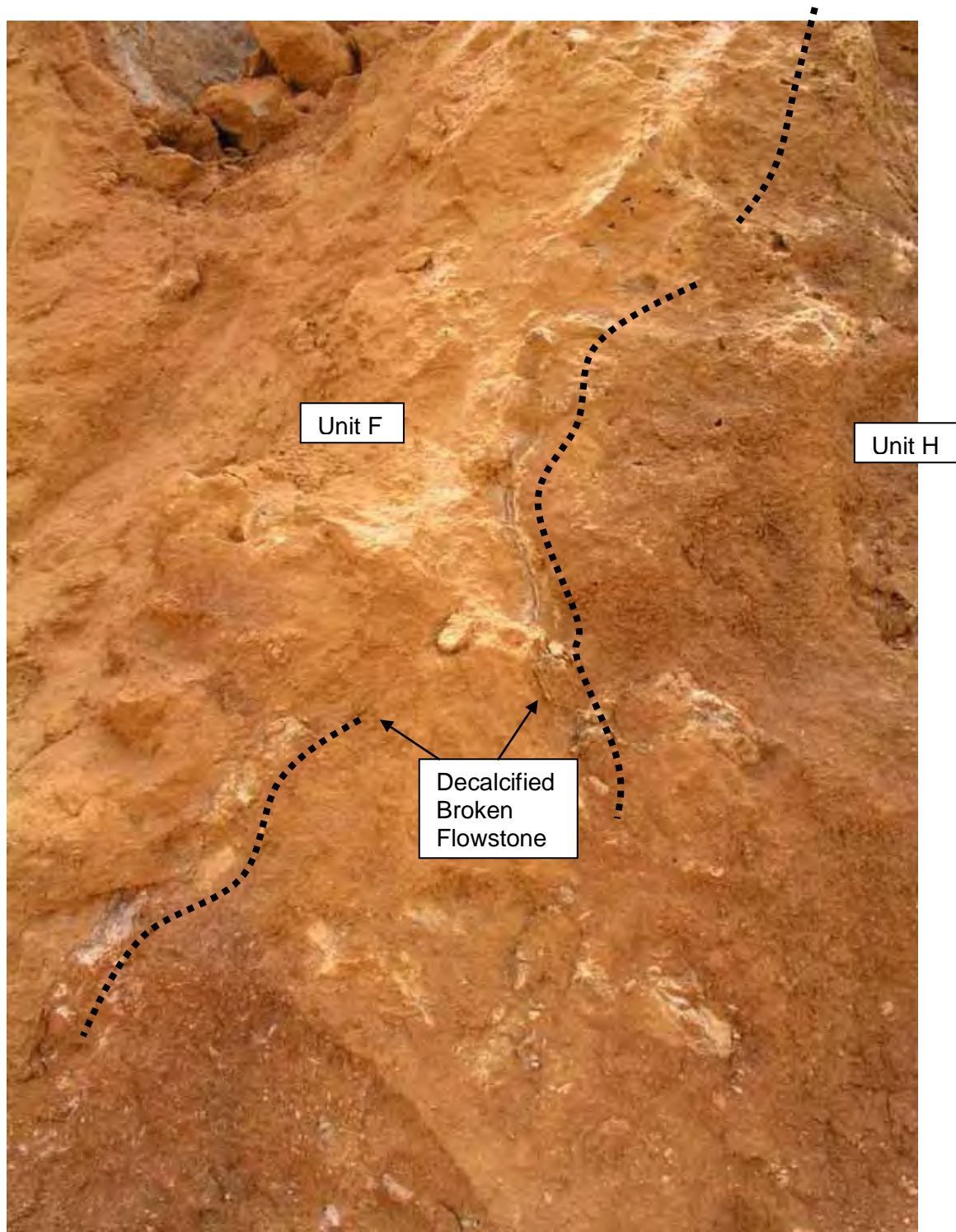


**Figure 3-37. QML1311 F & H, Bench 3. Showing decalcified flowstone contact between QML1311 F and H.**

QML1311H.

*Chronometric age.* Calcitic infill of bone and basal flowstone suggest that this deposit is >450,000 years old (Hocknull et al., 2007).





**Figure 3-38 QML1311 F&H, Bench 3. Close up of old flowstone of F now incorporated within H. Also shows sedimentological differences between F and H, notably the massive increase in surface allochthonous clasts.**

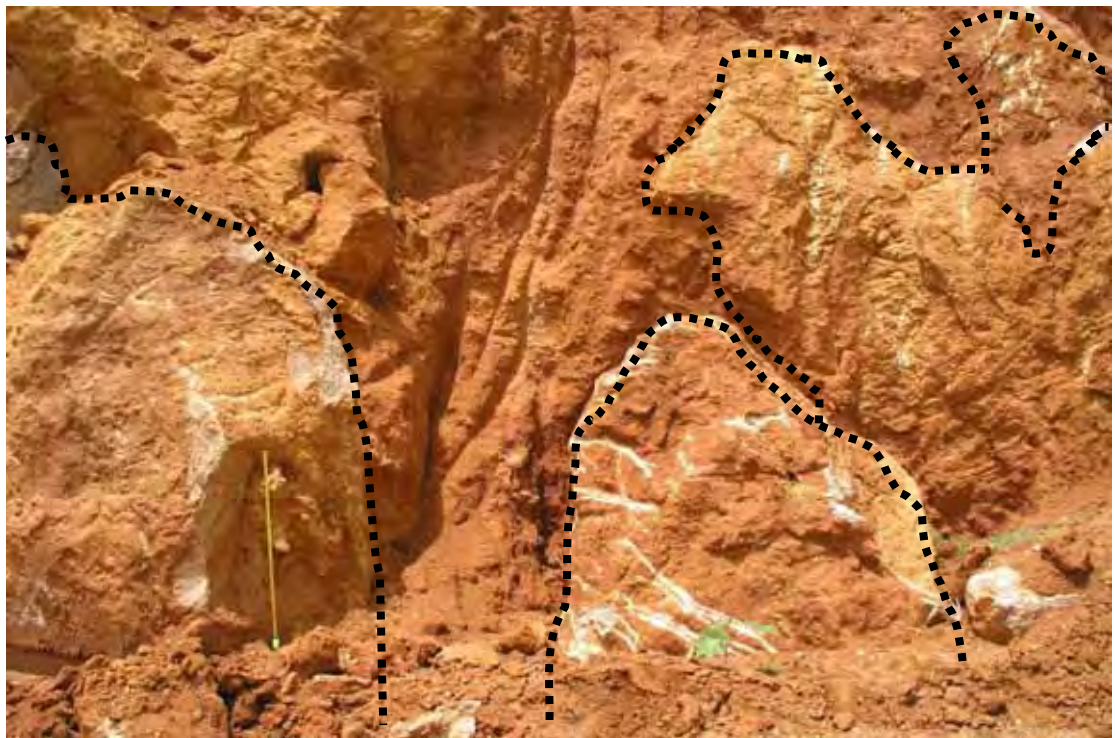


**Figure 3-39. QML1311H, Bench 3. Showing distinctive phreatic pendants within QML1311H sediment. Minimal, if any calcite precipitation indicative of a non-vadose system.**





**Figure 3-40. QML1311H, Bench 3. Matrix showing random bone orientations, increased percentage of allochthonous sediment with some post-depositional calcite formation with vugs and bone hollows.**



**Figure 3-41. QML1311F-H Contact zone with inter-layered calcite formations dated using U-Th techniques to >500ka.**



Figure 3-42. QML1311F. Calcitic Vug found within QML1311 F, used to determine minimum age of deposit. Returned an age ~280ka, which indicates speleothem deposition at this time.

QML1311J

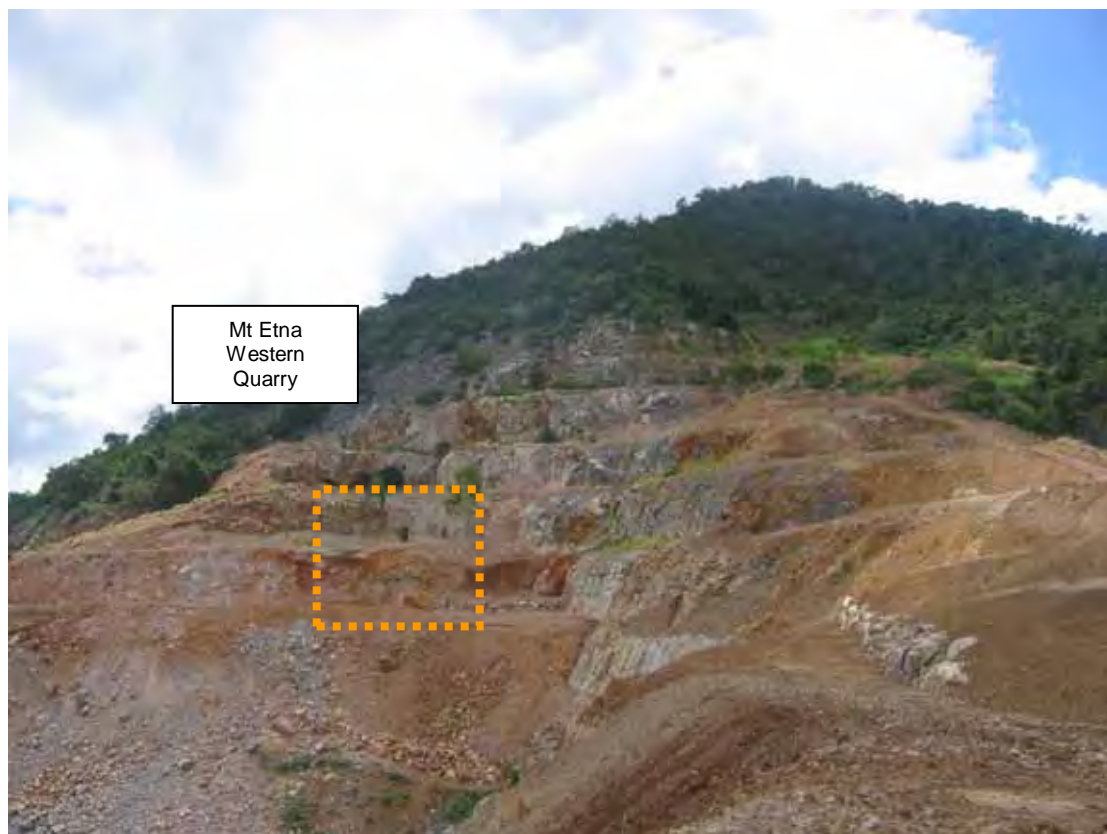
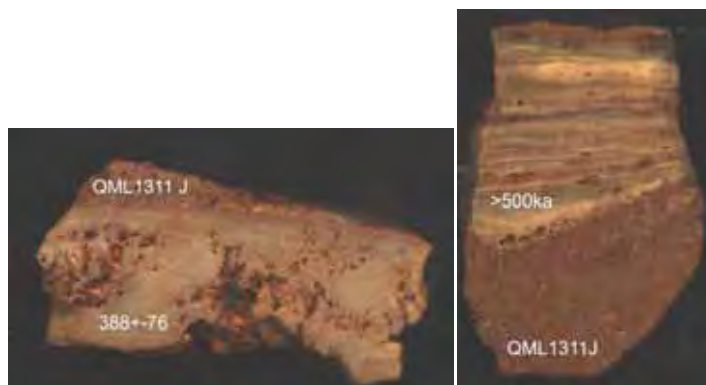


Figure 3-43. QML1311J, Bench 3. Location of QML1311J on western quarry face.



**Figure 3-44. QML1311J. Note the small size of this deposit. It may have been considerably larger before mining operations.**



**Figure 3-45. QML1311J. Speleothem used to date QML1311J. A. Calcite vug within QML1311J, used to provide a minimum age. B. Flowstone within QML1311J used to provide a close approximation of the deposits age.**



### 3.3.3 Elephant Hole Cave System (Figs 3-46, 3-47)



Figure 3-46. QML1384 UU and LU, Bench 3. Showing solution pipe and chamber being excavated for stockpiling.



Figure 3-47. QML1384UU. Capping flowstone considered to represent the minimum age of QML1384UU.



### 3.4 Limestone Ridge National Park

#### 3.4.1 Northern Limestone Ridge Section (Figs 3-48 – 3-50)

##### Johansen's Cave

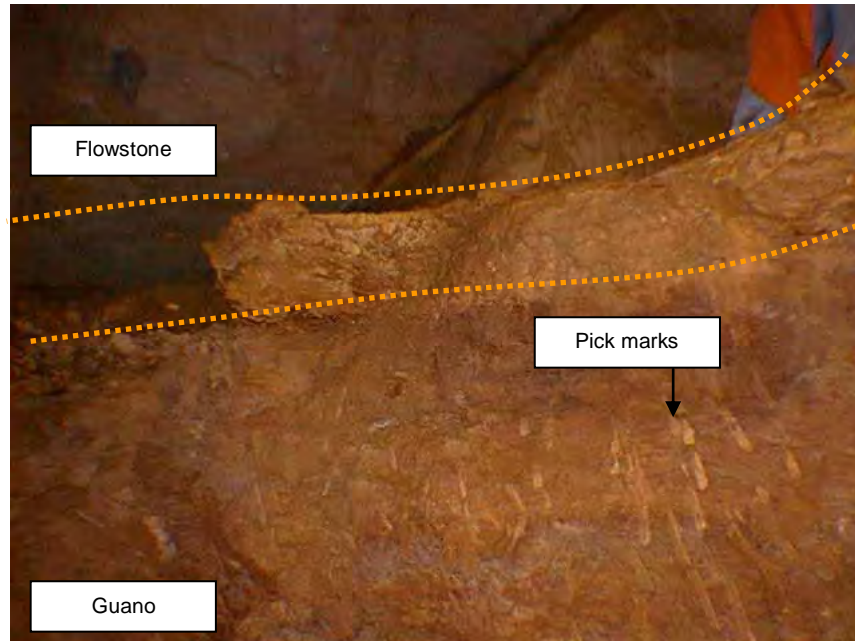


Figure 3-48. QML1314, Lower Johansen's Cave, Limestone Ridge (northern section). Showing capping flowstone and guano beneath.



Figure 3-49. QML1314, Lower Johansen's Cave flowstone lithified sediment in cross-section. Note, the cementation of the sediment below the flowstone indicating that the sediment deposit below the flowstone accumulated before the flowstone.



**Figure 3-50. QML1314, Lower Johansen's Cave Guano deposit below flowstone level. Note the distinct colouration difference between the guano floor sediment and the sediment wall (dotted orange line).**

#### 3.4.2 Southern Limestone Ridge (Eastern Face) (Figs 3-51 – 3-54)

##### Mini Cave



**Figure 3-51. QML1284, Mini Cave, Limestone Ridge (southern section). Example of cave wall flowstone, inter-bedded within fossiliferous deposit, used for dating the sequence presented in Hocknull et. al. (2007).**

**Above Mini Cave.**

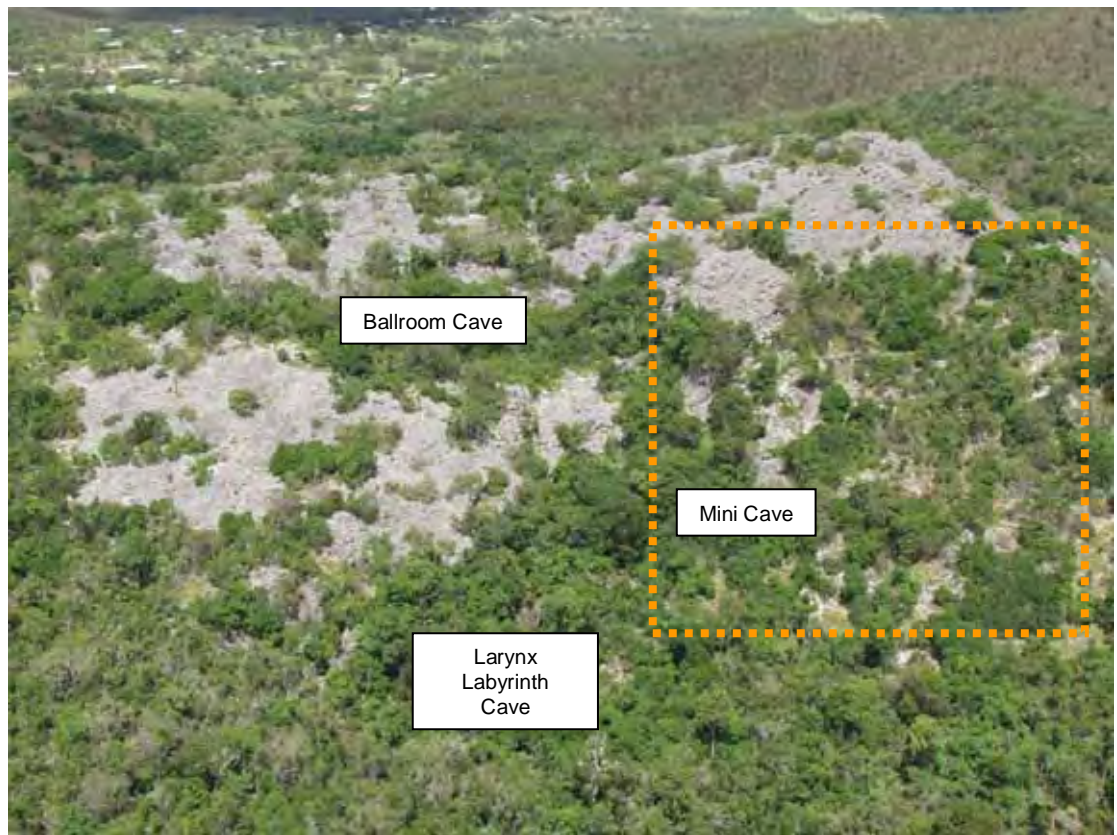


**Figure 3-52. Mini Cave – Lost Paradise – Lion’s Den Section of Limestone Ridge (southern section).**



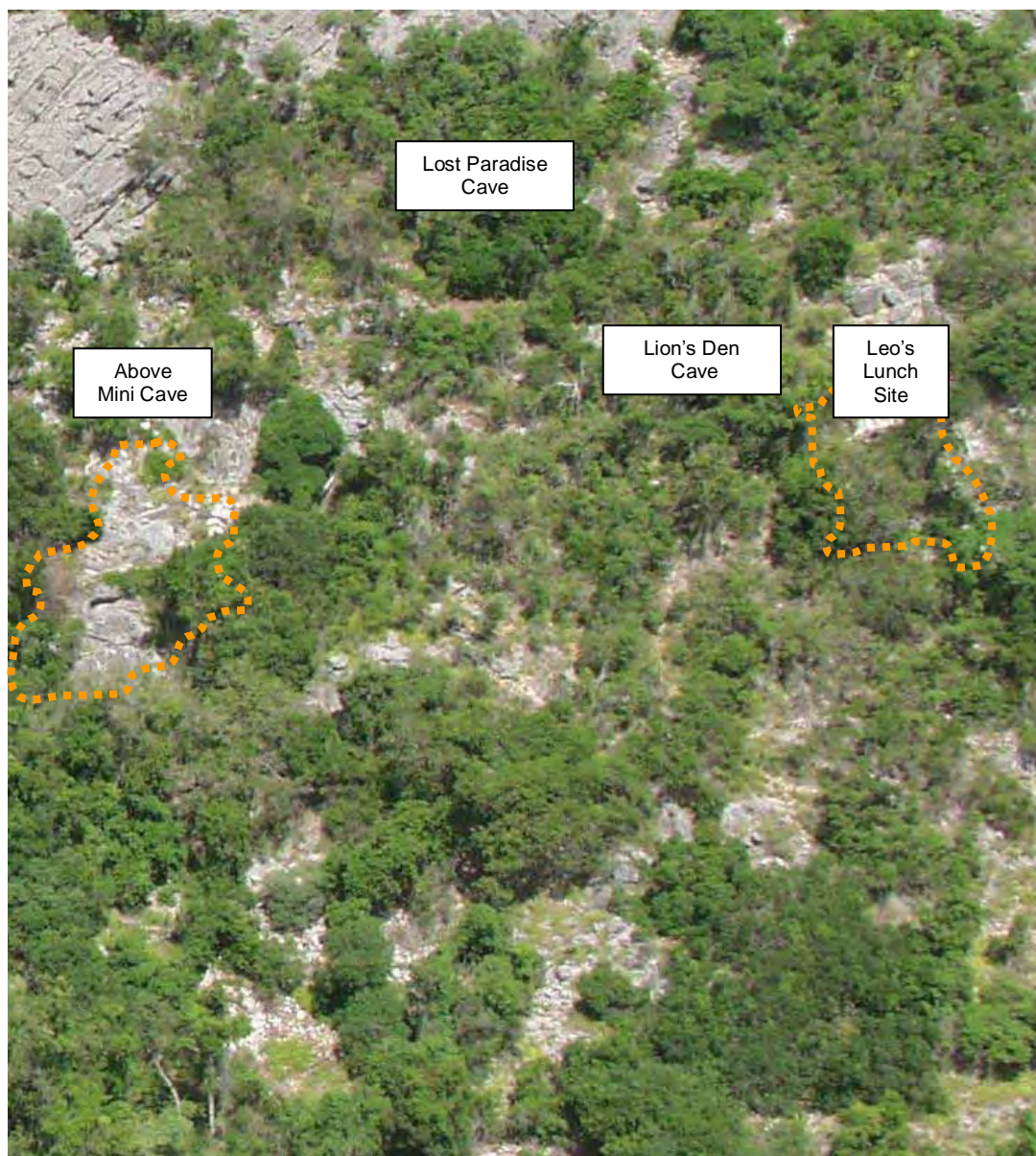


**Figure 3-53. Demarcation of karst exposed bone-bearing fossiliferous cave sediment deposits. QML1284a (Above Mini Cave) and QML1382 (Leo's Lunch Site).**

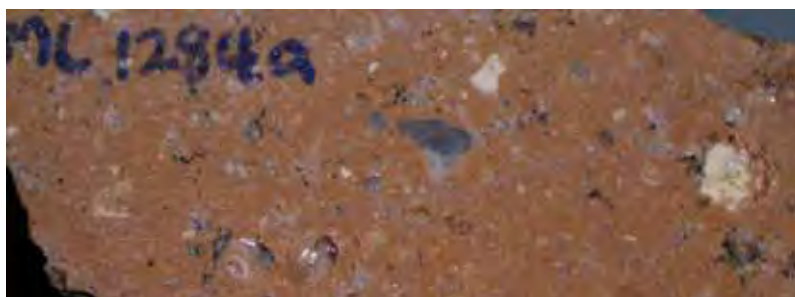


**Figure 3-54. QML1284a. Sedimentological sample cut in cross-section to show matrix composition.**

### 3.5 Karst Glen

Figs 3-55, 3-56



**Figure 3-55. QML1412, near KG3 B entrance, Karst Glen. Showing exposed bone-bearing fossiliferous deposits.**



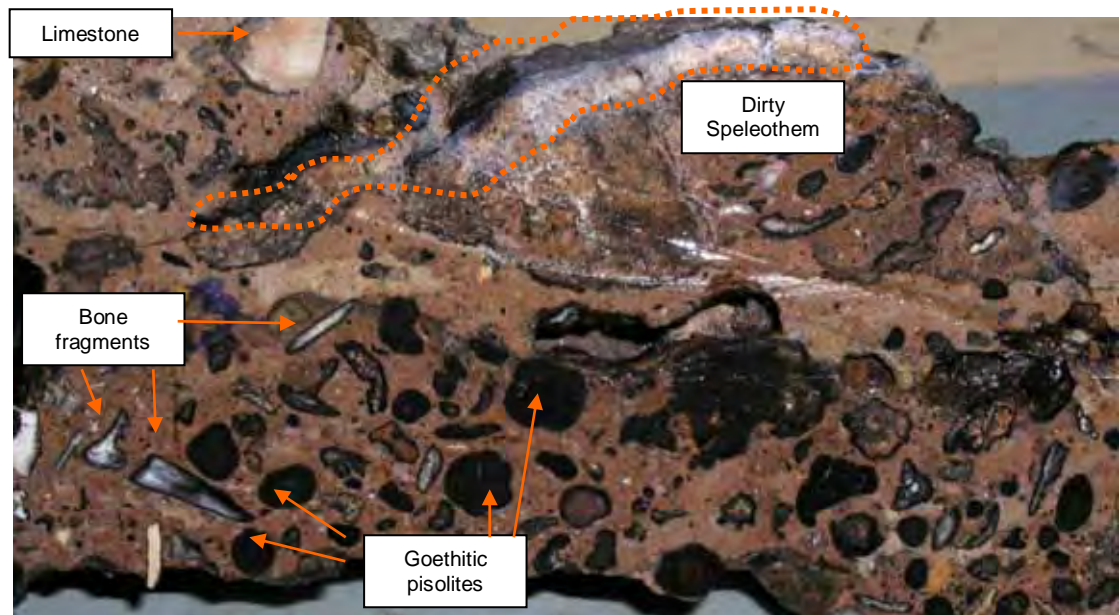


**Figure 3-56. QML1411, exposed fissure deposit, Karst Glen. Showing unique sedimentological deposit in cross-section. Goethitic pisolites, dirty speleothem, bone fragments, limestone clasts and clay matrix.**

### **3.6 Olsen's Cave System (Figs 3-57 – 3-59)**

Honey Moon Suite Chamber



**Figure 3-57. Honey Moon Suite Chamber deposit, Olsen's Cave.**

## QML1456, Colloseum Chamber

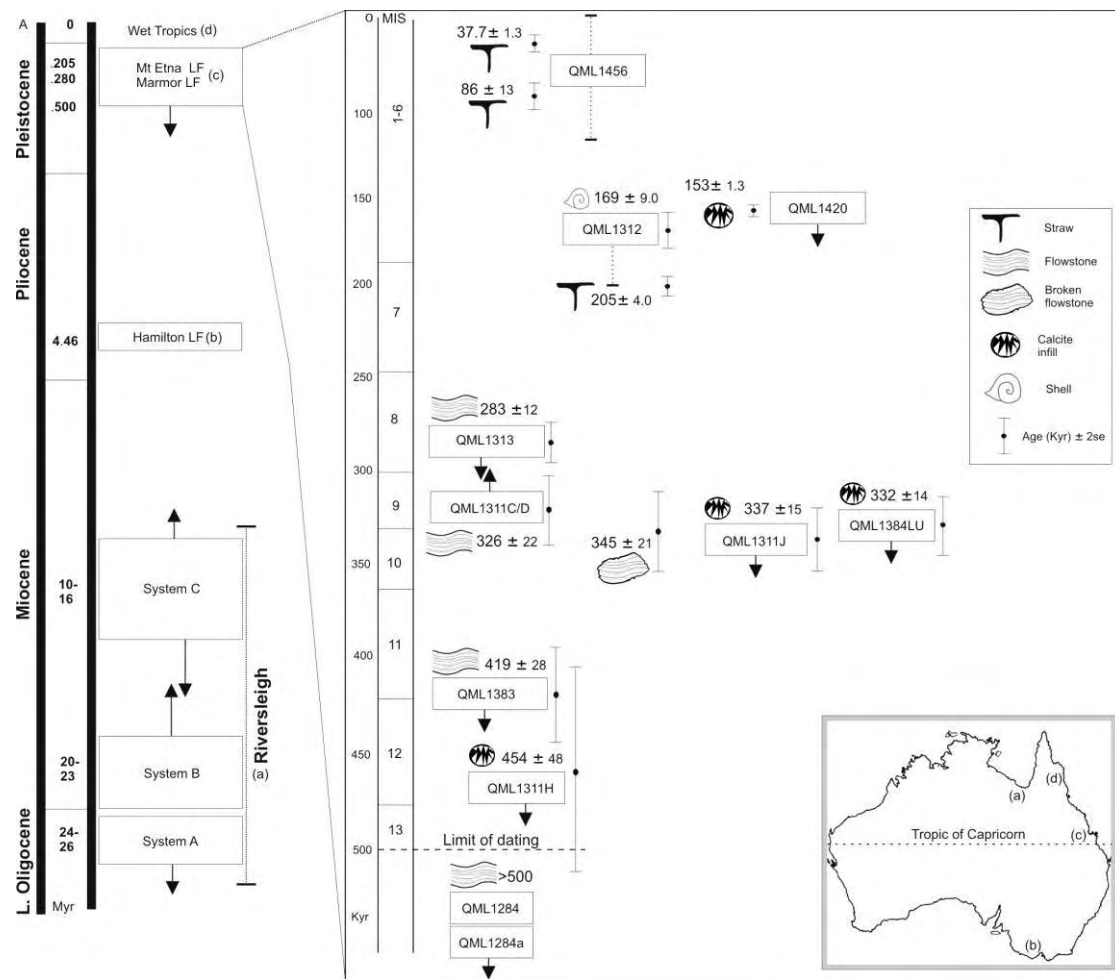


Figure 3-58. QML1456, Colloseum Chamber excavation.



Figure 3-59. QML1456, Colloseum Chamber dating materials. A. Lower incisor from a *Petrogale*. B. Straws. C. Snail shell.

### 3.7 Summary of Chronometric Ages.



**Figure 3-60. Summary of Chronometric ages discussed in text and throughout Chapters 1-7.**

### 3.8 Hypothesised Cave and Cave Deposit Formation

#### 3.8.1 Mount Etna

Cave system development at Mt Etna is dominated by the high angle of bedding plane within the parent limestone massif. These high angled bedding planes dictate the formation of near vertical open cave entrances and long vertical shafts. Due to the access afforded by limestone mining, a system of developmental sequences is proposed for the formation of caves and cave deposits on the western face of Mt Etna (Fig. 3-63).

##### A. Phreatic cave development and fissure breccias

Phreatic cave development at Mt Etna is interpreted to be a water table dominated phenomenon (Shannon, 1970a). Cave formation occurred at the water table where



dissolved acid corroded and eroded large blind-ending chambers. Solution pipes and fissures developed at or close to ground surface via collapse (fissure) or corrosion via meteoric water (solution pipes), where organic acids corroded and eroded the parent limestone along joints and bedding planes. Solution pipes penetrated deep within the limestone massif following the soluble vertical bedding planes of the limestone. Rare faunal accumulations occurred.

#### Phreatic Cave Development (Fig. 3-30, 3-39)

Numerous extant cave systems at Mt Etna preserve evidence of phreatic development, including phreatic pendants and passages, but most have undergone considerable overprinting by subsequent vadose development and their morphologies are generally hard to interpret. This is not true for the lower sections of Speaking Tube Cave system (QML1311 C, D, F, H) and Elephant Hole Cave system (QML1384LU, QML1385), which have been exposed through limestone mining. These exposed chambers have been completely in-filled with sediment, but they preserve phreatic chambers that have had minimal vadose development. Chamber deposits above and lateral to these lower infills preserve evidence of active vadose development (see below).

#### Fissure Development (Fig. 3-61)

Preserved fissure fills occur on the top mined bench of the western face of Mt Etna. These fissure fills do not appear to be solution pipes because the limestone contact zones do not have the distinctive solution-pipe wall morphology (corroded and scalloped surfaces). Instead, they are angular and irregular with breccia wedged against a fractured limestone wall. The sediment infill is a breccia and consists of angular parent limestone and allochthonous rock derived from the sedimentary sequences found laterally and above the limestone massif. Faunal remains are extremely rare, if present at all, with the only remains found so far being isolated, very badly preserved or crushed land snails. This form of breccia has only been found high on the western benches of Mt Etna, near the top of the limestone exposure. The fissure deposits are blind-ending and as such do not contribute significantly to the sedimentation of lower cavernous systems.



**Figure 3-61. An example of a fissure deposit high on the western face of Mt Etna mine, showing angular limestone clasts and irregular limestone wall.**

#### Solution Pipes (Fig. 3-62).

Solution pipes are preserved on the western face of Mt Etna and are exposed either through natural karst erosion or through limestone mining. Solution pipes preserve a different morphology and sediment infill type when compared with fissure deposits. The sediment infill is usually fine clay with some vadose development in the form of cave wall speleothem or sediment speleothem. Rare fauna has been recovered from these deposits. Although the total depth of any individual solution pipe remains unresolved, the depth (20-30m) and width (2-10m) of the preserved solution pipe sections suggest that they have significant influence on the delivery of sediment into the lower cavernous systems.



**Figure 3-62. An example of a sediment-filled solution pipe, Bench 0, Mt Etna Mine.**

**B. Phreatic chamber sedimentation and small vadose cave development**

Solution pipes penetrated the massive phreatic caverns through the dissolution of near vertical joint and fracture planes within the limestone. Sedimentation began, whilst vadose cave development occurred near the ground surface. At this stage the first significant faunal and vadose accumulations occurred. The water table was stable.

**Phreatic Chamber Sedimentation (Fig. 3-33)**

Normal cave development processes do not seem to explain the presence of massive homogenous, faunally rich, allochthonous derived sediments within a purely phreatic chamber. Usually, cave systems that begin to accumulate large amounts of external materials are also exposed to the air and therefore develop quickly into vadose systems dominated by speleothem formations and distinct sediment bedding (Shannon, 1970a & b). This can only be countered by the presence of a phreatic chamber that remains full of water, yet collects sediment from the surface.

Two scenarios may account for the retention of phreatic chamber conditions whilst connected, via solution pipes, to the surface and lacking substantial vadose development.

1. Water table. Traditionally the water table is hypothesised as the major corrosive and erosive mechanism for phreatic development, well below ground level

(Shannon, 1970a). This may well have been the case for the initial development of the caverns on Mt Etna, however, the lack of vadose development and the massive sedimentation that occurred in several of the lower chambers on the western face of Mt Etna call for additional explanation. Lack of corrosion on the fossil remains indicates a relatively stable alkaline environment. This feature suggests an absence of an acid-rich water table within the cave systems at the time of sediment deposition.

2. Meteoric waters. Large volumes of meteoric water appear to have coursed through the Mt Etna limestone during the depositional phase within the phreatic chambers. This is based on both the faunal remains indicating the presence of a high rainfall rainforest environment at the surface and the contemporaneous massive flowstones developed in vadose cave systems in the upper caverns. It is suggested here that once the solution pipes had penetrated the lower phreatic chambers, massive sediment loads and meteoric waters entered the phreatic chambers. Although the water table would have still dominated input into the chamber, additional meteoric waters carrying sediments from above would provide additional water to keep the chambers full and provide a relatively alkaline environment for fossilisation.

Sediment entering the phreatic chambers was of small particle size (clay fraction and grain-fraction) and apparently derived from the surface soil clays because it contains allochthonous materials such as non-limestone clasts and faunal remains. Subsequent widening of these solution pipes allowed the input of larger clasts into the phreatic chamber, including gravel and pebble-sized allochthonous clasts, clay and larger faunal remains.

#### Phreatic-Vadose Cycling – Wetting and Drying

There is evidence along the contact zones between individual deposits and within deposits that some vadose exposure – including erosion of older sediments, deposition of flowstones and precipitation of calcite within vacuities – occurred and hence the chambers were not always full of water. Most likely, they underwent a series of saturated and relatively dry periods, with saturated periods marked by sedimentation and water-full chambers and a lack of speleothem, and dry periods marked by a lack of sedimentation and development of speleothem (flowstones and calcitic vugs).

The distinctive speleothem associated with these deposits are capping flowstones, which demarcate the different deposits. Their morphology follows the surface topology of the sediment cone. These speleothems are relatively uniform and continuous, thin 'coatings' across each particular deposit. A secondary speleothem forms in vacuities within the chamber sediment deposit itself as either calcitic vugs within the sediment or within the hollow chambers left within bones and teeth. These precipitations occurred after the sediment was deposited and most likely within the same period of vadose development of capping flowstones.

The formation of these speleothems seems to have occurred when either the water table dropped and/or the amount of meteoric water entering the chamber dropped, which then exposed the chamber sediment to vadose erosion and speleothem genesis. There is also a nearly complete cessation of sedimentation at this time, which may reflect either a reduction in prevailing meteoric water availability or the consequential sealing of the solution pipes. These periods of vadose speleothem development and lack of sediment deposition were extensive, up to 120,000 years in duration, and yet complex speleothem genesis did not occur (e.g. stalagmite and stalactite formation). The porosity of the cave sediment also lends itself to the precipitation of calcite within it, converting it from soft clay to hard cemented sediment.

Subsequently the chambers once again became full of water, most likely via a rise in water table or via the return of large volumes of meteoric water. The return to previous conditions is evidenced by the return of massive homogenous sedimentation, lack of bedding and speleothem genesis, and post-depositional subsurface fracturing of faunal remains in the new deposits. The return of large volumes of water is also evidenced by the fractured and dislodged rafts of speleothem that had formed previously. These surficial flowstones underwent some degree of decalcification and pieces became incorporated as part of the contact zone morphology. Decalcification occurred on the dorsal surface of the flowstone. Sedimentation dominated the chamber fills once more.

The deposits recovered from QML1311 are evidence of a sequence of three phreatic-dominated sedimentation phases and two vadose-dominated capping/calcitic phases. QML1311F is the oldest sediment so far found and forms a sediment cone that has

undergone subsequent surficial erosion and flowstone deposition. QML1311 is also the most heavily cemented of the QML1311 deposits and contains massive veins and vugs filled with calcite. The ages of all of these deposits are beyond the range of U-Th dating, i.e. >500ka. Deposition of QML1311H occurred after this point and the contact zone between the two deposits contains significantly fractured and decalcified flowstones. Dating of this flowstone is equivocal because it is outside the applicability of U/Th (e.g. >500ka). Cessation of sedimentation of Unit H and the development of calcitic infills began at least  $454 \pm 48$ ka. This was followed by the deposition of a capping flowstone, which demarcates QML1311F and H from C/D, a new period of massive sedimentation. The period between the cessation of sedimentation of Unit H and the return of sedimentation producing Unit C/D is thus estimated to represent approximately 128,000 years ( $\sim 454$ -326ka).

The capping speleothem is not significantly fractured, the dorsal edge is irregular and interspersed within the sediment of unit C/D, indicating a rapid burial once sedimentation recommenced. This confirms that the age of the lower portions of QML1311C/D are very close to the minimum age of the speleothem ( $326 \pm 22$ ka).

The long periods when sedimentation in the chambers ceased, being replaced by only moderate speleothem genesis and calcite growth, suggests that the solution pipe activity for any particular chamber was limited and that deposition ceased once the solution pipe outflow was blocked. Therefore, although the age range of deposits for the entire western face of Mt Etna spans over ~500,000 years, individual deposits within particular chambers appear to have accumulated during relatively short periods, marked by long intervals ( $\geq 128,000$  years) when the chambers were cut off from major sediment input and underwent limited speleothem development.

### Faunal Deposition

The faunal remains consist of small-sized fragments of bone, teeth and land snail shell, plus more abundant small-sized, but complete, vertebrate and invertebrate fossils. The small fragments of bone possess angular breakage patterns and some rounding, indicating that the faunal remains travelled along the solution pipes into the chamber. It is considered here that the faunal remains have entered the solution pipes, via pit-fall or predator accumulation at the surface, possibly within a doline created by

exposed limestone with minimal karstic development. These entrance facies to the solution pipes have eroded away. There is no evidence that the faunal remains were derived from a higher vadose cave chamber and this is evidenced by the lack of reworked bone and speleothem within the chamber deposits. Reworked material would indicate the presence of a connected vadose chamber collecting material above the phreatic chamber and subsequently re-depositing this material lower down in the system. Thus, the phreatic chamber deposits are considered to be in situ accumulations with minimal temporal mixing.

The complete lack of distinct bone orientation and any indication of bedding plains within the phreatic deposits indicate a rapid deposition once the material entered the phreatic chamber. Fossil remains preserve evidence of depositional sediment that was particularly thixotropic. Post-depositional thixotropy and the lack of speleothem development indicate a water-logged (underwater) sedimentation. It is hypothesised that the rapid accumulation within the phreatic chambers formed crude sediment cones, with greater lateral extent, unlike those found in southern Australian cave systems (Reed, 2002).

The continuous sedimentation (sediment rain) within these chambers has resulted in a series of individually homogenous deposits (e.g. QML1311 (C, D, F, H); QML1384LU), however, each can be discriminated on the basis of colour, texture, bone preservation, allochthonous clasts and post-depositional calcitic formations.

#### Vadose Cave Formation

On the western face of Mt Etna, set back into the limestone face and above the phreatic chambers, are preserved sediment-filled vadose cave chambers. These chambers were not connected to the phreatic chambers until much later in their development. Mt Etna's vadose cave deposits are markedly different to those described above as part of the phreatic chamber system. Vadose chamber deposits are rich in speleothems, articulated faunal remains and preserve stratigraphic bedding planes throughout the profile. Vadose chamber deposition has occurred simultaneous with phreatic chamber deposition, deposits of very similar age being found above the phreatic system. Three main vadose deposits are conspicuous on the western face of Mt Etna mine: QML1310, QML1383 and QML1313. These deposits are described and discussed in Hocknull (2005), Hocknull et al. (2007) and above. All preserve

relatively different types of vadose chamber deposit, from aven deposits, to chamber floor and entrance facies.

#### C. Karstic development and extant large vadose cave development.

Post deposition of the phreatic and vadose chamber sediments karstic development then began to dominate the region. This is evidenced by the change in depositional materials, where the inclusion of allochthonous sediments transitions into less clay-rich deposits then more organic-rich deposits where the only rocky inclusions are that of the parent limestone. Faunal remains also change, with an almost complete lack of large vertebrates. Taxa such as chelid turtles, megafauna and mekosuchine crocodilians, which were found in both vadose and phreatic deposits, disappear from the record and this seems to represent a major change in the depositional settings of Mt Etna rather than a true absence of these taxa in the surrounding habitats. Karstic development would have occurred at the same time as significant loss of soil profile, and the development of exposed high karst. Cave entrances are isolated high above the surrounding ground surface and soil profile, therefore sedimentation via allochthonous materials ceased to dominate the new depositional environments. Instead, organic-rich deposits dominated. Karst collapse dominated the development of cave entrances, providing for large vertical entrances and establishment of significant chiropteran populations.

#### D. Major karst development and guano deposition.

The current Mt Etna karstic terrain is dominated by the open karst processes typical in dry, open karst terrains of tropical north Queensland (Shannon, 1970a). The massive cavernous systems previously only fed by relatively small vertical entrances and solution pipes, now collapsed in and provided massive vertical entrances. Their big entrances and newly enlarged chambers provided significant roosting chambers for bats and thus accumulation of significantly deep guano deposits. Enormous guano deposits typical of Mt Etna include those found at the base of Bat Cleft and Elysium Caves.



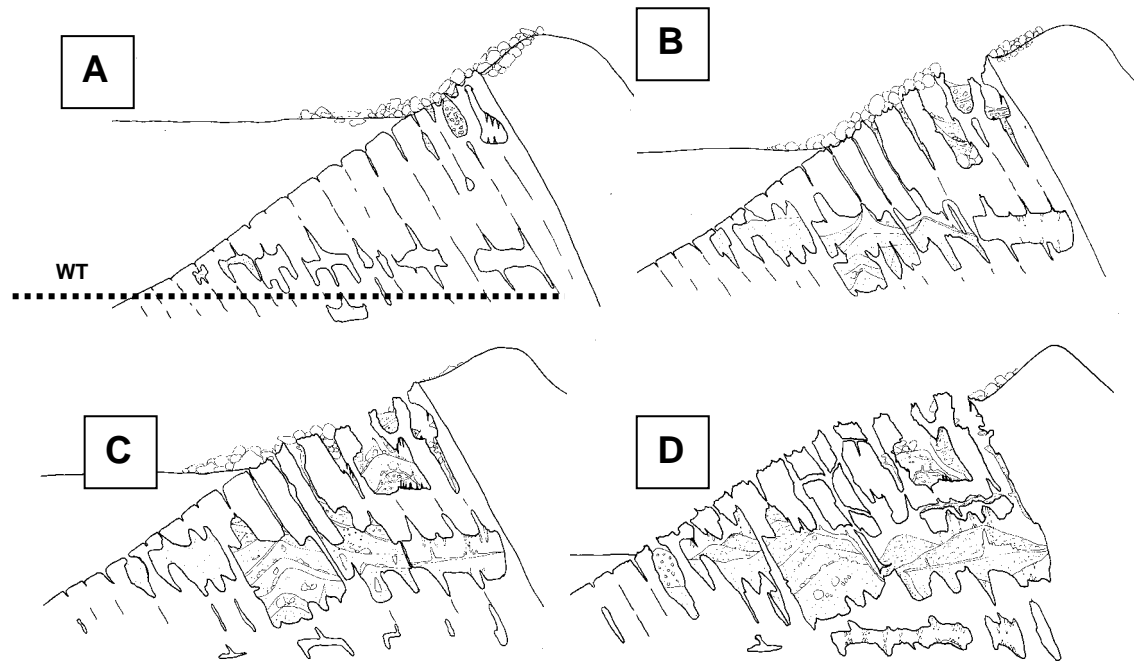


**Figure 3-63. Hypothesised cave formation, sedimentation and karst development on the western margin of Mt Etna. A. Phreatic and Fissure Development. B. Phreatic sedimentation and vadose cave development. C. Karstic and major vadose development. D. Karstic exposure and guano deposition. WT = water table.**

### 3.8.2 Limestone Ridge

Cave development on Limestone Ridge is unique amongst limestone blocks of the Mt Etna region. The limestone massif of Limestone Ridge has a relatively low angled bedding plane, compared with the near vertical bedding plane of Mt Etna, and hence the dominant cave development occurs to be near horizontal rather than vertical. Limestone Ridge also possesses significant volcanic intrusions that have penetrated the limestone and dictated the formation of some cave systems.

#### A. Phreatic development.

Evidence of phreatic development can be seen throughout many of the cave systems, including phreatic pendants and passageways.

#### B. Vadose cave and open doline development

Vadose cave development is extensive throughout Limestone Ridge and cave deposition in these caverns is very common. In particular, Mini Cave illustrates a

palaeocave deposition that is typically developed in horizontally developed, vadose chambers. These structures include definable stratigraphic sequences, where sediment deposits are interspersed between significant low-angle flowstones and cave floor formations (such as cave pearls and stalagmites). Sediment accumulation within these palaeocaves is typically allochthonous derived sediments which thus indicate the presence of a soil profile above the cave entrance. The faunal remains within these sediments are more often articulated and derive from pit-trap and predator accumulations as well as fauna living within the cave system itself.

Palaeocave sediments are also exposed on the surficial karst limestone as part of old dolines or cave collapses, indicating the past presence of cave chambers above the present cavernous system. Thus, older cave deposits are usually found above younger ones, something not observed at Mt Etna. These older palaeocaves also preserve allochthonous sediments, indicating that the soil profile of the region was once well above the current limestone surface.

### C. Extant cave development

The extant caves of Limestone Ridge have developed laterally as have the palaeocaves before them. These present caves cut through sections of the older palaeocaves that were developed at the same level. Other cave systems have developed along the area of intrusion by volcanics, the caves being distinctly horizontal. Ballroom Cave in the south-eastern section of Limestone Ridge most distinctly illustrates this phenomenon. Clastic material derived from these volcanic intrusions is yet to be discovered in any of the palaeocave deposits. It therefore seems unlikely that there were higher levels of volcanic intrusion and likely that this current sequence of cave development is the first to impact on the intruded rock units.

### D. Karst development

Subsequent to the deposition of the palaeocaves on Limestone Ridge significant soil loss has occurred, which has in turn exposed the bare limestone to karstic development. As at Mt Etna, the significant loss of clay-rich soil profiles has significantly altered the depositional materials available, therefore the majority of deposits consist of fine organic-rich sediments and cobbles of parent limestone.

Typical tropical karstic processes have produced the high karst of the ridge and this has in turn developed larger cave entrances and areas of collapse. As with Mt Etna, the opening of these cave systems has facilitated accumulation of significant guano deposits, derived from bats. Such caves include Johansen's Cave and Old Timbers Cave.

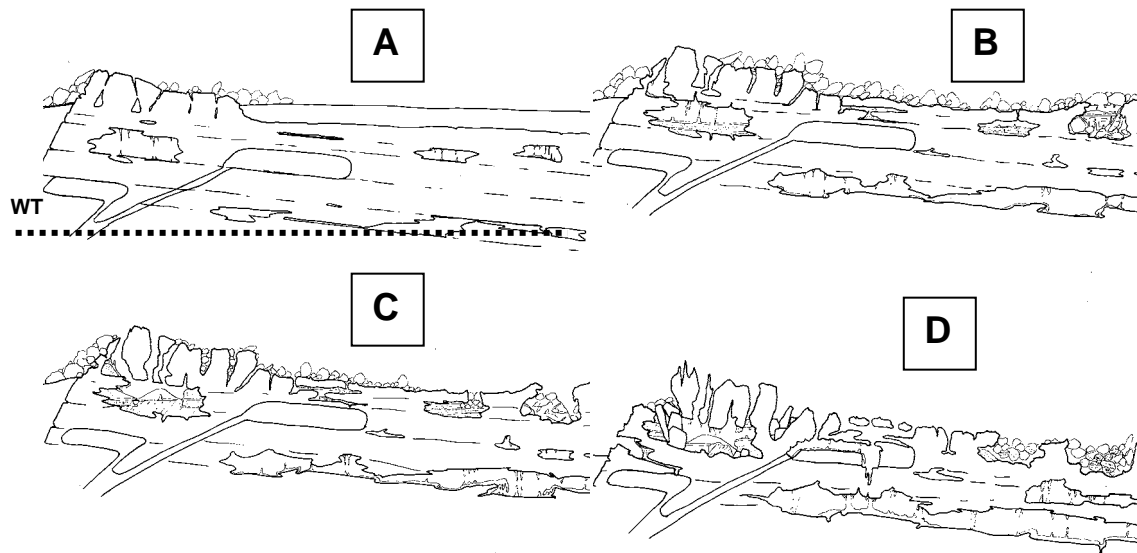


**Figure 3-64. Hypothesised cave formation, sedimentation and karst development at Limestone Ridge (southern section). A. Phreatic Development. B. Vadose cave and open doline development. C. Extant Cave development. D. Karstic exposure and guano deposition. WT = water table.**

### 3.8.3 Olsen's Cave

Olsen's Cave is a single limestone massif with an irregular and high-angled limestone bedding plane. This has dictated the overall large chamber development. However, unlike Mt Etna, Olsen's Cave has not developed significantly deep chambers. Instead, the cave possesses significantly large and high-roofed chambers, combined with massive entrance collapses.

#### A. Phreatic development

Phreatic development is evidenced by the overall shape of the cave systems, although much of the phreatic system has been altered by vadose formations.

#### B. Karstic and joint development

Deflation of the surrounding soil profiles and exposure of limestone to the surface allowed the development of karst and vadose chambers. Joints and fracture planes within the limestone dictate the gross collapse patterns typical in the cave. This has led to the development of several different levels to the cave chambers and several entrances to them.

### C. Cave sedimentation

Sedimentation and flowstone deposition in the chambers has undergone cycles of significant deposition followed by depositional hiatuses. Thick flowstones can be found throughout the cave system, in particular as a basal floor flowstone that is extensively developed in Colloseum, Honey Moon Suite and Cathedral Chambers. Deposition of sediment within the cave system does not seem to have been dominant nor of such long duration as at Mt Etna and Limestone Ridge. Vadose chamber development has produced highly decorated chambers, but development of decorations has significantly slowed allowing the sedimentation of chambers to dominate. Older sediments are present as false floors within Icicle Chamber, but little old lithified sediment can be located in this cave system. Late Pleistocene-Holocene deposits dominate the chamber sediments, including significant bone accumulations and guano deposits. Fossiliferous deposits can be found throughout the cave system, with high concentrations of bone material accumulated through predator and pit-trap processes being typical of Colloseum, Icicle and Honey Moon Suite Chambers.

### D. Karstic exposure and collapse. Massive cave entrances.

Exposed limestone karst has undergone significant collapse, which has provided large entrances at or near ground level to Olsen's Cave. These collapses have also provided entries for both Ghost Bat (*Macroderma*) and other bats, such as species of *Miniopterus*. Guano deposition has been significant in the past and is evidenced by the guano extraction that has taken place.

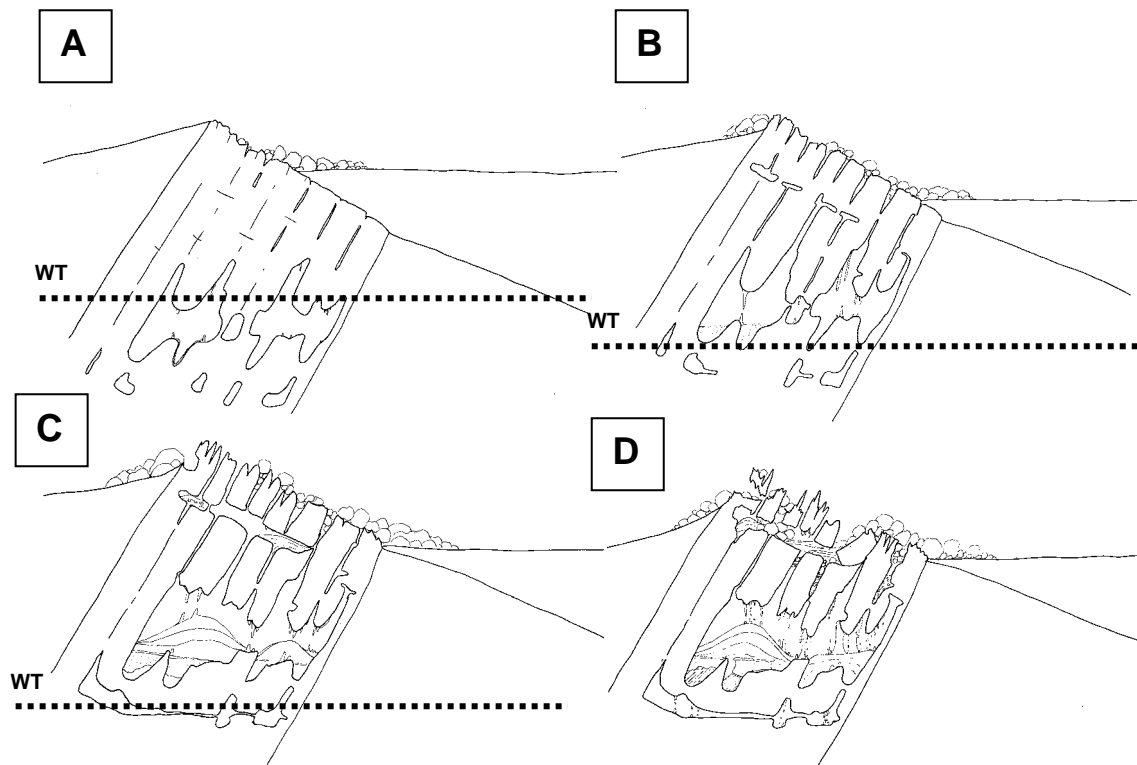


**Figure 3-65. Hypothesised cave formation, sedimentation and karst development at Olsen's Cave. A. Phreatic Development. B. Karstic and joint development. C. Cave sedimentation. D. Karstic exposure, collapse and guano deposition. WT = water table.**

#### 3.8.4 Karst Glen

Karst Glen is an isolated limestone massif with relatively vertical limestone bedding planes. The limestone karst terrain is of relatively low relief when compared with Mt Etna and Limestone Ridge.

##### A. Phreatic development and fissure deposition

Phreatic development appears to have developed the chambers in a similar way to Olsen's Cave. Karst Glen differs from Olsen's by possessing significant fissures that intersect the limestone bedding planes and have accumulated significant sediment deposits, including fossils.

##### B. Karst and joint development

Soil deflation and erosion has exposed the limestone which has developed into karst. Cave entrances tend to be vertical and only accessible via ropes or ladders. The cave chambers are complex and bedding plane and joint controlled chamber connections,

intersected by previous fissures. A very large fissure can be seen within Ladder Cave (KG3) and includes several fossiliferous deposits.

#### C. Vadose cave development

Minimal vadose development can be observed in this system and may be due to the immediate input of fissure sediments within the phreatically developed chambers.

#### D. Karst exposure and collapse

Along the leading edge of the exposed karst (the north-westerly margin), large fall-aways of karst are observed which have exposed significant fossil deposits. Most of these deposits are old fissure deposits, however, some are indicative of old cave chamber floor accumulations with the bone heavily broken up and mostly representing small vertebrates. These deposits are considered to be derived from an old predator accumulation, either from a Ghost Bat (*Macroderma*) or owl's (*Tyto* spp.) roost (or both). Several fissure deposits are exposed on the karst surface, including a deposit rich in pisolitic goethite and bone. This deposit is unique within all of the deposits so far investigated. There is currently no satisfactory explanation for this type of deposit.

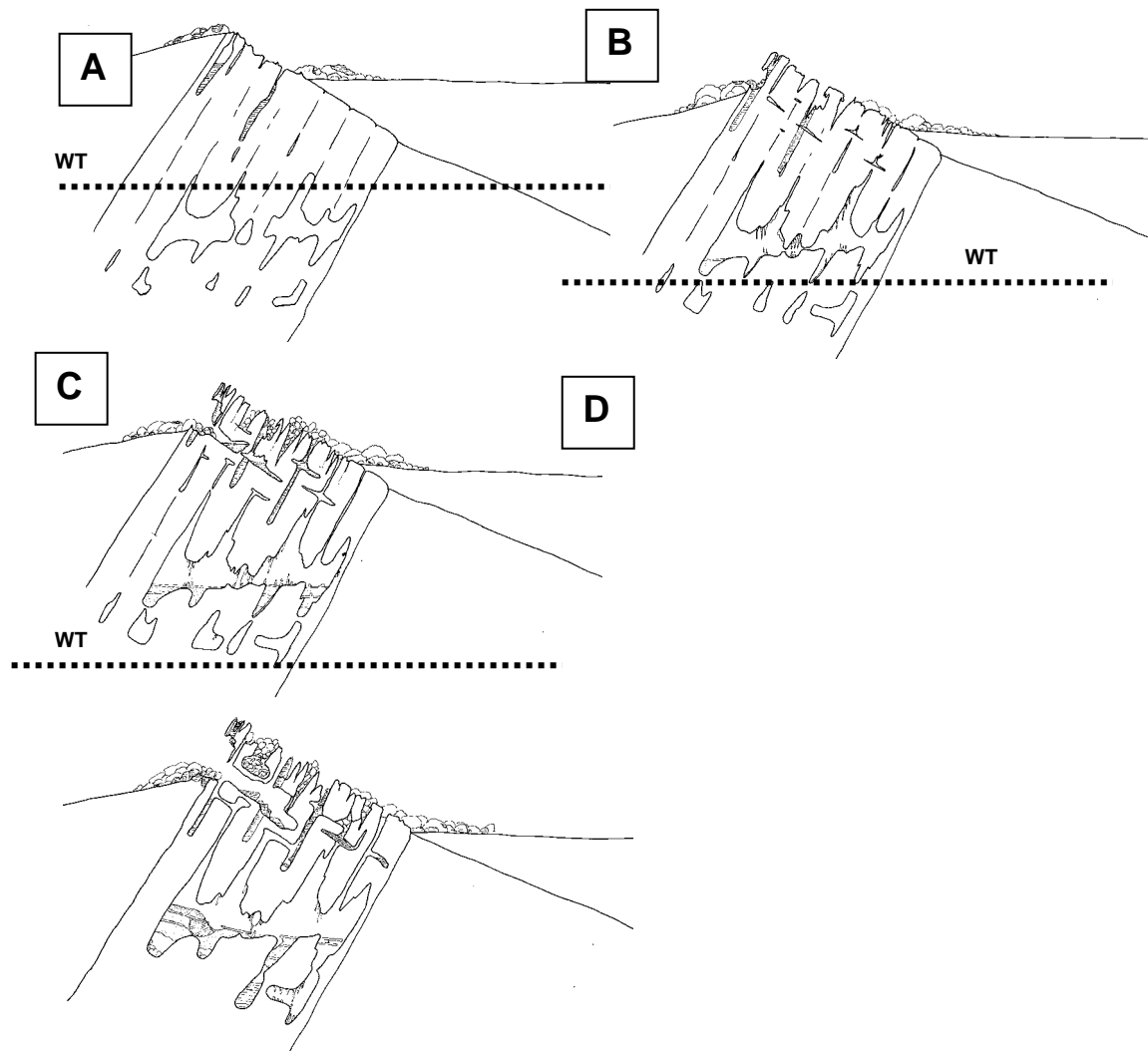


**Figure 3-66. Hypothesised cave formation, sedimentation and karst development at Karst Glen. A. Phreatic and Fissure deposition. B. Karst and joint development. C. Vadose cave development. D. Karstic exposure and collapse. WT = water table.**

## Chapter 4

### 4.1 Additional Pleistocene vertebrate fauna from central eastern Queensland, Australia.

### 4.2 Introduction

Cainozoic vertebrate faunas from rich cave deposits in central eastern Queensland were preliminarily reported by Hocknull (2005). These deposits were considered to be Pliocene and Pleistocene in age based on biocorrelation, however, more recently have been found to be restricted to the Pleistocene on the basis of direct chronometric dating (Hocknull et al 2007). Since Hocknull (2005), several new localities have been uncovered and faunas recovered from them. This chapter records these new taxa and updates the faunal groups reported by Hocknull (2005) and Hocknull et al., (2007). All systematics follow those methods outlined by Hocknull (2005). Faunal remains are all lodged within the Queensland Museum fossil collections within the Mt Etna collection (Hocknull Thesis Material).

Comparative collections investigated by Hocknull for the taxonomic identifications in Hocknull (2005) and this chapter include all of the skeletal collections available from the Queensland Museum, Australian Museum, Museum of Victoria, South Australian Museum and Western Australian Museum. Each collection was systematically surveyed for diagnostic skeletal remains of mammals, reptiles, amphibians and birds. Apomorphies were determined as best as possible for the extant and extinct taxa in collections and from the literature. Autapomorphic and synapomorphic features were determined as best possible using cladistic methodologies to return the most thorough taxonomic identification possible within the constraints of the available comparative collections. Where possible, the diagnostic features that differentiate these taxa were placed within a phylogenetic framework to produce a parsimonious phylogenetic tree of relationship.

Detail systematic descriptions of key groups await further study and the collection of more comparative data, especially for those extant and Quaternary taxa from New Guinea, where present day taxonomic accounts are poor. These descriptions will be



the subject of several research projects in the future by the author and will form part of several postgraduate and post-doctoral works, some of which have already commenced.

### 4.3 Systematic Palaeontology

Order ANURA Rafinesque, 1815

Family HYLIDAE Rafinesque, 1815

#### **Cyclorana**

Hocknull (2005) identified two ilia attributable to *Cyclorana* from Olsen's Cave. Since then, several dozen ilia have now been retrieved from an excavation within Colloseum Chamber of Olsen's Cave. *Cyclorana* has been found at all levels of 90cm deep excavation, which is considered to represent the latest Pleistocene and Holocene depositional timeframes. Two species are identified here. Two species of *Cyclorana* occur in the central eastern Queensland region in the present day, *Cyclorana novaehollandiae* and *Cyclorana brevipes*. Tyler *et al.*, (1994) redefined the species-level characteristics of *Cyclorana* and described a morphological dichotomy which allows placement of *Cyclorana* ilia into two groups of morphospecies. *C. australis* and *C. novaehollandiae* both possess a dorsal rim along the ilial shaft and inconspicuous dorsal prominence and protuberance. The remaining congeners do not possess a dorsal rim and possess very distinctive dorsal protuberances on long anteriorly placed prominences.

#### ***Cyclorana* sp. cf. *C. cultripes***

Fossil specimens possess diagnostic features attributable to *Cyclorana cultripes* as defined by Tyler (1976) and Tyler *et al.*, (1994). These features include; a long prominent dorsal prominence (as long as the diameter of the ilial section of the acetabulum), a laterally developed protuberance that is oriented at a very acute angle to the ilial shaft.



**Figure 4-1. *Cyclorana* sp. cf. *C. cultripes*, right partial ilium, QML1456.**

### ***Cyclorana* sp. 2**

*Cyclorana* sp. 2 differs from the other species of *Cyclorana* in the Colloseum Chamber excavation by possessing a more knob-like dorsal protuberance which is orientated at a greater angle to the ilial shaft than the same angle seen in *C. sp. cf. C. cultripes*. *Cyclorana* sp. 2 also differs from *C. cultripes* by possessing a more rounded acetabulum and a shorter dorsal acetabular expansion.



**Figure 4-2. *Cyclorana* sp. 2, right ilium, QML1456.**

## **Family MYOBATRACHIDAE**

### ***Neobatrachus***

Hocknull (2005) described an unidentified species of *Neobatrachus* from QML1385. Since then, additional specimens have been recovered including a relatively complete ilium from QML1312. Excavations in late Pleistocene-Holocene deposits have uncovered a second species identified herein.

### ***Neobatrachus* sp. 1**

*Neobatrachus* sp. 1 is much smaller than *N. sp. 2*, possesses a larger acetabulum and a smaller more posteriorly placed dorsal protuberance. The dorsal acetabular expansion is reduced.

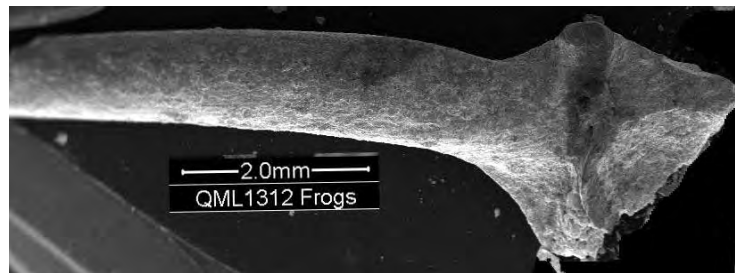


**Figure 4-3. *Neobatrachus* 1., left ilium, QML1312.**

### ***Neobatrachus* sp. 2**

*Neobatrachus* sp. 2 differs from *N. sp. 1* by being much larger, possessing a relatively smaller acetabulum, more distinct, anteriorly positioned, dorsal protuberance on a broad and distinct dorsal prominence. The ventral acetabular expansion and preacetabular zone is reduced .

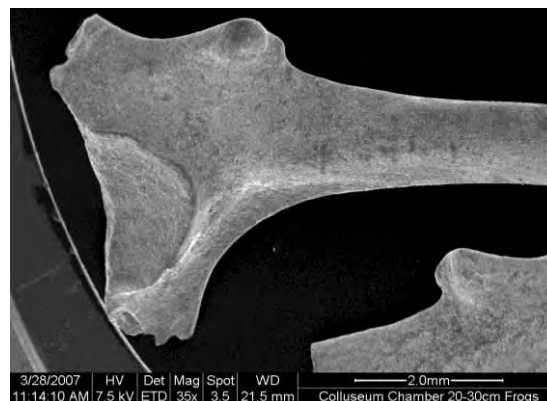


**Figure 4-4. *Neobatrachus* sp. 2., right ilium, QML1456.**

### **Uperoleia**

*Uperoleia* was identified on the basis of the following characteristics; Ilium small, short and relatively straight; indistinct acetabular rim; superior rim of acetabulum above the ventral margin of the ilial shaft; ventral acetabular expansion slightly dilated and a moderate preacetabular zone; dorsal prominence very slight and a small

ovoid dorsal protuberance; dorsal prominence and protuberance anterior of anterior rim of acetabular fossa.

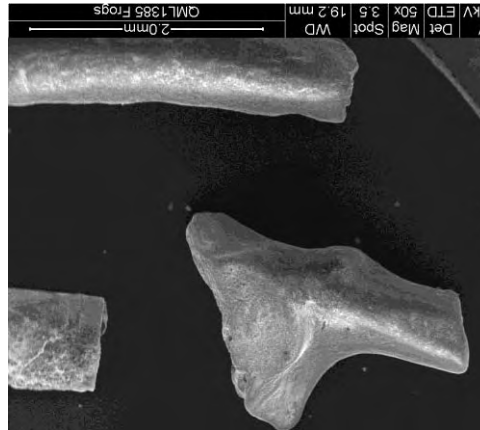


Figure 4-5. *Uperoleia* sp., right ilium, QML1385.

#### ***Taudactylus* sp. cf. *T. diurnus***

*Taudactylus* was identified on the basis of the following combined features considered by Tyler (1976) to be diagnostic for the genus. Small ilium. Slight curvature of the ilial shaft. Shaft simple, laterally compressed in cross section, without crest or rim and bearing a low elongate dorsal prominence. Dorsal protuberance ovoid and dorso-laterally projecting. Acetabular rim distinct forming deep cup and positioned above the level of the ventral margin of the ilial shaft. Over half of the dorsal prominence and protuberance anterior of anterior rim of acetabulum. Dorsal acetabular expansion directed posteriorly. Ventral acetabular expansion slightly dilated and a narrow preacetabular zone. On direct comparison with comparative specimens of *Taudactylus* the fossil species most closely allies with *T. diurnus* both in morphology and size.



Figure 4-6. *Taudactylus* sp. cf. *T. diurnus*, left ilium, QML1284.

#### *Assa* sp.

*Assa* was identified on the basis of the following combined characteristics diagnostic of the genus (Tyler, 1976). Small ilium. Iliac shaft slightly curved, circular in cross section, without dorsal crest, rim or groove. Dorsal prominence slightly defined with an inconspicuous but rounded dorsal protuberance. Dorsal prominence level with the anterior margin of the acetabular rim. Preacetabular zone developed through ventral acetabular expansion. Dorsal acetabular expansion poorly developed and short. Acetabular rim pronounced and large with the dorsal rim on level or slightly superior to the ventral margin of the iliac shaft.

A morphologically similar taxon, *Geocrinia*, differs from the fossil species by being much larger in size, having a more laterally compressed iliac shaft cross section and a poorly developed ventral acetabular zone and expansion.



**Figure 4-7. *Assa* sp., A. right ilium, B. left ilium, C. left ilium; QML1385.**

# Philoria

*Philoria* was identified based on the combination of features presented by Tyler (1976) as diagnostic for the genus. These features differ from a morphologically similar taxon, *Kyarranus*.

Small ilium. Large acetabulum with the superior margin on level with the ventral margin of ilial shaft. Ventral acetabular expansion not dilated, with narrow preacetabular zone. Dorsal prominence and protuberance indistinguishable from each other, with the prominence poorly developed and entirely anterior of the acetabular rim. Dorsal acetabular expansion developed and postero-dorsally directed.

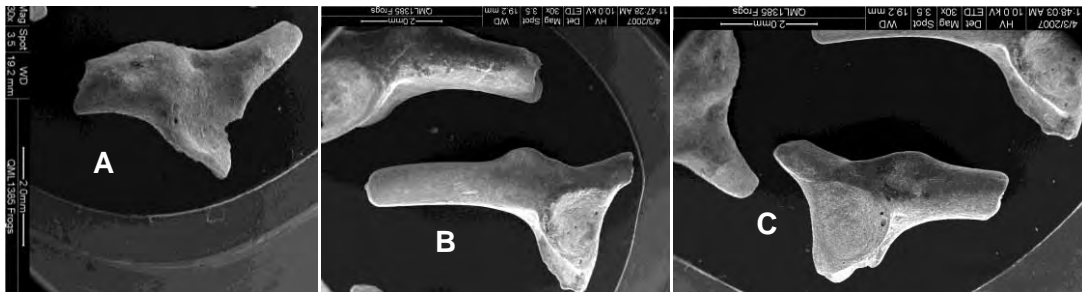


**Figure 4-8. *Phyloria* sp., A. Left ilium, B. Left ilium, C. Right ilium, QML1385.**

## Pseudophyrne

Two morpho-species of *Pseudophyrne* are identified here and both are diagnosed on the basis of combined characters that define *Pseudophyrne* (Tyler, 1976).

Small ilium. Shaft almost straight, circular in cross section, without crest or rim. Large acetabulum with distinct narrow acetabular rim. Superior margin of the acetabular rim lies above the ventral margin of the ilial shaft. Dilated and well developed ventral acetabular expansion and preacetabular zone. Dorsal acetabular expansion poorly developed, short and postero-dorsally directed. Dorsal prominence

slightly raised with a small knob-like or point-like tip to the dorsal protuberance.

Dorsal protuberance in line with the anterior margin of the acetabular rim.

*Pseudophryne* sp. 1 is smaller than *P.* sp. 2 and possesses a less developed dorsal protuberance. *Pseudophryne* sp. 2. is larger and possess a well developed, pointed, dorsal protuberance, which is directed antero-laterally.

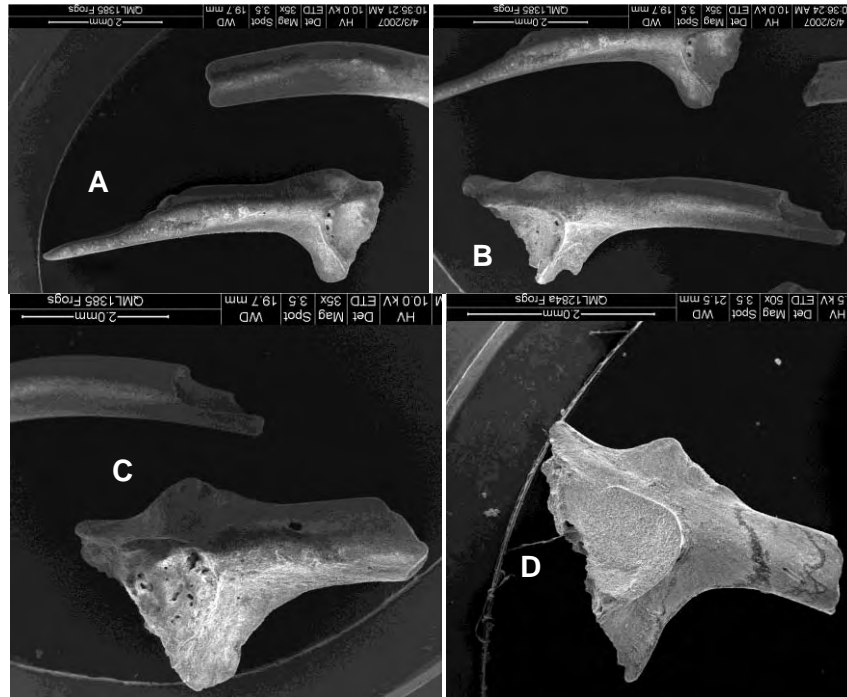


Figure 4-9. *Pseudophryne* sp.1, A. Left ilium, B. Right ilium, C-D. *Pseudophryne* sp. 2 Right ilium, QML1385. D. Right ilium, QML1284a

### Kyarranus

Hocknull (2005) identified a single species of *Kyarranus* from the Mt Etna deposits. Since then, several more specimens referable to *Kyarranus* have been recovered and two distinct taxa are present.

#### *Kyarranus* sp. 1

*Kyarranus* sp. 1 was original identified by Hocknull (2005). *K.* sp. 1 differs from *K.* sp. 2 by being larger and possessing a less elaborate and prominent dorsal prominence and protuberance.

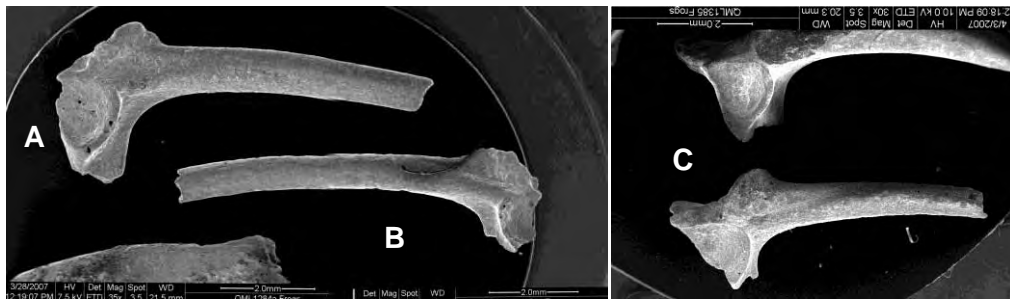


Figure 4-10. *Kyarranus* sp. 1, A. Right ilium, B. Left ilium, QML1284a; C. Right ilium, QML1385.

### *Kyarranus* sp. 2

*Kyarranus* sp. 2 differs from *K.* sp. 1, by being smaller, possessing a distinct antero-dorsally projecting dorsal protuberance which sit upon a broad crest-like prominence. The prominence is almost as long as the prominence and protuberance is high.

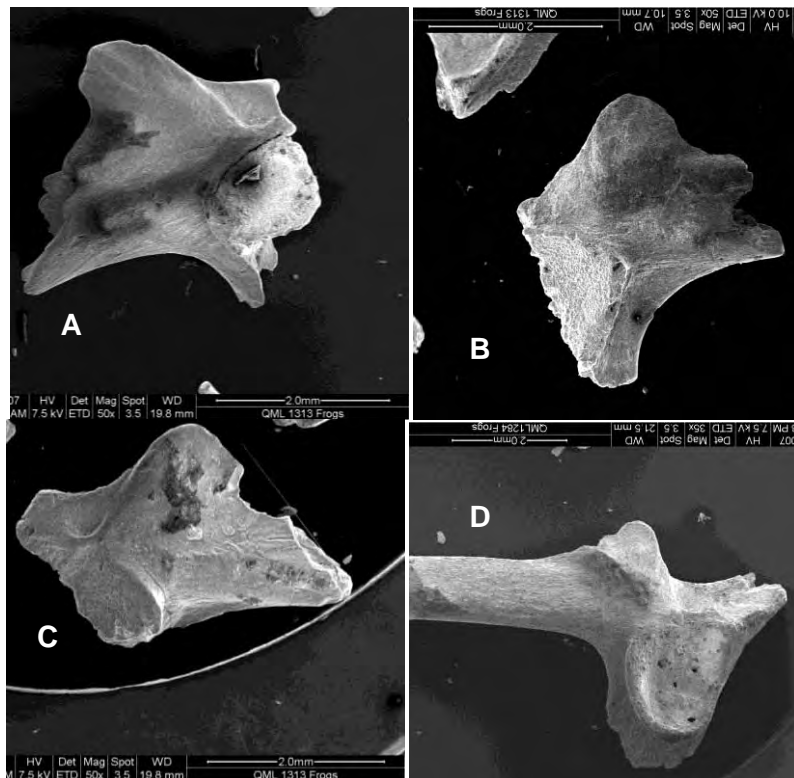
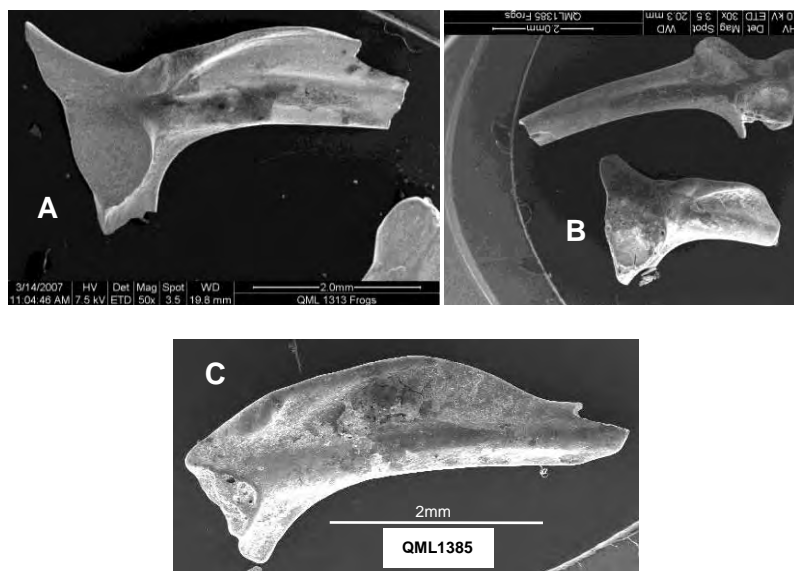


Figure 4-11. *Kyarranus* sp. 2, A. Left ilium, B. Right ilium, C. Right ilium, QML1313; D. Left ilium, QML1284.

### *Lechriodus* sp. cf. *L. platyceps*



Hocknull (2005) identified a species of *Lechriodus* from Mt Etna. Here we identify it as most closely resembling *Lechriodus platyceps*, based on its similar crest shape and distal crest tapering; overall similar size; similar dorsal prominence shape and similar degree of dorsal and ventral acetabular expansion.



**Figure 4-12.** *Lechriodus* sp. cf. *L. platyceps*, A. Right ilium, QML1313; B. Right ilium, C. Right ilium, QML1385.

## MICROHYLIDAE

Hocknull (2005) reported on three species of microhylid from Mt Etna. Review of these fossils has shown that microhylid sp. 1 and microhylid sp. 2 are in fact specimens referable to the myobatrachid genus *Pseudophryne*. However, subsequent to Hocknull (2005) two microhylids have been identified in addition to cf. *Hylophorbus*; species of *Cophixalus* and a new genus.

### **Cophixalus**

*Cophixalus* was identified based on the following combinations of features that characterise the genus. Small ilium. Medio-laterally compressed ilial shaft with no crest or rim. Slightly curved. Concave ventral acetabular expansion and very narrow preacetabular zone. Very large acetabulum and broad acetabular rim, which is positioned superior to the ventral margin of the ilial shaft. Dorsal protuberance indistinguishable from dorsal prominence, which is conspicuous and situated anterior of the acetabular rim. Dorsal acetabular expansion poorly developed.



**Figure 4-13. *Cophixalus* sp., A. Right ilium, B. Right ilium, C. Left ilium, QML1385.**

### **?Gen. Nov.**

A series of ilia recovered from the Mt Etna deposits represent a new genus of microhylid frog. The ilium is relatively small with a horizontal shaft. Iliac shaft elliptical in cross section without crest or rim. Dorsal acetabular expansion short and pointed with a parallel axis to iliac shaft axis, making the straight dorsal expansion a continuation of the straight shaft. Ventral acetabular expansion perpendicular to dorsal acetabular expansion and iliac shaft, producing a near 90° angle between the preacetabular zone and the ventral margin of the iliac shaft. Acetabulum large and sub-triangular in shape with a distinct rim. Preacetabular zone very narrow running into a ventrally dilated ventral acetabular expansion which is rounded ventrally well below the base of the acetabular rim. Dorsal prominence long and low with an indistinguishable dorsal protuberance. Dorsal prominence begins posteriorly over the level of the anterior rim of the acetabulum, ending well anterior.

The absence of a dorsal crest or distinct rounded dorsal protuberance excluded this taxon from being a hylid. The anteriorly developed dorsal prominence, indistinct dorsal protuberance and straight iliac shaft exclude this taxon from being a member of most myobatrachid genera. Those myobatrachid genera that possess a straight shaft (*Neobatrachus*, *Notaden*, *Pseudophryne*, *Uperoleia*) differ in the relative expression

of the dorsal prominence and protuberance. The combination of a distinctly straight shaft with straight dorsal acetabular expansion and elongate dorsal prominence without a distinct protuberance sets this new genus apart from all described myobatrachids and microhylids. The taxon may represent an extant microhylid from New Guinea which has yet to have its ilial osteology adequately described.

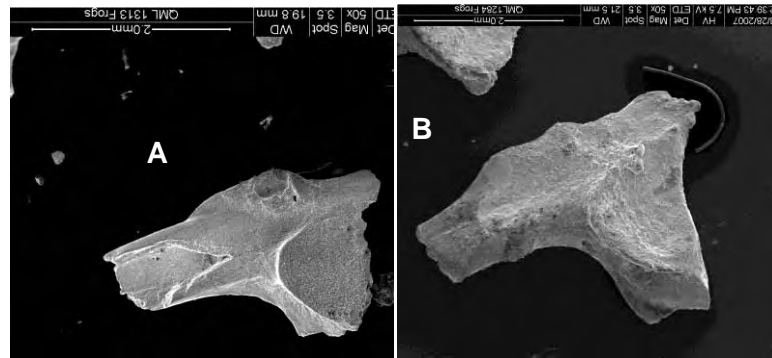


Figure 4-14. microhylid ?gen. nov. A. Left ilium, QML1313; B. Left ilium, QML1284.

The most up-to-date faunal list of frog taxa across the middle-late Pleistocene is presented in Chapter 7.

#### Order TESTUDINES Linnaeus, 1758

##### Family CHELIDAE, Gray 1825a

Chelids have only been recovered from Middle Pleistocene sites at Mt Etna. The majority of the specimens identifiable as chelid turtles include pieces of carapace and plastron, however, isolated vertebrae and limb bones are known. Based on carapace and plastron specimens, the chelid turtles would have been moderately large.

##### ***Rheodytes* sp. cf. *R. leukops***

*Rheodytes* has been identified from the middle Pleistocene deposits at Mt Etna. The remains of a first left pleural diagnose this chelid to the genus *Rheodytes* by possessing the following features considered diagnostic of the genus (Thomson, 2000); 10-15° angle between the anterior bridge strut and the rib/gomphosis of pleural one; anterior and posterior sutures run in parallel making up the of the bridge strut suture; no medial constriction of bridge strut.

There are only two described species of *Rheodytes*; the extant Fitzroy River Turtle (*R. leukops*) and an extinct Plio-Pleistocene species from the Darling Downs (*R. devisi*) (Thomson, 2000). On comparison with the type specimen of *R. devisi*, the pleural from Mt Etna is considerably more gracile, being thinner in cross-section and generally smaller. The bridge struts of the Mt Etna fossil are less robust than those of *R. devisi*. Essentially *R. leukops* was differentiated from *R. devisi* by Thomson (2000) on the basis of *R. devisi* having a much more robust shell and deeper insertion of the bridge strut sutures. Because the Mt Etna fossil is gracile in morphology it is here considered to be close to *R. leukops*. The presence of *R. leukops* at Mt Etna during the middle Pleistocene is not surprising as it exists in major tributaries of the Fitzroy River, one of which occurs only 4kms to the west of Mt Etna today.

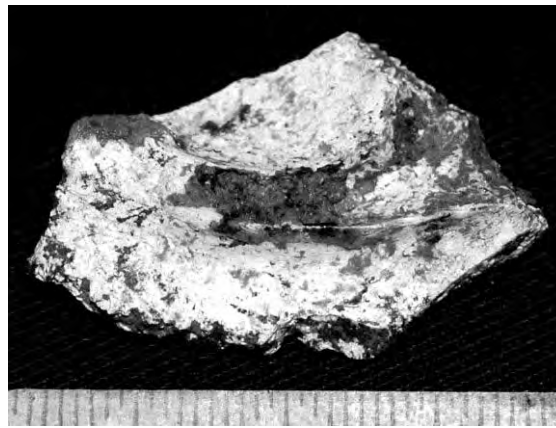


**Figure 4-15. *Rheodytes* sp. cf. *R. leukops*, first left pleural, QML1384LU.**

#### **Indeterminate chelids**

Several chelid fossils, including postcranial and vertebral elements, represent much larger contemporaneous sympatric taxa with *R. sp. cf. R. leukops*. At least two taxa occur alongside *R. sp. cf. R. leukops*. Both taxa are represented by isolated fragments of carapace and plastron, including peripherals. Two forms of peripheral are observed. One type of peripheral is thickly set and bears distinctly rugose shell ornamentation (non-trionychid); is steeply tapering in the proximo-distal plane, which would constitute a domed shell. The other type of peripheral is similarly thick in cross-section, however, tapers less steeply in the proximo-distal plane, which would constitute a less domed shell; this taxon does not possess rugose ornamentation at all. These features are shared within most genera of chelids and the rugose ornamentation

may be a function of size in particular groups, therefore, specific diagnosis will remain until more complete material is available.

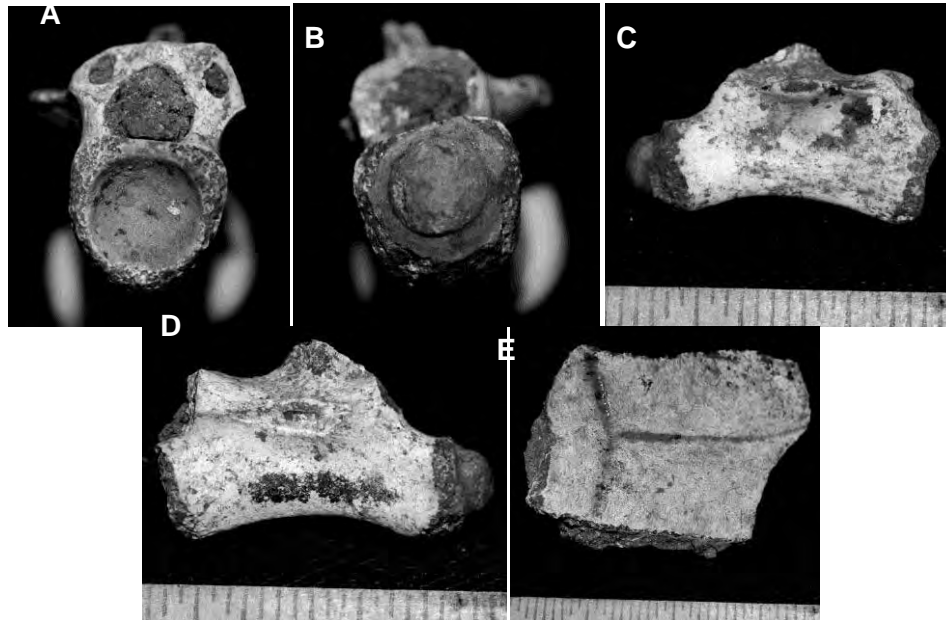


Figure 4-16. indeterminate chelid remains; A-D. dorsal vertebra in anterior (A), posterior (B), left lateral (C) and right lateral (D) views, QML1384LU. E. carapace fragment, QML1311H.

Order NEOSUCHIA Benton & Clark, 1988

Family CROCODYLIDAE Cuvier, 1807

### ***Quinkana* sp.**

Additional crocodylid specimens have been recovered from the Middle Pleistocene fossil deposits of Mt Etna since first recorded by Hocknull (2005). These new specimens include better preserved specimens of osteoderms, teeth and vertebrae. Based on the ziphodont dentition and the overall size and matching morphology, these new specimens most closely resemble *Quinkana*. This is not surprising because *Quinkana* has been found in cave deposits to the north and south of Mt Etna, in Chillagoe and Texas respectively (Molnar, 1981; Willis, 1995). The Texas specimen is considered to be Middle Pleistocene (Price et al 2009), and although the specimen of *Quinkana* from Chillagoe is yet to be firmly dated, it is most likely older than middle Pleistocene. Crocodilian remains from Mt Etna are currently restricted to the

Middle Pleistocene and older deposits with most remains being found in QML1311 H, C/D and QML1384 LU. Each of these sites are 330ka or older.

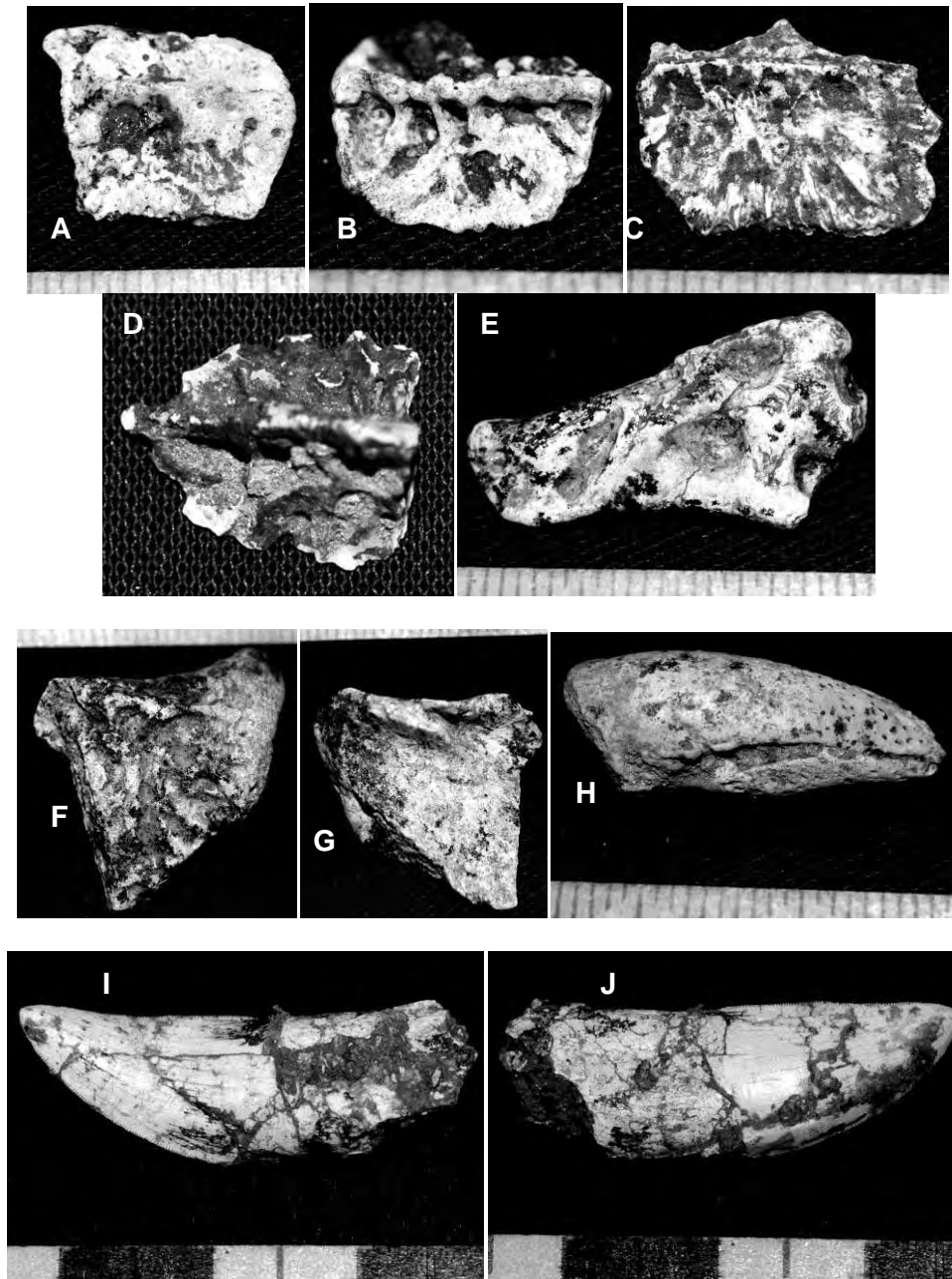


Figure 4-17. *Quinkana* sp. A-E. Isolate osteoderms from QML1384LU (A-C), QML1311CD (D), QML1311H (E). F-G. Postorbital bone in dorsal (F) and ventral (G) views. H. ungual, I-J. isolated tooth in mesial (I) and lateral view (J), QML1311H.

Order SQUAMATA Oppel, 1811

Family AGAMIDAE Hardwicke & Gray, 1827

### Middle Pleistocene

Agamid fossils are relatively rare in the Middle Pleistocene localities at Mt Etna, being represented by isolated fragments of maxillae and dentaries. The only exception to this is the youngest identified Middle Pleistocene site, QML1312 (see Hocknull 2005, Hocknull et al 2007). Most specimens from the older Middle Pleistocene deposits are unidentifiable pieces of acrodont dentition, however, two specimens can be referred to the genus *Hypsilurus*, a nearly complete dentary (Hocknull 2005) and an anterior portion of a maxilla preserving pleurodont dentition. Two pleurodont teeth are preserved,  $P^1$  is half the size of  $P^2$ , with  $P^2$  being caniniform and recurved. These features, combined with the absence of a nares ridge and a relatively angulate dorsal maxillary process allies this specimen to a member of the *Hypsilurus*/*Arua* group presently confined to New Guinea. The dentary may belong to this group also, however, its reduced pleurodont dentition suggests closer similarities to the Australian members of *Hypsilurus*, *H. boydii* and *H. spinipes*. Therefore, the agamid fauna in the middle Pleistocene bears striking resemblance to the typical rainforest agamids found in Australia and New Guinea. Hocknull (2005) reports on the agamids from younger middle Pleistocene sites, all of which are xeric-adapted taxa.

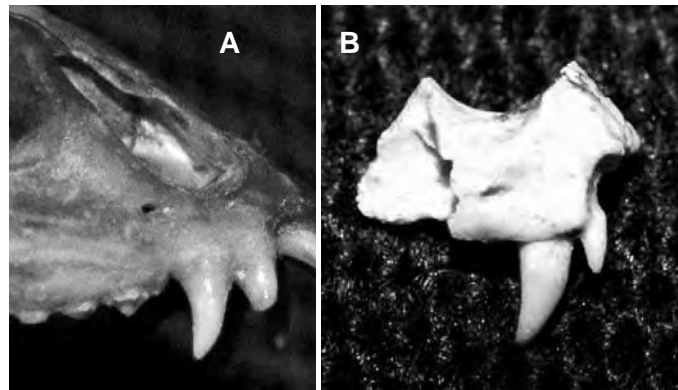


Figure 4-18. A. *Arua modestus* (modern Aru Island) anterior right maxilla. B. *Hypsilurus/Arua* sp. anterior right maxillary fragment, QML1313.

### Late Pleistocene

Late Pleistocene deposits at Mt Etna contain more abundant agamid remains, especially those deposits derived from Owl roost accumulations. Abundant remains of agamids have been recovered from several late Pleistocene – Holocene deposits, including QML1456 (Colloiseum Chamber). Most of these maxillae are small-sized

and represent at least two taxa. Several specimens bear a single large caniniform pleurodont tooth associated with an angulate dorsal maxillary process and an absent nares ridge. These features ally these specimens most closely with *Diporiphora*. Other small maxillae bear two maxillary pleurodont teeth, with P<sup>1</sup> being half the size of P<sup>2</sup>, P<sup>2</sup> caniniform. A short nares ridge is usually present at the base of a relatively vertical dorsal maxillary process. These combined features ally these specimens most closely with *Tympanocryptis*.

### Family Scincidae Oppel, 1811

#### Middle Pleistocene

Skinks are relatively common faunal elements within each of the Quaternary deposits throughout the Mt Etna region. Hocknull (2005) reported on several taxa represented in the faunas, including a distinctive, new species of *Tiliqua* (Fig. 4-19 and 4-20). Few additional remains of this new taxon have been recovered from Middle Pleistocene deposits, however, an osteoderm recovered from QML1384LU may represent this species. In overall morphology, the osteoderm resembles *Tiliqua rugosa*, however, it does not possess as distinctively punctuate dorsal surface.

#### ***Tiliqua* sp. nov.**

Members of the *Tiliqua* lineage can be divided into four distinct morphologies based on tooth crown shape and the relative sizes of posterior-most teeth.

1. *Tiliqua nigrolutea* & *Tiliqua adelaidensis*.
2. *Tiliqua rugosa*, *Tiliqua occipitalis* & *Tiliqua multifasciata*
3. *Tiliqua scincoides*, *Tiliqua gigas* & *Tiliqua* sp. nov.
4. *Cyclodomorphus gerrardii* & *Cyclodomorphus maximus*

#### Morphology 1.

Homodont dentition along entire tooth row; occlusal profile elongate-ovoid where elongation is directed antero-posteriorly; tooth crowns bear small cuspule with cristid; posterior-most teeth with crown tips oriented lingually, producing a lingually curved tooth in mesial profile; very fine striae.



### Morphology 2.

Homodont dentition along entire tooth row, size increasing slightly toward posterior margin; occlusal profile of tooth crowns, ovoid; tooth crowns bear cuspule with cristid; tooth crown with distinct cristae.

### Morphology 3.

Homodont dentition along anterior portion of tooth row, posterior teeth much larger and durophagous; posterior-most teeth very small in comparison to largest durophagous tooth; occlusal profile of tooth crowns, elongate-ovoid and inflated; elongation labio-lingually, inflation begins at base of tooth; distinct cristae.

### Morphology 4.

Homodont dentition along anterior portion of tooth row, posterior teeth much larger and durophagous, with massive singular ovoid durophagous tooth; tooth crowns ovoid, bearing small central cuspule within shallow basin; dental sulcus convex along midlength; dentary symphysis distinct.

*Tiliqua* sp. nov. possesses tooth crown features most similar to Morphology 3. *Tiliqua* sp. nov. differs from the only other species bearing this morphology, *Tiliqua scincoides* and *Tiliqua gigas*, by being; more robust, with a deeper dental sulcus along the entire length; broader dentary along entire length; less anterior curvature to the dentary; longer postero-ventral expansion of the dentary symphysis; straighter superior margin of the dental sulcus (similar to *Cyclodomorphus* spp.). The absence of a massive durophagous tooth in the posterior quadrant of the dentary precludes *Tiliqua* sp. nov. from being a member of *Cyclodomorphus*.

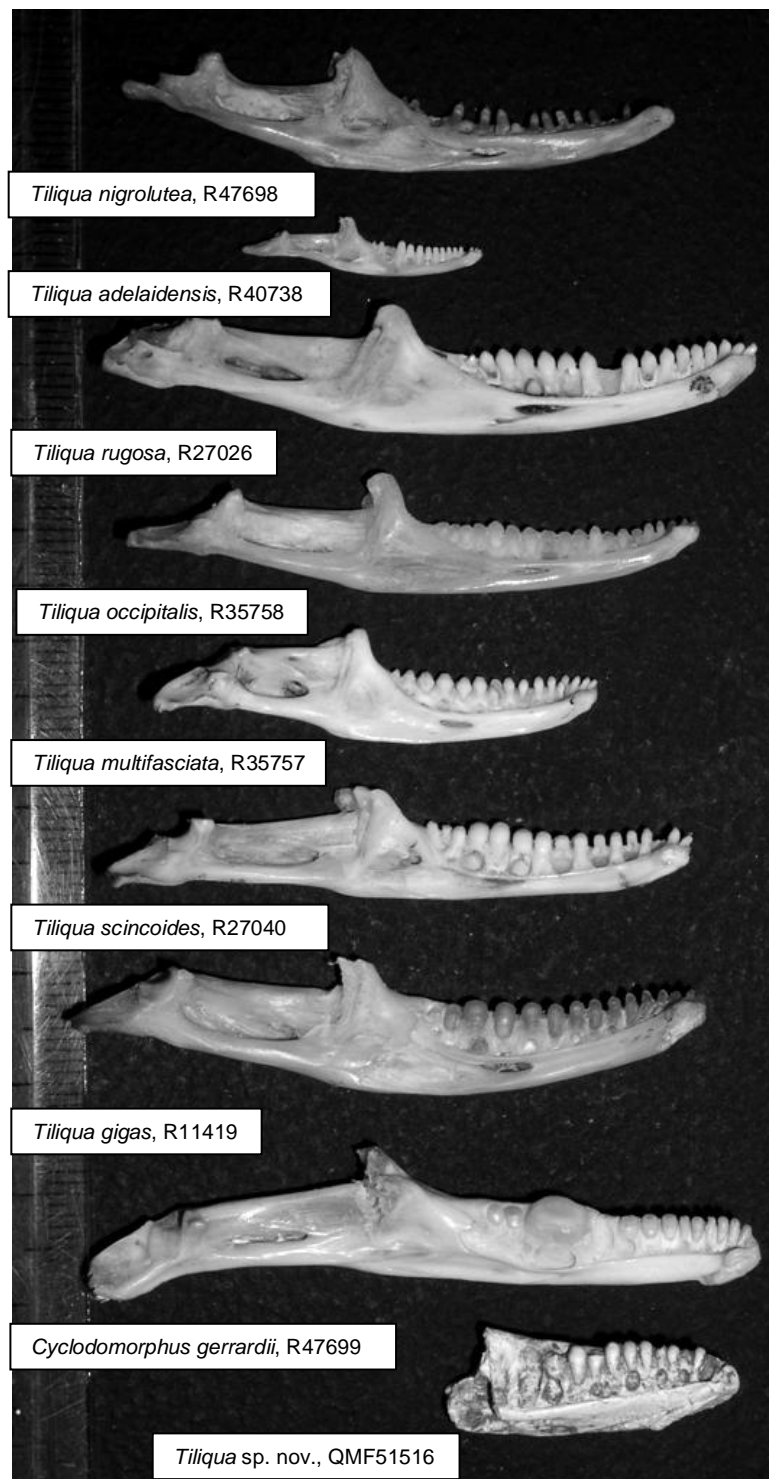


**Figure 4-19.** *Tiliqua* sp. nov.. (QMF 51516) Fossil dentary compared with dentaries of extant species of *Tiliqua* and *Cyclodomorphus* (lingual view).



**Figure 4-20.** *Tiliqua* sp. nov.. Fossil dentary compared with dentaries of extant species of *Tiliqua* and *Cyclodomorphus* (dorsal (occlusal) view). Species comparisons as above.

### ***Cyclodomorphus gerrardii***

The most abundant skink from the middle Pleistocene fossil deposits, *Cyclodomorphus gerrardii*, has been recovered at most life-history body-sizes, from juveniles to large adults. See Hocknull (2005), Chapter 2.

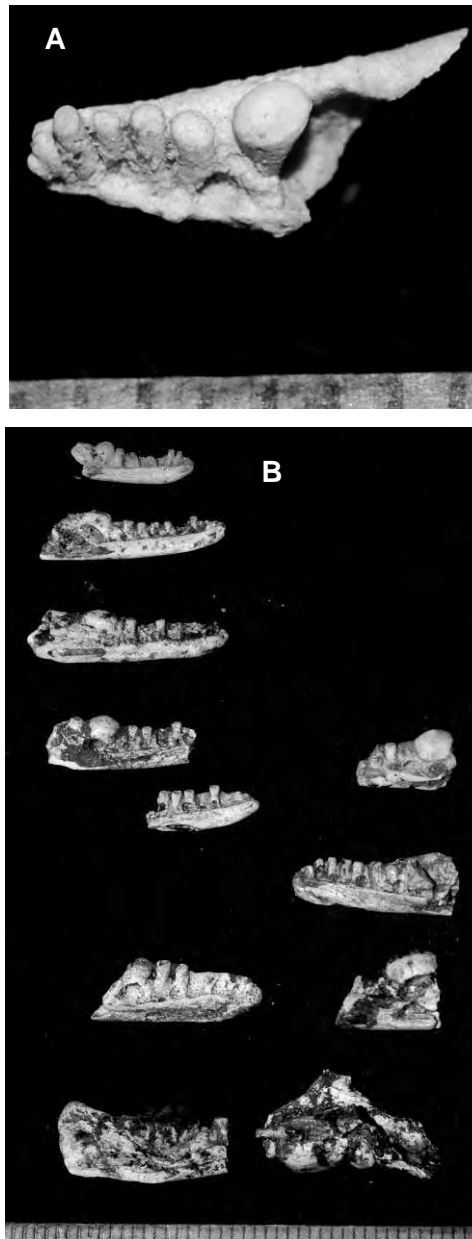
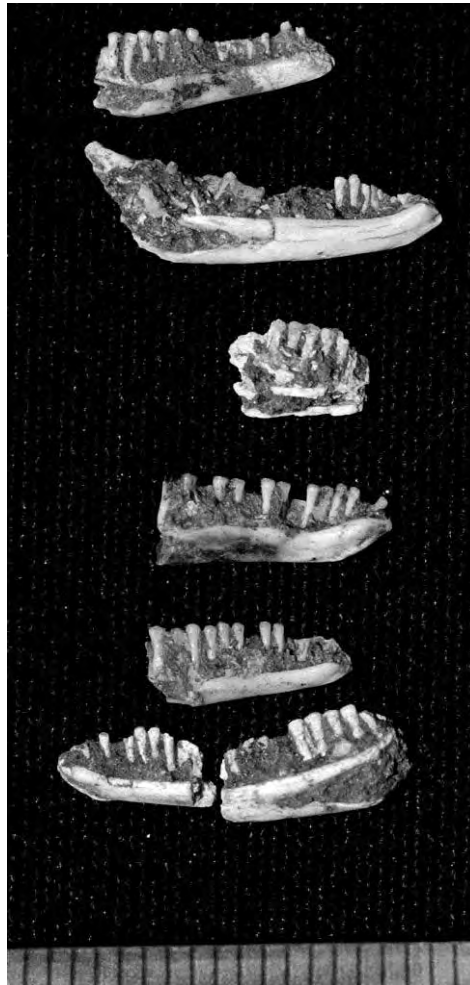


Figure 4-21. *Cyclodomorphus gerrardii*. A. Left maxilla (QML1313), B. Ontogenetic series from QML 1311 H.

### ***Egernia major***

Hocknull (2005) reported of the presence of *Egernia* spp at Mt Etna. Comparison of these specimens to extant species of *Egernia* has shown that the largest specimens of *Egernia* are very similar in overall morphology to the large skink, *Egernia major*. *Egernia major* dentaries and maxillae are distinguished from almost all other members of *Egernia* by the presence of a robust chisel-like dentition and dental

sulcus. *E. major* possesses a deep posterior to the denary and closely-spaced homodont teeth.



**Figure 4-22. *Egernia major*. Isolated dentaries from QML 1311 H.**

### **Sphenomorphus Group skinks**

Hocknull (2005) identified two forms of small skink referable to the Sphenomorphus group (sensu Hutchinson, 1992). Fig. 4-23 presents the overall variation seen in these skink taxa indicating that they may represent more than two taxa.

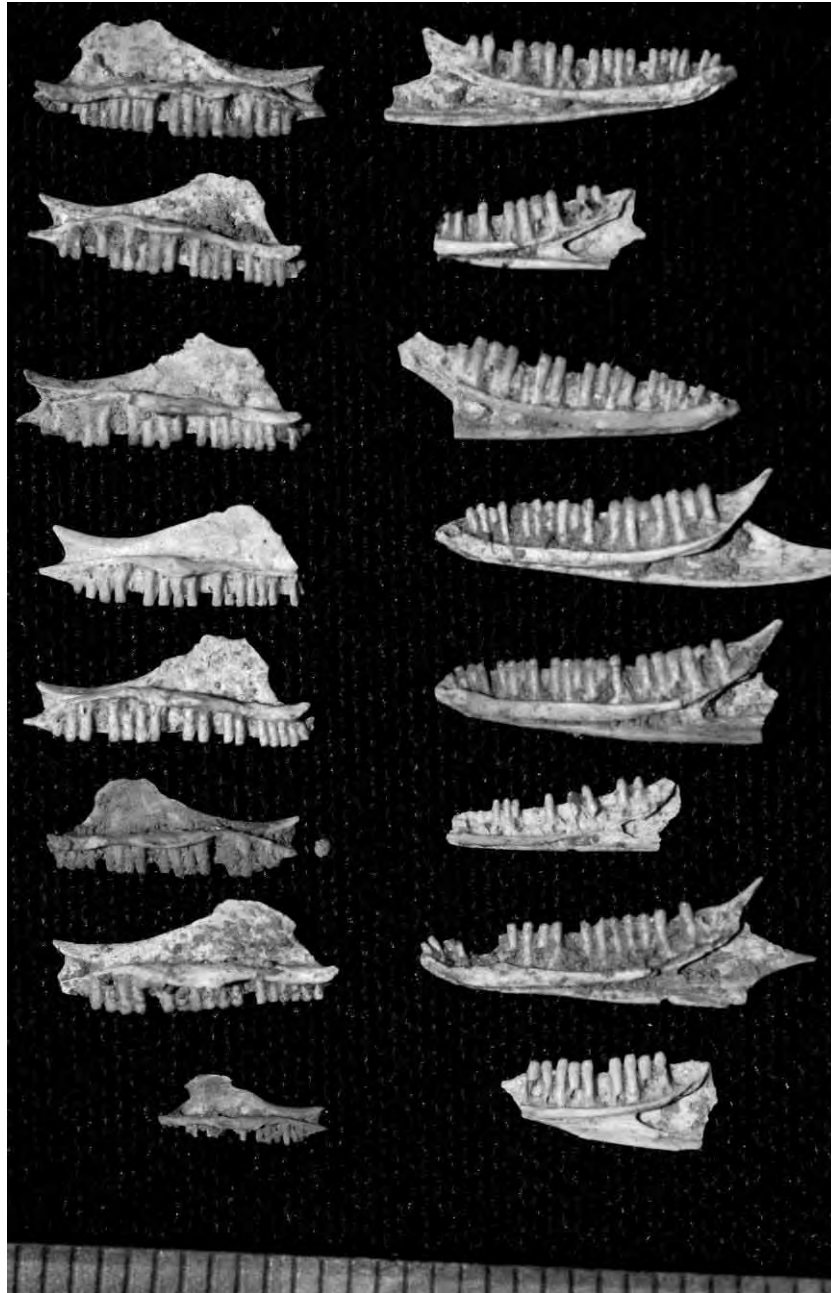


Figure 4-23. *Sphenomorphus* group skinks. Isolated maxillae (left column) and dentaries (right column) from QML1312.

### Late Pleistocene

Late Pleistocene to Holocene deposits possess a diverse extant skink fauna. *Tiliqua scincoides* has been recovered and is distinguished from most other species of *Tiliqua* on the basis of its posterior durophagous dentition in both the maxillae and dentaries. Direct comparison of the fossil specimens with *Tiliqua* species allies the fossils most closely in both size and morphology to *T. scincoides*, which is not surprising as this species is extant in the region today. The most common large skink in both middle

and late Pleistocene deposits is *Cyclodomorphus gerrardii*. Easily identified by the massive posterior durophagous tooth in both maxillae and dentaries. *C. gerrardii* also possesses a distinctively straight to convex dental sulcus, which is concave in *Tiliqua*.

#### Family Gekkonidae Oppel, 1811

Gekkonid fossils are numerous in sites older than 280ka, however, they are not well enough preserved to determine any taxonomic affiliations. Most specimens are small fragmentary maxillae and dentaries, however, some jaw elements indicate the presence of very large gekkonids, similar in size to the large *Phyllurus* and *Saltuarius* gekkonids found in eastern Australian rainforests.

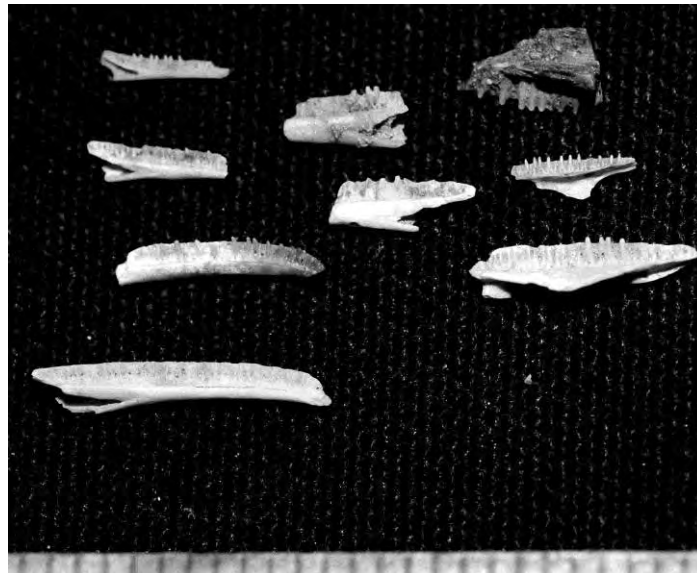


**Figure 4-24. gekkonid fossils. Isolated maxillae and dentary fragments from QML1313.**

#### Family Varanidae Hardwicke & Gray, 1827

##### **Varanus spp.**

Varanid fossils occur throughout all Middle and Late Pleistocene – Holocene deposits, usually represented by isolated vertebrae. In the older Middle Pleistocene localities at Mt Etna preserve several size-classes of vertebrae, ranging from small-sized specimens up to those within the range of *V. komodoensis* (Hocknull, Chapter

5). Based on other postcranial remains, it is suggested that three species of *Varanus* occurred during the Middle Pleistocene of Mt Etna. A small to medium-sized form, similar in size to *Varanus varius*, a large-sized form close to *V. giganteus* and a very large form referred to in Chapter 5 as *V. sp. cf. V. komodoensis*. These larger forms are also represented by isolated vermiform osteoderms. Massive vertebrae of *V. priscus* are yet to be found at Mt Etna, however, a single distal caudal was reported to the south at Marmor Quarry (Hocknull, 2005).

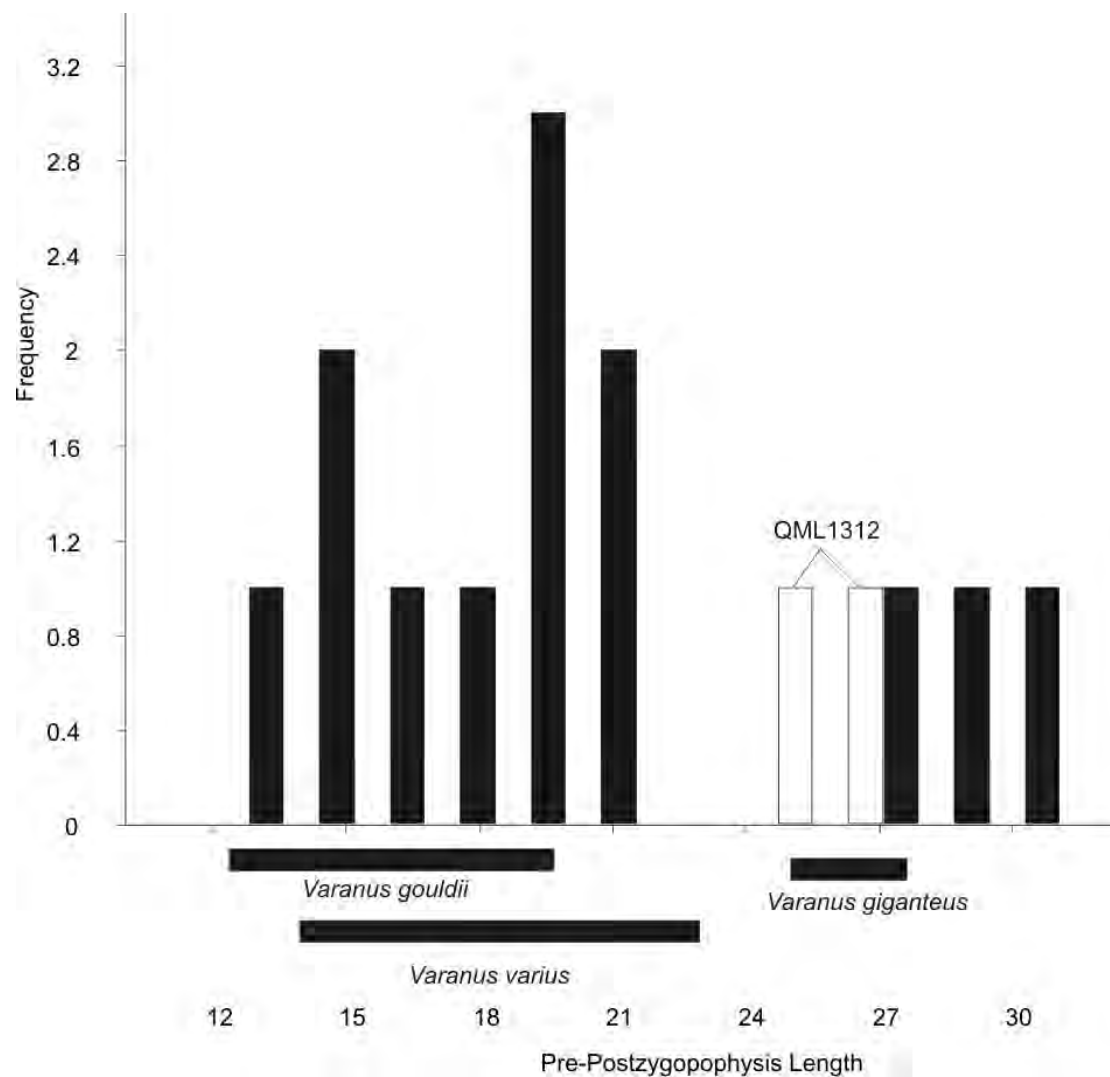


**Figure 4-25. Histogram of fossil varanid dorsal vertebral measurements (Pre-Postzygopophys Length), compared with variation seen in three different-sized varanids (*V. gouldii*, *V. varius* and *V. giganteus*)**



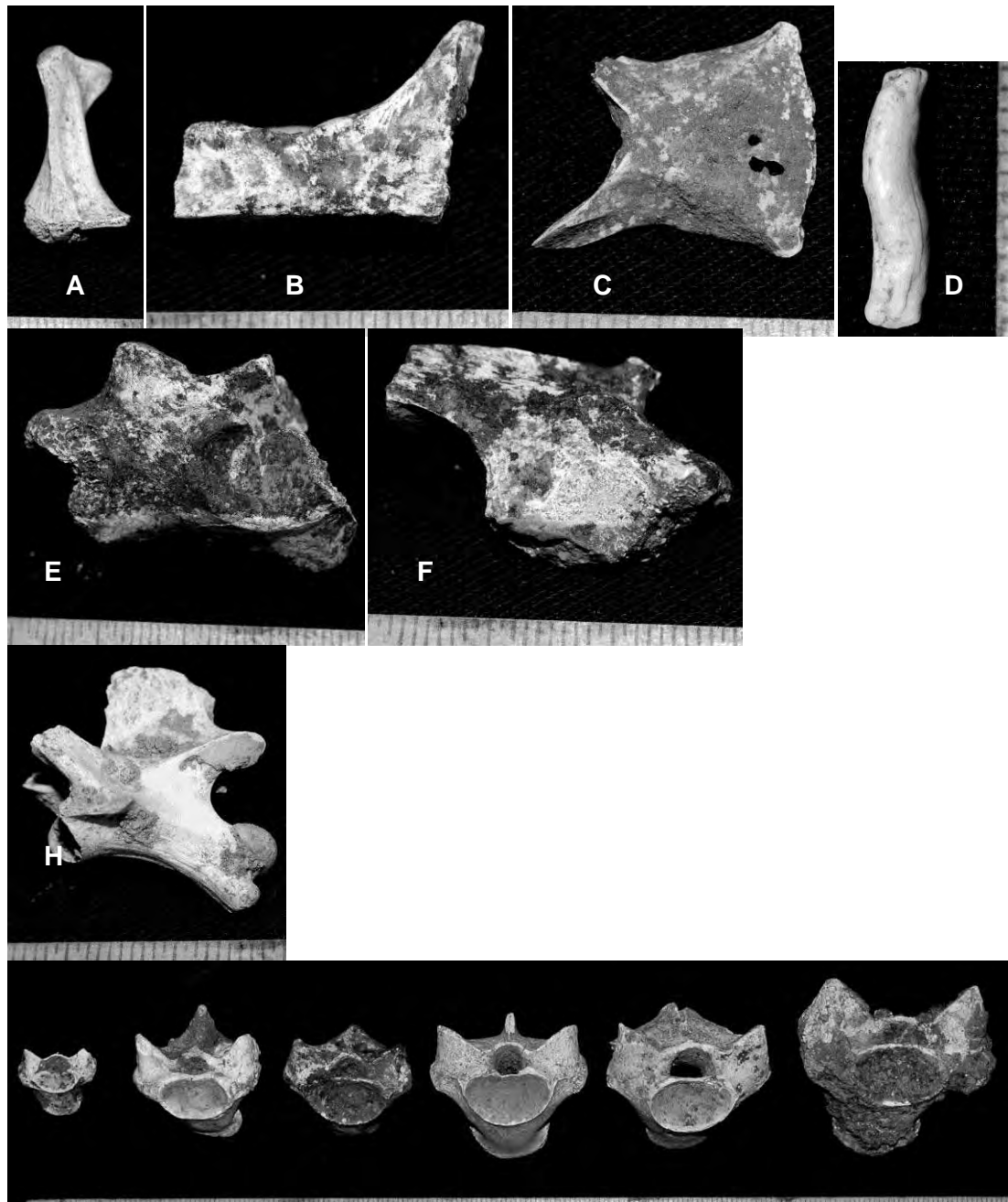


Figure 4-26. Varanid fossils. A. Quadrate (QML1312), B. Frontal (QML1311H), C. Parietal (QML1312), D. Osteoderm (QML1311J), E. Sacral vertebra (QML1311H), F. Ilium (QML1311H), G. Cervical (QML1312), H. Dorsal vertebrae (left to right): QML1311 H, QML1311 C/D, QML1384LU, QML1312, QML1312, QML1311 H.

Family ELAPIDAE Boie, 1827

***Pseudechis* sp.**

An isolated right maxilla is referable to a species of *Pseudechis*. Following the morphological characteristics of the maxilla provided by Scanlon et al., (2003) I was able to score the maxilla and determine the generic level assignment of the elapid

maxilla. The maxilla bears a single large pleurodont tooth with venom groove, plus four smaller posterior accessory teeth also possessing grooves. This feature, along with the presence of a hypopophysis on trunk vertebrae diagnose elapid snakes. Scanlon (2003) describes 13 characteristics of the elapid maxilla which can be used in identification. I have scored the fossil maxilla for these 13 characters; 1. (0); 2. (1); 3. (1); 4. (1); 5. (0); 6. (0); 7. (0); 8. (2); 9. (1); 10. (0); 11. (0); 12. (1); 13. (0). This series of character states are unique to *Echiopsis* and *Pseudechis* species. On comparison, the specimen most closely resembled species of *Pseudechis*. *Echiopsis* is much smaller than the fossil specimen (see Fig. 35.7 in Shea et al (1993)) and differs morphologically by possessing a more pointed anterior process, more mesially angled ectopterygoid process, larger posterior teeth and a shallow anterior fang recess. On comparison with published illustrations and available imagery (Scanlon pers. obs.) the maxilla conforms closely with *P. guttatus* (see Fig. 35.6 in Shea et al (1993)) although the fossil is larger, has more posterior teeth (4 vs 3) and possesses a distinct foramen positioned antero-dorsally of the first posterior tooth. On comparison with *P. porphyriacus* (see Greer (1997)), the fossil is larger in size, possessing fewer posterior teeth and is missing the antero-dorsal foramen. Maximum body lengths for *Pseudechis* range from 1.5-2.0m, with *P. australis* being the largest taxon. Measurements taken from a large sample of fossil elapid vertebrae indicate the presence of a very large elapid in the Middle Pleistocene of Mt Etna. Using a regression of total body length versus pre-postzygopophysis length I returned a positive correlation with a high  $R^2$  value (0.97). The equation of this linear regression allowed me to estimate the maximum total body lengths for vertebrae measured from the Middle Pleistocene deposits (Fig. 4-27). Fig. 4-28 shows that several specimens reached maximum body length estimates of 2100mm (2.1m). It is for this reason that it is considered here that the fossil taxon is most likely a large species of *Pseudechis*. Extant *Pseudechis australis* commonly reach 2m total body length, however, it is not unreasonable to consider the possibility that other extant species of *Pseudechis* reached this size in the past, or that there were other large taxa now extinct.

The majority of vertebral remains indicate a spread of body lengths, ranging from 60cm – 2.1m. This distribution looks to be trimodal, with three distinct body classes; small to medium-sized (<100cm), large (100-180cm), very large (~200cm) (Fig. 4-28). The majority of extant elapid species fall below 100cm in length and this is

reflected in the highest frequency of estimated body-lengths being elapids under 100cm predicted body-length. Interestingly, very-large body-lengths of around 2m are not uncommon and are as frequent as most of the smaller size classes.

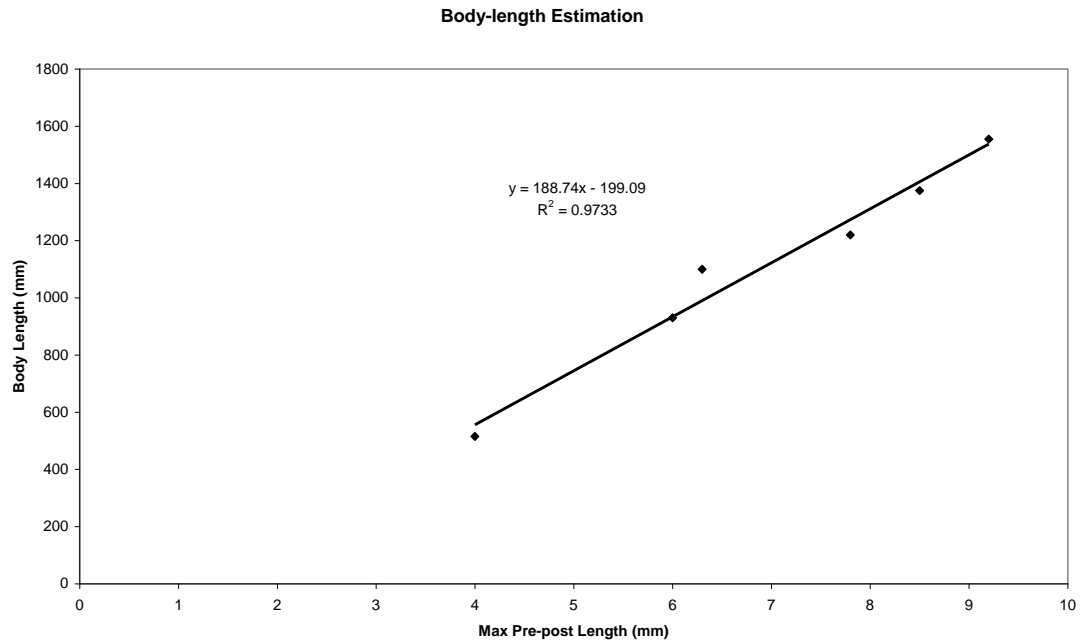


**Figure 4-27. Bivariate plot of total Body Length to maximum pre-postzygopophysis length (dorsal vertebrae) for Australian elapids. Used to estimate the total body length of fossil elapid vertebrae.**

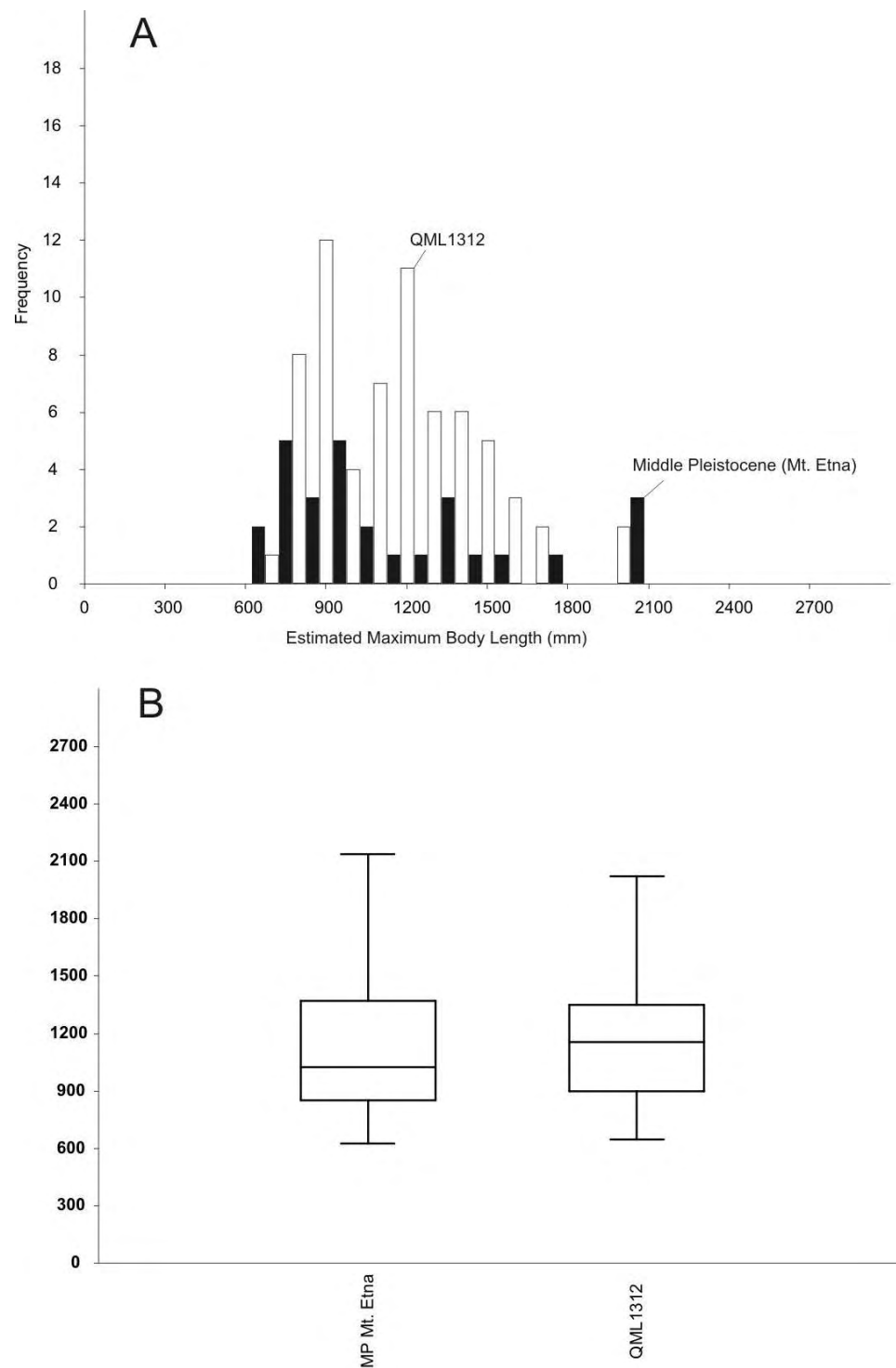


**Figure 4-28. A** Histogram of estimate body lengths for fossil elapid dorsal vertebrae from middle Pleistocene sites at Mt Etna. **B.** Comparison between the size range of elapids from older middle Pleistocene rainforest sites to arid fauna of QML1312.

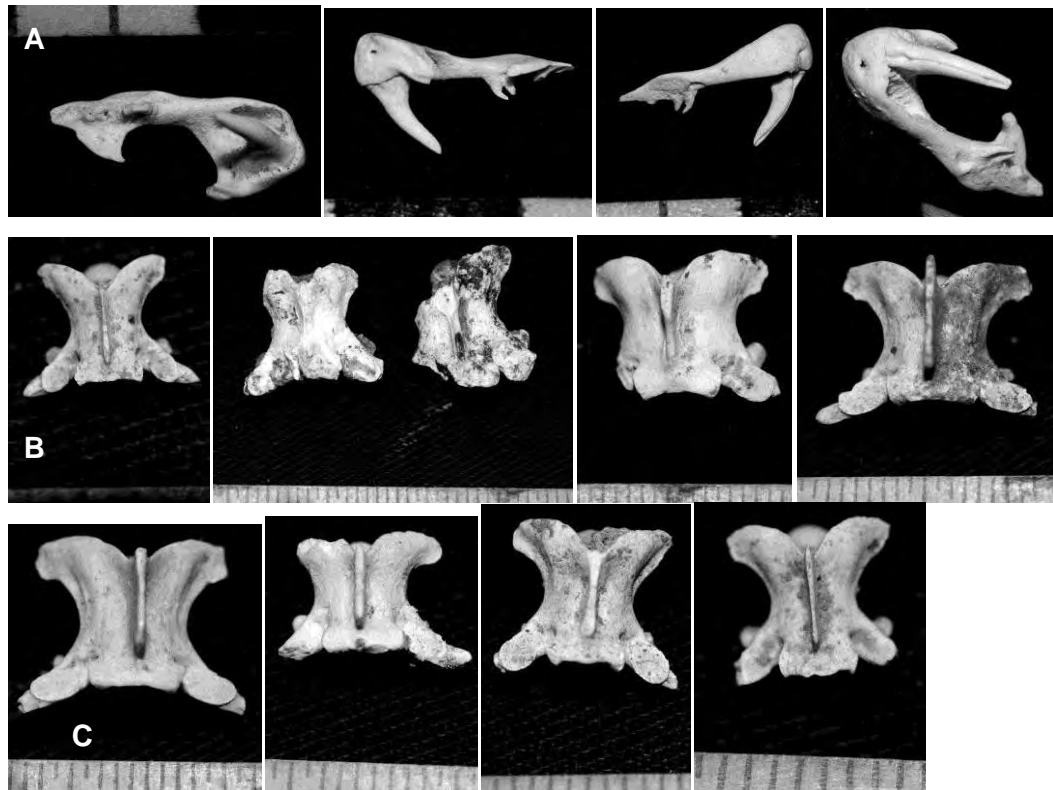


**Figure 4-29.**Elapid fossils. A. Maxilla from QML1313 in ventral, mesial, lateral and anterior views. B. Elapid dorsal vertebrae in dorsal view from (left to right) QML1312, QML1311 H, QML1384LU, QML1311 J, QML1312. C. Elapid dorsal vertebrae in dorsal view from (left to right) QML1312, QML1313, QML1312, QML1312.

#### Subfamily PYTHONINAE Fitzinger, 1826

Python remains are common in middle and late Pleistocene deposits. A large sample of vertebrae was measured from middle Pleistocene localities to determine the size range in pythons from Mt Etna. Figure 4-30 shows the frequency distribution as a histogram of measured python vertebrae. It is immediately obvious that the size range of vertebrae from the sites varies considerably (<4mm up to 15mm in pre-postzygopophysis length). The distribution of frequencies does not follow a typical normal distribution, which indicates that there are several modes within the single sample. The spread of data recovers three or four modes, which interestingly correspond to the distribution of vertebral sizes for a variety of different-sized python taxa, ranging from relatively small species, such as *Morelia viridis* (Total Length 1-2m) to the largest extant Australian python, *Morelia amethystina* (Total Length up to 5m, perhaps as much as 8.5m). The distribution of vertebral sizes suggests that there

were at least three or four python body-sizes accumulating in the deposits, which may reflect three or four species of python. This would not be surprising as each of these size-classes would fill a different body-size guild as is present in modern ecologies today. Structurally and faunally, the sites and ecology would have also provided ample location and prey diversity for such guild partitioning, allowing for guilds in arboreal, cave-dwelling or ground-dwelling constrictors. The presence of a giant python, the size of *Morelia amethystina*, is not surprising as this taxon is found in a number of different tropical environments of the present day, including rainforest.

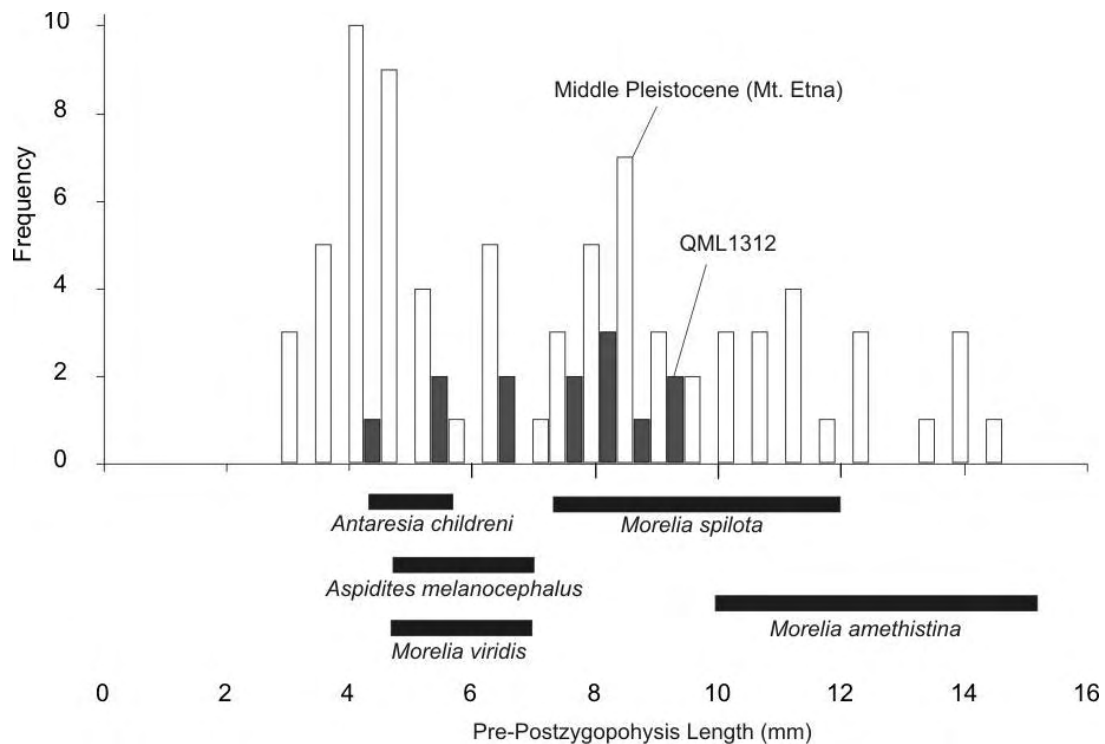


**Figure 4-30. Histogram of pythonine fossil vertebral lengths (Pre-postzygopophysis Length) compared with the variation in lengths seen in a variety of python species.**

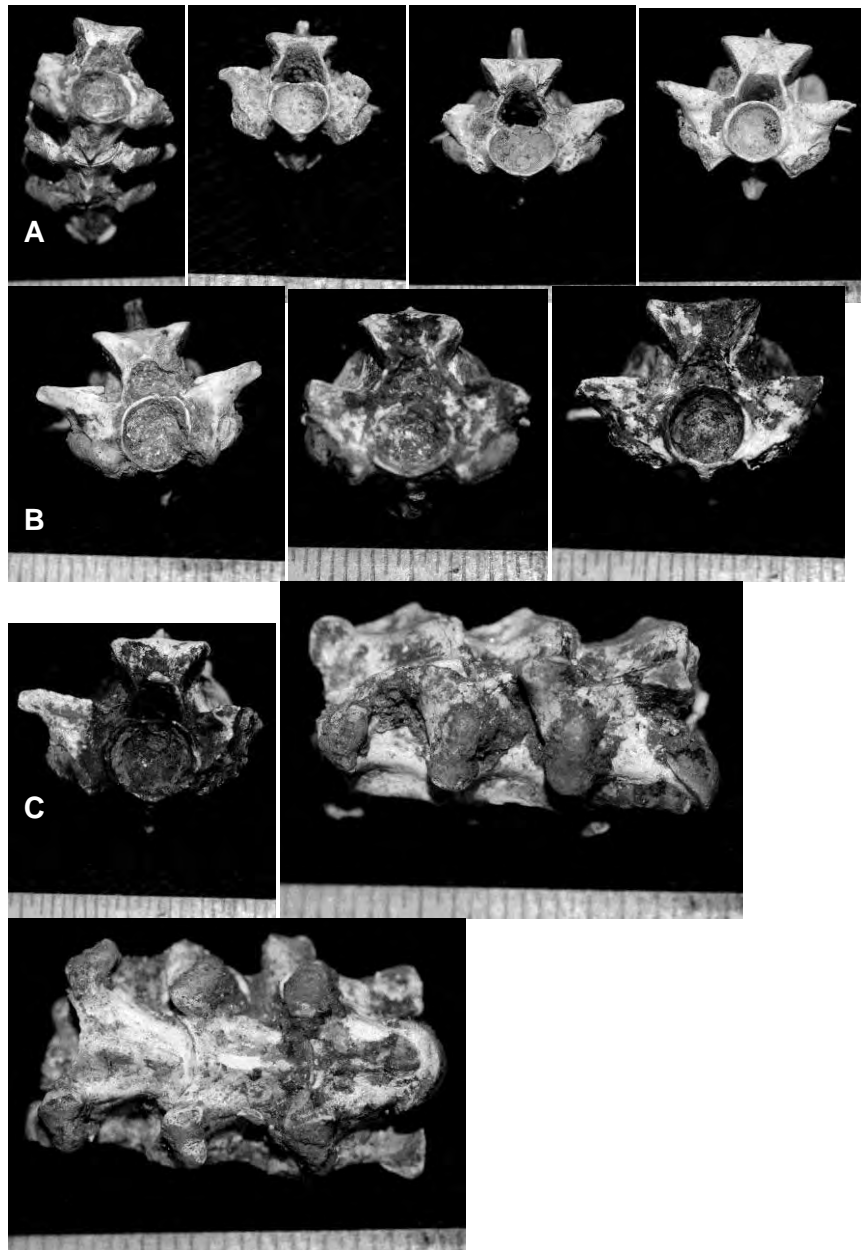


**Figure 4-31. Pythonine fossils. A** Dorsal vertebrae in anterior view from (left to right) QML1311H, QML1312, QML1312, QML1312. **B.** QML1311H, QML1384LU, QML1311CD, QML1311H. **C.** Articulated series in lateral and ventral view (QML1311 H).

#### Family TYPHOLOPIDAE Gray, 1825

Typholopids were reported by Hocknull (2005). Better imagery is now available of these taxa which verify the characteristics used by Hocknull to identify them as typholopids.

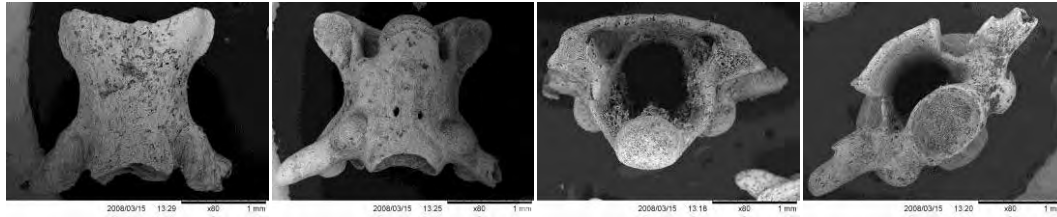


**Figure 4-32. Typhlopoid vertebrae in dorsal, ventral posterior and anterior views (QML1284).**

### Family MADTSOIIDAE

Madtsioids were not recorded by Hocknull (2005), however, subsequent collections made from Mt Etna have turned up isolated remains of these gigantic snakes.

Madtsioids are exceptionally rare within the deposits, being represented by few remains, mostly complete or fragments of vertebrae, partial ribs and a single quadrate. These remains have been identified as madtsoiid by use of the extensive diagnostic features detailed by Scanlon (1996) and Scanlon & Lee (2000).

#### **Yulunggur sp.**

The madtsoiid remains have been preliminarily identified to the genus *Yulunggur* on the basis of diagnostic features detailed in Scanlon (1992), Scanlon & Lee (2000) and Mackness & Scanlon (1992). The vertebrae most closely resembles specimens of *Y. camfieldensis*, *Yulunggur* sp. (Mackness & Scanlon, 1992) and ‘*Wonambi* sp. cf. *W. naracoortensis*’ (McNamara, 1990) = *Yulunggur* (Scanlon, 1995). In particular, the neural spine extends as a low, dorsally concave crest beginning just posterior of the zygosphenes and sloping postero-dorsally to the tip of the neural spine. The neural spine continues as a high and narrow point. This differs from *Wonambi* and *Nanowana*, which have neural spines that extend antero-posteriorly along almost the entire length of the neural arch, rising steeply behind the zygosphenes. The kidney-shaped diapophyses are typical of *Yulunggur* and differ from *Wonambi*, which have dorsal concavities.

Specimen	Locality	Pre-Post	Pre-Pre	Centrum L	Zygo L/W
<i>Yulunggur</i> sp.	QML1384LU			13.13	
<i>Yulunggur</i> sp.	QML1384LU	21.48	31.23	15.69	
<i>Yulunggur</i> sp.	QML1311J				8.09/13.10
<i>Yulunggur</i> sp.	QML1311H				7.87/10.81



<i>Yulungur</i> sp.	Chinchilla Sands	19.5	32.9	14.0	
<i>Yulungur camfieldensis</i>	Northern Territory	22	35	17	7/10

**Table 4-1. Fossil madtsoiid vertebral measurements compared with published fossil specimens.**

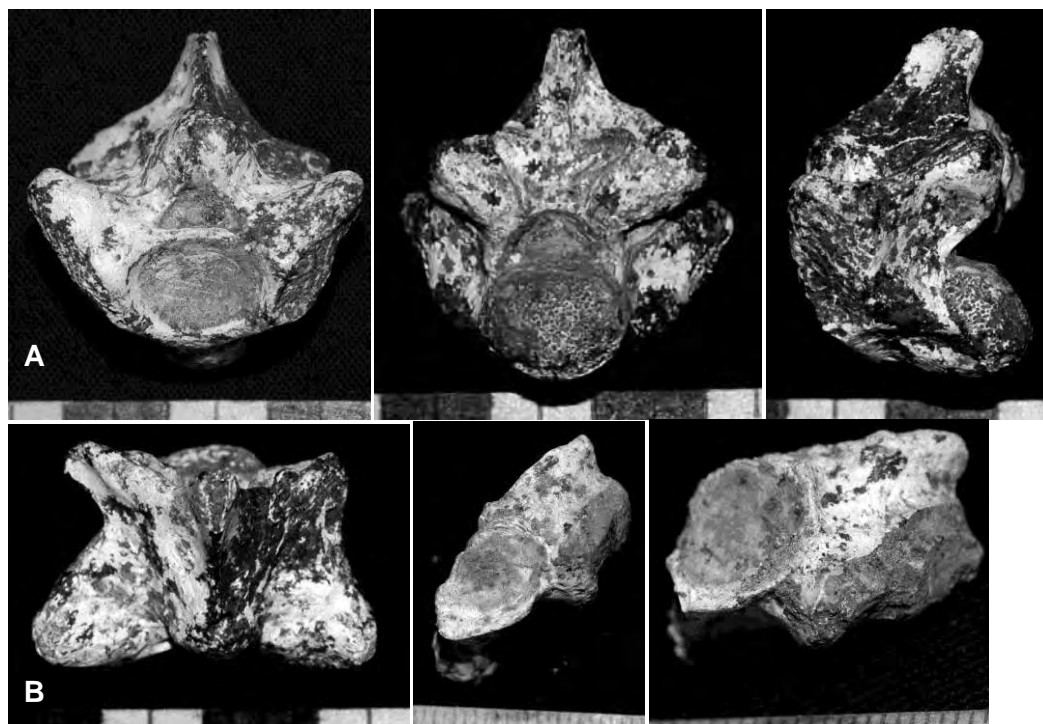


**Figure 4-33. Madtsoiid vertebrae in, A. anterior, posterior and lateral views (QML1384LU). B. Dorsal (QML1384LU) and anterior views (QML1311H, QML1311J) .**

The most up-to-date faunal list of reptile taxa across the middle-late Pleistocene is presented in Chapter 7.

## MAMMALIA

### TACHYGLOSSIDAE

Monotremes were not reported by Hocknull (2005). Tachyglossidae is represented by a single manus ungual recovered from QML1311 J. Based on the overall size of the ungual it is expected that it represents a species of *Tachyglossus* or *Zaglossus*.

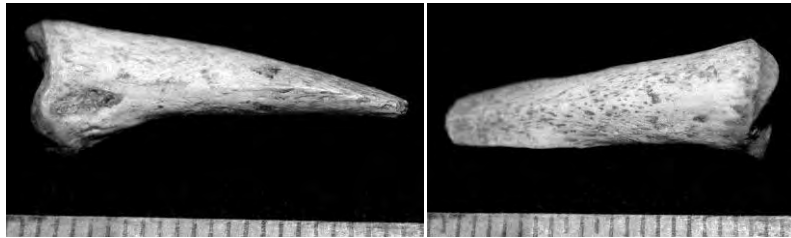


**Figure 4-34. Fossil tachyglossid ungual (QML1311J).**

#### PERAMELOMORPHIA

The oldest described ‘bandicoots’ are the yaraloids from the Oligo-Miocene of Riversleigh and Bullock Creek Faunas. *Yarala* is considered to be a plesiomorphic bandicoot with uncertain relationships to the three extant perameloid families; Peramelidae, Peroryctidae and Thylacomyidae. The first peramelids and thylacomyids appear in the early Pliocene and occur in several Pliocene sites throughout eastern Australia (QLD, NSW, VIC and SA).

Thylacomyids first appear in the early-middle Pliocene Palankarinna Local Fauna, South Australia, represented by *Ischnodon australis* (Stirton, 1955), however, the extant thylacomyid, *Macrotis*, is only known from the Quaternary, being found in Pleistocene and Holocene deposits throughout central Australia and eastern Queensland (Hocknull, 2005a & Hocknull 2005b).

Peramelids are better represented in Neogene sites, with three species of extinct *Perameles* currently described and named. The New South Wales Bow and Big Sink Local Faunas record a species of plesiomorphic *Perameles*, *Perameles bowensis*, which also has been recorded from the Pliocene Chinchilla Sands Local Fauna, in southern Queensland. A derived species of *Perameles*, *P. allinghamensis* (Archer &

Wade, 1976) is recorded alongside a highly apomorphic perameloid-like marsupial, *Numbigilga ernielundelius* (Beck et al., 2008), from the early Pliocene Bluff Downs Local Fauna of northern Queensland. An extinct Pleistocene species of *Perameles*, *Perameles sobbei*, was recorded by Price (2002) from the eastern Darling Downs. *Isoodon* is only known from the Quaternary with no extinct species currently described. *Chaeropus ecaudatus* only has a Quaternary record, found throughout central and southern Australia, and as far east as Mt Etna, central eastern Queensland (Hocknull, 2005) and Chillagoe, north-eastern Queensland (Muirhead & Godthelp, 1995).

Originally Hocknull (2005) considered the perameloid fauna from the Mt Etna region to comprise the Peramelidae, Thylacomyidae and several new perameloid taxa, including plesiomorphic taxa similar to the Oligo-Miocene genus *Yarala*. Since then, revision of the perameloid material and characteristics, and with the description of early Pliocene members of the Peroryctidae from Victoria, it is considered here that these new taxa should be included within the Peroryctidae as the only Pleistocene record of this family on mainland Australia.

#### PERORYCTIDAE

Peroryctids are an enigmatic group of bandicoots usually associated with dense rainforest habitats of Papua New Guinea and the northern tip of Cape York, Queensland (Flannery, 1994). Nine species of peroryctid are currently recognised in Papua New Guinea, with several new taxa remaining undescribed. These species currently represent four recognised genera; *Microperoryctes*, *Peroryctes*, *Echymipera* and *Rhincomeles*, however, the taxonomic status of many new taxa remain equivocal, therefore this number could be much higher. One species of peroryctid, *Echymipera rufescens*, occurs in far north Queensland as the only peroryctid to currently inhabit the Australian mainland. This species is considered to have only recently arrived on mainland Australia through a land connection through Cape York to Papua New Guinea, where the species has a greater distribution.

Three peroryctid taxa are identified from the Mt Etna middle Pleistocene fossil assemblage. The characteristics of these three taxa are provided in Table 4-2, which formed the basis of a phylogenetic reconstruction (Fig. 4-39). Peroryctid 1 and 2 are nested within a very well supported clade (83% bootstrap) containing the early

Pliocene peroryctid (cf. *Peroryctes* Large) from the Hamilton Local Fauna, Victoria. Peroryctid 1 & 2 are similar in overall morphology but differ by being slightly larger in overall size. These taxa are nested within a clade containing *Peroryctes* and *Microperoryctes*, therefore, the resolution of this group will depend on a more detailed analysis of all of the Papua New Guinea peroryctid taxa. What is certain is that the fossil peroryctids are not related to *Echymipera*, the only peroryctid extant in Australia.

Peroryctid 3 has good support (>60% bootstrap) as the sister taxon to all others within a clade to the exclusion of *Echymipera* and *Rhynchomeles*. Therefore, it seems that peroryctids are most likely paraphyletic from this analysis. Discussions of these results require a more detailed morphological analysis, however, it is clear that the Pleistocene species of peroryctid are related to the *Peroryctes*/*Microperoryctes* clade and not to that which includes *Echymipera*/*Rhynchomeles* and the Peramelidae.

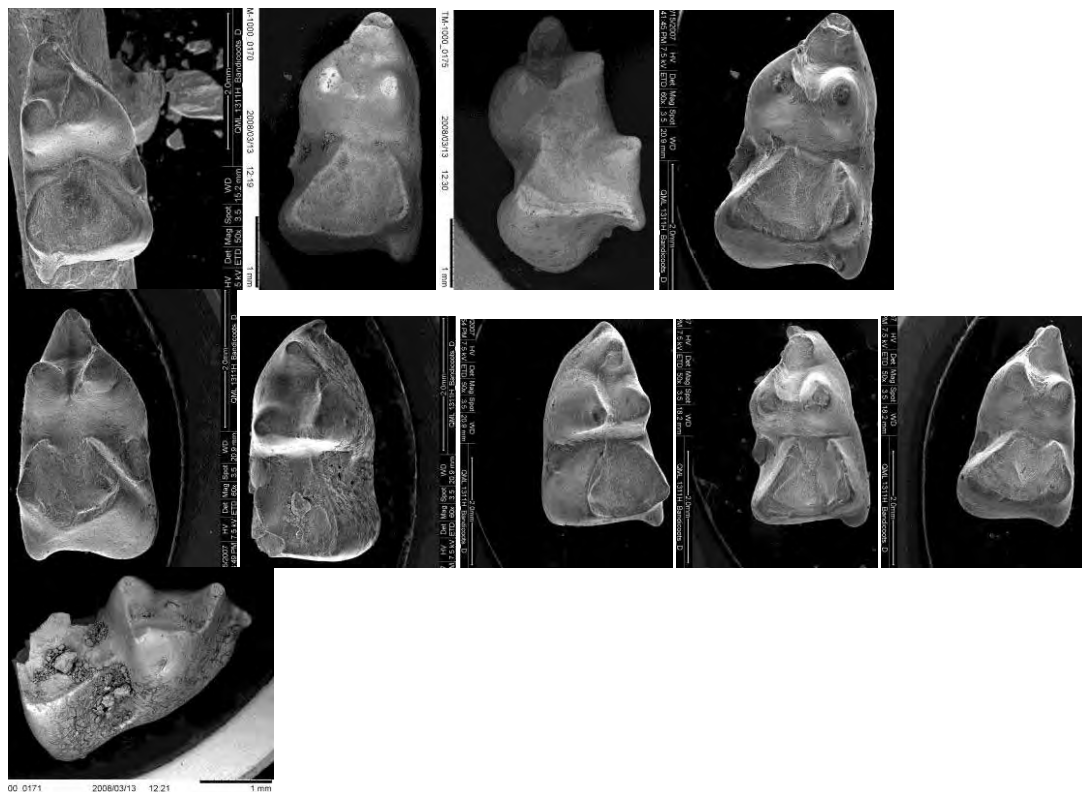


Figure 4-35. Fossil peroryctid M<sub>1</sub>s in occlusal view.

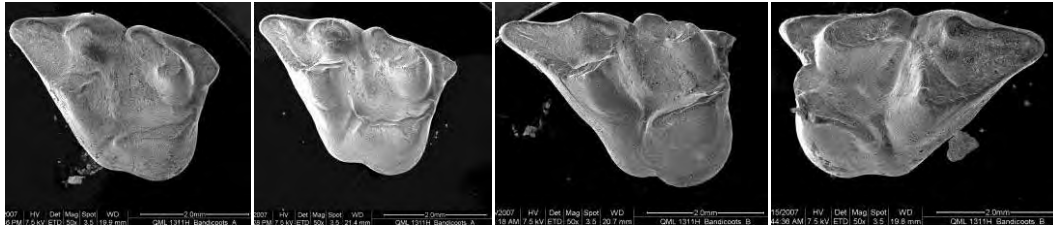
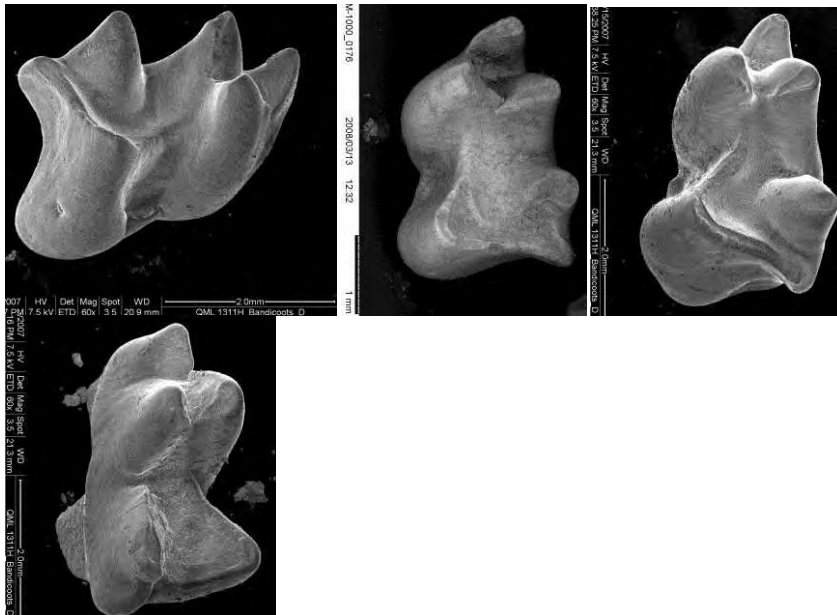
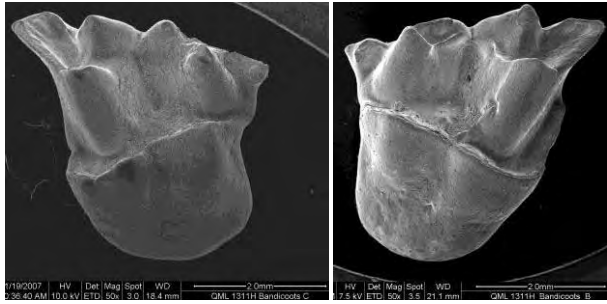


Figure 4-36. Fossil peroryctid M<sup>1</sup>s in occlusal view.

### Family PERAMELIDAE Gray, 1803

Two new species of *Perameles* were identified by Hocknull (2005). This consideration remains here under the current character analysis of peramelid relationships. Characteristics of these species are given in Table 4-2. Phylogenetic reconstruction of these new species of *Perameles* reveals that both taxa are plesiomorphic to the remaining taxa, including *P. bowensis* (Fig. 4-39). There is little resolution within this clade, however, it remains well-supported (73% bootstrap). The two new species have good support as the sister taxa to the remaining *Perameles*. *P. allinghamensis* was not included in this analysis so its position remains equivocal.





**Figure 4-37. Fossil peramelid lower  $M_1$ s in occlusal view and  $M^1$ s in near-occlusal view.**

#### 4.3.1 *Perameloid Characters and Character States*

##### $M_1$

1. Pre-entocristid: Bladed, running to base of metaconid (1). Absent or (antero-buccal) (1)
2. Protoconid-metaconid-paraconid approximation; equally spaced (0), metaconid-paraconid closely spaced, paraconid anteriorly positioned (1), equally spaced with metaconid posteriorly positioned (2), metaconid-protoconid-paraconid widely spaced with paraconid anteriorly positioned and metaconid posteriorly positioned (3), metaconid-protoconid wider spaced than both are to paraconid (4), paraconid lost (5).
3. Paracristid connection of paraconid to metaconid. Continuous cristid (0), Incised cristid (1).
4. Posthypocristid termination; hypoconulid (0), entoconid base (1).
5. Size of hypoconulid; distinct (0), reduced (1), absent (2)
6. Anterior cingulum. Present as full cingulum (0), Present as small cingulid (1), Anterior buldge (2), Completely absent (3).

##### $M^1$

7. Anterior cingulum; absent (0), present (1).
8. Posterior cingulum; cleft between metaconule and metacone (0); clear cingulum running from metaconule to antero-lingual margin of

metasytlar corner (1); cingulum running from metaconule to postero-lingual base of metacone (2); distinct cingulum connects to metasytlar corner (3).

9. Paracone orientation; antero-posterior (0); bucco-lingually (1).

10. Metaconule development;  $\frac{1}{4}$  -  $\frac{1}{3}$  the size of protocone (0);  $\frac{1}{2}$  the size of protocone (1); equal to the protocone (2); absent (3).

11. Preprotocrista; runs to base of paracone (0); runs buccal of paracone base to the anterior cingulum (1); runs to anterior cingulum and forms part of it (2).

12. Metastylar corner; metastyle projects postero-buccally from tooth crown (0); metastyle simple and conical, oriented vertically and within the confines of the tooth crown (1).

	1	2	3	4	5	6	7	8	9	10	11	12
<i>Yarala burchfieldi</i>	1	3	1	0	0	0	1	0	0	3	2	0
<i>Perameles gunnii</i>	1	0	1	0	1	3	0	2	1	2	2	0
<i>Perameles nasuta</i>	1	0	1	0	1	3	0	2	1	2	2	0
<i>Perameles bowensis</i>	1	0	1	0	1	3	1	2	1	2	1	1
<i>Perameles bougainville</i>	1	0	1	0	1	3	0	2	1	2	2	0
<i>Perameles sobbei</i>	1	0	1	0	1	3	?	?	?	?	?	?
<i>Macrotis lagotis</i>	0	5	1	0	1	0	1	3	0	3	2	1
<i>Chaeropus ecaudatus</i>	1	4	1	0	0	2	0	0	1	2	2	0
<i>Ischnodon australis</i>	1	4	1	1	1	?	?	?	?	?	?	?
<i>Rhynchomeles prattorum</i>	0	2	0	0	1	2	1	2	0	1	2	0
<i>Peroryctes raffayanna</i>	0	3	0	0	0	2	0	0	0	0	0	0
<i>Microperoryctes longicaudata</i>	0	1	1	0	0	2	0	0	0	0	0	0
<i>Echymipera clara</i>	0	2	0	1	1	3	0	2	0	1	2	0
<i>Echymipera rufescens</i>	0	2	0	0	1	3	1	2	0	1	2	0
<i>Echymipera kaluba</i>	0	2	0	0	0	3	0	2	0	1	2	0
Cf. <i>Peroryctes tedfordi</i>	0	0	1	1	2	2	0	0	0	0	0	0
Cf. <i>Peroryctes</i> Large	0	1	1	1	0	1	0	0	0	0	0	0
<i>Perameles</i> 1	1	0	1	0	0	3	0	2	1	1	2	0
<i>Perameles</i> 2	1	0	1	1	1	2	0	2	1	1	2	0
Peroryctid 1	0	1	1	1	0	0	0	0	0	0	0	0
Peroryctid 2	0	1	1	1	0	1	0	0	0	0	0	0
Peroryctid 3	1	1	1	0	0	1	0	0	0	1	1	0

**Table 4-2. Table of Character states for fossil peroryctid and peramelid fossils from Mt Etna.**

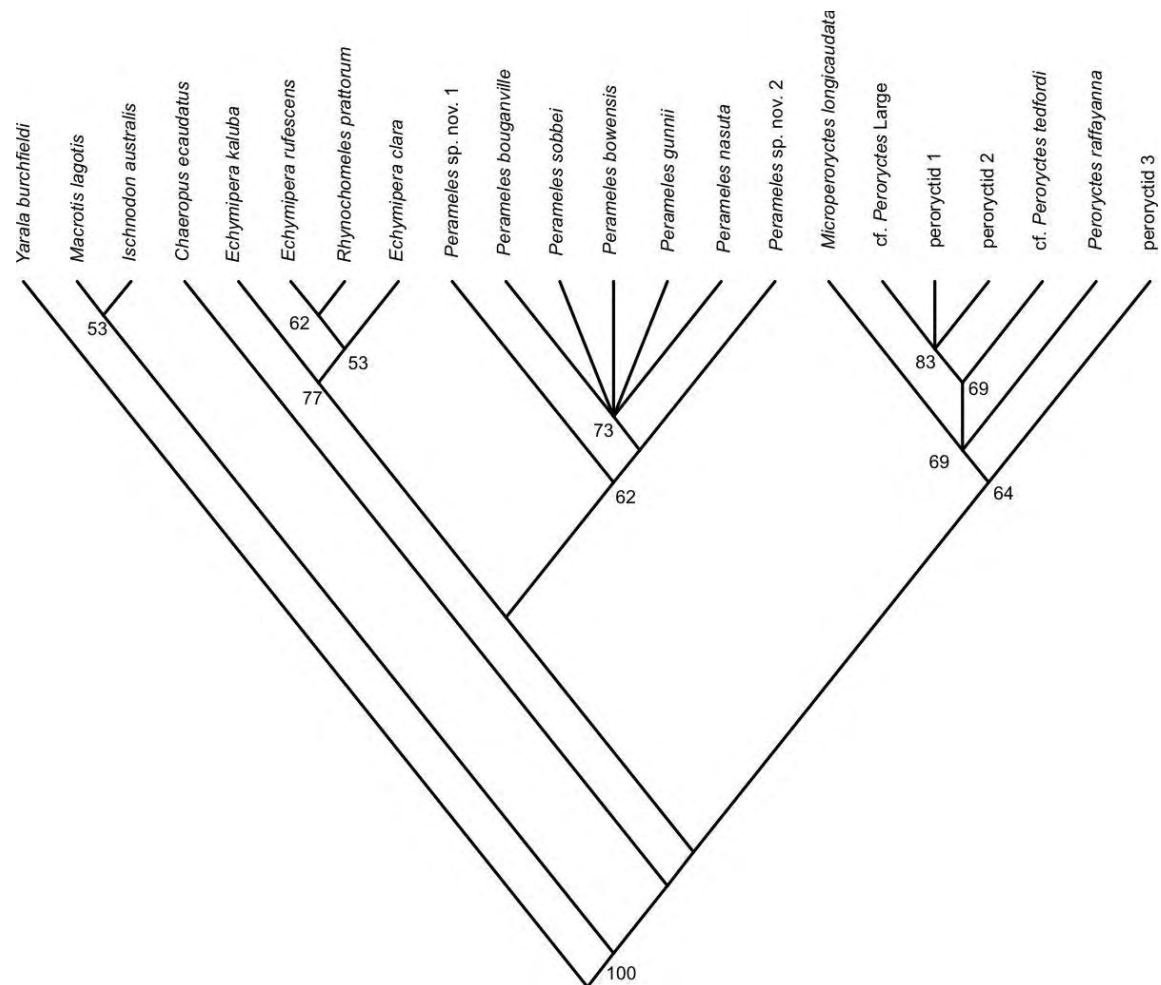


**Figure 4-39. Consensus phylogeny of Mt Etna perameloid taxa, including bootstrap values over 50%.**

### Family DASYURIDAE

Dasyurids presented in Hocknull (2005) and Hocknull et al., (2007) have recently been reviewed by Cramb, Hocknull & Webb (2009).

### Family THYLACINIDAE

Additional specimens have been recovered that represent *Thylacinus cynocephalus*, including a partial skeleton which includes a fragmentary skull, cervical vertebrae, scapula, thoracic vertebrae, ribs and humerus. This partial articulated skeleton comes from QML1313. Other sites have now recorded isolated molars, premolars and calcanea, all within the morphological and morphometric variation of *T. cynocephalus*.



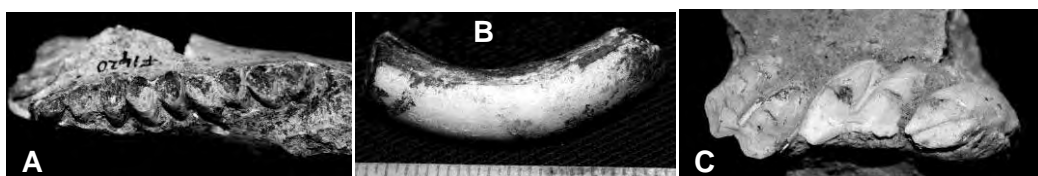


Figure 4-40. Fossil thylacinid specimens, including, A. Right maxillary molar row, B. Proximal humerus and C. Calcaneum (QML1313).

#### Family VOMBATIDAE

##### ***Vombatus ursinus mitchelli***

Additional remains of *Vombatus* have been recovered from QML1311J deposit of Mt Etna. This specimen is markedly smaller than the specimens assigned previously to *V. ursinus mitchelli* and are most similar to *V. ursinus ursinus*, the extant Common Wombat. This new specimen raises the possibility that there were two different sized species of *Vombatus* present at Mt Etna during the middle Pleistocene. Both taxa are exceptionally rare in the deposits with only two specimens known from the middle Pleistocene and two specimens from the late Pleistocene.



**Figure 4-41. Fossil vombatids, A. Left mandible (QMF 1420), B. Isolated molar (QML1311 H), C. Right maxillary fragment (QML1311 J).**

**Vombatid *gen. et sp. nov.***

A small collection of bones recovered from an upper chamber in Lower Johannsen's Cave, Northern Limestone Ridge section has recovered fragmentary remains of a large-sized vombatid. Material recovered included both lower incisors, fragments of incisor enamel, molar enamel and highly fragmented dentary alveoli and dentary symphysis. Isolated post-cranial remains presumably associated with the vombatid specimen include epiphyses of limb elements and pes phalanges. The lower incisors are very long, relatively straight, and laterally compressed with an elongate-ovoid occlusal wear facets.

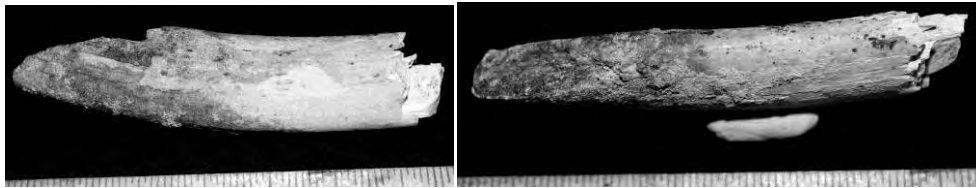


**Figure 4-42. Possible new vombatid (isolated incisor from skull) (Lower Johansen's Cave).**

**Family PALORCHESTIDAE**

**Palorchestes sp. cf. *P. pickeringi***

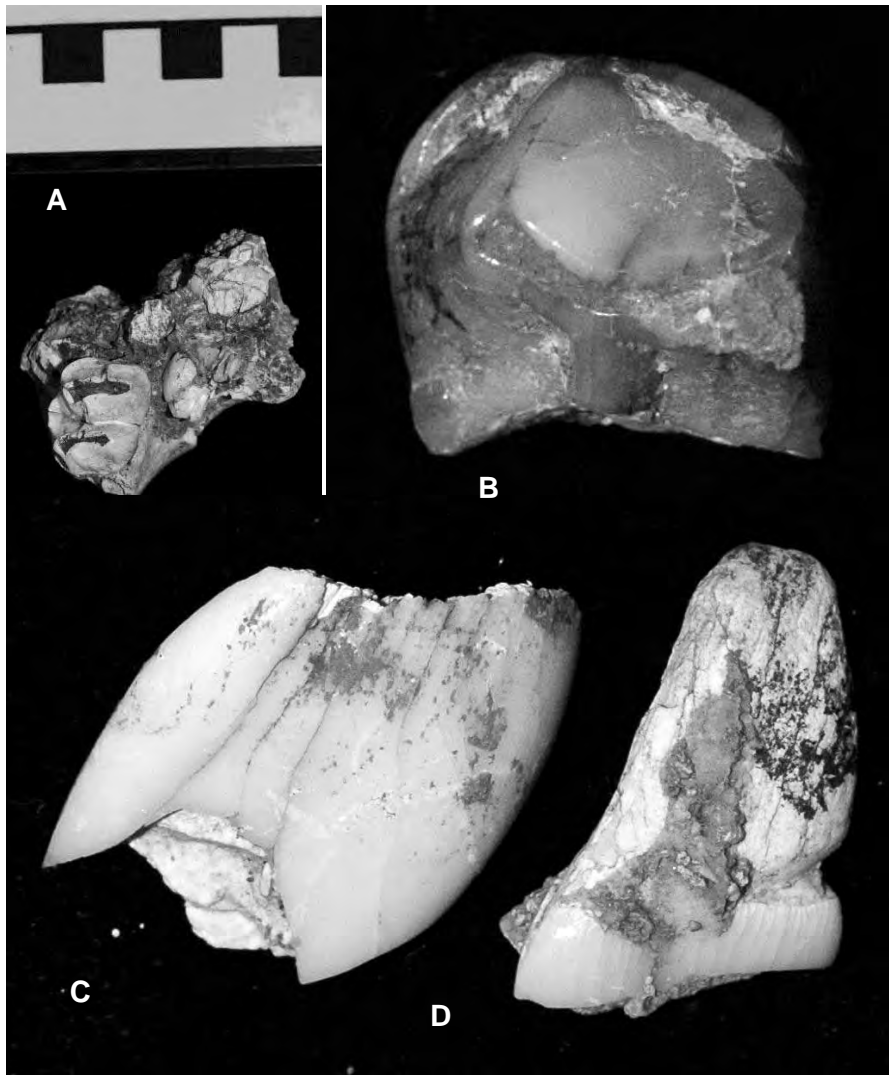


Figure 4-43. *Palorchestes* sp. cf. *P. pickeringi* from Mt Etna. A. QMF 51759 RM<sup>2</sup>, partial M<sup>1</sup>. B. M<sub>3</sub> (QML1384LU). C-D. QMF 51760, LI<sup>1-2</sup>.

Hocknull (2005) described the remains of *Palorchestes* at Mt Etna, allying them with *P. parvus* based primarily on size. Since then, Piper (2006) described *Palorchestes pickeringi* has been described from the early Pleistocene Nelson Bay Fauna, to which the fossil specimens share closest morphology. Piper (2006) provides a detailed description of *P. pickeringi* and a comparison of this taxon to its closest morphological and morphometric taxa, *P. parvus* and *P. painei*. Based on M<sup>2</sup> length versus width, the Mt Etna taxon is within the size range of *P. parvus*, *P. painei* and *P. pickeringi*. It is within the lower range of *P. parvus*, closest to the members of this taxon that come from the middle-late Pliocene Chinchilla Sands Fauna. It is as wide

as specimens of *P. painei*, however, much more elongate. When compared with *P. pickeringi*, it is only slightly larger. On morphological grounds the Mt Etna *Palorchestes* differs from *P. painei* by possessing higher crowned lophs; having a relatively longer  $M^2$ ; better developed links and cingulae; deeper postero-lingual fossette on  $M^1$  and  $M^2$ ; lacking a posterior cingulum on  $M^2$ . The Mt Etna *Palorchestes* differs from *P. parvus* by being lower crowned, although the specimens referred to *P. parvus* from Chinchilla approach the Mt Etna specimens; being smaller than Pleistocene *P. parvus*; lacking a distinctive postero-buccal cingulum; lacking the buccal cingulum between the loph valley; lacking a posterior cingulum. The Mt Etna *Palorchestes* differs from *P. pickeringi* the least, both lacking the distinctive posterior cingulum seen in both *P. parvus* (Pliocene and Pleistocene) and *P. painei*. It is similarly low crowned. The  $M_3$  protoloph is morphologically identical to *P. pickeringi*, only slightly larger.

#### ***Palorchestes* sp. cf. *P. parvus***

Hocknull (2005) did not report on *Palorchestes* from Marmor Quarry. A single left  $M_3$  (cast) was located in the Queensland Museum collection having been recovered from Marmor Quarry and sent to the British Museum of Natural History. The molar is imbedded in matrix, which obscures the lingual side of the tooth, however, most features are preserved. The tooth is high crowned with a distinctive mid-link and posterior-link and cingulid. Based on size alone, the specimen is large and falls outside the range of variation observed in *P. pickeringi* and the Mt Etna *Palorchestes*, within the upper range of *P. parvus*. The specimen is too small to be referable to *P. azael* and does not possess the distinctive cingula of this taxon. The fossil most closely allies *P. parvus* in both size and morphology, especially the high-crowned lophs. Due to the significant confusion surrounding *Palorchestes* taxonomy I will only tentatively refer this specimen to *P. parvus*, however, it is most likely not the same taxon found in the middle Pleistocene of Mt Etna.

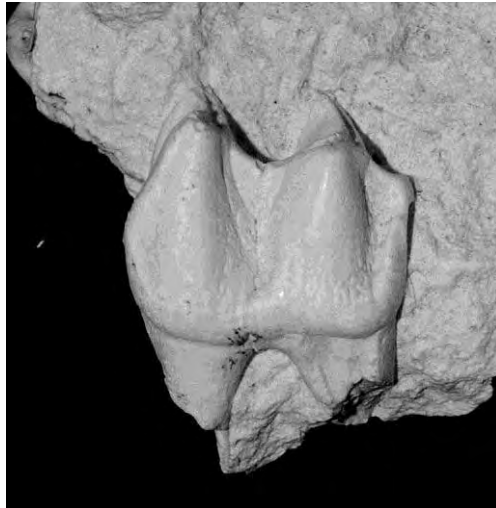


Figure 4-44. *Palorchestes* sp. cf. *P. parvus*, Marmor Quarry LM<sub>3</sub>.

#### Family DIPROTODONTIDAE

A small lophodont molar fragment and a fragment of maxilla preserving tooth roots are the only representative fossils of the Diprotodontidae so far recognised from Mt Etna. The fragment of molar loph is very quadrangular in ventral view, with a sloped loph occlusal face, which is both indicative of a low-crowned dentition. The enamel is not punctate. Only two low-crowned diprotodontids are known from the Pleistocene of Australopapua, *Hulitherium thomasettii* and ‘*Kolopsis*’ *watutense* from Papua New Guinea. Although it is speculation of the possibility of New Guinean rainforest megafauna present on mainland Australia, these fossils strongly indicate a guild of low-crowned, browsing diprotodontids that inhabited tropical rainforests of mainland Australia during the Quaternary.

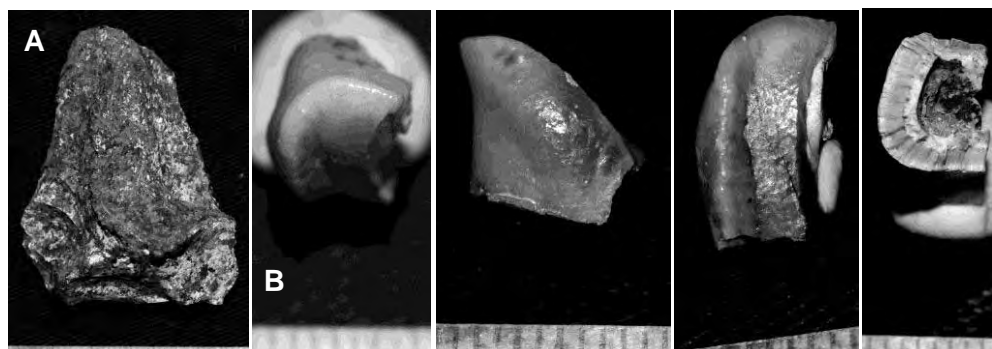


Figure 4-45. Fossil diprotodontid fragments from Mt Etna. A. Fragment of maxilla (QML1311 H). B. molar loph (QMF 51761)

## Family MACROPODIDAE Gray, 1821

**Troposodon** sp. cf. **T. minor**

An isolated RP<sup>2</sup> represents a large-sized species of *Troposodon*. Superficially the P<sup>2</sup> matches the P<sup>3</sup> of *T. bluffensis* and *T. bowensis*, however, on comparison of all species of *Troposodon*, and the identity of this specimen as a P<sup>2</sup> allies it closest to *T. minor*. The P<sup>2</sup> matches in many respects QMF3711, one of the only preserved P<sup>2</sup>s available for study from *T. minor*. The P<sup>2</sup> is very similar in overall morphology to the P<sup>3</sup>, being elongate and narrow with a low-crowned main crest with indistinct cusps; low lingual cingulum and shallow basin; lingual cingulum terminating at the base of the anterior-most cusp; buccal cingulum absent; anterior margin pointed and posterior margin rounded. P<sup>2</sup> morphology differs from P<sup>3</sup> morphology by the possession of a distinctive postero-lingual cusp which bounds the lingual margin of a posterior-lingual pocket. This pocket is heavily reduced or absent in the P<sup>3</sup>s of all species of *Troposodon* so far described. The P<sup>2</sup> is intermediate in size between the P<sup>3</sup>s of *T. bowensis*/*T. bluffensis* and the remaining species *Troposodon minor* and *T. kenti*. This specimen is closest to

the P<sup>2</sup> from *T. minor*.

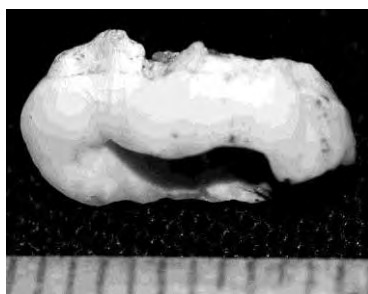
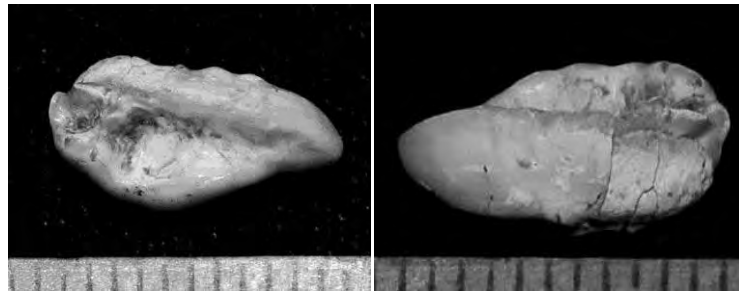


Figure 4-46. *Troposodon* sp. cf. *T. minor* from Mt Etna, RP<sup>3</sup> (QML1311 H).

cf. **Lagostrophus**

Several isolated lower molars show features common to *Troposodon* and *Lagostrophus*, including, high-crowned lophids, premetacristid and parametacristid running from the metaconid; broad and high anterior cingulae forming a third lophid

for each molar; no posterior cingulae and 's'-shaped lophids. The molars are very small in size and are closer to *Lagostrophus* than any described species of *Troposodon*. At this stage the molars are comparable to *Lagostrophus*, however, may represent a different, but related taxon.



Figure 4-47. cf. *Lagostrophus* sp. LM<sub>2</sub>.

### **Protemnodon**

Hocknull (2005) identified *Protemnodon* sp. cf. *P. devisi* from Mt Etna. Subsequently Hocknull et al (2007) list a second species of *Protemnodon*. Both of these are now represented by more specimens and required further comparison and identification.

#### **Protemnodon sp. cf. *P. devisi***

Isolated P<sup>2</sup>s, P<sup>3</sup>s, dP<sup>3</sup>s and molars represent this taxon. Based on size, the fossil specimens most closely approximate *P. anak* and *P. devisi*. The fossil specimen more closely reflect the morphology of *P. devisi* than that of *P. anak* by possessing lower crowned molars; similarly shaped P<sup>2</sup> and P<sup>3</sup>; distinct postparacristae and premetacristae; less developed and lower midlink; lower molars with no posterior cingulae.

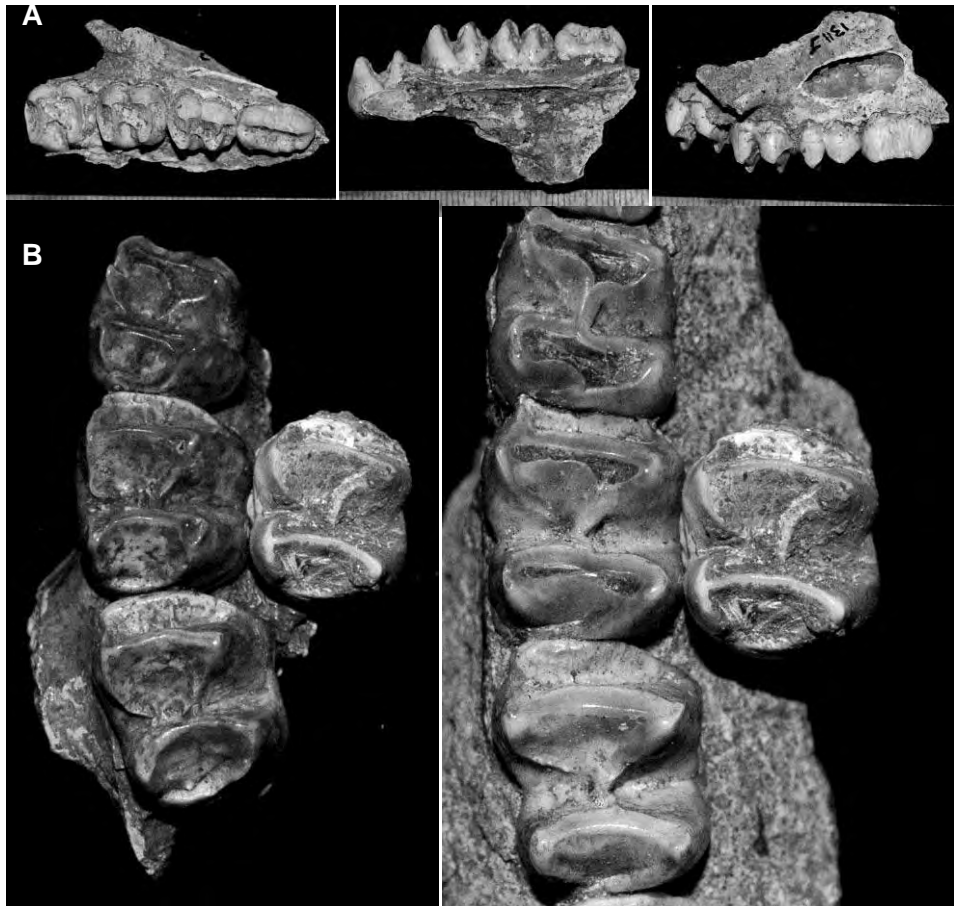


Figure 4-48. *Protamnodon* sp. cf. *P. devisi* from Mt Etna. A. Right maxilla with P<sup>2</sup>- M<sup>2</sup> in occlusal, lingual and buccal views (QML1311J). Isolated M<sup>1</sup> (QML1311 H) compared with *P. devisi* (left) and *P. anak* (right).

#### ***Protamnodon* sp. nov.**

A new species of large *Protamnodon* is represented by isolated upper and lower molars and an elongate RP<sub>3</sub> retained within the jaw fragment which preserves the diastema between I<sub>1</sub> and P<sub>3</sub>, the depth of the dentary at this point, the mental foramen and the posterior portion of the dentary symphysis. In size, this species of *Protamnodon* is most similar to *P. brehus*, however, features of both the dentary and the upper molars sets this taxon apart from most other species of *Protamnodon*. The mental foramen is placed very close to the anterior root of the P<sub>3</sub>, a feature only observed in *P. hopei* and *P. tumbuna*, and a synapomorphy of these taxa within *Protamnodon*. The position of the posterior margin of the dentary symphysis is situated in the fossil specimen below the anterior root of the P<sub>3</sub>. This is a unique feature of this taxon, however, some species of *Protamnodon* come close to this morphology, including *P. tumbuna*, *P. nome* and *P. hopei*. The posteriorly placed



posterior margin of the dental symphysis is a synapomorphy of these four taxa. The depth of the dentary below the  $P_3$  is seen in the larger species of *Protemnodon*. The  $P_3$  of the fossil specimen is a typically elongate premolar, being long and narrow, similar to that of *P. hopei*, *P. anak*, *P. devisi* and *P. brehus*. The upper molars are very low crowned, similar to that seen in *P. hopei* and *P. otibandus*; much more low crowned than that seen in *P. chinchillaensis* and *P. devisi*. The upper molars are very broad and possess distinct postparacristae and premetacristae; and a short urocrista.

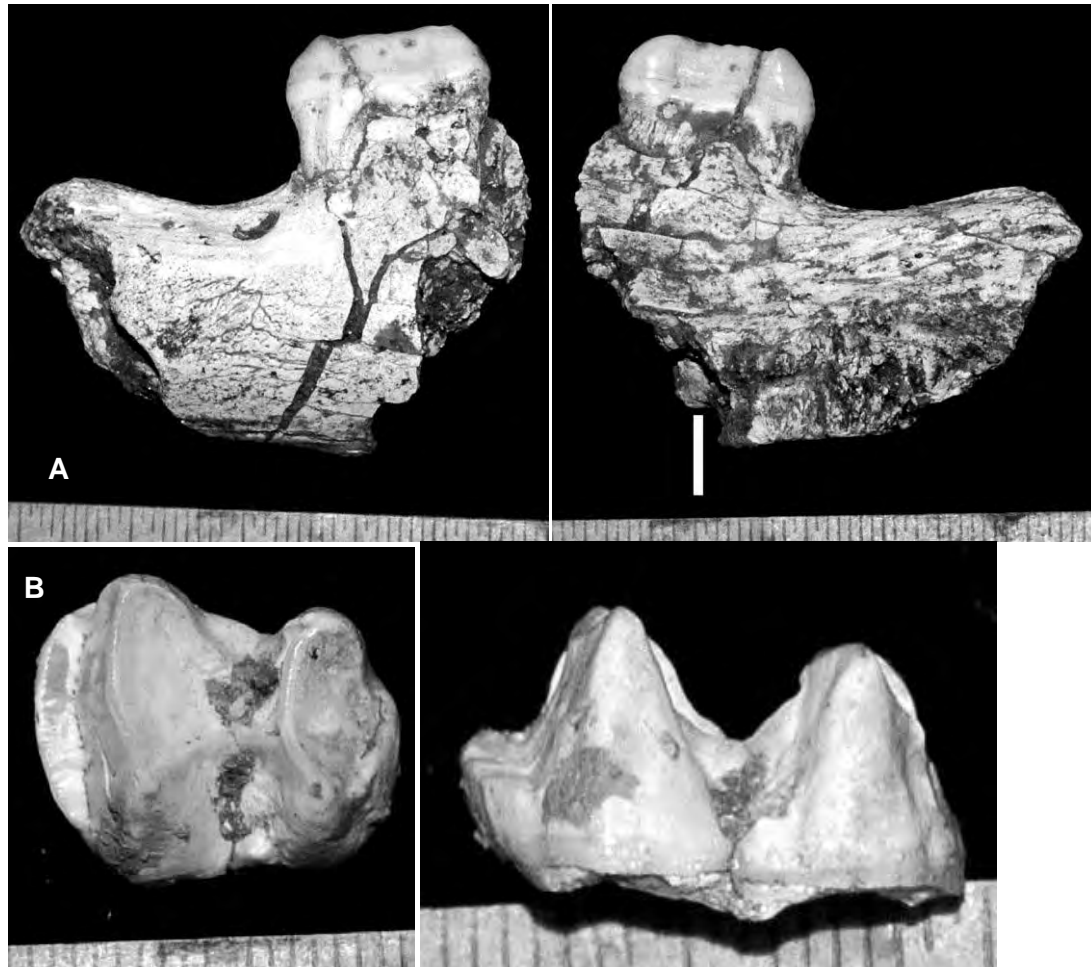


**Figure 4-49. *Protemnodon* sp. nov. Mt Etna, A. Left partial mandible showing posterior position of the mental foramen, close to the base of  $P_3$  (left) and the posterior placement of the dental symphysis (right) (QML1311 H). B. Isolated low-crowned  $M^{2or3}$  (QML1311 H)**

### ***Protemnodon brehus***

A partial skull bearing left  $P^3$ - $M^4$  and right  $M^{2-4}$  represents *Protemnodon brehus*, being characteristic of the typical *Protemnodon* skull shape and including a dentition similar in size to that which diagnoses *P. brehus* (Batholomai, 1973). This specimen

differs from the other two species represented at Mt Etna by being larger in overall dimensions, possessing higher-crowned molars and a distinctive elongate P<sup>3</sup>.

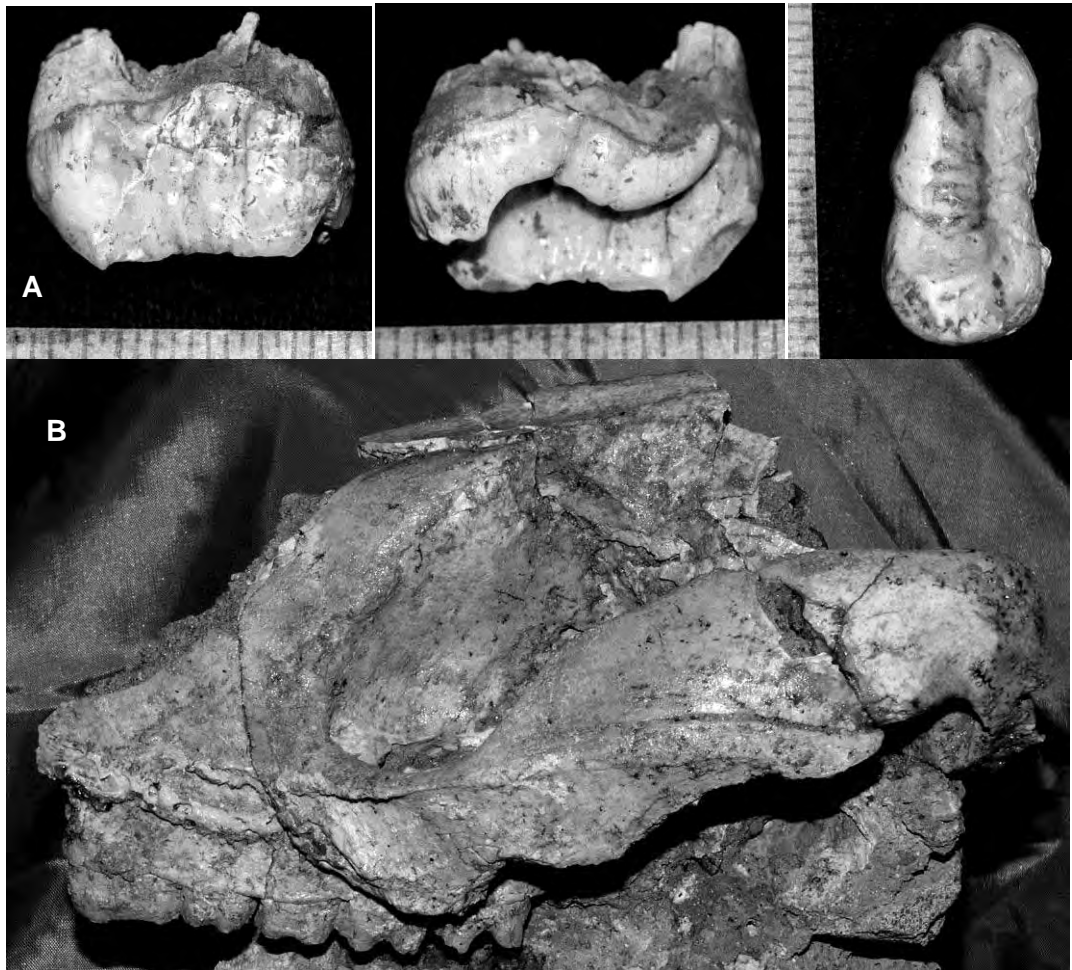


Figure 4-50. *Protomnodon brehus* from Mt Etna, isolated P<sup>3</sup> (QML1311H) and partial skull (QML1311J).

### **Wallabia** sp.

Two upper premolars are considered to represent a species of *Wallabia* based of the following combination of features unique to *Wallabia* that are present in the fossils; lingual cingulum present by not well developed; >3 ridges running down the flanks of a straight main crest; >2 distinct cuspules between the main anterior and posterior cusps of the main crest; deep postero-lingual pocket; tall postero-lingual cusp; postero-buccal cuspule absent; blade-like posterior cusp of main crest; rounded anterior and posterior margins making the tooth look evenly ovoid in occlusal view,

with the posterior margin broader. The specimens are very close in size and morphology to *Wallabia bicolor*.

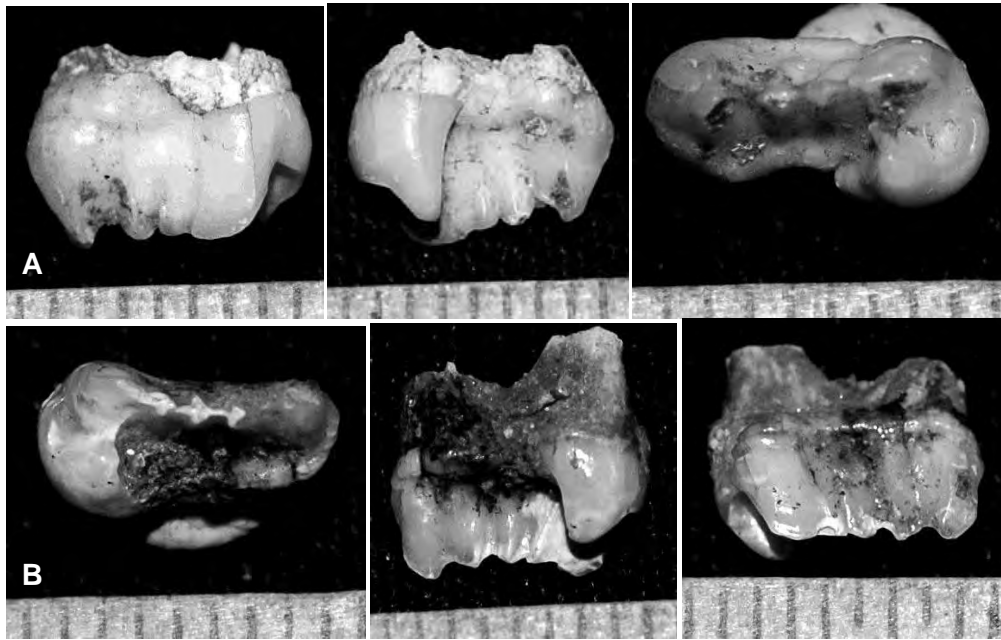
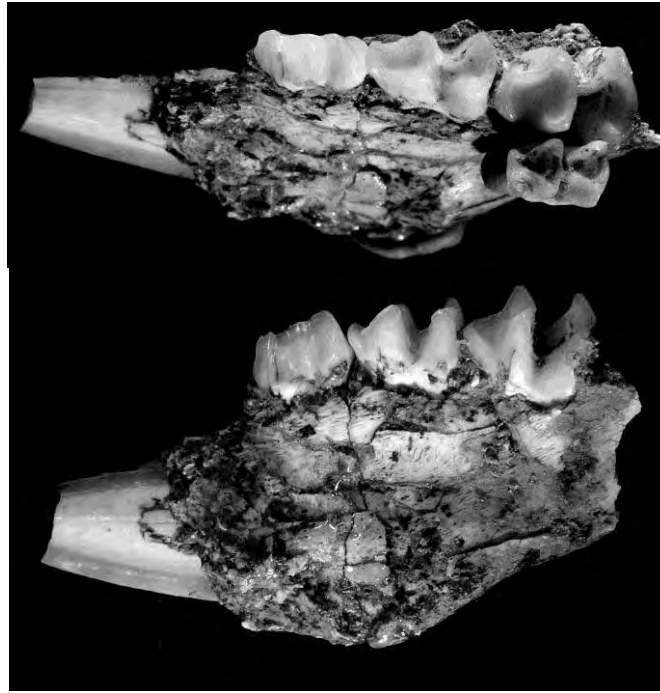


Figure 4-51. *Wallabia* sp. from Mt Etna, isolated P<sup>3</sup>s, A. QML1311 H; B. QML1311 H.

### ***Thylogale stigmatica***

Hocknull (2005) identified two species of *Thylogale*, one large species (*Thylogale* sp. 2) and the other a very small species (*Thylogale* sp 1). Based on the elongate nature of the dP<sub>3</sub>; anteriorly extended anterior cingulum and shape of the P<sub>2</sub> the larger of the two *Thylogale* species are referable to *Thylogale stigmatica* (Fig. 4-52).



**Figure 4-52. *Thylogale stigmatica* from Mt Etna, right mandible with P<sub>2</sub>-M<sub>1</sub> (compared with isolated molar of *Thylogale* sp. nov. (above).**

#### ***Thylogale* sp. nov.**

Hocknull (2005) identified a very small species of *Thylogale* (*Thylogale* sp. 1). Flannery et. al., (1992) considered the phylogenetic characteristics of *Thylogale* species, including two extinct taxa, *T. christenseni* and *T. ignis*. Of the currently recognised species of *Thylogale*, *T. christenseni*, *T. calabyi* and *T. ignis* are the smallest, with *T. christenseni* being the smallest of these. Fig. 4-53 shows how the *Thylogale* species present at Mt Etna is even smaller and narrower in dP<sub>3</sub> molar dimensions than *T. christenseni*, making it the smallest macropodid known, possessing a dP<sub>3</sub> only slightly longer than the M<sub>1</sub> of *Hypsiprymnodon moschatus* (3.4mm vs 3.2mm). The narrower protolophid of dP<sub>3</sub> in *Thylogale* sp. nov. reflects the morphological feature diagnostic of this new species; an almost entirely coalesced protolophid, forming a triangular anterior to the dP<sub>3</sub> trigonid where the preprotocristid and premetacristid join medially along the central axis of the molar, which then runs as a blade to the anterior margin. The molars are relatively high crowned and in all molars the cristid obliqua almost contacts an equally developed preentocristid, where both cristids run medially from the apex of the hypolophid to the middle of the

median valley. These cristids almost coalesce, similar to the protolophid. These features are not seen in any described species of *Thylogale*. The preentocristid is well developed in *T. brunii*, however, they run along the margin of the molar and not to its centre. Based on the characteristics considered by Flannery et al (1992) and Flannery (1989), the new species of *Thylogale* would fit phylogenetically into the ‘primitive’ group of thylogales, including *T. billardierii*, *T. ignis* and *T. christenseni*. Discussion of these features will need to await a more detailed morphological analysis of *Thylogale* species, however, it seems reasonable to consider that the smallest species of *Thylogale* are in fact highly derived relative to their sister taxa and may represent yet another convergent reversal in character states of the dentition in macropods. The functional implications of the development of singular cutting blades in  $P_{2-3}$  and  $dP_3$  and nearly cingular in  $M_1$  in such a small-sized macropod suggests that this species of *Thylogale* had specialised its dentition from its inherited high-crowned lophodont ancestry. This may have been used to process vegetation in a very different way to the ‘standard’ macropodine system. It is speculated here that the ‘normal’ tiny fungivorous-frugivorous macropod guild, which is usually filled in other Australian habitats by species of *Hypsiprymnodon* and/or *Bettongia* (absent from the Mt Etna fossil record), was instead filled by a specialised, small-bodied species of *Thylogale*. This small-bodied macropod would need to eat vegetation with higher levels of nutritional over grass simply due to its small body-size. The retention of bladed premolars and molars may have provided this small species of *Thylogale* the opportunity to take advantage of an available resource with minimal competition, other than with rodents.

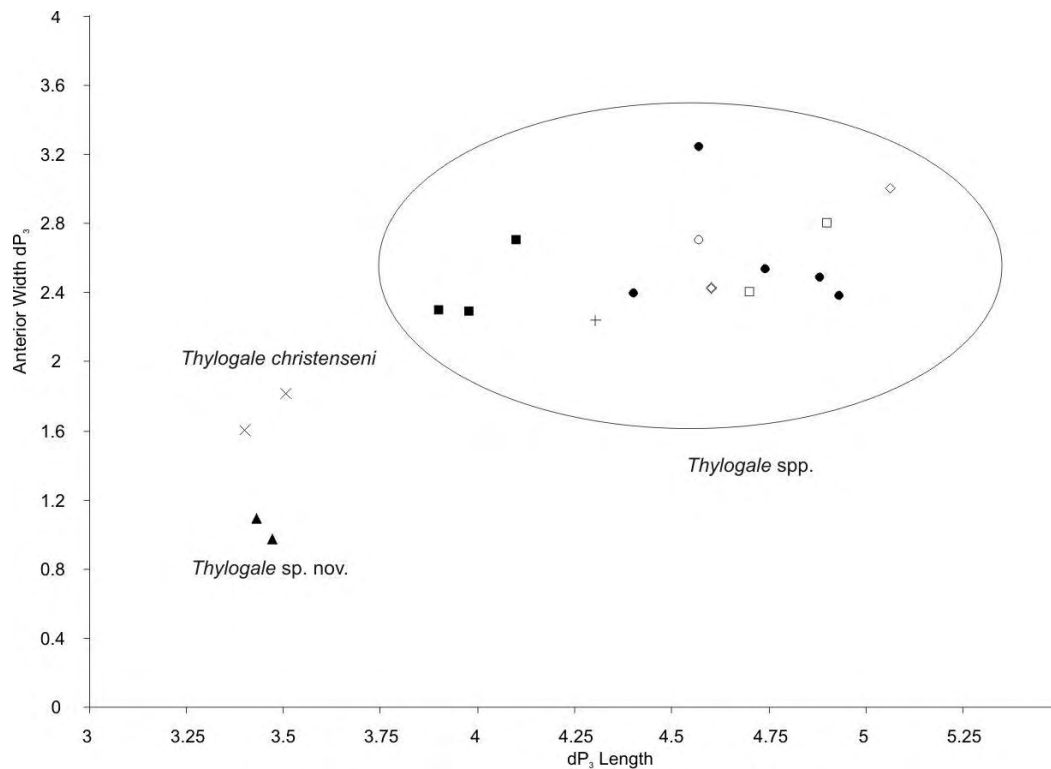


Figure 4-53. Bivariate plot of dP<sub>3</sub> length to anterior width, showing the very small size of *Thylogale* sp. nov. from Mt Etna, compared with *T. christenseni* and all other species of *Thylogale*.

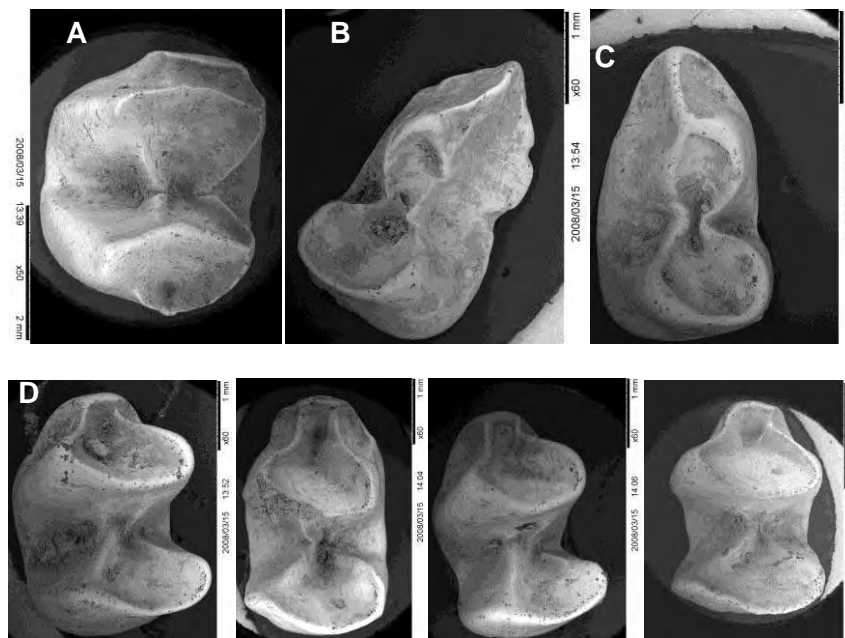


Figure 4-54. *Thylogale* sp. nov. from Mt Etna. A. Isolated upper M<sup>2or3</sup>. B-C, isolated dP<sub>3</sub>s. D. four isolated lower M<sub>2-3</sub>s.

## **Dendrolagus**

Hocknull (2005) identified *Dendrolagus* from the Mt Etna fossil deposits, considering there to be one taxon, whilst Hocknull et al., (2007) listed four species of *Dendrolagus*. As additional material has become available revision of these taxa has yielded yet another species, totalling five species. These species are briefly described and compared below.

*Dendrolagus* species are easily distinguished on the basis of P3 and M1 morphology, in particular upper dentition. Three premolar shapes are common within *Dendrolagus*;

1. Posteriorly broadened; where the posterior width is markedly wider than the anterior width. This is usually due to the corresponding lack of a buccal and/or lingual cingulum, which produces an occlusal outline that is rounded on the anterior end, narrowed along its length and bulbous at the posterior end.
2. Sub-rectangular; where the premolar is equally as wide along its entire length with a rounded anterior margin.
3. Sub-rectangular with tapered and pointed anterior margin; where the premolar is equally as wide along its entire length with a pointed anterior margin, with corresponding anterior crista from the large anterior median cusp.

Morphotype 1. P<sup>3</sup> posteriorly broadened.

Described species of *Dendrolagus* with premolar morphotype 1 include; *D. inustus*, *D. mbasio*, *D. scottae* and *D. spadix*. All three fossil species of *Dendrolagus* possess a buccal cuspule or cuspule that has merged with the buccal edge of the main premolar crest, therefore, these species are immediately differentiated from *D. inustus* because this species does not possess a buccal cuspule. Preliminary identification of these two taxa includes species that share very close morphology to *D. mbasio* and *D. spadix*.

### ***Dendrolagus* sp. cf. *D. mbasio***

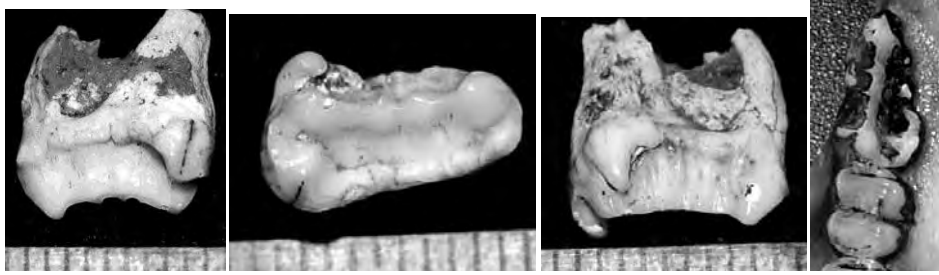


Figure 4-55. *Dendrolagus* sp. cf. *D. mbasio* from Mt Etna, isolated RP<sup>3</sup>, compared with modern specimen (right).

#### ***Dendrolagus* sp. cf. *D. spadix***

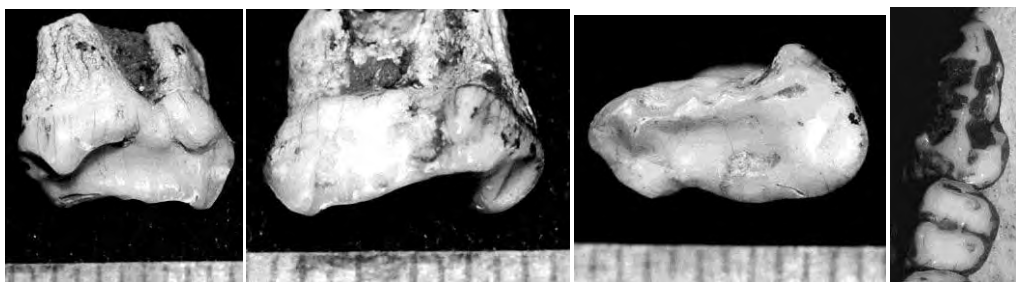


Figure 4-56. *Dendrolagus* sp. cf. *D. spadix* from Mt Etna, isolated LP<sup>3</sup>, compared with modern specimen.

Morphotype 2. P<sup>3</sup> sub-rectangular, rounded anterior margin.

Described species of *Dendrolagus* bearing premolar morphotype 2 include *D. matschiei*, *D. ursinus*, *D. lumholtzi* and *D. bennettianus*. These four species can be differentiated by the relative development of the lingual basin and lingual cingulum of P<sup>3</sup>. A shallow basin and a simple lingual cingulum are present in *D. matschiei*, *D. ursinus* and *D. lumholtzi*, whilst *D. bennettianus* has a well developed basin and a high, crenulated lingual cingulum. PM37 possesses a shallow basin and simple lingual cingulum, therefore, closest in morphology to *D. matschiei*, *D. ursinus* and *D. lumholtzi*.

#### ***Dendrolagus* sp. cf. *D. ursinus***





**Figure 4-57. *Dendrolagus* sp. cf. *D. ursinus* from Mt Etna, RP<sup>3</sup>-M<sup>1</sup> QMF51771.**

Similarities with *D. matschiei* include; shallow lingual basin; relatively smooth lingual basin (uncrenulated); lobate lingual cingulum; lacks a buccal cingulum; lacks an antero-lingual pocket; lacks a distinct posterior pocket; possesses two main ridgelets between major crest cusps; similar in size. Differs from *D. matschiei* by; buccal cuspule isolated and discrete instead of being merged with the main crest; less distinct mid-line crest ridgelets; posterior width of premolar wider than anterior width of M<sup>1</sup>.

Similarities with *D. ursinus* include; overall similar size; antero-lingual pocket absent; shallow lingual basin; lobate lingual cingulum; premolar posterior width subequal to anterior width of M<sup>1</sup>; isolated posterior buccal cuspule; buccal cingulum reduced or absent; two mid-crest ridgelets. Differs from *D. ursinus* by; greater development of posterior-lingual pocket; buccal cuspule isolated but linked to main crest of premolar.

Similarities with *D. lumholtzi* include; posterior-lingual pocket reduced or absent; anterior-lingual pocket absent; shallow lingual basin; lobate lingual cingulum (not crenulated); similar in size; premolar posterior width subequal to anterior width of M<sup>1</sup>. Differs from *D. lumholtzi* by; isolated posterior-buccal cuspule; buccal cingulum present in *D. lumholtzi*; two distinct mid-crest ridgelets versus only a single distinct ridgelet in *D. lumholtzi*.

*Dendrolagus* sp. cf. *D. ursinus* differs significantly from *D. lumholtzi* and *D. matschiei*, whilst possesses very close morphology to *D. ursinus*. It is for this reason that this species of *Dendrolagus* is comparable to *D. ursinus* until a more detailed review is undertaken.

#### ***Dendrolagus* sp. nov. 1**

*Dendrolagus* sp. nov. 1 possesses a combination of features of the P<sup>3</sup> and M<sup>1</sup> that are currently not described for any species of *Dendrolagus*, therefore this taxon is considered to represent a new species. The features of this new species include; sub-rectangular P<sup>3</sup>; buccal cingulum absent; buccal cuspule merged with lateral margin of main premolar crest; anterior-lingual pocket absent; small posterior-lingual fossette; lingual basin shallow; lingual cingulum incipient; 2 main crest ridgelets; anterior

ridgelet distinct, posterior ridgelet smaller; very simplified morphology; posterior width of  $P^3$  subequal anterior width of  $M^1$ .

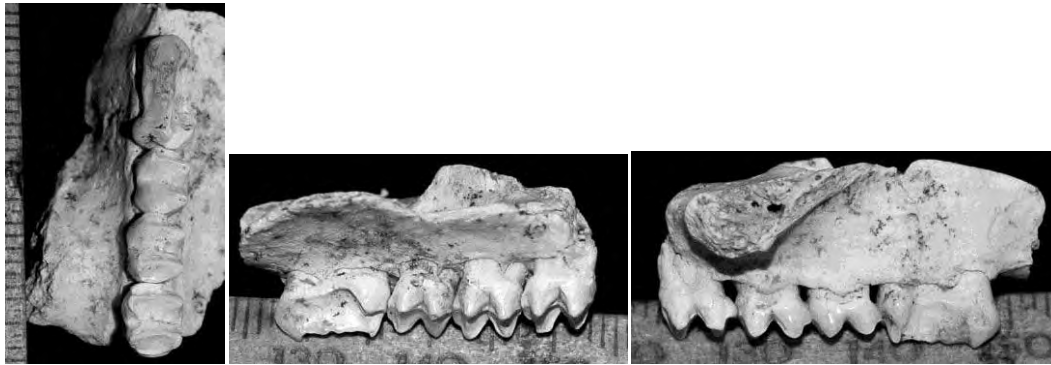


Figure 4-58. *Dendrolagus* sp. nov. 1 from Mt Etna, right maxilla  $P^3$ - $M^3$ , QML1313.

### *Dendrolagus* sp. nov. 2

Morphotype 3.  $P^3$  sub-rectangular, pointed (tapered) anterior margin.

Described species of *Dendrolagus* with premolar morphotype 1 include; *D. dorianus* and *D. goodfellowi*.



Figure 4-59. *Dendrolagus* sp. nov. 2 from Mt Etna. A. Isolated  $RP^3$  (QML1311 H) compared with modern specimens, B. *D. dorianus* and C. *D. goodfellowi*.

### Bohra

Hocknull (2005) identified *Bohra* from the middle Pleistocene deposits at Mt Etna on the basis of a single large dendrolagin calcaneum. Since then large-sized premolars

and molars have been recovered that possess distinctly dendrolagin morphology. These are here referred to as species of *Bohra*. Prideaux (2008) diagnosed *Bohra* dentition along with post-cranial remains. Based on this diagnosis all three of the premolars presented here would be considered to fall outside the range of variation seen in the genus. However, considering the degree of variation of premolar morphology between species of *Dendrolagus*, it is suggested that these taxa be referred to *Bohra* and the diagnostic features of *Bohra* expanded to encompass these new species. Comparisons were made between these three new species and the two species that have associated P<sup>3</sup>s, *B. wilkinsonorum* and *B. illuminata*. The three Mt Etna taxa differ most from *B. illuminata* by being much larger and having the anterior margin of the P<sup>3</sup> similar in width to the posterior margin. *B. illuminata* is wider posteriorly. Each of the three species described here have well developed lingual cingulae (as does *B. wilkinsonorum*), however, *B. illuminata* does not. Based on the obvious differences between *B. illuminata* and the three species here, only *B. wilkinsonorum* will be specifically compared between each species.

***Bohra* sp. nov. 1**

QML1311H

*Bohra* sp. nov. 1 is presently represented by a right P<sup>3</sup>. The occlusal profile of the premolar is elongate-ovoid with rounded anterior and posterior extremities. The posterior width of the premolar is slightly wider than the anterior width. The greatest width of the premolar is at approximately 2/3 the length of the premolar between the buccal cuspule and the lingual cingulum. Main crest of premolar begins anterior to the anterior-most cusp as a crest running from the base of the tooth crown. The main crest bears two smaller cuspules and associated ridgelets. Posterior-most cusp less distinct than anterior-most cusp with a buccally crest that runs perpendicular to the main crest axis. This crest merges with the posterior-buccal cuspule so that the cuspule is not isolated from the main crest. Anterior to the base of this merged crest is a distinct isolated buccal cuspule. This cuspule begins a very short incipient buccal cingulum which terminates below the second ridgelet of the main crest. Anterior-buccal cingulum absent. Antero-lingual pocket well-developed. A crest runs lingually from the anterior-most cusp of the main crest to form the posterior margin of the antero-lingual pocket. The posterior margin of the antero-lingual pocket is boarded by a tall crest. Lingual cingulum well developed, high and lobate. Lingual basin deep with

distinct basin cristae running buccally, perpendicular from the axis of the main crest. Postero-lingual pocket well developed and low on the tooth crown in posterior aspect. Similarities with *Bohra wilkinsonorum* include; merged postero-buccal cuspule; deep postero-lingual pocket; anterior crest of anterior-most cusp of main crest carries to crown base; antero-buccal cingulum absent; well-developed postero-lingual cusp; similar length.

Differences to *Bohra wilkinsonorum* include; possession of accessory postero-buccal cuspule; deeper lingual basin; better developed lingual cingulum; broader postero-lingual pocket; distinct perpendicular cristae within lingual basin; antero-lingual basin present; lingual cingulum bowed lingually at approximately  $\frac{1}{2}$  the length of premolar; wider posterior margin.

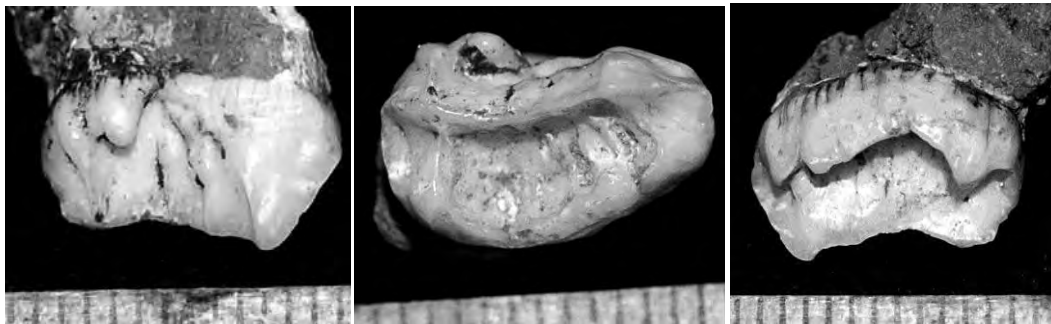


Figure 4-60. *Bohra* sp. nov. 1 from Mt Etna (QML1311 H), isolated RP<sup>3</sup>.

#### ***Bohra* sp. nov. 2.**

QML1311C/D

*Bohra* sp. nov. 2 is represented by a right P<sup>3</sup>, M<sup>2 or 3</sup> & M<sup>4</sup>.

The occlusal profile is sub-rectangular with rounded anterior and posterior margins with a main crest dividing the premolar into two sections. The main crest originates anteriorly at the base of the tooth crown, connects with the anterior-most distinct cusp, then forming a long straight crest to the posterior-most cusp. One small indistinct cuspule is central on the main crest with a single ridgelet. The posterior-most cusp possesses a postero-lingual crista running along the posterior margin of the postero-lingual cusp. Postero-buccal cusp distinct, connected to the buccal margin of the main crest via a short horizontal link. Buccal cingulum incipient, made up of isolated large buccal cuspules, the largest of which is toward the middle (buccally) of

the main crest. Two smaller cuspules are placed posterior to this largest cuspule. Antero-lingual basin absent. Lingual cingulum well developed starting from the anterior-most lingual margin and terminating anterior of the postero-lingual cusp. Lingual cingulum divided between the 1<sup>st</sup> and 2<sup>nd</sup> third; and 2<sup>nd</sup> and 3<sup>rd</sup> third of length by distinct clefts. Lingual cingulum lobate. Lingual basin well developed with low perpendicular crests. Postero-lingual cuspule broad with crest connecting lingual margin of main crest.

Similarities with *B. wilkinsonorum*: Similar overall length and width; anterior crest of anterior-most main crest cusp runs to the base of the crown; antero-lingual pocket absent; lingual cingulum present and well-developed; lingual cingulum straight and lobate; less distinct perpendicular lingual basin crests; deep postero-lingual pocket.

Differences from *B. wilkinsonorum*: better developed margin of the lingual cingulum; deeper lingual basin; broader postero-lingual pocket; distinct buccal cuspules; distinct postero-lingual cusp; reduced cuspules on main crest (1 cuspule vs 3 in *B. wilkinsonorum*).

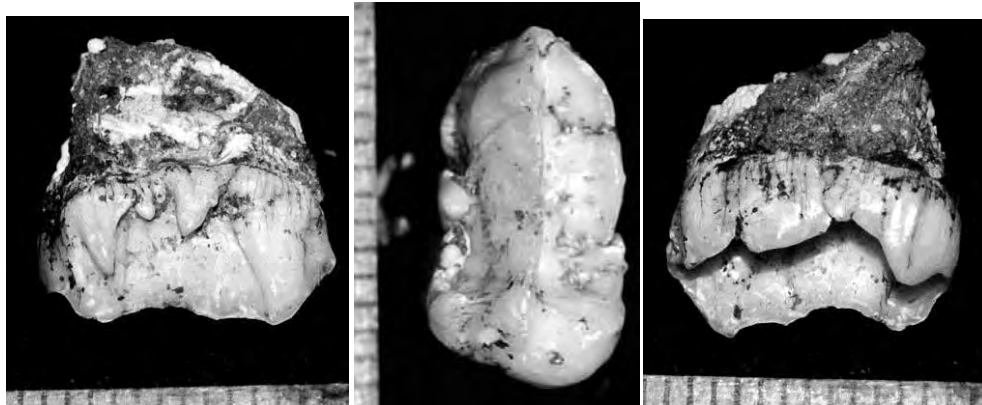


Figure 4-61. *Bohra* sp. nov. 2 from Mt Etna (QML1311 CD), isolated RP<sup>3</sup>.

### ***Bohra* sp. nov. 3**

QML1311H

*Bohra* sp. nov. 3 is represented by a right P<sup>3</sup>.

Profile in occlusal view, inflated and ovoid with main crest running along centre of premolar with two distinct cusps at anterior and posterior margins. Two indistinct cuspules at the centre of the main crest running between the anterior and posterior-most cusps. Anterior crest of anterior-most cusp runs anteriorly to the crown base.

Posterior crest runs from the posterior-most cusp to the crown base. Postero-buccal cuspule merged with buccal edge of the main crest. Buccal cingulum runs along buccal margin to midway along tooth. No anterior buccal cingulum. Lingual cingulum well developed and lobate. Perpendicular crests run from lingual margin of main crest to buccal edge of lingual cingulum. Postero-lingual cusp distinct with an accessory cuspule anterior of it. Postero-lingual pocket shallow and divided by crest.

Similarities with *B. wilkinsonorum*: antero-lingual pocket absent; postero-buccal cingulum present; postero-buccal cuspule merged with buccal margin of main crest; antero-lingual cingulum not well developed.

Differences from *B. wilkinsonorum*: occlusal profile ovoid and inflated; fewer main crest cuspules and ridgelets; shallower postero-lingual pocket which is divided; presence of an accessory cusp anterior to postero-lingual cusp; distinct perpendicular cristae within lingual basin; lingual cingulum better developed and lobate.

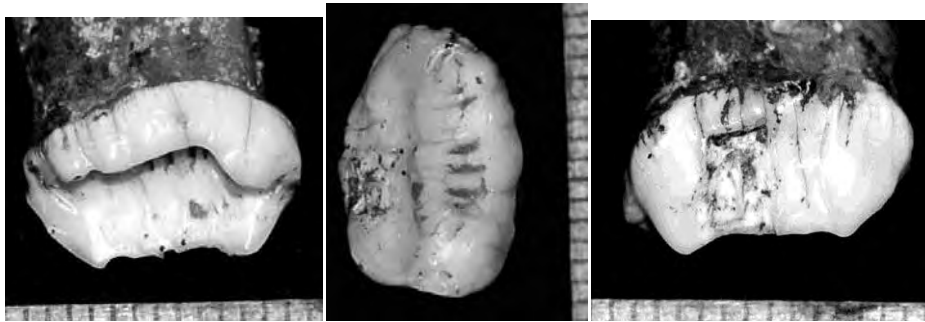


Figure 4-62. *Bohra* sp. nov. 3 from Mt Etna QML1311 H, isolated RP<sup>3</sup>.

### **Kurrabi** sp. 1

*Kurrabi* sp. 1 is here defined on the basis of two upper premolars, a RP<sup>3</sup> and a LP<sup>3</sup>. These specimens represent a species of *Kurrabi* that possess the following features; elongate-ovoid premolar in occlusal view; main crest with distinct anterior-most cusp; anterior-most crest gently slopes to the anterior margin, producing a pointed anterior margin; 2 small cuspules and associated ridgelets along the midline of the main crest; a blade-like posterior-most cusp; shallow and low postero-lingual pocket and low rounded postero-lingual cusp; postero-buccal cusp absent; lingual cingulum well-developed running to below the anterior-most cusp; a crest connects the postero-lingual cusp with the lingual flank of the main crest; a small cuspule is found at the midline of this crest.

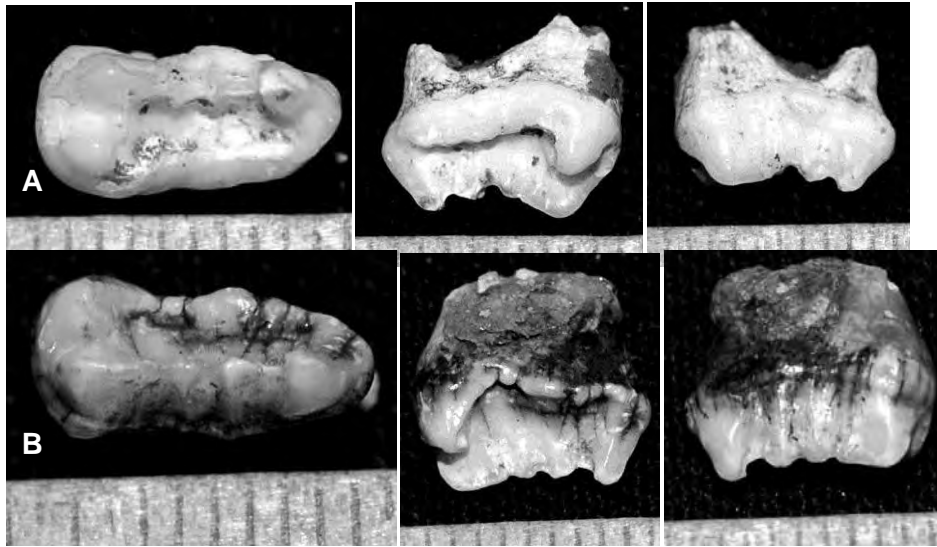


Figure 4-63. *Kurrabi* sp. 1 from Mt Etna, isolated P<sup>3</sup>s. A. QML1311 H and B. QML1311 H.

#### ***Kurrabi* sp. 2**

*Kurrabi* sp. 2 is identified here and differentiated from *Kurrabi* sp. 1 on the basis of the following features; elongate-ovoid premolar in occlusal view; anteriorly tapered (more so than *Kurrabi* sp. 1); main crest straight and blade-like with the anterior-most cusp contributing to the crest (versus a distinct cusp in *Kurrabi* sp. 1); 2 very small cuspules on the main crest with very short indistinct ridgelets; lingual cingulum well developed and widest posteriorly (versus equal width along its length); anterior margin of lingual cingulum connects to base of anterior crest of the central crest; buccal cingulum absent; postero-buccal cuspule absent; postero-lingual cuspule attaches to main crest via a short crest.

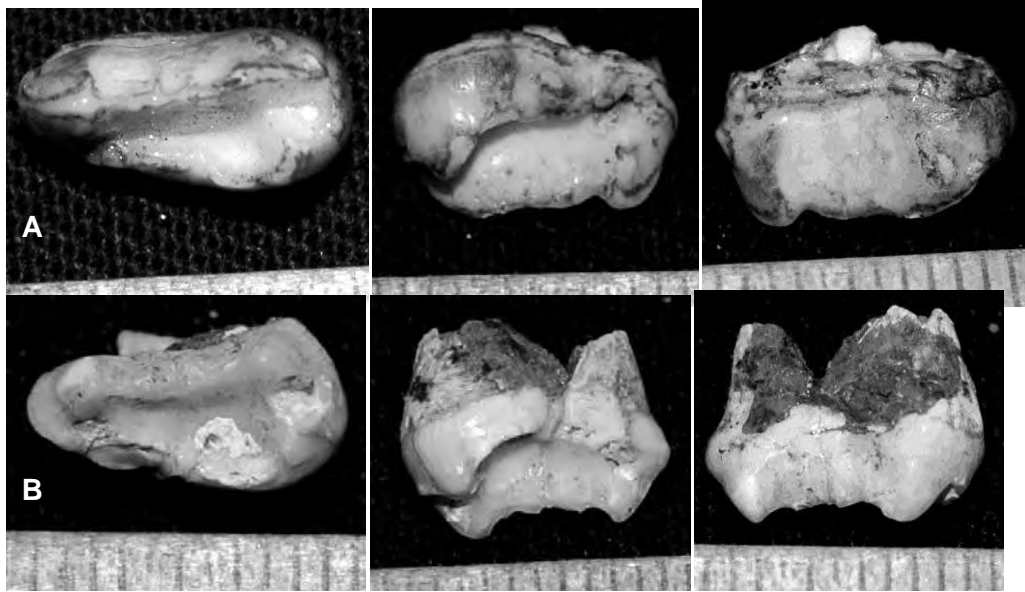


Figure 4-64. *Kurrabi* sp. 2 from Mt Etna, isolated P<sup>3</sup>s. A, QML1311 H, B. QML1311H.

#### STHENURINAE

Sthenurine indet.

cf. *Simosthenurus* sp.

Although macropod dental remains are common from the deposits at Mt Etna, only a single anterior half of a lower molar represents the Sthenurinae. This in stark contrast to the similar-aged Middle Pleistocene deposits of southern Australia (Prideaux et., al., 2007), where sthenurines are diverse and common elements within the fauna. The single molar is tentatively referred to *Simosthenurus* based on its low-crown, overall size and relatively weak anterior crenulations running anterior of the protolophid.



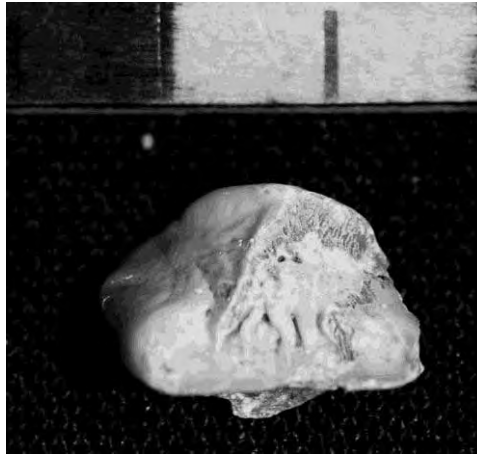


**Figure 4-65. cf. *Simosthenurus* sp. from Mt Etna, isolated M<sub>1or2</sub>. (QML1311 H)**

#### Family PSEUDOCHEIRIDAE (Winge, 1893)

Pseudocheirids are among the most abundant and diverse marsupials within the Middle Pleistocene ( $\geq 280\text{ka}$ ) localities at Mt Etna. Additional specimens have been recovered since Hocknull (2005) which allow for a better understanding of overall diversity and morphological variation, including isolated specimens of new additional taxa.

#### **Gen. et sp. nov.**

**MATERIAL.** An isolated left M<sub>2</sub> or M<sub>3</sub>, QML1311 CD

An isolated molar represents this new genus, which is distinguished from all other pseudocheirids by the combination of the following unique features; 1. Presence of a unique cristid originating from the anterior termination of the cristid obliqua and the posterior termination of the postprotocristid, running lingually into a pocket developed by the lingual emargination of the metastylid. 2. A distinctly lingual metastylid, with lingual margin being the lingual-most margin of the entire lingual molar edge. 3. Distinct entostylid crest contacting postentocristid. 4. Blade-like premetacristid. 5. Minor crenulations.

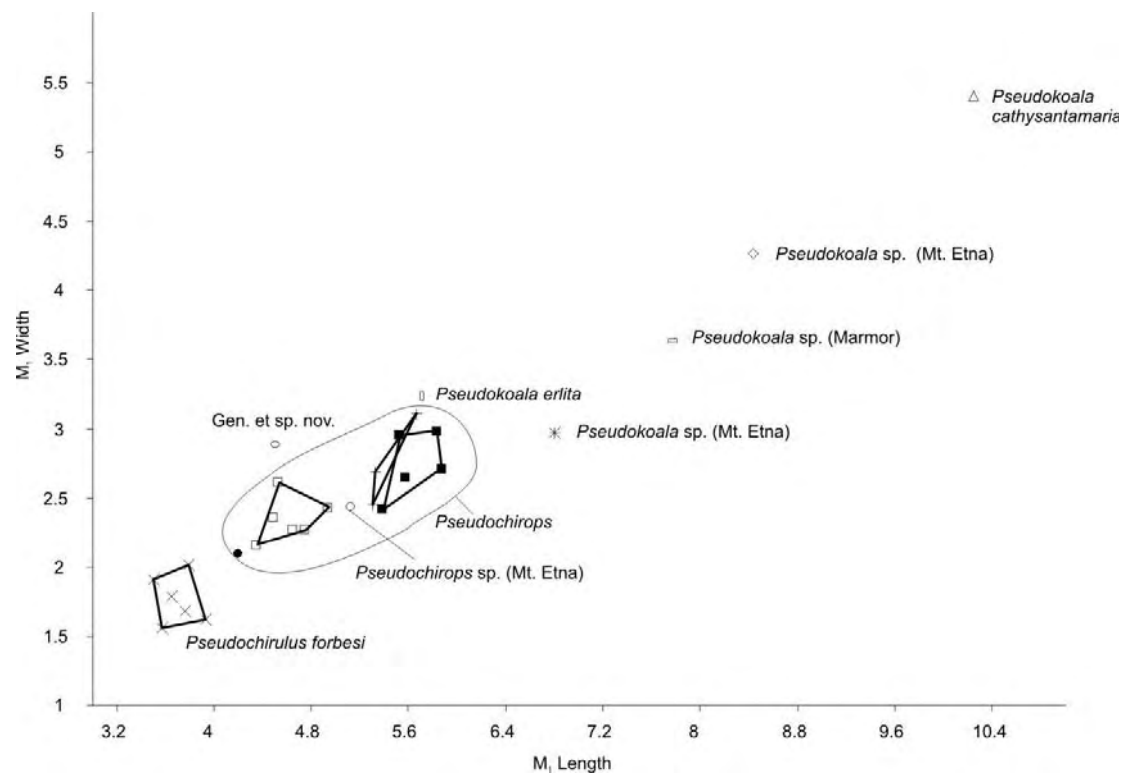


Figure 4-66. Bivariate plot of  $M_1$  Length to Width of large pseudocheirids, including a new genus, *Pseudochirops* and *Pseudokoala* from Mt Etna.

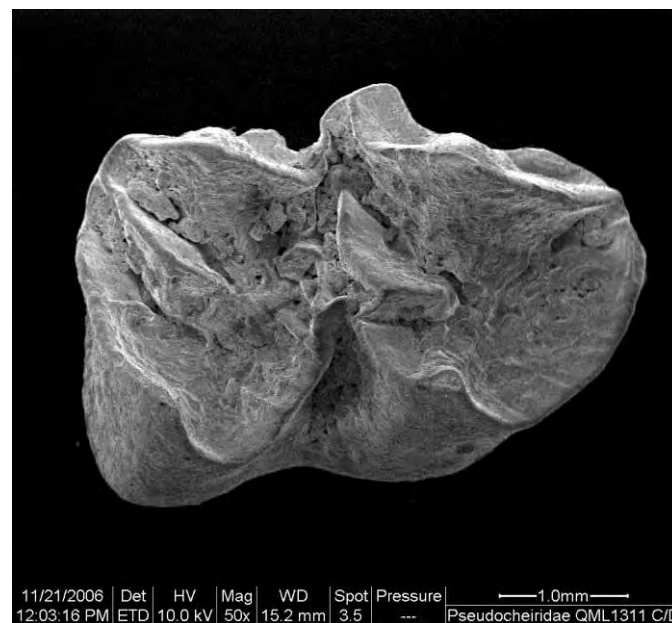


Figure 4-67. New genus of pseudocheirid from Mt Etna, isolated  $M_{2or3}$  from Mt Etna (QML1311 C/D).

### Pseudokoala

Three species of *Pseudokoala* are represented in the Middle Pleistocene sites at Mt Etna and Marmor Quarry. Each differs in overall size (Fig. 4-66) and morphology. Detailed descriptions of these taxa will await a fuller review of the pseudocheirids from Mt Etna and Marmor Quarry. Below is a short comparative analysis of the taxa so far recognised.

### ***Pseudokoala* sp. nov. 1**

The largest member referable to *Pseudokoala* is represented from two deposits (QML1384LU and QML1311 H) by two isolated lower molars, a right M<sub>1</sub> and a right M<sub>2</sub> respectively. Based on size alone, these specimens fall between *P. curramulkensis* and *P. cathysantamaria*. On morphological grounds they are closest to *P. erlita*, however, easily differentiated from this taxon. The M<sub>1</sub> does not possess the buccal buttressing of the protoconid as seen in *P. cathysantamaria*. It also does not possess a posteriorly extended postentocristid, which is present to a small degree in *P. curramulkensis* and a great degree in *P. cathysantamaria*. The new species uniquely possesses a greater degree of crenulations and buccal cuspules within the median valley anterior-buccal of the cristid obliqua.

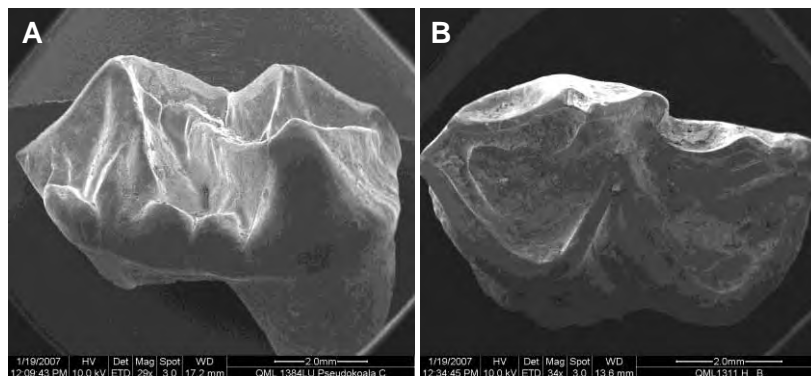


**Figure 4-68. *Pseudokoala* sp. nov. 1 from Mt Etna. A. RM<sub>1</sub> QML1384LU, B. RM<sub>2</sub> QML1311H.**

### ***Pseudokoala* sp. cf. *P. curramulkensis***

The second largest species of *Pseudokoala* from the Middle Pleistocene is represented from two localities (QML1311 C/D and Marmor Quarry) by two isolated lower molars, a RM<sub>2 or 3</sub> and a LM<sub>2 or 3</sub> respectively. The molars are generally more elongate than those available for *P. erlita* and *P. cathysantamaria* (only known from M<sub>1</sub>). The specimens compare most favourably with *P. curramulkensis* in size and relative

proportions. In addition the lack of crenulations, high bladed cristids and lack of elongate postentocristid suggest that there is a very close morphological correspondence with *P. curramulkensis*.

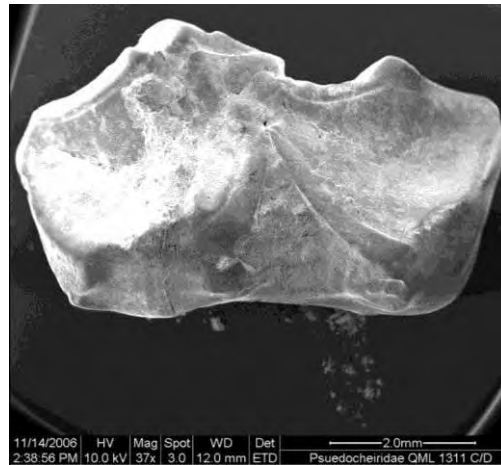


Figure 4-69. *Pseudokoala* sp. cf. *P. curramulkensis* from Mt Etna QML1311C/D (RM<sub>2</sub>).

#### ***Pseudokoala* sp. cf. *P. erlita***

The smallest species of *Pseudokoala* is only currently known from a single locality (QML1385) and is represented by three or possibly four specimens. A LM<sub>2</sub> is the best preserved specimen and is close in size to *P. erlita*. Although heavily worn, it still preserves the remains of crenulations in the taloned, which is most similar to *P. erlita*, relative to all other described taxa. It does not possess any posterior extension of the postentocristid, which it shares with *P. erlita*. Based on these very similar morphological and morphometric features it will be compared here to *P. erlita* until better material of all *Pseudokoala* taxa is known.

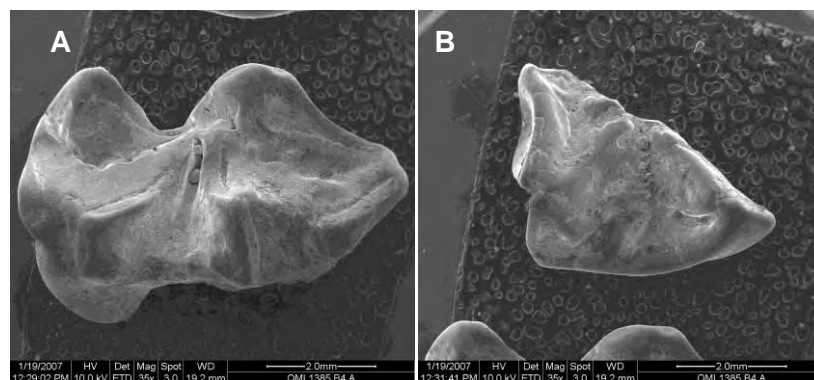


Figure 4-70. *Pseudokoala* sp. cf. *P. erlita* from Mt Etna. A. LM<sub>2</sub> (QML1385), B. M<sup>2or3</sup> (QML1385).

## Pseudochirops

At least three, and possibly several more, species of *Pseudochirops* are known from the Middle Pleistocene sites at Mt Etna. Based on upper molar size alone, there are two morphometric size classes, however, morphologically lower dentition conveys a broader arrangement of taxa, including a very small-sized taxon referable to *Pseudochirops*.

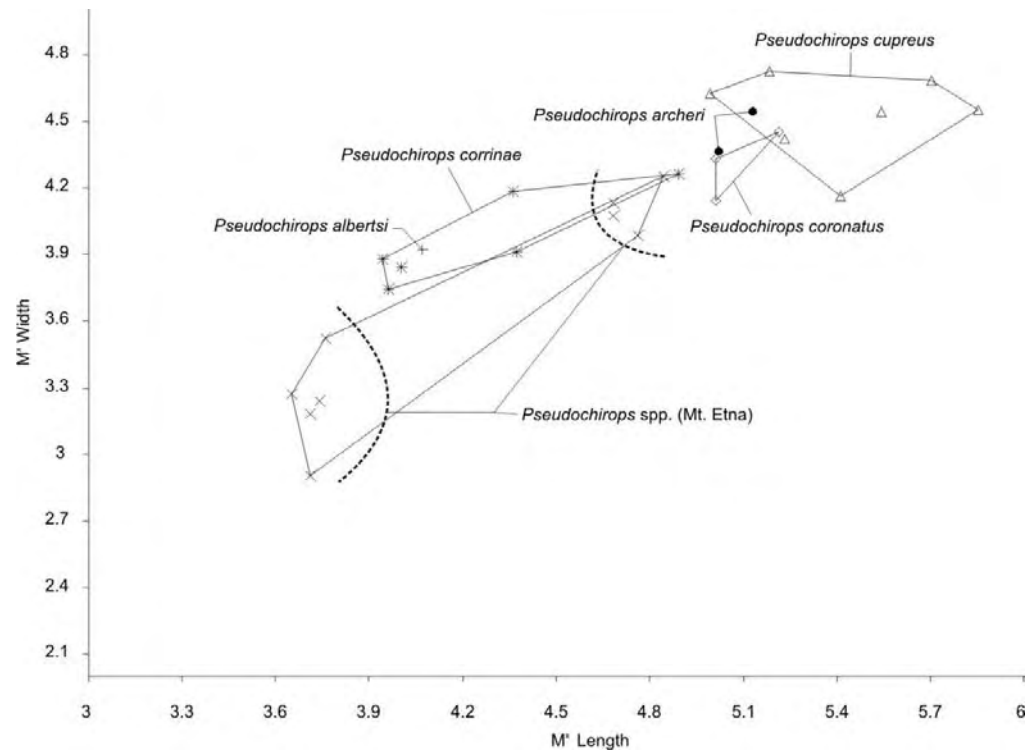
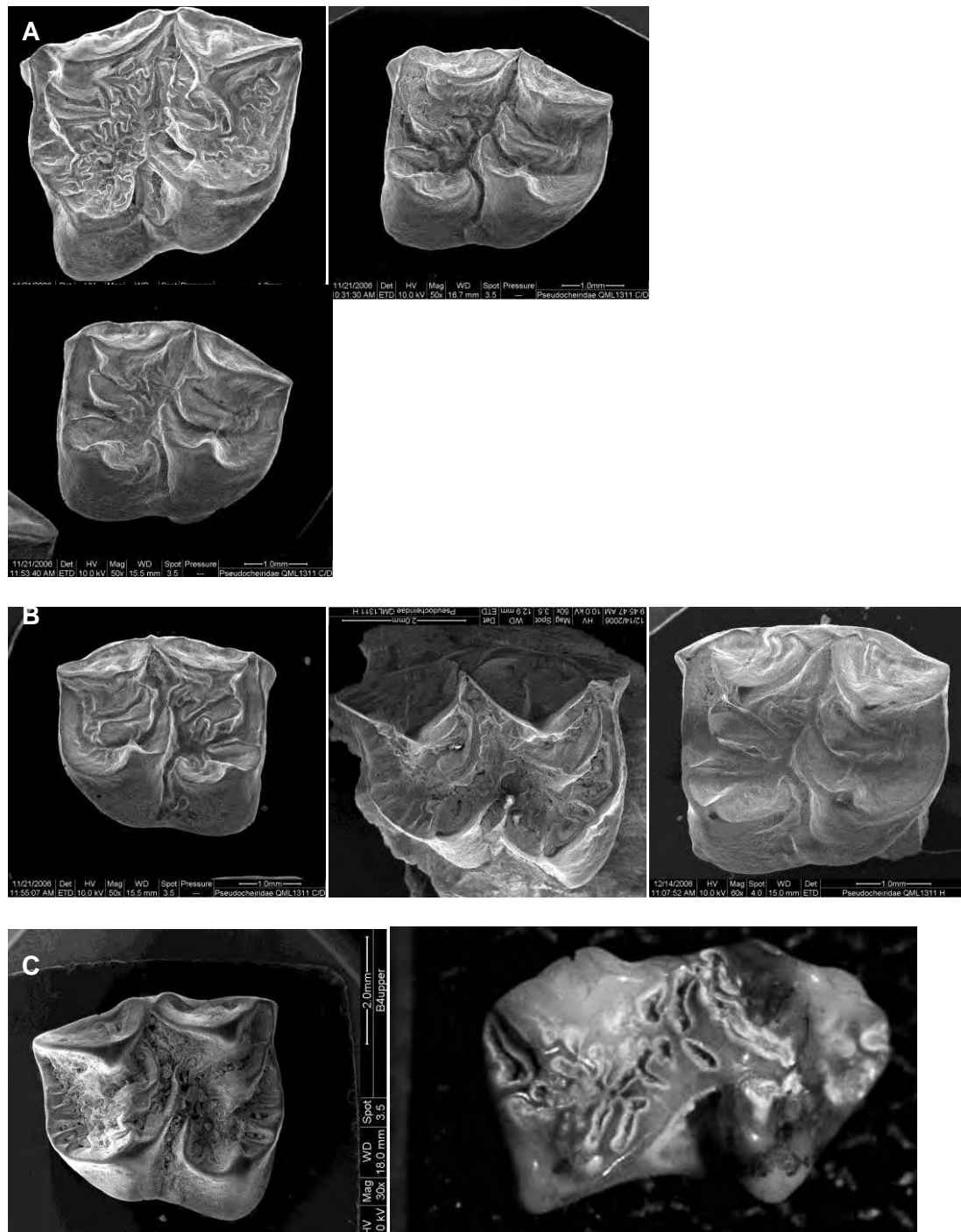


Figure 4-71. Bivariate plot of M<sup>1</sup> length to width for fossil and modern *Pseudochirops*.

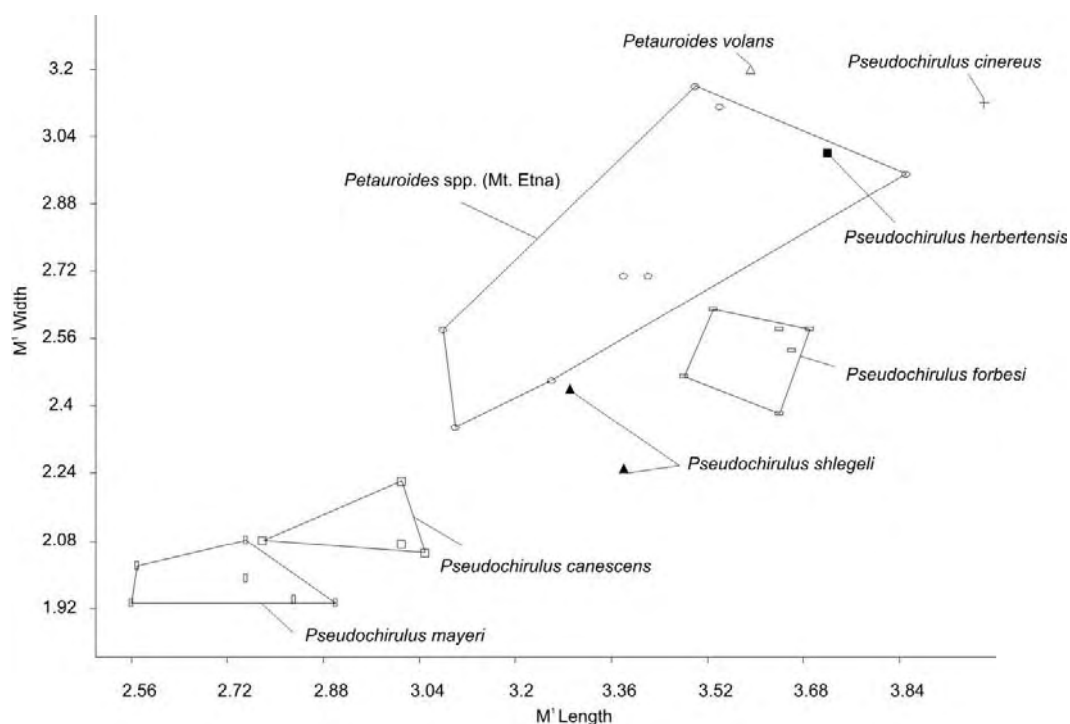


**Figure 4-72. Fossil *Pseudochirops* from Mt Etna, isolated upper molars. A. M<sup>1</sup>s QML1311CD, QML1311CD, QML1311CD. B. M<sup>2</sup> QML1311CD, M<sup>1</sup> QML1311H, M<sup>1</sup> QML1311H. C. M<sup>x</sup>s QML1385, QML1385.**

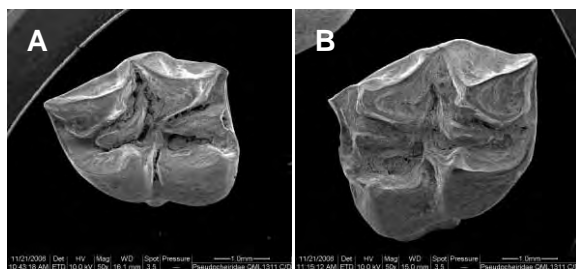
### Petauroides

Hocknull (2005) and Hocknull et. al (2007) identified *Petauroides* from Mt Etna. Morphometric analysis of upper molars referable to *Petauroides* show distinctions of taxa on the basis of size-class, with small-sized *Petauroides* close in size to

*Pseudochirulus schlegeli*, medium-sized *Petauroides* close to *Pseudochirulus forbesi* and large *Petauroides* close to *Pseudochirulus herbertensis* and *Petauroides volans* (Fig. 4-73).



**Figure 4-73.** Bivariate plot of M<sup>1</sup> length to width for fossil and modern *Petauroides* and *Pseudochirulus*.



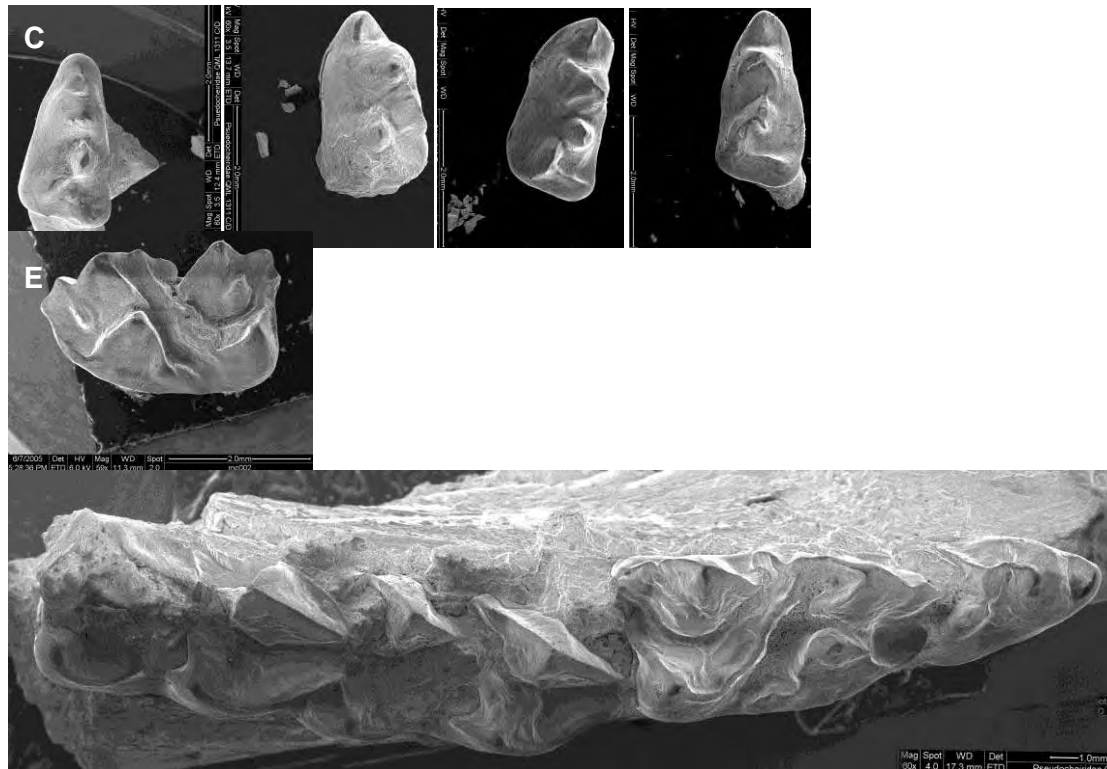
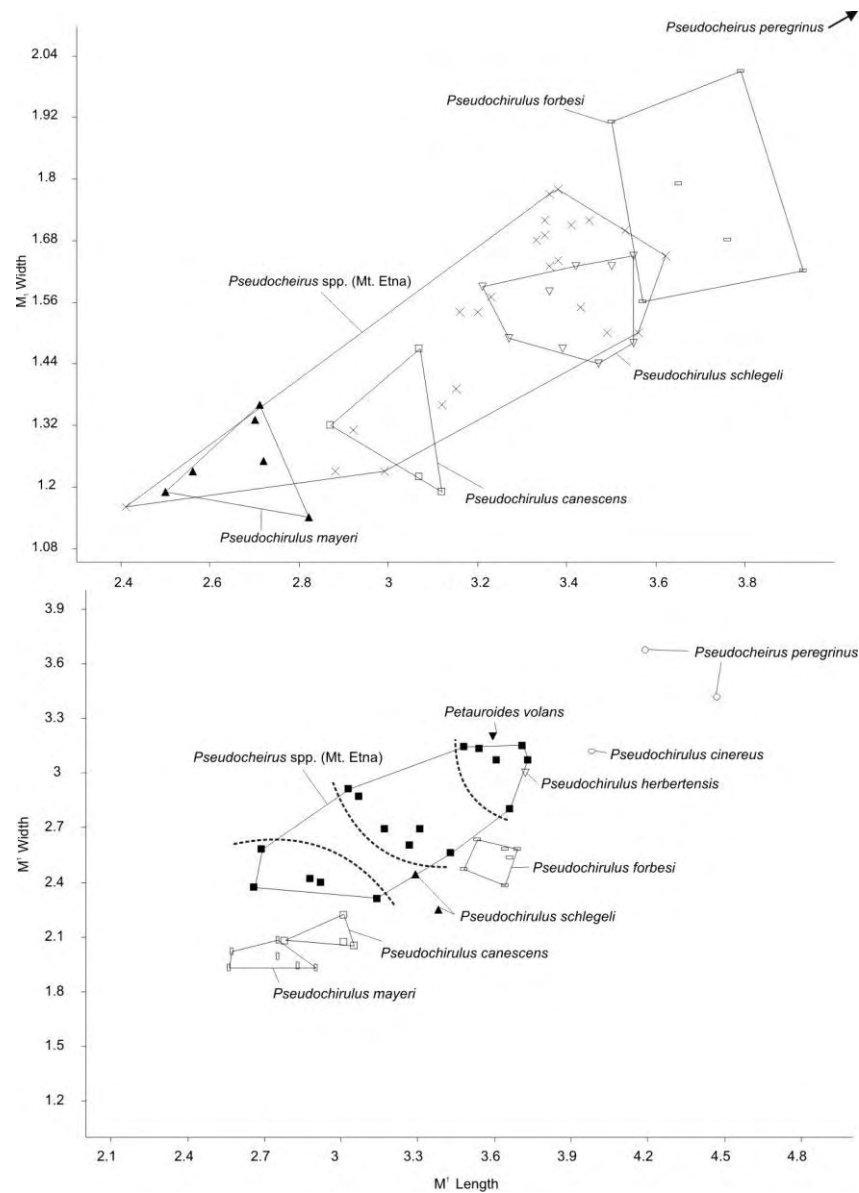


Figure 4-74. Fossil *Petauroides* from Mt Etna. A. M<sup>1</sup> QML1311CD, B. M<sup>1</sup> QML1311CD. C, P<sub>3</sub> QML1311CD, QML1311CD, QML1311H, QML1311H, D. M<sub>1</sub> QML1284. E. RP<sub>3</sub>-M<sub>3</sub> QML1313.

### **Pseudocheirus**

Hocknull (2005) and Hocknull et al (2007) list three species of *Pseudocheirus* from Mt Etna. Morphometric analysis of *Pseudocheirus* upper and lower first molars show that there are three clearly distinct size-classes which correspond to the three taxa suggested by Hocknull (2005), all being markedly smaller than *Pseudocheirus peregrinus* and *Pseudocheirus occidentalis*. The three size classes are comparable to species-level size classes seen in *Pseudochirulus*. The small-size class is close to *P. mayeri* and *P. canescens*; the medium-size class is close to *P. schegeli* and *P. forbesi*; the large size class is close to *P. herbertensis* and *Petauroides volans* (Fig. 4-75).





**Figure 4-75. Bivariate plots of  $M_1/M_1$  length to width for fossil and modern *Petauroides*, *Pseudochirulus* and *Pseudocheirus*.**



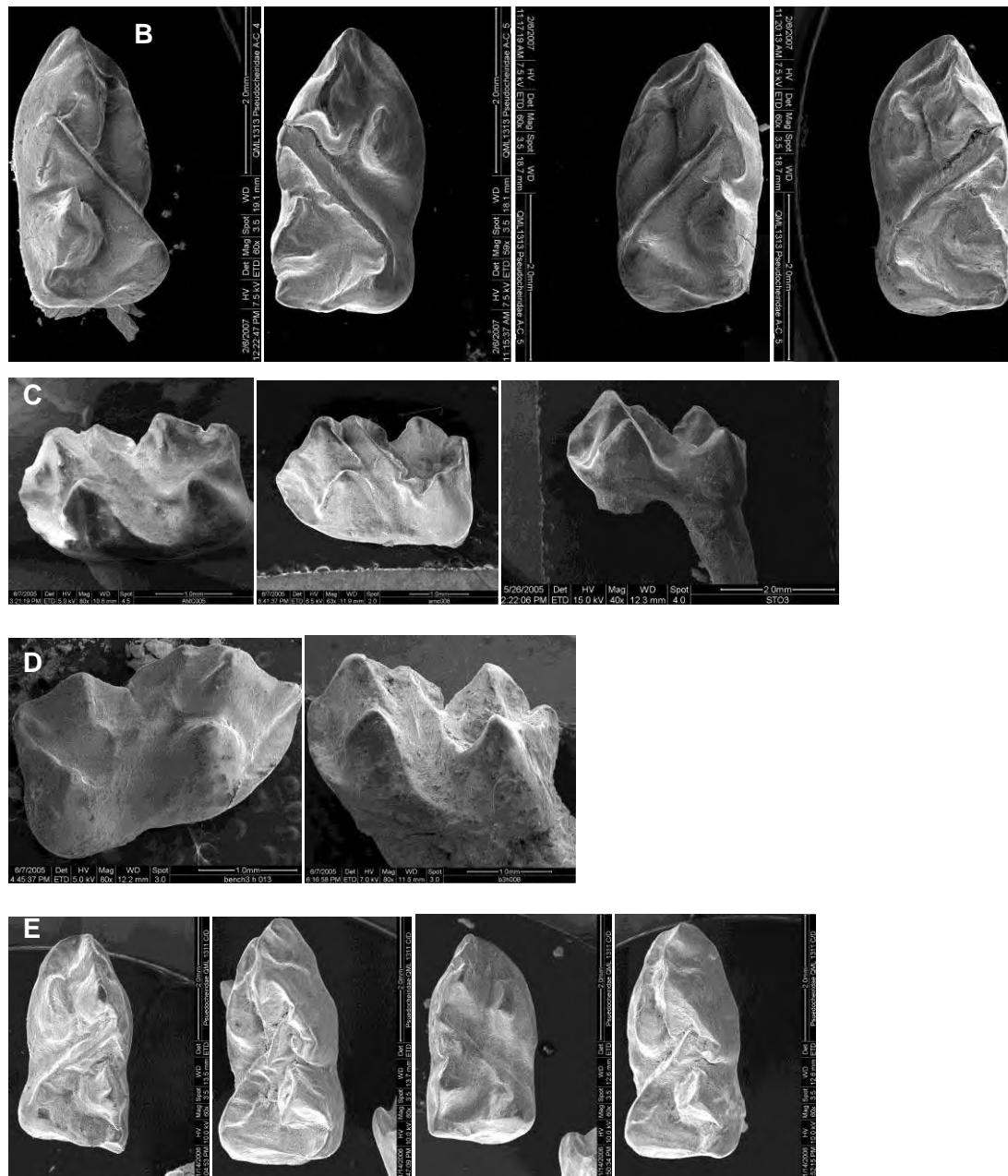
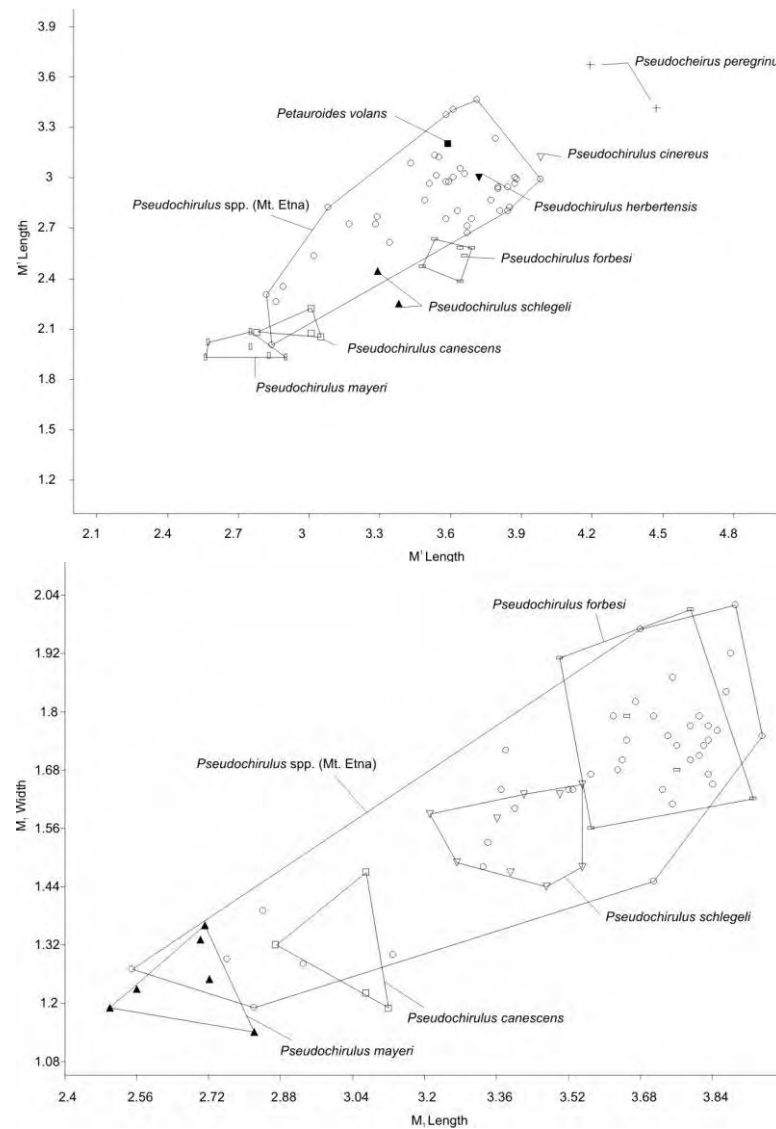


Figure 4-76. Fossil *Pseudochairus* from Mt Etna, lower dentition. A.  $P_3$ s, B-E.  $M_1$ s.

### **Pseudochirulus**

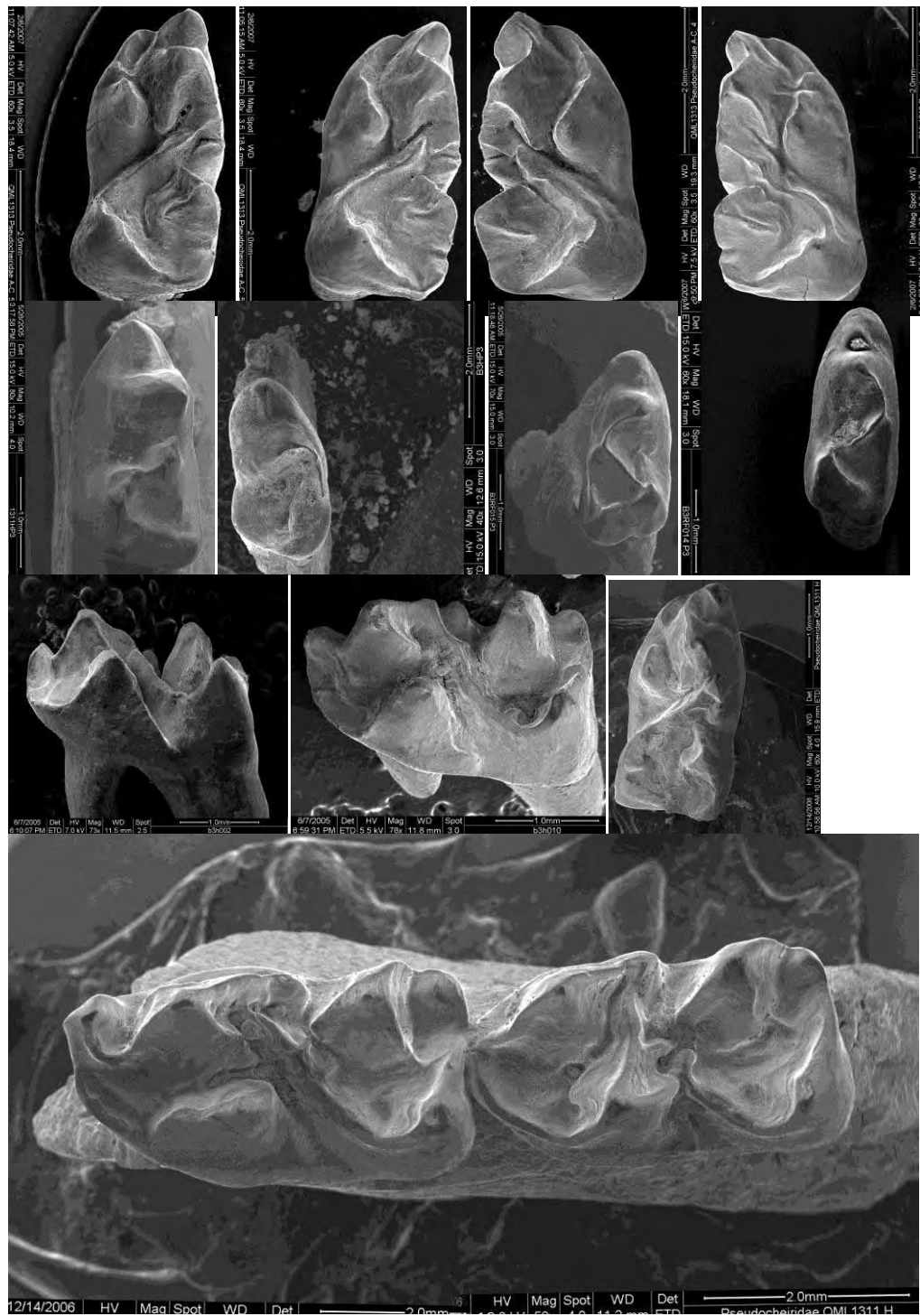
Hocknull (2005) and Hocknull et al (2007) list three species of *Pseudochirulus* from Mt Etna. Morphometric analysis of upper and lower first molars concur with this assignment and suggest an increase in the number of distinct taxa to four (Fig. 4-77). This will need to be verified on morphological grounds. Lower molars in particular elude to there being four distinct size classes within the sample from Mt Etna,

including two taxa clustering with *P. mayeri* and *P. canscens* respectively, and two taxa clustering with *P. schegeli* and *P. forbesi* respectively. Again, these will need to be verified on morphological grounds, however, strongly support the increased taxonomic diversity and size-class ranges seen at Mt Etna in morphologically distinct pseudocheirid lineages.



**Figure 4-77. Bivariate plots of  $M_1/M_1$  length to width for fossil and modern *Pseudochirulus*.**





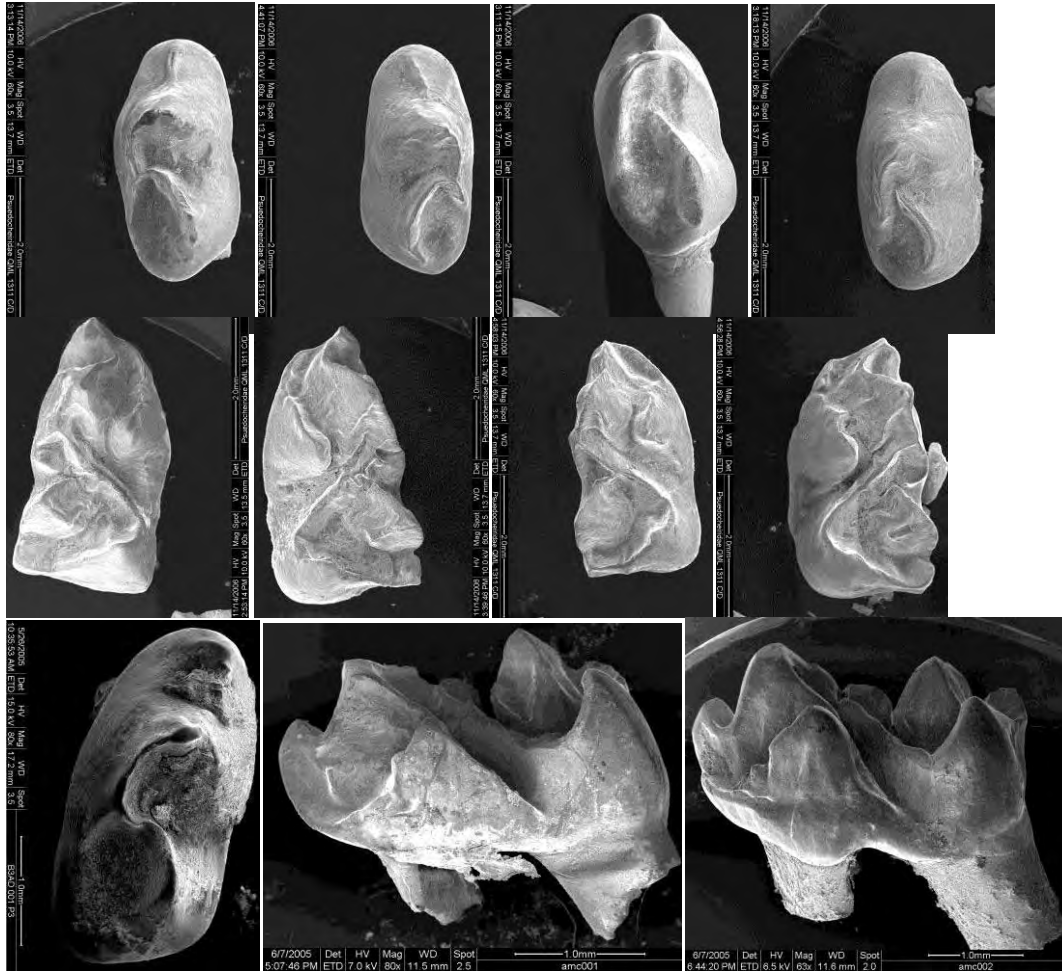


**Figure 4-78. Fossil *Pseudochirulus* from Mt Etna, lower dentition. P<sub>3</sub>s and M<sub>1</sub>s.**

### Characteristic of Pseudocheiridae

#### Lower Molars:

1. 1.[1] Protostylid, M1 (0) Absent, (1) Present.
2. Shape of protostylid, M1 (0) low and conical, (1) high and pyramidal, (2) high and blade-like.
3. Position of protostylid. (0) anterior of metaconid, (1) equal to metaconid.
4. [3] Protostylid basin, M1. (0) Absent, (1) Present.

5. Posterior ridge of protostylid basin (made up by the bprcd & popstd) M1. kinked medially (0), rounded medially (1).
6. Anterior ridge of protostylid basin (made up by the prpstd linking to the pacd). M1. Linked (0), not linked (1)
7. [14] Posterobuccal trigonid basin (on M2-4). Absent (0), Present (1)
8. Entostylid ridge (M1). absent (0), present, connected to pen (1), present, not connected to pen
9. [5] Preentocristid connected to the metasylid. Absent (0), Present (1).
10. [~6] Cristid obliqua M2-4. Connects to poprcdM2-4 (0), curves buccally to end at the base of the protoconid M2-4(1), Connects to poprcd M2-3 with M4 curving buccally to end at protoconid base (2).
11. Protocristid connects to metastylid M2-4. No (0), just buccally of metastylid (1), fully (2).

### P3

12. Crest (paracristid?) between paraconid and protoconid. (0) Absent, (1). Present
13. Crest (paracristid?) shape between paraconid and protoconid. (0) arcuate, (1) straight, blade-like, absent (2)
14. Posthypocristid. (0) Weak or absent (1) short and rounded posteriorly, (2) long and straight to posterior margin, tiny ending in a cleft (3).
15. Posterior protoconid basin. (0) Absent, (1) Present.
16. Relative length / width of P3

17. Tooth crenulations P3-M4. Absent (0), Present (1).

#### Upper Molars

18. Preprotoconule crista termination (M1). (0) base of the parastyle, (1) links to parastyle, (2) links to preprotocrista, (3) base of the paracone.

19. Preprotoconule crista termination (M2-4). (0) base of the parastyle (M2-4), (1) links to preprotocrista (M2-4), (2) links to preprotocrista (M3-4), (3) links to the base of the paracone (M2-4).

20. Protostyle (ps). Weak or absent (0), Present and strongly developed (1).

21. lingual cingulum between protocone and metaconule. Absent (0), Present (1).

22. Anterolingual paracristae (M1-4) (0) absent or not well developed, (1) well developed.

23. Anterolingual metacristae. (M1-4) (0) not well developed, (1) well developed.

24. Posterolingual paracristae. (0) not well developed, (1) Moderately developed, (2) well developed.

25. Posterolingual metacristae. (0) not well developed, (1) Moderately developed, (2) well developed.

26. Crest labial to protostyle. (0) Absent or weak, (1) Present.

27. Posterior bifurcation of protoconule. (0) Absent, (1) Present.

28. Neometaconule unites with metacone. (0) Absent, (1) Present on M1 and M2 only, (2) Present on all molars.

29. Mesostyle Twinning. (0) Weak or absent twinning, (1) Anterior style dominant (2) Equal dominance of styles, (3) posterior dominant.

### P3

30. Preparacristae. (0) Absent, paraconule conid shaped, (1) Present, postparaconule crista crest-like, terminating at the base of paracone, (2) Present, links to paraconule, (3) Present, links to anterolingual cuspule.

31. Anterolingual paracristae. Absent (0), Present (1)

32. Posterolingual paracrista. Absent (0), Present (1)

33. Anterobuccal paracrista. Absent (0) Present, short (1), Present links to paraconule (2)

34. Paraconule. Weak or absent (0), Cone shaped (1)

35. “Neoparaconule”. Absent (0), Present as conule (1), Present as crest enlargement (2).

36. Protocone. Weak or low crest (0), distinct conical cusp (1), cuspule (2).

37. P3 Shape. Ovoid (0), Elongate-ovoid (1), Rounded-triangular (2), constricted anterior, bulbous posterior – only in *Pseudocheirops* (3)

38. Tooth crenulations P3-M4. Absent (0), Present (1)

39. P3 Ridge running buccally from postparacrista. (0) Absent (1) Present.



40. Buccal cingulum on P3. Absent (0), Present on the posterior margin (1), Present as shallow basin (2), Present as basin with cuspule (3)

#### Lowers M1

41. Protostylid relation to protoconid on M1. (0) protostylid compressed laterally and against protoconid base, producing a distinct cleft. (1) protostylid distinct from protoconid producing a wide valley between the two cusps.
42. The preprotocristid running to the paraconid. (0) absent, (1) Present, as a continuous crest with indistinct paraconid cusp. (2) Present with a mediolingual kink with distinct paraconid cusp. (3) Present, broken by cleft at the base of the paraconid.

#### P3

43. Postparaconid basin. (0) Absent, (1) Present.
44. Posterobuccal crest (cingulum) from preparacristid (0) Absent, (1) Terminates anterior to the protostylid. (2) Present, contacts the protostylid. (3) Present, contacts the protostylid with a midline cuspule (anterior of protostylid).
45. Postmetaconid basin. (0) Absent, (1) Present.
46. [7] Anterolingual shelf (als). (0) Weak or absent, (1) Well developed.
47. Preentocristid crest. (0) Absent, (1) Present, oriented ant-medially, (2) Present, oriented ant-buccally.
48. P3. Metaconid posterobuccal to protoconid. (0) Absent, (1) Present, linked to the pcd, (2) Present, not linked to the pcd by a short gap – forming a cleft, (3) Present, not linked to the pcd by a wide valley, (4) Present, continuous crest of cristid obliqua to protoconid.

49. M1 Posterobuccal crest of paraconid. (0) Absent, (1) Present (broken midway to postprotostylid cristid, small cuspule), (2) Present (connects to preprotostylid cristid), (3) double crest linking to postprotostylid cristid.
50. Lingual parastyle on M1. (0) absent, (1) present as a bladed crest from paraconid, (2) developed as an enlargement of paraconid.
51. Protostylid connected to protoconid by cristid on M1. (0) Absent, (1) Present as a high distinct link, (2) present as a low weak link.
52. Orientation of anterior margin of cristid obliqua (0) oriented antero-buccally (1) oriented buccally, then laterally at position of protoconid.
53. Buccal cingulum running from anterior buccal cingulum to transverse valley. (0) Absent, (1) Continuous cingulum from anterior buccal cingulum to tv. (2) Cingulum with cuspule in transverse valley.

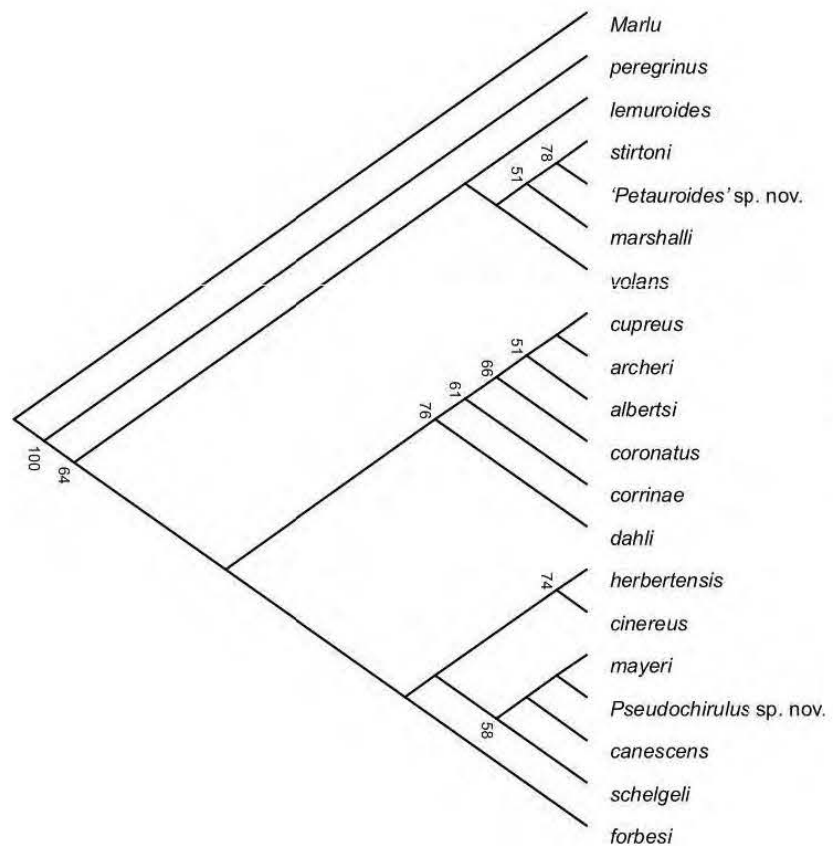
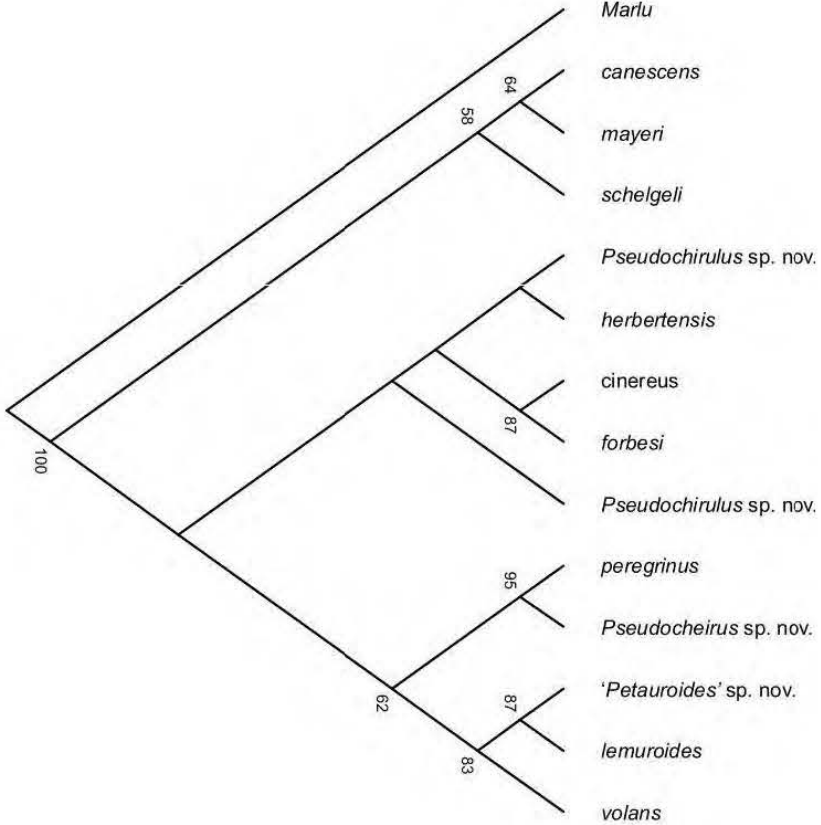


Figure 4-79. Phylogenetic analysis of pseudocheirids using upper dentition and lower dentitions. Both phylogenies report bootstrap values >50%.

## Upper Dentition

	1 8	1 9	2 0	2 1	2 2	2 3	2 4	2 5	2 6	2 7	2 8	2 9	3 0	3 1	3 2	3 3	3 4	3 5	3 6	3 7	3 8	3 9	4 0
<i>schelgeli</i>	0	0	0	0	0	0	0	0	0	0	0		1	0	0	0		0	0	2	0	0	2
<i>canescens</i>	0	0	0	0	0	0	0	0	0	0	0		0	0	0	0		0	0	1	0	0	2
<i>mayeri</i>	0	0	1	0	0	0	0	0	0	0	0		0	0	0	0		0	2	2	0	0	2
<i>peregrinus</i>	1	2	1	1	0	0	0	0	0	0	0		3	0	0	2		2	0	0	0	0	1
<i>volans</i>	1	1	0	0	0	0	1	1	0	0	0		2	1	1	0		0	2	0	0	1	2
<i>lemuroides</i>	2	1	0	0	0	0	1	1	0	0	0		1	0	1	3		0	0	3	0	0	1
<i>marshalli</i>	0	0	0	1	0	0	0	0	0	0	0		1	0	0	0		0	0	2	0	0	1
<i>stirtoni</i>	2	1	0	2	0	0	1	1	0	0	0		1	0	1	0		0	0	2	0	0	1
<i>archeri</i>	0	0	1	0	0	1	1	1	1	0	0		2	0	0	3		0	1	3	1	1	2
<i>dahli</i>	2	1	0	0	0	0	0	0	0	0	0		2	0	0	0		0	2	0	0	0	1
<i>cupreus</i>	0	0	1	1	1	1	1	1	1	1	0		2	0	0	0		0	1	3	1	0	1
<i>coronatus</i>	0	2	1	1	1	1	1	1	1	0	1		2	0	0	1		0	1	3	1	1	1
<i>corrinae</i>	0	0	1	1	0	1	1	1	0	0	0		2	0	0	0		0	2	3	0	1	1
<i>albertsi</i>	0	0	0	1	1	1	1	1	1	1	0		2	0	0	0		0	2	3	1	1	1
<i>herbertensis</i>	0	2	0	0	0	0	0	0	0	0	0		1	0	0	1		0	0	2	0	0	1
<i>forbesi</i>	3	3	0	0	0	0	0	0	0	0	0		1	0	0	1		0	0	1	0	0	1
<i>cinereus</i>	3	3	0	0	0	0	0	0	0	0	0		1	0	0	1		0	0	2	0	0	1
<i>Marlu</i>	3	0	0	0	0	0	0	0	0	0	0		2	0	0	0		0	0	0	0	0	0
<i>Pseudochirulus</i> <i>sp</i>	3	1	0	0	0	0	0	0	0	0	0		0	0	0	1		0	2	2	0	0	2
<i>Pseudochirulus</i>	3	1	1	0	0	0	0	0	0	0	0		1	0	0	1		0	0	2	0	0	1
<i>Pseudocheirus</i>	1	2	0	1	0	0	0	0	0	0	0		3	0	0	0		1	0	0	0	0	1
<i>Petauroides</i>	2	1	0	0	0	0	1	1	0	0	0		1	0	1	0		0	0	0	0	0	2

Table 4-3, pseudocheirid character matrix for upper dentition.

## Lower Dentition

	1 1	2 2	3 3	4 4	5 5	6 6	7 7	8 8	9 9	10 0	11 1	12 2	13 3	14 4	15 5	16 6	17 7	18 8	19 9	20 0	21 1	22 2	23 3
<i>schelgeli</i>	1	2	0	0	0	0	2	1	0	0	2	1	0	0	0	0	0	0	2	1	0	0	0
<i>canescens</i>	1	0	0	0	0	0	2	1	0	0	2	1	0	1	0	0	0	0	2	1	0	0	0
<i>mayeri</i>	1	0	0	0	0	0	2	1	0	0	0	1	0	0	0	0	0	0	2	1	0	0	0
<i>peregrinus</i>	1	0	0	0	0	0	0	0	0	0	1	1	1	0	0	0	0	1	4	1	0	3	0
<i>volans</i>	1	0	0	0	0	2	0	2	1	0	3	1	0	0	0	0	0	1	1	2	0	0	0
<i>lemuroides</i>	1	2	0	0	0	0	0	2	1	0	2	1	0	0	1	0	1	1	1	1	0	4	0
<i>marshalli</i>	1	0	0	0	0	3	1	2	1	0	3	1	0	0	1	0	1	1	1	1	0	0	0
<i>stirtoni</i>	1	0	0	0	0	3	1	2	1	0	3	1	0	0	1	0	0	2	0	0	2	0	0
<i>archeri</i>	1	1	1	0	1	1	0	0	1	1	3	1	1	0	0	1	1	0	2	0	3	0	0
<i>dahli</i>	1	1	1	0	1	0	0	0	0	1	2	1	0	0	0	0	1	0	2	0	0	0	0
<i>cupreus</i>	1	1	1	1	1	1	0	0	1	1	3	1	1	0	0	2	1	0	2	0	4	0	0
<i>coronatus</i>	1	1	1	1	1	2	0	0	0	1	2	1	1	1	1	2	1	0	2	0	4	0	0
<i>corrinae</i>	1	1	1	0	1	2	0	0	1	1	2	0	0	1	1	0	1	0	2	1	0	0	0
<i>albertsi</i>	1	1	1	1	1	1	0	0	0	1	3	1	1	1	0	1	1	0	2	0	4	0	0
<i>herbertensis</i>	1	2	0	0	0	0	0	1	0	1	2	1	0	0	2	0	1	0	1	0	1	0	1
<i>forbesi</i>	1	2	0	0	0	0	0	1	0	0	2	1	0	1	2	0	1	0	1	0	4	0	0
<i>cinereus</i>	1	2	0	0	0	0	0	1	0	1	2	1	0	0	2	0	1	0	1	0	1	0	1
<i>Marlu</i>	0	?	0	0	0	0	0	0	0	0	1	4	1	0	1	0	1	1	2	0	0	0	0

<i>Pildra</i>	0	?	0	0	0	4	2	0	0	0	2	0	0	1	0	0	1	1	2	0	0
<i>Petauroides</i> sp.	1	0	0	0	0	3	1	2	1	0	3	3	0	0	0	0	0	2	0	0	2
<i>Pseudochirulus</i> sp.	1	0	0	0	0	0	0	1	?	0	0	4	2	1	0	0	0	2	3	0	0

**Table 4-4, pseudocheirid character matrix for lower dentition.**

### Family PETAURIDAE (Gill, 1872)

Hocknull (2005) and Hocknull et al (2007) list four petauroids from Mt Etna.

Williams & Hocknull are currently working on the taxonomy and phylogeny of these taxa, including a distinctly new genus with at least two new species and new species of *Dactylopsila*.

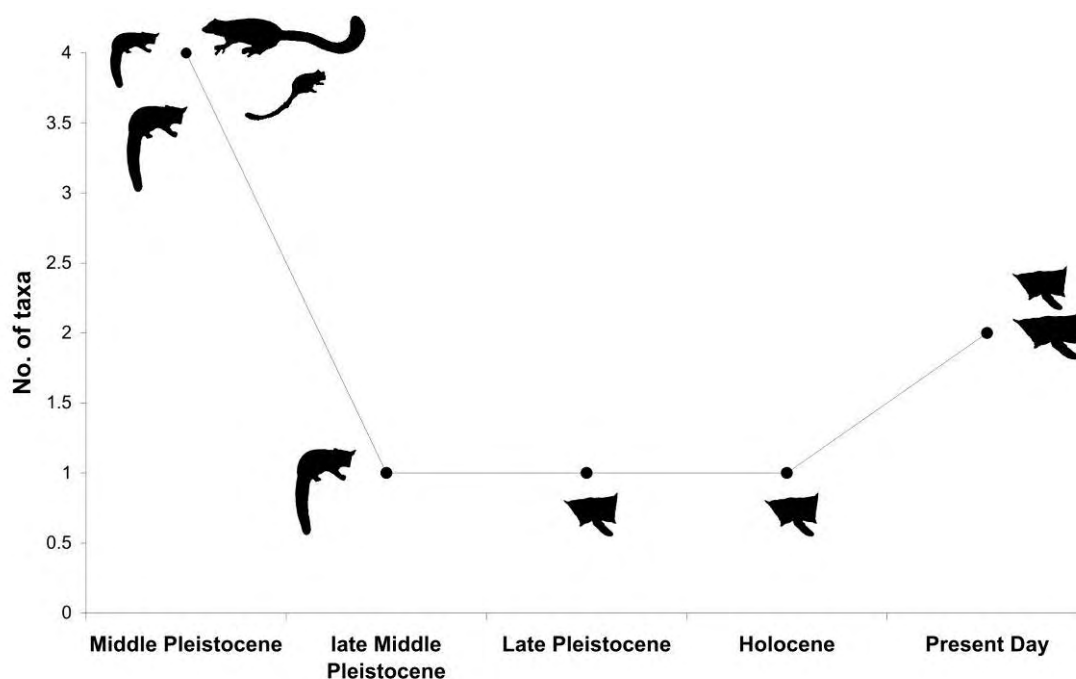


**Figure 4-80. Taxonomic diversity of petaurids through the Middle Pleistocene to present day at Mt Etna.**

	1	2	3	4	5	6	7	8	9	10	11	12	13	14	15	16	17	18	19
<i>Djaluganji</i>	1	0	0	0	0	0	0	0	0	0	0	1	0	0	0	0	0	0	0
Gen. et. sp. nov.	1	0	1	0	1	1	0	1	0	1	1	2	0	1	1	0	0	1	0
<i>Dactylopsila</i>	0	1	0	1	0	0	0	1	0	2	0	0	2	1	2	1	0	2	1
<i>breviceps</i>	1	0	1	2	1	1	1	0	1	2	1	0	1	1	2	0	1	1	1
<i>australis</i>	1	0	1	1	1	1	1	1	1	2	1	2	2	1	2	0	1	1	1
<i>norfolcensis</i>	1	0	1	2	1	1	1	1	1	2	1	1	2	1	1	0	1	1	1
<i>gracilis</i>	1	0	1	2	1	1	1	1	1	2	1	2	2	1	1	0	1	1	1
<i>Gymnobelidius</i>	0	1	2	2	1	1	1	1	1	2	1	2	2	1	2	0	1	1	1

**Table 4-4, Character matrix for petaurids (from Williams & Hocknull, in Prep).**

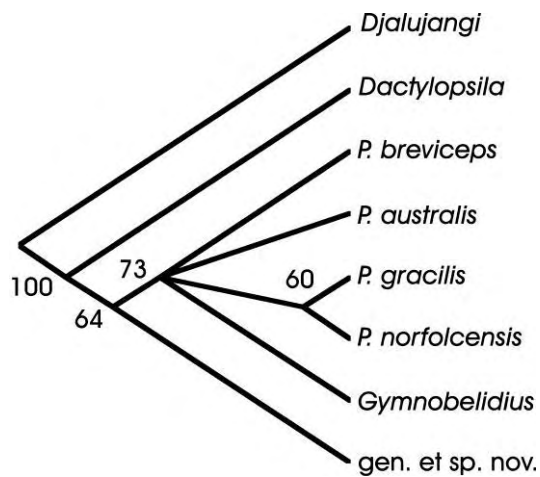
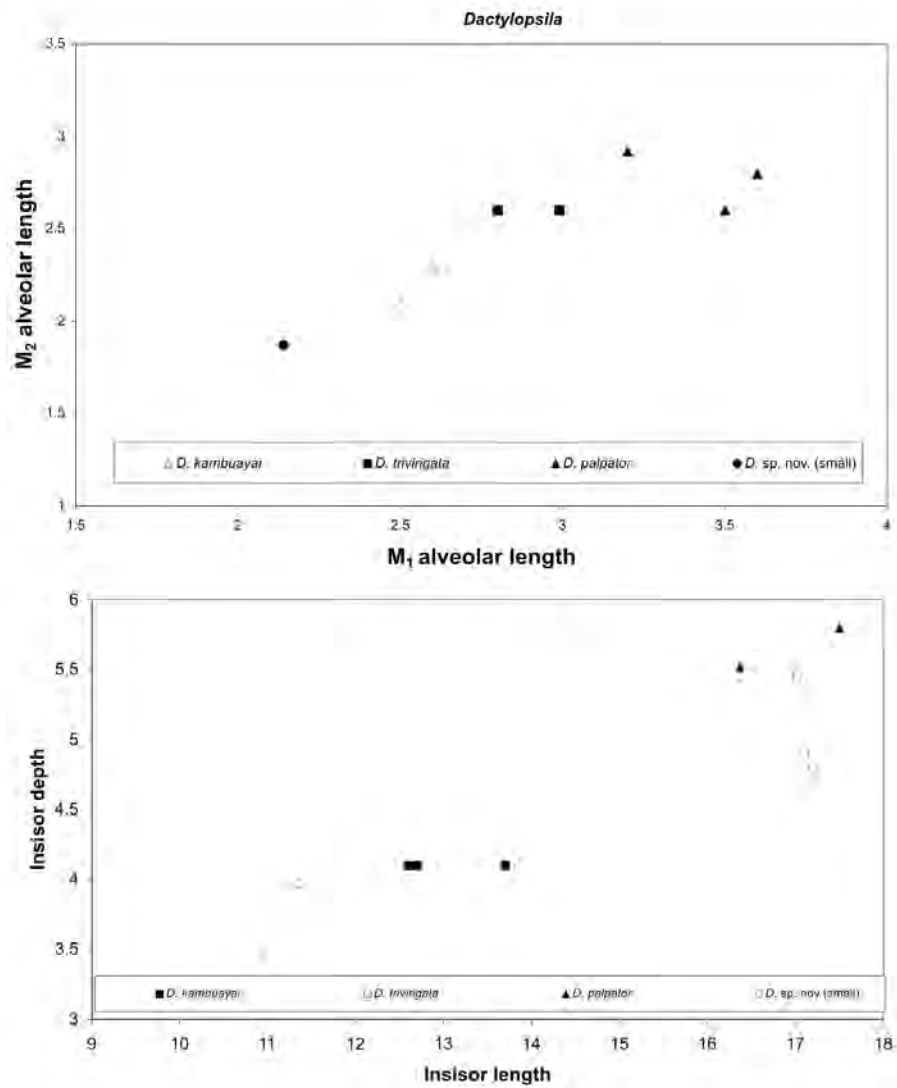


Figure 4-81 Phylogeny of petaurids at Mt Etna, showing bootstrap values over 50%.

### **Dactylopsila**

Morphometrically the fossil specimens of *Dactylopsila* fall within two distinct size classes, one very small and the other medium-sized (Fig. 4-82, 4-83). There are yet to be specimens representing the large-sized *Dactylopsila* species (*D. trivirigata* and *D. palpator*). Instead there is a species similar in size and overall morphology to *D. tatei* and another which is very small, closer to *D. kambuayai* (Holocene) from the Vogelkop of New Guinea (Aplin et al 1999).



**Figure 4-82. Bivariate plots of Incisor length to depth for fossil and modern *Dactylopsila*.**

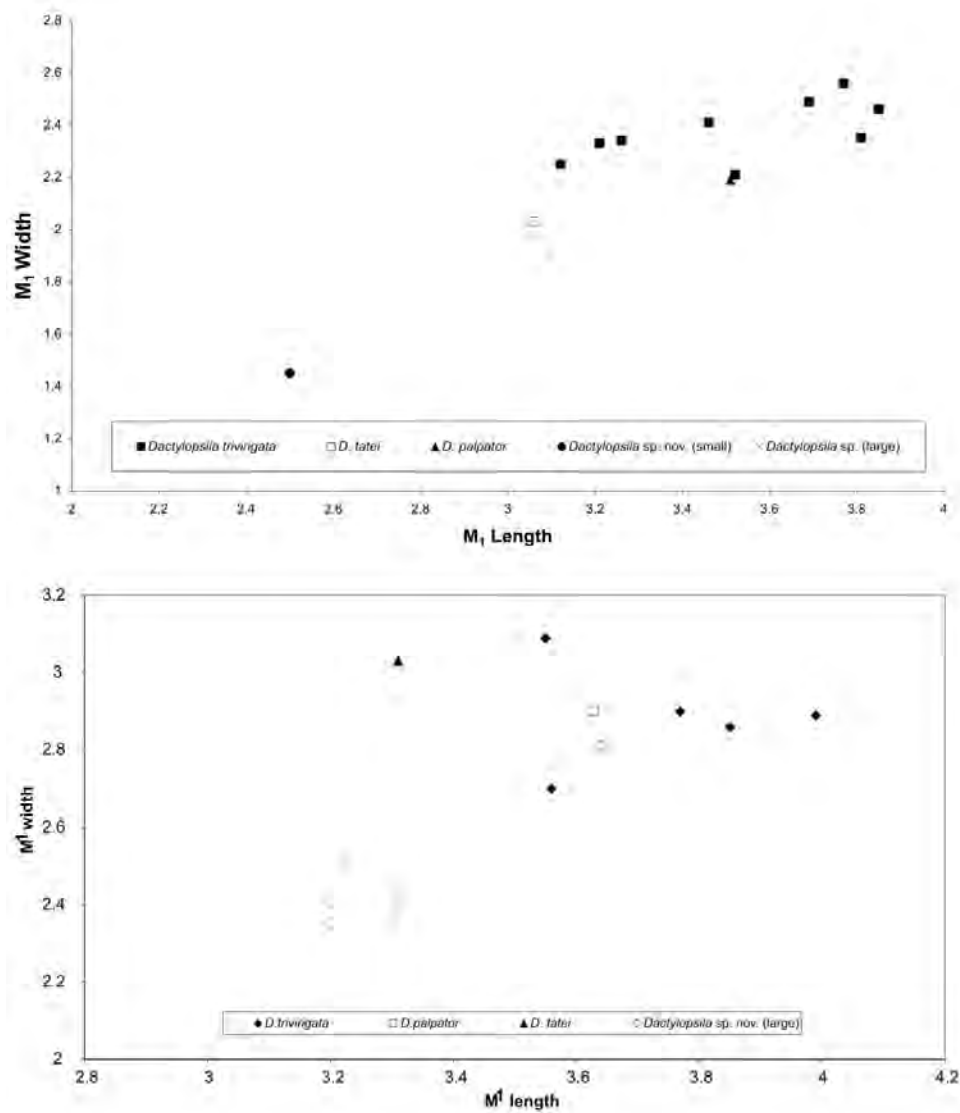
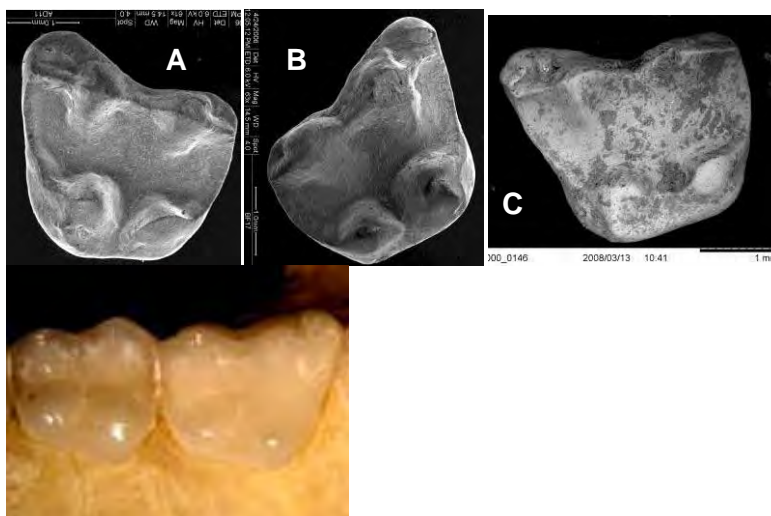


Figure 4-83. Bivariate plots of  $M_1/M^1$  length to width for fossil and modern *Dactylopsila*.





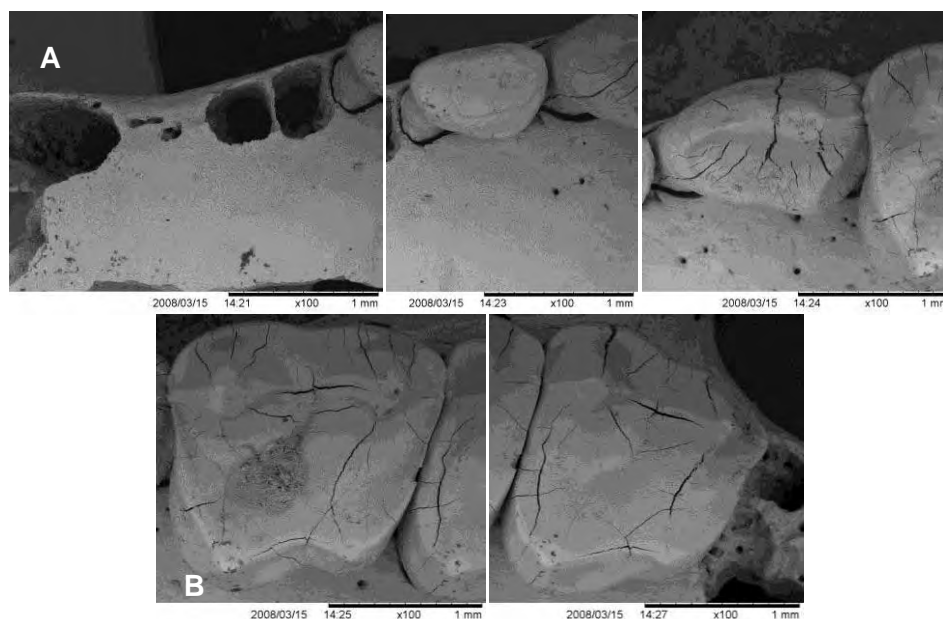
**Figure 4-84. Fossil *Dactylopsila* from Mt Etna. A-C. M<sup>1</sup>s (QML1284, QML1284a, QML1311H). D. *D. tatei*.**

Family BURRAMYIDAE (Broom, 1898)

Hocknull (2005) alluded to the relationships of the fossil burramyids from the middle Pleistocene sites at Mt Etna. In particular Hocknull (2005) identified a single taxon that shared most morphological features with *Cercartetus caudatus*, however, differed enough to represent a distinct species. Since then, more specimens referable to *Cercartetus* have been found and revision is warranted, in particular the description of a second new species of *Cercartetus*.

***Cercartetus* sp. nov. 1**

*Cercartetus* sp. nov. 1 is referable to the taxon described by Hocknull (2005), distinguished on the basis of the following combination of characteristics; short diastema between C<sup>1</sup> and P<sup>1</sup>, with C<sup>1</sup> being large; P<sup>1</sup> and P<sup>2</sup> are both double-rooted; P<sup>1</sup> and P<sup>2</sup> elongate-ovoid in occlusal view; P<sup>3</sup> ovoid with a single cusp; M<sup>1</sup>-M<sup>4</sup> present and elongate, gracile cusps. P<sub>3</sub> sub-triangular in occlusal view; relatively broad posterior of P<sub>3</sub> relative to M<sub>1</sub> anterior width. Mandible gracile and constricted posteriorly near the beginning of the ascending process.



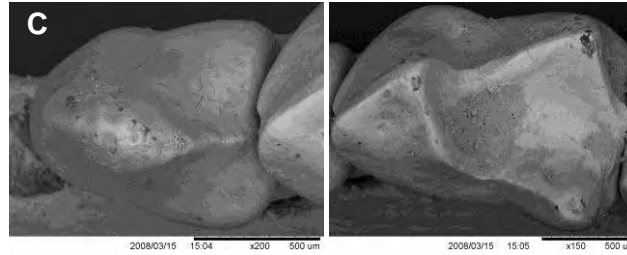


**Figure 4-85. *Cercartetus* sp. nov. 1 from Mt Etna QML1313. A. Left maxilla showing alveoli for  $P^1$ , preserved  $P^{2-3}$ . B.  $M^{1-2}$ . C.  $P_3$ - $M_1$ .**

### ***Cercartetus* sp. nov. 2**

A second species of *Cercartetus* is recognisable from the middle Pleistocene deposits at Mt Etna. This species shares most features with *Cercartetus* sp. 1 and *Cercartetus caudatus*, however, it is much more robust and larger in almost all dimensions.

*Cercartetus* sp. nov. 2 differs from *C. sp. nov. 1* in the following ways; larger in all dimensions; narrower  $P_3$  with long anterior and posterior crests; reduced  $P_{1-2}$  distance, significantly more bunched when compared with *C. sp. nov. 1* and *C. caudatus*;  $M_1$  more elongate with the anterior with narrower and with a cristid obliqua with a greater lingual curvature;  $M_1$  metaconid crest posterior to protoconid;  $M_{2-4}$  relatively broader between cusps. Mandible deeper throughout its length especially below the  $M_4$  and ascending process. Overall dimensions robust.

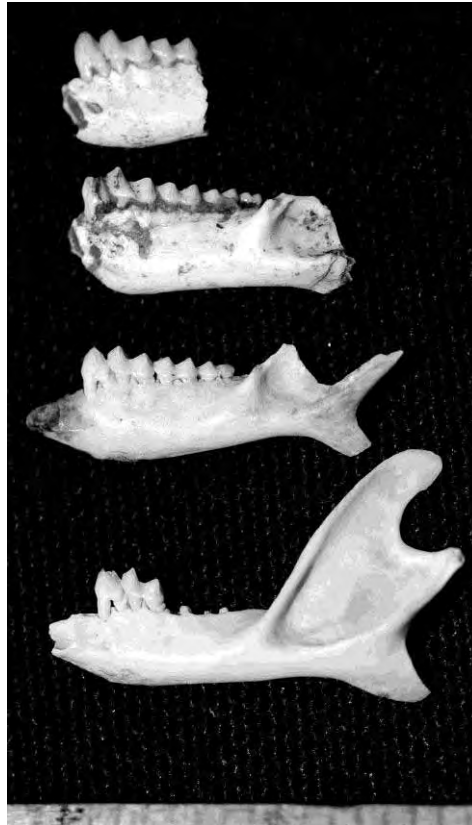


**Figure 4-86.** Fossil *Cercartetus* from Mt Etna, *Cercartetus* sp. nov. 2 (top two mandibles) compared with *C. sp. nov. 1* (lower two mandibles).

#### Family INCERTAE SEDIS

Since Hocknull (2005) additional remains of this new taxon have been recovered.  $M^1$  morphological variation indicates that there are two species of this new taxon found within the Middle Pleistocene deposits at Mt Etna. It remains uncertain as to whether this new taxon represents a new family of marsupials or should be placed within the Burramyidae or Acrobatidae. Inclusion in either of these families would require a review of all taxa currently considered within each, including several undescribed taxa from the Oligo-Miocene deposits of Riversleigh, far north Queensland.

#### **Gen. nov.**

Hocknull (2005) provided characteristics that diagnosed this new taxon.

### Sp. nov. 1

Sp. nov. 1 is diagnosed by the following combination of unique features; double-rooted  $P^2$  and  $P^3$ ,  $M^1$  sub-rectangular in occlusal view bearing four main cusps (paracone, protocone, metacone, hypocone) with a shallow central basin.

Postparacrista connects to the premetacrista in shallow basin forming a continuous shallow crest. Buccal margin of the tooth parallels the ectoloph forming a continuous 'wave' on the buccal margin. Anterior width slightly wider than posterior width.  $M^2$  similar to  $M^1$ , however, the paracone is buccally positioned making the anterior width greater than the posterior width. Molar row straight in lateral profile with no posterior dorsal inflexion. Sp. nov. 1 differs from the only other member of its genus by being slightly larger and possessing a continuous postparacrista-premetacrista on  $M^{1-2}$ ; a less distinct anterior cingulum  $M^{1-3}$ ; more elongate molar profile  $M^{1-4}$ .

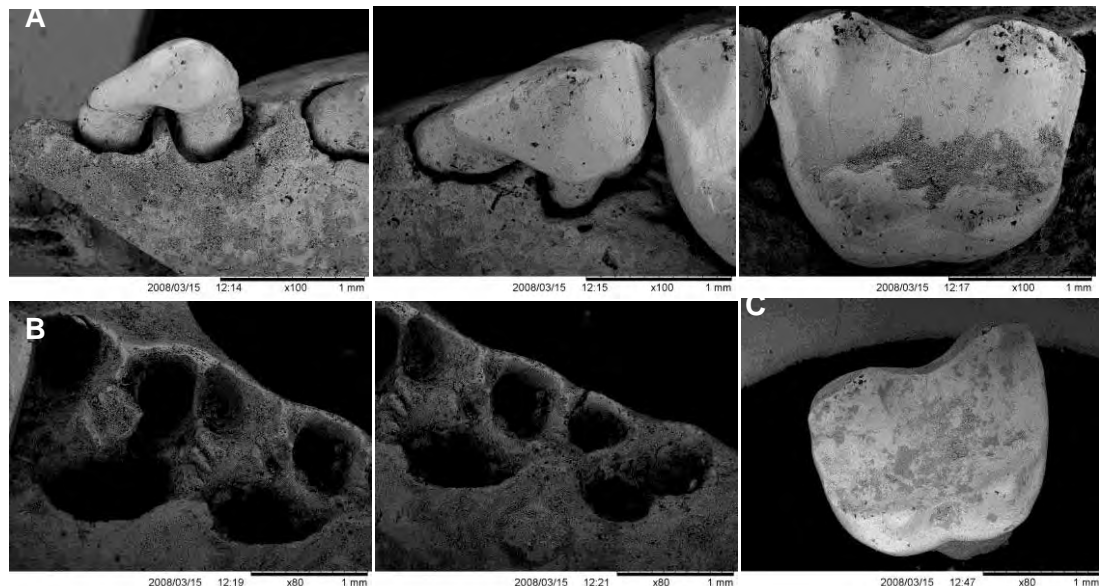


**Figure 4-87.** Fossil acrobatoid (sp. nov. 1) from Mt Etna (QML1313). A.  $P^2$ ,  $P^3$ ,  $M^1$ . B.  $M^{2-3}$  (alveoli),  $M^{3-4}$  alveoli. C. Isolated  $M^1$ .

### Sp. nov. 2

Sp. nov. 2 is diagnosed on the basis of the following combined features;  $M^{1-2}$  with the postparacrista and premetacrista terminating in the midline of the tooth's central shallow basin; paracone oriented antero-buccally; distinct anterior cingulum; buccal margin of  $M^{1-2}$  distinctly 'm' shaped. Sp. nov. 2 differ from Sp. nov. 1 by being slightly smaller; squarer in occlusal profile; possessing an 'm' shaped buccal margin;

a broken postpara-premetacrista; a more pronounced anterior cingulum and a more buccally oriented paracone.

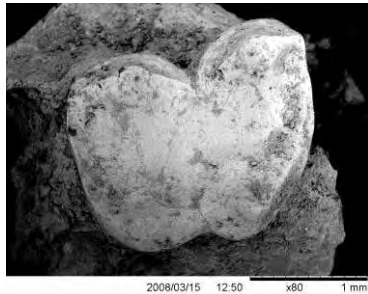


**Figure 4-88. Fossil acrobatoid (sp. nov. 2) from Mt Etna, isolated M<sup>1</sup>.**

#### Family ACROBATIDAE Aplin, 1987

##### ***Acrobates* sp.**

*Acrobates* sp. does not vary considerably from the comparative material available to this study. However, some of the fossil specimens exhibit and more robust and overall larger in size. The cristid obliqua is directed buccally instead of lingually. Whether these features are enough to split this taxon specifically from *Acrobates pygmaeus* will depend on more detailed morphological studies and a greater number of fossil specimens.

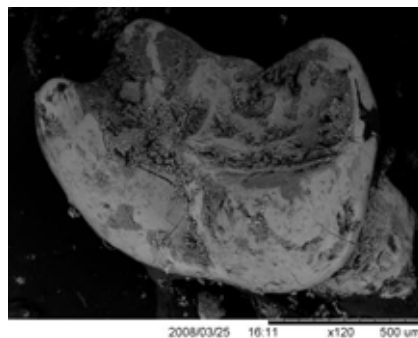


**Figure 4-89. Fossil *Acrobates* from Mt Etna, isolated M<sub>1</sub>.**

#### Family PHASCOLARCTIDAE

Price et al (submitted) and Price and Hocknull (submitted) are determining the taxonomic status of the Mt Etna and Marmor Quarry phascolarctids.

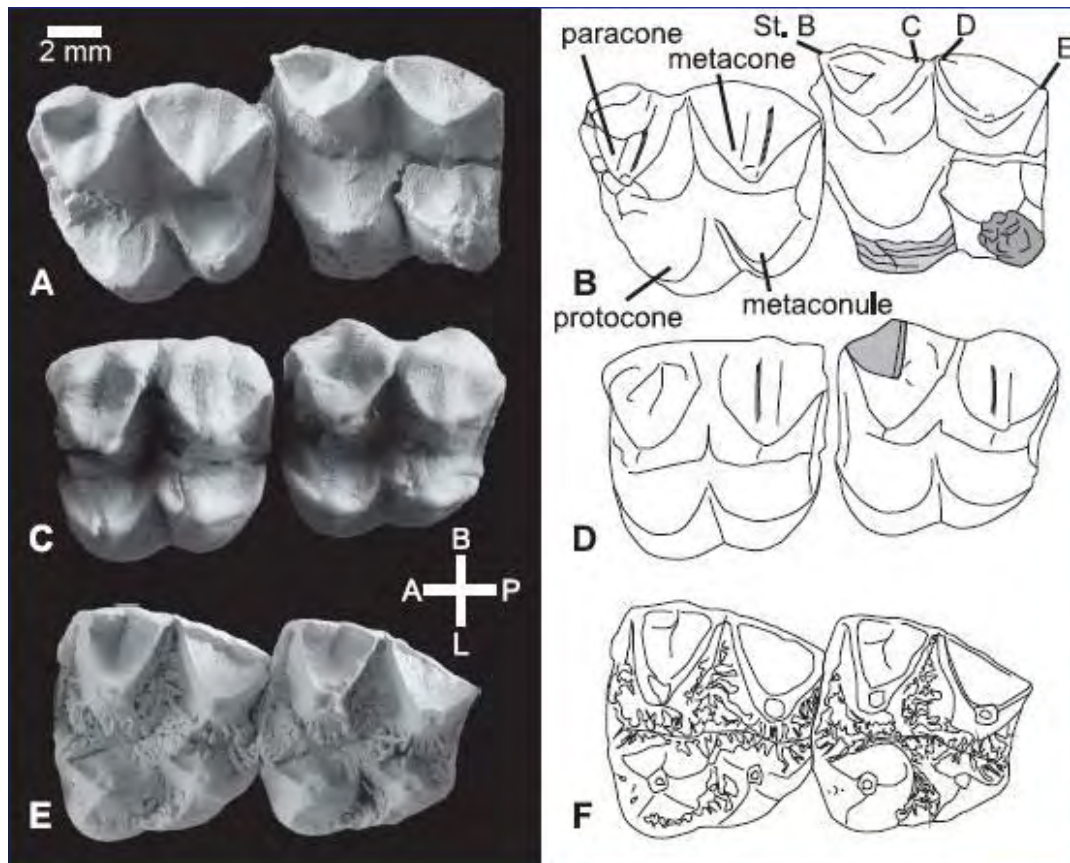


Figure 4-90. *Madakoala* sp. nov. 1 from Mt Etna (A&B) compared with *M. devisi* (C&D) and *Phascolarctos* (E&F), from Price & Hocknull (submitted).

#### Family POTOROIIDAE

#### “*Milliyowi* / *Aepyprymnus*” sp. nov.

Subsequent to Hocknull (2005), a single dentary specimen was discovered representing the only potoroiid so far recovered from the Middle Pleistocene of Mt Etna. The specimen is a right dentary preserving the base of the  $I_1$ , an erupting  $P_3$  and fully erupted  $M_{1-2}$ . The  $P_3$  preserves the distinctive premolar ridgelets and bunolophodont molars typical of potorooids.  $M_{1-2}$  are bunolophodont and low-crowned, relative to macropodids. The dentary compares very closely with *Aepyprymnus rufescens* and *Milliyowi bunganditj* both in  $P_3$  and molar morphology. Prideaux (1999) provided synapomorphies that unite *Aepyprymnus* and *Milliyowi*, which are also present in the fossil taxon. These features include; elongate molars relative to length with trigonid antero-posteriorly elongated; molars relatively high crowned (relative to other bettongins) and molars sublophodont. Within this clade the fossil taxon shares features with both *Milliyowi* and *Aepyprymnus* that were

considered to be autapomorphies by Prideaux (1999). Unfortunately there are no known specimens of  $M_1$  or  $M_2$  known from *Milliyowi*, therefore direct comparison is not available. However, features preserved in the molariform  $dP_3$  and  $M_3$  show features shared between *Milliyowi* and the fossil, to the exclusion of *Aepyprymnus*. These features include, mid lophid kinks in both the protolophid and hypolophid of molars, posterior cingulid cleft at the mid-line of the cingulid; more elongate molars and similar molar size (Fig. 4-92). Features shared between the fossil and *Aepyprymnus* to the exclusion of *Milliyowi* include, the absence of subsidiary ridges on the  $P_3$ , however, this may be considered a variable feature possibly present in *Aepyprymnus*; reduced precingulid; less elongate  $P_3$  to  $M_1$  ratio. The length of the  $P_3$  corresponds to the variation seen in *Aepyprymnus*, however, it's anterior and posterior widths are narrower. The molars are larger in overall dimensions and fit closely with those molar dimensions available for *Milliyowi* (Fig. 4-92). The cross-sectional shape of the incisor does not match that of *Aepyprymnus rufescens*.

Further material of this exceptionally rare potoroiid will be needed to determine its phylogenetic and taxonomic placement, however, based on the significant differences it shows between *Aepyprymnus rufescens* and *Milliyowi bunganditj*, it is most likely a separate taxon, within a clade containing both *Aepyprymnus* and *Milliyowi*. Whether the features that differentiate these three taxa are considered to be enough to warrant generic level status is debatable due to the shared features of all three taxa. This may require the synonymy of *Milliyowi* into *Aepyprymnus*, an increase in the known variation within *Aepyprymnus*, and the recognition of three distinct species.

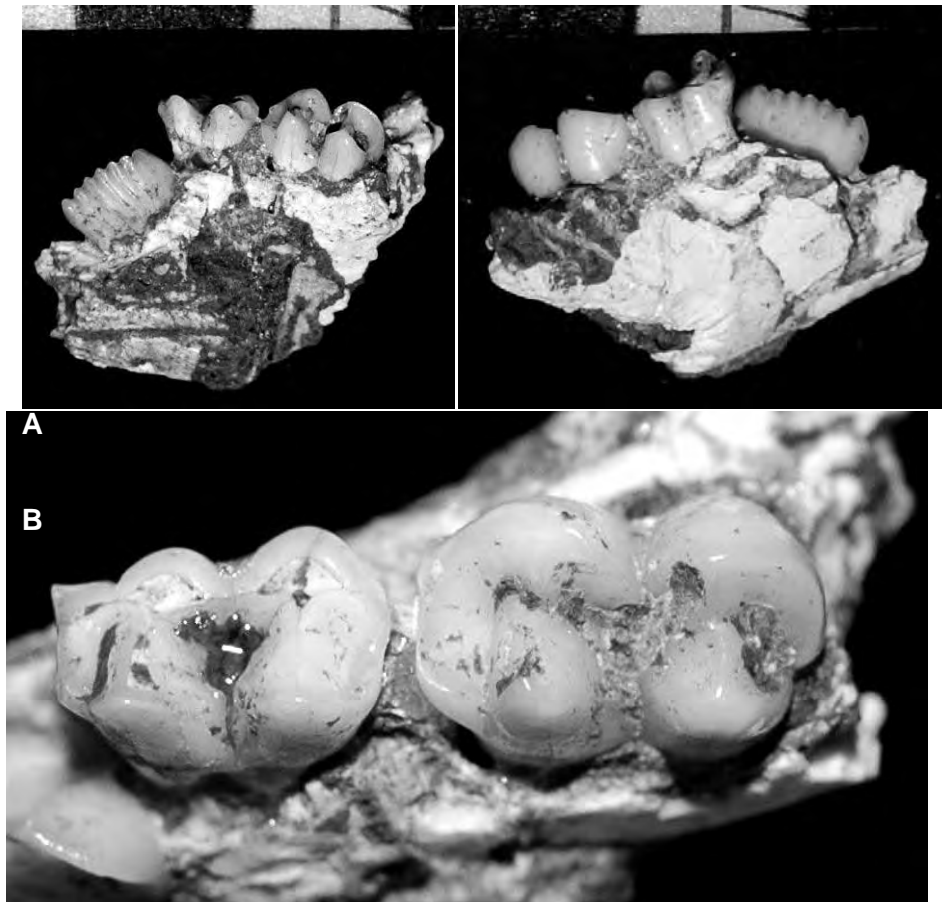
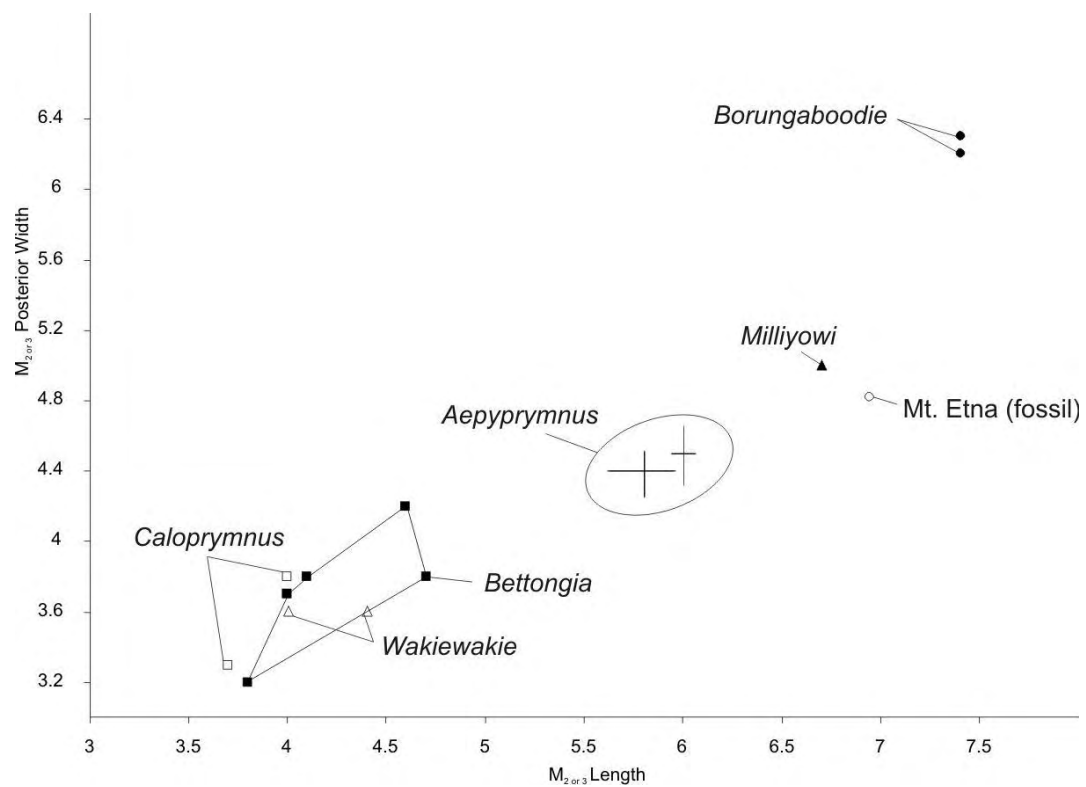


Figure 4-91. “*Milliyowi/Aepyprymnus*” sp. nov. from Mt Etna. A.  $P_3$ - $M_2$  (buccal and lingual views). B.  $M_{1-2}$  occlusal view.





**Figure 4-92. Bivariate plot of lower molar length vs width of fossil and modern potorooids, compared with the new species from Mt Etna.**

#### Family PHALANGERIDAE Thomas, 1888

Hocknull (2005) identified two phalangerids from the middle Pleistocene deposits at Mt Etna and a single species from younger late Pleistocene – Holocene deposits. Since then several isolated molars and premolars have been recovered from middle Pleistocene deposits that warrant further attention.

*Strigoscus* sp. of Hocknull (2005) was subsequently referred to by Hocknull et al (2007) as *Phalanger* sp. 1. This was due to the rearrangement of the taxonomy of *Strigoscus* since 2005, with the inclusion of '*Strigoscus*' *gymnotis* within *Phalanger* (Osborne & Christidis, 2002) and '*Strigoscus*' *reidi* and '*Strigoscus*' *notialis* within *Onirotiscus* (Crosby, 2007). Originally Hocknull (2005) considered *Strigoscus* sp. to most closely resemble '*Strigoscus*' *notialis* from the Pliocene Hamilton Fauna, however, since then several additional specimens have altered this designation.

#### **Phalanger gymnotis**

*Phalanger gymnotis* is represented by a right maxilla with alveoli for  $P^{1-2}$  and dentition  $P^3-M^2$ . Several isolated  $M^1$ s are considered to represent the taxon along with several partial mandibles. *Phalanger gymnotis* has been identified by the following combination of characteristics unique to *Phalanger gymnotis*.:  $P_3$  ovate in occlusal view;  $P_3$  hypertrophy;  $P^3$  with four cuspules,  $P_3$  with 5-6 cuspules;  $P_3$  at an oblique angle to molar row;  $P^2$  single-rooted;  $P_3$  crown higher anteriorly than posteriorly;  $M^1$  preprotocrista does not contact parastyle (midlength cleft);  $M^1$  parastyle distinct cuspule;  $M^1$  with faint crenulations in unworn specimens;  $M^1$  with distinct stylar crest and pocket running from postprotocrista;  $M_1$  metaconid not posteriorly placed; no neometaconule or protoconule on upper molars.

The lack of a double-rooted  $P^1$ , the presence of molar crenulations on unworn teeth, and the presence of a fissure dividing the paracone from the parastyle differentiate this taxon from members of the Oligo-Miocene genus, *Onirotiscus*. Crosby (2007) placed

both *S. reidi* and *S. notialis* within *Onirotociscus* although Crosby (2007) did not provide a differential diagnosis for *S. notialis* as a member of *Onirotociscus*. These two taxa were initially considered by Hocknull (2005) to be similar to the Mt Etna taxon, however, based on the morphology of the type species of *Onirotociscus* (*O. reidi*), it is certain that the Mt Etna taxon is not *Onirotociscus* (sensu stricto). Whether *S. notialis* (= *O. notialis*) is a member of the Oligo-Miocene genus is questionable due to the features used to diagnose the genus are based on cranial material not available for either *S. notialis* or the Mt Etna specimens. This will need to be discussed elsewhere.

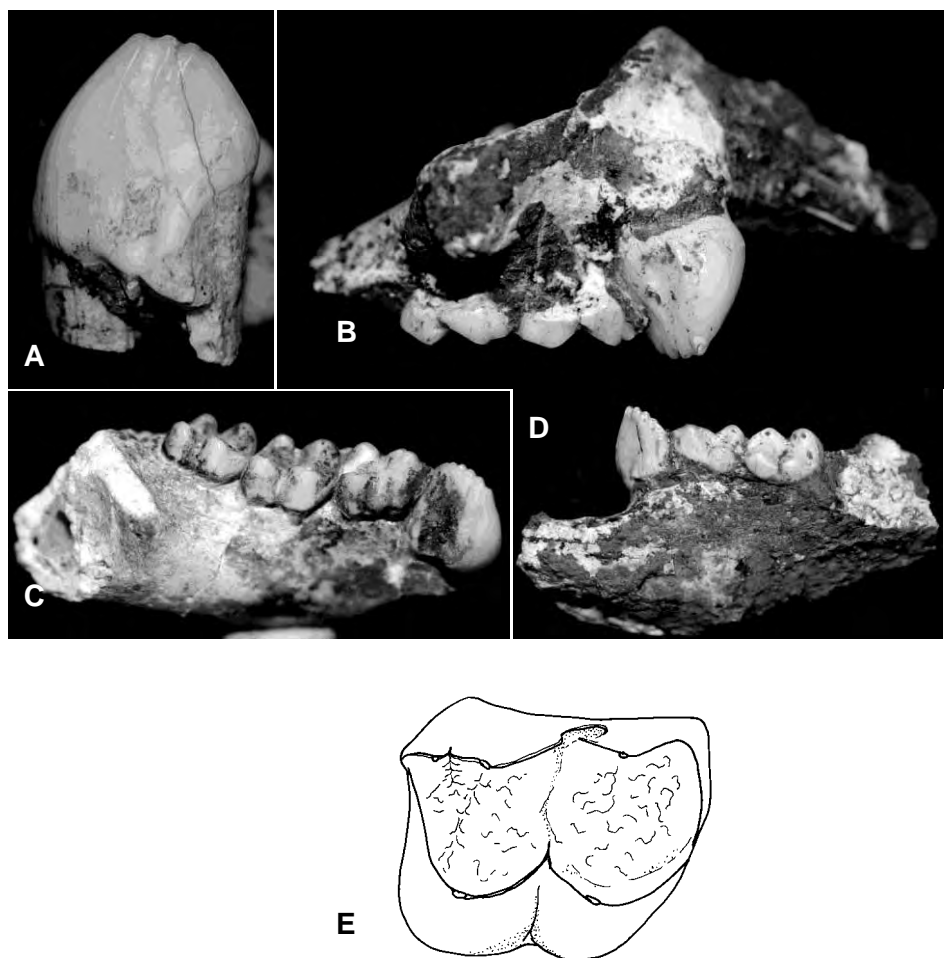


Figure 4-93. *Phalanger gymnotis* from Mt Etna. A. P<sup>3</sup> (QML1284), B. P<sup>3</sup>-M<sup>2</sup> (QML1311H), C. P<sub>3</sub>-M<sub>3</sub> (QML1284), D. P<sub>3</sub>-M<sub>2</sub> (QML1384LU). E. M<sup>1</sup> (QML1311CD).

#### *Phalanger* sp. cf. *P. mimicus*

*Phalanger* sp. 2 of Hocknull et al (2007) was based on a left maxilla with P<sup>3</sup>-M<sup>2</sup>.

Since then the re-description of *P. mimicus* from northern Australia and southern New

Guinea has prompted closer evaluation of the fossil taxon. Three specimens are considered to be close to *P. mimicus*, a left maxilla with  $P^3$ - $M^2$  (QMF52008), an isolated  $M^1$  and a left mandible with  $P^3$ - $M^1$  (QMF52005). The upper dentition is considered to be most diagnostic. The following features are shared with *P. mimicus*; Large  $P3$ ; oblique  $P3$  to molar row (not as much as *P. gymnotis*); preprotocrista with mid-length cleft; presence of a distinct buccal kink of the postprotocrista (sometimes developed into small styler cusp); lack of lingual cingulum on  $M^2$ ; minimal crenulations in unworn teeth. QMF52008 differs from measured *P. mimicus* by possessing a slightly wider  $P^3$ . This size difference may reflect greater size variation in the past or simply due to the small sample measured taken by Norris & Musser (2001). In addition, QMF52008 preserves an anterior portion of the zygomatic arch, which indicates that the rostral section of the arch was quite wide, thus similar to the feature of the zygomatic arch used to differentiate *P. mimicus* by Norris and Musser (2001).

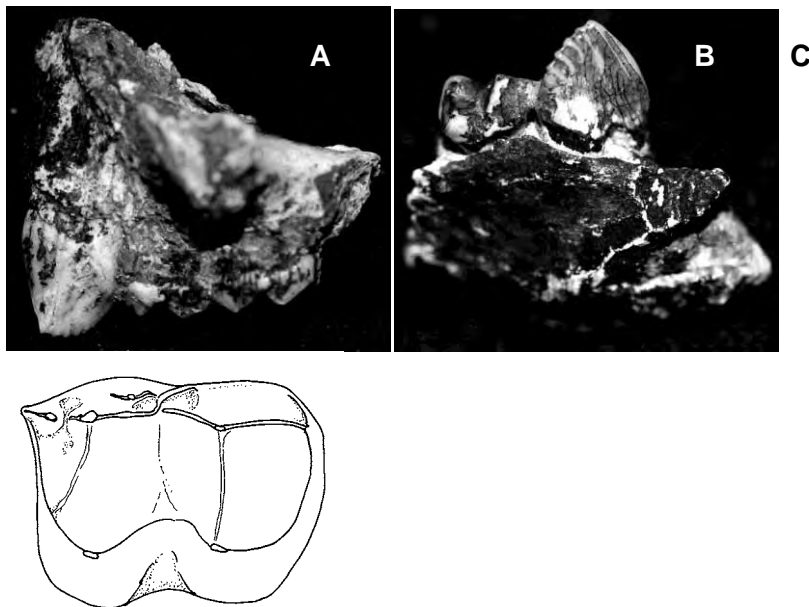
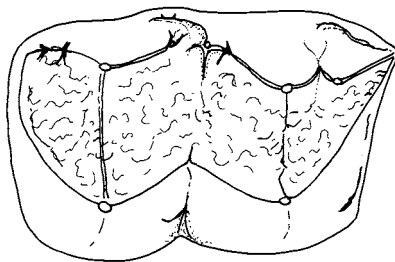


Figure 4-94. *Phalanger* sp. cf. *P. mimicus* from Mt Etna. A.  $P^3$ - $M^2$  (QML1384LU), B.  $P_3$ - $M_1$  (QML1284) C.  $M^1$  (QML1311H).

### ***Spilocuscus* sp.**

A third phalangerin, representing the only specimen of what is considered here to be a species of *Spilocuscus*. QMF52006 is a right M<sup>1</sup>, preserving a combination of features only known from species of *Spilocuscus*. The combination of features include; crenulated enamel; elongate M<sup>1</sup>; distinct stylar cuspules and buccal stylar basin; anterior cingulae (incipient or well developed); buccal cingulae (incipient or well developed); preprotocrista not contacting parastyle, divided by cleft; small cuspule on postmetacristae; absence of neometaconule and protoconule.

Three species of *Spilocuscus* were compared; *S. maculatus*, *S. rufoniger* and *S. wilsoni*. *S. wilsoni* is similar in most features to QMF52006, including similar size with less distinct crenulations on the upper molars (Helgen & Flannery, 2004). QMF52006 differs from *S. maculatus* and *S. rufoniger* on the basis of its smaller size and less distinct crenulations, and less well developed cingulae, both anterior and buccal. Both the fossil and *S. wilsoni* are generally less distinct in molar features, although each of them is still expressed to a degree.



**Figure 4-95. *Spilocuscus* sp. from Mt Etna, QMF52006 M<sup>1</sup>.**

### **Family MIRALINIDAE**

Two specimens have been recovered from the Middle Pleistocene of Mt Etna that are considered here to represent new members of a previously exclusive Oligo-Miocene marsupial family, the Miralinidae. Miralinids are known from central Australian and north-western Queensland Tertiary deposits. A typically rare, small-sized, phalangeroid possum, miralinids can be easily distinguished by the presence of a metaloph on all upper molars, distinct molar crenulations on unworn teeth, the development of a metaconule between the metalophs, and a blade-like parastylar

corner. These features are present in the two specimens so far recognised within the Middle Pleistocene deposits.

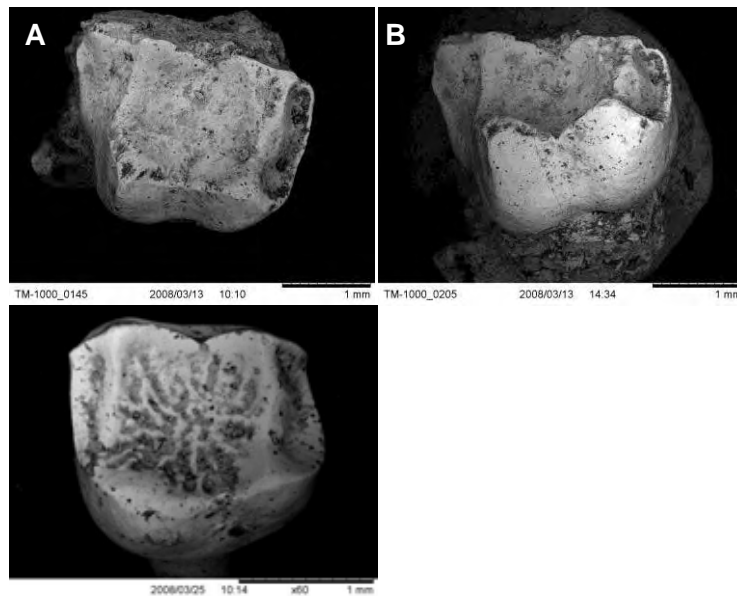


**Figure 4-96. Miralinid fossils from Mt Etna. A-B.  $M^1$  (QML1311H), C.  $M^{2 \text{ or } 3}$  (QML1311H)**

#### Family THYLACOLEONIDAE Gill, 1872

Australia's extant native mammalian carnivore diversity is exceptionally depauperate relative to other landmasses of similar size and to their known diversity in the past (Wroe et al., 2004). Understanding how Australia's marsupial carnivores have responded to past ecological changes underpins the long-term management of Australia's terrestrial predatory guilds. One noticeable absence from the extant native fauna is large mammalian carnivores, top predatory specialists. This niche was once filled by the marsupial 'lions', or thylacoleonids, which represent the most specialised mammalian carnivores so far known to inhabit Australia, having been relatively diverse in the past but are now totally extinct.

The Thylacoleonidae is a family of diprotodontian marsupial carnivores with a fossil record spanning the late Oligocene to late Pleistocene, and includes four genera and eleven species (Gillespie, 2007) ranging in size from the very small Oligo-Miocene thylacoleonids (<3kg) (Myers, 2001) to the largest species *Thylacoleo carnifex* (~105kg). Since the late Oligocene there is an observed trend in

thylacoleonids toward increasing body-size, decreasing species-level diversity, and greater hypertrophy (Gillespie 2007). The species diversity of thylacoleonids at any one site is low, ranging from one to at most four sympatric species (Gillespie, 2007). By the late Miocene a single genus is present (*Wakaleo*); by the Pliocene only *Thylacoleo* is known, represented by two species; and by late Pleistocene times a single species, *T. carnifex*, represents the last of member of this marsupial carnivore family.

*T. carnifex* was a cosmopolitan species during the Pleistocene, having been found in almost all Pleistocene vertebrate faunas and represented by complete skeletons (e.g. Prideaux et., al. 2007). Until recently, *Thylacoleo carnifex* was considered to be the only species of thylacoleonid present during the Pleistocene, having become the largest and most specialised of the family and thus sympatry of thylacoleonid species had not continued into the Pleistocene. New vertebrate localities from southern Australia have now recorded the presence of *Thylacoleo hilli* in the early Pleistocene, extending its range from the Mio-Pliocene into the Pleistocene (Piper, 2007).

The purpose of this section is to document the middle Pleistocene occurrence of *T. hilli* and to discuss its phylogenetic position and palaeoecological implications of sympatric species of thylacoleonid in the Pleistocene.

#### **New Material of *Thylacoleo hilli*.**

Subsequent to Hocknull (2005) new material identifiable as *Thylacoleo hilli* has been recovered from the middle Pleistocene Mt Etna fossil deposits. These new specimens include a partial right maxilla bearing the P<sup>2-3</sup> and alveoli for M<sup>1</sup>; anterior portion of a left dentary with alveoli for I<sub>1</sub>, P<sub>2</sub> and anterior alveoli of P<sub>3</sub>; isolated partial P<sub>3</sub> and a left calcaneum.

The holotype of *T. hilli* Pledge is an isolated left P<sup>3</sup>, being slightly longer posteriorly than the two P<sup>3</sup>s known from Mt Etna and an isolated P<sup>3</sup> from Childers Cove, Victoria. This slight difference in tooth crown length is considered here to illustrate variation within the species as opposed to any specific differences. This consideration

is based on the relatively variable  $P^3$  found in *T. carnifex* and *T. crassidentatus*. Both the Mt Etna and Childers Cove specimens are very close in both size and morphology.

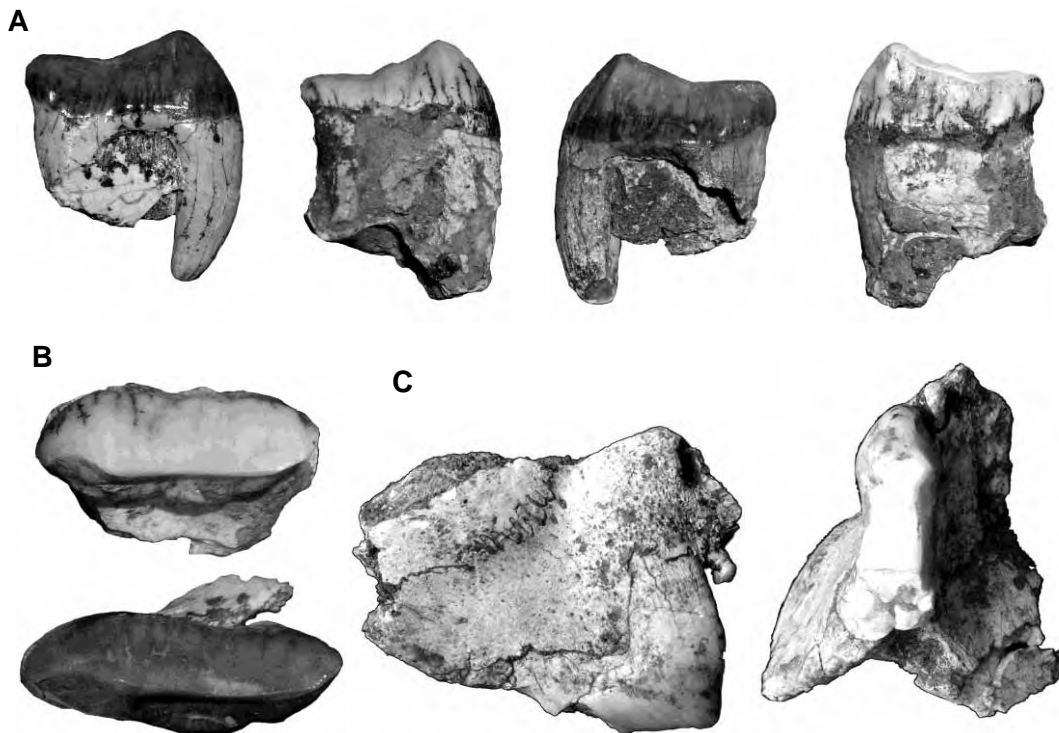


**Figure 4-97. *Thylacoleo hilli* from Mt Etna. A. QMF52013 compared with *T. hilli* from Childers Cove, Victoria (buccal and lingual views). B. QMF52013 compared with *T. hilli* from Childers Cove, Victoria (occlusal view). C. right maxillary fragment preserving  $P^2$ - $P^3$  and  $M^1$  alveolus (QML1311H)**

The  $P_3$  of *T. hilli* is known from two specimens, one from Bow in New South Wales and the other from Mt Etna. Both specimens compare very favourably and are considered here to represent the lower dentition of *T. hilli*. A partial anterior left dentary allies most closely with *T. hilli* based on overall size and position of incisor and premolar alveoli. Finally, a small left calcaneum possesses markedly similar features to *T. carnifex*, at about a third the size. It is considered to represent the first known specimen of a calcaneum assignable to *T. hilli*.



Figure 4-98. *Thylacoleo hilli* calcaneum from Mt Etna (QML1311H) compared with *T. carnifex* from the eastern Darling Downs.



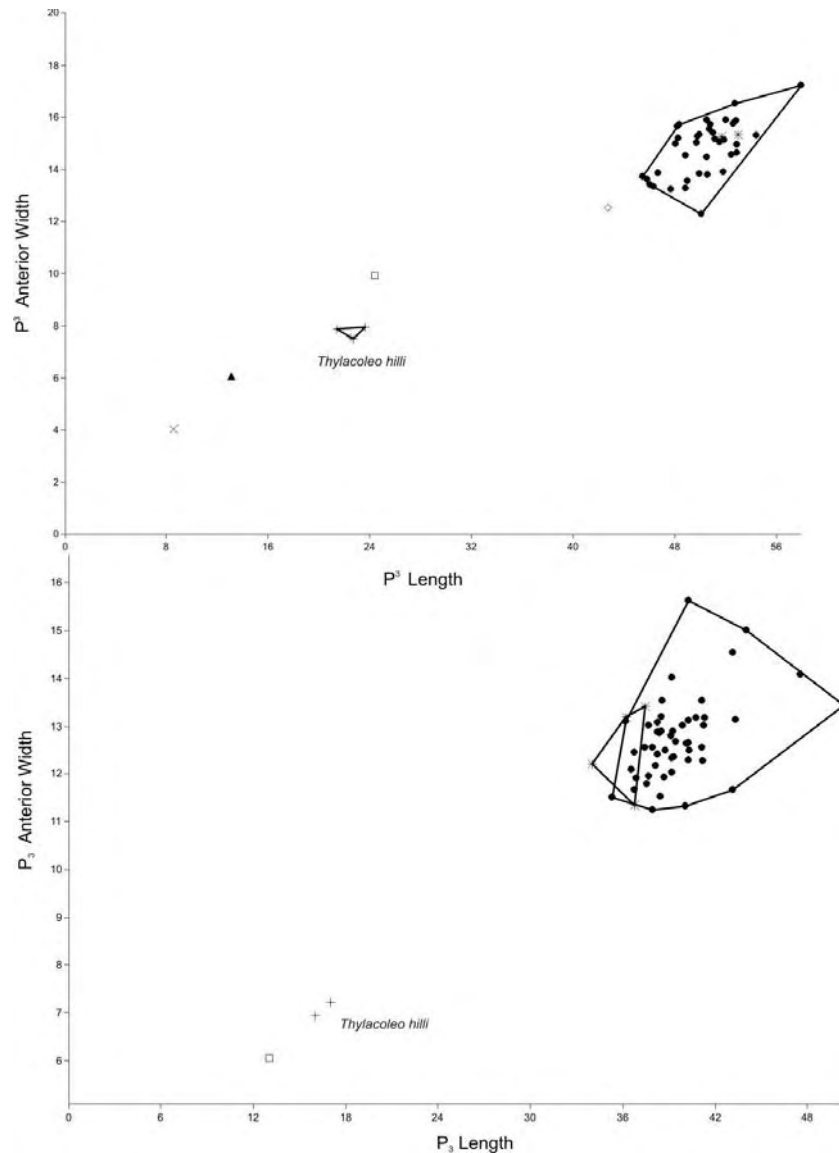


**Figure 4-99. Bivariate plot of P3 length to width for species of thylacoleonid, to compare against *T. hilli* specimens (marked).**

### **Phylogenetic Position of *T. hilli*.**

The following characteristics were scored for thylacoleonids in order to determine the phylogenetic position of *T. hilli*.

#### **Characters**

##### **Dentition**

1. Length of P<sup>3</sup> : <5mm (0); 7-10mm (1); 10-15mm (2), 15-25mm (3), >50mm (4).

2. Relative Width / Length of  $P^3$  : 0.55-0.65 (0); 0.45-0.55 (1); 0.35-0.45 (2); 0.2-0.35 (3).
3. Relative Width / Length of  $P_3$  : 0.50-0.60 (0); 0.40-0.50 (1); 0.30-0.40 (2).
4.  $P^{1-2}$  crown in line with base of  $P^3$  crown, inline (0); above (1) nb: maybe sexually dimorphic trait.
5.  $M^4$  Present (0); Absent (1)
6.  $M^3$  Present (0); Absent (1)
7.  $M^2$  Present (0); Absent (1)
8. Posterobuccal extension past  $M^1$  Absent (0), Present (1)
9.  $M^1 L / P^3 L$ ,  $>0.4$  (0);  $<0.4$  (1)

#### Gillespie (2007) Characters

10. Character 1,  $I_2$  and canine.
11. Character 2, Lower premolar number.
12. Character 3,  $P_3$  buccally deflected.
13. Character 4,  $P_3$  serrated.
14. Character 6, Upper premolar number.
15. Character 7,  $P_3$  posterolingual crest.
16. Character 8, Anterior crest of  $P_3$ .
17. Character 9, Anterobuccal crest of  $P_3$ .
18. Character 10, Posterobuccal crest of  $P_3$ .
19. Character 21,  $P^2$  position relative to  $P^3$ .
20. Character 22,  $P^3$  shearing facet.
21. Character 23,  $P^3$  crown length relative to cheektooth row ( $P^3$ - $M^4$ ).
22. Character 24,  $P^3$  longitudinal blade length:  $P^3$  crown length.
23. Character 25,  $P^3$  Longitudinal blade curvature.

- 24. Character 26, Presence and inclination of a posterior longitudinal blade on P<sup>3</sup>.
- 25. Character 27, P<sup>3</sup> mid-crown constriction.
- 26. Character 28, P<sup>3</sup> posterobuccal crest.
- 27. Character 29, P<sup>3</sup> anterolingual crest/cuspule.

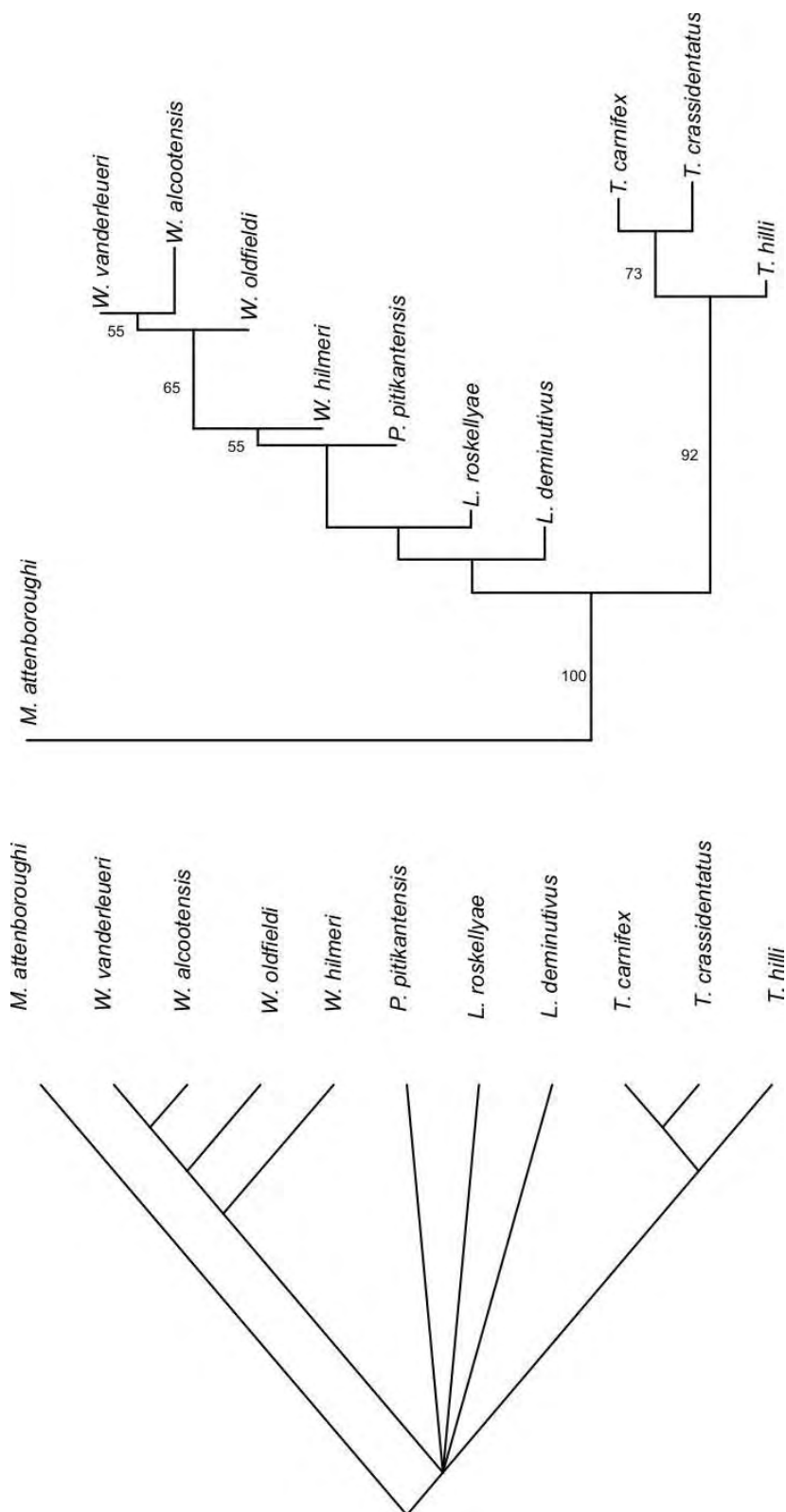


Figure 4-100. Phylogeny of thylacoleonids. Above, bootstrap valued phylogram showing supported groupings. Below, strict consensus tree.

The phylogenetic results show very strong support for the monophyly of *Thylacoleo*. Within *Thylacoleo*, *T. hilli* is considered most basal to the remaining two larger-bodied taxa, *T. carnifex* and *T. crassidentatus*. This basal position corresponds to the oldest presumed age of *T. hilli* being Mio-Pliocene of Curramulka. The basal position of *T. hilli* requires the loss of the posterior-most molar in both *T. hilli* and *T. carnifex*, a convergence on the posterior expansion of the P3s.

### **Sympatry in Pleistocene *Thylacoleo*.**

Sympatry in thylacoleonids was thought to be restricted to Oligo-Pliocene faunas with the Pleistocene dominated by a single very large carnivorous marsupial, *T. carnifex*. The present new records show that particular local faunas were able to sustain two species of *Thylacoleo* during the early and middle Pleistocene. A comparison was made between the faunas present at localities possessing two species of *Thylacoleo* with those only possess one. The absence of *T. hilli* from any one particular fauna could represent a taphonomic bias toward the collection of large-bodied specimens, both by the site dynamics or by fossil collection biases. To remove as much of this potential bias as possible only sites recording very small to megafaunal-sized taxa were used, with systematic collection so that a contemporary prey fauna would be available for comparison.

Mio-Pleistocene faunas where species of *Thylacoleo* are present were used to determine the relative proportion of prey types within the sympatric fauna. On face value the faunas that had more than one species of *Thylacoleo* tended to possess more arboreal taxa as part of the overall fauna, which lead to the hypothesis that *T. hilli* was most likely an arboreal prey specialist. This would allow the existence of two species of *Thylacoleo* within the same ecology, excluding the influence of competition.

Figure 4-101 presents the results of these analyses which clear demonstrates that faunas that possess a single species of *Thylacoleo* (almost exclusively *T. carnifex*) the proportion of prey species is dominated by terrestrial prey (herbivores) with minor arboreal taxa available, whereas in faunas that possess both *T. hilli* and a species of large *Thylacoleo* (either *carnifex* or *crassidentatus*) the proportion of prey species that are arboreal and terrestrial is almost equal. These data support the contention of *Thylacoleo* sympatry throughout the late Cainozoic, however, as habitats eventually

lost their diverse arboreal fauna *T. hilli* no longer was able to sustain its presents in the fauna. It is conceivable that the arboreal *Thylacoleo hilli* survived in regions of Australia well into the late Pleistocene, forming another part of the late Pleistocene faunal extinction within habitats that were marginalised through late Pleistocene glacial maxima and anthropogenic burning.

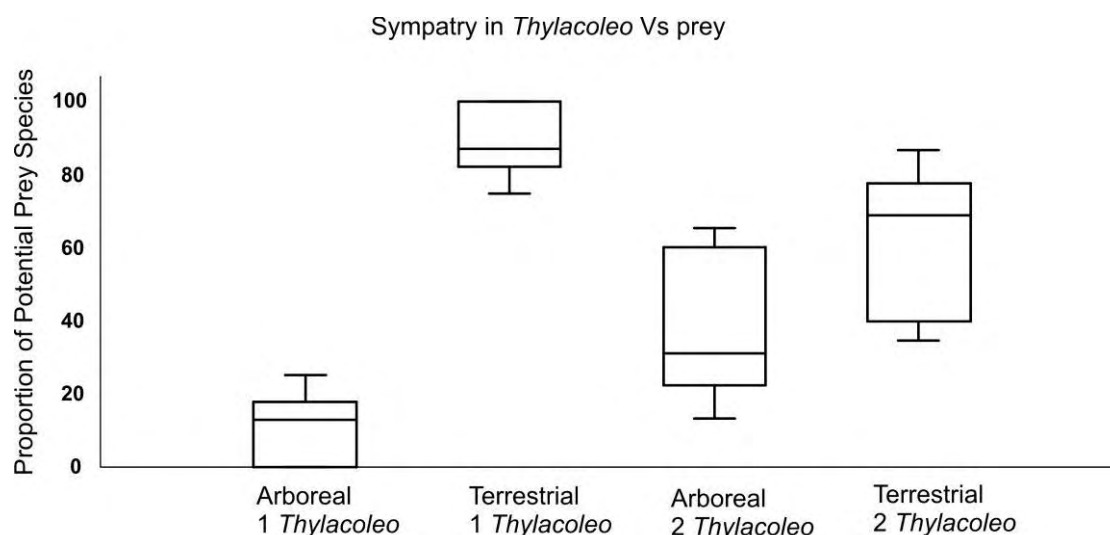


**Figure 4-101. Sympatry in *Thylacoleo*.** Box plot of proportional prey species (divided into terrestrial and arboreal herbivores) with the presence of 1 or 2 species of *Thylacoleo*.

## Family MURIDAE

### Leggadina

*Leggadina* has been identified on the basis of the following characteristics; small murid;  $M^1$  with distinctly chevroned molar crests (lophs); T3 and T6 oriented posteriorly as a long crested cusp at  $45^0$  posteriorly inflected from the main crests made by T1-2 and T4-5 respectively; presence of a distinct crest-like anterior cingulum; reduced T7 to very small cusps merged with T8.

QML1312

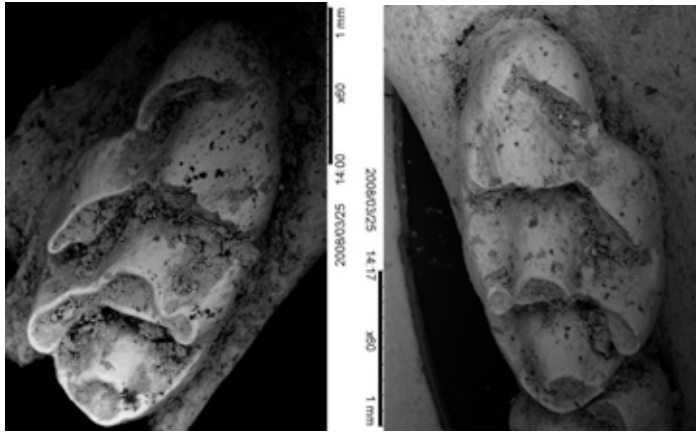


Figure 4-102. Fossil *Leggadina* from Mt Etna, M<sup>1</sup>s (QML1312).

### Pseudomys

Several different species of *Pseudomys* exist in the middle Pleistocene deposits at Mt Etna. Identification of these taxa is difficult due to the complex taxonomy of extant *Pseudomys* species.



Figure 4-103. Fossil *Pseudomys* from Mt Etna, M<sup>1</sup>s.

### *Zyzomys*

*Zyzomys* is easily distinguished from most other Australian murids by the presence of a T7 on the M<sup>1</sup>; subparallel lophs developed from the wearing down of T1-3; T4-6 and T7-9. In occlusal view, *Zyzomys* upper molars are elongate and sub-rectangular in profile with an enlarged T7, similar in size to the T8-9 complex. The fossil specimens are characterised by possessing an anterior cingulum anterior to T2-3; T1 is heavily reduced; enlarged T7 the coalesces with the T8-9 complex after wear. The fossil



specimens were compared with *Z. argurus*, the closest living species of *Zyzomys* to Mt Etna, which occur some 800kms to the north. On close comparison fossil species was markedly different. *Z. argurus* differs from the fossil taxon by the shape of the anterior margin of the zygomatic arch. In *Z. argurus*, the zygomatic arch curves smoothly to the posterior whilst in the fossil the anterior margin of the zygomatic arch is angulate and is ‘squared off’ to produce a more distinctive posterior inflection of the arch. In size, the fossil specimens are larger than *Z. argurus*. The other species of *Zyzomys* are restricted to the Northern Territory and Western Australia, therefore, if the fossil *Zyzomys* represents an extant species it will also represent a massive range extension for that species. Based on the taxa found within QML1312, it would be most plausible that the species represented at Mt Etna be *Z. pedunculatus*, as other species, like this one share a now central Australian distribution (e.g. *Chaeropus ecaudatus*, *Macrotis lagotis*, *Perameles bougainville* and *Tympanocryptis cephalus*). On comparison with the extinct Pliocene species, *Z. rackhami*, the fossils conform most closely in morphology, in particular with the development of the T1bis and the relatively reduced T1 and well developed T3, 6 and 9. However, *Z. rackhami* is smaller than the fossil. Godthelp (1997) considered *Z. rackhami* to be closest in morphology to *Z. pedunculatus*, however, smaller in size. Therefore, it may well be reasoned to consider *Z. pedunculatus* as a likely candidate for the Mt Etna fossil.



**Figure 4-104. Fossil *Zyzomys* from Mt Etna, M<sup>1</sup>s (QML1312).**

## Notomys

Three species of *Notomys* have been preliminarily identified from the middle Pleistocene of Mt Etna. The taxonomy of these species will require further work to determine the morphological features needed to differentiate *Notomys* spp. and some species of very similar *Pseudomys*. The identification of *Notomys* has been primarily based on the enlargement of the T1 and T4, along with the shape of the zygomatic arch. The fossil *Notomys* are pictured below alongside comparative specimens of extant *Notomys* species.

#### ***Notomys* sp. 1**

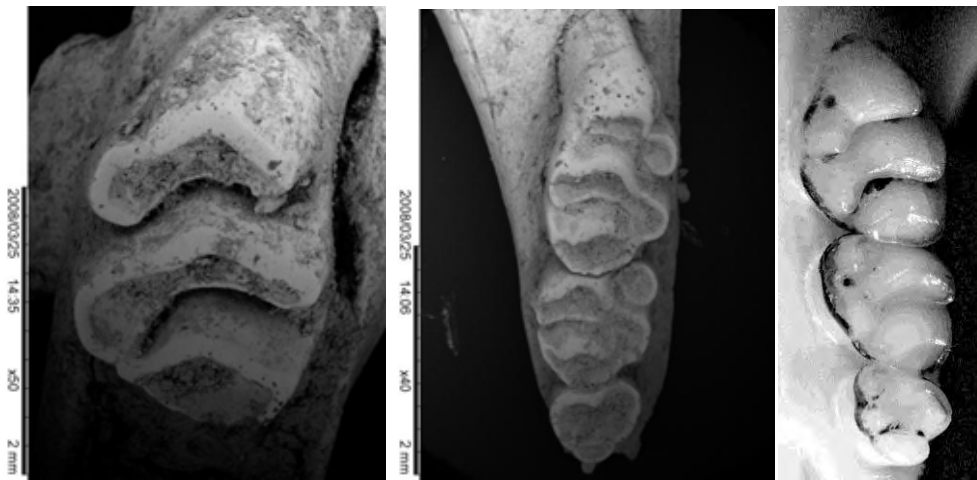


**Figure 4-105. Fossil *Notomys* from Mt Etna (QML1312) compared with *N. aquilo* (far right) M<sup>1</sup>s and maxillae.**

#### ***Notomys* sp. 2**



**Figure 4-106. Fossil *Notomys* from Mt Etna (QML1312) compared with *N. fuscus* (right) maxillae.**

### Notomys sp. 3



**Figure 4-107. Fossil *Notomys* from Mt Etna (QML1312) M<sup>1</sup> compared with *N. cervinus* (right) maxillae.**

### Pogonomys

*Pogonomys* is known from all middle Pleistocene sites older than 280ka. *Pogonomys* is easily identified within the murid fauna by the possession of the most complex, cuspidate dentition of any Australian murid. In particular, the M<sup>1</sup> morphology is very distinctive. The first row of cusps includes a T1, 1 bis, T2, an anterior cingular pocket between T2 and T3, a T3 crest connects to the base of T5; the second row of cusps include, a T4, T5, T6; whilst the third row contains T7, T8, T9, with T9 connecting to T6 via a crest and a posterior cingulum (developed as a cuspule).

On comparison with *P. mollipilosus* (= *loriae* AUS) it is obvious that the Mt Etna species is much smaller than it and possesses cusp morphologies not seen in the Australian *Pogonomys*. In particular, the anterior cingular pocket between T2 and T3, the close approximation of T6 and T9 such that when they are worn only slightly they coalesce. In addition the position of the palatal vacuity in *P. mollipilosus* is placed much further forward, the posterior margin of the vacuity lying anterior to the line of the posterior margin of the zygomatic arch. This is in contrast to the Mt Etna taxon, where the palatal vacuity is placed posterior, in line with the anterior margin of the first molar. The remaining species of *Pogonomys* were harder to compare due to the lack of comparative specimens available. These species were *P. championi*, *P. fergussoniensis*, *P. loriae*, *P. macrourus* and *P. sylvestris*. Aplin et., al. (1999)

describe the dentition of *P. loriae* and compares it against *P. macrourus* and *P. sylvestris*. Based on these descriptions I am able to differentiate the Mt Etna fossil from *P. loriae* because *P. loriae* lacks the T3-T5 crest and the close approximation of T6 and T9. *P. loriae* also possesses a more elongate posterior cingulum versus a cuspidate posterior cingulum in the fossil. Based on the figures provided in Aplin et al. (1999) the small form of *P. loriae* is much larger than the fossil species at Mt Etna, therefore, ruling out both the large and small-toothed forms described by Aplin et al (1999). Both *P. macrourus* and *P. sylvestris* are smaller than *P. loriae*, therefore, good candidates for the Mt Etna fossil. However, morphological features detailed in Aplin et al (1999) differ from those present in the fossil form at Mt Etna. In particular, the fossil form lacks an oblique crest between T1 and T5 which is considered to be present in *P. macrourus* and *P. sylvestris*; the fossil instead has an oblique crest between T3 and T5. The fossil does however, possess a basal anterior cingular pocket between T2 and T3, which are also shared with *P. macrourus* and *P. sylvestris*. *P. championi* is a similar size to *P. macrourus* and *P. sylvestris*, however, tooth morphology was not available to compare. Therefore, the species of *Pogonomys* at Mt Etna will remain unknown until comparisons can be made between all four small-sized species. What is certain is that the species present at Mt Etna is not the extant species found in the Wet Tropics of far north Queensland.

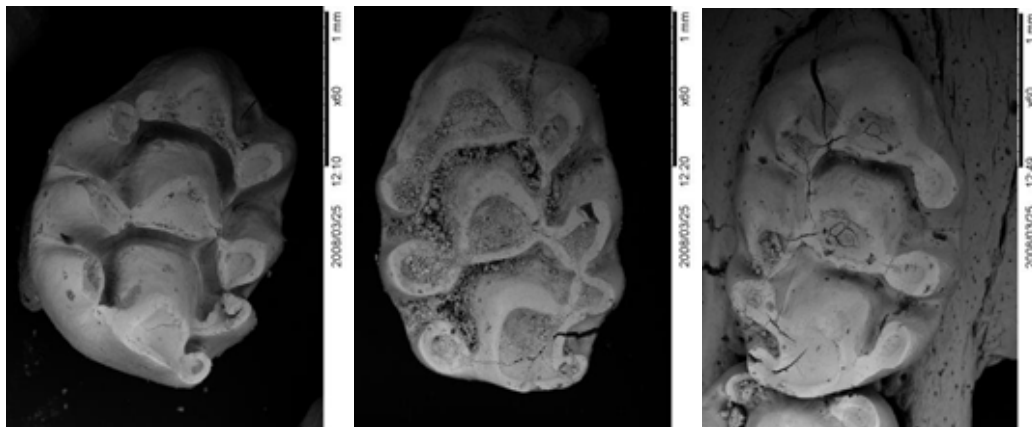


Figure 4-107. Fossil *Pogonomys* M<sup>1</sup>s from Mt Etna (QML1313).

“Mesembriomys”

Hocknull (2005) and Hocknull et al., (2007) preliminarily identified the presence of *Mesembriomys* within the fossil deposits at Mt Etna. A larger comparative sample and the discovery of a *Mesembriomys*-like murid from the Nelson Bay Formation in Victoria has led to the re-evaluation of murid fossils previously considered to be species of *Mesembriomys*.

Initially the presence of the T7 and the broadness of the tooth led to the placement of the largest specimens within *Mesembriomys*. However, with a greater understanding of the only two described species of *Mesembriomys*; *M. gouldii* and *M. macrourus*, it is now more likely that the specimens are not *Mesembriomys*, but instead represents a new extinct T7-bearing murid genus, which may have phylogenetic relationship to modern *Mesembriomys*. Therefore, for these fossil taxa to remain in *Mesembriomys*, the generic-level degree of variation would have to be expanded, which does not seem at this stage to be appropriate. Instead, the erection of a new taxon for a number of taxa bearing similar morphologies should be considered.

**sp. nov. 1**

Murid gen. et sp. nov. 1 possesses the following combination of unique features; very small  $M^1$ ; T3 heavily reduced or absent; T1 distinct and isolated; T4 distinct and isolated; T7 distinct and isolated, positioned just posterior of T4 and antero-laterally of T8; T9 reduced.

**sp. nov. 2**

Murid sp. nov. 2 possesses the following combination of unique features; very small  $M^1$ ; T3 present; accessory cusp 1bis present; T2-3, T5-6 and T8-9 form compressed loph; T7 present and positioned posteriorly to T4.

**sp. nov. 3**

Murid sp. nov. 3 possesses the following combination of unique features; medium-sized  $M^1$ ; T3 heavily reduced or absent; T1 small but present; T4 distinct and isolated; T7 distinct and isolated, positioned posterior of T4; T9 distinct and large, attached to T8.



Figure 4-108. Fossil '*Mesembriomys*' from Mt Etna (middle Pleistocene localities) compared with extant *Mesembriomys gouldii* (top right) and *M. macrurus* (bottom right), M<sup>1</sup>s.

## Uromys

### *Uromys* sp. nov.

A medium-sized species of *Uromys* is present throughout the middle Pleistocene deposits. Originally considered to be *U. caudimaculatus*, it is now thought to be a species similar to *U. caudimaculatus*, but considerably smaller (as illustrated in Fig. 4-110). A possible contender as both a taxon sharing close morphological similarities with *U. caudimaculatus*, however, being smaller in size, is the island endemic *Uromys emmae*. Unfortunately comparative specimens have not been available for this study, so determination of this species will need to await further work. Needless to say, it most likely represents either a new species with relationship to *U. caudimaculatus* and *U. emmae*.



Figure 4-109. *Uromys* sp. nov. from Mt Etna (QML1313), compared with *Melomys* sp. from Mt Etna (QML1313), maxillae.

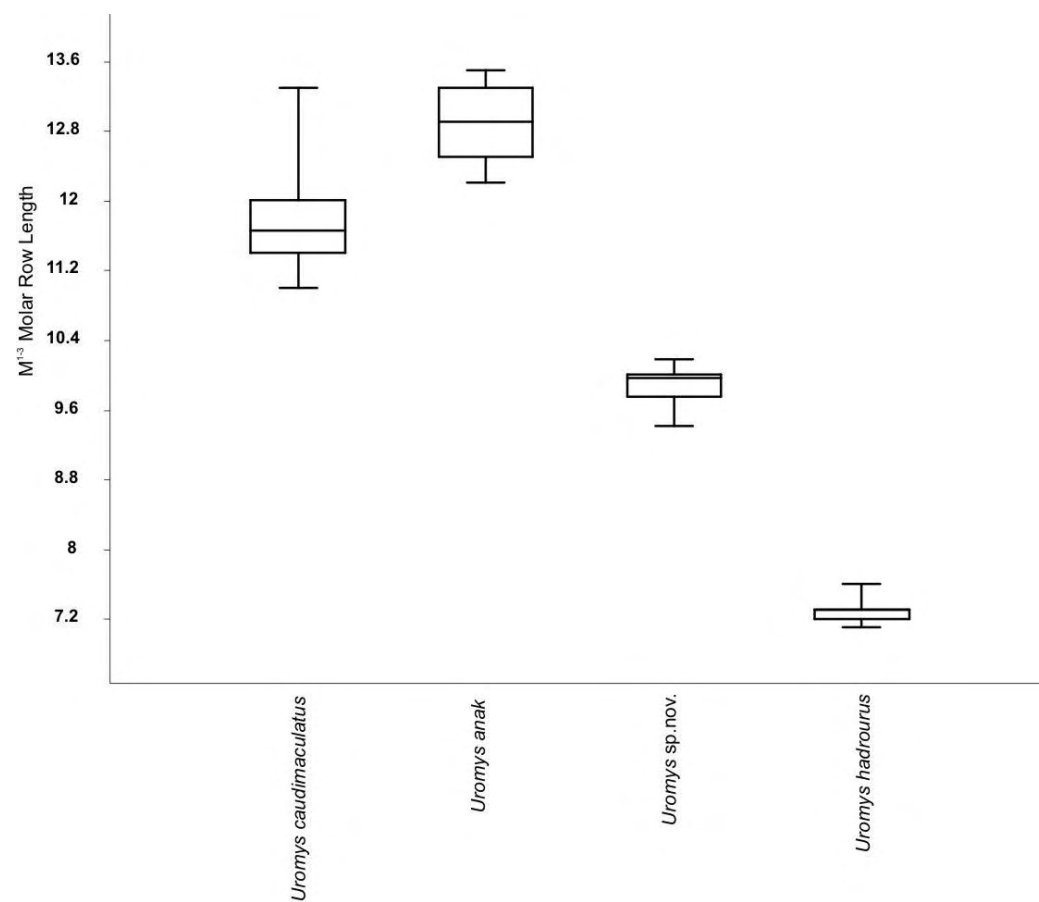
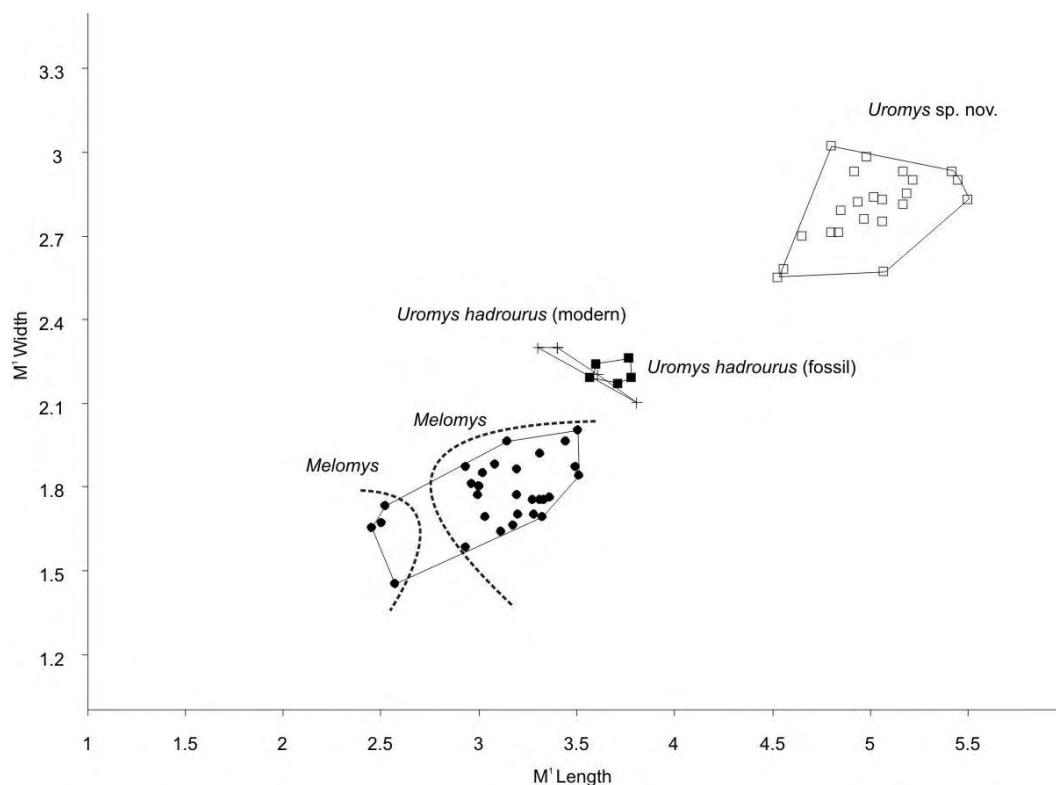


Figure 4-110. Box plot of  $M^{1-3}$  molar row length compared with extant species of *Uromys*.

### ***Uromys hadrourus***

*Uromys hadrourus* had been preliminarily identified by Godthelp when preparing Hocknull (2005), however, specific diagnostic characters awaited detailed analysis. Based primarily on molar size, the fossil specimens represent a very small species of *Uromys* within the morphometric range of *U. hadrourus*, being larger than all extant *Melomys* and representing the smallest species of *Uromys*. The molars are typical of *Uromys* being arcuate with distinctly joined crests of T1-3, T4-5 and T7-9. The molars are generally shallow with posteriorly-facing crests and the anterior portion of the zygomatic arch is broad and curved.



**Figure 4-111. Bivariate plot of M<sup>1</sup> length to width of fossil and modern *Uromys* and *Melomys* specimens.**



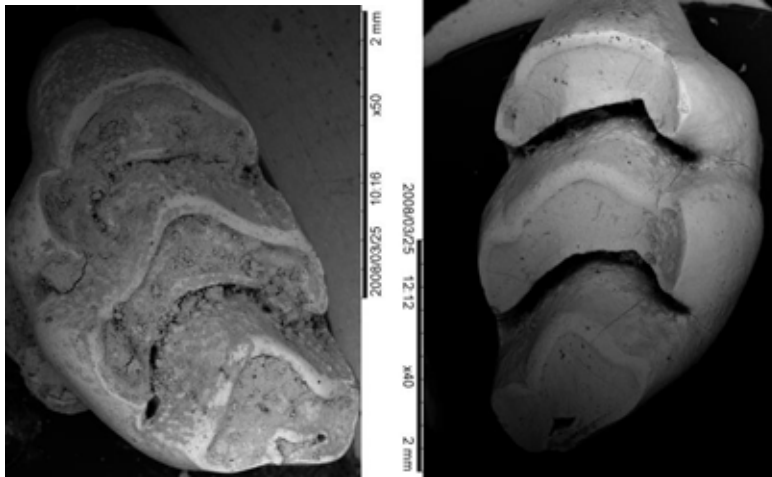


Figure 4-112. *Uromys hadrourus* from Mt Etna (QML1313) M<sup>1</sup>s.

### Melomys

Small arcuate crested molars represent *Melomys*. Based on the molar sizes it is most likely that there represent two species of *Melomys*, however, detailed morphometric and morphological comparisons will be needed, most likely with more complete maxilla and possible skulls. This is primarily due to the complex taxonomy of *Melomys*.

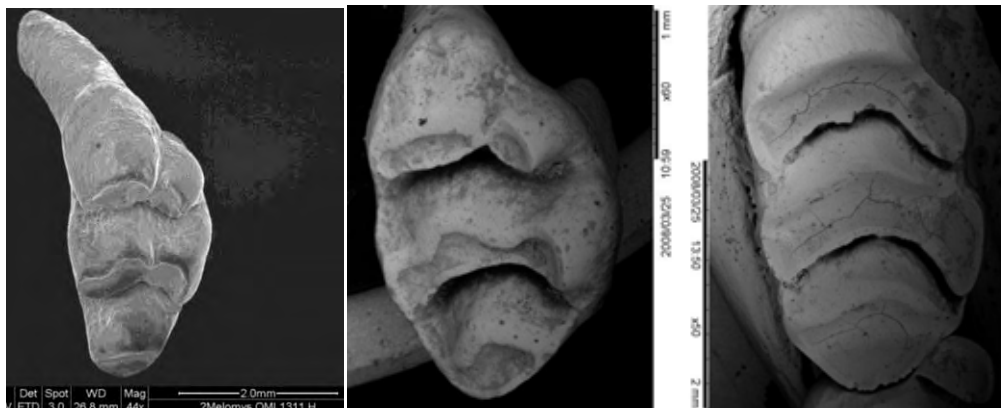


Figure 4-113. Fossil *Melomys* from Mt Etna QML1311H, QML1311 CD and QML1313, M<sup>1</sup>s.

The most up-to-date faunal list of mammalian taxa across the middle-late Pleistocene is presented in Chapter 7.

<b>Taxon</b>	<b>Identification</b>	<b>Direct comparison / Literature</b>	<b>Geographic/Geological Limitations</b>
<i>Litoria</i> sp. 1	Comparative	Direct & Literature	Australopapua Cainozoic – Extant
<i>Litoria</i> sp. 2	Comparative	Direct & Literature	Australopapua Cainozoic – Extant
<i>Litoria</i> sp. 3	Comparative	Direct & Literature	Australopapua Cainozoic – Extant
<i>Litoria</i> sp. 4	Comparative	Direct & Literature	Australopapua Cainozoic – Extant
<i>Litoria caerulea</i>	Comparative	Direct & Literature	Australopapua Cainozoic – Extant
<i>Nyctimystes</i> sp. 1	Comparative	Direct & Literature	Australopapua Cainozoic – Extant
<i>Nyctimystes</i> sp. 2	Comparative	Direct & Literature	Australopapua Cainozoic - Extant
<i>Cyclorana</i> sp. cf. <i>C. cultripes</i>	Comparative	Direct & Literature	Australian Cainozoic - Extant
<i>Cyclorana</i> sp. 2	Comparative	Direct & Literature	Australian Cainozoic - Extant
<i>Etnabatrachus maximus</i>	Comparative	Direct & Literature	Australopapua Cainozoic - Extant
<i>Crinia</i> sp.	Comparative	Direct & Literature	Australopapua Cainozoic - Extant
<i>Kyarranus</i> sp. 1	Comparative	Direct & Literature	Australian Cainozoic - Extant
<i>Kyarranus</i> sp. 2	Comparative	Direct & Literature	Australian Cainozoic - Extant
<i>Limnodynastes</i> sp. 1	Comparative	Direct & Literature	Australian Cainozoic - Extant
<i>Limnodynastes</i> sp. 2	Comparative	Direct & Literature	Australian Cainozoic - Extant
<i>Limnodynastes</i> sp. 3	Comparative	Direct & Literature	Australian Cainozoic - Extant
<i>Limnodynastes tasmaniensis</i> sp. Group	Comparative	Direct & Literature	Australian Cainozoic - Extant
<i>Limnodynastes spenceri</i> sp. Group	Comparative	Direct & Literature	Australian Cainozoic - Extant
<i>Limnodynastes peronii</i>	Comparative	Direct & Literature	Australian Cainozoic - Extant
<i>Lechriodus</i> sp. cf. <i>L. platyceps</i>	Comparative	Direct & Literature	Australian Cainozoic - Extant
<i>Neobatrachus</i> sp. 1	Comparative	Direct & Literature	Australopapua Cainozoic - Extant
<i>Neobatrachus</i> sp. 2	Comparative	Direct & Literature	Australian Cainozoic - Extant
<i>Assa</i> sp.	Comparative	Direct & Literature	Australian Extant
<i>Pseudophyrne</i> sp.	Comparative	Direct & Literature	Australian Extant
<i>Philoria</i> sp.	Comparative	Direct & Literature	Australian Extant
<i>Taudactylus</i> sp. cf. <i>T. diurnus</i>	Comparative	Direct & Literature	Australopapua Cainozoic - Extant
<i>Uperoleia</i> sp.	Comparative	Direct & Literature	Australopapua Extant
cf. <i>Hylephorbus</i>	Comparative	Direct & Literature	Australopapua Cainozoic - Extant
<i>Cophixalus</i> sp.	Comparative	Direct & Literature	Australopapua Cainozoic - Extant
New Genus	Comparative	Direct & Literature	Australopapua Cainozoic - Extant
<i>Vombatus ursinus mitchelli</i>	Comparative	Direct & Literature	Australian Cainozoic
<i>Vombatus ursinus ursinus</i>	Comparative	Direct & Literature	Australian Cainozoic - Extant
<i>Plorchestes</i> sp. cf. <i>P. pickeringi</i>	Comparative	Direct & Literature	Australian Cainozoic
diprotodontid	Comparative	Direct & Literature	Australopapua Cainozoic - Extant
<i>Troposodon</i> cf. <i>minor</i>	Comparative	Direct & Literature	Australian Cainozoic
<i>Protemnodon</i> cf. <i>devisi</i>	Comparative	Direct & Literature	Australopapua Cainozoic - Extant
<i>Protemnodon</i> sp. nov.	Comparative	Direct & Literature	Australopapua Cainozoic - Extant
<i>Protemnodon brehus</i>	Comparative	Direct & Literature	Australopapua Cainozoic – Extant

<b>Taxon</b>	<b>Identification</b>	<b>Direct comparison / Literature</b>	<b>Geographic/Geological Limitations</b>
<i>Wallabia</i> sp.	Comparative	Direct & Literature	Australopapua Cainozoic – Extant
<i>Kurrabi</i> sp. 1	Comparative	Direct & Literature	Australopapua Cainozoic – Extant
<i>Kurrabi</i> sp. 2	Comparative	Direct & Literature	Australopapua Cainozoic – Extant
cf. <i>Simosthenurus</i>	Comparative	Literature	Australopapua Cainozoic – Extant
<i>Macropus agilis</i>	Comparative	Direct & Literature	Australopapua Cainozoic – Extant
<i>Thylogale stigmatica</i>	Comparative	Direct & Literature	Australopapua Cainozoic – Extant
<i>Thylogale miniroo</i> sp. nov.	Comparative	Direct & Literature	Australopapua Cainozoic – Extant
<i>Petrogale</i> sp.	Comparative	Direct & Literature	Australian Cainozoic - Extant
cf. <i>Lagostrophus</i>	Comparative	Direct & Literature	Australian Cainozoic - Extant
<i>Aepyprymnus/Milliyowi</i> sp.	Comparative	Direct & Literature	Australian Cainozoic - Extant
<i>Bohra</i> sp. 1	Comparative	Direct & Literature	Australian Cainozoic
<i>Bohra</i> sp. 2	Comparative	Direct & Literature	Australian Cainozoic
<i>Bohra</i> sp. 3	Comparative	Direct & Literature	Australian Cainozoic
<i>Dendrolagus</i> sp. cf. <i>D. ursinus</i>	Comparative	Direct & Literature	Australopapua Cainozoic – Extant
<i>Dendrolagus</i> sp. cf. <i>D. mbasio</i>	Comparative	Direct & Literature	Australopapua Cainozoic – Extant
<i>Dendrolagus</i> sp. cf. <i>D. spadix</i>	Comparative	Direct & Literature	Australopapua Cainozoic – Extant
<i>Dendrolagus</i> sp. nov. 1	Comparative	Direct & Literature	Australopapua Cainozoic – Extant
<i>Dendrolagus</i> sp. nov. 2	Comparative	Direct & Literature	Australopapua Cainozoic – Extant
<i>Phascolarctos</i> cf. <i>stirtoni</i>	Comparative	Direct & Literature	Australian Cainozoic - Extant
<i>Madakoala</i> sp. nov.	Apomorphic (cladistic)	Direct & Literature	Australian Cainozoic - Extant
gen. et sp nov.	Apomorphic (cladistic)	Direct & Literature	Australopapua Cainozoic / Extant
<i>Pseudocheirus</i> sp. 1	Apomorphic (cladistic)	Direct & Literature	Australopapua Cainozoic / Extant
<i>Pseudocheirus</i> sp. 2	Apomorphic (cladistic)	Direct & Literature	Australopapua Cainozoic / Extant
<i>Pseudocheirus</i> sp. 3	Apomorphic (cladistic)	Direct & Literature	Australopapua Cainozoic / Extant
<i>Pseudochirulus</i> sp. 1	Apomorphic (cladistic)	Direct & Literature	Australopapua Cainozoic / Extant
<i>Pseudochirulus</i> sp. 2	Apomorphic (cladistic)	Direct & Literature	Australopapua Cainozoic / Extant
<i>Pseudochirulus</i> sp. 3	Apomorphic (cladistic)	Direct & Literature	Australopapua Cainozoic / Extant
<i>Petauroides</i> sp. 1	Apomorphic (cladistic)	Direct & Literature	Australopapua Cainozoic / Extant
<i>Petauroides</i> sp. 2	Apomorphic (cladistic)	Direct & Literature	Australopapua Cainozoic / Extant
<i>Petauroides</i> sp. 3	Apomorphic (cladistic)	Direct & Literature	Australopapua Cainozoic / Extant
<i>Pseudochirops</i> sp. 1	Apomorphic (cladistic)	Direct & Literature	Australopapua Cainozoic / Extant
<i>Pseudochirops</i> sp. 2	Apomorphic (cladistic)	Direct & Literature	Australopapua Cainozoic / Extant
<i>Pseudochirops</i> sp. 3	Apomorphic (cladistic)	Direct & Literature	Australopapua Cainozoic / Extant
<i>Pseudokoala</i> sp. 1	Apomorphic (cladistic)	Direct & Literature	Australian Cainozoic
<i>Pseudokoala</i> sp. 2	Apomorphic (cladistic)	Direct & Literature	Australian Cainozoic
<i>Pseudokoala</i> sp. 3	Apomorphic	Direct & Literature	Australian Cainozoic

	(cladistic)		
<b>Taxon</b>	<b>Identification</b>	<b>Direct comparison / Literature</b>	<b>Geographic/Geological Limitations</b>
<i>Phalanger</i> sp. nov.	Comparative	Direct & Literature	Australopapua Cainozoic / Extant
<i>Phalanger</i> cf. <i>P. mimicus</i>	Comparative	Literature	Australopapua Cainozoic / Extant
<i>Spilocuscus</i> sp.	Comparative	Direct & Literature	Australopapua Cainozoic / Extant
<i>Trichosurus</i> sp. 1	Comparative	Direct & Literature	Australopapua Cainozoic / Extant
<i>Trichosurus</i> sp. 2	Comparative	Direct & Literature	Australopapua Cainozoic / Extant
miralinid	Apomorphic (cladistic)	Literature	Australopapua Cainozoic / Extant
<i>Dactylopsila</i> sp. 1	Apomorphic (cladistic)	Direct & Literature	Australopapua Cainozoic / Extant
<i>Dactylopsila</i> sp. 2	Apomorphic (cladistic)	Direct & Literature	Australopapua Cainozoic / Extant
<i>Cercartetus</i> sp. 1	Apomorphic (cladistic)	Direct & Literature	Australopapua Cainozoic / Extant
<i>Cercartetus</i> sp. 2	Apomorphic (cladistic)	Direct & Literature	Australopapua Cainozoic / Extant
<i>Acrobates</i> sp.	Comparative	Direct & Literature	Australopapua Cainozoic / Extant
gen 1 et sp nov 1	Apomorphic (cladistic)	Direct & Literature	Australopapua Cainozoic / Extant
gen 1 et sp nov 2	Apomorphic (cladistic)	Direct & Literature	Australopapua Cainozoic / Extant
<i>Sarcophilus lanarius</i>	Comparative	Direct & Literature	Australian Cainozoic - Extant
<i>Sarcophilus harissii</i>	Comparative	Direct & Literature	Australian Cainozoic - Extant
<i>Antechinus</i> sp. nov. 1	Comparative	Direct & Literature	Australopapua Cainozoic / Extant
<i>Antechinus</i> sp. nov. 2	Comparative	Direct & Literature	Australopapua Cainozoic / Extant
<i>Antechinus flavipes</i>	Comparative	Direct & Literature	Australopapua Cainozoic / Extant
<i>Sminthopsis murina</i>	Comparative	Direct & Literature	Australopapua Cainozoic / Extant
<i>Sminthopsis macroura</i>	Comparative	Direct & Literature	Australopapua Cainozoic / Extant
<i>Planigale</i> sp.	Comparative	Direct & Literature	Australopapua Cainozoic / Extant
<i>Planigale maculata</i>	Comparative	Direct & Literature	Australopapua Cainozoic / Extant
<i>Planigale tenurostris</i>	Comparative	Direct & Literature	Australopapua Cainozoic / Extant
<i>Micromurexia</i> cf. <i>M. habbema</i>	Comparative	Direct & Literature	Australopapua Cainozoic / Extant
gen 1 et sp nov. 1	Comparative	Direct & Literature	Australopapua Cainozoic / Extant
gen 2 et sp nov 2	Comparative	Direct & Literature	Australopapua Cainozoic / Extant
gen 3 et sp. nov 3	Comparative	Direct & Literature	Australopapua Cainozoic / Extant
<i>Phascogale</i> sp. nov. 1	Comparative	Direct & Literature	Australopapua Cainozoic / Extant
<i>Phascogale topoatafa</i>	Comparative	Direct & Literature	Australopapua Cainozoic / Extant
<i>Dasyurus</i> sp. nov. 1	Comparative	Direct & Literature	Australopapua Cainozoic / Extant
<i>Dasyurus vivverinus</i>	Comparative	Direct & Literature	Australopapua Cainozoic / Extant
<i>Dasyurus hallucatus</i>	Comparative	Direct & Literature	Australopapua Cainozoic / Extant
<i>Dasyurus maculatus</i>	Comparative	Direct & Literature	Australopapua Cainozoic / Extant
<i>Leggadina</i>	Comparative	Direct & Literature	Australian Extant
<i>Pseudomys</i> 'small'	Comparative	Direct & Literature	Australian Extant

<b>Taxon</b>	<b>Identification</b>	<b>Direct comparison / Literature</b>	<b>Geographic/Geological Limitations</b>
<i>Pseudomys 'large'</i>	Comparative	Direct & Literature	Australian Extant
<i>Zyzomys</i> sp.	Comparative	Direct & Literature	Australian Extant
<i>Notomys</i> sp. 1	Comparative	Direct & Literature	Australian Extant
<i>Notomys</i> sp. 2	Comparative	Direct & Literature	Australian Extant
<i>Notomys</i> sp. 3	Comparative	Direct & Literature	Australian Extant
<i>Pogonomys</i> sp.	Comparative	Direct & Literature	Australopapua Cainozoic / Extant
" <i>Mesembriomys</i> " 1	Comparative	Direct & Literature	Australopapua Cainozoic / Extant
" <i>Mesembriomys</i> " 2	Comparative	Direct & Literature	Australopapua Cainozoic / Extant
" <i>Mesembriomys</i> " 3	Comparative	Direct & Literature	Australopapua Cainozoic / Extant
" <i>Mesembriomys</i> " 4	Comparative	Direct & Literature	Australopapua Cainozoic / Extant
<i>Uromys</i> sp. nov.	Comparative	Direct & Literature	Australopapua Cainozoic / Extant
<i>Uromys hadrourus</i>	Comparative	Direct & Literature	Australopapua Cainozoic / Extant
<i>Melomys</i> sp.	Comparative	Direct & Literature	Australopapua Cainozoic / Extant
<i>Melomys cervinipes</i>	Comparative	Direct & Literature	Australopapua Cainozoic / Extant
<i>Conilurus albipes</i>	Comparative	Direct & Literature	Australian Extant
<i>Conilurus</i> sp. nov.	Comparative	Direct & Literature	Australian Extant
<i>Rattus</i> spp.	Comparative	Direct & Literature	Australopapua Cainozoic / Extant
?new genus	Comparative	Direct & Literature	Australopapua Cainozoic / Extant
<i>Hydromys</i>	Comparative	Direct & Literature	Australian Extant
? <i>Peroryctes</i> sp. 1	Apomorphic (cladistic)	Direct & Literature	Australopapua Cainozoic / Extant
? <i>Peroryctes</i> sp. 2	Apomorphic (cladistic)	Direct & Literature	Australopapua Cainozoic / Extant
<i>Peroryctid</i> 3	Apomorphic (cladistic)	Direct & Literature	Australopapua Cainozoic / Extant
<i>Perameles</i> sp. 1	Apomorphic (cladistic)	Direct & Literature	Australopapua Cainozoic / Extant
<i>Perameles</i> sp. 2	Apomorphic (cladistic)	Direct & Literature	Australopapua Cainozoic / Extant
<i>Perameles bouganville</i>	Comparative	Direct & Literature	Australian Extant
<i>Perameles nasuta</i>	Comparative	Direct & Literature	Australian Extant
<i>Isodon obesulus</i>	Comparative	Direct & Literature	Australian Extant
<i>Isodon</i> sp. 1	Comparative	Direct & Literature	Australian Extant
<i>Chaeropus ecaudatus</i>	Comparative	Direct & Literature	Australian Extant
<i>Macrotis lagotis</i>	Comparative	Direct & Literature	Australian Extant
<i>Isodon macrourus</i>	Comparative	Direct & Literature	Australian Extant
<i>Ampibolurus</i>	Comparative	Direct & Literature	Australian Extant
<i>Pogona</i> sp. (small)	Comparative	Direct & Literature	Australian Extant
<i>Tympanocryptis</i> cf. <i>cephalus</i>	Comparative	Direct & Literature	Australian Extant
<i>Hypsilurus</i> sp.	Comparative	Direct & Literature	Australopapua Cainozoic / Extant

<b>Taxon</b>	<b>Identification</b>	<b>Direct comparison / Literature</b>	<b>Geographic/Geological Limitations</b>
<i>Diporiphora</i>	Comparative	Direct & Literature	Australian Extant
<i>Tiliqua scincoides</i>	Comparative	Direct & Literature	Australian Extant
<i>Cyclodomorphus gerrardii</i>	Comparative	Direct & Literature	Australian Extant
<i>Tiliqua</i> sp. nov.	Comparative	Direct & Literature	Australian Extant
<i>Egernia major</i>	Comparative	Direct & Literature	Australian Extant
<i>Egernia</i> sp.	Comparative	Direct & Literature	Australian Extant
<i>Sphenomorphus</i> group robust	Comparative	Direct & Literature	Australian Extant
<i>Sphenomorphus</i> group gracile	Comparative	Direct & Literature	Australian Extant
<i>Varanus</i> sp.	Comparative	Direct & Literature	Australian Extant
<i>V. komodoensis</i>	Apomorphic (cladistic)	Direct & Literature	Wallacea
gekkonidae	Comparative	Direct & Literature	Australian Extant
elapid small	Comparative	Direct & Literature	Australian Extant
elapid large	Comparative	Direct & Literature	Australian Extant
<i>Pseudechis</i>	Apomorphic (cladistic)	Direct & Literature	Australian Extant
pythonine small	Comparative	Direct & Literature	Australian Extant
pythonine large	Comparative	Direct & Literature	Australian Extant
<i>Yurlunggur</i>	Apomorphic (cladistic)	Direct & Literature	Australopapua Cainozoic / Extant
typhlopidae	Comparative	Direct & Literature	Australian Extant
<i>Rheodactyles</i>	Comparative	Direct & Literature	Australian Extant
chelid	Comparative	Direct & Literature	Australian Extant
<i>Quinkana</i> sp.	Apomorphic (cladistic)	Direct & Literature	Australian Cainozoic

**Table 4-5. Taxonomic methodology and coverage for the taxa identified during this work. Apomorphy-based versus comparative-based method for identification; literature-based or direct comparisons to extant and extinct taxa; geographical and temporal coverage of comparisons.**

## Chapter 5

### 5.1 Dragon's Paradise Lost: Palaeobiogeography, Evolution and Extinction of the Largest-Ever Terrestrial Lizards (Varanidae).

### 5.2 Preface

The following chapter is a published work:

Hocknull SA, Piper PJ, van den Bergh GD, Due RA, Morwood MJ, et al. (2009)  
Dragon's Paradise Lost: Palaeobiogeography, Evolution and Extinction of **the  
Largest-Ever Terrestrial Lizards (Varanidae)**. **PLoS ONE 4(9): e7241.**  
**doi:10.1371/journal.pone.0007241**

It details the evolution, extinction and palaeobiogeography of large-bodied varanid lizards, which includes the only of Pleistocene *Varanus komodoensis* from mainland Australia. This record occurs in the Mt Etna fossil record and forms part of a long record of *V. komodoensis* on mainland Australia since the Early Pliocene.

### 5.3 Authors

Scott A. Hocknull, <sup>1\*</sup> Philip J. Piper, <sup>2</sup> Gert D. van den Bergh, <sup>3</sup> Rokus Awe Due, <sup>4</sup>  
Michael J. Morwood, <sup>3</sup> Iwan Kurniawan <sup>5</sup>

<sup>1</sup> Geosciences, Queensland Museum, PO Box 3300 Brisbane, Qld 4000, Australia

<sup>2</sup> Archaeological Studies Program, Basement Palma Hall, University of the Philippines, 1101 Diliman, Quezon City, Philippines.

<sup>3</sup> School of Earth and Environmental Sciences, University of Wollongong, Wollongong, New South Wales 2522, Australia.

<sup>4</sup> Indonesian Centre for Archaeology, Jl. Raya Condut Pejaten No. 4, Jakarta 12001, Indonesia

<sup>5</sup> Geological Survey of Indonesia, Jl Diponegoro, No. 57, Bandung 40122, Indonesia

\* Corresponding Author: scott.hocknull@qm.qld.gov.au

## 5.4 Abstract

*Background:* The largest living lizard species, *Varanus komodoensis* Ouwens 1912, is vulnerable to extinction, being restricted to a few isolated islands in eastern Indonesia, between Java and Australia, where it is the dominant terrestrial carnivore.

Understanding how large-bodied varanids responded to past environmental change underpins long-term management of *V. komodoensis* populations.

*Methodology/Principal Findings:* We reconstruct the palaeobiogeography of Neogene giant varanids and identify a new (unnamed) species from the island of Timor. Our data reject the long-held perception that *V. komodoensis* became a giant because of insular evolution or as a specialist hunter of pygmy *Stegodon*. Phyletic giantism, coupled with a westward dispersal from mainland Australia, provides the most parsimonious explanation for the palaeodistribution of *V. komodoensis* and the newly identified species of giant varanid from Timor. Pliocene giant varanid fossils from Australia are morphologically referable to *V. komodoensis* suggesting an ultimate origin for *V. komodoensis* on mainland Australia (>3.8 million years ago). *Varanus komodoensis* body size has remained stable over the last 900,000 years (ka) on Flores, a time marked by major faunal turnovers, extinction of the island's megafauna, the arrival of early hominids by 880 ka, co-existence with *Homo floresiensis*, and the arrival of modern humans by 10 ka. Within the last 2000 years their populations have contracted severely.

*Conclusions/Significance:* Giant varanids were once a ubiquitous part of Subcontinental Eurasian and Australasian faunas during the Neogene. Extinction played a pivotal role in the reduction of their ranges and diversity throughout the late Quaternary, leaving only *V. komodoensis* as an isolated long-term survivor. The events over the last two millennia now threaten its future survival.

## 5.5 Introduction

Fossils of giant varanids ( $\geq 3\text{m}$  Total Body Length) were first reported in the 1850s with the description of *Megalania prisca* from the Pleistocene of Australia [1, 2]. Since that time, and with the discovery of living Komodo Dragons (*V. komodoensis*)



on the east Indonesian islands of Flores, Rinca and Komodo [3] considerable attention was paid in trying to understand the evolution of body size in monitor lizards [4-6]. Though several processes are proposed to explain the evolution of giantism in varanids, two competing hypotheses dominate the literature: autapomorphic giantism (i.e. Island Rule) and phyletic giantism (i.e. Cope's Rule) [7]. Both processes were previously invoked for the evolution of *V. komodoensis* [4, 6, 7].

It is commonly thought that *V. komodoensis* is a classic example of autapomorphic giantism having evolved large body size sometime in the past from a small-bodied ancestor that arrived on isolated Indonesian islands, which were devoid of predatory competition [3, 8]. Some proposals suggest that *V. komodoensis* attained large body size on Flores as a specialist hunter of pygmy *Stegodon* [3, 9], the only large-bodied prey inhabiting Flores throughout the middle and late Pleistocene to as recently as 12,000 years ago [10, 11]. The alternative, phyletic giantism, is supported by independent phylogenetic studies of morphology [12-14] and genetics [15, 16], which nest *V. komodoensis* within an Australopapuan clade of varanids containing the two large-sized living species, *V. salvadorii* and *V. varius*, and the largest of all known lizards *Megalania prisca* (= *Varanus prisca*) [14]. Thus, large body size is a synapomorphy of the clade and is not an autapomorphic trait of *V. komodoensis*. The implications of the phyletic model are that: 1. The extant populations of *V. komodoensis* are relictual, having had a much wider geographic distribution in the past [17, 18]. 2. *Varanus komodoensis* arrived on Flores already large and did not evolve giantism there through the processes of insular evolution [7].

We aim to reconstruct the palaeobiogeography and geochronology of Neogene large-bodied varanids by using the fossil remains available from deposits in India, Java, Flores, Timor and Australia.

## 5.6 Methods

### Morphometrics

Five measurements were taken of fossil and modern *Varanus* cervical, dorsal, sacral and anterior caudal vertebrae (Figure 1). Measurements were undertaken using dial or digital callipers to 0.5mm resolution. See Table S1 for specimen list and data.

Measurements are in millimetres (mm) and include:

1. Prezygapophysis to postzygapophysis length (Pre-Post), measured from the anterior margin of the prezygapophyses to the posterior margin of the postzygapophyses (Figure 1, A).

2. Centrum length (CL), measured from the posterior margin of the cotyle to the posterior margin of the condyle (Figure 1, B).

3. Cotylar width (CW), measured from the left lateral margin of the cotyle to the right lateral margin of the cotyle (Figure 1, C).

4. Postzygapophysis to postzygapophysis width (Post-Post), measured from the lateral margin of the left postzygapophysis to the lateral margin of the right postzygapophysis (Figure 1, D).

5. Prezygapophysis to prezygapophysis width (Pre-Pre), measured from the lateral margin of the left prezygapophysis to the lateral margin of the right prezygapophysis (Figure 1, E).

Two measurements were taken of fossil and modern *Varanus* teeth (Figure 1).

1. Crown height, measured from the base of the tooth plicidentine to the crown tip if preserved (Figure 1, F).

2. Basal width, measured from the anterior margin to the posterior margin of the base of the tooth (Figure 1, G).

Two measurements were taken from the humerus of fossil and modern *Varanus* (Figure 1) [19].

1. Maximum diaphysis width of humeri (Figure 1, H).

2. Maximum width of the distal end (Figure 1, I).

### Capturing Maximal Size Variation

Our modern sample of *V. salvator* may not represent the maximal size limit seen in the largest *V. salvator* individuals. Our comparative sample of *V. salvator* was close to the maximal snout-vent lengths (SVL) recorded in a large sample of this taxon; however, the largest specimen from our sample had a total length approximately 15-20% shorter than the total length of the longest recorded *V. salvator* (321cm) [20]. Therefore, we took the measurements of our largest *V. salvator* vertebral specimens and increased them by 20%, adding these additional measurements to the main dataset. This provided a more accurate estimate of *V. salvator* maximal size limits.

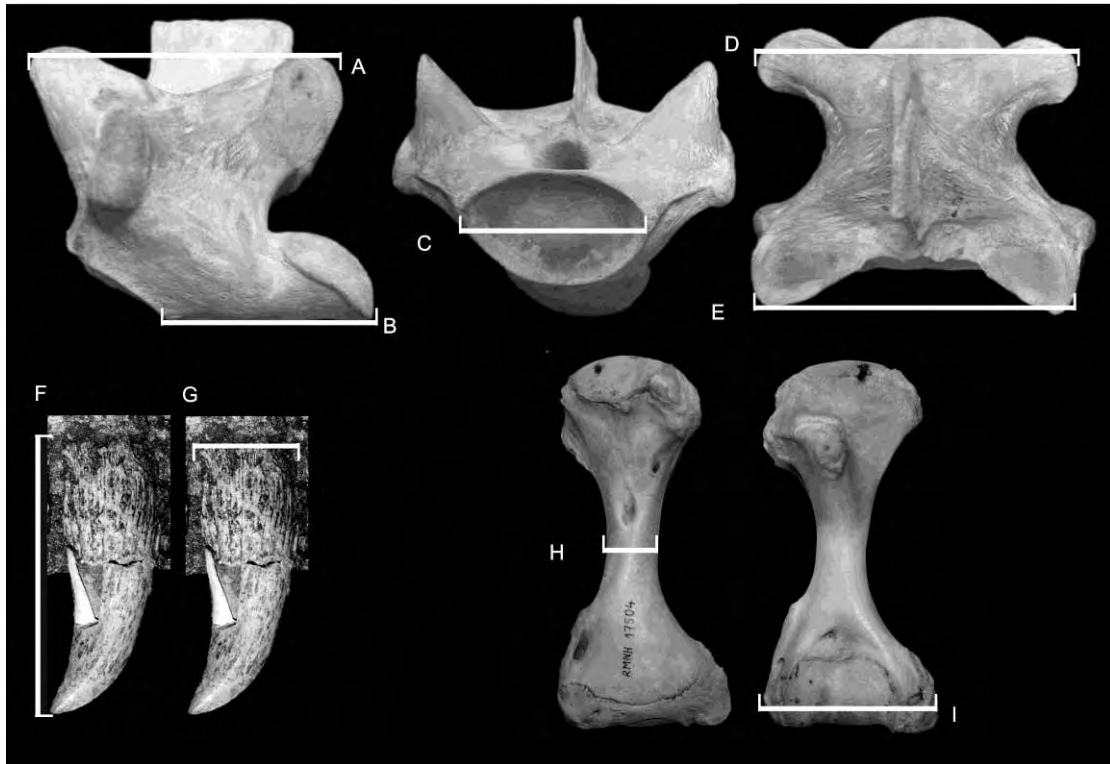


**Figure 5-1.** Morphometric measurements. **A.** Pre-postzygapophysis length. **B.** Centrum length. **C.** Cotylar width. **D.** Post-postzygapophysis width. **E.** Pre-prezygapophysis width. **F.** Tooth crown height. **G.** Tooth base length. **H.** Diaphysis width (humerus). **I.** Distal condyle width (humerus).

### Descriptive Statistics

Bivariate plots of morphometric data were plotted to determine the position of fossil specimens in relation to the modern samples taken of *Varanus*. Convex hulls were drawn to delineate the area of maximal variation observed in the samples. Due to the different preservation states of many of the specimens, only a single measurement might be available (univariate data). For these data frequency distribution histograms or box-plots showing the median value, 25-75% quartiles and the minimal and maximal values, were produced to determine where in the range of variation the fossil specimens plotted out. Principle components analysis (PCA) was applied to analyse multivariate data; however, most multivariate analyses were uninformative due to the large amount of missing data from the fossil specimens.

Where possible statistical tests were carried out where fossil sample sizes were sufficient to return an informative result. Descriptive statistics and tests were conducted using PAST software version 1.82b [21].

## 5.7 Results

*Varanus komodoensis* Ouwens 1912

Australia (Early Pliocene – middle Pleistocene).

Fossil specimens from Pliocene and Pleistocene-aged sites in Australia (Table 1) were identified as belonging to *Varanus komodoensis* on the basis of the following combination of unique cranial and post-cranial characteristics. Overall similar size and proportions of all preserved skeletal elements. Maxilla contributes to the labial margin of the premaxillary-maxillary aperture (pmp). Maxillary margin of the pmp shallow. Premaxillary-maxillary suture faces antero-lingually. Angulate maxillary crest. Labio-lingually compressed, closely-set recurved and serrated dentition both on maxillae and dentaries. At least 12 tooth loci in dentary. Parietal with distinct supratemporal crests, with fronto-parietal suture interlocking. Humerus stockier than all other members of *Varanus*, except *V. prisca*.

**Maxillae (Figure 2, B-D and Figure 3, H-I).** Three maxillae; a near complete right maxilla (QMF 874), the anterior section of a right maxilla (QMF 42105) and the posterior portion of a left maxilla (QMF 54605) share closest morphology and size with *Varanus komodoensis*. QMF42105 represents a marginally larger individual than specimens QMF874 and QMF 54605. All three share with *V. komodoensis* closely-spaced, labio-lingually compressed, recurved dentition with finely grooved plicidentine, and serrated mesial and distal margins. The teeth are morphometrically similar to the modern *V. komodoensis* sample (Figure S1).

QMF 874 and QMF 42105 also share with *V. komodoensis* a distinct interlocking premaxillary-maxillary suture with an open premaxillary-maxillary aperture (pmp) and an angulate narial crest. The circumference of the premaxillary-maxillary aperture is made up by the premaxilla and maxilla to varying degrees in different *Varanus* groups (Figure S2). In the fossil maxillae only the posterior and labial margins of the pmp are enclosed by the maxilla, the remainder is enclosed by the premaxilla. This key feature allies the fossils to taxa where the premaxilla contributes to the anterior and lingual margin of the pmp (*V. indicus*, *V. varius* group and *V. gouldii* group). The fossils differ morphologically from *V. indicus* by possessing an interlocking and anterolingually oriented premaxillary-maxillary suture articulation, more labially

angulate maxillary crest and more recurved dentition. Morphometrically, the fossils are also much larger.

Morphologically the fossil specimens are most similar to members of the *V. varius* group and to some members of the *V. gouldii* group, in particular *V. varius*, *V. komodoensis*, *V. panoptes* and *V. mertensi* (Figure S2). The maxillary margin of the pmp in the *V. varius* group is shallower than those from the *V. gouldii* group. The pmp is similarly shallow in both fossil maxillae, allying them closer to the *V. varius* group. The only taxon present in either the *gouldii* or *varius* groups that reaches the large size of the fossils and possesses the closely-spaced, recurved dentition, is *V. komodoensis*.

**Table 1.** Pliocene – Pleistocene fossils from Queensland representing *Varanus komodoensis*.

Specimen	Registration	Location (Fauna)	Age	Age Reference
Cervical vertebra	QMF 23684	Bluff Downs Local Fauna, north-eastern Queensland	Early Pliocene	[32]
Dorsal vertebra	QMF 23686	Bluff Downs Local Fauna, north-eastern Queensland	Early Pliocene	[32]
Right maxilla	QMF 874	Chinchilla Sands Local Fauna, south-east Queensland	Middle Pliocene	[33]
Right maxilla (partial)	QMF 42105	Chinchilla Sands Local Fauna, south-east Queensland	Middle Pliocene	[33]
Left dentary (partial)	QMF 870+QMF 871	Chinchilla Sands Local Fauna, south-east Queensland	Middle Pliocene	[33]
Quadrate	QMF 42156	Chinchilla Sands Local Fauna, south-east Queensland	Middle Pliocene	[33]
Supraorbital	QMF 25392	Chinchilla Sands Local Fauna, south-east Queensland	Middle Pliocene	[33]
Parietal	QMF 53956	Chinchilla Sands Local Fauna, south-east Queensland	Middle Pliocene	[33]
Scapulocoracoid	QMF 866	Chinchilla Sands Local Fauna, south-east Queensland	Middle Pliocene	[33]
Left humerus (partial)	QMF 53954	Chinchilla Sands Local Fauna, south-east Queensland	Middle Pliocene	[33]
Right humerus (partial)	QMF 53955	Chinchilla Sands Local Fauna, south-east Queensland	Middle Pliocene	[33]
Vertebrae	QM Colln (numerous)	Chinchilla Sands Local Fauna, south-east Queensland	Middle Pliocene	[33]
Left maxilla (partial)	QMF 54605	Mt Etna Local Fauna, central eastern Queensland	Middle Pleistocene	[28]
Supraoccipital	QMF 54607	Mt Etna Local Fauna, central eastern Queensland	Middle Pleistocene	[28]
Quadrate (right)	QMF 54606	Mt Etna Local Fauna, central eastern Queensland	Middle Pleistocene	[28]
Tibia	QMF 54608	Mt Etna Local Fauna, central eastern Queensland	Middle Pleistocene	[28]
Ulna diaphysis	QMF 54604	Mt Etna Local Fauna, central eastern Queensland	Middle Pleistocene	[28]
Dorsal vertebra	QMF 54120	Mt Etna Local Fauna, central eastern Queensland	Middle Pleistocene	[28]
Caudal vertebra	QMF 1418	Marmor Quarry, eastern Queensland	Middle Pleistocene	[34]

**Supraorbital (Figure 2, E).** QMF 25392 is a complete left supraorbital bone, which matches closely *V. komodoensis*, including the possession of a thick postorbital bar which projects postero-laterally, is shallowly curved and is suboval in cross-section. Proximally, the supraorbital flares in an antero-posterior direction, producing a ‘Y’ shaped bone. The dorsal surface is smooth, whilst the ventral surface preserves a rugose margin.

**Parietal (Figure 2, F).** QMF 53956 possesses distinct dorsally expressed supratemporal crests which ally this specimen to large-sized members of the *V. varius* group (*V. salvadorii*, *V. komodoensis* and *V. prisca*). QMF 53956 is smaller than *V.*

*prisca* with less defined crests and a broader central roof. Based on overall size, QMF 53956 is most similar to *V. komodoensis* and larger than *V. salvadorii*. It also possesses an interlocking frontal-parietal suture articulation, which is only seen in *V. komodoensis* and *V. prisca*.

**Quadrates (Figure 2, G-H. Figure 3, J).** Two right quadrates are known, including a complete specimen (QMF 42156) and the proximal half of another (QMF 54606). Both are similar in overall morphology and size to one another and to *V. komodoensis*. In both specimens and in *V. komodoensis*, the proximal condyle is antero-posteriorly expanded into two articular facets, both rounded basins that are relatively smooth. One or two thin laminae run ventrally to the distal condyle which is medio-laterally expanded into two similar-sized condyles. A distinct medial crest originates from the midline of the proximal articular end and runs medio-distally along the medial side of the quadrate, terminating at the antero-medial corner of the disto-medial condyle. A broad, rounded and straight ridge originates at the antero-lateral corner of the proximal articular face and runs distally to the antero-lateral corner of the disto-lateral condyle.



Figure 5-2. *Varanus komodoensis* (Pliocene, Australia). A. Modern *V. komodoensis* skull in dorsal view (NNM 17504). B. QMF 874, right maxilla in lateral view. C. QMF 42105, partial right maxilla in dorsal view. D. QMF 42105, right maxilla in dorsal view. E. QMF 25392, complete left supraorbital in dorsal view. F. QMF 53956, partial parietal in dorsal view. G-H. QMF 42156, right quadrate in anterior and lateral views. I-J. QMF 870+871, partial left dentary in lingual view, J illustrating the tooth loci. Abbreviations: mcrst, dorsal maxillary crest; pmp, premaxillary-maxillary aperture; pms, premaxilla-maxilla suture; sym, dentary symphysis; mg, Meckalian groove. Dashed line represents broken edge of maxilla. Scale bar = 5cm

**Supraoccipital (Figure 3, K).** QMF 54607 is an isolated but complete supraoccipital bone from the skull of a large species of *Varanus*. In dorsal view, it is trapezoidal in shape with a ventral width wider than the dorsal width. A ridge occurs in the midline of the bone oriented dorso-ventrally and constricted toward the middle. A cup-like recess is present on the dorsal face of the bone, which would have received the *processus ascendens*, which seems to have been unossified or at least not attached to the supraoccipital (as it is in *V. priscus*). The angle of the supraoccipital in relation to the parietal, and to the paraoccipitals would be more acute than seen in *V. priscus*, similar to that of *V. komodoensis* and less so than most other species of *Varanus*.

**Dentary (Figure 2, I-J).** QMF 870 and QMF 871 represent either a single left dentary, which is badly broken at its midline, or two separate fragments of two left dentaries. Although not noted as the same specimen, preservation and size indicates that these two specimens come from a very similar, if not the same, individual. QMF 871 is an anterior-most portion of a left dentary preserving the dentary symphysis and the first six tooth loci. The first tooth occurs just postero-dorsal of the dentary symphysis, which is rounded and bisected by the proximal origin of the Meckelian groove. The second tooth is complete and the best preserved of both specimens. The tooth is compressed labio-lingually, has a rounded distal margin and a constricted and serrate mesial cutting edge. QMF 870 is a portion of the posterior section of a left dentary, preserving five tooth loci. The dentary is missing below the dorsal margin of the Meckelian groove. The dorsal half of the posterior mental foramen can be seen in labial profile. Considered together, these two specimens indicate that the dentary preserved 12-13 tooth loci, where the teeth are closely-spaced, labio-lingually compressed, distinctly recurved and serrated. When compared to a range of *Varanus* species, it is clear that adult *V. komodoensis* possesses 12 or 13 tooth loci for each dentary; whereas other species of *Varanus* possess 11 or fewer tooth loci. *V. salvator* (10-11); *V. albigularis* (9-10); *V. indicus* (9-10); *V. varius* (9-10); *V. salvadorii* (10-11); *V. panoptes* (10-11); *V. tristis* (10-11). The only complete dentary of *V. priscus* possesses 11 tooth loci.



**Humeri (Figure 3, A-B, E-F).** A right (QMF 53955) and a left (QMF 53954) humerus, both missing the proximal and distal-most epiphyses are of similar size and morphology to *V. komodoensis*. The humeri of *V. priscus* and *V. komodoensis* are stocky and robust when compared to humeri found in all other members of *Varanus*. Both fossil humeri indicate a stout humerus with broad proximal and distal epiphyses. When comparing the maximum diaphyseal width of the two specimens with species of extant and fossil *Varanus*, both specimens fall within the size range of *V. komodoensis* and outside that of small and large *Varanus prisca* (Figure S3).

**Vertebrae (Figure 3, M-P. Figure 4).** Thirty eight dorsal vertebrae were measured from two Pliocene localities, Chinchilla (n= 37) and Bluff Downs (n= 1). All of these vertebrae fell within the size range of modern *V. komodoensis* ( $p>0.8$ ) (Figure S4). In all features, the fossil sample reflects directly similar features seen in *V. komodoensis*. A partial dorsal vertebra (QMF 54120) and a caudal vertebra collected from middle Pleistocene-aged sites at Mt. Etna and Marmor Quarry respectively represent a large-bodied varanid which is much smaller than *V. prisca*, but larger than any living varanid on mainland Australia and New Guinea (e.g. *Varanus giganteus*, *V. varius*, *V. salvadorii*) (Figure 4). QMF 54120 is a fragmentary dorsal vertebra, preserving the left lateral half of the cotyle and the left lateral portion of the postzygapophysis. On direct comparison with *V. komodoensis* it shares similar size and morphology. QMF1418 is a near complete proximal mid-caudal vertebra and falls within the size range of *V. komodoensis* (Figure S9).

**Other postcranial elements (Figure 3, L-M).** In addition to the above diagnostic skeletal elements, several other postcranial remains recovered from these Pliocene and Pleistocene sites match *V. komodoensis* in over size and general morphology. These specimens include the proximal end of a left tibia (QMF 54608), the proximal end of a dorsal rib (QMF 54603), the diaphysis of an ulna (QMF 54604) and a partial scapulocoracoid (QMF866).

Flores (early Pleistocene - Holocene)

Fossil specimens of *V. komodoensis* were recovered from the early-middle Pleistocene Ola Bula Formation in central Flores (Tangi Talo, Dhozo Dhalu) and from a late

Pleistocene-Holocene cave deposit in central-western Flores (Liang Bua) [10, 22]. Fossil specimens of *V. komodoensis* include many cranial and postcranial elements (Table S1).

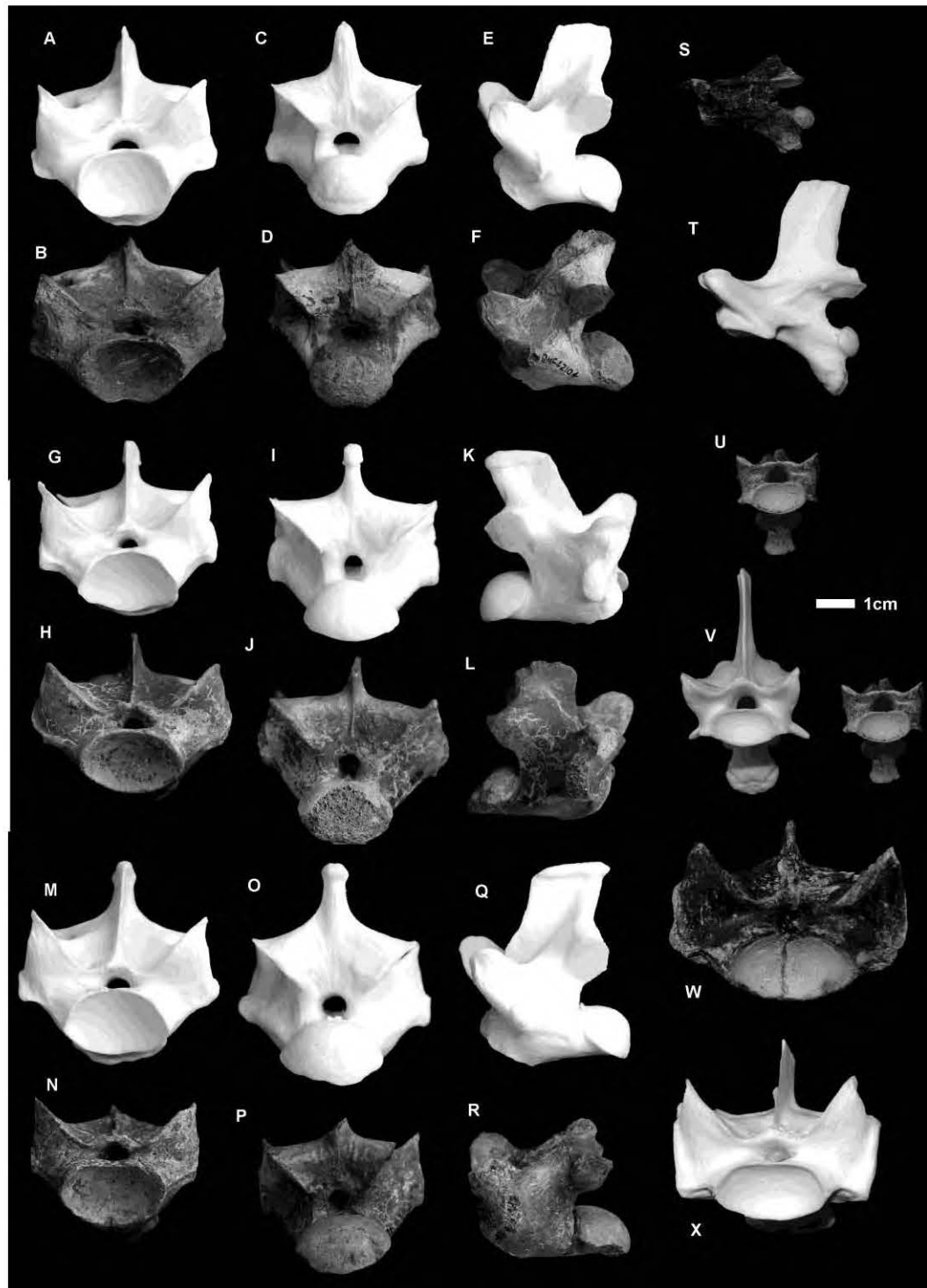


**Figure 5-3.** *Varanus komodoensis* (Neogene, Australia). A-B, E-G. Pliocene *V. komodoensis* (Australia) A-B. QMF 53955, partial left humerus in dorsal view showing position of insertion for the *latissimus dorsi* (lat dors). C-D. Left and right humerus of a modern *V. komodoensis* (NNM 17504). E-F. QMF 53954, partial right humerus in ventral

and dorsal views, showing the position of the ectepicondyle (ect). G. QMF 866, partial scapulocoracoid. H-P. Pleistocene *V. komodoensis* (Australia). H-I. QMF 54605, partial left maxilla in lingual and labial views. J. QMF 54606, partial right quadrate in anterior view. K. QMF 54607, supraoccipital bone in posterior view. L. QMF 54608, proximal left tibia. M. QMF 54604, ulna diaphysis. N-P. QMF 1418, proximal mid-caudal in cranial, oblique lateral and dorsal views. Scale bar = 1cm.

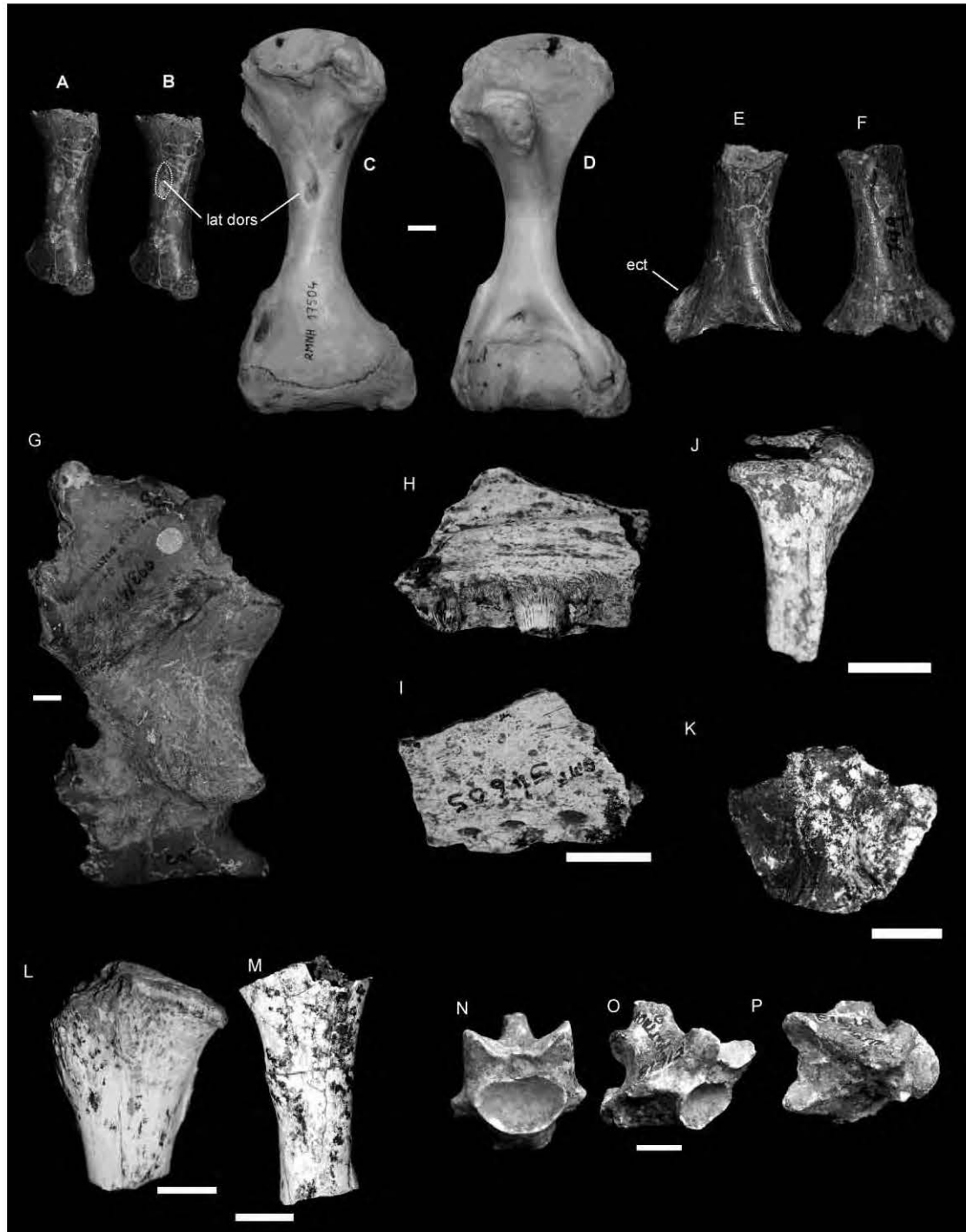


**Figure 5-4.** *Varanus komodoensis* (Pliocene, Australia). A-F. QMF 42104, posterior dorsal vertebra compared with modern *V. komodoensis* (white), in anterior (A-B), posterior (C-D) and left lateral (E-F) views. G-L. QMF 42096, mid-dorsal vertebra compared with modern *V. komodoensis* (white), in anterior (G-H), posterior (I-J) and right lateral (K-L) views. M-R. QMF 42102, mid-dorsal vertebra compared with modern *V. komodoensis*

(white), in anterior (M-N), posterior (O-P) and left lateral (Q-R) views. S-V. QMF 23684, cervical vertebra compared with modern *V. komodoensis* (white), in left lateral (S-T) and anterior (U-V) views. W-X. QMF 23686, anterior dorsal vertebra compared with modern *V. komodoensis* (white) in anterior view. Scale bar = 1 cm.

**Teeth (Figure 5, E).** Twelve teeth were studied from the Pleistocene of Flores, including six isolated teeth from early Pleistocene Tangi Talo and six teeth from late Pleistocene-Holocene Liang Bua. Morphometrically these teeth fall within the size range of *V. komodoensis* (Figure S1). Morphologically, the teeth bear the unique features of being greatly recurved and compressed labio-lingually. This feature is only present in modern *V. komodoensis* and fossil specimens referable to *V. komodoensis*.

**Cervical vertebrae (Figure 5, D).** Four well preserved cervical specimens were used in this study, including one from early Pleistocene Tangi Talo and three from late Pleistocene-Holocene Liang Bua. The Tangi Talo specimen is only slightly larger than the modern *V. komodoensis* sample (Figure S5, A). Two Liang Bua specimens are only slightly larger and one is within the morphometric range of our modern *V. komodoensis* sample (Figure S5, B). No statistical test was conducted due to the very small sample sizes for each site (1 and 3 respectively).

**Dorsal vertebrae (Figure 5, C).** Fifteen dorsal vertebrae were used in this study, all coming from Liang Bua. Due to the differing preservation states of each vertebra the only available measurement for all dorsal vertebrae was the cotylar width. When the Liang Bua fossil sample is compared to our sample of modern *V. komodoensis* the mean value for cotylar width is significantly different ( $p < 0.001$ ). When comparing the maximal size limits of our two samples the Liang Bua fossil sample is most-likely biased toward large individuals (Figure S6). Therefore, we consider the significant difference in mean cotylar width to be related to a taphonomic bias toward large individuals being preserved at the Liang Bua site, not an overall larger size. These large individuals are still within the maximal size limits of our modern sample of *V. komodoensis*. In addition, three well-preserved specimens were used in a bivariate plot of prezygapophysis – postzygapophysis (Pre-post) length over prezygapophysis – prezygapophysis (Pre-pre) width. The fossils fall within the morphometric range of modern *V. komodoensis*, with the exception of a single specimen that possesses a

slightly broader pre-pre width (Figure S7). Morphologically, the vertebrae are identical to modern *V. komodoensis*.

**Sacral vertebrae (Figure 5, B).** A single sacral vertebra from Liang Bua is directly comparable in size to *V. komodoensis* and places morphometrically within the sample of modern *V. komodoensis* (Figure S8). No statistical tests were able to be carried out due to the small sample size (n=1).

**Anterior caudal vertebrae.** Six anterior caudal vertebrae were studied from Liang Bua, all of which fall within the morphometric and morphological variation of modern *V. komodoensis*; their mean sizes not significantly different ( $p > 0.67$ ) (Figure S9).

**Humerus.** A single humeral diaphysis represents *V. komodoensis* from Tangi Talo both in size and morphology. When compared to modern *V. komodoensis* and humeri from Chinchilla, the Tangi Talo specimen has a slightly broader diaphysis (Figure S3). This may simply reflect the biased preservation of larger individuals within this deposit, as is seen in the Liang Bua collection.

**Other postcranial elements (Figure 5, H-I).** In addition to the above diagnostic specimens several other remains recovered from Liang Bua are considered to represent *V. komodoensis*, including fragments of ilia, metapodials, a phalanx, partial right mandible, and the diaphyses of an ulna and a radius (Table S1). These remains will form part of a future review of *V. komodoensis* fossils from Liang Bua.



**Figure 5-5.** *Varanus komodoensis* (Pleistocene, Flores). **A-B.** Sacral vertebrae from modern (A) and fossil (LB558a) *V. komodoensis* in anterior view. **C.** Articulated dorsal vertebrae (LB19/20-9-04) in dorsal view. **D.** Cervical vertebra (LB517b) in dorsal view. **E.** Four isolated teeth (LB04 unreg) in lingual view. **F-H.** Ulna diaphysis (LB-447a/16.8.04) in medial (F), cranial (G) and lateral (H) views. **I.** Radius diaphysis (LB-28.7.03) in medial view. Scale bar = 1cm.

*Varanus* sp. cf. *V. komodoensis*

Java (Middle Pleistocene).

A single anterior dorsal vertebra (CD6392) of a large-bodied varanid is recorded from the middle Pleistocene Kedung Brubus deposit (Figure 6, A-F). Morphometrically this specimen falls within the middle range of modern and fossil *V. komodoensis* and is

well outside the largest *V. salvator* (+20%) sample (Figure S7). CD6392 was considered to be *V. komodoensis* [17]. It is remarkably similar to *V. komodoensis* in both size and morphology, possessing steep zygapophyses, dorsally oriented condyles, distinct precondylar constriction and an open neural canal. Although the specimen is close in morphology, assignment to *V. komodoensis* is tentative and should await more specimens for verification.

*Varanus sivalensis* Falconer 1868

India, (Pliocene - early Pleistocene)

Three specimens were previously described to represent *Varanus sivalensis* [23 – 25], a distal humerus and two dorsal vertebrae (anterior and mid-dorsal vertebrae).

Whether these three specimens represent a single taxon (*V. sivalensis*) will depend on the discovery of more fossil specimens referable to this taxon. The humerus is morphologically distinct from *Varanus komodoensis* to warrant its unique taxonomic status; however, the two referred dorsal vertebrae fall within the variation of modern and fossil *V. salvator*. Therefore, it is unlikely that these three specimens represent the same taxon.

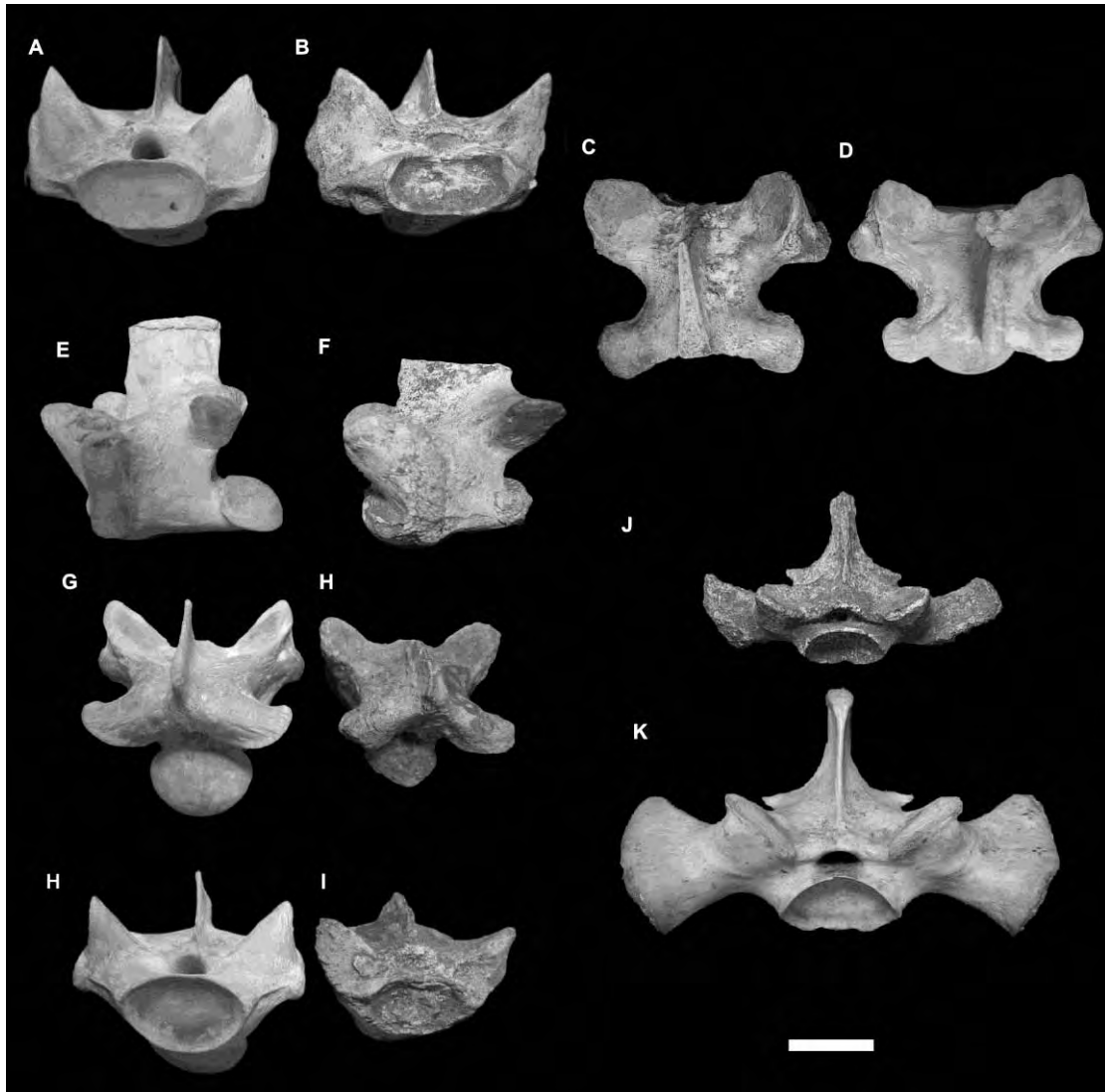


**Figure 5-6.** *Varanus* sp. cf. *V. komodoensis* and *V. salvator* (Pleistocene, Java). **A-F.** *V. sp. cf. V. komodoensis*. Anterior dorsal vertebra (CD 6392) compared with modern *V. komodoensis* in anterior (A-B), dorsal (C-D) and left lateral view (E-F). **G-K.** *V. salvator*. G-I. CD 8873, mid-dorsal vertebra, compared with modern *V. komodoensis* in dorsal (G-H) and anterior (H-I) views. J-K. CD 216, sacral vertebra, compared with modern *V. komodoensis* in anterior view. Scale bar = 1cm.

**Humerus (Figure 7, C-D).** Morphologically the humerus differs from *V. komodoensis* by features already described [12]. NHMR40816 plots in the middle range of *V. komodoensis* and outside *V. salvator*.

**Dorsal vertebrae (Figure 7, F, H, I-J, L, N).** NHMR739 is an anterior dorsal vertebra and plots within the fossil sample of *V. salvator* and is only slightly larger than the extant sample of *V. salvator* (Figure S7). NHMR740 was originally designated as a cervical vertebra; however, it is clearly a mid-dorsal vertebra, lacking any features allying it to the cervical region. Morphometrically it plots within the



lower range of *V. komodoensis* and outside the sample of modern *V. salvator*. The specimen does fit within the size range of fossil *V. salvator* from the early Pleistocene of Trinil, Java (Figures S6, S7). Both dorsal vertebrae are not considered to be significantly different to either the Trinil fossil sample or the modern *V. salvator* sample (Table 2). Both vertebrae are early Pleistocene in age, therefore, they match the Trinil specimens in morphology, size and age.

*Varanus salvator* Laurenti, 1768

Java (Early Pleistocene).

The sample of large-bodied varanid fossils from the early Pleistocene deposits of Trinil, Java include dorsal, sacral and caudal vertebrae (Figure 6, G-K). Both the sacral and caudal vertebrae fall within the variation observed in modern *V. salvator* (Figures S8, S9). The majority of dorsal vertebrae fall within the variation of modern *V. salvator* whilst three specimens fall within the lower range of the *V. komodoensis* sample used in this study. Originally considered to be *V. komodoensis* [17], these few larger specimens are considered here to represent very large individuals of *V. salvator* even though they tend to be wider than the *V. salvator* (+20%) sample (Figure S7). This may be accounted for through allometric changes of the vertebrae in the largest individuals, where breadth of vertebra increases to a greater proportion with increased length (pers. obs.). Morphologically the vertebrae are similar to the comparative sample of *V. salvator*, being more gracile than *V. komodoensis* and *V. sivalensis*, the only two varanids closest in size to *V. salvator* and the fossil specimens. Statistically, the Trinil sample is not considered to be significantly different to the modern *V. salvator* sample, or the specimens derived from the Siwalik Hills (Table 2).

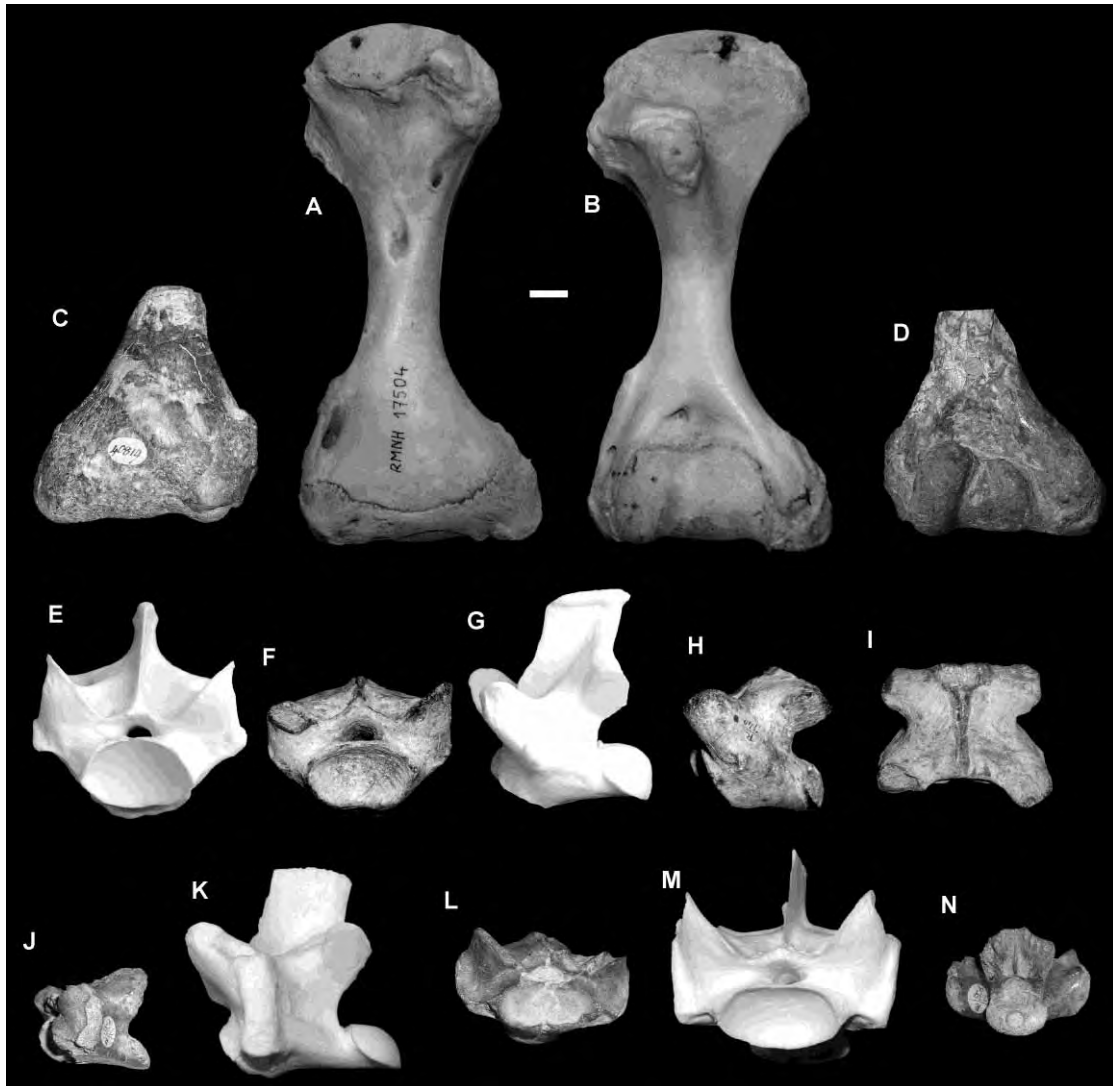


**Figure 5-7.** *Varanus sivalensis* (Pliocene, India). **A-B.** NNM 17504, modern *Varanus komodoensis* humerus. **C-D.** NHMR 40819, distal humerus in dorsal (C) and ventral (D) views. **E-I.** NHMR 740, posterior dorsal vertebra compared with modern *V. komodoensis* (white) in anterior (E-F), left lateral (G-H) and dorsal (I) views. **J-N.** NHMR 739, anterior dorsal compared with modern *V. komodoensis* (white) in left lateral (J-K), anterior (L-M) and posterior (N) views. Scale bar = 1cm.

*Varanus* sp. nov.

Timor (Middle Pleistocene)

Three massive varanid vertebrae are known from collections recovered from Timor, including a dorsal, sacral and anterior caudal vertebra (CV Collection, NNM). A mid-dorsal and anterior caudal were originally assigned to *V. komodoensis* [17]. The dorsal specimen falls within the upper morphometric range of *V. komodoensis*, but it possesses less vertically oriented condyles, has a reduced neural canal and is robust – features characteristic of *V. prisca* (Figures 8, S7). A sacral (not recorded previously)

and an anterior caudal vertebra are morphologically similar to *V. prisca*, possessing rounded condyle-cotyles, stout transverse processes and thick cortical bone. They are both intermediate in size between *V. komodoensis* and *V. prisca* (sensu stricto) and possess zygapophyses that are at a lower angle (Figures 8, S8, S9). The combination of intermediate size and unique morphology indicate that these specimens most likely represent a new unnamed taxon of large-bodied varanid.

#### Central Australia (Middle-Late Pleistocene)

**Vertebrae.** A large sample of dorsal vertebrae were measured from collections of Pleistocene varanids from central Australia. The morphometric variation encompassed by these specimens indicates the presence of a varanid intermediate in size between *V. komodoensis* and *V. prisca* (sensu stricto) (Figure S10, S11). The three samples of vertebrae were significantly different to one another with the central Australian sample showing significantly smaller size when compared to the eastern Australian *V. prisca* (sensu stricto) sample ( $p < 0.0002$ ) and significantly larger size when compared to modern and fossil *V. komodoensis* ( $p < 0.004$ ). Whether these specimens represent a diachronous sample across the middle to late Pleistocene, or a morphocline of Pleistocene giant varanids from smaller central Australian forms toward larger eastern Australian forms is yet to be determined. Regardless, these specimens indicate a giant varanid present in central Australia during the Pleistocene that resembles, at least in size, the taxon present on Timor during the middle Pleistocene.

**Table 2.** Tukey's pairwise comparisons (ANOVA) table of fossil and modern *Varanus* dorsal vertebrae, pre-post length measurements.

	Liang Bua	Siwaliks	<i>V. komodoensis</i>	<i>V. salvator</i> (n = 29)
Trinil (n = 11)	$p < 0.0004^*$	$p > 0.9$	$p < 0.002^*$	$p > 0.9$
Liang Bua (n = 3)		$p < 0.006^*$	$p > 0.9$	$p < 0.0002^*$
Siwaliks (n = 2)			$p < 0.03^*$	$p > 0.7$
<i>V. komodoensis</i> (n = 74)				$p < 0.0007^*$

\*Indicates a significant difference between samples.  
doi:10.1371/journal.pone.0007241.t002

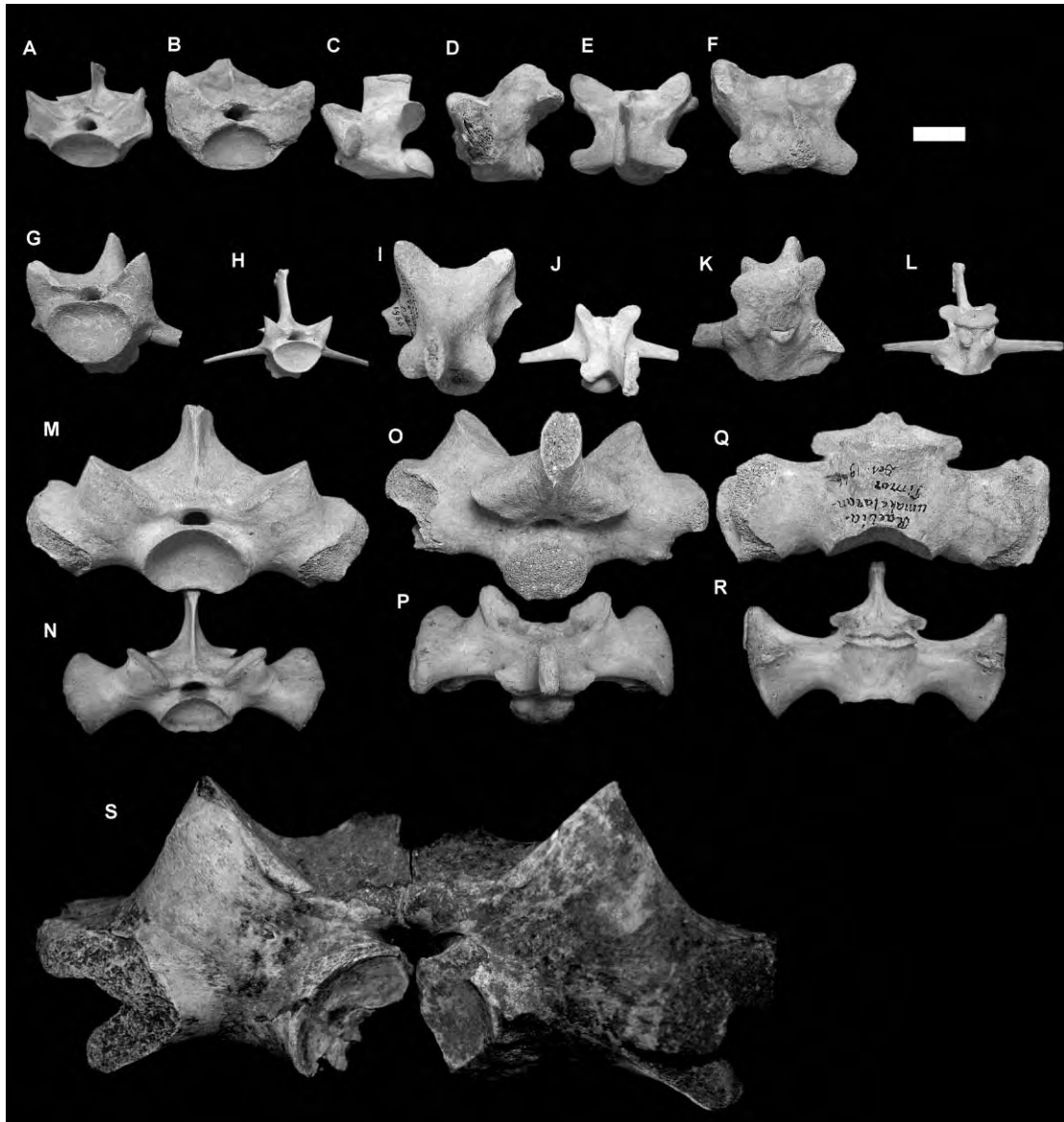


**Figure 5-8.** *Varanus* sp. nov. (Pleistocene, Timor). **A-F.** Mid-dorsal vertebra (CV Raebia 1) compared with modern *V. komodoensis* in anterior (A-B), left lateral (C-D), dorsal (E-F) views. **G-L.** Anterior caudal vertebra (CV Raebia 2) compared with modern *V. komodoensis* in anterior (G-H), dorsal (I-J) and oblique posterior (K-L) views. **M-R.** Sacral vertebra (CV Raebia 3) compared with modern *V. komodoensis* in anterior (M-N), dorsal (O-P) and ventral (Q-R) views. **S.** QMF 8968, sacral vertebra of *Varanus prisca* in anterior view.

## 5.8 Discussion.

Archaeological and paleontological excavations at sites in central and western Flores produced teeth and post-cranial elements of *V. komodoensis* dating from the early Pleistocene to the late Holocene (~900 - 2 ka) [10, 22]. This fossil record provides an opportunity to evaluate long-term morphological and morphometric changes in *V.*

*komodoensis* on Flores over ca. 900,000 years. Comparisons between fossil and extant *V. komodoensis* show that there are few morphometric or morphological differences between the fossil specimens and those of modern *V. komodoensis*. Therefore, maximal body size of this species remained stable for at least 900,000 years despite the fact that the biostratigraphic sequence on Flores records at least three faunal turnovers, marked by the extinction of the giant tortoise *Colossochelys* [26], two species of *Stegodon* and *Homo floresiensis*, as well as the arrival of hominins by 880 ka and modern humans by 10 ka [22]. Even in the absence of any moderately-sized prey between the extinction of *Stegodon florensis insularis* (~12. ka) [10, 11] and the introduction of the pig from Sulawesi (~7 ka) [10] *V. komodoensis* was able to persist on Flores. The stability of *V. komodoensis* body size over a long temporal sequence and during periods of major ecological change implies that insular evolutionary processes had limited effect, and more importantly illustrate the adaptive flexibility and resilience of a generalist carnivore, rather than a specialist predator of the island's pygmy *Stegodon*.

So, if *V. komodoensis* did not evolve on an isolated island in Wallacea, from where did it disperse? India and Australia are the only regions that preserve a giant varanid fossil record older than 900 ka, and are the only identifiable sources for large-bodied *Varanus* [2]. The oldest recorded large-bodied *Varanus* from both regions occur in the Pliocene, suggesting a relatively synchronous yet independent evolution of lizard giantism. In India large-bodied varanid fossils are rare, being represented by two vertebrae and a partial humerus, each assigned to the extinct *V. sivalensis* [24]. Both vertebrae probably represent *Varanus salvator*. The humerus is of similar size to *V. komodoensis* but differs morphologically [12]. The absence of *V. sivalensis* from younger deposits at the same locales suggests that large-bodied varanids were either very rare or more likely extinct on the Indian sub-continent by the end of the early Pleistocene. Therefore, based on both morphology and chronology, *V. sivalensis* is an unlikely source for *V. komodoensis* on Flores. *Varanus sivalensis* is associated with a Late Pliocene Siwalik fauna that includes diverse mammalian megafauna, including the placental carnivores *Crocota*, *Hyaena* and *Panthera* [27]. This record alone demonstrates that varanids can evolve giantism on continental landmasses with competition from large placental carnivores.

Varanids appear in the Australian fossil record by the Miocene and possess a more or less continuous record of large-bodied forms from the early Pliocene (~3.8mya) through to the late Pleistocene [2]. Varanids most likely dispersed eastward from Asia to Australia, then radiated to produce a clade containing *V. komodoensis* [15, 16, 18]. Although the taxonomy of the Australian Miocene-Pleistocene varanids remains largely unresolved [2], it is most likely that they are contained within this monophyletic clade. There are at least three giant varanid taxa present in Australia during the Neogene, including one species from the Pliocene, one from the Pleistocene of central Australia and *Varanus prisca* (sensu stricto) from the middle-late Pleistocene. On the basis of both size and a unique combination of morphological features shared only with *V. komodoensis* the Pliocene taxon is here considered to be conspecific with *V. komodoensis*. Newly recovered large-bodied varanid fossils from middle Pleistocene [28] deposits in north-eastern Australia are also referable to *V. komodoensis*, demonstrating the longevity of *Varanus komodoensis* on mainland Australia and the coexistence of two giant varanids, *V. prisca* and *V. komodoensis*. In combination, the evidence from the fossil record as well as the morphological and molecular phylogenetic studies clearly supports Australia as the ancestral source for *V. komodoensis*.

Large-bodied varanid fossils were previously recovered from two middle Pleistocene sites along the Solo River in Java, west of the Wallace Line - the Trinil (~900ka) and Kedung Brubus (800-700 ka) Faunas [22]. Although large, the Trinil vertebrae fall closest to the variation of modern *V. salvator*, with a few specimens comparable in size with the smallest modern *V. komodoensis*. These few larger specimens, considered previously to be *V. komodoensis* [17], more likely represent very large individuals of *V. salvator*. A single vertebra from the younger Kedung Brubus site is much bigger, comparable closely in both size and morphology with large *V. komodoensis*. We therefore conclude that it is likely that *V. komodoensis*, having reached Flores by the early Pleistocene, dispersed westward, across Wallace's Line to arrive in Java sometime during the middle Pleistocene.

Differential timing for the initial appearance of Komodo dragon in Australia, Flores and Java, therefore indicates that *V. komodoensis* dispersed from east to west, perhaps reaching Java during a period of lowered sea-level. At the time of Kedung Brubus,

Java was part of the Asian mainland, and the fauna included large placental carnivores such as *Panthera* and *Hyaena* [22], further illustrating the ability of giant varanids to exist as part of a continental, placental-dominated fauna. There is currently no evidence that giant varanids survived on Java beyond the middle Pleistocene.

Further support for the westward dispersal of giant varanids comes from Timor, an island between Flores and Australia. Three vertebral specimens from Raebia in the Atambua Basin, central Timor, represent a new unnamed species of giant varanid intermediate in size between *V. komodoensis* and *V. prisca (sensu stricto)*. The Timor specimens were derived from the uppermost part of the folded, regressive Noele Formation, of which the marine part correlates with planktonic foraminifera zones N18-N22 [29, 30]. This suggests that the specimens are at least middle Pleistocene in age. Pleistocene varanid fossils from central Australia, usually identified as *V. prisca*, are also intermediate in size between *V. komodoensis* and *V. prisca (sensu stricto)*, and may represent the same intermediate taxon present in Timor. Formal description of the new Timor-Australian varanid waits until more diagnostic specimens are available.

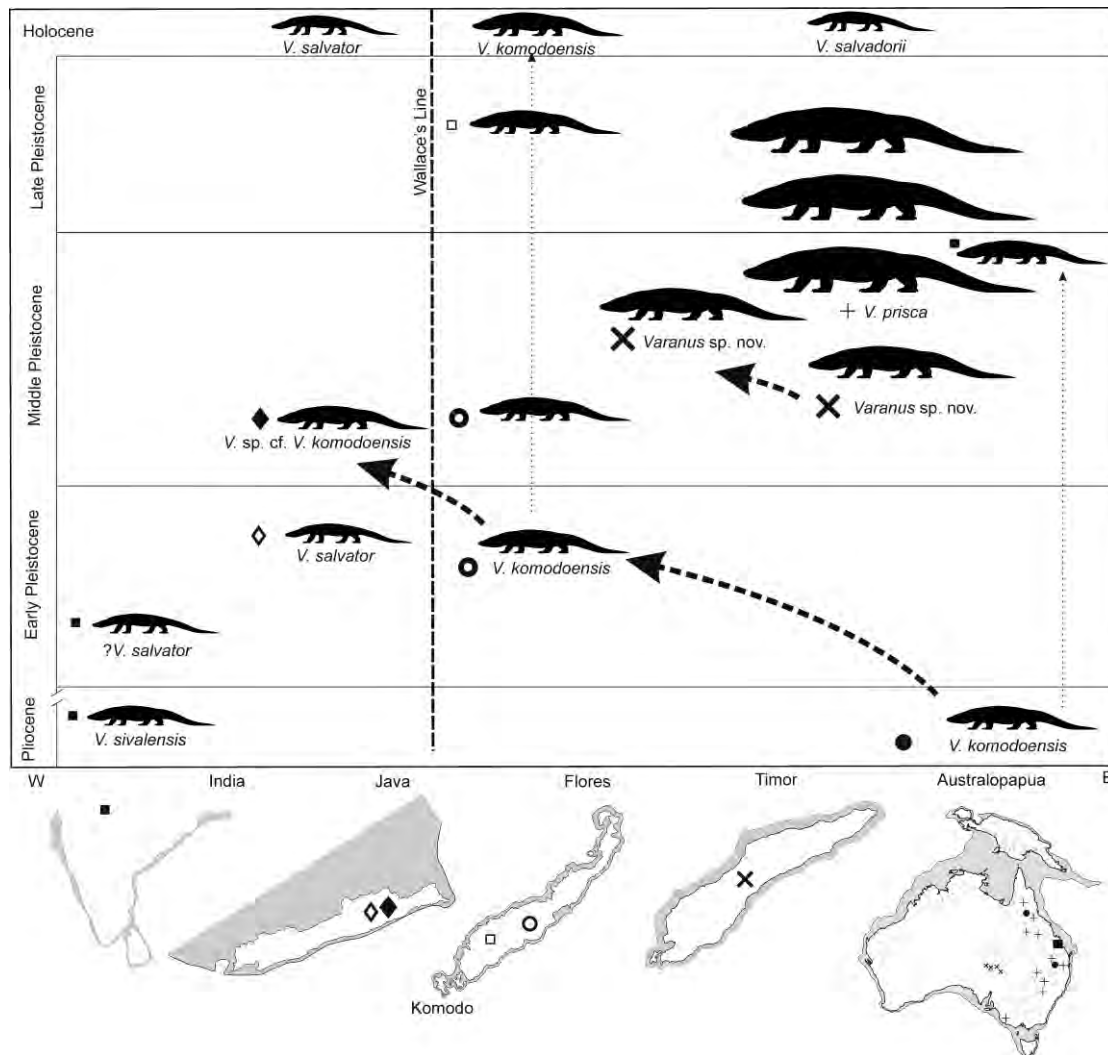


**Figure 5-9.** Palaeogeography and chronology of giant varanids. **Schematic diagram illustrating the proposed taxonomy, chronology and dispersal sequence of giant varanids from mainland Australia to the Indonesian islands of Timor, Flores and Java during the Pliocene-Pleistocene.**

## 5.9 Conclusion

The fossil record suggests that giant varanids evolved independently on mainland Asia and the island-continent of Australia during the Pliocene, alongside large-bodied mammalian carnivores. Only the Indonesian-Australian giant varanids appear to have survived beyond the early Pleistocene.

We conclude that *V. komodoensis* evolved in Australia by the early Pliocene and dispersed west as far as Flores by 900 ka and Java by 800-700 ka. It is likely that the



Timor varanid represents another large-bodied varanid lineage, attaining a larger body size than that of *V. komodoensis*, having evolved on mainland Australia and dispersed west to Timor. Continuing along this same evolutionary trajectory, *Varanus prisca*, reached gigantic proportions by the late-Middle Pleistocene, but was extinct in Australia by the end of the Pleistocene (Figure 9).

We conclude that *V. komodoensis* is the last of a clade of giant varanids that was once a ubiquitous part of Australasia, distributed from Australia across Wallacea, as far as continental Asia (Java). There is now only a relict population on Flores and a few small adjacent islands. Komodo dragon distribution has also retracted significantly on Flores itself; being present at Liang Bua in the uplands of West Flores until ~2 ka, but now only occurring in isolated habitats along the northern and western coastal lowlands [3, 31]. The retraction is likely due to habitat loss and persecution by modern humans over the last few millennia and emphasizes the continuing threat of extinction to this, the last of the giant varanids.

## 5.10 Acknowledgements

We thank Addison Wynn, Chris Thacker, Gasso Miracle, George Zug, Jeffrey Seigel, Jennie McGuire, Jim Mead, Liz Reed, Ryan Rabett and Traci Hartsell for assistance in attaining varanid morphometric data. John de Vos, Bob Jones, Tom Rich, Chris Smeenk, John McCarthy, Pim Arntzen, Michael Lee, Mark Hutchinson, Patrick Couper and Andrew Amey are thanked for access to fossil and comparative varanids held at their various institutions. Fachroel Aziz, Suyono, Ruli Setiawan, Slamet Sudiarwadi assisted with fieldwork in Timor.

## 5.11 References

1. Owen R (1859) Description of some remains of a gigantic land-lizard (*Megalania prisca*, Owen) from Australia. Philosophical Transactions of the Royal Society of London, 149: 43-48.

2. Molnar RE (2004) Dragons in the Dust: The palaeobiology of the Giant Monitor Lizard *Megalania*. (Indiana Uni. Press, Indiana) Pp210.
3. Auffenberg W (1981) The Behavioural Ecology of the Komodo Monitor. (Uni. Press of Florida, Gainesville FL) Pp406.
4. Pianka ER (1995) Evolution of body-size: Varanid lizards as a model system. *American Naturalist* 146(3), 398-414.
5. Christian A, Garland Jr (1996) Scaling of Limb Proportions in Monitor Lizards (Squamata: Varanidae). *Journal of Herpetology*, 30(2), 219-230.
6. Pianka ER (2004) Evolution of Body Size and Reproductive Tactics. In ER Pianka, DR King (Eds): *Varanoid Lizards of the World*. (Indiana University Press. Bloomington, Indiana)
7. Gould GC, MacFadden BJ (2005) Gigantism, Dwarfism and Cope's Rule: "Nothing in Evolution Makes Sense without a Phylogeny". *Bulletin of the American Museum of Natural History* 285(1), 219-237.
8. Burness GP, Diamond J, Flannery T (2001) Dinosaurs, dragons, and dwarfs: The evolution of maximal body size. *PNAS* 98(25), 14518-14523.
9. Diamond JM (1987) Did Komodo dragons evolve to eat pygmy elephants? *Nature* 326, 832.
10. van den Bergh GD, et al (2008) The youngest *stegodon* remains in Southeast Asia from the Late Pleistocene archaeological site Liang Bua, Flores, Indonesia. *Quaternary International* 182, 16-48.
11. Morwood, MJ, et al (2004) Archaeology and age of *Homo floresiensis*, a new hominin from Flores in eastern Indonesia. *Nature* 431,1087–1091.
12. Dunn, ER (1927) Results of the Douglas Burden Expeditions to the Island of Komodo, I. Notes on *Varanus komodoensis*. *American Museum Novitates*, 286, 1-10.

13. Conrad J (2008) Phylogeny and systematics of Squamata (Reptilia) based on morphology. *Bulletin of the American Museum of Natural History*. 310, 182pp.
14. Head JJ, Barrett PLS, Rayfield EJ (2009) Neurocranial osteology and systematic relationships of *Varanus (Megalania) prisca* Owen, 1859 (Squamata: Varanidae). *Zoological Journal of the Linnean Society*, 155, 445-457.
15. Ast J (2001) Mitochondrial DNA evidence and evolution in Varanoidea (Squamata). *Cladistics*, 17, 211–226.
16. Fitch AJ, Goodman AE, Donnellan, SC (2006) A molecular phylogeny of the Australian monitor lizards (Squamata: Varanidae) inferred from mitochondrial DNA sequences. *Australian Journal of Zoology* 54, 253-269.
17. Hooijer D (1972) *Varanus* (Reptilia, Sauria) from the Pleistocene of Timor. *Zoologische Mededelingen*. 47, 445-447.
18. Fuller S, Braverstock P, King D (1998) Biogeographic origins of goannas (Varanidae): A molecular perspective. *Molecular Phylogenetics and Evolution*, 9(2), 294-307.
19. Reed EH, Hutchinson, MN (2005) First record of a giant varanid (*Megalania*, Squamata) from the Pleistocene of Naracoorte, South Australia. *Memoirs of the Queensland Museum*. 51(1), 203-214.
20. Gaulke M, Horn HG (2004) *Varanus salvator* (nominate form). In E.R. Pianka & D. R. King (Eds.): *Varanoid Lizards of the World*. (Indiana University Press. Bloomington, Indiana).
21. Hammer O, Harper DAT, Ryan PD (2001) PAST: Palaeontological Statistics software package for education and data analysis. *Palaeontologica Electronica* 4(1): 9pp.

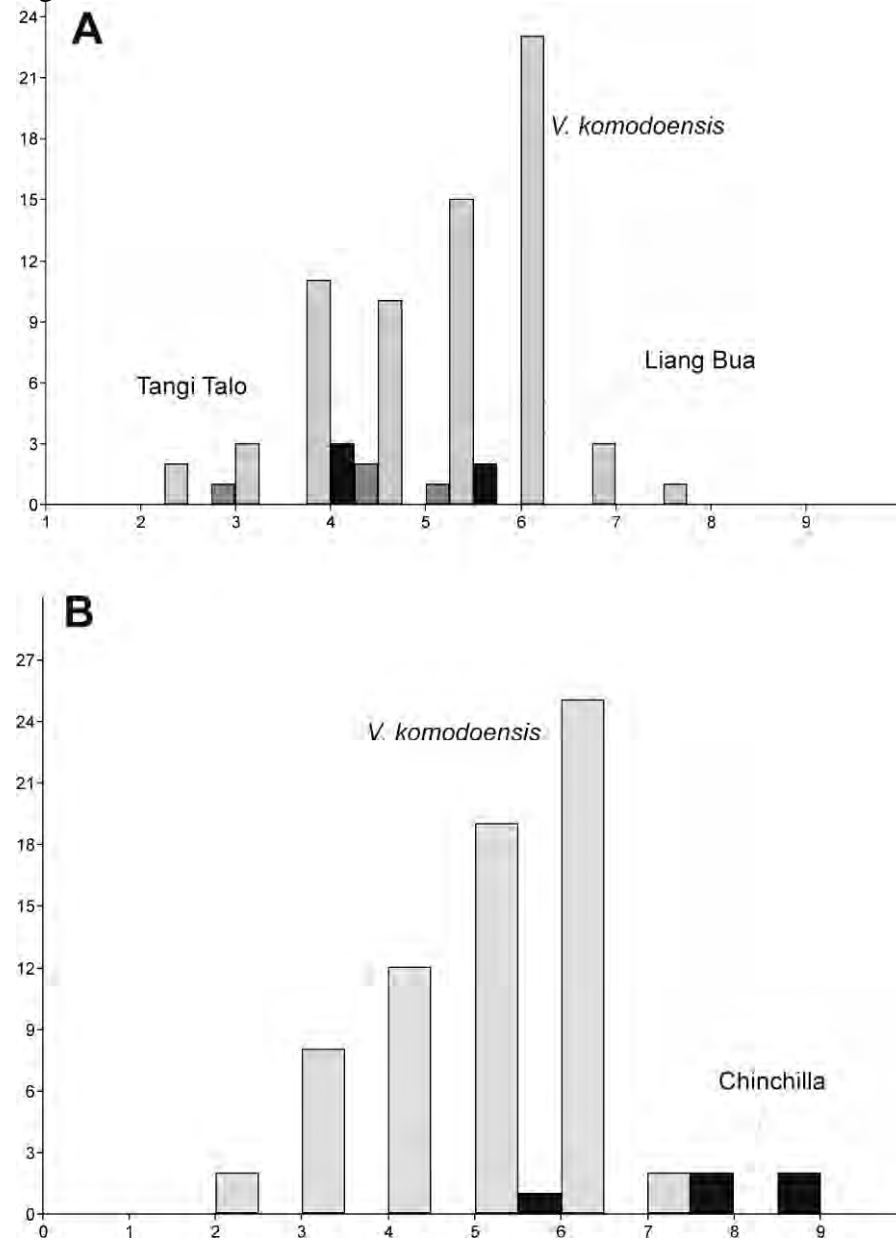
22. van den Bergh GD, de Vos J, Sondaar PY (2001) The Late Quaternary palaeogeography of mammal evolution in the Indonesian Archipelago. *Palaeogeography, Palaeoclimatology, Palaeoecology*, 171, 385-408.
23. Falconer HP (1868). *Paleontological Memoirs and Notes of the Late Hugh Falconer, A. M., M. D. with a Biographical Sketch of the Author* (C. Murchison, ed.). Volume I, *Fauna antiqua Sivalensis*. Robert Hardwicke Publishers, Picadilly.
24. Lydekker R (1886) Fauna of the Karnul caves. *Palaeontologica Indica* 10(4), 1-58.
25. Lydekker R (1888) Catalogue of the fossil Reptilia and Amphibia in the British Museum (Natural History), Cromwell Road, S.W. Pt. 1. The Orders Ornithosauria, Crocodilia, Dinosauria, Squamata, Rhynchocephalia, and Preterosauria. London: The Trustees.
26. Setiyabudi E (2006) Paleontological study on fossil giant tortoises from the Indonesian islands. (unpublished Thesis, Kagoshima University, Japan).
27. Dennell RR, Coard D, Turner A (2006) The biostratigraphy and magnetic polarity zonation of the Pabbi Hills, northern Pakistan: An Upper Siwalik (Pinjor Stage) Upper Pliocene–Lower Pleistocene fluvial sequence. *Palaeogeography, Palaeoclimatology, Palaeoecology*, 234, 168-185.
28. Hocknull SA, Zhao J-x, Feng Y-x, Webb GE (2007). Responses of Quaternary rainforest vertebrates to climate change in Australia, *Earth and Planetary Science Letters*, 264, 317-331.
29. Suwitodirdjo K, Tjokrosapoetro S (1975) Geologic Quadrangle Map, Timor, (GRDC , Bandung (1974/75).
30. de Smet MEM (1990). Detection of collision related vertical movements in the outer Banda Arc (Timor, Indonesia) using micropaleontological data. *J. SE Asian Earth Sci.*, 4(4), 337-356.

31. Murphy JB et al. (2002) Komodo Dragons: Biology and Conservation. Smithsonian Institution Press, Washington.
32. Mackness BS, Whitehead PW, McNamara GC (2000) New Potassium-Argon basalt date in relation to the Pliocene Bluff Downs Local Fauna, northern Australia. Australian Journal of Earth Sciences, 47: 807-811.
33. Dawson L, Muirhead J, Wroe S (1999) The Big Sink Fauna: a lower Pliocene mammalian fauna from the Wellington Caves complex, Wellington, New South Wales. Records of the Western Australian Museum. Supplement No. 57, 265-290.
34. Price GJ, Zhao, J-x, Feng Y-x, Hocknull, SA (2009) New Records of Plio-Pleistocene Koalas from Australia: Palaeoecological and Taxonomic Implications. Records of the Australian Museum, 61: 39-48.

## 5.12 Supporting Online Material

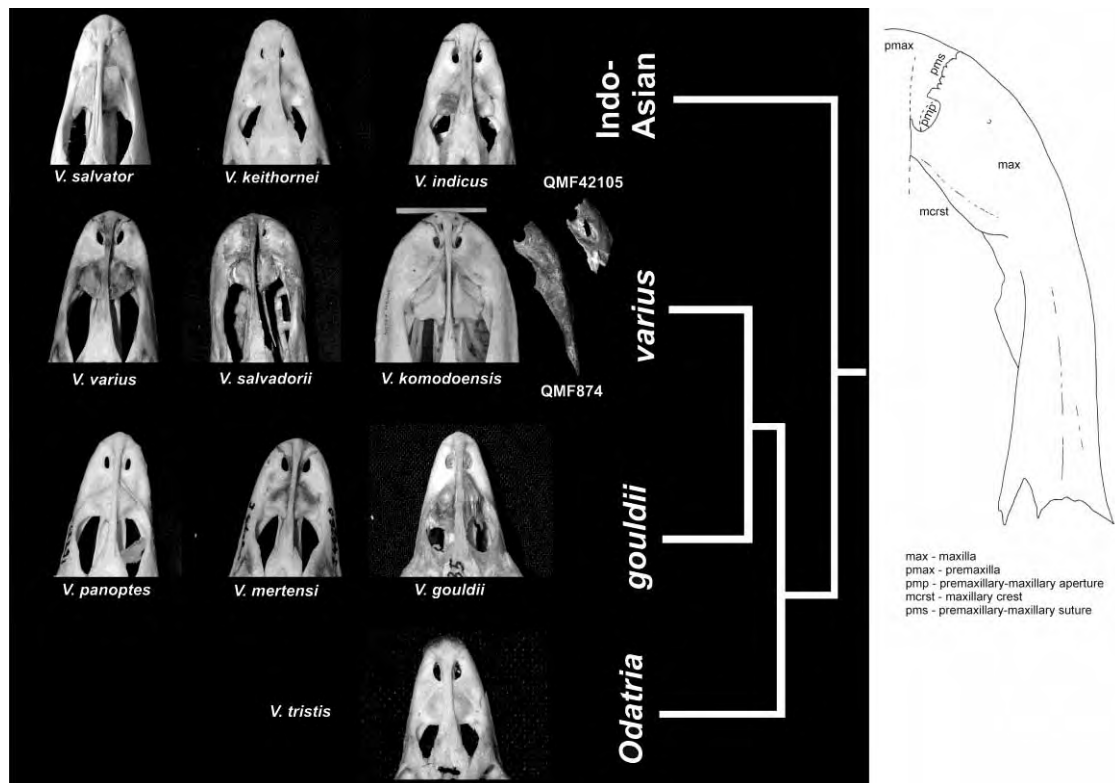
## 5.13 Supplementary Figures

Figure S1.



**Figure S1. Histogram of tooth base length measurements for modern (A-B), Pleistocene (A) and Pliocene (B) *V. komodoensis*. Tangi Talo (n = 4), Liang Bua (n = 5), Chinchilla (n = 5) and *V. komodoensis* (n = 68). Measurements in mm.**

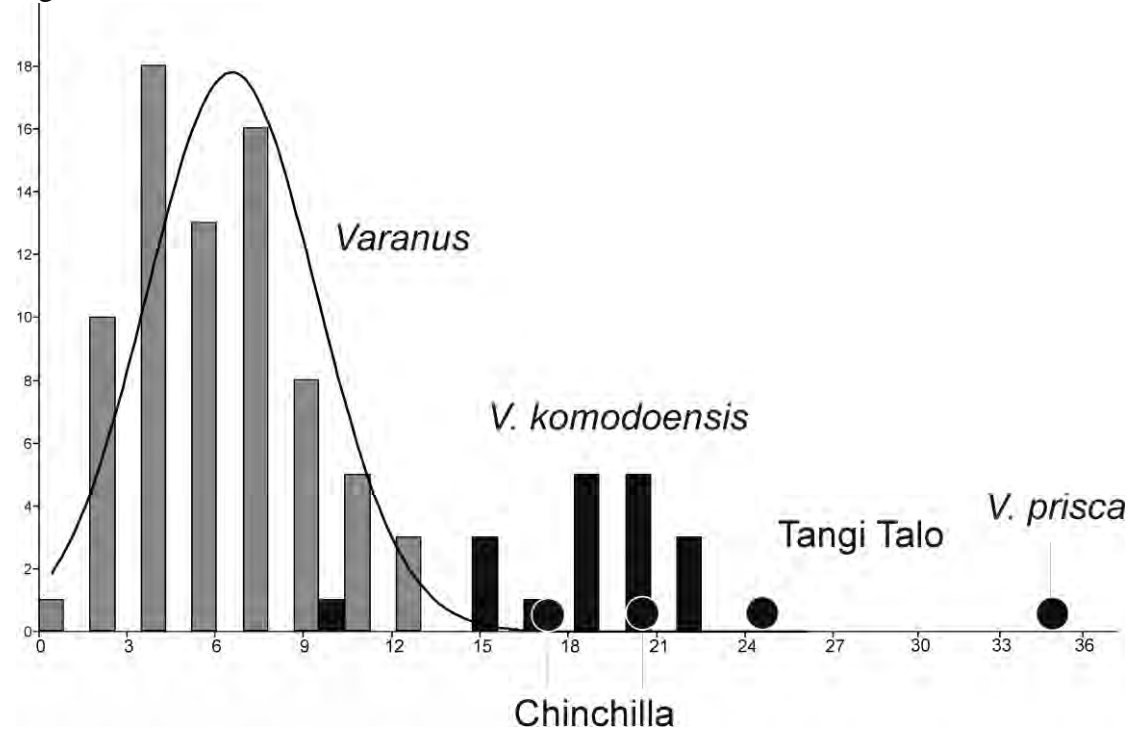
Figure S2.



**Figure S2. Morphological comparisons between Indo-Asian and Indo-Australian varanid maxillae based on the phylogenetic reconstruction of Ast (2001). *Varanus varius* group with fossil specimens for comparison (to scale with *V. komodoensis*).**

Ast, J.C. 2001. Mitochondrial DNA Evidence and Evolution in Varanoidea (Squamata). *Cladistics*, 17, 211–226.

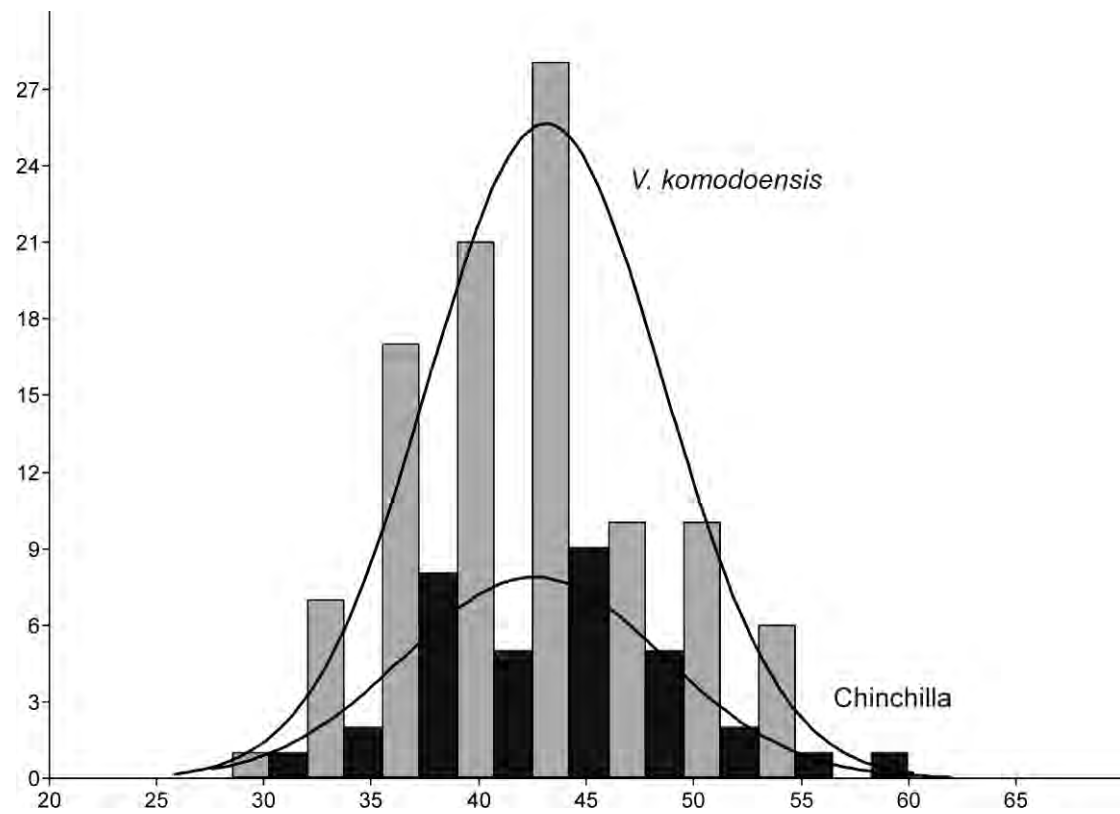
Figure S3.



**Figure S3.** Histogram of humerus maximum diaphysis width with normal curve fitted to *Varanus* sample. *Varanus* spp. (n = 71), *Varanus komodoensis* (n = 18) (see Hutchinson & Reed (2005) for taxa used) . Measurements in mm.

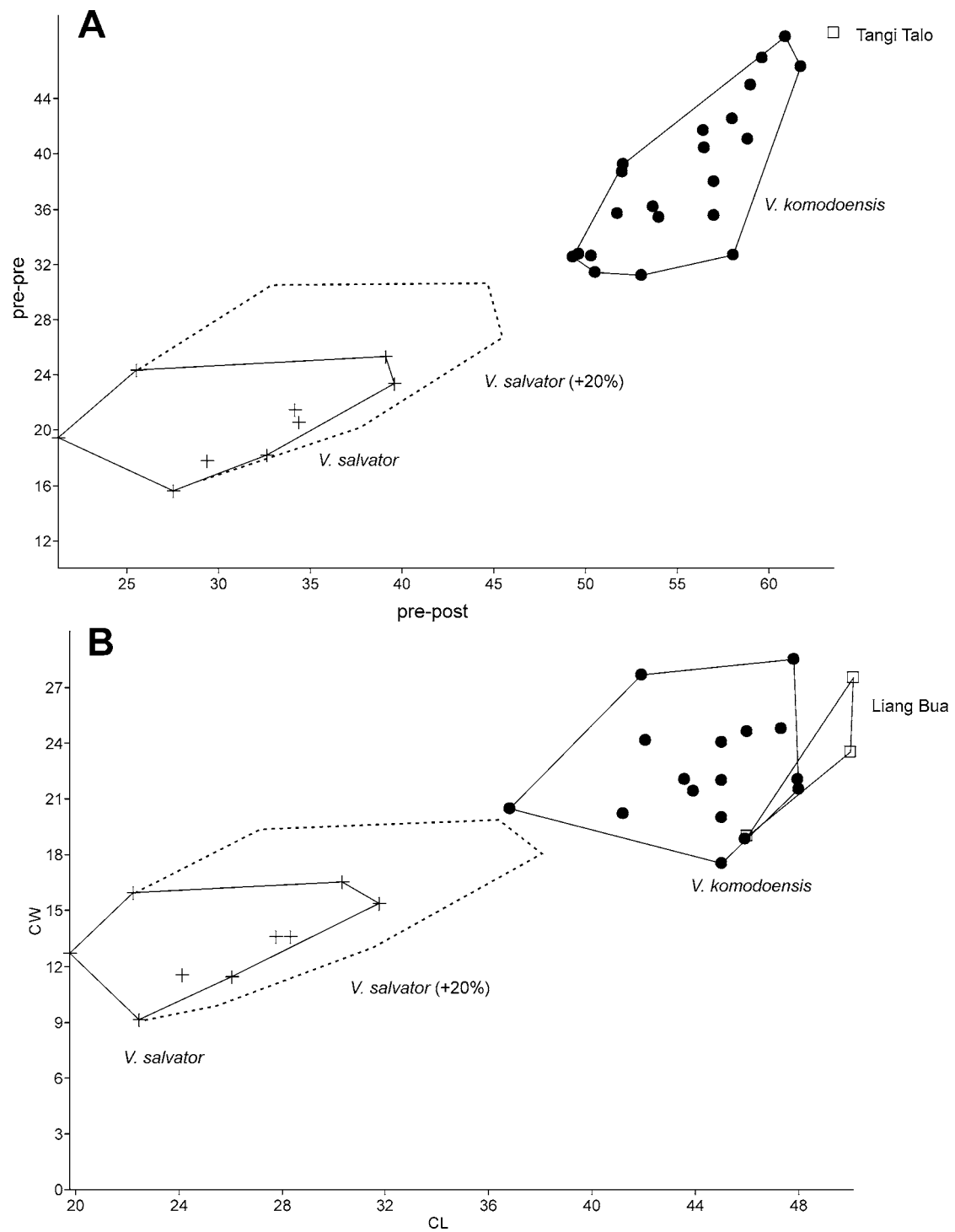


Figure S4



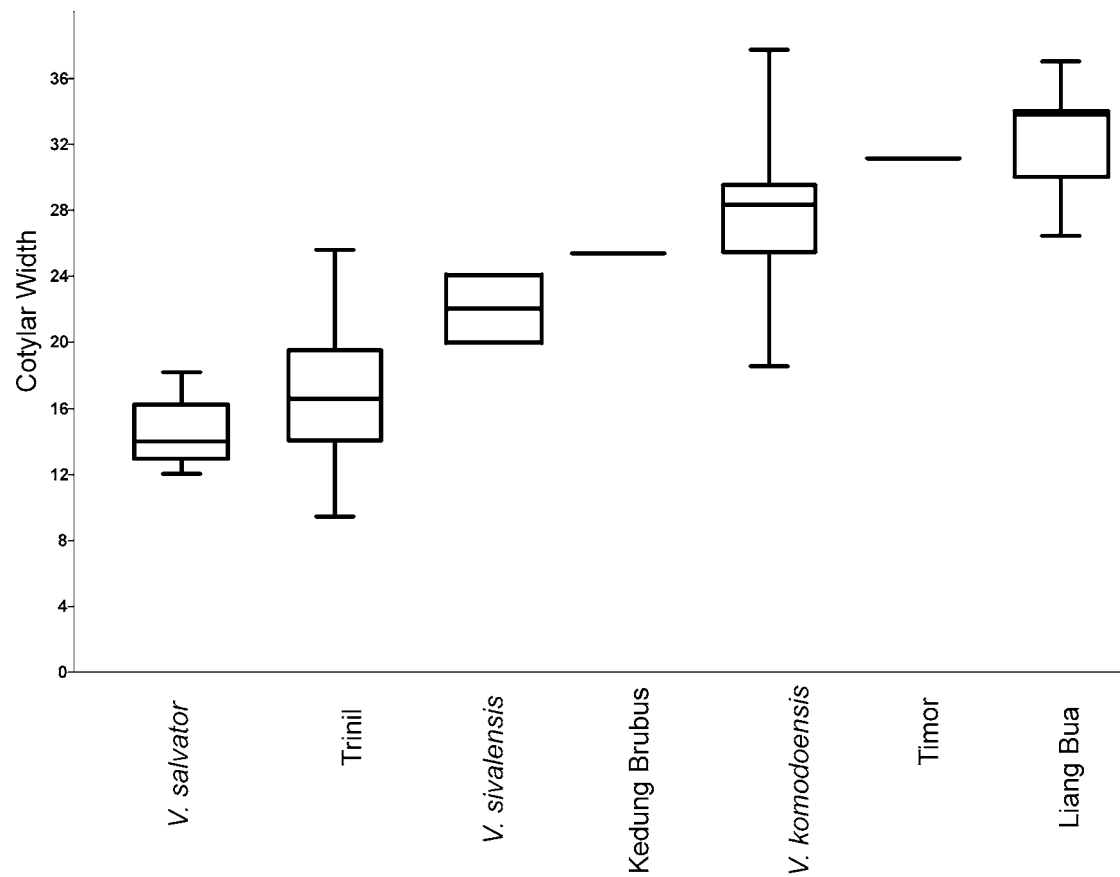
**Figure S4. Histogram of dorsal vertebrae pre-post measurements with normal curve fitted. *Varanus komodoensis* modern (n = 100), Pliocene (Chinchilla & Bluff Downs) (n = 38). Measurements in mm.**

Figure S5.



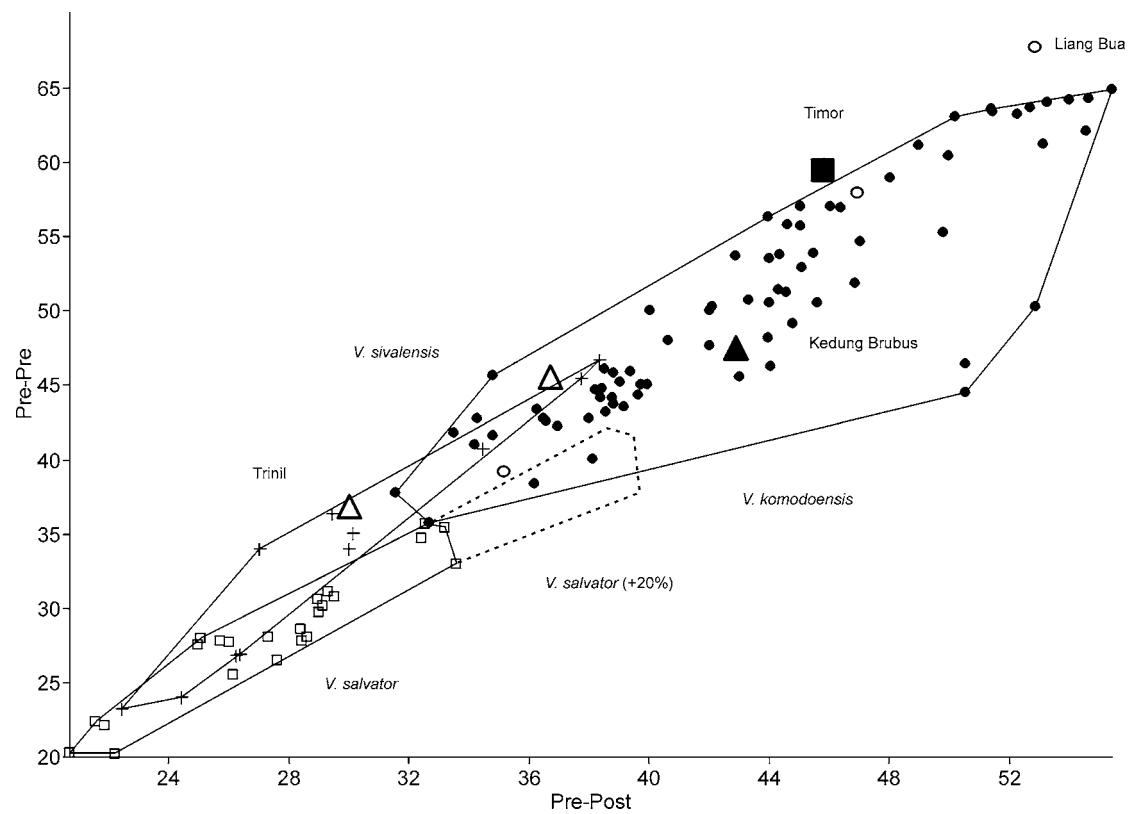
**Figure S5. Measurements of varanid cervical vertebrae. A. Bivariate Plot of pre-pre length vs pre-post length. B. Bivariate Plot of cotylar width vs centrum length. Convex hulls applied to show limits of sample variation. Measurements in mm.**

Figure S6.



**Figure S6. Box-plot of dorsal vertebrae cotylar width measurements. *Varanus salvator* (n = 24), Trinil (n = 15), *Varanus sivalensis* (n=2), modern *Varanus komodoensis* (n = 112). Liang Bua (n = 16). Measurements in mm.**

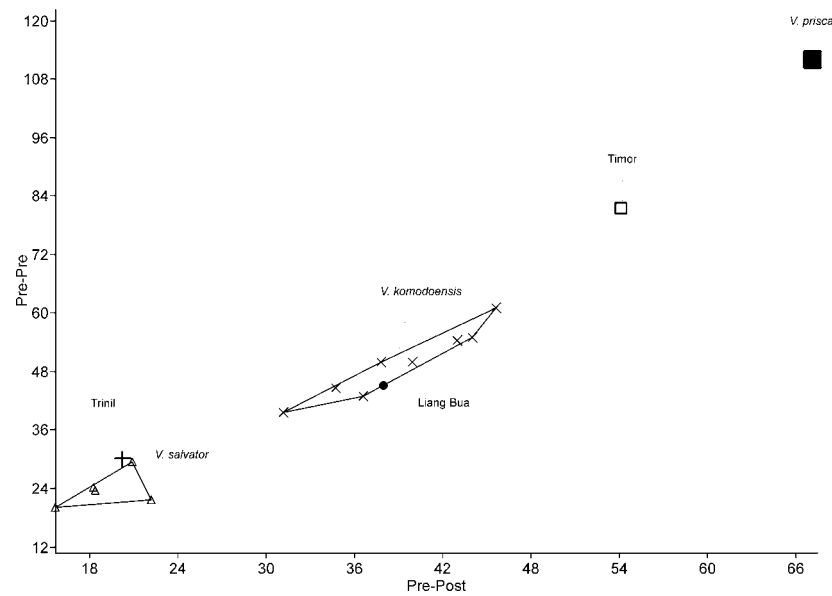
Figure S7



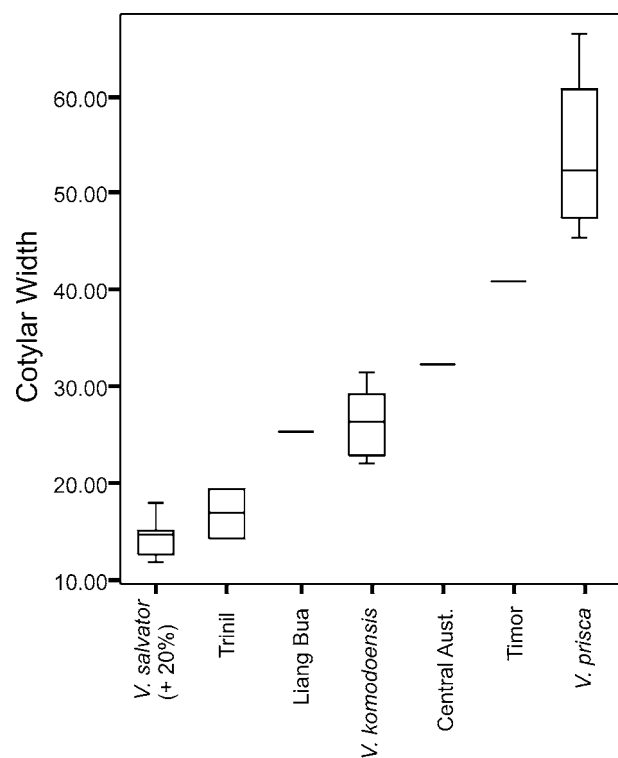
**Figure S7. Measurements of varanid dorsal vertebrae. Bivariate Plot of pre-pre length vs pre-post length. Convex hulls applied to show limits of sample variation. Measurements in mm.**

Figure S8.

A.



B.



**Figure S8. Measurements of varanid sacral vertebrae. A. Bivariate plot of pre-pre length vs pre-post length. Convex hulls applied to show limits of sample variation. B. Box-plot of sacral vertebrae cotylar width measurements. *Varanus salvator* (n = 10), Trinil (n = 2), *Varanus komodoensis* (n = 9), *V. prisca* (n = 4). Measurements in mm.**

Figure S9.

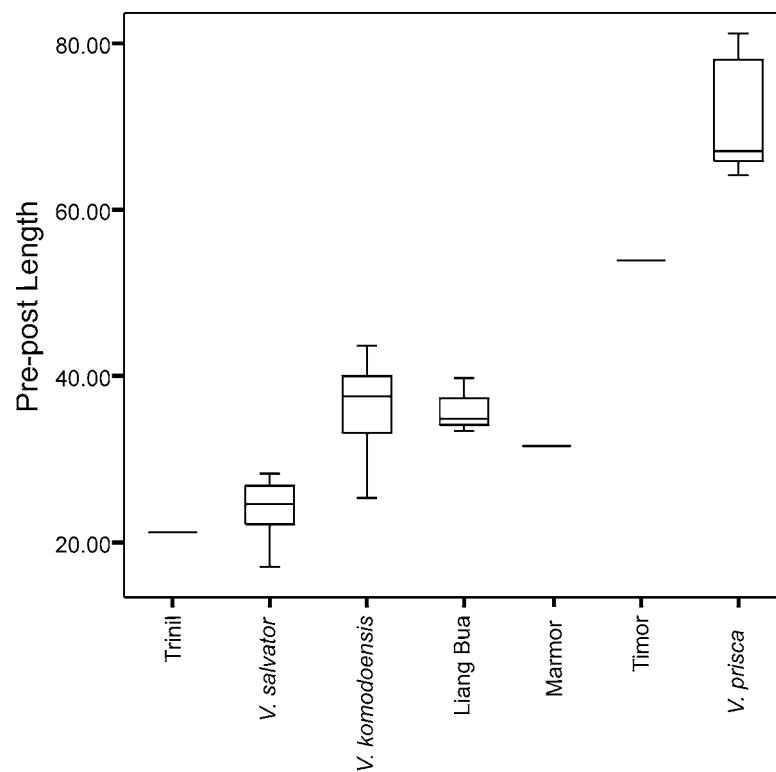


Figure S9. Box-plot of caudal vertebrae prezygapophysis-postzygapophysis length measurements. *Varanus salvator* (n = 9), *Varanus komodoensis* (n = 24), Liang Bua (n = 4), *V. prisca* (n = 8). Measurements in mm.

Figure S10.

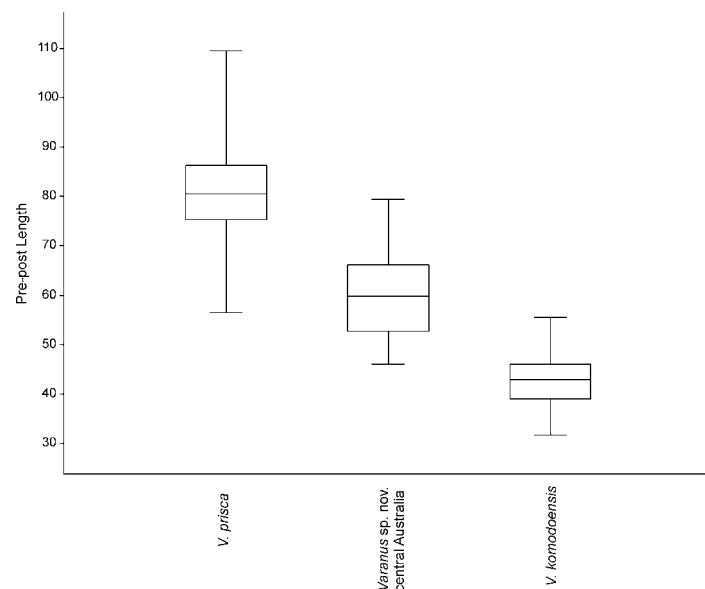
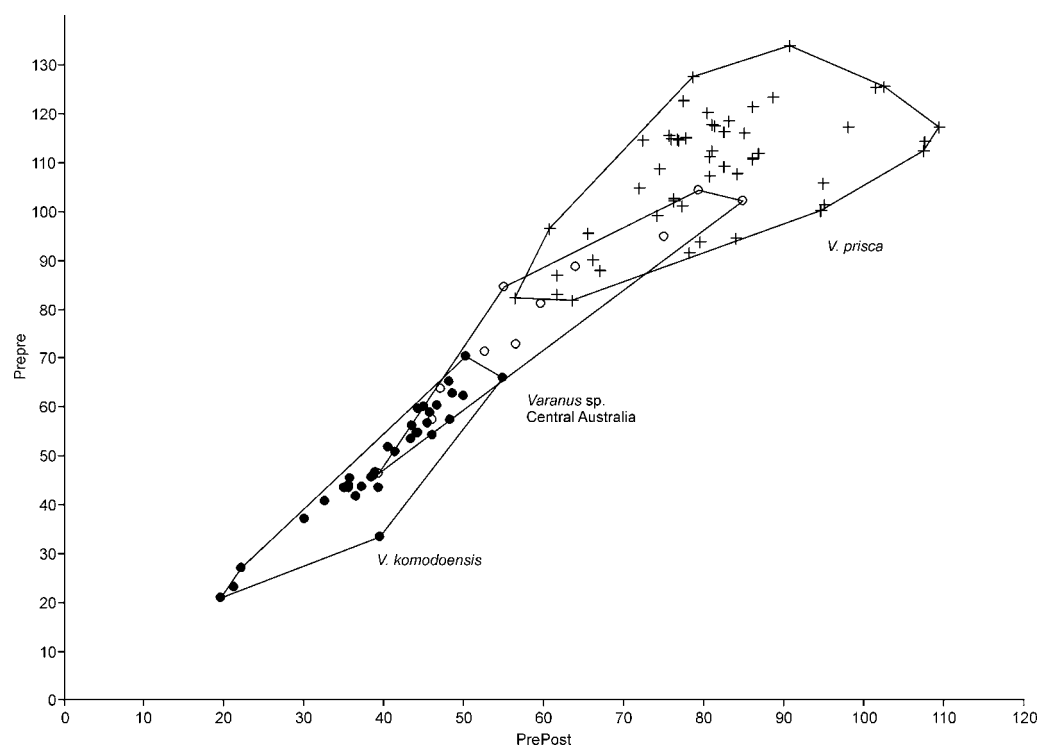


Figure S10. Box plot of dorsal vertebra pre-postzygapophysis length for *V. prisca* (n= 53), *Varanus sp. nov.* (n = 11) and modern *V. komodoensis* (n= 32). Measurements in mm.

Figure S11.



**Figure S11. Measurements of varanid dorsal vertebrae. Bivariate plot of pre-pre length vs pre-post length. Convex hulls applied to show limits of sample variation. Measurements in mm.**

Table S1. Specimens used in this study.

Taxon	Specimen No.	Specimen Description	Age	Locality / Formation	Province / Country
<i>V. komodoensis</i>	LB 1-9-03	Dorsal vertebra	Late Pleistocene	Liang Bua	Flores
<i>V. komodoensis</i>	LB 485	Dorsal vertebra	Late Pleistocene	Liang Bua	Flores
<i>V. komodoensis</i>	LB19/20-8-04	Dorsal vertebra	Late Pleistocene	Liang Bua	Flores
<i>V. komodoensis</i>	LB244	Dorsal vertebra	Late Pleistocene	Liang Bua	Flores
<i>V. komodoensis</i>	LB298	Dorsal vertebra	Late Pleistocene	Liang Bua	Flores
<i>V. komodoensis</i>	LB307	Dorsal vertebra	Late Pleistocene	Liang Bua	Flores
<i>V. komodoensis</i>	LB31/07/2004	Dorsal vertebra	Late Pleistocene	Liang Bua	Flores
<i>V. komodoensis</i>	LB413	Dorsal vertebra	Late Pleistocene	Liang Bua	Flores
<i>V. komodoensis</i>	LB418	Dorsal vertebra	Late Pleistocene	Liang Bua	Flores
<i>V. komodoensis</i>	LB420	Dorsal vertebra	Late Pleistocene	Liang Bua	Flores
<i>V. komodoensis</i>	LB447	Dorsal vertebra	Late Pleistocene	Liang Bua	Flores
<i>V. komodoensis</i>	LB468	Dorsal vertebra	Late Pleistocene	Liang Bua	Flores
<i>V. komodoensis</i>	LB517	Dorsal vertebra	Late Pleistocene	Liang Bua	Flores
<i>V. komodoensis</i>	LB623	Dorsal vertebra	Late Pleistocene	Liang Bua	Flores

Taxon	Specimen No.	Specimen Description	Age	Locality / Formation	Province / Country
<i>V.</i>			Late		
<i>komodoensis</i>	LB751	Dorsal vertebra	Pleistocene	Liang Bua	Flores
<i>V.</i>			Late		
<i>komodoensis</i>	LB398	Caudal vertebra	Pleistocene	Liang Bua	Flores
<i>V.</i>			Late		
<i>komodoensis</i>	LB503c, 18-8-04	Caudal vertebra	Pleistocene	Liang Bua	Flores
<i>V.</i>			Late		
<i>komodoensis</i>	LB18/08/2004	Caudal vertebra	Pleistocene	Liang Bua	Flores
<i>V.</i>			Late		
<i>komodoensis</i>	LB117d	Caudal vertebra	Pleistocene	Liang Bua	Flores
<i>V.</i>			Late		
<i>komodoensis</i>	LB21.8.03	Caudal vertebra	Pleistocene	Liang Bua	Flores
<i>V.</i>			Late		
<i>komodoensis</i>	LB558b	Caudal vertebra	Pleistocene	Liang Bua	Flores
<i>V.</i>			Late		
<i>komodoensis</i>	LB503d	Cervical vertebra	Pleistocene	Liang Bua	Flores
<i>V.</i>			Late		
<i>komodoensis</i>	LB517b	Cervical vertebra	Pleistocene	Liang Bua	Flores
<i>V.</i>			Late		
<i>komodoensis</i>	LB503b	Cervical vertebra	Pleistocene	Liang Bua	Flores
<i>V.</i>			Early		
<i>komodoensis</i>	TT4062	Cervical vertebra	Pleistocene	Tangi Talo	Flores
<i>V.</i>			Late		
<i>komodoensis</i>	LB558a	Sacral vertebra	Pleistocene	Liang Bua	Flores
<i>V.</i>			Late		
<i>komodoensis</i>	no No.	Tooth	Pleistocene	Liang Bua	Flores
<i>V.</i>			Late		
<i>komodoensis</i>	no No.	Tooth	Pleistocene	Liang Bua	Flores
<i>V.</i>			Late		
<i>komodoensis</i>	no No.	4 x teeth	Pleistocene	Liang Bua	Flores
<i>V.</i>			Early		
<i>komodoensis</i>	TT-3854A	Tooth	Pleistocene	Tangi Talo	Flores
<i>V.</i>			Early		
<i>komodoensis</i>	TT-3854B	Tooth	Pleistocene	Tangi Talo	Flores
<i>V.</i>			Early		
<i>komodoensis</i>	TT-3854C	Tooth	Pleistocene	Tangi Talo	Flores
<i>V.</i>			Early		
<i>komodoensis</i>	TT-3854D	Tooth	Pleistocene	Tangi Talo	Flores
<i>V.</i>			Early		
<i>komodoensis</i>	TT-3854E	Tooth	Pleistocene	Tangi Talo	Flores
<i>V.</i>			Early		
<i>komodoensis</i>	TT-3854F	Tooth	Pleistocene	Tangi Talo	Flores
<i>V.</i>		right humerus	Early		
<i>komodoensis</i>	TT-4097	diaphysis	Pleistocene	Tangi Talo	Flores
<i>V.</i>			Late		
<i>komodoensis</i>	LB-28.7.03	radius diaphysis	Pleistocene	Liang Bua	Flores
<i>V.</i>		2 ilium fragments	Late		
<i>komodoensis</i>	LB-289a/10.5.01	of 1 individual	Pleistocene	Liang Bua	Flores
<i>V.</i>		2 metapodials	Late		
<i>komodoensis</i>	LB-578	and 1 phalanx	Pleistocene	Liang Bua	Flores
<i>V.</i>			Late		
<i>komodoensis</i>	LB-19.7.04	right mandible	Pleistocene	Liang Bua	Flores
<i>V.</i>		left ulna	Late		
<i>komodoensis</i>	LB-447a/16.8.04	diaphysis	Pleistocene	Liang Bua	Flores
<i>V. salvator</i>	CD1908.3	Dorsal vertebra	Early		
			Pleistocene	Trinil	Java
<i>V. salvator</i>	CD207	Dorsal vertebra	Early		
			Pleistocene	Trinil	Java
<i>V. salvator</i>	CD3	Dorsal vertebra	Early		
			Pleistocene	Trinil	Java
<i>V. salvator</i>	CD5676	Dorsal vertebra	Early		
			Pleistocene	Trinil	Java
<i>V. salvator</i>	CD5731	Dorsal vertebra	Early		
			Pleistocene	Trinil	Java
<i>V. salvator</i>	CD5782	Dorsal vertebra	Early		
			Pleistocene	Trinil	Java
<i>V. salvator</i>	CD5793	Dorsal vertebra	Early		
			Pleistocene	Trinil	Java
<i>V. salvator</i>	CD5835	Dorsal vertebra	Early		
			Pleistocene	Trinil	Java
<i>V. salvator</i>	CD5917	Dorsal vertebra	Early		
			Pleistocene	Trinil	Java



Taxon	Specimen No.	Specimen Description	Age	Locality / Formation	Province / Country
<i>V. salvator</i>	CD6384	Dorsal vertebra	Early Pleistocene	Trinil	Java
<i>V. salvator</i>	CD6877	Dorsal vertebra	Early Pleistocene	Trinil	Java
<i>V. salvator</i>	CD6902	Dorsal vertebra	Early Pleistocene	Trinil	Java
<i>V. salvator</i>	CD6904	Dorsal vertebra	Early Pleistocene	Trinil	Java
<i>V. salvator</i>	CD8873	Dorsal vertebra	Early Pleistocene	Trinil	Java
<i>V. salvator</i>	CD11194	Dorsal vertebra	Early Pleistocene	Trinil	Java
<i>V. salvator</i>	CD6189	Caudal vertebra	Early Pleistocene	Trinil	Java
<i>V. salvator</i>	CD8432	Sacral vertebra	Early Pleistocene	Trinil	Flores
<i>V. salvator</i>	CD5742	Sacral vertebra	Early Pleistocene	Trinil	Flores
<i>V. sivalensis</i> (= <i>V. salvator</i> )	NHMR740	Dorsal vertebra	Early Pleistocene	Siwalik Hills	India
<i>V. sivalensis</i> (= <i>V. salvator</i> )	NHMR739	Cervical vertebra (= Dorsal vertebra)	Early Pleistocene	Siwalik Hills	India
<i>V. sivalensis</i>	NHMR40819	Distal Humerus	Early Pleistocene	Siwalik Hills	India
<i>Varanus prisa</i>	QM & AM Collections	Cranial & post cranial specimens	Late Pleistocene	Eastern Darling Downs	Australia
<i>Varanus prisca</i>	QM & MOV Collections	Cranial & post cranial specimens	Middle-Late Pleistocene	Wyandotte Fmn	Australia
<i>Varanus prisca</i>	AM Collections	Postcranial specimens	Late Pleistocene	Cuddie Springs	Australia
<i>Varanus</i> sp. nov.	SAM & UCMP Collection	Postcranial specimens	Middle-Late Pleistocene	Katapiri / Kutjitarra Fmn	Australia
<i>Varanus</i> sp. nov.	CV Collection, NNM	Dorsal vertebra	>Middle Pleistocene	Raebia	Timor
<i>Varanus</i> sp. nov.	CV Collection, NNM	Sacral vertebra	>Middle Pleistocene	Raebia	Timor
<i>Varanus</i> sp. nov.	CV Collection, NNM	Caudal vertebra	>Middle Pleistocene	Raebia	Timor
<i>V. komodoensis</i>	QM Collection	Numerous vertebrae	late Early Pliocene	Chinchilla	Australia
<i>V. komodoensis</i>	QMF874	right maxilla	late Early Pliocene	Chinchilla	Australia
<i>V. komodoensis</i>	QMF870+871	left mandible	late Early Pliocene	Chinchilla	Australia
<i>V. komodoensis</i>	QMF866	right scapulocoracoid	late Early Pliocene	Chinchilla	Australia
<i>V. komodoensis</i>	QMF42156	left quadrate	late Early Pliocene	Chinchilla	Australia
<i>V. komodoensis</i>	QMF53956	parietal	late Early Pliocene	Chinchilla	Australia
<i>V. komodoensis</i>	QMF53955	right humerus	late Early Pliocene	Chinchilla	Australia
<i>V. komodoensis</i>	QMF53954	left humerus	late Early Pliocene	Chinchilla	Australia
<i>V. komodoensis</i>	QMF42105	right maxilla	late Early Pliocene	Chinchilla	Australia
<i>V. komodoensis</i>	QMF 25392	supraorbital	Early Pliocene	Chinchilla Bluff	Australia
<i>V. komodoensis</i>	QM23686	Dorsal vertebra	Early Pliocene	Downs Bluff	Australia
<i>V. komodoensis</i>	QMF23684	Cervical vertebra	Early Pliocene	Downs Bluff	Australia
<i>V. komodoensis</i>	QMF 54605	Maxilla	Middle Pleistocene	Mt. Etna	Australia
<i>V. komodoensis</i>	QMF 54607	Supraoccipital	Middle Pleistocene	Mt. Etna	Australia

<b>Taxon</b>	<b>Specimen No.</b>	<b>Specimen Description</b>	<b>Age</b>	<b>Locality / Formation</b>	<b>Province / Country</b>
<i>V. komodoensis</i>	QMF 54606	Quadrate	Middle Pleistocene	Mt. Etna	Australia
<i>V. komodoensis</i>	QMF 54608	Tibia	Middle Pleistocene	Mt. Etna	Australia
<i>V. komodoensis</i>	QMF 54604	Ulna	Middle Pleistocene	Mt. Etna	Australia
<i>V. komodoensis</i>	QMF54120	Dorsal vertebra	Middle Pleistocene	Mt. Etna	Australia
<i>V. komodoensis</i>	QMF 1418	Caudal vertebra	Middle Pleistocene	Marmor Quarry	Australia
<i>V. komodoensis</i>	CD6392	Dorsal vertebra	Middle Pleistocene	Kedung Brubus	Java
<b>Comparative Specimens</b>					
<i>Varanus komodoensis</i>	NNM17504	Skeleton	Modern	Flores	Indonesia
<i>Varanus komodoensis</i>	NNM17494	Skeleton	Modern	Rinca	Indonesia
<i>Varanus komodoensis</i>	NNM6994	Skeleton	Modern	West Flores	Indonesia
<i>Varanus komodoensis</i>	NNM21-11-38	Skeleton	Modern	?	Indonesia
<i>Varanus komodoensis</i>	NNM35517	Skeleton	Modern	?	Indonesia
<i>Varanus komodoensis</i>	NNM35518	Skeleton	Modern	?	Indonesia
<i>Varanus komodoensis</i>	NNM35515	Skeleton	Modern	?	Indonesia
<i>Varanus komodoensis</i>	NNM35510	Skeleton	Modern	Komodo	Indonesia
<i>Varanus komodoensis</i>	USNM228163	Skeleton	Modern	?	Indonesia
<i>Varanus komodoensis</i>	USNM101444	Skeleton	Modern	?	Indonesia
<i>Varanus komodoensis</i>	NHM934.9.2	Skeleton	Modern	Komodo	Indonesia
<i>Varanus komodoensis</i>	USNM220286	Skeleton	Modern	?	Indonesia
<i>Varanus komodoensis</i>	USNM220287	Skeleton	Modern	?	Indonesia
<i>Varanus komodoensis</i>	USNM221892	Skeleton	Modern	?	Indonesia
<i>Varanus komodoensis</i>	LACM	Skeleton	Modern	?	Indonesia
<i>Varanus salvator</i>	USNM220287	Skeleton	Modern	Borneo	Indonesia
<i>Varanus salvator</i>	NAU QSP	Skeleton	Modern	?	Indonesia
<i>Varanus salvator</i>	NAU QSP	Skeleton	Modern	?	Indonesia
<i>Varanus salvator</i>	NNM9505906	Skeleton	Modern	West Java	Indonesia
<i>Varanus salvator</i>	NHM64.92.77	Skeleton	Modern	Borneo	Indonesia
<i>Varanus salvator</i>	NHMB1972	Skeleton	Modern	Ceylon	Indonesia
<i>Varanus salvator</i>	NHM2160	Skeleton	Modern	Ceylon	Indonesia
<i>Varanus salvator</i>	NHM?314	Skeleton	Modern	?	?
<i>Varanus salvator</i>	NHM17.4.42	Skeleton	Modern	Ceylon	Indonesia
<i>Varanus salvadorii</i>	QMJ14498	Skeleton	Modern	PNG	PNG
<i>Varanus</i> spp.	QM Collection	Skeletons	Modern	Various	Australia

**Collection Abbreviations**

<b>Taxon</b>	<b>Specimen No.</b>	<b>Specimen Description</b>	<b>Age</b>	<b>Locality / Formation</b>	<b>Province / Country</b>
<b>ARKENAS</b>		National Archaeological Research Centre, Jakarta, Indonesia			
<b>NHMR</b>		British Museum of Natural History Fossil			
<b>NHM</b>		British Natural History Museum Extant			
<b>CD</b>		Dubois Collection, NNM			
<b>CV</b>		Verhoeven Collection, NNM			
<b>NNM</b>		Naturalis National Museum of Natural History The Netherlands			
<b>LB</b>		Liang Bua Collection, ARKENAS			
<b>TT</b>		Tangi Talo Collection, GSI			
<b>GSI</b>		Geological Survey Institute, Bandung Indonesia (formerly GRDC)			
<b>USNM</b>		United States National Museum Smithsonian Institute Washington, United States of America			
<b>NAU</b>		Northern Arizona University Quaternary Sciences Program Collection Flagstaff, United States of America			
<b>UCMP</b>		University of California Museum of Palaeontology Collection, Berkeley California, United States of America			
<b>QMF</b>		Queensland Museum Fossil			
<b>SAM</b>		South Australian Museum Adelaide			
<b>AM</b>		Australian Museum Sydney			
<b>MOV</b>		Museum of Victoria Melbourne Australia			

## 5.14 Chapter Conclusions

The Plio-Pleistocene record for giant varanids has been underestimated by most authors, with new forms now recognised in the Pliocene and middle Pleistocene. The existence of at least two giant varanid species during the middle Pleistocene of eastern Australia illustrates the continental dominance of varanids in their environment, being the largest bodied carnivore from the arid-zone to mesothermic lowland rainforests. The ecophysiological abilities shown in modern varanids shows how adaptable they are to almost any environment, including the ability to disperse across water to insular islands. Giant varanids are one of the very few vertebrate groups to have successfully made the oceanic dispersal from west to east, then return east to west across Wallace's Line.

The stability in body-size across these ecological gradients and through time for particular taxa, such as the *V. komodoensis* lineage, illustrates the overall stability in the evolutionary advantages provided to a large terrestrial reptilian carnivore. Dominance from mekosuchine crocodilians during the early-mid Tertiary illustrates the ability of another reptile group to have taken advantage of a terrestrial ecology not filled by mammals or birds prior to the arrival of varanids. The long-term existence of the *V. komodoensis* lineage on mainland Australia brings to light the question of its extinction and isolation on Indonesian islands to the west. Impacts from human activities are considered the most likely reason for the extinction of *V. komodoensis* populations on Flores, after ca. 900,000 years of relative body-size and population stability. This too seems to be the case for *V. komodoensis* on mainland Australia, having been relatively stable for over 3.5 million years only being segregated into more closed habitats by the dominant *Varanus priscus* during the end of the Pleistocene. Both *V. komodoensis* and *V. priscus* were most likely driven extinct sometime since the middle Pleistocene, and probably as part of the late Pleistocene 'megafauna' extinction chronology. The extinction of *Varanus priscus* from open habitats would have opened up considerable areas for a giant varanid of smaller body size, like *V. komodoensis*. The extinction of megafaunal prey species would also not affect *V. komodoensis* as it would *V. priscus*, as *V. komodoensis* can exist without large-bodied prey, whilst remaining large-bodied itself. This suggests that the process

that drove *V. priscus* extinct was also the same process that drove *V. komodoensis* extinct on mainland Australia.

## Chapter 6

### 6.1 Responses of Quaternary rainforest vertebrates to climate change in Australia.

#### 6.2 Abstract

A new middle Pleistocene vertebrate fossil record from eastern Australia, dated by U disequilibrium series, records the first Quaternary record of an Australian tropical rainforest fauna. This exceptionally rich fauna underwent extinction after a long period of relative faunal stability, spanning several glacial cycles, and persisted probably until 280 000 years ago. Some time between 280 000 and 205 000 years ago the rainforest fauna was replaced by a xeric-adapted fauna. Since that time, the xeric-adapted fauna was replaced by a mesic-adapted fauna which was established by the Holocene. This is the first vertebrate faunal evidence in Australia of the middle Pleistocene Mid-Brunhes Climatic Event (MBE), a major climatic reorganisation that led to increased aridity in northern Australia from around 300 000 years ago. Several independent palaeoclimate proxies suggest that the climatic shift to aridity was due to increased climatic variability and weakened northern monsoons, which may be manifested in the extinction of the aseasonal rainforest fauna and its replacement by an arid-adapted fauna. We extend the temporal ranges of several taxa from the Pliocene into the middle Pleistocene. We also reveal a longer palaeobiogeographic connection of rainforest taxa and lineages shared between New Guinea and Australia than was previously thought and show that their extinction on mainland Australia occurred sometime after 280 000 years ago.

#### 6.3 Introduction

Understanding the influence of climate change on the biogeography, evolution and extinction of faunas is critical for development of conservation strategies for modern habitats under threat from climate change and human disturbance [1,2]. This is of

particular importance in Australia, where intensified aridity has shaped large portions of the continent and where habitats, such as tropical rainforests, are considered to be under threat of extinction from climate change and human impact [3-5].

In spite of progressively more detailed Quaternary palaeoclimatic and palynological records in the Australian region, there remains a fundamental gap in our knowledge of faunal response to past climate change. This is primarily due to the scarcity of accurately dated, temporally extensive fossil faunas that sample a variety of palaeoecologies. Australia, in particular, has a paucity of chronometrically dated sites and a complete absence of a Quaternary rainforest vertebrate fossil record.

The post-middle Miocene rainforest vertebrate fossil record from the Australopapuan region is extremely poor, possibly reflecting the onset of progressive continent-wide aridity in the late Miocene [6-8]. A single vertebrate locality (Hamilton Local Fauna) from south-eastern Australia indicates the only mainland rainforest record dated to the Pliocene [9]. Restriction of the Quaternary rainforest vertebrate fossil record to sites in New Guinea, even though Quaternary vertebrate fossils sites are found across mainland Australia, has led to the proposition that Australian rainforest habitats were close to their present refugial status before the end of the Pliocene [10].

In the absence of a Quaternary fossil record, studies of modern Australian rainforest faunas have resorted to combine palaeoclimate records inferred from pollen and isotope records [11,12] with phylogeographies and molecular clocks inferred from genetic studies [2,13] to interpret the affects of Quaternary climate cycles on faunal biogeography.

Without direct evidence from a fossil record, these interpretations and hypotheses cannot be adequately tested. Furthermore, it is impossible without a fossil record to accurately infer the presence of extinct taxa, their ecological roles, and the mitigating circumstances that led to their extinction, climate or otherwise. The purpose of this paper is to document a globally rare palaeofauna (e.g. rainforest), via a suite of Quaternary fossil deposits from a single locality in central-eastern Queensland, Australia, which span an interval of intense climate change and fill a major temporal gap in our knowledge of vertebrate faunas from northern Australia.

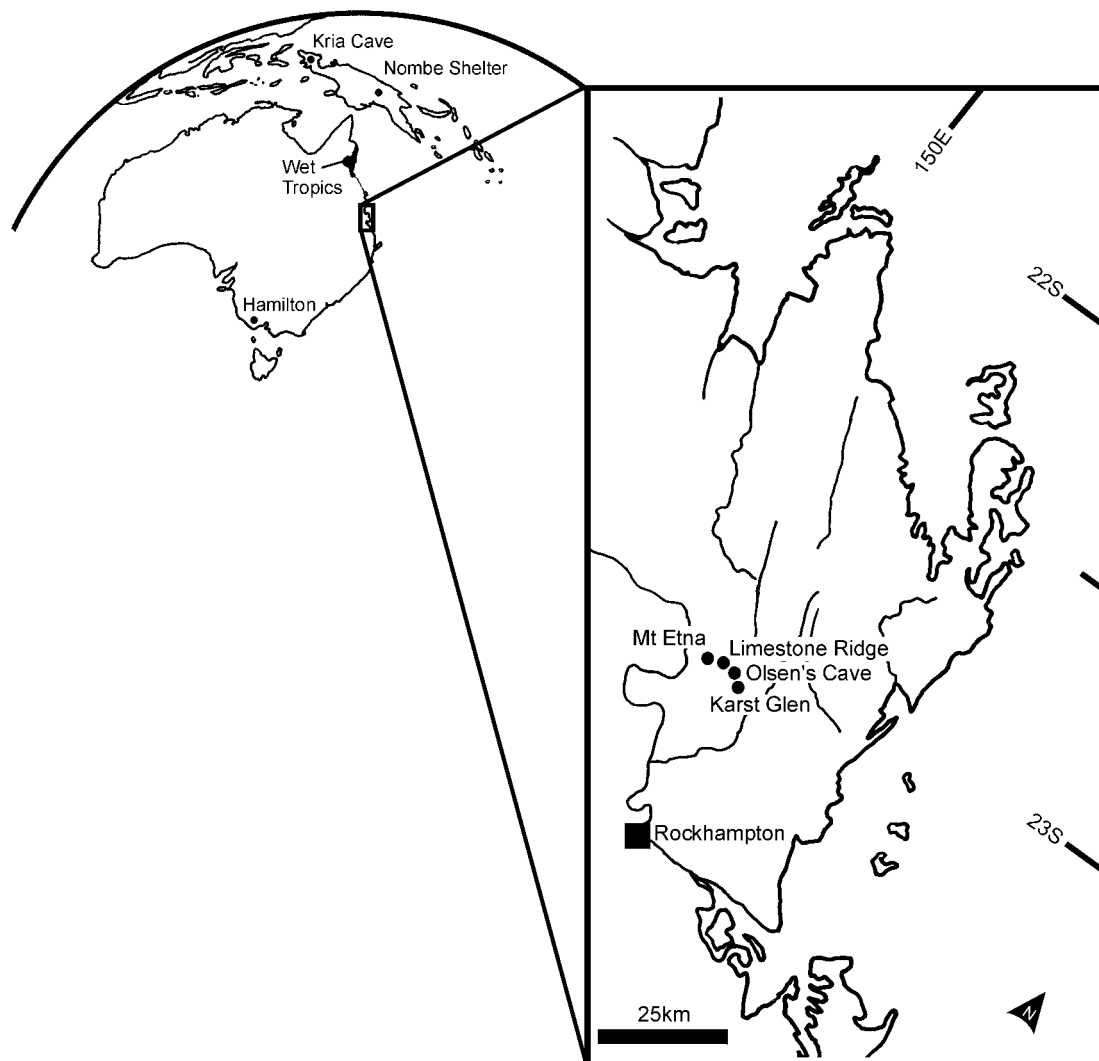


**Figure 6-1. Location of the post-Miocene Australopapuan rainforest vertebrate fossil record in relation to the present day Wet Tropics rainforests of north-eastern Australia, including the early Pliocene Hamilton fauna from south-eastern Australia, the Quaternary faunas from New Guinea and the eastern Australian Quaternary fauna presented herein.**

## **6.4 Methods**

### *6.4.1 Geologic Settings*

Caves formed within isolated Devonian limestone massifs north of Rockhampton, central-eastern Queensland, were systematically surveyed for bone-bearing sediments and breccias (Fig. 1). Vertical and horizontal joints, dictated by the gross orientation of limestone strata and structural features, have produced very deep cave systems with vertical shaft entrances and large chambers [14]. Limestone quarrying on the



northwest face of Mt Etna has exposed in cross-section the deep sediment-filled chambers of at least two cave systems, exposing extensive and abundant fossil remains and associated speleothems. Additional cave deposits occur in nearby karst, including Limestone Ridge, Olsen's Caves and Karst Glen (Fig. 1). Systematic collections and site descriptions are reported elsewhere [15] with additional information and amendments presented herein. Site sedimentology and taphonomy is summarised in Appendix A.

#### 6.4.2 *Thermal Ionization Mass Spectrometry (TIMS) uranium-series dating.*

TIMS uranium-series dating was undertaken using analytical procedures described elsewhere [16], except the known  $^{236}\text{U}/^{233}\text{U}$  ratio in a  $^{229}\text{Th}$ - $^{233}\text{U}$ - $^{236}\text{U}$  mixed spike was used for mass fractionation correction for the unknown samples.  $^{234}\text{U}/^{238}\text{U}$  and  $^{230}\text{Th}/^{238}\text{U}$  activity ratios of the samples are normalised to the corresponding ratios measured for the secular-equilibrium HU-1 standard and their ages calculated using half-lives of 75,380 years ( $^{230}\text{Th}$ ) and 244,600 years ( $^{234}\text{U}$ ).

Sites chosen for dating include those with minimal transportation and reworking of sediments and with available speleothem, either basal to, within, or capping the fossil deposit. Capping or basal flowstones yielding ages within the dating window were used to bracket deposit ages, with basal flowstone dates representing maximum ages and capping flowstone dates representing the minimum ages of the enclosed deposit. Ages outside the dating window were assigned an age of >500 thousand years (ka). Broken flowstones and straws incorporated within the deposits are considered to be maximum ages; the youngest of these from a given deposit was used to establish maximum bracket ages of that deposit.

Where speleothem was not available, bone, teeth, shell, and calcite fillings of these, were analysed. Calcite fillings in bones and teeth yield minimum ages of the fossils because the calcite grows within the specimens post deposition. The bones, teeth and shell are considered to yield minimum ages because U is taken up subsequent to deposition, and the system is most likely to be closed in respect to U loss after uptake. This interpretation was tested and substantiated by the dating of both the bone and calcite fillings within the bone, where we show that calcite yielded an older age than the bone (Table 1). Thus, U uptake in the bone occurred during or continued after

calcite deposition. Therefore, the oldest age recovered using all of these materials was taken as the minimum age of the deposit.

#### 6.4.3 Faunal Analysis

Only non-volant vertebrate species of mammals, frogs and agamid lizards were used as proxies for habitat type. Fossils sharing generic and specific-level identity with living taxa were assumed to be representative of the habitat types and climates presently occupied by extant taxa and therefore are used as habitat proxies. All fossils used in the analyses are considered to represent species derived from proximal habitats to the fossil deposit; based primarily on the restricted foraging ranges of the two predator accumulators present in the deposits (Owl (*Tyto* sp.) and Ghost Bat (*Macroderma gigas*)) [15], and the pit-trap accumulation mode for non-volant, large-sized taxa. Cave entrances were all located high on exposed karst, with a single exception (Olsen's Cave), however, none of the sites possess fluvially transported sediments.

Analyses of faunal diversity and similarity include only mammalian taxa with body weight less than 3 kg (e.g. equal to, or smaller than, *Pseudochirops*), due to the body-size bias apparent in deposits derived predominantly from predator accumulators. Amounts of sediment sorted for vertebrate remains varied from site to site, ranging from less than 0.1 m<sup>3</sup> to more than 4 m<sup>3</sup>. Hence, relative abundances were not analysed (Appendix A).

Pair-wise, Euclidean cluster analysis of mammalian presence/absence data was utilised to determine the similarity of fossil faunas to one another and to known modern and fossil faunas from a broad range of habitat types. Generic-level mammal lists were generated from the literature and included taxa from hydric, mesic and xeric habitats, such as; tropical rainforest, dry vine forests, open-forests, open woodlands, heathlands, shrublands, grasslands and chenopod shrublands. Vegetation classifications follow Webb and Tracey [17] for closed-forest vegetation (e.g. tropical rainforest, dry vine forest) and Specht [18] for all other open vegetation types. Cluster analyses were performed using PAST software [19].

## 6.5 Results

### 6.5.1 Faunal Ages

Sites within the study area that have produced dated faunas range in age from ~7 ka to greater than 500 ka, at the limit of the uranium-series technique employed. Table 1 summarises site ages with a full listing and imagery available as supplementary materials in Appendix A.

Queensland Museum Locality (QML)1284 and QML1284a, considered to be the two oldest faunas, are located on Limestone Ridge, east of Mt Etna. QML1284 has been dated based on several *in situ* flowstone layers associated within the fossil beds. Layer B is stratigraphically the oldest and Layer J the youngest, with calcite fillings from within bone derived from the fossil bed in between flowstone layers G and H. Such dates, especially those for purer flowstone samples with higher U contents and higher  $^{230}\text{Th}/^{232}\text{Th}$  activity ratios, (e.g. MC-02mid & MC-09) and thus more precise results, approximate the application limit (~500 ka) of the TIMS U-series dating method. The analytical precisions for the calcite fillings are poor due to small sample sizes and extremely low U, and thus the age results are only indicative, but they are consistent with the ~500 ka assignment for the site. The capping flowstone MC-01, which covers patches of the underlying fossil deposit, yields an age of  $284 \pm 9$  ka, suggesting that the fossil-bearing horizons were exposed in cross-section prior to ~280 ka. Subsequently a capping flowstone formed over this wall, which has once again been eroded to expose the underlying bone-bearing sediments. Fauna was collected in blocks from the wall and floor having come from the area bracketed by Layers B and G.

QML1284a is located on open karst above and to the northwest of QML1284.

QML1284a is considered to be older than QML1284 as it occurs in weathered karst terrain outside the main entrance to QML1284 indicating an older collapsed chamber [15].

QML1311H yielded a minimum age of  $454 \pm 48$  ka based on calcite infilling of bone and is directly below QML1311J which yielded a minimum age of  $337 \pm 15$  ka.

Unfortunately the speleothem associated with QML1311H was too contaminated by detritus or decalcified to retrieve a reliable basal age. However, it is suspected to be close to the limits of U-series technique (~500 ka) because the speleothem of QML1311H contacts QML1311F, which has a minimum age of  $432 \pm 54$  ka.

A minimum age of QML1383A was obtained from a flowstone that divides the lower unit A from B (ROK F) and yielded a basal age of  $419 \pm 28$  ka. The base of the flowstone is inter-laminated within the top sediments of QML1383A. Therefore, speleothem deposition occurred as sedimentation was slowing down, and thus QML1383A fauna is considered to be close to the age of the flowstone's base. Two sites were deposited at least 330 000 years ago: QML1311J and QML1384LU. QML1311J and QML1384LU are separate deposits located on the western side of Mt Etna. Both sites have yielded minimum ages close to 330-340 ka based on calcite fillings in bone (e.g. ROK24, ROK27 cal).

One site located on the western side of Mt Etna was deposited after 330 ka (QML1311C/D). QML1311C/D contacts with QML1311F deposit via a large continuous basal flowstone layer. The maximum age of QML1311C/D is based on the minimum age ( $326 \pm 22$  ka) of the basal flowstone (ROK04/04), which is also supported by stratigraphically consistent dates for ROK04/15 and ROK04/46 (Table 1).

A capping flowstone of QML1313 provides a minimum age of  $283 \pm 7$  ka based on the weighted mean of two dates (ROK02-4 & 5). The base of the flowstone is inter-laminated with the uppermost centimetres of the bone-bearing sediment. Therefore, the flowstone is considered to have begun deposition as sedimentation rates decreased and not a considerable time after that. Thus, the fauna of QML1313 is considered to date close to 280 000 years old.

QML1312 was dated using bone, teeth, shell and incorporated pieces of broken flowstone and straw. The oldest age derived from bone, teeth and shell provided a minimum age for the deposit, whereas the youngest dated broken flowstone pieces and straw provided a maximum age. Thus the deposit dates between  $169 \pm 9$  ka (snail shell, ROK-10) and  $205 \pm 4$  ka (calcite straw, QML1312-6).

Floor sediments (0-10cm) from within Icicle and Honey Moon Suite Chambers (Olsen's Cave) yielded a diverse subfossil fauna. Calcite cement was used to date the Icicle Chamber deposit, returning an age of  $7.6 \pm 0.2$  ka (OC-07), whilst macropod enamel returned an age of  $6.3 \pm 0.2$  ka (ROK-07) for the Honey Moon Suite Chamber deposit. Both deposits are considered to be Holocene in age.

### 6.5.2 *Site Faunal Groupings*

To test whether the chronology of deposits was consistent with the fossil faunas within them, a chronometrically constrained, bootstrapped, cluster analysis was performed using the dated faunas (Fig. 2). The analysis returned very strong support (99% bootstrap value) for two main clusters, those sites that are older than ~280 ka, and those sites that are younger than ~205 ka. Within the cluster of sites older than ~280 ka, there was very strong support (91%) for the position of deposits aged between ~280 ka and ~330 ka and good support (60%) for the position of deposits considered to be between ~450 ka and ~500 ka. The remaining sites, QML1384LU, QML1383A and QML1284a, were not faunally supported in their chronological position. This lack of support may reflect the presence of transitional faunas in the case of QML1383A where the age of this deposit is better defined, or incorrect chronological placement in the case of QML1384LU and QML1284a where we only have minimum ages. Within the sites younger than ~205 ka there was very strong support for the entire chronological sequence.

Similarities between fossil and modern faunas are summarised in a cluster analysis (Fig. 3). Three main faunal groupings are observed for modern habitats; 1) Faunas occurring in New Guinean and northern Australian hydric habitats (tropical rainforest), 2) Faunas occurring in Australian mesic habitats (dry vine forests to woodlands), and 3) Faunas occurring in Australian xeric habitats (open woodlands, arid grasslands and shrublands). Fossil faunas from the present study cluster amongst each of these three groupings.

All of the dated sites older than ~280 ka cluster together and with the New Guinean and northern Australian tropical rainforest faunas. Several fossil taxa of frogs, lizards and mammals are presently restricted to rainforest environments and are considered to be rainforest specialists (Table 2), which strongly supports the previous contention that these faunas represent a tropical rainforest habitat [15]. The high diversity of mammalian arboreal folivores and hyliid frog species reflects a palaeoecology with complex vegetative structure, whilst the presence of microhylid frogs and freshwater turtles indicates permanent water bodies [15].

A single fauna (QML1312), dated to between 205-170 ka, clusters with xeric habitats of central and southern Australia. These arid and semi-arid faunas occur in a great

variety of habitats (e.g. Open woodlands, hummock grasslands, tussock grasslands and chenopod shrublands). Several of the taxa present in this deposit are considered to be arid-adapted taxa that specialise in arid habitats (Table 2). Contrary to the dominant arid/semi-arid signal, a proportion of the fauna does not occur in these dry regions today and are indicative of more mesic environments. For example, a single calcaneum represents a species of *Dendrolagus*, an arboreal rainforest-dwelling macropod, and as it is unlikely to be reworked, the taxon was rare but present in the surrounding habitat. The presence of this, and other arboreal taxa, indicates that treed habitat occurred proximal to the cave entrance, possibly in the form of a refugium. Two fossil faunas (Icicle Chamber and Honey Moon Suite Chamber) cluster with the modern mesic habitat in the study area, which includes grassy open-forests with refugial dry vine forests (semi-evergreen vine-thickets). This is not surprising as both deposits are considered to be Holocene in age.

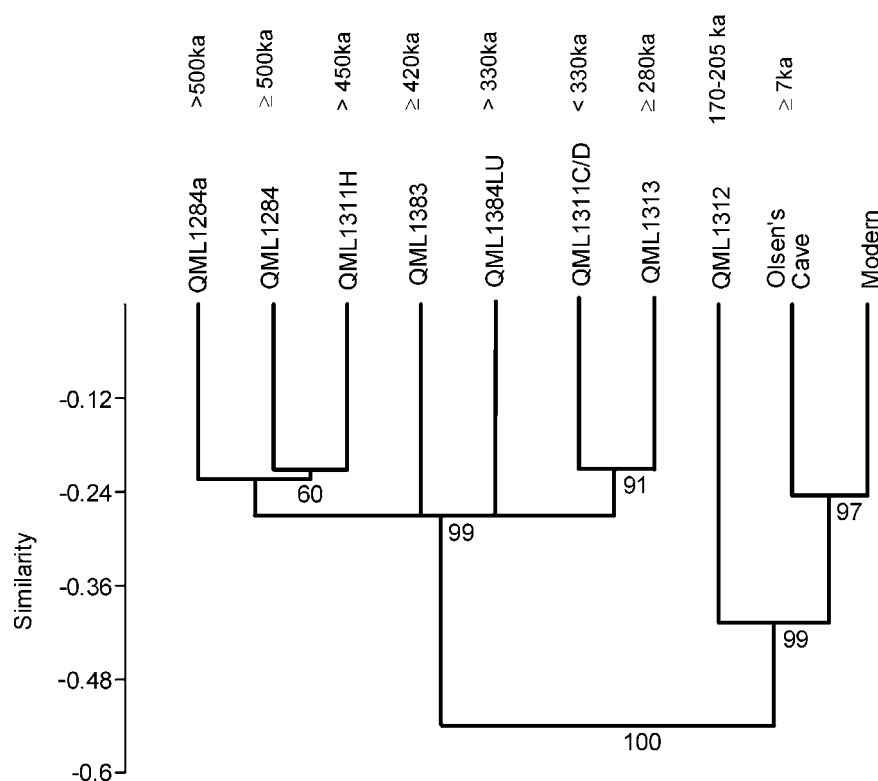


**Figure 6-2. Chronometrically constrained, bootstrapped, similarity cluster analysis of dated fossil and modern faunas of the present study.**

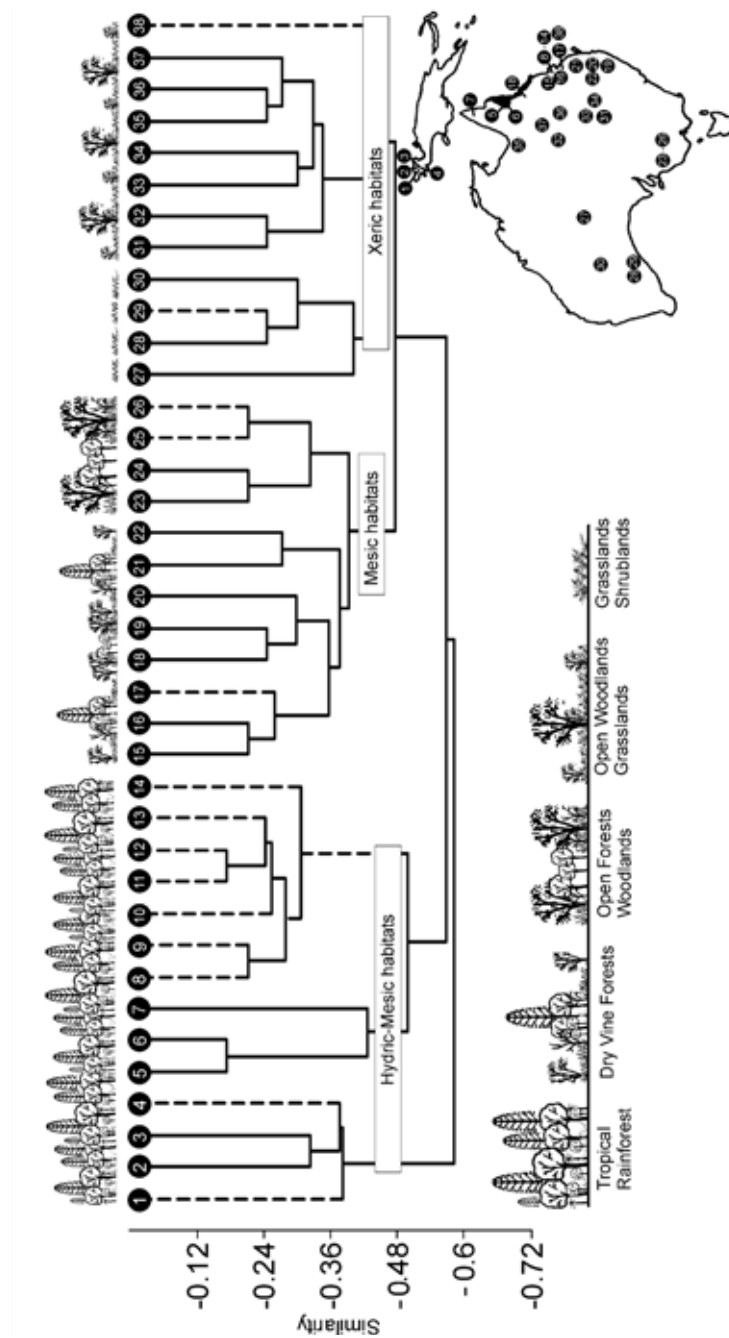


Figure 6-3. Similarity cluster analysis of modern and fossil faunas associated with hydric (1-14), mesic (15-26) and xeric (27-38) habitats. Dashed lines indicate fossil faunas. Site locations and references are provided as a supplementary table in Appendix A.

### 6.5.3 Faunal Succession

The middle Pleistocene is characterised by two distinct faunas; 1) a tropical rainforest fauna that existed at least between 500 ka and ~280 ka ago, spanning three glacial cycles from Marine Isotope Stage (MIS) 8 through MIS13, and 2) a xeric-adapted fauna with refugial elements, dated to 205-170 ka ago. Sites considered to represent the latest Pleistocene are yet to be adequately dated and will be the focus of future work. Holocene sites are characterised by a typically modern mesic-adapted fauna. Approximately 50% reduction in species richness of small to medium-sized mammal species was observed between the older rainforest faunas (>280 ka; 28-35 spp.) and those of the Holocene and present day (16-12 spp. respectively) (Fig. 4a). This reduction in species richness is not considered to be an artefact of taphonomy or collection size because deposits with similar accumulation modes and collection sizes show markedly different species richness [e.g., QML1284 (30 spp.) vs Icicle Chamber (16 spp.)].

Furthermore, the middle Pleistocene deposits that preserve large to megafaunal-sized mammalian taxa illustrate a similar massive reduction in species richness compared with the present day fauna at Mt Etna. The reduction includes the total extinction of megafaunal species (>100 kg) and a reduction of more than 50% species richness for both large-sized (3-15 kg) and very large-sized (15-100 kg) mammalian species. Although the overall species richness of mammals decreased by more than 50% since the middle Pleistocene to present day levels, the loss and replacement of taxa was at times proportionally much greater. Loss of taxa in deposits dated between >500 ka and ~280 ka was low, varying between 0 and 13 %, whilst replacement with new taxa was similarly low (0-14 %), suggesting a relatively low rate of faunal turnover and a stable level of species richness for over 200 000 years (Fig. 4a). Between ~280 ka and ~205 ka major faunal reductions occurred with the loss of over 80% of small to medium-sized mammalian taxa (Fig. 4c). Losses also occurred in frog and lizard faunas with local extinction of the lizard *Hypsilurus* and the frogs, *Crinia*, *Etnabatrachus*, *Kyarranus*, *Lechriodus*, *Nyctimystes* and microhylids. Replacement of new mammalian taxa was proportionally lower than species losses, but it was still very high at over 75% (Fig. 4b), which accounts for the overall decrease in species richness from 33 to 21 spp. Frog species richness decreased overall with replacement by some new forms, such as *Cyclorana* and *Neobatrachus*. Lizard species richness



increased with appearance of new xeric-adapted taxa, including *Amphibolurus*, *Tympanocryptis* and *Pogona*.

The local extinction of more than 65% of small to medium-sized mammalian species occurred between the youngest middle Pleistocene fauna (205-170 ka) and the Holocene fauna (<10 ka). Replacement with new species was low, approximately 38%, which accounts for another drop in overall species richness from 21 to 13 spp. (Fig. 4a). Frog and lizard species richness remained relatively stable over this period of time, but the three agamids present at 205-170 ka were replaced by three others, *Pogona barbata*, *Chlamydosaurus kingii* and *Diporiphora bilineata*.

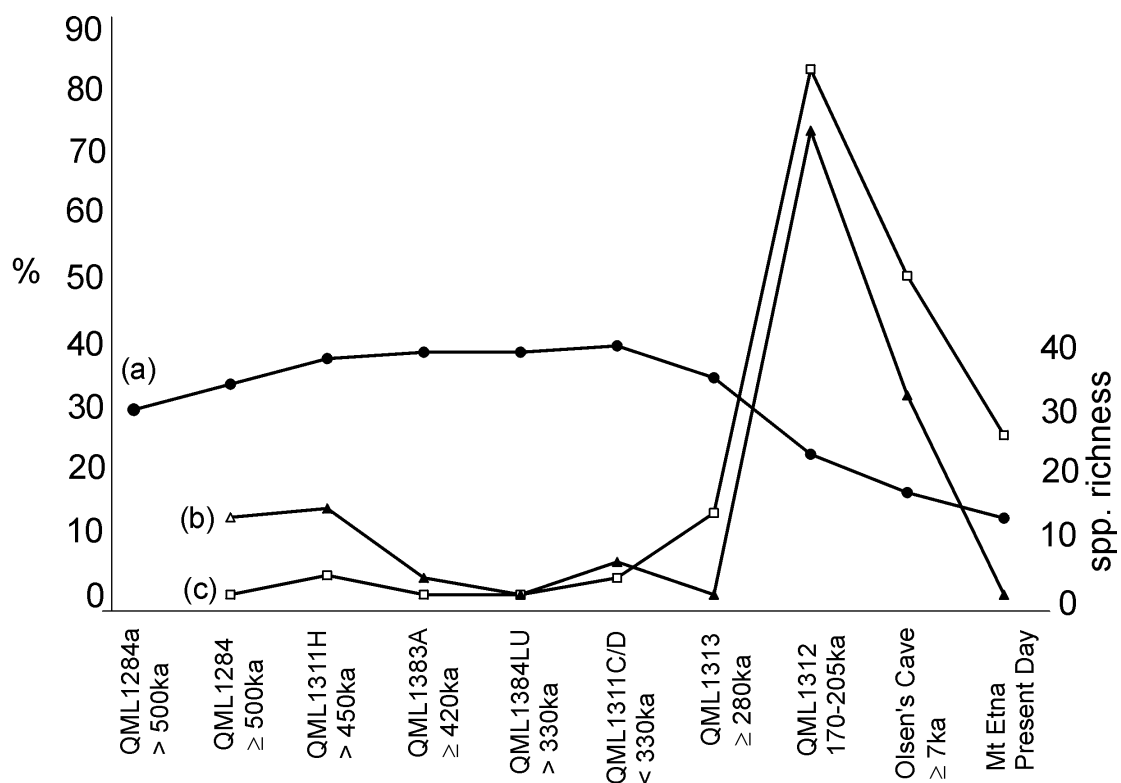


**Figure 6-4. Species richness and faunal turnover through time for medium and small-sized mammal species for the study area. (a) species richness (count of spp.), (b) percentage of new species, (c) percentage of species loss.**

#### 6.5.4 *Speleothem formation*

U-Th isotopic data for all speleothems (e.g., *in situ* and broken flowstones and straws, and calcite fillings) are listed in Appendix A, where a  $^{230}\text{Th}/^{238}\text{U}$  vs.  $^{234}\text{U}/^{238}\text{U}$  evolution diagram is illustrated. The data from the Mt Etna sites show that (1) the

growth of all such speleothems occurred mainly during interglacials or interstadials, consistent with relatively wetter climatic conditions during those times; and (2) 23 (or more than 68 %) of the 34 dated Pleistocene speleothem samples (randomly collected) are older than 300 ka, implying that climate conditions were wetter and more favourable for speleothem development prior to 300 ka. Indeed, most of the >300 ka speleothems are either *in situ* or broken flowstones that are volumetrically more significant than those younger than 300 ka, which are mainly calcite fillings or capping flowstones.

Table 1  
Representative U/Th dates for fossil sites at Mt Ema, central-eastern Queensland

QML	Locality	Sample name	Description	Age interpretation	( <sup>230</sup> Th/ <sup>232</sup> Th)	Corr. <sup>230</sup> Th age (ka)	±2σ
Olsen's	Honey Moon Suite	ROK-07	<i>Petrogale</i> incisor	Min. age	33.7	6.3	0.2
Olsen's	Icicle Chamber	OC-07	Calcite cement	Close to real	19.3	7.6	0.2
1312	Elephant Hole Cave	ROK 10	Snail shell	Min. age	16.3	169	9
1312	Elephant Hole Cave	QML1312-6	Broken straw	Max. age	17.3	205	4
1313	Speaking Tube Cave	ROK02-4	Flowstone	Min. age	66.9	283	9
1313	Speaking Tube Cave	ROK02-5	Flowstone	Min. age	352	283	12
1383	Unit A	ROK F	Flowstone	Max. age of Unit A	31.0	419	28
1311	Deposit C/F contact	ROK04/04	Flowstone	Max. age of C	16.0	326	22
1311	Deposit C/F contact	ROK04/15	Flowstone	Mid flowstone	13.8	347	26
1311	Deposit C/F contact	ROK04/46	Flowstone	Min. age of F	24.6	432	54
1311	H deposit	ROK20-1 bone	Macropod bone	Min. age	5470	216	4
1311	H deposit	ROK20-4 cal	Calcite filling in bone	Min. age	749	454	48
1384	Lower Unit	ROK27 bone	Macropod bone	Min. age	1278	267	5
1384	Lower Unit	ROK27 cal	Calcite filling in bone	Min. age	38.6	332	14
1284	Mini Cave Layer A	MC/01	Capping flowstone	Min. age	92.6	284	9
1284	Layer B	MC-02 mid	Oldest flowstone	Max. age	22.3	484	85
1284	Layer J	MC-10	Youngest flowstone	Min. age	6.8	447	74

Note: Ratios in parentheses are activity ratios calculated from the atomic ratios. The ages are calculated using Ken Ludwig's Isoplot/EX program. Corr. and uncorr. denote corrected and uncorrected. The corrected <sup>230</sup>Th ages and initial (<sup>234</sup>U/<sup>238</sup>U) ratios include a negligible to small correction for non-radiogenic Th using average crustal <sup>232</sup>Th/<sup>238</sup>U atomic ratio of 3.8 ± 1.9 (<sup>230</sup>Th, <sup>234</sup>U and <sup>238</sup>U are assumed to be in secular equilibrium).

**Table 6-1. Representative U/Th dates for fossil sites at Mt Etna, central-eastern Queensland.**

## 6.6 Discussion

### 6.6.1 Implications for biocorrelation

The present sites previously were interpreted as a suite of early Pliocene, Plio-Pleistocene and Holocene sites, and the rainforest assemblages were considered to be Pliocene in age on the basis of biocorrelation [15]. Biocorrelation of these sites was based primarily on the very few chronometrically dated Pliocene sites in Australia. Since that time, several of the Pliocene-aged taxa that were once considered robust markers are now recorded in younger early Pleistocene sites [20].

Likewise, the new radiometric dates presented here extend the temporal ranges of several taxa into the middle Pleistocene. In particular, we present the youngest Australian records for the following taxa: *Pseudokoala* (Early Pliocene-early Pleistocene), '*Petauroides*' (Early Pliocene) *Kurrabi* (Pliocene), *Thylacoleo hilli* (Miocene-early Pleistocene), *Palorchestes* cf. *P. pickeringi* (Early Pliocene-early Pleistocene) and *Protemnodon* cf. *P. devisi* (Pliocene). In addition this study fills a significant gap in the Australian fossil record of extant vertebrate lineages with a fossil record previously restricted to the Oligo-Miocene and Pliocene; such as *Dactylopsila*, *Dendrolagus*, *Pseudochirops*, *Kyarranus* and *Lechriodus*. Moreover, we provide the first fossil record in Australia for several extant lineages; such as *Pseudochirulus*, *Pogonomys*, *Uromys*, *Mesembriomys*, *Hypsilurus* and *Nyctimystes*. One important implication of these results is that other sites in Australia that have been dated only on the basis of biocorrelation may have incorrectly assigned ages. Importantly, it illustrates the need for, 1) a more robust biocorrelative synthesis of the temporal and geographic ranges of Australian Neogene vertebrate taxa and 2) more extensive chronometric dating of Neogene sites.

#### 6.6.2 Responses of middle Pleistocene vertebrate faunas to climate change.

Understanding the responses of middle Pleistocene vertebrate communities to Quaternary climate change is of crucial importance when attempting to infer the affects of late Pleistocene climate change on fauna without the superimposition of anthropogenic activities. Well-dated and faunally rich middle Pleistocene faunas from Australia are rare with three exceptions - two localities from southern Australia, Naracoorte [21,22] and Nullarbor Caves [23] and the present study area (Fig. 5). The Cathedral Cave record from the Naracoorte Caves World Heritage Area, South Australia, is of particular importance because it spans a similar timeframe to the present study [22]. Demonstrated faunal stability at Naracoorte during the middle Pleistocene suggests that the influence of glacial cycles at that time were not severe enough to cause extinctions there. However, it was shown that relative abundance and community composition did fluctuate with climate [22]. Furthermore, a large proportion of the modern non-megafaunal taxa found in the area today are the same taxa found in the middle Pleistocene deposits, suggesting that faunal stability continued throughout the middle and late Pleistocene to the present day. These results

inferred a faunal resilience to climate change in southern Australia. This trend is also suggested for the fossil record from the Nullarbor Caves [23]. We corroborate this faunal stability in the faunal cluster analysis where middle Pleistocene faunas from the Naracoorte and Nullarbor caves cluster most closely with their respective modern day faunas (Fig. 3).

The faunal succession documented in southern Australia contrasts with that documented here, where after an interval of faunal stability for over 200 000 years, a major faunal turnover occurred, which replaced the majority of taxa present in the area prior to 280 ka. Since before 500 ka until ~280 ka, the Mt Etna area possessed a diverse tropical rainforest habitat. However, between ~280 ka and ~205 ka large proportions of the vertebrate fauna were driven locally extinct, being replaced by a xeric-adapted fauna. The presence of xeric-adapted taxa indicates a marked drop in precipitation during the faunal turnover at Mt Etna, presumably a greater reduction in precipitation than what had occurred during previous glacials. Interestingly, this period of faunal turnover and reduced precipitation approximates a period of aridity observed at Naracoorte indicated by both speleothems and local faunal composition [22]. The striking difference between the northern and southern records is that the northern non-megafaunal fauna was driven extinct during this arid event, whilst the southern non-megafaunal fauna was resilient through to the present day.

Sometime after ~205-170 ka the xeric-adapted taxa were lost, and by the Holocene (~7ka) a more mesic fauna had established. The late Pleistocene record for Mt Etna is not securely dated and thus the record is missing the last two glacial maxima, a time of extreme climatic change [24] the arrival of humans and extinction of megafauna [25]. Therefore, the Holocene mesic fauna most likely represents the local habitat returning to an interglacial state and may reflect one of many faunal changes since the middle Pleistocene. The return to mesic conditions did not result in the return of the wet-adapted fauna present prior to ~280 ka.

The interval for the major faunal turnover at Mt Etna (~280-205 ka) occurred during an hypothesised shift towards greater El Niño-Southern Oscillation (ENSO) variability [26] and a weakening of the northern monsoon [27], culminating in intensifying aridity throughout northern Australia (Fig. 5). Our data support a large body of accumulating evidence for a long-term shift towards increasing aridity overlain on a more abrupt shift to greater amplitude of climatic change in individual glacial cycles initiated at the mid-Brunhes Climate Event (MBE) (~430-300 ka).

Dome C (Antarctica) ice core data show a strong contrast in climate before and after ~430 ka (MBE) [24]. The ice core  $\delta D\%$  data show an overall warming trend after ~430 ka and much higher amplitude swings in glacial-interglacial temperatures, suggesting a less equitable climate after ~430 ka. Dust records also show increasing dust volume at glacial maxima after ~430 ka [24].

Sediment core data from MD97-2140 [28], Western Pacific, show greater amplitude and closer swings in Sea Surface Temperatures (SST) between glacial and interglacials after ~450 ka. Sediment core data from Ocean Drilling Program (ODP) hole 806B [29], Western Pacific, also show greater amplitude swings in glacial-interglacial SST after around 450 ka.

Records of terrigenous dust transported by aeolian processes into the Indian Ocean (SO-14-08-05) [30], Tasman Sea (E26.1 core) [31] and Coral Sea (GR100 core) [32] all suggest increased aridity in Australia after 350 ka, with particular peaks after 300 ka, 200 ka and 50 ka.

The Lake Woods and Gregory basins illustrate increased aridity through the progressive reduction of lake sizes and development of playas and lunettes since 300 ka [33]. Magela Ck., Northern Territory records a shift to aridity after 300 ka by a net increase in sedimentation throughout the tributary after a long period of incision and sediment evacuation [34]. Such a shift is consistent with a decrease in long-term discharge.

SSTs over the last 800 000 years or so have been reconstructed for the western Coral [35-38] and Tasman Seas [39], illustrating an increase in SST leading up to, and during, the period of faunal turnover. This suggests that the SST along the entire East Australian Current was rising at the time, and rising SST has been invoked as evidence for the onset of ENSO activity [26,40]. Although increased SST does not indicate mainland aridity directly, increased ENSO activity would produce a climatic variability not conducive for rainforest habitat, which requires a relatively aseasonal climate [41]. Timing of initiation of the growth of the Great Barrier Reef supports the increases in Coral Sea SSTs that are inferred from  $\delta^{18}O$  records and may be associated with the initiation of the western Pacific warm pool [42,43]. Intermittent carbonate deposition dominated by coralline algal facies began in outer shelf regions around  $600 \pm 280$  ka, but true vertically accreting reef facies only began to accumulate between 452 and 365 ka [43,44]. Thus, initiation of true reef growth may coincide with an increase in Coral Sea SST.

Palynological records from northern Australia indicate a progressive increase in open-arid vegetation, beginning ~300 ka and intensifying further since ~180 ka [27]. Pollen records to the south [45] and north [46] of the study site record shifts from rainforest taxa to drier-land taxa reflecting increased aridity from ~275 ka and ~250 ka ago respectively.

We hypothesise that the trend toward drier and more variable climate ~300-200 ka ago in northern Australia made rainforest habitats unsustainable in central-eastern Queensland, particularly during the increasingly dry glacial maxima, and that pattern contrasts strongly with earlier long periods of more equable climates and relative faunal stability.

In contrast, southern and central Australia experienced increased aridity earlier than northern Australia with records showing aridification starting from 600-500 ka in southern regions and as early as 4-2 million years ago (Ma) in central regions.

In central Australia, Gibber and Stony Deserts were formed 4-2 Ma [47], whilst Lake Amadeus underwent an arid shift from uniform lacustrine clays to evaporites and dunes after ~1.2-1.0 Ma [48-50].

In the south, Lake Bungunnia underwent an arid shift from lacustrine clays to saline clays and dunes after ~600 ka [48, 51, 52]. Lake Lefroy preserves evidence of an arid shift from freshwater clays to evaporitic gypsum-dominated sediments around 500 ka [48, 53]. Lake Lewis underwent a shift from uniform lacustrine clays to more heterogenous deposits representing greater aridity and fluctuating salinity (between 600-500 ka) [48, 54]. Sellicks Beach and Kangaroo Island preserve weathered dune systems that show a change to aridity 600-500 ka ago characterised by oxide-weathering zones changing to carbonate-weathering zones [55].

The faunal stability demonstrated at Naracoorte throughout the middle Pleistocene to present day may reflect a prolonged adaptation to this earlier onset of climatic variability and aridity, where entire faunal assemblages became resilient to increased climatic variability. Conversely, northern faunas responding to a later onset of aridity would not have had as much time to adapt to a new climatic regime, and as such, may remain relatively unstable to change, climate or otherwise.

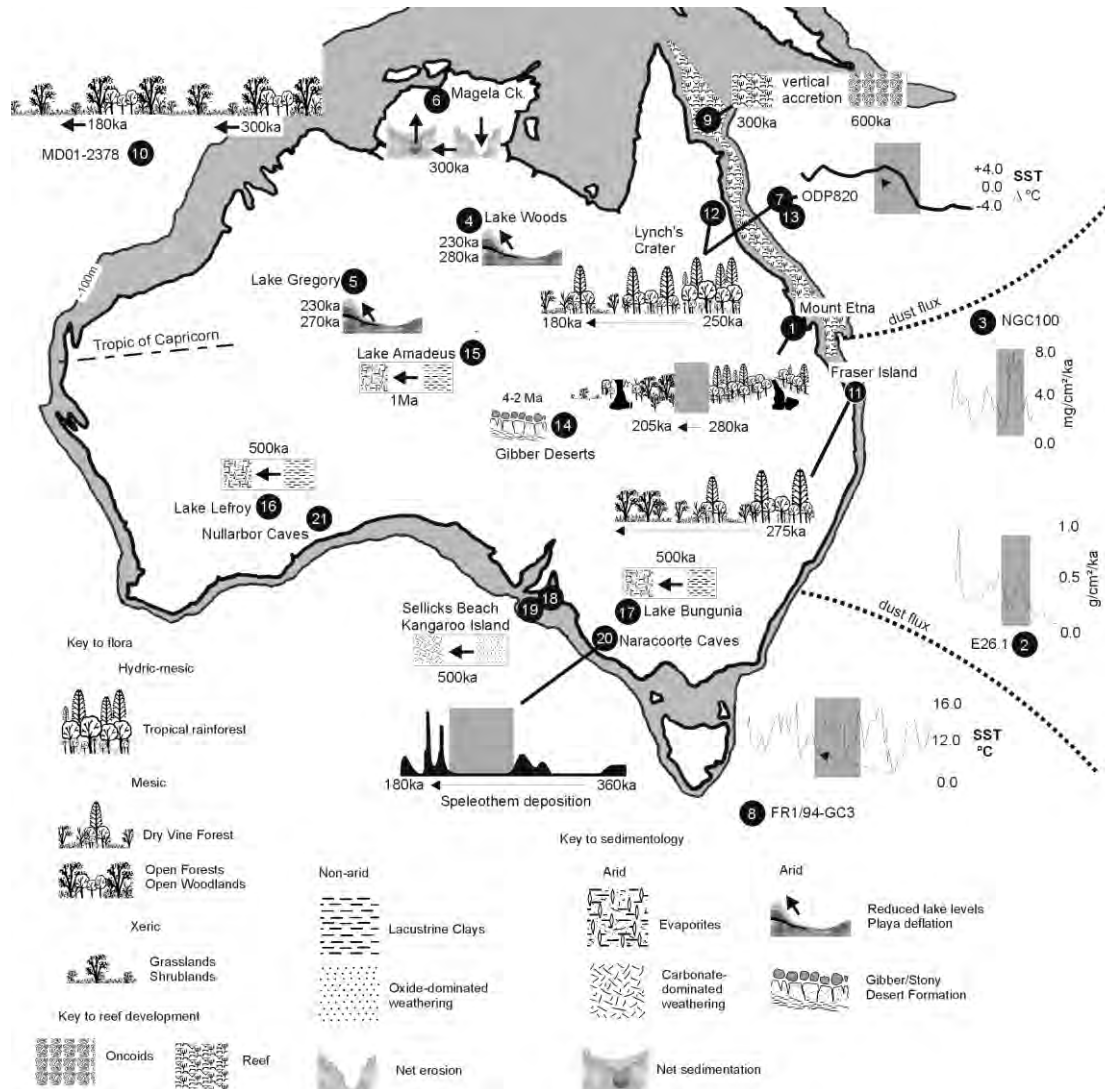


**Figure 6-5. Australia's middle Pleistocene palaeoclimatic record showing the differential timing of the shift to intensifying aridity and climatic variability in northern, central and southern Australia. The vertical grey bar represents the time of faunal turnover during the middle Pleistocene at Mt Etna (~280-205 ka). 1-13. Intensifying aridity in northern Australia since ~300 ka; 1. Mt Etna faunal turnover, 2-3. Aeolian dust records from the Tasman [31] and Coral Seas [32], 4-5. Lake level reduction and playa deflation [33], 6. Magela Ck. net sedimentation post 300 ka [34], 7-9. Sea Surface Temperature (SST) increase along the East Australian Current with reef development [35, 38, 39, 43, 44], 10-13. Palynological records from northwest Australia [27,45,46]. 14-15. Intensifying aridity in central Australia since 4 Ma; 14. Gibber-Stony desert formation [47], 15. Lake Amadeus arid shift [49]. 16-20. Intensifying aridity in southern Australia since ~600 ka; 16-17. Southern lakes shift to aridity [50-54], 18-19. Southern weathering shift to aridity [55], 20. Dry phase between 270-220 ka at the Naracoorte Caves recorded from speleothems [21,22].**

Table 2  
Middle Pleistocene fossil taxa considered to be rainforest or arid specialists with the annual precipitation range\* of their closest living relatives

Rainforest taxa			
Taxon	Closest living relative	Rainforest location	Annual precipitation (mm)*
<i>Cercartetus</i> sp.	<i>Cercartetus caudatus</i>	WT/New Guinea (NG)	1879–3060
<i>Dactylopsila</i> sp. 1	<i>Dactylopsila palpator</i>	NG	1091–5544
<i>Dactylopsila</i> sp. 2	<i>Dactylopsila kambuayai</i>	NG (Holocene)	Montane
<i>Dendrolagus</i> sp. 1	<i>Dendrolagus matschiei</i>	NG	1261–3644
<i>Dendrolagus</i> sp. 2	<i>Dendrolagus</i> spp.	NG	1261–3644
<i>Dendrolagus</i> sp. 3	<i>Dendrolagus</i> spp.	NG	1261–3644
<i>Dendrolagus</i> sp. 4	<i>Dendrolagus</i> spp.	NG	1261–3644
<i>Hypsilurus</i> sp.	<i>Hypsilurus</i> spp.	NG/WT/Southeast QLD (SEQ)	1074–5427
<i>Kyarranus</i> spp.	<i>Kyarranus</i> spp.	SEQ	1092–2110
<i>Lechriodus</i> spp.	<i>Lechriodus</i> spp.	SEQ/NG	1301–2074
Microhylids	Microhylids	WT/NG	1017–4005
<i>Nyctimystes</i> spp.	<i>Nyctimystes</i> spp.	WT/NG	1099–6795
<i>Petauroides</i> sp. 1	<i>Petauroides ayamaruensis</i>	NG (Holocene)	Montane
<i>Petauroides</i> sp. 2	<i>Petauroides ayamaruensis</i>	NG (Holocene)	Montane
<i>Petauroides</i> sp. 3	<i>Petauroides ayamaruensis</i>	NG (Holocene)	Montane
<i>Phalanger</i> sp. 1	<i>Phalanger gymnotis</i>	NG	2119–6580
<i>Phalanger</i> sp. 2	<i>Phalanger</i> spp.	NG	1706–6580
<i>Pogonomys</i> sp.	<i>Pogonomys</i> spp.	WT/NG	1675–5692
<i>Pseudochirops</i> sp. 1	<i>Pseudochirops</i> spp.	WT/NG	1261–5544
<i>Pseudochirops</i> sp. 2	<i>Pseudochirops</i> spp.	NG	1261–5544
<i>Pseudochirops</i> sp. 3	<i>Pseudochirops</i> spp.	NG	1261–5544
<i>Pseudochirulus</i> sp. 1	<i>Pseudochirulus canescens/mayeri</i>	NG	2722–5544
<i>Pseudochirulus</i> sp. 2	<i>Pseudochirulus forbesi</i>	NG	1296–5544
<i>Pseudochirulus</i> sp. 3	<i>Pseudochirulus</i> spp.	WT/NG	1296–5544
<i>Thylogale</i> sp. (small)	<i>Thylogale christenseni</i>	NG (Holocene)	Montane
<i>Uromys</i> sp.	<i>Uromys hadrourus</i>	WT	1211–3436
Arid taxa			
Taxon	Closest living relative		Annual precipitation (mm) <sup>a</sup>
<i>Chaeropus ecaudatus</i>	<i>Chaeropus ecaudatus</i>		144–333
<i>Macrotis lagotis</i>	<i>Macrotis lagotis</i>		132–722
<i>Notomys</i> spp.	<i>Notomys</i> spp.		129–1273
<i>Perameles bouganville</i>	<i>Perameles bouganville</i>		208–391
<i>Planigale</i> sp. 2	<i>Planigale tenuirostris</i>		140–743
<i>Pogona</i> sp.	<i>Pogona minor/michelli</i>		163–996
<i>Sminthopsis macroura</i>	<i>Sminthopsis macroura</i>		129–996
<i>Tympanocryptis</i> sp.	<i>Tympanocryptis cephalus</i>		181–539

<sup>a</sup> Annual precipitation range (mm) was determined for closest living relatives by using DIVA-GIS 5.2 bioclimatic software (Hijmans et al., 2005) and taxon distribution data taken from OZCAM BioMaps online databases (OZCAM community, 2006).

**Table 6-2. Middle Pleistocene fossil taxa considered to be rainforest or arid specialists with the annual precipitation range\* of their closest living relatives.**

### 6.6.3 Implications for megafaunal extinction hypotheses

We provide the first direct evidence of Quaternary rainforest megafauna in Australia. Therefore, any hypotheses of megafaunal extinction must take into account their extinction from rainforest habitats. Evidence will need to determine whether the reduction of rainforest habitat to its present state was primarily due to pre-human climate change and that this was sufficient to drive the megafauna extinct from rainforest habitat, or whether the addition of human hunting and habitat modification was necessary to tip the balance.

Faunal stability throughout the middle-late Pleistocene, during periods of climate change and prior to human arrival, has been used to argue against climate change as a



mitigating factor in the extinction of the late Pleistocene megafauna [22, 23]. It is argued that the southern faunas, including megafauna, were resilient to climate change and thus the extinction of megafauna must have included other factors, of which anthropogenic impacts are favoured [22, 23].

Our results cannot preclude climate change, in particular increased climatic variability and aridity, as a mitigating factor in the extinction of Pleistocene fauna in northern Australia. Although we are yet to determine the direct affects of climate change on megafaunal species, we argue that the climate changes during the middle, and presumably late Pleistocene, in northern Australia dramatically influenced the composition and stability of both the flora and fauna before first human occupation ~50 ka. Hence, the response of fauna and flora to climate change and the impacts of human occupation may have been very different in different regions of Australia owing to differential timing of major climate-induced habitat modifications.

#### 6.6.4 *Palaeobiogeographic Implications*

The middle Pleistocene rainforest faunas of Mt Etna provide new data on the paleobiogeography of taxa endemic to the tropical rainforests of New Guinea and the Wet Tropics bioregion of Australia. Of particular interest are the small, herbivorous, arboreal and terrestrial mammals that are common in Holocene deposits and in extant montane rainforests throughout New Guinea (e.g. †*Thylogale christenseni*, *Thylogale calabyi*, †*Dactylopsila kambuyai*, †*Petauroides* *ayamauruensis* and *Pseudochirulus mayeri* [56-58]). These small-bodied taxa are absent from the existing Wet Tropics rainforests of northern Australia, however, closely related taxa are found approximately 800kms to the south of the Wet Tropics in the middle Pleistocene deposits at Mt Etna [15]. This indicates that they were present in Australia during the Pleistocene, however, were driven extinct on mainland Australia sometime after ~280 ka.

Similarly, middle Pleistocene species of possum (*Pseudochirulus* and *Phalanger*) and tree-kangaroo (*Dendrolagus* “short-foot” clade) from Mt Etna share closer phylogenetic relationships with New Guinean taxa than they do with extant Wet Tropics taxa, suggesting that they too were driven extinct on mainland Australia after ~280 ka. Therefore, the continental extinction of several taxa, including entire guilds,

and not just those that were megafauna, occurred within Australian rainforests during the Pleistocene.

Palaeoclimatic models have been used to hypothesise relatively recent (i.e. 7500-6000 years ago) arrivals of New Guinean taxa into the Wet Tropics region (e.g. *Cercartetus caudatus*, *Dactylopsila trivirgata*, *Uromys caudimaculatus*, and *Pogonomys mollipilosus*) [11]. However, species from each of these genera occur in the middle Pleistocene of Mt Etna, and, with the exception of *Uromys* sp., none of them are considered to be conspecific with modern forms. This suggests a complex interchange of faunas between New Guinea and Australia during the Quaternary, with the current “New Guinea species” in the Wet Tropics representing one of at least two possible invasions, the first arriving before the middle Pleistocene and reaching as far south as Rockhampton. Alternatively, “New Guinea species” that presently occur in the Wet Tropics may share a refugial status with the Wet Tropics endemics, representing species and/or lineages present on mainland Australia for much longer than previously was thought.

The Wet Tropics bioregion possesses a group of mammals that are not present in either New Guinea or the middle Pleistocene sites of Mt Etna (e.g. *Hypsiprymnodon*, *Bettongia* and *Hemibelideus*). The absence of these mammals from the Mt Etna deposits is an enigma and cannot be explained taphonomically because collecting has been thorough and similarly-sized taxa are found in abundance in most of the deposits. Each of these three genera represent deeply divergent clades [7], two of which are monotypic rainforest specialists (*Hypsiprymnodon* and *Hemibelideus* [11]), and two possess a long fossil record associated with interpreted rainforest palaeoecologies (i.e. *Hypsiprymnodon* and *Bettongia* (Oligo-Pliocene) [7]). Likewise, *Dorcopsis*, now endemic to New Guinea has an early Pliocene record in Australia, however, it is absent from the middle Pleistocene deposits at Mt Etna [9]). Thus, the middle Pleistocene rainforest faunas at Mt Etna represent a mixture of taxa that are now differentially isolated in New Guinea and the Wet Tropics. This mixture has included or excluded taxa with long histories associated with rainforests, illustrating the complex taxonomic filters operating in Australopapuan rainforests throughout the Neogene. The extinct rainforest assemblage presented here illustrates a diversity of taxa and guilds unlike that found in present day Australian tropical rainforests. These results emphasise the dominance of extinction, via climate change, as the major driving force in shaping Australia’s present day tropical rainforest faunas.

## 6.7 Conclusions

Fossiliferous cave deposits from Mt Etna, central-eastern Queensland represent the only Quaternary rainforest vertebrate fossil record known in Australia. The deposits were previously thought to be Pliocene in age based on biocorrelation, but direct chronometric dating has revealed that most of these sites are in fact middle Pleistocene in age, dating from before 500 ka to approximately 280 ka. This result extends the temporal range of several Pliocene and early Pleistocene taxa into the middle Pleistocene.

After a long period of relative faunal stability at Mt Etna, a major faunal turnover occurred between ~280 ka and ~205 ka, wherein a diverse rainforest fauna was replaced by a xeric-adapted fauna, lending the first vertebrate fossil evidence to the large-scale climatic shifts to aridity in northern Australia, documented by numerous other palaeoclimatic methods. At least one more faunal change occurred since that time to produce the Holocene and modern mesic-adapted fauna, which we suggest is a continued response of northern Australian habitats to the sustained shift to increased climatic variability. However, additional anthropogenic influences are not ruled out in the most recent faunal changes.

These results contrast with Quaternary records from southern Australia which show remarkable faunal stability over the last 500 ka. That stability may reflect long term adaptation to increasing aridity, which began earlier in southern Australia.

Our results illustrate the presence of a suite of rainforest taxa without any present day Australian representative and indicate a longer connectivity between the faunas of northern Australia and New Guinea than previously was thought. Understanding the causes for the extinction of these taxa on mainland Australia is fundamental when considering the vulnerabilities of present day rainforest taxa in far north Queensland, a bioregion under several climatic and human induced threats.

We demonstrate here that Quaternary climate change influenced regions of the Australian continent in different ways over a similar period of time and to a degree previously not recorded. Although this is in itself an intuitive statement, it does illustrate the inherent complexity in determining what the responses of fauna and flora to climate change may be in the future.

## 6.8 Acknowledgements

This project was funded by the Australian Research Council (LP0453664) with the support of Industry Partners (Queensland Museum, Cement Australia, Rockhampton Regional Development, Australian Museum, Central Queensland Speleological Society and the Outback Isa Riversleigh Interpretative Centre). We thank S. Hand, M. Archer, H. Godthelp, T. Barrows, P. Moss, G. Prideaux, A. Cook, S. Marks, G. Price, L. Deer, B. Cooke, K. Spring, J. Wilkinson, P. Tierney, N. Sands, P. Berrill, B. Bauer, K. Lawrence, C. White, J. Cramb, J. Williams, S. Martinez and D. Lewis for their support and discussion during the progress of this research.

## 6.9 Appendix A. Supplementary material

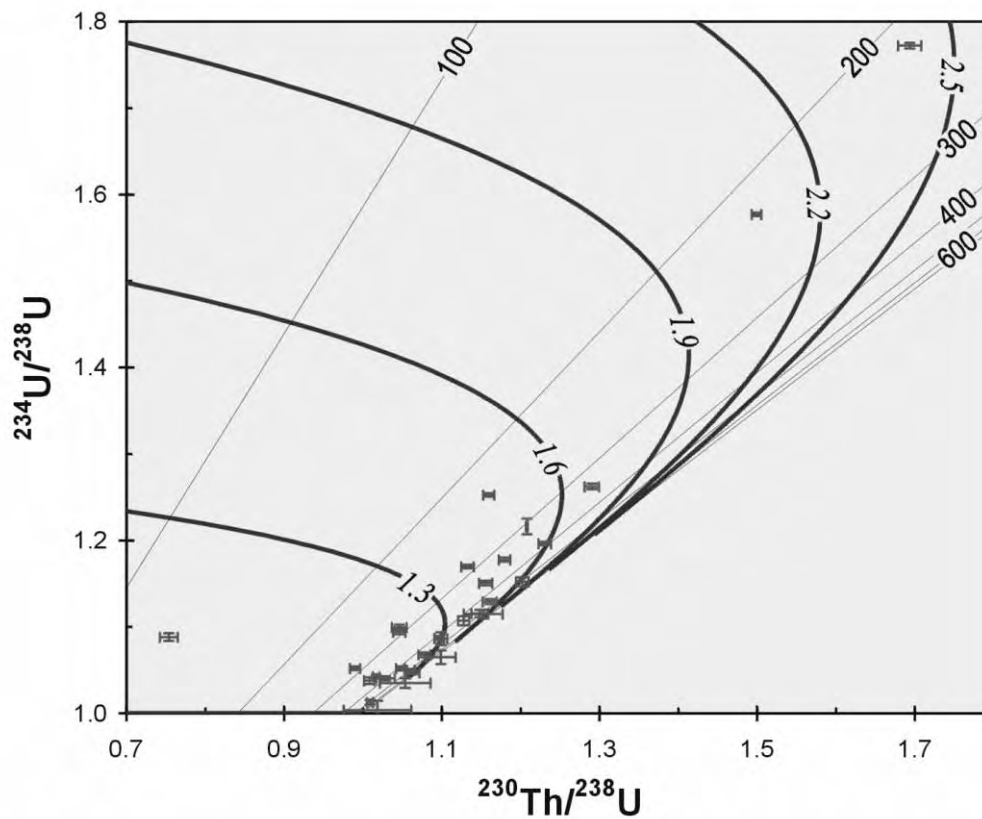


**Figure 6-6.**  $^{230}\text{Th}/^{238}\text{U}$  vs.  $^{234}\text{U}/^{238}\text{U}$  evolution diagram for flowstone and calcite filling samples from Mt Etna. Curved lines are closed-system isotopic evolution for initial  $^{234}\text{U}/^{238}\text{U}$  activity ratios of 1.3, 1.6, 1.9, 2.2 and 2.5. Straight lines are isochrons with numbers corresponding to isochron ages (ka). The plot shows that the vast majority of samples plot in between the 300 and 600 ka isochrons.

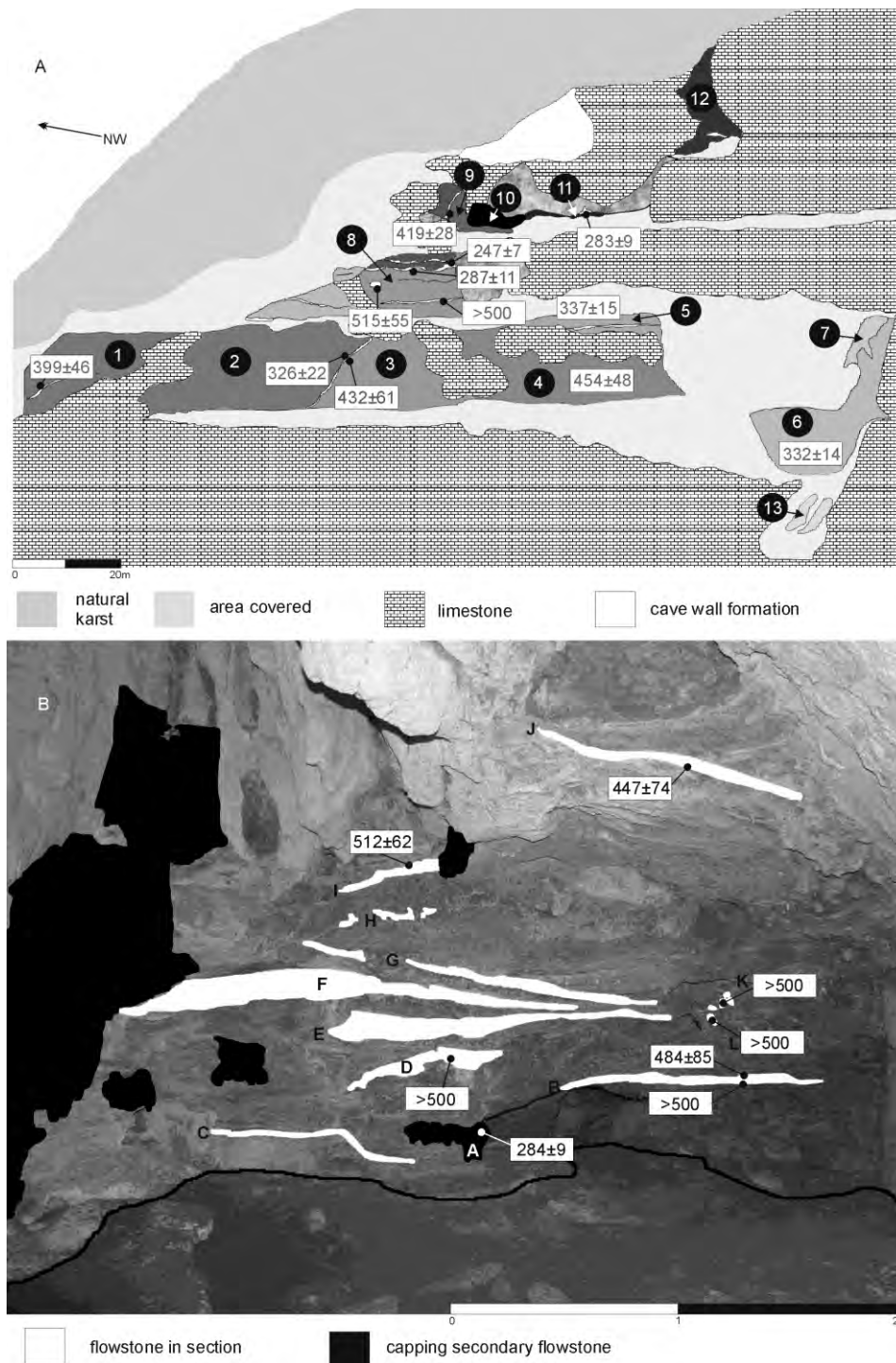


**Figure 6-7. Stratigraphy of Mt Etna Limestone Mine and QML1284 with dates, adapted and revised [15]. A. Exposed fossil deposits at Mt Etna Limestone Mine, western benches. 1-5 QML1311; 1. A/B, 2. C/D, 3. F, 4. H, 5. J. 6-7 QML1384; 6. LU, 7. UU. 8. QML1310 Unit 2, 9. QML1383 A, 10. Open chamber to Speaking Tub Cave System, 11. QML1313, 12. Bench 0 (A/B), 13. QML1385. Blue coloured text represent minimum ages, red coloured text represents maximum ages.**

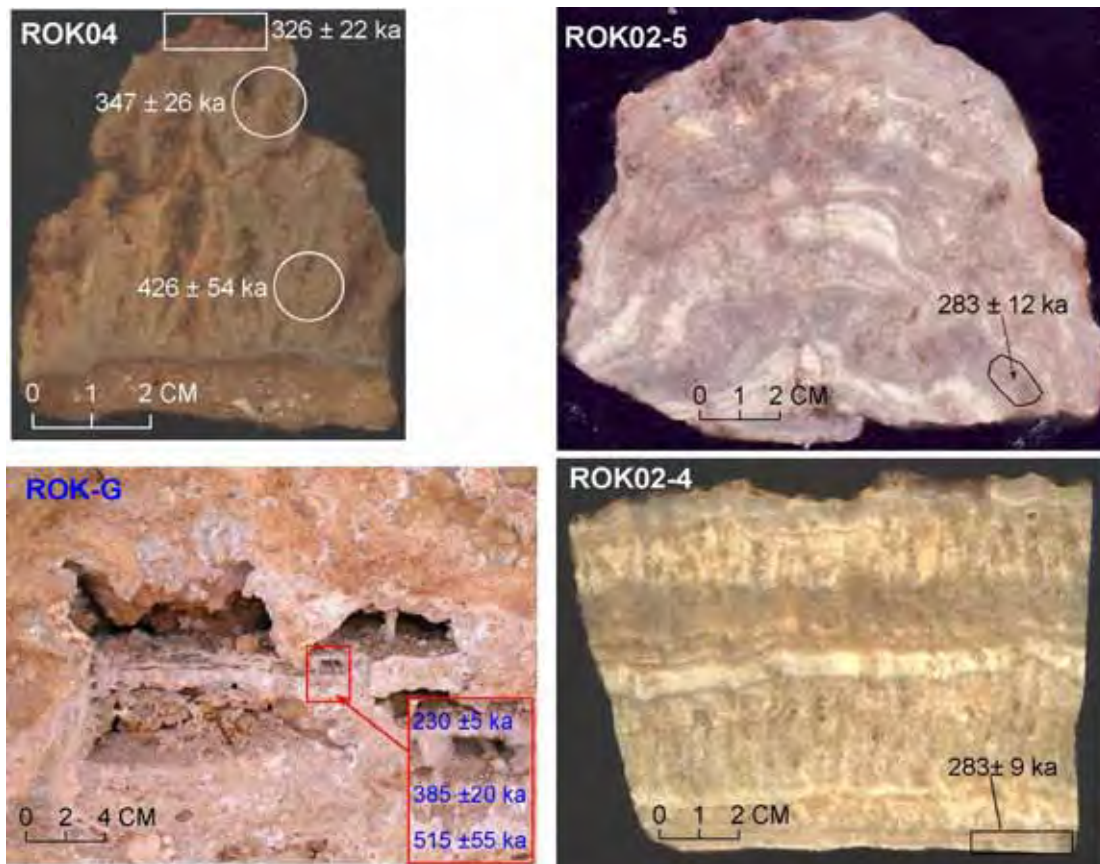


**Figure 6-8. Images of selected flowstones with dating loci. Flowstone ROK04 was dated at three loci, i.e. ~4, 15 and 46 mm below the top surface of the flowstone. Samples ROK02-4 and 02-5 represent different sections of one flowstone (ROK02), and the bottom parts of both samples yield identical ages. ROK-G is a flowstone-like calcite vug growing within the void of Unit-2 deposits at site QML1310 (somehow like a micro-cave). Its top, middle and bottom portions yield three different ages corresponding to Marine Isotope Stages 7, 11 and 13.**

Site	Site Age	Accumulation Mode	Predator Accumulators	Bone Associations	Bone Modification	Dominant Sedimentology	Transportation	Reworking	Size Filter	Quantity Sorted
<b>Olsen's Cave</b>										
Iceberg Chamber	~ 7ka	Predator	<i>Felis sp.</i>	Disarticulated	digestive	Lightly cemented cave clay and guano	Minimal		>15 $\mu$	<0.1m <sup>3</sup>
Heavy Moon Suite	> 6ka	PB Trap	<i>Macrodontomys gipps</i>	Semi-associated	exchng				Megalomys	
<b>Mt Etna</b>										
QML1312	170-207 ka	Predator	<i>Macrodontomys gipps</i>	Disarticulated	Bone punctures	Lightly compacted cave clay	Minimal		>15 $\mu$	<0.2m <sup>3</sup>
		PB trap	<i>Felis sp.</i>	Semi-associated	digestive				Megalomys	
QML1313	$\geq$ 280ka	PB trap	<i>Macrodontomys gipps</i>	2 bone articulations	exchng	broken flowstone, calcite				
		Predator	<i>Felis sp.</i>	>2 bone articulation	digestive	Heavily cemented cave clays	Minimal		>15 $\mu$	<0.5m <sup>3</sup>
QML1313C-D	<310 ka	PB trap	<i>Macrodontomys gipps</i>	Associated	exchng	with parent flowstone clasts			Megalomys	
		Predator	<i>Felis sp.</i>	Disarticulated	digestive	Moderately cemented	Moderate			4m <sup>3</sup> -6
				Semi-associated	exchng	cave clays				
QML1311 J	> 330ka	PB trap	<i>Macrodontomys gipps</i>	2 bone articulations	Bone punctures	Moderately cemented cave clays	Minimal			<0.1m <sup>3</sup>
		Predator	<i>Felis sp.</i>	Disarticulated	digestive	with flowstone				
QML1384 LU	> 330ka	PB Trap	<i>Macrodontomys gipps</i>	Semi-associated	exchng	New Site	Moderate			4m <sup>3</sup> -6
		Predator	<i>Felis sp.</i>	Disarticulated	digestive	Moderately cemented				
QML1383 A	$\geq$ 420ka	Predator	<i>Macrodontomys gipps</i>	Minor articulations	exchng	cave clays				
QML1311 H	> 450ka	PB trap	<i>Macrodontomys gipps</i>	Disarticulated	Bone punctures	Heavily cemented cave clays	Minimal		>15 $\mu$	<0.2m <sup>3</sup>
		Predator	<i>Felis sp.</i>	Fragmented	digestive		Moderate		Megalomys	4m <sup>3</sup> -6
			<i>Macrodontomys gipps</i>	Disarticulated	exchng	Moderately cemented				
QML1310 Unit 2	~250-300ka	PB Trap	<i>Felis sp.</i>	Semi-associated		cave clays				
				2 bone articulations						
QML1385	7- 800ka	PB Trap	<i>Macrodontomys gipps</i>	Articulated	Bone punctures	Heavily cemented cave clays	Minimal			<0.1m <sup>3</sup>
		Predator		Disarticulated		Heavily cemented cave clays	Major	Moderate	>15 $\mu$	<0.1m <sup>3</sup>
				Fragmented					Megalomys	
<b>Limestone Ridge</b>										
QML1284	$\geq$ 500ka	PB Trap	<i>Felis sp.</i>	Articulated	digestive	Heavily cemented cave clays	Minimal			<0.2m <sup>3</sup>
		Predator	<i>Macrodontomys gipps</i>	Associated	exchng					
QML1284a	> 500ka	Predator	<i>Macrodontomys gipps</i>	Disarticulated	Bone punctures	Heavily cemented cave clays	Minimal		>15 $\mu$	<0.2m <sup>3</sup>
				Fragmented					Megalomys	
<b>Karet Glen</b>										
QML1411	?	PB Trap	<i>Macrodontomys gipps</i>	Disarticulated	Bone punctures	Heavily cemented cave clays	Major	Considerable		<0.1m <sup>3</sup>
		Channel fill			Rounding	Profilic Conglomerate				
					Bone pebbles					



Q08.141.5.1413	γ	Predator	Macrodontia gigas	Disarticulated Fragmented	Heavily cemented case days	Minimal	> 45g Myeloma	< 0.1m2
----------------	---	----------	-------------------	------------------------------	----------------------------	---------	------------------	---------



Petauridae											
gen et sp nov. 1	0	0	1	1	1	1	1	1	1	1	S
gen et sp nov. 2	0	0	0	1	1	0	1	1	1	1	S
<i>Dactylopsila</i> sp. 1	0	0	0	1	0	0	1	1	1	1	S
<i>Dactylopsila</i> sp. 2	0	0	0	0	1	0	0	0	1	0	S
<i>Petaurus</i> sp.	1	1	0	0	0	0	0	0	0	0	S
Burramyidae											
<i>Cercartetus</i> sp.	0	0	0	1	1	1	1	1	1	1	S
Acrobatidae		0									
<i>Acrobates</i> sp.	0	0	0	1	1	0	0	0	1	0	S
gen et sp nov.	0	0	0	1	1	1	1	1	1	1	S
Phascolarctidae											
<i>Phascolarctos</i> *	1	0	0	0	0	1	0	0	0	0	L
gen et sp nov. *	0	0	0	0	1	0	0	0	0	0	L
Pseudocheiridae											
gen. et sp nov. *	0	0	0	0	1	0	0	0	0	0	M
<i>Pseudocheirus</i> sp. 1	0	0	0	1	1	1	1	1	1	1	S
<i>Pseudocheirus</i> sp. 2	0	0	0	1	1	1	1	1	1	1	M
<i>Pseudocheirus</i> sp. 3	0	0	0	1	1	1	1	1	1	1	M
<i>Pseudocheirus peregrinus</i>	1	1	0	0	0	0	0	0	0	0	M
<i>Pseudochirulus</i> sp. 1	0	0	0	1	1	1	1	1	1	1	S
<i>Pseudochirulus</i> sp. 2	0	0	0	1	1	1	1	1	1	1	M
<i>Pseudochirulus</i> sp. 3	0	0	0	1	1	1	0	1	1	1	M
<i>Petauroides</i> sp. 1	0	0	0	1	1	1	1	1	1	1	M
<i>Petauroides</i> sp. 2	0	0	0	1	1	1	1	1	1	1	M
<i>Petauroides</i> sp. 3	0	0	0	1	1	1	1	1	1	1	M
<i>Pseudochirops</i> sp. 1	0	0	0	0	1	1	0	1	0	0	M
<i>Pseudochirops</i> sp. 2	0	0	0	0	0	0	0	0	1	0	M
<i>Pseudochirops</i> sp. 3	0	0	0	0	1	0	0	0	0	0	M
<i>Pseudokoala</i> sp. 1	0	0	0	0	1	0	0	0	0	0	L
<i>Pseudokoala</i> sp. 2*	0	0	0	0	1	1	0	0	0	0	L
Vombatidae											
<i>Vombatus</i>	0	0	0	0	1	1	0	0	0	0	VL
Diprotodontidae											

diprotodont indet	0	0	0	0	0	0	0	0	0	0	MF
Phalangeridae											
<i>Phalanger</i> sp. 1	0	0	0	1	1	1	1	1	1	1	L
<i>Phalanger</i> sp. 2*	0	0	0	0	0	0	0	1	0	0	L
<i>Trichosurus</i> sp. 1	1	1	1	0	0	0	0	0	0	0	L
<i>Trichosurus</i> sp. 2	0	0	0	0	0	1	0	0	0	0	L
DASYUROMORPHIA											
Thylacimidae											
<i>Thylacinus</i> sp.	0	0	1	1	1	1	0	1	0	0	VL
Dasyuridae											
<i>Sarcophilus</i> sp.	0	0	1	0	1	1	0	1	0	0	L
<i>Antechinus</i> sp. 1	0	0	0	1	1	1	1	1	0	1	S
<i>Antechinus</i> sp. 2	0	0	0	1	1	1	0	1	1	1	S
<i>Antechinus flavipes</i>	1	1	1	0	0	0	0	0	0	0	S
<i>Antechinus swainsoni</i>	0	0	1	0	0	0	0	0	0	0	S
<i>Sminthopsis murina</i>	1	1	1	1	0	0	0	0	1	0	S
<i>Sminthopsis</i> sp.	0	0	0	0	0	1	1	1	0	0	S
<i>Sminthopsis macroura</i>	0	1	1	0	0	0	0	0	0	0	S
<i>Planigale</i>	0	0	0	1	1	0	1	0	0	0	S
<i>Planigale maculata</i>	1	1	1	0	0	0	0	0	0	0	S
<i>Planigale</i> sp. 2*	0	0	1	0	0	0	0	0	0	0	S
gen et sp nov.	0	0	0	1	1	1	1	1	1	1	S
<i>Phascogale</i> sp. 1	0	0	0	1	0	1	1	1	1	1	S
<i>Phascogale topoatafa</i>	1	1	1	0	0	0	0	0	0	0	S
<i>Dasyurus</i>	0	0	0	1	1	1	1	1	0	1	M
<i>Dasyurus viverrinus</i>	0	0	1	0	0	0	0	0	0	0	M
<i>Dasyurus hallucatus</i>	1	1	1	0	0	0	0	0	0	0	M
<i>Dasyurus maculatus</i>	1	1	0	0	0	0	0	0	0	0	L
PERAMELOMORPHIA											
Perameloid											
gen et sp nov. 1	0	0	0	1	1	1	1	1	0	1	M
gen et sp nov. 2	0	0	0	1	1	1	1	1	0	0	M
Peramelidae											
<i>Perameles</i> sp. 1	0	0	0	1	1	1	0	1	1	1	M

<i>Perameles</i> sp. 2	0	0	0	1	1	0	0	1	1	1	M
<i>Perameles bougainville</i>	0	0	1	0	0	0	0	0	0	0	M
<i>Perameles nasuta</i>	1	1	0	0	0	0	0	0	0	0	M
<i>Isoodon obesulus</i>	0	1	1	0	0	0	0	0	0	0	M
<i>Isoodon</i> sp. 1	0	0	1	1	1	1	1	1	0	0	M
<i>Chaeropus ecaudatus</i>	0	0	1	0	0	0	0	0	0	0	M
<i>Macrotis lagotis</i>	0	0	1	0	0	0	0	0	0	0	M
<i>Isoodon macrourus</i>	1	1	0	0	0	0	0	0	0	0	M
RODENTIA											
Muridae											
<i>Pogonomys</i>	0	0	0	1	1	1	1	1	1	1	S
<i>Mesembriomys</i>	0	0	0	1	1	1	1	1	1	1	M
<i>Uromys</i>	0	0	0	1	1	1	1	1	1	1	M
<i>Melomys</i>	0	0	0	1	1	1	1	1	1	1	M
<i>Zyzomys</i>	0	0	1	1	1	1	1	1	1	1	S
<i>Leggadina</i>	0	1	1	0	0	0	0	0	0	0	S
<i>Rattus</i>	1	1	1	0	0	0	0	0	0	0	S
<i>Notomys</i>	0	0	1	0	0	0	0	0	0	0	S
<i>Conilurus</i>	0	0	1	0	0	0	0	0	0	0	S
<i>Pseudomys</i>	1	1	1	1	1	1	1	1	1	1	S
<i>Mastacomys</i>	0	1	0	0	0	0	0	0	0	0	M
ANURA											
<i>Crinia</i>	0	0	0	1	0	0	1	0	1	0	S
<i>Cyclorana</i>	1	1	1	0	0	0	0	0	0	0	S
<i>Etanatrachus</i>	0	0	0	0	1	0	0	1	1	0	M
<i>Kyarranus</i>	0	0	0	1	1	1	1	1	1	1	S
<i>Lechriodus</i>	0	0	0	1	1	1	1	0	1	1	S
<i>Limnodynastes</i>	1	1	1	1	1	1	1	1	1	1	S
<i>Litoria</i>	1	1	0	1	1	1	1	1	1	1	S
<i>Neobatrachus</i>	0	1	0	0	0	0	0	0	0	0	S
<i>Nyctimystes</i>	0	0	0	1	0	1	1	1	1	1	S
microhylids	0	0	0	1	0	0	1	0	1	1	S

Table 6-4. Faunal lists for fossil sites and present day. 0=absent, 1= present.

SQUAMATA											
Agamidae											
<i>Amphibolurus</i>	0	0	1	0	0	0	0	0	0	0	S
<i>Chlamydosaurus kingii</i>	1	0	0	0	0	0	0	0	0	0	M
<i>Diporiphora bilineata</i>	1	1	0	0	0	0	0	0	0	0	S
<i>Hypsilurus</i>	0	0	0	1	0	0	0	0	1	1	M
indet agamid	1	1	1	1	1	1	1	1	1	1	S
<i>Pogona barbata</i>	1	1	0	0	0	0	0	0	0	0	M
<i>Pogona</i> sp. ( <i>mitchelli/minori</i> )	0	0	1	0	0	0	0	0	0	0	S
<i>Tympanocryptis</i> cf. <i>T. cephalus</i>	0	0	1	0	0	0	0	0	0	0	S
<i>Tympanocryptis lineata</i>	0	1	0	0	0	0	0	0	0	0	S

\*fauna identified subsequently to [15]. Size classes: S, small <500g; M, medium 500g-3kg; L, large 3kg-15kg; VL, very-large 15kg-100kg; MF, megafauna >100kg.

Detailed uranium-series analytical data and dates for fossil sites at Mt Etna, eastern-central Queensland.

QML Locality	Sample Name	Description	Age interpretation	U (ppm) $\pm 2\sigma$	$^{232}\text{Th}$ (ppb) $\pm 2\sigma$	$^{230}\text{Th}/^{232}\text{Th}$ $\pm 2\sigma$	$^{234}\text{U}/^{238}\text{U}$ $\pm 2\sigma$	$^{230}\text{Th}/^{238}\text{U}$ $\pm 2\sigma$	uncorr.	$^{230}\text{Th}$ Age (ka) $\pm 2\sigma$	$^{230}\text{Th}$ Age (ka) $\pm 2\sigma$	Initial ( $^{234}\text{U}/^{238}\text{U}$ ) $\pm 2\sigma$	
Olsen's Honey Moon Suite	ROK-07	<i>Petrogale</i> incisor	min. age	0.4406 0.0003	3.74	33.7	1.6126 0.0036	0.09435 0.0021	6.5	0.2	6.3	0.2	1.625 0.003
Olsen's scicle Chamber	OC-07	Calcite cement	close to real	0.0071 0.0002	0.220	19.3	2.7695 0.0112	0.1954 0.0039	7.9	0.2	7.6	0.2	2.823 0.013
1312 Elephant Hole Cave	ME-KT-1	<i>Petrogale</i> incisor	min. age	3.3451 0.0025	2.71	3682	1.2664 0.0025	0.9821 0.0032	149	1	149	1	1.407 0.003
1312 Elephant Hole Cave	ME-KB-1	macropod bone	min. age	4.4746 0.0041	1.69	3974	1.0843 0.0021	0.4944 0.0058	66	1	66	1	1.102 0.002
1312 Elephant Hole Cave	ROK 1 0	snail shell	min. age	0.0366 0.0001	8.18	16.3	1.4228 0.0065	1.2042 0.0218	173	7	169	9	1.727 0.022
1312 Elephant Hole Cave	ROK 1 1	<i>Petrogale</i> incisor	min. age	3.5621 0.0030	56.9	150	1.1646 0.0024	0.7890 0.0033	118	1	118	1	1.231 0.003
1312 Elephant Hole Cave	ROK26-1	broken flowstone	max. age	0.0783 0.0001	10.9	22.7	1.0518 0.0023	1.0475 0.0055	415	26	411	27	1.173 0.012
1312 Elephant Hole Cave	ROK26-2	broken flowstone	max. age	0.0496 0.0001	6.01	25.3	1.0378 0.0038	1.0081 0.0068	348	20	345	21	1.104 0.009
1312 Elephant Hole Cave	ROK26-3	broken flowstone	max. age	0.4056 0.0004	3.77	332	1.0425 0.0019	1.0168 0.0042	355	12	355	12	1.116 0.005
1312 Elephant Hole Cave	QML1312-3	broken flowstone	max. age	0.1854 0.0001	65.6	9.00	1.0835 0.0016	1.0489 0.005	314	8	305	13	1.220 0.009
1312 Elephant Hole Cave	QML1312-4	broken flowstone	max. age	0.0786 0.0001	131.1	2.06	1.1513 0.0058	1.1334 0.024	314	36	269	143	1.594 0.163
1312 Elephant Hole Cave	QML1312-6	broken straw	max. age	0.2151 0.0002	39.1	17.3	1.1735 0.0026	1.0393 0.0053	209	3	205	4	1.326 0.007
1313 Speaking Tube Cave	ROK02-4	flowstone	min. age	0.019560 0.0001	0.88	66.9	1.0521 0.0021	0.9898 0.0065	284	9	283	9	1.118 0.005
1313 Speaking Tube Cave	ROK02-5	flowstone	min. age	0.018910 0.0002	0.17	352	1.0995 0.0032	1.0461 0.0093	283	12	283	12	1.222 0.008
1383 Bench 1 NW (Unit A)	ROK F	flowstone	max. age of Unit A	0.0499 0.0001	5.35	31.0	1.0870 0.0022	1.0965 0.0057	422	26	419	28	1.294 0.020
1310 Unit 2	ROK 1 5	flowstone	max. age of Unit 2	0.1962 0.0002	1.99	318	1.0470 0.0015	1.0625 0.0090	602	202	602	202	1.239 0.147
1310 Unit 2	ROK 1 6 top	flowstone	min. age	0.1894 0.0003	6.52	109	1.2945 0.0023	1.2347 0.0104	247	7	247	7	1.598 0.012
1310 Unit 2	ROK 1 8 bottom	flowstone	min. age of Unit 2	0.0186 0.0000	2.92	20.2	1.0941 0.0026	1.0439 0.0078	291	11	287	12	1.222 0.008
1310 Unit 2	ROK G top	vug in void	youngest age of vug	0.0439 0.0000	0.54	284	1.2525 0.0020	1.1594 0.0071	230	4	230	5	1.485 0.006
1310 Unit 2	ROK G middle	vug in void		0.0245 0.0000	0.25	362	1.1964 0.0019	1.2305 0.0080	385	20	385	20	1.587 0.032
1310 Unit 2	ROK G bottom	vug in void	max. age of vug	0.0432 0.0000	0.10	1464	1.0499 0.0015	1.0606 0.0049	515	55	515	55	1.215 0.031
1311 deposit A/B contact	ROK03 top	flowstone	max. age of B	0.0228 0.0000	0.67	105.9	1.0405 0.0023	1.0285 0.0118	399	46	399	46	1.126 0.016
1311 deposit C/F contact	ROK04/04	flowstone	max. age of C	0.0895 0.0000	20.7	16.0	1.2162 0.0092	1.2078 0.0010	331	14	326	22	1.559 0.028
1311 deposit C/F contact	ROK04/15	flowstone	mid flowstone	0.0415 0.0000	10.5	13.8	1.1507 0.0027	1.1555 0.0085	352	18	347	26	1.432 0.025
1311 deposit C/F contact	ROK04/46	flowstone	min. age of F	0.0249 0.0001	3.37	24.6	1.0863 0.0074	1.0987 0.0082	436	60	432	54	1.305 0.036
1311 H deposit	ROK20-1 bone	macropod bone	min. age	11.486 0.0167	9.45	5470	1.5742 0.0026	1.4825 0.0089	216	4	216	4	2.039 0.010
1311 H deposit	ROK20-1 cal	calcite filling in bone	min. age	1.1058 0.0012	22.8	221	1.5771 0.0021	1.4991 0.0062	221	3	221	3	2.085 0.008
1311 H deposit	ROK20-2	calcite filling in bone	min. age	0.0854 0.0001	5.56	35.1	1.0882 0.0045	0.7536 0.0113	125	4	123	4	1.127 0.006
1311 H deposit	ROK20-4 bone	macropod bone	min. age	10.982 0.0209	4.95	8951	1.3324 0.0027	1.3294 0.0076	285	7	285	7	1.746 0.014
1311 H deposit	ROK20-4 cal	calcite filling in bone	min. age	0.1800 0.0002	0.85	749	1.1291 0.0029	1.1609 0.0091	454	48	454	48	1.468 0.060
1311 H deposit	ROK21	calcite filling in bone	min. age	10.255 0.0153	18.5	2849	1.7722 0.0032	1.6933 0.0148	215	5	215	5	2.421 0.019
1384 Lower Unit	ROK27 bone	macropod bone	min. age	4.6035 0.0048	15.1	1278	1.3991 0.0027	1.3856 0.0069	267	5	267	5	1.851 0.011
1384 Lower Unit	ROK27 cal	calcite filling in bone	min. age	0.0822 0.0001	7.61	38.6	1.1777 0.0024	1.1795 0.0073	333	13	332	14	1.466 0.016
1284 Layer A	MC/01	capping flowstone	min. age	0.0163 0.0000	0.606	92.6	1.1697 0.0022	1.1325 0.0079	285	9	284	9	1.384 0.010
1284 Mini Cave Layer B	MC-02 base	flowstone oldest	max. age	0.0332 0.0001	18.6	6.5	1.1521 0.0053	1.2022 0.0080	511	79	500	208	1.741 0.389
1284 Layer B	MC-02 mid	flowstone	max. age	0.0545 0.0001	8.53	22.3	1.1155 0.0041	1.1480 0.0105	487	79	484	85	1.475 0.105
1284 Layer D	MC-04	flowstone	mid	0.011230 0.0002	6.31	5.9	1.0649 0.0080	1.0987 0.0186	>500		>500		

1284	Layer E	MC-05	flowstone	mid	0.025530.00004	21.1	4.1	1.1072	0.0053	1.1276	0.0069	438	44	418	134	1.453	0.129
1284	Layer H	MC-08	calcite filling (cracks)	mid	0.015580.00002	12.0	4.5	1.1148	0.0049	1.1523	0.0246	527	234	511	362	1.618	0.589
1284	Layer I	MC-09	flowstone	min. age	0.0715 0.0001	2.04	107	1.0129	0.0028	1.0090	0.0037	513	62	512	62	1.055	0.008
1284	Layer J	MC-10	flowstone youngest	min. age	0.0557 0.0001	26.8	6.8	1.0677	0.0027	1.0780	0.0075	459	50	447	74	1.277	0.047
			calcite filling in	min. age													
1284	between layer G & H	MC-11 bc	bone		0.004690.00001	0.48	30.2	1.0038	0.0108	1.0183	0.0429	>500		>500			
			calcite filling in	min. age													
1284	between layer G & H	MC-11 sbc	bone		0.007530.00001	1.88	12.8	1.0350	0.0057	1.0534	0.0322	>500		>500			

Note: Ratios in parentheses are activity ratios calculated from the atomic ratios. The ages are calculated using Ken Ludwig's Isoplot/EX program. Corr. and uncorr. denote corrected and uncorrected. The corrected <sup>230</sup>Th ages and initial (<sup>234</sup>U/<sup>238</sup>U) ratios include a negligible to small correction for non-radiogenic Th using average crustal <sup>232</sup>Th/<sup>238</sup>U atomic ratio of 3.8±1.9 (<sup>230</sup>Th, <sup>234</sup>U and <sup>238</sup>U are assumed to be in secular equilibrium). Ages assigned as >500 ka are those that are too old and cannot be calculated using Isoplot/EX program. Refer to Appendix A, Fig 1. for their actual ranges.

Table 6-5. Detailed U-series data for fossil sites.











## Chapter 7

### 7.1 Responses of Australian Neogene rainforest vertebrates to late Cainozoic environmental change: a synthesis of current knowledge.

#### 7.2 Introduction

Assessing the likely impact of future environmental changes on biodiversity requires knowledge of past climatic patterns and processes and their influence on the fauna and flora (Archer et al., 1991, 1998; Birmingham & Dick, 2005; Moritz et al., 2005). Past climatic patterns and processes are preserved in the geological record via a suite of independent proxies, however, the record of past fauna and flora relies solely on the fossil record and inferences from modern biogeography and phylogeography. These records provide an accurate assessment of the current condition of the modern environment and underpin the assumptions and robustness of modelling future environmental change. Therefore, a detailed knowledge of the Neogene is paramount to testing and corroborating future predictions.

This is most apparent on the Australian continent (Australia-New Guinea) where Neogene environmental change has significantly shaped its modern biota, both terrestrial and marine, and where anthropogenic influences have been available for at least 40,000 years. The Neogene palaeoenvironmental history of Australia is dominated by palaeoclimatic records that indicate long-term drying trends through intensifying aridity and greater climatic variability (Archer et al., 1999; Greenwood & Christophell, 2005; McGowran et al., 2000). Neogene floral records also indicate the dominant trend of increasingly open vegetation and greater influence of scleromorphic (pyrophylic) taxa. Although not as well documented as the other proxies, the Neogene vertebrate fossil record illustrates a general trend from closed-habitat faunas to a dominance of open-habitat faunas through time (Archer et al., 1999; Hocknull et al., 2007).

These general trends mask a more complex system of palaeoenvironmental change that will only become apparent with more detailed documentation of the Neogene

fossil record and the combination of both faunal and floral records in palaeoenvironmental reconstructions.

This paper brings together relevant proxies of geology, tectonics and climate that correspond to floral and faunal change throughout the Australian Neogene in an effort to better understand the responses of rainforest vertebrates to changes within the Neogene environment of Australia and Papua New Guinea. In particular it summarises the findings of Hocknull (2005), Hocknull et al. (2007) and Chapters 2-6 and synthesises this as a hypothetical reconstruction of rainforest vertebrate evolution in Australopapua.

### **7.3 The Australian Neogene vertebrate literature (1960-2008).**

A search of the Zoological Record was undertaken to survey the record for papers published between 1960 and 2008 regarding five main topics concerning Neogene vertebrates. These are: 1, taxonomic and phylogenetic papers covering the description or revision of Neogene vertebrate fossils; 2, faunal and palaeoecological papers covering Neogene faunal lists and palaeoecological reconstructions; 3, papers focused solely on the megafauna extinction debate; 4, papers considering topics not covered by 1-3, such as biomechanics, body-size estimation and taphonomy; and 5, papers focused on the molecular systematics and phylogeography of vertebrate fauna with mention of Neogene diversification.

Figure 7-1 graphically illustrates the results of this survey where each category is a proportion of the total number of articles published on topics 1-5 surveyed per decade. This proportional comparison was used instead of total counts to standardise the data to take into account the increase in total number of published articles. The total number of articles is a reflection of the total number of workers for any one decade, which varied from decade to decade.

These results show an overall trend over the five decades toward the proportional reduction of alpha-taxonomy and traditional phylogenetic studies in Neogene vertebrate fossil studies. Correspondingly, there has been a proportional increase in

papers focused solely on the megafauna extinction debate. The use of molecular techniques to recover phylogenetic and phylogeographic information from extant groups without using a fossil record has had a massive increase in proportional representation of this type of study in reconstructing past responses of lineages to changing environments.

These results document the overall trend in Australian vertebrate palaeontology away from traditional alpha-taxonomy, systematics and palaeoecology towards the highly polarised megafauna extinction debate and focused topical studies such as biomechanics and taphonomy. This trend is the reverse of that shown by studies of molecular phylogenetics, which are nevertheless experiencing increased demand for a better fossil record to test molecular-based phylogenies and phylogeographic hypotheses (e.g. Meredith et al., 2008).

The long-term trends observed here need to be reversed if the massive explosion of molecular studies are to be adequately tested using palaeoecological, palaeobiogeographical and geo-climatic data. Without increased understanding of alpha-taxonomy and palaeoecology derived from the fossil record through a return to proportionally higher numbers of such studies, working in sync with molecular studies or integrated with them, standard scientific methods of cross-checking and hypothesis testing will fail. This will ultimately lead to circular reasoning within molecular studies based on no new tests of fundamental hypotheses of faunal and floral diversification.

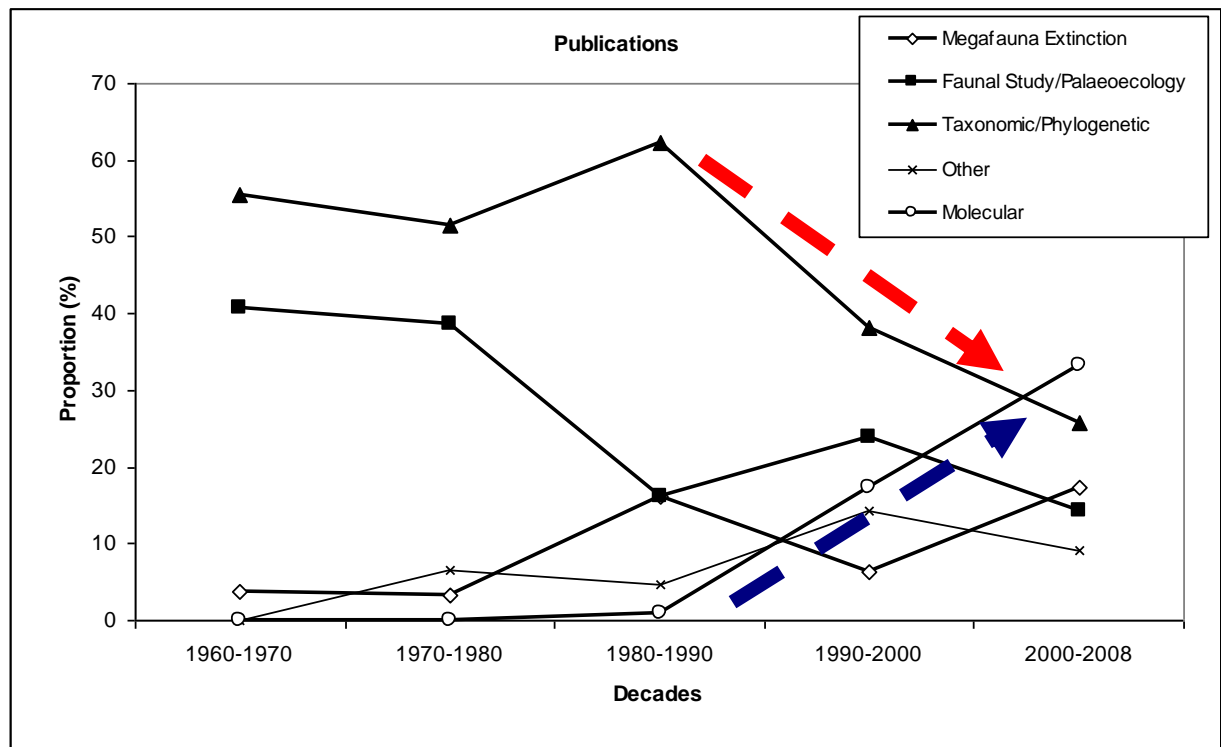


**Figure 7-1. Publications relating to the Neogene vertebrate record showing the marked decline (red arrow) over the last ca. 20 years in the study of vertebrate faunas, alpha-taxonomy and palaeoecology. This is compared with the significant proportional shift with increasing (blue arrow) molecular studies and a focus on megafauna extinction.**

#### **7.4 Temporal and spatial coverage of Neogene vertebrate fossil sites.**

The Australian Neogene terrestrial vertebrate fossil record is derived from fossil sites with markedly different depositional environments, including marine, estuarine, lacustrine, fluvial, swamp, spring, dune, cave and fissure settings. Each depositional environment presents markedly different interpretative difficulties and even within similar depositional environments interpretation can be difficult and misleading. Much of this can be overcome with systematic collection of in situ taphonomic, sedimentologic and chronometric samples and data (Price & Webb, 2006; Reed, 2002). Unfortunately large numbers of Neogene vertebrate localities have not been treated with adequate systematic collection and are interpretatively limited for most current research. These collections usually include spot site collections, either as



single specimens or a grab bag of specimens from a single, or several sites, within a particular locality (e.g. Molnar & Kurz, 1997).

Although such records (e.g. a single taxonomic record with no fixed age) serve the general purpose of understanding past taxonomic diversity, they offer little, if any, palaeoenvironmental data. This has led to the general conclusion that Australia's Neogene vertebrate record is temporally and spatially patchy and relatively useless in comparison to other techniques that provide longer temporal records for biogeographical and palaeoenvironmental reconstruction (e.g. palynology; Kershaw et al., 2003; 2005). Indeed, if we only consider systematically collected, dated and faunally representative collections, this conclusion may be justified. However, this situation is an historical artefact and is reflective of gross collecting techniques, rather than being representative of the potential resource available at any particular site.

Faunally representative sites would include collections of vertebrate remains from taxa of varying body-sizes, not simply fauna represented by large-bodied megafauna. Similarly, fauna only preserving small-sized taxa, such as those derived from owl-roost and ghost bat deposits, are also under-representative. In addition, well documented faunas would include species lists across most taxonomic groups represented as fossils in an individual fauna. Therefore, few Australian Neogene faunas can be considered to be well represented, well documented and also chronometrically dated.

Conceding the limitations outlined above, this chapter attempts to synthesise to available palaeobiogeographic, palaeogeographic and palaeoclimatic information to integrate the fossil record with the geological, tectonic and climatic records, in conjunction with evolutionary hypotheses derived from molecular studies. This study specifically focuses on the history of rainforest vertebrates in an attempt to better determine the evolutionary trajectories of several of Australia's most vulnerable vertebrate groups to past and present environmental change.

## **7.5 Palaeogeographic evolution of the Australopapuan region.**

Understanding the past geographical extent and position of present day areas of major biogeographic significance is integral to understanding the adaptive radiation,

dispersal and vicariance of faunal groups through time. This has been a particularly important issue for reconstructing the evolutionary history of rainforest vertebrates on mainland Australia, the New Guinea landmass, and surrounding oceanic and continental islands. The geology and tectonic history of the northern margin of the Australian Plate is very complex, especially throughout the mid-late Cainozoic when the development of present day landforms began. This period is of major significance for biogeographers and evolutionary biologists because it also marks a major radiation of vertebrate groups throughout the Australopapuan region in regions now restricted to relatively small areas of the continental plate (Heinsohn & Hope, 2006). Some groups are thought to have dispersed from Southern Asia to Australia via a series of island hops or dispersal across oceanic barriers (Aplin, 2006). Other groups are endemic to the Australopapuan region, having their origins when Australia was connected to Antarctica as part of Gondwana, or having evolved in isolation as an island continent (Archer et al., 1998). Teasing apart this chronology is integral to understanding the evolutionary trajectories of the Australopapuan biota and possible future influences of environmental change. In particular, the Neogene is of great importance because this is also a time of major climatic, geographical and sea level change.

The mainland of Australia has been relatively stable over the Cainozoic (Davies et al., 1996), but the northern margin of the Australian Plate has undergone a very complex history. The Australopapuan region is comprised of continental crust (Australian Plate), oceanic crust (Pacific Plate) and a series of different-aged accretionary terranes of island arc origin that have docked with the Australian Plate over the last 30 million years (Pigram & Davies, 1987). The docking terranes occurred along the northern margin of the Australian Plate in the regions now made up of the islands east of Wallace's Line, including Timor, Sulawesi, New Guinea, New Britain and the Solomon Islands. Several accreting terranes docked to form the northern margin of New Guinea whilst the southern margin is derived from up-thrusted continental crust, which is reflected in the island's extremely complex tectonic and geological history (Davies et al., 1996; Febo, 2007; Haig & Medd, 1996; Pigram & Davies, 1987; Pigram et al., 1989; Sandiford, 2007; Tcherepanov et al., 2008).

Palaeogeographic information relevant to the evolution of Australopapuan rainforest vertebrates encompasses the Oligocene to present. Figure 7-2 provides a simplified cross-section of the Australopapuan component of the Australian Plate from south to

north. This figure illustrates the subduction zone tectonics of the Australian Plate margin and the development of the complex New Guinean terranes, being both continental and oceanic in origin. These components provided the major east-west 'spine' of New Guinea, also termed the New Guinea Orogen (fold belt). Of palaeobiogeographic interest, this region makes up the highest mountainous terrains of New Guinea, which also possess the most diverse vertebrate faunas (Heads, 2002). These high terrains are climatically distinctive, occurring in the mesothermic to microthermic archipelago as defined by Nix (1982). In general, these isolated highland rainforests are considered to preserve the remnants of a once more expansive mesothermic rainforest zone that occurred throughout Australia and is now restricted to cool high altitudinal zones of eastern Australia and New Guinea (Greenwood & Christophel, 2006).

Of particular interest to palaeobiogeographers is knowing when parts of New Guinea became emergent from the ocean surface and remained emergent throughout their history, thereby providing viable habitat for dispersing fauna and flora.

There is no direct evidence of emergent landmasses in the New Guinea Orogen prior to the Late Miocene. Direct evidence relies on well-documented and well-dated sequences of stratigraphy that show a change from marine to emergent conditions, by exposure and erosion producing unconformities and followed by the deposition of terrigenous silici-clastic sediments (Chivas et al., 2001). Oligocene-Pliocene sedimentary basins and carbonate platforms record the best evidence for emergent land in the New Guinea Orogen, pointing to initial emergence during the Late Miocene. The emergent land area was most likely relatively small, but post-Late Miocene saw major uplift and subsequent wasting of the emergent lands with significant clastic in fill. By the Pliocene much of the central Orogen was evidently exposed and available for colonisation (Pigram et al., 1989; Figs 7-5, 7-6). These sequences demonstrate the continuous emergence of land, evidenced most conspicuously by mass sedimentation of carbonate platforms with silici-clastic sequences and the presence of internal fluvial deposited basins (Chivas et al., 2001; Tcherepanova et al., 2008).

Two such silici-clastic sediment infills are of particular importance to palaeobiogeographic reconstructions of Australopapua: the Gulf of Carpentaria (Karumba Basin) and the Gulf of Papua (Papuan Basin). Both sedimentary infills

show a Mesozoic basement followed by extensive Oligo-Miocene carbonate platform development, contemporaneous to carbonate platform development along the northeast of Australia (Queensland Plateau and Marion Plateau; Chivas et al., 2001; Davies et al., 1996; Muller, 2000; Pigram & Davies, 1987; Tcherepanova et al., 2008). . These carbonate platforms consist of continuous shallow to deep marine sequences indicating permanent marine conditions between northern mainland Australia and the developing New Guinea Orogen. It is therefore unlikely that there was any emergent land on the northern Australian margin, and certainly not of substantial size.

The youngest carbonate platforms date from the Middle to Late Miocene, being shortly followed by significant and continuous silici-clastic infills. These infill deposits are of terrestrial origin and therefore indicate the close proximity of emergent land. Sedimentation of this magnitude does not occur along the Queensland and Marion Plateaus, suggesting that the origin of the sediments was almost exclusively from an emergent island/s to the north of the basin rather than erosion of the northern margin of mainland Australia.

Terrestrial evidence of emergent landmasses includes central New Guinean sedimentary basins, which also date from the Late Miocene to Pliocene. The discovery of vertebrate fossils interpreted as Late Miocene in age provide not only direct evidence of emergent landmasses, but the ability of large-bodied non-volant vertebrates to disperse to these landmasses from mainland Australia (Menzies et al., 2008).

Based on these data, it seems most parsimonious that emergent islands were not available to be colonised by most non-volant vertebrates in the Middle Miocene. However, significant uplift along the New Guinea Orogen enabled colonisation of emergent landmasses from northern Australia since the Late Miocene. Colonisation occurred rapidly and by the Late Pliocene to Pleistocene the non-volant rainforest vertebrate fauna of New Guinea was well-established (Plane, 1967). Rapid colonisation of New Guinea suggests dispersal over vegetated land connections rather than random and diffuse oceanic dispersals.

Land connections between New Guinea and northern Australia were well established throughout the Pleistocene (Chivas et al., 2001), but earlier connections remain equivocal. Although the presence of emergent landmasses north of the mainland during the Late Miocene to Early Pliocene has been documented, they were not

necessarily connected to northern Australia as evidenced by the presence of a deep northern (cratonic) basin (Chivas et al., 2001). The rapid uplift that created the emergent land also corresponds to significant cratonic basin development and northern margin subsidence. Subsidence occurs throughout the entire northwest to northeast margin of Australia (Sandiford, 2007). These subsiding basins then became the depo-centres for the silici-clastic sediments eroding off the newly established emergent landmasses to the north. Therefore, although eustatic sea level was 100m lower than present during Late Miocene times, the subsidence of these basins outstripped sea level fall, in effect leaving the landmasses separated from each other via an oceanic barrier. By Middle to Late Pliocene times the cratonic basin (Gulf of Carpentaria) sedimentation rate had outpaced the subsidence and this led to the shallowing of these northern basins, which then allowed any significant sea level fall to expose the basin floor for the first time. Seismic profiling of the Gulf of Carpentaria shows an abrupt change from sedimentation to sedimentation and channel-cutting associated with the aerial exposure of the sea floor (Chivas et al., 2001). This change is believed to have occurred during the Mid to Late Pliocene when sea level fell below 100m.

Almost continuous land connection has been available since this time as evidenced by the extensive fluvial deposits and channel cutting throughout the Gulf of Carpentaria, especially during the Quaternary. Investigation of the Eustatic Sea Level Curve over the Cainozoic (using Bintanja et al., 2005; Haq et al., 1987) shows that lowered sea levels below the present day began during the Late Miocene to the present day (Fig. 7-3). By Middle Pliocene times it is likely that a fall in sea level of only 10-20m would connect the northern Australian mainland to New Guinea via Cape York Peninsula.

Therefore it is most likely that overland dispersal of non-volant rainforest vertebrates was almost continuously available for 3.6 million years, only being disconnected when interglacial conditions mirrored that of the present day. A closer inspection of the last million years of sea level change shows a near continuous connection of land between New Guinea and northern Australia between 900,000 and 400,000 years ago as even interglacials were 10-30m lower than the more recent interglacial sea level high stands (Bintanja et al., 2005). More frequent separations occurred in the last 400,000 years as interglacial sea levels increased in amplitude. Thus, over the last ~3.5 million years, land connection between New Guinea and Australia was the norm,

with separations being the exception to the rule and only becoming more frequent during the later part of the Pleistocene. Figure 7-2 diagrammatically summarises the palaeogeography of northern Australia during the mid-late Cainozoic, together with the hypothesised distribution of micro, meso- and megathermic floras during periods of sea level high and low stands.

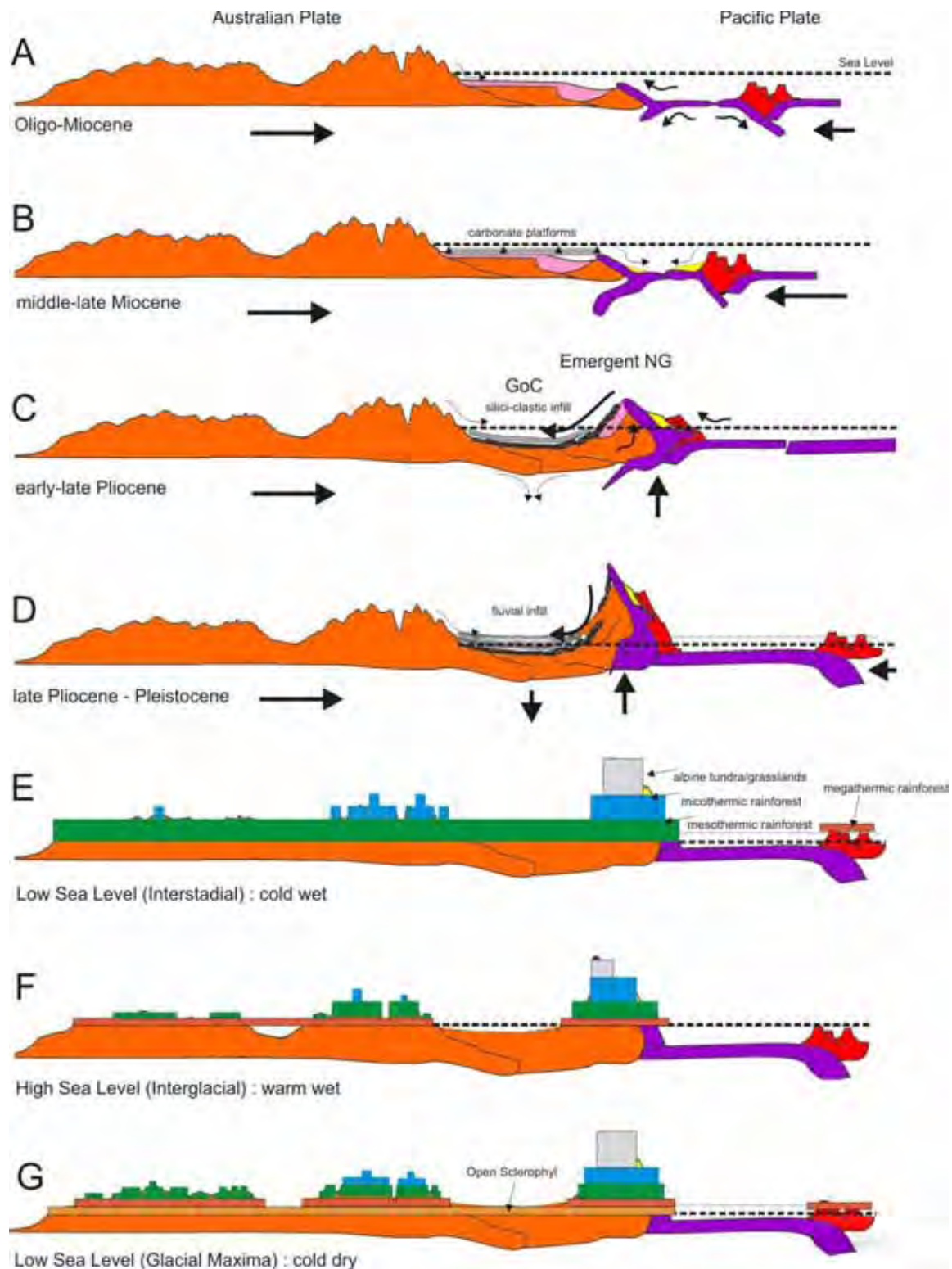


**Figure 7-2. Palaeogeographic reconstruction of the northern Australian region through the mid-late Cainozoic. A. Oligo-Miocene (convergent margins, subduction zone), B. Middle-Late Miocene, carbonate platform development, C. early-Late Pliocene, cratonic basin subsidence and silici-clastic in fill (emergent northern islands) D. Late Pliocene-Pleistocene, upthrust and basin filling (orogen fully developed), exposed basin floor during lowered sea level. E. Late Pliocene-Pleistocene during lowered Sea Level (cool and wet), F. Late Pliocene-Pleistocene during high sea level (warm and wet), G. Late Pliocene-Pleistocene during low sea level (cold and dry).**

Presented below is a series of palaeogeographic maps to illustrate the concepts discussed above.

1)



**Figure 7-3. Middle Miocene palaeogeographic map showing plate movements and the development of carbonate platforms.**



2)



**Figure 7-4. Late Miocene, showing the beginning of emergent land and cratonic basin sedimentation. Arrival of other oceanic terranes from the north.**

3)

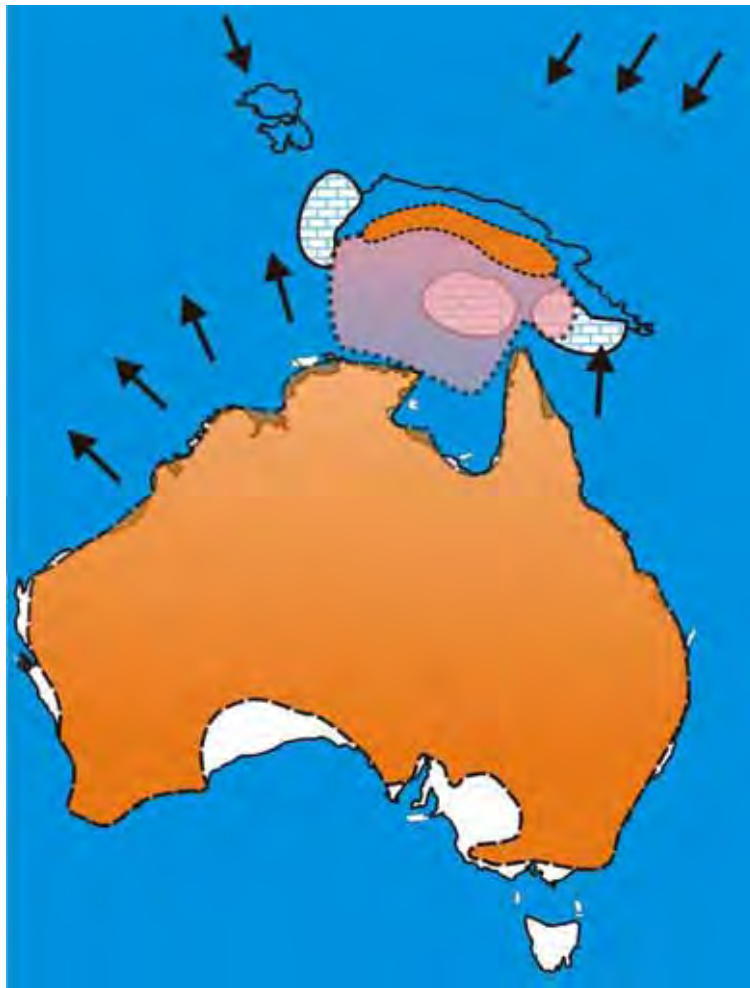


**Figure 7-5. Early Pliocene, burial of carbonate platforms and subsidence of the intracratonic basin (Gulf of Carpentaria), lateral development of carbonate platforms off Gulf of Papua.**

4)

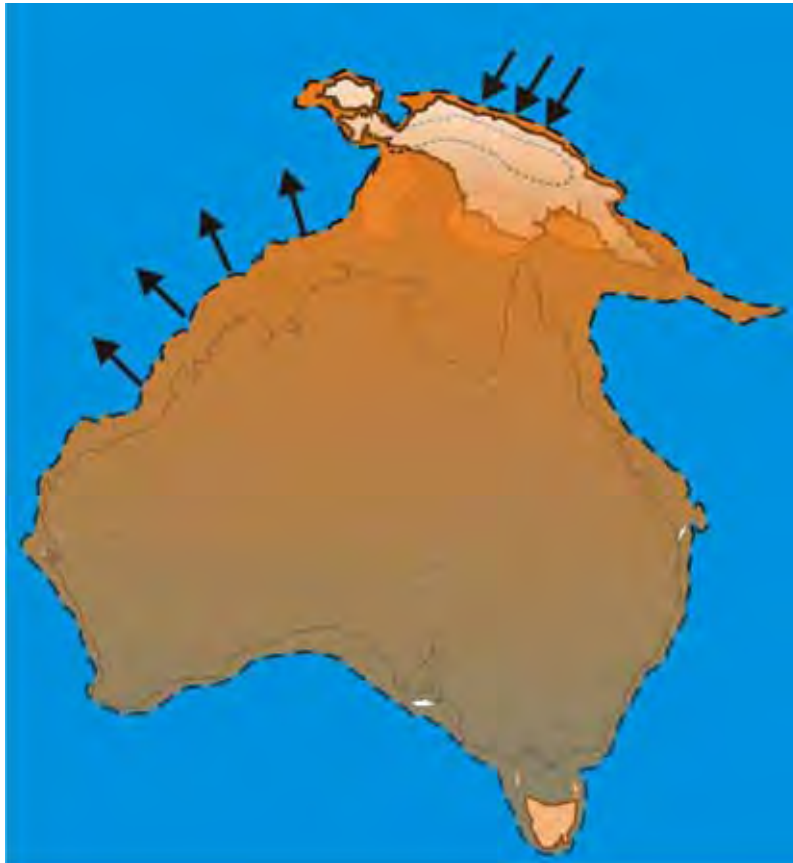


**Figure 7-6. Late Pliocene, major up thrust and basin fill, lowered sea level exposes basin, total land connection for the first time.**

5)



**Figure 7-7. Pleistocene, Last Glacial Maximum margin (100-120m) lowered sea level. Lake Carpentaria, Bass Strait Lake. Black represents the present day mesothermic rainforest archipelago.**

### Eustatic Sea-Level Change

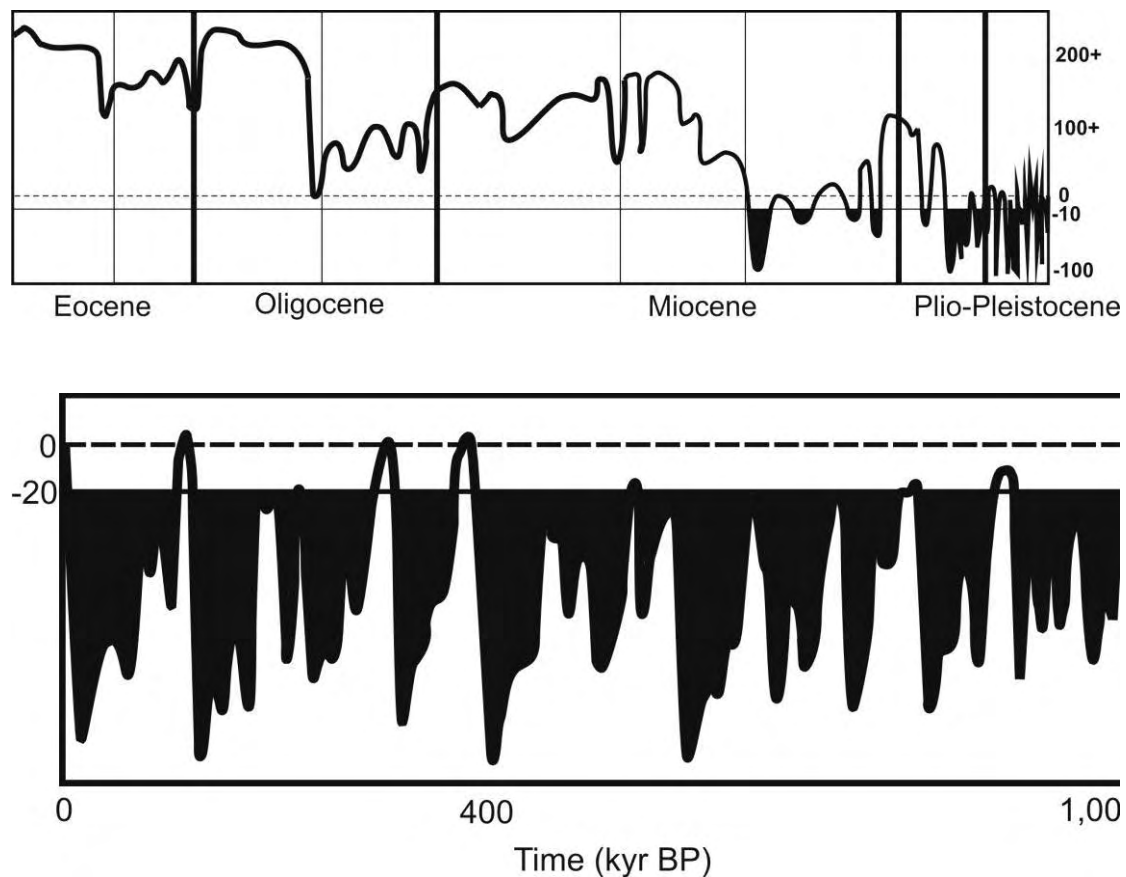


**Figure 7-8. Mid-late Cainozoic Sea Level Change from Bintanja et al (2005) and Haq et al (1987).**

## 7.6 Palaeoclimatic and rainforest floral evolution of the Australopapuan region.

The northern Australopapuan region is dominated by a summer monsoonal climate coupled with the effects of El Nino Southern Oscillation (ENSO). This climatic regime dominates the distribution of rainforest floral assemblages (Herbert et al., 2007; Kershaw et al. 2007; Moss & Kershaw, 2007; Nix 1987). The majority of Australopapua occurs in a region classified as megathermal dominant ( $>24^{\circ}\text{C}$  Mean Annual Temperatures), but there are significant areas in both New Guinea and northern Australia that persist under mesothermal ( $14\text{--}24^{\circ}\text{C}$  MAT) and microthermal climates ( $<14^{\circ}\text{C}$  MAT). These areas are restricted to high altitudes, above 800-1000m, thereby typically temperate rainforests can escape rising lowland temperatures with increased altitude. This temperature gradient significantly shapes the rainforest vertebrate communities, even though the floral assemblages remain relatively stable

taxonomically but vary physiognomically across the meso-megathermic gradient (Kanowski et al., 2001, 2003; Willams, 1997).

The combination of palaeoproxies for climate and flora, such as isotopic and palynologic records, allows for a relatively well defined chronology of events to be reconstructed throughout the late Cainozoic in this region. Recently reviewed by MacPhail (2007), the palaeoflora and climate will only be summarised here.

Late Cainozoic climates and flora are dominated by the overall trend to increasing climatic variability, intensifying aridity and higher temperatures in northern Australia (Hocknull et al., 2007). Climate and flora are dominated by three main parameters, temperature, precipitation and seasonality. All three parameters are locally influenced by global and regional changes, and all palaeoclimatic proxies can shed light on the prevailing climate of any particular time in the past.



**Figure 7-9. Middle Miocene, illustrated extent of rainforest vegetation based on records available (most-likely more extensive than this).**

Northern Australian climate during the Early to Middle Miocene is considered to have been relatively cooler than the present day with much greater rates of precipitation

and a more uniform, aseasonal climate. This is reflected in the diversity of rainforest floras recovered in on-shore and off-shore records (Fig. 7-9). The Early to Middle Miocene of northern Australia is a long period of relatively climate stability, termed the Miocene Climatic Optimum. However, by the early-Late Miocene climatic systems had changed. Although ambient temperatures in northern Australia remained relatively cool, the overall precipitation rate decreased dramatically, accompanied by the beginning of significant seasonality. The causes of this climatic change have been attributed to numerous coincidental phenomena.

1. Substantial growth of the Antarctic Ice Sheet (McGowran et al., 2000)
2. Blocking of the Indonesia Seaway (Li et al., 2006)
3. Development of the Western Pacific Warm Pool (Li et al., 2006)
4. Initiation of the dominant monsoonal climate (Macphail, 2007)
5. Beginning of ENSO activity (Li et al., 2006)

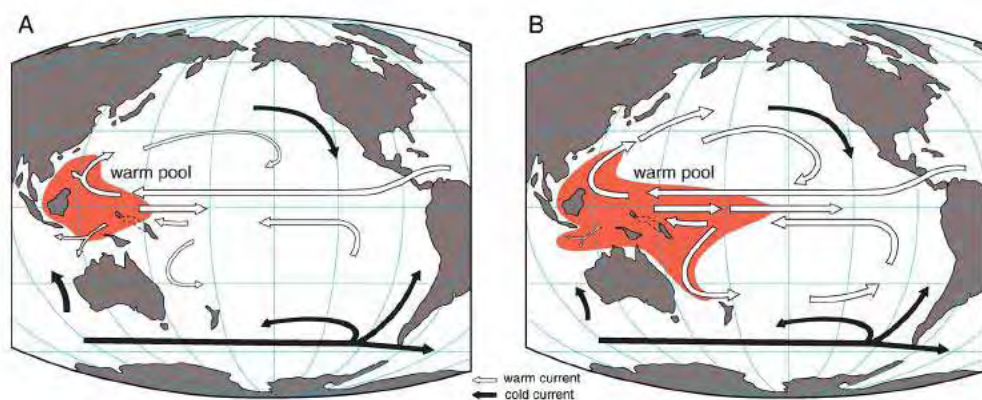


Fig. 8. Interpreted circulation pattern in the low latitude Pacific from ~10 to 8 Ma (modified from Kennett et al., 1985). (A) First warm pool began to form at ~10 Ma as a result of Indonesian seaway closure and warm surface water pileup over the far western Pacific. (B) Warm pool expansion to wider regions. White arrows = warm currents; black arrows = cold currents.

**Figure 7-10. Middle-late Miocene development of the western Pacific warm pool (From Li et al, 2006).**

Increase in the Antarctic Ice Sheet would certainly reduce the available meteoric waters available globally, however, development of monsoonal seasons and initiation of ENSO activity does not necessarily correspond to lowered precipitation in northern Australia, unless the system is dominated by El Nino-like activity. However, the development of ENSO and monsoonal activity would produce defined seasonality that may have dramatically influenced the distribution of aseasonal rainforest vegetation. El Nino activity requires the eastward extension of the Western Pacific Warm Pool via warm waters amassing along the South American western coastal margin, with a weak



equatorial current pushing warm water across to the west. El Nino activity brings drier conditions to northern and eastern Australia, and therefore the initiation of a dominant El Nino system could explain the Late Miocene climatic shift in Australia.

A potential catastrophic event could provide a mechanism for the weakening of the east-west equatorial current and the development of seasonal El Nino-like conditions. Located in the eastern equatorial Pacific is a gigantic submarine impact crater that dates to the Late Miocene. The crater has an estimated 150km diameter, making it one of the three largest meteorite craters so far found on Earth. The impact of such a massive meteor would seem to provide ample evidence for a mechanism that would stop the east-west equatorial current and allow the eastern equatorial Pacific to heat up, initiating El Nino conditions. Rainforests were severely affected during the Late Miocene climate change, retracting to eastern Australia and to small riparian sections of the Lake Eyre Basin. North-western and south-western Australian pollen records indicate intensified drying and development of sclerophyllic vegetation.

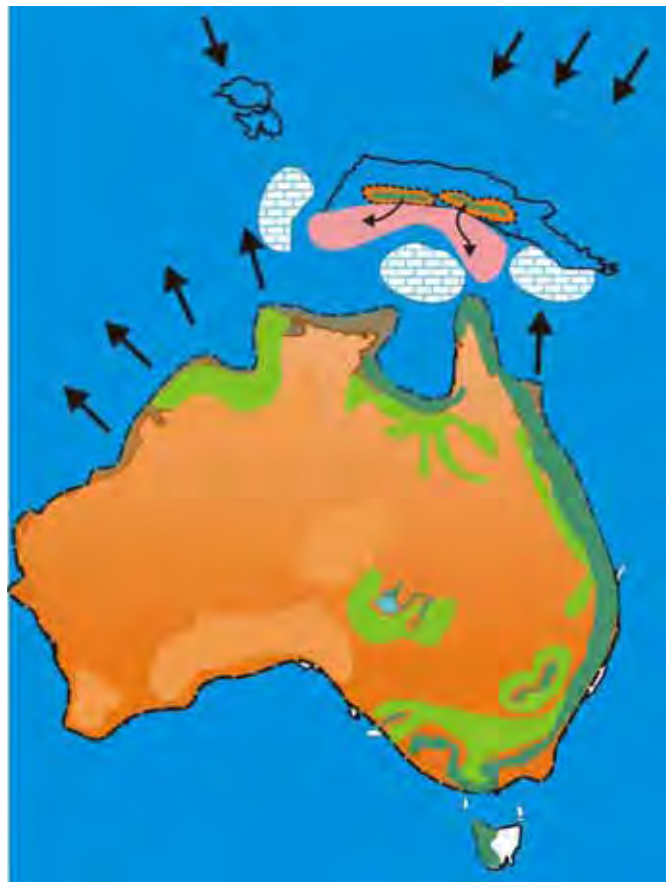


**Figure 7-11. Late Miocene vegetation, showing the reduction in western, central and northern rainforest habitats.**



Early Pliocene times saw the return of relatively wetter conditions throughout Australia, however, the prevailing seasonality continued, only allowing for small expansions of rainforest in north-eastern and south-eastern Australia (Greenwood & Christophell, 2005; Macphail, 2007). The climate in the western part of the continent remained dry, with continued development of open floral habitats. Pliocene floral records from north-eastern Queensland indicate the prevalence of rainforest gymnosperm and angiosperm floras, which are of major biogeographic significance because this was at a time when emergent landmasses had, or were, appearing off the northern edge of the continental margin (New Guinea). A possible coastal expansion of rainforest during wetter Early Pliocene times may have provided greater opportunities for diffuse dispersal over oceanic barriers to island landmasses.



**Figure 7-12. Early Pliocene vegetation, only marginal increase in rainforests during the early Pliocene. Continued aridification in the southwest and central Australia. Expansion of dry-adapted flora.**

Middle and Late Pliocene climate was much more variable than any other time in the Cainozoic as the globe entered the glacial cycles typical of the Pleistocene. The abrupt uplift of New Guinea and the almost entire closure of the Indonesian Sea Way initiated the permanent ENSO activity that dominates the modern tropical and equatorial zones. The Pliocene was thought to be a time of almost permanent El Nino conditions, even through the warm early Pliocene, although this remains controversial (Wara et al., 2005). As in the Late Miocene, the presence of a massive submarine crater (Eltanin) dated to the Late Pliocene and located off the south-western coast of South America provides a possible trigger for initiation of intensified El Nino activity. An impact in the southern Pacific may shut down the south-north current along the South American coast, thereby allowing the eastern development of the equatorial warm pool, leading to El Nino. Once again, increased temperatures of the eastern equatorial Pacific would lead to dominant El Nino conditions across Australopapua. Coincident with the newly emergent landmasses across the northern margin of Australia, the western equatorial warm pool extended east to its present position. A dominant, or permanent, El Nino climate, coupled with massive increases in continental and sea ice in Antarctic and the Arctic, dramatically impacted the climatic systems of Australopapua (Sato et al., 2008). The uplift of New Guinea also produced an additional rain shadow across mainland Australia, reconfiguring the prevailing monsoonal system from the Western Pacific Warm Pool and shifting it to the South China Sea, further reducing the viable rainfall on mainland Australia. Even so, evidence from terrestrial and ocean cores provides evidence of a relatively continuous and stable rainforest environment in north-eastern Australia (Kershaw et al., 2005; Moss & Wild, 2005).

Near-permanent land connection of New Guinea and northern Australia during the Late Pliocene and Pleistocene would have provided adequate time for rainforests to establish connections and the dispersal of taxa between the two regions. Intensifying aridity continued within western and central Australia, with sclerophyllic floras dominating inland eastern and southern Australia. Based on the palynoflora of southern Queensland (MacPhail, 2007), it is most likely that the connection between middle eastern Queensland and southern Queensland rainforests split at this time and this division continued to the present day.

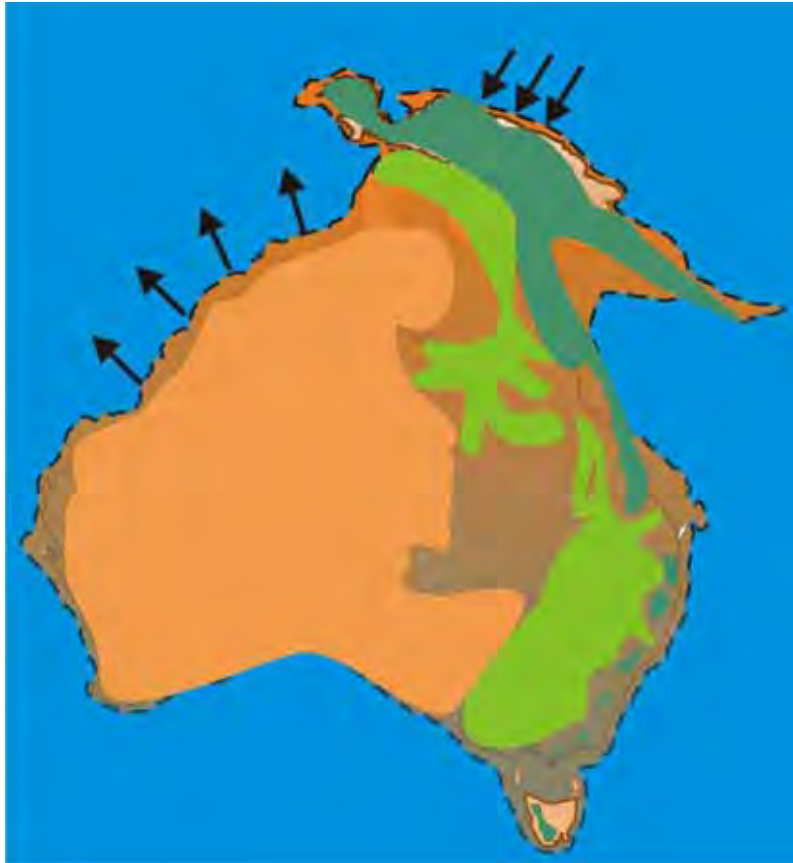


**Figure 7-13. Mid-late Pliocene vegetation. Disconnection of the southern rainforests, still relatively continuous connection of northern rainforests, allowing for southern expansion of New Guinea rainforest fauna (e.g. rainforest-obligate rodents and microhylids).**

Throughout the Quaternary intensifying aridity dominated the entire continent and caused the last divisions of north-eastern Australian rainforests, including the separation of middle eastern Queensland rainforests from those to the north. This separation probably occurred sometime after 280,000 years ago when diverse lowland rainforest faunas became extinct in central eastern Queensland (Hocknull et al., 2007). Northern Queensland rainforests remained relatively stable until approximately 240,000 years ago when climatic changes introduced major floral shifts over the last two glacial-interglacial cycles (Hocknull et al., 2007; Kershaw et al., 2007; Moss & Kershaw, 2007). During the Last Glacial Maximum (LGM) massive reductions of rainforests and intense forest fires marked the greatest retraction of rainforest so far recorded, with only very recent (~8,000 years) subsequent expansion (Herbert et al., 2007; Kershaw et al., 2007).



**Figure 7-14. Present-day mesothermic rainforest patches in northern Australia, associated with uplands ~600m +.**

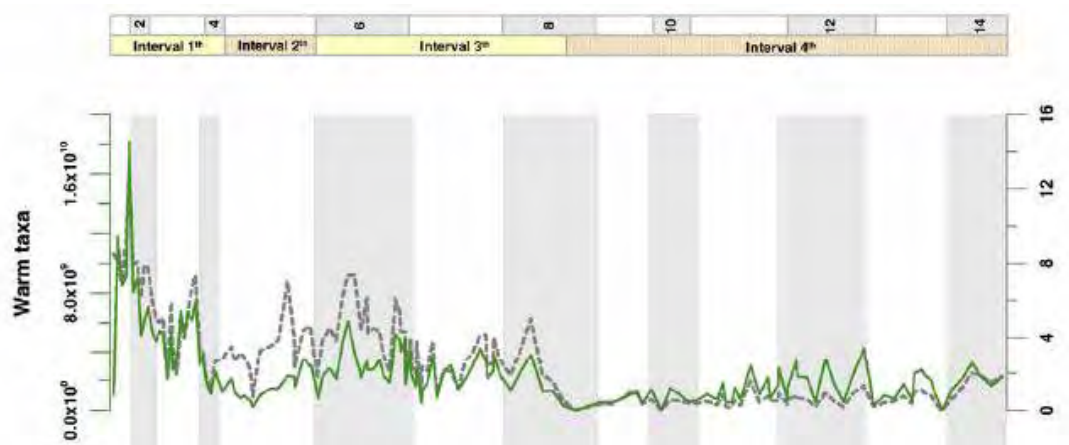


**Figure 7-15. Abundance of warm-water planktonic foraminiferans, showing dramatic increase from ~283ka. From Lopez-Otalvaro et al (2008).**

Major climatic changes across northern Australia during the Middle to Late Pleistocene are similar to those outlined above for the Late Miocene and Late Pliocene, and have been described in detail by Hocknull et al. (2007). The influence of a weakened monsoon, increasingly variable climate and impact of altered ENSO activity, especially intensified El Nino activity since ~283,000 years ago (López-Otalvaro et al., 2008; Fig 7-15), all had significant impacts on the mesothermic rainforests of north-eastern Australia. In addition to these sustained changes, there were other global and regional phenomena coincidental with these major changes. Of major interest are the impact and volcanic records in the Australasian region during the Middle Pleistocene. Approximately 800-817,000 years ago two impacts occurred, one in the south-western margin of Tasmania (Darwin Crater; Haines, 2005) and the other somewhere on the mainland of southern China or ocean floor near the South China Sea (Australasian microtektites; Glass & Koeberl, 2006). Both events caused widespread tektite ejecta across southern and central Australia, southern Asia, the Indian Ocean and western Pacific.

Shortly after these impacts a super-eruption of the Toba caldera occurred in south-eastern Asia, located to the south of one of the suspected impact sites (Glass & Koeberl, 2006). Although major faunal turnovers occurred after this time in Southern Asia these have been considered to be in response to land connections being established between south-eastern Asian continental islands with mainland Asia and the influence of immigration of mainland taxa onto these islands (Van den berg et al., 2001; Hocknull et al., in press; Chapter 5). Investigations of these turnovers may

reveal a closer association with two, possibly three, catastrophic events happening very closely in time and space. The impacts and volcanism occurred during the Middle Pleistocene Transition, a period when the Earth's orbital frequencies changed from 41ka dominant glacial-interglacial cycles to 100ka cycles. The impacts are not considered to have been drivers of these orbital changes because they preceded the impacts by ~100,000 years, however, a massive impact in the South China Sea may have caused severe alterations to the Western Pacific Warm Pool. Interestingly, SSTs ~800,000 in the equatorial Pacific were frequently high but reverted to more frequently cool periods until the mid-Brunhes event ~500-400,000 years ago when they began to rise again (Jansen et al., 1986). Global cooling has been associated with land-based meteor impacts (Haines, 2005), and therefore this lowering of SST within the equatorial region may well have been in response to the three catastrophic events recorded in the region at the time.

Cooler equatorial waters led to La Nina dominated climatic patterns, which have been recorded to be dominant in the Pacific equatorial region from 550 – 283,000 years ago; changing to dominantly El Nino conditions after 283,000 years ago (Lopez-Otálvaro et al., 2008). These cooler, La Nina conditions would be much more suitable for mesothermic rainforest providing greater precipitation to continental Australia. The pollen record in northern Queensland for this period is poorly known, with most detailed records extending back only to 250,000 years ago. Therefore, it is unknown at this stage whether or not the changes prior to the mid-Brunhes event caused major changes to the rainforest flora or fauna.

Figure 7-16 summarises the climatic changes that occurred from the Late Miocene to the present day. Climatic change impact on the distribution of mesothermic rainforests can be tracked through the palynological and faunal remains throughout this period. The dominant influences centre around the relative warming or cooling of the equatorial Pacific and ENSO activity, both La Nina dominant and El Nino dominant periods. The establishment of El Nino conditions was severely detrimental to mesothermic rainforests during the Late Miocene, Late Pliocene and Late to Middle Pleistocene. Layered upon this climatic instability were global and regional trends towards increased aridity (decreased precipitation) driven regionally by the weakening monsoons, the emerging New Guinea rain shadow and the more intense Pleistocene glacial maxima. All of these climatic changes worked against the long-term stability

of mesothermic rainforests in Australopapua, which evidently impacted on the diversity and evolutionary trajectory of most vertebrate lineages (Schneider & Williams, 2005).

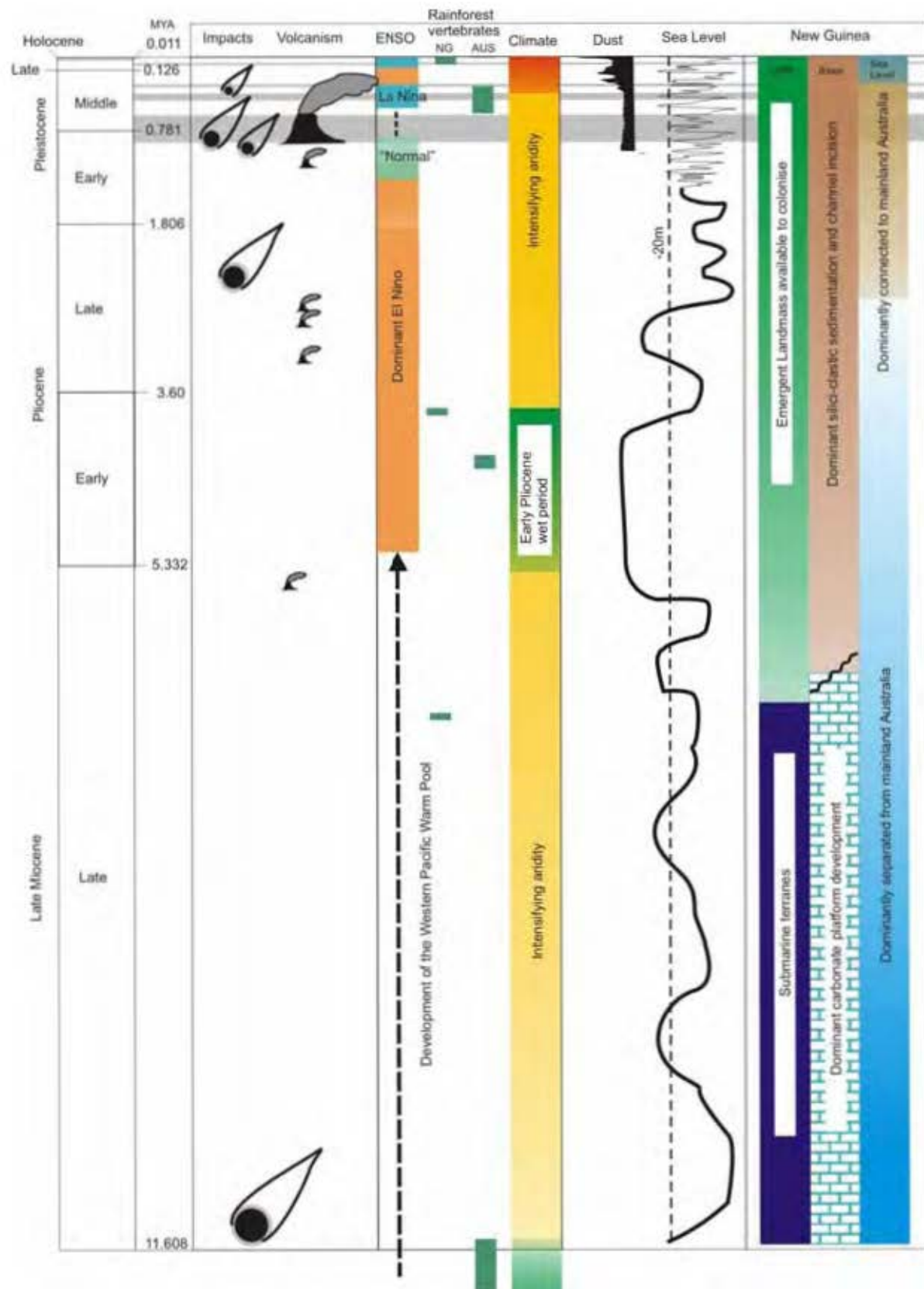


Figure 7-16. Summarised palaeogeography, palaeoclimate, sea level and impact history of the Australasian region.



## 7.7 Biochronology and evolutionary radiations of vertebrate groups during the Cainozoic.

Seven time periods have representative rainforest vertebrate faunas in the Australopapuan region as follows: 1, Late Oligocene (AUS); 2, Early Miocene (AUS); 3, Middle Miocene (AUS); 4, Early Pliocene (AUS); 5, Early to Middle Pliocene (NG); 6, Middle Pleistocene (AUS); and 7, Late Pleistocene (NG). These periods illustrate the relative influence of major faunal turnovers and the radiation of non-volant vertebrate groups within rainforests during periods of relative rainforest stability.

### 7.7.1 Frog radiations

The oldest Australian frog fossils derive from Eocene sediments in south-eastern Queensland (~55 Mya), near the township of Murgon (Tyler, 2006). This frog fauna includes the extant genera *Lechriodus*, *Limnodynastes* and *Litoria* (Tyler, 2006) and extinct taxa such as *Australobatrachus* (Tyler, 1976). This ancient origin for many of today's most speciose frog genera suggests that these groups have dominated the frog faunas for over 55 million years. Evidence from Oligo-Miocene, Pliocene and Pleistocene frog faunas supports this contention, with most fossil taxa being attributable to these same genera and the appearance of modern lineages. The current exceptions to this are *Australobatrachus* (Tyler, 1976) and *Etnabatrachus* (Hocknull, 2003), which represent two extinct genera possibly from the Hylidae. Hocknull (Chapter 4) also records a possible new genus of microhylid frog, but as noted therein this may represent a New Guinea taxon not yet available for comparison.

The endemic radiations with Gondwanan heritage in Australia include the Hylidae, Myobatrachinae and Limnodynastinae. The remaining two families currently found in Australopapua are the Microhylidae and Ranidae. Both of these families do not have a pre-Pleistocene fossil record and are thought to be arrivals from southern Asia. Until the faunal record at Mt Etna was established there was no confirmed fossil evidence of microhylids on mainland Australia (Hocknull, 2005; Hocknull et al., 2007, Chapter 4). Ranids remain elusive in the Australian mainland fossil record, and are only known from a single extant species.

The most obvious difference between the frog radiations within the Cainozoic rainforests of New Guinea and Australia are the major adaptive radiations of ranids

and microhylids that has occurred on New Guinea but not in Australia (Menzies, 2006). Although microhylids dispersed into northern Australia, along with a single species of ranid, their diversification in northern Queensland rainforests is nowhere near that in New Guinea. This suggests that microhylids and ranids have had a long period of isolated radiation on New Guinea, followed by relatively recent connections to northern Queensland whilst experiencing major dispersal filters. The likely timings of these connections are discussed below.

The Middle Pleistocene rainforest frog fauna from Mt Etna testifies to a once greater diversity of frog taxa in northern rainforest environments, with significant reductions in diversity occurring in the last 280,000 years.

### 7.7.2 *Squamate radiations*

Lizard groups with origins in Laurasia that dispersed to Australia during the Oligo-Miocene, such as the water dragons (hydrosaurines) and monitors (varanids), are characterised by monophyletic radiations from a single founding taxon. Since their arrival, radiations have occurred on mainland Australia, seemingly dominated by adaptive radiations into open and arid habitats throughout the Late Miocene to present day.

### 7.7.3 *Agamidae*

Agamid fossils are easily identified fossils and generally indicate the presence of an open, dry habitat, with the exception of the rainforest-obligate *Hypsilurus* and riparian-obligate *Physignathus* species. Agamid dental remains are relatively easy to identify to genus using features detailed by Hocknull (2002) for maxillae and dentaries. Oligo-Miocene agamid fossils represent several undescribed taxa related to the hydrosaurines (Hocknull, 2000) and indicate the arrival of riparian, water-loving dragons to mainland Australia before the Early Miocene and oceanic dispersal for the group. The Plio-Pleistocene agamid fossil record is dominated by arid-adapted taxa, suggesting their preadaptation to dry warm environments (Hocknull, 2000). Two Pleistocene records from Queensland are the only fossil records of the rainforest-obligate *Hypsilurus* species. One record is from the Late Pleistocene Russenden Cave Fauna of south-eastern Queensland, the second from the Middle Pleistocene Mt Etna Fauna (Hocknull, 2000, 2005; Hocknull et al., 2007; Chapter 4).

#### 7.7.4 *Varanidae*

Miocene records of varanids include isolated remains from northern Queensland, all of which represent relatively small lizards. These oldest records, along with the monophyly of the entire Australopapuan clade (Ast, 2001), strongly indicate a single dispersal event that brought a founding varanid taxon to Australia across an oceanic barrier from Asia. Small varanids are usually adept swimmers and could potentially survive long distance dispersal events.

As for agamids, the Plio-Pleistocene record for varanids is indicative of their adaptation and extension into the arid-zone. However, a steady increase in body size also testifies to an Australian radiation of varanids as large terrestrial carnivores, culminating in the evolution of the gigantic *Varanus priscus* during the Middle to Late Pleistocene. The presence of the *V. komodoensis* lineage in Australia since the Early Pliocene is remarkable and attests to its successful adaptive strategy. Hocknull (Chapter 5) argues for an ecological segregation of *V. komodoensis* from *V. priscus* based primarily on competitive partitioning. During the Middle and Late Pleistocene *V. komodoensis* seems to disappear from the record and is replaced by *V. priscus*. The Middle Pleistocene fossil record suggests that *V. komodoensis* had not disappeared from the ecology of Australia, it had simply occupied ecologies *V. priscus* could not, thereby possibly existing on mainland Australia well into the Pleistocene.

The presence of a diverse squamate fauna in a Middle Pleistocene rainforest, rather than drier habitat, conflicts with the notion that squamates diversified only in response to aridification. Instead, I argue that similar levels of diversification occurred in both habitats, but subsequent extinctions in closed environments, and reference typically only to the modern Australian environment, have together skewed perspective on longer-term adaptive radiations of Australian squamates.

#### 7.7.5 *Mekosuchines*

Mekosuchine crocodiles represent an endemic radiation in the southern Pacific, with Australia as a centre of radiation. Faunal transitions of crocodilian taxa during the Neogene seems to have occurred at least four times: 1, between the Middle and Late Miocene; 2, between the Late Miocene and Early Pliocene; 3, sometime during the Middle to Late Pliocene; and 4, towards the end of the Late Pleistocene.

The mekosuchines that failed to survive the Middle to Late Miocene transition are of small to medium body size (e.g. less than 2m long - *Mekosuchus* and *Trilophosuchus* species) and are both considered to have been at least partially terrestrial and possibly even arboreal (Willis, 1995). The arrival and rapid diversification of varanids, a group of terrestrial, arboreal and aquatic lizards, in Australia occurred sometime during the Middle Miocene (Archer et al., 1995b) and provided, for the first time since the Cretaceous, a terrestrial carnivorous reptile competitor for crocodylians. The mid-Late Miocene is marked by the onset of dry conditions that evidently reduced suitable habitat for smaller terrestrial mekosuchines, yet aided diversification of varanids. The large aquatic mekosuchines, such as species of *Baru*, seem to have been replaced during the Mio-Pliocene transition with their body-size equivalent, *Pallimnarchus*. The diversification of varanids continued throughout the Mio-Pliocene climatic transition and by the Early Pliocene varanids had reached *V. komodoensis* size (Hocknull, Chapter 5) whilst mekosuchines had undergone further significant extinction.

The post-Miocene occurrence of the plesiomorphic *Australosuchus* species in the Pliocene of central and eastern Australia confirm that these mekosuchines survived two climatic transitions, but does not seem to have survived into the Pleistocene. The arrival of *Crocodylus* species in Australia did not seem to alter the diversity of aquatic mekosuchines during the Pliocene, and perhaps filled an ecological niche left by a former large mekosuchine.

Fossil remains of ziphodont crocodylians are found throughout the Pleistocene of Queensland and most likely represent species of the genus *Quinkana*. *Quinkana* has been confirmed from sites in southern Queensland, notably Texas Caves, central eastern Queensland (Mt Etna) and northern Queensland (Chillagoe). Quaternary records of ziphodont crocodylians are exclusively known from cave deposits, with the exception of a possible giant *Quinkana* species from undated, presumably Pleistocene, fossil beds on the eastern Darling Downs.

Gigantism in the *Quinkana* lineage occurred during the Plio-Pleistocene, although mekosuchine diversity apparently never fully recovered. We argue that varanids were better able to adapt to the increased aridity throughout the Pleistocene, as suggested by their high diversity today in arid central and western Australia, independent

gigantism in several endemic varanid lineages (Pianka, 1995) and the Pleistocene restriction of the large-bodied *Quinkana fortirostrum* to north-eastern Australia. In the remnant rainforest palaeohabitats *Quinkana* occurs alongside small to very large terrestrial and arboreal varanids, suggesting that mekosuchines never again filled the rainforest niches they once had during the mid-Tertiary.

Extant crocodile species are confined to the coastal and inland regions of northern Australia. The majority of Pleistocene crocodylian fossils are derived from fluvial and lacustrine deposits throughout Queensland, northern New South Wales and South Australia, attesting to a massive extinction of crocodylians during the Pleistocene. Crocodylians were once an abundant component of the Pleistocene faunas of the Lake Eyre, Murray-Darling and northern Australian flood plains, but no longer occur in the Lake Eyre and Murray Darling systems. The causes of the Late Pleistocene extinction of the mekosuchines (species of *Pallimnarchus* and *Quinkana*) has yet to be resolved, but it is clear that whatever caused their demise did not seem to affect the distribution of *Crocodylus* species.

#### 7.7.6 Mammalian radiations

Figure 7-17 presents a biochronology of non-volant mammal families throughout the late Cainozoic of Australopapua, illustrating the family-level impact of major climatic changes occurring in the Late Miocene and Late Pleistocene. Although the Late Pliocene climatic changes were substantial, there does not seem to be a

correspondingly severe impact on diversity, at least at family level.

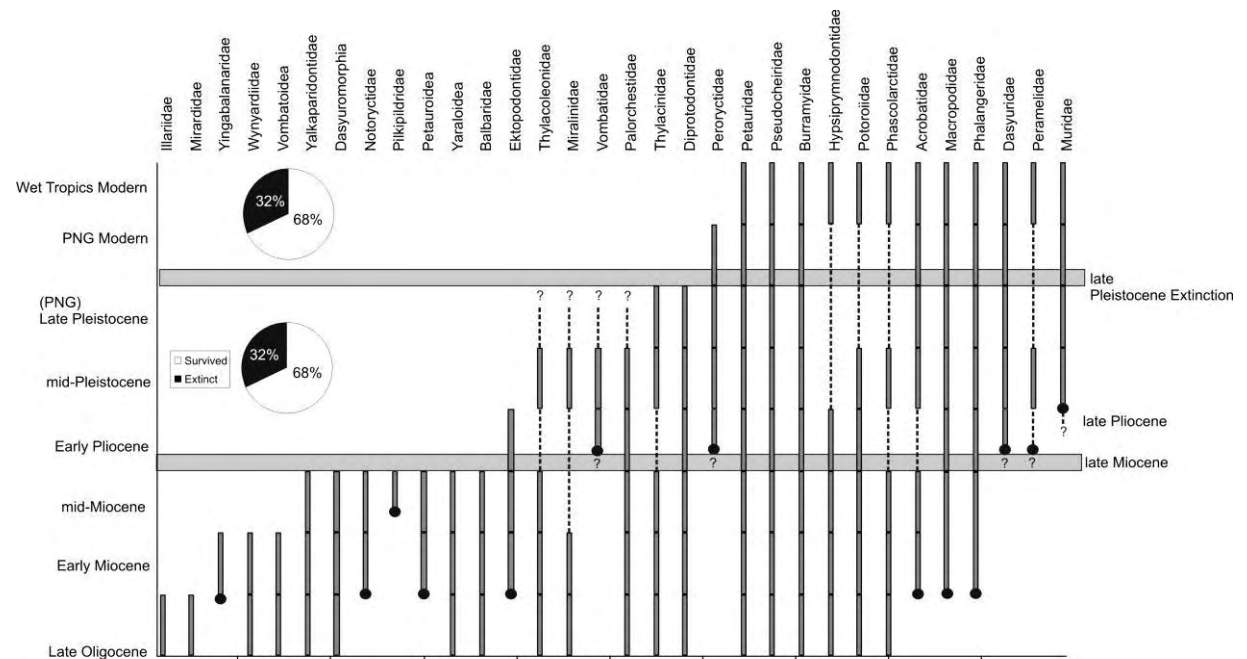


**Figure 7-17. Biochronology of non-volant marsupial families from the Late Oligocene to the present day.**

Presented below is a review of key mammalian groups represented in the Australian Neogene and their hypothesised responses to major climatic changes during the Late Miocene, Pliocene and Quaternary. To investigate these groups thoroughly I have attempted to bring together disparate information from both the fossil record and current phylogenetic/phylogeographic studies that pertain to each major group. Here I discuss the conflicts and correlations of these data and consider the overall trends throughout the Neogene, with specific attention to the Quaternary record.

#### 7.7.7 *Bandicoots*

Bandicoots are a diverse group of omnivorous and herbivorous, small to medium-sized marsupials with a continental distribution, including New Guinea and surrounding islands. The extant groups of bandicoots include open habitat xeric-adapted to closed-forest mesic-adapted taxa. The evolutionary history of peramelomorphians is long, with the oldest member possibly occurring in the Early Eocene (Archer et al., 1999). A large radiation of bandicoots, mostly (or exclusively)

members of the extinct family Yaralidae, dominate the faunas of the Oligo-Miocene (Archer et al., 1999) but they do not persist into the Neogene. Currently, no extant bandicoot lineage has a fossil record older than Early Pliocene, however, molecular evidence points to a much earlier radiation of the extant lineages, perhaps during the Early Miocene (Meredith et al., 2008). Where Early Miocene mammal-bearing deposits exist, bandicoots are diverse and relatively abundant, but they are exclusively represented by yaralids or other extinct families, so the absence of the modern lineages is an enigma.

The basal-most lineages among the extant bandicoots (*Macrotis* spp. and *Chaeropus ecaudatus*) are both adapted to xeric, open-habitats, indicating adaptive radiation of these taxa into these environments sometime in the Middle to Late Miocene. By the Pliocene, all extant lineages are represented in the fossil record, with the exception of the *Chaeropus* (pig-footed bandicoot) lineage that is only known from the Middle to Late Pleistocene. The absence of the *Chaeropus* lineage in the older fossil record may simply be due to inadequate sampling of Miocene fossil localities, especially those that represent the most arid habitats of the time (e.g. Alcoota Local Fauna and Encore Site Local Fauna). A rapid diversification post Middle Miocene and pre-Early Pliocene of the extant bandicoot lineages began with those adapted to and confined to xeric habitats today (thylacomyids and *Chaeropus*), followed by an open-arid radiation (peramelids), and then a radiation (back) into rainforests (peroryctids). Based on molecular divergence times, species-level diversification is thought to have occurred throughout the Pliocene (Meredith et al., 2008).

Quaternary bandicoot faunas in southern Australia generally reflect this, with *Perameles bouganville* and *P. gunnii* present in southern Victoria by the Early Pleistocene (Piper, 2007). Northern Australian Pleistocene bandicoot faunas indicate that species-level diversification may have continued into the Pleistocene with extinct lineages present in the Middle and Late Pleistocene (Hocknull et al., 2007; Price & Webb, 2006). New species of *Perameles* from Middle Pleistocene deposits in central eastern Queensland also show that *Perameles* diversified within closed-forest (rainforest) habitats alongside peroryctids (Hocknull, Chapter 4). These diverse rainforest bandicoots indicate that post-Miocene rainforests in eastern Australia were also species-rich, retaining this high diversity of bandicoots into the Quaternary. Sometime between 280 and 205,000 years ago these lineages became extinct in central-eastern Queensland due primarily to intensifying aridity and increased climatic

variability (Hocknull et al., 2007). Whether these same lineages persisted in Late Pleistocene rainforests further north is unknown, however, only a single bandicoot today inhabits the Wet Tropics rainforests, *Perameles nasuta*. It seems most likely that *Perameles nasuta* dispersed into rainforests in more recent times because it is a generalist rather than specialist in Wet Tropics rainforests (Winter, 1988).

Three arid-adapted southern and central Australian bandicoot species have greater palaeodistributions in the Middle and Late Pleistocene than today. Both *Chaeropus ecaudatus* and *Mactois lagotis* have been found in north-eastern Queensland Pleistocene faunas (Muirhead & Godthelp, 1995; Hocknull et al., 2007). In central-eastern Queensland *Chaeropus ecaudatus*, *Macrotis lagotis* and *Perameles bougainville* occur in a Middle Pleistocene fauna, indicating arid conditions extended eastwards across the Great Dividing Range sometime between 205 and 170,000 years ago (Hocknull et al., 2007). These arid-adapted taxa were replaced by more mesic-adapted bandicoots in the Late Pleistocene-Holocene, most likely as part of an interglacial fauna (Hocknull, Chapter 4). In south-eastern Queensland *Perameles bougainville* is part of a Late Pleistocene fauna (Price & Webb, 2006) that includes a mixture of mesic and xeric-adapted taxa, indicating a mosaic of habitats in the region at the time. These records suggest that arid-adapted bandicoots have responded to late Tertiary and Quaternary climate cycles by extending their ranges during aridification and either retracting their range or remaining in mosaic habitats during interglacials. The mesic-xeric adapted *Isodon obesulus* has widely disjunct extant populations in northern (*I. obesulus peninsulae*) and southern (*I. obesulus obesulus*) Australia. Molecular evidence suggests that these populations have not been divergent for very long and that they share a close phylogenetic relationship, and even conspecific status, with *I. auratus* in the centre and west of Australia (Pope et al., 2001). As a single species, *I. obesulus/auratus* has the widest distribution of any extant bandicoot species, being found in both xeric and mesic habitats (Fig. 7-18). Pleistocene-Holocene records of *I. obesulus* reflect this previous massive range and extend it even further with Queensland sites recording *I. obesulus* along the eastern seaboard. Central Australian distributions are extended further east with Pleistocene records of *I. auratus* at Lake Victoria (Tedford, 1994). Modern annual precipitation and mean annual temperature records for the combined range of *I. auratus* and *I. obesulus* predicts a near continent-wide distribution today



and is reflective of the modern, historical and fossil records (Fig. 7-18). It would seem, therefore, a once continental species has been impacted by major range retractions not necessarily related to climate change.

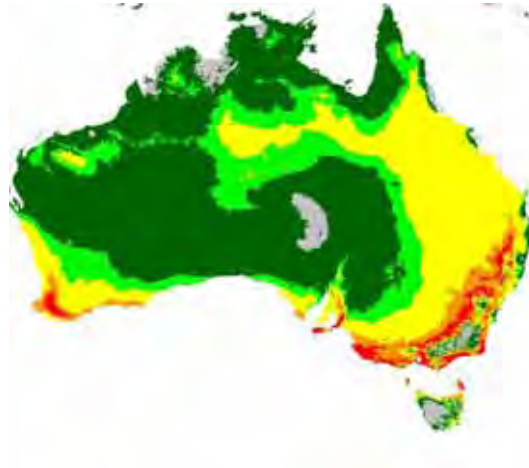


**Figure 7-18. Bioclimatic distribution prediction map for *I. obseulus* and *I. auratus* based on mean annual precipitation and mean monthly temperature.**

#### 7.7.8 *Peroryctidae*.

The early diversification of peroryctids in rainforests is evidenced by their presence in the Early Pliocene of the southern Australia Hamilton Local Fauna (Turnbull & Lundelius, 2003). Once thought to be an exclusively New Guinean group of bandicoots, peroryctids have a fossil record on mainland Australia in the Early Pliocene and Middle Pleistocene (Trunbull et al., 2003; Chapter 4), with peroryctids presumably diversifying to fill the gaps left after extinction of yaraloids in the Late Miocene turnover. Peroryctids were the only perameloid group to disperse into New Guinea, where they further speciated. The absence of *Perameles* species from New Guinea rainforest faunas is a puzzle in light of their long Australian fossil record (Early Pliocene to present) and presence in central Queensland Pleistocene rainforests. The Early Pliocene Hamilton Local Fauna of Victoria may hold some clues to this. In that fauna, only peroryctids occur, and these bear morphological features very similar to those of the Middle Pleistocene Mt Etna rainforest bandicoots. The most plesiomorphic and oldest *Perameles* fossils come from the Early Pliocene Bluff Downs and Bow Local Faunas, both interpreted as mesic palaeoecologies (Mackness & Hutchinson, 2000) but neither specifically as a rainforest environment (in the sense of mesothermic rainforest). It is hypothesised here that the ancestry of the peramelids

that diversified in Middle Pleistocene Mt Etna rainforests lay within the mesic non-rainforest habitats of the Pliocene. Dispersal of fauna from Australian mesothermic rainforests to New Guinea during the Pliocene perhaps did not include peramelids because peroryctids occupied that habitat in New Guinea. Subsequent retraction and loss of mesic rainforest habitat in Australia may have reduced peroryctid diversity facilitating the rise of another bandicoot lineage, such as *Perameles*, pre-adapted to mesic habitats but tolerant of a more variable climate. Both of Mt Etna's fossil *Perameles* species appear to be more plesiomorphic than *P. bowensis*, and corroborate the hypothesis that their ancestry lies outside mesothermic rainforests but they subsequently diversified within those habitats during the latest Pliocene or Pleistocene. This late invasion and differentiation does not seem to have been very successful or long-lasting, because neither the northern or southern Australian mesothermic rainforests, nor the New Guinean rainforests, support a plesiomorphic species of *Perameles*.

#### 7.7.9 *Dasyurids (marsupial mice, quolls)*

The oldest dasyurid fossils are Early Miocene in age (Wroe, 1999), but representatives of extant lineages are only known from Early Pliocene Australian localities (Cramb & Hocknull, 2009). This contrasts with molecular divergence dates that predict modern clades and species lineages diverged in the Miocene and Early Pliocene (Krajewski et al., 2000). The diversification of dasyurids during the end of the Miocene to Early Pliocene is more or less mirrored by bandicoots, where archaic lineages present in Oligo-Miocene times become extinct during a major faunal turnover towards the end of the Miocene and are replaced by what is essentially modern taxa by Early Pliocene times. The radiation of modern dasyurid lineages appears to be a macroevolutionary response to a drying climate during the later Miocene, with basal modern lineages diversifying within arid environments. However, Middle Pleistocene closed-forest (rainforest) vertebrate faunas include a diversity of dasyurids similar to that found in modern arid regions and in dasyuromorphian groups present in the rainforests of the Oligo-Miocene (Cramb & Hocknull, 2009). This suggests that the post-Miocene radiation of dasyurids occurred in arid and was further developed in mesic habitats and not necessarily as a unidirectional response to increasing aridity. Extinction of these mesic-adapted

dasyurids since the Middle Pleistocene has led to the modern primarily arid-adapted dasyurid fauna. Extant dasyurids restricted to rainforest habitats include *Sminthopsis leucopus* (northern population), *Antechinus adustus* and *Antechinus godmani*.

Phylogenetically *Sminthopsis leucopus* (northern population) nests high within the *Sminthopsis* radiation, suggesting that its restriction to rainforest in northern Australia is due to a recent dispersal into and isolation within northern rainforests rather than being part of a long-term refugium. The rainforest-restricted species of *Antechinus* exhibit conflicting phylogenies (molecular vs morphological), and could therefore represent either recent dispersals and isolation events within northern rainforests, or represent refugial holdouts of a basal adaptation to rainforest habitats.

The Middle Pleistocene rainforest dasyurid assemblage from Mt Etna is evidence of a highly diverse radiation of rainforest dasyurids by the Pleistocene (Cramb & Hocknull, 2009). The post-Miocene diversification of dasyurids was not solely driven by aridification, and instead this misconception appears to be an artefact of Late Pleistocene extinction of rainforest forms.

Both *Dasyurus maculatus* and *Phascogale topoatafa* have modern distributions that are currently disjunct, both having isolated populations in north-eastern Australia. Molecular evidence suggests that the *D. maculatus* population has not been isolated for very long showing minimal genetic divergence (Firestone et al., 1999), but northern and southern *Phascogale topoatafa* populations are thought to have diverged 5-8 million years ago (Krajewski et al., 2000). This may simply reflect genetic sampling, in which only Northern Territory and not Cape York populations of *P. topoatafa* were tested. Pleistocene-Holocene fossils of *D. maculatus* and *Phascogale topoatafa* have been recovered from cave sites in central eastern Queensland indicating that there were viable populations of both species where there is now a significant gap. The bioclimatic parameters of each dasyurid species cannot explain the north-south division because northern and southern Australia experience extremely different climatic regimes. Therefore the absence of these species today in central eastern Queensland is most likely not climatically related.

The largest known dasyurids are the marsupial devils (*Sarcophilus* species), with a fossil record that spans the Late Pliocene to present day. With the possible exception of *Glaucodon*, this is the only dasyurid lineage to evolve giantism relative to all other

members of the family. Molecular divergence estimates have the *Sarcophilus* lineage diverging in the Miocene, but no fossil specimens are known. Morphological change was significant during the Plio-Pleistocene as members of this lineage became very large, possibly reflecting diversification into new open habitats. By the late Quaternary *Sarcophilus* was a relatively broad-ranging taxon with a wide bioclimatic and habitat tolerance across open xeric to closed, mesic habitats.

The dasyurids have successfully diversified into most habitats and bioclimatic zones since the Miocene, in response to major climatic changes throughout the Late Miocene and Pliocene. Combined molecular and fossil evidence supports the view that dasyurids are exceptionally adaptable, having repeatedly entered and diversified within habitats left open by extinct dasyuromorphian or dasyurid occupants. The most recent radiation of medium-sized to large dasyurids (lineages of *Phascogale*, *Dasyurus* and *Sarcophilus*) seem to be most vulnerable to environmental change, whether it is the result of climatic or anthropogenic impact.

#### 7.7.10 Kangaroos

Diverse plesiomorphic kangaroo lineages characterise the pre-Late Miocene faunas of Australia, including the highly diverse and entirely extinct Oligo-Miocene balungamayine and balbarine macropodoids. Modern families of macropodoids are present in the Oligo-Miocene, including members of the Hypsiprymnodontidae, Potoroidae and Macropodidae (Archer, et al., 1999). Molecular evidence is generally congruent with the fossil record that most lineages are ancient and had diverged by the Miocene (Westerman et al., 2002). *Hypsiprymnodon* is morphologically conservative, apparently little changed from the Miocene through to the present day, low in species diversity and restricted to closed-forest environments throughout its history. Intriguingly, *Hypsiprymnodon* is not found extant or as fossils in the extensive New Guinean rainforests, nor does it have an Australian Pleistocene record even though a Pleistocene rainforest fauna is known (Hocknull et al., 2007). Having survived the major climatic upheavals of the Late Miocene and Pleistocene, it survives as a monotypic genus in small rainforest fragments in far north Queensland. Such taxonomic stability in the face of major climatic change is not reflected in the macropodids, which rapidly diversify throughout the Pliocene and are the most

specious marsupial herbivore family. By the Early Pliocene, most extant macropodid lineages are present in the Australian fossil record, having developed a unique series of ecomorphological traits that reflect their adaptation to a drying, seasonal and open environment. In particular, the dual major adaptive radiations of the sthenurine and macropodine kangaroos within new open habitats developed during the Pliocene when grasslands and xeromorphic habitat expanded rapidly.

Additionally, macropodines successfully developed arboreality and became the largest arboreal marsupials to have ever existed. These arboreal kangaroos diversified mostly in mesic habitats, but larger forms occurred in dry, open habitat and included the megafaunal form *Bohra*. One feature common amongst most of the macropodid lineages was the evolution of large body-size, whether arboreal or terrestrial, browsers, grazers or omnivores. The evolution of large body-size is considered to be a response to low-nutrient xeromorphic vegetation, which in itself is a floristic response to increasing aridity and nutrient-poor soils (Archer, 1984).

The radiation of the sthenurine and macropodine macropodids occurred during the Pliocene and Pleistocene. These kangaroos are thus two of the few marsupial groups in which genus and species-level lineages arose after the Late Miocene faunal turnover. Sthenurine kangaroos are one of the very few marsupial groups that continued to diversify up until their extinction in the Late Pleistocene. In particular, the diversification of *Procoptodon* species during the Pleistocene illustrates what is essentially an arid-adaptation of a browsing kangaroo lineage, reaching enormous size and most likely adapted to feed on xeromorphic herbage and shrubs (Prideaux, 2004). On the other hand, several macropodine lineages in the Plio-Pleistocene (e.g. *Macropus*, *Petrogale*, *Onychogalea* species) developed adaptations for grazing, as a response to the expansion of grasslands throughout Australia. These morphological adaptations include the development of hypsodont-lophodont molars and molar-row progression that enabled these macropodines to process the abrasive, phytolith-rich, grasses. However, macropodine diversification was not a unidirectional response to increasing aridity; some macropodine lineages diversified in closed and alpine habitats as browsers or browser-grazers. Forest wallabies (*Dorcopsis* and *Dorcopsulus* species), the tree kangaroos (*Dendrolagus* and *Bohra* spp) and pademelons (*Thylogale* spp) are three such groups, having diversified during the Pliocene-Pleistocene into closed-habitat environments. Giant forest wallabies (*Protemnodon* spp) show considerable divergence between New Guinea and Australian forms (Plane, 1967;

Flannery, 1992), which has led the conclusion that isolated evolution of this group occurred outside mainland Australia. However, Hocknull (Chapter 4) has identified a new species of rainforest *Protemnodon* from the Middle Pleistocene of Mt Etna which is most closely related to New Guinea *protemnodons*, demonstrating once again connectivity between rainforest faunas of northern Queensland and New Guinea. The present day distribution of the Dendrolagini, with only two extant species present in Australia, would lead to the conclusion that the major diversification occurred in isolation within the rainforests of New Guinea. Recent discoveries of Plio-Pleistocene dendrolagins paint a different picture of dendrolagin evolution in Australopapua. *Dendrolagus* and *Bohra* species occur in Australia in the Pliocene and Pleistocene, with at least one taxon of each present in the Late Pliocene and at least three or four species of each genus in the Pleistocene. Flannery & Szalay (1982) and Groves (1982) consider the short foot clade to be unique to New Guinea, but Hocknull *et al.* (2007) and Hocknull (Chapter 4) demonstrate that there has been greater connectivity between these two regions throughout the Pleistocene and potentially earlier, with the diversity of dendrolagins equivalent to that in New Guinea and several taxa sharing close morphological and phylogenetic relationships. These records come from palaeoenvironments that have rarely been sampled and it seems that the Pleistocene diversity of dendrolagins on mainland Australia has been greatly underestimated.

The small-sized forest macropodid lineage, *Thylogale*, is relatively diverse in New Guinea ranging greatly in size and including diminutive forms extinct in the Holocene (e.g. *Thylogale christenseni*). The smallest species of *Thylogale* occur in the Early Pliocene of Victoria (*T. ignis*), Middle Pleistocene of Queensland (*T. sp. nov.*) and the Holocene of New Guinea (*T. christenseni*). Considered to be the most plesiomorphic of the thylogales, this group has a long history in Pliocene to Holocene rainforests across New Guinea and Australia. The extinction of these diminutive thylogales occurred sometime in the Late Pleistocene-Holocene in Australia and the Holocene of New Guinea.

#### 7.7.11 *Burramyoidea* (Pygmy possums) *Burramys*, *Cercartetus* + other undescribed taxa

The extant pygmy possum lineages are represented by two morphologically conservative, yet distinct genera, *Burramys* and *Cercartetus*, both of which have a fossil record extending back to the Oligo-Miocene (Archer et al., 1999). Both *Burramys* and *Cercartetus* are recorded in Early Pliocene sites, but the Middle Pliocene to Middle Pleistocene fossil record for burramyids is completely lacking. Molecular divergence estimates for species of *Cercartetus* are 27-16 million years ago (Osborne & Christidis, 2002), which significantly pre-dates the Late Miocene faunal turnover. Populations of individual species within *Cercartetus*, such as the NG population of *Cercartetus caudatus* versus the mainland Australia population, are thought to have diverged 4-3 million years ago (Osborne & Christidis, 2002). This is in stark contrast to biogeographic models using palaeoclimatic modelling that propose a 7000-6500 year old dispersal of *C. caudatus* into Australia from NG via a cool wet rainforest corridor (Winter, 1997). Middle Pleistocene *Cercartetus* fossils from central eastern Queensland appear to be closely related to *C. caudatus*, indicating a much larger palaeodistribution of this lineage during the Pleistocene and possible Pleistocene differentiation.

Faunal connectivity of the Middle Pleistocene rainforest community with that of the NG rainforest communities is evidenced by the presence in the Middle Pleistocene fauna of NG derived taxa, such as the rainforest specialist murid *Pogonomys*, which is thought to have arrived in Australia during the Late Pliocene no earlier than 2.5-2 million years ago (Aplin, 2006). The Early to Middle Pliocene divergence estimate for New Guinea and Australian *C. caudatus* populations are thus in conflict with these other lines of evidence.

#### 7.7.12 *Phalangerioidea* (*Cuscuses*, *Brushtails*, *Ektopodons* and *Miralinids*)

The phalangeroids include four known families (Pilkipildridae, Phalangeridae, Miralinidae and Ektopodontidae), with only representatives of one family extant (Phalangeridae). All families are present in the Oligo-Miocene and molecular data suggests that most generic lineages had diverged between 15-25 million years ago (Ruedas & Morales, 2005). Only the pilkipildrids have a fossil record restricted to the Miocene, with ektopodontids surviving into the Early Pleistocene in southern

Australia (Piper, 2007), and miralinids into the Middle Pleistocene of northern Australia (Chapter 4). Within the phalangeroids, the phalangerids are the most diverse family across the entire late Tertiary and Quaternary, and thus it is of little surprise that they have survived to the present day.

Ektopodontids are generally low in diversity throughout the Cainozoic, having a specialised dentition and presumably specialised diet. Even so, their survival through the Late Miocene faunal turnover and increased aridity throughout the Neogene suggests that their final extinction sometime in the Early to Middle Pleistocene was not necessarily climate related. It has been suggested that their specialised diet resulted in competition with murids and this proved their demise. However, rodents have been recorded in contemporaneous deposits with ektopodontids in the Early Pleistocene (Piper, 2007) and possibly in the Middle Pliocene (Chinchilla Sands Local Fauna) (Hocknull, pers. Obs.), thus casting doubt on that scenario.

Miralinids show very little diversity with only a few species present in the Oligo-Miocene (Archer et al., 1999) and a single species in the Middle Pleistocene deposits of central eastern Queensland (Hocknull, Chapter 4). This Middle Pleistocene record illustrates yet another family of marsupials with its origins in the Tertiary and possessing a ghost lineage through to the Pleistocene. Miralinids and ektopodontids are interpreted to be sister taxa (Archer et al., 1999), and therefore their combined lineage is one of the very few to survive the Late Miocene extinction event. Interestingly, miralinids are only known in northern Australia post-Late Miocene, whilst ektopodontids are found only as far north as Chinchilla in the post-Late Miocene. This suggests that whatever dietary specialisations these two groups shared, they were subsequently driven apart during the Neogene, with one lineage restricted to Pleistocene temperate regions and the other seemingly restricted to the Pleistocene tropics.

Of the phalangerins, *Phalanger gymnotis* is considered to be a basal member of the extant genus *Phalanger*. The taxonomic placement of fossil phalangerids has undergone significant review recently, with several fossil taxa previously interpreted to be members of extant genera now placed in separate tribes with no close relationship (Crosby, 2007). The oldest fossil remains of any extant phalangerid



genera are now shared between *Wyulda* and *Trichosurus* and are from the Oligo-Miocene of northern Australia (Crosby, 2007). The presence of species of *Phalanger* and *Spilocuscus* in the Middle Pleistocene of Australia suggests that these taxa may have evolved on mainland Australia before dispersing to New Guinea. Molecular divergence of these taxa is thought to be earlier than the Late Pliocene, and hence divergence most likely occurred on mainland Australia with subsequent dispersal to New Guinea (see discussion below).

#### 7.7.13 *Petauroidea* (Ringtails and Gliders)

Gliders and ringtail possums are the most diverse of Australian arboreal herbivores, with an ancestry dating back to the Late Oligocene. The Oligo-Miocene ringtails (Pseudocheiridae) include several diverse lineages that are restricted to the Late Oligocene to Middle Miocene (Archer et al., 1999). The Late Miocene faunal turnover saw the extinction of most of these Oligo-Miocene lineages, but by Early Pliocene times all extant lineages have a fossil record, with the exception of *Pseudochirulus* and *Hemibelidius*. The evolution of these extant genera would have had to have occurred sometime between the late-Middle and Late Miocene, suggesting that the extant arboreal folivore genera diversified at a time dominated by a drying climate. Within closed-forest environments, pseudocheirids continued to diversify, producing adaptive radiations within *Pseudocheirus*, *Pseudochirulus* and *Petauroides*, as well as new genera (Hocknull, Chapter 4). The *Pseudokoala* lineage had appeared by the Early Pliocene and attained large body-size by the Early Pleistocene, continuing on into the Middle Pleistocene. By Middle Pleistocene times Australia was home to at least 5 species of *Pseudocheirus*, 3-4 species of *Petauroides*, 3-5 species of *Pseudochirulus*, 3 species of *Pseudochirops*, 2 species of *Pseudokoala* and a single species of an undescribed genus. This does not take into account the two genera without a Middle Pleistocene fossil record, *Petropseudes* and *Hemibelidius*. Including these, there are at least 22 species of pseudocheirid present during the Middle Pleistocene of Australia. This is in contrast to Australia's eight extant species, and documents a reduction of over 60% species-level diversity since the Middle Pleistocene. Such a great reduction in diversity is possibly due to the major reductions in closed-forest habitat during the last two glacial maxima and the increased seasonality of climate, which resulted in

replacement of many of the aseasonal closed-forest habitats present along the eastern seaboard by deciduous, seasonal vegetation during the Middle Pleistocene. Such a reduction in available foliage for obligate folivores may have made much of the eastern forests unviable for high diversities of pseudocheirids. Further, dietary specialisations in pseudocheirids over long periods of habitat stability has sustained significant morpho-physiological segregation in the modern dietary diversity in surviving pseudocheirid species. These historical specialisations seem to have significantly restricted the ability of surviving lineages to expand in present rainforest habitats.

The gliders (Petauridae) are a diverse group of possums with several undescribed genera from Oligo-Miocene sites (Archer et al., 1999). The extant petaurid genus, *Dactylopsila*, has been recorded in Oligo-Miocene sites at Riversleigh, northern Queensland, and *Petaurus* occurs earliest in the Early Pliocene sites of southern Victoria (Turnbull & Lundelius, 1970). Molecular evidence suggests the divergence of species of *Dactylopsila* some 10 million years ago and species of *Petaurus* as much as 6 million years ago. There is therefore reasonable congruence between the petaurid fossil record and molecular phylogenies and possible divergence dates.

#### 7.7.14 *Thylacoleonidae*

Two species of marsupial lions are known from the Pleistocene of Australia, *Thylacoleo carnifex* and *Thylacoleo hilli*. *Thylacoleo carnifex* was a ubiquitous element of all Pleistocene vertebrate faunas, whilst *Thylacoleo hilli* was restricted to two Pleistocene assemblages: the Early Pleistocene Nelson Bay Fauna and the Middle Pleistocene Mt Etna Fauna (Piper, 2007; Hocknull, 2005, Hocknull et al., 2007). Both Nelson Bay and Mt Etna faunas preserve both large and small species of *Thylacoleo*, illustrating that for some palaeoecologies of the Pleistocene two species of thylacoleonids lived in sympatry. However, for most Pleistocene vertebrate faunas only a single large thylacoleonid was present. *Thylacoleo hilli* is associated with faunas that possess diverse arboreal taxa, ranging in size from small possums to large tree kangaroos and pseudocheirids.

### 7.7.15 *Muridae*

Murids are present in the Australian fossil record by the Early Pliocene (Archer et al., 1999) and a fossil record exists for most Australian genera by the Middle to Late Pleistocene. All Quaternary murid fossils have been allocated to modern genera, although there are several new species that became extinct sometime since the Pleistocene. Most of the identifiable murid fossil taxa occurred in open habitats. The Mt Etna fossil fauna, however, represents the only fossil record of rainforest murids in Australia.. This Middle Pleistocene fauna of rainforest murids includes new species of *Melomys*, *Uromys*, *Pogonomys* and a group close to *Mesembriomys*, which suggests that there was a rapid radiation of murids into rainforest habitats sometime during the Late Pliocene to Early Pleistocene. This trend mimics the rainforest radiations evident in dasyurids, bandicoots and possums post Late Miocene fauna turnover.

## 7.8 Palaeobiogeography of Australopapuan rainforest vertebrates

Palaeodistributions can assist in the testing of phylogeographic hypotheses derived from molecular or biogeographic studies. Previous distributions of rainforest vertebrates also provide a relative indication of the degree of rainforest habitat reduction and retraction to refugial centres.

### 7.8.1 *Palaeobiogeography of rainforest frogs (Figure 7-19).*

*Lechriodus* has one of the longest fossil records of any frog genus in the world, with extinct species recorded from the Eocene, Oligo-Miocene and Middle Pleistocene (Tyler, 2007; Chapter 4). Extant *Lechriodus* species are rainforest frogs presently found in southern Queensland and New Guinea. Thus the Middle Pleistocene record of *Lechriodus* at Mt Etna, central eastern Queensland, indicates massive range retractions for this genus in the Pleistocene to the north and south.

By the Middle Pleistocene (>500ka) microhylids were diverse at Mt Etna, central eastern Queensland, suggesting that they had been established in the area for considerable time. The absence of microhylids in southern Queensland rainforests, or its fossil record, indicates that by the time microhylids had reached middle eastern

Queensland (MEQ) the connectivity of mesothermic rainforest between MEQ and southern Queensland had been severed. Microhylids have declined in their southern range since 280,000 years ago when they became locally extinct at Mt Etna. Their retraction north and isolation in mesothermic rainforest habitats reflects the impact of the last two glacial cycles on northern rainforest vertebrate distributions.

Although the hylids, myobatrachines and limnodynastines have diversified into the drier parts of the continent, the microhylids and ranids have not. Microhylids are confined to closed habitats, with many of the endemic species restricted to microtherm-mesothermic rainforests on mountain tops in the Wet Tropics (Cogger, 2000).

For example, *Cophixalus* occurs today only in restricted rainforest patches in the Wet Tropics but was once found as far south as Mt Etna. The relatively recent arrival on mainland Australia of microhylids, together with their very narrow bioclimatic tolerance, suggests that they colonised Australia during a period when mesothermic rainforests stretched from MEQ through the Wet Tropics (WT) to New Guinea (NG). This would have had to occur during a time of lowered sea level but also when temperatures were micro-mesothermic and the precipitation rate high.

Land connection between New Guinea and northern Australia during the Late Pliocene-Pleistocene was almost continuous, and dispersal of these small frogs could have occurred any time during that period. Rainforest pollen in upland and off-shore records attests to a relatively continuous presence of rainforest in northern Australia, being significantly reduced by climatic changes only in the last 280,000 years (Kershaw et al., 2003; 2005). Based on these data, microhylids probably arrived in Australia before 500,000 years ago but after ~2.4 million years during the Late Pliocene-early Pleistocene. Microhylid diversification evidently occurred within these rainforests, followed by their isolation due to rainforest retractions and elevation of mesothermic habitats from lowlands to highland isolates.

The genus *Kyarranus* also has a long fossil record, spanning at least the Oligo-Miocene to the present day (Tyler, 1991). *Kyarranus* is restricted today to well-watered areas including rainforest and wet sclerophyll forests in south-eastern Queensland and northern New South Wales. The Quaternary record of *Kyarranus* species, however, includes the Mt Etna and eastern Darling Downs faunas, illustrating a considerable southern range retraction into small pockets of wet habitat.

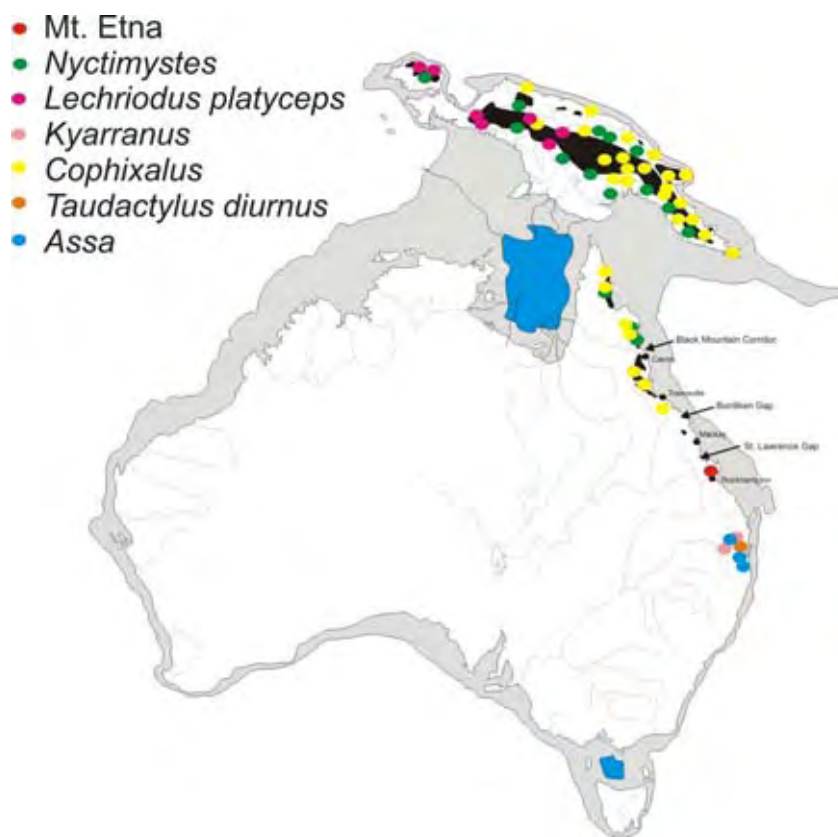


**Figure 7-19.** Palaeobiogeography of Middle Pleistocene and present day frog species.

7.8.2 Palaeobiogeography of rainforest squamates (Figure 7-20; 7-21).

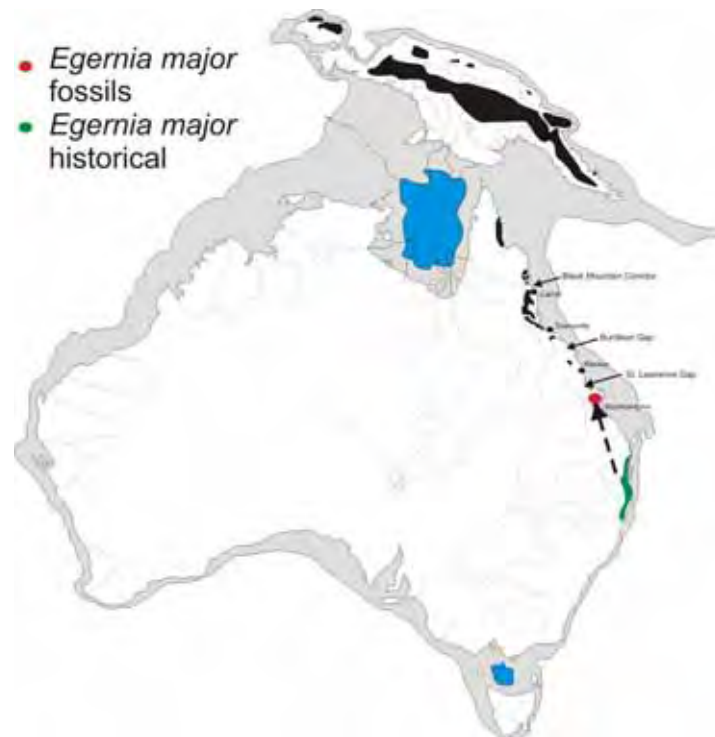


Figure 7-20. Palaeobiogeography of Middle Pleistocene and present *Egernia major*.



Figure 7-21. Palaeobiogeography of Middle Pleistocene and present day species of *Hypsilurus*.

### 7.8.3 *Agamidae*

Hocknull (2005) and Hocknull et al., (2007) record a faunal shift in agamid taxa during the Middle Pleistocene at Mt Etna, central eastern Queensland, during which species of *Hypsilurus* were replaced by those of *Amphibolurus*, *Pogona* and *Tympanocryptis*. *Hypsilurus* species now occur in rainforests in northern and southern Queensland, approximately 1000kms and 700kms to the north and south of Mt Etna respectively.

### 7.8.4 *Scincidae*

*Cyclodomorphus gerrardii* is a large extant skink associated with wet and closed forests. The Quaternary fossil record of *Cyclodomorphus gerrardii* is restricted to a few sites in eastern Australia, in particular Mt Etna, central eastern Queensland, where it is the most common skink (Hocknull, 2005). A less common new robust species of *Tiliqua* is also represented in these deposits.

### 7.8.5 *Palaeobiogeography of rainforest mammals (Figure 7-22 to 7-38).*

Presented below is a series of palaeobiogeographic maps of the Australopapuan region showing the distribution of fossil sites and extant mammal taxa with closest phylogenetic relationship to the fossil species present at Mt Etna during the Middle Pleistocene. The examples are divided into three groups: 1, taxa sharing both southern and northern distributions during the Neogene and present day; 2, taxa sharing a southern distribution during the Neogene and present day; and 3, taxa sharing a northern distribution (NG + WT).

# 1. SOUTHERN-NORTHERN TAXA

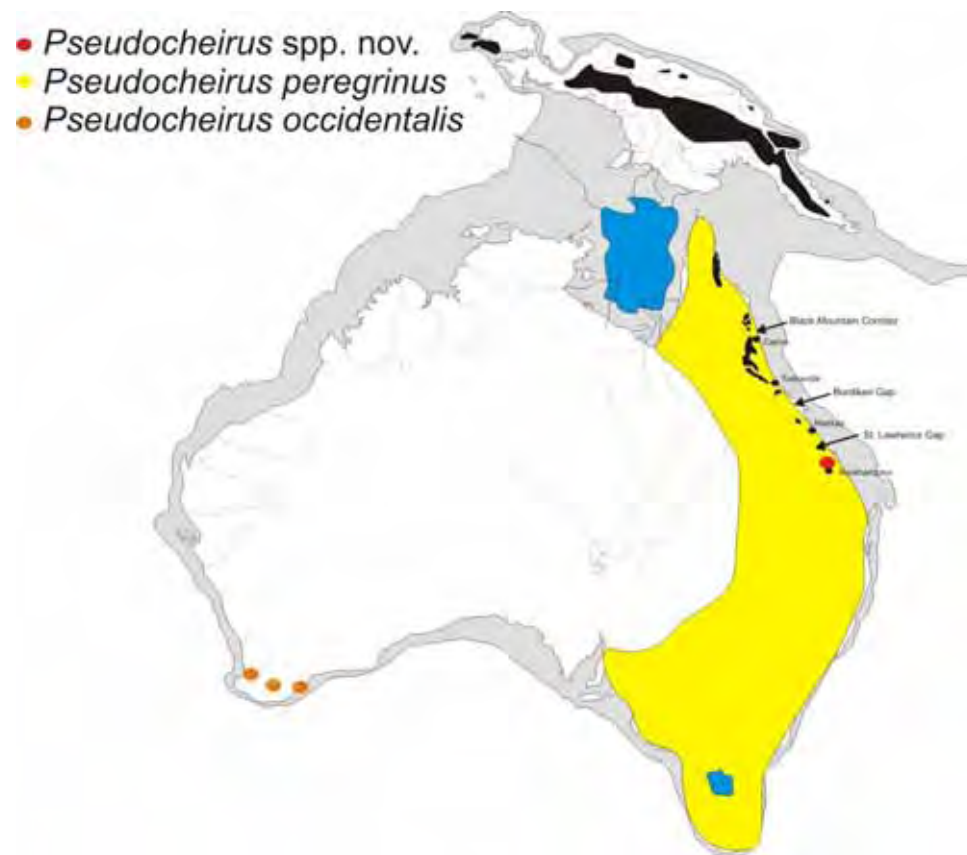


Figure 7-22. Palaeobiogeography of Middle Pleistocene and present day *Pseudocheirus*.



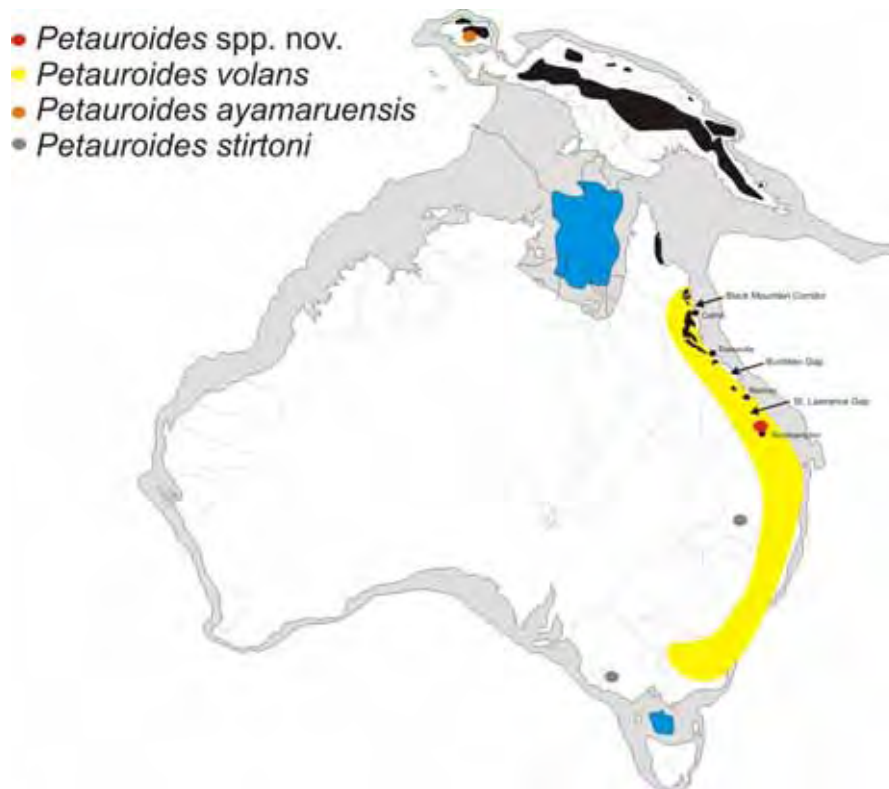


Figure 7-23. Palaeobiogeography of Early Pliocene, Middle Pleistocene, Holocene and present day *Petauroides*.

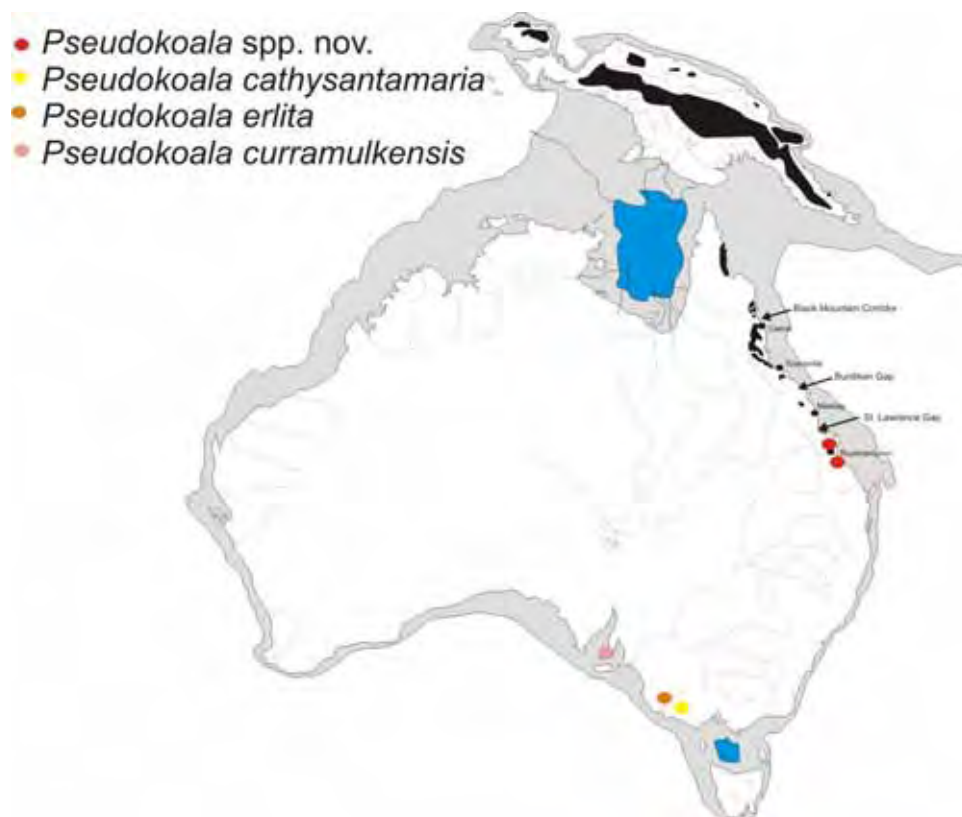


Figure 7-24. Palaeobiogeography of Mio-Pliocene, Early Pliocene, early Pleistocene and Middle Pleistocene species of *Pseudokoala*.

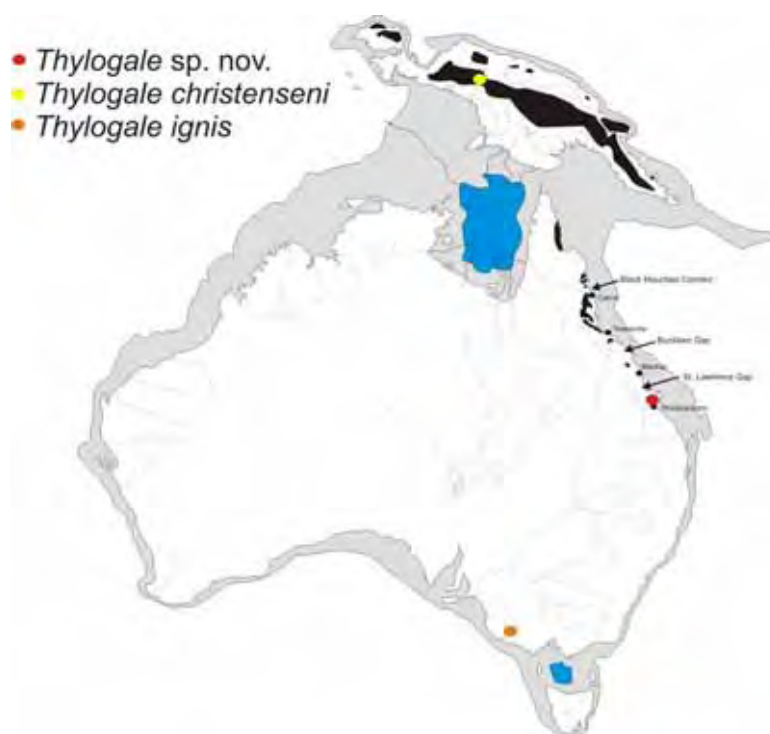


Figure 7-25. Palaeobiogeography of Early Pliocene, Middle Pleistocene, Holocene species of 'plesiomorphic' thylogale.

## 2. SOUTHERN TAXA



Figure 7-26. Palaeobiogeography of Early Pliocene, late Pliocene and Middle Pleistocene species of *Bohra*.



Figure 7-27. Palaeobiogeography of Mio-Pliocene, Early Pliocene, early Pleistocene and Middle Pleistocene *Thylacoleo hilli*.

### 3. NORTHERN TAXA

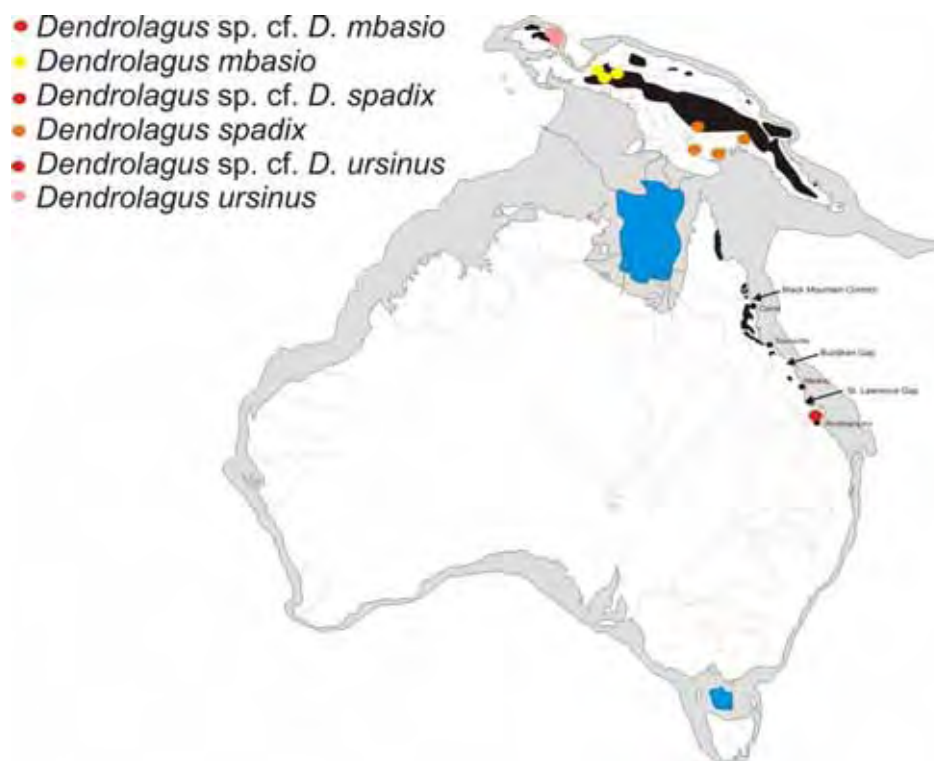


Figure 7-28. Palaeobiogeography of Middle Pleistocene and present day species of *Dendrolagus*.



Figure 7-29. Palaeobiogeography of Middle Pleistocene, Holocene and present day species of *Dactylopsila*.



Figure 7-30. Palaeobiogeography of Middle Pleistocene and present day *Micromurexia*.

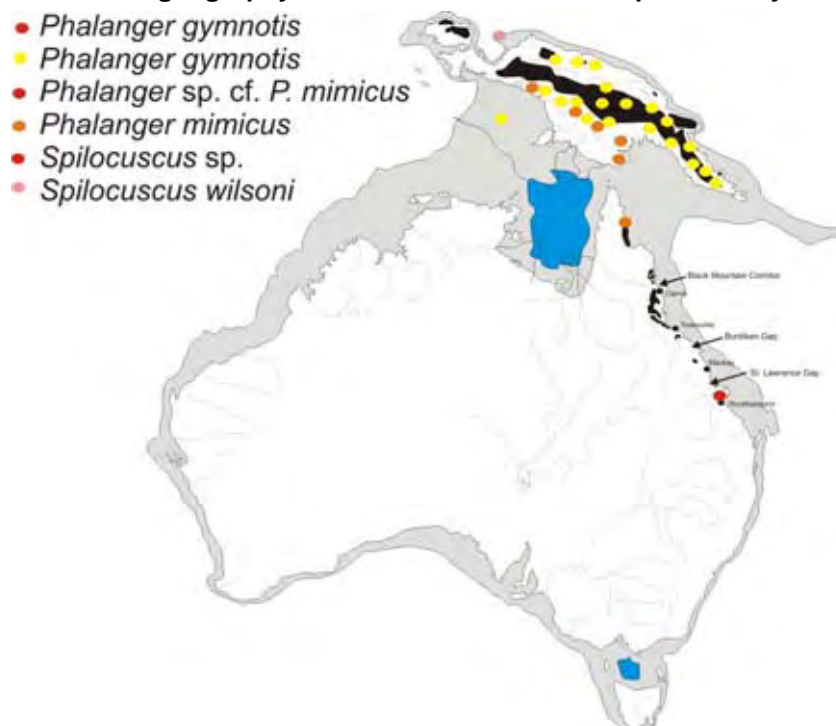


Figure 7-31. Palaeobiogeography of Middle Pleistocene and present day species of *Phalanger* and *Spilocuscus*.

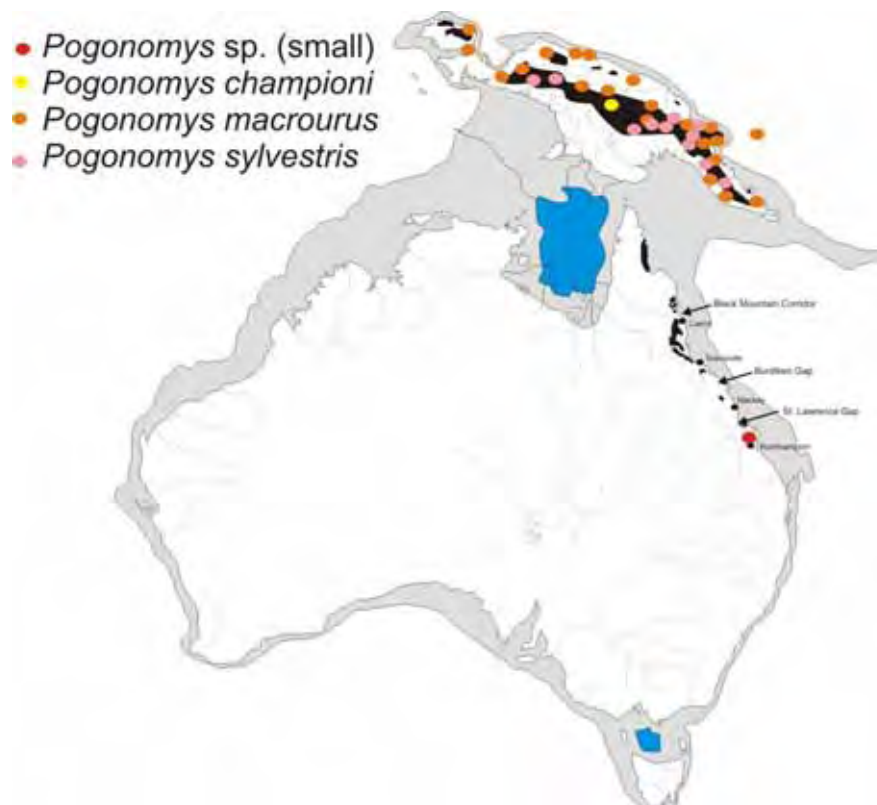


Figure 7-32. Palaeobiogeography of Middle Pleistocene and present day species of *Pogonomys*.



Figure 7-33. Palaeobiogeography of Pleistocene species of *Protemnodon*.





Figure 7-34. Palaeobiogeography of Middle Pleistocene and present day species of *Pseudochirops*.

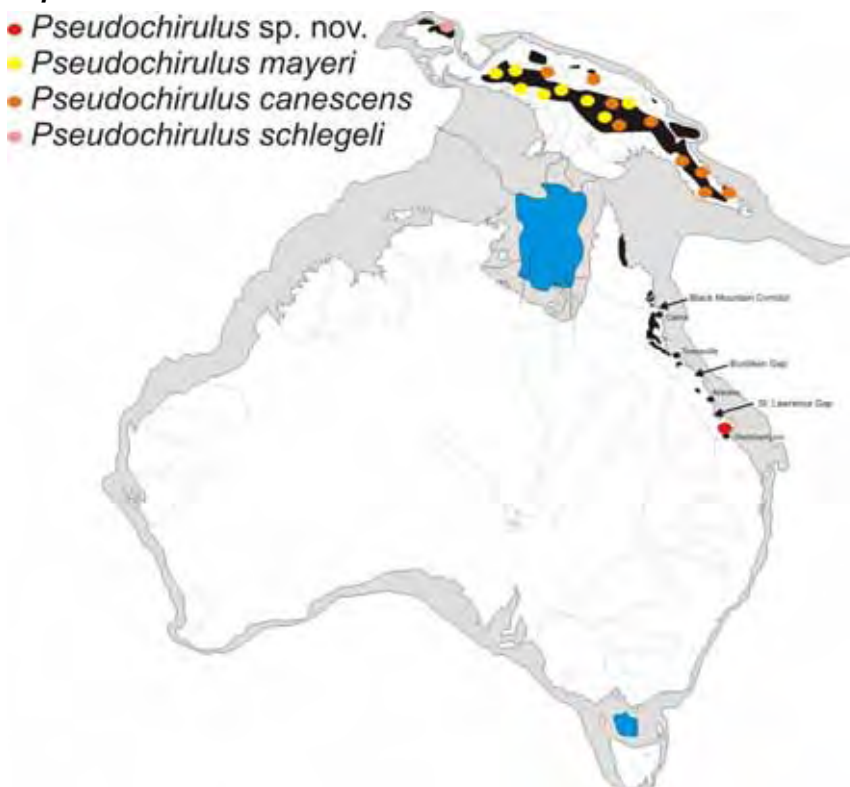


Figure 7-35. Palaeobiogeography of Middle Pleistocene and present day species of *Pseudochirulus*.

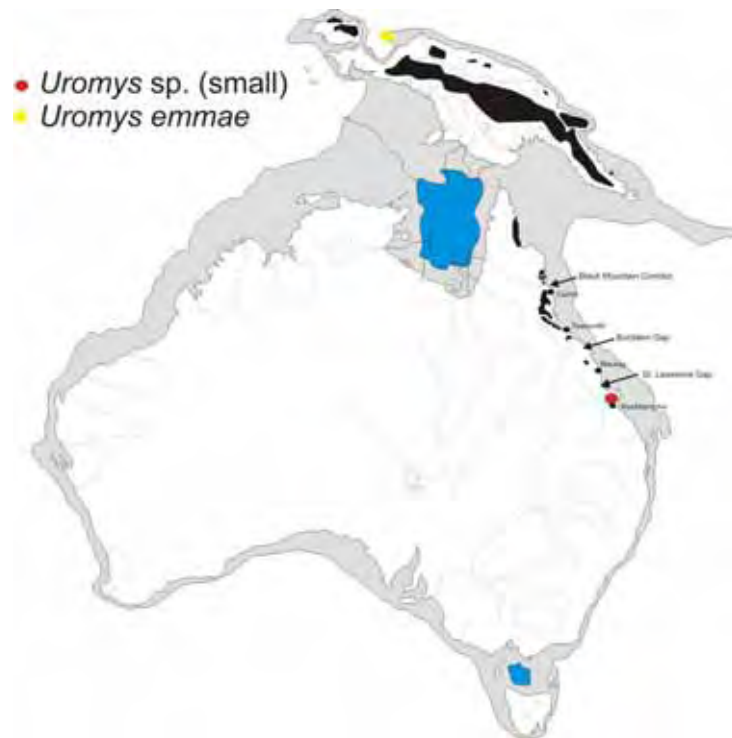


Figure 7-36. Palaeobiogeography of Middle Pleistocene and present day species of *Pseudochirulus*.



Figure 7-37. Palaeobiogeography of Middle Pleistocene and present day *Uromys hadrourus*.





**Figure 7-38. Palaeobiogeography of Middle Pleistocene and present day species of *Uromys*.**

## **7.9 New Guinean rainforest connectivity to northern Australian rainforest.**

Faunal connection between northern Australian rainforests and those of New Guinea have been proposed to have occurred in two major ways; 1, via over-water dispersal to founding islands that eventually became New Guinea; or 2, during periods of lowered sea-level when land bridges were available for terrestrial dispersal and colonisation. As presented above, palaeogeographic reconstructions over the Neogene show that over-water dispersal to off-shore islands could have occurred in the Late Miocene with the emergence of New Guinea, whilst land was almost continuously available for over land dispersal since ~2.5 million years ago in the Late Pliocene.

If over-water dispersal was the only avenue for faunal dispersal to New Guinea then fauna that successfully made it to New Guinea might be expected to be biased toward taxa better able to cross water-barriers. Alternatively, if the dominant dispersal mechanism was across land within habitat corridors, then successful fauna might simply reflect the proportion (subset) of those fauna or guilds available to disperse. Thus, fauna or guilds with the greatest representation in northern Australian

rainforests would be more likely to have founded new habitats and have proportionately higher dispersal success rate. Within those guilds, it would be expected that the most vagile taxa would more successfully colonise New Guinea than those less vagile.

I took the families of marsupials that survived the Late Miocene faunal turnover as candidates for dispersal to New Guinea. By that time, New Guinea was available to colonise via over-water dispersal (see *Palaeogeography* section). Soon after that time, in the Late Miocene to Early Pliocene, New Guinea was available to be colonised via a near permanent land-bridge (see *Palaeogeography* section). Each family was allocated guild types according to locomotion, body-size and diet; the proportional representation of each guild type was then calculated. The most representative locomotory guild type was terrestrial, comprising over 53% of all such guilds (Fig. 7-39), the most representative body-size guild was small, comprising over 30% of the body-size guilds (Fig. 7-40); and the most representative dietary guild was herbivorous, representing over 45% of dietary guilds (Fig. 7-41).

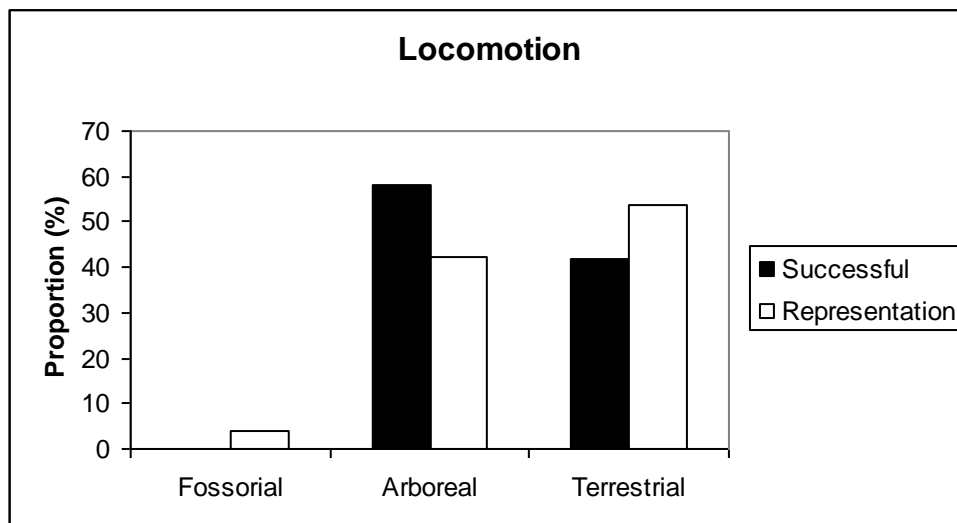


**Figure 7-39. Locomotary guilds for marsupial family dispersal to New Guinea (NG).**

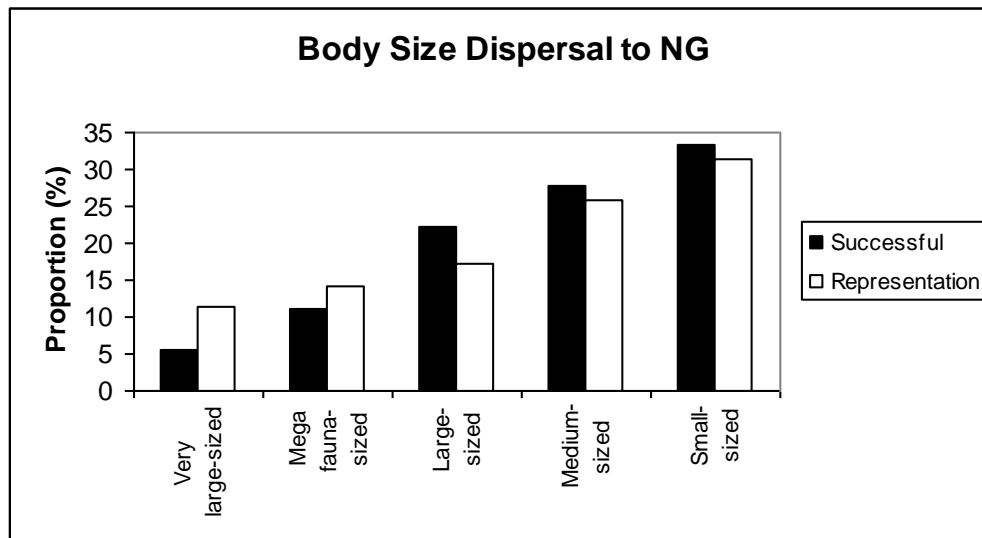


**Figure 7-40. Body-size guilds for marsupial family dispersal to NG.**

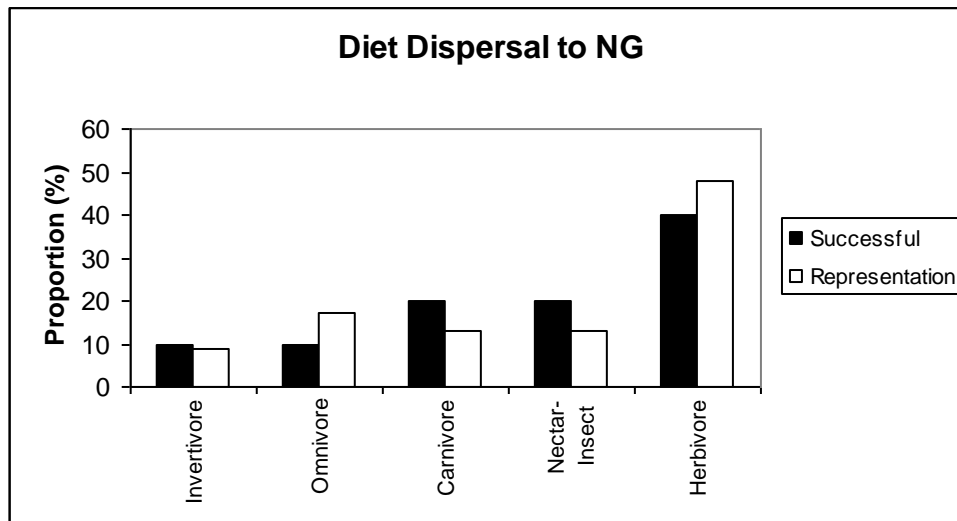


**Figure 7-41. Dietary guilds for marsupial family dispersal to NG.**

The analysis shows a positive correlation between the proportional representation within a guild and the success of that guild to disperse to New Guinea (Fig. 7-42), such that the greater representation of a guild type within a mammalian family, the more likely it is for that guild type to have dispersed to New Guinea. The overall trend observed between candidate and successful families thus simply reflects the proportional distribution of the different guilds within the candidate fauna. These data support the contention that the dominant dispersal mechanism of rainforest mammals from northern Australia to New Guinea was via land connection, not over-water dispersal.

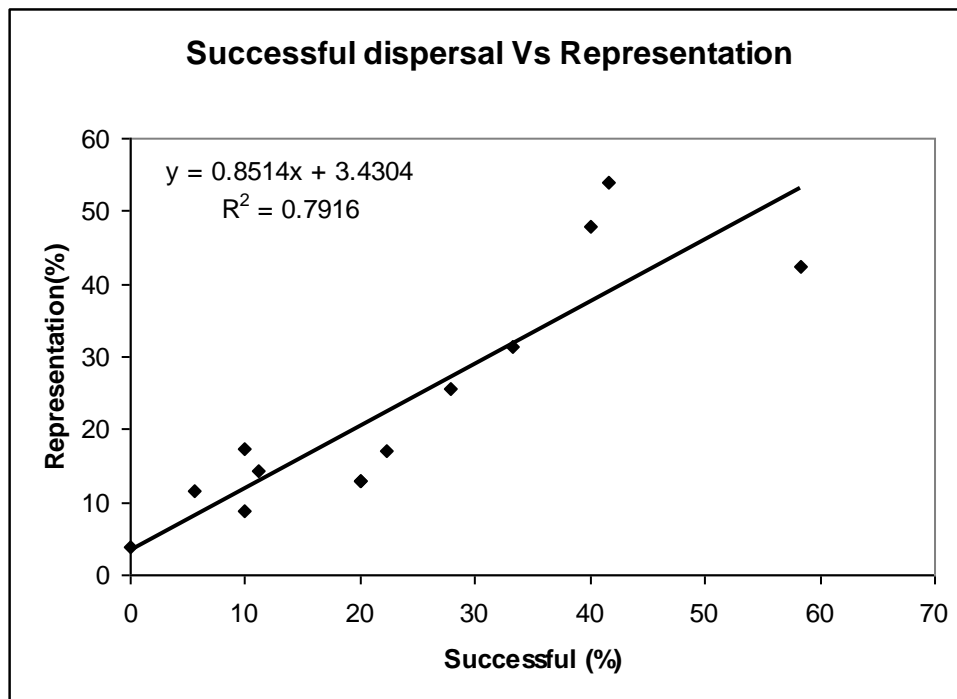


**Figure 7-42. Linear regression of Successful dispersal versus candidate representation, showing a positive relationship between candidate representation versus success in dispersing to NG.  $R^2$  value high: 0.79.**

The presence of a diprotodontid in New Guinea in the Late Miocene record (Menzies et al., 2008) may reflect an early over-water dispersal event that was successful, but terrestrial megafaunal herbivores represent a very limited component of the candidate fauna and likewise a limited component of the successfully dispersed fauna.

Therefore, although this early fossil record falsifies a 'land-bridge only' dispersal of mammalian groups to New Guinea it does not impact on the dominant role that land-bridge dispersal has played in the establishment of the New Guinea fauna.

Interestingly, the most successful dispersalists to New Guinea were arboreal mammals, in spite of this not being the most representative guild group in the candidate fauna. Arboreality it seems has assisted dispersal success to New Guinea.

Only four of the eleven candidate arboreal families evidently did not successfully disperse to New Guinea (Phascolarctidae, Ektopodontidae, Miralinidae and Tarsipedidae) although it is also possible that they may simply have not yet been found in the New Guinea fossil record.

Throughout the Early Pliocene to Early Pleistocene, ektopodontids had a mostly southern distribution, with the most northerly record occurring in southern Queensland (pers. obs.). If a viable northern Australian habitat for this family had been missing since the end of the Miocene, it would not be surprising to find that they did not disperse to New Guinea.

Miralinids occurred in northern and southern Australian rainforest faunas from Oligocene to Pleistocene times and therefore, like other arboreal possums such as pseudocheirids, phalangerids, petaurids, burramyids and acrobatids, good candidates for dispersal. However, miralinids, like ektopodontids, were dietary specialists and were perhaps adapted to particular plant species that did not establish in New Guinea. They are also rare elements in Australian Oligo-Miocene and Pleistocene deposits, and might yet be found in NG fossil deposits.

Tarsipedids do not have a fossil record older than the Pleistocene and are confined to Western Australia. Their absence from other Australian habitats is enigmatic, but it is likely that they were already restricted to the south-west of the continent during the period when New Guinea was most accessible for colonisation.

Phascolarctids pose perhaps the most interesting problem. Prior to discovery of species of *Madakoala* in the Middle Pleistocene rainforests of Mt Etna, any biogeographic analysis of phascolarctids would revolve around the dietary specialisation of the only phascolarctid lineage present post-Middle Miocene, *Phascolarctos*. Highly derived and specialists on eucalypt foliage, with a dominantly eastern and southern distribution, the absence of *Phascolarctos* species from New Guinea is easily reconciled. However, *Madakoala* species have been present in Australian rainforests, and absent from non-rainforest palaeoenvironments, since the Late Oligocene (Price & Hocknull, submitted). Why then did these koalas not disperse to New Guinea like other arboreal folivores? The fossil record in New Guinea is too poorly known to preclude the possibility that rainforest koalas did not disperse, establish and subsequently become extinct in New Guinea. However, the vagility of phascolarctids, their diets and early diversity may provide other clues. During the Oligo-Miocene, several phascolarctids lived sympatrically and appear to have specialised on a variety of different plant groups as evidenced by their dentitions (Black et al., in review), just as modern rainforest possum groups do so today. It is likely that early phascolarctids specialised on various myrtaceous vegetation within

the rainforest flora, in effect tying koala distribution to certain dietary trees. I speculate here that *Madakoala* species specialised on rainforest understory myrtaceaceous vegetation whilst *Phascolarctos* specialised on *Eucalyptus*-type myrtaceaceous vegetation, both of low vagility and together inhibiting long-distance dispersals by koalas.

## 7.10 Extinction of Neogene rainforest faunas

### 7.10.1 Late Miocene Vs Late Pleistocene extinctions.

Based on current taxonomic understanding, the proportion of families to go extinct in the Late Miocene and Late Pleistocene was equal, with 32% of families present in Middle Miocene rainforests becoming extinct by the Early Pliocene, and 32% of families present in Middle Pleistocene rainforests extinct by the present day (Fig. 7-43). The intervening periods witnessed major climatic change, with the Late Pleistocene additionally experiencing anthropogenic influences resulting from the human occupation of mainland Australia and New Guinea by 40,000 years ago (Archer et al., 1998). The pattern of climatic change that impacted the Late Miocene rainforests was similar to that of the Middle to Late Pleistocene. The development of the Western Pacific Warm Pool, which led to major ENSO activity, overall global cooling, heavily reduced precipitation and increased seasonality, were experienced in both Late Miocene and Late Pleistocene times. Late Pleistocene aridity was considerably more intense than that in the Late Miocene (McGowran et al., 2000), but the inferred response to climatic changes would be relatively similar. This being the case, faunas might be expected to respond in similar ways during both times and this should be reflected in the taxa driven extinct.

Figure 7-43 gives the breakdown of family guild types that disappeared in the Late Miocene and Late Pleistocene extinction windows. These extinctions appear to have little in common. During the Late Miocene, the body-size in extinct families was heavily biased to small-bodied taxa, whereas in the Late Pleistocene it was biased towards families of mostly large taxa. The Late Pleistocene rainforest megafaunal extinction directly corresponds to the large-bodied extinction bias experienced across all terrestrial palaeohabitats across the continent, including New Guinea and Tasmania. The Late Pleistocene extinction was also biased towards terrestrial forms,

whereas Late Miocene extinctions were shared between terrestrial and arboreal families. Late Miocene extinctions were also evenly suffered by all feeding guilds with almost equal proportions of herbivores, omnivores and carnivores going extinct. This is in sharp contrast to Late Pleistocene extinctions during which there was a very clear bias toward the extinction of herbivores.

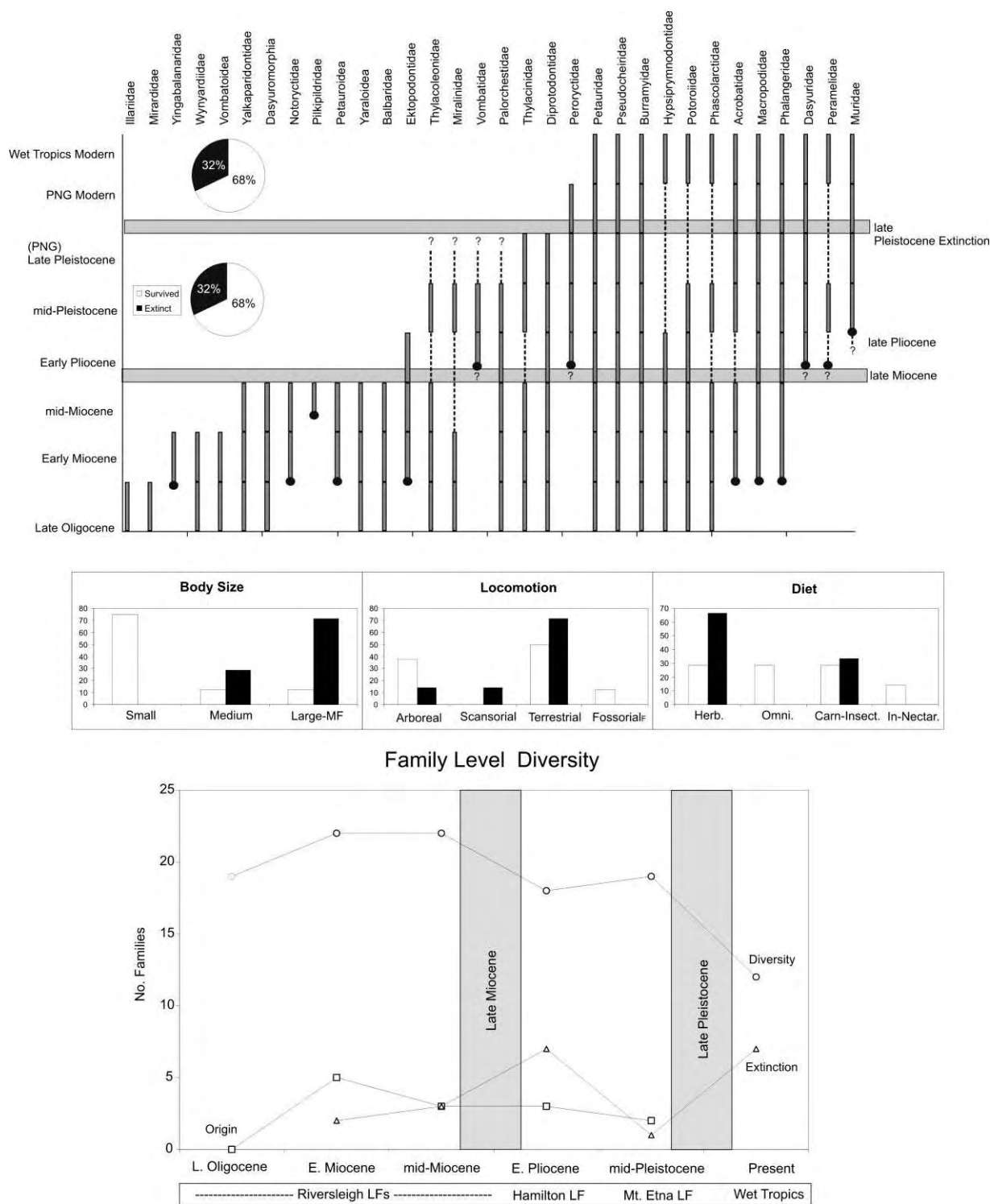


**Figure 7-43. Biochronology of non-volant marsupial families from the late Oligocene to present day, showing extinctions during the late Miocene and late Pleistocene. Extinction events broken down into guild types (body-size, locomotion and diet). Overall family-level diversity has fallen through time to the present levels with extinction peaking both during the late Miocene and late Pleistocene.**



At face value, differences between the two extinction events could be used to argue for the additive influence of humans in the extinction of particular families, such as very large and megafaunal terrestrial herbivores. However, when the origination (appearance) of new families is also considered, there appears to be a steady decline in new forms that might have replaced extinct ones. Over time, family-level diversity decreased as extinct families were not replaced, thus proportionately large-bodied forms that survived the Late Miocene extinction became better represented at the family level. Nevertheless, the large-bodied families of the Middle Miocene are the same large-bodied families that occur in the Middle Pleistocene, suggesting something different occurred during the Late Pleistocene extinction event which drove these previously resilient large-bodied families to extinction. The two main culprits appear to be related to reduced rainforest area and/or the influence of human hunting/burning.

The reduction of rainforests occurred throughout the Neogene as intensifying aridity spread across Australia. The Middle Pleistocene rainforest vertebrate record at Mt Etna suggests that lowland rainforest faunas included a complement of large-bodied taxa as well as an extraordinary diversity of small species and therefore,, at least at that time, the rainforest area must have been sufficient to sustain a broad range of vertebrate body-sizes. Fossil evidence suggests that the north-eastern Queensland rainforests were severely reduced during the Last Glacial Maximum (LGM) (Kershaw et al., 2003; 2005). Models of north-eastern Queensland rainforest area during the Late Pleistocene and Holocene show how significant these reductions may have been. The LGM model shows severe rainforest reductions in the Wet Tropics, but it does not reconstruct the potential distribution of rainforest extending onto the continental shelf that was exposed at this stage (Hilbert et al., 2007). The extension of mesothermic rainforests onto the continental shelf should be recognisable in off-shore pollen cores by a proportional increase in rainforest angiosperm taxa representing core rainforest habitat. However, off-shore pollen records consistently show the Late Pleistocene record dominated by greater coastal representation of grasslands and swamps, rather than lowland rainforest or dry rainforest gymnosperms (Moss & Kershaw, 2007). These peaks in grasses and herbs are out of phase with peaks in charcoal, and it remains unclear whether burning physically increased open areas or whether grasslands grew independently but subsequently burnt more readily. Humans

have been implicated in causing the peak in charcoal at 40,000 years ago, and perhaps also at 130,000 years ago (Kershaw et al., 2003; 2005). Either way, over the 250,000 year record, grasslands and open sclerophyll habitats, rather than rainforests, dominate the lowlands. Therefore, with any temperature and precipitation reduction during the LGM sclerophyll trees and herbs would benefit to the detriment of mesothermic rainforest expanding into the lowlands.

Lowland dominance of grasslands would effectively keep mesothermic rainforests restricted to upland areas of higher rainfall. Thus, during the LGM mesothermic rainforest would most likely be restricted to very small refugia as suggested by the modelling in Hilbert et al. (2007) with the possible modification of a proportional increase in open sclerophyll herbs. A lack of comparable mammalian diversity in modern rainforests suggests that the small size of rainforest refugia had a significant filtering process such that few taxa survived the LGM reduction in habitat area.

Living arboreal possums of the Wet Tropics mesothermic rainforests also present intriguing data that appear to reflect loss of arboreal herbivore diversity and lack of post-extinction expansion and adaptation. Pseudocheirids in particular are today relatively specialised on specific rainforest plants, and hence curiously partitioned by diet in a rainforest with relatively few arboreal herbivores. These specialisations appear to be a retention from a previous time when significantly more arboreal herbivores partitioned the rainforest environment according to body-size and diet. This probably occurred in post-Late Miocene rainforests and is corroborated by the Middle Pleistocene rainforest record of Mt Etna.

All extinctions of rainforest vertebrates raise questions regarding the most parsimonious reason/s for their ultimate demise. This is especially true for large rainforest vertebrates and in particular the iconic Komodo Dragon *Varanus komodoensis*. As presented in Chapter 5, the Komodo Dragon lineage has had a long history on mainland Australia, having first appeared in the fossil record in the Early Pliocene, already at modern body-size. Over time, the Komodo Dragon remained exceptionally constant in body-size, whether as an isolated island relict throughout the Pleistocene or in the Early Pliocene to Middle Pleistocene of continental Australia. Evidence from the fossil record of Flores and mainland Australia indicate the exceptional resilience of this lineage to major changes to its environment, surviving the Pliocene aridification of Australia and major faunal turnovers both on Flores and

central eastern Queensland. On Flores, *V. komodoensis*, survived periods of aridity, arrival and extinction of several megafauna species, volcanism and the arrival of three hominid lineages. Only in the last 2000 years has this species declined significantly on Flores, with human persecution the major driving force (Hocknull, in press (Chapter 5)).

The presence of *V. komodoensis* in Australia during the Pleistocene raises the question of why it became extinct in Australia when other large carnivorous varanid lizards continue to thrive. Its lack of specialisation as a generalist carnivore, long-term climatic resilience and disappearance on a continent many times larger than Flores arguably suggests that the Komodo Dragon was most likely driven to extinction by human activities on mainland Australia (see Chapter 5).

### **7.11 Guild decline and extinction in tropical rainforests during the Quaternary**

Taxonomic decline and extinction in tropical rainforest habitats throughout the Quaternary, as discussed above, only partially reflects the patterns of extinction in regard to ecological changes. Division of rainforest faunas into their respective guilds enables changes in diversity to be related directly to an ecological correlate, whether that is a change in dietary guild, locomotory guild or body-size. Presented below is a direct comparison between the guild diversity of mammals, lizards and frogs of the Middle Pleistocene rainforest fauna represented at Mt Etna versus the modern northern Queensland Wet Tropics rainforest fauna. Understanding past guild loss will better help predict the most vulnerable guild types to future environmental changes and focus attention on these groups in any conservation attempt.

Extinction of certain body sizes has been shown above to have affected mammals at the family-level, whereby extinction of entire megafaunal mammal families occurred during the Late Pleistocene. This is reflected at lower taxonomic levels where 100% of megafaunal guilds were driven to extinction across all groups (mammals, reptiles and frogs), demonstrating that megafaunal extinctions in Australian Pleistocene rainforests were not taxonomically biased toward mammals. Figure 7-44 shows the relative proportion of body sizes to have gone extinct in rainforests sometime in the

Late Pleistocene. The greatest proportional extinction (100%) corresponds to the least representative group (<10%). Body-size decrease corresponds to increasing representation but with reduced proportion of extinction, except for small body size. The greatest proportion of extinction was biased in the Late Pleistocene toward megafauna and small-bodied guilds, leaving medium-sized guilds relatively untouched. These data suggest that the most vulnerable taxa during the Late Pleistocene extinctions were the very large and small vertebrate taxa within the rainforests.

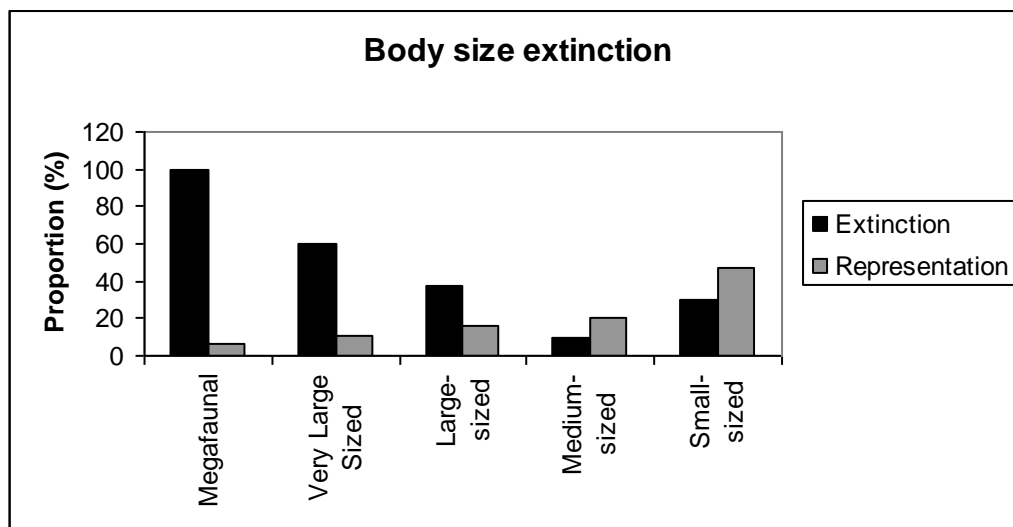


**Figure 7-44. Body-size guild extinction between the Quaternary rainforests (Mt Etna) and present day Wet Tropics rainforests (species-level).**

Extinct dietary guilds illustrate an intriguing relationship, with the greatest proportion of vertebrates to go extinct being carnivores, then herbivores and then invertivores, even though the representation of each guild showed the opposite trend (Fig. 7-45) with low and high representative guilds showing lower levels of extinction. It seems likely, therefore, that Late Pleistocene extinctions in rainforests were biased toward carnivores and herbivores over other better or less represented groups.

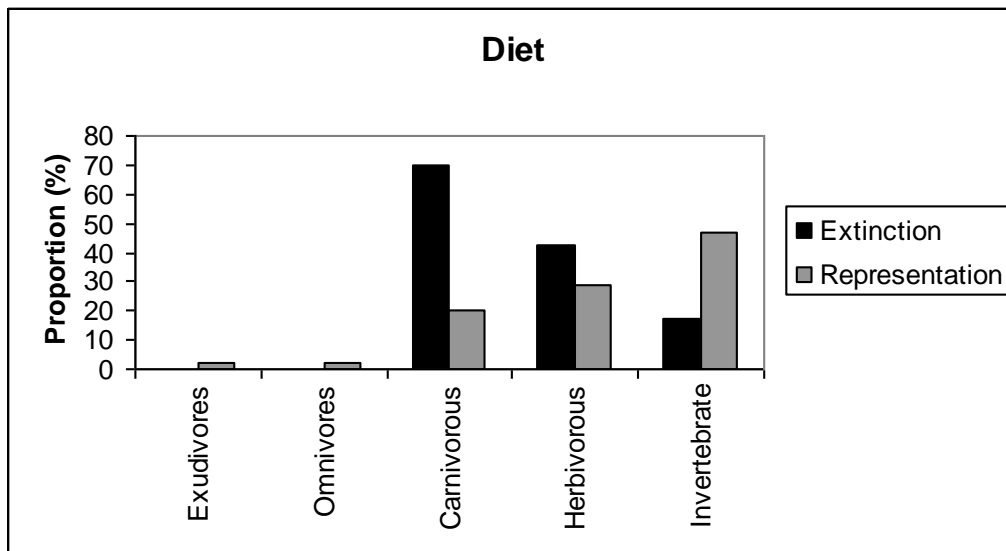


**Figure 7-45. Dietary guild extinction between the Quaternary rainforests (Mt Etna) and present day Wet Tropics rainforests (species-level).**

Locomotory adaptations showed a relatively predictable trend, where the best represented guilds were the ones to undergo the greatest extinction (Fig. 4-46). This excludes the fossorial guild, which was represented by a single taxon. Terrestrial guilds were best represented and suffered the greatest proportion of extinction.

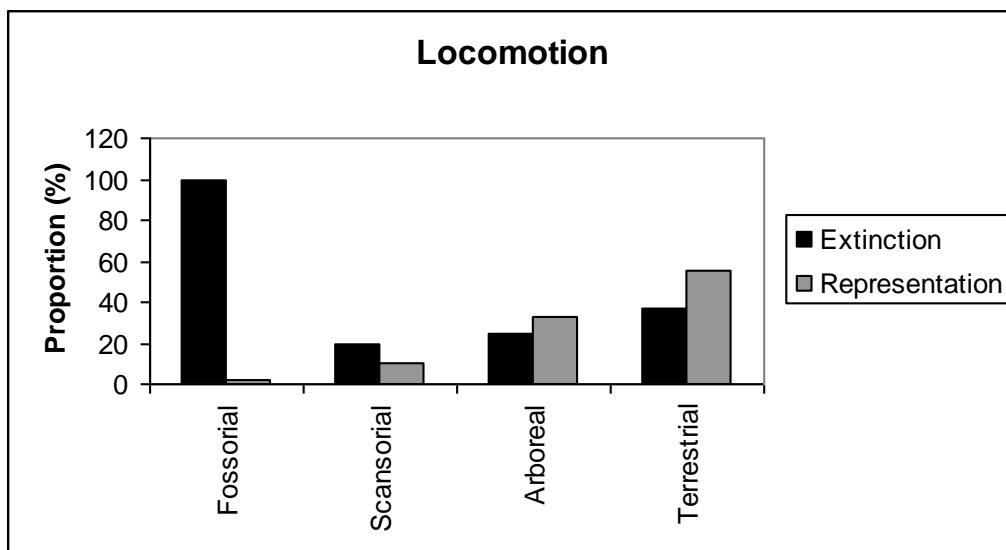


**Figure 7-46. Locomotory guild extinction between the Quaternary rainforests (Mt Etna) and present day Wet Tropics rainforests (species-level).**

### 7.11.1 Frogs

Although overall generic frog diversity in rainforests was reduced by half between Middle Pleistocene and present day, guild diversity was only reduced by 1/6, or only two of the twelve guild types (i.e. the small terrestrial (pouch-brooding) *Assa* and the medium-sized burrowing *Neobatrachus*). Assessing overall taxonomic differences is difficult due to issues in identifying fossil species *Litoria*. If *Litoria* species were reduced in both time periods as suggested in Table 7-1, a direct comparison between total frog diversity shows a reduction of 55% of species-level diversity between the Middle Pleistocene and present day. However, if species-level diversity of fossil *Litoria* is taken as currently understood, this reduction is only 23%. Therefore the presence of *Litoria* species in the present day may be significantly altering the calculated decline in diversity. There are two possibilities to explain this difference: 1, fossil diversity of *Litoria* at Mt Etna has been significantly underestimated and is much greater than four species; or 2, modern *Litoria* diversity in the Wet Tropics rainforests has increased post extinction to possibly fill vacated niches left by other Pleistocene frog taxa. Support for the second scenario comes from the greater capacity of *Litoria* species to disperse between small patches of rainforests, expanding post refugia, compared with that of less vagile frogs.

Guild	Taxa	Middle Pleistocene	Present Day Wet Tropics
1: small <30mm arboreal (hylid)	<i>Litoria</i>	Present	Present
2/5: medium- sized 25-55mm arboreal (hylid)	<i>Litoria</i> <i>Nyctimystes</i>	Present Present	Present Present
3: Large 90- 120mm arboreal hylid	<i>Litoria</i>	Present	Present
4: Medium – sized. Terrestrial	<i>Limnodynastes</i> <i>Rana</i> <i>Crinia</i> <i>Lechriodus</i>	Present Absent Present Present	Present Present Present Present
6: small <20mm microhylid	<i>Cophixalus</i> <i>Sphenophryne</i> New Genus	Present Absent Present	Present Present <b>Absent</b>
7: >20mm microhylid- myobatrachid	<i>Cophixalus</i> <i>Philoria</i> <i>Kyarranus</i>	Present Present Present	Present <b>Absent</b> <b>Absent</b>
8: Large	<i>Mixophyes</i>	Absent	Present

Terrestrial >70mm	<i>Emabatrachus</i>	Present	<b>Absent</b>
9: small terrestrial (25-30) stream	<i>Taudactylus</i>	Present	Present
10: small terrestrial (25-30) pouch	<i>Assa</i>	Present	<b>Absent</b>
11: medium- sized burrowers	<i>Neobatrachus</i>	Present	<b>Absent</b>
12: small terrestrial (congregation – grassy marsh)	<i>Pseudophryne</i> / <i>Uperoleia</i>	Present	Present

**Table 7-1. Middle Pleistocene and Present day (Wet Tropics) frog fauna and guilds.**

Hylidae	MP1	RF
<i>Litoria</i> sp. 1		
<i>Litoria</i> sp. 2		
<i>Litoria</i> sp. 3		
<i>Litoria</i> sp. 4		
<i>Litoria bicolour</i>		
<i>Litoria fallax</i>		
<i>Litoria genimaculata</i>		
<i>Litoria infraenata</i>		
<i>Litoria lesueurii</i>		
<i>Litoria lorica</i>		
<i>Litoria annotis</i>		
<i>Litoria nykalensis</i>		
<i>Litoria revelata</i>		
<i>Litoria rheocola</i>		
<i>Litoria xanthomera</i>		
<i>Nictimystes dayi</i>		
<i>Nyctimystes</i> sp. 1		
<i>Nyctimystes</i> sp. 2		
<i>Emabatrachus maximus</i>		
<b>Myobatrachidae</b>		
<i>Crinia</i> sp. (spp. = 1)		
<i>Kyarranus</i> sp. 1		
<i>Kyarranus</i> sp. 2		
<i>Limnodynastes</i> sp. 1		
<i>Limnodynastes</i> sp. 2		
<i>Limnodynastes</i> sp. 3		
<i>Limnodynastes tasmaniensis</i> sp. Group		
<i>Limnodynastes spenceri</i> sp. Group		
<i>Limnodynastes peronii</i>		
<i>Lechrionus</i> sp. cf. <i>L. platyceps</i>		
<i>Neobatrachus</i> sp. 1		

<i>Mixophyes schevilli</i>		
<i>Assa</i> sp. (spp. = 1)		
<i>Pseudophyrne</i> sp. (spp. =1)		
<i>Philoria</i> sp. (spp.= 1)		
<i>Taudactylus</i> sp. cf. <i>T. diurnus</i>		
<i>Taudactylus acutirostris</i>		
<i>Taudactylus rheophilus</i>		
<i>Uperoleia</i> sp. (spp. = 1)		
Microhylidae		
cf. <i>Hylophorbus</i>		
<i>Cophixalus</i> spp. (spp. = 1)		
<i>Sphenopryne</i> spp. (spp. = 1)		
New Genus (spp = 1)		
Ranidae		
<i>Rana daeneli</i>		
Total taxonomic richness	26	20
Total taxonomic richness		
( <i>Litoria</i> spp. = 1)	22	10
Total Generic Richness	16	8
Family Richness	3	4

**Table 7-2. Middle Pleistocene and Present day (Wet Tropics) frog fauna.**

### 7.11.2 Reptiles

Of the reptiles the only guild missing from present day rainforests that was present in Middle Pleistocene rainforests is the very large terrestrial ectotherm guild (Table 7-3). This was made up of three distinctive taxa: the terrestrial crocodile *Quinkana*; the large madtsoiid snake *Yurlunggur*; and the giant varanid *Varanus komodoensis*. Overall reptilian taxonomic diversity decreased, with the extinction of two families (Madtsoiidae and Mekosuchinae).

Guild	Taxa	Middle Pleistocene	Present Day Wet Tropics
1: small terrestrial/arboreal arthropod	All small skinks and geckoes	Present	Present
2: medium terrestrial arthropods	<i>Egernia</i>	Present	Present
3: medium terrestrial mollusc	<i>Tiliqua</i> <i>Cyclodomorphus</i>	Present Present	Present Present
4: medium arboreal arthropod	<i>Hypsilurus</i>	Present	Present
5: large terrestrial	<i>Varanus</i>	Present	Present



vertebrate	Large elapids	Present	Present
6: large-very large arboreal vertebrate	Pythonine snakes	Present	Present
7: very large terrestrial vertebrate	<i>Quinkana</i>	Present	<b>Absent</b>
	<i>Varanus</i>	Present	<b>Absent</b>
	<i>komodoensis</i>		
	<i>Yurlunggur</i>	Present	<b>Absent</b>
8: very small fossorial arthropods	Typhlopidae	Present	Present

**Table 7-3. Middle Pleistocene and Present day (Wet Tropics) reptile fauna and guilds.**

Reptiles	MP1	RF
<i>Hypsilurus</i> sp. (spp. =1)		
<i>Hypsilurus boydii</i>		
<i>Tiliqua scincoides</i>		
<i>Cyclodomorphus gerrardii</i>		
<i>Tiliqua</i> sp. nov.		
<i>Egernia major</i>		
<i>Egernia</i> sp. (spp. = 1)		
<i>Sphenomorphus</i> group robust (spp. = 1)		
<i>Sphenomorphus</i> group gracile (spp. = 1)		
<i>Varanus</i> sp. (spp. = 1)		
<i>Varanus</i> cf. <i>V. komodoensis</i>		
Gekkonidae (spp. = 1)		
elapid small (spp. = 1)		
elapid large (spp. = 1)		
pythonine small (spp. = 1)		
pythonine large (spp. = 1)		
<i>Yurlunggur</i> sp.		
Typhlopidae (spp. = 1)		
<i>Rheodactyles</i> sp.		
Chelid (spp. = 1)		
<i>Quinkana</i> sp.		
Total Taxonomic Richness	19	13
Generic Level Richness	15	12
Family Level Richness	10	8

**Table 7-4. Middle Pleistocene and Present day (Wet Tropics) reptile fauna.**

### 7.11.3 Endo-Ectotherm Carnivore Guilds

All endothermic obligate-carnivore guilds are absent from present day rainforests following post-Middle Pleistocene extinction of the large to megafaunal endothermic and ectothermic carnivores (Table 7-5). *Dasyurus maculatus* is the only remaining endotherm that is primarily carnivorous. The loss of all large to megafaunal carnivores corresponds to the entire loss of very large scansorial and terrestrial herbivores from present day rainforests. The largest arboreal Australian rainforest herbivores are now two arboreal tree-kangaroos and a very large forest kangaroo (e.g. *Wallabia*).

Carnivores	MP1	RF	Size	Body Temp	Habit
<i>Thylacoleo</i> sp. (Large)			MF	Endo	T
<i>Thylacoleo hilli</i>			L	Endo	S
<i>Thylacinus cyanocephalus</i>			VL	Endo	T
<i>Varanus</i> sp.			L	Ecto	A
<i>Varanus</i> cf. <i>V. komodoensis</i>			VL	Ecto	T
elapid small			M	Ecto	T
elapid large			L	Ecto	T
pythonine small			M	Ecto	A
pythonine large			L	Ecto	A
<i>Yurlunggur</i>			VL	Ecto	T
<i>Quinkana</i> sp.			MF	Ecto	T
<i>Sarcophilus lanianus</i>			L	Endo	T

**Table 7-5. Middle Pleistocene and Present day (Wet Tropics) carnivore fauna and guilds.**

Carnivore Guilds	MP RF	PD RF
MFENT	1	*
MFECT	1	*
VLENT	1	*
VLECT	2	*
LENS	1	*
LENT	1	*
LECA	2	2
LECT	1	*
MECT	1	1
MECA	1	1
Total Taxa	12	4

Total Guilds	10	3
Guild Loss		7

**Table 7-6. Middle Pleistocene and Present day (Wet Tropics) carnivore guilds.**

#### 7.11.4 Endothermic Herbivore Guilds

##### Terrestrial Herbivores

Three guilds of terrestrial herbivores were lost: 1, megafaunal herbivores; 2, medium-sized grazers; and 3, small browsers (Table 7-7). The extinction of the megafaunal herbivores is reflected in the loss of megafaunal carnivores, but the loss of the small browsers (i.e. *Thylogale* lineage) is an enigma. This guild did exist in the rainforests of New Guinea until relatively recently in the Holocene. Its extinction appears to be related to human hunting or the introduction of wild dogs (Hope, 1981; Hope et al., 1993; Flannery, 1995). Therefore the extinction of this guild on mainland Australia may have been very late in the history of Australian northern rainforests. The discovery of mesothermic Holocene rainforest fossil faunas will be needed to determine whether these taxa survived the majority of extinctions in the Late Pleistocene.

Terrestrial Herbivores	MP1	RF	Size	Diet
<i>Vombatus ursinus mitchelli</i>			VL	Grazer
<i>Vombatus ursinus ursinus</i>			VL	Grazer
<i>Palorchestes</i> sp. cf. <i>P. pickeringi</i>			MF	Browser
diprotodontid			MF	Browser
<i>Troposodon</i> cf. <i>minor</i>			MF	Browser
<i>Protemnodon</i> cf. <i>devisi</i>			MF	Browser
<i>Protemnodon</i> sp. nov.			MF	Browser
<i>Protemnodon brehus</i>			MF	Browser
<i>Wallabia</i> sp.			VL	Browser
<i>Wallabia bicolor</i>			VL	Browser
<i>Kurrabi</i> sp. 1			VL	Browser
<i>Kurrabi</i> sp. 2			VL	Browser
cf. <i>Simosthenurus</i>			VL	Browser
<i>Macropus agilis</i>			VL	Grazer
<i>Macropus giganteus</i>			VL	Grazer
<i>Thylogale stigmatica</i>			L	Grazer
<i>Thylogale miniroo</i> sp. nov.			S	Browser
<i>Petrogale</i> sp.			L	Browser
<i>Petrogale mareeba</i>			L	Browser
cf. <i>Lagostrophus</i>			M	Grazer
				Browser-
<i>Aepyprymnus/Milliyowi</i> sp.			M	Fungivore

<i>Bettongia</i> sp.			M	Browser- Fungivore
<i>Hypsiprymnodon</i>			S	Browser- Fungivore

**Table 7-7. Middle Pleistocene and Present day (Wet Tropics) terrestrial herbivore fauna and guilds.**

Terrestrial Herbivores		MP1	RF
MF	Browser	6	*
VL	Grazer	3	1
VL	Browser	4	1
L	Grazer	1	1
L	Browser	1	2
M	Grazer	1	*
M	Browser- Fungivore	1	2
S	Browser	1	*
S	Browser- Fungivore		1
	Total Taxa	18	8
	Total Guilds	8	6
	Guild Loss		3(- 1)

**Table 7-8. Middle Pleistocene and Present day (Wet Tropics) terrestrial herbivore guilds.**

#### Arboreal Herbivores

As with terrestrial herbivores, three guilds of arboreal herbivores were lost between the Middle Pleistocene and present day: 1, very large folivore-frugivores; 2, small folivore-bryophytivores; and 3, small folivore-frugivores (Table 7-9). The loss of these guilds underscores the biased extinction of very large and very small taxa during this period. The first guild is comprised of *Bohra*, the ‘megafaunal’ tree-kangaroo. This guild is representative of the largest arboreal guild to have gone extinct in the Australian Pleistocene across all habitats, and therefore can be regarded as the megafaunal equivalent of terrestrial herbivores. The small-sized arboreal guilds are represented by the smallest pseudocheirid species and miralinids. Both groups were probably dietary specialists, which may have left them vulnerable to perturbations in the availability of their food source.

Arboreal Herbivores	MP1	RF	Size	Diet
<i>Bohra</i> sp. 1			VL	Folivore-Frugivore
<i>Bohra</i> sp. 2			VL	Folivore-Frugivore
<i>Bohra</i> sp. 3			VL	Folivore-Frugivore
<i>Dendrolagus</i> sp. cf. <i>D. ursinus</i>			L	Folivore-Frugivore
<i>Dendrolagus</i> sp. cf. <i>D. mbasio</i>			L	Folivore-Frugivore
<i>Dendrolagus</i> sp. cf. <i>D. spadix</i>			L	Folivore-Frugivore
<i>Dendrolagus</i> sp. nov. 1			L	Folivore-Frugivore
<i>Dendrolagus</i> sp. nov. 2			L	Folivore-Frugivore
<i>Dendrolagus bennettianus</i>			L	Folivore-Frugivore
<i>Dendrolagus lumholtzi</i>			L	Folivore-Frugivore
<i>Phascolarctos</i> cf. <i>stirtoni</i>			L	Folivore
<i>Phascolarctos cinereus</i>			L	Folivore
<i>Madakoala</i> sp. nov.			L	Folivore
gen. et sp nov.			M	Folivore
<i>Pseudocheirus</i> sp. 1			S	Folivore-bryophyta
<i>Pseudocheirus</i> sp. 2			M	Folivore
<i>Pseudocheirus</i> sp. 3			M	Folivore
<i>Pseudocheirus peregrinus</i>			M	Folivore
<i>Pseudochirulus</i> sp. 1			S	Folivore-bryophyta
<i>Pseudochirulus</i> sp. 2			M	Folivore
<i>Pseudochirulus</i> sp. 3			M	Folivore
<i>Pseudochirulus herbertensis</i>			M	Folivore
<i>Pseudochirulus cinereus</i>			M	Folivore
<i>Petauroides volans</i>			M	Folivore
<i>Petauroides</i> sp. 1			M	Folivore
<i>Petauroides</i> sp. 2			M	Folivore
<i>Petauroides</i> sp. 3			M	Folivore
<i>Pseudochirops</i> sp. 1			M	Folivore
<i>Pseudochirops</i> sp. 2			M	Folivore
<i>Pseudochirops</i> sp. 3			M	Folivore
<i>Pseudochirops archeri</i>			M	Folivore
<i>Pseudokoala</i> sp. 1			L	Folivore
<i>Pseudokoala</i> sp. 2			L	Folivore
<i>Hemibelidius lemuroides</i>			M	Folivore
<i>Phalanger</i> sp. nov.			L	Folivore-Frugivore
<i>Phalanger</i> cf. <i>P. mimicus</i>			L	Folivore-Frugivore
<i>Phalanger intercastellanus/mimicus</i>			L	Folivore-Frugivore
<i>Spilocuscus</i> sp.			L	Folivore-Frugivore
<i>Spilocuscus maculatus</i>			L	Folivore-Frugivore
<i>Trichosurus</i> sp. 1			L	Folivore-Frugivore
<i>Trichosurus vulpecula</i>			L	Folivore-Frugivore

<i>Trichosurus</i> sp. 2		L	Folivore-Frugivore
miralinid		S	Folivore-Frugivore
Total taxonomic richness	30	11	

**Table 7-9. Middle Pleistocene and Present day (Wet Tropics) arboreal herbivore fauna and guilds.**

Size	Arboreal Herbivores	MP1	RF
VL	Folivore-Frugivore	3	*
L	Folivore-Frugivore	9	4
L	Folivore	4	1
M	Folivore	11	6
S	Folivore-bryophyta	2	*
S	Folivore-Frugivore	1	*
	Total Taxa	30	11
	Total Guilds	6	3
	Guild Loss		3

**Table 7-10. Middle Pleistocene and Present day (Wet Tropics) arboreal herbivore guilds.**

#### 7.11.5 Ecto-Endothermic Invertebrate Eater Guilds

Here, the only guild to be lost was the small arboreal endotherm, represented by a new species of *Dactylopsila* (Table 7-11). Although this guild is missing in present day Wet Tropics it is present in Holocene deposits in western New Guinea suggesting that, like the small species of *Thylogale*, this guild may have survived into the Holocene and its demise perhaps caused by hunting.

Invertebrate Eaters	MP1	RF	Size	Habit	Temp
<i>Dactylopsila</i> sp. 1			M	A	Endo
<i>Dactylopsila</i> sp. 2			S	A	Endo
<i>Dactylopsila trivirgata</i>			M	A	Endo
<i>Cercartetus</i> sp. 1			VS	A	Endo
<i>Cercartetus</i> sp. 2			VS	A	Endo
<i>Cercartetus caudatus</i>			VS	A	Endo
<i>Acrobates</i> sp.			VS	A	Endo
gen 1 et sp nov 1			M	A	Endo
gen 1 et sp nov 2			M	A	Endo
<i>Hypsilurus</i> sp.			M	A	Ecto
<i>Hypsilurus boydii</i>			M	A	Ecto

<i>Tiliqua scincoides</i>		M	T	Ecto
<i>Cyclodomorphus gerrardii</i>		M	T	Ecto
<i>Tiliqua</i> sp. nov.		M	T	Ecto
<i>Egernia major</i>		M	T	Ecto
<i>Egernia</i> sp.		S	T	Ecto
<i>Sphenomorphus</i> group robust		S	S	Ecto
<i>Sphenomorphus</i> group gracile		S	S	Ecto
gekkonidae		S	A	Ecto
typhlopidae		VS	F	Ecto
<i>Sarcophilus lanarius</i>		L	T	Endo
<i>Antechinus</i> sp. nov. 1		S	S	Endo
<i>Antechinus</i> sp. nov. 2		S	S	Endo
<i>Antechinus flavipes</i>		S	S	Endo
<i>Antechinus godmani</i>		S	S	Endo
<i>Antechinus leo</i>		S	S	Endo
<i>Sminthopsis 'murina'</i>		S	T	Endo
<i>Sminthopsis macroura</i>		S	T	Endo
<i>Planigale</i> sp.		S	T	Endo
<i>Planigale maculata</i>		S	T	Endo
<i>Planigale tenurostris</i>		S	T	Endo
<i>Micromurexia</i> cf. <i>M. habbema</i>		S	S	Endo
gen 1 et sp nov. 1		S	T	Endo
gen 2 et sp nov 2		S	T	Endo
gen 3 et sp. nov 3		S	T	Endo
<i>Phascogale</i> sp. nov. 1		M	A	Endo
<i>Phascogale topoatafa</i>		M	A	Endo

**Table 7-11. Middle Pleistocene and Present day (Wet Tropics) 'invertivore' fauna and guilds.**

Invertebrate Eaters	MP	RF
MAEN	4	2
MAECT	1	1
MTECT	4	2
STECT	1	1
STEND	5	2
SSEND	3	3
SAEND	1	*
SSECT	1	2
VSAEN	3	2
VSFECT	1	1
Total Taxa	24	16
Total Guilds	10	9
Guild Loss		1

**Table 7-12. Middle Pleistocene and Present day (Wet Tropics) 'invertivore' guilds.**

#### 7.11.6 *Endothermic Exudivores and Omnivores*

Of all of Middle Pleistocene rainforest fauna as represented at Mt Etna, the only guilds not affected by major extinctions and faunal turnovers were the small to medium-sized arboreal exudivores and medium-sized omnivores (Table 7-13). Both guild types remain within the rainforests of the Wet Tropics and New Guinea, although the taxa that make up these guilds have changed. The exudivore guild type was filled by an extinct petaurid during the Middle Pleistocene, being replaced by species of *Petaurus* in modern rainforests. Omnivores are dominated by rodents and perameloids in both the Middle Pleistocene and present day rainforests. Although the guild itself was not driven extinct, the majority of Middle Pleistocene taxa filling this guild have been replaced by new ones within the modern rainforests. Perameloids included extinct species of peroryctids and peramelids during the Middle Pleistocene, being replaced in modern rainforests by species of *Perameles* and *Isodon*. Neither taxa are considered to be rainforest specialists, although *P. nasuta* does have rainforest as its core habitat in northern Queensland. Overall perameloid diversity decreased by over half.

Rodent diversity also decreased but less so than for perameloids. Three species and one genus were lost. This apparent small reduction in overall diversity masks the considerable faunal turnover in rodents between the Middle Pleistocene and present day. The most conspicuous change is in the appearance of *Rattus* in modern rainforests, following their absence from Middle Pleistocene rainforests. *Rattus* species seem to replace *Pseudomys* and 'Mesembriomys' lineages, both of which no longer exist in the Wet Tropics rainforests. The only rodent species retained between Middle Pleistocene and modern rainforests is *Uromys hadrourus*. Although *Uromys*, *Melomys* and *Pogonomys* occur in both Middle Pleistocene and modern rainforests the species are not conspecific, the original taxa inhabiting Middle Pleistocene rainforests being replaced – *Uromys* sp. nov. with *U. caudimaculatus*, *Pogonomys* sp. nov. with *Pogonomys ?loriae* (AUS) and *Melomys* sp. with *Melomys cervinipes*. Thus, although omnivore guilds per se were not severely reduced by changes in Australian Quaternary rainforests, the taxa occupying this guild were, with significant Late Pleistocene turnover producing the present day fauna.



Petauridae	MP1	RF	Size	Habit
gen et sp nov. 1			M	A
gen et sp nov. 2			M	A
<i>Petaurus</i> spp.			M	A

**Table 7-13. Middle Pleistocene and Present day (Wet Tropics) exudivore fauna and guilds.**

Exudivore Guilds	MP RF	PD RF
MAEx	2	2
Total Taxa	2	2
Total Guilds	1	1
Guild Loss		0

**Table 7-14. Middle Pleistocene and Present day (Wet Tropics) exudivore guilds.**

Peramelomorpha	MP1	RF
?Peroryctes sp. 1		
?Peroryctes sp. 2		
Peroryctid 3		
<i>Perameles</i> sp. 1		
<i>Perameles</i> sp. 2		
<i>Perameles nasuta</i>		
<i>Isoodon macrourus</i>		
Total Taxa	5	2
Total Guilds	1	1
Guild Loss		0

**Table 7-15. Middle Pleistocene and Present day (Wet Tropics) omnivore (perameloid) fauna and guilds.**

Muridae	MP1	RF
<i>Pseudomys</i> 'small'		
<i>Pseudomys</i> 'large'		
<i>Pogonomys</i> sp.		
<i>Pogonomys</i> sp.		
" <i>Mesembriomys</i> " 1		
" <i>Mesembriomys</i> " 2		
" <i>Mesembriomys</i> " 3		
" <i>Mesembriomys</i> " 4		
<i>Uromys</i> sp. nov.		
<i>Uromys caudimaculatus</i>		
<i>Uromys hadrourus</i>		
<i>Melomys</i> sp.		
<i>Melomys cervinipes</i>		
<i>Rattus fuscipes</i>		
<i>Rattus leucopus</i>		
?new genus		
<i>Hydromys</i>		

11 8

Total Species Richness

Total Generic Richness

6

5

**Table 7-16. Middle Pleistocene and Present day (Wet Tropics) murid (omnivore-granivore) fauna.**

## **7.12 Responses of Pleistocene rainforest vertebrates to climate change**

### *7.12.1 Taxonomic turnover and decline at Mt Etna*

Rainforest vertebrate decline between the Middle Pleistocene rainforest faunas and those of the present day Wet Tropics has been documented above. The comparisons chart the overall decline in diversity and guild richness for rainforest vertebrates. However, to better understand the role that climate plays in shaping vertebrate faunas, comparisons should be made within the same geographical area in order to remove possible geographic variation. Below I document faunal and guild decline and response to environmental changes for Mt Etna across five time periods (Middle Pleistocene rainforest fauna (MP1), Middle Pleistocene turnover fauna (MP2), Late Pleistocene fauna (LP), Holocene Fauna (H) and present day fauna (PD)). These time periods witnessed major climatic changes as well as the first anthropogenic influence sometime in the Late Pleistocene, and therefore impacts of both should correspond with the faunal record. One major limitation of this approach lies in the taphonomic biases of the deposits, where younger deposits are almost exclusively from predator accumulations and therefore biased against the preservation of megafaunal remains. These significantly bias our understanding of very large and megafaunal species diversity, and thus the analysis cannot resolve the extinction and turnover chronologies for such groups. For small to large species, taphonomy will have had relatively minor influences on their representation in the fossil record, and therefore they should respond in ways reflective of prevailing environmental changes. Figure 7-47 provides a summary of the climatic changes that impacted the Australian continent before, during and after the faunal turnovers experienced at Mt Etna throughout the Middle and Late Pleistocene.

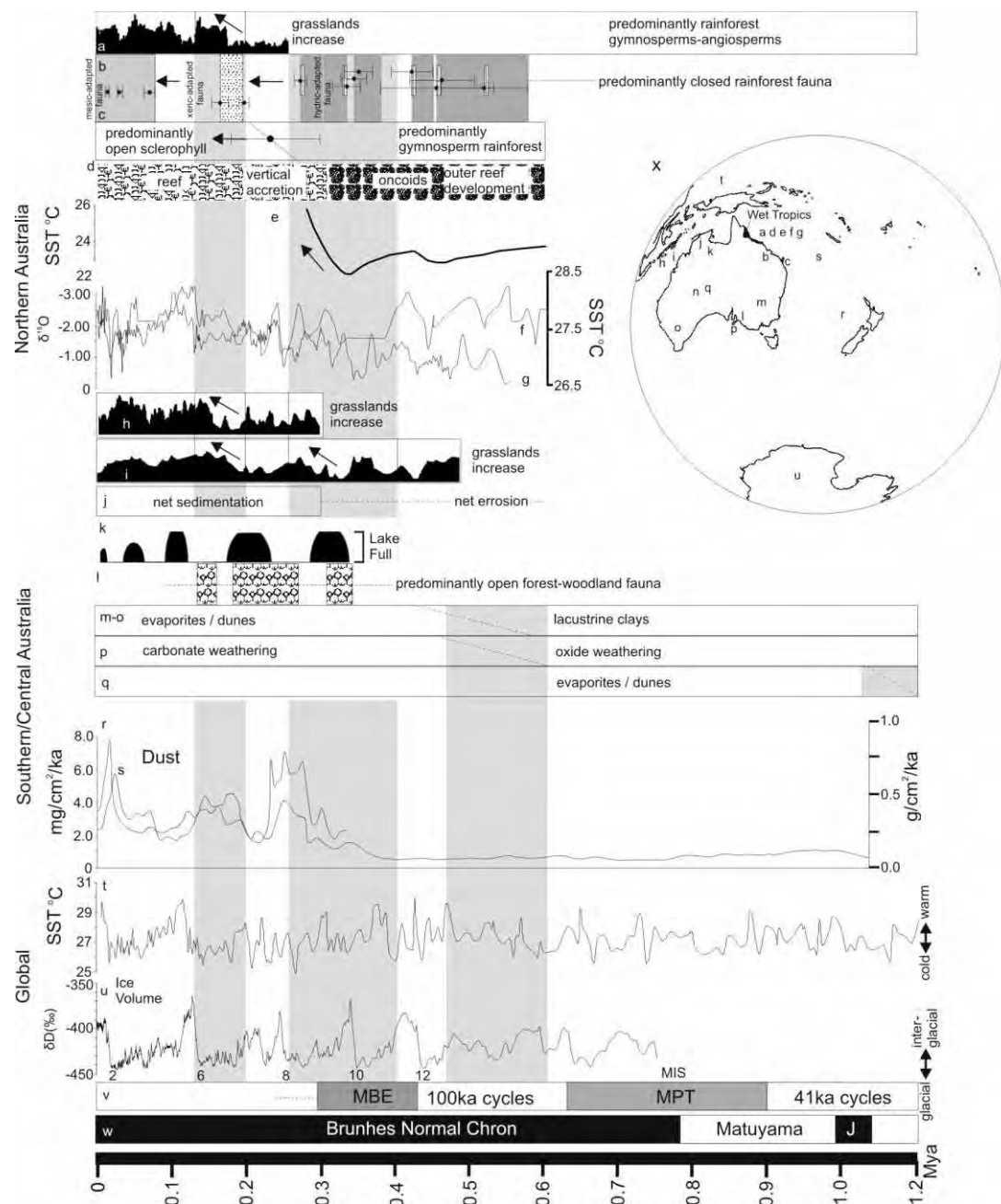


**Figure 7-47. Summary of prevailing climatic changes over the last 1.2 million years in the Australasian region.**

Fauna itself can provide some degree of palaeoclimatic data because extant species present in the fossil record can be used as climatic proxies. Figure 7-48 presents two bioclimatic profiles of taxa across the MP1-MP2 faunal turnover: 1, the entire fauna; and 2, only fauna known to be obligates in their respective habitats. Bioclimatic data were collected for all extant fossil taxa at the generic rather than species level so as to provide the broadest possible resolution and to take into account any potential

taxonomic inconsistencies. Using annual precipitation (mm) as the climate proxy, taxa were arranged according to ascending precipitation minima. In other words, taxa were ranked according to the lowest known annual precipitation of their habitat, thus providing the absolute minimum precipitation rate for presence of the extant species. In the first analysis, the highest minimum precipitation rate was taken for MP2 taxa, whilst the lowest maximum precipitation rate was taken for MP1 taxa, providing the minimum precipitation rate needed to encompass all MP1 extant taxa and maximum precipitation rate needed to encompass all MP2 taxa. These levels predicted a change in precipitation rate of at least 1200mm.

In the second analysis, only habitat-obligate taxa were used, thereby reducing possible variation. Here, instead of using minima and maxima, box-plots were used to determine the largest amount of data that could be encompassed for all taxa. The annual precipitation rate returned values for MP1 between 1500 and 4000mm, and results for MP2 returned annual precipitation ranges between 100 and 600mm. This represents a minimum reduction in annual precipitation of approximately 600mm or nearly half.

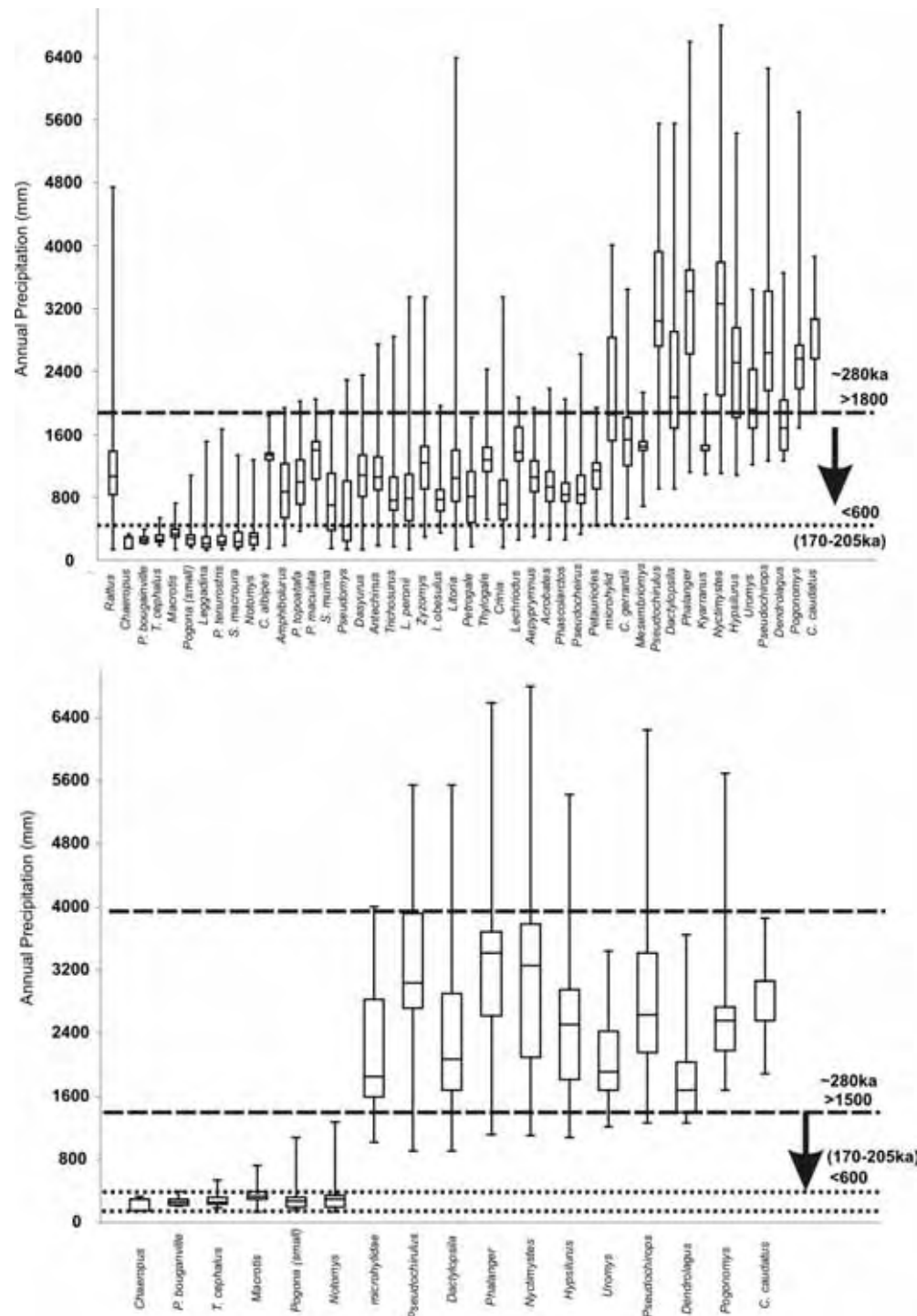


**Figure 7-48. Bioclimatic distribution of fauna between middle Pleistocene rainforest fauna and the xeric-adapted QML1312 fauna. Showing overall decrease in mean annual precipitation (see text for explanation). Top (all taxa), Bottom (obligate taxa only).**

### 7.12.2 Frogs

Massive declines in frog fauna occur between MP1 and MP2, illustrating the importance of rainforest habitat to the majority of frogs (Fig. 7-49). Those surviving

the faunal turnover include species of *Litoria* and *Limnodynastes*, perhaps not surprising since these taxa represent respectively the most speciose hylid and limnodynastine genera present in Australia today.

A conspicuous arrival within the new MP2 fauna is the burrowing frog genus *Cyclorana*, usually associated with open and dry habitats. This *Cyclorana* species continues into the LP and is joined by a congener and an additional open-arid burrowing frog of the genus *Neobatrachus*. After the LP, frog diversity declines with the local disappearance of one species each of *Cyclorana* and *Neobatrachus*, without replacement (Fig 7-50). The difference between H and PD frog faunas is most likely a reflection of taphonomy rather than real ecology. Here the PD frog fauna is bolstered by an large number of species of *Litoria* which may simply reflect the lack of taxonomic certainty surrounding the diversity of fossil *Litoria* species. On balance, the frog faunas of MP1 were driven locally extinct and remained so even when more mesic climates returned during the Holocene.

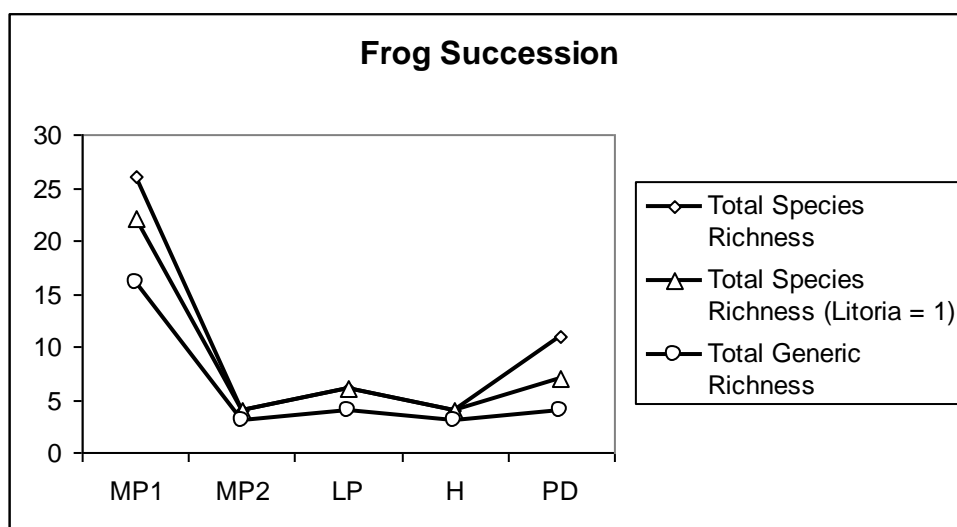


**Figure 7-49. Frog succession at Mt Etna between the middle Pleistocene and present day. MP1 (>280ka), MP2 (205-170ka), LP (<80ka), H (<10ka) PD (present).**

Hylidae	MP1	MP2	LP	H	PD
<i>Litoria</i> sp. 1					
<i>Litoria</i> sp. 2					
<i>Litoria</i> sp. 3					
<i>Litoria</i> sp. 4					
<i>Litoria rubella</i>					
<i>Litoria nasuta</i>					
<i>Litoria gracilentia</i>					

<i>Litoria fallax</i>					
<i>Litoria caerulea</i>					
<i>Nyctimystes</i> sp. 1					
<i>Nyctimystes</i> sp. 2					
<i>Cyclorana</i> sp. cf. <i>C. cultripes</i>					
<i>Cyclorana brevipes</i>					
<i>Cyclorana novaehollandiae</i>					
<i>Cyclorana</i> sp. 2					
<i>Etmabatrachus maximus</i>					
Myobatrachidae					
<i>Crinia</i> sp.					
<i>Kyarranus</i> sp. 1					
<i>Kyarranus</i> sp. 2					
<i>Limnodynastes</i> sp. 1					
<i>Limnodynastes</i> sp. 2					
<i>Limnodynastes</i> sp. 3					
<i>Limnodynastes tasmaniensis</i> sp. Group					
<i>Limnodynastes spenceri</i> sp. Group					
<i>Limnodynastes peronii</i>					
<i>Limnodynastes salmini</i>					
<i>Lechriodus</i> sp. cf. <i>L. platyceps</i>					
<i>Neobatrachus</i> sp. 1					
<i>Neobatrachus</i> sp. 2					
<i>Assa</i> sp.					
<i>Pseudophryne</i> sp.					
<i>Philoria</i> sp.					
<i>Taudactylus</i> sp. cf. <i>T. diurnus</i>					
<i>Uperoleia rugosa</i>					
<i>Uperoleia</i> sp.					
Microhylidae					
cf. <i>Hylophorbus</i>					
<i>Cophixalus</i> sp.					
New Genus					
Total Species Richness	26	4	6	4	11
Total Species Richness ( <i>Litoria</i> = 1)	22	4	6	4	7
Total Generic Richness	16	3	4	3	4

Table 7-17. Mt Etna frog succession.

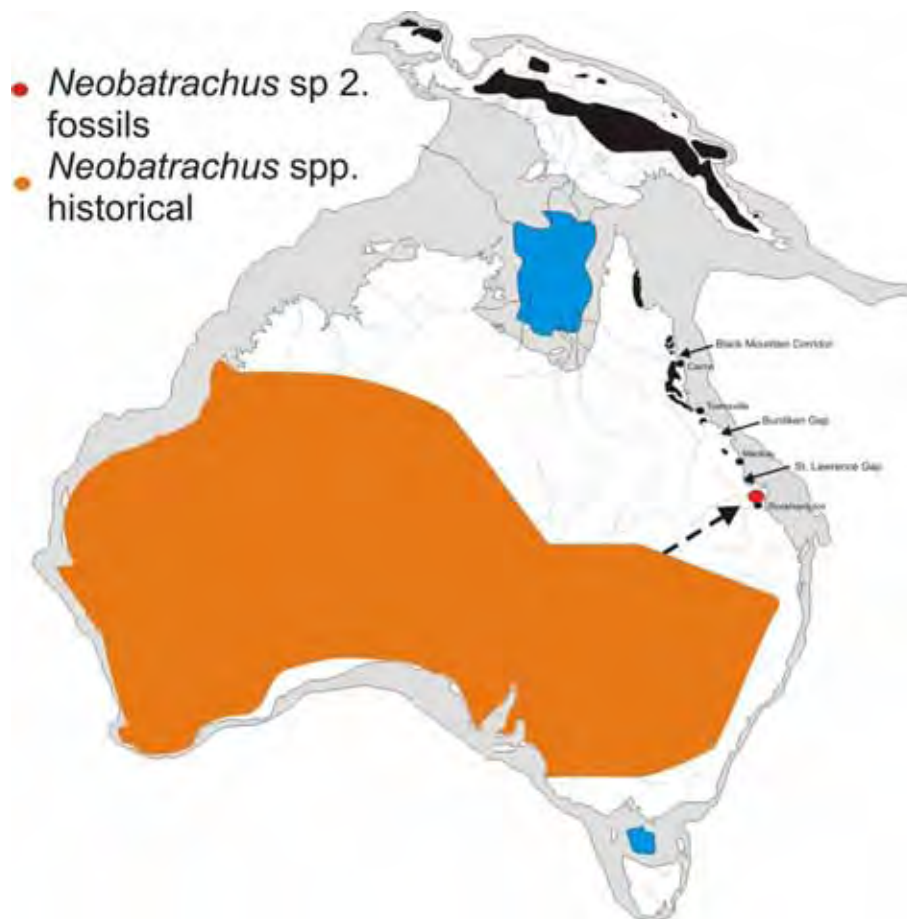


**Figure 7-50. Middle Pleistocene (Mt Etna) and present day occurrence of *Neobatrachus*.**

### 7.12.3 Mammals

### 7.12.4 Rodents

Rodent diversity across MP1, MP2 and LP remain relatively stable, even though the taxonomic composition of the rodent faunas changes dramatically. For example more than 80% of the MP1 rodent fauna becomes locally extinct, being replaced in MP2 by a similarly rich fauna (Fig 7-51). MP2 and LP rodent faunas remain relatively similar, but by LP times the fauna has recruited an additional genus. Between LP, H and PD, rodent diversity decrease dramatically with the loss of two species per time period and a reduction of three genera. These reductions are not easy to explain other than to suggest that, because rodent diversity is highest in rainforest and arid-zone habitats, the return of relatively mesic climates saw overall diversity decline. Alternatively, the taxonomy of *Pseudomys* species may play a large role in skewing known diversity. Like *Litoria* in frog faunas, *Pseudomys* is difficult to distinguish on the basis of



skeletal morphology, and hence its true taxonomic diversity is hard to discern. The more mesic habitats of the Holocene may have supported more species of *Pseudomys* than rainforests and arid-zone habitats. With further morphological work, it is expected that changes in rodent diversity throughout the Middle Pleistocene to present day will reflect changes in habitat, but that total diversity will not alter substantially through time.

Muridae	MP1	MP2	LP	H	PD
<i>Leggadina</i>					
<i>Pseudomys</i> 'small'					
<i>Pseudomys</i> 'large'					
<i>Zyzomys</i> sp.					
<i>Notomys</i> sp. 1					
<i>Notomys</i> sp. 2					
<i>Notomys</i> sp. 3					
<i>Pogonomys</i> sp.					
" <i>Mesembriomys</i> " 1					
" <i>Mesembriomys</i> " 2					
" <i>Mesembriomys</i> " 3					
" <i>Mesembriomys</i> " 4					
<i>Uromys</i> sp. nov.					
<i>Uromys hadrourus</i>					
<i>Melomys</i> sp.					
<i>Melomys cervinipes</i>					
<i>Conilurus albipes</i>					
<i>Conilurus</i> sp. nov.					
<i>Rattus</i> spp.					
?new genus					
<i>Hydromys</i>					
Total Species Richness	11	9	9	7	5
Total Generic Richness	6	6	7	6	4

**Table 7-18. Mt Etna murid succession.**

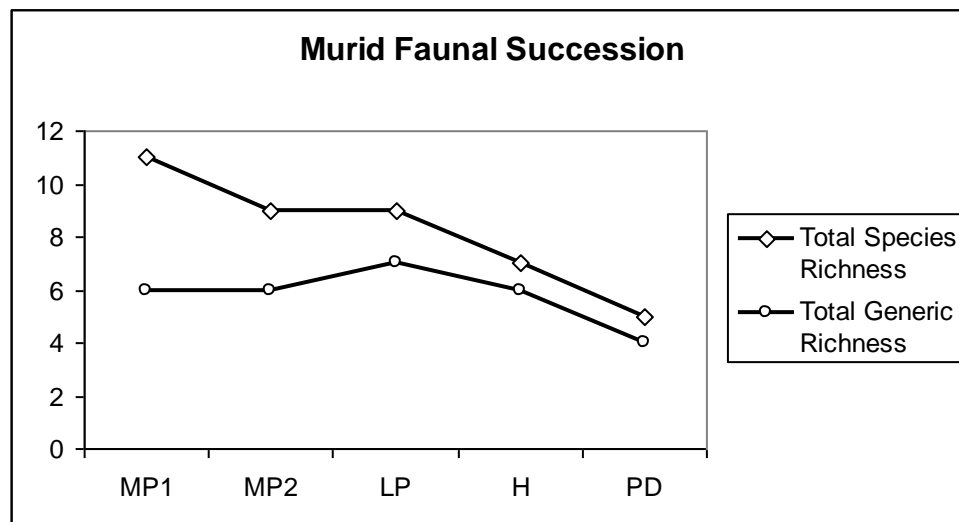


Figure 7-51. Murid succession at Mt Etna between the middle Pleistocene and present day. MP1 (>280ka), MP2 (205-170ka), LP (<80ka), H (<10ka) PD (present).

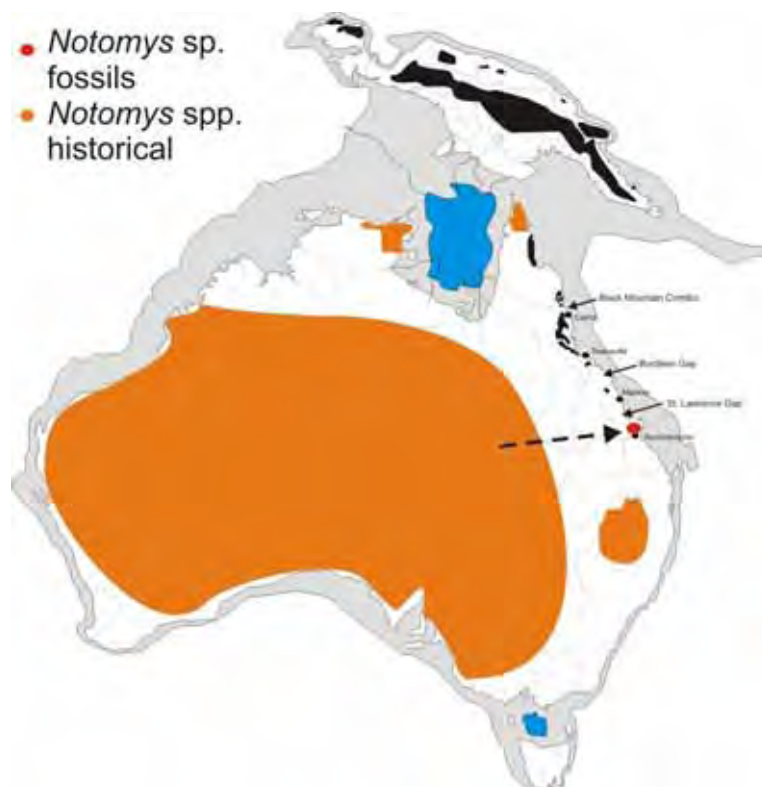


Figure 7-52. Middle Pleistocene (Mt Etna) and present day occurrence of *Notomys*.

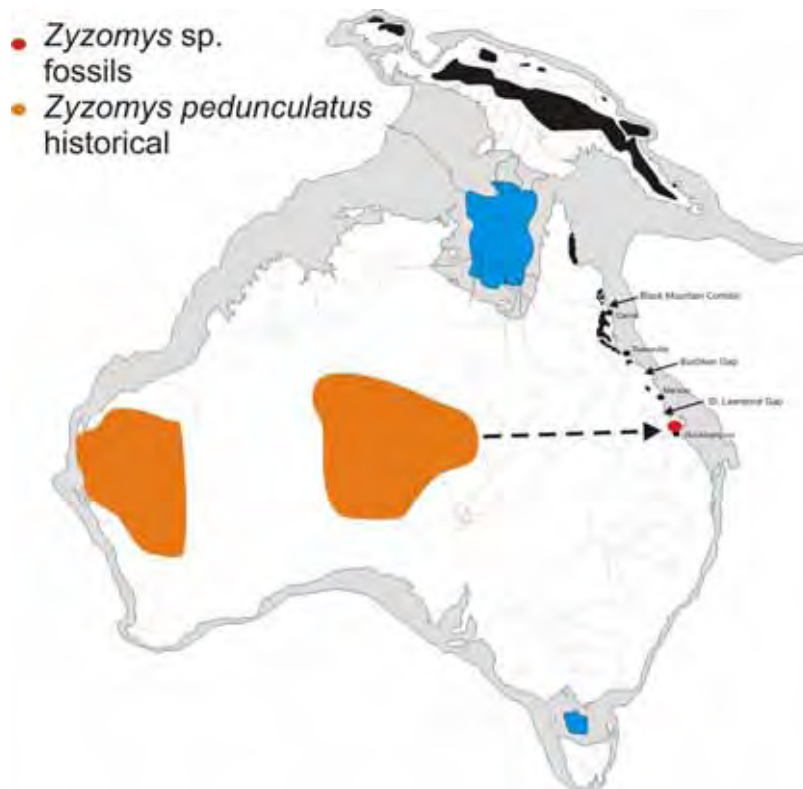


Figure 7-53. Middle Pleistocene (Mt Etna) and present day occurrence of *Zyzomys*.

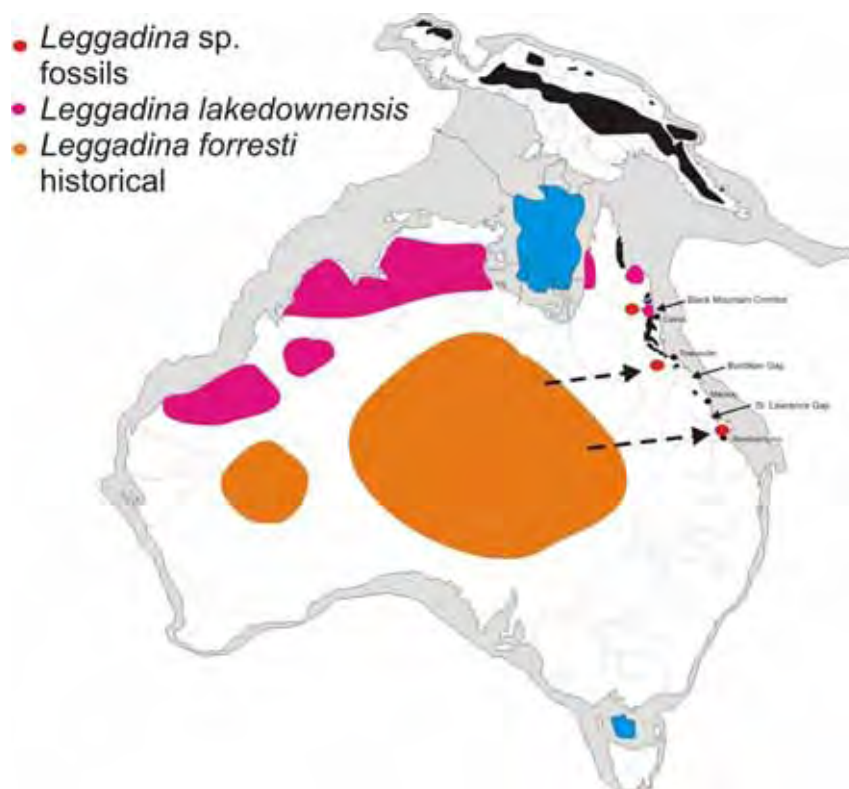


Figure 7-54. Middle Pleistocene (Mt Etna) and present day occurrence of *Leggadina*.



**Figure 7-55.** Middle Pleistocene (Mt Etna) and present day occurrence of *Conilurus*.

#### 7.12.5 Arboreal 'Possums'

97% of arboreal possum species become locally extinct between MP1 and MP2. The only survivor of this turnover to continue into MP2 is a single petauroid species (Fig 7-56). This taxon is extinct today but it appears to have been an exudivore based on its dental similarities with *Petaurus* species. The survival of an exudivore into MP2 is intriguing because this is also one of only two guilds to be unaffected by overall rainforest faunal extinctions. Exudivore guilds survived the Late Miocene turnover, this local Middle Pleistocene turnover and the Late Pleistocene contractions of rainforests in northern Queensland and New Guinea, reflecting its tolerance to major changes in climate.

Arboreal taxa do not recover from this massive extinction event, remaining low in diversity throughout the rest of LP to PD. The exudivore guild not only remains stable throughout this time but is the only taxonomic group to increase in species-level diversity, with an increase in petaurid taxa from 1 to potentially 3. This increase most likely reflects the LP to PD expansion of sclerophyllic, pyrophylic exudate-vegetation, such as *Eucalyptus*, *Banksia* and *Acacia* species, on which these petaurids

thrive. The impact of Late Pleistocene burning in northern Queensland has been implicated in the expansion and dominance of pyrophylic vegetation, which would also facilitate the increased distribution of possum species associated with them, such as the species of *Petaurus*. A relatively recent expansion of range may be reflected in future genetic studies of exudivorous marsupials in perhaps limited genetic structuring in populations.

Petauridae	MP1	MP2	LP	H	PD
gen et sp nov. 1					
gen et sp nov. 2					
<i>Dactylopsila</i> sp. 1					
<i>Dactylopsila</i> sp. 2					
<i>Petaurus</i> spp.					
Burramyidae					
<i>Cercartetus</i> sp. 1					
<i>Cercartetus</i> sp. 2					
Acrobatidae					
<i>Acrobates</i> sp.					
gen 1 et sp nov 1					
gen 1 et sp nov 2					
Phascolarctidae					
<i>Phascolarctos</i> cf. <i>stirtoni</i>					
<i>Phascolarctos cinereus</i>					
<i>Madakoala</i> sp. nov.					
Pseudocheiridae					
gen. et sp nov.					
<i>Pseudocheirus</i> sp. 1					
<i>Pseudocheirus</i> sp. 2					
<i>Pseudocheirus</i> sp. 3					
<i>Pseudocheirus peregrinus</i>					
<i>Pseudochirulus</i> sp. 1					
<i>Pseudochirulus</i> sp. 2					
<i>Pseudochirulus</i> sp. 3					
<i>Petauroides</i> sp. 1					
<i>Petauroides</i> sp. 2					
<i>Petauroides</i> sp. 3					
<i>Pseudochirops</i> sp. 1					
<i>Pseudochirops</i> sp. 2					
<i>Pseudochirops</i> sp. 3					
<i>Pseudokoala</i> sp. 1					
<i>Pseudokoala</i> sp. 2					
Phalangeridae					
<i>Phalanger gymnotis</i>					
<i>Phalanger</i> cf. <i>P. mimicus</i>					
<i>Spilocuscus</i> sp.					

<i>Trichosurus</i> sp. 1					
<i>Trichosurus vulpecula</i>					
<i>Trichosurus</i> sp. 2					
Miralinidae					
miralinid					
Total Species Richness	31	2	4	3	5
Total Generic Richness	17	2	4	3	5

**Table 7-19. Mt Etna possum succession.**

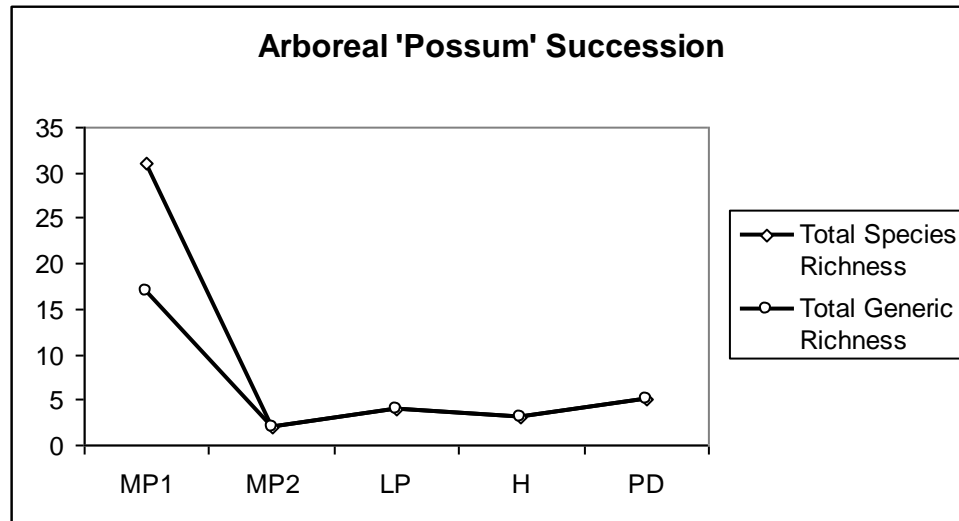


**Figure 7-56. 'Possum' succession at Mt Etna between the middle Pleistocene and present day. MP1 (>280ka), MP2 (205-170ka), LP (<80ka), H (<10ka) PD (present).**

#### 7.12.6 (Non-megafaunal) Small-Large macropods

Between MP1 and MP2 there was a large reduction of small-large kangaroos, but after this time the total taxonomic diversity remains relatively stable with the retention of the largest species of *Thylogale* and *Petrogale*, along with the addition of *Aepyprymnus* in the fauna from LP to PD (Fig 7-57). The presence of *Petrogale* species throughout time almost certainly reflects the stability of their major habitat preference, rocky outcrops. Habitat for this lineage would have increased in overall area throughout the MP and LP as the immediate land surface topography changed in response to major erosion and exposure of karstic limestone (Hocknull, Chapter 3). The presence of *Thylogale* suggests stability of small patches of closed forest within the limestone area, suggesting that even when surrounding habitats were significantly reduced small viable refugia existed.

Macropodidae	MP1	MP2	LP	H	PD
<i>Thylogale</i> cf. <i>T. thetis</i>					
<i>Thylogale miniroo</i> sp. nov.					
<i>Dendrolagus</i> sp. cf. <i>D. ursinus</i>					
<i>Dendrolagus</i> sp. cf. <i>D. mbasio</i>					
<i>Dendrolagus</i> sp. cf. <i>D. spadix</i>					
<i>Dendrolagus</i> sp. nov. 1					
<i>Dendrolagus</i> sp. nov. 2					
<i>Dendrolagus</i> sp.					
<i>Petrogale</i> sp.					
cf. <i>Lagostrophus</i>					
Potoroiidae					
<i>Aepyprymnus/Milliyowi</i> sp.					
Total Species Richness	10	3	2	3	3
Total Generic Richness	5	3	2	3	3

**Table 7-20. Mt Etna kangaroo-potoroo succession.**

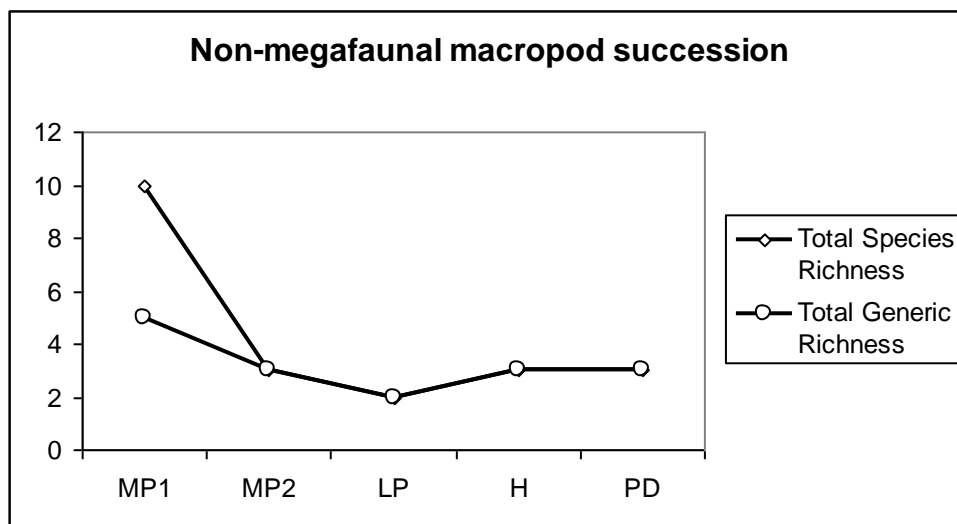


**Figure 7-57. Non-megafaunal macropod succession at Mt Etna between the middle Pleistocene and present day. MP1 (>280ka), MP2 (205-170ka), LP (<80ka), H (<10ka) PD (present).**

#### 7.12.7 Very Large- Megafaunal Mammals

Very large and megafaunal mammals are significantly biased against representation in the Mt Etna MP2 and LP fossil record because taphonomic factors mitigate against their accumulation in these particular (karstic) deposits. For this reason, the fossil record from the Middle Pleistocene Marmor Quarry locality, from the same region, is compared with MP1, LP, H and PD records for this particular guild (Table 7-21). Between the megafaunal record of MP1 and Marmor Quarry there is a reduction in total diversity of very large to megafaunal mammals and a replacement of typically

closed-forest dwelling species (e.g. *Protemnodon* species) with more open-dwelling taxa (e.g. *Macropus* species), indicating a response to the overall opening up of the habitat (Fig 7-58). The LP deposit does not record a very large or megafaunal component, and hence the timing of extinction of local megafauna in the central eastern Queensland region cannot yet be determined.

Mammalian "Megafauna"	MP1	Marmor	LP	H	PD
<i>Palorchestes</i> sp. cf. <i>P. pickeringi</i>	■				
<i>Palorchestes</i> sp. cf. <i>P. parvus</i>		■			
diprotodontid	■				
zygomaturine		■			
<i>Troposodon</i> cf. <i>minor</i>	■				
<i>Protemnodon</i> cf. <i>devisi</i>	■				
<i>Protemnodon</i> sp. nov.	■				
<i>Protemnodon brehus</i>	■				
<i>Wallabia</i> sp.	■				
<i>Wallabia bicolor</i>					■
<i>Bohra</i> sp. 1	■				
<i>Bohra</i> sp. 2	■				
<i>Bohra</i> sp. 3	■				
<i>Kurrabi</i> sp. 1	■				
<i>Kurrabi</i> sp. 2	■				
cf. <i>Simosthenurus</i>	■	■			
<i>Thylacoleo</i> sp. (Large)	■	■			
<i>Thylacoleo hilli</i>	■				
<i>Thylacinus cyanocephalus</i>	■	■			
<i>Macropus agilis</i>	■	■	■	■	■
<i>Macropus titan</i>		■	■	■	■
<i>Macropus giganteus</i>		■	■	■	■
<i>Macropus parryi</i>				■	■
Total Species Richness	17	6	2	2	4
Total Generic Richness	11	5	1	1	2

**Table 7-21. Mt Etna 'megafauna' succession.**



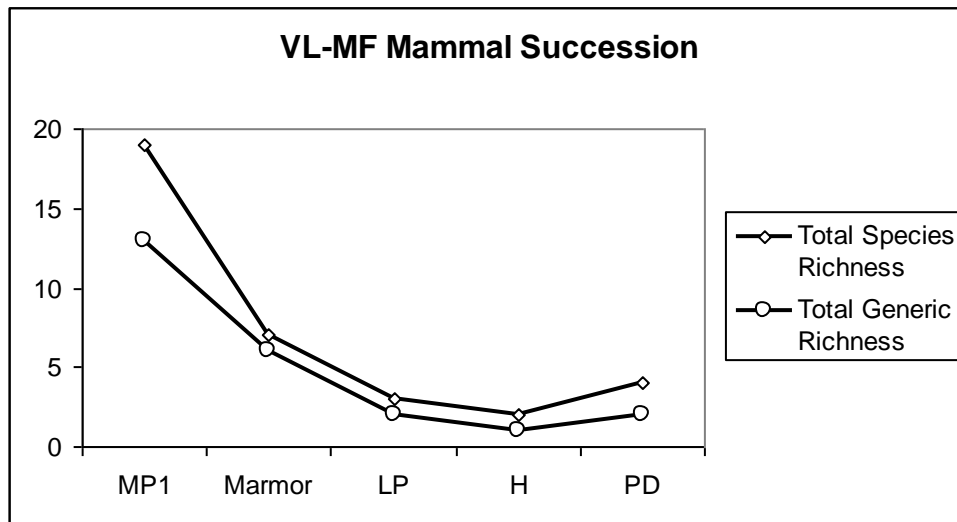


**Figure 7-58.** Very large and megafaunal mammal succession at Mt Etna between the middle Pleistocene and present day. MP1 (>280ka), MP2 (205-170ka), LP (<80ka), H (<10ka) PD (present).

#### 7.12.8 Carnivorous-Insectivorous Mammals

The diversity of carnivorous and insectivorous mammals drops between MP1 and MP2, is constant between MP2 and LP, the drops to PD (Fig 7-59). This pattern is nearly identical to that found for rodent diversity through time and possibly reflects similar preferred habitats, with diversity in rainforest and arid habitats being greater than that in mesic habitats. However, taxonomic certainty is much better resolved in dasyurids, allowing closer inspection of faunal changes through time. Between MP1 and MP2 seven taxa go extinct and are replaced by four, with a total species drop of four. Two of these (*Planigale tenurostris* and *Sminthopsis macroura*) are today restricted to the arid zone, whilst the other two are found along the eastern seaboard. Between MP2 and LP, four species go extinct and are replaced by four, keeping overall diversity constant. During this period older species of *Antechinus* are replaced by *A. flavipes*, a generalised antechinus found throughout the eastern seaboard, and *Sarcophilus laniarius* replaced by *S. harissii*. Between LP and H, only two dasyurid species become locally extinct, *Dasyurus vivverinus* and *D. maculatus*, both of which today have highly disjunct populations (see discussion of *D. maculatus* above). Overall, from the Middle Pleistocene to present day, dasyurid diversity remains high, although generic-level diversity is evidently declining in eastern Australia.

Dasyuridae	MP1	MP2	LP	H	PD
<i>Sarcophilus lanarius</i>					
<i>Sarcophilus harissii</i>					
<i>Antechinus</i> sp. nov. 1					
<i>Antechinus</i> sp.nov. 2					
<i>Antechinus flavipes</i>					
<i>Sminthopsis murina</i>					
<i>Sminthopsis macroura</i>					
<i>Planigale</i> sp.					
<i>Planigale maculata</i>					
<i>Planigale tenurostris</i>	?				
<i>Micromurexia</i> cf. <i>M. habbema</i>					
gen 1 et sp nov. 1					
gen 2 et sp nov 2					
gen 3 et sp. nov 3					
<i>Phascogale</i> sp. nov. 1					
<i>Phascogale topoatafa</i>					
<i>Dasyurus</i> sp. nov. 1					
<i>Dasyurus vivverinus</i>					
<i>Dasyurus hallucatus</i>					
<i>Dasyurus maculatus</i>					
Total Species Richness	13	8	8	7	5
Total Generic Richness	10	6	6	6	5

**Table 7-22. Mt Etna dasyurid succession.**

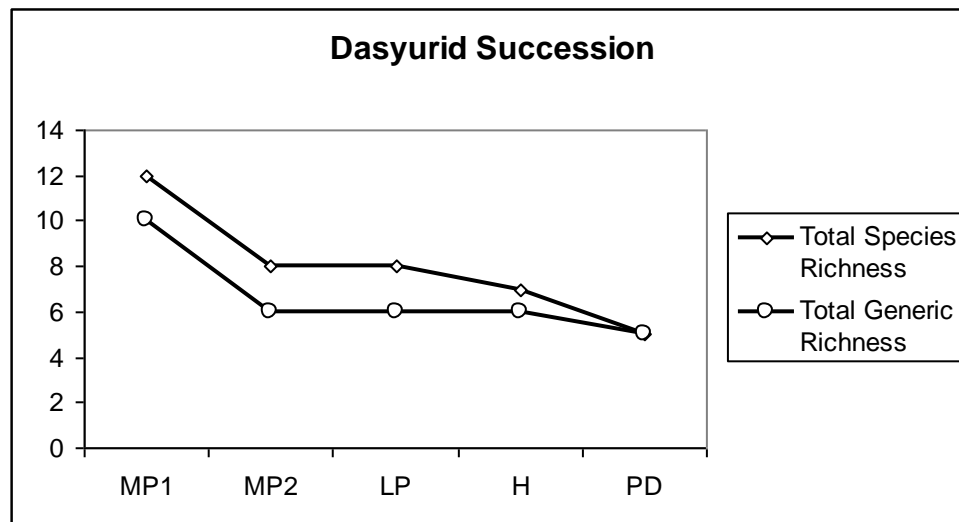


**Figure 7-59. Dasyurid succession at Mt Etna between the middle Pleistocene and present day. MP1 (>280ka), MP2 (205-170ka), LP (<80ka), H (<10ka) PD (present).**

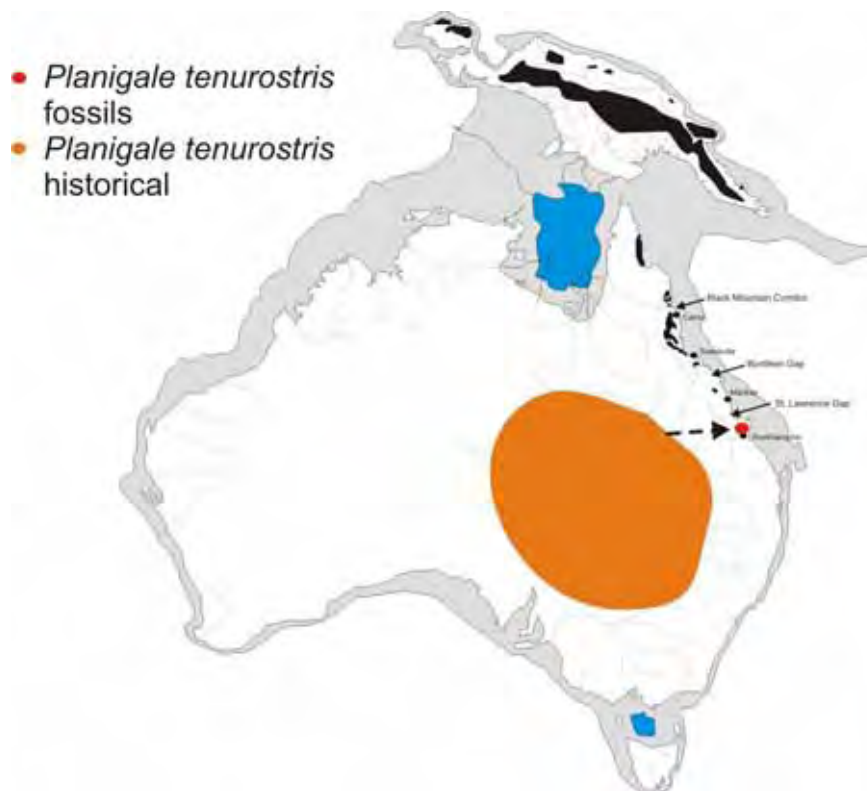


Figure 7-60. Middle Pleistocene (Mt Etna) and present day occurrence of *Planigale tenurostris*.

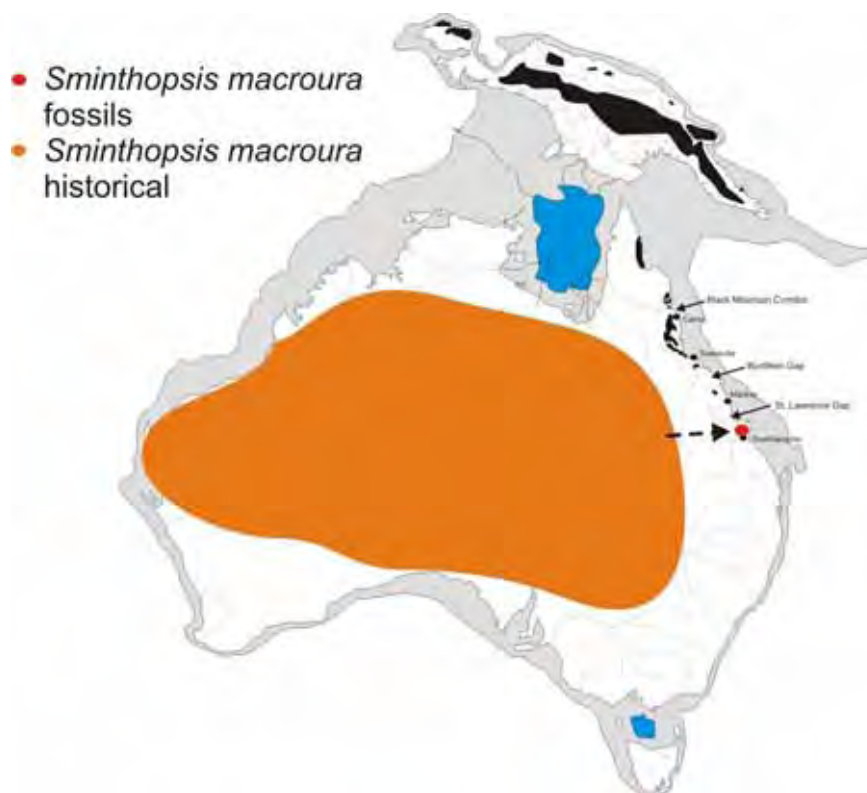


Figure 7-61. Middle Pleistocene (Mt Etna) and present day occurrence of *Sminthopsis macroura*.

### 7.12.9 Terrestrial Omnivores (*perameloids*)

Perameloids exhibit remarkable stability in diversity across the MP1 and MP2 faunal turnover. There is a 100% taxonomic turnover but replacement with an equally diverse MP2 fauna and an increase in generic-level diversity (Fig 7-62). Post-MP2, perameloid diversity declines toward PD levels, with species diversity decreasing stepwise by one taxon each time period, and a sharp decline in generic-level richness stabilising between LP and PD. Like exudivorous petaurids, omnivorous perameloids show remarkable guild-level stability during a period of major taxonomic turnover. After this major turnover, perameloid diversity declines to the present day level of just two species. This pattern, like that seen in dasyurids and rodents, suggests a bimodal level of diversity with arid-zone and rainforest faunas supporting the most diverse faunas, and intermediate, mesic habitats retaining little diversity.

Peramelomorpha	MP1	MP2	LP	H	PD
?Peroryctes sp. 1	■				
?Peroryctes sp. 2	■				
Peroryctid 3	■				
<i>Perameles</i> sp. 1	■				
<i>Perameles</i> sp. 2	■				
<i>Perameles bouganville</i>		■	■		
<i>Perameles nasuta</i>				■	■
<i>Isoodon obesulus</i>		■	■	■	
<i>Isoodon</i> sp. 1		■	■		
<i>Chaeropus ecaudatus</i>		■			
<i>Macrotis lagotis</i>		■			
<i>Isoodon macrourus</i>			■	■	■
Total Species Richness	5	5	4	3	2
Total Generic Richness	3	4	2	2	2

**Table 7-23. Mt Etna bandicoot succession.**

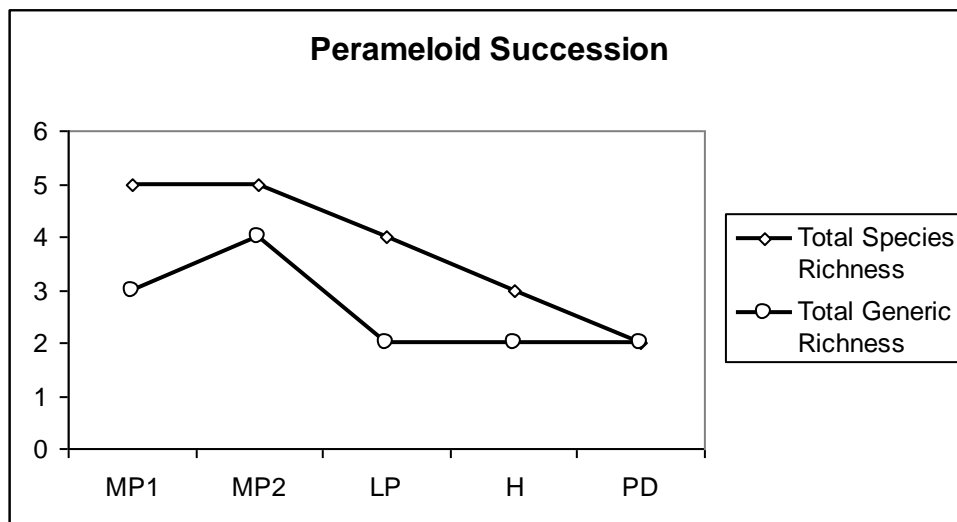


**Figure 7-62.** Perameloid succession at Mt Etna between the middle Pleistocene and present day. MP1 (>280ka), MP2 (205-170ka), LP (<80ka), H (<10ka) PD (present).

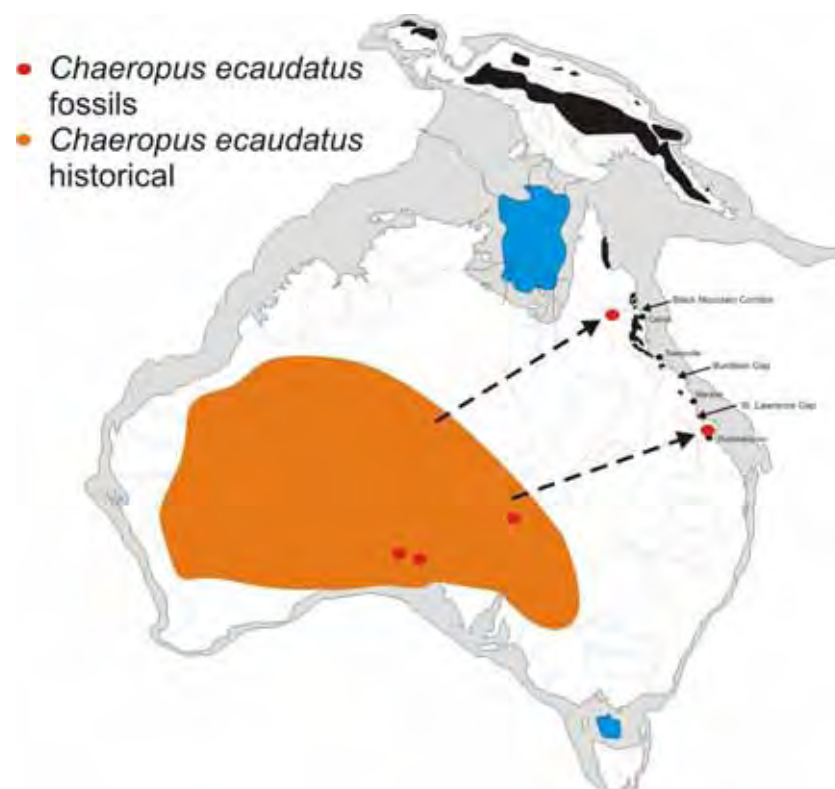


**Figure 7-63.** Middle Pleistocene (Mt Etna & Chillagoe) and present day occurrence of *Chaeropus ecaudatus*.

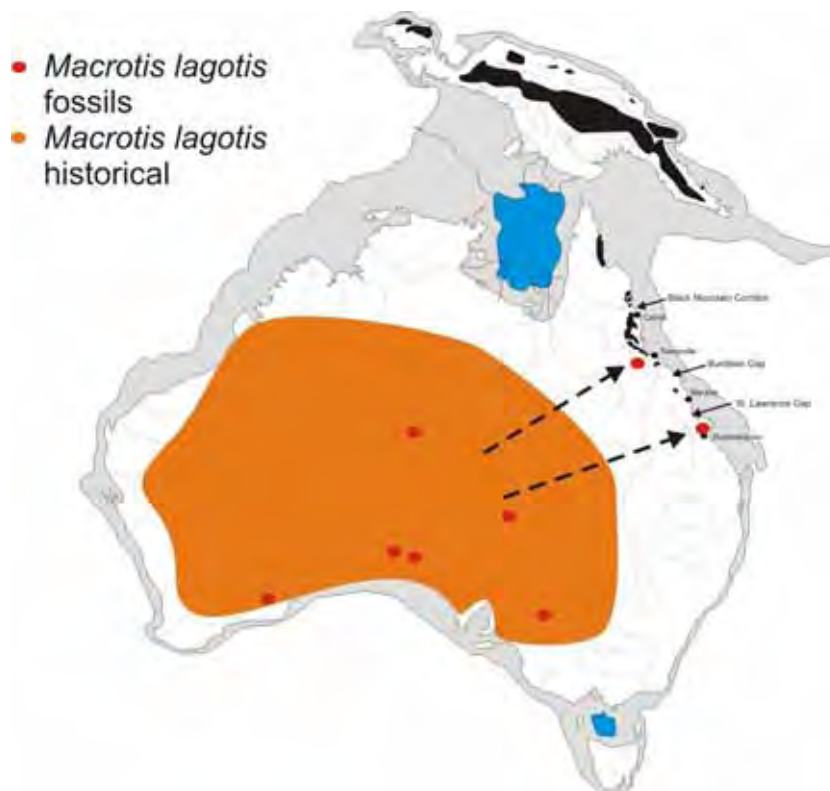


Figure 7-64. Middle Pleistocene (Mt Etna) and late Pleistocene (Broken River) and present day occurrence of *Macrotis lagotis*.

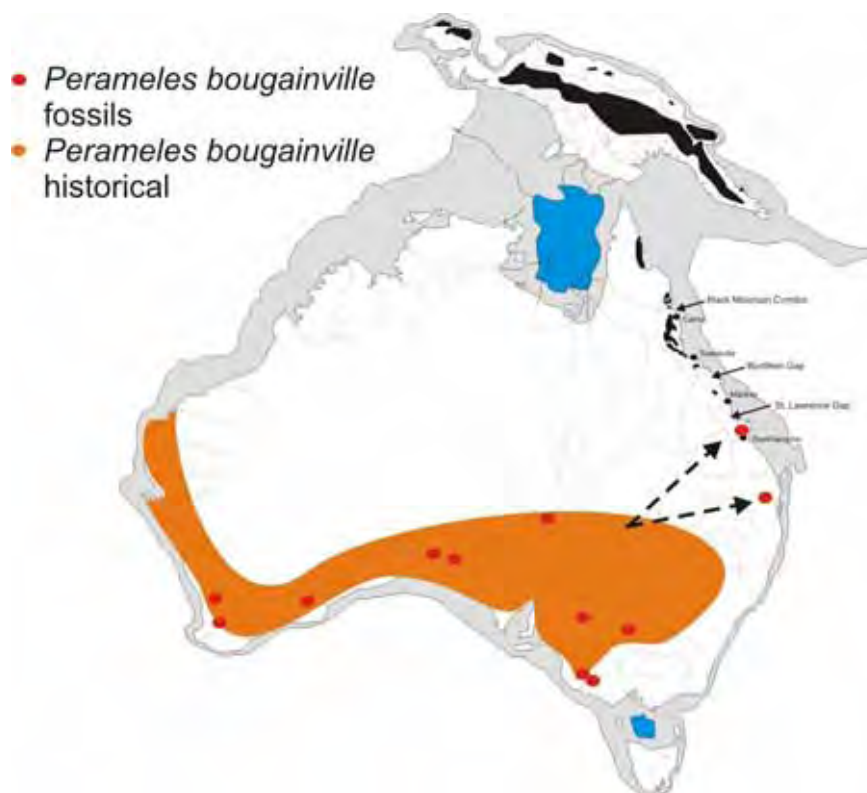


Figure 7-65. Middle Pleistocene (Mt Etna) and late Pleistocene (Darling Downs) and present day occurrence of *Perameles bougainville*.

### 7.12.10 *Reptiles*

Reptiles appear to respond in a similar way to mammals with generally significant loss of diversity during the MP1-MP2 turnover. However, taxonomic uncertainty in large groups of reptiles such as gekkonids and scincids almost certainly biases these results. Nevertheless, localised extinctions between MP1 and MP2 appear to reflect the change from a rainforest-adapted to arid-adapted fauna with the extinction of species of *Hypsilurus*, *Cyclodomorphus* and *Egernia major*. Very large to megafaunal reptiles are biased taphonomically from being represented in MP2 to LP deposits so their true absence remains equivocal. Agamid taxa show the most conspicuous faunal turnover throughout the time period, with *Hypsilurus* species being replaced by three new arid-adapted agamids in MP2. This arid fauna subsequently disappears and is replaced between MP2 and LP by *Diporiphora* species and *Pogona barbata*. The addition of the *Chlamydosaurus* lineage to this group completes the PD agamid fauna.

Reptiles	MP1	MP2	LP	H	PD
<i>Ampibolurus</i>					
<i>Pogona</i> sp. (small)					
<i>Tympanocryptis</i> cf. <i>cephalus</i>					
<i>Hypsilurus</i> sp.					
<i>Diporiphora</i>					
<i>Chlamydosaurus</i>					
<i>Pogona barbata</i>			X	X	
<i>Tiliqua scincoides</i>					
<i>Cyclodomorphus gerrardii</i>					
<i>Tiliqua</i> sp. nov.					
<i>Egernia major</i>					
<i>Egernia</i> sp.					
<i>Sphenomorphus</i> group robust					
<i>Sphenomorphus</i> group gracile					
<i>Varanus</i> sp.					
<i>Varanus</i> cf. <i>V. komodoensis</i>					
gekkonidae					
elapid small					
elapid large					
pythonine small					
pythonine large					
<i>Yurlunggur</i>					
typhlopidae					
<i>Rheodectyes</i>					
chelid					
<i>Quinkana</i> sp.			?		
Total Taxonomic Richness	19	11	8-9	8-9	16
Total Generic Richness	15	10	8-9	8-9	16

**Table 7-24. Mt Etna reptile succession.**

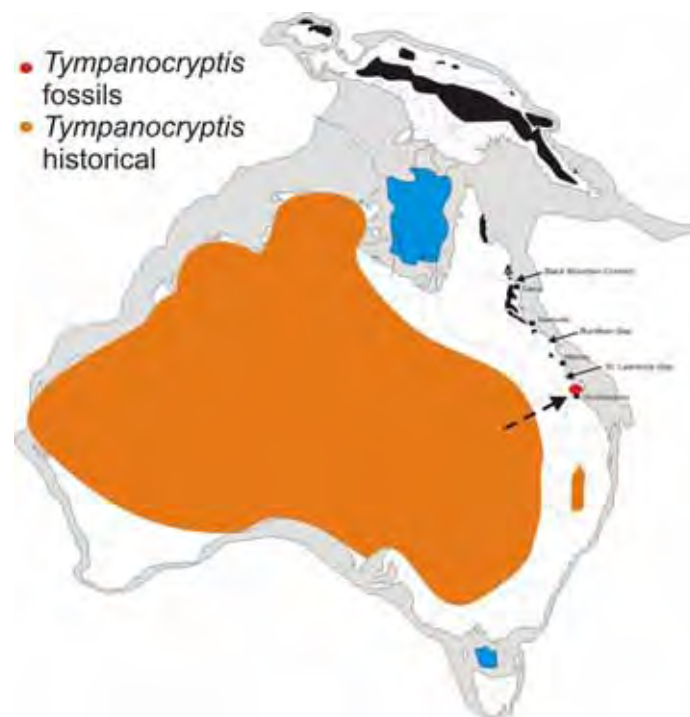


Figure 7-66. Middle Pleistocene (Mt Etna) and present day occurrence of *Tympanocryptis*.

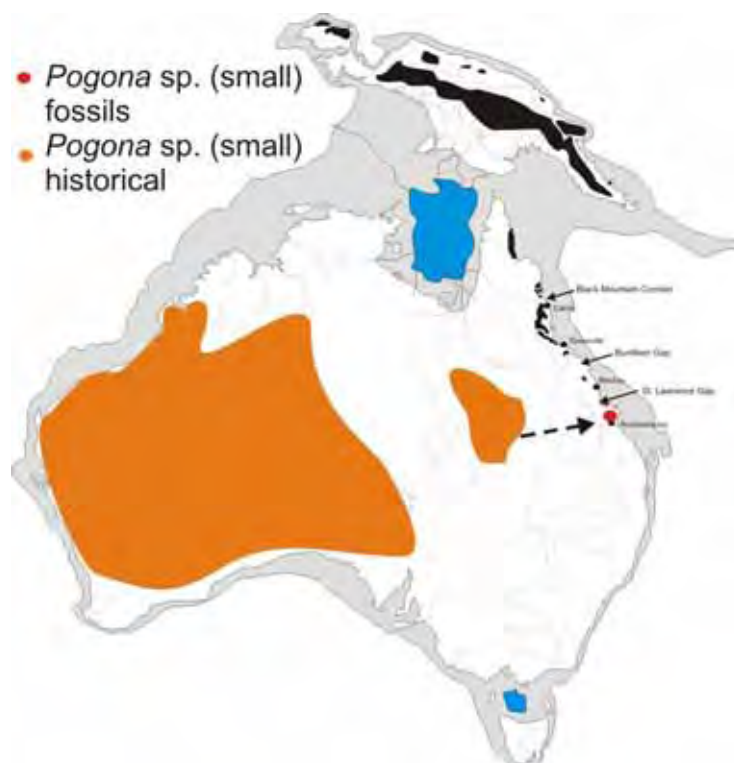


Figure 7-67. Middle Pleistocene (Mt Etna) and present day occurrence of *Pogona* (small).



### 7.13 Conclusions

The Neogene rainforest vertebrate record is an exceptionally rare component of the vertebrate fossil record of Australia. Where present, these localities yield rich and diverse faunas that provide crucial taxonomic, phylogenetic and biogeographic links to modern lineages and entire bioregions.

There is an overall disturbing trend away from primary alpha taxonomy and palaeoecology in Australian vertebrate palaeontology, at a time when it is needed most. Determining the baseline health of ecosystems, their fauna and flora, through recent (Quaternary) times is critical to understanding the natural trajectories with an overprint of climatic change. The addition of anthropogenic modification of the environment also needs to be determined so that future models are robust and account for what is part of the natural cycle and unavoidable.

The long-term trend for Australian rainforests has been to reduce in overall size following a long drying trend and increased climatic variability. However, this has not been reflected in a decrease in species-level diversity in rainforest fauna. Instead, rainforests have held onto their species-level diversity well into the middle Pleistocene, whilst losing higher taxonomic groups, at the genus, family and even super-family level.

The penultimate and last glacial maxima seem to have been the most severe in their impact on northern Australian mesothermic rainforest faunas, with an overall trend since approximately 300,000 years to reduce significantly with no equivalent expansion in times of more equable climate. Here the significant losses are seen between those rainforests of the mid-Pleistocene and present day. This trend over the last ca. 300,000 years has led to an extremely unstable environment in the north, in comparison to more stable environments in the south of the continent. These trends are particularly concerning when considering future climate models and responses of the present fauna to additional change and variability.

The lead up to the present day northern fauna is considered here to be marked by a series of whole-scale faunal turnovers punctuated throughout the last ca. 300,000 years, where any particular prevailing habitat persists and then is completely (or

nearso) replaced by an entirely different fauna. Only a small proportion of the fauna survives these turnovers. Therefore the new replacement fauna is not derived by sympatric evolution of ancestral forms in response to the changing environment. Instead, better adapted taxa replace those of the previous fauna. Therefore, the prevailing responses to the changing environments is not evolution via adaptation. Rather, it is marked by their extinction and replacement by forms already suited to the new climatic regime.

On balance the work presented above indicates that the insitu adaptive ability of mesic fauna in northern Australia is naturally extremely poor, with adaptation not being possible even in times of natural (non-anthropogenic) environmental change. The natural rate of climatic change seems to outstrip the adaptive abilities of the fauna. It, therefore, should not be expected that any particular fauna will adaptively respond to future natural (or human driven) climate change. Instead it might be expected that fauna already adapted to the predicted future climatic regime (e.g. dry and variable) will completely replace the present mesic faunas.

## Chapter 8

### 8.1 Conclusions

Figure 8-1 presents a summarised chronology of key events during the Late Miocene to present day that significantly influenced the evolution, diversification and extinction of mesothermic rainforest faunas in Australia and New Guinea.

The mesothermic rainforests of Australia have undergone a long and complex history of change, including periods of major retraction and extinction. However, following each past period of retraction subsequent, rapid radiations have occurred to fill the voids left by extinct taxa. Across the Middle to Late Miocene, vertebrate extinctions were dominated by small-bodied dietary specialists that were eventually replaced by a variety of taxa with broader diets and more varied body-size.

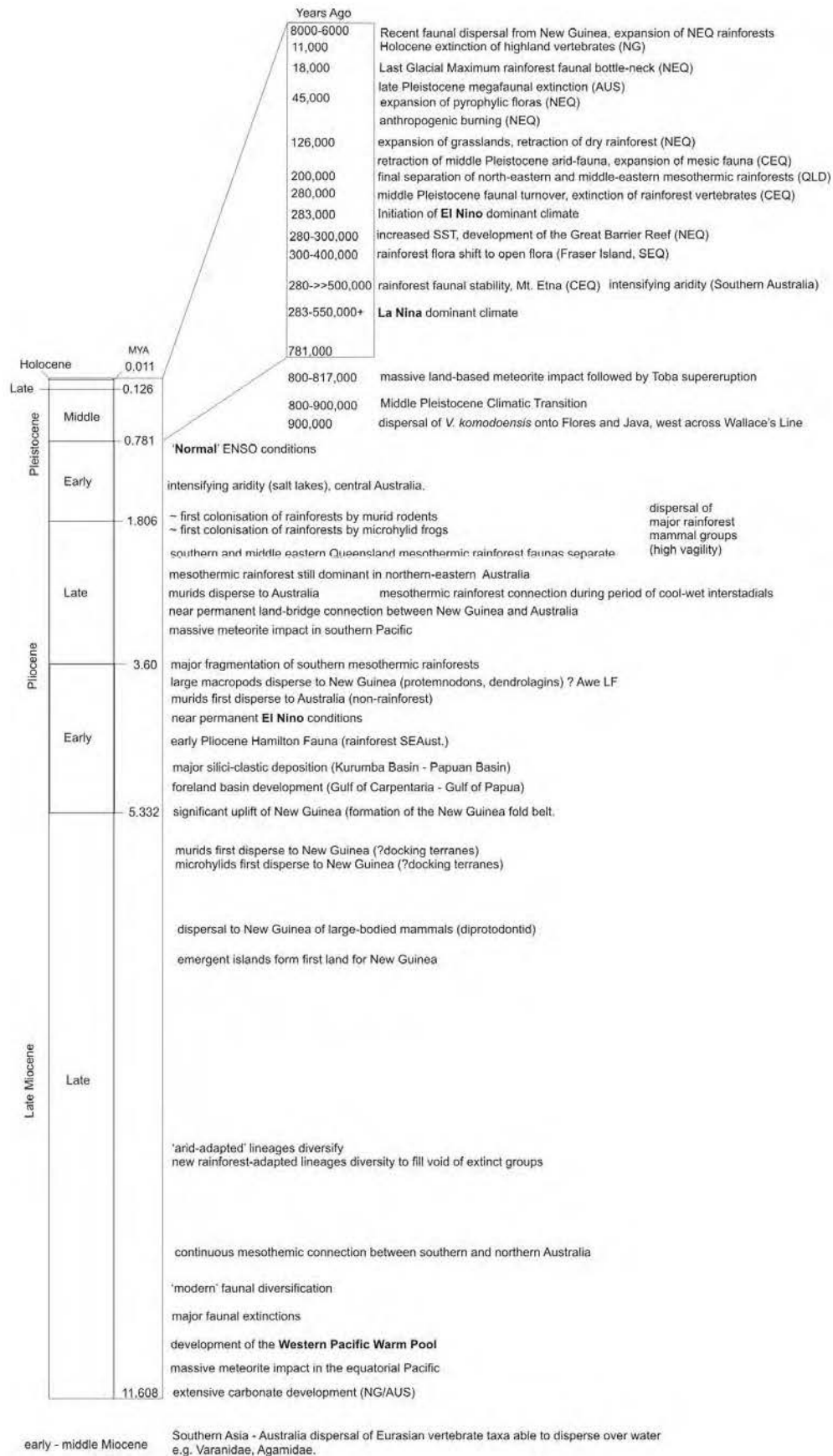


**Figure 8-1. Summary of major events since the Late Miocene that shaped Australian mesothermic rainforest vertebrate faunas**

The Plio-Pleistocene radiations that occurred within mesothermic rainforests echo those from earlier periods. Diverse and numerous taxa derive from relatively few ancestors, mainly due to family-level extinctions. Further, although family-level extinctions were many, morphological diversity also remained high, with morphological equivalents representing almost all Oligo-Miocene families that went extinct. This is reflected in overall species-level diversity in the Plio-Pleistocene, which is on par with the earlier, diverse Oligo-Miocene rainforest faunas. These speciose radiations are in sharp contrast to those of the present day Wet Tropics and New Guinea rainforests, where, for example, non-volant marsupial diversity is exceptionally poor compared with that of the Miocene and Middle Pleistocene. Between the Early Pliocene and Middle Pleistocene very little change in diversity seems to have taken place in mesothermic rainforest faunas. This reflects a relatively long period of stability for mesothermic rainforests in north-eastern Australia, which perhaps acted as important refugia while the rest of the continent underwent major climatic and environmental changes. Stability of mesothermic rainforest in north-eastern Australia appears to have facilitated diversification of modern rainforest vertebrate groups, enabling sympatric speciation and fostering long-term divergence across geographic areas.

During the Pliocene, the new landmass of New Guinea became connected to northern Australia enabling the mainland's diverse rainforest fauna to colonise new terrains to the north. Subsequent climatic and tectonic changes in the region would make this newly emergent land an important refuge for the Australian Plio-Pleistocene rainforest fauna.

Emergence of New Guinea also facilitated the colonisation of Australia by several northern vertebrate groups, two of which diversified in Australopapuan rainforests – microhylid frogs and murid rodents. These groups appear to have arrived in Australian rainforests sometime during the Late Pliocene to Early Pleistocene, when a cool-wet land-bridge existed between Australia and New Guinea. Both groups reached central eastern Queensland by the Middle Pleistocene, but evidently spread no further south. Ultimately these first colonists became locally extinct, and their lineages retracted north, either being driven continentally extinct or into upland refugia in north-eastern Queensland (for example the murid *Uromys hadrourus*). The rise of the New Guinea Highlands and the increased glacial maxima combined with a dominant El Niño system during the Middle to Late Pleistocene to drive the

remaining mesothermic rainforest in north-eastern Queensland into small isolated highland refugia. Mesothermic rainforests in southern and central eastern Queensland lowlands became extinct, whilst smaller refugia in central eastern Queensland hung on in higher altitude mesothermic zones. Rainforest declined significantly in these areas, driving large-bodied elements of the fauna to extinction and leaving the smallest taxa (e.g. microhylid frogs, gekkonids and scincids) as isolated refugees. Mammalian diversity plummeted during the last two glacial maxima, leaving the southern-most refugia in north-eastern Queensland's Wet Tropics with few endemic species. Mesothermic rainforest in north-eastern Queensland finally succumbed during the last glacial maximum when this rainforest was reduced to its smallest ever area. Again mammalian diversity declined to the few endemic refugees today found in the uplands of the Wet Tropics bioregion. A conspicuous example of this is the overall taxonomic richness decline documented between mesothermic Middle Pleistocene rainforest mammals and those of present day rainforests. Comparing the small to large arboreal herbivores present in the Middle Pleistocene rainforests of Mt Etna to the same guild today in the entire Wet Tropics and Cape York, the number of arboreal herbivores has dropped by two-thirds, from 30 to 11 species. Considering only mesothermic rainforest arboreal herbivores, the comparison is even more striking, with 30 versus 7 species being represented, or one quarter the original diversity surviving.

The legacy of this massive decline in rainforest arboreal herbivores may be reflected in dietary specialisations in the arboreal possums of the Wet Tropics. These possums exhibit strict dietary preferences despite a sea of plant diversity, evidently reflecting a phylogenetic constraint left over from a time when the very high diversity of arboreal herbivores in rainforests dictated very fine dietary partitioning. The apparent lack of subsequent dietary expansion suggests relatively recent loss of other arboreal herbivores, probably in the Late Pleistocene or perhaps during the Last Glacial Maximum when mesothermic rainforests were at their smallest viable size for herbivorous mammals.

The Australian continental trend for mesothermic rainforest has been to retract, retract, retract, with rainforest refugia clinging to Australia's eastern margin until climatic thresholds were reached and their extinction followed. Alternatively, these forests became so reduced in size that their vertebrate faunas became extinct and they formed 'ghost' refugia that were subsequently recolonised by other non-rainforest

mesic-adapted fauna. In some cases, these areas continued to enable speciation to occur acting as ‘species pumps’. However, it seems that the pace of climate change has outstripped the capacity of even these long-term refugia to generate new taxa, shifting from being species pumps during the Pliocene to Middle Pleistocene to predominantly ‘species filters’ characterised by taxonomic resilience during the Late Pleistocene to Holocene.

This phenomenon has affected even the most recent arrivals to the mesothermic rainforests, the rodents. The fossil record of rainforest rodents suggests that they arrived sometime before the Middle Pleistocene, which allowed them to speciate within the Australian mesothermic rainforests of northern Australia. However, since the Middle Pleistocene murid diversification in Australian mesothermic rainforests appears to have virtually ceased with any new species representing dispersals from New Guinea.

Probably the most striking conclusion of this research is the clear recognition of the substantial connection of Australian and New Guinea rainforest faunas throughout the Late Miocene and into the Holocene. New Guinea can no longer be considered an isolated island experiment that received from Australia a few early dispersals during the mid-Tertiary with minimal connection until the Late Pleistocene. Instead it must be regarded as a contiguous part of northern Australia and the shared mesothermic rainforests part of the same bioregion – the Tumbuna Biogeographical Province. This study has attempted to bring together a large body of data regarding the evolution, diversification and extinction of Australia’s mesothermic rainforest vertebrates. As with most studies that bring together new information across disciplines, it raises more questions than it answers. Future research should focus on establishing better understanding of these important time periods in the evolution of Australia’s rainforest biota, especially during periods of major climatic change, faunal turnover and extinction, and particularly in the Pleistocene. This includes improved understanding about the specific thresholds tipped to transform rainforest environments from predominantly areas of diversification (species pumps) to refuges from extinction (species filters). Research thus focused will inevitably provide data

essential to test current hypotheses regarding likely threats to extant rainforest habitats under future scenarios of climatic change and environmental disturbance.

Where can these data be found? Fossil evidence must be sought in northern Queensland and New Guinea. Arguably New Guinea offers a greater, virtually untapped, opportunity for gathering data to help understand the impacts of more recent (e.g. Late Pleistocene) climatic changes than might be gathered on mainland Australia. However, integrating data from both New Guinea and northern Australia will undoubtedly provide a better understanding of the conservation status of, and the immediate and long-term strategies needed to protect, the shared biodiversity of both regions.



## References

Abbott, D. H, 2001. Ewing Structure: A Possible Abyssal Impact Crater. *American Geophysical Union*, Fall Meeting 2001, Abstract #P22D-04.

An, Z.S, J.M. Bowler, N.D. Opdyke, P.G. Macumber , J.B. Firman, 1986.  
Palaeomagnetic stratigraphy of Lake Bungunnia: Plio–Pleistocene precursor of aridity in the Murray Basin, southeastern Australia, *Palaeogeograph.*,  
*Palaeoclimatol.*, *Palaeoecol.* 54 (1986) 219-239.

Aplin K.P., J.M. Pasveer, W.E. Boles, 1999. Late Quaternary vertebrates from the Bird's Head Peninsula, Irian Jaya, Indonesia, including the descriptions of two previously unknown marsupial species. *Rec. West. Aust. Mus. Supp.* 57 351-387.

Aplin, K.P. 2006. Chapter 31. Ten million years of rodent evolution in Australasia: phylogenetic evidence and a speculative historical biogeography. (Pp707-744) in *Evolution and Biogeography of Australasian Vertebrates*, J.R. Merrick, M. Archer, G.M. Hickey & M.S.Y. Lee (eds) Auscipub, Oatlands, Australia.

Archer M., R. Arena, M. Bassarova, K. Black, J. Brammall, B. Cooke, P. Creaser, K. Crosby, A. Gillespie, H. Godthelp, M Gotti, S.J. Hand, B. Kear, A. Krikmann, B. Mackness, J. Muirhead, A. Musser, T. Myers, N. Pledge, Y. Wang, S. Wroe. The evolutionary history and diversity of Australian mammals, *Aust. Mamm.* 21(1999) 1-45.

Archer M., S.J. Hand, H. Godthelp, 1995. In: D. Lunney (Ed), *Conservation of Australia's forest fauna*. Royal Society of New South Wales, Mosman, 1991, pp. 67-80.

Archer M., S.J. Hand, H. Godthelp, in: E.S. Vrba, G.H. Denton, T.C. Partridge, L.H. Burckle (Eds.), *Paleoclimate and Evolution, with Emphasis on Human Origins*. Yale Univ. Press, New Haven, 1995, pp. 77-90.

Archer, M. & Dawson, L. 1982 Revision of Marsupial Lions of the genus *Thylacoleo* Gervais (Thylacoleonidae, Marsupialia) and thylacoleonid evolution in the late Cainozoic. In *Carnivorous Marsupials*, Archer M. (ed). Royal Zoological Society of New South Wales. 2: 477-494.

Archer, M. 1981 Results of the Archbold expeditions. No 104. Systematic revision of the marsupial genus *Sminthopsis* Thomas. *Bulletin of the American Museum of Natural History* 168: 61-224.

Archer, M. A. & Wade, M. 1976 Bluff Downs Local Fauna. *Memoirs of the Queensland Museum* 17: 383-398.

Archer, M. A. 1976 The dasyurid dentition and its relationships to that of didelphids, thylacinids, borhyaeniids (Marsupicanivora) and peramelids (Peramelina: Marsupialia). *Australian Journal of Zoology Supplementary Series* No. 39: 1-34.

Archer, M. A. 1984 The Australian marsupial radiation. In *Vertebrate Zoogeography and Evolution in Australasia*. (Animals in space and time). M Archer and G Clayton eds. Hesperian Press. Carlisle. p 633 – 808.

Archer, M. et al., 1998. From Plesiosaurs to People: 100 Million years of Australian Environmental Change. Technical Papers Series, State of the Environment, Australia Canberra, 66pp.

Archer, M., Hand, S.J & Godthelp, H. 1995a. Tertiary Environmental and Biotic Change in Australia. In *Palaeoclimat and evolution, with emphasis on human origins*, Vrba, E.S., Denton, G.H., Partridge, T.C. & Burckle, L.H. (eds). Yale University Press, New Haven.

Archer, M., Hand, S.J. & Godthelp, H. 1995b. *Riversleigh*. Reed Books: Sydney.

Archer, M.A. 1978 Quaternary vertebrate faunas from the Texas Caves of southeastern Queensland. *Memoirs of the Queensland Museum* 19: 61-109.

Archer, M.A., Black, K. & Nettle, K. 1997 Giant Ringtail Possums (Marsupialia, Pseudocheiridae) and Giant Koalas (Phascolarctidae) from the late Cainozoic of Australia. *Proceedings of the Linnean Society of New South Wales* 117: 3-16.

Ast J.C. 2001. Mitochondrial DNA Evidence and Evolution in Varanoidea (Squamata). *Cladistics*, 17, 211–226 (2001).

Auffenberg W, 1981. *The Behavioural Ecology of the Komodo Monitor*. (Uni. Press of Florida, Gainesville FL, 1981) Pp406.

Ayliffe, L.K. & Veeh, H.H. 1988. Uranium-series dating of speleothems and bones from Victoria Cave, Naracoorte, South Australia.

Azzaroli, A., De Giuli, C, Fuccarelli, G. & Torre, D. 1988 Late Pliocene to early-mid Pleistocene mammals in Eurasia: Faunal Succession and dispersal events. *Palaeogeography, Palaeoclimatology, Palaeoecology* 66(1-2): 77-100.

Barker, R.M., Blake, P.R., Burrows, P.E., Crouch, S.B.S., Fordham, B.G.F, Hayward, M.A., Livingstone, M.D., Morwood, D.A., Murray, C.G., Parfrey, S.M., Robertson, A.D.C., Simpson, G.A., Taube, A., Domagala, J. & Randall, R.E. 1997. New insights into the geology of the northern New England Orogen in the Rockhampton-Monto

region, central coastal Queensland: progress report on the Yarrol project. *Queensland Government Mining Journal* 98 (1146): 11-26.

Batholomai, A. 1975 The genus *Macropus* Shaw (Marsupialia: Macropodidae) in the upper Cainozoic deposits of Queensland. *Memoirs of the Queensland Museum* 16(3): 309-363.

Batholomai, A. 1977 The fossil vertebrate fauna from Pleistocene deposits at Cement Mills, Gore, South eastern Queensland. *Memoirs of the Queensland Museum* 18(1): 41-51.

Beck et al., 2008. A bizarre new family of Marsupialia (insertae sedis) from the early Pliocene of northeastern Australia: implications for the phylogeny of bunodont marsupials. *Journal of Palaeontology* 82(4) 749-762.

Bishop, W.W., Chapman, G.R., Hill, A. & Miller, J.A. 1971. Succession of Cainozoic vertebrate assemblages from the northern Kenya Rift Valley. *Nature* 233 (5319): 389-394.

Black, K. 2000 A new species of Palorchestidae (Marsupialia) from the late middle to early late Miocene Encore Local Fauna, Riversleigh, northwestern Queensland. *Memoirs of the Queensland Museum* 41 (2): 181-186.

Black, K., Archer, M., Hand, S.J. (in review). A new Tertiary koala (Marsupialia, Phascolarctidae) from Riversleigh: closer to the roots of the family tree. *Palaeontology*.

Bourke, R.M 1970. A case for conservation – The Mt Etna and Limestone Ridge Caving Area. In: *Mount Etna caves*, Sprent J.K. (ed) p98-114, University of Queensland Speleological Society, St. Lucia, Brisbane.

Bowler J.M, K-H Wyrwoll, Y. Lu, 2001. Variations of the northwest Australian summer monsoon over the last 300,000 years: the paleohydrological record of the Gregory (Mulan) Lakes System. *Quat. Int.* 83-85, 63-80.

Bowler J.M., 1981. Australian salt lakes: a palaeohydrological approach, *Hydrobiologia* 82 (1981) 431-444.

Bowler, J.M. 1982. Aridity in the late Tertiary and Quaternary of Australia. In *Evolution of the Flora and Fauna of Arid Australia*, Barker, W.R. & Greenslade, P.J.M. (eds), 35-45. Peacock Publications, Australian Systematic Botany Society, ANZAAS, South Australian Division: Adelaide.

Braithwaite, R.W., Winter, J.W., Taylor, J.A. & Parker, B.S. 1985 Patterns of diversity and structure of mammalian assemblages in the Australian Tropics. *Australian Mammalogy* 8: 171-186.

Brammal, J.R. 1998. A new petauroid possum from the Oligo-Miocene of Riversleigh, northwestern Queensland. *Alcheringa* 23: 31-50.

Burness G.P., J. Diamond, T. Flannery 2001. *PNAS* 98(25), 14518-14523.

Chen X.Y., C.E.Barton, 1991. Onset of aridity and dune-building in Central Australia: sedimentological and magnetostratigraphic evidence from Lake Amadeus, *Palaeogeograph., Palaeoclimatol., Palaeoecol.* 84 (1991) 55-71.

Chivas, A.R. et al., 2001. Sea-level and environmental changes since the last interglacial in the Gulf of Carpentaria, Australia: an overview. *Quaternary International* 83-85 (2001) 19-46.

Cogger, H.G. 2000. Reptiles and amphibians of Australia 5<sup>th</sup> ed. (Reed: Melbourne) 796p.

Conrad J, 2008. *Bull. Am. Mus. Nat. Hist.* 310, 182pp (2008).

Cramb, J. Hocknull, S.A. & Webb, G. E. 2009. High diversity Pleistocene rainforest dasyurid assemblage with implications for the radiation of the Dasyuridae. *Austral Ecology*, 2009 in Press.

Crosby, K. 2007. Rediagnosis of the fossil species assigned to *Strigocuscus* (Marsupialia: Phalangeridae), with description of a new genus and three new species. *Alcheringa* 31: 33-58.

Davies P.J., F.M. Peerdeman, 1998. In: G.F. Camoin, P.J. Davies, (Eds.) Reef and carbonate platforms in the Pacific and Indian Oceans. International Association of Sedimentologists Special Publication 25, Oxford, Blackwell International, 1998, pp. 22-33.

Davies, H. L., Winn, R.D., & KenGemar, P. 1996. Evolution of the Papuan Basin – a View from the Orogen. Petroleum Exploration, Development and Production in Papua New Guinea: Proceedings of the Third PNG Petroleum Convention, Port Moresby. 53-61.

Dawson, L. & Augee, M.L. 1997 The Late Quaternary sediments and fossil vertebrate fauna from Cathedral Cave, Wellington Caves, New South Wales. *Proceedings of the Linnean Society of New South Wales* 117: 51-78.

Dawson, L. & Flannery, T.F. 1985 Taxonomic and phylogenetic status of living and fossil kangaroos of the genus *Macropus* Shaw (Macropodidae: Marsupialia), with new subgeneric name for the larger wallabies. *Australian Journal of Zoology* 33: 473-498.

Dawson, L. 1982a Taxonomic status of fossil devils (*Sarcophilus*: Dasyuridae, Marsupialia) from the late Quaternary eastern Australia localities. In *Carnivorous Marsupials*, Archer, M. (ed). Surrey Beatty & Sons 2: 516-525.

Dawson, L. 1982b The taxonomic status of fossil thylacines (*Thylacinus*, Thylacinidae, Marsupialia) from late Quaternary deposits in eastern Australia. In *Carnivorous Marsupials*, Archer, M. (ed). Surrey Beatty & Sons 2: 527-536.

Dawson, L. 1983 The taxonomic status of small fossil wombats (Vombatidae: Marsupialia) from the Quaternary deposits, and of related modern wombats. *Proceedings of the Royal Society of New South Wales* 107: 101-123.

Dawson, L. 2004. A new Pliocene tree kangaroo species (Marsupialia, Macropodinae) from the Chinchilla Local Fauna, southeastern Queensland. *Alcheringa* 28: 267-273.

Dawson, L., Muirhead, J. & Wroe, S. 1999. The Big Sink Fauna: a lower Pliocene mammalian fauna from the Wellington Caves complex, Wellington, New South Wales. *Records of the Western Australian Museum*. Supplement No 57: 265-290.

de Garidel-Thoron T., Y. Rosenthal, F. Bassinot, L. Beaufort, 2005. Stable sea surface temperatures in the western Pacific warm pool over the past 1.75million years, *Nature* 433 (2005) 294-298.

de Smet M.E.M *et al.*, 1990. *J. SE Asian Earth Sci.*, 4(4), 337-356.

Dennell R *et al.* 2006, *Palaeogeo. Palaeoclim., Palaeoeco.*, 234, 168-185.

Diamond J.M, 1987 *Nature* 326, 832.

Dunn E.R, 1927. Results of the Douglas Burden into the Island of Komodo, I – Notes on *Varanus komodoensis*, *Am. Mus. Novitates*, 286, 1-10.

Dwyer, P. 1970. Mammals of the Mount Etna Caves. In *Mount Etna caves*, Sprent, J.K. (ed), University of Queensland Speleological Society, St. Lucia, Brisbane.

English P., N.A. Spooner, J. Chappell, D.G. Questiaux, N.G. Hill, 2001. Lake Lewis basin, central Australia: environmental evolution and OSL chronology, *Quat. Int.* 83-85 (2001) 81-101

EPIC Community Members, 2004. Eight glacial cycles from an Antarctic ice core, *Nature* 429 (2004) 623-628.

Fensham, R. J. 1995. Floristics and environmental relations of inland dry rainforest in north Queensland, Australia. *Journal of Biogeography* 22(6): 1047-1063.

Fitch A.J. *et al.*, *Aust. J. Zool.* 54, 253-269.

Flannery T., *Mammals of New Guinea*. Reed Books, Sydney, 1995.

Flannery, T. F. & Szakay, F. S., 1982 *Borha paulae*, a new giant fossil tree kangaroo (Marsupialia: Macropodidae) from New South Wales, Australia. *Australian Mammalogy* 5: 83-94.

Flannery, T. F. 1989. Phylogeny of the Macropodoidea; a study in convergence. Pp 146 in G.C. Grigg, P.J. Jarman & I.D. Hume (eds). *Kangaroos, Wallabies and Rat-kangaroos*. Sydney, Surrey Beatty & Sons.

Flannery, T.F, 1984. Re-examination of the Quanbun Local Fauna, A late Cenozoic Vertebrate Fauna from Western Australia. *Records of the West Australian Museum* 11(2): 119-128.



Flannery, T.F. & Archer, M. 1984 The macropodoids (Marsupialia) of the Pliocene Bow Local Fauna, central eastern New South Wales. *The Australian Zoologist* 7: 193-204.

Flannery, T.F. & Archer, M. 1987. *Strigocuscus reidi* and *Trichosurus dicksoni* , two new fossil phalangerids (Marsupialia: Phalangeridae) from the Miocene of northwestern Queensland. In *Possums and Opossums: studies in evolution*. Archer, M (ed), Surrey Beatty & Sons, Chipping Norton 2: 527-536.

Flannery, T.F. 1992. New Pleistocene marsupials (Macropodidae, Diprotodontidae) from subalpine habitats in Irian Jaya, Indonesia. *Alcheringa* 16: 321-331.

Flannery, T.F., Rich, TH., Turnbull, W.D. & Lundelius, E.L. Jr. 1992. The Macropodoidea (Marsupialia) of the Early Pliocene Hamilton Local Fauna, Victoria, Australia. *Fieldiana, Geology Series* No 25:1-37.

Flannery, T.F., Turnbull, W.D., Rich, T.H.V. & Lundelius, E.L. Jr. 1987. The phalangerids of the early Pliocene Hamilton Local Fauna, southwestern Victoria, pp537-546. In Archer, M ed., *Possums and Opossums: Studies in Evolution*. Surrey Beatty and Sons and the Royal Society of New South Wales, Sydney.

Flynn, L.J., Tedford, R.H. & Zhanxiang, Q 1991. Enrichment and stability in the Pliocene mammalian fauna of north China. *Paleobiology*. 17(3): 246-265.

Freedman, L. & Joffe, A.D. 1966. Skull and tooth variation in the genus *Perameles* Part 3: Metrical Features of *P. gunnii* and *P. bougainville*. *Records of the Australian Museum* 27: 197-217.

Fujioka T., J. Chappell, M. Honda, I. Yatsevich, K. Fifield, D. Fabel, 2005. Global cooling initiated stony deserts in central Australia 2–4 Ma, dated by cosmogenic <sup>21</sup>Ne-<sup>10</sup>Be *Geology* 33(12) 2005 993–996.

Fuller S., P. Braverstock, D. King, 1998. *Mol. Phyl. Evol.*, 9(2), 294-307.

Gaulke M., H.G. Horn, 2004. *Varanus salvator* (n nominate form). In E.R. Pianka & D. R. King (Eds.): *Varanoid Lizards of the World*. (Indiana University Press. Bloomington, Indiana, 2004)

Gerdtz, W.R. & Archbold, N.W. 2003 An early occurrence of *Sarcophilus laniarius harrisii* (Marsupialia, Dasyuridae) from the Early Pleistocene of Nelson Bay, Victoria. *Proceedings of the Royal Society of Victoria* 115 (2): 45-54.

Gersonde, R. 1997. Geological record and reconstruction of the late Pliocene impact of the Eltanin asteroid in the Southern Ocean. *Nature* 390 (357-363).

Gilbert, B.M., Martin, L.D. & Savage, H.G. 1981. *Avian Osteology*. B.Miles Gilbert Publisher: Wyoming Pp 252.

Gillespie, A.K. 2007. Diversity and systematics of marsupial lions from the Riversleigh World Heritage Area and the evolution of the Thylacoleonidae. UNSW, Unpublished PhD Thesis, Sydney, 394pp.

Glass, B.P. & Koeberl, C. 2006. Australasian microtektites and associated impact ejecta in the South China Sea and the Middle Pleistocene super eruption of Toba. *Meteoritics & Planetary Science* 41, (2) 305–326.

Gould G.C, B.J. MacFadden, 2004. *Bull. Am. Mus. Nat. Hist.* 285(1), 219-237.

Greenwood D.R., D.C. Christophel, in: E. Bermingham, C.W. Dick, C. Moritz (Eds.), *Tropical Rainforests Past, Present, and Future*. Univ. Chicago Press, Chicago, 2005. pp. 336-373.

Greer, A.A. 1979 A phylogenetic subdivision of Australian scincid lizards. *Records of the Australian Museum* 32 339-371.

Haines, P.W. 2005. Impact cratering and distal ejecta: the Australian record. *Australian Journal of Earth Sciences* 52, (481–507).

Hammer Ø., D.A.T. Harper, P. Ryan, PAST: Paleontological Statistics Software Package for Education and Data Analysis, *Palaeo. Elect.* 4(1) (2001) 1-9  
[http://palaeo-electronica.org/2001\\_1/pastissue1\\_01.htm](http://palaeo-electronica.org/2001_1/pastissue1_01.htm).

Haq, B.U., Hardenbol, J., & Vail, P.R. 1987. Chronology of fluctuating sea-levels since the Triassic. *Science* 235: 1156-1167.

Heads, M 2002. Regional patterns of biodiversity in New Guinea animals. *Journal of Biogeography* 29: 285-294.

Hecht, M 1975 The morphology and relationships of the largest known terrestrial lizard, *Megalania prisca* Owen, from the Pleistocene of Australia. *Proceedings of the Royal Society of Victoria* 87: 239-250.

Heinshon, T. & Hope, G. 2006. Chapter 5. The Torresian Connections: Zoogeography of New Guinea: (Pp71-94) in Evolution and Biogeography of Australasian Vertebrates, J.R. Merrick, M. Archer, G.M. Hickey & M.S.Y. Lee (eds) Auscipub, Oatlands, Australia.

Hekel, H. 1972 Pollen and spore assemblages from Queensland Tertiary sediments. *Geological Survey of Queensland*, Publications 355, Palaeontology Paper, 30.

Helgen, K.M. & Flannery, T.F. 2004. Notes on the phalangerid marsupial genus *Spilocuscus*, with description of a new species from Papua. *Journal of Mammalogy*, 85(5): 825-833.

Hesse P.P., G.H. McTainsh, Australian dust deposits: modern processes and the Quaternary record, *Quat. Sci. Rev.* 22 (2003) 2007-2035.

Hesse P.P., The record of continental dust from Australia in Tasman Sea sediments, *Quat. Sci. Rev.* 13 (1994) 257-272.

Hijmans R.J., L. Guarino, A. Jarvis, R. O'Brien, P. Mathur, C. Bussink, M. Cruz, I. Barrantes, E. Rojas, DIVA-GIS 5.4 software. (2005) [www.diva-gis.org](http://www.diva-gis.org)

Hilbert, D. W., Graham, A., & Hopkins, M.S. 2007. Glacial and interglacial refugia within a long-term rainforest refugium: The Wet Tropics Bioregion of NE Queensland, Australia. *Palaeogeo. Palaeoclim. & Palaeoecol.* 251: 104-118.

Hocknull, S.A. 2002. Comparative maxillary and dentary morphology of the Australian dragons (Agamidae: Squamata): A framework for fossil identification. *Memoirs of the Queensland Museum.* 48 (1): 125-145.

Hocknull, S.A. 2003 *Etnabatrachus maximus* gen. et sp. nov., a Plio-Pleistocene frog from Mount Etna, central eastern Queensland. *Memoirs of the Queensland Museum* 49(1): 327-330.

Hocknull S.A., 2005. Ecological succession during the late Cainozoic of central eastern Queensland: extinction of a diverse rainforest community, *Mem. Queensland Mus.* 51(1) 39-122.

Hocknull, S.A., J.X. Zhao, Y.X. Feng, G.E. Webb 2007. Responses of middle Pleistocene rainforest vertebrates to climate change in Australia, *Earth Planet. Sci. Lett.* (2007) 264: 317-331.

Holman, J.A. 2000. Fossil snakes of North America: origin, evolution, distribution, paleoecology. Indiana University Press, Indiana.

Hooijer D., *Varanus* (Reptilia, Sauria) from the Pleistocene of Timor. *Zool. Meded.* 47, 445-447 (1972).

Hope G., T. Flannery, and Boeardi. A preliminary report of changing Quaternary mammal faunas in subalpine New Guinea, *Quat. Res.* 40 (1993) 117-126.

Hope, J. H. 1978 Pleistocene mammal extinctions: the problem of Mungo and Menindee, New South Wales. *Alcheringa* 2: 65-82.

Hope, J.H. 1981 A new species of *Thylogale* (Marsupialia: Macropodidae) from Mapala Rock Shelter, Jaya (Carstenz) Mountains, Irian Jaya (Western New Guinea), Indonesia. *Records of the Australian Museum* 33 (8): 369-387.

Horsup, A., James, C. & Porter, G. 1993 Vertebrates of dry rainforest of south and mideastern Queensland. *Memoirs of the Queensland Museum* 34(1): 215-228.

Hutchinson, M.N & Mackness, B.S. 2002. Fossil lizards from the Pliocene Chinchilla Local Fauna, Queensland, with a description of a new species. *Records of the South Australian Museum* 35(2): 169-184.

Hutchinson, M.N. 1992 Origins of the Australian scincid lizards: a preliminary report on the skinks of Riversleigh. *The Beagle, Records of the Northern Territory Museum of Arts and Sciences* 9: 61-69.

Hutchinson, M.N. 1997 The first fossil pygopod (Squamata, Gekkota), and a review of mandibular variation in living species. *Memoirs of the Queensland Museum* 41: 355-366.

International Consortium for Great Barrier Reef Drilling. New constraints on the origin of the Australian Great Barrier Reef: Results from an international project of deep coring, *Geology* 29 (2001) 483-486.

Isern A.R., J.A. McKenzie, D.A. Feary, The role of sea-surface temperature as a control on carbonate platform development in the western Coral Sea, *Palaeogeograph., Palaeoclimatol., Palaeoecol.* 124 (1996) 247-272.

Jansen J.H.F., A. Kuijpers, S.R. Troelstra, A Mid-Brunhes Climatic Event: Long-Term Changes in Global Atmosphere and Ocean Circulation, *Science* 232 (1986) 619-622.

Kanowski, J., Hopkins, M.S., Marsh, H. & Winter, J.W. 2001 Ecological correlates of folivore abundance in north Queensland rainforests. *Wildlife Research* 28: 1-8.

Kawahata H., Shifts in oceanic and atmospheric boundaries in the Tasman Sea (Southwest Pacific) during the Late Pleistocene: evidence from organic carbon and lithogenic fluxes, *Palaeogeograph., Palaeoclimatol., Palaeoecol.* 184 (2002) 225-249.

Kawamura H., A. Holbourn, W. Kuhnt, Climate variability and land-ocean interactions in the Indo Pacific Warm Pool: A 460-ka palynological and organic geochemical record from the Timor Sea, *Mar. Micropaleo.* 59 (2006) 1-14.

Kershaw A.P., S. van der Kaars, P.T. Moss. Late Quaternary Milankovitch-scale climate change and variability and its impact on monsoonal Australasia. *Mar. Geol.* 201 (2003) 81-85.

Kershaw A.P., P.T. Moss, R. Wild, in: E. Bermingham, C.W. Dick, C. Moritz (Eds.), *Tropical Rainforests Past, Present, and Future*. Univ. Chicago Press, Chicago, 2005, pp. 374-400.

Kershaw P., P. Moss, S. van der Kaars, Causes and consequences of long-term climatic variability on the Australian continent, *Fresh. Biol.* 48 (2003) 1274-1283.

Kershaw, A.P. 1986 The last two glacial-interglacial cycles from northeastern Australia: implications for climatic change and Aboriginal burning. *Nature* 322:47-49.

Kershaw, A.P., Bretherton, S.C. & van der Kaars, S. 2007. A complete pollen record of the last 230 ka from Lynch's Crater, north-eastern Australia. *Palaeogeo. Palaeoclim. & Palaeoecol.* 251: 23-45.

Kirkegaard, A.G., Shaw, R.D. & Murray, C.G. 1970. Geology of the Rockhampton and Port Clinton 1:250000 sheet areas. *Geological Survey of Queensland Report* 38: 1-137.

Laurance, W.F. 1997 Responses of mammals to rainforest fragmentation in tropical Queensland: a review and sythesis. *Wildlife Research* 24: 603-612.

Lawrence K.T., T.D. Herbert, Late Quaternary sea-surface temperatures in the western Coral Sea: Implications for the growth of the Australian Great Barrier Reef, *Geology* 33 (2005) 677-680.

- Lee, M.S.Y. 1996. Possible affinities between *Varanus giganteus* and *Megalia prisca*. *Memoirs of the Queensland Museum* 39(2):232.
- Li, Q., et al., 2006. Late Miocene development of the western Pacific warm pool: Planktonic foraminifer and oxygen isotopic evidence. *Palaeogeography, Palaeoclimatology, Palaeoecology* 237 (2006) 465–482.
- Lindsey, T.R. 1992. Encyclopedia of Australian Animals, Birds. Angus & Robertson : NSW Pp469.
- Long, J., Archer, M., Flannery, T. & Hand, S. 2002 Prehistoric Mammals of Australia and New Guinea (One hundred million years of evolution). UNSW Press: Sydney Pp 244.
- Long, J.A. & Mackness, B.S. 1994. Studies of the late Cainozoic diprotodontid marsupials of Australia. 4. The Bacchus Marsh Diprotodons – geology, sedimentology and taphonomy. *Records of the South Australian Museum*. 27: 95-110.
- Longman 1925a Fossil marsupials from Marmor. *Memoirs of the Queensland Museum*. 8(2): 109-110
- Longman 1925b Ophidian vertebrae from cave deposits at Marmor Quarry. *Memoirs of the Queensland Museum* 8(2): 111-112.
- Longman, H. 1921 A new genus of fossil marsupial. *Memoirs of the Queensland Museum* 7: 65-80.
- Longman, H. 1924 Some Queensland fossil vertebrates. *Memoirs of the Queensland Museum*. 8(1):16-28.



Longmore M.E., H. Heijnis, Aridity in Australia: Pleistocene records of Palaeohydrological and Palaeoecological change from the perched lake sediments of Fraser Island, Queensland, Australia, *Quat. Int.* 57-58 (1999) 35-47.

López-Otálvaro, G-E et al., 2008. Variations in coccolithophorid production in the Eastern Equatorial Pacific at ODP Site 1240 over the last seven glacial–interglacial cycles. *Marine Micropaleontology* 69 (2008) 52–69.

Luckett, P.W. 1993. An ontogenetic assessment of dental homologies in therian mammals. In *Mammal Phylogeny; Mesozoic Differentiation, Multituberculates, Monotremes, Early Therians and Marsupials*. Szalay, S.F., Novacek, M.J. & McKenna, M.C. (eds) Springer-Verlag, New York, 182-284.

Lundelius, E.L. Jr. 1989 The implications of disharmonious assemblages for Pleistocene extinctions. *Journal of Archaeological Science*. 16: 407-417.

Lundelius, E.L., Jr. 1983 Climate implications of late Pleistocene and Holocene faunal associations in Australia. *Alcheringa* 7: 125-149.

Lydekker R, Mem. Geol. Surv. India, Palaeo. Indica, 10(3), 1-32 (1886).

Mackness, B.S. & Hutchinson, M.N. 2000. Fossil lizards from the Early Pliocene Bluff Downs Local Fauna. *Transactions of the Royal Society of South Australia*. 124 (1): 17-30.

Mackness, B.S. Scanlon, J.D. 1999. The first Pliocene record of the madtsoiid snake genus *Yurlunggur* Scanlon, 1992 from Queensland. *Memoirs of the Queensland Museum* 43(2): 783-785.

Mackness, B.S. Whitehead, P.W. & McNamara, G.C. 2000 New potassium-argon basalt date in relation to the Pliocene Bluff Downs Local Fauna, northern Australia. *Australian Journal of Earth Sciences*. 47: 807-811.

Macphail, M. 2007. Australian palaeoclimates: Cretaceous to Tertiary A review of palaeobotanical and related evidence to the year 2000. CRCLEME Special Report, *CRC LEME Open File Report* 151. 279pp.

Macphail, M.K. 1996 Neogene environments in Australia, 1: re-evaluation of microfloras associated with important Early Pliocene marsupial remains at Grange Burn, southwest Victoria. *Review of Palaeobotany and Palynology* 92: 307-328.

Macphail, M.K. 1997 Late Neogene Climates in Australia: Fossil Pollen– and Spore-based Estimates in Retrospect and Prospect. *Australian Journal of Botany* 45: 425-464.

Maddison, D.R. & Maddison, W.P. 2000. MacClade Version 4.02. Sinauer Associates Inc. Publishers, Massachusetts.

Martin, H.A. & McMinn, A. 1993 Palynology of sites 815 and 823. The Neogene vegetation history of coastal vegetation of coastal northeast Australia. *Proceedings of the ODP Sciences Results* 133: 115-125.

McGowran, B et al., 2000. Australasian palaeobiogeography: the Palaeogene and Neogene Record. *Mem. Assoc. Australasian Palaeontologists* 23: 405-470.

McNamara, G.C. 1990. The Wyandotte Local Fauna: a new, dated Pleistocene vertebrate fauna from northern Queensland. *Memoirs of the Queensland Museum*. 28 (1): 285-297.

Medina-Elizalde M., D.W. Lea, The mid-Pleistocene transition in the tropical Pacific, *Science* 310 (2005) 1009-1012.

Menzies, J. 2006. The frogs of New Guinea and the Solomon Islands. Pensoft, Bulgaria. 345pp.

Menzies, J. et al., 2008. Possible early age for a diprotodon (Marsupialia: Diprotodontidae) fossil from the Papua New Guinea highlands. *Alcheringa*. 32, 129–147.

Menzies, J.I, Russell, L., Tyler, M.J. & Mountain, M.-J. 2002. Fossil frogs from the central highlands of Papua New Guinea. *Alcheringa* 26: 341-351.

Meredith, R. Westerman, M. & Springer, M.S. 2008. A timescale and phylogeny for ‘bandicoots’ (Peramelomorpha: Marsupialia) based on sequences for five nuclear genes. *Molecular Phylogeny and Evolution* 47(2008): 1-20.

Molnar R.E., *Dragons in the Dust: The palaeobiology of the Giant Monitor Lizard Megalania*. (Indiana Uni. Press, Indiana, 2004) Pp210.

Molnar, R. E. & Kurz, C. 1997. The distribution of Pleistocene vertebrates on the eastern Darling Downs, based on the Queensland Museum collections. *Proceedings of the Linnean Society of New South Wales*. 117: 107-134.

Molnar, R.E. 1982. Pleistocene ziphodont crocodilians of Queensland. *Records of the Australian Museum*. 33: 803-834.

Molnar, R.E. 1990, New cranial elements of a giant varanid from Queensland. *Memoirs of the Queensland Museum* 29 (2): 437-444.

Moriarty, K.C., McCulloch, M.T., Wells, R.T., McDowell, M.C., 2000. Mid-Pleistocene cave fills, megafaunal remains and climate change at Naracoorte, South Australia: Towards a predictive model using U-Th dating of speleothems, *Palaeogeograph., Palaeoclimatol., Palaeoecol.*, 159 (2000) 113–143.

Moritz, C.W. Dick, E. Bermingham, 2005. From the Past to the Future: Evolution, Ecology and Conservation of Tropical Rainforests, in: E. Bermingham, C.W. Dick, C. Moritz, (Eds.), *Tropical Rainforests Past, Present, and Future*, Univ. of Chicago Press, Chicago, 2005, pp. 1-3.

Morwood M.J *et al.*, 2004. *Nature* 431, 1087–1091.

Moss, P.T. & Kershaw, A.P. 2007. A late Quaternary marine palynological record (oxygen isotope stages 1 to 7) for the humid tropics of northeastern Australia based on ODP Site 820. *Palaeogeo. Palaeoclim. & Palaeoecol.* 251: 4-22.

Muirhead, J. & Filan, S.L. 1995. *Yarala burchfieldi*, a plesiomorphic bandicoot (Marsupialia: Peramelemorphia) from the Oligo-Miocene deposits of Riversleigh, northwestern Queensland. *Journal of Palaeontology* 69: 127-134.

Muirhead, J. & Godthelp, H 1995. Fossil bandicoots of Chillagoe (Northeastern Queensland) and the first known specimens of the Pig-Footed Bandicoot *Chaeropus* Ogilby, 1838 from Queensland. *Australian Mammalogy* 19:73-76.

Muirhead, J. 1994. Systematics, evolution and palaeobiology of recent and fossil bandicoots (Peramelemorphia: Marsupialia). PhD thesis, University of New South Wales, Sydney, NSW.

Muirhead, J. 1999. Bandicoot diversity and evolution (Peramelemorphia: Marsupialia): the fossil evidence. *Australian Mammalogy* 21:11-13.

Muirhead, J. 2000, Yaraloidea (Marsupialia, Peramelemorphia), a new superfamily of marsupial and a description and analysis of the cranium of the Miocene *Yarala burchfieldi*. *Journal of Palaeontology* 74: 512-523.

Muirhead, J., Dawson, L. & Archer, M. 1997. *Perameles bowensis*, a new species of *Perameles* (Peramelemorphia, Marsupialia) from the Pliocene faunas of Bow and Wellington Caves, New South Wales. *Proceedings of the Linnean Society of New South Wales* 117: 163-173.

Muller, R.D., Lim, V.S.L. & Isern, A.R. 2000. Late Tertiary tectonic subsidence on the northeast Australian passive margin: response to dynamic topography? *Marine Geology* 162: 337–352

Murphy J.B. *et al.*, 2002. *Komodo Dragons: Biology and Conservation*. (Smithsonian Press, Washington, 2002) Pp 268.

Murray, P.F. 1998. Palaeontology and Palaeobiology of wombats. In Wombats Wells, RT. & Pridmore, P.A. (eds). Surrey Beatty & Sons, Chipping Norton 1:1-33.

Myers, T.J. 2001. Prediction of marsupial body mass. *Australian Journal of Zoology*, 49: 99-118.

Nanson G.C., T.J. East, R.G. Roberts, 1993. Quaternary stratigraphy, geochronology and evolution of the Magela Creek catchment in the monsoon tropics of northern Australia, *Sed. Geol.* 83 (1993) 277-302.

Nelson, J. E. 1989. Megadermatidae. In Fauna of Australia Volume 1B Mammalia, Walton, D.W. & Richardson, B.J. (eds) ABRS & Australian Government Publishing Service: Canberra

Nix H.A. 1982. Environmental determinants of biogeography and evolution in Terra Australis, in: W.R. Barker, P.J.M. Greenslade (Eds.), *Evolution of the Flora and Fauna of Arid Australia*. Peacock Publications and the Australian Systematic Botany Society, Adelaide, 1982, pp. 35-45.

Nix, H.A. & Switzer, M.A. 1991. *Rainforest Animals: Atlas of Vertebrates Endemic to Australia's Wet Tropics*. Kowari 1. Australian National Parks and Wildlife Service: Canberra.

Norris, C.A. & Musser, G.G. 2001. Systematic revision within the *Phalanger orientalis* complex (Diprotodontia: Phalangeridae): a third species of lowland Gray Cuscus from New Guinea and Australia. *American Museum Novitates* (3356): 20pp.

Osborne, M.J. & Christidis, L. 2002. Molecular relationships of the cuscuses, brushtail and scaly-tailed possums (Phalangerinae). *Australian Journal of Zoology*, 50: 135-139.

Owen, R. 1859. *Phil. Trans. Roy. Soc. London*, 161, 213-266.

OZCAM community, BioMaps. (2006) [www.biomaps.net.au/biomaps](http://www.biomaps.net.au/biomaps)

Peerdeman F.M, P.J. Davies, P.J. A.R. Chivas, 1993. The stable oxygen isotope signal in shallow-water, upper slope sediments off the Great Barrier Reef (Hole 820A), *Proc. Ocean Drill. Pro. Sci. Res.* 133 (1993) 163-173.

Pelejero C., E. Calvo, T.T. Barrows, G.A. Logan, P. De Deckker, 2006. South Tasman Sea alkenone palaeothermometry over the last four glacial/interglacial cycles *Mar. Geol.* 230 (2006) 73–86.

Philip, G.M. and Pedder, A.E.H., 1967. Stratigraphical correlation of the principal Devonian limestone sequence of eastern Australia. In *International Symposium on the*

Devonian System, D.H. Oswald (ed), Calgary, Alberta Society of Petroleum Geologists, v.2: 1025-1041.

Pianka E.R, 1995. *Am. Nat.* 146(3), 398-414.

Pigram, C.J. & Davies, H.L. 1987. Terranes and the accretion history of the New Guinea orogen. *BMR Journal of Australian Geology and Geophysics*, 10: 193-211.

Pillans B., R. Bourman, 2001. Mid Pleistocene arid shift in southern Australia, dated by magnetostratigraphy, *Aust. J. Soil Res.* 39 (2001) 89-98.

Piper K.J., 2007. Early Pleistocene Mammals from The Nelson Bay Local Fauna, Portland, Victoria, Australia, *J. Vert. Palaeo.* 27(2):492-503.

Plane, M.D. 1967. Stratigraphy and vertebrate fauna of the Otibanda Formation, New Guinea. Bureau of Mineral Resources, Geology & Geophysics Bulletin, No. 86, Pp 1-64.

Pledge, N. S. 1977 A new species of *Thylacoleo* (Marsupialia: Thylacoleonidae) with notes on the occurrences and distribution of Thylacoleonidae in South Australia. *Records of the South Australian Museum.* 17: 277-283.

Pledge, N.S. 1987. *Phascolarctos maris*, a new species of koala (Marsupialia: Phascolarctidae) from the Early Pliocene of South Australia. In Possums and opossums: Studies in evolution, Archer, M (ed), p327-330. Royal Zoological Society of New South Wales and Surrey Beatty & Sons Pty Ltd, Sydney.

- Pledge, N.S. 1992. The Curramulka Local Fauna: a new late Tertiary fossil assemblage from Yorke Peninsula, South Australia. *The Beagle, Records of the Northern Territory Museum of Arts and Sciences*. 9(1): 111-113.
- Pope L, Storch D, Adams M, Moritz C and Gordon G. 2001. A phylogeny for the genus *Isoodon* and a range extension for *I. obesulus peninsulae* based on mtDNA control region and morphology. *Australian Journal of Zoology* **49**, 411–434
- Price, G. J. et al., 2009. New U/Th ages for Pleistocene megafauna deposits of southeastern Queensland, Australia. *Journal of Asian Earth Sciences*, 34 (2009), 190-197.
- Price, G.J. & Webb, G.E., 2006. Late Pleistocene sedimentology, taphonomy and megafauna extinction on the Darling Downs, southeastern Queensland, Australia. *Australian Journal of Earth Sciences*, 53 (6): 947-970.
- Price, G.J. 2002. *Perameles sobbei* sp. nov. (Marsupialia: Peramelidae) a Pleistocene bandicoot from the Darling Downs, south-eastern Queensland. *Memoirs of the Queensland Museum* 48: 193-197.
- Prideaux G.J., J.A. Long, L.K. Ayliffe, J.C. Hellstrom, B. Pillans, W.E. Boles, Hutchinson M.N., R.G. Roberts, M.L. Cupper, L.J. Arnold, P.D. Devine, N.M. Warburton, 2007. An Arid-Adapted Middle Pleistocene Vertebrate Fauna from South-Central Australia *Nature* 445 (2007) 422-425.
- Prideaux G.J., R.G. Roberts, D. Megirian, K.G. Westaway, J.C. Hellstrom, J.M. Olley, 2007. Mammalian responses to Pleistocene climate change in southeastern Australia, *Geology* 35(1) (2007) 33-36.
- Prideaux, G. J. & Warburton, N.M. 2008. A new Pleistocene tree kangaroo (Diprotodontia: Macropodidae) from the Nullarbor Plains of southern central Australia. *Journal of Vertebrate Palaeontology* 28(2): 463-478.



Prideaux, G.J. 1999. *Borungaboodie hatcheri* gen. et sp. nov., a very large bettong (Marsupialia: Macropodidae) from the Pleistocene of south western Australia. Records of the Western Australian Museum Suppl. Series 57: 317-329.

Reed E.H., M.N. Hutchinson, First record of a giant varanid (*Megalania*, Squamata) from the Pleistocene of Naracoorte, South Australia. *Mem. Qld. Mus.* 51(1):203-214 (2005).

Reed, E.H. & Bourne, S.J. 2000 Pleistocene fossil vertebrate sites of the south east region of South Australia. *Transactions of the Royal Society of South Australia.* 124(2): 61-90.

Reed, E.H. 2002. Vertebrate taphonomy of large mammal bone deposits, Naracoorte Caves World Heritage Area. Unpublished PhD Thesis, Flinders University.

Rich, T.H. 1991 Monotremes, placentals and marsupials: their record in Australia and its biases. In *Vertebrate palaeontology of Australasia*. Vickers-Rich, P., Monaghan, J.M., Baird, R.F., Rich, T.H. (eds) Pioneer Design Studio, Studio, Melbourne: 1005-1058.

Sandiford, M. 2007. The tilting continent: A new constraint on the dynamic topographic field from Australia. *Earth and Planetary Science Letters* 261 (2007) 152–163.

Sato, K., et al., 2008. Establishment of the western Pacific warm pool during the Pliocene: Evidence from planktic foraminifera, oxygen isotopes, and Mg/Ca ratios. *Palaeogeography, Palaeoclimatology, Palaeoecology* 265 (2008) 140–147.

- Scanlon, J.D. & Lee, MSY. 2000. The Pleistocene serpent *Wonambi* and the early evolution of snakes. *Nature* 403 (416-420).
- Scanlon, J.D. 1992. A new large madtsoiid snake from the Miocene of the Northern Territory. *The Beagle* 9: 49-60.
- Scanlon, J.D. 1995. First records from Wellington Caves, New South Wales, of the extinct madtsoiid snake, *Wonambi naracoortensis* Smith 1976. *Proc. Linn. Soc. NSW* 115: 233-238.
- Scanlon, J.D., Lee, MSY & Archer, M. 2003. Mid-Tertiary elapid snakes (Squamata: Colubroidea) from Riversleigh, Northern Australia: early steps in a continental-wide adaptive radiation. *Geobios* 36(5), 573-601.
- Schneider C.J., S.E. Williams, 2005. in: E. Bermingham, C.W. Dick, C. Moritz (Eds.), *Tropical Rainforests Past, Present, and Future*. Univ. Chicago Press, Chicago, 2005, pp. 401-424.
- Shannon, C.H.C. 1970a Cave descriptions. In: *Mount Etna caves*, Sprent, J.K. (ed) p22-36, University of. Queensland Speleological Society, St. Lucia, Brisbane.
- Shannon, C.H.C. 1970b Geology of the Mount Etna area. In: *Mount Etna caves*, Sprent, J.K. (ed) p11-21, University of. Queensland Speleological Society, St. Lucia, Brisbane.
- Shea, G.M. 1990. The genera *Tiliqua* and *Cyclodomorphus* (Lacertilia: Scincidae): generic diagnoses and systematic relationships. *Memoirs of the Queensland Museum* 29: 495-520.

Simpson, G.A., Crouch, S.B.S., Murray, C.G., Withnall, I.W. & Blight, R.K.J. 2001. Ridgeland, Queensland Sheet 8951; first edition (1:100 000 Geological Series). Department of Natural Resources and Mines, Brisbane.

Smith, M.J. 1972 Small fossil vertebrates from Victoria Cave, Naracoorte, South Australia. II. Peramelidae, Thylacinidae and Dasyuridae (Marsupialia). *Transactions of the Royal Society of South Australia*. 96(2): 71-84.

Smith, M.J. 1976 Small fossil vertebrates from Victoria Cave, Naracoorte, South Australia. IV. Reptiles. *Transactions of the Royal Society of South Australia*. 100(1): 39-51.

Specht R.L., 1981. Major vegetation formations in Australia, in: A. Keast (Ed.), Ecological Biogeography of Australia. Dr. W. Junk, The Hague, 1981, pp. 165-295.

Stephenson A.E. 1986, Lake Bungunna – a Plio-Pleistocene megalake in southern Australia, *Palaeogeograph., Palaeoclimatol., Palaeoecol.* 57 (1986) 137-156.

Stirton, R.A. 1936. Succession of North American Continental Pliocene faunas. *American Journal of Science*. 32 (189) 161-206.

Strahan, R (ed) 1995. The Mammals of Australia. Australian Museum and Reed Books: Sydney.

Suwitodirdjo K., S. Tjokrosapoetro. *Geologic Quadrangle Map, Timor*, (GRDC , Bandung (1974/75).

Swofford, D.L. 2000. PAUP: phylogenetic analysis using parsimony. Version 4.0b10. Illinois Natural History Survey, Champaign, Australia.

Tcherepanov, E.N et al, 2008. Carbonate seismic stratigraphy of the Gulf of Papua mixed depositional system: Neogene stratigraphic signature and eustatic control. *Basin Research* 20, 185–209.

Tedford, R.H. 1994 Succession of Pliocene through Medial Pleistocene mammal faunas of Southeastern Australia. *Records of the South Australian Museum* 27 (2): 79-93.

Tedford, R.H., Wells, R.T. & Barghoorn, S.F. 1992 Tirari Formation and contained faunas, Pliocene of the Lake Eyre Basin, South Australia. *The Beagle, Records of the Northern Territory Museum of Arts and Sciences* 9 (1): 173-193.

Thomas, C. D., Cameron, A., Green, R. E., Bakkenes, M., Beaumont, L. J., Collingham, Y. C., Erasmus, B. F. N., de Siqueira, M. F., Grainger, A., Hannah, L., Hughes, L., Huntley, B., van Jaarsveld, A. S., Midgley, G. F., Miles, L., Ortega-Huerta, M. A., Peterson, A. T., Phillips, O. L., Williams, S. E., 2004. Extinction risk from climate change. *Nature* 427 (2004) 145-148.

Thomson, S.A. 2000. A revision of the fossil chelid turtles (Pleurodira) described by C.W. Devis (1897). *Memoirs of the Queensland Museum* 43: 593-598.

Toop, J. 1985 Habitat requirements, survival strategies and ecology of the Ghost bat *Macroderma gigas* Dobson, (Microchiropteran, Megadermatidae) in central coastal Queensland. *Macroderma* 1: 37-44.

Turbull, W.D., Lundelius, E.L. Jr. & Archer, M.A. 2003. Dasyurids, perameloids, phalangeroids and vombatoids from the Early Pliocene Hamilton Fauna, Victoria, Australia. Chapter 18. *Bulletin American Musuem of Natural History* 279: 513-540.

Turnbull, W.D. & Lundelius, E.L. Jr. 1970 The Hamilton fauna. A late Pliocene mammalian fauna from the Grange Burn, Victoria, Australia. *Fieldiana: Geology, New Series* No 19. 1-163.

Turnbull, W.D., Lundelius, E.L. Jr. & Tedford, R.H. 1992. A Pleistocene marsupial fauna from Limeburner's Point, Victoria, Australia. *The Beagle, Records of the Northern Territory Museum of Arts and Sciences*. 9: 143-172.

Tyler, M. J. & Lee, M.S.Y. 2006. Chapter 12 The origins of Australian frogs. (Pp237-240) in *Evolution and Biogeography of Australasian Vertebrates*, J.R. Merrick, M. Archer, G.M. Hickey & M.S.Y. Lee (eds) Auscipub, Oatlands, Australia.

Tyler, M.J. 1976. Comparative osteology of the pelvic girdle of Australian frogs and description of a new fossil genus. *Transactions of the Royal Society of South Australia* 100(1): 3-14.

Tyler, M.J. 1988. *Neobatrachus pictus* (Anura: Leptodactylidae) from the Miocene/Pliocene boundary of South Australia. *Transactions of the Royal Society of South Australia* 112: 91.

Tyler, M.J. 1991. *Kyarannus* Moore (Anura, Leptodactylidae) from the Tertiary of Queensland. *Proceedings of the Royal Society of Victoria* 103(1): 47-51.

Tyler, M.J., Davis, A.C. & Williams, C.R. 1998. Pleistocene frogs from near Cooma, New South Wales. *Proceedings of the Linnean Society of New South Wales* 119: 107-113.

Tyler, M.J., Godthelp, H. & Archer, M. 1994. Frogs from a Plio-Pleistocene site at Floraville Station, Northwestern Queensland. *Records of the South Australian Museum* 27(2): 169-173.

van den Bergh G.D *et al.* 2008, *Quat. Intern.* 182, 16-48.

van den Bergh G.D., *et al.*, 2008. The youngest *Stegodon* remains in Southeast Asia from the Late Pleistocene archaeological site Liang Bua, Flores, Indonesia. *Quat. Intern.* 182, 16-48 (2008).

van den Bergh G.D., J. de Vos, P.Y. Sondaar, 2001. The Late Quaternary palaeogeography of mammal evolution in the Indonesian Archipelago. *Palaeogeog. Palaeoclim., Palaeoeco.*, 171, 385-408.

Van Dyck, S. 1982 The relationships of *Antechinus stuartii* and *A. flavipes* (Dasyuridae, Marsupialia) with special reference to Queensland. In Archer, M (ed) *Carnivorous Marsupials*: 723-766, Surry Beatty & Sons, Chipping Norton, NSW.

Van Dyck, S. 2002. Morphology-based revision of *Murexia* and *Antechinus* (Marsupialia: Dasyuridae). *Memoirs of the Queensland Museum* 48(1): 239-330.

Van Dyck, S. & Crowther, M.S. 2000. Reassessment of northern representatives of the *Antechinus stuartii* complex (Marsupialia: Dasyuridae): *A. subtropicus* sp. nov. and *A. adustus* new status. *Memoirs of the Queensland Museum* 45(2): 611-636.

Vavryn, J.M.C 1987. The fight to save Mount Etna Caves from limestone mining. *Helectite* 25(2): 47-50.

Wara, M.W. *et al.*, 2005. Permanent El Niño-Like Conditions During the Pliocene Warm Period. *Science* 309, 758 (2005).

Webb L.J & J.G. Tracey, 1981. Australian rainforests: patterns and changes, in: A. Keast (Ed.), *Ecological Biogeography of Australia*. Dr. W. Junk, The Hague, 1981, pp. 605-694.

Webster J.M., P.J. Davies, 2003. Coral variation in two deep drill cores: significance for the Pleistocene development of the Great Barrier Reef, *Sediment. Geol.* 159 (2003) 61-80.

Westerman, M. , Burk A., Amrine-Madsen, H-M, Prideaux, G.J., Case, J.A., Springer, M.S.S. (2002) Molecular Evidence for the Last Survivor of an Ancient Kangaroo Lineage *Journal of Mammalian Evolution*, Vol. 9, No. 3 209-223.

Williams, S. E. 1997. Patterns of Mammalian Species Richness in the Australian Tropical Rainforests: Are Extinctions during Historical Contractions of the Rainforest the Primary Determinants of Current Regional Patterns in Biodiversity? *Wildlife Research* 24: 513-530.

Williams, S. E. and Hilbert, D. 2006. Climate change threats to the biodiversity of tropical rainforests in Australia, in: W. F. Laurance and C. Peres (Eds.), *Emerging threats to tropical forests*. Chicago University Press, Chicago, United States of America, 2006.

Williams, S. E., Bolitho, E. E., Fox, S, 2003. Climate change in Australian tropical rainforests: an impending environmental catastrophe. *Proc. Royal Soc. London Series B – Biol. Sci.* 270 (2003) 1887-1892.

Willis, P.A. 1995 The phylogenetic systematics of Australian crocodilians. PhD thesis, University of New South Wales, Sydney.

Willmott, W.F., O'Flynn, M.L. & Trezise, D.L. 1986. 1:100000 geological map commentary Rockhampton Region, Queensland. *Geological Survey of Queensland*: Brisbane.

Winter, J.W. 1988 Ecological specialization of mammals in Australian tropical and sub-tropical rainforest: refugial or ecological determinism? *Proceedings of the Ecological Society of Australia*. 15: 127-138.

Winter, J.W. 1997 Responses of Non-volant Mammals to Late Quaternary Climate Changes in the Wet Tropics Region of North-eastern Australia. *Wildlife Research* 24: 493-511.

Woodburne, M.O., Tedford, R.H., Archer, M., Turnbull, W.D., Plane, W.D., Plane, M.D. & Lundelius, E.L., Jr. 1985 Biochronology of the continental mammal record of Australia and New Guinea. *Special Publication, South Australian Department of Mines and Energy* 5: 347-365.

Wroe S. (1999) The geologically oldest dasyurid, from the Miocene of Riversleigh, North-west Queensland. *Palaeontology* **42**, 501-27.

Wroe , S., Field, J., Fullagar, R. & Jermin, L.S., 2004. Megafaunal extinction in the late Quaternary and the global overkill hypothesis. *Alcheringa* 28, 291-331.

Wroe, S. & Mackness, B.S. 1998. Revision of the Pliocene dasyurid, *Dasyurus dunmalli* (Dasyuridae: Marsupialia). *Memoirs of the Queensland Museum* 42(2): 605-612.

Wroe, S., Argot, C. & Dickman, C. 2004. On the rarity of big fierce carnivores and primacy of isolation and area: tracking large mammalian carnivore diversity on two



isolated continents. *Proceedings of the Royal Society of London (Biology)* (Published On-line 1-9).

Wroe, S., Ebach, M., Ahyong, S., De Muizon, C. & Muirhead, J. 2000. Cladistic analysis of Dasyuromorphian (Marsupialia) phylogeny using cranial and dental characters. *Journal of Mammalogy*, 81 (4): 1008-1024.

Zheng H., C.Mc. A Powell, H. Zhao, 2002. Eolian and lacustrine evidence of late Quaternary palaeoenvironmental changes in southwestern Australia, *Glob. Planet. Change* 35, 75-92.

Zhoa, J-xin., Hu, K., Collerson, K.D. & Xu, H. 2001. Thermal ionization mass spectrometry U-series dating of a hominid site near Nanjing, China. *Geological Survey of America* 29(1): 27-30.

## Appendices

### 8.2 Submitted/Published Papers by S. Hocknull as part of PhD work.

8.2.1 Hocknull, S.A. 2003. *Etnabatrachus maximus* gen. et sp. nov., a Plio-Pleistocene frog from Mt Etna, central eastern Queensland. *Memoirs of the Queensland Museum* **49**(1): 327-330.

8.2.2 Hocknull S.A., Ecological succession during the late Cainozoic of central eastern Queensland: extinction of a diverse rainforest community, *Mem. Queensland. Mus.* 51(1) (2005) 39-122.

8.2.3 Hocknull, S.A., J.X. Zhao, Y.X. Feng, G.E. Webb, 2007. Responses of middle Pleistocene rainforest vertebrates to climate change in Australia, *Earth Planet. Sci. Lett.* (2007) 264: 317-331.

8.2.4 Hocknull, S.A. 2005 Late Pleistocene-Holocene occurrence of Chaeropus (Peramelidae) and Macrotis (Thylacomyidae) from Queensland, Australia. *Memoirs of The Queensland Museum* 51(1) 38.

8.2.5 Hocknull, S.A. 2005. Additional Specimens of Bohra (Marsupialia: Macropodidae) from the Pliocene of Queensland. *Memoirs of the Queensland Museum* 51(1) 26

8.2.6 Cramb, J, Hocknull, S.A. & Webb, G.E. 2009. High diversity Pleistocene rainforest dasyurid assemblages with implications for the radiation of the Dasyuridae. *Austral Ecology*. *Austral Ecology* In Press.

8.2.7

Hocknull SA, Piper PJ, van den Bergh GD, Due RA, Morwood MJ, et al. (2009) Dragon's Paradise Lost: Palaeobiogeography, Evolution and Extinction of The Largest-Ever Terrestrial Lizards (Varanidae). *PLoS ONE* 4(9): e7241. doi:10.1371/journal.pone.0007241



VOLUME 51

PART 1

# MEMOIRS

OF THE

# QUEENSLAND MUSEUM

BRISBANE

31 MAY 2005

© Queensland Museum

PO Box 3300, South Brisbane 4101, Australia

Phone 06 7 3840 7555

Fax 06 7 3846 1226

Email [qmlib@qm.qld.gov.au](mailto:qmlib@qm.qld.gov.au)

Website [www.qmuseum.qld.gov.au](http://www.qmuseum.qld.gov.au)

National Library of Australia card number

ISSN 0079-8835

## NOTE

Papers published in this volume and in all previous volumes of the *Memoirs of the Queensland Museum* may be reproduced for scientific research, individual study or other educational purposes. Properly acknowledged quotations may be made but queries regarding the republication of any papers should be addressed to the Director. Copies of the journal can be purchased from the Queensland Museum Shop.

A Guide to Authors is displayed at the Queensland Museum web site [www.qmuseum.qld.gov.au/resources/resourcewelcome.html](http://www.qmuseum.qld.gov.au/resources/resourcewelcome.html)

**A Queensland Government Project**

Typeset at the Queensland Museum

# ECOLOGICAL SUCCESSION DURING THE LATE CAINOZOIC OF CENTRAL EASTERN QUEENSLAND: EXTINCTION OF A DIVERSE RAINFOREST COMMUNITY

SCOTT A. HOCKNULL

Hocknull, S.A. 2005 05 31: Ecological succession during the late Cainozoic of central eastern Queensland: extinction of a diverse rainforest community. *Memoirs of the Queensland Museum* **51**(1): 39-122. Brisbane. ISSN 0079-8835.

New late Cainozoic faunal assemblages are preliminarily identified and described from central eastern Queensland. Biocorrelation of the sites has determined that the oldest faunal assemblages are Early Pliocene in age, with younger faunas from the Plio-Pleistocene, late Pleistocene and Holocene. Pliocene faunal assemblages are characterised by rainforest-specialist frog, squamate and mammalian taxa. These include new Pliocene records for frogs; *Kyarranus*, *Lechriodus*, *Nyctimystes* and microhylids, squamates; *Cyclodomorphus gerrardii*, a new species of *Tiliqua* and typhlopids, and mammals; *Bohra* sp., *Pseudochirulus* spp., new petaurids and dasyurids, *Dactylopsila*, petauroid *incertae sedis*, *Acrobates*, *Cercartetus*, *Uromys/Melomys*, *Mesembriomys* and *Pogonomys*. Ecological signals derived from the faunal assemblages correlate well with dated palynological records from central eastern and northern Queensland (ODP815, Aquarius Well and Lynch's Crater). Combined Early Pliocene palynological and faunal records strongly indicates a nonseasonal, mesothermal, angiosperm-dominant rainforest with emergent gymnosperms at Mount Etna. A Plio-Pleistocene seasonal, open ecology indicated by the palynological record is corroborated by fauna from similar-aged sites, although several rainforest taxa persist. Increasing aridity during the late Pleistocene is suggested by a distinctly arid-adapted faunal assemblage in late Pleistocene sites, including eastern-most records of *Tympanocryptis*, *Macrotis lagotis*, *Chaeropus ecaudatus*, *Perameles bougainville*, *Sminthopsis macroura* and *Notomys*. Faunal succession from the Early Pliocene to Holocene is characterised by the extinction of most rainforest groups by the late Pleistocene, being replaced by more xeric-adapted forms. Several of the Early Pliocene taxa show resilience to extinction by remaining, albeit rare, in the late Pleistocene fauna, probably in local refugia. These include *Dendrolagus* sp., a new petauroid, *Thylogale*, *Macroderma gigas*, *Sarcophilus lanarius* and *Thylacinus*. Presence of rainforest murids in the Early Pliocene of Australia significantly predates previous estimates for their dispersal onto mainland Australia. □ *Pliocene, Pleistocene, ecological succession, rainforest fauna, Queensland, Australia, fossil vertebrates.*

Scott A. Hocknull, Queensland Museum, 122 Gerler Rd Hendra 4011; 1 August 2004.

The succession of faunal assemblages during the late Cainozoic of Australia is unknown for large parts of the continent. Where present, the records are extremely patchy when compared to similar-aged faunal records for other continents (e.g. North America (Stirton, 1936); Africa (Bishop et al., 1971); China (Flynn et al., 1991); and Eurasia (Azzaroli et al., 1988)). A majority of the Australian late Cainozoic Local Faunas have either been the focus of long term, low yield, sporadic collecting with little systematic documentation or once-off, large-scale excavations of a single fossil specimen, site or horizon (Rich, 1991). Typical examples of these sites include the Plio-Pleistocene sites of the Darling Downs southeast Queensland, which, for over 150 years have yielded large collections of specimens with little or no field data due to the ad

hoc nature of the collecting (Molnar & Kurz, 1997). These specimens are usually collected as single miscellaneous finds from along creek banks and riverbeds and have, until recently, possessed little documentation associated with the specimen. Such specimens are mostly out of stratigraphic context making them basically useless for detailed palaeoecological reconstruction and biostratigraphy.

In contrast, one-off large-scale excavations have either occurred in response to a major find, such as a complete skeleton(s), or the impending destruction of a fossil site by human impact (Archer, 1978; Long & Mackness, 1994). Material recovered from these sites usually possesses good field data, however, very rarely spans the temporal scale needed to document the

succession of faunas for a single region over large periods of time.

There have been several attempts to tie together Pliocene and Pleistocene sites in an effort to develop a biochronological and evolutionary framework for the late Cainozoic fossil communities of Australia (Archer & Wade 1976; Lundelius, 1983, 1989; Woodburne et al., 1985; Rich, 1991; Tedford et al., 1992; Tedford, 1994; Archer et al., 1995a; Archer et al., 1999; Dawson et al., 1999).

A review of literature for Australian Plio-Pleistocene faunas show some distinctive trends: 1) The majority of sites determined as Pliocene in age are considered to be from the Early Pliocene (5.2-3.4 Mya); Bluff Downs (Mackness et al., 2000); Chinchilla (Tedford et al., 1992); Rackham's Roost (Archer et al., 1995b): QLD; Curramulka (Pledge, 1992; Tedford, 1994), Tirari Formation (Tedford et al., 1992), Sunlands (Pledge, 1987): SA; Forsyth's Bank (Tedford, 1994); Hamilton (Rich, 1991); Parwan (Tedford, 1994); Boxlea (Tedford, 1994); Coimadai (Turnbull et al., 1992) VIC; Big Sink (Dawson et al., 1999); and Bow (Flannery & Archer, 1984) NSW. These sites include the only radiometrically or magnetostratigraphically dated sites of the Pliocene: Bluff Downs 3.6 Mya; Hamilton 4.5 Mya and the Tirari Formation 3.4-3.9 Mya. 2) When Early Pliocene faunas are compared with the few identified Late Pliocene sites (3.4-2.0 Mya): Dog Rocks in Victoria (Tedford, 1994); Bone Gultch and Fisherman's Cliff in New South Wales (Tedford, 1994); and Quanbun in Western Australia (Flannery, 1984; Rich, 1991), there is a distinct 'modernisation' of the fauna as suggested by Tedford (1994). These faunas possess several extant and extinct genera and species that become dominant during the Pleistocene and are the typical suite of taxa found in the late Pleistocene (Bartholomai, 1977; Archer, 1978; Hope, 1978; McNamara, 1990; Dawson & Augee, 1997; Molnar & Kurz, 1997; Reed & Bourne, 2000). The apparent faunal mixing of plesiomorphic and stratigraphically older taxa with younger, derived taxa, makes biochronology of the Late Pliocene and early Pleistocene difficult via stage-of-evolution criteria. Direct dates are needed to calibrate the timing of faunal changeover from the Pliocene to Pleistocene.

One notable near absence from the Pliocene to Pleistocene record is that of the diverse rainforest communities that distinguished many of the older

Oligo-Miocene faunas of Australia (Archer et al., 1995a; Archer et al., 1999). A palaeoecological succession for the Pliocene through medial Pleistocene of southeastern Australia has been proposed by Tedford (1994). This includes the Early Pliocene Hamilton Fauna (Turnbull & Lundelius, 1970; Flannery, 1992; Rich, 1991; Macphail, 1996), the only representation of a post Early Miocene rainforest community in southern Australia. Additional Pliocene and Pleistocene faunas from southeastern Australia support several rainforest components, however, these accounts are usually interpreted as part of a patchy assemblage and do not dominate the ecological reconstruction (Tedford, 1994; Archer et al., 1999).

Tedford (1994) concluded that the rainforest communities of southeastern Australia are missing by the Late Pliocene. Archer et al. (1995a) reviewed the Tertiary biotic change in Australia and concluded that by the Late Pliocene central Australia was becoming arid, coastal regions were forested and open, and rainforest persisted in northeastern Queensland as refugia. Macphail (1997) showed distinctly drier-adapted flora throughout the Late Pliocene of Australia.

A unique opportunity to access a late Cainozoic terrestrial fossil record from central eastern Queensland has been made possible via a series of open-cut limestone quarries and cavernous systems running along the coast to the north and south of Rockhampton (Fig. 1). Exposures of extensive fossiliferous deposits in stratigraphic context allow for this first account of a faunal succession spanning the Pliocene to Holocene in Queensland, including a distinctive Pliocene-aged rainforest community.

#### HISTORY OF COLLECTION

Collection of vertebrate remains from cave and fissure deposits in central eastern Queensland (CEQ) occurred sporadically for over 90 years, but few papers have appeared on fossils collected from these sites (Longman 1921, 1924, 1925a, 1925b; Hocknull, 2003).

Central eastern Queensland contains several limestone blocks with known karstification. Of these, Marmor and The Caves are the only two areas where vertebrate fossils have been found prior to 2002.

In 1910 G.E. Blundell collected a tooth from Marmor Quarry, S of Rockhampton, which made its way to the British Museum of Natural History

(BMNH10257) identified as *Macropus brehus*, now identified as *Palorchestes*.

First vertebrate remains acquired by the Queensland Museum QM were from guano mining in caves on Reserve Holding 272, Limestone Ridge, east of Mount Etna (R444), between 1920-1921. A mandible assigned to *Sarcophilus lanianus* was presented to Heber A. Longman in 1921 by P.H. Ebbott of Mount Etna Fertilisers Ltd (Longman, 1921). Shortly thereafter, Samuel Evans, mine manager of Marmor Quarry, presented several small collections of fossils unearthed during quarrying. In 1924, Longman collected the QM's first representative samples from CEQ; from Olsen's Cave, SE of Mt Etna and Marmor Quarry, publishing the combined material collected from Marmor Quarry (Longman, 1924, 1925a & b). Longman's faunal records from Marmor Quarry included; *Diprotodon australis* (herein ?Zyngaturinae), *Phascolumys* sp. (herein, *Vombatus urinus mitchellii*), *Thylacoleo carnifex* (herein *Thylacoleo* sp.), *Thylacinus spelaeus* (herein *Thylacinus cynocephalus*), *Sarcophilus lanianus*, *Macropus anak* (herein *Macropus titan*), *Phascogale flavipes* (herein *Antechinus* sp. 2), *Petrogale* sp. cf. *P. inornata* (herein *Petrogale* sp.) and *Megalanina prisca*. Smaller fauna included snake and rodent remains. Fossils collected from Olsen's Cave remained unpublished.

In 1925 Evans presented a second Marmor Quarry collection to Longman. F.W. Whitehouse collected bones from Johannsens Cave on Limestone Ridge in 1926, during the peak of guano mining. A hiatus of nearly 30 years followed. In 1954 and 1957 two collections of bones were presented to the QM from Marmor Quarry, by O. Anderson and J.E. Joyce, respectively. Final collections of large pieces of bone-bearing cave breccia were taken from Marmor Quarry in 1964-5 by Bartholomai and Joyce. This breccia is currently being prepared and contains remains of some very large vertebrates, including *Macropus titan*, as well as many smaller-sized species. No collecting has been possible from Marmor Quarry since 1964.

In 1972, Mike Murray donated small surficial collections from Old Timbers, Lion's Den and Johansen's Cave, Mount Etna area.

A second hiatus from the 1970's to mid 1980's occurred when concerns regarding the conservation of several caves on Mount Etna were at their greatest (Bourke, 1970; Vavryn, 1987). Two cave systems, Speaking Tube Cave

and Elephant Hole Cave, were under threat from quarrying operations on the W flank of Mt Etna. In 1986, Kerry Williamson & Dianne Vavryn removed two sacks of loose bone and sediment from the floor of Elephant Hole Cave before mining operations broke into the cave. The small collection was sent to the QM later that year.

Mining operations continued on the western ridge of Mount Etna until early 2004. During the initial stages of operation, the two known caves were broken into and cave breccias exposed. A deposit was unearthed in 1992 when breaking into Speaking Tube Cave. Then mine manager M. Barton, with assistance from David Kershaw and Don Kime, kindly donated bone-breccia samples to the QM and kept a stockpile of bone breccia material on the eastern side of Mount Etna on a flat bench below Main Cave (QML1313).

The author, Paul Tierney and members of the Central Queensland Speleological Society, mounted expeditions to Mt. Etna in 1998, 2000 and 2001. Several sites were successfully located and collected within the Mt. Etna Caves National Park and Mt. Etna Limestone Mine.

Extensive fossiliferous deposits on Limestone Ridge were found in 1998 which included considerably diverse faunas from several distinct ecologies, including rainforest. Twice in 2000, the QM and University of New South Wales systematically collected material from sites on Limestone Ridge and Mt. Etna.

In 2001 collections were made from the Mt Etna Limestone Mine, with the discovery of, inter alia, faunal assemblages of similar diversity and age to those from Limestone Ridge. Deposits represent a series of cave-fills exposed in cross-section by mining operations. Examination of these units has enabled development of a preliminary chronology of the faunas. Continued fieldwork in 2002 and 2003 increased the number of distinct sites on the mining lease and located a remnant chamber of Speaking Tube Cave. In mid-2002 a limestone at Mount Princhester, 50kms north of Mount Etna, was investigated and small deposits of exposed fossiliferous cave floor sediment collected. Further fieldwork (2003) resulted in discovery of new sites in Olsen's Cave and Karst Glen, SE of the main Mount Etna and Limestone Ridge blocks.

## METHODS

FOSSIL SITES (Figs. 1-3). Preliminary site geology, including simplified sedimentological descriptions are provided herein. Cave names

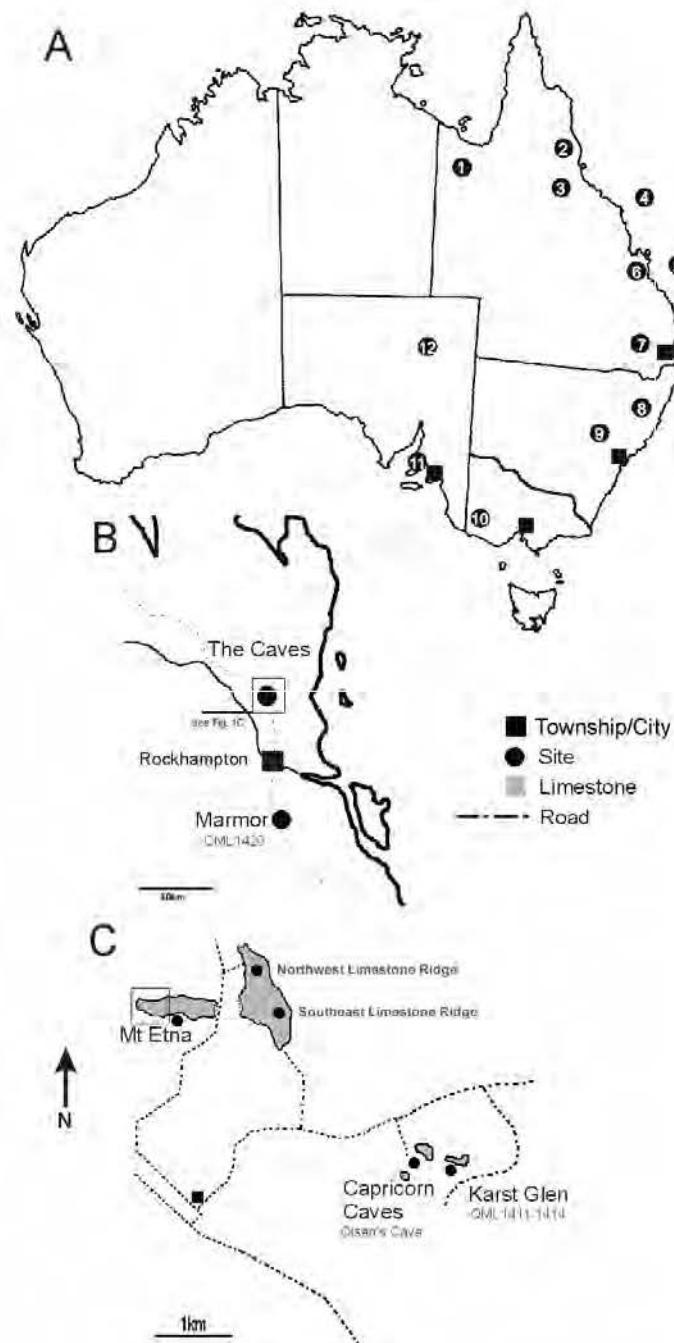


FIG 1. Map of fossil localities. A, Major localities mentioned in text, 1. Riversleigh; 2. Lynch's Crater; 3. Bluff Downs; 4. ODP815, Marion Plateau; 5. Aquarius Well, Capricorn Trough; 6. Mt Etna/Marmor; 7. Chinchilla; 8. Bow; 9. Big Sink, Wellington; 10. Hamilton; 11. Curramulka; 12. Tirari Formation, Lake Eyre. B, 6. expanded. C, The Caves area.



follow (Shannon, 1970b). Fossil sites are given a QML number (Queensland Museum Locality). Superpositional and stratigraphic data was collected from all localities with the exception of Marmor Quarry. Data collected included, stratigraphic context, breccia components, bone preservation, tooth preservation, shell preservation and a facies interpretation. Where possible, sampling bias was reduced by collecting and processing equal amounts of material from each site.

**TAXONOMY.** A brief systematic account of the taxa found from each site is tabulated (Table 1-3, Appendix 1) with abbreviated systematic descriptions of relevant taxa given below. A selection of the best-preserved specimens was used to provide the identifications that follow. All specimens are held at the Queensland Museum, (prefix QMF). Frog osteological nomenclature and taxonomy follows Tyler (1976) and Cogger (2000) respectively. Squamate nomenclature follows; Hutchinson (1992) for scincids, Hutchinson (1997) for pygopodids and gekkonids, Hecht (1975) for varanids, Hocknull (2002) for agamids, Smith (1976) for elapids and Holman (2000) for typhlopids. Squamate taxonomy follows Cogger (2000); crocodylian nomenclature and taxonomy follows Willis (1995); mammalian nomenclature follows Archer (1984) for tooth morphology and Luckett (1993) for tooth positions. Mammalian taxonomy follows Strahan (1995) and Flannery (1994). Fossil mammal taxonomy follows Long et al. (2002). Avian nomenclature follows Gilbert et al. (1981) and taxonomy Lindsey (1992).

**FAUNAL ASSEMBLAGES (LOCAL FAUNA).** Similarities between site faunas were computed using PAUP (Swofford, 2000) and MacClade software (Maddison & Maddison, 2000), where sites defined as 'taxa' and the taxa as 'characters'. 'Characters' were given the states of either being absent (0) or present (1) (Appendix 1).

Small-sized mammals (smaller than and including *Petrogale*) were chosen for the analysis because they were represented in all of the sites and are least affected by taphonomic bias. The dominant accumulating agent for each site was either via a pit-trap and/or owl/bat roosts. This biases the preservation of large-sized vertebrate taxa, thus they are excluded from the analysis.

A mammal list was constructed to define the present day small mammal fauna for Mount Etna. This list was derived from mammal species surveyed directly at Mount Etna (Horsup et al.,

1993; Dwyer, 1970) and those species found in habitat similar to that of present day Mount Etna (semi-evergreen vine thicket), which are also found within the central eastern Queensland region today (Horsup et al., 1993). The present day fauna was fixed in position for the analysis as the 'outgroup'. Present day mammal species not found in the fossil record were excluded from the 'ingroup' analysis because they were simply counted as autapomorphies and uninformative. A dendrogram of relationship was constructed using both PAUP and MacClade parsimony analyses (heuristic search; 1000 replicates).

**FAUNAL ASSEMBLAGE AGE.** Biocorrelated taxa were used to provide an estimated date for each of the sites. Palaeoecological signals generated from well-constrained palynological records off the coast of central eastern Queensland (Hekel, 1972; Martin & McMinn, 1993) were correlated with palaeoecological signals generated from site faunas. Direct dating of one site, QML1312, was possible via Thermal Ionisation Mass Spectrometry (TIMS) Uranium-series dating. Dating was carried out on a *Petrogale* jaw. The date is considered to be a minimum age based on late-stage uptake of Uranium into bone and dentine (Ayliffe & Veeh, 1988; Shen et al., 2001; Zhao et al., 2002).

## GEOLOGICAL SETTINGS

The geological history of the limestone blocks containing cave and fissure deposits of the present study have been subject to debate (Kirkgaard et al., 1970; Shannon, 1970a; Willmott et al., 1986; Barker et al., 1997; Simpson et al., 2001). Sites occur in cavern and fissure systems within Early Devonian limestone blocks (Philip & Pedder, 1967) of the Mount Alma Formation (*sensu* Barker et al., 1997). Limestone blocks are irregular in shape and are scattered randomly throughout the formation. The southern extremity of the limestone blocks occurs in the Marmor-Raglan area 50 kms S of Rockhampton. The northern extension of the limestone outcrops as a series of small limestone bluffs at The Caves township (25km N of Rockhampton) and at Princhester (50km N). Sediments from these sites have yielded an enormous and varied vertebrate fossil record.

Palaeontological and structural evidence suggests the limestones are allochthonous blocks within Late Devonian Mount Alma Formation (Barker et al., 1997).

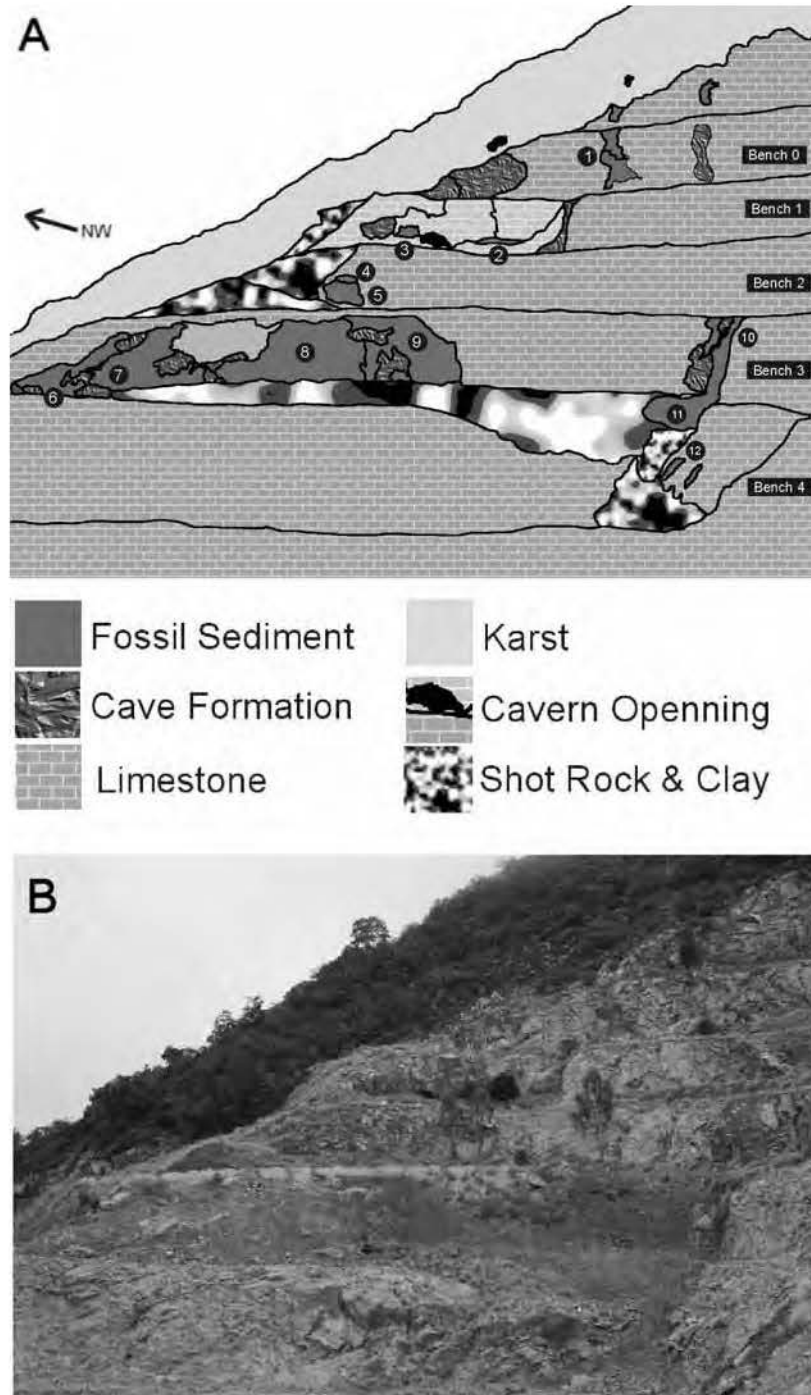


FIG. 2. Fossil localities on the western benches of Mount Etna Limestone Mine. 1. QML1419; 2. QML1313, 3. QML1383, 4. QML1310 Unit 1, 5. QML1310 Unit 2, 6. QML1311 A/B, 7. QML1311 C/D, 8. QML1311 F, 9. QML1311 H, 10. QML1398U, 11. QML1384L, 12. QML1385.

The structural history of these limestone blocks which includes their distance and position from one another, irregular bedding planes, faulting, and complex joint systems, has had a direct influence on the sedimentology of the varying vertebrate fossil deposits found within them (Willmott et al., 1986). Structural history has also influenced the terrestrial communities occupying the limestone (caverns and surrounds) through the past and in the present. Modern ecologies on these limestones strongly reflect this influence because most of the bluffs act as present day refugia for flora and fauna (Horsup et al., 1993).

#### SITE LIST

##### **Mount Etna Limestone Mine and National Park**

###### *Speaking Tube Cave System*

Bench 0, QML1419\*

Bench 1, QML1313 (=QML1313 & QML1288)\*\*

Bench 1, QML1383\*

Bench 2, QML1310 Unit 1

Bench 2, QML1310 Unit 2\*

Bench 3, QML1311 Unit A\*

Bench 3, QML1311 Unit B\*

Bench 3, QML1311 Unit C\*\*

Bench 3, QML1311 Unit D\*\*

Bench 3, QML1311 Unit F\*

Bench 3, QML1311 Unit H\*\*

###### *Elephant Hole Cave System*

Williamson & Vavryn Collection, QML1312\*\*

Bench 3, QML1384 Upper Unit\*\*

Bench 3, QML1384 Lower Unit\*\*

Bench 4, QML1385\*\*

##### **Northwest Limestone Ridge**

###### *Johansen's Cave System*

QML1314, Guano deposit\*\*

QML368, Flowstone (False Floor) Unit\*\*

Southeast Limestone Ridge

###### *Mini Cave System*

Mini Cave Chamber Deposit, QML1284\*\*

Mini Cave Surface Deposit, QML1284a\*\*

Leo's Lunch Site, QML1382\*

##### **Olsen's Cave System\*\***

Karst Glen System

KG3 Surface Deposits, QML1411-1414\*

##### **Marmor Quarry**

Marmor Bone Breccia collection, QML1420\*\*

\* Sites with fauna

\*\* Sites with fauna presented herein

##### **MOUNT ETNA LIMESTONE MINE AND NATIONAL PARK**

Approximately 40% of Mount Etna is massive recrystallised limestone with the remainder a combination of faulted sedimentary and volcanogenic units of the Mount Alma Formation (Shannon, 1970a; Barker et al., 1997). Limestone on Mount Etna dips steeply to the SW, with major joints oriented along a NW axis. Joints are predominantly vertical and control cave development (Shannon, 1970b). Phreatic enlargement has occurred along these vertical planes producing deep chambers with sculptured phreatic pendants. Vadose cave development is marked by extensive speleothem formation and cave entrance development. Bone breccias and cemented cave floors are common throughout, occurring within functional cave systems or exposed on weathered and collapsed dolines. Two major cave systems on Mount Etna are the focus of the present study; Speaking Tube and Elephant Hole Cave systems.

Speaking Tube Cave system occupies two major joint controlled rifts running down the mountain in a NW-SE direction. Phreatic chambers developed at depth are linked to the surface by long solution pipes. Elephant Hole Cave system is a third joint-controlled rift to the SE of the Speaking Tube Cave system. It is also linked to the surface by large solution pipes. A geochronological summary of sites found on the western benches of Mount Etna Limestone Mine is provided in Fig. 3.

##### **Speaking Tube Cave System**

SPEAKING TUBE CAVE: E7. "This cave has nine entrances at middle to highest levels on the West flank of Mt. Etna. It is a very complicated active inflow cave with three active sumps." (Shannon, 1970b: 25)

It is obvious from the many and varied bone breccias recovered that Speaking Tube Cave system has had a long and complex history. No substantial collections were made from Speaking Tube Cave before it was broken into by mining operations. In 1992, bone breccias were exposed close to surface karst and stockpiled by Pacific Lime Pty Ltd operators. A small sample of these bone breccia blocks was sent to the Queensland Museum marked "Speaking Tube Cave". In 2000 the stockpile was located on the eastern side of

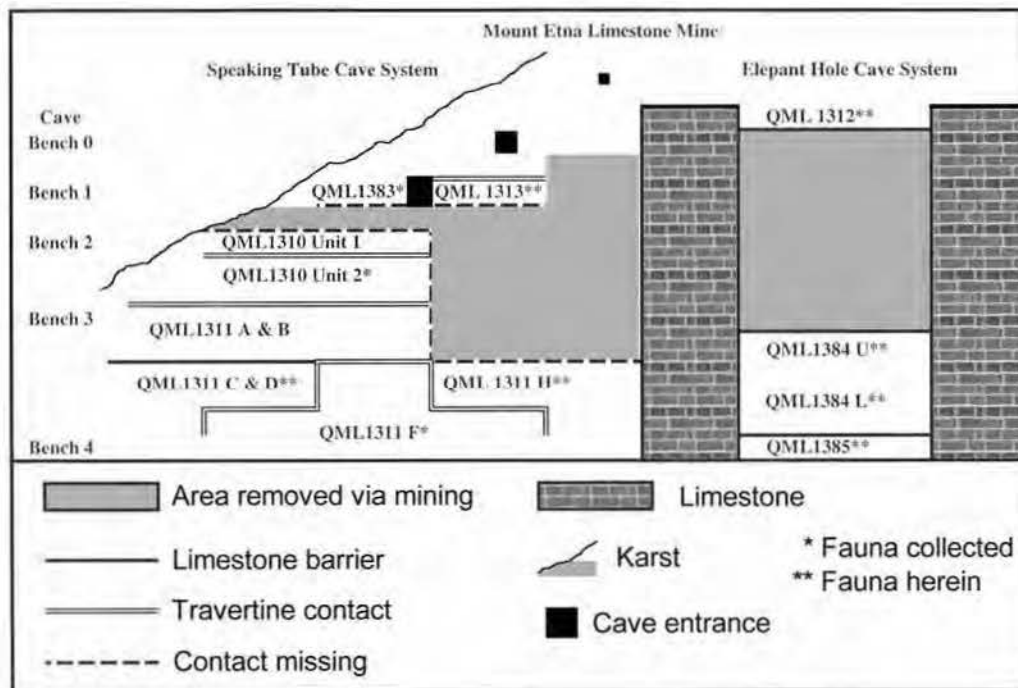


FIG 3. Schematic diagram illustrating the relationships between fossil deposits on the western benches of the Mount Etna Limestone Mine, Mount Etna. \* Fauna collected. \*\* Fauna presented herein.

Mount Etna by the QM and collected, given the site name 'Mat's Menagerie' (QML1313). The original location of the bone breccia was unknown until 2002 when equivalent material was found in situ on Bench 1 of the western benches. Five main benches are considered to preserve portions of the Speaking Tube Cave system, including an entrance to the cave through an exposed chamber on Bench 1.

**BENCH 0, QML1419.** A thin veneer of limestone covered a solution tube until 2003 when it collapsed and revealed a breccia-filled tube. It was discovered in mid 2003. The solution pipe contains several levels of varyingly indurated fossiliferous sediment.

**BENCH 1, QML1313 (=QML1313 & QML1288).** A small amount of bone breccia received from Pacific Lime in 1992 and labeled as 'Speaking Tube Cave' (QML1288) was rediscovered by the Queensland Museum as a stockpile on the eastern face of Mount Etna, subsequently named "Mat's Menagerie Site" (QML1313). The bone breccia originated on the

western benches where its exact locality was unknown. Inspection of the Bench 1 cliff line relocated lithologically identical bone breccia adhering to an exposed cave chamber wall. The material follows a cave wall demarcated by cave formations along the middle length of the bench. The breccia runs in a northwest/southeast axis toward an opened chamber. The chamber constitutes a known chamber within Speaking Tube Cave. Bone breccia received by the museum, stockpiled on the eastern face and adhering to the southeast side of the cave wall on Bench 1, western benches, constitutes the same unit.

**Stratigraphic context.** There is no preserved contact of this unit with any of the other deposits on the mountain. The area in which a contact may have occurred has been mined. There are no clasts of other bone breccias within the matrix. The only breccia that shows similarities in sedimentology to QML1313 is QML1311 (Unit A) of Bench 3, which indicates that this unit was very extensive and formed deep within the system. It is sedimentologically distinct from the



only other breccia found on Bench 1 (QML1383), which occurs to the northwest of the open chamber.

*Breccia components.* Distinctly bright yellow to orange coloured, heavily cemented containing large angular clasts of parent limestone, flowstone and smaller clasts of allochthonous rock; abundant bone, teeth and skulls of variable sizes; snails common; large calcite vugs. Small clasts of red to brown clay; pisolites of ironoxide and calcite; bedding chaotic.

*Bone preservation.* Articulated and semi-associated skeletal elements; well-preserved material with no apparent dominant bone orientation; calcite growth within bone vacuities; bones variable in size, from large limb bones (10-15cm) to grain-sized bone fragments.

*Tooth preservation.* Teeth usually in jaws.

*Shell preservation.* Shells complete and isolated.

*Facies Interpretation.* Abundant large angular clasts, articulated and semi-articulated large-sized bones, large complete shells and no dominant bedding or clasts indicates an entrance facies talus and scree.

**BENCH 1, QML1383.** Located to the northwest of the open chamber, QML1383 is a large fossiliferous unit.

*Stratigraphic context.* Sedimentologically this unit is similar to QML1311 (Unit B) of Bench 3 and QML1310 (Unit 2) of Bench 2. QML1310 (Unit 1) of Bench 2 divides the contact between QML1383 and QML1310 (Unit 2) so it is suggested here that QML1383 is stratigraphically younger than both QML1310 and QML1311. The site has an analogous depositional facies.

*Breccia components.* Dark red to pink clay, heavily cemented with minor clasts of decalcified limestone, allochthonous sediments and pisolites; abundant bones, teeth and shell.

*Bone preservation.* Bones fragmentary and small; no distinct large bone orientation; smaller bone fragments occur in fine lenses which are horizontally bedded.

*Tooth preservation.* Usually isolated and well preserved.

*Shell preservation.* Abundant in small lenses.

*Facies Interpretation.* Lack of large angular clasts, large bones and the lack of distinct large bone orientation indicates a depositional facies away from an entrance and having not been subject to significant water transport. Abundance

of small fragments of bones and isolated teeth indicates a possible predator accumulation. Thin irregular lenses of material suggest that accumulation occurred from slumping of upper roost deposits, probably *Macroderma*. The deposit seems to occur within an old aven when viewed in sectional profile.

**BENCH 2, QML1310.** Bench 2 lacks large deposits of breccia, with the two units described here only found on a small pinnacle left from mining operations.

*Unit 1; Stratigraphic context.* Unit 1 is younger than Unit 2 with a distinct cave floor formation between the two horizons.

*Breccia components.* Mottled red/grey horizons; lacks bone and teeth; small clasts of allochthonous sediments; heavily cemented.

*Bone, tooth and shell preservation.* Rare to nil.

*Facies Interpretation.* Lack of fossil material and major clasts indicates a non-entrance facies. The mottling of the rock indicates the presence of dense rootlets and thus the base of a chamber.

*Unit 2; Stratigraphic context.* Occurs below and is older than Unit 1. Several thick bands of flowstone occur through the top of this unit, demarcating different levels of formation. Toward the base there is a considerable reduction in flowstone. The base of Unit 2 appears to be very similar in depositional style to QML1311 (Unit B) of Bench 3 and is interpreted as the top of this unit.

*Breccia components.* Flowstone-dominated light red coloured, heavily cemented bone breccia; flowstones irregular in shape and domed at the middle of the exposure; bones abundant and small; shell abundant in small lenses, associated with flowstones; small, grain-sized clasts of allochthonous sediment.

*Bone preservation.* Disarticulated, disassociation within the accumulation; large numbers of bones from small animals, usually broken into grain-sized particles.

*Tooth preservation.* Isolated teeth, well preserved, no rounding.

*Shell preservation.* Small snail shells, in bands usually associated with flowstone unit.

*Facies Interpretation.* The mass of banded flowstones at the top of QML1310 Unit 2 indicates a major increase in speleothem genesis over that found in QML1311, Unit B. It is unknown whether this was a rapid phase of precipitation or it was a gradual increase over time. The reason for this is because the contact

between QML1311, Unit B and the base of QML1310 Unit 2 has been removed by mining. The presence of the flowstones and a domed lamination indicates a series of cave floors, probably in the shape of a sediment cone. Absence of large angular clasts and large bones indicates a chamber facies. The sediment cone was probably produced at the base of a bat roost because there are no additional chambers above the deposit that could have acted as a sump.

#### BENCH 3, QML1311

**Unit A; Stratigraphic context.** Unit A in contact with Unit B. Unit A formed before Unit B. Unit A is considered lithologically equivalent to QML1313 sediment although found deeper within the system. This is reflected in the breccia components, bone preservation, greater bedding and speleothem genesis of Unit A sediments.

**Breccia components.** Yellow, grey and pink coloured clay; heavily cemented; massive flowstones and travertine throughout (ranging from 5-20cm thick); cave formations preserved within breccias. Large clasts of allochthonous sediments and semi-rounded parent limestone. Drusy calcite vugs and well preserved bone.

**Bone preservation.** A semi-articulated, associated accumulation with some patches of sorted large bone; limb bones well preserved with most elements complete; small bones in apparent association; bone vacuities infilled with calcite.

**Tooth preservation.** Teeth usually found in complete or near complete jaws.

**Shell preservation.** Snails abundant, isolated, and well preserved.

**Facies Interpretation.** Unit A is considered a talus accumulation below the entrance facies of QML1313.

**Unit B; Stratigraphic context.** Unit B occurs in two areas along Bench 3. Unit B contacts Unit A on its north-western extremity and occurs above Unit C/D toward the center of Bench 3. Unit B is divided from Unit C/D by a massive limestone wall, varying from 5-10m thick. Unit B is considered so close in lithology to the sediment at the base of QML1310 Unit 2, Bench 2, that it is considered here to have had a conformable contact between these two units.

**Breccia components.** Light red heavily cemented clay; numerous clasts of decalcified parent limestone, cave wall travertine and allochthonous sediments, including gravel. Cave formation dominates the clasts, followed by allochthonous sediment and parent limestone.

Bone and tooth fragments abundant; small drusy calcite vugs; isolated iron-oxide pisolites.

**Bone preservation.** Disarticulated accumulation with some sorting of small bone elements. Sorting is localised and not common; large bones are rare; small bone well preserved with teeth in jaws. Long bones badly preserved, mostly broken at both proximal and distal ends; numerous grain-sized bone particles occur in irregularly graded lenses. Calcite growth within bone vacuities.

**Tooth preservation.** Well preserved tooth rows.

**Shell preservation.** Shell abundant and usually associated with bone sorting.

**Facies Interpretation.** Unit B is considered the base of a talus from a well-developed sediment cone. The base being Unit B and the top being QML1310 Unit 2 Bench 2. The lack of large bone accumulations and the abundance of small bone fragments suggest a similar predator accumulation as to QML1310 Unit 2 Bench 2 within an aven chamber.

**Unit C; Stratigraphic context.** Unit C grades into Unit D but with less mottling. Unit C and D are considered equivalent in age. Unit C is separated from Unit A & B by a large limestone wall, varying from 5-10m thick. Units C and D unconformably overlies Unit F on a decalcified and eroded travertine surface formed on Unit F and included as clasts in Units C & D. Units C and D are thus considered to be younger than Unit F.

**Breccia components.** Red/yellow/grey clay, moderately cemented; drusy calcite vugs formed within rootlet vacuities; isolated iron-oxide pisolites; small clasts of decalcified parent limestone and allochthonous sediments. Isolated clasts of broken and transported travertine; large bones, isolated teeth and numerous complete small bones; large bones fractured and exploded by clay matrix; no travertine formation other than calcite formation between Unit C and F. Small clasts of Unit F at the southeast extremity of unit C.

**Bone preservation.** Disarticulated accumulation with little bone sorting; large long bones missing proximal and distal ends; vertebrae missing processes. Large bones have been transported some distance. Small bones variably preserved; complete elements to grain-sized particles; bone vacuities filled with clay.

**Tooth preservation.** Large teeth usually preserved within the jaw. Small teeth usually isolated and associated with edentulous jaws.

*Shell preservation.* Rare to absent.

*Facies Interpretation.* Unit C is considered to be a deep chamber deposit based on the lack of large angular inclusions and large well-preserved, semi articulated or associated bone. There are no indications that this deposit is a predator accumulation. The lack of sorting of clasts and no distinct bedding planes indicate that stream and channel action was not the main mode of transport and deposition here. The presence of large bones and very few well-preserved snails indicates a deposit where the larger elements have been transported from an entrance facies into a lower chamber probably via extensive slumping, requiring little water transport.

**Unit D; Stratigraphic context.** Unit D is a mottled breccia very close in lithology to Unit C and is considered equivalent in age. Unit D conformably grades into Unit C without any distinctive demarcation.

*Breccia components.* Mottled red/yellow/grey clay, loosely cemented; drusy calcite vugs formed within rootlet vacuities. Unit D possesses distinctive mottling due to penetration of the clay load by rootlets. Isolated iron-oxide pisolites; small clasts of decalcified parent limestone and allochthonous sediments; rare large bones and isolated teeth; no travertine formation other than calcite formation between Unit C/D and F.

*Bone preservation.* Disarticulation accumulation with little bone sorting; large long bones missing proximal and distal ends. Bone vacuities filled with clay.

*Tooth preservation.* Small teeth usually isolated and associated with edentulous jaws.

*Shell preservation.* Rare to absent.

*Facies Interpretation.* As for Unit C but with a greater influence from rootlets altering the general colouration and texture of the sediments.

**Unit F; Stratigraphic context.** Unit F is located between Units C & D and Unit H. There are contacts between Unit F and Unit C on the northwest flank, and with Unit H on the southeast flank. These contacts are demarcated by cave wall formation in the form of travertine and decalcified, detached flowstones with Units C, D and H. All three Units have been secondarily capped by a more recent travertine. Based on the contact zone, Unit F formed before Units C, D and H.

*Breccia components.* Bright yellow sandy, clay-rich; cemented; travertine distinct and demarcates contacts with younger sediment;

little internal flowstone formation. Interspersed small, rootlet-shaped drusy calcite vugs; minor clasts (0.5-2cm) of decalcified parent limestone with chalky texture. Small patches of highly fragmented bones and teeth.

*Bone preservation.* Disarticulated accumulation with no bedding or sorting; bones small and hollow in cross section; no large elements, mostly postcranial.

*Tooth preservation.* Mostly fragmented rodent incisors.

*Shell preservation.* Shell absent.

*Facies Interpretation.* The sediment is unlike any other found in the study area. The paucity of bone, internal speleothem genesis and clasts indicates a possibly dry accumulation. Further investigation of this deposit is needed. The lack of fossil specimens may also indicate a relatively old age for the deposit, before there was major connection of the solution pipes with the surface and well before karstification.

**Unit H; Stratigraphic context.** Unit H contacts the travertine wall enclosing Unit F and is younger. Unit H has formed at a similar depth to Units C, D and QML1384 Lower Unit, however, their superpositional relationships are unknown, possibly contemporaneous.

*Breccia components.* Red to dark brown clay, heavily compacted but not heavily cemented; numerous small clasts of altered serpentinite, clasts of decalcified parent limestone and iron-oxide pisolites; large and small bone fragments; isolated teeth and jaws. Minor travertine inclusions from Unit F.

*Bone preservation.* Dissarticulated accumulation with no distinct bedding or sorting of elements. Tightly packed bone accumulations; large bones are commonly long bones. Long bones usually with broken proximal and distal ends; shafts fractured and exploded by clay matrix; vertebrae usually missing transverse processes and neural spines; metatarsals commonly missing one distal end; small bones include variously fragmented skeletal elements; usually preserving epiphyses. Ranging from complete bone elements to grain-sized bone particles.

*Tooth preservation.* Mostly edentulous jaws and numerous isolated teeth. Large (e.g. large macropodid) teeth usually remain within the jaw. Teeth variably preserved with tooth roots.

*Shell preservation.* Nil.

*Facies Interpretation.* Absence of angular limestone blocks and dipping beds indicates a

non-entrance facies. The lack of cementation indicates a period of saturation of the sediment or the inclusion of humic acids into the cavern, both similarly retarding the precipitation of calcite within the sediment, however, geochemical analyses will be needed to clarify this.

### Elephant Hole Cave System

**ELEPHANT HOLE CAVE: E8.** *"On the West flank of Mt Etna. The cave [Elephant Hole Cave] has three middle level entrances, all containing vertical pitches. An active inflow cave. From the main entrance a talus slope leads to the drop into two large caverns. ...The cave has little decoration, but has some breccia deposits which include bone material."* Shannon (1970b: 25)

**Williamson & Vavryn Collection, QML1312;** a sample of unconsolidated floor sediment from an earth floor within Elephant Hole Cave in 1986.

*Stratigraphic context.* Of unknown stratigraphic context. TIMS U-series date based on *Petrogale* dentition (minimum age)  $149,000 \pm 611$  ybp. Considered to be young based on the preservation state of the material. Younger than QML1384 and QML1385 deposits.

*Breccia components.* Sediment and bone that was collected is derived from a loosely compacted cave floor (Vavryn & Williamson pers coms.) which is almost entirely made-up of fine, dark to light brown or red clay. Sediment breaks down easily in water and contains small, angular fragments of cave wall and roof, which show some signs of weathering and decalcification. Bone appears to be subfossil, with minimal bone discolouration, except for black manganese-oxide surface stains.

*Bone preservation.* Disarticulated, semi associated; bone small to medium-sized (<100mm in length) with portions of larger limb elements; very well preserved with most of the long bones retaining epiphyses and skull bones intact. Bone cavities free of calcite and sediment.

*Tooth preservation.* Most mandibles and maxillae retain teeth and most molar rows.

*Shell preservation.* Fragmentary and rare.

*Facies Interpretation.* Abundance of small bones of mammals, lizards, frogs and passerine birds suggests that a fraction of the deposit be derived from a predator accumulation. Some gnaw marks have been found and identified as rodent gnawings. Present in the deposit are owl (*Tyto* sp.) and ghost bat (*Macroderma gigas*) remains indicating that typical cave dwelling predators were present in Elephant Hole Cave during

deposition. Well-preserved and semi-associated large vertebrate remains attaining a maximum size of the macropodine *Petrogale*, indicate an accumulation close to an entrance.

No orientations of the bones were taken with the collection so it is unclear whether water was involved in the accumulation. No speleothem or cementing has occurred, suggesting the sediment was not water transported. Some sediment clods remained within the deposit and were not broken down during collection, transport or preparation. These compacted sediment clods are thick with bones and teeth with their orientations relatively random. The lack of water transport, compaction and calcite precipitation indicates a very dry accumulation close to an entrance, with input from a predator's roost.

**BENCH 3, QML1384 UPPER UNIT.** In 2000 whilst collecting on the western benches of Mount Etna Mine, a site (QML 1384U) was discovered with a similar sedimentology to that seen in the material recovered from Elephant Hole Cave by Williamson & Vavryn in 1986 (QML1312). Based on the position of the deposit on the mine site, it would have occupied a deep chamber within the Elephant Hole Cave system.

*Stratigraphic context.* QML 1384 is considered to be older than QML1312 because it is found much deeper and is more compacted and lightly cemented. There is no distinct reworking of bone material and the bone has a greater degree of alteration than the bone from QML1312.

*Breccia components.* Cave earth compacted, only lightly cemented, breaking down easily in weak acidic solution. Sediment possesses a strikingly similar colour and texture to QML1312, including an abundance of brown to red clay, angular cave wall and roof inclusions.

*Bone preservation.* Bones disarticulated; subfossil preservation; similar in preservation to QML1312, especially by the presence of the black manganese oxide staining. The completeness of cranial and postcranial bones also indicates close similarities because no other site at Mt Etna, other than the Elephant Hole Cave collection, has such a high density of perfectly preserved elements. Bones infilled with clay.

*Tooth preservation.* Complete jaws with tooth rows preserved.

*Shell preservation.* Rare and fragmentary.

*Facies Interpretation.* The chambers of Elephant Hole Cave were large and vertical. It is therefore



considered that QML1384U is simply a lower and older extension of the entrance and predator accumulation identified as the QML1312 deposit.

#### BENCH 3, QML1384 LOWER UNIT.

*Stratigraphic Context.* QML1384L is lithologically similar to QML1384U. There is no distinct contrast between the upper and lower unit except for a darker colour of the clay in the Lower Unit. The Lower Unit is considered to be continuous with and therefore older than the sediments collected from the upper unit.

*Breccia components.* Sediment unconsolidated, extremely clay-rich, dark brown in colour. The clay is very greasy in texture; isolated allochthonous cobbles and gravel are dispersed throughout the clay load. Bone rare; little flowstone and few autochthonous clasts are present in the sediment.

*Bone preservation.* Bone rare and fragmented, where present relatively unaltered, possessing simple manganese staining. Larger bone vacuities free of clay. Similar in preservation to the upper unit, except for greater manganese staining.

*Tooth preservation.* Rare and isolated.

*Facies interpretation.* Lower Unit is simply an extension of a large vertically oriented solution pipe which fed into a large chamber housing phreatic pendants. The lack of distinctive vadosely developed flowstones within the sediment suggest that, like QML1311 Units C, D and H, the lower unit was accumulating within a water-saturated chamber, or one with sufficient acidity to prevent carbonate precipitation. This would also explain the lack of carbonate to indurate the clay sediment. The sediment looked to continue deeper within the system and certainly down to the level of Bench 4 (QML1385) deposit. This lower unit may contact QML1385 and be a source for the bone accumulations in it.

BENCH 4, QML 1385. In 2002 a small deposit of bones was discovered further down the mine site benches, in a direct line below QML1384L. The deposit is the lowest found so far on Mount Etna. This deposit is unlike any found on Mount Etna, however, it occurs closest to the base of the QML1384L. It is here considered to be part of the Elephant Hole Cave system, however, it may be independent of all accumulations on the mountain. A large wedge of limestone covers any potential connection between QML1384L and QML 1385 below it.

*Stratigraphic context.* Although the relationship of the deposit to the Elephant Hole Cave system is unclear, it is considered older than both QML1312 and QML1384 based primarily on the preservation of the bones, cementing of the breccia and great depth on the mountain.

*Breccia components.* The bone breccia contains deep red coloured clays, well sorted, well rounded pebbles and gravel and abundant fossilised bones and teeth. The breccia is heavily cemented but lacks distinctive speleothem genesis. Clasts of gravels are distinctly allochthonous with few parent limestone fragments.

*Bone preservation.* Disarticulated, slight reworking and rounding of dark-coloured bones. The majority of the bones are discoloured to some degree with crystallisation occurring within the bone. Long bones are usually found in parallel orientations but are not associated.

*Tooth preservation.* Variably preserved either within jaws, isolated and complete, or isolated and tumbled with smoothed edges.

*Shell preservation.* Rare.

*Facies Interpretation.* QML1385 is a complex mixture of accumulation processes. Bones and teeth are variably preserved and show differing degrees of preservation and alteration. A small portion of the bones and teeth are tumbled and rounded indicating stream or channel deposition. Many bones, especially frog ilia and mammal and bird limb bones show signs of predation, including bite marks (bat) and semi digestion (owl). The site is interpreted as a mixed deposit of material accumulated by reworking and water transportation of a predator accumulation. The material was then washed deep within the mountain to form well-sorted stream gravel deposits. Lack of travertine clasts or travertine development may indicate the deposition into a water-filled pool or a recently opened chamber.

#### LIMESTONE RIDGE

Limestone Ridge occurs directly to the east and southeast of Mount Etna (Fig 1, C) and may have been connected to Mt. Etna in the past. The ridge is bisected by a large siltstone/mudstone unit of the Mount Alma Formation, therefore, the cave systems presented herein are best described in two sections, northwest Limestone Ridge and southeast Limestone Ridge. The limestone blocks do not dip to the southeast as seen at Mount Etna and overall cave system development is along a horizontal joint axis.

Within a horizontally controlled joint system phreatic enlargement has developed long, 'ballroom' shaped and sized chambers. The presence of massive speleothems illustrates a long vadose history. Some horizontal development of the caves has been due to the influence of intrusive sills of volcanogenic material, such as Ball Room Cave J8 and Lost Paradise Cave J7 (Shannon, 1970a).

#### NORTHWEST LIMESTONE RIDGE

##### Johansen's cave system

JOHANSEN'S CAVE J1 AND J2. "*This is at present the largest cave in the Mt Etna district*" Shannon (1970b: 29).

Johannsens Cave is characterised by its abundance of bat guano. In 1919 guano mining began in Johansen's Cave. A discovery by P.H. Ebbott of a mandible of *Sarcophilus lanianus* (Longman, 1921) from within a guano matrix may be attributed to guano mining in Johansen's or Bee Cave. In 1926 Whitehouse recovered a small surface collection of bones from the guano in Johansen's Cave, all being from modern local species. In 1972 Mike Murray collected kangaroo mandibles, an edentulous *Sarcophilus harrisii* mandible and a crocodilian premaxilla from Lower Johansen's Cave. The mandibles were obviously from guano accumulations as guano still adheres to the bone. A note on the specimen label for the crocodile premaxilla (QMF17071) reads "In flowstone bed, above Tas. Devil level, Lower Johansen's Cave."

In 2002 the author visited Johansen's Cave, in particular Lower Johansen's Cave (J2), to relocate the flowstone bed with a guano unit below it. A distinctive thick (10-30cm) flowstone bed occurs along a small section of the back chamber with a large unit of mined guano below it. Preliminary inspection of the chamber located large vertebrate bones, including macropod metatarsals within the flowstone and similar-sized but differently preserved bone in the guano. The flowstone bed forms a false floor across a small portion of the chamber with a secondary filling of guano.

QML1314, Guano bed below flowstone *Stratigraphic context.* Guano occurs throughout the cave and has an amorphous sedimentological structure. It is considered younger than the flowstone unit because of the false floor nature of the flowstone.

*Breccia component.* Fine-grained dark brown to black guano, heavily organic; large and small bones of variable size and parent limestone fragments.

*Bone preservation.* Disarticulated, well preserved bone with long bones preserving epiphyses.

*Tooth preservation.* Variably preserved jaws with teeth preserved or isolated.

*Snail preservation.* Abundant, complete snail shells. Colour patterning present.

*Facies Interpretation.* A guano deposit with minor stream and channel movement within a large chamber.

QML368, FLOWSTONE (FALSE FLOOR) UNIT *Stratigraphic context.* A distinct false floor developed over an older sediment, which has been subsequently eroded leaving the false floor. Guano fills within a vacuity under the false floor. Thus, the flowstone unit is considered to be older than the guano beneath it.

*Breccia components.* Fine-grained yellow to brown clays with very well preserved, heavily cemented travertine. Numerous large bones and land snails occur within these flowstone bands.

*Bone preservation.* Disarticulated. Well preserved bones with most epiphyses preserved.

*Facies Interpretation.* Flowstone false floor.

*Surface collection:* no stratigraphic context.

SHUFFLE CAVE NO E NO: bone collection QML371

OLDER TIMBERS CAVE J31: surface collection QML372 & 1315

#### SOUTHEAST LIMESTONE RIDGE

##### Mini cave system

MINI CAVE J12. "*Small horizontal ... active inflow cave. The single entrance leads to a tunnel cavern 60 feet long then a short crawl to an end [second] chamber*" (Shannon, 1970b: 32).

At the end of the first chamber is a small shelf of heavily cemented bone breccia. The existing breccia is the remainder of a more substantial deposit that would have filled at least 40% of the first chamber.

QML1284, MINI CAVE CHAMBER BRECCIA, *Stratigraphic context.* The chamber breccia occurs lower on Limestone Ridge than both surface breccias (QML1284a and QML1382), however, they are considered to be

contemporaneous deposits. QML1284a illustrates an entrance facies, which would be expected to occur above the QML1284 section, feeding material into the chamber.

*Breccia components.* Consists of fine-grained yellow to red coloured clay, bedded travertine, small angular clasts of parent limestone, allochthonous siltstone and serpentinite, small black goethitic and lighter coloured carbonate pisolites. The oxide pisolites are considered to be allochthonous, the carbonate pisolites autochthonous (cave pearls). The sediments are layered with speleothem, producing distinct sections throughout the deposit. These layers are continuous throughout the deposit and are interpreted as a series of sump deposits flowing into permanent rim pools.

*Bone preservation.* An articulated assemblage of small cave dwelling species such as snakes, frogs and bats. Bones well preserved in a halo of carbonate. Bones vary in size from tiny osteoderms to pockets of larger bone up to 100mm in size. All skeletal elements are well preserved, even the minute osteoderms from skinks. Little evidence of bone gnawing or digestion from predators.

*Tooth preservation.* Teeth usually in jaws and well preserved tooth rows, mostly molar rows and isolated incisors. Majority of teeth are from small taxa, however, isolated teeth from large-sized taxa occur randomly in the lenses.

*Shell preservation.* Snail shells well preserved, usually complete shells of varying sizes.

*Facies Interpretation.* Presence of distinct rim pool formations (basin-shaped travertine, abundant carbonate pisolites, and sorting of sediment matrix) indicates the deposit was at the base of a chamber being fed from above. The entrance is thought to have been higher than the current Mini Cave entrance and QML1284a is in a suitable position to be this entrance facies. The abundance of articulated or associated specimens indicates that many vertebrates including frogs, bats, rodents and snakes inhabited the chamber.

**QML1284A, ABOVE MINI CAVE.** Located above and to the northwest of the Mini Cave entrance is a heavily weathered bone breccia, which is interpreted as the upper level of the Mini Cave System, and an old cave chamber collapse.

*Stratigraphic context.* QML1284a deposit sits above QML1284 sediments but is considered to be relatively contemporaneous as it is believed that QML1284a is the entrance facies for the

same series of accumulations making up the deeper rip pool deposits of QML1284. QML1382 is a lateral extension of the QML1284a entrance facies, therefore, is of similar age also.

*Breccia components.* Pink-grey coloured clay, heavily cemented with thinly bedded travertine throughout. Irregular bedding within breccia blocks. Large clasts of parent limestone, with smaller clasts of oxide and carbonate pisolites, allochthonous gravels and large calcite vugs.

*Bone preservation.* Well preserved, complete bones and associated specimens. Bones showing predation and partial digestion. Snail shells complete and associated with travertine.

*Tooth preservation.* Teeth usually in jaws and well preserved.

*Shell preservation.* Well preserved, complete.

*Facies Interpretation.* Large angular limestone clasts and irregular bedding suggests a facies close to an entrance. The presence of a distinct predator accumulation and a small contribution of larger vertebrate remains suggests a chamber was close to an entrance, which was big enough to support a bat or owl's roost.

**QML1382, LEO'S LUNCH SITE.** Located to the north of QML1284a, QML1382 is interpreted as a lateral extension of the QML1284a collapse line.

*Breccia components.* A grey-pink, heavily cemented bone breccia with large clasts of parent limestone, smaller clasts of flowstone, pisolites and allochthonous sediment.

*Bone preservation.* Small grain-sized fragments, isolated limbs and vertebrae within flowstones.

*Tooth preservation.* Isolated teeth.

*Shell preservation.* Snail shells associated with flowstone.

*Facies Interpretation.* A lateral extension of the entrance facies of QML1284a, with greater flowstone development and irregular bone accumulations.

*Surface collections:* no stratigraphic context.

**LOST PARADISE CAVE J7:** bone collection, stream channel first chamber.

**BALL ROOM CAVE J8:** bone collection, stream channel southern end of main chamber.

#### OLSEN'S CAVE SYSTEM

##### Olsen's cave.

*"Essentially only one cave system of sixteen interconnected caverns, usually joint-controlled*

*and of varying dimensions...*” Shannon (1970b: 36).

*Stratigraphic context.* Unknown, however, bone preservation suggests relatively young deposit.

*Breccia components.* Dark brown coloured clay sediment. Loosely consolidated and cemented cave floor sediment. No major clasts present.

*Bone preservation.* A mass of disarticulated, unsorted, tightly compacted fragmentary bone.

*Tooth preservation.* Jaws with teeth and most molar rows. Exclusively small vertebrates.

*Shell preservation.* Nil.

*Facies Interpretation.* Tightly compacted bone accumulation of predominantly small vertebrate remains suggests a typical predator accumulation such as an owl's roost accumulation. Some incorporation of isolated macropod teeth.

#### KARST GLEN SYSTEM

To the southwest of Olsen's Cave is another isolated outcrop of limestone known as Karst Glen. Several small to medium sized caves occur in this limestone block and possess associated fossil deposits. Tall karst towers on the northern aspect of the limestone outcrop demarcate a collapsed cliff line following an intersecting vertically jointed system. These collapses have exposed a series of bone breccias and cemented cave floor sediments. Amongst the karst scree, several *in situ* fossil deposits can be found, generally near to, or beneath, a present cave entrance. Within the chambers, deep sequences of breccia are associated with extensive speleothems. Collections were not made within the caves of these breccias, however, outcrops of surface breccia were located and collected.

#### QML1411-1414, KG3 surface breccia

**QML1411, KG3 BRECCIA UPPER BRECCIA SITE.** Located as an exposed fissure deposit near the top of the karst limestone at Karst Glen, QML1411 connects with the sediment found deeper within the limestone caverns. Lithologically it is unique amongst the cave deposits for central eastern Queensland being a markedly pisolitic conglomerate rather than a breccia.

*Stratigraphic context.* QML1411 occurs high on the open karst as a fissure deposit dipping at approximately 45° and running the length of a NW joint. It is stratigraphically higher than any of the other units currently at Karst Glen and is considered to be a very old fissure fill system.

The age of the sites in relation to the other sites on Karst Glen is unknown.

*Breccia components.* The rock unit at QML1411 is best considered a pisolitic conglomerate. The majority of the unit contains large and small, well rounded conglomerate of black oxide pisolites. The rock is heavily cemented with the matrix a grey-coloured carbonate clay. Small clasts of parent limestone occur throughout the conglomerate.

*Bone preservation.* Very well rounded and reworked medium-sized bones that are heavily oxidised and shiny black in colour and lustre.

*Tooth preservation.* Nil.

*Shell preservation.* Nil.

*Facies Interpretation.* A heavily reworked channel fill occurring within the confines of a limestone fissure.

#### QML1412 & QML1413, KG3 B ENTRANCE BRECCIA.

QML1412 and QML1413 occurs beneath and to the southeast of “B” entrance within the KG3 Cave complex at Karst Glen. The unit follows a collapsed joint running NE-SW. The breccia is the remnant sediment fill within the vertical joint that has collapsed. Several of the blocks are *in situ*, forming the source for a large breccia scree found working its way downslope throughout the thick vegetation. Large patches of flowstone exposed on the surface can also be found closer to the present cliff line.

*Stratigraphic context.* QML1412 and QML1413 are of unknown stratigraphic context to other sites on KG3 and within the Cave systems. As the deposits are all joint controlled, each joint may contain contemporaneous sediment without stratigraphic contact.

*Breccia components.* A fine grained, red coloured matrix that is heavily cemented. Very small allocthonous gravel and pisolite clasts. Sediment is clay dominant. Weathered flowstone found in patches throughout the site.

*Bone preservation.* Bone mostly small and well sorted into fine lenses forming the main irregular bedding planes. Finest portion of bone material, small and sand grain-sized. Bone well preserved, however, most elements are fragmentary with epiphyses missing.

*Tooth preservation.* Teeth usually associated with jaws. Almost entirely comprised of small jaws of rodents, possums, bats and dasyurids. Very few larger vertebrates present.



*Shell preservation.* Very little shell present. Some well preserved isolated large snails.

*Facies Interpretation.* The lack of large angular limestone clasts, patchy travertine and abundant clay load indicates a non-entrance facies. The fine lenses of grain-sized bones and massive accumulation of small vertebrates indicates a possible predator accumulation.

#### MARMOR QUARRY

##### QML1420.

Bone breccia collected by Bartholomai in 1964

*Stratigraphic context.* Unknown. QML1420 has been treated as a single fauna because none of the fossils are in stratigraphic context. Two factors suggest that the fossils have been derived from similarly aged sediment, probably the same breccia: 1. The lithology of the matrix adhering to all of the material collected is very similar. When known sites of different age are compared at Mount Etna, the matrix differs dramatically in sediment colour, cementation and bone preservation (e.g. QML1312 versus QML1311). Therefore, it seems likely that the material from Marmor Quarry is derived from the same unit. 2. Two collections have been used for this analysis: One by Longman in the 1920's and one by Bartholomai in the 1960's. Both collections used the mine manager of-the-day as a source of historical knowledge for site location, plus they both collected similar fauna, such as *Macropus titan*, *M. agilis siva*, and *Sarcophilus laniarius*.

Both collections contain similar species of rodents and bandicoots, with the small mammals derived from Bartholomai's collection via acid etching of bone breccia. This breccia also contained megafauna such as *Macropus titan*.

*Breccia components.* Grey to brown clay, lightly cemented; clasts of limestone only.

*Bone preservation.* Bone preserved as grain-sized fragments, isolated large long bone elements and occasional large vertebrate remains.

*Tooth preservation.* Small-sized vertebrates are generally preserved as isolated teeth without jaws. Large-sized vertebrates present as isolated mandibles and maxillae with preserved teeth.

*Shell preservation.* Isolated large snails.

*Facies Interpretation.* The sediment type and bone preservation is very similar to the guano found in Lower Johansen's Cave, the major difference being the degree of cementation. Marmor Quarry sediment is considerably more cemented than the guano found at Lower

Johannsen's Cave. It is therefore considered that the breccia recovered by Bartholomai in 1964 comes from a cemented guano deposit.

#### FAUNAS

Many of the sites individually represent diverse faunas and their constituent taxa are tabulated (Tables 1-3, Appendix 1). Higher level taxa which are represented by few or one elements but are noteworthy are listed below. In addition the murids are listed below but will be described in another work.

#### UNDESCRIBED TAXA

Teleost indet. QMF51442, vertebra, QML368.

Microchiropterans; QMF48001-48108; QMF48160-QMF48165; All localities (except QML1420).

Bats are found in all faunal assemblages except QML1420 and range in size from very small species of *Miniopterus*, to the very large *Macroderma gigas* (Fig. 29A-E.). Identification of the numerous small species of bats was outside the scope of the present study.

Murids: Rodents are a conspicuous element of all sites and faunal assemblages. At least ten genera have been identified (Author and H. Godthelp). The taxa range in size from the large arboreal *Melomys/Uromys* and aquatic *Hydromys*, to the very small arboreal *Pogonomys* and terrestrial *Leggadina*. Specific identifications will be determined in a full review of the rodents. A preliminary list is provided below with identified specimens.

**Conilurus** sp. Fig. 30A: QMF52052; QML1312.

**Hydromys** sp. QMF52056; QML1420.

**Leggadina** sp. Fig. 30B: QMF52040-QMF52042, QML1312; Olsen's Cave; QML1314.

**Uromys/Melomys** sp. Fig. 30C-D: QMF52014-QMF52021; QML1284; QML1284a; QML1313; QML1420; QML1311; QML1384L.

**Mesembriomys** spp. QMF52028-QMF52032, QML1284; QML1384L; QML1385; QML1313; QML1311.

**Notomys** spp. Fig. 30I: QMF52036-52039; QML1312.

**Pogonomys** sp. nov. Fig. 30G QMF52022-QMF52027; QML1313; QML1284; QML1284a; QML1384U; QML1384L; QML1385; QML1311.

**Pseudomys** spp. Fig. 30E-F; QMF52043-QMF52051; All Localities.

**Rattus** spp. Fig. 30J; QMF52033- QMF52035; QML1312; QML1384U; Olsen's Cave; QML1420.

**Zyzomys** spp. Fig. 30H; QMF52053- QMF52055; QML1284; QML1284a; QML1312.

#### SYSTEMATIC PALAEONTOLOGY

Order ANURA Rafinesque, 1815

Family HYLIDAE Rafinesque, 1815

**Cyclorana** Steindachner, 1867

**Cyclorana** sp.  
(Fig. 4G)

MATERIAL. QMF51443 & QMF51444 ; Olsen's Cave.

Two ilia represent this genus. Both ilia possess very large acetabular fossae with thin acetabular rims; distinct but small dorsal acetabular expansion; small and rounded ventral acetabular expansion; narrow preacetabular zone; slight curvature of the ilium; distinct dorsal prominence; anteroventrally and laterally orientated dorsal protuberance. Dorsal prominence almost entirely anterior of the acetabular rim. Superior acetabular rim margin above the level of the ventral margin of the ilial shaft. Lateral rim and medial groove absent. Ilial crest absent.

Identified as *Cyclorana* on comparison with Tyler's description of the genus (Tyler, 1976; Tyler et al., 1994). Identified as being close to *Cyclorana cultripes* by the presence of the large acetabular fossa, distinct dorsal prominence and protuberance and laterally projecting protuberance. Comparative specimens of the many species of *Cyclorana* were not available for this study, therefore, no specific assignment is warranted.

#### **Litoria/Nyctimystes**

Menzies et al. (2002) illustrated the problems associated with identifying fossil hylids from their pelvic elements, especially differentiating species of *Litoria* and *Nyctimystes*. Using the diagnostic features described by Tyler (1976) and Menzies et al. (2002) for *Litoria* and *Nyctimystes*, it was clear that both these taxa are present within the faunal assemblages. Identification to species level was not possible, except for those fossil specimens closely allying taxa with available comparative specimens such as *Litoria caerulea*.

Specimens assigned to *Litoria* were so based on the presence of the following distinctive

features; 1. Ovoid dorsal protuberance, 2. Dorsal ilial crest absent, 3. Large acetabular fossa. Specimens assigned to *Nyctimystes* were so based on the presence of the following additional features to those seen in *Litoria*; 1. Ventral acetabular expansion rounded. 2. Very broad preacetabular zone.

**Litoria** Tschudi, 1838

**Litoria** sp. 1  
(Fig. 4D)

MATERIAL. QMF51445; QML1385.

Small *Litoria* with: 1. acetabular fossa large and shallow with distinct peripheral rim. 2. dorsal prominence anterior to acetabular rim. 3. dorsal protuberance a distinct ovoid, laterally developed, knob. 4. small fossa posterior of the protuberance and at the base of prominence. 5. ridge runs anteriorly from base of protuberance to medial side of ilial shaft. 6. Ilial shaft slightly curved. 7. dorsal acetabular expansion and ventral acetabular expansion reduced. 8. narrow preacetabular zone. 9. broad ilial shaft.

Differs from all other *Litoria* within the assemblages by possessing an anterior ridge of the dorsal prominence running from the base of the dorsal protuberance to the medial side of the ilial shaft. Differs from *Litoria* sp 2 by possessing a narrow preacetabular zone and a shorter dorsal acetabular expansion. Differs from *Litoria* sp. 3 by being smaller and possessing a smaller dorsal protuberance and a narrower preacetabular zone. Differs from *Litoria* sp. 4 by being smaller and having a more ovoid, and better-developed dorsal protuberance.

**Litoria** sp. 2  
(Fig. 4E)

MATERIAL. QMF51446; QML1385.

Medium-sized *Litoria* with the following: 1. broad, oval, and shallow acetabular fossa. 2. distinct acetabular rim. 3. Narrow preacetabular zone. 4. Elongate dorsal acetabular expansion. 5. Well developed and rounded ventral acetabular expansion. 6. Low dorsal prominence. 7. Dorsal protuberance ovoid and laterally developed. 8. Ilial shaft straight.

Differs from *Litoria* sp. 3 by being larger, having a smaller dorsal protuberance and an elongate dorsal acetabular expansion, which extends superiorly of the line of the dorsal protuberance. Differs from *Litoria* sp. 4 by being

larger, possessing a well-developed dorsal protuberance and broad preacetabular zone.

***Litoria* sp. 3**  
(Fig. 4B)

MATERIAL: QMF51447-51449; QML1385.

A medium-sized *Litoria* possessing the following features: 1. Large, half-moon shaped acetabular fossa. 2. Reduced dorsal acetabular expansion. 3. Ventral acetabular expansion well developed and rounded. 4. Narrow preacetabulae zone. 5. Dorsal prominence reduced. 6. Dorsal protuberance as a massive ovoid knob with a distinct ventral groove.

Differs from *Litoria* sp. 4 by being larger and possessing an enormous ovoid dorsal protuberance with a ventral groove.

***Litoria* sp. 4**  
(Fig. 4C)

MATERIAL. QMF51450-51456; QMF51463-51464, QML1385; QML1284.

A small-sized *Litoria* possessing the following features; 1. Reduced, triangular-ovoid acetabular fossa. 2. Dorsal acetabular expansion and ventral acetabular expansion reduced. 3. Dorsal prominence reduced. 4. Dorsal protuberance conical-shaped and laterally produced. 5. Iliac shaft straight.

Differs from *Litoria conicula* by possessing a larger conical protuberance, smaller acetabular fossa, less developed ventral acetabular expansion and a narrow preacetabular zone.

***Litoria caerulea* (White, 1790)**

MATERIAL. QMF51457-51462; QML1314.

A large-sized *Litoria*, possessing the following features: 1. Medial and lateral groove absent. 2. Dorsal acetabular expansion reduced. 3. Ventral acetabular expansion gently curved. 4. Dorsal prominence and protuberance low on the iliac shaft. 5. Dorsal protuberance elongate-ovoid and slightly produced laterally.

Closely resembles comparative material available for *L. caerulea* from Queensland, especially the distinctly low dorsal prominence and ovoid protuberance.

Two smaller morphs of *Litoria* are present in subfossil accumulations from QML1314. It is uncertain whether these represent different taxa or a highly variable *Litoria caerulea*.

***Nyctimystes* Stejneger, 1916**

***Nyctimystes* sp. 1**  
(Fig. 4F)

MATERIAL. QMF51465; QML1385.

A large *Nyctimystes* possessing the following features of the ilium; 1. Moderately large triangular acetabular fossa. 2. Reduced dorsal acetabular expansion. 3. Ventral acetabular expansion gently rounded and expanded, spatulate-shaped. 4. Preacetabular zone broad. 5. Dorsal prominence low with small indistinct ovoid protuberance. 6. Posterior ridge of dorsal prominence tapers to anterior base of dorsal acetabular expansion. 7. Iliac shaft straight, medio-laterally compressed and broad.

TABLE 1. Faunal lists for fish and amphibians

	QML368	QML1284	QML1284a	QML1312	QML1314	QML1384U	QML1385	Olsen's Cave
Teleosti indet	x							
<i>Cyclorana</i> sp.								x
<i>Litoria</i> sp. 1							x	
<i>Litoria</i> sp. 2							x	
<i>Litoria</i> sp. 3							x	
<i>Litoria</i> sp. 4		x					x	
<i>Litoria caerulea</i>					x			
<i>Nyctimystes</i> sp. 1							x	
<i>Nyctimystes</i> sp. 2		x	x					
<i>Etnabatrachus maximus</i>		x					x	
<i>Crinia</i> sp.							x	
<i>Kyarranus</i> sp.		x	x			x	x	
<i>Limnodynastes</i> sp. 1							x	
<i>Limnodynastes</i> sp. 2		x		x			x	
<i>Limnodynastes</i> sp. 3			x					
<i>L. tasmaniensis</i> sp. grp.							x	
<i>L. spenceri</i> sp. grp.							x	
<i>L. sp. cf. L. peronii</i>		x		x				
<i>Lechriodus</i> sp.		x						
<i>Neobatrachus</i> sp.							x	
microhylid sp. 1		x	x					
microhylid sp. 2		x	x					
microhylid sp. 3		x						

Differs from *Nyctimystes* sp. 2 by lacking a well-developed dorsal prominence and laterally developed dorsal protuberance. Further differs by lacking a distinctive groove ventral of the dorsal protuberance.

***Nyctimystes* sp. 2**

MATERIAL. QMF51466-51468; QMF51469-51471, QML1284; QML1284a.

A large *Nyctimystes* possessing the following features of the ilium; 1. Large ovoid acetabular fossa. 2. Reduced and pointed dorsal acetabular expansion. 3. Ventral acetabular expansion rounded and very broad. 4. Preacetabular zone broad and gently curved to the base of the ilial shaft. 5. Dorsal prominence and protuberance low on the ilial shaft. 6. Dorsal protuberance distinct and laterally developed into an elongate-ovoid knob. 7. Beneath the dorsal protuberance runs a distinct lateral groove. 8. Dorsal protuberance above anterior-most margin of acetabular rim.

*Nyctimystes* sp. 2 most closely resembles *N. disrupta* and *N. zweifeli* from illustrations and descriptions available from Tyler (1976) and Menzies et al. (2002).

***Etnabatrachus* Hocknull, 2003**

***Etnabatrachus maximus* Hocknull, 2003  
(Fig. 6B)**

MATERIAL. QMF44207, QMF44208; QML1385, QML1284.

A giant frog probably from the Hylidae, based on the large rounded dorsal protuberances. Previously described by Hocknull (2003) and currently endemic to the Plio-Pleistocene of Mount Etna and Limestone Ridge.

Family LEPTODACTYLIDAE Werner, 1896

***Crinia* Tschudi, 1838**

***Crinia* sp.  
(Fig. 4A)**

MATERIAL. QMF51472, QML1385.

A small leptodactylid. Only the rim of acetabular fossa preserved, indicating a large rounded and shallow fossa. Other features include: 1. Dorsal acetabular expansion short and pointed. 2. Ventral acetabular expansion broken and insignificant. 3. Preacetabular zone narrow. 4. Dorsal prominence low and long, running halfway anterior of the acetabular rim. 5. Dorsal protuberance inconspicuous. 6. Long thin

median groove running the length of the ilial shaft. 7. Ilial shaft curved and slender.

*Crinia* sp. is identified as *Crinia* based on its small-size, reduced dorsal prominence and protuberance, slender curved ilial shaft, large acetabular fossa and longitudinal medial groove.

***Kyarranus* Moore, 1958**

***Kyarranus* sp.  
(Fig. 5F)**

MATERIAL. QMF51488, QMF51489, QMF51490, QMF51491; QML1284a; QML1284, QML1385, QML1384U.

Large sub-triangular acetabular fossa. Acetabular rim distinct and high. Dorsal acetabular expansion expressed as a triangular point at an equivalent height to the dorsal prominence and protuberance. Ventral acetabular expansion narrow and anteriorly projecting. Preacetabular zone narrow. Dorsal prominence high and anterior of acetabular rim. Dorsal protuberance is an elongate antero-dorsally projecting process from dorsal prominence. Small fossa at the posterior base of the dorsal prominence. Ilial shaft long, slender and curved.

*Kyarannus* is a distinctive leptodactylid, possessing an elaborate dorsal prominence and anteriorly projecting protuberance. The combination of this feature with a long, curved ilial shaft and a high acetabular rim identify *Kyarranus* here. Specific placement will be considered in later works.

***Limnodynastes* Fitzinger, 1843**

Tyler et al. (1998) describes all species of *Limnodynastes* as possessing an extremely large dorsal prominence and protuberance, and a high and steep dorsal acetabular expansion of the ilium. Within the genus there is considerable variation of these features, with the development of an ilial crest in some taxa (Tyler 1976). Specimens possessing these features are here assigned to *Limnodynastes*.

***Limnodynastes* sp. 1**

MATERIAL. QMF51473-51474; QML1385.

Acetabular fossa large and high, with a distinct acetabular rim. Dorsal acetabular expansion rises steeply from the shaft to an acute point. Ventral acetabular expansion is gracile and rounded. Preacetabular zone narrow and runs beneath the rim of the acetabulum. Dorsal prominence rises high above ilial shaft and positioned anterior of the acetabular margin. Dorsal prominence antero-dorsally oriented and distinct. A short



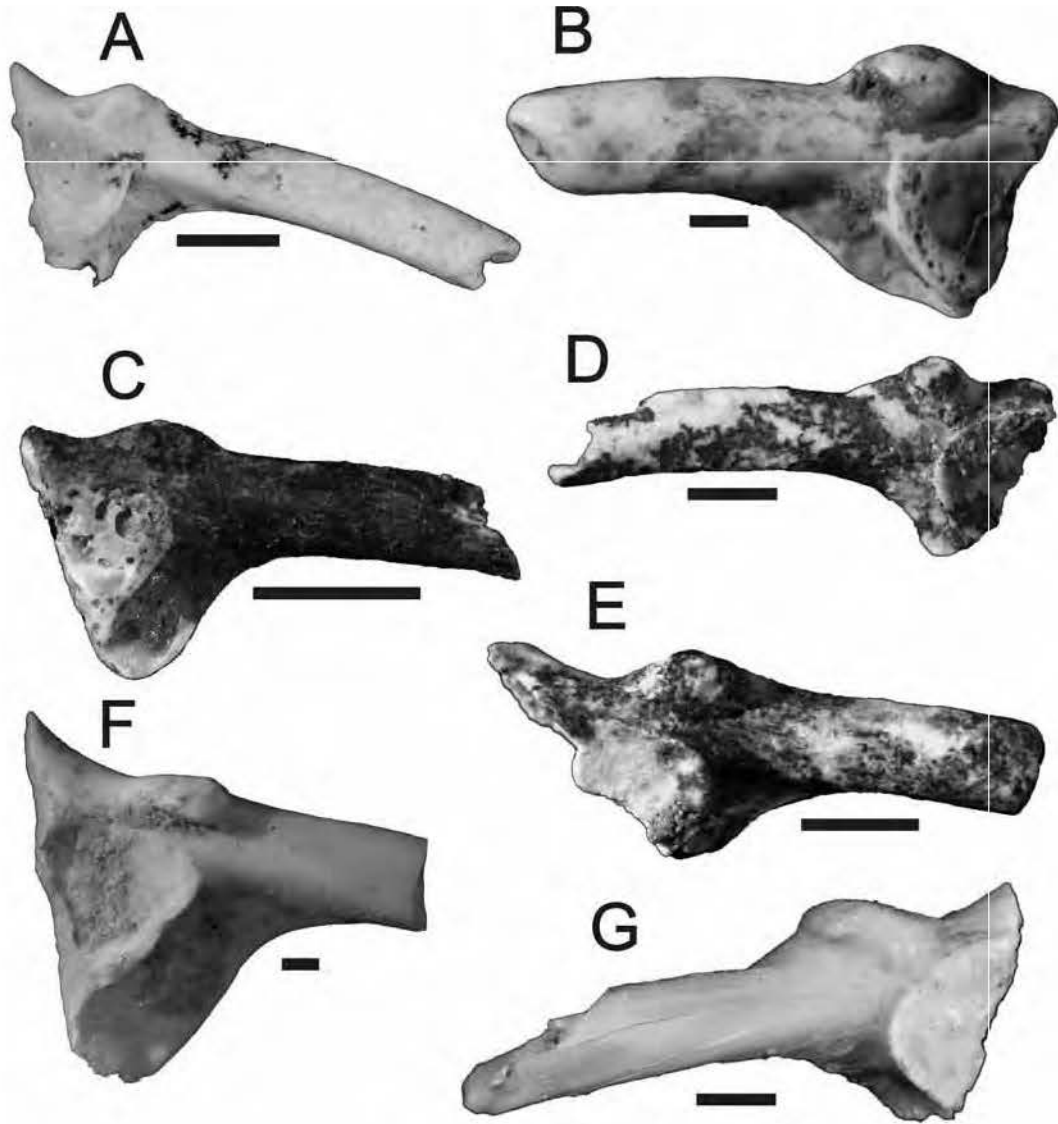


FIG. 4. A, *Crinia* sp.; QMF51472, right ilium. B, *Litoria* sp. 3; QMF51447, left ilium. C, *Litoria* sp. 4; QMF51450, right ilium. D, *Litoria* sp. 1; QMF51445, left ilium. E, *Litoria* sp. 2; QMF51446, left ilium. F, *Nyctimystes* sp. 1; QMF51465, left ilium. G, *Cyclorana* sp.; QMF51443, left ilium. Scale bar = 1mm.

lateral groove runs 1/3 the length of the ilial shaft, originating just anterior to the base of the dorsal prominence. A long median groove runs the length of the ilial shaft. Iliac shaft slightly curved.

Differs from *Limnodynastes* sp. 2 by possessing a median groove, a larger dorsal prominence and protuberance and missing a

pocket on the ventral acetabular expansion, situated beneath the acetabular rim. Differs from *Limnodynastes* sp. 3 by lacking a lateral groove ventral to the dorsal prominence and possessing a better-developed dorsal protuberance. Differs from *Limnodynastes tasmaniensis* sp. group by possessing a median groove on the ilium. Differs

from *Limnodynastes spenceri* sp. group by lacking a dorsal ilial crest. Differs from *Limnodynastes peronii* by being much smaller and lacking the massive development of the dorsal prominence and protuberance.

***Limnodynastes* sp. 2**  
(Fig. 5E)

MATERIAL. QMF51476-51477, QMF51478-51481, QMF41864, QMF41856, QMF33383; QML1284, QML1385, QML1312.

Acetabular fossa broad and shallow, subtriangular in lateral view. Acetabular rim high. Dorsal acetabular expansion elongate and pointed reaching much higher than the tip of the

dorsal protuberance. Ventral acetabular expansion rounded. Preacetabular zone narrow, running beneath the acetabular rim. A dorsal pocket occurs beneath the rim and at the origin of the ventral acetabular expansion. Dorsal prominence low and inconspicuous. A small fossa is located at the posterior base of the prominence. Dorsal protuberance equally inconspicuous being low and only slightly conical. Iliac shaft laterally compressed, narrow and curved.

Differs from *Limnodynastes* sp. 3 by possessing a pocket on the ventral acetabular expansion and a lower dorsal prominence. Differs from *Limnodynastes tasmanensis* group

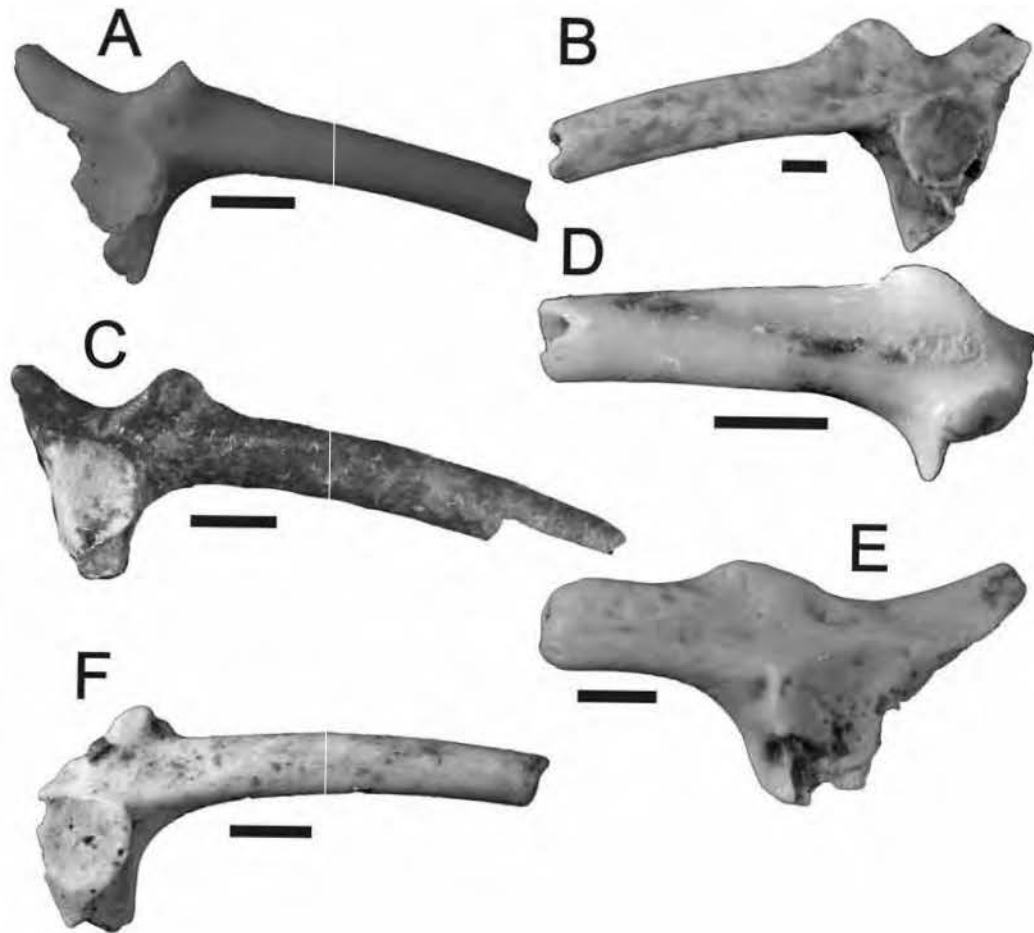


FIG. 5. A, *Limnodynastes* sp. 3; QMF51486, right ilium. B, *Limnodynastes* sp. cf. *L. peronii*; QMF41793, left ilium. C, *Limnodynastes* sp. 1; QMF51473, right ilium. D, *Limnodynastes spenceri*; QMF51484, left ilium. E, *Limnodynastes* sp. 2; QMF51476, right ilium. F, *Kyarranus* sp.; QMF51489, right ilium. Scale bar = 1mm.

by possessing a lower prominence, indistinct protuberance and lacking a lateral groove. Differs from *Limnodynastes spenceri* group by lacking a dorsal ilial crest. Differs from *Limnodynastes peronii* by lacking a massively developed dorsal prominence and protuberance.

**Limnodynastes sp. 3**  
(Fig. 5A)

MATERIAL. QMF51486; QML1284a.

Acetabular fossa ovoid and deep, rim elevated. Dorsal acetabular expansion elongate and pointed dorsally. Ventral acetabular expansion rounded and gracile. Preacetabular zone narrow. Lateral groove absent. Dorsal prominence low. Dorsal protuberance distinct, as a point projecting antero-dorsally from the prominence. Iliac shaft slightly curved. Median groove running the length of the iliac shaft.

Differs from *Limnodynastes tasmaniensis* group by possessing a median groove along the shaft and lacking a lateral groove. Differs from *Limnodynastes spenceri* group by lacking an ilial crest. Differs from *Limnodynastes peronii* by lacking a massive dorsal prominence and protuberance.

**Limnodynastes tasmaniensis** Günther, 1858  
sp. group.

MATERIAL. QMF51482-51483; QML1385.

Acetabular fossa distinctly rounded and elevated from the shaft. Dorsal acetabular expansion elongate, tapering to a point at an equivalent level to the dorsal protuberance. Ventral acetabular expansion narrow and tapered. Preacetabular zone narrow and concave. Lateral groove present on the shaft just ventral to the dorsal prominence. Dorsal prominence distinct, triangular shaped. Dorsal protuberance elongate, ovoid and projecting antero-dorsally. Iliac shaft curved.

Differs from *Limnodynastes spenceri* group by lacking a dorsal ilial crest. Differs from *Limnodynastes peronii* by lacking the massive dorsal prominence distinctive of *L. peronii*.

**Limnodynastes spenceri** Parker, 1940 sp.  
group.  
(Fig. 5D)

MATERIAL. QMF51484-51485; QML1385.

Small ilium possessing a distinct dorsal ilial crest and prominent antero-dorsally oriented dorsal protuberance. Acetabular fossa small and rounded. Acetabular rim distinct. Dorsal acetabular expansion unknown in the specimens. Ventral acetabular expansion unknown in

specimens. Preacetabular zone narrow and close to the acetabular rim. Iliac shaft relatively straight.

Differs from all other *Limnodynastes* species by possessing an ilial crest. Differs from the only other taxa with ilial crests, *Rana*, *Mixophyes* and *Lechriodus*, by lacking the extreme dorsal development of the crests.

**Limnodynastes sp. cf. L. peronii** Duméril & Bibron, 1841  
(Fig. 5B)

MATERIAL. QMF41793, QMF41801, QMF41812, QMF41821, QMF41827, QMF33380, QMF41863, QMF41865-41866; QML1284; QML1312.

Acetabular fossa large and rounded. Rim elevated and thick. Dorsal acetabular expansion elongate and tapered, steeply pointed. Ventral acetabular expansion rounded and broad. Preacetabular zone narrow and concave. Fossa present at the posterior base of the dorsal prominence. Dorsal prominence distinct and anterior of acetabular rim. Dorsal protuberance large and well developed. Protuberance anterior projecting. Iliac shaft broad and slightly curved.

Specimens assigned to *L. peronii* from QML1284 differ from conspecific specimens from QML1312 in possessing a distinct fossa and a more anteriorly projecting dorsal prominence. This variation is considered to be within the possible range of variation for this taxon.

**Lechriodus** Boulenger, 1882

**Lechriodus sp.**  
(Fig. 6A)

MATERIAL. QMF51492; QML1284.

Iliac crest present. Dorsal protuberance ovoid and level with the acetabular rim. Dorsal acetabular and ventral acetabular expansions narrow and short. Preacetabular zone narrow. Broad semicircular acetabular fossa. Shallow lateral groove runs the length of the iliac crest.

**Neobatrachus** Peters, 1863

**Neobatrachus sp.**  
(Fig. 6C)

MATERIAL. QMF51487; QML1385.

Acetabular fossa very small and rounded. Acetabular rim low and distinct from preacetabular zone. Dorsal acetabular expansion very broad and high, coalescing with the posterior margin of the dorsal prominence. Ventral acetabular expansion narrow and pointed. Preacetabular zone narrow and close to

acetabular rim. Dorsal prominence is large with a tiny point making up the dorsal protuberance. Iliac shaft nearly straight and laterally compressed.

*Neobatrachus* possesses distinct iliac characteristics not found in other leptodactylids, including the elaboration of the dorsal acetabular expansion and its coalescence with the dorsal prominence, small acetabular fossa and reduced ventral acetabular expansion. Specific assignment is not justified at this stage due to the lack of comparative specimens.

Family MICROHYLIDAE Günther, 1858

Microhylids have been identified from some of the faunal assemblages based on their small size, very large acetabular fossa, curved shaft and diminutive posteriorly placed dorsal prominence and protuberance.

microhylid sp. 1  
(Fig. 6C)

MATERIAL. QMF51493-51494, QMF51495; QML1284, QML1284a.

Large rounded acetabular fossa which is distinct from the shaft and possesses a distinct acetabular rim. Dorsal acetabular expansion short and pointed. Ventral acetabular expansion short and rounded. Preacetabular zone narrow and constricted toward the acetabular rim. Dorsal prominence low with a conical protuberance posterior of acetabular rim. Iliac shaft recurved without dorsal crest.

Differs from microhylid 2 by possessing a curved shaft and less ridged dorsal protuberance. Differs from microhylid 3 by lacking a dorsal crest.

microhylid sp. 2  
(Fig. 6F)

MATERIAL. QMF51496, QMF51497; QML1284, QML1284a.

Acetabular fossa large and rounded. Distinct acetabular rim. Dorsal acetabular expansion and ventral acetabular expansion unknown, however, inferred to be reduced. Preacetabular zone narrow. Dorsal prominence low, dorsal protuberance small and ridged. Iliac shaft slightly curved and slender. Differs from microhylid 3 by lacking a dorsal crest.

microhylid sp. 3 cf. *Hylophorbus* Macleay,  
1878  
(Fig. 6D-E)

MATERIAL. QMF51498; QML1284.

Large rounded acetabular fossa. Distinct acetabular rim, set high above iliac shaft. Dorsal acetabular expansion elongated to a sharp dorsal point. Ventral acetabular expansion anteriorly deflected and rounded. Preacetabular zone narrow. Dorsal prominence inconspicuous, forming the posterior margin of a dorsal crest. Dorsal protuberance elongate and antero-dorsally projecting. Iliac shaft curved. Dorsal crest laterally compressed, angled medially, running almost the entire length of the iliac shaft.

The form of the ilium, distinct iliac crest, and curvature of the shaft ally this taxon very closely to *Hylophorbus* from Papua New Guinea as described and figured in Menzies et al. (2002). More specimens and access to comparative *Hylophorbus* will be needed to clarify its taxonomic placement within the Microhylidae.

Order TESTUDINES Linnaeus, 1758

Family CHELIDAE Gray, 1825a

chelid indet.  
(Fig. 7G-H)

MATERIAL. QMF52061, QMF52062, QMF52063; QML1311(H); QML1384L; QML1311(C/D).

Several pieces of carapace and plastron represent remains of freshwater turtles. The portions of carapace are thick, with distinct suture lines. A single posterior portion of a plastron is very thin and preserves pelvic sutures from the left side.

Order NEOSUCHIA Benton & Clark, 1988

Family CROCODYLIDAE Cuvier, 1807

Mekosuchinae indet.  
(Fig. 7A-F)

MATERIAL. QMF51499-51505, QMF52064-52065, QMF17071; QML1311 (H), QML1384L, QML368, QML1313.

Fragmentary remains, including a serrated ziphodont tooth, a portion of an edentulous premaxilla, two partial vertebrae, three scutes, the proximal end of a femur and an ungual represent crocodilians. The tooth has a distinctly serrate carinae and is ziphodont in form. A wear facet can be seen on the mesial margin of the tooth. The premaxilla is rounded with three alveoli, linked to one another by thick ridges on the lateral premaxillary margin. The vertebrae are antero-posteriorly compressed and squat, preserving both the condyle and cotyle. Scutes, small and thin, with a flat ventral surface and a keeled dorsal surface. Rows of pits occur on the dorsal surface of the scutes.

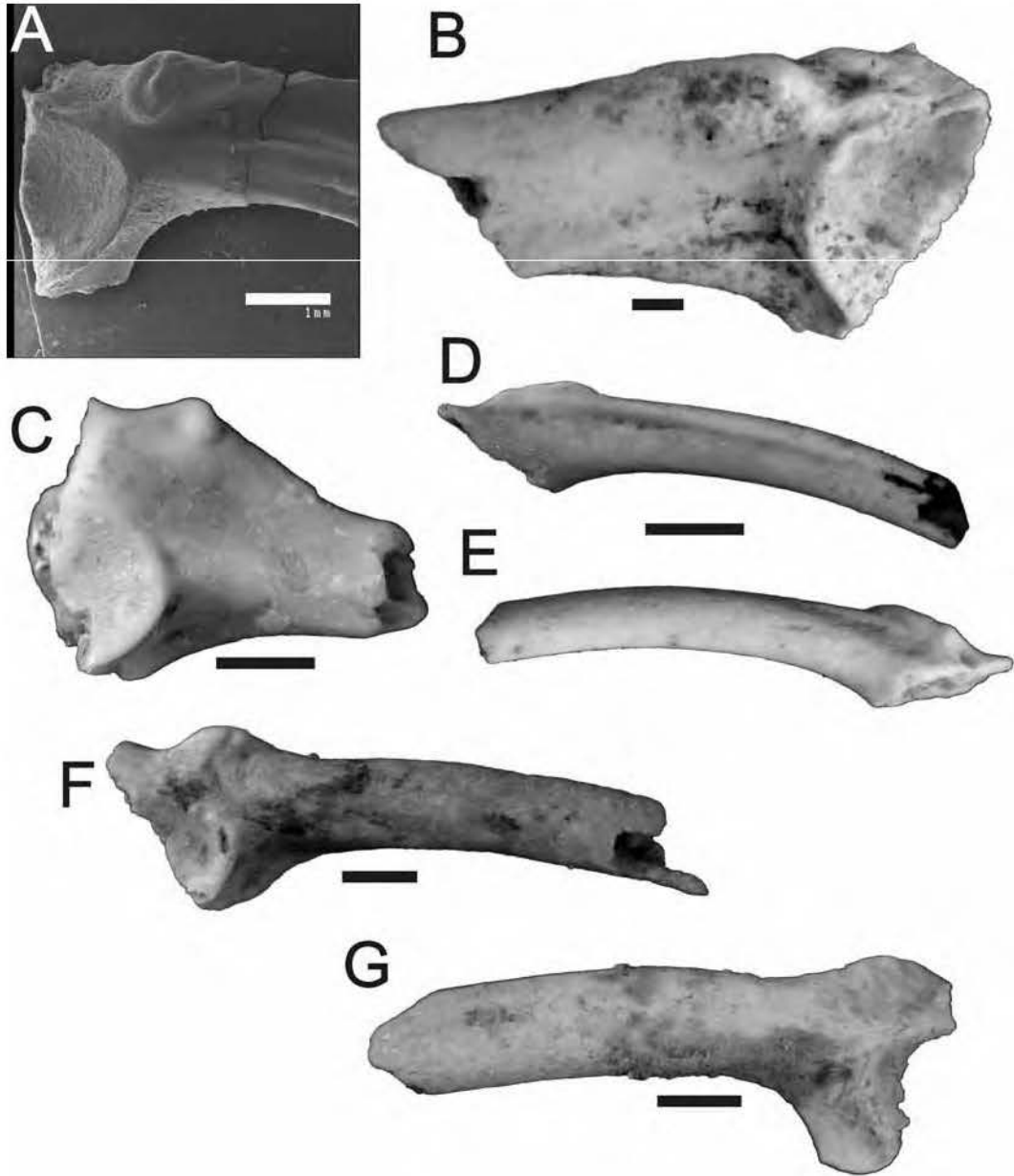


FIG 6. A, *Lechriodus* sp.; QMF51492, right ilium. B, *Etnabatrachus maximus*; QMF44208, left ilium. C, *Neobatrachus* sp.; QMF51487, right ilium. D-E, microhylid sp. 3; QMF51498, left ilium in mesial and lateral view. F, microhylid sp. 2; QMF51496, left ilium. G, microhylid sp. 1; QMF51493, right ilium. Scale bar = 1 mm.



The overall shape and size of the premaxillary bone, tooth and femur are similar to that of *Baru huberi* (QMF31061) but differs by having a deep reception pit for the first dentary tooth, that breaks the dorsal surface of the premaxilla.

Order SQUAMATA Oppel, 1811

Family AGAMIDAE Hardwicke & Gray, 1827

**Amphibolurus** Wagler, 1830

**Amphibolurus** sp.

(Fig. 8D)

MATERIAL. QMF43893; QML1312.

Right maxilla bearing two pleurodont tooth loci, both broken at the base. Nine acrodon tooth loci. The dorsal maxillary process is broken dorsal to the narial basin.

QMF43893 is placed within *Amphibolurus* on the basis of the following combined features: 1. Possessing a significantly reduced, near absent, naris ridge. 2. Dorsal maxillary process constricted superiorly and broad inferiorly. 3. Two pleurodont teeth with P<sup>1</sup> approximately three quarters the size of P<sup>2</sup>. 4. Less than fifteen acrodon teeth. 5. Angular dorsal maxillary process. 6. Hooked anterior profile.

**Diporiphora** Gray, 1842

**Diporiphora** group 2 (*sensu* Hocknull, 2002)

(Fig. 8)

MATERIAL. QMF51507; Olsen's Cave.

A left maxilla bearing one large pleurodont and six acrodon teeth. Maxilla broken posterior to A<sup>6</sup>. Pleurodont tooth large, recurved and orientated labially. Angulate dorsal maxillary process.

Identified as a species within *Diporiphora* group 2 *sensu* Hocknull (2002) on the basis of the following combined features: 1. Naris ridge absent. 2. Broad dorsal maxillary process, narrowed superiorly. 3. One large caniniform maxillary pleurodont tooth.

**Hypsilurus** Peters, 1867

**Hypsilurus** sp.

MATERIAL. QMF51506; QML1313.

Half of a badly preserved right dentary (Length: 12.13+mm) bearing 11 acrodon and one tiny pleurodont tooth represents a medium-sized agamid. The dentary is broken posteriorly of A<sub>11</sub> and is gracile, tapering anteriorly with little curvature. Four visible foramina are present on the labial side of the dentary, with the last

occurring below A<sub>11</sub>. The dental sulcus is narrow along its length and tapers markedly anteriorly. The dentary symphysis is small and ovoid. Acrodon dentition is badly weathered, however, there are distinct mesoconids and small antero and posterconids. Tooth size changes markedly between tooth position A<sub>5</sub> and A<sub>6</sub>.

Agamid dentaries are difficult to identify, however, only five Australian agamid genera possess such distinctively diminutive pleurodont dentition of the dentary; *Chelosania*, *Hypsilurus*, *Physignathus*, *Moloch* and *Pogona* (Hocknull, 2002). The fossil is most similar to *Hypsilurus* by sharing one very tiny pleurodont tooth (*Hypsilurus* possesses one or two) and a very gracile, tapered dentary outline. The fossil dentary differs from all of the other four genera by possessing a much more gracile dentary and narrowly tapered dental sulcus. The fossil specimen differs further from *Chelosania* by being larger and possessing less tricuspid acrodon dentition. The fossil differs further from *Physignathus* by being smaller and possessing one versus three pleurodont dentary teeth. The fossil differs further from *Pogona* by possessing less rounded acrodon dentition and relatively shallower posterior and anterior margins.

**Pogona** Storr, 1982

**Pogona** sp. (small morphotype)

(Fig. 8C)

MATERIAL. QMF41969; QML1312.

Left maxilla with the anterior and posterior margins broken. Twelve acrodon teeth present.

*Pogona* has been identified from QML1312 by the presence of the following feature of the maxilla: 1. Posterior region deep. 2. Rounded acrodon teeth with large mesocones. Based on its size, the specimen allies the smaller *Pogona* species, such as *P. mitchelli* and *P. minor*.

**Tympanocryptis** Peters, 1863

**Tympanocryptis** sp. cf. **T. cephalus** Günther, 1867

(Fig. 8A)

MATERIAL. QMF41963; QML1312.

A nearly complete right maxilla, which is broken posteriorly to A<sup>12</sup>. Twelve acrodon and two pleurodont teeth preserved. Dorsal maxillary process broken at the dorsal margin.

Specimens referred here to a species of *Tympanocryptis* have been identified based on the following combined features; 1. Naris ridge present. 2. Naris ridge borders narial basin. 3.

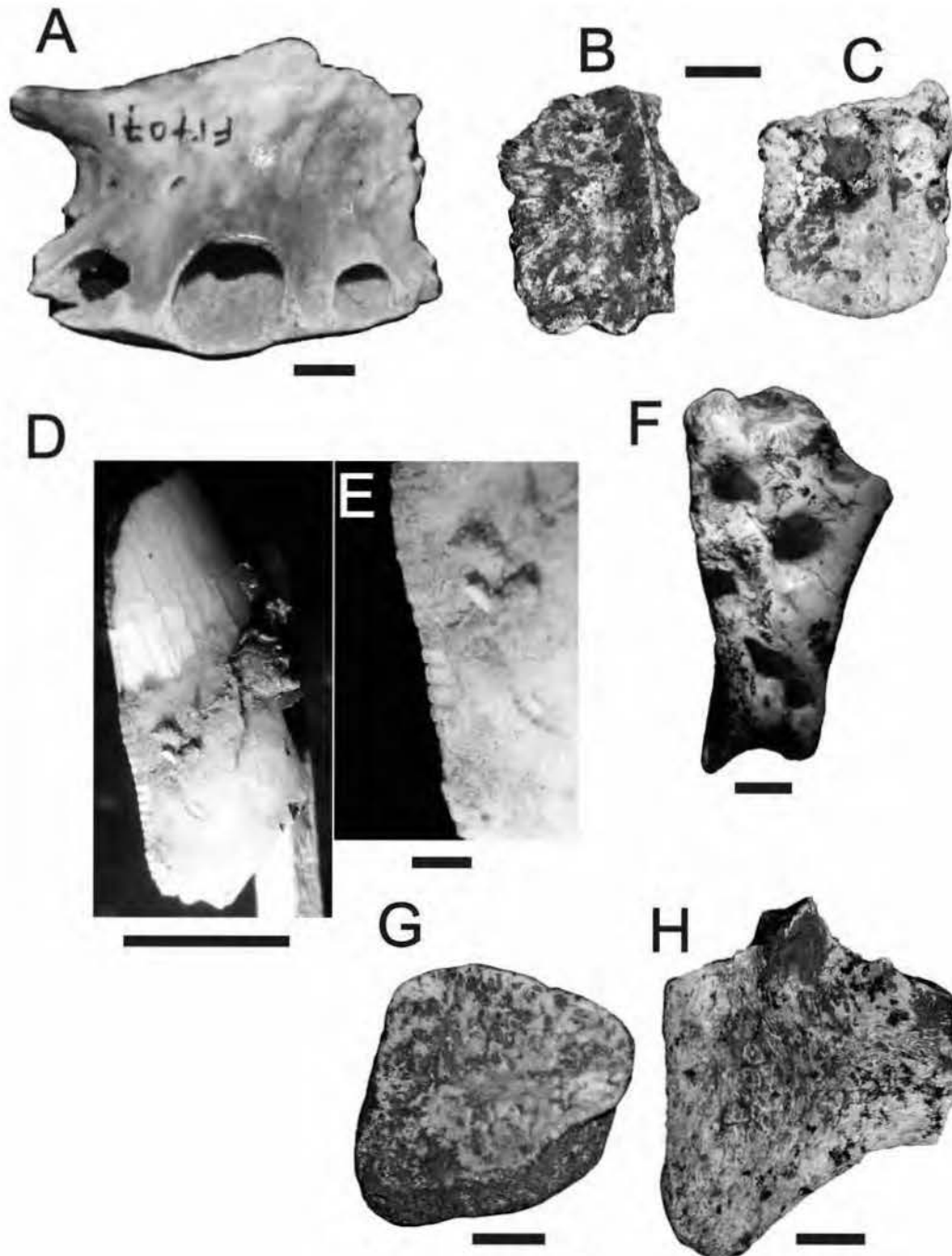


FIG. 7. A-F, Mekosuchinae; A, QMF17071, premaxillary. B, QMF52064, scute. C, QMF52065, scute. D, QMF51503, zipodont tooth. Scale bar = 5mm. E, QMF51593 closeup of carinae (Scale bar = 1mm). F, QMF51505, scute. G-H, Chelidae; G, QMF52061, carapace. H, QMF52062, plastron.

TABLE 2. Faunal lists for reptiles and birds.

	QML368	QML1284	QML1284a	QML1311H	QML1311CD	QML1312	QML1313	QML1314	QML1384U	QML1384L	QML1385	QML1420	Olsens Cave
chelid indet.				x	x					x			
mekosuchine indet.	x			x			x			x			
<i>Amphibolurus</i> sp.						x							
<i>Diporiphora</i> sp.													x
<i>Hypsilurus</i> sp.							x						
<i>Pogona</i> sp.						x							
<i>Tympanocryptis</i> sp. cf. <i>T. cephalus</i>						x							
agamid indet.	x	x	x	x	x	x	x		x	x	x	x	
<i>Tiliqua</i> sp.		x											
<i>Tiliqua scincoides</i>							x	x					
<i>Cyclodomorphus gerrardii</i>		x	x	x	x		x		x	x	x	x	x
<i>Egernia</i> spp.	x	x	x	x	x	x	x	x	x	x	x	x	x
<i>Eugongylus</i> Group		x	x										
<i>Sphenomorphus</i> Group (gracile)		x	x			x	x				x		
<i>Sphenomorphus</i> Group (robust)						x							x
gekkonid (large)		x	x				x						
gekkonid (small)	x	x	x	x	x	x	x	x	x	x	x	x	x
<i>Varanus</i> sp. 1				x		x							
<i>Varanus</i> sp. 2				x	x	x	x						
<i>Megalania prisca</i>												x	
elapid indet.	x	x	x	x	x	x	x	x	x	x	x	x	x
pythonine indet.	x	x	x	x	x	x	x	x	x	x	x	x	x
typholopid		x	x										
Galliformes						x							
Gruiformes						x							
Passeriformes		x				x							
Strigiformes	x	x	x	x	x	x	x	x	x	x	x		x

Two unequally-sized pleurodont teeth with P<sup>2</sup> caniniform. 4. Distinct notch anterodorsally of P<sup>1</sup>. QMF41963 shares very close similarities to *T. cephalus*. P<sup>1</sup> and P<sup>2</sup> are parallel to one another, which is not found in *T. tetraporophora* and *T. intima*. Also, *T. intima* is considerably larger than the specimen and comparative *T. cephalus*. The posterior “molar” acrodont teeth do not show the marked size change typical of *T. lineata* and *T. intima* (Hocknull, 2002). The lateral margin of the premaxillary/maxillary suture is higher and the naris ridge contributes more to this than it does in *T. lineata*. The P<sup>1</sup> is very small, which is more usual in *T. cephalus* specimens, than *T. lineata*. The total number of acrodont teeth is unknown in this specimen, however, judging from the amount of missing maxilla, the number of teeth would be thirteen or more. Thirteen or more acrodont teeth in the maxilla is more

commonly found in *T. cephalus* with tooth counts of 13-14 than *T. lineata* with 11-13.

agamid indet.

MATERIAL: QML1284, QML1284a, QML1311, QML1313, QML1384, QML1385; QML1420

Several maxillary and dentary fragments bearing acrodont dentition are recorded in most sites, however, most of these are unidentifiable because they do not preserve the anterior diagnostic elements needed (Hocknull, 2002). The majority of the specimens show characteristics typical of juvenile agamids, including large acrodont teeth relative to jaw depth, lack of distinct wear facets on the acrodont teeth and dental bone, and overall bone fragility.



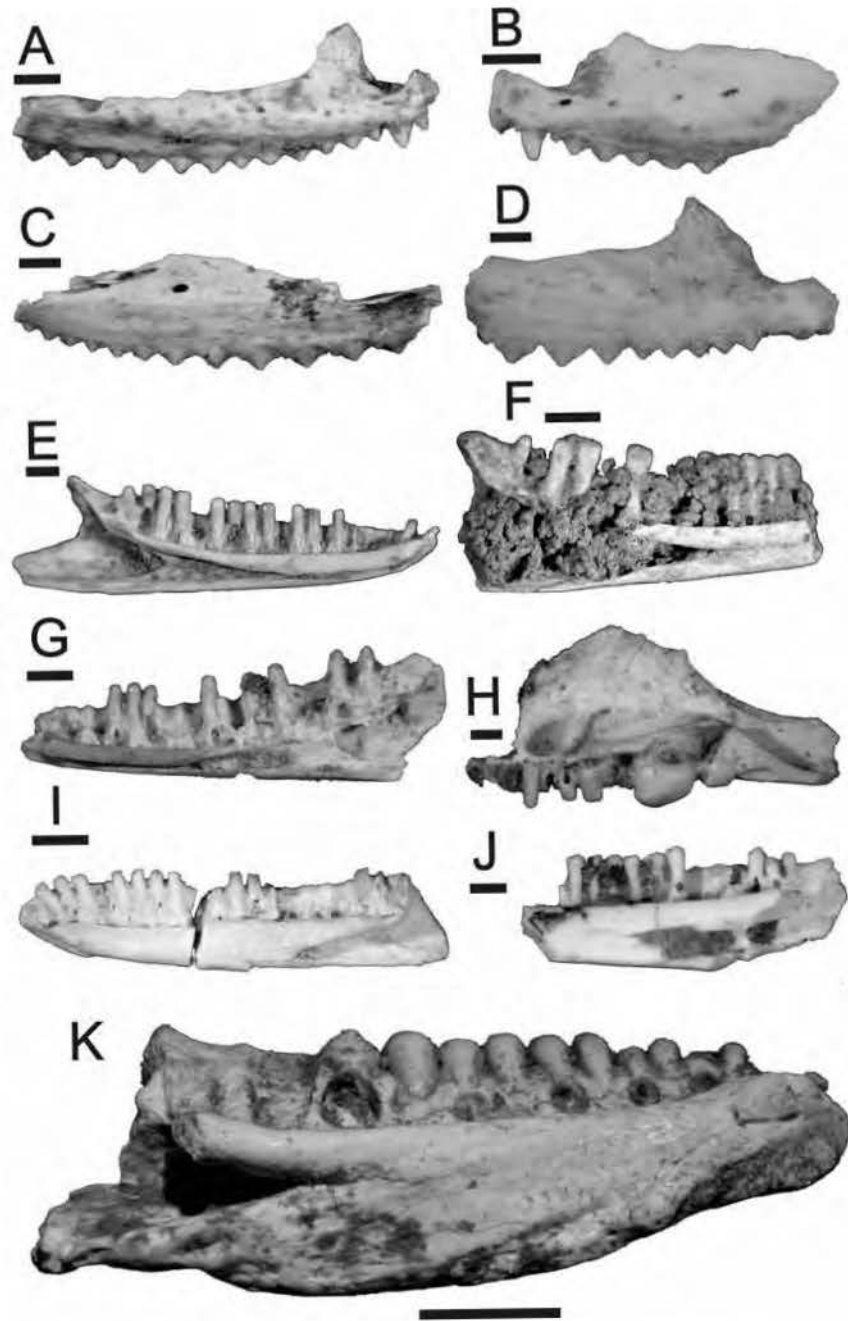


FIG. 8. A-D, Agamidae; A, *Tympanocryptis* sp. cf. *T. cephalus*; QMF41963, right maxilla. B, *Diporiphora* group 2; QMF51507, left maxilla. C, *Pogona* sp.; QMF41969, left maxilla. D, *Amphibolurus* sp.; QMF43893, right maxilla. E-K, Scincidae; E, *Sphenomorphus* group (robust morph); QMF51543, left dentary. F, *Egernia* sp.; QMF51529, left dentary. G, *Sphenomorphus* group (gracile morph); QMF51537, right dentary. H, *Cyclodomorphus gerrardii*; QMF51519, right maxilla. I-J, *Eugongylus* group; QMF51535 & QMF51536, right dentaries. K, *Tiliqua* sp.; QMF51516, left dentary. Scale bar = 5mm.

Family SCINCIDAE Oppel, 1811

**Egernia** Group *sensu* Greer, 1979

**Tiliqua** Gray, 1825

**Tiliqua** sp. nov.  
(Fig. 8K)

MATERIAL. QMF51516; QML1284.

A robust left dentary, broken posterior to the splenial notch. Eleven conical, haplodont teeth are preserved with four addition tooth loci. Symphyseal crest extends to below the eighth haplodont tooth locus. Symphysis elongate, tapering sharply to the posterior and rounded anteriorly. The labial side of the dentary bone is distinctly inflated to the posterior, giving the dentary a very robust appearance in lateral view. Teeth gradually increase in width toward the posterior, all retaining their conical grooved tooth crowns. Dental shelf deep along its length.

The closed Meckelian groove places this specimen with the *Egernia* and *Eugongylus* groups within the Lygosominae (Greer, 1979). The enlarged posterior conical teeth place this specimen within the *Tiliqua* lineage (Shea, 1990). The presence of a long symphyseal crest, bunched haplodont dentition and the absence of a single massive posterior durophagous tooth excludes this specimen from being *Cyclodomorphus*. *Tiliqua* sp. differs markedly from all living and fossil *Tiliqua* so far described and is most probably a new species.

**Tiliqua scincoides** (White, 1790)

MATERIAL. QMF51517; QMF51518; QML1313, QML1314.

*Tiliqua scincoides* is best represented by a single right dentary possessing nine teeth and twelve tooth loci. The largest tooth is toward the posterior and is characterised by having a rounded durophagous tooth crown. The elongate symphyseal crest places this specimen within *Tiliqua*, its size and tooth morphology place it firmly within *Tiliqua scincoides* by being much smaller and more gracile than both *T. gigas* and the large *Tiliqua* species from Mini Cave.

**Cyclodomorphus** (Fitzinger, 1843)

**Cyclodomorphus gerrardii** (Gray, 1845)  
(Fig. 8H)

MATERIAL. QMF51519-QMF51527; Olsen's Cave, QML1284, QML1284a, QML1311(H), QML1311(C/D), QML1384 U, QML1313, QML1385, QML1420.

Several isolated maxillae and dentaries possess a massively rounded posterior tooth in both jaw

elements, a short symphyseal crest and a concave anterior portion of the dental sulcus. Maxillae preserve up to ten haplodont teeth in varying degrees of replacement. Dentaries usually exhibit some form of abrasion on the smaller anterior haplodont teeth.

The identification of *Cyclodomorphus gerrardii* was based on the presence a single massive durophagous maxillary and dentary tooth, concave anterior dental sulcus and short symphyseal crest.

**Egernia** Gray, 1838

**Egernia** spp.  
(Fig. 8F)

MATERIAL. QMF51529-51534; all localities.

Dentaries and maxillae large, possessing at least 12 haplodont teeth with chisel-shaped crowns. Meckelian groove closed. Posterior portion of the jaw robust and deep. Large inferior mental foramen.

**Eugongylus** group (*sensu* Hutchinson, 1992)  
(Fig. 8I-J)

MATERIAL. QMF51535-QMF51536; QML1284, QML1284a.

Large-sized scincid possessing a slender dentary, wedge-shaped, tightly spaced haplodont teeth and a closed Meckelian groove.

The large size, slender dentary, closed Meckelian groove ally these specimens to the *Eugongylus* Group *sensu* Hutchinson (1992).

**Sphenomorphus** Group (*sensu* Greer, 1979)

gracile morphotype  
(Fig. 8G)

MATERIAL. QMF51537-QMF51541; QML1284a; QML1284, QML1312, QML1313, QML1385.

Small-sized dentary with closely-spaced haplodont teeth. Teeth with pointed crowns. Meckelian groove open along its length to symphysis. Dentary shallow and symphysis small.

The small gracile form of the dentary and the open Meckelian groove place these specimens within the gracile morphotype of *Sphenomorphus* Group *sensu* Hutchinson (1992).

robust morphotype  
(Fig. 8E)

MATERIAL. QMF51543, QMF51544; QML1312, Olsen's Cave.

Large-sized dentary with elongate blunt-crowned haplodont teeth. Meckelian groove open along its length to symphysis. Dentary deep at posterior, tapering markedly to ovoid symphysis.

The open Meckelian groove, large size, robust tooth morphology and deep jaw place these specimens within the robust morphotype of *Sphenomorphus* Group sensu Hutchinson (1992).

#### Family GEKKONIDAE Oppel, 1811

Fossil gekkonids have been found in several deposits and are abundant throughout. Unfortunately most of the maxillae and dentaries are preserved as fragments, which make identification very difficult. In addition to this, there is no premise for identification of fossil Australian gekkonid taxa based on maxillary and dentary characteristics, therefore, gekkonid specimens described here were only compared to the limited comparative collection available to the author.

##### gekkonid (large) (Fig. 9A-C)

MATERIAL. QMF51508, QMF51509, QMF51510; QML1284, QML1284a, QML1313.

Several large maxillary and dentary fragments preserving rows of closely-set, needle-like homodont teeth. Maxillae possess a dorsal process of the maxilla, which lies anterior to the orbit and contacts the nasal bones. The process borders the posterior margin of the narial opening. The morphology of this margin varies between gekkonid taxa and is distinctly broad in the fossil specimens. The most complete fossil dentaries indicate the presence of a very large gekkonid. The dentaries are characterised by being long and curved mesially, possessing many closely-spaced homodont teeth, a splenial notch and a small dental symphysis.

Based on its overall very large size, the fossil taxon must have reached a snout-to-vent length of 16 cm or more, making it similar in size to the largest extant Australian gekkonids (*Phyllurus*, *Cryptodactylus*). The maxillae and dentaries of all three genera show similarities with the fossil taxon.

##### gekkonid (small) (Fig. 9B)

MATERIAL. QMF51511-51515; All localities.

Several small fragmentary dentaries and maxillae are preserved throughout the deposits,

probably representing several taxa. A small maxilla (QMF51511; QML1284) is distinctive in possessing a relatively narrow dorsal process originating posterior of the narial opening and tapering markedly to the posterior of the maxilla. The dentition is simple, however several of the teeth are bicuspid. Dentaries are small, curved and slender.

On comparison with small-sized gekkonids, most of the gekkonid specimens cannot be adequately identified.

#### Family VARANIDAE Hardwicke & Gray, 1827

Varanids are a conspicuous member of the lizard fauna. Varanids have been identified from isolated, recurved small and large-sized serrated teeth, an isolated parietal, quadrate, femur, dentary fragments and several isolated cervical, dorsal and caudal vertebrae.

##### *Varanus* Merrem, 1820

###### *Varanus* sp. 1

MATERIAL. QMF51546, QMF51547; QML1312, QML1311(H).

A medium-sized species of *Varanus* is represented by a parietal, two dentary fragments, an isolated dorsal and several caudal vertebrae. The fossils compare favourably with a similarly sized *Varanus varius*, particularly in the broad flat parietal with narrow, slender temporal ridges; small-sized teeth and a dorsal vertebrae that falls within measurements provided by Smith (1976) for *Varanus*. The dorsal vertebrae compare in size to either *V. varius* or *V. gouldi*.

###### *Varanus* sp. 2 (Fig. 9D-E, G-H)

MATERIAL. QMF51548-QMF51550, QMF52066; QML1312, QML1311(H), QML1311(C/D), QML1313.

A very large varanid is represented by an isolated right quadrate, a cervical and several dorsal and caudal vertebrae. On prezygopophysis to postzygopophysis length alone, these specimens fall within the range of dorsal vertebral measurements provided by Smith (1976) for *V. giganteus* and below the range provided for a small species of *Megalania* from Chinchilla provided by Hutchinson & Mackness (2002). The dorsal vertebrae are most similar in length to *V. giganteus*, however, differ remarkably in the ratio defined by Smith (1976) as prezygopophysis- prezygopophysis (Pr-Pr) width over prezygopophysis- postzygopophysis (Pr-Po) length. In particular, when comparing this ratio to modern and fossil varanids the dorsal

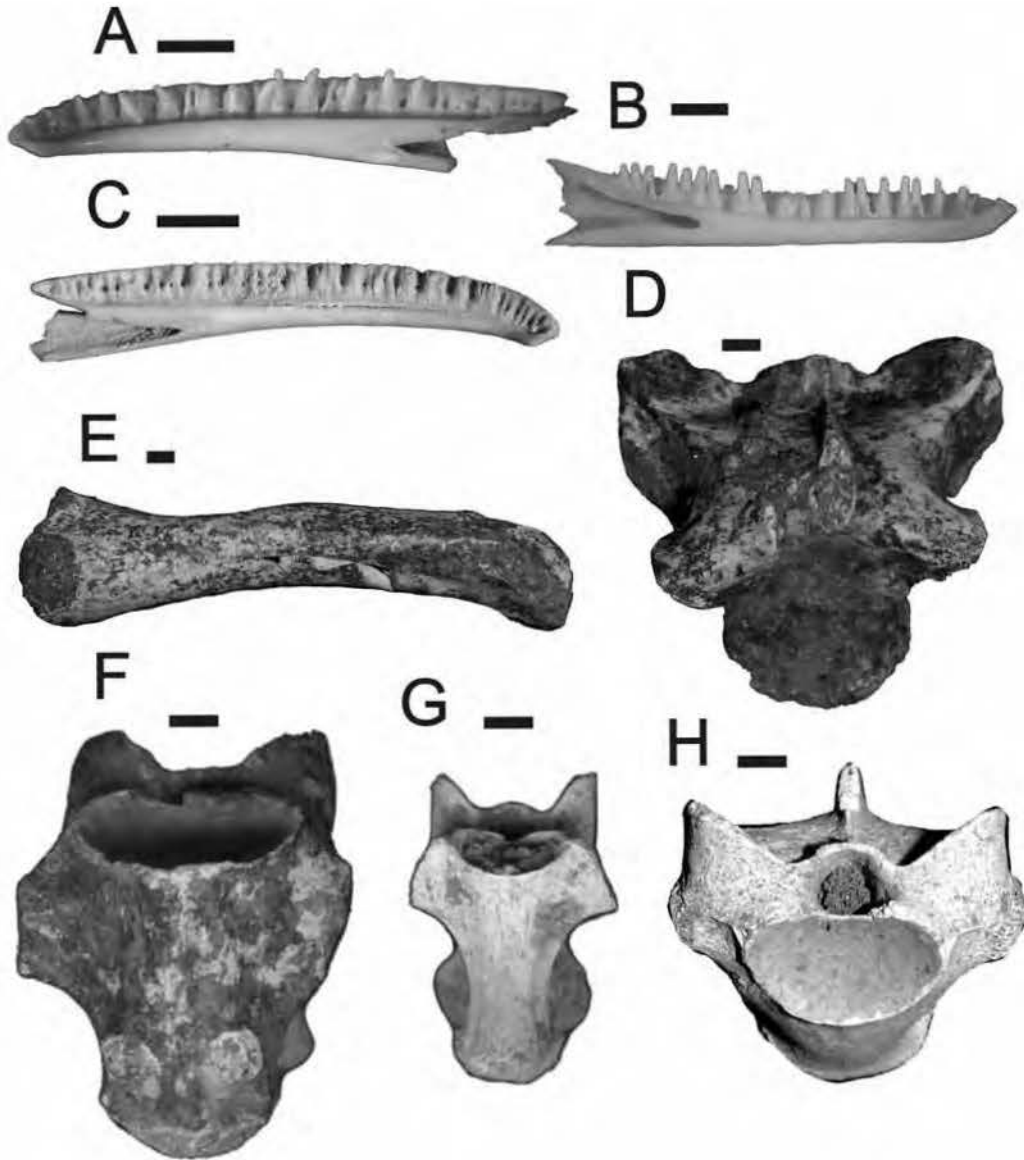


FIG 9. A-C, Gekkonidae; A&C, gekkonid (large morph); QMF51508, right dentary, QMF51510, left dentary. B, gekkonid (small morph); QMF51511, left dentary. Scale bar = 1mm. D-H, Varanidae; D-E, *Varanus* sp. 2; D, QMF51548, dorsal vertebra. E, QMF51549, femur. F, *Megalania prisca*; QMF1418, caudal vertebra. G-H, *Varanus* sp. 2; G, QMF51550, cervical vertebra. H, QMF52066, dorsal vertebra. Scale bar = 5mm.

vertebrae measured here attain a ratio of between 1.07 and 1.22. This indicates that the Pr-Pr width of the vertebrae are generally wider than the Pr-Po length. Interestingly, the measurements provided by Smith (1976) show that dorsal vertebrae of extant *Varanus* are mostly longer

than broad with some being nearly equally as long as broad. Very few measured slightly broader than long.

Specimens referable to *Megalania* from both Chinchilla, Bluff Downs (Mackness &



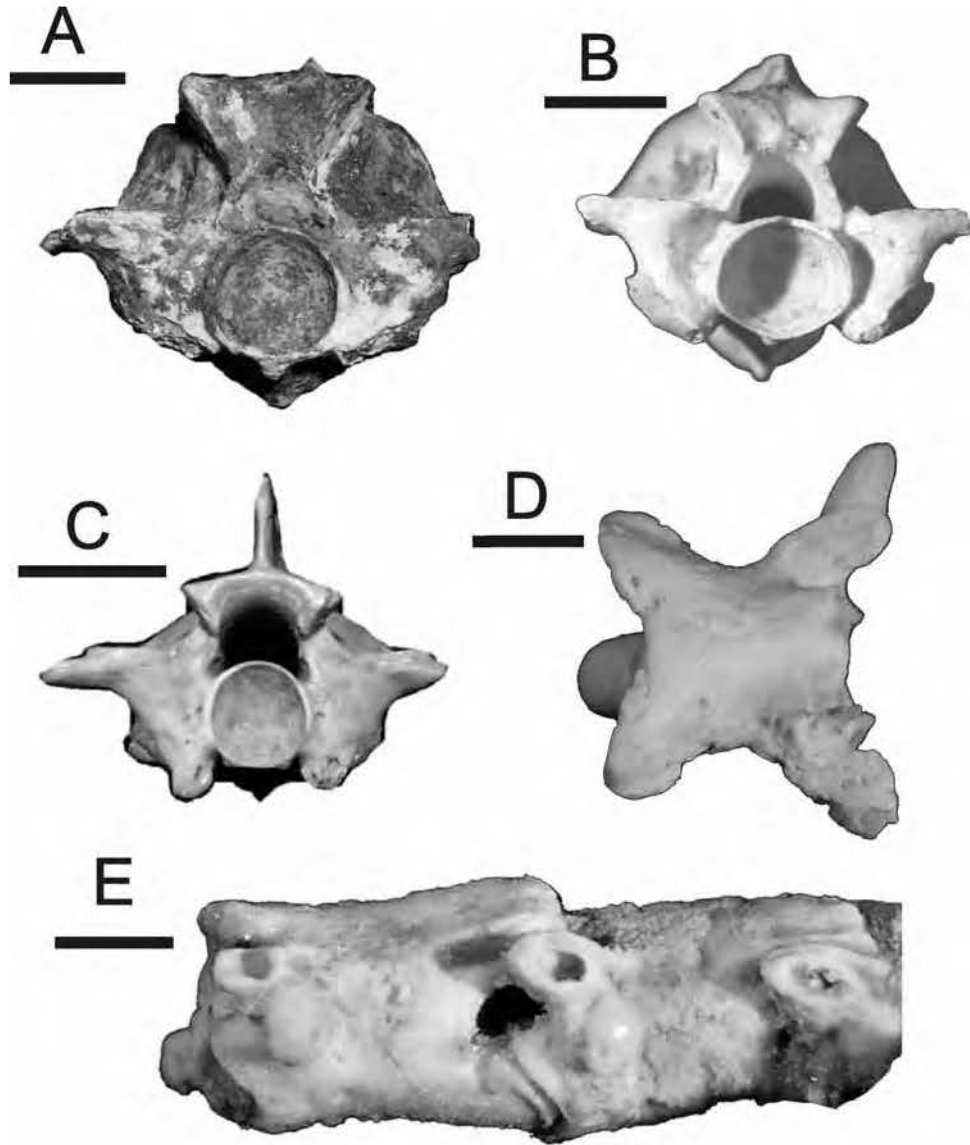


FIG 10. A-B, Pythoninae; A, QMF51560, dorsal vertebra. B, QMF51561, dorsal vertebra. C, Elapidae; QMF51551, dorsal vertebra. Scale bar = 5mm. D-E, Typhlopidae; D, QMF51578, dorsal vertebra. E, QMF51579, three articulated dorsal vertebrae. Scale bar = 1mm.

Hutchinson, 2000; Hutchinson & Mackness, 2002) and the Darling Downs (Hecht 1975; pers. obs.) possess dramatically broader than long dorsal vertebrae. This feature is easily seen in the largest *Megalanias prisca* dorsal vertebrae. Further comparisons of *Varanus* spp larger than *V. giganteus*, such as *V. komodoensis*, will be needed to verify the validity of these differences.

#### **Megalanias** (Owen, 1860)

#### **Megalanias prisca** (Owen, 1860) (Fig. 9F)

MATERIAL. QMF1418; QML1420.

*Megalanias prisca* is represented by a single varanid distal caudal vertebra, cotyle-condyle length: 28.80mm. The massive size of the

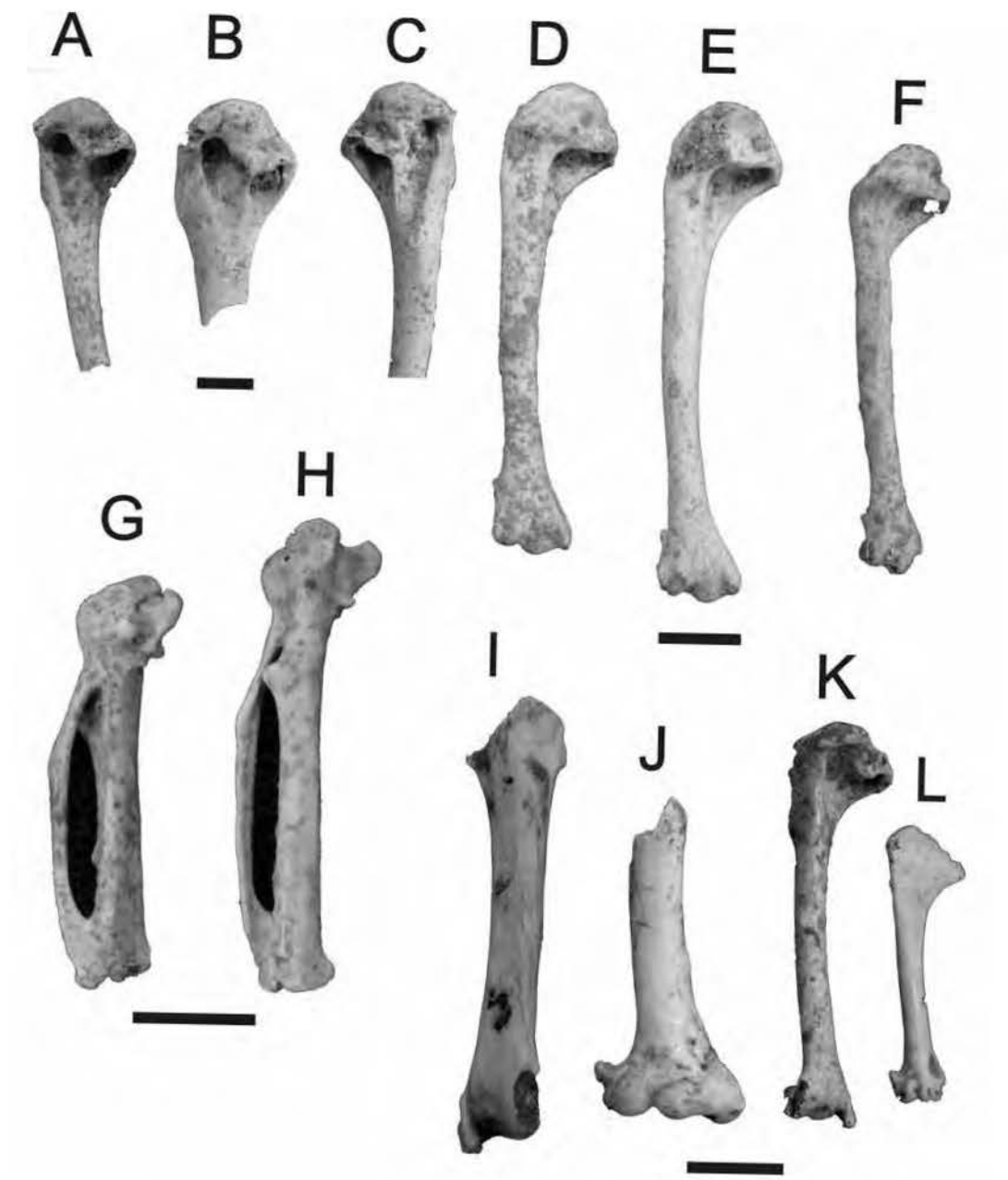


FIG 11. A-C, Galliformes; QMF51607-51609 (left to right), humeri. D-H, Gruiformes; D-F, QMF51610-51612 (left to right), humeri. G-H, QMF33458 & QMF33460 (left to right), carpometacarpi. I-L, Passeriformes; QMF51601-51604 (left to right), humeri. Scale bar = 5mm.

vertebra and the fact that it is a distal caudal vertebra indicates that the varanid was enormous, attaining the dimensions only seen in *Megalania*. Until the debate surrounding the generic validity of *Megalania* is resolved (Hecht, 1975; Molnar, 1990; Lee, 1996), this giant varanid will be placed within *Megalania*.

Family ELAPIDAE Boie, 1827

elapid indet.

Fig. 10C

MATERIAL. QMF51551-51559; All Localities.

Elapids have been identified based on the following features of the trunk vertebrae: 1. Elongate and high vertebrae, longer than broad. 2. Distinct hypopophyses. 3. High neural spine. 4. Accute prezygopophyses. 5. Spherical condyle-cotyle articulation. Elapid specimens are variable in size with the largest specimen from QML1312, being at least twice the size of the the largest elapids from QML1284, 1284a and 1311.

Subfamily PYTHONINAE Fitzinger, 1826

pythonine indet.  
(Fig. 10A-B)

MATERIAL. QMF51560-51569; All Localities.

In addition to maxillary and dentary remains, pythonines have been identified from the deposits based on the following features of the trunk vertebrae: 1. Short, stout vertebrae, as wide as long. 2. Robust zygantrum. 3. Thick zygosphenes. 4. Ovoid condylar-cotylar articulation. 5. Hypopophysis tiny or absent. 6. Large ovoid prezygopophyses. 7. High neural spines with overhanging anterior and posterior margins.

Family TYPHOLOPIDAE Gray, 1825

typholopid indet.  
(Fig. 10D-E)

MATERIAL. QMF51578-51582, QMF51583-51587; QML1284, QML1284a.

Typholopids have been identified on the basis of the following features of the trunk vertebrae: 1. Neural spine absent. 2. Neural arch low and thin. 3. Zygantrum narrow and deep. 4. Accute prezygopophyses. 5. Hypopophysis absent. 6. Hemal keel abent or only slight. 7. Neural canal very large relative to vertebral size.

AVES

Bird postcranial elements are numerous throughout all of the sites, especially from those sites interpreted as predator accumulations with owls as the major accumulator. The largest bird elements are currently attributed to the owls (Strigiformes), the smallest from the song birds (Passeriformes).

Galliformes  
(Fig. 11A-C)

MATERIAL. QMF51607-51609; QML1312.

Quails are represented by several postcrania, including very distinctive humeri and carpometacarpi. The size of the humeri and presence of two proximal pneumatic fossae in the head of the humerus suggests the presence of a species of *Coturnix*.

Gruiformes  
(Fig. 11D-H)

MATERIAL. QMF33458, QMF33460, QMF51610-QMF51612; QML1312.

Buttonquails are represented by several postcrania, including humeri, carpometacarpi, femora, tarsometatarsi and sternal fragments. The distinctive larger pneumatic fossa in at the proximal head of the humerus and the large triangular intermetacarpal tuberosity ally these specimens closest to a species of *Turnix*.

Passeriformes  
(Fig. 11I-L)

MATERIAL. QMF51601, QMF51602-51606; QML1284 QML1312.

Passeriformes were identified from humeri possessing a distinct entepicondylar prominence, ectepicondyle distinct and distal to internal condyle, and a shallow pneumatic fossae.

Strigiformes  
(Fig. 12 A-K)

MATERIAL. QMF51578-51587; All localities except QML1420.

Owls were identified from numerous postcranial specimens including humeri, ulnae, carpometacarpi, phalanges, claws, femora and tarsometatarsi. Owls possess a distinct first phalange of the pes digits, with four tuberosities in each corner of the phalange. The phalange tends to be short and squat with a deep facet on the dorsal and distal margin.

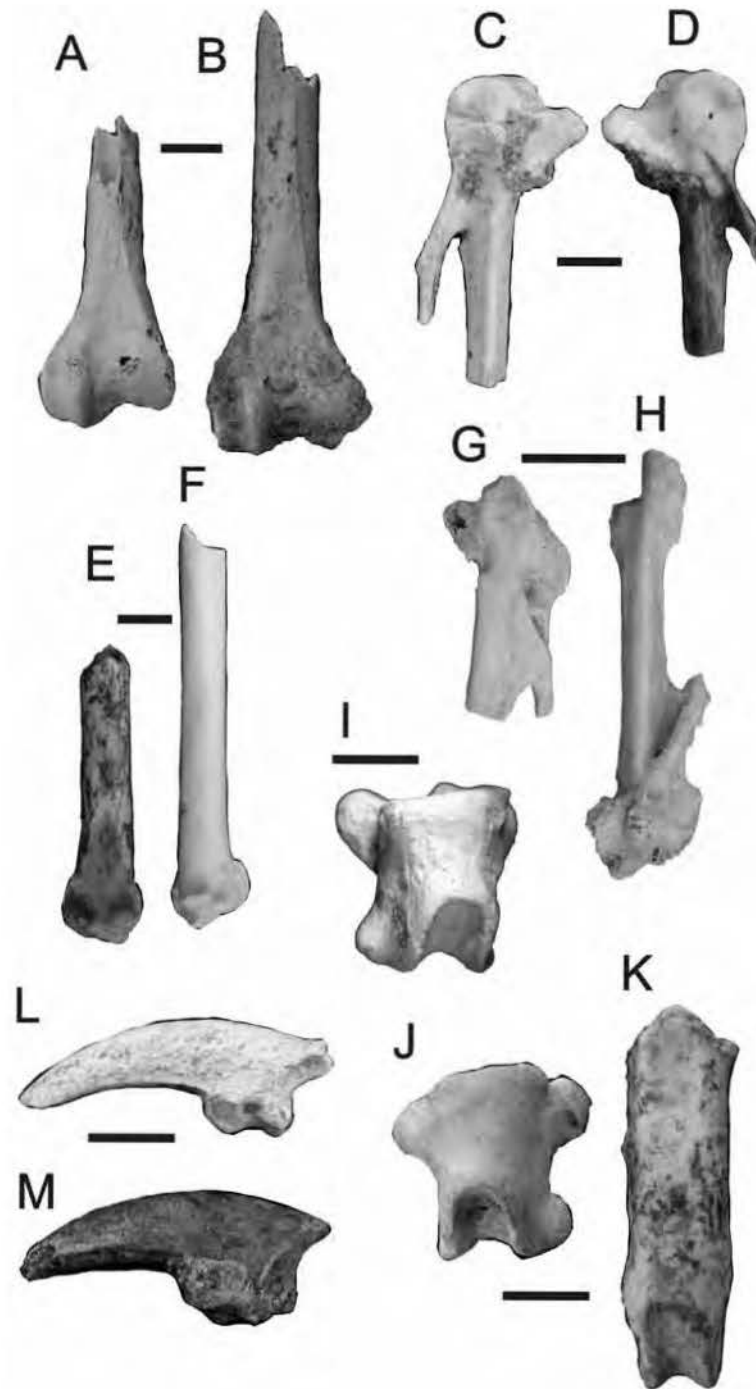


FIG. 12. A-K, Strigiformes; A-B, QMF51578 & 51579, femora. C-D, QMF51580 & 51581, carpometacarpi. E-F, QMF51582 & 51583, ulnae. G-H, QMF51584 & 51585, carpometacarpi. I-K, QMF51586, 51581, 33361, phalanges. L-M, QMF33863 & 33864, claws. Scale bar = 5mm.



## MAMMALIA

## Family PERAMELIDAE Gray, 1825b

**Perameles** Geoffroy, 1803**Perameles** sp. 1  
(Fig. 13A)

MATERIAL. QMF51613-QMF51620; QML1284, QML1284a, QML1311(H), QML1313, QML1384U, QML1385, QML1420, QML1311(C/D).

A species of *Perameles* on the basis of the following combination of features: 1. Presence of fully developed anterior and posterior cingulae on  $M^{1-3}$ . 2. Triangular tooth crown with the para and metastylar corners outside the margin of the tooth crown. 3. Equidistant protoconid-metaconid, protoconid-paraconid distances on  $M_{1-4}$ . 4. Absence of the anterior cingulid on  $M_1$ .

When compared to the modern species of *Perameles* the fossils differ as follows:

*Perameles* sp. 1 is larger than *P. bougainville* and has a more buccally developed posterior cingulum on  $M^{1-3}$ . The posthypocristid runs to the hypoconulid on  $M_{1-3}$  whereas the posthypocristid only runs to the hypoconulid in  $M_{1-2}$  of *P. bougainville*.

*Perameles* sp. 1 is smaller than *P. nasuta*. The meta- and parastylar corners in unworn molars of the fossil taxon are bicuspid whereas *P. nasuta* possess single conical meta- and parastyle.

*Perameles* sp. 1. is smaller than *P. gunnii* and possesses a more buccally developed posterior cingulum on  $M^{1-4}$ . The posthypocristid runs to the hypoconulid on all lower molars in the fossil *Perameles*, whereas it only runs to the hypoconulid in  $M_{2-3}$  of *P. gunnii*.

*Perameles* sp. 1. differs from *P. bowensis* by being larger, possessing larger hypoconulids, and a posthypocristid that runs to the hypoconulid on  $M_3$ . *Perameles* sp. 1. differs from *P. allinghamensis*, which is only known by an isolated upper molar, by being much smaller and possessing a posterior cingulum that terminates below and buccal to the metacone. *Perameles* sp. 1. differs from *P. sobbei*, which is only known from lower dentition, by possessing larger hypoconulids on  $M_{1-3}$ , a posthypocristid that runs to the hypoconulid on  $M_{1-3}$ , and by being smaller.

**Perameles** sp. 2  
(Fig. 13B)

MATERIAL. QMF51621-QMF51626; QML1284, QML1284a, QML1311(H), QML1313, QML1384U, QML1385.

A second medium-sized species of *Perameles* possesses the following features: 1. Anterior cingulid of  $M_1$  absent. 2. Hypoconulid reduced on  $M_{1-3}$ . 3. Posthypocristid contacts the base of the entoconid  $M_{1-3}$ . 4. Trigonid cusps approximated. 5. Entoconid conical with a small preentocristid crest. *Perameles* sp. 2 differs from *Perameles* sp. 1 by being larger, possessing a posthypocristid that contacts the entoconid and a preentocristid crest. *Perameles* sp. 2 differs from *P. nasuta*, *P. bougainville*, *P. eremiana*, *P. bowensis* by possessing an  $M_1$  with a posthypocristid that contacts the entoconid instead of the hypoconulid. *Perameles* sp. 2 differs from *P. gunnii* by being markedly smaller, possessing a more mesially terminating cristid obliqua and not possessing a simple conical entoconid. *Perameles* sp. 2 differs from *P. sobbei* by its smaller size, larger hypoconulid on  $M_1$ , narrower protoconid-metaconid distance and smaller paraconid.

**Perameles bougainville** Quoy & Gaimard,  
1824  
(Fig. 12C-E)

MATERIAL. QMF51627-51630, QMF51631; QML1312; Olsen's Cave.

A small species of *Perameles* is present in the fauna recovered from QML1312 and a single specimen in Olsen's Cave. The fossils are identified as *Perameles* on the basis of the following combined features: 1. Para- and metastylar corners angular, occurring outside the peripheral margin of the tooth crown base. 2. The presence of a variably complete posterior cingulum. 3. Anterior cingulum on  $M_{2-4}$  that originates well below the apex of the paraconid. 4. Gently curved ascending ramus. 5. Reduced metaconule.

When compared to the three available species of modern *Perameles* (*P. nasuta*, *P. gunnii* and *P. bougainville*) this fossil species was closest to *P. bougainville* in size. The fossils referred to here as *P. bougainville* differ from both *P. nasuta* and *P. gunnii* by; being considerably smaller; possessing small, isolated parastyles on  $M^1$  instead of large, curved parastyles that are connected to the main tooth crown by a distinct preparacrista; possessing distinct protocones and metaconules on  $M^{1-3}$ ; acute angle made by the postprotocrista and premetaconule crista; possessing a lower angle of the postmetacrista to the longitudinal axis of the tooth crown; more lingually oriented stylar cusp B & D. They differ from *P. allinghamensis* by being much smaller

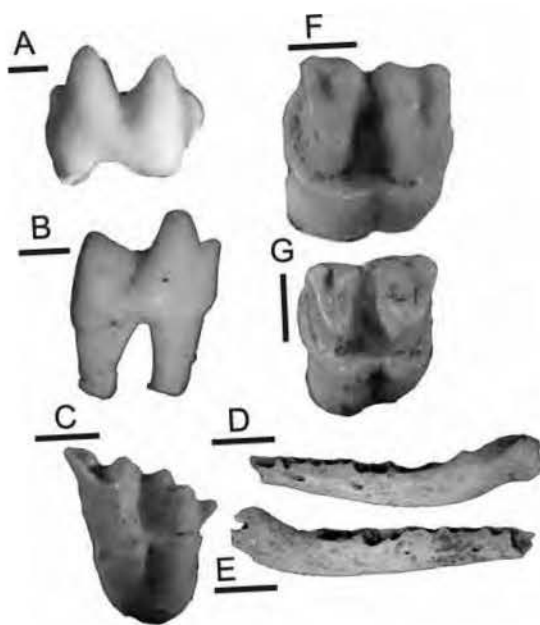


FIG. 13. A-G, Peramelidae; A, *Perameles* sp. 1; QMF51613, LM<sub>1</sub>. B, *Perameles* sp. 2; QMF51621, RM<sub>1</sub>. C-E, *Perameles bougainville*; QMF51627, RM<sub>1</sub>. Scale bar = 1mm. D, QMF51628, left mandible. E, QMF51529, right mandible. Scale bar = 5mm. F, *Isoodon obesulus*; QMF51632, RM<sub>2</sub>. G, *Isoodon* sp.; QMF51635, RM<sub>2</sub>. Scale bar = 1mm.

and possessing a more triangular outline in occlusal view. They differ from *P. bowensis* by being larger and better developed posterior cingulum on M<sup>3</sup>.

The fossils compare favourably with *P. bougainville* on the basis of: 1. Small size, though they are slightly larger than the samples measured by Freedman & Joffe (1966). 2. Form of the parastyle on M<sup>1</sup>, being small, isolated and not connected to the preprotocrista. 3. Higher angle of the postmetacrista to the longitudinal axis of the tooth crown. 4. Lingually oriented stylar cusps B & D. 5. Incomplete posterior cingulum on M<sup>1-2</sup> with a short posterior cingulum on M<sup>3</sup>.

The identification presented here is made with some caution due to the absence of *P. eremiana* from comparative collections available. However, Muirhead (1994) provides characteristics to split these two species. These features included the development of the

posterior cingulum (complete on M<sup>1</sup> in *P. eremiana* and incomplete on M<sup>1</sup> of *P. bougainville*) and the hypoconulid. Features characteristic of *P. bougainville* are shared with the fossil over *P. eremiana*. It is unlikely that the fossil taxon represents an extinct species based on the closeness in morphology to *P. bougainville*. Instead, it may represent a larger-sized eastern population of the arid-adapted *P. bougainville*. This record represents the most easterly and northerly record of the small-sized, arid-adapted members of *Perameles*.

#### **Isoodon Desmarest, 1817**

##### **Isoodon obesulus (Shaw, 1797)** (Fig. 13F)

MATERIAL. QMF51632-QMF51634; QML1312, QML1384U, QML1420.

*Isoodon* fossils are abundant in the QML1384U and QML1312 deposits. These specimens are referred to *Isoodon* based on the following combined features: 1. Well developed anterior and posterior cingulae on M<sup>1-3</sup>; 2. Stylar corners well within the tooth crown margins on M<sup>2-3</sup>; 3. Stylar cusps B & D oriented lingually; 4. Deep, dumb-bell shaped lingual root on upper molars; 5. Cuspid at the anterobuccal base of the hypoconid, 6. Anterior cingulae on M<sup>2-4</sup> terminates just ventral to the paraconid.

Morphologically, the fossils differ from *I. macrourus* and *I. auratus* in possessing distinct metaconules and protocones on M<sup>1-3</sup>, where the postprotocrista and premetaconule crista form an acute angle between the two cusps. They also agree in size with modern *I. obesulus*.

##### **Isoodon sp.** (Fig. 13G)

MATERIAL. QMF51635-QMF51636; QML1384U, QML1312.

Specimens of a species of *Isoodon* represent a second species. The specimens are smaller than all three extant *Isoodon* species, being closer to *I. obesulus* than *I. macrourus* and *I. auratus*. In morphology the specimens differ from all species of *Isoodon* by possessing an incomplete anterior cingulum on M<sup>2</sup> and narrower metastyle-stylar cusp D and parastyle-stylar cusp B distances. The fossil specimens are all smaller than those teeth assigned to *I. obesulus* from the same deposit.

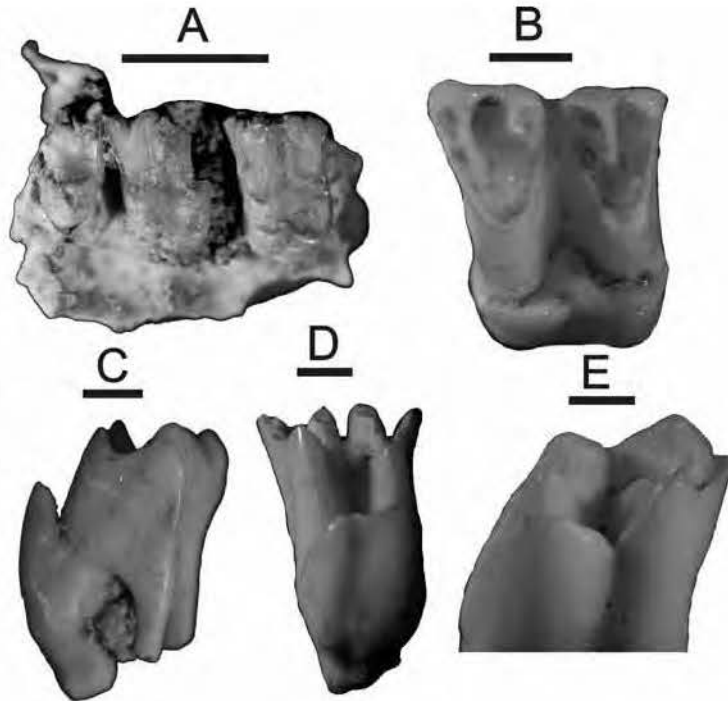


FIG 14. A-D, Peramelidae; A-D, *Chaeropus ecaudatus*; A, QMF51637, RM<sup>3-4</sup>. Scale bar = 5mm. B-C, QMF515638, RM<sup>2</sup>, occlusal & anterior views. D, QMF51639, RM<sup>3</sup>. E, Thylacomyidae; *Macrotis lagotis*; QMF51642, RM<sup>1</sup>. Scale bar = 1mm.

#### **Chaeropus** Ogilby, 1838

##### ***Chaeropus ecaudatus*** (Ogilby, 1838) (Fig. 14A-D)

MATERIAL. QMF51637-51641; QML1312.

*Chaeropus ecaudatus* is only known from QML1312 and is the third most abundant bandicoot in that deposit. *C. ecaudatus* has been identified from upper molars using the following combination of characteristics defined by Muirhead and Godthelp (1995): 1. Near parallel preparacristae and postmetacristae to each other and almost perpendicular to the long axis of the tooth crown. 2. Absence of both an anterior and posterior cingulae. 3. Very tall and slender molar crowns. 4. Preprotocristae and postprotocristae terminate at the base of the paracone and metacone respectively. 5. Preparacristae straight with no anterior curvature.

#### Family THYLACOMYIDAE (Bensley, 1903)

##### **Macrotis** Reid, 1837

##### ***Macrotis lagotis*** (Reid, 1837) (Fig. 14E)

MATERIAL. QMF51642-51643; QML1312.

The Greater Bilby is an enigmatic species of bandicoot with a highly specialised and distinctive tooth morphology. Two molars have been recovered from QML1312. Identification of the teeth as *M. lagotis* was based on the following combination of features. 1. Absence of the paraconid, 2. Absence of the metaconule, 3. Rectangular-ovoid molar crowns, 4. Dumbbell-shaped molar roots and 5. Large cuspid on the anterobuccal side of the lower molars (considerably larger than that found in *Isoodon*).

#### Family INCERTAE SEDIS

Two new bandicoots are present in the fauna with uncertain family-level taxonomic position. Several indications of new bandicoot groups within the Late Tertiary have been made in the literature (Muirhead, 1994, 1999; Dawson et al.,

1999; Long et al., 2002) without formal description. One family, the Yaralidae, are described from the Oligo-Miocene (Muirhead, 2000) and are thought to occur into the Pliocene (Long et al., 2003). Based on dentition alone, family-level taxonomy becomes complicated with several perviously diffinitive features now thought to be plesiomorphies (Muirhead, 1994; 2000; Muirhead & Filan, 1995). It is for this reason that these two distinct bandicoots will remain *incertae sedis* with the possibility of their placement within the plesiomorphic family Yaralidae.

Recently, Turnbull et al., (2003) erected a new bandicoot taxon, cf. *Peroryctes tedfordi* from the Early Pliocene Hamilton Fauna. Although they place the taxon in the Peroryctidae, they did note its plesiomorphic features and similarity to *Yarala*. The taxa identified below are morphologically very similar to cf. *Peroryctes tedfordi*, however, I reserve the placement of these taxa into any perameloid family until a full revision of both the Hamilton and Mt. Etna material is available.

Gen. et sp. nov. 1  
(Fig. 15A)

MATERIAL. QMF51644; QML1311 (H).

A large species of perameloid, similar in size to *Echymipera rufescens*, possessing the following features: 1. A distinct anterior cingulum on  $M_1$ . 2. Trigonid extremely compressed with protoconid and metaconid cusps high and approximated. 3. Paraconid small. 4. Bladed entoconid. 5. Hypoconulid heavily reduced on  $M_{1-2}$ , less so on

$M_3$ . 6.  $M_{2-3}$  trigonid with protoconid-metaconid relatively more broader than corresponding cusps on  $M_1$ . 7. Posthypocristid contacts the base of the entoconid on  $M_{1-3}$ . 8. Cristid obliqua terminates on the posterior trigonid flank, buccally of the tooth midline.

This taxon shares a complete and distinctive anterior cingulum with only one other published bandicoot, *Yarala burchfieldi* from the Oligo-Miocene of Riversleigh, Far North Queensland (Muirhead & Filan 1995). It differs from *Yarala burchfieldi* by possessing a bladed entoconid, smaller hypoconulids, posthypocristid that contacts the entoconid and a less posteriorly placed metaconid.

Gen et sp. nov. 2

(Fig. 15B)

MATERIAL. QMF51645-QMF51650; QML1284, QML1284a, QML1311(H), QML1384U, QML1313, QML1385, QML1311 (C/D).

A medium-sized bandicoot possessing the following dental characteristic: 1.  $M_1$  with anterior cingulid present as distinct antero-dorsally projecting cuspule. 2. A small buccal cuspule between metaconid and hypoconid. 3. Compressed trigonid with all three main cusps closely approximated. 4. Bladed entoconid on  $M_1$ . 5. Posthypocristid runs to the base of the entoconid on  $M_{1-3}$ . 6. Hypoconulid reduction on  $M_1$ , further reduction on  $M_2$  and near absent on  $M_3$ . 7. Cristid obliqua runs to the middle of the posteroventral flank of the trigonid. 8. Talonid broadens consecutively along molar row.

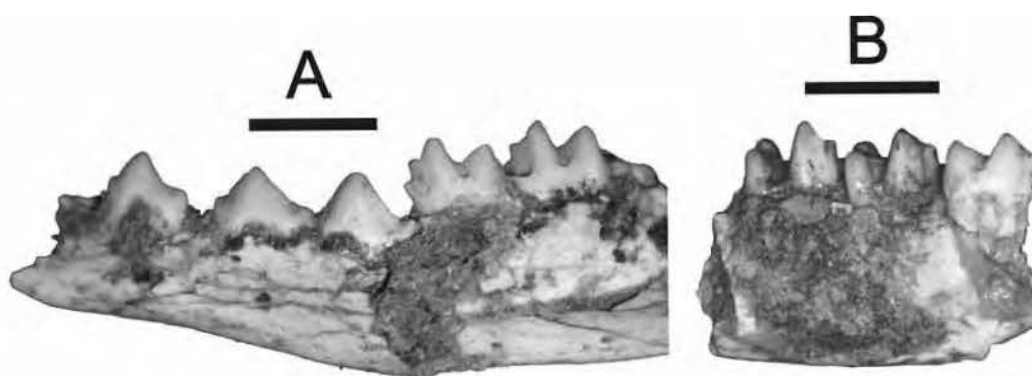


FIG 15. A-B, Family incertae sedis; A, Gen. et sp. nov. 1; QMF51644,  $LP_1-M_3$ . B, Gen. et sp. nov. 2; QMF51645,  $RM_{1-3}$ . Scale bar = 5mm



Family DASYURIDAE Goldfuss, 1820 *sensu* Waterhouse, 1838

Dasyurids are a conspicuous part of all of the faunas, being represented by isolated teeth, nearly complete mandibles and maxillae, or even partial skulls. Identification of dasyurids follows the character states defined by Wroe and Mackness (1998) for *Dasyurus*, Van Dyck (2002) for *Antechinus*, Archer (1981) for *Sminthopsis*, Dawson (1982a) for modern and fossil *Sarcophilus*, Archer (1976) for *Planigale* and Wroe et al. (2000) for other dasyurid genera.

***Antechinus* Macleay, 1841**

*Antechinus* is a morphologically diverse group as defined by Van Dyck (2002). Specimens were identified as *Antechinus* on the basis of the combined features: 1. Complete posterior cingulum on upper molars. 2.  $P_3 / P^3$  reduced. 3. Meta- and hypocristids not transverse to the longitudinal axis of the jaw. 4. Entoconid variably present.

***Antechinus* sp. 1**  
(Fig. 16A)

MATERIAL. QMF51651-51653, QMF51654-51657; QML1313, QML1284a.

*Antechinus* sp. 1 is allied very closely to *Antechinus adustus* based on maxillary morphology. The fossil maxillae possessed the greatest number of maxillary character-states provided by Van Dyck (2002) for *A. adustus*, which included characters; 18-19, 22, 25-28, 30, 33, 36-37. Mandibles and isolated lower molars conform in size to the maxillary specimens, however, they do not conform in the character-states that are present in *A. adustus*. Instead, the mandibles show a greater similarity to *A. godmani* or *A. minimus* (characters 40-46; 48-54). Due to the very small sample size, these morphological variations may either constitute a single morphologically distinct new taxon or two similarly-sized known species of modern *Antechinus*. The most convincing characteristics seem to be from the maxilla, thus *A. adustus* would be considered the most likely taxon present in the deposits.

***Antechinus* sp. 2**

MATERIAL. QMF51663-51680; QML1284a, QML1385, QML1311(C/D), QML1420, QML1311(H), QML1313, QML1284.

A second species of *Antechinus* is present and differs from *Antechinus* sp. 1 by being larger in overall dimensions and possessing a relatively

larger  $P_3$ . This species of *Antechinus* does not possess any greater similarity to any of the modern species of *Antechinus*.

***Antechinus flavipes* (Waterhouse, 1838)**  
(Fig. 16B)

MATERIAL. QMF51681-51685; QML1312, QML1384U.

*Antechinus flavipes* has been identified by numerous fragmentary and complete maxillae and mandibles. The most complete specimens, which are also the easiest to identify, are the mandibles. Using the characteristics provided by Van Dyck (1982, 2002) and Smith (1972), which included: 1. Tiny and crowded  $P_3$ . 2. Transversely orientated  $P_3$ . 3. Small entoconids. 4. Small paraconid. 5. Size (7.54-7.66mm  $M_{1-4}$  Length), I am able to differentiate this species from a second species present in the same deposit, *Antechinus swainsoni*.

***Antechinus swainsoni* (Waterhouse, 1840)**  
(Fig. 16C)

MATERIAL. QMF51686-51688; QML1312.

*Antechinus swainsoni* is also represented by numerous maxillae and mandibles. Using features in Van Dyck (1982) that differentiate *A. flavipes* from *A. swainsoni*, this smaller species was able to be distinguished. The premolar row is not crowded as in *A. flavipes*, the mandible is gracile and  $M_{1-4}$  length reaches 7.30-7.34mm.

***Dasyurus* Geoffroy, 1796**

*Dasyurus* was identified by the absence of  $P^3$  or  $P_3$  (except *Dasyurus dunmalli*) and its moderately large-sized molars and total mandibular dimensions (larger than *Phascogale*, smaller than *Sarcophilus* and *Glaucodon*).

***Dasyurus hallucatus* Gould, 1842**

MATERIAL. QMF51689, QML1312.

A small-sized *Dasyurus*, differing from other modern and extinct *Dasyurus* by possessing a relatively shorter metacrista length on  $M^3$  than  $M^2$ , and a metacone on  $M^1$  perpendicular to stylar cusp D.

***Dasyurus viverrinus* (Shaw, 1800)**  
(Fig. 16K)

MATERIAL. QMF51690-51695; QML1312; QML1384U.

A medium-sized *Dasyurus*, differing from other modern and extinct *Dasyurus* by possessing a longer metacrista on  $M^3$  than on  $M^2$ ; metacone anterior to stylar cusp D; reduced paracones; not

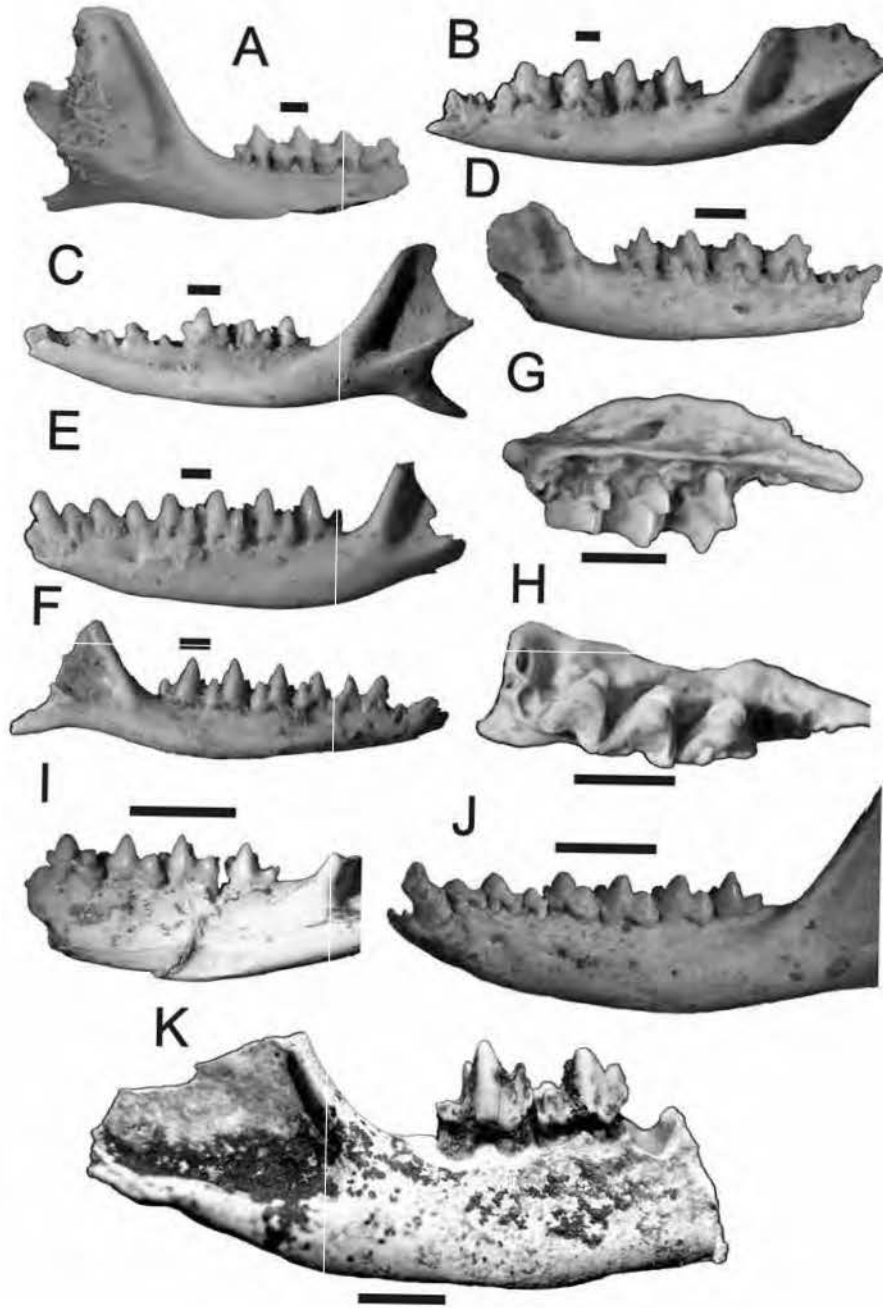


FIG 16. A-K, Dasyuridae; A-C, *Antechinus*; A, *Antechinus* sp. 1; QMF51651, RM<sub>1-4</sub>. B, *Antechinus flavipes*; QMF51681, LP<sub>3</sub>-M<sub>4</sub>. C, *Antechinus swainsoni*; QMF51686, LM<sub>2-4</sub>. D, *Planigale maculate*; QMF51707, RM<sub>1-4</sub>. E-F, *Sminthopsis*; E, *Sminthopsis macroura*; QMF51715, LC<sub>1</sub>-M<sub>4</sub>. F, *Sminthopsis murina*, QMF51724, RP<sub>2</sub>-M<sub>4</sub>. G-H, Gen et sp. nov.; QMF51743, lingual and occlusal views. Scale bar = 1mm. I-J, *Phascogale*; I, *Phascogale* sp.; QMF51704, LM<sub>1-4</sub>. J, *Phascogale topoatafa*; QMF51699, LC<sub>1</sub>-M<sub>4</sub>. K, *Dasyurus viverrinus*; QMF51690, RM<sub>3-4</sub>. Scale bar = 5mm.

bulbous (as in *D. maculatus*); reduced metaconid. Differs specifically from *D. geoffroyi*, a species most similar to *D. viverrinus*, by having relatively longer metacristae. Fossil specimens show similarities to *D. maculatus*, including a small entoconid and a reduced posterior cingulid on  $M_{1-3}$ . These features are intriguing and with more specimens may constitute further review, however, at the present time there are significantly more morphological features shared with *D. viverrinus*.

***Dasyurus* sp.**

MATERIAL. QMF51696-51698; QML1313.

A medium-sized species of *Dasyurus* is represented by an isolated  $M_2$ ,  $M^{2+3}$ . There are not enough features available on the specimen to warrant specific placement at the present time.

***Phascogale* Temminck, 1824**

Species of *Phascogale* are distinguished from other similar dasyurids by the  $P_3$  being higher than  $P_2$  and by being considerably larger than the only other dasyurid exhibiting the former trait, *Sminthopsis*.

***Phascogale topoatafa* (Meyer, 1793)  
(Fig. 16J)**

MATERIAL. QMF51699-51703; QML1312.

*Phascogale topoatafa* is distinguished from *Phascogale calura* by being larger, possessing a small posterior cusp on  $P_3$  and possessing a smaller protocone on  $M^{1-3}$ .

***Phascogale* sp.  
(Fig. 16I)**

MATERIAL. QMF51704-51706; QML1420, QML1313.

A small, possibly undescribed, species of *Phascogale* is tentatively identified here based on the great number of similarities (as defined by Van Dyck (2002)) shared with both *P. topoatafa* and *P. calura*. Its smaller size seems to differentiate it from the two extant species of *Phascogale*, however, further analysis of *P. calura* is needed to determine whether the fossil specimens are within the variation for this species.

***Planigale* Troughton, 1928**

***Planigale maculata* (Gould, 1851)  
(Fig. 16D)**

MATERIAL. QMF51707-QMF51711, QML1312; Olsens Cave.

A species of *Planigale* was identified based on its diminutive size, reduced single-rooted  $P_3$ , absent entoconid, present posterior cingulum and reduced stylar cusps, especially stylar cusp D on  $M^{2-3}$ . *P. maculata* was distinguished by its size, being smaller than *P. novaeguineae*, larger than *P. ingrami* and *P. tenuostris*, and by possessing  $P_3$  (versus *P. gilesi*, which does not).

***Sarcophilus* Cuvier, 1837**

Species of *Sarcophilus* were determined by using criteria described by Dawson (1982a) for *Sarcophilus lanarius* and *Sarcophilus harrisii*. No site has yet been found where both taxa can be said to occur sympatrically, however, a fragment of a mandible which is referred to here as

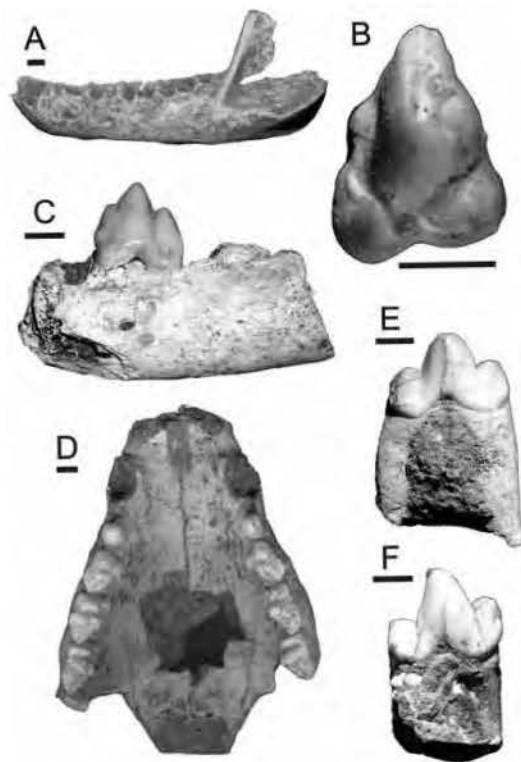


FIG 17. A-D, Dasyuridae; *Sarcophilus*; A, *Sarcophilus harrisii*; QMF51712, left mandible. B-D, *Sarcophilus lanarius*; B, QMF41997,  $LM^1$ . C, QMF51713,  $LM_1$ . D, QMF1872, partial skull. E-F, Thylacinidae; *Thylacinus cynocephalus*; E, QMF1737,  $RM_2$ . F, QMF51755,  $RM_1$ . Scale bar = 5mm.

*Sarcophilus lanarius* may have been derived from sediments from within Lower Johansen's Cave, a site containing the only representative of *Sarcophilus harrisii*.

***Sarcophilus harrisii* (Boitard, 1841)**  
(Fig. 17A)

MATERIAL. QMF51712; QML1314.

*Sarcophilus harrisii* is represented by an edentulous left mandible ( $M_{1-4}$  alveoli length: 39.50mm). The specimen differs markedly from *Sarcophilus lanarius* known from the Darling Downs and specimens from Marmor Quarry by being much smaller in size and having a more gracile lateral profile.

***Sarcophilus lanarius* (Owen, 1838)**  
(Fig. 17B-D)

MATERIAL. QMF693, QMF1872, QMF51713-QMF51714, QMF41997; QML1420, QML1311(H), QML1312, QML1384U, QML1384L.

*Sarcophilus lanarius* is represented by isolated molars, a partial mandible and an almost complete palate. The distinctive large triangular dasyurid molars unquestionably place these specimens within *Sarcophilus*. The large size and robust nature of the palate and molars allies these specimens with those of typical *Sarcophilus lanarius* from the eastern Darling Downs and those measured by Dawson (1982a).

***Sminthopsis* Thomas, 1887**

Archer (1981) reviewed the taxonomy of *Sminthopsis*, providing keys to the species using either external or skeletal features. Species of *Sminthopsis* were identified on the basis of their compressed upper and lower molars; absent posterior cingulum on upper molars; transverse meta- and hypocristids; and subequal premolar heights.

***Sminthopsis macroura* (Gould, 1845)**  
(Fig. 16E)

MATERIAL. QMF51715-QMF51723; QML1312, QML1384, QML1314.

*Sminthopsis macroura* was identified by possessing the following features: large and distinct entoconid; hypocristid that does not contact the entoconid;  $C_1$  not enlarged; premolars longer than broad; medium-sized species ( $M_{1-4}L = 5.8\text{mm}$ ).

***Sminthopsis murina* (Waterhouse, 1838)**  
(Fig. 16F)

MATERIAL. QMF51724-51739; QML1312, QML1313, QML1420, QML1284, QML1284a, QML1385, Olsen's Cave.

Difficulty was experienced in identifying a second species of *Sminthopsis*, distinguished by the absence of the entoconid. Very few features were available from Archer (1981) to distinguish species of this group based simply on mandibular or maxillary features. Three species were possible candidates; *S. butleri*, *S. leucopus* and *S. murina*. *S. butleri* was excluded because it apparently shows signs of tiny entoconids on  $M_{1-3}$ , the fossil specimens do not. *S. leucopus* was excluded because the fossil specimens show premolars that do slightly contact each other, a feature generally not seen in *S. leucopus*, however, this is a relatively variable trait. *S. murina* is preferred until further analysis is possible.

**Gen. et sp. nov.**  
(Fig. 16G-H)

MATERIAL. QMF51743-51754; QML1311(H), QML1385, QML1284, QML1284a, QML1313, QML1384U.

A tiny dasyurid, similar in size to *Planigale* and *Ningaui*, possesses heavily reduced upper dentition, including a significantly reduced protocone on  $M^{1-5}$ ; an extremely reduced paracone on  $M^1$ ; absent styler cusps D and B on all molars; and a distinct ectoloph indentation. There are only four roots found between the canine root and  $M^1$  suggesting the loss of  $P^3$  as in *Planigale gilesi*. The possession of these distinctly derived traits (*sensu* Wroe et al., 2000) suggests the possible need to erect a new genus of dasyurid to accommodate this highly distinctive taxon. More complete material will soon be available and a more formal description and analysis is underway.

**Family THYLACINIDAE Bonaparte, 1838**

***Thylacinus* Temminck, 1824**

***Thylacinus cynocephalus* (Harris, 1808)**  
(Fig. 17E-F)

MATERIAL. QMF1737, QMF51755-QMF51757; QML1420, QML1313, QML1311(H), QML1311 (C/D), QML1312.

Several isolated molars and an almost complete skull and mandibles represent the marsupial carnivore, *Thylacinus cynocephalus*. They compare favourably with modern and fossil



TABLE 3. Faunal lists for large-sized mammal species

	QML1284	QML1284a	QML1311H	QML1311CD	QML1312	QML1313	QML1384U	QML1384L	QML1420
<i>Thylacinus cynocephalus</i>			x	x	x	x			x
<i>Vombatus ursinus mitchellii</i>				x					x
?zygomaturine									x
<i>Palorchestes</i> sp. cf. <i>P. parvus</i>			x	x					x
?diprotodontid indet.			x						
<i>Bohra</i> sp.				x					
<i>Kurrabi</i> sp.			x	x					
<i>Protomnodon</i> sp. cf. <i>P. devisi</i>	x		x	x					
macropodine indet.	x	x	x				x	x	x
<i>Macropus</i> sp. 1					x				x
<i>Macropus</i> sp. cf. <i>M. agilis siva</i>			x						x
<i>Macropus titan</i>									x
<i>Thylacoleo</i> sp.								x	x
<i>Thylacoleo hilli</i>			x						

specimens assigned to *T. cynocephalus*, falling within the variation provided by Dawson (1982b).

#### Family VOMBATIDAE Burnett, 1830

##### *Vombatus* Geoffroy, 1803

##### *Vombatus ursinus mitchellii* (*sensu* Dawson, 1983) (Fig. 18A)

MATERIAL. QMF51758, QMF1420; QML1311 C/D, QML1420.

The only large marsupial with hypsodont molars, wombats are easily identified from any deposit. *Vombatus* is represented from QML1420, Marmor Quarry, by an incomplete left mandibular ramus with molars and insisor root preserved, and a partial right maxilla. A single tooth, within a partial maxilla has also been recovered from QML1311 Unit C/D. Based on size comparisons, the three specimens are much smaller than *Phascolonus* and slightly smaller than *Phascolomys medius*, falling within the size range of the Late Pleistocene *Vombatus ursinus mitchellii* (*sensu* Dawson 1983; Murray 1998) from the eastern Darling Downs.

#### Family DIPROTODONTIDAE Gill, 1872

##### ?zygomaturine (Fig. 18B)

MATERIAL. QMF1419, QML1420.

Tooth fragments of a diprotodontid from Marmor Quarry which were initially identified by Longman (1925a) as *Diprotodon australis* are revised to ?zygomaturine. Two of the three tooth fragments come from the same molar. The fragments consist of a protolophid which possesses a narrow anterior cingulum. The third tooth fragment may come from the same molar and represents the posterior lingual side of the molar, preserving the lingual edge of the hypolophid. The tooth is low crowned and the lophs are relatively straight and narrow. Based on this, and comparing the molars to specimens of *Zygomaturus*, *Euryzygoma* and *Diprotodon*, it seems most likely that the tooth came from a species *Zygomaturus*. Phalanges and fragments of vertebrae have also come from Marmor Quarry, however, these do not aid in the identification of this relatively large form of diprotodontid.

#### Family PALORCHESTIDAE (Tate, 1948)

##### *Palorchestes* Owen, 1873

##### *Palorchestes* sp. cf. *P. parvus* De Vis, 1895 (Fig. 18C-D)

MATERIAL. QMF51759-51760, QMF42635 (cast) / BMNH10257; QML1311(H); QML1311 (C/D), QML1420.

*Palorchestes* is represented by an isolated M<sub>2</sub>, a left maxillary fragment preserving the posterior portion of M<sup>1</sup> and a complete M<sup>2</sup>, and a left I<sup>1-2</sup>. Left I<sup>1</sup> large, curved and broad distally. LI<sup>2</sup> broad with tapering root. LM<sup>1</sup> preserves a double midlink and a posterior-lingual fossette. LM<sup>2</sup> ovo-rectangular in occlusal view, lophs relatively narrow with the metaloph slightly narrower than paraloph. Single mid- and forelink. Anterior cingulum deep and completely running the length of the molar, bisected by forelink. Buccal cingulum present between paracone and metacone. Postero-lingual pocket. No posterior cingulum. M<sub>2</sub> rectangular in occlusal view, lophs high and narrow, distinct fore- and midlink, posterior cingulid absent.

These specimens cannot be assigned to a species of *Palorchestes* because they lack diagnostic features of the M<sup>1</sup> (Black, 1997). Based simply on size, the specimens are from a small species of *Palorchestes*, much smaller than

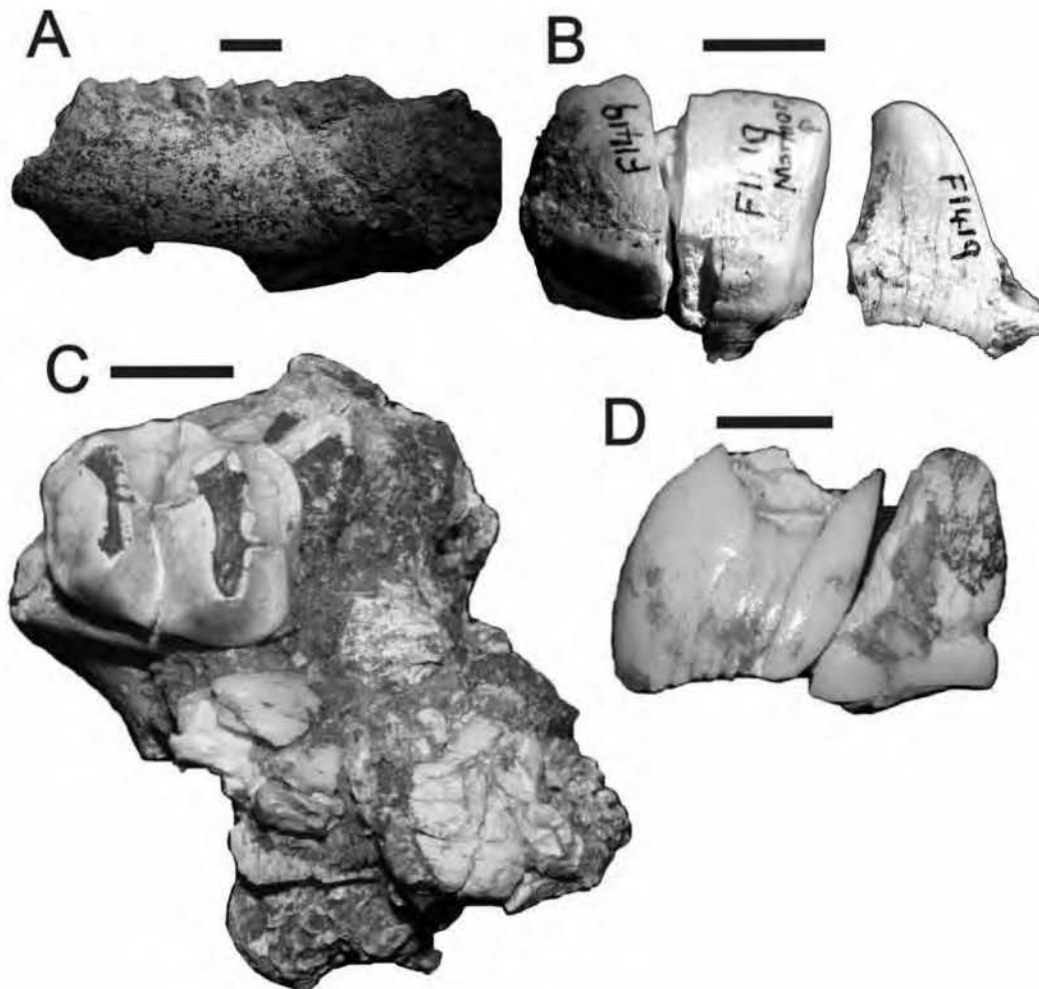


FIG 18. A, Vombatidae; *Vombatus ursinus mitchelli*; QMF1420, LM<sub>1-4</sub>. B, ?Zygomaturine; QMF1419, fragmentary molar. C-D, Palorchestidae; *Palorchestes* sp. cf. *P. parvus*; C, QMF51759, RM<sup>2</sup> (partial M<sup>1</sup>). D, QMF51760, LI<sup>1-2</sup>. Scale bar = 10mm.

*P. azael* and very similar in size to *P. parvus*. The M<sub>2</sub> is larger than the species recovered from the Hamilton LF, which was considered by Turnbull & Lundelius (1970) to be *Palorchestes painei*. This identification has been challenged by Rich (1991) who considers it to represent a new taxon, illustrating the taxonomic uncertainty surrounding the smaller members of the Palorchestidae.

?diprotodontid indet.

MATERIAL. QMF51761; QML1311H.

Approximately a quarter of a lower molar possibly represents a small diprotodontid. The tooth is low crowned, lophodont and bears thick slightly crenulated enamel distinctive in several diprotodontian groups. The molar is distinctly not macropod based on the thickness of the enamel and the crenulations are not as distinct as those found in the Sthenurinae. The lophids are lower than those found in palorchestids.

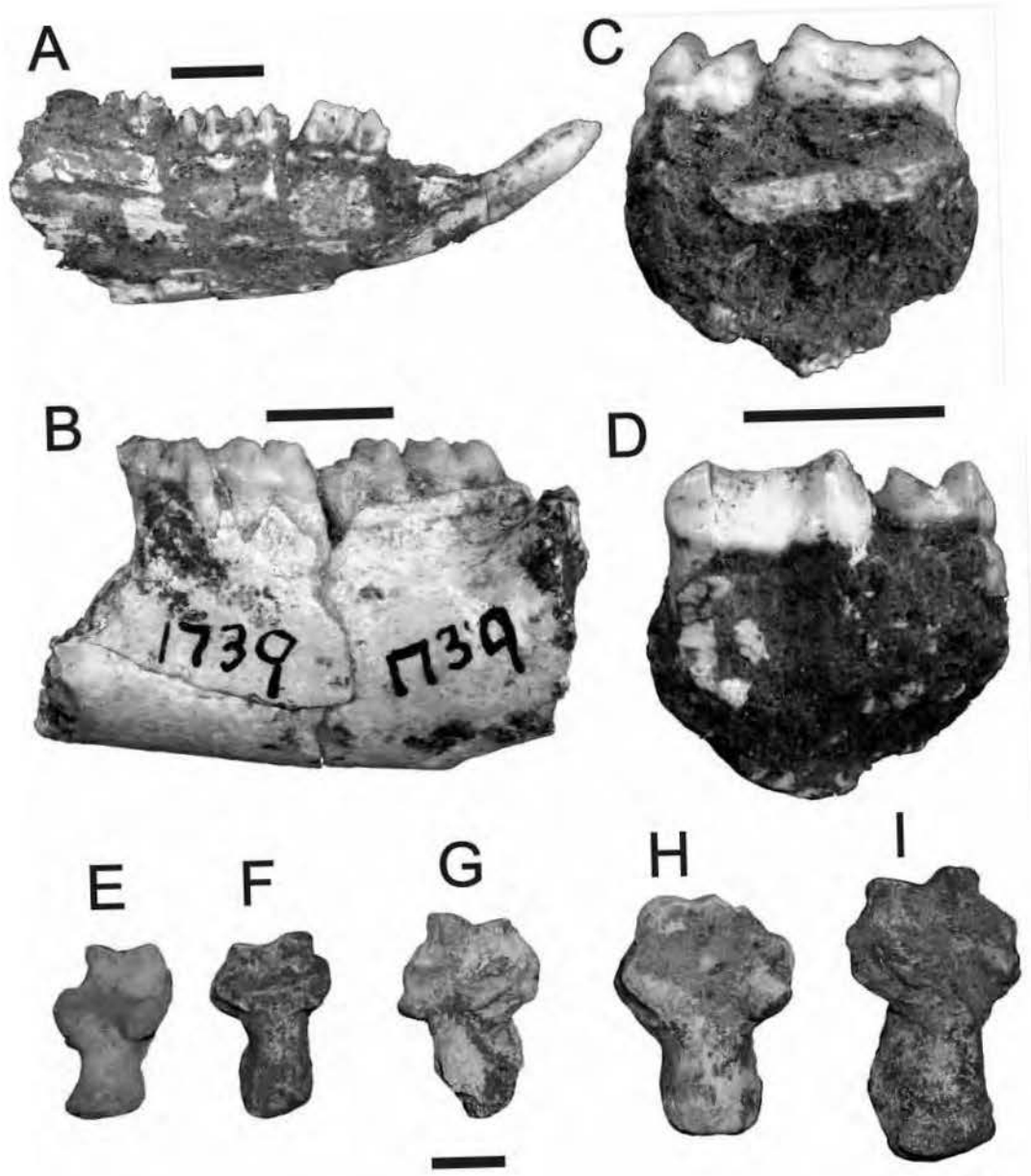


FIG19. A-I, Macropodidae. A-H, *Dendrolagus* sp.; A, QMF51770, RI<sub>1</sub>-M<sub>4</sub>. B, QMF1739, LM<sub>1-4</sub>. C-D, QMF51771, RP<sup>3</sup>-M<sup>1</sup> in lingual and buccal view (showing postero-buccal cuspule on P<sup>3</sup>). E-H, Calcanea; QMF51772-51775 (left to right). I. *Bohra* sp.; QMF51783, calcaneum. Scale bar = 5mm.

Family MACROPODIDAE Gray, 1821

**Bohra** Flannery & Szakay, 1982

**Bohra** sp.  
(Fig. 19I)

MATERIAL. QMF51762; QML1311C/D.

*Bohra* sp. is represented by a complete right calcaneum (Calcaneal Length: 46.79mm; Calcaneal-Cuboid articulation height 12.43mm and width 18.96; Astragalar-calcaneal articulation length 23.01mm). The calcaneum is placed within *Bohra* on the basis of the following features it shares with *Bohra paulae*: 1. Massive calcaneal size relative to all other dendrolagine macropods. 2. Height to width of calcaneal-cuboid articulation (Flannery & Szakay, 1982) (0.65). 3. Calcaneal length to astragalar-calcaneal articular length (Flannery & Szakay, 1982) (0.49).

**Dendrolagus** Muller & Schkegel, 1839

**Dendrolagus** sp.  
(Fig. 19A-H)

MATERIAL. QMF51770-QMF51783; QML1284, QML1311(H), QML1311(C/D), QML1312, QML1385, QML1420.

*Dendrolagus* is represented by two nearly complete mandibles, three maxillary fragments, isolated premolars, molars and three calcanea. The mandibles are characterised by possessing low crowned, square molars and an elongate, blade-like P<sub>3</sub>. P<sub>3</sub> blade bounded by a large anterior cusp and posterior cusp. A single intermediate cuspule is situated a third the way along the crest. The upper dentition is characterised by an ovo-rectangular P<sup>3</sup> in occlusal view, possessing low-crowned square molars with weak midlinks and absent forelinks. P<sup>3</sup> with both postero-buccal and postero-lingual cuspules. Paracone linked to metacone via a crested blade. A single vertical ridge runs to a small cuspule near the centre of the blade. A tiny accessory cuspule is present posterior to the main cuspule. Lingual cingulum runs the length of the tooth, terminating below the paracone. When compared to extant species of *Dendrolagus* the fossil taxon shares closest lower dentition morphology with *D. matschiei*, whereas the upper dentition most closely resembles *D. ursinus*. At present there are no morphological or morphometric features that suggest that the mandibles represent one taxon and the maxillae another. Further material will be needed to clarify the specific placement of these specimens,

however, it seems most probable that the fossils represent an extinct taxon with phylogenetic links to both *D. matschiei* and *D. ursinus*.

Calcanea have been identified by possession of a distinctive squat shape, short calcaneal tuberosity, and broad anterior articular facets. Four specimens have been recovered so far and all four are distinctly different in size. The largest is from QML1420 Marmor Quarry (QMF51781), the second largest from QML1311 (QMF51780) and the smallest from QML1312. With so few calcanea available to compare, morphometric comparison with extant populations was not possible, however, the great difference in size between the largest and smallest calcanea may illustrate the presence of several species.

**Kurrabi** Flannery & Archer, 1984

**Kurrabi** sp.  
(Fig. 20A-D)

MATERIAL. QMF51767-51769; QML1311(H), QML1311 (C/D).

Three isolated P<sup>3</sup>'s represent a species of *Kurrabi*. Each premolar is elongate with two small vertical ridges on the longitudinal crest between the paracone and metacone. A moderate-sized fossette occurs on the posterior lingual side of the tooth. A lingual cingulum runs the length of the tooth, terminating just posterior of the base of the paracone. In size, the specimens are closest to *K. merriwaensis* (L: 9.2-11.5mm). Without more material specific diagnosis is not warranted.

**Protemnodon** Owen, 1874

**Protemnodon** sp. cf. **P. devisi** Bartholomai,  
1973  
(Fig. 20E-H)

MATERIAL: QMF41737, QMF41953, QMF51763-QMF51766, QMF52068; QML1284, QML1311(H), QML1311 (C/D).

*Protemnodon* sp. cf. *P. devisi* has been identified from an isolated premolar; a badly preserved palate with portions of RP<sup>2</sup>, RdP<sup>3</sup>, RM<sup>1-3</sup> and LdP<sup>3</sup>, RM<sup>1-2</sup> preserved; a left mandible with M<sub>2+3</sub>; left mandible preserving P<sub>3</sub>; isolated RM<sup>1</sup>, LM<sup>3</sup>, LM<sup>4</sup>, LdP<sub>3</sub>, LM<sub>2</sub>, LM<sub>3</sub> and an isolated I<sub>1</sub>. Dimensions of the premolar and molars are within the range given for *P. devisi* by Bartholomai (1973). However, the specimens here differ from *P. devisi* from Chinchilla, but are similar to those of *P. sp. cf. P. devisi* described by Dawson et al. (1999) from Big Sink, in the



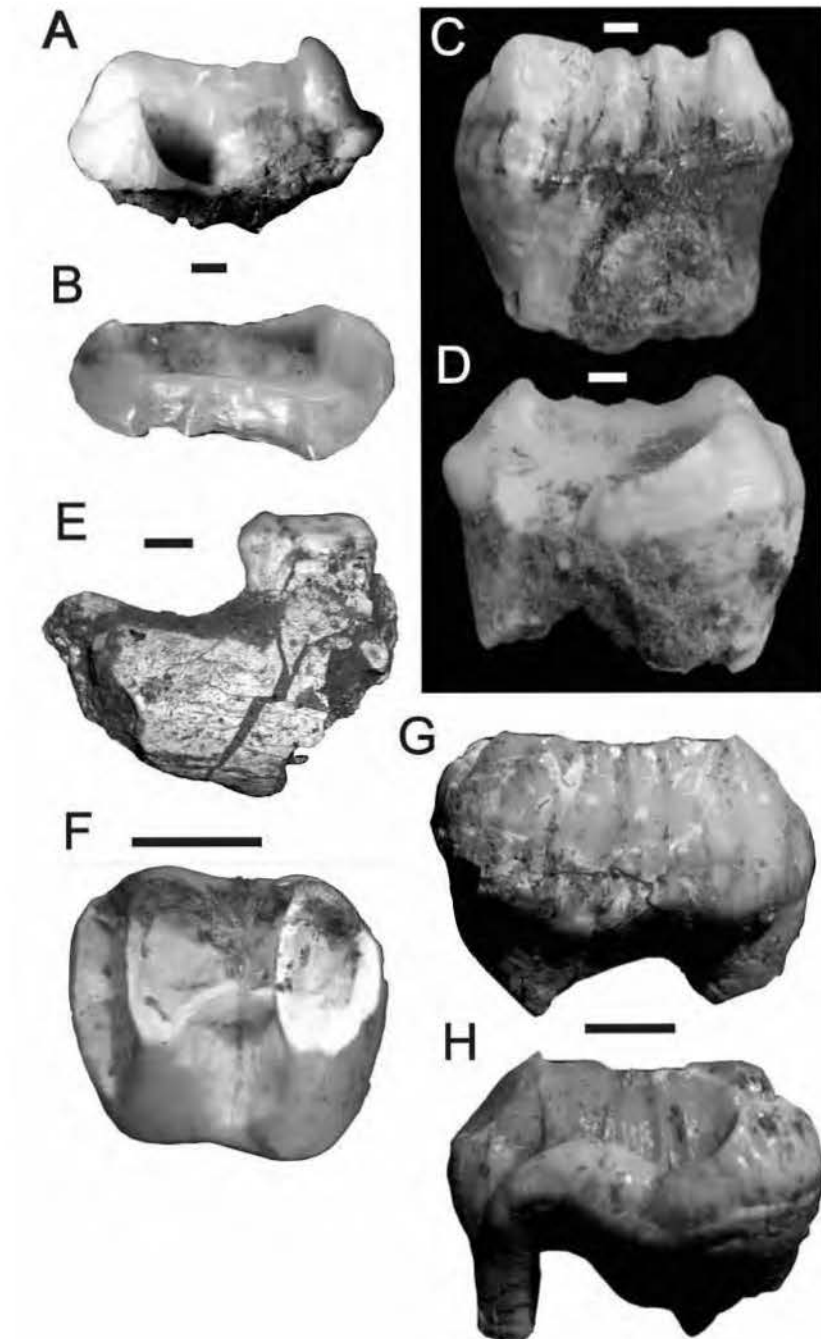


FIG 20. A-H, Macropodidae. A-D, *Kurrabi* sp.; A-B, QMF51767; RP<sup>3</sup> in lingual & occlusal views. C, QMF51768, LP<sup>3</sup>. D, QMF51769, LP<sup>3</sup>. Scale bar = 1mm. E-H, *Protomnodon* sp. cf. *P. devisi*; E, QMF41737, LP<sub>3</sub>. F, QMF41953, LM<sup>3</sup>. G-H, QMF51763; LP<sup>3</sup> in buccal & lingual views. Scale bar = 5mm.

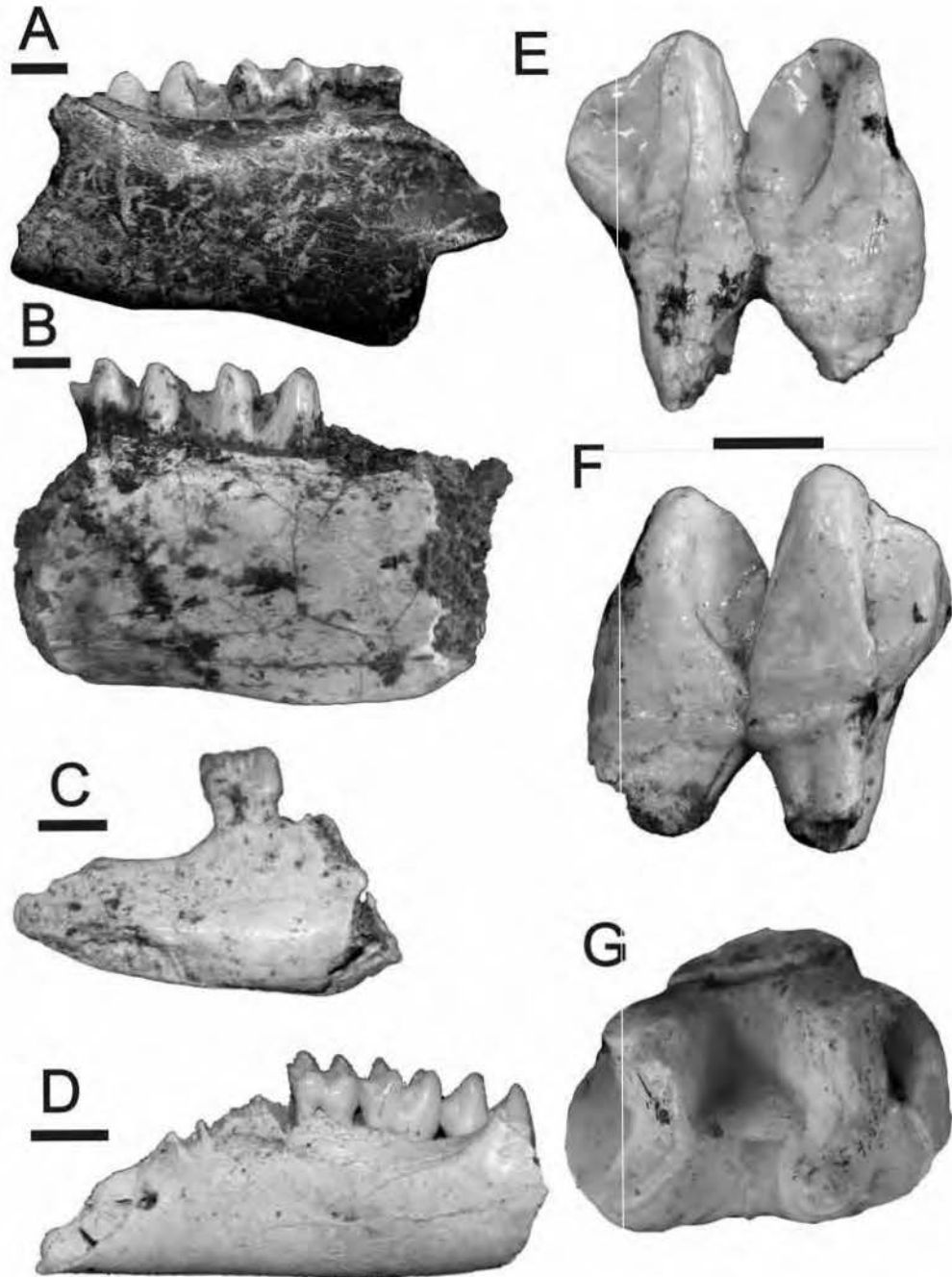


FIG 21. A-G, Macropodidae; A-B, *Macropus* sp. cf. *M. agilis siva*; A, QMF51829, RM<sub>1-3</sub>. B, QMF51830, LM<sub>1-2</sub>. C-D, *Petrogale* sp.; C, QMF51812, RP<sub>3</sub>. D, QMF51813, LM<sub>2-4</sub>. E-G, *Macropus titan*; QMF1697 in lingual (E), buccal (F) & occlusal (G) views. Scale bar = 5mm.

following ways: 1. Lower molars lack a posterior cingulum. 2. Upper molars lack a secondary link across the median valley. 3.  $P^3$  has weak vertical ridges. The specimens do possess premetacristae, which the Big Sink specimens do not. The overall variation seen in the specimens of *P. devisi* from Chinchilla, Big Sink and Mount Etna is within that seen for similar cosmopolitan species such as *P. anak*.

macropodine sp. indet

MATERIAL. QMF51802-51811; QML1284, QML1284a, QML1420, QML1384, QML1311(H).

Several isolated molars appear to represent a large species similar to species of *Thylogale*, however, being much greater in size. Other distinctive features of the molars include sharply crested postpara- and premetacrista running into the median valley; a sharply crested preparacrista linking onto the anterior cingulum, and a well-developed forelink.

The molar is high crowned, and similar in shape to some species of *Macropus*, however, the midlink is weakly developed and the cristae are sharp and elaborated unlike *Macropus*.

***Petrogale* Gray, 1837**

***Petrogale* sp.**  
(Fig. 21C-D)

MATERIAL. QMF51812-51824; All localities.

*Petrogale* is represented by dozens of isolated mandibles, maxillae, molars, premolars, insisors and postcrania. The only taxa close to *Petrogale* are *Thylogale* and small members of *Macropus*. *Petrogale* differs from *Thylogale* in having lower-crowned molars, in the  $I^3$  morphology (not having a longitudinal groove along the length of the  $I^3$  crown) and the anterior morphology of the

$P^3$  (not having a well-developed lingual cingulum with an anterior-lingual pocket). *Petrogale* differs from small-sized *Macropus* by being generally smaller, having a relatively longer  $P^3$  and smaller  $I^3$ . The taxonomic diversity of modern species of *Petrogale* is not reflected in dental morphology, thus species placement is not warranted on the basis of available material.

***Macropus* Shaw, 1790**

Isolated molars and partial jaws represent species of *Macropus*. Bartholomai (1975), Archer (1978) and Dawson & Flannery (1985) illustrate the difficulty in identifying species of *Macropus* on the basis of isolated molars or jaws without premolars and insisors. Distinction of different species of *Macropus* requires almost complete mandibles or maxillae. When dealing with isolated teeth, absolute size comparisons are the only features available for comparison to available data such as Bartholomai (1975). More complete specimens are required before specific allocations can be made.

***Macropus* sp. 1**

MATERIAL. QMF51825-51828; QML1312, QML1420.

A medium-sized *Macropus*, close to *Macropus dorsalis*, is represented by isolated molars that are larger in absolute size than those species of *Petrogale* but smaller than modern species of the size of *Macropus agilis*.

***Macropus* sp. cf. *M. agilis siva* (De Vis, 1895)**  
(Fig. 21A-B)

MATERIAL. QMF51829-51834; QML1420, QML1311(H).

Isolated molars and a partial right mandible represent a medium-sized species of *Macropus*.

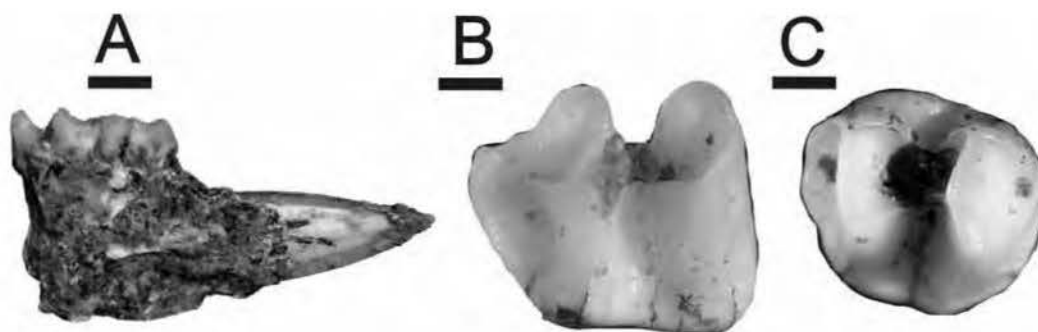


FIG 22. A-C, Macropodidae; *Thylogale* sp.; A, QMF51784,  $LI_1$ - $M_2$ . Scale bar = 5mm. B, QMF51785,  $LM_2$ . C, QMF51786,  $LM^2$ . Scale bar = 1mm.

*Macropus agilis agilis* is closest in overall size to the fossil specimens from Marmor Quarry, however, there is overlap with *Macropus agilis siva* when comparing the mandible from Lost Paradise Cave (J7) and the maxilla and mandible from QML1311. All dental measurements fall within the range for *Macropus agilis siva* defined by Bartholomai (1975).

**Macropus titan** (Owen, 1838)  
(Fig. 21 E-G)

MATERIAL. QMF1697, QMF51835-51837; QML1420. *Macropus titan* is a large macropod easily distinguished by its large high crowned molars, distinct mid- and fore-links and posterior hypolophid groove. Specimens referred to here are placed within *M. titan* based on these features and their similar size to samples taken from the Darling Downs (Bartholomai, 1975).

**Thylogale** Gray, 1837

Two species of *Thylogale* have been identified based on the presence of high-crowned (relative to *Dendrolagus*), rectangular molars, poorly developed midlinks, an anterior cingulum that does not extend across the entire width of the upper molars, and an I<sup>3</sup> that has a complete longitudinal groove on the occlusal face. They have been differentiated from *Petrogale* by having weaker midlinks, an incomplete anterior cingulum on upper molars, smaller-sized molars, and better-developed cristae on dP3s and upper molars.

**Thylogale** sp. 1  
(Fig. 22A-C)

MATERIAL. QMF51784-51797; QML1284, QML1284a, QML1385, QML1384U.

A very small-sized new species of *Thylogale*, smaller than any extant or extinct species, including the smallest known species, *Thylogale christenseni* from Irian Jaya. The upper molars possess weakly developed midlinks, a reduced forelink and an anterior cingulum that only extends slightly more than half way across the front of the molar. These features are shared to a greater extent with *T. christenseni* and *T. billardieri*. With further specimens, this taxon will probably be a new species closely related to *Thylogale christenseni*.

**Thylogale** sp. 2

MATERIAL. QMF51798-51801; QML1312, QML1420. On the basis of molar size and morphology, differentiation of *Thylogale thetis* and *Thylogale*

*stigmatica* is extremely difficult. The fossil specimens are within the range of both taxa and are very similar in overall morphology.

Family PSEUDOCHEIRIDAE (Winge, 1893)

Pseudocheirids are represented by hundreds of isolated premolars and molars, molar rows and jaw fragments. The apparent morphological diversity in the collection is corroborated by the diversity in sizes, ranging from very small ringtails of similar size to *Pseudochirulus mayeri*; medium-sized similar to *Pseudochirulus forbesi*; large-sized *Pseudocheirops* and giant *Pseudokoala*. On reviewing the morphology of modern and Tertiary pseudocheirid taxa it became obvious that the most useful features for identification are found in the P3 and M1 of the upper and lower dentition. Based on characters from these key teeth, several groups emerged. More specific formal taxonomy will be provided in a future analysis as more complete material becomes available.

**Pseudochirulus** Matschie, 1915

*Pseudochirulus* has been identified based on the following combined features: P<sup>3</sup> morphology; elongate-ovoid, preparacrista variably linked to paraconule by blade or valley, only two cusps, posterolingual cingulum variably expressed. M<sup>1</sup> morphology; molar profile elongate-rectangular, preprotoconule crista variably expressed, lingual cingulum absent. P<sub>3</sub> morphology; metaconid blade-like or absent, paraconid distinct and not linked to protoconid by blade, cristid obliqua distinct running from the hypoconid to protoconid. M<sub>1</sub> morphology; distinct paraconid; preprotocristid kindred buccally to paraconid, metaconid variably expressed, entostylid absent. Three species of *Pseudochirulus* have been identified, two small species similar in size to *Pseudochirulus mayeri* and one medium-sized species similar in size to *Pseudochirulus forbesi*.

**Pseudochirulus** sp. 1  
(Fig. 23 G-I, Fig. 24 E)

MATERIAL. QMF51838-51870; QML1385, QML1311(H), QML1311(C/D), QML1284, QML1284a, QML1313, QML1385L.

*Pseudochirulus* sp. 1 is the smallest of the pseudocheirid taxa represented and possesses the following distinctive features that distinguish it and differentiate this species from *Pseudochirulus* sp. 2 and 3: 1. Simple preprotoconule that does not connect to any other



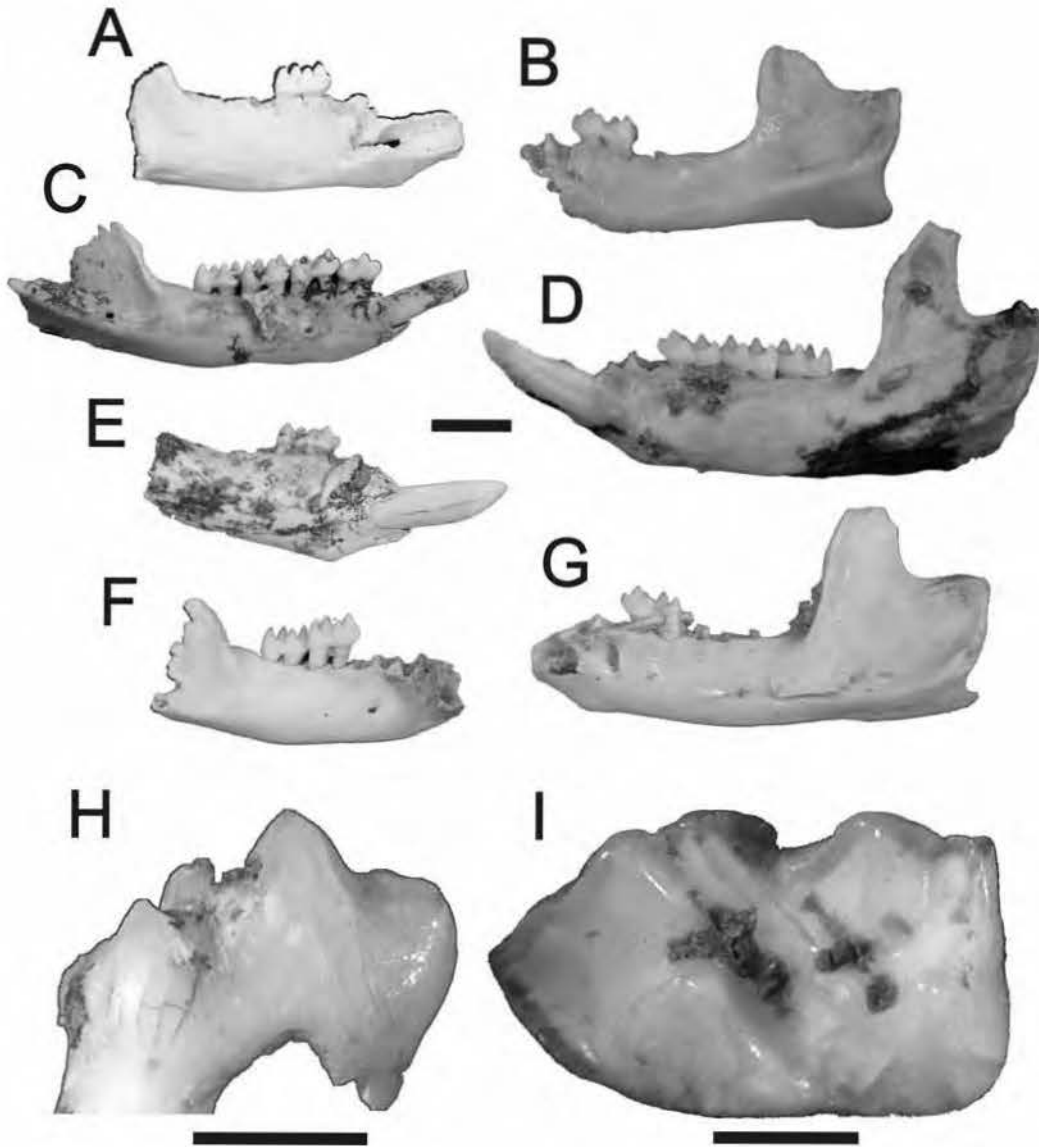


FIG 23. A-I, Pseudocheiridae. A, B, D, E & H, *Pseudocheirus* spp.: A, QMF51898, RM<sub>1</sub>. B, QMF51899, RI<sub>1</sub>-M<sub>3</sub>. D, QMF51900, RM<sub>2,3</sub>. E, QMF51901, RP<sub>3</sub>. Scale bar = 5mm. H, QMF51840, LM<sub>1</sub>. (Scale bar = 1mm). C, *Pseudochirulus* sp. 2; QMF51871, RI<sub>1</sub> & M<sub>1</sub>. F, G & I, *Pseudochirulus* sp. 1; F, QMF51838, LM<sub>1</sub>. G, QMF51839, LI<sub>1</sub> & M<sub>1,3</sub>. Scale bar = 5mm. I, QMF51841. Scale bar = 1mm.

cristae. 2. Protostyle absent. 3. Lingual cingulum absent. 4. Anteriorlingual para- and metacristae absent. 5. Posterolingual para- and metacristae absent. 6. P<sup>3</sup> elongate-ovoid in occlusal view. 7.

P<sup>3</sup> preparacrista does not connect to paraconule. 8. Distinct posterolingual cingulum on P<sup>3</sup>.

*Pseudochirulus* sp. 1 is closest in morphology to the living *Pseudochirulus canescens* and

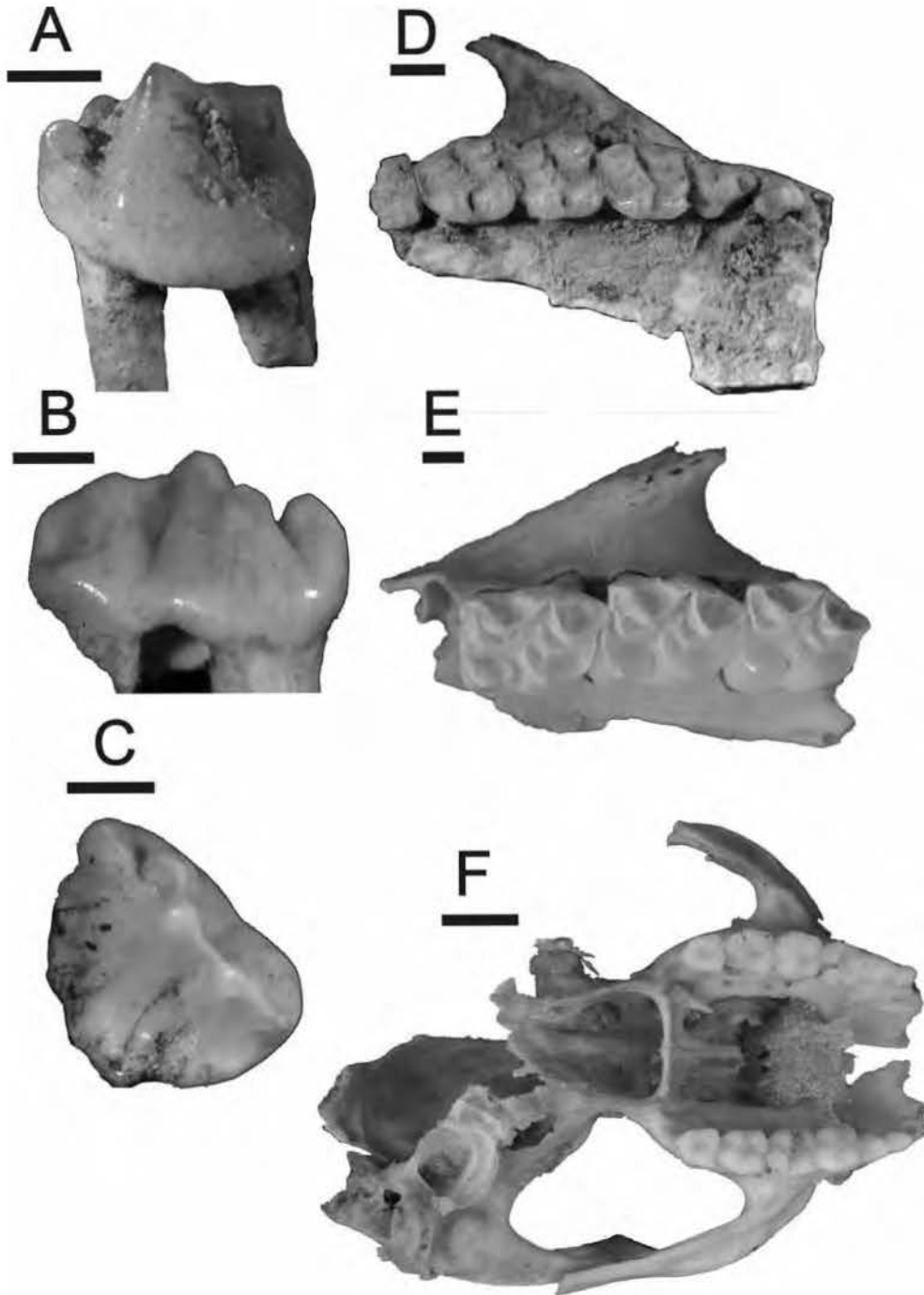


FIG 24. A-F, Pseudocheiridae; A-D, *Pseudocheirus* sp.; A, QMF51920, LP<sup>3</sup>. B-C, QMF51921, LP<sup>3</sup> in buccal & occlusal views. E, *Pseudochirulus* sp. 1; QMF51870, RP<sup>3</sup>-M<sup>3</sup> (broken). Scale bar = 1mm. F, *Pseudochirulus* sp. 2; QMF51887, partial skull. Scale bar = 5mm.

*Pseudochirulus mayeri* and the Early Pliocene *Pseudocheirus marshalli*.

**Pseudochirulus sp. 2**  
(Fig. 23C, Fig. 24F)

MATERIAL. QMF51871-51887; QML1284, QML1284a, QML1313, QML1311(H), QML1384U, QML1384L, QML1385.

*Pseudochirulus* sp. 2 possesses the following distinctive features, that when combined differentiate it from *Pseudochirulus* sp. 1 and 3: P<sup>3</sup> morphology; 1. P<sup>3</sup> elongate-ovoid. 2. Distinct paraconule. 3. Preparacrista contacts paraconule. 4. Broad posterolingual margin with indistinct cingulum. 5. Postparaconule crista distinct and terminates at the base of the paracone. M<sup>1</sup> morphology; 1. Preprotoconule crista contacts paracone buttress. 2. Protostyle present and well-developed. Overall size larger than *Pseudochirulus* sp. 1.

When compared to modern species the fossil taxon is most similar to *Pseudochirulus cinereus* and *Pseudochirulus forbesi* in overall size. The P<sup>3</sup> of *Pseudochirulus* sp. 2 is distinctly more ovoid than the morphology seen in the modern species. The P<sup>1</sup> has large double roots, a feature seemingly unique to this taxon, having not being observed in any of the modern or fossil taxa.

**Pseudochirulus sp. 3**

MATERIAL. QMF51888-51897; QML1284, QML1284a, QML1313, QML1311(H), QML1385, QML1384U, QML1384L.

*Pseudochirulus* sp. 3 possesses the following features that in combination differentiate it from *Pseudochirulus* sp. 1 and 2: P<sup>3</sup> morphology; 1. P<sup>3</sup> elongate-ovoid. 2. Preparacrista contacts paraconule. 3. Distinct posterolingual cingulum, variably cuspidate. 3. Kink in the posterobuccal end of the postparacrista.

When compared to modern species, the fossils are closest in morphology to both *Pseudochirulus mayeri* and *Pseudochirulus herbertensis*. The fossil specimens differ from these species in being larger than *Pseudochirulus mayeri* and smaller than *Pseudochirulus herbertensis*.

**Pseudocheirus Ogilby, 1837**

**Pseudocheirus spp.**  
(Fig. 23A-B, D-E, H, Fig. 24A-D)

MATERIAL. QMF51898-51922; QML1284, QML1284a, QML1313, QML1311(H), QML1385, QML1384U, QML1384L.

*Pseudocheirus* has been identified on the basis of the following combined features: P<sup>3</sup> morphology; 1. Tricuspid, possessing a paracone, paraconule and an accessory cusp between and buccal to them. 2. Ovoid shape to the premolar in occlusal view. 3. Shallow, indistinct posterolingual basin. M<sup>1</sup> morphology; 1. Preprotoconule terminating at the base of the parastyle. 2. Protostyle distinct. 3. Lingual cingulum present between protocone and metaconule. 4. Lack postero- and anterolingual para- and metacristae. P<sub>3</sub> morphology; 1. Metaconid present as a distinct and high cusp. M<sub>1</sub> morphology; 1. Preprotocristid blade-like running to tip of paraconid. 2. Paraconid in line with protoconid. 3. Protostylid tall and crested, closely set against protoconid. 4. Entostylid absent. There are three species of *Pseudocheirus* represented from the sites, all three being markedly different in size but all significantly smaller than extant *Pseudocheirus*. Three species are considered to be new extinct species.

**Petauroides Thomas, 1888**

**Petauroides spp.**  
(Fig. 25A-C)

MATERIAL. QMF51923-51935; QML1284, QML1284a, QML1313, QML1311(H).

*Petauroides* has been identified on the basis of the following combined features: P<sup>3</sup> morphology; 1. Ovoid shape in occlusal view. 2. Distinctly straight blade made by the crests running between the paraconule, paracone and posterobuccal margin of the premolar. 3. Posterolingual postparacrista running into posterolingual basin. 4. Posterolingual cingulum present. M<sup>1</sup> morphology; 1. Preprotoconule connects to preprotocrista. 2. Posterolingual para- and metacristae well developed as crests. 3. Protostyle absent. 4. Lingual cingulum absent. P<sub>3</sub> morphology; 1. Paraconid, protoconid and metaconid in a line along the longitudinal axis of the tooth crown. 2. Cristids variably expressed and probably constitute several species. 3. Small posterior pocket below the metaconid developed in some specimens.

The morphological diversity seen in specimens referred to here as *Petauroides* indicates a very complex fossil history leading to the modern *Petauroides* and *Hemibelideus*. The only P<sup>3</sup> specimen available is closest in morphology to *Hemibelideus*. P<sub>3</sub> morphology shows great degrees of morphological diversity albeit retaining typical *Petauroides* characteristics.

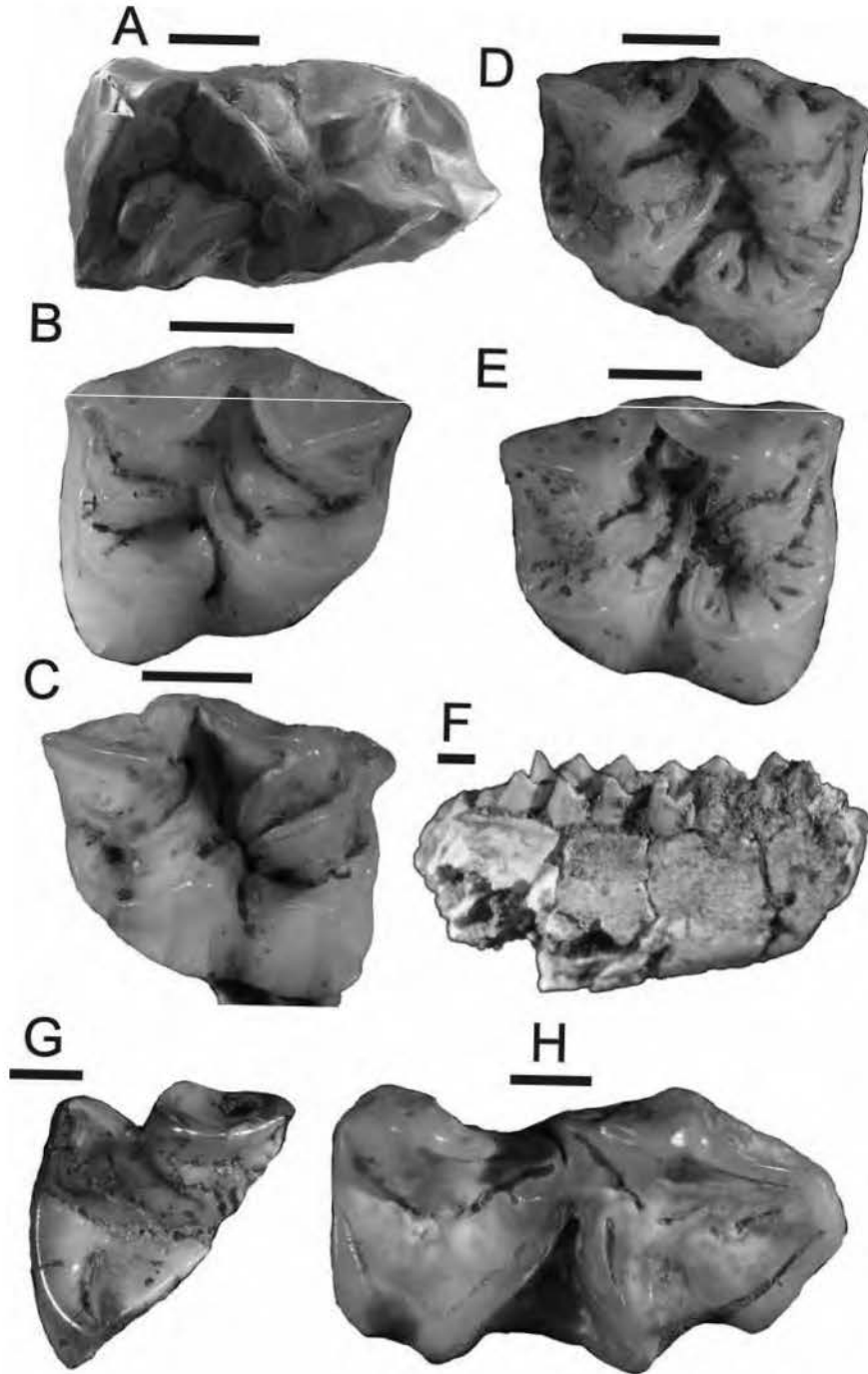


FIG 25. A-H, Pseudocheiridae; A-C, *Petauroides* sp.; A, QMF51923, RM<sub>1</sub>. B, QMF51924, LM<sup>2</sup>. C, QMF51925, RM<sup>2</sup>. D-F, *Pseudocheirops* sp.; D-E, *Pseudocheirops* sp. 1; D, QMF51934, RM<sup>3</sup>. E, QMF51935, RM<sup>2</sup>. Scale bar = 1mm. F, *Pseudocheirops* sp. 2; QMF51937, RM<sub>2</sub>. Scale bar = 5mm. G-H, *Pseudokoala* sp.; G, QMF51934, RM<sup>7</sup>. H, QMF51939, RM<sub>2</sub>. Scale bar = 1mm.

Five distinct morphologies are present, however, these will be treated as polymorphic until a larger collection is available. Even so, no  $P_3$  clearly represents known species of *Petauroides* or *Hemibelideus*.  $M_1$  morphology shares greater similarities with extinct species of *Petauroides* (*Petauroides stirtoni* and *Petauroides ayamaruensis*, see Long et al., (2002)) than with the modern *Petauroides volans* and *Hemibelideus lemuroides*.

#### **Pseudocheirops Matschie, 1915**

*Pseudocheirops* has been identified on the basis of the following features: 1. Protostylid basin on  $M_{1-3}$ . 2. Elaborate crenulations on upper and lower molars. 3. Entostylid present. 4. Posterior bifurcation of protoconule. 5. Protostyle present. 6. Crest present labial to protostyle. Two species of *Pseudocheirops* have been identified so far.

##### **Pseudocheirops sp. 1** (Fig. 25D-E)

MATERIAL. QMF51936, QMF51934-51935; QML1311(H), QML1384L.

*Pseudocheirops* sp. 1 is a right mandible preserving a partial  $M_1$ , complete  $M_{2-3}$  and a partial  $M_4$ . Two upper right molars are also considered to be conspecific. The fossils compare favourably with *Pseudocheirops archeri* both in size, crenulations and development of the protostylid basin.

##### **Pseudocheirops sp. 2** (Fig. 25F)

MATERIAL. QMF51937; QML1284.

The second, much smaller species *Pseudocheirops* sp. 2, is only known from a right  $M_2$ . The crenulations are indistinct with a narrow entostylid and very small protostylid basin. The fossil is much smaller than any of the modern *Pseudocheirops* available to study, yet it is similar in size to the Pliocene *Pseudocheirops winteri* from Bluff Downs. The fossil differs from *Pseudocheirops winteri* by possessing a complete preentocristid-metacristid connection.

#### **Pseudokoala Turnbull & Lundelius, 1970**

##### **Pseudokoala sp.** (Fig. 25G-H)

MATERIAL. QMF51938-51939; QML1385; QML1311 (C/D).

*Pseudokoala* has been identified from an isolated  $M_2$  and a fragment of upper molar. It has been placed within *Pseudokoala* based on the

following combined features: 1. Very large size. 2. Crenulations present but forming large buttresses, less crenulated than *Pseudocheirops* spp. 3. Lack of an entostylid. 4. Truncated posthypocristid. 5. Buccally buttressed protoconid.

When compared to the three species of *Pseudokoala*, *Pseudokoala* sp. is closest to *Pseudokoala erlita* in size ( $M_2L$ : 6.78mm *Pseudokoala* sp.,  $M_2L$ : 6.2-7.3mm *Pseudokoala erlita* Turnbull & Lundelius (1970),  $M_1L$ : 10.7mm *Pseudokoala curramulkensis*,  $M_1L$ : 10.9mm *Pseudokoala cathysantamaria* Archer et al. (1997). The molar crown is simplified as in *Pseudokoala erlita*, however, due to the worn nature of the tooth no more specific comparisons can be made.

pseudocheirid indet.

MATERIAL. QMF51940; Olsen's Cave.

A posterior fragment of an upper molar with distinctly selenodont morphology represents the only material of a pseudocheirid from the Olsen's Cave collection. The lack of crenulations and an anterolingual metacrista allies the specimen to a large member of *Pseudochirulus* or *Pseudocheirus peregrinus*.

#### **Family PETAURIDAE (Gill, 1872)**

Petaurids are represented by several nearly complete maxillae, fragmentary mandibles, isolated insisors, premolars, molars and postcrania. Two genera are recorded, *Dactylopsila* and a new undescribed genus.

#### **Dactylopsila Gray, 1858**

*Dactylopsila* has been identified based on the following combined features: 1. Possession of a distinct and large  $M^1$  parastyle. 2. Reduction of the styler margin with a distinct indentation between the paracone and metacone. 3. Reduced metaconule. 4. Procumbent  $I_1$ . 5. Bulbous, rectangular-ovoid lower molars.

##### **Dactylopsila sp. 1** (Fig 26E)

MATERIAL. QMF51943-QMF51946; QML1284; QML1284a; QML1384U; QML1385.

*Dactylopsila* sp. 1 is 10-12% smaller than the species of *Dactylopsila* available for study, *Dactylopsila trivirigata* and *Dactylopsila palpator*. The fossil species also differs from *D. trivirigata* and *D. palpator* by possessing less rounded and more gracile lower molars, a more buccal placement of the protoconid on  $M_1$  and a



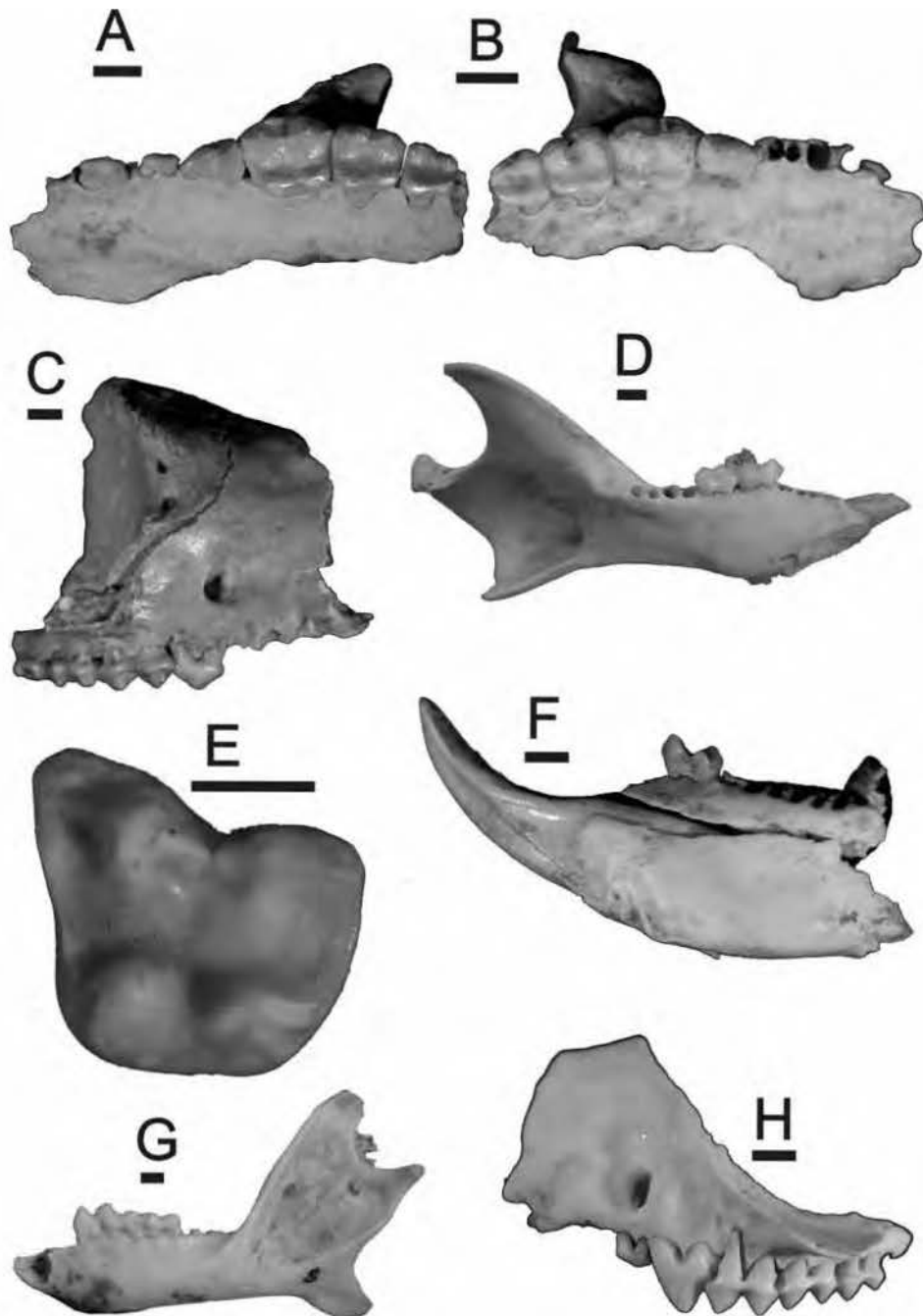


FIG 26. A-F, Petauridae, A-D, Gen. et sp. nov.; A, QMF51949, LP<sup>1</sup>-M<sup>3</sup>. B, QMF51950, RP<sup>3</sup>-M<sup>3</sup>. C, QMF54951, partial skull. D, QMF54952, left mandible (M<sub>1,2</sub>). E, *Dactylopsila* sp. 1; QMF51947, LM<sup>1</sup>. F, *Dactylopsila* sp. 2; QMF51948, RI<sub>1</sub> & M<sub>1</sub>. G-H, Burramyidae; *Cercartetus* sp.; G, QMF51984, LP<sub>3</sub>-M<sub>2</sub>. H, QMF51985, LP<sup>2</sup>-M<sup>3</sup>. Scale bar = 1mm.

less distinct postprotocristid. When compared to the extinct *D. kambuayai* the fossil is approximately 20% larger, however, it does possess a similar gracile profile of the  $M_2$ .

***Dactylopsila* sp. 2**  
(Fig. 26F)

MATERIAL. QMF51947-51948; QML1284.

A second, smaller species of *Dactylopsila* is represented by a fragmentary left mandible with  $I_1$  and  $M_1$ . The  $I_1$  is large and recurved, procumbent.  $M_1$  gracile in occlusal profile, rectangular ovoid with conids without bulbous exterior margins. Protoconid mesially produced. Masseteric fossa inserts below  $M_{2-3}$ . Very small alveoli for  $P_{2-3}$ .

When compared to *D. trivirigata* and *D. palpator*, *Dactylopsila* sp. 2 differs by being much smaller, a less recurved  $I_1$ , possessing a more gracile and unbuttressed hypoconid, and a more mesially oriented protoconid on  $M_1$ . *Dactylopsila* sp. 2 is similar in size and  $I_1$  morphology to *D. kambuayai*, however, there are no specimens of  $M_2$  available for direct comparison.

Gen. et sp. nov. 1 & 2  
(Fig. 26A-F)

MATERIAL. Sp 1: QMF51949-51969; QML1284, QML1284a, QML1313, QML1312, QML1385, QML1384U; QML1384L; QML1420, QML1311.

MATERIAL. Sp 2: QMF51970-51973; QML1284, QML1284a.

Two species of a new medium-sized petauroid are characterised by a dentition that possesses a combination of both plesiomorphic features found in Oligo-Miocene petauroid *Djaluganji yadjana* (Brammal, 1998), and the derived characteristics seen in modern *Petaurus*. The upper molar row is distinctly straight, not possessing the upward inflexion toward the posterior as seen in all modern petaurids. The presence of a distinct stylar basin in  $M^1$  and  $M^2$  distinguish this taxon from both the modern and described Oligo-Miocene petaurids. The reduction of the premolars and molar gradient is shared with *Petaurus* and *Gymnobelidius*, but not to the extent seen in these taxa. Two distinct species are present from the sites and can be distinguished from each other (and the Hamilton Fauna petaurids) on the state of the metaconule, postprotocristae, premetaconule cristae and stylar basin. The greater number of features shared with *Petaurus* and *Gymnobelidius*

warrant its placement in the Petauridae at the present time.

Family BURRAMYIDAE (Broom, 1898)

Burramyids were identified on the basis of their small-sized, square molars with reduced stylar shelf and distinctly high paracone and metacone. They were differentiated from acrobatids by possessing reduced  $P_1$  and  $P_2$  and the presence of  $M_4$ . Burramyid specimens comprise the majority of the very small possums collected from the possum-rich localities of the present study. A conspicuous absence from the burramyid fauna is *Burramys*, with all of the specimens being placed within *Cercartetus*.

***Cercartetus* Gloger, 1841**

***Cercartetus* sp.**  
(Fig. 26G-H)

MATERIAL. QMF51984-52002; QML1284, QML1284a, QML1385, QML1311(H), QML1313.

Several nearly complete mandibles, well preserved maxillae, dozens of isolated molars and premolars represent *Cercartetus*. These specimens have been placed within *Cercartetus* based on their size and the absence of the distinctly plagiaulacoid  $P^3/P_3$ , which is distinct in the only other burramyid, *Burramys*. On comparison with the four known species of *Cercartetus*, the fossil specimens differ least from *Cercartetus caudatus* by being very close in size, retaining  $M_4$  and possessing a  $P^3$  with a single conical cusp. The specimens differ from all other species of *Cercartetus* by possessing an  $M_4$ . *Cercartetus* sp. differs from *Cercartetus caudatus* by possessing a larger and double rooted  $P^1$  and  $P^2$ , a larger  $C^1$  root and a shorter diastema between  $C^1$  and  $P^1$ . Additionally, it differs from all extant species of *Cercartetus* by only possessing two individual roots between  $I_1$  and  $P_3$ , instead of three. The homology of the missing root is unknown. With further analysis, *Cercartetus* sp. probably represents a new extinct species closely related to *Cercartetus caudatus*.

SUPERFAMILY INCERTAE SEDIS

Gen et sp. nov.  
(Fig. 27B-C)

MATERIAL. QMF51974-51981; QML1284, QML1284a, QML1311(H), QML1385.

A medium-sized possum, similar in size to *Petaurus*, represents a new taxon of uncertain affinities. The closest morphologies to this taxon can be found within both the Acrobatidae and the

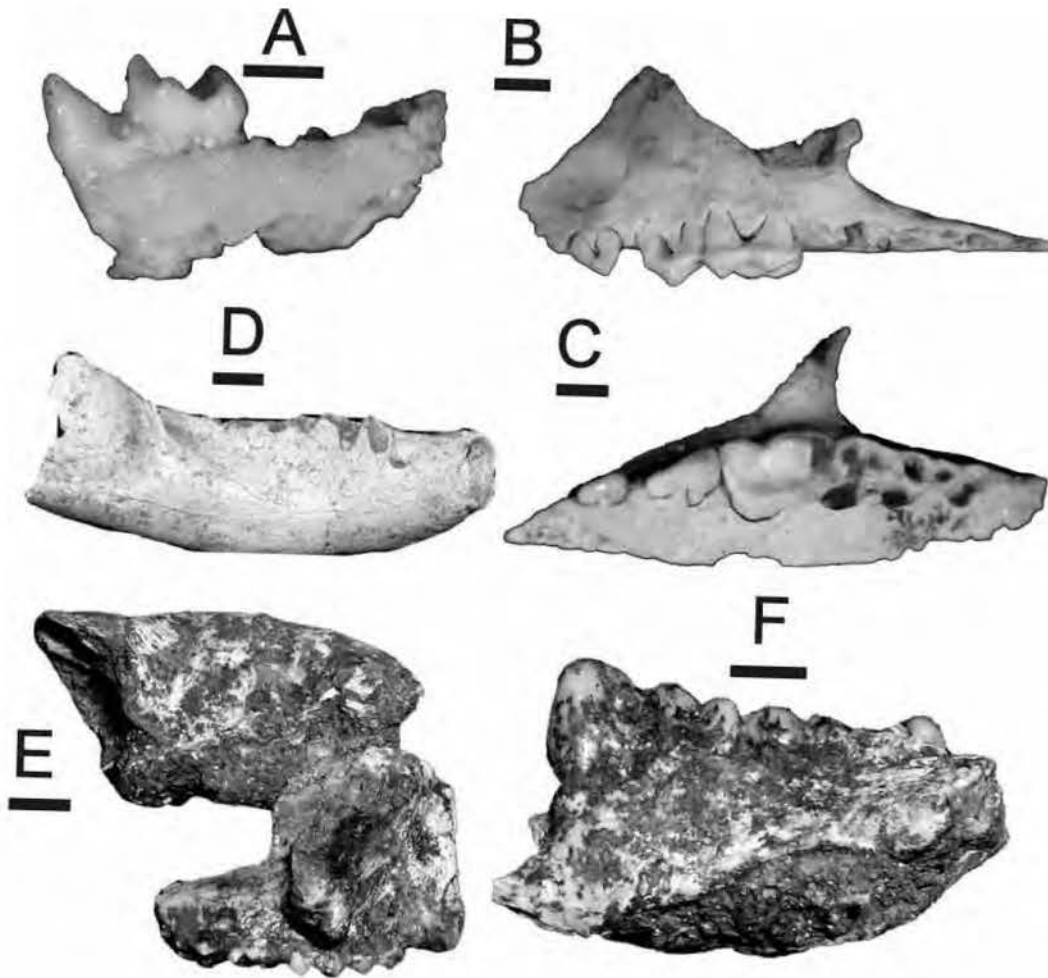


FIG 27. A, Acrobatidae; *Acrobates* sp.; QMF51982,  $RP_3$ - $M_1$ . Scale bar = 1mm. B-C, Superfamily incertae sedis; QMF51974 in buccal & occlusal view. Scale bar = 1mm. D-F, Phalangeridae; D, *Trichosurus* sp. 1; QMF52009, right mandible. E, *Trichosurus* sp. 2; QMF52012, partial skull. F, *Strigocuscus* sp.; QMF52003,  $LP_3$ - $M_3$ . Scale bar = 5mm.

Burramyidae, where features they share include: 1. Enlarged paracones and metacones on  $M^{1-4}$ . 2. Very reduced styler margin. 3. Distinct molar size gradient from  $M^{1-4}$ . 4. Double-rooted  $P^{2-3}$ . The taxon differs from the majority of these taxa by features that are considered plesiomorphic within the two families (Archer, 1984), including: 1. Presence of  $M^4$  (*Burramys parvus* and *Cercartetus caudatus*). 2. Subequal metaconule with protocone. 3. Double-rooted  $P^2$ .

The taxonomic placement within either of these families would require further material and a review of pygmy-possum higher taxonomy, which is under considerable confusion at present (Archer, 1984; Strahan, 1998).

#### Family ACROBATIDAE Aplin, 1987

Acrobatids are easily distinguished and are here represented by the very small-sized *Acrobates*. The fossil specimens have been



identified as acrobatid based on the large sized premolars and the premolariform shape to the  $M_1$  trigonid (Archer, 1984).

**Acrobates** Desmarest, 1818

**Acrobates** sp.  
(Fig. 27A)

MATERIAL. QMF51982- QMF51983; QML1385, QML1284.

*Acrobates* sp. has been identified based on its diminutive size and the presence of a large  $P_3$ , which distinguishes it from the only other member of the Acrobatidae, the New Guinea genus *Distoechurus*. On comparison with *Acrobates*, the specimens are very similar in size and overall morphology. There is only a slight difference in the posterobuccal morphology of the  $P_3$ . The variation of this feature is unknown, therefore, the identification will remain conservative.

Family PHALANGERIDAE Thomas, 1888

Phalangerids have been found in most localities and either represent rainforest phalangerids or the more sclerophyl woodland species of *Trichosurus*. There is considerable difficulty when identifying phalangerids from partial jaws and isolated teeth because the best diagnostic features seem to be from the periotic (Crosby, pers.com.) and basicranial region (Flannery et al., 1987). Morphological conservatism obvious in fossil phalangerid taxa, including the Miocene *Strigocuscus reidi* and Early Pliocene *Strigocuscus notialis*, makes identification of this material particularly difficult. However, using features defined by Flannery et al. (1987) it is possible to refine the identification of phalangerids to generic level.

**Strigocuscus** Gray, 1862

**Strigocuscus** sp.  
(Fig. 27F)

MATERIAL. QMF52003-QMF52008, QMF52071; QML1284, QML1284a, QML1384U, QML1385, QML1384L.

*Strigocuscus* sp. is represented by two partial right mandibles, a partial left mandible and several isolated premolars and molars. The specimens are placed within *Strigocuscus* based on the presence of the following features: 1.  $P_3$  at an oblique angle to the molar row. 2.  $P_3$  has more than four cuspules. 3.  $P_3$  hypertrophic. 4.  $P_3$  highest anteriorly. 5. Molars without complex crenulations. 6. Preprotocrista contacts parastyle

on  $M^1$ . The fossils share their greatest similarity with *S. gymnotis* and *S. notialis*, which includes a distinctly large, antero-buccally oriented  $P_3$  and a single-rooted  $P_2$ . The specimens differ from *S. gymnotis* by being only slightly larger, possessing more cuspules on  $P_3$  and having a distinct contact of the preprotocrista to parastyle. [Note: AMR22155, *S. gymnotis* from Parkop Village PNG does possess an  $M^2$  with a preprotocrista contacting the parastyle albeit not as distinct as the fossil]. *S. reidi* Flannery & Archer, 1987 from the Miocene and *S. notialis* Flannery et al., 1987 from the Early Pliocene are phenetically very similar to *S. gymnotis*, however both possess distinct preparacristae contacting the parastylar corner of  $M^1$ . Additionally *S. reidi* is larger than *S. gymnotis* and *S. notialis* is smaller. On balance, *Strigocuscus* sp. shares most features with *S. notialis*, except for being larger.

**Trichosurus** Lesson, 1828

**Trichosurus** sp. 1  
(Fig. 27D)

MATERIAL. QMF52009-QMF52011; QML1312, QML1314, QML1420.

*Trichosurus* sp. 1 is represented by an edentulous right and a partial left mandible, two left partial maxillae, isolated molars and premolars. *Trichosurus* sp. 1 has been identified based on the following combined features: 1.  $P_2$  absent. 2.  $P_3$ , rectangular-shaped in lateral profile (as high anteriorly as posteriorly). 3. Gracile mandible in lateral profile.

Archer (1978) could not adequately differentiate modern species of *Trichosurus* based on molar morphology and size, this mainly being due to the extreme variation seen in the cosmopolitan *T. vulpecula*. One feature of note, present in both fossil mandibles, is a large cavity situated above the posterodorsal margin of the mandibular symphysis, which penetrates the lower incisor alveolus. This feature has not been seen in any phalangerid examined for this study yet the feature is present in both mandibles referred to *Trichosurus* sp. 1. Also, both jaws are from different faunas, being split by almost 100km. The association of the cavity with the incisor root suggests that this may be a pathology, which affected a large population of *Trichosurus* in central eastern Queensland.

**Trichosurus** sp. 2  
(Fig. 27E)

MATERIAL. QMF52012, QMF52070; QML1311(H), QML1384L.

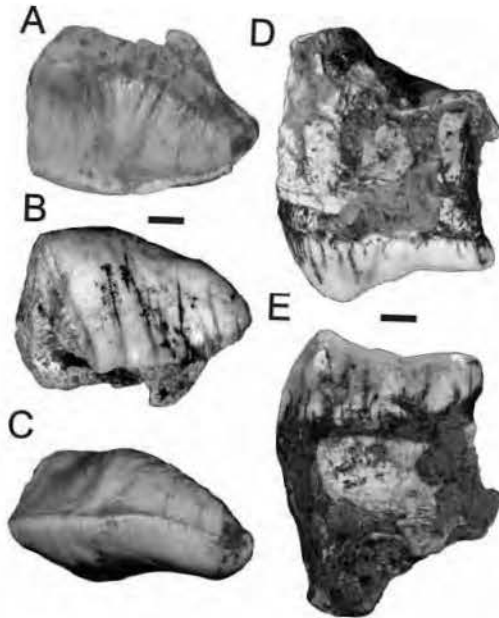


FIG 28. A-E, Thylacoleonidae; A-C, *Thylacoleo* sp.; QMF52069, RP<sup>3</sup> in lingual, buccal & occlusal views. D-E, *Thylacoleo hilli*; QMF52013, RP<sup>3</sup> in buccal & lingual views. Scale bar = 5mm.

A second, small species of *Trichosurus* is known from a single left mandible fragment preserving P<sub>3</sub> and M<sub>1</sub> and a portion of skull with right maxilla (P<sup>3</sup>-M<sup>4</sup>). The specimen is placed within *Trichosurus* based on: 1. A rectangular P<sub>3</sub> in lateral profile. 2. M<sub>1</sub> with distinct metaconid, positioned posterolingually to protoconid. 3. Reduced P<sub>3</sub> cuspules. 4. P<sub>3</sub> smaller than M<sub>1</sub>. 5. Preprotocristid crest to paraconid. When compared to *T. vulpecula* and *T. caninus*, the fossil species is markedly smaller with a relatively larger M<sub>1</sub> to P<sub>3</sub>. *Trichosurus* sp. 2 differs from the Early Pliocene *T. hamiltonensis* by possessing a smaller P<sub>3</sub> relative to M<sub>1</sub> and by being smaller in overall size. *Trichosurus* sp. is closest in morphology and size to *T. dicksoni* from the Miocene of Riversleigh. Because direct comparison to all trichosurin phalangerids, such as *T. arnhemensis*, was not possible a specific assignment will be left for a later analysis.

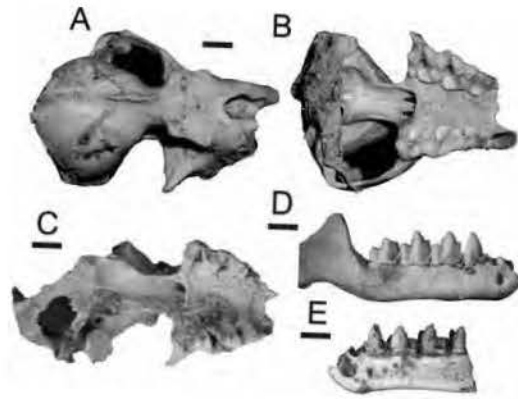


FIG 29. A-E, Megadermatidae; *Macroderma gigas*; A-B, QMF48021, partial skull in dorsal & ventral views. C, QMF48022, partial skull. D, QMF48006, RP<sub>3</sub>-M<sub>3</sub>. E, QMF48591, LP<sub>4</sub>-M<sub>3</sub>. Scale bar = 5mm.

#### Family THYLACOLEONIDAE Gill, 1872

##### *Thylacoleo* Gervais, 1852

##### *Thylacoleo* sp. (Fig. 28A-C)

MATERIAL. QMF1338, QMF52069; QML1420, QML1384L.

An isolated P<sub>3</sub> (QMF1338) and P<sup>3</sup> (QMF52069) represent the distinctive marsupial carnivore, *Thylacoleo*. Comparison of the premolars with *Thylacoleo carnifex* and *T. crassidentatus* does not resolve its taxonomic position, because the posterior portions of both premolars are broken, thus a full morphometric analysis was not possible. Interestingly, both specimens show very little wear.

##### *Thylacoleo hilli* Pledge, 1977 (Fig. 28D-E)

MATERIAL. QMF52013; QML1311(H).

A single left P<sup>3</sup> represents the smallest known species of *Thylacoleo*, *Thylacoleo hilli*. Identification of small thylacoleonid P<sub>3</sub>'s has been subject to speculation that they may be deciduous premolars of larger species (Pledge, 1977; Archer, 1984; Archer & Dawson, 1982b). Archer & Dawson (1982) suggest that *Thylacoleo* probably did not have a significant deciduous premolar since no thylacoleonid material so far found preserves a dP<sup>3</sup>. The lack of a molariform premolar, resorption pits for the

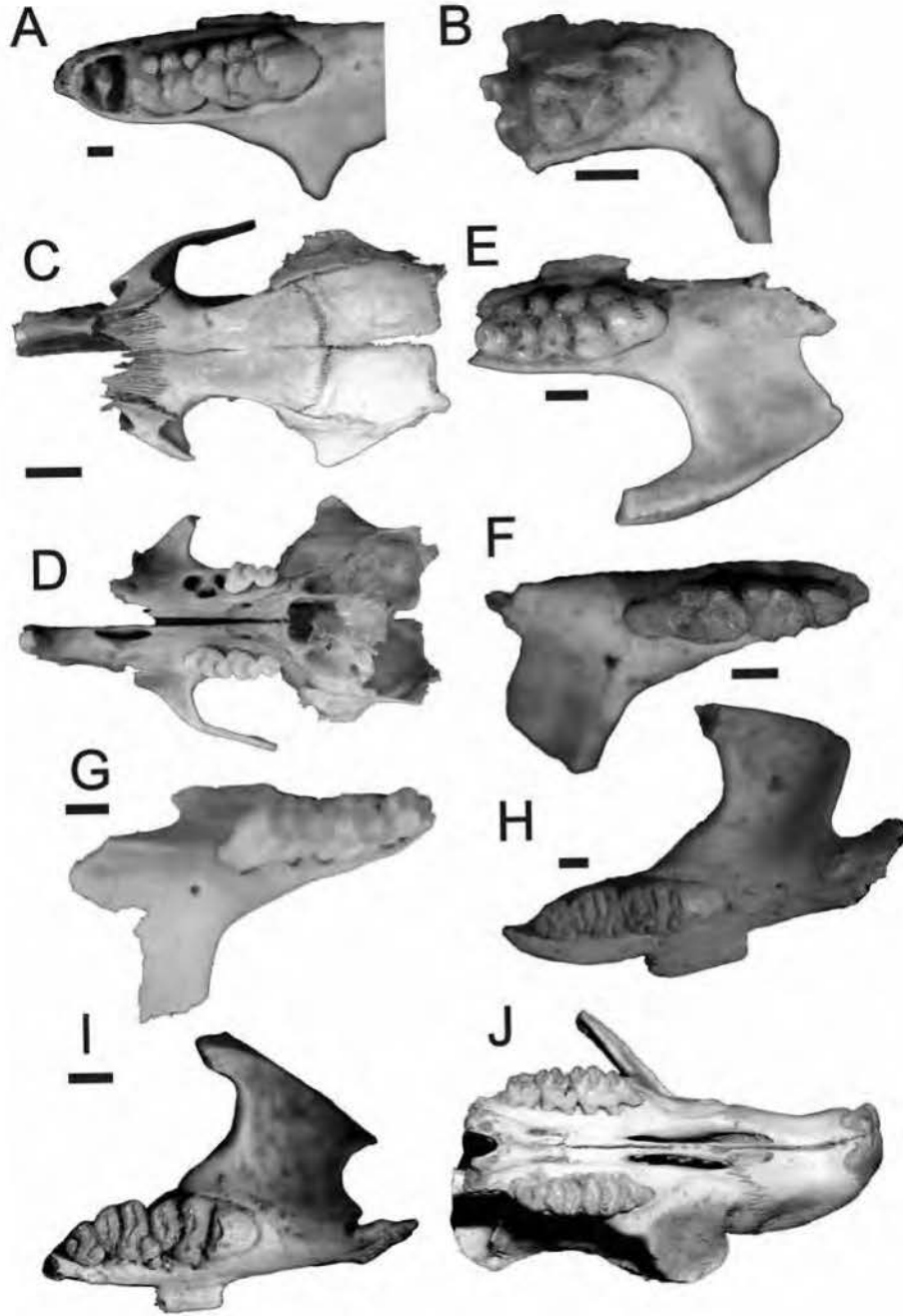


FIG 30. A-I, Muridae; A, *Conilurus* sp.; QMF52052, LM<sup>1-2</sup>. B, *Leggadina* sp.; QMF52040, LM<sup>1</sup>. Scale bar = 1mm. C-D, *Uromys/Melomys* sp.; QMF52014, skull in dorsal & ventral views. Scale bar = 5mm. E-F, *Pseudomys* spp.; E, QMF52043, LM<sup>1-2</sup>. F, QMF52044, RM<sup>1-3</sup>. G, *Pogonomys* sp.; QMF52022, RM<sup>1-3</sup>. H, *Zyzomys* sp.; QMF52053, RM<sup>1-3</sup>. Scale bar = 1mm. I, *Notomys* sp.; QMF52036, RM<sup>1-3</sup>. J, *Rattus* sp.; QMF52033, partial skull. Scale bar = 5mm.

premolar roots and the presence of a relatively well used wear facet along the longitudinal shearing blade of the fossil premolar indicate that this specimen was from an adult. Comparison to obvious juvenile *T. carnifex* from Naracoorte Caves, shows that *Thylacoleo* did not have any deciduous dentition (pers. obs.). The specimen is therefore assigned to the Late Miocene to Pliocene *T. hilli* based on its diminutive size (24.4mm in *T. hilli* (Pledge, 1977) and 22.23mm for QMF52013), simplified posterior margin of the premolar and overall similarity to the holotype described by Pledge (1977).

### BIOCHRONOLOGY

In order to develop a faunal chronology of the sites, each site needed to be grouped based on their faunal similarity and these groups placed in geochronological order. Presence/absence data was used to produce a dendrogram of similarity for sites using small-sized mammalian taxa (excluding bats) represented at each site (Appendix 1; Fig. 31). The analysis grouped sites with progressively dissimilar faunas from those of the present day. Fig. 31 shows the relationship of sites based on small-sized mammal fauna.

Olsen's Cave fauna shares the greatest similarity with the present day fauna. Five faunas fall successively further away from the Olsen's Cave fauna, first QML1312, then QML1420, QML1384U, QML1384L and QML1311C/D. A

final group of five faunas (QML1284, 1284a, 1385, 1313 and 1311H) remain unresolved (polytomy) by the analysis and are considered to possess, equally, the least number of taxa shared with the present day.

When compared to the available site geochronologies, the faunal dendrogram correlates well with the sites from the Elephant Holes Cave System but not as well with the sites from the Speaking Tube Cave System. Geochronologically, the Elephant Hole Cave System sites range from the oldest (QML1385) through QML1384L and QML1384U to the youngest (QML1312). The faunal dendrogram correlates with the geochronology, by QML1312 sharing the most taxa with the present day and QML1385 the least. Within the Speaking Tube Cave System, QML1311(H) and QML1311(C/D) are considered to be geochronologically contemporaneous, with QML1313 possibly being younger. The faunal dendrogram does not provide any further resolution to these sites, all of which share similarly few taxa with the present day.

### ASSEMBLAGE AGE

A complete absence from the sites of mammalian taxa known from the Oligocene-Miocene (possible exceptions being *Thylacoleo hilli* and *Trichosurus* sp. 2) confines biocorrelation to sites of post Late Miocene age. Radiometrically-dated and biocorrelated vertebrate faunas from the Pliocene were used to hypothesise the age of the oldest of the sites at Mount Etna and Limestone Ridge. Table 4 presents a summary of the taxa shared between the Mount Etna and Limestone Ridge sites and other Pliocene vertebrate communities throughout eastern Australia. Two sites possessed mixed faunas of Pliocene and Pleistocene taxa. These two sites were simply classified as Plio-Pleistocene, being younger than the biocorrelated Early Pliocene sites and older than the dated late Pleistocene, QML1312. Table 5 summarises the hypothesised ages for each site yielding fauna identified herein.

**Early Pliocene.** The most dissimilar assemblages to those of the present day fauna possess several taxa confined to the Pliocene in other parts of Australia. These taxa include, *Thylacoleo hilli*, *Kurrabi* sp., *Protemnodon* sp. cf. *P. devisi* and the new perameloids. Of these taxa, *Thylacoleo hilli* and *Kurrabi* sp. are confined elsewhere in Australia to the Early

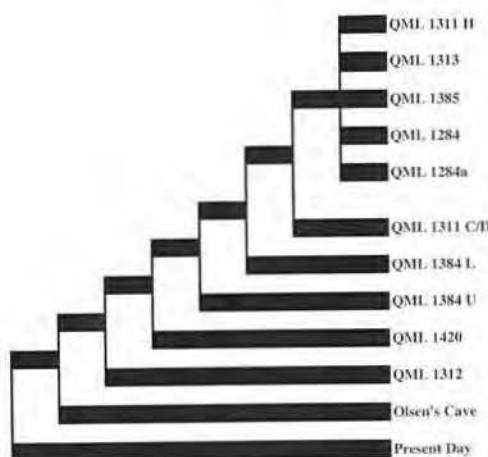


FIG 31. Dendrogram illustrating faunal similarity derived from small-sized mammal species from sites presented herein. Present day small-sized mammal fauna placed as the outgroup.



Pliocene (Pledge, 1977; Flannery & Archer, 1984; Flannery et al., 1992). Several undescribed taxa presented here share their closest morphological similarities with taxa only known from the Early Pliocene. These taxa include, *Strigoscus* sp. close to *Strigoscus notialis* (Hamilton LF); *Trichosurus* sp. 2 close to *Trichosurus hamiltonensis* (Hamilton LF); *Petauroides* spp. close to *Petauroides stirtoni* (Hamilton LF; Big Sink LF); *Pseudochirulus* sp. 1 close to *Pseudocheirus marshalli* (Hamilton LF); *Pseudokoala* sp. close to *P. erlita* (Hamilton LF); and *Kurrabi* sp. close to *K. merriwaensis* (Bow LF; Big Sink LF).

Noticeable occurrences of believed Pleistocene-aged taxa are also present in these assemblages, including *Macropus agilis siva* and *Sarcophilus lanianus*. There is uncertainty surrounding the identification of *Macropus agilis siva* in the fauna, therefore it may be incorrectly identified. *Sarcophilus lanianus* is positively identified here and is considered to be the earliest age for this taxon, rather than a younger age of the fauna. The previously oldest record of *Sarcophilus* is from the early Pleistocene of Nelson Bay (Gerdtz & Archbold, 2003) although Tedford (1994) has identified possible *Sarcophilus* from Parwan (Early Pliocene). Gerdtz & Archbold (2003) record the presence of *Sarcophilus harrisii* and *Sarcophilus moornaensis* during the early Pleistocene of Victoria, indicating a pre-Pleistocene origin of *Sarcophilus* and supporting the presence of *Sarcophilus* in the Pliocene of Australia.

Overall, the majority of biocorrelatable taxa indicate an Early Pliocene age for the following sites: QML1284, QML1284a, QML1384L, QML1311 C/D, QML1311 H, QML1313 and QML1385.

**Plio-Pleistocene.** Two sites, QML1384U and QML1420 are considered to be dated sometime between the Late Pliocene and middle Pleistocene. Both sites possess similar small mammal faunas, with QML1384U sharing a similar large portion of its small mammal fauna with the Early Pliocene sites. Unfortunately QML1384U is yet to yield megafauna, however, it is considered to be faunally intermediate between the Early Pliocene assemblage and QML1420. QML1420 fauna lacks the restricted Early Pliocene taxa and possesses Plio-Pleistocene and Pleistocene species, including; *Palorchestes* cf. *P. parvus*, *Macropus titan*, *Macropus agilis siva*, and *Megalanina*

*prisca*. Additionally, QML1420 is considered to be pre-late Pleistocene in age based on its intermediate small mammal fauna between the Pliocene-aged assemblages and the dated late Pleistocene QML1312 fauna.

**Late Pleistocene.** QML1312 has been TIMS U-series dated using *Petrogale* dentition, providing a minimum age of 149,000  $\pm$  611 ybp. Faunally, QML1312 is intermediate between QML1420 and Olsen's Cave. The only distinctly Pleistocene taxon within the deposit is *Sarcophilus lanianus*. There are some elements of the fauna that show a lingering relationship to the older faunas, namely *Dendrolagus*, new genus of petauroid and *Thylacinus cynocephalus*.

**Holocene.** Olsen's Cave and QML1314 are considered to be post-late Pleistocene and probably Holocene in age based on the complete lack of megafauna (even though QML1314 site does collect large-sized macropodines) and the exclusive presence of extant taxa. Olsen's Cave fauna possesses the most similar small mammal fauna to the present day and the accumulation is subfossil in preservation.

#### FAUNAL SUCCESSION

To adequately reconstruct the faunal and palaeoecological succession from Early Pliocene through to the present day taphonomic processes must be considered and the maximum available source area of fauna must be estimated for each fossil site. This may be predicted by examining the gross taphonomic processes dominating the deposition of each faunal assemblage.

Two predominantly allochthonous accumulation modes are identified as accounting for all of the sites; these being pit-trap and/or predator accumulations. Thus, all large-sized fauna, which would have been too large for owls and Ghost Bats to dispatch, would have been derived from the immediate vicinity of the cave/fissure entrance. There is no indication for denning of large marsupicarnivores or major fluvial deposition as evidenced by the lack of gnaw marks on long bones and fluvially transported sediments. Smaller vertebrates would have been collected from the vicinity of the cave entrances as either allochthonous or autochthonous (cave dwelling) assemblages. Additionally, small vertebrates would have also been collected within the hunting ranges of both the Ghost Bat and owl, the only known cave-dwelling predators within the deposits.

	Mount Etna LF	Bluff Downs LF	Rackham's Roost LF	Chinchilla LF	Big Sink LF	Bow LF	Kanunka LF	Town Well Cave	Hamilton LF
MYA	QLD Early Pliocene	QLD 3.8	QLD Early Pliocene 3-5	QLD late Early Pliocene 3.4	NSW Early Pliocene 3-5	NSW Early Pliocene 3-5	SA Late Pliocene 3.4	Mio-Pliocene	VIC Early Pliocene 4.46
<i>Thylacinus</i>	<i>cynocephalus</i>			<i>cynocephalus</i>	sp.				sp.
<i>Antechinus</i>	spp.				sp.				
<i>Smynthopsis</i>	<i>murina</i>		sp.		spp.				
<i>Dasyurus</i>	sp.	<i>dunmalli</i>		<i>dunmalli</i>		<i>dunmalli</i>			
<i>Perameloid</i>	gen. nov.				gen. nov.	gen. nov.			cf. <i>Peroryctes tedfordi</i>
<i>Perameles</i>	sp. 1 & sp. 2			<i>bowensis</i>		<i>bowensis</i>			
		<i>allinghamensis</i>				<i>allinghamensis</i>			
<i>Thylacoleo</i>	sp.	<i>crassidentatus</i>		<i>crassidentatus</i>		<i>crassidentatus</i>			
<i>Thylacoleo</i>	<i>hilli</i>					<i>hilli</i>		<i>hilli</i>	
<i>Protomiodon</i>	cf. <i>devisi</i>	<i>snewini</i>	cf. <i>snewini</i>	<i>devisi</i>	<i>devisi</i>	<i>chinchillaensis</i>	cf. <i>devisi</i>		sp.
<i>Kurrabi</i>	sp.			cf. <i>merriwaensis</i>	cf. <i>merriwaensis</i>	<i>merriwaensis</i>	sp.		<i>plechenorum</i>
<i>Bobra</i>	sp.			<i>wilkinsonorum</i>					
<i>Dendrolagus</i>	sp.					sp.	sp.		sp.
<i>Macropus</i>	sp.					spp.	spp.		sp.
<i>Thylagale</i>	spp.								<i>ignis</i>
<i>Palorchestes</i>	cf. <i>parvus</i>	<i>selestiae</i>		<i>parvus</i>		cf. <i>parvus</i>			sp. nov.
Vombatidae	<i>Vombatus</i>	<i>Ramsayia</i>		? <i>Vombatus</i>		<i>Phascolumus</i>	<i>Vombatus</i>		gen. indet.
<i>Srigocuscus</i>	sp.								<i>notialis</i>
<i>Trichosurus</i>	sp. 2								<i>hamiltonensis</i>
Burramyidae	<i>Cercartetus</i>				<i>Cercartetus</i>				<i>Burramys</i>
<i>Pseudokooda</i>	sp.								<i>erlita</i>
<i>Pseudocheirus</i>	spp.								<i>marshalli</i>
<i>Petauroides</i>	spp.				cf. <i>stirtoni</i>				<i>stirtoni</i>
<i>Pseudocheirops</i>	spp.	<i>winteri</i>							
Petauridae	gen. nov.								<i>Petaurus</i>
<i>Macroderma</i>	<i>gigas</i>		<i>gigas</i>		<i>koppa</i>				

TABLE 4. Biocorrelations of taxa in the hypothesised Early Pliocene Mount Etna Local Fauna.

Owls have hunting ranges of up to 10km<sup>2</sup> (Lindsey, 1992) and *Macroderma gigas* ranges over an area of 2km<sup>2</sup> (Toop, 1985; Nelson, 1989). Thus owls would have had the potential to collect vertebrates from both the limestone bluff and the surrounding lowlands. The present day range of an owl at Mount Etna would encompass both closed vegetation typical of limestone bluffs out into lowland open vegetation. Small creeks are present within the owl's range and thus provide a third possible hunting habitat along riverine areas. Ghost Bat foraging areas would be considerably smaller and source the majority of its prey from the immediate vicinity of the feeding roost.

Owls are not considered to be an active accumulator at Marmor Quarry and Ghost Bats are considered to have had little input into the small vertebrate accumulation, therefore, Marmor Quarry is considered to have collected most of its fauna from the immediate vicinity of the pit-trap entrance.

Where possible, fossil sites were equally sampled to remove any potential collecting bias at each of the sites. Only presence/absence data are used for faunal and palaeoecological successions, with no analysis of relative abundance, which would be most affected by sample size. Collections from QML1312 are restricted due to the site's destruction prior to the expeditions in 2000.

On balance, the majority of faunas described here are considered to have been representative of the ecologies in direct vicinity of the cave entrances for both Mt Etna and Marmor Quarry.

*Anurans.* Greatest diversity of frogs occurs in the Early Pliocene sites from Mount Etna and Limestone Ridge. Of the 22 frog taxa identified here, 20 are found in the Early Pliocene sites. *Cyclorana* is restricted to the Holocene Olsen's Cave fauna and is not present in any of the older sites. New fossil frog records for Australia include the Early Pliocene species of *Nyctimystes*, *Etnabatrachus maximus* and microhylids. New frog records for the Early Pliocene include species of *Crinia*, *Kyarannus*, *Lechriodus*, *Limnodynastes* and *Litoria*. The majority of the species present in the Early Pliocene are locally extinct by the late Pleistocene, leaving only a single species of *Limnodynastes*. Species of *Litoria* and *Cyclorana* occur in the Holocene assemblages. The present day frog fauna includes at least, *Cyclorana*, *Litoria*, *Limnodynastes* and

TABLE 5. Summarised ages for The Caves & Marmor fossil sites.

Holocene	Olsen's Cave QML1314
Late Pleistocene	QML1312
Plio-Pleistocene	QML1420 QML1384U
Early Pliocene	QML1313 QML1384L QML1311C/D QML1311H QML1284 QML1284a QML1385

*Pseudophryne*. The retention of *Litoria* and *Limnodynastes* into the present day fauna is not surprising as these genera are cosmopolitan in their distribution and habitat preferences.

Occurrence of *Neobatrachus* in the Early Pliocene is peculiar, representing a burrowing frog with a present day distribution restricted to arid areas. *Neobatrachus* has been recorded from the Pliocene of South Australia (Tyler, 1988; Tyler, 1994) in a palaeoecology that was wetter than today. Its presence within a predominantly rainforest frog fauna may be explained in a similar way as to the presence of the marsupial mole family, Notoryctidae, which occurs in a predominantly rainforest mammal fauna in the Oligo-Miocene of Riversleigh, yet it is confined to the arid zone of Australia today (Long et al., 2002). Adaptation for burrowing in soft rainforest soils may have allowed notoryctids to be pre-adapted to a later arid environment with soft sands. Similarly, it may be conceived that a burrowing frog that originated in rainforest would then be pre-adapted to life in the arid zone.

*Chelids.* Turtle fossils are restricted to the Early Pliocene localities and are a rare component of the assemblages. Freshwater turtles occur throughout the region today and are almost never encountered on the limestone karst. Turtle fossils would become absent from the record as karstification developed inhospitable ground for turtles to traverse.

*Crocodylians.* Crocodile specimens are generally restricted to the Early Pliocene sites and are rare. A single specimen is known from QML368 which has yet to yield a contemporaneous large-sized fauna that can be biocorrelated, however, the small-mammal fauna suggests a Pleistocene age.

*Squamates*. Agamids (Dragons) are rare, but have been found in all deposits from the Early Pliocene through to the present. Early Pliocene agamid remains are mostly unidentifiable, however, a single specimen is referable to a species of *Hypsilurus*. Diversity of agamids is greatest in the late Pleistocene with species of *Amphibolurus*, *Pogona* (small-morph) and *Tympanocryptis* present. *Diporiphora* replaces these in the Holocene. The present agamid fauna includes, *Diporiphora*, *Chlamydosaurus* and *Pogona barbata* (large-morph).

Gekkonids (Geckoes) have been found throughout the Pliocene to present, except in QML1420. Absence of gekkonids from QML1420 is considered an artefact of small collection size and the absence of a distinct predator accumulation. The large gekkonid form is present in the Early Pliocene sites but missing in the late Pliocene to present day. Due to their general rareness within the Early Pliocene sites, it is uncertain whether the absence of the large gekkonid from younger sites is a taphonomic bias or a Plio-Pleistocene extinction. The small gekkonid forms are present throughout the Pliocene to the present, however, they probably constitute several distinct taxa.

Large scincids (Skinks) are conspicuous in the Early Pliocene deposits. *Tiliqua* is known from the Early Pliocene and Holocene, but does not occur in the Late Pliocene-Pleistocene or late Pleistocene faunas. Species of *Tiliqua* are rare within any assemblage, represented by single specimens. Its absence from sites cannot be determined as either ecological or taphonomic. *Cyclodomorphus gerrardii* is the most common large skink and is found from the Early Pliocene to the present day, with the exception of site QML1312. The absence of *Cyclodomorphus* from QML1312 is not considered to be due to taphonomic bias because abundant remains of other large-sized skinks are present in this fauna. Instead, *Cyclodomorphus* is considered to have become locally extinct due to late Pleistocene aridity. By the present day, *Cyclodomorphus* had dispersed back into the Mt. Etna region. *Egernia* sp. is present throughout the Early Pliocene to Holocene. Large skinks found at Mount Etna today include *Tiliqua scincoides* and *Cyclodomorphus gerrardii*.

Varanids (Goannas & Monitors) are found from the Early Pliocene to the present day, with the exception of the Holocene faunal assemblage. This absence at Olsen's Cave is considered to be a taphonomic bias against large squamates (as with

large mammals) because the deposit is derived from an owl roost. Two varanids are present in the Early Pliocene, one the size of modern *Varanus varius*, the second much more massive but not attaining the size of Pliocene or Pleistocene species of *Megalania*. These two taxa persist into the late Pleistocene, however, are missing from QML1420. Varanids are represented at QML1420 by the giant varanid *Megalania prisca*.

Elapids (Venomous snakes) are found from the Early Pliocene to the present day. Conspicuous size difference can be seen when comparing the largest vertebrae of elapids in the Pliocene-Pleistocene with those from the late Pleistocene. The late Pleistocene elapids are up to twice the size of their Early Pliocene relatives.

Pythonines are found from the Early Pliocene to the present day. Madtsoiids have not been found. Python vertebrae tend to remain large-sized throughout the Pliocene to present day.

Typhlopids (Blind snakes) are only found in the Early Pliocene sites. This is the second record of fossil blind snakes in Australia and the first from the Pliocene. The first record was from the Oligo-Miocene Riversleigh deposits from far north Queensland (Archer et al., 1995b).

Typhlopids are a peculiar fossorial group with a cosmopolitan range today. A nocturnal ant/termite feeder, typhlopids represent a specialised niche within the Early Pliocene faunal assemblage at Mount Etna. The typhlopids seem to represent yet another group of fossorial animals, like the notoryctids (marsupial moles) and leptodactylids (*Neobatrachus*), which have utilised their adaptation for burrowing in ancient rainforests as an adaptive advantage with subsequent increasing aridity.

*Aves*. Four bird groups have been identified, including the quails (Galliformes), button quails (Gruiformes), song birds (Passeriformes) and owls (Strigiformes). The owls are a conspicuous component of all the fossil assemblages except QML1420. Their absence at QML1420 is considered to be due to taphonomic processes. All four groups exist in the area today. The Early Pliocene occurrence of owls is the oldest known in Australia.

*Thylacinidae*. *Thylacinus cynocephalus* is present from the Early Pliocene to late Pleistocene. *Thylacinus cynocephalus* is absent



from the Plio-Pleistocene site QML1384U, which is probably due to the taphonomic bias in that deposit toward smaller-sized mammals. *Thylacinus* is absent by the Holocene.

*Dasyuridae*. *Antechinus* spp. are present from the Early Pliocene through to the present day. During the Early Pliocene, *Antechinus* is represented by two species. By the late Pleistocene, these two species are extinct, having been replaced by *Antechinus flavipes* and *Antechinus swainsoni*. *Dasyurus* spp. are also present from the Early Pliocene through to the present day. During the Pliocene *Dasyurus* is represented by a medium-sized species. This species is replaced by *Dasyurus hallucatus* and *Dasyurus viverrinus* during the late Pleistocene. *Dasyurus hallucatus* and *Dasyurus maculatus* are found in the Holocene and present day fauna respectively. *Phascogale* has a possible appearance in the Early Pliocene with a small undescribed species. This species continues into the Pleistocene, however, it is extinct by the late Pleistocene, having been replaced with *Phascogale topoatafa*. *Planigale maculata* appears in the late Pleistocene and remains in the Holocene and present day fauna. An extinct, undescribed, small planigale-like dasyurid is present in the Pliocene but is extinct by the Pleistocene. Species of *Sarcophilus* are present from the Early Pliocene to late Pleistocene and possibly Holocene. *Sarcophilus lanianus* is known to occur from the Early Pliocene to late Pleistocene. A single specimen of *Sarcophilus harrisii* is present in the late Pleistocene-Holocene from Lower Johansen's Cave (QML1314). Species of *Sminthopsis* occur in the Early Pliocene but are rare within the Pliocene assemblages. During the late Pleistocene *Sminthopsis* represents the most abundant small-sized dasyurid, represented by two species, *Sminthopsis murina* and *Sminthopsis macroura*.

*Vombatidae*. A species of *Vombatus* is represented by three specimens, one in the Early Pliocene and two in the Plio-Pleistocene site QML1420. *Vombatus* is not present in the area by the late Pleistocene.

?*Zygomaturine*. This large-sized diprotodont is only known in the region from the Plio-Pleistocene (QML1420).

*Palorchestidae*. *Palorchestes* sp. cf. *P. parvus* is present in the Early Pliocene and in the Plio-Pleistocene (QML1420).

*Macropodidae*. *Bohra* sp. is only present in the Early Pliocene. Species of *Dendrolagus* are present from the Early Pliocene to late Pleistocene. Species of *Thylogale*, *Petrogale* and *Macropus* are all present from the Early Pliocene to the present day. *Protemnodon* sp. cf. *P. devisi* and *Kurrabi* are only present in the Early Pliocene. *Macropus titan* is restricted to the Plio-Pleistocene of Marmor Quarry and is absent from the late Pleistocene. This is the first record in Australia of *Dendrolagus* in the Pleistocene and the second record of *Bohra* in the Pliocene (Dawson, 2004).

A conspicuous absence from the macropod fauna are the morphologically distinct potoroids, in particular *Potorous* and *Hypsiprymnodon*. Although they may turn up in future collections, the sample sizes at present suggest that this may be unlikely and that this group of macropods was absent from the Early Pliocene of Mt. Etna. Interestingly, the small macropod fauna at Mt. Etna includes several small-sized macropodids, namely *Thylogale* sp. 1, which is very similar to the Irian Jaya *Thylogale christenseni*. Furthermore, there are no potoroids known from the present day or fossil record of Papua New Guinea and Irian Jaya, yet the small macropodid faunas tend to be either species of *Thylogale* or *Dorcopsis*. The disjunct nature of this macropodid fauna, where the Early Pliocene Mt. Etna fauna more closely resembles those from Papua New Guinea and Irian Jaya, is also seen in the Pseudocheiridae.

*Pseudocheiridae*. Pseudocheirids are considerably diverse during the Pliocene but are locally extinct by the late Pleistocene, returning in the Holocene as a rarity and abundant in the present day as a single taxon, *Pseudocheirus peregrinus*.

*Pseudochirulus* spp. are present in the Early Pliocene, including *Pseudochirulus* sp. 1 which is very similar to the Early Pliocene Hamilton Fauna *Pseudochirulus marshalli* and the modern Papua New Guinean *Pseudochirulus canescens* and *Pseudochirulus mayeri*. Similarly, taxa referred to here as *Petauroides* share closer taxonomic affinities with species from both the Early Pliocene Hamilton Fauna and the late Pleistocene Irian Jaya Fauna, than they do to the modern *Petauroides* and *Hemibelideus* from far north Queensland forests and rainforests.

*Petauridae*. The new genus of petaurid is present with two species in the Pliocene and one species in the Plio-Pleistocene and late Pleistocene. It is

extinct by the Holocene. *Dactylopsila* is present in the Pliocene but is locally extinct by the Pleistocene. This is the first post Miocene, and pre Holocene, record of *Dactylopsila* in Australia. *Dactylopsila* sp. 2 is diminutive in size relative to any living species, however, it is very close to the extinct Irian Jayan taxon, *Dactylopsila kambuayai*, which along with the macropodids and pseudocheirids illustrates a possible faunal connection to Papua New Guinea and Irian Jaya during the Early Pliocene.

*Superfamily* incertae sedis. A new genus and species of possum with unknown phylogenetic and taxonomic affinities is present in the Early Pliocene but has yet to turn up in younger sediments.

*Acrobatidae*. *Acrobates* occurs in the Early Pliocene and has not been found in younger sediments. This is the first record of acrobatids in the Pliocene of Australia.

*Burramyidae*. *Cercartetus* occurs in the Pliocene but is not found in younger sediments. The only other Pliocene record of *Cercartetus* is from the Big Sink Fauna (Dawson et al., 1999).

*Phalangeridae*. *Strigocuscus* is present in the Pliocene but is absent by the Pleistocene. *Trichosurus* is represented by two species, the first confined to the Early Pliocene and the second found in the Pleistocene, Holocene and present day.

*Thylacoleonidae*. Two species of *Thylacoleo*, one small and one large species, occur in the Early Pliocene whilst one large species has been found in the Plio-Pleistocene (QML1420). No remains of *Thylacoleo* have yet been found in late Pleistocene deposits.

*Peramelidae*. Species of *Perameles* occur throughout the Pliocene and into the present day. During the Pliocene and Plio-Pleistocene times, *Perameles* was represented by two extinct species. By the late Pleistocene to Holocene, these species were replaced by *Perameles bougainville* and eventually *Perameles nasuta*. *Isodon* occurs in the Plio-Pleistocene to present day. *Isodon* is represented by two small-sized species in the Plio-Pleistocene and late Pleistocene sites, *Isodon obesulus* and *Isodon* sp. During the Holocene, small-sized *Isodon* were replaced with the larger *Isodon macrourus*. During the late Pleistocene both *Chaeropus* and *Macrotis* appeared, leaving no further record.

*Perameloid* incertae sedis. An enigmatic family of bandicoots possibly related to the Oligo-Miocene Yaralidae are restricted to the Pliocene-aged deposits.

*Muridae*. Rodents are a conspicuous element of every deposit. Early Pliocene rodents include the first records of many rainforest taxa with no previous fossil records in Australia. Several taxa are found to dominate the Pliocene sites with possible Plio-Pleistocene records. These include *Melomys/Uromys*, *Pogonomys* and *Mesembriomys*. *Zyomys* is present from the Pliocene to late Pleistocene. *Leggadina* is found in the late Pleistocene to Holocene. *Conilurus* is found in the late Pleistocene. *Rattus* is found from the Plio-Pleistocene to present day. *Pseudomys* is found from the Pliocene to present day. *Notomys* is restricted to the late Pleistocene. *Hydromys* has been recovered from the Early Pliocene, Plio-Pleistocene (QML1420) and present day faunas.

*Microchiropterans*. Bats are found in all deposits, except QML1420. *Macroderma gigas* is found from Early Pliocene to the present day.

## PALAEOECOLOGICAL SUCCESSION

### EARLY PLIOCENE.

*Nonseasonal, Mesothermal, angiosperm-dominant rainforest with emergent gymnosperms; minor grassy understory.*

Rainforest has been indicated both locally by the fauna and regionally through palynological studies of the Early Pliocene. Two pollen cores, Aquarius Well (Fig. 1A,5) (Hekel, 1972) and ODP815 (Fig. 1A,4) (Martin & MacMinn, 1993), located off the central eastern Queensland coast are close to the fossil sites. The Aquarius Well core was taken from the edge of the Capricorn Trough, which is located to the NE of Mount Etna and Marmor Quarry (Fig 1). Hekel (1972) published the palynological record of Aquarius Well, showing a dramatic increase in rainforest flora in the region post Late Miocene and dominating the entire Early Pliocene.

ODP815 drill core (Martin & MacMinn, 1993) from the Marion Plateau to the NE of Mount Etna shows an Early Pliocene dominated by rainforest flora. Macphail (1997) reviewed both the Aquarius Well and ODP815 records and concluded that the dominant vegetation type during the Early Pliocene would have been an angiosperm-dominated mesotherm rainforest with Araucaraceae. Low pollen counts for

rainforest angiosperm taxa were considered to be an artefact of taphonomic bias toward more dispersible taxa, however, no conclusions could be drawn as to how dominant or complex the rainforest angiosperms were. Macphail (1997) suggests that the climate required to support such a vegetation structure would include temperatures greater than 20°C, and an annual precipitation rate of between 1300 and 2000mm.

Fauna recovered from Early Pliocene-aged sites within the local area of Mount Etna and Limestone Ridge support the presence of rainforest at the time, as follows;

*Anurans.* Microhylids are recorded from the Early Pliocene deposits and, although rare, indicate a very moist rainforest environment. *Nyctimystes* is presently known from rainforests of far north Queensland and Papua New Guinea, whilst *Lechriodus* is known from rainforest in southeastern Queensland and Papua New Guinea. *Kyarranus*, although not exclusively rainforest dwelling, is restricted to areas of constant moisture in areas close to or within montane rainforest or wet sclerophyll. Interestingly, the suite of frog genera identified in the Early Pliocene is similar to that recorded from the interpreted rainforest ecologies present during the Oligo-Miocene of Riversleigh (*Litoria*, *Limnodynastes*, *Kyarranus*, *Lechriodus*, and *Crinia*) (Tyler, 1991; Tyler 1994) and to those identified from the montane rainforests of Papua New Guinea (Menzies et al., 2002).

The overall abundance and diversity of small-sized frogs and the presence of only a single, rare, monotypic giant frog (*Etnabatrachus maximus*) indicates that the area experienced a reliable (non-seasonal) precipitation regime (Tyler, 1994).

*Squamates.* Several squamates indicate a predominantly rainforest ecology during the Early Pliocene. The most abundant large-sized squamate present in any of the Early Pliocene deposits is *Cyclodomorphus gerrardii*. Although also found in dry sclerophyllous vegetation today, *Cyclodomorphus gerrardii* is most frequently encountered in wet sclerophyll and rainforest. *Hypsilurus* sp. has been identified from the Early Pliocene. This agamid genus is rainforest-restricted, present only in rainforests of southeastern Queensland, the Wet Tropics and Papua New Guinea.

*Mammals.* Several analyses of Australian mammal biogeography have focussed on determining correlative values that describe the patterns seen in rainforest mammal distributions (Braithwaite et al., 1985; Williams, 1997; Kanowski et al., 2001; Kanowski et al., 2003; Winter, 1988; Winter, 1997; Laurance, 1997; Nix & Switzer, 1991). These correlative values encompass several different categories into which the mammals found in rainforests have been placed. These categories include broad definitions such as "Rainforest Specialists Species", "Forest Generalists Species", "Rainforest Ecotone Species", "Generalist Species" and "Independent Species" (Winter, 1988); or more specific definitions, such as the eleven defined tropical mammal guilds of Braithwaite et al. (1985). Williams (1997) used Braithwaite et al.'s guilds to describe patterns seen in mammal species of the Wet Tropics rainforest. Other authors (Kanowski et al., 2001; Kanowski et al., 2003; Winter, 1997; Laurance, 1997; Nix & Switzer, 1991) have either focussed on a single or a combination of ecological parameters to describe patterns in rainforest mammal species-richness. These parameters include; modelled palaeoclimate, floristics, altitude, geology, precipitation, rainforest shape and size, latitude, temperature, habitat fragmentation and predators. These criteria developed for modern rainforest mammals have been utilised here in identifying the palaeoecological parameters of the Early Pliocene environment, since several extant mammal genera (and possibly species) with obvious rainforest affinities occur in the Early Pliocene sites.

#### *Ecological Specialisation.*

Forteen extant mammal species were identified by Winter (1988) to be rainforest specialists and restricted to northern Queensland. Of these taxa, eight are considered to be rainforest specialist genera (*Phalanger*, *Uromys*, *Pogonomys*, *Pseudocheirops*, *Pseudochirulus*, *Hypsiprymnodon*, *Hemibelideus* and *Dendrolagus*). In the Early Pliocene assemblages, five of these eight genera are present, with the absence of *Phalanger*, *Hypsiprymnodon* and *Hemibelideus*.

Rainforest-restricted mammal species were determined for Australia and New Guinea by using Strahan (1995) and Flannery (1994) respectively. The genera *Strigocusus* and

Fossil Taxon	Present Day Analogue	Guild
Thylacinidae		
<i>Thylacinus</i>	<i>Thylacinus cynocephalus</i>	VLTC
Dasyuridae		
<i>Antechinus sp. 1</i>	<i>Antechinus</i>	SSI
<i>Antechinus sp. 2</i>	<i>Antechinus</i>	SSI
<i>Dasyurus sp.</i>	<i>Dasyurus</i>	MSI/C
<i>Phascogale sp.</i>	<i>Phascogale</i>	SSI
<i>Sarcophilus laniarius</i>	<i>Sarcophilus harrisii</i>	LTC
<i>Sminthopsis murina</i>	<i>Sminthopsis murina</i>	SSI
dasyurid new	<i>Planigale</i>	STI
Vombatidae		
<i>Vombatus ursinus mitchelli</i>	<i>Vombatus ursinus</i>	VLTH
<i>Palorchestes sp. cf. P. parvus</i>	None	VLTH
diprotodont indet	None	VLTH
Macropodidae		
<i>Bohra sp.</i>	None	LSH
<i>Dendrolagus spp.</i>	<i>Dendrolagus</i>	LAH
<i>Thylogale sp. 1</i>	<i>Thylogale christenseni</i>	MTH
<i>Thylogale sp. 2</i>	<i>Thylogale stigmata</i>	LTH
<i>Petrogale</i>	<i>Petrogale</i>	LTH
<i>Macropus sp. 1</i>	<i>Macropus dorsalis</i>	LTH
<i>Protemnodon cf. P. devisi</i>	None	VLTH
<i>Kurrabi</i>	None	LTH
Pseudocheiridae		
<i>Pseudocheirulus sp. 1</i>	<i>Pseudocheirulus mayeri</i>	SAH
<i>Pseudocheirulus sp. 2</i>	<i>Pseudocheirulus canescens</i>	MAH
<i>Pseudocheirulus sp. 3</i>	<i>Pseudocheirulus herbertensis</i>	SAH
<i>Pseudocheirus spp</i>	<i>Pseudocheirus spp.</i>	SAH
<i>Petauroides</i>	<i>Petauroides/Hemibelidius</i>	SAH
<i>Pseudocheirops sp. 1</i>	<i>Pseudocheirops</i>	MAH
<i>Pseudocheirops sp. 2</i>	<i>Pseudocheirops</i>	MAH
<i>Pseudokoala</i>	None	LAH
Petauridae		
gen. et sp. nov. 1	<i>Petaurus</i>	SAN-I
gen. et sp. nov. 2	<i>Petaurus</i>	SAN-I
<i>Dactylopsila sp. 1</i>	<i>Dactylopsila</i>	SSI
<i>Dactylopsila sp. 2</i>	<i>Dactylopsila</i>	SSI
Incerti Sedis		
gen. et sp. nov.	None	SAN-I
Acrobatidae		
<i>Acrobates sp</i>	<i>Acrobates</i>	SAN-I
Burramyidae		
<i>Cercatetus sp.</i>	<i>Cercatetus</i>	SAN-I
Phalangeridae		
<i>Strigocuscus</i>	<i>Strigocuscus</i>	LAH
<i>Trichosurus sp. 2</i>	<i>Trichosurus</i>	LAH

Fossil Taxon	Present Day Analogue	Guild
Thylacoleonidae		
<i>Thylacoleo hilli</i>	None	LSC
<i>Thylacoleo sp.</i>	None	VLSC
Peramelidae		
<i>Perameles sp. 1</i>	<i>Perameles</i>	MTO
<i>Perameles sp. 2</i>	<i>Perameles</i>	MTO
Perameloid fam. Incertae sedis		
gen. et sp. nov. 1	<i>Perameles/Peroryctes</i>	MTO
gen. et sp. nov. 2	<i>Perameles/Peroryctes</i>	MTO
Muridae		
<i>Hydromys</i>	<i>Hydromys</i>	MQO
<i>Pseudomys spp</i>	<i>Pseudomys</i>	STO
<i>Zyzomys</i>	<i>Zyzomys</i>	STO
<i>Uromys/Melomys</i>	<i>Uromys/Melomys</i>	SSH
<i>Pogonomys</i>	<i>Pogonomys</i>	SSH
<i>Mesembriomys</i>	<i>Mesembriomys</i>	MSO

TABLE 6. Mammalian guilds defined for the Early Pliocene. Guild traits expanded from Braithwaite et al., (1985). Abbreviations: Size; S. Small, <200g; M. Medium 200g-3kg; L. Large 3kg-20kg, VL Very Large >20kg. Microhabitat: A. Arboreal, T. Terrestrial, S. Scansorial, Q. Semi-aquatic. Diet: N - Nectarivore, I - Insectivore, O - Omnivore, C - Carnivore, H - Herbivore.

*Dactylopsila* are presently rainforest-restricted and are found in the Early Pliocene at Mt Etna.

Additionally, *Cercartetus* sp. is considered to be very close to, if not conspecific with, *Cercartetus caudatus*, and although *Cercartetus* is not a rainforest-restricted genus, *Cercartetus caudatus* is a distinct rainforest specialist (Winter, 1988). *Antechinus* sp. 1 is considered to be very close to the rainforest-restricted *Antechinus adustus* (Van Dyck & Crowther, 2000).

#### Mammal guilds and species richness

Palaeoecological reconstruction using extant rainforest-restricted and specialist taxa as analogues provides good evidence for the presence of rainforest during the Early Pliocene. Defining the different mammalian guilds and the species richness present at sites allows for an extension of the palaeoecological reconstruction to include possible correlations with floristic diversity and climate as seen in modern day rainforest studies (Braithwaite et al., 1985; Heads, 2002; Williams, 1997).

Braithwaite et al. (1985) defined Australian tropical mammal guilds on the basis of three



traits; 1. Body size (small <200g, medium 200-3kg, and large 3kg-10kg); 2. Microhabitat (arboreal, scansorial and terrestrial); and 3. Diet (insectivore, nectavore, folivore/frugivore (here classed as herbivore), carnivore, omnivore and granivore). Allocation of these three traits to the taxa from the Early Pliocene was achieved by choosing the closest living analogue or determining each trait from morphology. Table 6 lists the Early Pliocene mammalian fauna, their modern analogues and defined guild type based on Braithwaite et al's traits.

Most of the fossil taxa were able to be assigned to their equivalent modern day analogue by means of genus-level identity. Most species within the analogue genus shared traits defined for that genus' guild, with the possible exception of size. For genera with unknown modern analogues, the closest living taxon to the extinct taxon was used, with inferences drawn for each trait based on family-level trait similarity. For example, *Pseudokoala* was defined as being a large-sized (>3kg), arboreal herbivore, based on its much larger size when compared to the largest living pseudocheirid (*Pseudocheirops* - <3kg); and because all living pseudocheirids are arboreal and herbivorous.

The remaining taxa are those with no family-level trait similarities to modern groups (Diprotodontidae, Palorchestidae and Thylacoleonidae). All three of these families are characterised by being very large-sized (>20kg), with the exception of *Thylacoleo hilli*, which is considered here to be large-sized (between 10 and 20kg) (Wroe et al., 2004). Based on the very-large size of these mammals, a fourth body size trait is added here. Two mammal families are considered to be terrestrial in their microhabitat due to their very large size, with the acception of *Thylacoleo*, which is here considered to be scansorial. Diprotodontidae and Palorchestidae are considered to be herbivores and members of the Thylacoleonidae to be carnivores.

All of the guilds defined by Braithwaite et al. (1985) were present in the Early Pliocene at Mt Etna. Nine new guilds were identified that did not fit the 11 guilds defined by Braithwaite et al. (1985) and are here considered to be either present in the Wet Tropics, Papua New Guinea/Irian Jaya or extinct from rainforests today. These nine guilds were; 1. Small-sized, arboreal, herbivore (SAH) (e.g. *Pseudochirulus mayeri*, *Pseudochirulus* sp 1., *Pseudocheirus* sp.

1-2). This guild is present today in Papua New Guinea and Irian Jaya; 2. Medium-sized arboreal herbivore (MAH) (e.g. *Pseudochirulus* spp., *Pseudocheirops* spp.). Today present in the The Wet Tropics, Papua New Guinea and Irian Jaya; 3. Large-sized, scansorial carnivore (LSC) (e.g. *Thylacoleo hilli*), which is extinct; 4. Medium-sized terrestrial herbivore (MTH) (e.g. *Thylogale* sp. 1, *Thylogale christenseni*), recently extinct in Irian Jaya (Hope, 1981); 5. Medium-sized, semi-aquatic omnivore (MQO) (e.g. *Hydromys*), present in the Wet Tropics, PNG and Irian Jaya; 6. Large-sized, scansorial herbivore (e.g. *Bohra* sp.), which is now extinct; 7. Very large-sized, terrestrial herbivore (VLTH) (e.g. *Palorchetes*, diprotodont), extinct; 8. Very large-sized terrestrial carnivore (VLTC) (e.g. *Thylacinus*), extinct; and 9. Very large-sized scansorial carnivore (VLSC) (e.g. *Thylacoleo*), extinct.

Braithwaite et al. (1985) illustrates that the greatest number of mammalian guilds found in the Australian tropics are located in the habitat classified as rainforest. Williams (1997) illustrates that three guilds; small, scansorial, insectivores; large, arboreal, herbivores; and small, scansorial, omnivores, are important in determining species richness in modern rainforest of the Wet Tropics and are also the most extinction prone. All three of these guilds are present in each of the interpreted Early Pliocene sites at Mt. Etna.

Williams (1997) also shows that overall species richness in rainforest is positively influenced by guild diversity, rainforest shape, area and habitat diversity (rainfall and vegetation diversity). According to Williams (1997), the number of small to large-sized mammalian guilds present in the most species rich locations of the present day Wet Tropics is nine. The number of small to large sized mammalian guilds from individual sites in the Early Pliocene of Mount Etna ranges from ten to thirteen.

Williams (1997) identifies two regions of the northern Queensland Wet Tropics that possess the greatest species richness (21-26 spp), greatest number of endemic mammal species (4-8 spp.) and thus the greatest number of guilds (9) of rainforest mammals in Australia. These two areas are defined by Williams as the Windsor and Carbine Uplands, and the Lamb, Atherton, Bellenden-Ker/Bartle-Frere & Kirrama Uplands. Both regions have their greatest area above 1000m altitude and possess the greatest

vegetation diversity of the Wet Tropics. The present day climatological parameters needed to sustain such a large number of guilds and high species richness for these two upland regions is a high consistent (nonseasonal) precipitation rate (>2000mm) with a moderately cool to cool annual temperature regime (meso-megathermal; 21-23°C) (Nix, 1982; Winter, 1997).

Rainforest areas of the Papua New Guinean central highlands show similar species richness of mammals (24-29 spp) (Heads, 2002). These regions are defined by Nix (1982) as a nonseasonal mesothermal-microthermal (12-14°C) climate.

The similarities seen here for both the Wet Tropics and Papua New Guinea suggest that both regions possess their greatest mammalian species richness and guild diversity in areas that have a relatively cool climate with nonseasonal high annual rainfall. Each of the Early Pliocene sites from Mt. Etna possess from at least 21 to 30 small to large-sized mammal species. This species richness is similar to that found in Papua New Guinea and the Wet Tropics of today, however, this does not account for the very large-sized taxa also present in the Early Pliocene.

When considered together; guild diversity, species richness, specialist and endemic taxa, the Early Pliocene faunal assemblage strongly indicates the presence of a diverse rainforest habitat, which was subject to regular nonseasonal high rainfall in a mesothermal climate regime (20-23°C). The entire fauna strongly indicates a vegetation structure that included several levels of complexity to house diverse guilds containing, arboreal, scansorial, terrestrial, fossorial, semi-aquatic and aquatic niches. On the basis that the fossil sites are not found higher than 200m above sea level today, the Early Pliocene rainforest could be considered to be lowland rainforest. The diversity of mammalian nectavores, herbivores and insectivores indicates the presence of an equally diverse angiosperm flora, possibly more diverse than what is indicated in the ODP 815 and Aquarius Well pollen cores. The very rare occurrence of grazing macropods and a single wombat specimen indicates the presence of small areas of grasslands or grassy understorey within the Mt. Etna area.

#### PLIO-PLEISTOCENE.

*Seasonal, mesothermal, mosaic rainforest-sclerophyll forest with chenopod, asteraceae and grassy understorey.*

The Plio-Pleistocene pollen record for central eastern Queensland shows an increased seasonality toward the end of the Late Pliocene and into the Pleistocene with an increase in the sclerophyllous vegetation and decrease in several rainforest groups (Martin & McMinn, 1993). Podocarps, araucarians and ferns decrease with an increase in Casuarinaceae in the Aquarius Well core (Hekel, 1972). Similarly gymnosperms, rainforest angiosperms and ferns decrease during the Plio-Pleistocene of ODP815. A sudden increase in Chenopodaceae and Asteraceae is seen in the Plio-Pleistocene Aquarius Well record (Hekel, 1972), and a steady increase in these two floristic groups is seen toward the Late Pliocene and Pleistocene in the ODP815 core (Martin & McMinn, 1993).

Two sites record the Plio-Pleistocene vertebrate record of central eastern Queensland (QML1384U and QML1420). This is due to the intermediate faunal similarity between the Early Pliocene rainforest faunal assemblage and the late Pleistocene faunal assemblage. QML1384U retains the distinct rainforest signal found in the Early Pliocene, however, there are a number of differences that may reflect a more seasonal climate. Additionally, QML1420, has a fauna that shows a more seasonal, open habitat.

*Frogs.* Only two frog species have been identified in the Plio-Pleistocene faunal assemblage, *Litoria* and *Kyarranus*. Although specimens are abundant at QML1384U, the presence of so few frog taxa may reflect a less complex vegetation and precipitation regime during this time. Neither taxon is specifically rainforest-dwelling, however, *Litoria* sp. indicates an arboreal environment and *Kyarranus* sp. indicates areas of permanent moisture.

*Squamates.* The presence of *Cyclodomorphus gerrardii* indicates a closed, wet, forest system.

*Mammals.* Although the mammal species are similar to those from the Early Pliocene, several taxa have been replaced by species with a broader environmental tolerance. *Antechinus flavipes* is present in the Plio-Pleistocene and possibly possesses a broader ecological range than that hypothesised for *Antechinus* sp. 1 and *Antechinus* sp. 2, which it replaces. *Sminthopsis macroura* also appears in Plio-Pleistocene, which may indicate a dry, open environment based on its present day distribution. Extant *Sminthopsis macroura* are commonly found in chenopod shrublands throughout central Australia

(Strahan, 1998), therefore the presence of chenopods in the Plio-Pleistocene pollen record could have provided suitable habitat for this species.

Arboreal possums continue to constitute a large portion of the QML1384U fauna, less so QML1420. Pseudocheirids are represented by three genera (*Pseudochirulus*, *Pseudocheirus* and *Petauroides*), petaurids with two genera (*Dactylopsila* and new genus), burramyids by *Cercartetus*, and phalangerids by *Strigocuscus*. The abundance of arboreal herbivores, insectivores and nectavores, indicates the retention of some rainforest and a dominance of angiosperms in the vicinity of Mt Etna.

Bandicoot diversity shows changes from the Early Pliocene with the appearance of two species of *Isodon*. *Isodon obesulus* possibly indicates a more mosaic vegetation structure (Strahan, 1998).

Macropod diversity remains high at QML1420, with a strong component of grazing macropodids, indicating the presence of more extensive grasslands at Marmor Quarry.

The mammal assemblage at QML1420 indicate a mosaic of environments present in the area, including open areas with grasses (*Macropus* spp, *Vombatus*, *Megalanis prisca*, zygomaturine), closed forest (*Dendrolagus*, *Thylogale* sp. 2, *Trichosurus*, Petauroid new genus and *Melomys/Uromys*) and semi-aquatic (*Hydromys*).

#### LATE PLEISTOCENE (ca. 149, 000 ybp)

*Dry, open arid-zone with closed 'refugial' forest.*

The pollen record for the late Pleistocene is absent at Aquarius Well and ODP815, demarcated by a hiatus of deposition and correlated with sea level fall (Hekel, 1972; Martin & McMinn, 1993). As an alternative, Lynch's Crater (Fig. 1A, 2), far north Queensland provides a better late Pleistocene record for Queensland (Kershaw, 1986). Kershaw (1986) estimates an annual precipitation rate which is 50% lower than the present day approximately 150,000 years ago. If it is hypothesised that the Mt. Etna area experienced a similar relative decrease in annual precipitation rate during this period of time, then the annual precipitation rate would have been less than 500mm (present day annual rainfall is between 800-1000mm, Data from Bureau of Meteorology: [www.bom.gov.au](http://www.bom.gov.au)). An annual precipitation rate of below 500mm is equivalent to the precipitation rate currently recorded in central western Queensland,

approximately 600kms to the west of Rockhampton. The late Pleistocene faunal assemblage reflects the very dry components of this ecology, however, it also records remnants of more mesic, probably refugial, environments.

*Frogs.* Frog diversity is low with only a single taxon so far positively identified and a complete absence of hylids (tree frogs).

*Squamates.* Squamate diversity is high, with most taxa identified, presently existing in the Australian arid zone. The squamates comprise, three agamids, all of which are currently restricted to the arid zone of central Australia; at least three species of skink; two large-sized varanids and several elapids. The absence of *Cyclodomorphus gerrardii* supports the contention for a very dry habitat.

*Mammals.* A distinct faunal change demarcates the late Pleistocene mammal assemblage from the older faunas of the same area. The small to large-sized dasyurids illustrate a diversity of insectivorous and carnivorous niches available within the ecology. There is retention of *Antechinus flavipes*, *Dasyurus hallucatus*, *Sminthopsis murina* and *Sminthopsis macroura* from older assemblages, with the addition of *Antechinus swainsonii*, *Dasyurus viverrinus*, *Planigale maculata* and *Phascogale topoatafa*. *Antechinus swainsonii* indicates the presence of closed wet environments, as do *Antechinus flavipes*, *Sminthopsis murina* and *Planigale maculata*. The remaining three new taxa lend evidence to the presence of dry sclerophyll in the region because all three extend into these environments today. Macropodines also indicate the presence of both open and closed environments with *Macropus* indicating grasses and *Thylogale* sp. 2 and *Dendrolagus* occupying closed forest. Possums are almost entirely absent with only two taxa present, *Trichosurus* sp. 1 and the new genus of petauroid.

*Perameles bougainville* appears in the record during the late Pleistocene, indicating the presence of dry open environments with shrubby, possibly chenopod-dominant ground cover. *Isodon obesulus* remains in the faunal assemblage, supporting the mosaic nature of the palaeoenvironment. *Chaeropus ecaudatus* and *Macrotis lagotis* both strongly indicate a dry climate. Additionally, they illustrate the presence of grasses, possibly tussock grasses, in the area (Strahan, 1998). The rodent fauna also suggests a combination of distinctive dry and woodland species. The presence of species of *Notomys* and

*Leggadina* suggest an open environment, whilst *Conilurus* sp. suggests woodland.

On balance, the faunal assemblage indicates mosaic vegetation with areas of open grassland/chenopod shrubland, sclerophyll forest and a closed refugial forest. Such refugial forest is seen today in the semi-evergreen vine forest on Mount Etna, where the vine thickets are restricted to the wetter microclimates of limestone, whilst being surrounded by dry sclerophyll woodlands.

### CONCLUSION

Analysis of faunal and palaeoecological succession spanning the Early Pliocene to Holocene in central eastern Queensland is made possible by the long accumulation histories of cave and fissure systems in this region. As with the Wellington Caves of New South Wales (Dawson et al., 1999), Mount Etna provides a unique opportunity to document environmental change over ca. 4 million year period and the fauna associated with this change.

The Pliocene sites from Mount Etna are distinguished from all other sites in Australia of similar age by the presence of a distinct and dominant rainforest fauna, with the exception of the Hamilton Local Fauna. All other Pliocene sites in Australia differ from those at Mount Etna and Hamilton by possessing none or minor components of the fauna which are rainforest-adapted. In addition, the Mount Etna Fauna provides biogeographic links to Papua New Guinea and Irian Jaya by possessing taxa that are now restricted to these areas today or have only recently gone extinct there.

The mammalian fauna of the Early Pliocene at Mount Etna suggests biogeographic connectivity to Papua New Guinea and Irian Jaya during or just prior to this time. The murid fauna indicates a much earlier dispersal event of rainforest murids into Australia and questions the late Pleistocene or Holocene arrival previously suggested (Flannery, 1995; Winter, 1997). Combining an Early Pliocene record of rainforest specialist murids at Mount Etna with the incredibly diverse and endemic murid fauna from Rackham's Roost, Riversleigh, far north Queensland, substantially increases the probability that murids entered Australia before the Early Pliocene and probably in the Late Miocene (Archer et al., 1991; Long et al., 2002). The Pliocene possum and macropod faunas from Mount Etna illustrate connectivity between New

Guinea and Australia also, by possessing taxa (or lineages) with affinities to taxa now extant or recently extinct in New Guinea.

Although the fossil record is patchy between the Early Pliocene and late Pleistocene, there is a distinct trend in the fauna to become arid-adapted, with an arid-adapted fauna by the late Pleistocene. The late Pleistocene fauna adds new records for the palaeodistribution of arid-adapted taxa, with several extant central Australian taxa being found extremely close to the eastern Australian coastline. Evenso, several mesic-adapted taxa persist into the late Pleistocene, probably existing in refugia offered by the limestone bluffs in the Mount Etna area, as is seen today.

The Mount Etna and surrounding fossil deposits offer a unique opportunity to document the evolution of the central Queensland environment over 4 million years of climate change, including the extinction of a diverse rainforest community, the expansion of the arid zone interior and the isolating effects on fauna utilising the refugial nature of limestone bluffs.

### ACKNOWLEDGEMENTS

Henk Godthelp is thanked for his assistance in rodent identifications. Jian-xin Zhao is thanked for his provision of preliminary dating results. The following people and groups are acknowledged for their encouragement and assistance in developing this study: Aaron Sands, Alex Cook, Amy Sands, Aust. Skeptics, Ayla Tierney, Bernie Cooke, Chris White, Deb Lewis, Gilbert Price, Gregg Webb, Henk Godthelp, Jan Williams, Jeannette Sands, Jian-xin Zhao, Joanne Wilkinson, John Hocknull, John Walsh, Jonathan Cramb, Kristen Spring, Liz Reed, Lyndall Dawson, Mary Dettmann, Merv Barton, Michael Archer, Mina Bassarova, Morag Hocknull, Noel Sands, Paul Tierney, Peter Jell, Shona Marks, Steve Bourne, Sue Hand and numerous volunteers. This study (in part) has been assisted by funds provided by an Australian Research Council Linkage Grant LP0453664, with the following Industry Partners: Queensland Museum, Cement Australia, Central Queensland Speleological Society, Rockhampton Regional Development. Tourism Queensland is thanked for additional funding.

### LITERATURE CITED

- APLIN, K.P.1987. Basicranial anatomy of the early Miocene Diprotodontian *Wynyardia bassiana* (Marsupialia: Wynyardiidae) and its implications



- for wynyardiid phylogeny and classification. Pp 369-391. In Possums and opossums: studies in evolution. 1 Archer, M. (ed) (Surrey Beatty & Sons, Chipping Norton).
- ARCHER, M. A. 1976. The dasyurid dentition and its relationships to that of didelphids, thylacinids, borhyaeniids (Marsupicanivora) and peramelids (Peramelina: Marsupialia). Australian Journal of Zoology Supplementary Series No. 39: 1-34.
1978. Quaternary vertebrate faunas from the Texas Caves of southeastern Queensland. Memoirs of the Queensland Museum 19: 61-109. 1981. Results of the Archbold expeditions. No 104. Systematic revision of the marsupial genus *Sminthopsis* Thomas. Bulletin of the American Museum of Natural History 168: 61-224.
1984. The Australian marsupial radiation. Pp. 633 – 808. In Vertebrate Zoogeography and Evolution in Australasia. (Animals in space and time). M Archer and G Clayton eds. (Hesperian Press, Carlisle).
- ARCHER, M. & DAWSON, L. 1982. Revision of Marsupial Lions of the genus *Thylacoleo* Gervais (Thylacoleonidae, Marsupialia) and thylacoleonid evolution in the late Cainozoic. Pp. 477-494. In Archer M. (ed). Carnivorous Marsupials 2. (Royal Zoological Society of New South Wales, Sydney)
- ARCHER, M. A. & WADE, M. 1976. Bluff Downs Local Fauna. Memoirs of the Queensland Museum 17: 383-398.
- ARCHER, M., HAND, S.J. & GODTHELP, H. 1995a. Tertiary Environmental and Biotic Change in Australia. Pp. XX-XX ) In Vrba, E.S., Denton, G.H., Partridge, T.C. & Burckle, L.H. (eds). Palaeoclimate and evolution, with emphasis on human origins, (Yale University Press, New Haven).
- ARCHER, M., HAND, S.J. & GODTHELP, H. 1995b. Riversleigh. (Reed Books: Sydney).
- ARCHER, M.A., BLACK, K. & NETTLE, K. 1997. Giant Ringtail Possums (Marsupialia, Pseudocheiridae) and Giant Koalas (Phascolarctidae) from the late Cainozoic of Australia. Proceedings of the Linnean Society of New South Wales 117: 3-16.
- ARCHER, M., ARENA, D.A., BASSAROVA, M., BLACK, K., BRAMMAL, J.R., COOKE, B.N., CREASER, P.H., CROSBY, K., GILLESPIE, A.K., GODTHELP, H., GOTT, M., HAND, S. J., KEAR, B.P., KRIKMANN, A., MACKNESS, B.S., MUIRHEAD, J., MUSSER, A. M., MYERS, T.J., PLEDGE, N.S., WANG, Y., & WROE, S. 1999. The evolutionary history and diversity of Australian mammals. Australian Mammalogy 21:1-45.
- AYLIFFE, L.K. & VEEH, H.H. 1988. Uranium-series dating of speleothems and bones from Victoria Cave, Naracoorte, South Australia.
- AZZAROLI, A., DE GIULI, C, FUCCARELLI, G. & TORRE, D. 1988. Late Pliocene to early-mid Pleistocene mammals in Eurasia: Faunal Succession and dispersal events. Palaeogeography, Palaeoclimatology, Palaeoecology 66(1-2): 77-100.
- BARKER, R.M., BLAKE, P.R., BURROWS, P.E., CROUCH, S.B.S., FORDHAM, B.G.F, HAYWARD, M.A., LIVINGSTONE, M.D., MORWOOD, D.A., MURRAY, C.G, PARFREY, S.M., ROBERTSON, A.D.C., SIMPSON, G.A., TAUBE, A., DOMAGALA, J. & RANDALL, R.E. 1997. New insights into the geology of the northern New England Orogen in the Rockhampton-Monto region, central coastal Queensland: progress report on the Yarrol project. Queensland Government Mining Journal 98 (1146): 11-26.
- BARTHOLOMAI, A. 1975. The genus *Macropus* Shaw (Marsupialia: Macropodidae) in the upper Cainozoic deposits of Queensland. Memoirs of the Queensland Museum 16(3): 309-363.
1977. The fossil vertebrate fauna from Pleistocene deposits at Cement Mills, Gore, South eastern Queensland. Memoirs of the Queensland Museum 18(1): 41-51.
- BENSLEY, B.A. 1903. On the evolution of the Australian Marsupialia; with remarks on the relationships of the marsupials in general. The Transactions of the Linnean Society of London. Zoology. 9:83-217.
- BISHOP, W.W., CHAPMAN, G.R., HILL, A. & MILLER, J.A. 1971. Succession of Cainozoic vertebrate assemblages from the northern Kenya Rift Valley. Nature 233 (5319): 389-394.
- BLACK, K. 1997. A new species of Palorchestidae (Marsupialia) from the late middle to early late Miocene Encore Local Fauna, Riversleigh, northwestern Queensland. Memoirs of the Queensland Museum 41 (2): 181-186.
- BONAPARTE, C.L.J.L. 1838. Synopsis of vertebratorum systematis. Nuovi Annali delle Scienze, Bologna. 2(1): 105-133.
- BOURKE, R.M. 1970. A case for conservation – The Mt Etna and Limestone Ridge Caving Area. Pp. 98-114, In Sprent J.K. (ed) Mount Etna caves. (University of Queensland Speleological Society, St. Lucia, Brisbane).
- BOWLER, J.M. 1982. Aridity in the late Tertiary and Quaternary of Australia. Pp. 35-45. In Barker, W.R. & Greenslade, P.J.M. (eds), Evolution of the Flora and Fauna of Arid (Australia, Peacock Publications, Australian Systematic Botany Society, ANZAAS, South Australian Division, Adelaide).
- BRAITHWAITE, R.W., WINTER, J.W., TAYLOR, J.A. & PARKER, B.S. 1985. Patterns of diversity and structure of mammalian assemblages in the Australian Tropics. Australian Mammalogy 8: 171-186.
- BRAMMAL, J.R. 1998. A new petauroid possum from the Oligo-Miocene of Riversleigh, northwestern Queensland. Alcheringa 23: 31-50.

- BROOM, R. 1896. On a small fossil marsupial with large grooved premolars. *Proceedings of the Linnean Society of New South Wales* 2 (10): 563-567.
- BURNETT, G.T. 1830. Illustrations of the Quadrupeda, or quadrupeds, being the arrangement of the true four-footed beasts indicated in outline. *Quarterly Journal of Literature Science and the Arts* 28: 336-353.
- COGGER, H.G. 2000. *Reptiles and amphibians of Australia* 5<sup>th</sup> ed. (Reed: Melbourne)
- CUVIER, G. 1807. Sur les ossements fossiles de crocodiles et particulièrement sur des environs du Havre de Honfleur, accedes remarques sur les squelettes des sauriens de la Thuringie: *Annales du Museum d'Histoire Naturelle*, Paris. 12 73-110.
- DAWSON, L. 1982a. Taxonomic status of fossil devils (*Sarcophilus*: Dasyuridae, Marsupialia) from the late Quaternary eastern Australia localities. Pp. 516-525. In Archer, M. (ed). *Carnivorous Marsupials 2*, (Surrey Beatty & Sons, Chipping Norton).
- 1982b. The taxonomic status of fossil thylacines (*Thylacinus*, Thylacinidae, Marsupialia) from late Quaternary deposits in eastern Australia. Pp. 527-536. In Archer, M. (ed). *Carnivorous Marsupials 2* (Surrey Beatty & Sons, Chipping Norton).
1983. The taxonomic status of small fossil wombats (Vombatidae: Marsupialia) from the Quaternary deposits, and of related modern wombats. *Proceedings of the Royal Society of New South Wales* 107: 101-123.
2004. A new Pliocene tree kangaroo species (Marsupialia, Macropodinae) from the Chinchilla Local Fauna, southeastern Queensland. *Alcheringa* 28: 267-273.
- DAWSON, L. & AUGEE, M.L. 1997. The Late Quaternary sediments and fossil vertebrate fauna from Cathedral Cave, Wellington Caves, New South Wales. *Proceedings of the Linnean Society of New South Wales* 117: 51-78.
- DAWSON, L. & FLANNERY, T.F. 1985. Taxonomic and phylogenetic status of living and fossil kangaroos of the genus *Macropus* Shaw (Macropodidae: Marsupialia), with new subgeneric name for the larger wallabies. *Australian Journal of Zoology* 33: 473-498.
- DAWSON, L., MUIRHEAD, J. & WROE, S. 1999. The Big Sink Fauna: a lower Pliocene mammalian fauna from the Wellington Caves complex, Wellington, New South Wales. *Records of the Western Australian Museum. Supplement No 57*: 265-290.
- DWYER, P. 1970. Mammals of the Mount Etna Caves. In *Mount Etna caves*, Sprent, J.K. (ed), (University of Queensland Speleological Society, St. Lucia, Brisbane).
- FITZINGER, L.I. 1826. *Neue Classification der Reptilien nach ihren natürlichen Verwandtschaften*. J.G. Hubner, Vienna.
- FLANNERY, T.F. 1984. Re-examination of the Quambun Local Fauna, A late Cenozoic Vertebrate Fauna from Western Australia. *Records of the West Australian Museum* 11(2): 119-128.
1992. New Pleistocene marsupials (Macropodidae, Diprotodontidae) from subalpine habitats in Irian Jaya, Indonesia. *Alcheringa* 16: 321-331.
1995. *Mammals of New Guinea*. (Reed Books, Sydney).
- FLANNERY, T.F. & ARCHER, M. 1984. The macropodoids (Marsupialia) of the Pliocene Bow Local Fauna, central eastern New South Wales. *The Australian Zoologist* 7: 193-204.
1987. *Strigocuscus reidi* and *Trichosurus dicksoni*, two new fossil phalangerids (Marsupialia: Phalangeridae) from the Miocene of northwestern Queensland. Pp. 527-536. In Archer, M (ed), *Possums and Opossums: studies in evolution 2*. (Surrey Beatty & Sons, Chipping Norton)
- FLANNERY, T.F., RICH, TH., TURNBULL, W.D. & LUNDELIUS, E.L. JR. 1992. The Macropodoidea (Marsupialia) of the Early Pliocene Hamilton Local Fauna, Victoria, Australia. *Fieldiana, Geology Series No 25*: 1-37.
- FLANNERY, T. F. & SZAKAY, F. S., 1982. *Borha paulae*, a new giant fossil tree kangaroo (Marsupialia: Macropodidae) from New South Wales, Australia. *Australian Mammalogy* 5: 83-94.
- FLANNERY, T.F., TURNBULL, W.D., RICH, T.H.V. & LUNDELIUS, E.L. JR. 1987. The phalangerids of the early Pliocene Hamilton Local Fauna, southwestern Victoria, Pp. 537-546. In Archer, M (ed.), *Possums and Opossums: Studies in Evolution*. (Surrey Beatty and Sons and the Royal Society of New South Wales, Sydney).
- FLYNN, L.J., TEDFORD, R.H. & ZHANXIANG, Q. 1991. Enrichment and stability in the Pliocene mammalian fauna of north China. *Paleobiology*. 17(3): 246-265.
- FREEDMAN, L. & JOFFE, A.D. 1966. Skull and tooth variation in the genus *Perameles* Part 3: Metrical Features of *P. gunnii* and *P. bougainville*. *Records of the Australian Museum* 27: 197-217.
- GERDTZ, W.R. & ARCHBOLD, N.W. 2003. An early occurrence of *Sarcophilus lanianus harrisii* (Marsupialia, Dasyuridae) from the Early Pleistocene of Nelson Bay, Victoria. *Proceedings of the Royal Society of Victoria* 115 (2): 45-54.
- GILBERT, B.M., MARTIN, L.D. & SAVAGE, H.G. 1981. *Avian Osteology*. (B.Miles Gilbert Publisher, Wyoming).
- GILL, T. 1872. Arrangement of the families of mammals with analytical table. *Smithsonian Miscellaneous Collection*. 2: I-VI, 1-98.
- GOLDFUSS, G.A. 1820. *Handbuch der Zoologie*. J. L. Schrag, Nürnberg.

- GRAY, J.E. 1821. On the natural arrangement of vertebrate animals. London Medical Repository. 15(1): 296-310.
- 1825a. A synopsis of the genera of reptiles and Amphibia, with a description of some new species. Annals of Philosophy. 10: 193-217.
- 1825b. Outline of an attempt at the disposition of the Mammalia into tribes and families with a list of the genera apparently appertaining to each tribe. Annals of Philosophy. 10(2): 337-344.
- GREER, A.A. 1979. A phylogenetic subdivision of Australian scincid lizards. Records of the Australian Museum 32 339-371.
- HARDWICKE, M.G. & J.E. GRAY. 1827. A Synopsis of the Species of Saurian Reptiles, collected in India by Major-General Hardwicke. Zoological Journal
- HEADS, M. 2002. Regional patterns of biodiversity in New Guinea animals. Journal of Biogeography 29: 285-294.
- HECHT, M. 1975. The morphology and relationships of the largest known terrestrial lizard, *Megalania prisca* Owen, from the Pleistocene of Australia. Proceedings of the Royal Society of Victoria 87: 239-250.
- HEKEL, H. 1972. Pollen and spore assemblages from Queensland Tertiary sediments. Geological Survey of Queensland, Publications 355, Palaeontology Paper, 30.
- HOCKNULL, S.A. 2002. Comparative maxillary and dentary morphology of the Australian dragons (Agamidae: Squamata): A framework for fossil identification. Memoirs of the Queensland Museum. 48 (1): 125-145.
2003. *Etnabatrachus maximus* gen. et sp. nov., a Plio-Pleistocene frog from Mount Etna, central eastern Queensland. Memoirs of the Queensland Museum 49(1): 327-330.
- HOLMAN, J.A. 2000. Fossil snakes of North America: origin, evolution, distribution, paleoecology. (Indiana University Press, Indiana).
- HOPE, J. H. 1978. Pleistocene mammal extinctions: the problem of Mungo and Menindee, New South Wales. Alcheringa 2: 65-82.
1981. A new species of *Thyligale* (Marsupialia: Macropodidae) from Mapala Rock Shelter, Jaya (Carstenz) Mountains, Irian Jaya (Western New Guinea), Indonesia. Records of the Australian Museum 33 (8): 369-387.
- HORSUP, A., JAMES, C. & PORTER, G. 1993. Vertebrates of dry rainforest of south and mideastern Queensland. Memoirs of the Queensland Museum 34(1): 215-228.
- HUTCHINSON, M.N. 1992. Origins of the Australian scincid lizards: a preliminary report on the skinks of Riversleigh. The Beagle, Records of the Northern Territory Museum of Arts and Sciences 9: 61-69.
1997. The first fossil pygopod (Squamata, Gekkota), and a review of mandibular variation in living species. Memoirs of the Queensland Museum 41: 355-366.
- HUTCHINSON, M.N. & MACKNESS, B.S. 2002. Fossil lizards from the Pliocene Chinchilla Local Fauna, Queensland, with a description of a new species. Records of the South Australian Museum 35(2): 169-184.
- KANOWSKI, J., HOPKINS, M.S., MARSH, H. & WINTER, J.W. 2001. Ecological correlates of folivore abundance in north Queensland rainforests. Wildlife Research 28: 1-8.
- KANOWSKI, J., IRVINE, A.K. & WINTER, J.W. 2003. The relationship between the floristic composition of rainforests and the abundance of folivorous marsupials in north-east Queensland. Journal of Animal Ecology 72: 627-632.
- KERSHAW, A.P. 1986. The last two glacial-interglacial cycles from northeastern Australia: implications for climatic change and Aboriginal burning. Nature 322:47-49.
- KIRKEGAARD, A.G., SHAW, R.D. & MURRAY, C.G. 1970. Geology of the Rockhampton and Port Clinton 1:250000 sheet areas. Geological Survey of Queensland Report 38: 1-137.
- LAURANCE, W.F. 1997. Responses of mammals to rainforest fragmentation in tropical Queensland: a review and synthesis. Wildlife Research 24: 603-612.
- LEE, M.S.Y. 1996. Possible affinities between *Varanus giganteus* and *Megalania prisca*. Memoirs of the Queensland Museum 39(2):232.
- LINDSEY, T.R. 1992. Encyclopedia of Australian Animals, Birds. (Angus & Robertson, Sydney).
- LONG, J., ARCHER, M., FLANNERY, T. & HAND, S. 2002. Prehistoric Mammals of Australia and New Guinea (One hundred million years of evolution). (UNSW Press, Sydney).
- LONG, J.A. & MACKNESS, B.S. 1994. Studies of the late Cainozoic diprotodontid marsupials of Australia. 4. The Bacchus Marsh Diprotodons – geology, sedimentology and taphonomy. Records of the South Australian Museum. 27: 95-110.
- LONGMAN, H. 1921. A new genus of fossil marsupial. Memoirs of the Queensland Museum 7: 65-80.
1924. Some Queensland fossil vertebrates. Memoirs of the Queensland Museum. 8(1):16-28.
- 1925a. Fossil marsupials from Marmor. Memoirs of the Queensland Museum. 8(2): 109-110
- 1925b. Ophidian vertebrae from cave deposits at Marmor Quarry. Memoirs of the Queensland Museum 8(2): 111-112.
- LUCKETT, P.W. 1993. An ontogenetic assessment of dental homologies in therian mammals. Pp. 182-284. In Szalay, S.F., Novacek, M.J. & McKenna, M.C. (eds). Mammal Phylogeny; Mesozoic Differentiation, Multituberculates, Monotremes, Early Therians and Marsupials. (Springer-Verlag, New York)

- LUNDELIUS, E.L., JR. 1983. Climate implications of late Pleistocene and Holocene faunal associations in Australia. *Alcheringa* 7: 125-149.
1989. The implications of disharmonious assemblages for Pleistocene extinctions. *Journal of Archaeological Science*. 16: 407-417.
- MACKNESS, B.S. & HUTCHINSON, M.N. 2000. Fossil lizards from the Early Pliocene Bluff Downs Local Fauna. *Transactions of the Royal Society of South Australia*. 124 (1): 17-30.
- MACKNESS, B.S. WHITEHEAD, P.W. & MCNAMARA, G.C. 2000. New potassium-argon basalt date in relation to the Pliocene Bluff Downs Local Fauna, northern Australia. *Australian Journal of Earth Sciences*. 47: 807-811.
- MACPHAIL, M.K. 1996. Neogene environments in Australia, 1: re-evaluation of microfloras associated with important Early Pliocene marsupial remains at Grange Burn, southwest Victoria. *Review of Palaeobotany and Palynology* 92: 307-328.
- 1997 Late Neogene Climates in Australia: Fossil Pollen- and Spore-based Estimates in Retrospect and Prospect. *Australian Journal of Botany* 45: 425-464.
- MADDISON, D.R. & MADDISON, W.P. 2000. MacClade Version 4.02. (Sinauer Associates Inc. Publishers, Massachusetts).
- MARTIN, H.A. & MCMINN, A. 1993. Palynology of sites 815 and 823. The Neogene vegetation history of coastal vegetation of coastal northeast Australia. *Proceedings of the ODP Sciences Results* 133: 115-125.
- MCNAMARA, G.C. 1990. The Wyandotte Local Fauna: a new, dated Pleistocene vertebrate fauna from northern Queensland. *Memoirs of the Queensland Museum*. 28 (1): 285-297.
- MENZIES, J.I, RUSSELL, L., TYLER, M.J. & MOUNTAIN, M.J. 2002. Fossil frogs from the central highlands of Papua New Guinea. *Alcheringa* 26: 341-351.
- MOLNAR, R.E. 1990. New cranial elements of a giant varanid from Queensland. *Memoirs of the Queensland Museum* 29 (2): 437-444.
- MOLNAR, R. E. & KURZ, C. 1997. The distribution of Pleistocene vertebrates on the eastern Darling Downs, based on the Queensland Museum collections. *Proceedings of the Linnean Society of New South Wales*. 117: 107-134.
- MUIRHEAD, J. 1994. Systematics, evolution and palaeobiology of recent and fossil bandicoots (Peramelemorphia: Marsupialia). PhD thesis, University of New South Wales, Sydney. Unpubl.
1999. Bandicoot diversity and evolution (Peramelemorphia: Marsupialia): the fossil evidence. *Australian Mammalogy* 21:11-13.
2000. Yaraloidea (Marsupialia, Peramelemorphia), a new superfamily of marsupial and a description and analysis of the cranium of the Miocene *Yarala burchfieldi*. *Journal of Palaeontology* 74: 512-523.
- MUIRHEAD, J. & FILAN, S.L. 1995. *Yarala burchfieldi*, a plesiomorphic bandicoot (Marsupialia: Peramelemorphia) from the Oligo-Miocene deposits of Riversleigh, northwestern Queensland. *Journal of Palaeontology* 69: 127-134.
- MUIRHEAD, J. & GODTHELP, H. 1995. Fossil bandicoots of Chillagoe (Northeastern Queensland) and the first known specimens of the Pig-Footed Bandicoot *Chaeropus* Ogilby, 1838 from Queensland. *Australian Mammalogy* 19:73-76.
- MURRAY, P.F. 1998. Palaeontology and Palaeobiology of wombats. Pp.1-33. In Wells, R.T. & Pridmore, P.A. (eds). *Wombats*, 1. (Surrey Beatty & Sons, Chipping Norton).
- NELSON, J. E. 1989. Megadermatidae. Pp. 852-856. In Walton, D.W. & Richardson, B.J. (eds) *Fauna of Australia Volume 1B Mammalia*, (ABRS & Australian Government Publishing Service, Canberra).
- NIX, H.A. 1982. Environmental determinants of biogeography and evolution in Terra Australis. Pp35-45. In Barker, W.R & Greenslade, P.J.M. (eds). *Evolution of the Flora and Fauna of Arid Australia*, (Peacock Publications and the Australian Systematic Botany Society: Adelaide).
- NIX, H.A. & SWITZER, M.A. 1991. *Rainforest Animals: Atlas of Vertebrates Endemic to Australia's Wet Tropics*. Kowari 1. (Australian National Parks and Wildlife Service, Canberra)
- OPPEL, M. 1811. *Die Ordnungen, Familien, und Gattungen de Reptilien*: Munich.
- PHILIP, G.M. & PEDDER, A.E.H. 1967. Stratigraphical correlation of the principal Devonian limestone sequence of eastern Australia. Pp. 1025-1041. In D.H. Oswald (ed), *International Symposium on the Devonian System*. (Alberta Society of Petroleum Geologists, Calgary)
- PLEDGE, N. S. 1977. A new species of *Thylacoleo* (Marsupialia: Thylacoleonidae) with notes on the occurrences and distribution of Thylacoleonidae in South Australia. *Records of the South Australian Museum*. 17: 277-283.
1987. *Phascolarctos maris*, a new species of koala (Marsupialia: Phascolarctidae) from the Early Pliocene of South Australia. Pp. 327-330. In Archer, M (ed.). *Possums and opossums: Studies in evolution*. (Royal Zoological Society of New South Wales and Surrey Beatty & Sons Pty Ltd, Sydney).
1992. The Curramulka Local Fauna: a new late Tertiary fossil assemblage from Yorke Peninsula, South Australia. *The Beagle, Records of the Northern Territory Museum of Arts and Sciences*. 9(1): 111-113.
- REED, E.H. & BOURNE, S.J. 2000. Pleistocene fossil vertebrate sites of the south east region of South Australia. *Transactions of the Royal Society of South Australia*. 124(2): 61-90.



- RICH, T.H. 1991. Monotremes, placentals and marsupials: their record in Australia and its biases. Pp. 1005-1058. In Vickers-Rich, P., Monaghan, J.M., Baird, R.F., Rich, T.H. (eds) Vertebrate palaeontology of Australasia. (Pioneer Design Studio, Studio, Melbourne).
- SHANNON, C.H.C. 1970a. Cave descriptions. Pp. 22-36. In Sprent, J.K.(ed.) Mount Etna caves. (University of. Queensland Speleological Society, St. Lucia, Brisbane).
- 1970b. Geology of the Mount Etna area. Pp.11-21. In Sprent, J.K.(ed.) Mount Etna caves. (University of. Queensland Speleological Society, St. Lucia, Brisbane).
- SHEA, G.M. 1990. The genera *Tiliqua* and *Cyclodomorphus* (Lacertilia: Scincidae): generic diagnoses and systematic relationships. Memoirs of the Queensland Museum 29: 495-520.
- SHEN, G.-J., WANG, W., WANG, Q., ZHAO, J.-X., COLLERSON, K.D., ZHOU, C.-L., TOBIAS, P.V. 2001. U-series Dating of Liujiang Hominid Site in Guangxi, Southern China. Journal of Human Evolution 43: 817-829.
- SIMPSON, G.A., CROUCH, S.B.S., MURRAY, C.G., WITHNALL, I.W. & BLIGHT, R.K.J. 2001. Ridglands, Queensland Sheet 8951; first edition (1:100 000 Geological Series). (Department of Natural Resources and Mines, Brisbane).
- SMITH, M.J. 1972. Small fossil vertebrates from Victoria Cave, Naracoorte, South Australia. II. Peramelidae, Thylaciniidae and Dasyuridae (Marsupialia). Transactions of the Royal Society of South Australia. 96(2): 71-84.
1976. Small fossil vertebrates from Victoria Cave, Naracoorte, South Australia. IV. Reptiles. Transactions of the Royal Society of South Australia. 100(1): 39-51.
- STIRTON, R.A. 1936. Succession of North American Continental Pliocene faunas. American Journal of Science. 32 (189) 161-206.
- STRAHAN, R. (ed) 1998. The Mammals of Australia. (Australian Museum and Reed Books, Sydney).
- SWOFFORD, D.L. 2000. PAUP: phylogenetic analysis using parsimony. Version 4.0b10. (Illinois Natural History Survey, Champaign).
- TATE, G.H.H. 1948. Results of the Archibold Expeditions. No. 59. Studies on the anatomy and phylogeny of the Macropodidae (Marsupialia). Bulletin of the American Museum of Natural History. 91: 233-351.
- TEDFORD, R.H. 1994. Succession of Pliocene through Medial Pleistocene mammal faunas of Southeastern Australia. Records of the South Australian Museum 27 (2): 79-93.
- TEDFORD, R.H., WELLS, R.T. & BARGHOORN, S.F. 1992. Tirari Formation and contained faunas, Pliocene of the Lake Eyre Basin, South Australia. The Beagle, Records of the Northern Territory Museum of Arts and Sciences 9 (1): 173-193.
- THOMAS, O. 1888. Catalogue of Marsupialia and Monotremata in the collection of the British Museum (Natural History), London, i-xiii: 1-401.
- TOOP, J. 1985. Habitat requirements, survival strategies and ecology of the Ghost bat *Macroderma gigas* Dobson, (Microchiroptera, Megadermatidae) in central coastal Queensland. Macroderma 1: 37-44.
- TURNBULL, W.D. & LUNDELIUS, E.L. JR. 1970. The Hamilton fauna. A late Pliocene mammalian fauna from the Grange Burn, Victoria, Australia. Fieldiana: Geology, New Series No 19. 1-163.
- TURBULL, W.D., LUNDELIUS, E.L. JR. & ARCHER, M.A. 2003. Dasyurids, perameloids, phalangeroids and vombatoids from the Early Pliocene Hamilton Fauna, Victoria, Australia. Chapter 18. Bulletin American Museum of Natural History 279: 513-540.
- TURNBULL, W.D., LUNDELIUS, E.L. JR. & TEDFORD, R.H. 1992. A Pleistocene marsupial fauna from Limeburner's Point, Victoria, Australia. The Beagle, Records of the Northern Territory Museum of Arts and Sciences. 9: 143-172.
- TYLER, M.J. 1976. Comparative osteology of the pelvic girdle of Australian frogs and description of a new fossil genus. Transactions of the Royal Society of South Australia 100(1): 3-14.
1988. *Neobatrachus pictus* (Anura: Leptodactylidae) from the Miocene/Pliocene boundary of South Australia. Transactions of the Royal Society of South Australia 112: 91.
1991. *Kyarannus* Moore (Anura, Leptodactylidae) from the Tertiary of Queensland. Proceedings of the Royal Society of Victoria 103(1): 47-51.
1994. Australian Frogs a Natural History. (Reed New Holland, Sydney)
- TYLER, M.J., DAVIS, A.C. & WILLIAMS, C.R. 1998. Pleistocene frogs from near Cooma, New South Wales. Proceedings of the Linnean Society of New South Wales 119: 107-113.
- TYLER, M.J., GODTHELP, H. & ARCHER, M. 1994. Frogs from a Plio-Pleistocene site at Floraville Station, Northwestern Queensland. Records of the South Australian Museum 27(2): 169-173.
- VAN DYCK, S. 1982. The relationships of *Antechinus stuartii* and *A. flavipes* (Dasyuridae, Marsupialia) with special reference to Queensland. Pp723-766In Archer, M (ed) Carnivorous Marsupials (Surrey Beatty & Sons, Chipping Norton).
2002. Morphology-based revision of *Murexia* and *Antechinus* (Marsupialia: Dasyuridae). Memoirs of the Queensland Museum 48(1): 239-330.
- VAN DYCK, S. & CROWTHER, M.S. 2000. Reassessment of northern representatives of the *Antechinus stuartii* complex (Marsupialia: Dasyuridae): *A. subtropicus* sp. nov. and *A. adustus* new status. Memoirs of the Queensland Museum 45(2): 611-636.

- VAVRYN, J.M.C. 1987. The fight to save Mount Etna Caves from limestone mining. *Helectite* 25(2): 47-50.
- WATERHOUSE, G.R. 1838. Catalogue of the Mammalia Preserved in the Museum of the Zoological Society. 2<sup>nd</sup> Edition. Richard and John Taylor. London.
- WILLIAMS, S. E. 1997. Patterns of Mammalian Species Richness in the Australian Tropical Rainforests: Are Extinctions during Historical Contractions of the Rainforest the Primary Determinants of Current Regional Patterns in Biodiversity? *Wildlife Research* 24: 513-530.
- WILLIS, P.A. 1995. The phylogenetic systematics of Australian crocodilians. PhD thesis, University of New South Wales, Sydney. Unpubl.
- WILLMOTT, W.F., O'FLYNN, M.L. & TREZISE, D.L. 1986. 1:100 000 geological map commentary Rockhampton Region, Queensland. (Geological Survey of Queensland: Brisbane).
- WINGE, H. 1893. Jordfunde og nulevende Pungdyr (Marsupialia) Fra Lagoa Santam Minas Geras, Brasilien: med udsigt over Pangdyrenes slægtskab *E Museo Lundii* 11(2): 1-149.
- WINTER, J.W. 1988. Ecological specialization of mammals in Australian tropical and sub-tropical rainforest: refugial or ecological determinism? *Proceedings of the Ecological Society of Australia*. 15: 127-138.
1997. Responses of Non-volant Mammals to Late Quaternary Climate Changes in the Wet Tropics Region of North-eastern Australia. *Wildlife Research* 24: 493-511.
- WOODBURNE, M.O., TEDFORD, R.H., ARCHER, M., TURNBULL, W.D., PLANE, W.D., PLANE, M.D. & LUNDELIUS, E.L., JR. 1985. Biochronology of the continental mammal record of Australia and New Guinea. Special Publication, South Australian Department of Mines and Energy 5: 347-365.
- WROE, S. & MACKNESS, B.S. 1998. Revision of the Pliocene dasyurid, *Dasyurus dunmalli* (Dasyuridae: Marsupialia). *Memoirs of the Queensland Museum* 42(2): 605-612.
- WROE, S., EBACH, M., AHYONG, S., DE MUIZON, C. & MUIRHEAD, J. 2000. Cladistic analysis of Dasyuromorphian (Marsupialia) phylogeny using cranial and dental characters. *Journal of Mammalogy*, 81 (4): 1008-1024.
- WROE, S., ARGOT, C. & DICKMAN, C. 2004. On the rarity of big fierce carnivores and primacy of isolation and area: tracking large mammalian carnivore diversity on two isolated continents. *Proceedings of the Royal Society of London (Biology)* (Published On-line 1-9).
- ZHOA, J-XIN., HU, K., COLLERSON, K.D. & XU, H. 2002. Thermal ionization mass spectrometry U-series dating of a hominid site near Nanjing, China. *Geological Survey of America* 29(1): 27-30.

QML	1311H	1311CD	1313	1385	1384L	1384U	1312	1284	1284a	1420	Olsens	Present
<i>Antechinus</i> sp. 1	0	0	1	0	0	0	0	0	1	0	0	0
<i>Antechinus</i> sp. 2	1	1	1	1	1	0	0	1	1	1	0	0
<i>Antechinus flavipes</i>	0	0	0	0	0	1	1	0	0	0	0	1
<i>Antechinus swainsoni</i>	0	0	0	0	0	0	1	0	0	0	0	0
<i>Dasyurus hallucatus</i>	0	0	0	0	0	0	1	0	0	0	0	1
<i>Dasyurus viverrinus</i>	0	0	0	0	0	1	1	0	0	0	0	0
<i>Dasyurus</i> sp.	0	0	1	0	0	0	0	0	0	0	0	0
<i>Phascogale</i> sp.	0	0	1	0	0	0	0	1	0	1	0	0
<i>Phascogale topoatafa</i>	0	0	0	0	0	0	1	0	0	0	0	1
<i>Planigale maculata</i>	0	0	0	0	0	0	1	0	0	0	1	1
<i>Sarcophilus lanarius</i>	1	1	0	0	1	1	1	0	0	1	0	0
<i>Sarcophilus harrisii</i>	0	0	0	0	0	0	0	0	0	0	0	0
<i>Sminthopsis macroura</i>	0	0	0	0	0	1	1	0	0	0	1	0
<i>Sminthopsis murina</i>	0	0	1	1	0	1	1	1	1	1	1	1
dasyurid (gen. et sp. nov.)	1	0	1	1	0	1	0	1	1	0	0	0
<i>Dendrolagus</i> spp.	1	1	1	1	1	0	1	1	1	1	0	0
<i>Thylogale</i> sp. 1	1	1	0	1	1	1	0	1	1	0	0	0
<i>Thylogale</i> sp. 2	0	0	0	0	0	0	1	0	0	1	0	0
<i>Petrogale</i>	1	1	1	1	1	1	1	0	0	1	1	1
<i>Pseudochirulus</i> sp. 1	1	1	1	1	1	0	0	1	1	0	0	0
<i>Pseudochirulus</i> sp. 2	1	1	1	1	0	1	0	1	1	0	0	0
<i>Pseudochirulus</i> sp. 3	1	1	1	1	0	1	0	1	1	0	0	0
<i>Pseudocheirus cf peregrinus</i>	0	0	0	0	0	0	0	0	0	0	1	1
<i>Pseudocheirus</i>	1	1	1	1	0	1	0	1	1	0	0	0
<i>Petauroides</i>	1	1	1	1	0	0		1	1	0	0	0
<i>Pseudocheirops</i> sp. 1	1	0	0	0	1	0	0	0	0	0	0	0
<i>Pseudocheirops</i> sp. 2	0	0	0	0	0	0	0	1	0	0	0	0
<i>Pseudokoala</i>	0	1	0	1	0	0	0	0	0	0	0	0
gen. et sp. nov. 1	1	1	1	1	1	1	1	1	1	1	0	0
gen. et sp. nov. 2	1	0	1	0	0	0	0	1	1	0	0	0
<i>Dactylopsila</i> sp. 1	1	0	1	1	0	1	0	1	1	0	0	0
<i>Dactylopsila</i> sp. 2	0	0	0	0	0	0	0	1	0	0	0	0
Incerti sedis gen. et sp. nov.	1	0	0	1	0	0	0	1	1	0	0	0
<i>Acrobates</i> sp.	0	0	0	1	0	0	0	1	0	0	0	0
<i>Cercatetus</i> sp.	1	1	1	1	1	0	0	1	1	0	0	0
<i>Strigocuscus</i>	1	1	0	1	1	1	0	1	1	0	0	0
<i>Trichosurus</i> sp. 1	0	0	0	0	0	0	1	0	0	1	0	1
<i>Trichosurus</i> sp. 2	1	0	0	0	1	0	0	0	0	0	0	0
<i>Perameles</i> sp. 1	1	1	1	1	1	1	0	1	1	1	0	0
<i>Perameles</i> sp. 2	1	1	1	1	0	1	0	1	1	0	0	0
<i>Perameles bouganville</i>	0	0	0	0	0	0	1	0	0	0	1	0
<i>Isodon obesulus</i>	0	0	0	0	0	1	1	0	0	1	0	0
<i>Isodon</i> sp.	0	0	0	0	0	1	1	0	0	0	0	0
<i>Chaeropus ecaudatus</i>	0	0	0	0	0	0	1	0	0	0	0	0
<i>Macrotis lagotis</i>	0	0	0	0	0	0	1	0	0	0	0	0
perameloid gen. et sp. nov. 1	1	1	1	1	1	1	0	1	1	0	0	0

QML	1311H	1311CD	1313	1385	1384L	1384U	1312	1284	1284a	1420	Olsens	Present
perameloid gen. et sp. nov. 2	1	0	0	0	0	0	0	0	0	0	0	0
<i>Notomys</i> sp. 1	0	0	0	0	0	0	1	0	0	0	0	0
<i>Notomys</i> sp. 2	0	0	0	0	0	0	1	0	0	0	0	0
<i>Hydromys</i>	0	0	0	0	0	0	0	0	0	1	0	1
<i>Pseudomys</i>	1	1	1	1	1	1	1	1	1	1	1	1
<i>Rattus</i>	0	0	0	0	0	1	1	0	0	1	1	1
<i>Conilurus</i>	0	0	0	0	0	0	1	0	0	0	0	0
<i>Zyzomys</i>	1	1	0	1	0	0	1	0	0	0	0	0
<i>Leggadina</i>	0	0	0	0	0	0	1	0	0	0	1	0
<i>Uromys/Melomys</i>	1	1	1	1	1	1	0	1	1	1	0	0
<i>Pogonomys</i>	1	1	1	1	1	1	0	1	1	0	0	0
<i>Mesembriomys</i>	1	1	1	1	0	0	0	1	1	0	0	0
<b>Microchiropteran</b>	1	1	1	1	1	1	1	1	1	0	1	1
<i>Macroderma gigas</i>	1	1	1	1	1	1	1	1	1	0	1	1

Appendix 1. Small-sized mammalian fauna data matrix. 0 = Absent, 1 = Present.



VOLUME 51

PART 1

# MEMOIRS

OF THE

# QUEENSLAND MUSEUM

BRISBANE  
31 MAY 2005

© Queensland Museum

PO Box 3300, South Brisbane 4101, Australia  
Phone 06 7 3840 7555  
Fax 06 7 3846 1226  
Email [qmlib@qm.qld.gov.au](mailto:qmlib@qm.qld.gov.au)  
Website [www.qmuseum.qld.gov.au](http://www.qmuseum.qld.gov.au)

National Library of Australia card number  
ISSN 0079-8835

## NOTE

Papers published in this volume and in all previous volumes of the *Memoirs of the Queensland Museum* may be reproduced for scientific research, individual study or other educational purposes. Properly acknowledged quotations may be made but queries regarding the republication of any papers should be addressed to the Director. Copies of the journal can be purchased from the Queensland Museum Shop.

A Guide to Authors is displayed at the Queensland Museum web site [www.qmuseum.qld.gov.au/resources/resourcewelcome.html](http://www.qmuseum.qld.gov.au/resources/resourcewelcome.html)

**A Queensland Government Project**  
Typeset at the Queensland Museum

LATE PLEISTOCENE-HOLOCENE OCCURRENCE OF *CHAEROPUS* (PERAMELIDAE) AND *MACROTIS* (THYLACOMYIDAE) FROM QUEENSLAND. *Memoirs of the Queensland Museum* 51(1): 38. Recent collections of vertebrate remains from cave systems in central-eastern and north-eastern Queensland have yielded diverse small-sized mammalian taxa. Within these faunas, four perameloid genera are present and include species of *Isoodon*, *Perameles*, *Chaeropus* and *Macrotis*. The presence of *Perameles* and *Isoodon* in these deposits is not surprising because they occur at the localities in the present day. However, Hocknull (2005) and Price (2004) report on the most easterly extent of *Perameles bougainville*, a typically arid distributed taxon. In addition, the presence of *Macrotis* and *Chaeropus* significantly increases the easterly distributions of these distinctly arid-adapted taxa. Muirhead & Godthelp (1995) reported on fossil *Chaeropus ecaudatus* from Chillagoe, northeastern Queensland, considering the age of the material to be late Pleistocene. Hocknull (2005) reported late Pleistocene *Chaeropus ecaudatus* and *Macrotis lagotis* from Mount Etna, central eastern Queensland. A new locality has yielded a specimen of *Macrotis* Thomas, 1887 and is presented herein. The locality (QML1287) is considered to be Late Pleistocene - Holocene in age based on the subfossil preservation of the excavated specimens, distinctly modern associated fauna, and the lack of associated megafauna.

Family THYLACOMYIDAE (Bensley, 1903)

*Macrotis* sp. (Fig 1)

Locality. QML1287, 'Dodgey's Cave', Dosey Limestone Kart, Broken River Province, 120km NW Charters Towers.

**Description.** QMF41971 is a left M<sup>2</sup> with little ware, broken root base. Max. length, 4.66mm; ant. width, 3.42mm; post. width, 2.67mm. Bulbous, sub-rectangular tooth in occlusal aspect, bearing three distinct anterior cusps (protocone, paracone and conical stylar cusp '?B'); two distinct posterior cusps (metacone and conical stylar cusp '?D'). Metaconule absent. Open, dumbbell-shaped roots. Anterior cingulum present.

**Remarks.** Identification of the tooth as *Macrotis* was based on the massively inflated, rectangular-ovoid occlusal crown, dumbbell-shaped molar roots, absence of the metaconule and conical stylar cusps. Muirhead (1994) listed characteristics of the dentition for both species of *Macrotis*, *M. lagotis* and *M. leucura*. Unfortunately, comparative specimens of *M. leucura* were not available for study, therefore, verification of *M. leucura* requires additional specimens and a morphometric appraisal of both species' dentition. Figure 2 illustrates the distributions (recent and fossil) of *M. lagotis*, *M. leucura* and *Chaeropus ecaudatus*. This is the second record of *Macrotis* in the fossil record of Queensland.



FIG 1. QMF41971, LM<sup>2</sup> in occlusal view. Scale bar = 4mm.

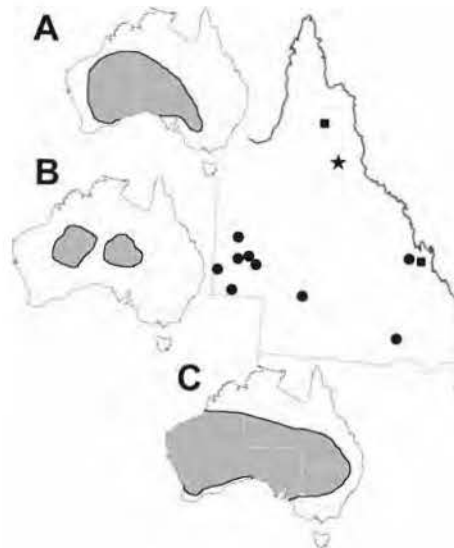


FIG 2. Distribution map of fossil and recent populations of A. *C. ecaudatus* (solid square), B. *M. leucura*, C. *M. lagotis* (solid circle) and *Macrotis* sp. (solid star). Recent bandicoot distributions from Strahan (1998).

The massive difference in the ranges of these three taxa when comparing late Pleistocene-Holocene to pre-European distributions indicates considerable contraction into the arid interior during the Holocene. A more detailed chronology of retraction is required to elucidate the factors influencing such a massive decline prior to European arrival, whether they be climatic, biotic and/or anthropogenic.

#### Literature Cited

- BENSLEY, B.A. 1903. On the evolution of the Australian Marsupialia: with remarks on the relationships of marsupials in general. *The Transactions of the Royal Society of London, Zoology* 9: 83-217.
- HOCKNULL, S.A. 2005. Ecological succession during the late Cainozoic of central eastern Queensland: extinction of a diverse rainforest community. *Memoirs of the Queensland Museum* 51: 39-122.
- MUIRHEAD, J. 1994. Systematics, evolution and palaeobiology of recent and fossil bandicoots (Peramelemorphia: Marsupialia). PhD thesis, University of New South Wales, Sydney. Unpubl.
- MUIRHEAD, J. & GODTHELP, H. 1995. Fossil bandicoots of Chillagoe (Northeastern Queensland) and the first known specimens of the Pig-Footed Bandicoot *Chaeropus* Ogilby, 1838 from Queensland. *Australian Mammalogy* 19:73-76.
- PRICE, G. J. 2004. Fossil bandicoots (Marsupialia: Peramelidae) and environmental change during the Pleistocene on the Darling Downs, southeastern Queensland, Australia. *Journal of Systematic Palaeontology* 2(4): 347-356.
- STRAHAN, R. (ed) 1998. *The Mammals of Australia*. (Australian Museum and Reed Books, Sydney).
- THOMAS, O. 1887. Description of a second species of rabbit-bandicoot (*Peragale*). *Annual Magazine of Natural History* 19 (5): 397-399.
- Scott A. Hocknull, *Queensland Museum, 122 Gerler Rd. Hendra, Queensland 4011, Australia ; 1 January 2005.*

VOLUME 51

PART 1

# MEMOIRS

OF THE

# QUEENSLAND MUSEUM

BRISBANE  
31 MAY 2005

© Queensland Museum

PO Box 3300, South Brisbane 4101, Australia  
Phone 06 7 3840 7555  
Fax 06 7 3846 1226  
Email [qmlib@qm.qld.gov.au](mailto:qmlib@qm.qld.gov.au)  
Website [www.qmuseum.qld.gov.au](http://www.qmuseum.qld.gov.au)

National Library of Australia card number  
ISSN 0079-8835

## NOTE

Papers published in this volume and in all previous volumes of the *Memoirs of the Queensland Museum* may be reproduced for scientific research, individual study or other educational purposes. Properly acknowledged quotations may be made but queries regarding the republication of any papers should be addressed to the Director. Copies of the journal can be purchased from the Queensland Museum Shop.

A Guide to Authors is displayed at the Queensland Museum web site [www.qmuseum.qld.gov.au/resources/resourcewelcome.html](http://www.qmuseum.qld.gov.au/resources/resourcewelcome.html)

**A Queensland Government Project**  
Typeset at the Queensland Museum

ADDITIONAL SPECIMENS OF *BOHRA* (MARSUPIALIA: MACROPODIDAE) FROM THE PLIOCENE OF QUEENSLAND. *Memoirs of the Queensland Museum* 51(1): 26. *Bohra paulae* Flannery & Szalay, 1982 was erected for a macropodine taxon considered to be a giant tree kangaroo. Holotype AMF62099, a large calcaneum, has relative dimensions found only in dendrolagin taxa (Flannery & Szalay, 1982; 84, Table 1) and relative calcaneal length (cl) to calcaneal tuberosity length (ctl) (Flannery & Szalay, 1982; 87, Table 3). Dentition in the type species is unknown.

Dawson (2004) described *Bohra wilkinsonorum* from the Pliocene, Chinchilla Sands, south east Queensland, based on a juvenile right maxillary fragment (QMF43277). Dentition shows features plesiomorphic within Dendrolagini and given its much larger size than *Dendrolagus*, it was considered to be *Bohra*. Recent discovery of *Bohra* from Chinchilla is intriguing because of a long history of collecting and abundance of macropodid material recovered (Rich, 1991; Hocknull, pers. obs.). Hocknull (2005) identified *Bohra* from the Early Pliocene of Mt Etna, central eastern Queensland, basing identification on a calcaneum which has relative dimensions similar to *B. paulae* but smaller in size. Audit of Chinchilla collections at the Queensland Museum was made to determine the additional material referable to members of the Dendrolagini. A calcaneum confirms the presence of *Bohra* in the Chinchilla Local Fauna. Abbreviations used in the text: AMF (Australian Museum Fossil); QMF (Queensland Museum Fossil).

**Description.** (Fig. 1) QMF49453; right calcaneum bearing a stout calcaneal tuberosity, broad astragular-fibular articulation, shallow and narrow calcaneal-cuboidal articulation, and broad rugose, plantar surface. Posterior medial and lateral margins of the tuberosity abraded, ventral portion of the calcaneal-cuboid articulation missing to the plantar surface. Dimensions cl: 43.64mm; ccaw: 18.72mm; ccch: 11.31mm (est.); calcaneal-astragular articulation length: 21.01mm.

**Remarks.** QMF49453 is similar in morphology to *Bohra paulae* except it is approximately 20% smaller. QMF49453 differs from *Bohra paulae* by a relatively narrower cca (e.g. ccch/ccaw; QMF49453, 0.604 versus *Bohra paulae*, 0.686

and species of *Dendrolagus* 0.601-0.702); and a relatively longer ct (e.g. ctl/cl; QMF49453, 0.481 versus *Bohra paulae*, 0.442 and species of *Dendrolagus* 0.46-0.512 (data from Flannery & Szalay, 1982)). QMF49453 is most similar to *Bohra* sp. (QMF51762) from Mt Etna but differs by a relatively narrower fibular-calcaneal articulation.

A low representation of *Bohra* within the Chinchilla Local Fauna (1 calcaneum, 1 maxilla) is apparent when compared to other macropodids (68 or more calcanea; 120 or more maxillae) from Chinchilla. This may explain why *Bohra* has not been previously recorded from Chinchilla. A greater representation of dendrolagin calcanea in the Early Pliocene Mt Etna Local Fauna is due to the abundance of *Dendrolagus* (Hocknull, 2005). Yet *Bohra* remains rare in both Queensland sites. Representation of *Bohra* from the type locality is unknown due to the uncertainty surrounding its stratigraphic context. Flannery & Szalay (1982) considered *Bohra paulae* not to be a rainforest taxon, however, it probably inhabited wooded areas due to its size and hypothesised arborealism. Dawson (2004) considered *Bohra* to be plesiomorphic to *Dendrolagus*, possessing a broad ecological tolerance and inhabiting a mosaic of vegetation including forest and open woodlands. Hocknull (2005) identified *Bohra* sp. as sympatric with *Dendrolagus* and other specialist taxa inhabiting rainforest. Considered together, *Bohra* represents a rare taxon with possible specialisations for arborealism, whilst possessing a broad habitat tolerance throughout the Plio-Pleistocene.

#### Literature Cited.

- DAWSON, L. 2004. A new Pliocene tree kangaroo species (Marsupialia, Macropodinae) from the Chinchilla Local Fauna, southeastern Queensland. *Alcheringa* 28: 267-273.
- FLANNERY, T.F. & SZALAY, F.S. 1982. *Bohra paulae*, a new giant fossil tree kangaroo (Marsupialia: Macropodidae) from New South Wales, Australia. *Australian Mammalogy* 5: 83-94.
- HOCKNULL, S.A. 2005. Ecological succession during the late Cainozoic of central eastern Queensland: extinction of a diverse rainforest community. *Memoirs of the Queensland Museum* 51: 39-122.
- RICH, T.H. 1991. Monotremes, placentals and marsupials: their record in Australia and its biases. Pp. 1005-1058. In Vickers-Rich, P., Monaghan, J.M., Baird, R.F., Rich, T.H. (eds) *Vertebrate palaeontology of Australasia*. (Pioneer Design Studio, Studio, Melbourne).

Scott A. Hocknull, Queensland Museum, 122 Gerler Rd. Hendra, Queensland 4011; 1 January 2005

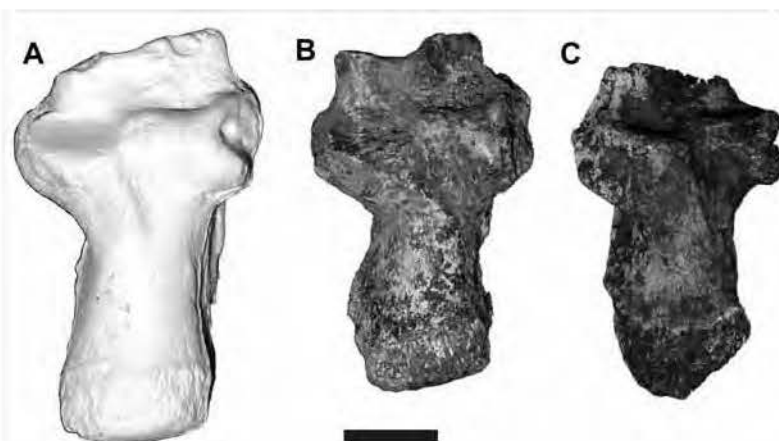


FIG 1. A, *Bohra paulae*, right calcaneum (cast of AMF62099). B, *Bohra* sp.; QMF51762, right calcaneum. C, *Bohra* sp.; QMF49453, right calcaneum. Scale bar = 10mm.

# High diversity Pleistocene rainforest Dasyurid assemblages with implications for the radiation of the dasyuridae

JONATHAN CRAMB,<sup>1</sup>\* SCOTT HOCKNULL<sup>2</sup> AND GREGORY E. WEBB<sup>1</sup>

<sup>1</sup>*School of Natural Resource Sciences, Queensland University of Technology GPO Box 2434, Brisbane, Qld 4001, Australia (Email: j2.cramb@student.qut.edu.au), and* <sup>2</sup>*Geosciences, Queensland Museum, Brisbane, Queensland, Australia*

**Abstract** It is commonly accepted that dasyurids (Marsupialia: Dasyuridae) radiated in the late Miocene or early Pliocene in response to a drying trend in Australia's climate as evidenced from the high diversity of dasyurids from modern arid environments compared with Miocene rainforest assemblages. However, mid-Pleistocene dasyurid assemblages from cave deposits at Mt Etna, Queensland are more diverse than any previously known from rainforest habitats. New taxa will be described elsewhere, but include three new genera as well as new species of *Dasyurus*, *Antechinus* and *Phascogale*. Comparison of dasyurids from Mt Etna sites that are interpreted as rainforest palaeoenvironments with fossil and extant assemblages indicate that they are at least as diverse as those from modern arid environments. Thus Neogene diversification of dasyurids occurred in both arid and rainforest habitats, but only the former survived continuing aridification. Hence, aridification cannot be invoked for the diversification of all dasyurid lineages.

**Key words:** dasyurid, extinction, Mt Etna, Pleistocene, rainforest.

## INTRODUCTION

The diversification of mammalian lineages in the fossil record has commonly been linked to environmental change. Climate has a powerful influence on the biota, and climatic changes in geological time have been invoked as drivers of both faunal diversification and extinction (Clemens *et al.* 1989; Janis 1993; Archer *et al.* 1999; Long *et al.* 2002; Dawson & Dawson 2006; Johnson 2006). In this way, a global cooling trend during the Neogene promoted the radiation of grazing macropodine kangaroos in Australia but also caused the decline of forest-adapted folivores, such as pilkipildrids, miralinids and pseudocheirids (Archer *et al.* 1994, 1999; Long *et al.* 2002; Archer & Hand 2006). Dasyurids (Marsupialia: Dasyuridae) have been touted as an example of one Australian lineage that was able to capitalize on the cooling, drying climate and successfully colonize the developing arid zone (Wroe 1996; Blacket *et al.* 1999; Crowther & Blacket 2003; Archer & Hand 2006; Johnson 2006).

Extant dasyurid assemblages are generally most diverse in arid regions (Fisher & Dickman 1993; Dickman 2003). However, the oldest definite dasyurid fossils are known from early Miocene rainforest deposits at Riversleigh, north-western Queensland, Australia, where they are low in diversity. The oldest fossils of

extant genera date to the early Pliocene (Wroe 1999; Wroe & Muirhead 1999) and include the genera *Sminthopsis*, *Planigale*, *Antechinus*, and possibly *Dasycercus* and *Phascomurexia* (Dawson *et al.* 1999; Archer *et al.* 2006; Van Dyck unpub. 1996). The early Pliocene dasyurid genera are found in a range of palaeohabitats, from the interpreted rainforest habitats of the Hamilton Local Fauna, in southern Australia, to the more open, drier habitats of the Rackham's Roost Local Fauna, in northern Australia. Hence, many extant dasyurid genera were established in a variety of habitats by the early Pliocene. This distribution, coupled with the drying trend in Australia's climate beginning in the late Miocene and intensifying throughout the Pleistocene, has led to the conclusion that dasyurids radiated during the Neogene in response to increasing aridity in Australia's climate (Wroe 1996; Blacket *et al.* 1999; Crowther & Blacket 2003; Johnson 2006).

Several mid-Pleistocene fossil assemblages from cave sites at Mt Etna near Rockhampton, Queensland, Australia have been interpreted as representing closed rainforest communities (Hocknull 2005; Hocknull *et al.* 2007) on the basis of faunal assemblages. Faunal indicators of closed rainforest conditions include a diverse guild of arboreal folivores and rainforest specialist genera such as *Dactylopsila*, *Pseudochirops*, *Pseudochirulus*, *Phalanger*, *Uromys* and *Pogonomys*; and a diverse range of frog taxa, including several that are rainforest-restricted (e.g. *Kyarranus*, *Lechriodus*, *Nyctimystes* and microhylids), (Hocknull 2005; Hocknull

\*Corresponding author.

Accepted for publication September 2008.

*et al.* 2007). Hocknull (2005, p. 108) considered that these sites represent nonseasonal, mesothermal, angiosperm-dominant rainforest with emergent gymnosperms with a minor grassy understory. Dasyurid assemblages from these sites proved to be unexpectedly diverse, thus questioning the commonly accepted hypothesis of dasyurid radiation outlined above.

The purpose of this paper is to provide a preliminary description of dasyurid assemblages from representative sites in the Mt Etna area and demonstrate their unusual nature and implications for ecological biogeography.

## METHODS

### Setting

The geological context of the Mt Etna Caves (23°09'24"S 150°26'58"E) has been summarized by Hocknull (2005) and Hocknull *et al.* (2007). Some caves acted as pit traps, and most deposits also received input from the feeding activities of owls and carnivorous ghost bats (*Macroderma gigas*). Published analyses (Hocknull 2005; Hocknull *et al.* 2007) identified sites representing a range of different ages and interpreted palaeoenvironments. Uranium-series dating of speleothems was used to establish maximum and minimum ages of the deposits [see Hocknull *et al.* (2007) for discussion of methods]. Palaeoenvironmental interpretations indicate a transition from closed rainforest environments represented from sites ranging in age from >500 000 years ago (ka) to 280 ka, to open, dry and perhaps arid environments in more recent sites (205 ka to recent) (Hocknull *et al.* 2007). Sites selected for this study were chosen to represent different palaeoenvironments, as interpreted by Hocknull (2005) (Table 1). We have tested the hypothesis that the most diverse dasyurid assemblages would occur in sites interpreted as representing drier habitats.

### Preparation and systematics

Consolidated cave sediments were processed by digestion in acetic acid, and loose cave sediments were sieved. Residues were picked for bones and teeth. Dasyurids were identified on the basis of dental morphology and size after comparisons with published literature and recent specimens held by the Queensland Museum and Australian Museum. Identifications of taxa were based on easily distinguishable morphological characters. Thus diversity is unlikely to be inflated because of excessive taxonomic splitting.

Dasyurid names follow Strahan and Conder (2007); Long *et al.* (2002). Full taxonomic descriptions will be published elsewhere. Specimens are held by the Queensland Museum and are listed in Appendix S1.

### Statistical analysis

The minimum number of individuals of each taxon was calculated based on the largest number of any one element (e.g. mandibles) attributed to the taxon. Differing sample sizes between sites made use of diversity indices untenable. For this reason diversity was compared using rarefaction analysis (Krebs 1989). Rarefaction allows the diversity of different samples to be compared when sample sizes differ. It does this by estimating the expected diversity of smaller samples based on that seen in larger samples.

Bias was accounted for where it could be reasonably assumed to exist. For example, *Sarcophilus lanianus* was not found in all sites. This is probably because of taphonomic bias, as it is the largest dasyurid and is not preyed upon by owls or ghost bats. Thus, it may have been excluded preferentially from accumulations formed largely by flying predators (particularly QML1456). The relatively small number of taxa present in all sites (10 or less) makes the addition of one species potentially significant in terms of species richness. Thus, *Sarcophilus* was removed from the analysis of all sites to eliminate this potential bias.

**Table 1.** Sites with dasyurid assemblages analysed in this work. Palaeoenvironmental interpretations from Hocknull (2005) and dates from Hocknull *et al.* (2007)

Site name	QML no.	Age (ka)	Interpretation
H Deposit	1311 H	>330	Closed rainforest
Speaking Tube Cave	1313	>280	Closed rainforest, most recent rainforest site at Mt Etna
Elephant Hole Cave	1312	205–170	Open dry grassland/woodland possibly with remnant rainforest
Colluseum Chamber	1456	Late Pleistocene-Holocene	Grassland/woodland, probably similar to modern environment



Rarefaction analysis was performed using PAST 1.54 palaeontological statistics software (Hammer *et al.* 2001).

## RESULTS

### Species richness

Taxon counts are presented in Table 2. Dasyurid diversity was greatest in QML1311 H in regards to raw species richness and in having the greatest number of genera. The number of species remained stable through QML1313, 1312 and 1456, but declined in the modern (extant) fauna (Fig. 1). The number of genera did not change greatly over the same time interval. Comparisons of species richness of the study sites and other fossil and extant assemblages are shown in Figure 1. Note that species richness of QML1311 H was similar to that of some arid assemblages (Fig. 2).

### Rarefaction analysis

QML1456 had by far the most specimens, but analysis showed that the other three study sites plotted above the 95% confidence interval in terms of having higher diversity (Fig. 3). This suggests that the QML1456 assemblage was the least diverse of the four sites. However, more than one-half of the specimens from QML1456 were assigned to only two species of *Smin-*

*thopsis*. These species may have been favoured prey items of the owls responsible for the deposit, thus introducing bias into the assemblage. No such bias is evident in the other study sites, so an analysis of the QML1313 assemblage was also undertaken. QML1312 plots within the 95% confidence interval of QML1313, suggesting that it was not significantly more diverse. However, QML1311 H plots above the confidence interval, suggesting that it was the most diverse assemblage among the study sites. Thus QML1311 H was the most diverse assemblage, while QML1456 was the least diverse. Assemblages from QML1312 and QML1313 fall in between, but could not be resolved further. The extant assemblage appears to be less diverse still, but could not be meaningfully compared with the fossil assemblages because of differences in survey technique.

## DISCUSSION

The Mt Etna sites show a temporal pattern of decreasing diversity, manifest at both the specific and generic level. QML1311 H represents a rich assemblage associated with a closed rainforest environment. QML1313 is essentially the same assemblage, but has been impoverished by the loss of several species (such as cf. *Micromurexia habbema*). This rainforest assemblage lost additional species, although it was still recognisable by the time of QML1312, but the diversity of the assemblage in the site was bolstered by the

**Table 2.** Minimum numbers of individuals of each species in the study sites

Dasyurid species	1311H	1313	1312	1456	Extant
<i>Antechinus flavipes</i>	0	0	0	12	1
<i>Antechinus</i> sp. nov. 1	3	25	0	0	0
<i>Antechinus</i> sp. nov. 2	23	24	7	0	0
<i>Dasyurus hallucatus</i>	0	0	0	0	1
<i>Dasyurus maculatus</i>	0	0	0	1	0
<i>Dasyurus ?viverrinus</i>	0	0	0	1	0
<i>Dasyurus</i> sp. nov.	2	1	3	0	0
<i>Phascogale topoatafa</i>	0	0	3	2	1
<i>Phascogale</i> sp. nov.	5	1	0	0	0
<i>Planigale maculate</i>	0	0	5	0	1
<i>Planigale tenuirostris</i>	2?	0	3	8	0
<i>Planigale</i> sp.	0	3	0	0	0
<i>Sarcophilus laniarius</i>	1	0	1	0	0
<i>Sminthopsis macroura</i>	0	0	8	180	0
<i>Sminthopsis 'murina'</i>	19	18	13	120	1
dasyurid cf. <i>Micromurexia habbema</i>	1	0	0	0	0
dasyurid (gen. et sp. nov. A)	2	0	0	0	0
dasyurid (gen. et sp. nov. C)	1	1	0	0	0
Total MNI	59	73	43	324	NA
Total no. of taxa	10	7	8	7	5

MNIs were not known for the extant fauna so these are listed as one. *Sminthopsis 'murina'* could not be separated from either *S. murina* or *S. leucopus*.

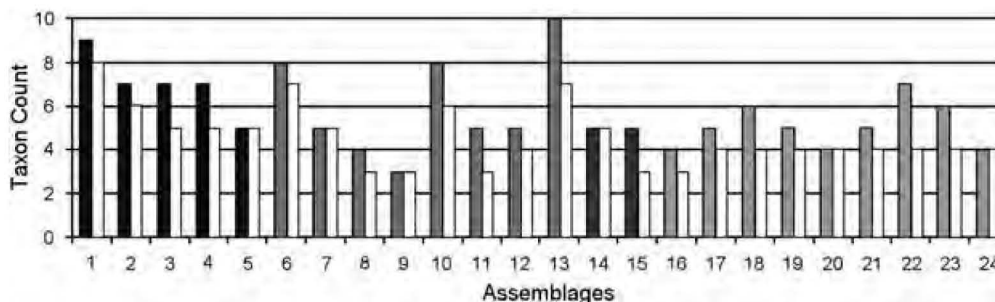


**Fig. 1.** Species and genera counts for 24 fossil and extant dasyurid assemblages. Filled bars: species richness; open bars: genus richness. Sites are grouped into the following categories (demarcated by different shading): Mt Etna assemblages (1–5), arid assemblages (6–13), rainforest assemblages (14–15), and non-arid assemblages (sclerophyll forest and woodland, 16–24). *Sarcophilus* has been removed from all assemblages. Assemblages are: 1, QML1311 H; 2, QML1313; 3, QML1312; 4, QML1456; 5, modern assemblage, Mt Etna; 6, D Cave, Flinders Ranges; 7, Big Morrow, Flinders Ranges; 8, Black's Point Sinkhole level C; 9, Thylacoleo Caves; 10, Sandringham Station; 11, Fowlers Gap; 12, Koonchera; 13, Uluru Kata-Tjuta National Park; 14, Upper Site, Riversleigh; 15, Atherton Tableland; 16, Big Sink, Wellington Caves; 17, Pyramids Cave reddish fraction; 18, Flowerpot Cave; 19, Russenden Cave; 20, Henschke Fossil Cave; 21, Cathedral Fossil Chamber upper fan, Naracoorte; 22, Cathedral Cave, Wellington; 23, Nettle Cave; 24, Devil's Lair layer O. Additional site information is given in Appendix 2. Data sources for figures 1 and 2 are referenced in Appendix S2.

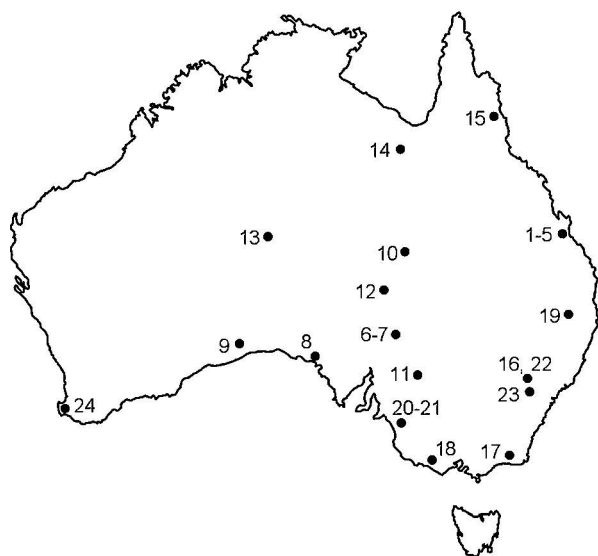


**Fig. 2.** Map of extant and fossil dasyurid sites used in Fig. 1.

addition of arid-adapted forms (such as *Sminthopsis macroura*). The mixture of taxa present in older sites with newly arrived arid-adapted species supports the contention that QML1312 represents a palaeoenvironment which included forest refugium proximal to the cave entrance, surrounded by xeric habitat (Hocknull *et al.* 2007). By the late Pleistocene (represented by QML1456) all rainforest taxa had been replaced by woodland or arid-adapted dasyurids.

The discovery of a diverse dasyurid assemblage associated with a closed rainforest environment has several important implications. Few dasyurids are known from the Oligo-Miocene deposits at Riversleigh

(Archer *et al.* 1994, 2006), and the majority of them do not appear to be closely related to any extant group. Therefore, the modern dasyurid fauna (i.e. all extant dasyurid species) evolved since that time. It has been suggested that this massive radiation was a response to continental aridification (Wroe 1996; Blacket *et al.* 1999; Crowther & Blacket 2003; Johnson 2006). The high diversity of arid-adapted extant dasyurids supports this view. Although it is generally agreed that arid assemblages contain the highest diversity of dasyurids, there is little consensus as to how many species may coexist. Morton (1982) stated that the most diverse arid zone assemblages contain as many as five species. However, Dickman (1989) claimed that as many as nine species of small carnivorous marsupials may coexist in the arid zone. This apparent confusion may result from differences in surveying techniques. Ecological surveys relying on trapping may not sample an entire assemblage because of the low abundance of dasyurids in arid environments (Morton 1982). Additionally, extant assemblages may have been greatly altered by anthropogenic impacts (primarily since European arrival) and thus may not represent the 'original' assemblage. Anthropogenic factors likely to have adversely affected dasyurid diversity in the late Holocene include habitat modification, introduction of exotic species and direct persecution.

Rather than traditional survey methods, such as trapping, analysis of owl feeding roost deposits seems to be a more effective method for the survey of small mammal communities (e.g. all but one of the assemblages shown in Fig. 1 that contain seven or more species are fossil or subfossil assemblages derived from owl roosts). Unfortunately, this does not inform the researcher about microhabitat use in the wider region, a feature of dasyurid assemblages that has been com-



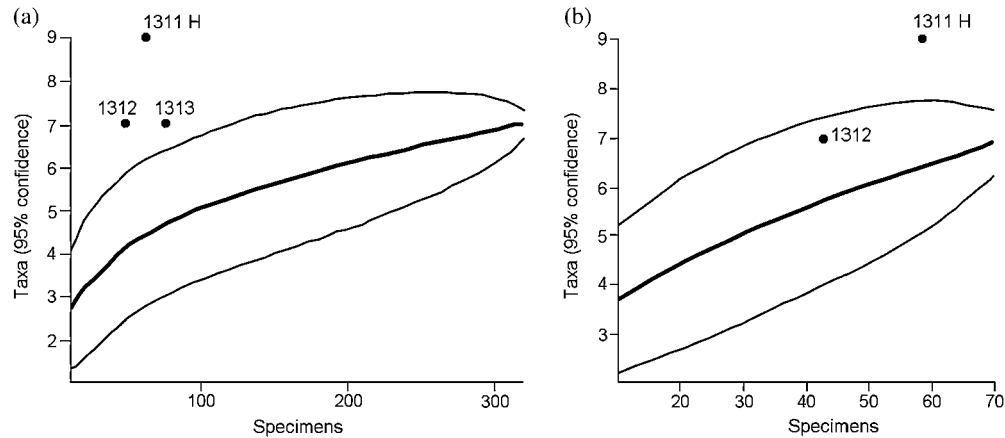


**Fig. 3.** Rarefaction plots of (a) QML1456 and (b) QML1313 with 95% confidence intervals. For numerical data see Appendix 3. Note that QML1311 H displays greater diversity than all other sites, while QML1313 and 1312 are more diverse than QML1456 but can not be further separated.

monly found to increase species richness (Morton 1982). An owl may hunt in multiple nearby habitats, effectively ‘surveying’ more species than a researcher focusing on a single habitat. Most fossil sites that contain dasyurids are owl feeding roosts, and this can make comparisons between fossil and extant assemblages difficult. The possibility thus arises that the diverse dasyurid assemblages from Mt Etna were sourced from multiple adjacent palaeohabitats. However, we consider this unlikely, as the other fossil faunas from Mt Etna are generally diverse assemblages of rainforest-adapted species (Hocknull 2005; Hocknull *et al.* 2007). This would seem to indicate that closed rainforest was extensively distributed across the region. Therefore, it is likely that most of the fossil faunas were sourced from the same palaeohabitat (with the exception of QML1312, which seems to represent an assemblage sampled from both relictual rainforest and dry, open habitat species). Regardless, all deposits at Mt Etna were produced by similar processes (pitfall trapping and the actions of flying predators), and most are from the same cave system making them easily comparable.

The diverse assemblages of dasyurids in mid-Pleistocene sites at Mt Etna suggest that the late Tertiary dasyurid radiation produced diverse assemblages in both closed rainforest and arid environments. Thus, the initial post Riversleigh dasyurid radiation may not have been associated with aridification. The current situation in which most dasyurid species are arid-adapted may be an artefact of extinction, caused when the majority of rainforest-adapted species disappeared in the mid-late Pleistocene as those habitats contracted to the present.

Dasyurids are mostly generalised small predators, yet some degree of resource partitioning must occur to allow multiple species to coexist. This seems to be

accommodated mainly through interspecific size differences and intraspecific sexual dimorphism (Fox, 1982; Dickman 1986a,b,c; Jones 1997, 2003; Jones and Barmuta 1998, 2000). The study sites showed a pattern of size classes. Most sites have: one very large dasyurid (*Sarcophilus* sp. where present), one large dasyurid (*Dasyurus*), one medium-sized dasyurid (commonly a species of *Phascogale*), two sizes of small dasyurid (the larger a species of *Antechinus*, the smaller a species of *Sminthopsis*) and a very small dasyurid (*Planigale* sp.). However, some sites contained more than one species occupying the same size class. *Antechinus* sp. nov. 1 and cf. *Micromurexia habbema* were approximately the same size in QML1311 H. Also in QML1311 H, two undescribed genera were of similar size. Two species of *Dasyurus* were present in QML1456 (although they differ somewhat in size). QML1312 had two species of *Planigale* that differ only slightly in size. The two species of *Sminthopsis* in QML1312 and QML1456 were essentially the same size. Shared size classes in QML1312 can be explained by the likelihood that it represents a mixed assemblage derived from differing proximal palaeohabitats. Likewise, QML1456 probably contains fauna from both grassland and open forest/woodland, thus explaining the presence of two similarly sized species of *Sminthopsis*. Those in QML1311 H are more difficult to interpret. It is possible that species separated into microhabitats to avoid competition, as has been shown to occur in some modern assemblages (Morton 1982). This possibly indicates that mid-Pleistocene rainforest communities exhibited tighter niche packing than is commonly observed in extant dasyurid assemblages.

Assemblage diversity can also be increased by the presence of specialist taxa. These are rare among dasyurids, the most obvious example being *Sarcophilus*, a specialist carrion-feeder (Jones 1995). Some

deposits at Mt Etna (although none of the four study sites) contained a new genus of very small dasyurid with reduced dentition (Hocknull 2005). This may represent a specialist taxon, although its exact niche is currently unknown.

## CONCLUSIONS

Mid-Pleistocene dasyurid assemblages from Mt Etna are unusual in several aspects. Most importantly they include high diversity assemblages that were apparently adapted to closed rainforest environments. Results presented here indicate that currently accepted hypotheses regarding the late Tertiary radiation of the Dasyuridae in response to increasing aridity are too simplistic. Identification of a plausible driving force behind this radiation is therefore a subject for future research. The current situation of relatively high diversity in arid habitats reflects loss of rainforest habitats more than initial diversification in arid habitats.

## ACKNOWLEDGEMENTS

We thank H. Janetzki, S. V. Dyke and S. Ingleby for access to comparative material. Research was funded by Australian Research Council grant LP0453664, the Queensland Museum and Cement Australia as part of an Honours research project by J. C.

## REFERENCES

- Archer M. & Hand S. J. (2006) The Australian marsupial radiation. In: *Evolution and Biogeography of Australasian Vertebrates* (eds J. R. Merrick, M. Archer, G. M. Hickey & M. S. Y. Lee) pp. 575–646. Auscipub, Oatlands.
- Archer M., Hand S. J. & Godthelp H. (1994) *Riversleigh*. Reed, Sydney.
- Archer M., Arena D. A., Bassarova M. *et al.* (1999) The evolutionary history and diversity of Australian mammals. *Aust. Mammal.* **21**, 1–45.
- Archer M., Arena D. A., Bassarova M. *et al.* (2006) Current status of species-level representation in faunas from selected fossil localities in the Riversleigh World Heritage Area, Northwestern Queensland. *Alcheringa Special Issue 1*, 1–17.
- Blacket M. J., Krajewski C., Labrinidis A., Cambron B., Cooper S. & Westerman M. (1999) Systematic relationships within the Dasyurid Marsupial Tribe Sminthopsini – a multigene approach. *Molecular Phylogenetics and Evolution* **12**, 140–55.
- Clemens W. A., Richardson B. J. & Baverstock P. R. (1989) Biogeography and phylogeny of the metatheria. In: *Fauna of Australia. Mammalia 1B* (eds D. W. Walton & B. J. Richardson) pp. 527–48. Australian Government Publishing Service, Canberra.
- Crowther M. S. & Blacket M. J. (2003) Biogeography and speciation in the Dasyuridae: why are there so many kinds of dasyurids? In: *Predators with Pouches: The Biology of Carnivorous Marsupials* (eds M. Jones, C. Dickman & M. Archer) pp. 124–32. CSIRO Publishing, Collingwood.
- Dawson L., Muirhead J. & Wroe S. (1999) The Big Sink Local Fauna: a lower Pliocene mammalian fauna from the Wellington Caves complex, Wellington, New South Wales. *Rec. West. Aust. Mus. (Suppl 57)*, 265–90.
- Dawson T. J. & Dawson L. (2006) Evolution of arid Australia and consequences for vertebrates. In: *Evolution and Biogeography of Australasian Vertebrates*. (eds J. R. Merrick, M. Archer, G. M. Hickey & M. S. Y. Lee) pp. 51–70. Auscipub, Oatlands.
- Dickman C. R. (1986a) An experimental manipulation of the intensity of interspecific competition: effects on a small marsupial. *Oecologia (Berlin)* **70**, 536–43.
- Dickman C. R. (1986b) A experimental study of competition between two species of dasyurid marsupials. *Ecol. Monogr.* **56**, 221–41.
- Dickman C. R. (1986c) Niche compression: two tests of an hypothesis using narrowly sympatric predator species. *Aust. J. Ecol.* **11**, 121–34.
- Dickman C. R. (1989) Patterns in the structure and diversity of marsupial carnivore communities. In: *Patterns in the Structure of Mammalian Communities* (eds D. W. Morris, Z. Abramsky, B. J. Fox & M. R. Willig) pp. 241–51. Texas Tech University, Lubbock.
- Dickman C. R. (2003) Distributional Ecology of Dasyurid Marsupials. In: *Predators with Pouches: The Biology of Carnivorous Marsupials* (eds M. Jones, C. Dickman & M. Archer) pp. 318–31. CSIRO Publishing, Collingwood.
- Fisher D. O. & Dickman C. R. (1993) Diets of insectivorous marsupials in arid Australia: selection for prey type, size or hardness? *J. Arid Environ.* **25**, 397–410.
- Fox B. J. (1982) A Review of Dasyurid Ecology and Speculation on the role of Limiting Similarity in Community Organization. In: *Carnivorous Marsupials* (ed. M. Archer) pp. 97–116. Royal Zoological Society of New South Wales, Mosman.
- Hammer Ø., Harper D. A. T. & Ryan P. D. (2001) PAST: paleontological statistics software package for education and data analysis. *Palaeontol. Electron.* **4**, 9.
- Hocknull S. A. (2005) Ecological succession during the late Cainozoic of central eastern Queensland; extinction of a diverse rainforest community. *Mem. Queensl. Mus.* **51**, 39–122.
- Hocknull S. A., Zhao J.-x., Feng Y.-x. & Webb G. E. (2007) Responses of Quaternary rainforest vertebrates to climate change in Australia. *Earth Planet. Sci. Lett.* **264**, 317–31.
- Janis C. M. (1993) Tertiary mammal evolution in the context of changing climates, vegetation, and tectonic events. *Annu. Rev. Ecol. Syst.* **24**, 467–500.
- Johnson C. (2006) *Australia's Mammal Extinctions: A 50000 Year History*. Cambridge University Press, Melbourne.
- Jones M. (1995) Tasmanian devil. In: *Mammals of Australia* (ed R. Strahan) pp. 82–4. Australian Museum, Reed Books, Sydney.
- Jones M. E. (1997) Character displacement in Australian Dasyurid carnivores: size relationships and prey size patterns. *Ecology* **78**, 2569–87.
- Jones M. E. (2003) Convergence in ecomorphology and guild structure among marsupial and placental carnivores. In: *Predators with Pouches: the Biology of Carnivorous Marsupials* (eds M. Jones, C. Dickman & M. Archer) pp. 285–96. CSIRO publishing, Melbourne.

- Jones M. E. & Barmuta L. A. (1998) Diet overlap and relative abundance of sympatric dasyurid carnivores: a hypothesis of competition. *J. Anim. Ecol.* **67**, 410–21.
- Jones M. E. & Barmuta L. A. (2000) Niche differentiation among sympatric Australian dasyurid carnivores. *J. Mammal.* **81**, 434–47.
- Krebs C. J. (1989) *Ecological Methodology*. Harper & Row, New York.
- Long J., Archer M., Flannery T. & Hand S. (2002) *Prehistoric Mammals of Australia and New Guinea*. University of New South Wales Press, Sydney.
- Morton S. R. (1982) Dasyurid marsupials of the Australian Arid Zone: an ecological review. In: *Carnivorous Marsupials* (ed. M. Archer) pp. 117–30. Royal Society of New South Wales, Mosman.
- Strahan R. & Conder P. (2007) *Dictionary of Australian and New Guinean Mammals*. CSIRO Publishing, Collingwood.
- Wroe S. (1996) *Muribacinus Gadiyuli*, (Thylacinidae: Marsupialia), a very Plesiomorphic Thylacinid from the Miocene of Riversleigh, Northwestern Queensland, and the Problem of Paraphyly for the Dasyuridae (Marsupialia). *J. Paleontol.* **70**, 1032–44.
- Wroe S. (1999) The geologically oldest dasyurid, from the Miocene of Riversleigh, North-west Queensland. *Palaeontology* **42**, 501–27.
- Wroe S. & Muirhead J. (1999) Evolution of Australia's marsupicarnivores: Dasyuridae, Thylacinidae, Myrmecobiidae,

*Dasyuromorphia incertae sedis* and *Marsupialia incertae sedis*. *Aust. Mammal.* **21**, 10–1.

## SUPPORTING INFORMATION

Additional Supporting Information may be found in the online version of this article:

**Appendix S1.** Rarefaction data

**Appendix S2.** Dasyurid assemblages used in Figures 2 and 3: No.s 10–12 were modified by the addition of *Dasyurus geoffroyi*. No. 15 was modified by the addition of *D. hallucatus* and *D. maculatus*. These species should be present in the assemblages but have been excluded by historical local extinctions or sampling focus on smaller species. *Sarcophilus* has been removed from all assemblages

Please note: Wiley-Blackwell are not responsible for the content or functionality of any supporting materials supplied by the authors. Any queries (other than missing material) should be directed to the corresponding author for the article.

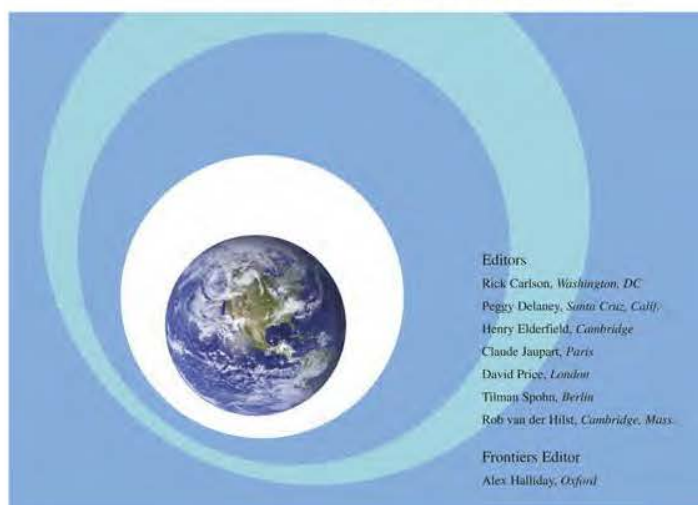


Volume 264, Issues 1–2

15 December 2007

ISSN 0012-821X

# EARTH & PLANETARY SCIENCE LETTERS



#### Editors

Rick Carlson, *Washington, DC*

Peggy Delaney, *Santa Cruz, Calif.*

Henry Elderfield, *Cambridge*

Claude Jaupart, *Paris*

David Price, *London*

Tilman Spohn, *Berlin*

Rob van der Hilst, *Cambridge, Mass.*

#### Frontiers Editor

Alex Halliday, *Oxford*

This article was published in an Elsevier journal. The attached copy is furnished to the author for non-commercial research and education use, including for instruction at the author's institution, sharing with colleagues and providing to institution administration.

Other uses, including reproduction and distribution, or selling or licensing copies, or posting to personal, institutional or third party websites are prohibited.

In most cases authors are permitted to post their version of the article (e.g. in Word or Tex form) to their personal website or institutional repository. Authors requiring further information regarding Elsevier's archiving and manuscript policies are encouraged to visit:

<http://www.elsevier.com/copyright>



# Responses of Quaternary rainforest vertebrates to climate change in Australia

Scott A. Hocknull<sup>a,\*</sup>, Jian-xin Zhao<sup>b</sup>, Yue-xing Feng<sup>b</sup>, Gregory E. Webb<sup>c</sup>

<sup>a</sup> *Geosciences, Queensland Museum, PO Box 3300 Brisbane, Qld 4000, Australia*

<sup>b</sup> *Radiogenic Isotope Laboratory, Centre for Microscopy and Microanalysis, The University of Queensland, Qld 4072, Australia*

<sup>c</sup> *School of Natural Resource Science, Queensland University of Technology, GPO Box 2434, Brisbane, Qld 4001, Australia*

Received 14 June 2007; received in revised form 3 October 2007; accepted 3 October 2007

Available online 10 October 2007

Editor: H. Elderfield

## Abstract

A new middle Pleistocene vertebrate fossil record from eastern Australia, dated by U disequilibrium series, records the first Quaternary record of an Australian tropical rainforest fauna. This exceptionally rich fauna underwent extinction after a long period of relative faunal stability, spanning several glacial cycles, and persisted probably until 280 000 years ago. Some time between 280 000 and 205 000 years ago the rainforest fauna was replaced by a xeric-adapted fauna. Since that time, the xeric-adapted fauna was replaced by a mesic-adapted fauna which was established by the Holocene. This is the first vertebrate faunal evidence in Australia of the middle Pleistocene Mid-Brunhes Climatic Event (MBE), a major climatic reorganisation that led to increased aridity in northern Australia from around 300 000 years ago. Several independent palaeoclimate proxies suggest that the climatic shift to aridity was due to increased climatic variability and weakened northern monsoons, which may be manifested in the extinction of the aseasonal rainforest fauna and its replacement by an arid-adapted fauna. We extend the temporal ranges of several taxa from the Pliocene into the middle Pleistocene. We also reveal a longer palaeobiogeographic connection of rainforest taxa and lineages shared between New Guinea and Australia than was previously thought and show that their extinction on mainland Australia occurred sometime after 280 000 years ago.

© 2007 Elsevier B.V. All rights reserved.

**Keywords:** Quaternary rainforest; palaeoclimate; U–Th dating; megafauna; Australia

## 1. Introduction

Understanding the influence of climate change on the biogeography, evolution and extinction of faunas is critical for development of conservation strategies for

modern habitats under threat from climate change and human disturbance (Archer et al., 1991; Moritz et al., 2005). This is of particular importance in Australia, where intensified aridity has shaped large portions of the continent and where habitats, such as tropical rainforests, are considered to be under threat of extinction from climate change and human impact (Thomas et al., 2004; Williams et al., 2003; Williams and Hilbert, 2006).

In spite of progressively more detailed Quaternary palaeoclimatic and palynological records in the Australian

\* Corresponding author. Tel.: +61 7 3406 8346; fax: +61 7 3406 8355.

E-mail addresses: [scott.hocknull@qm.qld.gov.au](mailto:scott.hocknull@qm.qld.gov.au) (S.A. Hocknull), [j.zhao@uq.edu.au](mailto:j.zhao@uq.edu.au) (J. Zhao), [y.feng@uq.edu.au](mailto:y.feng@uq.edu.au) (Y. Feng), [ge.webb@qut.edu.au](mailto:ge.webb@qut.edu.au) (G.E. Webb).



region, there remains a fundamental gap in our knowledge of faunal response to past climate change. This is primarily due to the scarcity of accurately dated, temporally extensive fossil faunas that sample a variety of palaeoecologies. Australia, in particular, has a paucity of chronometrically dated sites and a complete absence of a Quaternary rainforest vertebrate fossil record.

The post-middle Miocene rainforest vertebrate fossil record from the Australopapuan region is extremely poor, possibly reflecting the onset of progressive continent-wide aridity in the late Miocene (McGowran et al., 2000; Archer et al., 1999; Greenwood and Christophel, 2005). A single vertebrate locality (Hamilton Local Fauna) from south-eastern Australia indicates the only mainland rainforest record dated to the Pliocene (Turnbull and Lundelius, 1970). Restriction of the Quaternary rainforest vertebrate fossil record to sites in New Guinea, even though Quaternary vertebrate fossil sites are found across mainland Australia, has led to the proposition that Australian rainforest habitats were close to their present refugial status before the end of the Pliocene (Archer et al., 1995).

In the absence of a Quaternary fossil record, studies of modern Australian rainforest faunas have resorted to combine palaeoclimate records inferred from pollen and isotope records (Winter, 1997; Nix and Switzer, 1991) with phylogeographies and molecular clocks inferred from genetic studies (Moritz et al., 2005; Schneider and Williams, 2005) to interpret the affects of Quaternary climate cycles on faunal biogeography.

Without direct evidence from a fossil record, these interpretations and hypotheses cannot be adequately tested. Furthermore, it is impossible without a fossil record to accurately infer the presence of extinct taxa, their ecological roles, and the mitigating circumstances that led to their extinction, climate or otherwise. The purpose of this paper is to document a globally rare palaeofauna (e.g. tropical rainforest), via a suite of Quaternary fossil deposits from a single locality in central-eastern Queensland, Australia, which span an interval of intense climate change and fill a major temporal gap in our knowledge of vertebrate faunas from northern Australia.

## 2. Methods

### 2.1. Geologic settings

Caves formed within isolated Devonian limestone massifs north of Rockhampton, central-eastern Queensland, were systematically surveyed for bone-bearing sediments and breccias (Fig. 1). Vertical and horizontal joints, dictated by the gross orientation of limestone

strata and structural features, have produced very deep cave systems with vertical shaft entrances and large chambers (Shannon, 1970). Limestone quarrying on the northwest face of Mt Etna has exposed in cross-section the deep sediment-filled chambers of at least two cave systems, exposing extensive and abundant fossil remains and associated speleothems. Additional cave deposits occur in nearby karst, including Limestone Ridge, Olsen's Caves and Karst Glen (Fig. 1). Systematic collections and site descriptions are reported elsewhere (Hocknull, 2005) with additional information and amendments presented herein. Site sedimentology and taphonomy is summarised in Appendix A.

### 2.2. Thermal ionization mass spectrometry (TIMS) uranium-series dating

TIMS uranium-series dating was undertaken using analytical procedures described elsewhere (Zhao et al., 2001), except the known  $^{236}\text{U}/^{233}\text{U}$  ratio in a  $^{229}\text{Th}$ – $^{233}\text{U}$ – $^{236}\text{U}$  mixed spike was used for mass fractionation correction for the unknown samples.  $^{234}\text{U}/^{238}\text{U}$  and  $^{230}\text{Th}/^{238}\text{U}$  activity ratios of the samples are normalised to the corresponding ratios measured for the secular-equilibrium HU-1 standard and their ages calculated using half-lives of 75,380 years ( $^{230}\text{Th}$ ) and 244,600 years ( $^{234}\text{U}$ ).

Sites chosen for dating include those with minimal transportation and reworking of sediments and with available speleothem, either basal to, within, or capping the fossil deposit. Capping or basal flowstones yielding ages within the dating window were used to bracket deposit ages, with basal flowstone dates representing maximum ages and capping flowstone dates representing the minimum ages of the enclosed deposit. Ages outside the dating window were assigned an age of >500 thousand years (ka). Broken flowstones and straws incorporated within the deposits are considered to be maximum ages; the youngest of these from a given deposit was used to establish maximum bracket ages of that deposit.

Where speleothem was not available, bone, teeth, shell, and calcite fillings of these, were analysed. Calcite fillings in bones and teeth yield minimum ages of the fossils because the calcite grows within the specimens post deposition. The bones, teeth and shell are considered to yield minimum ages because U is taken up subsequent to deposition, and the system is most likely to be closed in respect to U loss after uptake. This interpretation was tested and substantiated by the dating of both the bone and calcite fillings within the bone, where we show that calcite yielded an older age than the

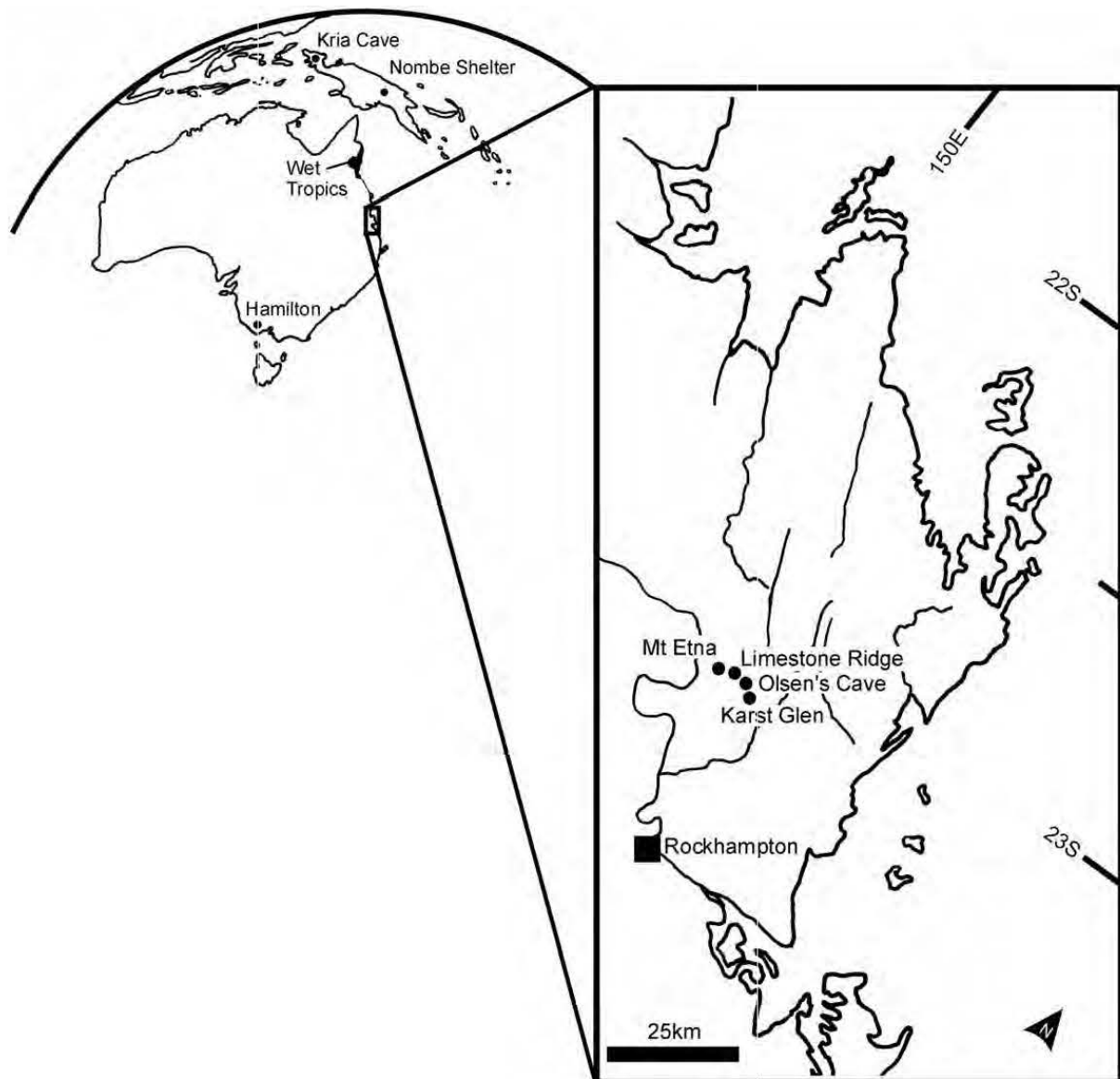


Fig. 1. Location of the post-Miocene Australopapuan rainforest vertebrate fossil record in relation to the present day Wet Tropics rainforests of north-eastern Australia, including the early Pliocene Hamilton fauna from south-eastern Australia, the Quaternary faunas from New Guinea and the eastern Australian Quaternary fauna presented herein.

bone (Table 1). Thus, U uptake in the bone occurred during or continued after calcite deposition. Therefore, the oldest age recovered using all of these materials was taken as the minimum age of the deposit.

### 2.3. Faunal analysis

Only non-volant vertebrate species of mammals, frogs and agamid lizards were used as proxies for habitat type. Fossils sharing generic and specific-level identity with living taxa were assumed to be representative of the habitat types and climates presently occupied by extant taxa and therefore are used as habitat proxies. All fossils used in the analyses are considered to represent species derived from

proximal habitats to the fossil deposit; based primarily on the restricted foraging ranges of the two predator accumulators present in the deposits (Owl (*Tyto* sp.) and Ghost Bat (*Macroderma gigas*)) (Hocknull, 2005), and the pit-trap accumulation mode for non-volant, large-sized taxa. Cave entrances were all located high on exposed karst, with a single exception (Olsen's Cave), however, none of the sites possess fluviially transported sediments.

Analyses of faunal diversity and similarity include only mammalian taxa with body weight less than 3 kg (e.g. equal to, or smaller than, *Pseudochirops*), due to the body-size bias apparent in deposits derived predominantly from predator accumulators. Amounts of sediment sorted for vertebrate remains varied from site to site, ranging

Table 1  
Representative U/Th dates for fossil sites at Mt Etna, central-eastern Queensland

QML	Locality	Sample name	Description	Age interpretation	( <sup>230</sup> Th/ <sup>232</sup> Th)	Corr. <sup>230</sup> Th age (ka)	±2σ
Olsen's	Honey Moon Suite	ROK-07	<i>Petrogale</i> incisor	Min. age	33.7	6.3	0.2
Olsen's	Icicle Chamber	OC-07	Calcite cement	Close to real	19.3	7.6	0.2
1312	Elephant Hole Cave	ROK 10	Snail shell	Min. age	16.3	169	9
1312	Elephant Hole Cave	QML1312-6	Broken straw	Max. age	17.3	205	4
1313	Speaking Tube Cave	ROK02-4	Flowstone	Min. age	66.9	283	9
1313	Speaking Tube Cave	ROK02-5	Flowstone	Min. age	352	283	12
1383	Unit A	ROK F	Flowstone	Max. age of Unit A	31.0	419	28
1311	Deposit C/F contact	ROK04/04	Flowstone	Max. age of C	16.0	326	22
1311	Deposit C/F contact	ROK04/15	Flowstone	Mid flowstone	13.8	347	26
1311	Deposit C/F contact	ROK04/46	Flowstone	Min. age of F	24.6	432	54
1311	H deposit	ROK20-1 bone	Macropod bone	Min. age	5470	216	4
1311	H deposit	ROK20-4 cal	Calcite filling in bone	Min. age	749	454	48
1384	Lower Unit	ROK27 bone	Macropod bone	Min. age	1278	267	5
1384	Lower Unit	ROK27 cal	Calcite filling in bone	Min. age	38.6	332	14
1284	Mini Cave Layer A	MC/01	Capping flowstone	Min. age	92.6	284	9
1284	Layer B	MC-02 mid	Oldest flowstone	Max. age	22.3	484	85
1284	Layer J	MC-10	Youngest flowstone	Min. age	6.8	447	74

Note: Ratios in parentheses are activity ratios calculated from the atomic ratios. The ages are calculated using Ken Ludwig's Isoplot/EX program. Corr. and uncorr. denote corrected and uncorrected. The corrected <sup>230</sup>Th ages and initial (<sup>234</sup>U/<sup>238</sup>U) ratios include a negligible to small correction for non-radiogenic Th using average crustal <sup>232</sup>Th/<sup>238</sup>U atomic ratio of 3.8±1.9 (<sup>230</sup>Th, <sup>234</sup>U and <sup>238</sup>U are assumed to be in secular equilibrium).

from less than 0.1 m<sup>3</sup> to more than 4 m<sup>3</sup>. Hence, relative abundances were not analysed (Appendix A).

Pair-wise, Euclidean cluster analysis of mammalian presence/absence data was utilised to determine the similarity of fossil faunas to one another and to known modern and fossil faunas from a broad range of habitat types. Generic-level mammal lists were generated from the literature and included taxa from hydric, mesic and xeric habitats, such as; tropical rainforest, dry vine forests, open-forests, open woodlands, heathlands, shrublands, grasslands and chenopod shrublands. Vegetation classifications follow Webb and Tracey (1981) for closed-forest vegetation (e.g. tropical rainforest, dry vine forest) and Specht (1981) for all other open vegetation types. Cluster analyses were performed using PAST software (Hammer et al., 2001).

### 3. Results

#### 3.1. Faunal ages

Sites within the study area that have produced dated faunas range in age from ~7 ka to greater than 500 ka, at the limit of the uranium-series technique employed. Table 1 summarises site ages with a full listing and imagery available as supplementary materials in Appendix A.

Queensland Museum Locality (QML)1284 and QML1284a, considered to be the two oldest faunas, are

located on Limestone Ridge, east of Mt Etna. QML1284 has been dated based on several *in situ* flowstone layers associated within the fossil beds. Layer B is stratigraphically the oldest and Layer J the youngest, with calcite fillings from within bone derived from the fossil bed in between flowstone layers G and H. Such dates, especially those for purer flowstone samples with higher U contents and higher <sup>230</sup>Th/<sup>232</sup>Th activity ratios, (e.g. MC-02mid and MC-09) and thus more precise results, approximate the application limit (~500 ka) of the TIMS U-series dating method. The analytical precisions for the calcite fillings are poor due to small sample sizes and extremely low U, and thus the age results are only indicative, but they are consistent with the ~500 ka assignment for the site. The capping flowstone MC-01, which covers patches of the underlying fossil deposit, yields an age of 284±9 ka, suggesting that the fossil-bearing horizons were exposed in cross-section prior to ~280 ka. Subsequently a capping flowstone formed over this wall, which has once again been eroded to expose the underlying bone-bearing sediments. Fauna was collected in blocks from the wall and floor having come from the area bracketed by Layers B and G. QML1284a is located on open karst above and to the northwest of QML1284. QML1284a is considered to be older than QML1284 as it occurs in weathered karst terrain outside the main entrance to QML1284 indicating an older collapsed chamber (Hocknull, 2005).



QML1311H yielded a minimum age of  $454 \pm 48$  ka based on calcite infilling of bone and is directly below QML1311J which yielded a minimum age of  $337 \pm 15$  ka. Unfortunately the speleothem associated with QML1311H was too contaminated by detritus or decalcified to retrieve a reliable basal age. However, it is suspected to be close to the limits of U-series technique ( $\sim 500$  ka) because the speleothem of QML1311H contacts QML1311F, which has a minimum age of  $432 \pm 54$  ka.

A minimum age of QML1383A was obtained from a flowstone that divides the lower unit A from B (ROK F) and yielded a basal age of  $419 \pm 28$  ka. The base of the flowstone is inter-laminated within the top sediments of QML1383A. Therefore, speleothem deposition occurred as sedimentation was slowing down, and thus QML1383A fauna is considered to be close to the age of the flowstone's base.

Two sites were deposited at least 330 000 years ago: QML1311J and QML1384LU. QML1311J and QML1384LU are separate deposits located on the western side of Mt Etna. Both sites have yielded minimum ages close to 330–340 ka based on calcite fillings in bone (e.g. ROK24, ROK27 cal).

One site located on the western side of Mt Etna was deposited after 330 ka (QML1311C/D), QML1311C/D contacts with QML1311F deposit via a large continuous

basal flowstone layer. The maximum age of QML1311C/D is based on the minimum age ( $326 \pm 22$  ka) of the basal flowstone (ROK04/04), which is also supported by stratigraphically consistent dates for ROK04/15 and ROK04/46 (Table 1).

A capping flowstone of QML1313 provides a minimum age of  $283 \pm 7$  ka based on the weighted mean of two dates (ROK02-4 and 5). The base of the flowstone is inter-laminated with the uppermost centimetres of the bone-bearing sediment. Therefore, the flowstone is considered to have begun deposition as sedimentation rates decreased and not a considerable time after that. Thus, the fauna of QML1313 is considered to date close to 280 000 years old.

QML1312 was dated using bone, teeth, shell and incorporated pieces of broken flowstone and straw. The oldest age derived from bone, teeth and shell provided a minimum age for the deposit, whereas the youngest dated broken flowstone pieces and straw provided a maximum age. Thus the deposit dates between  $169 \pm 9$  ka (snail shell, ROK-10) and  $205 \pm 4$  ka (calcite straw, QML1312-6).

Floor sediments (0–10 cm) from within Icicle and Honey Moon Suite Chambers (Olsen's Cave) yielded a diverse subfossil fauna. Calcite cement was used to date the Icicle Chamber deposit, returning an age of  $7.6 \pm 0.2$  ka (OC-07), whilst macropod enamel returned an age of  $6.3 \pm 0.2$  ka (ROK-07) for the Honey Moon Suite

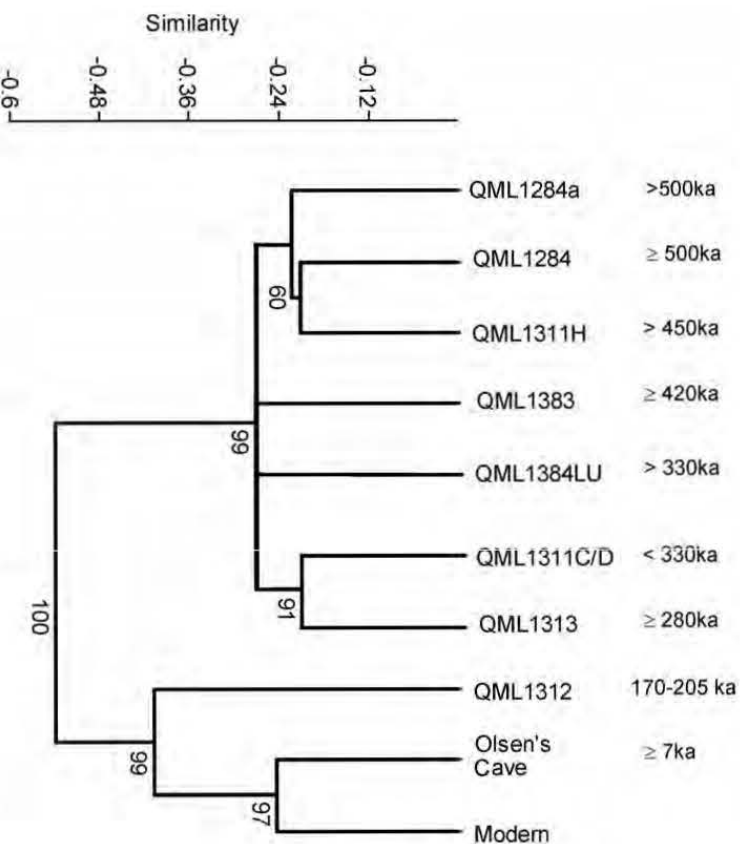


Fig. 2. Chronometrically constrained, bootstrapped, similarity cluster analysis of dated fossil and modern faunas of the present study.

Chamber deposit. Both deposits are considered to be Holocene in age.

### 3.2. Site faunal groupings

To test whether the chronology of deposits was consistent with the fossil faunas within them, a chronometrically constrained, bootstrapped, cluster analysis was performed using the dated faunas (Fig. 2). The analysis returned very strong support (99% bootstrap value) for two main clusters, those sites that are older than ~280 ka, and those sites that are younger than ~205 ka. Within the cluster of sites older than ~280 ka, there was very strong support (91%) for the position of deposits aged between ~280 ka and ~330 ka and good support (60%) for the position of deposits considered to be between ~450 ka and ~500 ka. The remaining sites, QML1384LU, QML1383A and QML1284a, were not faunally supported in their chronological position. This lack of support may reflect the presence of transitional faunas in the case of QML1383A where the age of this deposit is better defined, or incorrect chronological placement in the case of QML1384LU and QML1284a where we only have minimum ages. Within the sites younger than ~205 ka there was very strong support for the entire chronological sequence.

Similarities between fossil and modern faunas are summarised in a cluster analysis (Fig. 3). Three main

faunal groupings are observed for modern habitats; 1) Faunas occurring in New Guinean and northern Australian hydric habitats (tropical rainforest), 2) Faunas occurring in Australian mesic habitats (dry vine forests to woodlands), and 3) Faunas occurring in Australian xeric habitats (open woodlands, arid grasslands and shrublands). Fossil faunas from the present study cluster amongst each of these three groupings.

All of the dated sites older than ~280 ka cluster together and with the New Guinean and northern Australian tropical rainforest faunas. Several fossil taxa of frogs, lizards and mammals are presently restricted to rainforest environments and are considered to be rainforest specialists (Table 2), which strongly supports the previous contention that these faunas represent a tropical rainforest habitat (Hocknull, 2005). The high diversity of mammalian arboreal folivores and hylid frog species reflects a palaeoecology with complex vegetative structure, whilst the presence of microhylid frogs and freshwater turtles indicates permanent water bodies (Hocknull, 2005).

A single fauna (QML1312), dated to between 205 and 170 ka, clusters with xeric habitats of central and southern Australia. These arid and semi-arid faunas occur in a great variety of habitats (e.g. Open woodlands, hummock grasslands, tussock grasslands and chenopod shrublands). Several of the taxa present in this deposit are considered to be arid-adapted taxa that specialise in arid habitats (Table 2). Contrary to the dominant arid/semi-arid signal, a

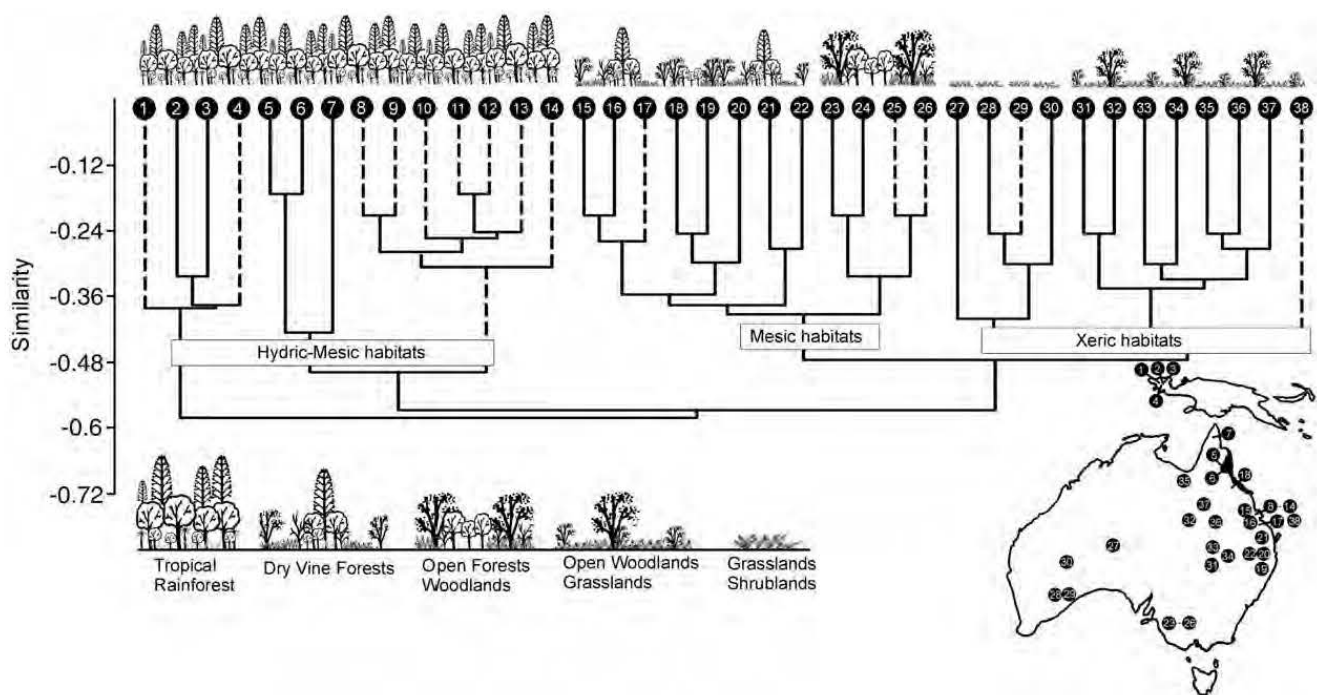


Fig. 3. Similarity cluster analysis of modern and fossil faunas associated with hydric (1–14), mesic (15–26) and xeric (27–38) habitats. Dashed lines indicate fossil faunas. Site locations and references are provided as a supplementary table in Appendix A.

Table 2

Middle Pleistocene fossil taxa considered to be rainforest or arid specialists with the annual precipitation range\* of their closest living relatives

Rainforest taxa			
Taxon	Closest living relative	Rainforest location	Annual precipitation (mm)*
<i>Cercartetus</i> sp.	<i>Cercartetus caudatus</i>	WT/New Guinea (NG)	1879–3060
<i>Dactylopsila</i> sp. 1	<i>Dactylopsila palpator</i>	NG	1091–5544
<i>Dactylopsila</i> sp. 2	<i>Dactylopsila kambuayai</i>	NG (Holocene)	Montane
<i>Dendrolagus</i> sp. 1	<i>Dendrolagus matschiei</i>	NG	1261–3644
<i>Dendrolagus</i> sp. 2	<i>Dendrolagus</i> spp.	NG	1261–3644
<i>Dendrolagus</i> sp. 3	<i>Dendrolagus</i> spp.	NG	1261–3644
<i>Dendrolagus</i> sp. 4	<i>Dendrolagus</i> spp.	NG	1261–3644
<i>Hypsilurus</i> sp.	<i>Hypsilurus</i> spp.	NG/WT/Southeast QLD (SEQ)	1074–5427
<i>Kyarranus</i> spp.	<i>Kyarranus</i> spp.	SEQ	1092–2110
<i>Lechriodus</i> spp.	<i>Lechriodus</i> spp.	SEQ/NG	1301–2074
Microhylids	Microhylids	WT/NG	1017–4005
<i>Nyctimystes</i> spp.	<i>Nyctimystes</i> spp.	WT/NG	1099–6795
<i>Petauroides</i> sp. 1	<i>Petauroides ayamaruensis</i>	NG (Holocene)	Montane
<i>Petauroides</i> sp. 2	<i>Petauroides ayamaruensis</i>	NG (Holocene)	Montane
<i>Petauroides</i> sp. 3	<i>Petauroides ayamaruensis</i>	NG (Holocene)	Montane
<i>Phalanger</i> sp. 1	<i>Phalanger gymnotis</i>	NG	2119–6580
<i>Phalanger</i> sp. 2	<i>Phalanger</i> spp.	NG	1706–6580
<i>Pogonomys</i> sp.	<i>Pogonomys</i> spp.	WT/NG	1675–5692
<i>Pseudochirops</i> sp. 1.	<i>Pseudochirops</i> spp.	WT/NG	1261–5544
<i>Pseudochirops</i> sp. 2	<i>Pseudochirops</i> spp.	NG	1261–5544
<i>Pseudochirops</i> sp. 3	<i>Pseudochirops</i> spp.	NG	1261–5544
<i>Pseudochirulus</i> sp. 1.	<i>Pseudochirulus canescens/mayeri</i>	NG	2722–5544
<i>Pseudochirulus</i> sp. 2	<i>Pseudochirulus forbesi</i>	NG	1296–5544
<i>Pseudochirulus</i> sp. 3	<i>Pseudochirulus</i> spp.	WT/NG	1296–5544
<i>Thylogale</i> sp. (small)	<i>Thylogale christenseni</i>	NG (Holocene)	Montane
<i>Uromys</i> sp.	<i>Uromys hadrourus</i>	WT	1211–3436
Arid taxa			
Taxon	Closest living relative		Annual precipitation (mm) <sup>a</sup>
<i>Chaeropus ecaudatus</i>	<i>Chaeropus ecaudatus</i>		144–333
<i>Macrotis lagotis</i>	<i>Macrotis lagotis</i>		132–722
<i>Notomys</i> spp.	<i>Notomys</i> spp.		129–1273
<i>Perameles bouganville</i>	<i>Perameles bouganville</i>		208–391
<i>Planigale</i> sp. 2	<i>Planigale tenurostris</i>		140–743
<i>Pogona</i> sp.	<i>Pogona minor/michelli</i>		163–996
<i>Sminthopsis macroura</i>	<i>Sminthopsis macroura</i>		129–996
<i>Tympanocryptis</i> sp.	<i>Tympanocryptis cephalus</i>		181–539

<sup>a</sup> Annual precipitation range (mm) was determined for closest living relatives by using DIVA-GIS 5.2 bioclimatic software (Hijmans et al., 2005) and taxon distribution data taken from OZCAM BioMaps online databases (OZCAM community, 2006).

proportion of the fauna does not occur in these dry regions today and are indicative of more mesic environments. For example, a single calcaneum represents a species of *Dendrolagus*, an arboreal rainforest-dwelling macropod, and as it is unlikely to be reworked, the taxon was rare but present in the surrounding habitat. The presence of this, and other arboreal taxa, indicates that treed habitat occurred proximal to the cave entrance, possibly in the form of a refugium.

Two fossil faunas (Icicle Chamber and Honey Moon Suite Chamber) cluster with the modern mesic habitat in the study area, which includes grassy open-forests with

refugial dry vine forests (semi-evergreen vine-thickets). This is not surprising as both deposits are considered to be Holocene in age.

### 3.3. Faunal succession

The middle Pleistocene is characterised by two distinct faunas; 1) a tropical rainforest fauna that existed at least between 500 ka and ~280 ka ago, spanning three glacial cycles from Marine Isotope Stage (MIS) 8 through MIS13, and 2) a xeric-adapted fauna with refugial elements, dated to 205–170 ka ago. Sites



considered to represent the latest Pleistocene are yet to be adequately dated and will be the focus of future work. Holocene sites are characterised by a typically modern mesic-adapted fauna.

Approximately 50% reduction in species richness of small to medium-sized mammal species was observed between the older rainforest faunas (>280 ka; 28–35 spp.) and those of the Holocene and present day (16–12 spp. respectively) (Fig. 4a). This reduction in species richness is not considered to be an artefact of taphonomy or collection size because deposits with similar accumulation modes and collection sizes show markedly different species richness [e.g., QML1284 (30 spp.) vs. Icicle Chamber (16 spp.)].

Furthermore, the middle Pleistocene deposits that preserve large to megafaunal-sized mammalian taxa illustrate a similar massive reduction in species richness compared to the present day fauna at Mt Etna. The reduction includes the total extinction of megafaunal species (>100 kg) and a reduction of more than 50% species richness for both large-sized (3–15 kg) and very large-sized (15–100 kg) mammalian species.

Although the overall species richness of mammals decreased by more than 50% since the middle Pleistocene to present day levels, the loss and replacement of taxa was at times proportionally much greater. Loss of taxa in deposits dated between >500 ka and ~280 ka was low, varying between 0 and 13%, whilst replacement with new taxa was similarly low (0–14%), suggesting a relatively low rate of faunal turnover and a stable level of species richness for over 200 000 years (Fig. 4a). Between

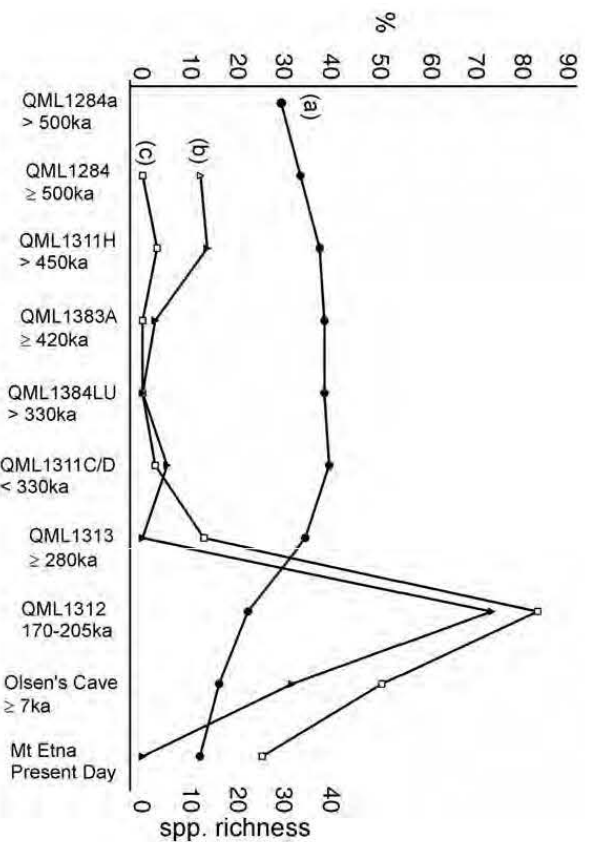


Fig. 4. Species richness and faunal turnover through time for medium and small-sized mammal species for the study area. (a) species richness (count of spp.), (b) percentage of new species, (c) percentage of species loss.

~280 ka and ~205 ka major faunal reductions occurred with the loss of over 80% of small to medium-sized mammalian taxa (Fig. 4c). Losses also occurred in frog and lizard faunas with local extinction of the lizard *Hypsilurus* and the frogs, *Crinia*, *Emmabatrachus*, *Kyarranus*, *Lechriodus*, *Nyctimystes* and microhylids. Replacement of new mammalian taxa was proportionally lower than species losses, but it was still very high at over 75% (Fig. 4b), which accounts for the overall decrease in species richness from 33 to 21 spp. Frog species richness decreased overall with replacement by some new forms, such as *Cyclorana* and *Neobatrachus*. Lizard species richness increased with appearance of new xeric-adapted taxa, including *Amphibolurus*, *Tympanocryptis* and *Pogona*.

The local extinction of more than 65% of small to medium-sized mammalian species occurred between the youngest middle Pleistocene fauna (205–170 ka) and the Holocene fauna (<10 ka). Replacement with new species was low, approximately 38%, which accounts for another drop in overall species richness from 21 to 13 spp. (Fig. 4a). Frog and lizard species richness remained relatively stable over this period of time, but the three agamids present at 205–170 ka were replaced by three others, *Pogona barbata*, *Chlamydosaurus kingii* and *Diporiphora bilineata*.

### 3.4. Speleothem formation

U–Th isotopic data for all speleothems (e.g., *in situ* and broken flowstones and straws, and calcite fillings)

are listed in Appendix A, where a  $^{230}\text{Th}/^{238}\text{U}$  vs.  $^{234}\text{U}/^{238}\text{U}$  evolution diagram is illustrated. The data from the Mt Etna sites show that (1) the growth of all such speleothems occurred mainly during interglacials or interstadials, consistent with relatively wetter climatic conditions during those times; and (2) 23 (or more than 68%) of the 34 dated Pleistocene speleothem samples (randomly collected) are older than 300 ka, implying that climate conditions were wetter and more favourable for speleothem development prior to 300 ka. Indeed, most of the >300 ka speleothems are either *in situ* or broken flowstones that are volumetrically more significant than those younger than 300 ka, which are mainly calcite fillings or capping flowstones.

## 4. Discussion

### 4.1. Implications for biocorrelation

The present sites previously were interpreted as a suite of early Pliocene, Plio-Pleistocene and Holocene sites, and the rainforest assemblages were considered to be Pliocene in age on the basis of biocorrelation (Hocknull, 2005). Biocorrelation of these sites was based primarily on the very few chronometrically dated Pliocene sites in Australia. Since that time, several of the Pliocene-aged taxa that were once considered robust markers are now recorded in younger early Pleistocene sites (Piper, 2007).

Likewise, the new radiometric dates presented here extend the temporal ranges of several taxa into the middle Pleistocene. In particular, we present the youngest Australian records for the following taxa: *Pseudokoala* (Early Pliocene–early Pleistocene), '*Petauroides*' (Early Pliocene) *Kurrabi* (Pliocene), *Thylacoleo hilli* (Miocene–early Pleistocene), *Palorchestes* cf. *P. pickeringi* (Early Pliocene–early Pleistocene) and *Protemnodon* cf. *P. devisi* (Pliocene). In addition this study fills a significant gap in the Australian fossil record of extant vertebrate lineages with a fossil record previously restricted to the Oligo-Miocene and Pliocene; such as *Dactylopsila*, *Dendrolagus*, *Pseudochirops*, *Kyarranus* and *Lechriodus*. Moreover, we provide the first fossil record in Australia for several extant lineages; such as *Pseudochirulus*, *Pogonomys*, *Uromys*, *Mesembriomys*, *Hypsilurus* and *Nyctimystes*.

One important implication of these results is that other sites in Australia that have been dated only on the basis of biocorrelation may have incorrectly assigned ages. Importantly, it illustrates the need for, 1) a more robust biocorrelative synthesis of the temporal and geographic ranges of Australian Neogene vertebrate taxa and 2) more extensive chronometric dating of Neogene sites.

### 4.2. Responses of middle Pleistocene vertebrate faunas to climate change

Understanding the responses of middle Pleistocene vertebrate communities to Quaternary climate change is of crucial importance when attempting to infer the affects of late Pleistocene climate change on fauna without the superimposition of anthropogenic activities. Well-dated and faunally rich middle Pleistocene faunas from Australia are rare with three exceptions—two localities from southern Australia, Naracoorte (Moriarty et al., 2000; Prideaux et al., 2007b) and Nullarbor Caves (Prideaux et al., 2007a) and the present study area (Fig. 5).

The Cathedral Cave record from the Naracoorte Caves World Heritage Area, South Australia, is of particular importance because it spans a similar time-frame to the present study (Prideaux et al., 2007b). Demonstrated faunal stability at Naracoorte during the middle Pleistocene suggests that the influence of glacial cycles at that time were not severe enough to cause extinctions there. However, it was shown that relative abundance and community composition did fluctuate with climate (Prideaux et al., 2007b). Furthermore, a large proportion of the modern non-megafaunal taxa found in the area today are the same taxa found in the middle Pleistocene deposits, suggesting that faunal stability continued throughout the middle and late Pleistocene to the present day. These results inferred a faunal resilience to climate change in southern Australia. This trend is also suggested for the fossil record from the Nullarbor Caves (Prideaux et al., 2007a). We corroborate this faunal stability in the faunal cluster analysis where middle Pleistocene faunas from the Naracoorte and Nullarbor caves cluster most closely with their respective modern day faunas (Fig. 3).

The faunal succession documented in southern Australia contrasts with that documented here, where after an interval of faunal stability for over 200 000 years, a major faunal turnover occurred, which replaced the majority of taxa present in the area prior to 280 ka. Since before 500 ka until ~280 ka, the Mt Etna area possessed a diverse tropical rainforest habitat. However, between ~280 ka and ~205 ka large proportions of the vertebrate fauna were driven locally extinct, being replaced by a xeric-adapted fauna. The presence of xeric-adapted taxa indicates a marked drop in precipitation during the faunal turnover at Mt Etna, presumably a greater reduction in precipitation than what had occurred during previous glacials. Interestingly, this period of faunal turnover and reduced precipitation approximates a period of aridity observed at Naracoorte (270–220 ka) indicated by both speleothems and local faunal

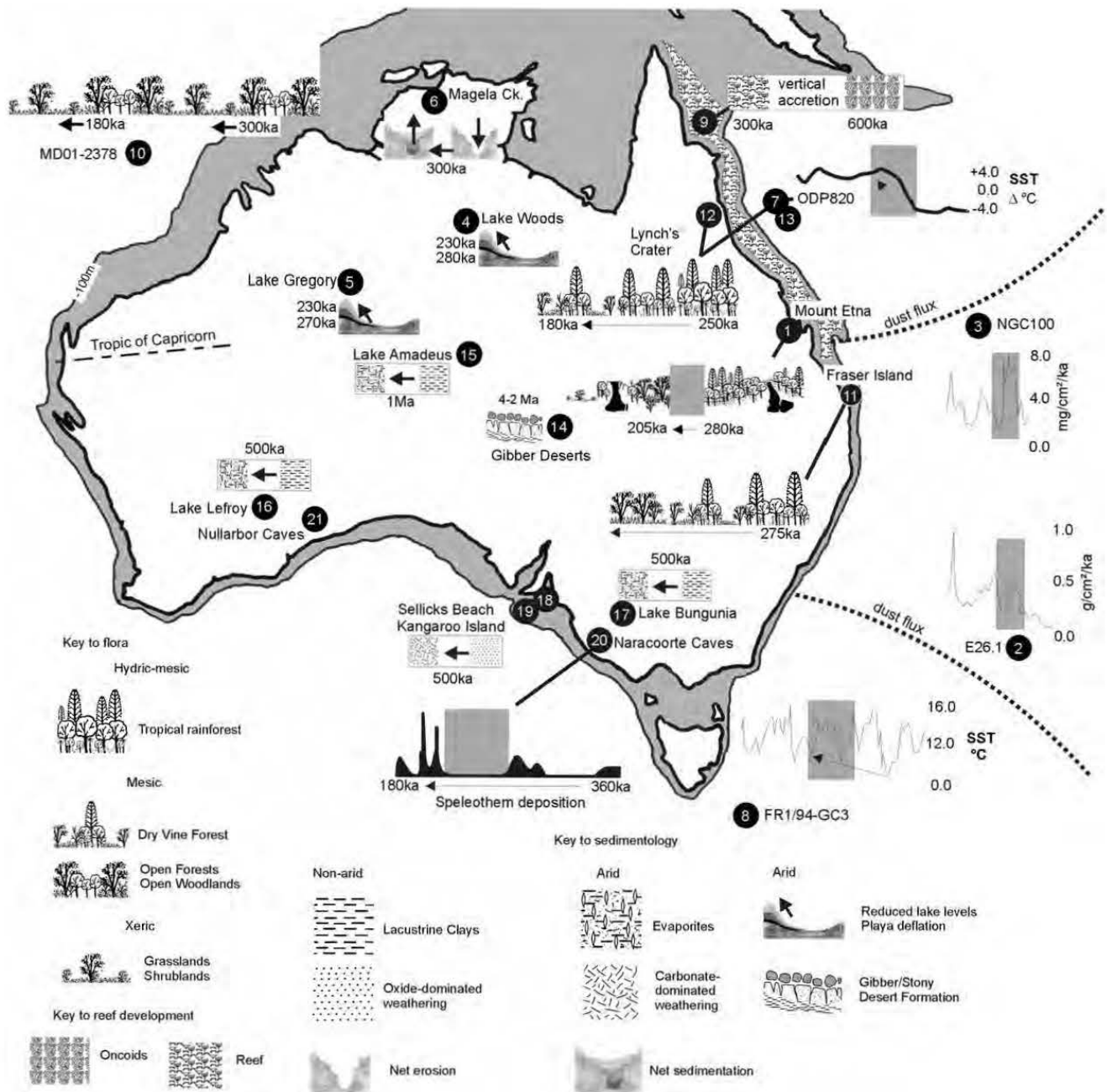


Fig. 5. Australia's middle Pleistocene palaeoclimatic record showing the differential timing of the shift to intensifying aridity and climatic variability in northern, central and southern Australia. The vertical grey bar represents the time of faunal turnover during the middle Pleistocene at Mt Etna (~280–205 ka). 1–13. Intensifying aridity in northern Australia since ~300 ka; 1. Mt Etna faunal turnover, 2–3. Aeolian dust records from the Tasman (Hesse, 1994) and Coral Seas (Kawahata, 2002), 4–5. Lake level reduction and playa deflation (Bowler et al., 2001), 6. Magela Ck. net sedimentation post 300 ka (Nanson et al., 1993), 7–9. Sea Surface Temperature (SST) increase along the East Australian Current with reef development (Peerdeman et al., 1993; Isern et al., 1996; Pelejero et al., 2006; International Consortium for Great Barrier Reef Drilling, 2001; Webster and Davies, 2003), 10–13. Palynological records from northwest Australia (Kawamura et al., 2006; Longmore and Heijnis, 1999; Moss and Kershaw, 2007). 14–15. Intensifying aridity in central Australia since 4 Ma; 14. Gibber–Stony desert formation (Fujioka et al., 2005), 15. Lake Amadeus arid shift (Chen and Barton, 1991). 16–20. Intensifying aridity in southern Australia since ~600 ka; 16–17. Southern lakes shift to aridity (Bowler, 1981; An et al., 1986; Stephenson, 1986; Zheng et al., 2002; English et al., 2001), 18–19. Southern weathering shift to aridity (Pillans and Bourman, 2001), 20. Dry phase between 270 and 220 ka at the Naracoorte Caves recorded from speleothems (Moriarty et al., 2000; Prideaux et al., 2007a).

composition (Prideaux et al., 2007b). The striking difference between the northern and southern records is that the northern non-mega faunal fauna was driven extinct during this arid event, whilst the southern non-

mega faunal fauna was resilient through to the present day.

Sometime after ~205–170 ka the xeric-adapted taxa were lost, and by the Holocene (~7 ka) a more mesic



fauna had established. The late Pleistocene record for Mt Etna is not securely dated and thus the record is missing the last two glacial maxima, a time of extreme climatic change (EPIC Community Members, 2004) the arrival of humans and extinction of megafauna (Wroe et al., 2004). Therefore, the Holocene mesic fauna most likely represents the local habitat returning to an interglacial state and may reflect one of many faunal changes since the middle Pleistocene. The return to mesic conditions did not result in the return of the wet-adapted fauna present prior to ~280 ka.

The interval for the major faunal turnover at Mt Etna (~280–205 ka) occurred during an hypothesised shift towards greater El Niño–Southern Oscillation (ENSO) variability (Kershaw et al., 2003a) and a weakening of the northern monsoon (Kawamura et al., 2006), culminating in intensifying aridity throughout northern Australia (Fig. 5). Our data support a large body of accumulating evidence for a long-term shift towards increasing aridity overlain on a more abrupt shift to greater amplitude of climatic change in individual glacial cycles initiated at the mid-Brunhes Climate Event (MBE) (~430–300 ka).

Dome C (Antarctica) ice core data show a strong contrast in climate before and after ~430 ka (MBE) (EPIC Community Members, 2004). The ice core  $\delta D_{\text{‰}}$  data show an overall warming trend after ~430 ka and much higher amplitude swings in glacial–interglacial temperatures, suggesting a less equable climate after ~430 ka. Dust records also show increasing dust volume at glacial maxima after ~430 ka (EPIC Community Members, 2004).

Sediment core data from MD97-2140 (de Garidel-Thoron et al., 2005), Western Pacific, show greater amplitude and closer swings in Sea Surface Temperatures (SST) between glacial and interglacials after ~450 ka. Sediment core data from Ocean Drilling Program (ODP) hole 806B (Medina-Elizalde and Lea, 2005), Western Pacific, also show greater amplitude swings in glacial–interglacial SST after around 450 ka.

Records of terrigenous dust transported by aeolian processes into the Indian Ocean (SO-14-08-05) (Hesse and McTainsh, 2003), Tasman Sea (E26.1 core) (Hesse, 1994) and Coral Sea (GR100 core) (Kawahata, 2002) all suggest increased aridity in Australia after 350 ka, with particular peaks after 300 ka, 200 ka and 50 ka.

The Lake Woods and Gregory basins illustrate increased aridity through the progressive reduction of lake sizes and development of playas and lunettes since 300 ka (Bowler et al., 2001). Magela Ck., Northern Territory records a shift to aridity after 300 ka by a net increase in sedimentation throughout the tributary after a

long period of incision and sediment evacuation (Nanson et al., 1993). Such a shift is consistent with a decrease in long-term discharge.

SSTs over the last 800 000 years or so have been reconstructed for the western Coral (Peerdeman et al., 1993; Davies and Peerdeman, 1998; Lawrence and Herbert, 2005; Isern et al., 1996) and Tasman Seas (Pelejero et al., 2006), illustrating an increase in SST leading up to, and during, the period of faunal turnover. This suggests that the SST along the entire East Australian Current was rising at the time, and rising SST has been invoked as evidence for the onset of ENSO activity (Kershaw et al., 2003a, 2005). Although increased SST does not indicate mainland aridity directly, increased ENSO activity would produce a climatic variability not conducive for rainforest habitat, which requires a relatively aseasonal climate (Nix, 1982). Timing of initiation of the growth of the Great Barrier Reef supports the increases in Coral Sea SSTs that are inferred from  $\delta^{18}\text{O}$  records and may be associated with the initiation of the western Pacific warm pool (Kershaw et al., 2003b; International Consortium for Great Barrier Reef Drilling, 2001). Intermittent carbonate deposition dominated by coralline algal facies began in outer shelf regions around  $600 \pm 280$  ka, but true vertically accreting reef facies only began to accumulate between 452 and 365 ka (International Consortium for Great Barrier Reef Drilling, 2001; Webster and Davies, 2003). Thus, initiation of true reef growth may coincide with an increase in Coral Sea SST.

Palynological records from northern Australia indicate a progressive increase in open-arid vegetation, beginning ~300 ka and intensifying further since ~180 ka (Kawamura et al., 2006). Pollen records to the south (Longmore and Hejnis, 1999) and north (Moss and Kershaw, 2007) of the study site record shifts from rainforest taxa to drier-land taxa reflecting increased aridity from ~275 ka and ~250 ka ago respectively.

We hypothesise that the trend toward drier and more variable climate ~300–200 ka ago in northern Australia made rainforest habitats unsustainable in central-eastern Queensland, particularly during the increasingly dry glacial maxima, and that pattern contrasts strongly with earlier long periods of more equable climates and relative faunal stability.

In contrast, southern and central Australia experienced increased aridity earlier than northern Australia with records showing aridification starting from 600–500 ka in southern regions and as early as 4–2 million years ago (Ma) in central regions.

In central Australia, Gibber and Stony Deserts were formed 4–2 Ma (Fujioka et al., 2005), whilst Lake

Amadeus underwent an arid shift from uniform lacustrine clays to evaporites and dunes after  $\sim 1.2$ – $1.0$  Ma (Jansen et al., 1986; Chen and Barton, 1991; Bowler, 1981).

In the south, Lake Bungunna underwent an arid shift from lacustrine clays to saline clays and dunes after  $\sim 600$  ka (Jansen et al., 1986; An et al., 1986; Stephenson, 1986). Lake Lefroy preserves evidence of an arid shift from freshwater clays to evaporitic gypsum-dominated sediments around 500 ka (Jansen et al., 1986; Zheng et al., 2002). Lake Lewis underwent a shift from uniform lacustrine clays to more heterogeneous deposits representing greater aridity and fluctuating salinity (between 600 and 500 ka) (Jansen et al., 1986; English et al., 2001). Sellicks Beach and Kangaroo Island preserve weathered dune systems that show a change to aridity 600–500 ka ago characterised by oxide-weathering zones changing to carbonate-weathering zones (Pillans and Bourman, 2001).

The faunal stability demonstrated at Naracoorte throughout the middle Pleistocene to present day for non-megafaunal taxa may reflect a prolonged adaptation to this earlier onset of climatic variability and aridity, where entire faunal assemblages became resilient to increased climatic variability. Conversely, northern faunas responding to a later onset of aridity would not have had as much time to adapt to a new climatic regime, and as such, may remain relatively unstable to change, climate or otherwise.

#### 4.3. Implications for megafaunal extinction hypotheses

We provide the first direct evidence of Quaternary rainforest megafauna in Australia. Therefore, any hypotheses of megafaunal extinction must take into account their extinction from rainforest habitats. Evidence will need to determine whether the reduction of rainforest habitat to its present state was primarily due to pre-human climate change and that this was sufficient to drive the megafauna extinct from rainforest habitat, or whether the addition of human hunting and habitat modification was necessary to tip the balance.

Faunal stability throughout the middle-late Pleistocene, during periods of climate change and prior to human arrival, has been used to argue against climate change as a mitigating factor in the extinction of the late Pleistocene megafauna (Prideaux et al., 2007a,b). It is argued that the southern faunas, including megafauna, were resilient to climate change and thus the extinction of megafauna must have included other factors, of which anthropogenic impacts are favoured (Prideaux et al., 2007a,b).

Our results cannot preclude climate change, in particular increased climatic variability and aridity, as a

mitigating factor in the extinction of Pleistocene fauna in northern Australia. Although we are yet to determine the direct effects of climate change on megafaunal species, we argue that the climate changes during the middle, and presumably late Pleistocene, in northern Australia dramatically influenced the composition and stability of both the flora and fauna before first human occupation  $\sim 50$  ka. Hence, the response of fauna and flora to climate change and the impacts of human occupation may have been very different in different regions of Australia owing to differential timing of major climate-induced habitat modifications.

#### 4.4. Palaeobiogeographic implications

The middle Pleistocene rainforest faunas of Mt Etna provide new data on the paleobiogeography of taxa endemic to the tropical rainforests of New Guinea and the Wet Tropics bioregion of Australia. Of particular interest are the small, herbivorous, arboreal and terrestrial mammals that are common in Holocene deposits and in extant montane rainforests throughout New Guinea (e.g. †*Thylogale christenseni*, *Thylogale calabyi*, †*Dactylopsila kambuyai*, †*Petauroides* *ayamauruiensis* and *Pseudochirulus mayeri* (Flannery, 1995; Hope et al., 1993; Aplin et al., 1999)). These small-bodied taxa are absent from the existing Wet Tropics rainforests of northern Australia, however, closely related taxa are found approximately 800 kms to the south of the Wet Tropics in the middle Pleistocene deposits at Mt Etna (Hocknull, 2005). This indicates that they were present in Australia during the Pleistocene, however, were driven extinct on mainland Australia sometime after  $\sim 280$  ka.

Similarly, middle Pleistocene species of possum (*Pseudochirulus* and *Phalanger*) and tree-kangaroo (*Dendrolagus* “short-foot” clade) from Mt Etna share closer phylogenetic relationships with New Guinean taxa than they do with extant Wet Tropics taxa, suggesting that they too were driven extinct on mainland Australia after  $\sim 280$  ka. Therefore, the continental extinction of several taxa, including entire guilds, and not just those that were megafauna, occurred within Australian rainforests during the Pleistocene.

Palaeoclimatic models have been used to hypothesise relatively recent (i.e. 7500–6000 years ago) arrivals of New Guinean taxa into the Wet Tropics region (e.g. *Cercartetus caudatus*, *Dactylopsila trivirgata*, *Uromys caudimaculatus*, and *Pogonomys mollipilosus*) (Winter, 1997). However, species from each of these genera occur in the middle Pleistocene of Mt Etna, and, with the exception of *Uromys* sp., none of them are considered to



be conspecific with modern forms. This suggests a complex interchange of faunas between New Guinea and Australia during the Quaternary, with the current “New Guinea species” in the Wet Tropics representing one of at least two possible invasions, the first arriving before the middle Pleistocene and reaching as far south as Rockhampton. Alternatively, “New Guinea species” that presently occur in the Wet Tropics may share a refugial status with the Wet Tropics endemics, representing species and/or lineages present on mainland Australia for much longer than previously was thought.

The Wet Tropics bioregion possesses a group of mammals that are not present in either New Guinea or the middle Pleistocene sites of Mt Etna (e.g. *Hypsiprymnodon*, *Bettongia* and *Hemibelideus*). The absence of these mammals from the Mt Etna deposits is an enigma and cannot be explained taphonomically because collecting has been thorough and similarly-sized taxa are found in abundance in most of the deposits. Each of these three genera represent deeply divergent clades (Archer et al., 1999), two of which are rainforest specialists (*Hypsiprymnodon* and *Hemibelideus* (Winter, 1997)), and two possess a long fossil record associated with interpreted rainforest palaeoecologies (i.e. *Hypsiprymnodon* and *Bettongia* (Oligo-Pliocene) (Archer et al., 1999)). Likewise, *Dorcopsis*, now endemic to New Guinea has an early Pliocene record in Australia, however, it is absent from the middle Pleistocene deposits at Mt Etna (Turnbull and Lundelius, 1970)). Thus, the middle Pleistocene rainforest faunas at Mt Etna represent a mixture of taxa that are now differentially isolated in New Guinea and the Wet Tropics. This mixture has included or excluded taxa with long histories associated with rainforests, illustrating the complex taxonomic filters operating in Australopapuan rainforests throughout the Neogene. The extinct rainforest assemblage presented here illustrates a diversity of taxa and guilds unlike that found in present day Australian tropical rainforests. These results emphasise the dominance of extinction, via climate change, as the major driving force in shaping Australia's present day tropical rainforest faunas.

## 5. Conclusions

Fossiliferous cave deposits from Mt Etna, central-eastern Queensland represent the only Quaternary rainforest vertebrate fossil record known in Australia. The deposits were previously thought to be Pliocene in age based on biocorrelation, but direct chronometric dating has revealed that most of these sites are in fact middle Pleistocene in age, dating from before 500 ka to approximately 280 ka. This result extends the temporal range of

several Pliocene and early Pleistocene taxa into the middle Pleistocene.

After a long period of relative faunal stability at Mt Etna, a major faunal turnover occurred between ~280 ka and ~205 ka, wherein a diverse rainforest fauna was replaced by a xeric-adapted fauna, lending the first vertebrate fossil evidence to the large-scale climatic shifts to aridity in northern Australia, documented by numerous other palaeoclimatic methods. At least one more faunal change occurred since that time to produce the Holocene and modern mesic-adapted fauna, which we suggest is a continued response of northern Australian habitats to the sustained shift to increased climatic variability. However, additional anthropogenic influences are not ruled out in the most recent faunal changes.

These results contrast with Quaternary records from southern Australia which show remarkable faunal stability over the last 500 ka for non-megafaunal taxa. That stability may reflect long-term adaptation to increasing aridity, which began earlier in southern Australia.

Our results illustrate the presence of a suite of rainforest taxa without any present day Australian representative and indicate a longer connectivity between the faunas of northern Australia and New Guinea than previously was thought. Understanding the causes for the extinction of these taxa on mainland Australia is fundamental when considering the vulnerabilities of present day rainforest taxa in far north Queensland, a bioregion under several climatic and human induced threats.

We demonstrate here that Quaternary climate change influenced regions of the Australian continent in different ways over a similar period of time and to a degree previously not recorded. Although this is in itself an intuitive statement, it does illustrate the inherent complexity in determining what the responses of fauna and flora to climate change may be in the future.

## Acknowledgements

This project was funded by the Australian Research Council (LP0453664) with the support of Industry Partners (Queensland Museum, Cement Australia, Rockhampton Regional Development, Australian Museum, Central Queensland Speleological Society and the Outback Isa Riversleigh Interpretative Centre). We thank S. Hand, M. Archer, H. Godthelp, T. Barrows, P. Moss, G. Prideaux, A. Cook, S. Marks, G. Price, L. Deer, B. Cooke, K. Spring, J. Wilkinson, P. Tierney, N. Sands, P. Berrill, B. Bauer, K. Lawrence, C. White, J. Cramb, J. Williams, S. Martinez and D. Lewis for their support and discussion during the progress of this research.

## Appendix A. Supplementary data

Supplementary data associated with this article can be found, in the online version, at [doi:10.1016/j.epsl.2007.10.004](https://doi.org/10.1016/j.epsl.2007.10.004).

## References

- An, Z.S., Bowler, J.M., Opdyke, N.D., Macumber, P.G., Firman, J.B., 1986. Palaeomagnetic stratigraphy of Lake Bungunnna: Plio-Pleistocene precursor of aridity in the Murray Basin, southeastern Australia. *Palaeogeogr. Palaeoclimatol. Palaeoecol.* 54, 219–239.
- Aplin, K.P., Pasveer, J.M., Boles, W.E., 1999. Late Quaternary vertebrates from the Bird's Head Peninsula, Irian Jaya, Indonesia, including the descriptions of two previously unknown marsupial species. *Rec. West. Aust. Mus., Supp.* 57, 351–387.
- Archer, M., Arena, R., Bassarova, M., Black, K., Brammall, J., Cooke, B., Creaser, P., Crosby, K., Gillespie, A., Godthelp, H., Gotti, M., Hand, S.J., Kear, B., Krikmann, A., Mackness, B., Muirhead, J., Musser, A., Myers, T., Pledge, N., Wang, Y., Wroe, S., 1999. The evolutionary history and diversity of Australian mammals. *Aust. Mammal.* 21, 1–45.
- Archer, M., Hand, S.J., Godthelp, H., 1991. In: Lunney, D. (Ed.), *Conservation of Australia's forest fauna*. Royal Society of New South Wales, Mosman, pp. 67–80.
- Archer, M., Hand, S.J., Godthelp, H., 1995. In: Vrba, E.S., Denton, G.H., Partridge, T.C., Burckle, L.H. (Eds.), *Paleoclimate and Evolution, with Emphasis on Human Origins*. Yale Univ. Press, New Haven, pp. 77–90.
- Bowler, J.M., 1981. Australian salt lakes: a palaeohydrological approach. *Hydrobiologia* 82, 431–444.
- Bowler, J.M., Wyrwoll, K.H., Lu, Y., 2001. Variations of the northwest Australian summer monsoon over the last 300,000 years: the paleohydrological record of the Gregory (Mulan) Lakes System. *Quat. Int.* 83–85, 63–80.
- Chen, X.Y., Barton, C.E., 1991. Onset of aridity and dune-building in Central Australia: sedimentological and magnetostratigraphic evidence from Lake Amadeus. *Palaeogeogr. Palaeoclimatol. Palaeoecol.* 84, 55–71.
- Davies, P.J., Peerdeman, F.M., 1998. In: Camoin, G.F., Davies, P.J. (Eds.), *Reef and Carbonate Platforms in the Pacific and Indian Oceans*. International Association of Sedimentologists Special Publication, vol. 25. Blackwell International, Oxford, pp. 22–33.
- de Garidel-Thoron, T., Rosenthal, Y., Bassinot, F., Beaufort, L., 2005. Stable sea surface temperatures in the western Pacific warm pool over the past 1.75 million years. *Nature* 433, 294–298.
- English, P., Spooner, N.A., Chappell, J., Questiaux, D.G., Hill, N.G., 2001. Lake Lewis basin, central Australia: environmental evolution and OSL chronology. *Quat. Int.* 83–85, 81–101.
- EPIC Community Members, 2004. Eight glacial cycles from an Antarctic ice core. *Nature* 429, 623–628.
- Flannery, T., 1995. *Mammals of New Guinea*. Reed Books, Sydney.
- Fujioka, T., Chappell, J., Honda, M., Yatsevich, I., Fifield, K., Fabel, D., 2005. Global cooling initiated stony deserts in central Australia 2–4 Ma, dated by cosmogenic  $^{21}\text{Ne}$ – $^{10}\text{Be}$ . *Geology* 33 (12), 993–996.
- Greenwood, D.R., Christophel, D.C., 2005. In: Bermingham, E., Dick, C.W., Moritz, C. (Eds.), *Tropical Rainforests Past, Present, and Future*. Univ. Chicago Press, Chicago, pp. 336–373.
- Hammer, Ø., Harper, D.A.T., Ryan, P., 2001. *PAST: Paleontological Statistics Software Package for Education and Data Analysis*. *Palaeontol. Electronica* 4 (1), 1–9 [http://palaeo-electronica.org/2001\\_1/pastissue1\\_01.htm](http://palaeo-electronica.org/2001_1/pastissue1_01.htm).
- Hesse, P.P., 1994. The record of continental dust from Australia in Tasman Sea sediments. *Quat. Sci. Rev.* 13, 257–272.
- Hesse, P.P., McTainsh, G.H., 2003. Australian dust deposits: modern processes and the Quaternary record. *Quat. Sci. Rev.* 22, 2007–2035.
- Hijmans, R.J., Guarino, L., Jarvis, A., O'Brien, R., Mathur, P., Bussink, C., Cruz, M., Barrantes, I., Rojas, E., 2005. *DIVA-GIS 5.4 Software*. [www.diva-gis.org](http://www.diva-gis.org).
- Hocknull, S.A., 2005. Ecological succession during the late Cainozoic of central eastern Queensland: extinction of a diverse rainforest community. *Mem. Queensl. Mus.* 51 (1), 39–122.
- Hope, G., Flannery, T., Boeardi, 1993. A preliminary report of changing Quaternary mammal faunas in subalpine New Guinea. *Quat. Res.* 40, 117–126.
- International Consortium for Great Barrier Reef Drilling, 2001. New constraints on the origin of the Australian Great Barrier Reef: results from an international project of deep coring. *Geology* 29, 483–486.
- Isern, A.R., McKenzie, J.A., Feary, D.A., 1996. The role of sea-surface temperature as a control on carbonate platform development in the western Coral Sea. *Palaeogeogr. Palaeoclimatol. Palaeoecol.* 124, 247–272.
- Jansen, J.H.F., Kuijpers, A., Troelstra, S.R., 1986. A mid-brunhes climatic event: long-term changes in global atmosphere and ocean circulation. *Science* 232, 619–622.
- Kawahata, H., 2002. Shifts in oceanic and atmospheric boundaries in the Tasman Sea (Southwest Pacific) during the Late Pleistocene: evidence from organic carbon and lithogenic fluxes. *Palaeogeogr. Palaeoclimatol. Palaeoecol.* 184, 225–249.
- Kawamura, H., Holbourn, A., Kuhn, W., 2006. Climate variability and land–ocean interactions in the Indo Pacific Warm Pool: a 460-ka palynological and organic geochemical record from the Timor Sea. *Mar. Micropaleontol.* 59, 1–14.
- Kershaw, P., Moss, P., van der Kaars, S., 2003a. Causes and consequences of long-term climatic variability on the Australian continent. *Fresh. Biol.* 48, 1274–1283.
- Kershaw, A.P., van der Kaars, S., Moss, P.T., 2003b. Late Quaternary Milankovitch-scale climate change and variability and its impact on monsoonal Australasia. *Mar. Geol.* 201, 81–85.
- Kershaw, A.P., Moss, P.T., Wild, R., 2005. In: Bermingham, E., Dick, C.W., Moritz, C. (Eds.), *Tropical Rainforests Past, Present, and Future*. Univ. Chicago Press, Chicago, pp. 374–400.
- Lawrence, K.T., Herbert, T.D., 2005. Late Quaternary sea-surface temperatures in the western Coral Sea: implications for the growth of the Australian Great Barrier Reef. *Geology* 33, 677–680.
- Longmore, M.E., Heijnis, H., 1999. Aridity in Australia: Pleistocene records of Palaeohydrological and Palaeoecological change from the perched lake sediments of Fraser Island, Queensland, Australia. *Quat. Int.* 57–58, 35–47.
- McGowran, B., Archer, M., Bock, P., Darragh, T.A., Godthelp, H., Hageman, S., Hand, S.J., Hill, R., Li, Q., Maxwells, P.A., Mcnamara, K.J., Macphail, M., Mildenhall, D., Partridge, A.D., Richardson, J., Shafiki, S., Truswell, E.M., Warne, M., 2000. Australasian palaeobiogeography: the Palaeogene and Neogene record. *Mem. Assoc. Aust. Palaeontol.* 23, 405–470.
- Medina-Elizalde, M., Lea, D.W., 2005. The mid-Pleistocene transition in the tropical Pacific. *Science* 310, 1009–1012.
- Moriarty, K.C., McCulloch, M.T., Wells, R.T., McDowell, M.C., 2000. Mid-Pleistocene cave fills, megafaunal remains and climate change at Naracoorte, South Australia: towards a predictive model using U–Th dating of speleothems. *Palaeogeogr. Palaeoclimatol. Palaeoecol.* 159, 113–143.

- Moritz, C., Dick, C.W., Bermingham, E., 2005. From the past to the future: evolution, ecology and conservation of tropical rainforests. In: Bermingham, E., Dick, C.W., Moritz, C. (Eds.), *Tropical Rainforests Past, Present, and Future*. Univ. of Chicago Press, Chicago, pp. 1–3.
- Moss, P.T., Kershaw, A.P., 2007. A late Quaternary marine palynological record (Oxygen Isotope Stages 1 to 7) for the Humid Tropics of northeastern Australia based on ODP Site 820. *Palaeoclimatology, Palaeoecology* 251 (1), 4–22.
- Nanson, G.C., East, T.J., Roberts, R.G., 1993. Quaternary stratigraphy, geochronology and evolution of the Magela Creek catchment in the monsoon tropics of northern Australia. *Sediment. Geol.* 83, 277–302.
- Nix, H.A., 1982. Environmental determinants of biogeography and evolution in Terra Australis. In: Barker, W.R., Greenslade, P.J.M. (Eds.), *Evolution of the Flora and Fauna of Arid Australia*. Peacock Publications and the Australian Systematic Botany Society, Adelaide, pp. 35–45.
- Nix, H.A., Switzer, M.A., 1991. *Rainforest Animals: Atlas of Vertebrates Endemic to Australia's Wet Tropics*. Australian National Parks and Wildlife Service, Canberra.
- OZCAM community, 2006. BioMaps. [www.biomaps.net.au/biomaps](http://www.biomaps.net.au/biomaps).
- Peerdeman, F.M., Davies, P.J., Chivas, A.R., 1993. The stable oxygen isotope signal in shallow-water, upper slope sediments off the Great Barrier Reef (Hole 820A). *Proc. Ocean Drill. Prog. Sci. Results* 133, 163–173.
- Pelejero, C., Calvo, E., Barrows, T.T., Logan, G.A., De Deckker, P., 2006. South Tasman Sea alkenone palaeothermometry over the last four glacial/interglacial cycles. *Mar. Geol.* 230, 73–86.
- Pillans, B., Bourman, R., 2001. Mid Pleistocene arid shift in southern Australia, dated by magnetostratigraphy. *Aust. J. Soil Res.* 39, 89–98.
- Piper, K.J., 2007. Early Pleistocene Mammals from The Nelson Bay Local Fauna, Portland, Victoria, Australia. *J. Vert. Palaeo.* 27, 492–503.
- Prideaux, G.J., Long, J.A., Ayliffe, L.K., Hellstrom, J.C., Pillans, B., Boles, W.E., Hutchinson, M.N., Roberts, R.G., Cupper, M.L., Arnold, L.J., Devine, P.D., Warburton, N.M., 2007a. An arid-adapted Middle Pleistocene vertebrate fauna from South-Central Australia. *Nature* 445, 422–425.
- Prideaux, G.J., Roberts, R.G., Megirian, D., Westaway, K.G., Hellstrom, J.C., Olley, J.M., 2007b. Mammalian responses to Pleistocene climate change in southeastern Australia. *Geology* 35 (1), 33–36.
- Schneider, C.J., Williams, S.E., 2005. In: Bermingham, E., Dick, C.W., Moritz, C. (Eds.), *Tropical Rainforests Past, Present, and Future*. Univ. Chicago Press, Chicago, pp. 401–424.
- Shannon, C.H.C., 1970. Geology of the Mount Etna area. In: Sprent, J.K. (Ed.), *Mount Etna Caves*. University of Queensland Speleological Society, St Lucia, Brisbane, pp. 11–21.
- Specht, R.L., 1981. Major vegetation formations in Australia. In: Keast, A. (Ed.), *Ecological Biogeography of Australia*. Dr. W. Junk, The Hague, pp. 165–295.
- Stephenson, A.E., 1986. Lake Bungunnia — a Plio-Pleistocene megalake in southern Australia. *Palaeogeogr. Palaeoclimatol. Palaeoecol.* 57, 137–156.
- Thomas, C.D., Cameron, A., Green, R.E., Bakkenes, M., Beaumont, L.J., Collingham, Y.C., Erasmus, B.F.N., de Siqueira, M.F., Grainger, A., Hannah, L., Hughes, L., Huntley, B., van Jaarsveld, A.S., Midgley, G.F., Miles, L., Ortega-Huerta, M.A., Peterson, A.T., Phillips, O.L., Williams, S.E., 2004. Extinction risk from climate change. *Nature* 427, 145–148.
- Turnbull, W.D., Lundelius Jr., E.L., 1970. The Hamilton fauna: a late Pliocene mammalian record from the Grange Burn, Victoria, Australia. *Fieldiana Geol.* 19, 1–163.
- Webb, L.J., Tracey, J.G., 1981. Australian rainforests: patterns and changes. In: Keast, A. (Ed.), *Ecological Biogeography of Australia*. Dr. W. Junk, The Hague, pp. 605–694.
- Webster, J.M., Davies, P.J., 2003. Coral variation in two deep drill cores: significance for the Pleistocene development of the Great Barrier Reef. *Sediment. Geol.* 159, 61–80.
- Williams, S.E., Bolitho, E.E., Fox, S., 2003. Climate change in Australian tropical rainforests: an impending environmental catastrophe. *Proc. Royal Soc. London Series B — Biol. Sci.* 270, 1887–1892.
- Williams, S.E., Hilbert, D., 2006. Climate change threats to the biodiversity of tropical rainforests in Australia. In: Laurance, W.F., Peres, C. (Eds.), *Emerging Threats to Tropical Forests*. Chicago University Press, Chicago, United States of America.
- Winter, J.W., 1997. Responses of non-volant mammals to Late Quaternary climate change in the wet tropics region of North-eastern Australia. *Wildl. Res.* 24, 493–511.
- Wroe, S., Field, J., Fullagar, R., Jeremiin, L.S., 2004. Megafaunal extinction in the late Quaternary and the global overkill hypothesis. *Alcheringa* 28, 291–331.
- Zhao, J.X., Hu, K., Collerson, K.D., Xu, H.K., 2001. Thermal ionization mass spectrometry U-series dating of a hominid site near Nanjing, China. *Geology* 29 (1), 27–30.
- Zheng, H., Powell, C.Mc.A., Zhao, H., 2002. Eolian and lacustrine evidence of late Quaternary palaeoenvironmental changes in southwestern Australia. *Glob. Planet. Change* 35, 75–92.

# MEMOIRS OF THE QUEENSLAND MUSEUM

BRISBANE

© Queensland Museum  
PO Box 3300, South Brisbane 4101, Australia  
Phone 06 7 3840 7555  
Fax 06 7 3846 1226  
Email [qmlib@qm.qld.gov.au](mailto:qmlib@qm.qld.gov.au)  
Website [www.qm.qld.gov.au](http://www.qm.qld.gov.au)

National Library of Australia card number  
ISSN 0079-8835

## NOTE

Papers published in this volume and in all previous volumes of the *Memoirs of the Queensland Museum* maybe reproduced for scientific research, individual study or other educational purposes. Properly acknowledged quotations may be made but queries regarding the republication of any papers should be addressed to the Editor in Chief. Copies of the journal can be purchased from the Queensland Museum Shop.

A Guide to Authors is displayed at the Queensland Museum web site

**A Queensland Government Project**  
Typeset at the Queensland Museum

*ETNABATRACHUS MAXIMUS* GEN. ET SP. NOV., A PLIO-PLEISTOCENE FROG  
FROM MOUNT ETNA, CENTRAL EASTERN QUEENSLAND

SCOTT A. HOCKNULL

Hocknull, S.A. 2003 06 30: *Etnabatrachus maximus* gen. et sp. nov., a Plio-Pleistocene frog from Mount Etna, central eastern Queensland. *Memoirs of the Queensland Museum* 49(1): 327-330. Brisbane. ISSN 0079-8835.

*Etnabatrachus maximus* gen. et sp. nov. is the first record of fossil frogs from the Mount Etna region of central eastern Queensland. *E. maximus*' very large size, divided prominences and lateral mid-shaft ridge distinguish it from all other Australian genera. The associated fauna from the type locality indicates a Plio-Pleistocene rainforest environment, making *E. maximus* the largest known species of rainforest frog from Australia. □ *Etnabatrachus maximus*, Plio-Pleistocene, Australia, Ilium, Cainozoic.

Scott A. Hocknull, Queensland Museum, PO Box 3300, South Brisbane, 4101 (e-mail: scotth@qm.qld.gov.au); 20 May 2003.

The first fossil frogs from Australia were described by Tyler in 1974 (Tyler, 1974). Since then, Tyler has published on taxa from the Eocene of southern Queensland through to the late Holocene deposits of South and Western Australia (Tyler, 1999). The dominating faunas exhibiting extinct taxa have been the Oligo-Miocene of Riversleigh Qld, Bullock Creek NT and Lake Palankarrina SA. The Pliocene to Holocene record is marked by the exclusively extant taxa illustrating an early establishment of the modern frog faunas.

Several new local faunas have been excavated from deposits from the Mount Etna Caves, Rockhampton, CE Queensland. These local faunas span the Pliocene to Holocene and preserve abundant frog remains, including species of *Lechriodus*, *Kyarannus*, *Litoria* and *Limnodynastes*. The age of the type locality for *Etnabatrachus maximus* gen. et sp. nov. is interpreted as late Pliocene to early Pleistocene based on taxa occurring across this boundary, including: *Petauroides* sp., close to *P. stirtoni* (Turnbull & Lundelius, 1970), *Pseudokoala* sp., close to *P. erlita* (Turnbull & Lundelius, 1970), *Palorchestes* sp., close to *P. parvus* (Tedford, 1994), *Perameles* sp., close to *P. bowensis* (Muirhead et al., 1997) and *Kurrabi* sp. (Flannery et al., 1992).

The type locality for *E. maximus* gen. et sp. nov. is interpreted as rainforest on the basis of sediments being at a time of major speleothem development, and taxa with distinct rainforest affinities, including: pseudocheirids – *Pseudochirulus mayeri*, *Pseudocheirops* spp. petaurids; *Dactylopsila* spp.; macropodids – *Dendrolagus* sp.; peramelimorphians –

peroryctid spp.; murids – *Uromys* sp. and *Pogonomys* sp. nov. (H. Godthelp, pers.comm.); and anurans – *Lechriodus* sp. and *Kyarannus* sp.

Specimens described herein are deposited in the Queensland Museum fossil collection (QMF). Ilial terminology and nomenclature follow Tyler (1976) and taxonomy follows Cogger (2000).

## SYSTEMATICS

Family ?HYLIDAE Gray, 1825

***Etnabatrachus* gen. nov.**

TYPE SPECIES. *Etnabatrachus maximus* sp. nov. from the Plio-Pleistocene of Mount Etna and Limestone Ridge, localities QML 1385 (Type) and QML1284.

ETYMOLOGY. Etna- in reference to Mount Etna, type locality and -batrachus for frog.

DIAGNOSIS. Large, robust ilium. Ilial crest absent, dorsal acetabular expansion poorly developed, rising slightly above dorsal margin of ilial shaft. Preacetabular zone broad and divided laterally by a mid-shaft ridge. Ridge runs anterior to the acetabular rim, orientated anterodorsally approximately halfway along its length. Ridge terminates at ventral margin of shaft, at approximately anterior ¼ of ilium length. Dorsal prominence divided into an anterior and a posterior prominence, bisected by a shallow valley running from the antero-medial side to the postero-lateral side. Anterior-most prominence laterally directed with elongate-ovoid protuberance in lateral profile. Anterior-most prominence placed well anterior of anterior acetabular rim. Posterior-most prominence smaller than anterior prominence with a more



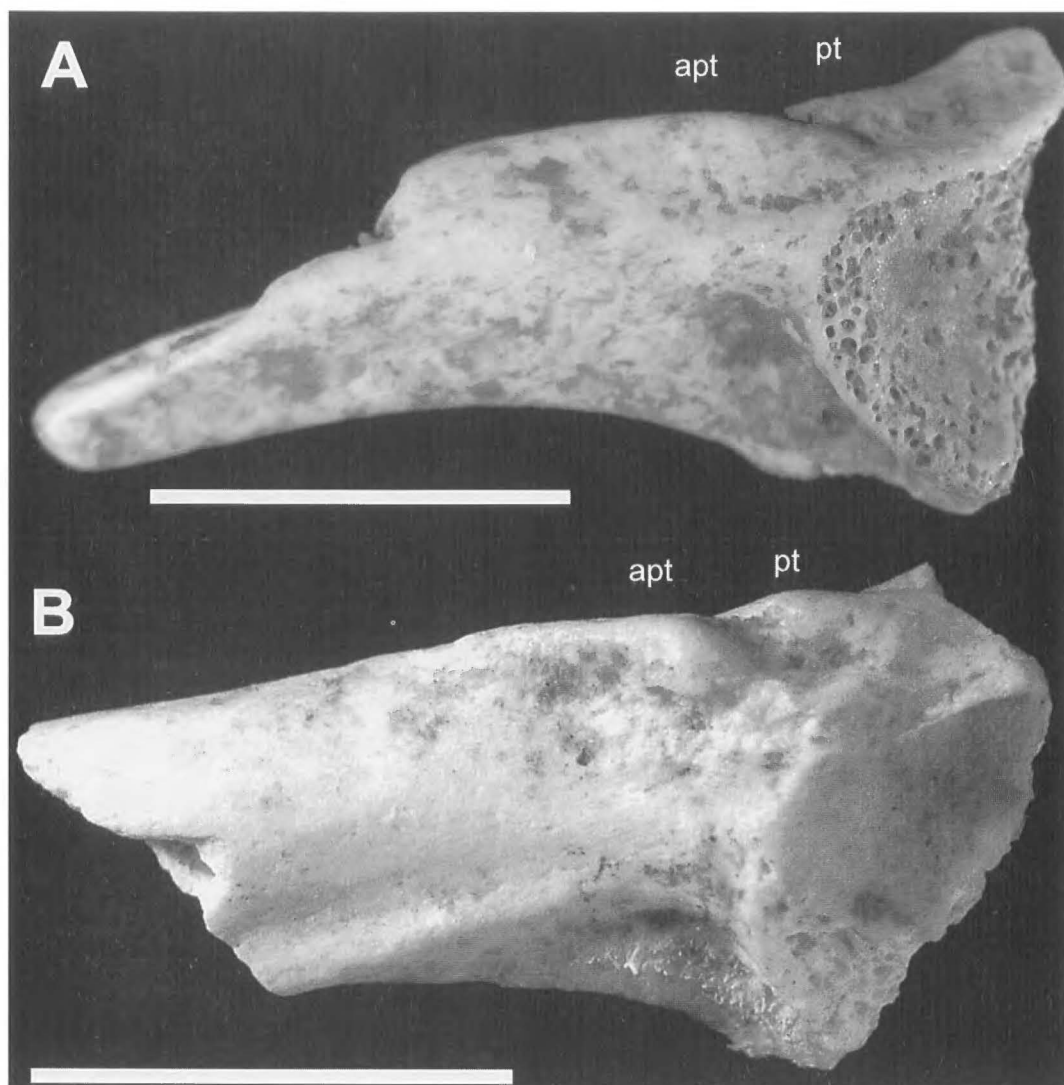


FIG. 1. *Etnabatrachus maximus* gen. et sp. nov. A, left ilium, Holotype QMF44207; B, left ilium, Paratype QMF44208. Scale = 5mm. apt, anterior-most protruberance; pt, proximal protruberance.

rounded protuberance in lateral profile. Posterior-most prominence placed superiorly and central to acetabular fossa. Iliac shaft broad posteriorly, tapering sharply to anterior end.

**DESCRIPTION.** Holotype, QMF44207, is a large, robust left ilium preserving approximately half the posterior end, including a portion of the shaft, acetabulum, dorsal and ventral expansions and prominences. Dorsal acetabular expansion small and rounded superiorly, making a short

iliac/ischial suture. Ventral acetabular expansion missing, broken on ventral margin, however, inferred as small with short iliac/pubic suture. Acetabular fossa large and well differentiated from iliac shaft. Acetabular rim narrow and produced laterally from the antero-posterior axis of the iliac shaft. Iliac shaft incomplete, broken approximately half way along its length, compressed medially and rounded laterally when viewed in cross-section. Preacetabular zone broad, broken postero-ventrally of acetabular

rim, superior to ventral acetabular expansion. Ridge runs antero-dorsally from ventral margin of acetabular rim, curves anteriorly half-way along its length positioned on the midline of the lateral side of the shaft. Curves antero-ventally along last 1/3 of its length, terminating on ventral margin of ilial shaft. Acetabular fossa eroded along posterior margin of fossa and anterior margin of acetabular rim. Dorsal prominence divided into two by a large groove running medio-laterally across ilial shaft. Groove terminates in a small basin, or insertion point, superior to dorsal acetabular rim. Anterior-most protuberance elongate-ovoid and laterally produced. Posterior-most protuberance ovoid in shape and antero-posterior in orientation, prominence terminating at the base of the dorsal acetabular expansion. Ilial shaft broad along its length, broken superiorly and perpendicular to the long axis of the ilium. Ilial length: 13.10+mm, dorsal acetabular expansion to ventral acetabular expansion height: 6.38+mm. Paratype QMF44208 is an incomplete left ilium, preserving the acetabulum, portions of both the dorsal and ventral acetabular expansions, divided prominences and preacetabular zone. Ilium large, robust along its length, broken approximately 1/3 its length. Ventral acetabular expansion unknown, inferred as diminutive in antero-posterior length and extending only slightly past ventral margin of acetabular rim. Acetabular fossa large with prominent narrow and high rim. Dorsal prominence divided into an anterior and a posterior prominence, bisected by a shallow valley running from the antero-medial side to the postero-lateral side. Valley terminates as a small basin (muscular insertion point) positioned superior to the dorsal acetabular rim. Anterior-most prominence laterally directed with an elongate-ovoid protuberance in lateral profile. Anterior-most prominence placed well anterior of anterior acetabular rim. Posterior-most prominence smaller than Anterior prominence with a more rounded protuberance in lateral profile. Prominence less laterally positioned, terminating at the base of the dorsal acetabular expansion. Posterior-most prominence placed superiorly and central to acetabular fossa. Ilial shaft broad posteriorly, tapering sharply to anterior end. Ilial length: 10.20+mm, dorsal acetabular expansion to ventral acetabular expansion height: 5.14+mm.

**REMARKS.** The large size, divided prominence, lateral mid-shaft ridge and reduced dorsal acetabular expansion distinguish *Etnabatrachus*

from all other known Australian genera. The rounded protuberance and lack of a dorsal crest ally this taxon closest to *Litoria* of Australia. However, specific placement in the Hylidae can only be tentative at this point. *Etnabatrachus* is considerably larger than the Oligo-Miocene *Litoria magna* Tyler, 1991, which Tyler (1991) considered to attain sizes of at least 120mm SVL. This puts *L. magna* in a size range greater than the largest extant *Litoria* (Cogger, 2000). It has been hard to estimate the SVL of *E. maximus* based on the lack of a complete ilium, however, the overall size of the ilium indicates a frog of considerable size, larger than 120mm SVL. The associated faunas recovered from the type locality indicate a palaeoenvironment of rainforest. Such a large species of frog in a rainforest deposit is not unusual as a number of species in present day rainforests attain large sizes (e.g. *Mixophyes* 115mm SVL and *Litoria* 120mm SVL).

***Etnabatrachus maximus* sp. nov.**  
(Fig. 1)

**ETYMOLOGY.** Latin, *maximus*, alluding to the large size of the species.

**MATERIAL.** HOLOTYPE: QMF44207, Paratype: QMF44208 from Plio-Pleistocene deposits, Mount Etna and Limestone Ridge (QML1284 & QML1385).

**DIAGNOSIS.** As for genus.

**DESCRIPTION.** As for genus.

**ACKNOWLEDGEMENTS**

I thank Rick Bell, Patrick Couper, Andrew Amey, Gilbert Price, Noel Sands and Paul Tierney for access to specimens, encouragement and help in preparing the material for this study.

**LITERATURE CITED**

- COGGER, H. 2000. Reptiles and Amphibians of Australia. 5th Ed. (Reed: Melbourne).
- FLANNERY, T.F., RICH, T.H., TURNBULL, W.D. & LUNDELIUS, E.L. Jr 1992. The macropodoidea (Marsupialia) of the early Pliocene Hamilton Local Fauna, Victoria, Australia. *Fieldiana Geology* NS 25: 1-37.
- MUIRHEAD, J., DAWSON, L. & ARCHER, M. 1997. *Perameles bowensis*, a new species of *Perameles* (Peremelandromphia: Marsupialia) from Pliocene faunas of Bow and Wellington Caves, New South Wales. *Proceedings of the Royal Society of New South Wales* 117: 163-173.
- TEDFORD, R.H. 1994. Succession of Pliocene through medial Pleistocene mammal faunas of southeastern Australia. *Records of the South Australian Museum*. 27(2): 79-93.

- TURNBULL, W.D. & LUNDELIUS, E.L. Jr 1970. The Hamilton Fauna: a late Pliocene mammalian fauna from the Grange Burn, Victoria, Australia. *Fieldiana: Geology* NS 19: 1-163.
- TYLER, M.J. 1974. First frog fossils from Australia. *Nature* 248 (5450): 711-712.
1976. Comparative osteology of the pelvic girdle of Australian frogs and description of a new fossil genus. *Transactions of the Royal Society of South Australia* 100(1): 3-14.
1982. Tertiary frogs from South Australia. *Alcheringa* 6: 101-103.
1985. Quaternary fossil frogs from Skull Cave and Devil's Lair in the extreme south-west of Western Australia. *Records of the Western Australian Museum* 12(2): 233-240.
1988. *Neobatrachus pictus* (Anura: Leptodactylidae) from the Miocene/Pliocene boundary of South Australia. *Transactions of the Royal Society of South Australia* 112: 91.
1989. A new species of *Lechriodus* (Anura: Leptodactylidae) from the Tertiary of Queensland, with a redefinition of the ilial characteristics of the genus. *Transactions of the Royal Society of South Australia* 113: 15-21.
1990. *Limnodynastes* Fitzinger (Anura: Leptodactylidae) from the Cainozoic of Queensland. *Memoirs of the Queensland Museum* 28(2): 779-784.
- 1991a. *Crinia* Tschudi (Anura: Leptodactylidae) from the Cainozoic of Queensland, with description of a new species. *Transactions of the Royal Society of South Australia* 115(2): 99-101.
- 1991b. *Kyarannus* Moore (Anura, Leptodactylidae) from the Tertiary of Queensland. *Proceedings of the Royal Society of Victoria* 103(1): 47-51.
- 1991c. A large new species of *Litoria* (Anura: Hylidae) from the Tertiary of Queensland. *Transactions of the Royal Society of South Australia* 115(2): 103-105.
1994. Hylid frogs from the mid-Miocene Camfield beds of Northern Australia. *The Beagle, Records of the Museum and Art Galleries of the Northern Territory* 11: 141-144.
1999. *Australian Frogs: a natural history*. (Reed: New Holland).
- TYLER, M.J., ASLIN, F.W. & BRYARS, S. 1992. Early Holocene frogs from the Tantanoola Cave, South Australia. *Transactions of the Royal Society of South Australia* 116(4): 153.
- TYLER, M.J. & GODTHELP, H. 1993. A new species of *Lechriodus* Boulenger (Anura: Leptodactylidae) from the early Eocene of Queensland. *Transactions of the Royal Society of South Australia* 117(4): 187-189.
- TYLER, M.J. & WALKLEY, R.W. 1996. First fossil record of the hylid frog *Litoria raniformis* (Keferstein). *Transactions of the Royal Society of South Australia* 120(2): 69.
- TYLER, M.J., DAVIS, A.C. & WILLIAMS, C.R. 1998. Pleistocene frogs from near Cooma, New South Wales. *Proceedings of the Linnean Society of New South Wales* 119: 107-113.
- TYLER, M.J., GODTHELP, H. & ARCHER, M. 1994. Frogs from a Plio-Pleistocene site at Floraville Station, Northwest Queensland. *Records of the South Australian Museum* 27(2): 169-173.



# Dragon's Paradise Lost: Palaeobiogeography, Evolution and Extinction of the Largest-Ever Terrestrial Lizards (Varanidae)

Scott A. Hocknull<sup>1\*</sup>, Philip J. Piper<sup>2</sup>, Gert D. van den Bergh<sup>3</sup>, Rokus Awe Due<sup>4</sup>, Michael J. Morwood<sup>3</sup>, Iwan Kurniawan<sup>5</sup>

**1** Geosciences, Queensland Museum, Brisbane, Queensland, Australia, **2** Archaeological Studies Program, University of the Philippines, Quezon City, Philippines, **3** School of Earth and Environmental Sciences, University of Wollongong, Wollongong, New South Wales, Australia, **4** Indonesian Centre for Archaeology, Jakarta, Indonesia, **5** Geological Survey of Indonesia, Bandung, Indonesia

## Abstract

**Background:** The largest living lizard species, *Varanus komodoensis* Ouwens 1912, is vulnerable to extinction, being restricted to a few isolated islands in eastern Indonesia, between Java and Australia, where it is the dominant terrestrial carnivore. Understanding how large-bodied varanids responded to past environmental change underpins long-term management of *V. komodoensis* populations.

**Methodology/Principal Findings:** We reconstruct the palaeobiogeography of Neogene giant varanids and identify a new (unnamed) species from the island of Timor. Our data reject the long-held perception that *V. komodoensis* became a giant because of insular evolution or as a specialist hunter of pygmy *Stegodon*. Phyletic giantism, coupled with a westward dispersal from mainland Australia, provides the most parsimonious explanation for the palaeodistribution of *V. komodoensis* and the newly identified species of giant varanid from Timor. Pliocene giant varanid fossils from Australia are morphologically referable to *V. komodoensis* suggesting an ultimate origin for *V. komodoensis* on mainland Australia (>3.8 million years ago). *Varanus komodoensis* body size has remained stable over the last 900,000 years (ka) on Flores, a time marked by major faunal turnovers, extinction of the island's megafauna, the arrival of early hominids by 880 ka, co-existence with *Homo floresiensis*, and the arrival of modern humans by 10 ka. Within the last 2000 years their populations have contracted severely.

**Conclusions/Significance:** Giant varanids were once a ubiquitous part of Subcontinental Eurasian and Australasian faunas during the Neogene. Extinction played a pivotal role in the reduction of their ranges and diversity throughout the late Quaternary, leaving only *V. komodoensis* as an isolated long-term survivor. The events over the last two millennia now threaten its future survival.

**Citation:** Hocknull SA, Piper PJ, van den Bergh GD, Due RA, Morwood MJ, et al. (2009) Dragon's Paradise Lost: Palaeobiogeography, Evolution and Extinction of the Largest-Ever Terrestrial Lizards (Varanidae). PLoS ONE 4(9): e7241. doi:10.1371/journal.pone.0007241

**Editor:** Samuel T. Turvey, Zoological Society of London, United Kingdom

**Received:** February 18, 2009; **Accepted:** August 24, 2009; **Published:** September 30, 2009

**Copyright:** © 2009 Hocknull et al. This is an open-access article distributed under the terms of the Creative Commons Attribution License, which permits unrestricted use, distribution, and reproduction in any medium, provided the original author and source are credited.

**Funding:** Australian Research Council LP0453664 and LP0883991. The funders had no role in study design, data collection and analysis, decision to publish, or preparation of the manuscript.

**Competing Interests:** The authors have declared that no competing interests exist.

\* E-mail: scott.hocknull@qm.qld.gov.au

## Introduction

Fossils of giant varanids ( $\geq 3$  m Total Body Length) were first reported in the 1850s with the description of *Megalanias prisca* from the Pleistocene of Australia [1,2]. Since that time, and with the discovery of living Komodo Dragons (*V. komodoensis*) on the east Indonesian islands of Flores, Rinca and Komodo [3] considerable attention was paid in trying to understand the evolution of body size in monitor lizards [4–6]. Though several processes are proposed to explain the evolution of giantism in varanids, two competing hypotheses dominate the literature: autapomorphic giantism (i.e. Island Rule) and phyletic giantism (i.e. Cope's Rule) [7]. Both processes were previously invoked for the evolution of *V. komodoensis* [4,6,7].

It is commonly thought that *V. komodoensis* is a classic example of autapomorphic giantism having evolved large body size sometime

in the past from a small-bodied ancestor that arrived on isolated Indonesian islands, which were devoid of predatory competition [3,8]. Some proposals suggest that *V. komodoensis* attained large body size on Flores as a specialist hunter of pygmy *Stegodon* [3,9], the only large-bodied prey inhabiting Flores throughout the middle and late Pleistocene to as recently as 12,000 years ago [10,11]. The alternative, phyletic giantism, is supported by independent phylogenetic studies of morphology [12–14] and genetics [15,16], which nest *V. komodoensis* within an Australopapuan clade of varanids containing the two large-sized living species, *V. salvadorii* and *V. varius*, and the largest of all known lizards *Megalanias prisca* (= *Varanus prisca*) [14]. Thus, large body size is a synapomorphy of the clade and is not an autapomorphic trait of *V. komodoensis*. The implications of the phyletic model are that: 1. The extant populations of *V. komodoensis* are relictual, having had a

much wider geographic distribution in the past [17,18]. 2. *Varanus komodoensis* arrived on Flores already large and did not evolve gigantism there through the processes of insular evolution [7].

We aim to reconstruct the palaeobiogeography and geochronology of Neogene large-bodied varanids by using the fossil remains available from deposits in India, Java, Flores, Timor and Australia.

## Methods

### Morphometrics

Five measurements were taken of fossil and modern *Varanus* cervical, dorsal, sacral and anterior caudal vertebrae (Figure 1). Measurements were undertaken using dial or digital callipers to 0.5 mm resolution. See Table S1 for specimen list and data. Measurements are in millimetres (mm) and include:

1. Prezygapophysis to postzygapophysis length (Pre-Post), measured from the anterior margin of the prezygapophyses to the posterior margin of the postzygapophyses (Figure 1, A).
2. Centrum length (CL), measured from the posterior margin of the cotyle to the posterior margin of the condyle (Figure 1, B).
3. Cotylar width (CW), measured from the left lateral margin of the cotyle to the right lateral margin of the cotyle (Figure 1, C).
4. Postzygapophysis to postzygapophysis width (Post-Post), measured from the lateral margin of the left postzygapophysis to the lateral margin of the right postzygapophysis (Figure 1, D).

5. Prezygapophysis to prezygapophysis width (Pre-Pre), measured from the lateral margin of the left prezygapophysis to the lateral margin of the right prezygapophysis (Figure 1, E).

Two measurements were taken of fossil and modern *Varanus* teeth (Figure 1).

1. Crown height, measured from the base of the tooth plicidentine to the crown tip if preserved (Figure 1, F).
2. Basal width, measured from the anterior margin to the posterior margin of the base of the tooth (Figure 1, G).

Two measurements were taken from the humerus of fossil and modern *Varanus* (Figure 1) [19].

1. Maximum diaphysis width of humeri (Figure 1, H).
2. Maximum width of the distal end (Figure 1, I).

### Capturing Maximal Size Variation

Our modern sample of *V. salvator* may not represent the maximal size limit seen in the largest *V. salvator* individuals. Our comparative sample of *V. salvator* was close to the maximal snout-vent lengths (SVL) recorded in a large sample of this taxon; however, the largest specimen from our sample had a total length approximately 15–20% shorter than the total length of the longest recorded *V. salvator* (321 cm) [20]. Therefore, we took the

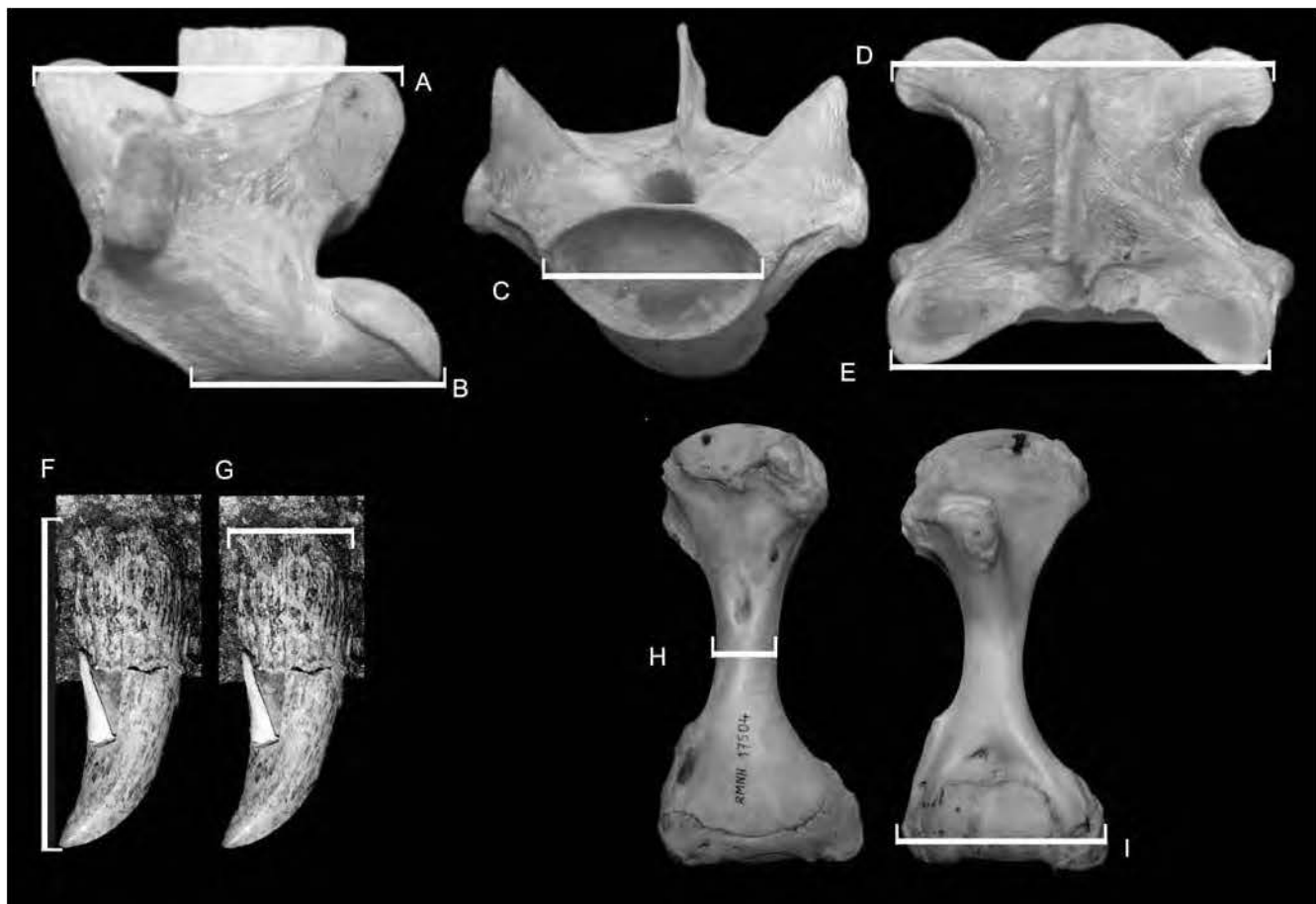


**Figure 1. Morphometric measurements.** A. Pre-postzygapophysis length. B. Centrum length. C. Cotylar width. D. Post-postzygapophysis width. E. Pre-prezygapophysis width. F. Tooth crown height. G. Tooth base length. H. Diaphysis width (humerus). I. Distal condyle width (humerus). doi:10.1371/journal.pone.0007241.g001

measurements of our largest *V. salvator* vertebral specimens and increased them by 20%, adding these additional measurements to the main dataset. This provided a more accurate estimate of *V. salvator* maximal size limits.

## Descriptive Statistics

Bivariate plots of morphometric data were plotted to determine the position of fossil specimens in relation to the modern samples taken of *Varanus*. Convex hulls were drawn to delineate the area of maximal variation observed in the samples. Due to the different preservation states of many of the specimens, only a single measurement might be available (univariate data). For these data frequency distribution histograms or box-plots showing the median value, 25–75% quartiles and the minimal and maximal values, were produced to determine where in the range of variation the fossil specimens plotted out. Principle components analysis (PCA) was applied to analyse multivariate data; however, most multivariate analyses were uninformative due to the large amount of missing data from the fossil specimens.

Where possible statistical tests were carried out where fossil sample sizes were sufficient to return an informative result. Descriptive statistics and tests were conducted using PAST software version 1.82b [21].

## Results

### *Varanus komodoensis* Ouwens 1912

**Australia (Early Pliocene – middle Pleistocene).** Fossil specimens from Pliocene and Pleistocene-aged sites in Australia (Table 1) were identified as belonging to *Varanus komodoensis* on the basis of the following combination of unique cranial and post-cranial characteristics. Overall similar size and proportions of all preserved skeletal elements. Maxilla contributes to the labial margin of the premaxillary-maxillary aperture (pmp). Maxillary

margin of the pmp shallow. Premaxillary-maxillary suture faces antero-lingually. Angulate maxillary crest. Labio-lingually compressed, closely-set recurved and serrated dentition both on maxillae and dentaries. At least 12 tooth loci in dentary. Parietal with distinct supratemporal crests, with fronto-parietal suture interlocking. Humerus stockier than all other members of *Varanus*, except *V. prisca*.

**Maxillae (Figure 2, B–D and Figure 3, H–I).** Three maxillae; a near complete right maxilla (QMF 874), the anterior section of a right maxilla (QMF 42105) and the posterior portion of a left maxilla (QMF 54605) share closest morphology and size with *Varanus komodoensis*. QMF42105 represents a marginally larger individual than specimens QMF874 and QMF 54605. All three share with *V. komodoensis* closely-spaced, labio-lingually compressed, recurved dentition with finely grooved plicidentine, and serrated mesial and distal margins. The teeth are morphometrically similar to the modern *V. komodoensis* sample (Figure S1).

QMF 874 and QMF 42105 also share with *V. komodoensis* a distinct interlocking premaxillary-maxillary suture with an open premaxillary-maxillary aperture (pmp) and an angulate narial crest. The circumference of the premaxillary-maxillary aperture is made up by the premaxilla and maxilla to varying degrees in different *Varanus* groups (Figure S2). In the fossil maxillae only the posterior and labial margins of the pmp are enclosed by the maxilla, the remainder is enclosed by the premaxilla. This key feature allies the fossils to taxa where the premaxilla contributes to the anterior and lingual margin of the pmp (*V. indicus*, *V. varius* group and *V. gouldii* group).

The fossils differ morphologically from *V. indicus* by possessing an interlocking and anterolingually oriented premaxillary-maxillary suture articulation, more labially angulate maxillary crest and more recurved dentition. Morphometrically, the fossils are also much larger.

**Table 1.** Pliocene – Pleistocene fossils from Queensland representing *Varanus komodoensis*.

Specimen	Registration	Location (Fauna)	Age	Age Reference
Cervical vertebra	QMF 23684	Bluff Downs Local Fauna, north-eastern Queensland	Early Pliocene	[32]
Dorsal vertebra	QMF 23686	Bluff Downs Local Fauna, north-eastern Queensland	Early Pliocene	[32]
Right maxilla	QMF 874	Chinchilla Sands Local Fauna, south-east Queensland	Middle Pliocene	[33]
Right maxilla (partial)	QMF 42105	Chinchilla Sands Local Fauna, south-east Queensland	Middle Pliocene	[33]
Left dentary (partial)	QMF 870+QMF 871	Chinchilla Sands Local Fauna, south-east Queensland	Middle Pliocene	[33]
Quadrate	QMF 42156	Chinchilla Sands Local Fauna, south-east Queensland	Middle Pliocene	[33]
Supraorbital	QMF 25392	Chinchilla Sands Local Fauna, south-east Queensland	Middle Pliocene	[33]
Parietal	QMF 53956	Chinchilla Sands Local Fauna, south-east Queensland	Middle Pliocene	[33]
Scapulocoracoid	QMF 866	Chinchilla Sands Local Fauna, south-east Queensland	Middle Pliocene	[33]
Left humerus (partial)	QMF 53954	Chinchilla Sands Local Fauna, south-east Queensland	Middle Pliocene	[33]
Right humerus (partial)	QMF 53955	Chinchilla Sands Local Fauna, south-east Queensland	Middle Pliocene	[33]
Vertebrae	QM Colln (numerous)	Chinchilla Sands Local Fauna, south-east Queensland	Middle Pliocene	[33]
Left maxilla (partial)	QMF 54605	Mt Etna Local Fauna, central eastern Queensland	Middle Pleistocene	[28]
Supraoccipital	QMF 54607	Mt Etna Local Fauna, central eastern Queensland	Middle Pleistocene	[28]
Quadrate (right)	QMF 54606	Mt Etna Local Fauna, central eastern Queensland	Middle Pleistocene	[28]
Tibia	QMF54608	Mt Etna Local Fauna, central eastern Queensland	Middle Pleistocene	[28]
Ulna diaphysis	QMF 54604	Mt Etna Local Fauna, central eastern Queensland	Middle Pleistocene	[28]
Dorsal vertebra	QMF 54120	Mt Etna Local Fauna, central eastern Queensland	Middle Pleistocene	[28]
Caudal vertebra	QMF 1418	Marmor Quarry, eastern Queensland	Middle Pleistocene	[34]

doi:10.1371/journal.pone.0007241.t001



**Figure 2.** *Varanus komodoensis* (Pliocene, Australia). A. Modern *V. komodoensis* skull in dorsal view (NNM 17504). B. QMF 874, right maxilla in lateral view. C. QMF 42105, partial right maxilla in dorsal view. D. QMF 42105, right maxilla in dorsal view. E. QMF 25392, complete left supraorbital in dorsal view. F. QMF 53956, partial parietal in dorsal view. G–H. QMF 42156, right quadrate in anterior and lateral views. I–J. QMF 870+871, partial left dentary in lingual view, J illustrating the tooth loci. Abbreviations: mcrst, dorsal maxillary crest; pmp, premaxillary-maxillary aperture; pms, premaxilla-maxilla suture; sym, dentary symphysis; mg, Meckalian groove. Dashed line represents broken edge of maxilla. Scale bar = 5 cm.  
doi:10.1371/journal.pone.0007241.g002



**Figure 3. *Varanus komodoensis* (Neogene, Australia).** A–B, E–G. Pliocene *V. komodoensis* (Australia) A–B. QMF 53955, partial left humerus in dorsal view showing position of insertion for the *latissimus dorsi* (lat dors). C–D. Left and right humerus of a modern *V. komodoensis* (NNM 17504). E–F. QMF 53954, partial right humerus in ventral and dorsal views, showing the position of the ectepicondyle (ect). G. QMF 866, partial scapulocoracoid. H–P. Pleistocene *V. komodoensis* (Australia). H–I. QMF 54605, partial left maxilla in lingual and labial views. J. QMF 54606, partial right quadrate in anterior view. K. QMF 54607, supraoccipital bone in posterior view. L. QMF 54608, proximal left tibia. M. QMF 54604, ulna diaphysis. N–P. QMF 1418, proximal mid-caudal in cranial, oblique lateral and dorsal views. Scale bar = 1 cm.  
doi:10.1371/journal.pone.0007241.g003

Morphologically the fossil specimens are most similar to members of the *V. varius* group and to some members of the *V. gouldii* group, in particular *V. varius*, *V. komodoensis*, *V. panoptes* and *V. mertensi* (Figure S2). The maxillary margin of the pmp in the *V. varius* group is shallower than those from the *V. gouldii* group. The pmp is similarly shallow in both fossil maxillae, allying them closer to the *V. varius* group. The only taxon present in either the *gouldii* or *varius* groups that reaches the large size of the fossils and possesses the closely-spaced, recurved dentition, is *V. komodoensis*.

**Supraorbital (Figure 2, E).** QMF 25392 is a complete left supraorbital bone, which matches closely *V. komodoensis*, including the possession of a thick postorbital bar which projects posterolaterally, is shallowly curved and is suboval in cross-section. Proximally, the supraorbital flares in an antero-posterior direction, producing a ‘Y’ shaped bone. The dorsal surface is smooth, whilst the ventral surface preserves a rugose margin.

**Parietal (Figure 2, F).** QMF 53956 possesses distinct dorsally expressed supratemporal crests which ally this specimen to large-sized members of the *V. varius* group (*V. salvadorii*, *V. komodoensis* and *V. prisca*). QMF 53956 is smaller than *V. prisca* with less defined crests and a broader central roof. Based on overall size, QMF 53956 is most similar to *V. komodoensis* and larger than *V. salvadorii*. It also possesses an interlocking frontal-parietal suture articulation, which is only seen in *V. komodoensis* and *V. prisca*.

**Quadrates (Figure 2, G–H. Figure 3, J).** Two right quadrates are known, including a complete specimen (QMF 42156) and the proximal half of another (QMF 54606). Both are similar in overall morphology and size to one another and to *V. komodoensis*. In both specimens and in *V. komodoensis*, the proximal condyle is antero-posteriorly expanded into two articular facets, both rounded basins that are relatively smooth. One or two thin laminae run ventrally to the distal condyle which is medio-laterally expanded into two similar-sized condyles. A distinct medial crest originates from the midline of the proximal articular end and runs medio-distally along the medial side of the quadrate, terminating at the antero-medial corner of the disto-medial condyle. A broad, rounded and straight ridge originates at the antero-lateral corner of the proximal articular face and runs distally to the antero-lateral corner of the disto-lateral condyle.

**Supraoccipital (Figure 3, K).** QMF 54607 is an isolated but complete supraoccipital bone from the skull of a large species of *Varanus*. In dorsal view, it is trapezoidal in shape with a ventral width wider than the dorsal width. A ridge occurs in the midline of the bone oriented dorso-ventrally and constricted toward the middle. A cup-like recess is present on the dorsal face of the bone, which would have received the *processus ascendens*, which seems to have been unossified or at least not attached to the supraoccipital (as it is in *V. prisca*). The angle of the supraoccipital in relation to the parietal, and to the paraoccipitals would be more acute than seen in *V. prisca*, similar to that of *V. komodoensis* and less so than most other species of *Varanus*.

**Dentary (Figure 2, I–J).** QMF 870 and QMF 871 represent either a single left dentary, which is badly broken at its midline, or two separate fragments of two left dentaries. Although not noted as the same specimen, preservation and size indicates that these two specimens come from a very similar, if not the same, individual. QMF 871 is an anterior-most portion of a left dentary preserving the dentary symphysis and the first six tooth loci. The first tooth occurs just postero-dorsal of the dentary symphysis, which is rounded and bisected by the proximal origin of the Meckelian groove. The second tooth is complete and the best preserved of both specimens. The tooth is compressed labio-lingually, has a rounded distal margin and a constricted and serrate mesial cutting edge. QMF 870 is a portion of the posterior section of a left

dentary, preserving five tooth loci. The dentary is missing below the dorsal margin of the Meckelian groove. The dorsal half of the posterior mental foramen can be seen in labial profile. Considered together, these two specimens indicate that the dentary preserved 12–13 tooth loci, where the teeth are closely-spaced, labio-lingually compressed, distinctly recurved and serrated. When compared to a range of *Varanus* species, it is clear that adult *V. komodoensis* possesses 12 or 13 tooth loci for each dentary; whereas other species of *Varanus* possess 11 or fewer tooth loci. *V. salvator* (10–11); *V. albigularis* (9–10); *V. indicus* (9–10); *V. varius* (9–10); *V. salvadorii* (10–11); *V. panoptes* (10–11); *V. tristis* (10–11). The only complete dentary of *V. prisca* possesses 11 tooth loci.

**Humeri (Figure 3, A–B, E–F).** A right (QMF 53955) and a left (QMF 53954) humerus, both missing the proximal and distal-most epiphyses are of similar size and morphology to *V. komodoensis*. The humeri of *V. prisca* and *V. komodoensis* are stocky and robust when compared to humeri found in all other members of *Varanus*. Both fossil humeri indicate a stout humerus with broad proximal and distal epiphyses. When comparing the maximum diaphyseal width of the two specimens with species of extant and fossil *Varanus*, both specimens fall within the size range of *V. komodoensis* and outside that of small and large *Varanus prisca* (Figure S3).

**Vertebrae (Figure 3, M–P. Figure 4).** Thirty eight dorsal vertebrae were measured from two Pliocene localities, Chinchilla (n = 37) and Bluff Downs (n = 1). All of these vertebrae fell within the size range of modern *V. komodoensis* (p > 0.8) (Figure S4). In all features, the fossil sample reflects directly similar features seen in *V. komodoensis*.

A partial dorsal vertebra (QMF 54120) and a caudal vertebra collected from middle Pleistocene-aged sites at Mt. Etna and Marmor Quarry respectively represent a large-bodied varanid which is much smaller than *V. prisca*, but larger than any living varanid on mainland Australia and New Guinea (e.g. *Varanus giganteus*, *V. varius*, *V. salvadorii*) (Figure 4). QMF 54120 is a fragmentary dorsal vertebra, preserving the left lateral half of the cotyle and the left lateral portion of the postzygapophysis. On direct comparison with *V. komodoensis* it shares similar size and morphology. QMF1418 is a near complete proximal mid-caudal vertebra and falls within the size range of *V. komodoensis* (Figure S9).

**Other postcranial elements (Figure 3, L–M).** In addition to the above diagnostic skeletal elements, several other postcranial remains recovered from these Pliocene and Pleistocene sites match *V. komodoensis* in over size and general morphology. These specimens include the proximal end of a left tibia (QMF 54608), the proximal end of a dorsal rib (QMF 54603), the diaphysis of an ulna (QMF 54604) and a partial scapulocoracoid (QMF866).

## Flores (early Pleistocene - Holocene)

Fossil specimens of *V. komodoensis* were recovered from the early-middle Pleistocene Ola Bula Formation in central Flores (Tangi Talo, Dhozo Dhalu) and from a late Pleistocene-Holocene cave deposit in central-western Flores (Liang Bua) [10,22]. Fossil specimens of *V. komodoensis* include many cranial and postcranial elements (Table S1).

**Teeth (Figure 5, E).** Twelve teeth were studied from the Pleistocene of Flores, including six isolated teeth from early Pleistocene Tangi Talo and six teeth from late Pleistocene-Holocene Liang Bua. Morphometrically these teeth fall within the size range of *V. komodoensis* (Figure S1). Morphologically, the teeth bear the unique features of being greatly recurved and compressed labio-lingually. This feature is only present in modern *V. komodoensis* and fossil specimens referable to *V. komodoensis*.

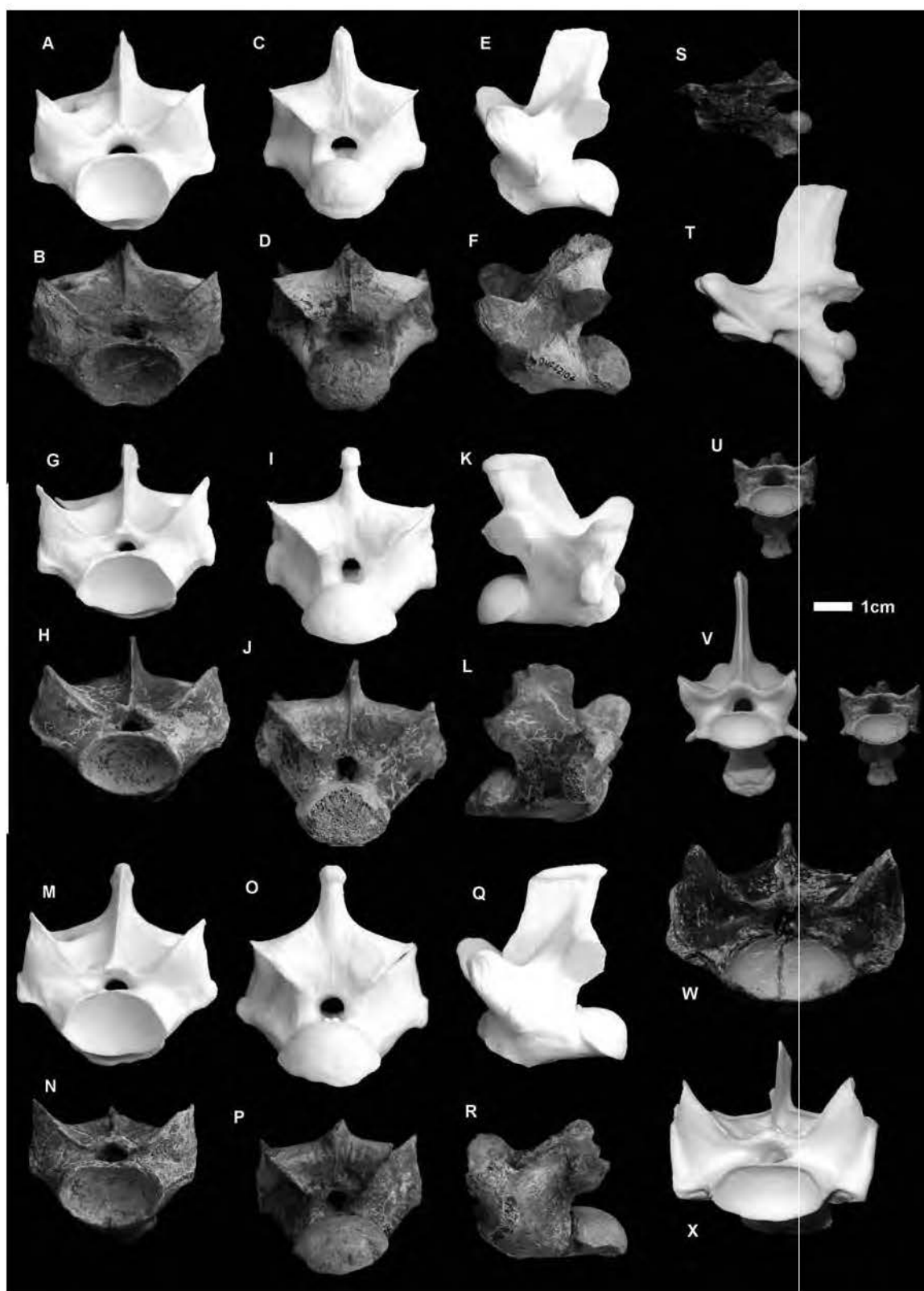


**Figure 4. *Varanus komodoensis* (Pliocene, Australia).** A–F. QMF 42104, posterior dorsal vertebra compared with modern *V. komodoensis* (white), in anterior (A–B), posterior (C–D) and left lateral (E–F) views. G–L. QMF 42096, mid-dorsal vertebra compared with modern *V. komodoensis* (white), in anterior (G–H), posterior (I–J) and right lateral (K–L) views. M–R. QMF 42102, mid-dorsal vertebra compared with modern *V. komodoensis* (white), in anterior (M–N), posterior (O–P) and left lateral (Q–R) views. S–V. QMF 23684, cervical vertebra compared with modern *V. komodoensis* (white), in left lateral (S–T) and anterior (U–V) views. W–X. QMF 23686, anterior dorsal vertebra compared with modern *V. komodoensis* (white) in anterior view. Scale bar = 1 cm.

doi:10.1371/journal.pone.0007241.g004



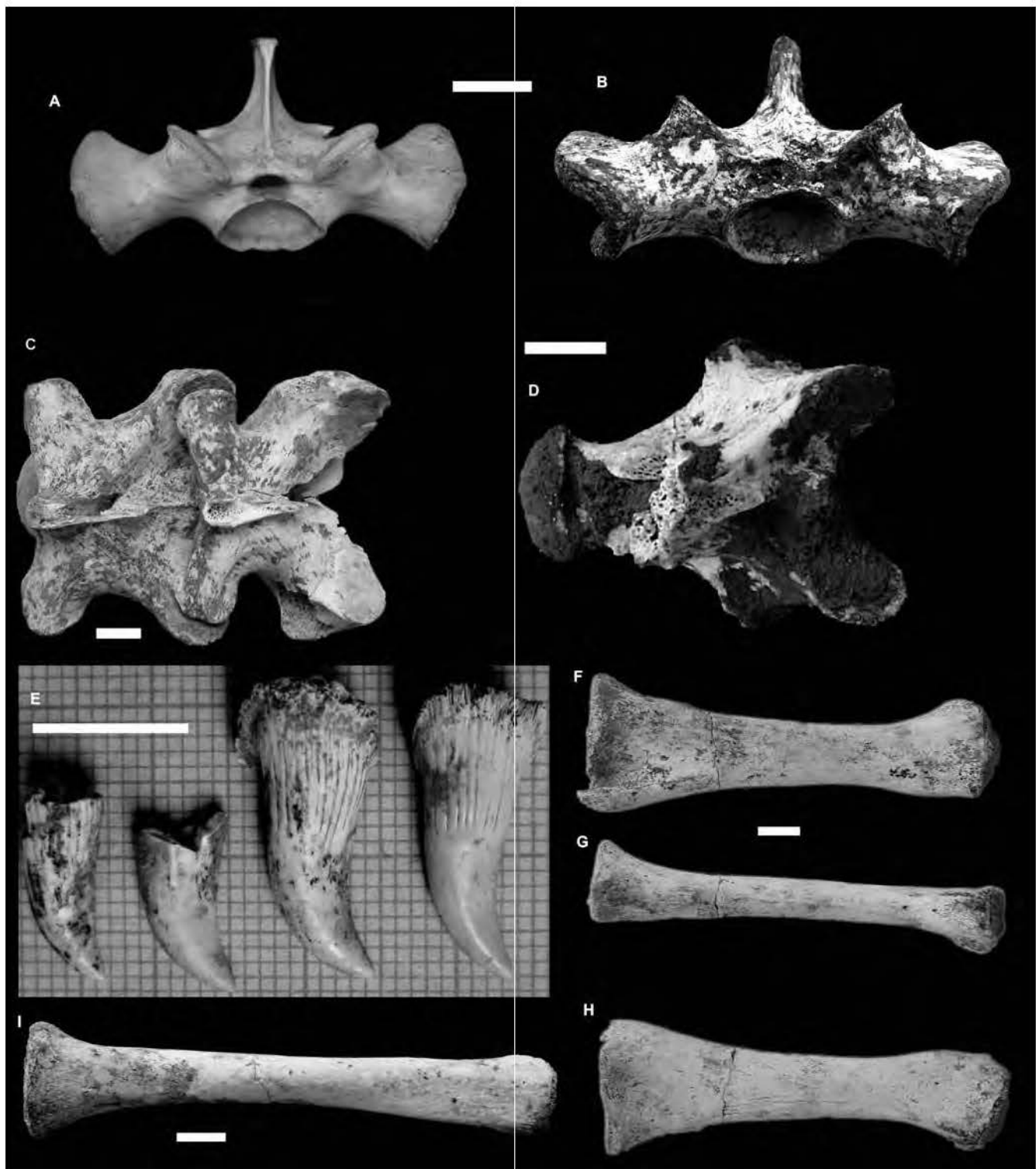


**Figure 5. *Varanus komodoensis* (Pleistocene, Flores).** A–B. Sacral vertebrae from modern (A) and fossil (LB558a) *V. komodoensis* in anterior view. C. Articulated dorsal vertebrae (LB19/20-9-04) in dorsal view. D. Cervical vertebra (LB517b) in dorsal view. E. Four isolated teeth (LB04 unreg) in lingual view. F–H. Ulna diaphysis (LB-447a/16.8.04) in medial (F), cranial (G) and lateral (H) views. I. Radius diaphysis (LB-28.7.03) in medial view. Scale bar = 1 cm.

doi:10.1371/journal.pone.0007241.g005

**Cervical vertebrae (Figure 5, D).** Four well preserved cervical specimens were used in this study, including one from early Pleistocene Tangi Talo and three from late Pleistocene-

Holocene Liang Bua. The Tangi Talo specimen is only slightly larger than the modern *V. komodoensis* sample (Figure S5, A). Two Liang Bua specimens are only slightly larger and one is within the



morphometric range of our modern *V. komodoensis* sample (Figure S5, B). No statistical test was conducted due to the very small sample sizes for each site (1 and 3 respectively).

**Dorsal vertebrae (Figure 5, C).** Fifteen dorsal vertebrae were used in this study, all coming from Liang Bua. Due to the differing preservation states of each vertebra the only available measurement for all dorsal vertebrae was the cotylar width. When the Liang Bua fossil sample is compared to our sample of modern *V. komodoensis* the mean value for cotylar width is significantly different ( $p < 0.001$ ). When comparing the maximal size limits of our two samples the Liang Bua fossil sample is most-likely biased toward large individuals (Figure S6). Therefore, we consider the significant difference in mean cotylar width to be related to a taphonomic bias toward large individuals being preserved at the Liang Bua site, not an overall larger size. These large individuals are still within the maximal size limits of our modern sample of *V. komodoensis*. In addition, three well-preserved specimens were used in a bivariate plot of prezygapophysis – postzygapophysis (Pre-post) length over prezygapophysis – prezygapophysis (Pre-pre) width. The fossils fall within the morphometric range of modern *V. komodoensis*, with the exception of a single specimen that possesses a slightly broader pre-pre width (Figure S7). Morphologically, the vertebrae are identical to modern *V. komodoensis*.

**Sacral vertebrae (Figure 5, B).** A single sacral vertebra from Liang Bua is directly comparable in size to *V. komodoensis* and places morphometrically within the sample of modern *V. komodoensis* (Figure S8). No statistical tests were able to be carried out due to the small sample size ( $n = 1$ ).

**Anterior caudal vertebrae.** Six anterior caudal vertebrae were studied from Liang Bua, all of which fall within the morphometric and morphological variation of modern *V. komodoensis*; their mean sizes not significantly different ( $p > 0.67$ ) (Figure S9).

**Humerus.** A single humeral diaphysis represents *V. komodoensis* from Tangi Talo both in size and morphology. When compared to modern *V. komodoensis* and humeri from Chinchilla, the Tangi Talo specimen has a slightly broader diaphysis (Figure S3). This may simply reflect the biased preservation of larger individuals within this deposit, as is seen in the Liang Bua collection.

**Other postcranial elements (Figure 5, H–I).** In addition to the above diagnostic specimens several other remains recovered from Liang Bua are considered to represent *V. komodoensis*, including fragments of ilia, metapodials, a phalanx, partial right mandible, and the diaphyses of an ulna and a radius (Table S1). These remains will form part of a future review of *V. komodoensis* fossils from Liang Bua.

#### *Varanus* sp. cf. *V. komodoensis*

**Java (Middle Pleistocene).** A single anterior dorsal vertebra (CD6392) of a large-bodied varanid is recorded from the middle Pleistocene Kedung Brubus deposit (Figure 6, A–F). Morphometrically this specimen falls within the middle range of modern and fossil *V. komodoensis* and is well outside the largest *V. salvator* (+20%) sample (Figure S7). CD6392 was considered to be *V. komodoensis* [17]. It is remarkably similar to *V. komodoensis* in both size and morphology, possessing steep zygapophyses, dorsally oriented condyles, distinct precondylar constriction and an open neural canal. Although the specimen is close in morphology, assignment to *V. komodoensis* is tentative and should await more specimens for verification.

#### *Varanus sivalensis* Falconer 1868

**India, (Pliocene - early Pleistocene).** Three specimens were previously described to represent *Varanus sivalensis* [23–25], a

distal humerus and two dorsal vertebrae (anterior and mid-dorsal vertebrae). Whether these three specimens represent a single taxon (*V. sivalensis*) will depend on the discovery of more fossil specimens referable to this taxon. The humerus is morphologically distinct from *Varanus komodoensis* to warrant its unique taxonomic status; however, the two referred dorsal vertebrae fall within the variation of modern and fossil *V. salvator*. Therefore, it is unlikely that these three specimens represent the same taxon.

**Humerus (Figure 7, C–D).** Morphologically the humerus differs from *V. komodoensis* by features already described [12]. NHMR40816 plots in the middle range of *V. komodoensis* and outside *V. salvator*.

**Dorsal vertebrae (Figure 7, F, H, I–J, L, N).** NHMR739 is an anterior dorsal vertebra and plots within the fossil sample of *V. salvator* and is only slightly larger than the extant sample of *V. salvator* (Figure S7). NHMR740 was originally designated as a cervical vertebra; however, it is clearly a mid-dorsal vertebra, lacking any features alluding it to the cervical region. Morphometrically it plots within the lower range of *V. komodoensis* and outside the sample of modern *V. salvator*. The specimen does fit within the size range of fossil *V. salvator* from the early Pleistocene of Trinil, Java (Figures S6, S7). Both dorsal vertebrae are not considered to be significantly different to either the Trinil fossil sample or the modern *V. salvator* sample (Table 2). Both vertebrae are early Pleistocene in age, therefore, they match the Trinil specimens in morphology, size and age.

#### *Varanus salvator* Laurenti, 1768

**Java (Early Pleistocene).** The sample of large-bodied varanid fossils from the early Pleistocene deposits of Trinil, Java include dorsal, sacral and caudal vertebrae (Figure 6, G–K). Both the sacral and caudal vertebrae fall within the variation observed in modern *V. salvator* (Figures S8, S9). The majority of dorsal vertebrae fall within the variation of modern *V. salvator* whilst three specimens fall within the lower range of the *V. komodoensis* sample used in this study. Originally considered to be *V. komodoensis* [17], these few larger specimens are considered here to represent very large individuals of *V. salvator* even though they tend to be wider than the *V. salvator* (+20%) sample (Figure S7). This may be accounted for through allometric changes of the vertebrae in the largest individuals, where breadth of vertebra increases to a greater proportion with increased length (pers. obs.). Morphologically the vertebrae are similar to the comparative sample of *V. salvator*, being more gracile than *V. komodoensis* and *V. sivalensis*, the only two varanids closest in size to *V. salvator* and the fossil specimens. Statistically, the Trinil sample is not considered to be significantly different to the modern *V. salvator* sample, or the specimens derived from the Siwalik Hills (Table 2).

#### *Varanus* sp. nov.

**Timor (Middle Pleistocene).** Three massive varanid vertebrae are known from collections recovered from Timor, including a dorsal, sacral and anterior caudal vertebra (CV Collection, NNM). A mid-dorsal and anterior caudal were originally assigned to *V. komodoensis* [17]. The dorsal specimen falls within the upper morphometric range of *V. komodoensis*, but it possesses less vertically oriented condyles, has a reduced neural canal and is robust – features characteristic of *V. prisca* (Figures 8, S7). A sacral (not recorded previously) and an anterior caudal vertebra are morphologically similar to *V. prisca*, possessing rounded condyle-cotyles, stout transverse processes and thick cortical bone. They are both intermediate in size between *V. komodoensis* and *V. prisca* (sensu stricto) and possess zygapophyses that are at a lower angle (Figures 8, S8, S9). The combination of

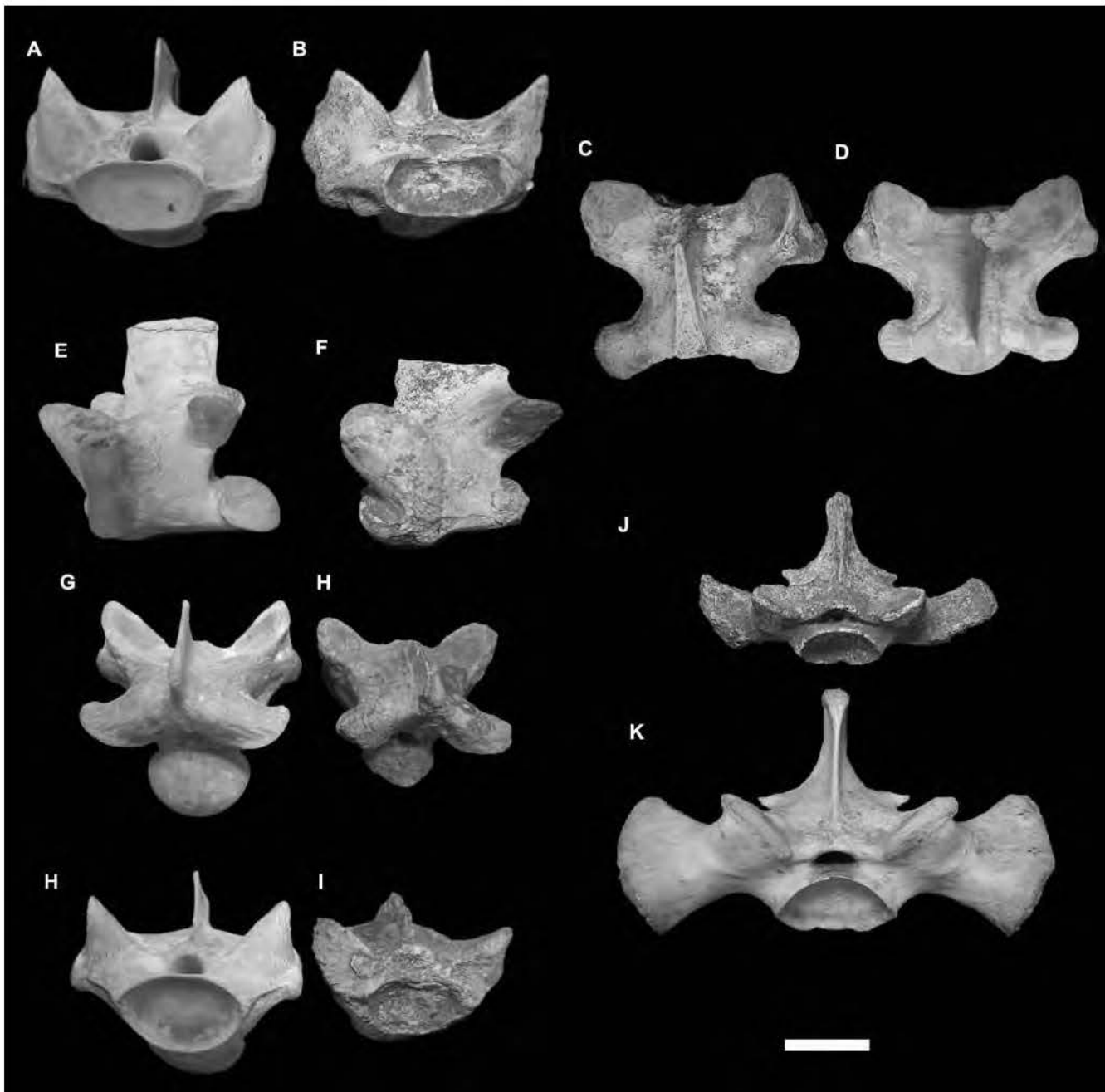


**Figure 6. *Varanus* sp. cf. *V. komodoensis* and *V. salvator* (Pleistocene, Java).** A–F. *V. sp. cf. V. komodoensis*. Anterior dorsal vertebra (CD 6392) compared with modern *V. komodoensis* in anterior (A–B), dorsal (C–D) and left lateral view (E–F). G–K. *V. salvator*. G–I. CD 8873, mid-dorsal vertebra, compared with modern *V. komodoensis* in dorsal (G–H) and anterior (H–I) views. J–K. CD 216, sacral vertebra, compared with modern *V. komodoensis* in anterior view. Scale bar = 1 cm.  
doi:10.1371/journal.pone.0007241.g006

intermediate size and unique morphology indicate that these specimens most likely represent a new unnamed taxon of large-bodied varanid.

#### Central Australia (Middle-Late Pleistocene)

**Vertebrae.** A large sample of dorsal vertebrae were measured from collections of Pleistocene varanids from central Australia. The morphometric variation encompassed by these specimens indicates the presence of a varanid intermediate in size between *V. komodoensis* and *V. prisca* (sensu stricto) (Figure S10,

S11). The three samples of vertebrae were significantly different to one another with the central Australian sample showing significantly smaller size when compared to the eastern Australian *V. prisca* (sensu stricto) sample ( $p < 0.0002$ ) and significantly larger size when compared to modern and fossil *V. komodoensis* ( $p < 0.004$ ). Whether these specimens represent a diachronous sample across the middle to late Pleistocene, or a morphocline of Pleistocene giant varanids from smaller central Australian forms toward larger eastern Australian forms is yet to be determined. Regardless, these specimens indicate a giant

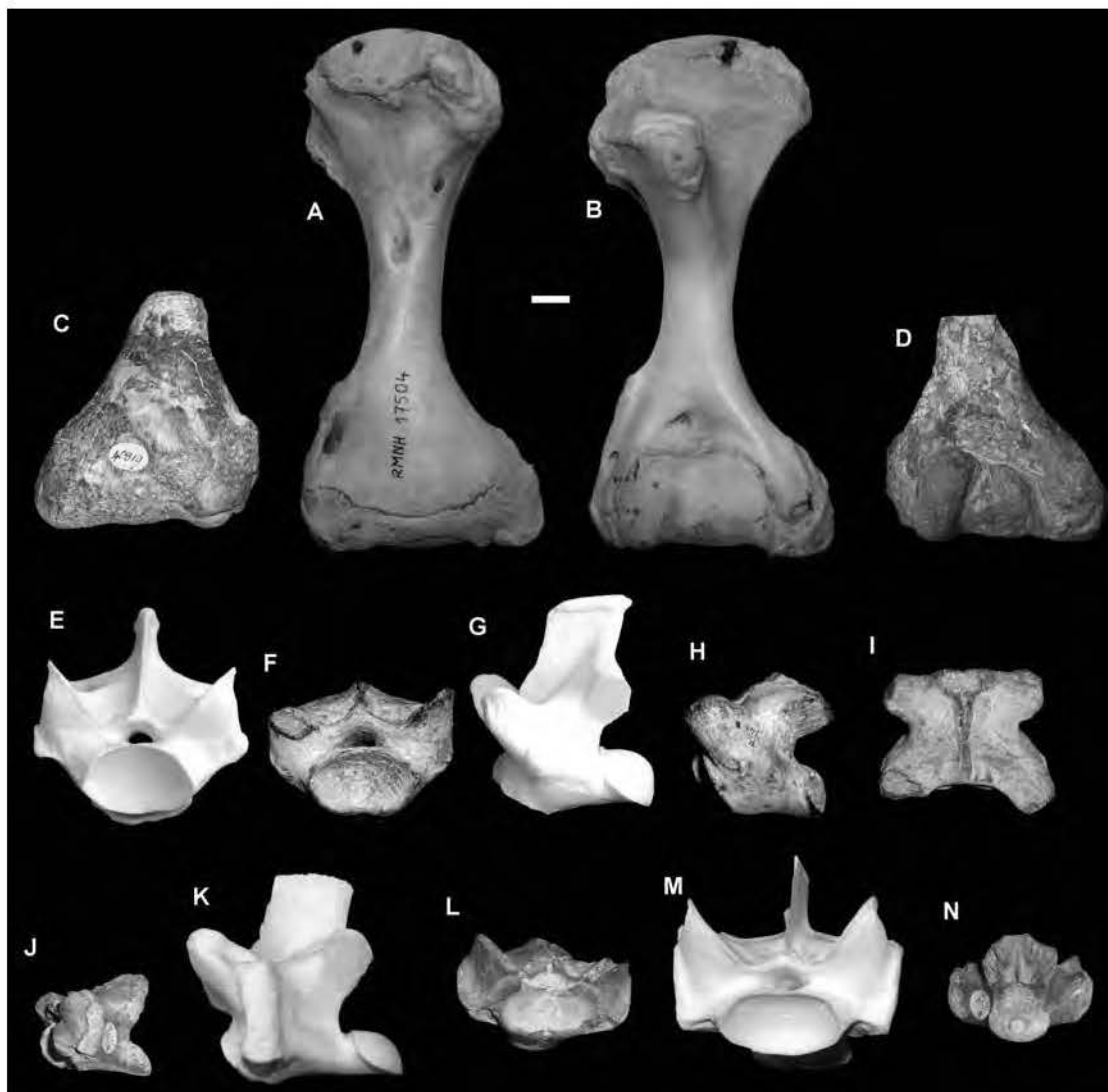


**Figure 7. *Varanus sivalensis* (Pliocene, India).** A–B. NNM 17504, modern *Varanus komodoensis* humerus. C–D. NHMR 40819, distal humerus in dorsal (C) and ventral (D) views. E–I. NHMR 740, posterior dorsal vertebra compared with modern *V. komodoensis* (white) in anterior (E–F), left lateral (G–H) and dorsal (I) views. J–N. NHMR 739, anterior dorsal compared with modern *V. komodoensis* (white) in left lateral (J–K), anterior (L–M) and posterior (N) views. Scale bar = 1 cm.  
doi:10.1371/journal.pone.0007241.g007

varanid present in central Australia during the Pleistocene that resembles, at least in size, the taxon present on Timor during the middle Pleistocene.

**Table 2.** Tukey's pairwise comparisons (ANOVA) table of fossil and modern *Varanus* dorsal vertebrae, pre-post length measurements.

	Liang Bua	Siwaliks	<i>V. komodoensis</i>	<i>V. salvator</i> (n = 29)
Trinil (n = 11)	p < 0.0004*	p > 0.9	p < 0.002*	p > 0.9
Liang Bua (n = 3)		p < 0.006*	p > 0.9	p < 0.0002*
Siwaliks (n = 2)			p < 0.03*	p > 0.7
<i>V. komodoensis</i> (n = 74)				p < 0.0007*

\* indicates a significant difference between samples.  
doi:10.1371/journal.pone.0007241.t002

## Discussion

Archaeological and paleontological excavations at sites in central and western Flores produced teeth and post-cranial elements of *V. komodoensis* dating from the early Pleistocene to the late Holocene (~900–2 ka) [10,22]. This fossil record provides an opportunity to evaluate long-term morphological and morphometric changes in *V. komodoensis* on Flores over ca. 900,000 years. Comparisons between fossil and extant *V. komodoensis* show that there are few morphometric or morphological differences between the fossil specimens and those of modern *V. komodoensis*. Therefore, maximal body size of this species remained stable for at least 900,000 years despite the fact that the biostratigraphic sequence on Flores records at least three faunal turnovers, marked by the extinction of the giant tortoise *Colossochelys* [26], two species of *Stegodon* and *Homo floresiensis*, as well as the arrival of hominins by 880 ka and modern humans by 10 ka [22]. Even in the absence of any moderately-sized prey between the extinction of *Stegodon floresiensis insularis* (~12. ka) [10,11] and the introduction of the pig

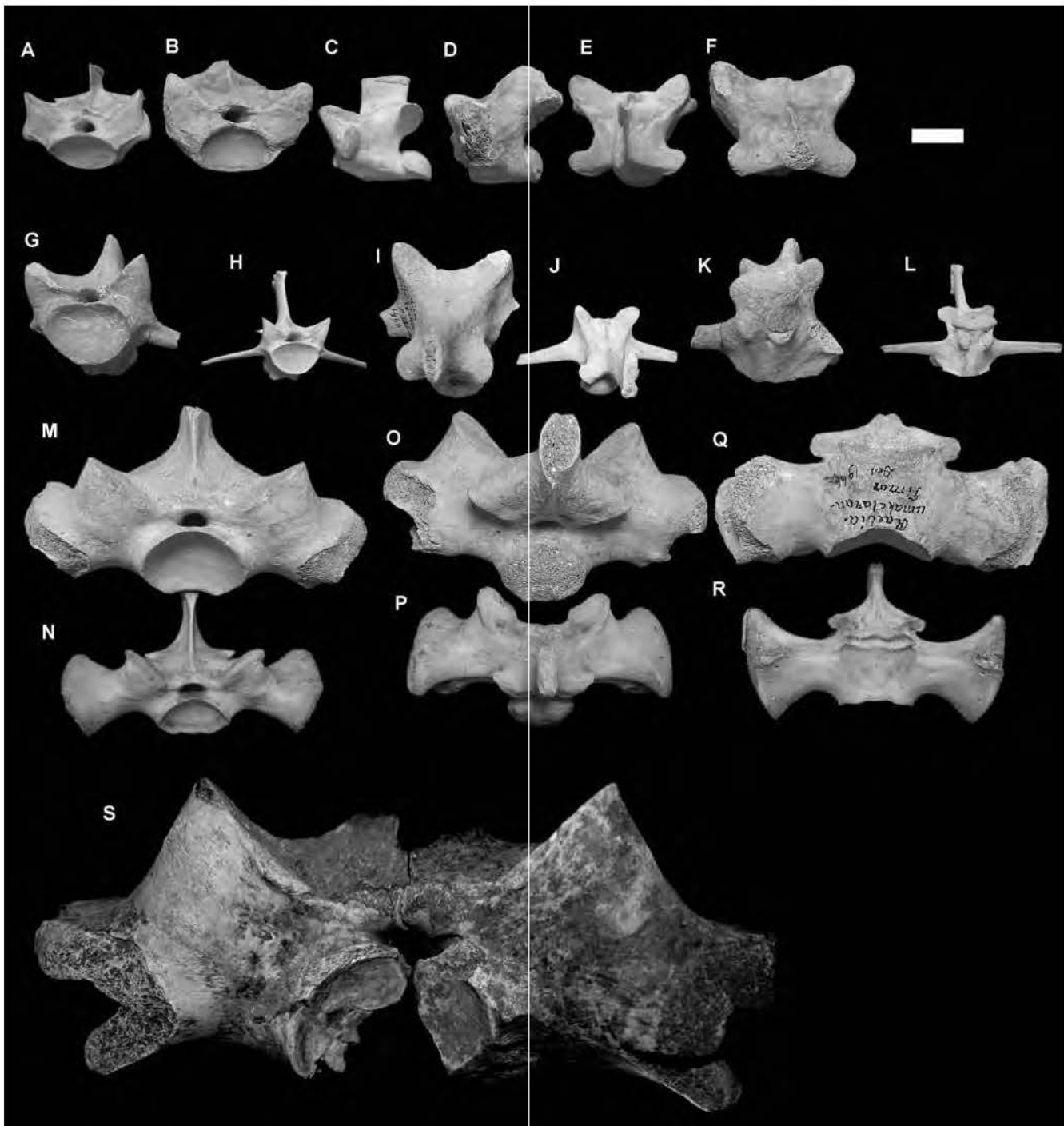


**Figure 8.** *Varanus* sp. nov. (Pleistocene, Timor). A–F. Mid-dorsal vertebra (CV Raebia 1) compared with modern *V. komodoensis* in anterior (A–B), left lateral (C–D), dorsal (E–F) views. G–L. Anterior caudal vertebra (CV Raebia 2) compared with modern *V. komodoensis* in anterior (G–H), dorsal (I–J) and oblique posterior (K–L) views. M–R. Sacral vertebra (CV Raebia 3) compared with modern *V. komodoensis* in anterior (M–N), dorsal (O–P) and ventral (Q–R) views. S. QMF 8968, sacral vertebra of *Varanus prisca* in anterior view.  
doi:10.1371/journal.pone.0007241.g008

from Sulawesi (~7 ka) [10] *V. komodoensis* was able to persist on Flores. The stability of *V. komodoensis* body size over a long temporal sequence and during periods of major ecological change implies that insular evolutionary processes had limited effect, and more importantly illustrate the adaptive flexibility and resilience of a generalist carnivore, rather than a specialist predator of the island's pygmy *Stegodon*.

So, if *V. komodoensis* did not evolve on an isolated island in Wallacea, from where did it disperse? India and Australia are the only regions that preserve a giant varanid fossil record older than 900 ka, and are the only identifiable sources for large-bodied *Varanus* [2]. The oldest recorded large-bodied *Varanus* from both regions occur in the Pliocene, suggesting a relatively synchronous yet independent evolution of lizard giantism. In India large-bodied

varanid fossils are rare, being represented by two vertebrae and a partial humerus, each assigned to the extinct *V. sivalensis* [24]. Both vertebrae probably represent *Varanus salvator*. The humerus is of similar size to *V. komodoensis* but differs morphologically [12]. The absence of *V. sivalensis* from younger deposits at the same locales suggests that large-bodied varanids were either very rare or more likely extinct on the Indian sub-continent by the end of the early Pleistocene. Therefore, based on both morphology and chronology, *V. sivalensis* is an unlikely source for *V. komodoensis* on Flores. *Varanus sivalensis* is associated with a Late Pliocene Siwalik fauna that includes diverse mammalian megafauna, including the placental carnivores *Crocota*, *Hyaena* and *Panthera* [27]. This record alone demonstrates that varanids can evolve gigantism on continental landmasses with competition from large placental carnivores.

Varanids appear in the Australian fossil record by the Miocene and possess a more or less continuous record of large-bodied forms from the early Pliocene (~3.8 mya) through to the late Pleistocene [2]. Varanids most likely dispersed eastward from Asia to Australia, then radiated to produce a clade containing *V. komodoensis* [15,16,18]. Although the taxonomy of the Australian Miocene-Pleistocene varanids remains largely unresolved [2], it is most likely that they are contained within this monophyletic clade. There are at least three giant varanid taxa present in Australia during the Neogene, including one species from the Pliocene, one from the Pleistocene of central Australia and *Varanus prisca* (sensu stricto) from the middle-late Pleistocene. On the basis of both size and a unique combination of morphological features shared only with *V. komodoensis* the Pliocene taxon is here considered to be conspecific with *V. komodoensis*. Newly recovered large-bodied varanid fossils from middle Pleistocene [28] deposits in north-eastern Australia are also referable to *V. komodoensis*, demonstrating the longevity of *Varanus komodoensis* on mainland Australia and the coexistence of two giant varanids, *V. prisca* and *V. komodoensis*. In combination, the evidence from the fossil record as well as the morphological and molecular phylogenetic studies clearly supports Australia as the ancestral source for *V. komodoensis*.

Large-bodied varanid fossils were previously recovered from two middle Pleistocene sites along the Solo River in Java, west of the Wallace Line - the Trinil (~900 ka) and Kedung Brubus (800–700 ka) Faunas [22]. Although large, the Trinil vertebrae fall closest to the variation of modern *V. salvator*, with a few specimens comparable in size with the smallest modern *V. komodoensis*. These few larger specimens, considered previously to be *V. komodoensis* [17], more likely represent very large individuals of *V. salvator*. A single vertebra from the younger Kedung Brubus site is much bigger, comparable closely in both size and morphology with large *V. komodoensis*. We therefore conclude that it is likely that *V. komodoensis*, having reached Flores by the early Pleistocene, dispersed westward, across Wallace's Line to arrive in Java sometime during the middle Pleistocene.

Differential timing for the initial appearance of Komodo dragon in Australia, Flores and Java, therefore indicates that *V. komodoensis* dispersed from east to west, perhaps reaching Java during a period of lowered sea-level. At the time of Kedung Brubus, Java was part of the Asian mainland, and the fauna included large placental carnivores such as *Panthera* and *Hyaena* [22], further illustrating the ability of giant varanids to exist as part of a continental, placental-dominated fauna. There is currently no evidence that giant varanids survived on Java beyond the middle Pleistocene.

Further support for the westward dispersal of giant varanids comes from Timor, an island between Flores and Australia. Three vertebral specimens from Raebia in the Atambua Basin, central Timor, represent a new unnamed species of giant varanid

intermediate in size between *V. komodoensis* and *V. prisca* (sensu stricto). The Timor specimens were derived from the uppermost part of the folded, regressive Noele Formation, of which the marine part correlates with planktonic foraminifera zones N18–N22 [29,30]. This suggests that the specimens are at least middle Pleistocene in age. Pleistocene varanid fossils from central Australia, usually identified as *V. prisca*, are also intermediate in size between *V. komodoensis* and *V. prisca* (sensu stricto), and may represent the same intermediate taxon present in Timor. Formal description of the new Timor-Australian varanid waits until more diagnostic specimens are available.

## Conclusion

The fossil record suggests that giant varanids evolved independently on mainland Asia and the island-continent of Australia during the Pliocene, alongside large-bodied mammalian carnivores. Only the Indonesian-Australian giant varanids appear to have survived beyond the early Pleistocene.

We conclude that *V. komodoensis* evolved in Australia by the early Pliocene and dispersed west as far as Flores by 900 ka and Java by 800–700 ka. It is likely that the Timor varanid represents another large-bodied varanid lineage, attaining a larger body size than that of *V. komodoensis*, having evolved on mainland Australia and dispersed west to Timor. Continuing along this same evolutionary trajectory, *Varanus prisca*, reached gigantic proportions by the late-Middle Pleistocene, but was extinct in Australia by the end of the Pleistocene (Figure 9).

We conclude that *V. komodoensis* is the last of a clade of giant varanids that was once a ubiquitous part of Australasia, distributed from Australia across Wallacea, as far as continental Asia (Java). There is now only a relict population on Flores and a few small adjacent islands. Komodo dragon distribution has also retracted significantly on Flores itself; being present at Liang Bua in the uplands of West Flores until ~2 ka, but now only occurring in isolated habitats along the northern and western coastal lowlands [3,31]. The retraction is likely due to habitat loss and persecution by modern humans over the last few millennia and emphasizes the continuing threat of extinction to this, the last of the giant varanids.

## Supporting Information

**Figure S1** Histogram of tooth base length measurements for modern (A–B), Pleistocene (A) and Pliocene (B) *V. komodoensis*. Tangi Talo (n = 4), Liang Bua (n = 5), Chinchilla (n = 5) and *V. komodoensis* (n = 68). Measurements in mm.

Found at: doi:10.1371/journal.pone.0007241.s001 (0.23 MB DOC)

**Figure S2** Morphological comparisons between Indo-Asian and Indo-Australian varanid maxillae based on the phylogenetic reconstruction of Ast (2001). *Varanus varius* group with fossil specimens for comparison (to scale with *V. komodoensis*).

Found at: doi:10.1371/journal.pone.0007241.s002 (4.69 MB DOC)

**Figure S3** Histogram of humerus maximum diaphysis width with normal curve fitted to *Varanus* sample. *Varanus* spp. (n = 71), *Varanus komodoensis* (n = 18) (see Hutchinson & Reed (2005) for taxa used). Measurements in mm.

Found at: doi:10.1371/journal.pone.0007241.s003 (0.14 MB DOC)

**Figure S4** Histogram of dorsal vertebrae pre-post measurements with normal curve fitted. *Varanus komodoensis* modern (n = 100),

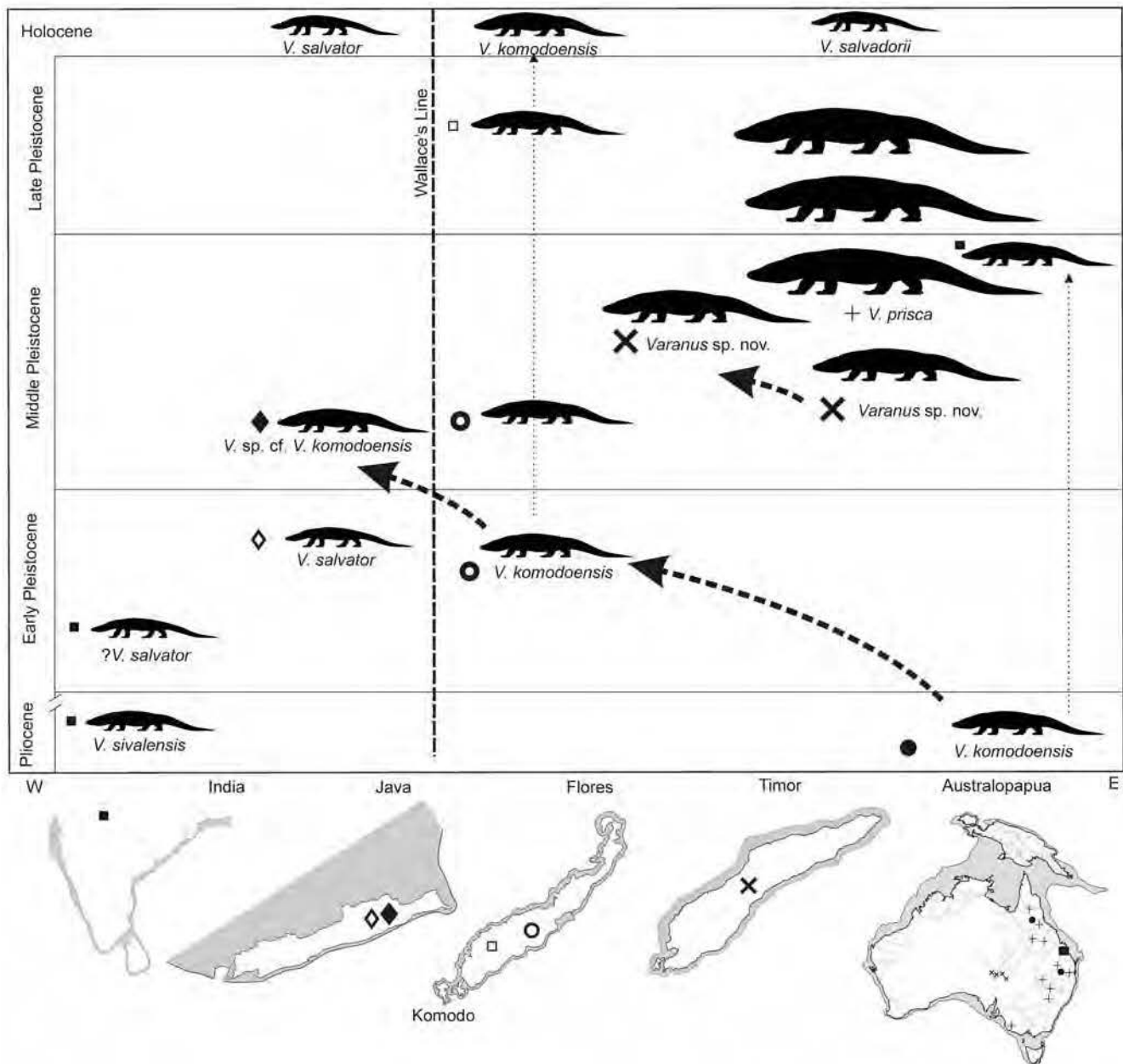


**Figure 9. Palaeogeography and chronology of giant varanids.** Schematic diagram illustrating the proposed taxonomy, chronology and dispersal sequence of giant varanids from mainland Australia to the Indonesian islands of Timor, Flores and Java during the Pliocene-Pleistocene. doi:10.1371/journal.pone.0007241.g009

Pliocene (Chinchilla & Bluff Downs) ( $n = 38$ ). Measurements in mm.

Found at: doi:10.1371/journal.pone.0007241.s004 (0.19 MB DOC)

**Figure S5** Measurements of varanid cervical vertebrae. A. Bivariate Plot of pre-pre length vs pre-post length. B. Bivariate Plot of cotylar width vs centrum length. Convex hulls applied to show limits of sample variation. Measurements in mm.

Found at: doi:10.1371/journal.pone.0007241.s005 (0.11 MB DOC)

**Figure S6** Box-plot of dorsal vertebrae cotylar width measurements. *Varanus salvator* ( $n = 24$ ), Trinil ( $n = 15$ ), *Varanus sivalensis* ( $n = 2$ ), modern *Varanus komodoensis* ( $n = 112$ ). Liang Bua ( $n = 16$ ). Measurements in mm.

Found at: doi:10.1371/journal.pone.0007241.s006 (0.05 MB DOC)

**Figure S7** Measurements of varanid dorsal vertebrae. Bivariate Plot of pre-pre length vs pre-post length. Convex hulls applied to show limits of sample variation. Measurements in mm.

Found at: doi:10.1371/journal.pone.0007241.s007 (0.09 MB DOC)

**Figure S8** Measurements of varanid sacral vertebrae. A. Bivariate plot of pre-pre length vs pre-post length. Convex hulls applied to show limits of sample variation. B. Box-plot of sacral vertebrae cotylar width measurements. *Varanus salvator* ( $n = 10$ ), Trinil ( $n = 2$ ), *Varanus komodoensis* ( $n = 9$ ), *V. prisca* ( $n = 4$ ). Measurements in mm.

Found at: doi:10.1371/journal.pone.0007241.s008 (0.10 MB DOC)

**Figure S9** Box-plot of caudal vertebrae prezygapophysis-postzygapophysis length measurements. *Varanus salvator* (n = 9), *Varanus komodoensis* (n = 24), Liang Bua (n = 4), *V. prisca* (n = 8). Measurements in mm.

Found at: doi:10.1371/journal.pone.0007241.s009 (0.06 MB DOC)

**Figure S10** Box plot of dorsal vertebra pre-postzygapophysis length for *V. prisca* (n = 53), *Varanus* sp. nov. (n = 11) and modern *V. komodoensis* (n = 32). Measurements in mm.

Found at: doi:10.1371/journal.pone.0007241.s010 (0.04 MB DOC)

**Figure S11** Measurements of varanid dorsal vertebrae. Bivariate plot of pre-pre length vs pre-post length. Convex hulls applied to show limits of sample variation. Measurements in mm.

Found at: doi:10.1371/journal.pone.0007241.s011 (0.07 MB DOC)

**Table S1** Specimens used in this study.

## References

- Owen R (1859) Description of some remains of a gigantic land-lizard (*Megalania prisca*, Owen) from Australia. Philosophical Transactions of the Royal Society of London 149: 43–48.
- Molnar RE (2004) Dragons in the Dust: The palaeobiology of the Giant Monitor Lizard *Megalania*. Indiana: Indiana University Press. 210 p.
- Auffenberg W (1981) The Behavioural Ecology of the Komodo Monitor. Gainesville FL: University Press of Florida. 406 p.
- Pianka ER (1995) Evolution of body-size: Varanid lizards as a model system. American Naturalist 146(3): 398–414.
- Christian A, Garland Jr (1996) Scaling of Limb Proportions in Monitor Lizards (Squamata: Varanidae). Journal of Herpetology 30(2): 219–230.
- Pianka ER (2004) Evolution of Body Size and Reproductive Tactics. In: Pianka ER, King DR, eds. Varanoid Lizards of the World. Bloomington, Indiana: Indiana University Press. pp 549–555.
- Gould GC, MacFadden BJ (2005) Gigantism, Dwarfism and Cope's Rule: "Nothing in Evolution Makes Sense without a Phylogeny". Bulletin of the American Museum of Natural History 285(1): 219–237.
- Burness GP, Diamond J, Flannery T (2001) Dinosaurs, dragons, and dwarfs: The evolution of maximal body size. PNAS 98(25): 14518–14523.
- Diamond JM (1987) Did Komodo dragons evolve to eat pygmy elephants? Nature 326: 832.
- van den Bergh GD, et al. (2008) The youngest *stegodon* remains in Southeast Asia from the Late Pleistocene archaeological site Liang Bua, Flores, Indonesia. Quaternary International 182: 16–48.
- Morwood MJ, et al. (2004) Archaeology and age of *Homo floresiensis*, a new hominin from Flores in eastern Indonesia. Nature 431: 1087–1091.
- Dunn, ER (1927) Results of the Douglas Burden Expeditions to the Island of Komodo, I. Notes on *Varanus komodoensis*. American Museum Novitates 286: 1–10.
- Conrad J (2008) Phylogeny and systematics of Squamata (Reptilia) based on morphology. Bulletin of the American Museum of Natural History 310: 1–182.
- Head JJ, Barrett PLS, Rayfield EJ (2009) Neurocranial osteology and systematic relationships of *Varanus (Megalania) prisca* Owen, 1859 (Squamata: Varanidae). Zoological Journal of the Linnean Society 155: 445–457.
- Ast J (2001) Mitochondrial DNA evidence and evolution in Varanoidea (Squamata). Cladistics 17: 211–226.
- Fitch AJ, Goodman AE, Donnellan SC (2006) A molecular phylogeny of the Australian monitor lizards (Squamata: Varanidae) inferred from mitochondrial DNA sequences. Australian Journal of Zoology 54: 253–269.
- Hooijer D (1972) *Varanus* (Reptilia, Sauria) from the Pleistocene of Timor. Zoologische Mededelingen 47: 445–447.
- Fuller S, Braverstock P, King D (1998) Biogeographic origins of goannas (Varanidae): A molecular perspective. Molecular Phylogenetics and Evolution 9(2): 294–307.
- Reed EH, Hutchinson, MN (2005) First record of a giant varanid (*Megalania*, Squamata) from the Pleistocene of Naracoorte, South Australia. Memoirs of the Queensland Museum 51(1): 203–214.
- Gaulke M, Horn HG (2004) *Varanus salvator* (nominate form). In: Pianka ER, King DR, eds. Varanoid Lizards of the World. Bloomington, Indiana: Indiana University Press. pp 244–255.
- Hammer O, Harper DAT, Ryan PD (2001) PAST: Palaeontological Statistics software package for education and data analysis. Palaeontologica Electronica 4(1): 1–9.
- van den Bergh GD, de Vos J, Sondaar PY (2001) The Late Quaternary palaeogeography of mammal evolution in the Indonesian Archipelago. Palaeogeography, Palaeoclimatology, Palaeoecology 171: 385–408.
- Falconer HP (1868) Paleontological Memoirs and Notes of the Late Hugh Falconer, A. M., M. D. Robert Hardwicke Publishers: Picadilly. 465 p.
- Lydekker R (1886) Fauna of the Karnul caves. Palaeontologica Indica 10(4): 1–58.
- Lydekker R (1888) Catalogue of the fossil Reptilia and Amphibia in the British Museum (Natural History), Cromwell Road, S.W. Pt. 1. The Orders Ornithosauria, Crocodilia, Dinosauria, Squamata, Rhynchocephalia, and Preterosauria. London: The Trustees. 245 p.
- Setiyabudi E (2006) Paleontological study on fossil giant tortoises from the Indonesian islands. (unpublished Thesis, Kagoshima University, Japan) 325 p.
- Dennell RR, Coard D, Turner A (2006) The biostratigraphy and magnetic polarity zonation of the Pabbi Hills, northern Pakistan: An Upper Siwalik (Pinjor Stage) Upper Pliocene–Lower Pleistocene fluvial sequence. Palaeogeography, Palaeoclimatology, Palaeoecology 234: 168–185.
- Hocknull SA, Zhao J-x, Feng Y-x, Webb GE (2007) Responses of Quaternary rainforest vertebrates to climate change in Australia, Earth and Planetary Science Letters 264: 317–331.
- Suwitodirdjo K, Tjokrosapoetro S (1975) Geologic Quadrangle Map, Timor, (GRDC, Bandung (1974/75).
- de Smet MEM (1990) Detection of collision related vertical movements in the outer Banda Arc (Timor, Indonesia) using micropaleontological data. Journal of South East Asian Earth Sciences 4(4): 337–356.
- Murphy JB, et al. (2002) Komodo Dragons: Biology and Conservation. Smithsonian Institution Press, Washington. 324 p.
- Mackness BS, Whitehead PW, McNamara GC (2000) New Potassium-Argon basalt date in relation to the Pliocene Bluff Downs Local Fauna, northern Australia. Australian Journal of Earth Sciences 47: 807–811.
- Dawson L, Muirhead J, Wroe S (1999) The Big Sink Fauna: a lower Pliocene mammalian fauna from the Wellington Caves complex, Wellington, New South Wales. Records of the Western Australian Museum Supplement No. 57: 265–290.
- Price GJ, Zhao J-x, Feng Y-x, Hocknull SA (2009) New Records of Pliocene Koalas from Australia: Palaeoecological and Taxonomic Implications. Records of the Australian Museum 61: 39–48.